CURRENT PROGRESS IN MESENCHYMAL STEM/ STROMAL CELL RESEARCH

EDITED BY: Lindolfo da Silva Meirelles, Karen Bieback and Marcela F. Bolontrade
PUBLISHED IN: Frontiers in Cell and Developmental Biology

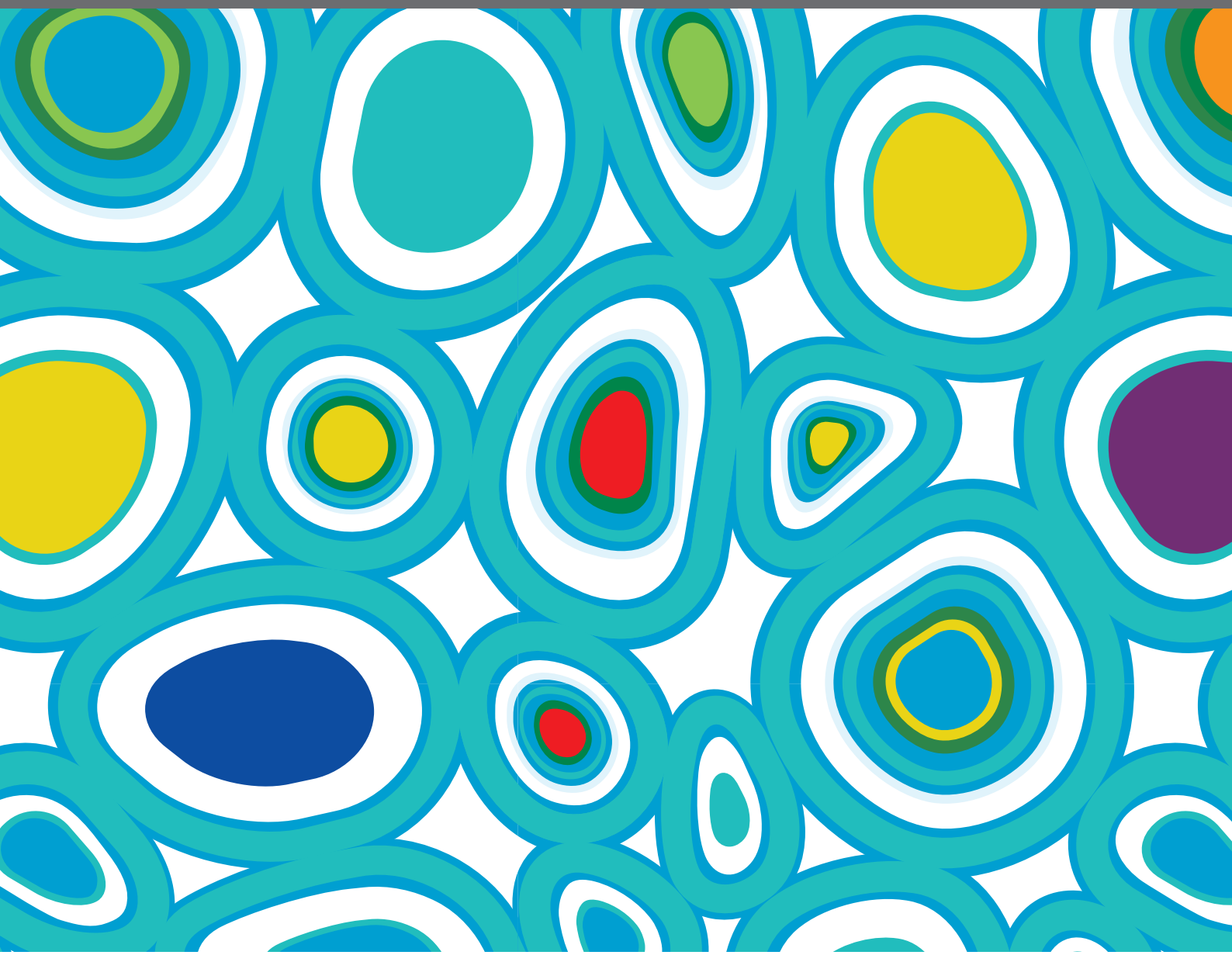

frontiers Research Topics

ISSN 1664-8714
ISBN 978-2-88966-625-6
DOI 10.3389/978-2-88966-625-6

About Frontiers

Frontiers is more than just an open-access publisher of scholarly articles: it is a pioneering approach to the world of academia, radically improving the way scholarly research is managed. The grand vision of Frontiers is a world where all people have an equal opportunity to seek, share and generate knowledge. Frontiers provides immediate and permanent online open access to all its publications, but this alone is not enough to realize our grand goals.

Frontiers Journal Series

The Frontiers Journal Series is a multi-tier and interdisciplinary set of open-access, online journals, promising a paradigm shift from the current review, selection and dissemination processes in academic publishing. All Frontiers journals are driven by researchers for researchers; therefore, they constitute a service to the scholarly community. At the same time, the Frontiers Journal Series operates on a revolutionary invention, the tiered publishing system, initially addressing specific communities of scholars, and gradually climbing up to broader public understanding, thus serving the interests of the lay society, too.

Dedication to Quality

Each Frontiers article is a landmark of the highest quality, thanks to genuinely collaborative interactions between authors and review editors, who include some of the world's best academicians. Research must be certified by peers before entering a stream of knowledge that may eventually reach the public - and shape society; therefore, Frontiers only applies the most rigorous and unbiased reviews.
Frontiers revolutionizes research publishing by freely delivering the most outstanding research, evaluated with no bias from both the academic and social point of view. By applying the most advanced information technologies, Frontiers is catapulting scholarly publishing into a new generation.

What are Frontiers Research Topics?

Frontiers Research Topics are very popular trademarks of the Frontiers Journals Series: they are collections of at least ten articles, all centered on a particular subject. With their unique mix of varied contributions from Original Research to Review Articles, Frontiers Research Topics unify the most influential researchers, the latest key findings and historical advances in a hot research area! Find out more on how to host your own Frontiers Research Topic or contribute to one as an author by contacting the Frontiers Editorial Office: frontiersin.org/about/contact

CURRENT PROGRESS IN MESENCHYMAL STEM/ STROMAL CELL RESEARCH

Topic Editors:
Lindolfo da Silva Meirelles, Universidade Luterana do Brasil, Brazil
Karen Bieback, Heidelberg University, Germany
Marcela F. Bolontrade, Consejo Nacional de Investigaciones Científicas y Técnicas (CONICET), Argentina

Citation: da Silva Meirelles, L., Bieback, K., Bolontrade, M. F., eds. (2021). Current Progress in Mesenchymal Stem/Stromal Cell Research. Lausanne: Frontiers Media SA. doi: 10.3389/978-2-88966-625-6

Table of Contents

frontiers in Cell and Developmental Biology

EDITORIAL
published: 18 February 2021
doi: 10.3389/fcell.2021.658903

Editorial: Current Progress in Mesenchymal Stem/Stromal Cell Research

Lindolfo da Silva Meirelles[1]*, *Karen Bieback*[2] and *Marcela F. Bolontrade*[3]

[1] Universidade Luterana do Brasil, Canoas, Brazil, [2] Institute for Transfusion Medicine and Immunology, Medical Faculty Mannheim, Heidelberg University, Heidelberg, Germany, [3] Instituto de Medicina Traslacional e Ingeniería Biomédica (IMTIB) CONICET, Instituto Universitario del Hospital Italiano, Hospital Italiano de Buenos Aires, Buenos Aires, Argentina

Keywords: mesenchymal stem cells, mesenchymal stromal (or stem) cells, mesenchymal stromal cells, basic research, MSC therapies

Editorial on the Research Topic

Current Progress in Mesenchymal Stem/Stromal Cell Research

Currently, mesenchymal stem/stromal cells (MSCs) are among the most used cell types in clinical trials. At the time this Editorial was written (mid-January 2021), a search at www.clinicaltrials.gov using the term "MSCs OR mesenchymal stem cells OR mesenchymal stromal cells" returned 10,407 registered clinical trials using these cells, 3,467 of which were active. While many characteristics of these cells have been described to date, aspects of their basic biology that may have an impact on their use in regenerative medicine are still under investigation. Likewise, in spite of the successful use of these cells in tissue engineering and cell therapy scenarios, further work on ways to enhance their aptitude for therapeutic purposes are still under development.

The aim of this Research Topic was to provide a venue for high-quality research articles and reviews that could broaden the knowledge on the biology of mesenchymal stem/stromal cells, including mechanisms that can affect their role as agents in cell therapy and tissue engineering. Manuscripts submitted to this Research Topic were expected to contain information to better understand how MSCs behave, and how they exert their therapeutic properties, whether such information would come from *in vitro* or *in vivo* studies. Consequently, suggested subjects for submitted manuscripts included (a) novel features of MSCs from different tissues; (b) molecular aspects of MSC differentiation; (c) processes for the enhancement of MSC differentiation and expansion in culture; (d) identification of MSCs, or cells that can give rise to them, *in situ*; (e) acellular MSC-derived products such as extracellular vesicles; (f) immunomodulatory properties of MSCs; (g) molecular interactions between MSCs and other cell types *in vitro* or *in vivo*; and (h) reviews of achievements and challenges in translating MSCs from the bench to bedside, including the development of authorized advanced therapy medicinal products. Consequently, this Research Topic received 26 manuscripts. Seventeen of these manuscripts were accepted; eight of these were original research reports, and nine were reviews or mini-reviews.

The review articles in this Research Topic cover a wide range of subjects in the MSC field. The review by Bozorgmehr et al. highlights biological properties and clinical applications of endometrial and menstrual blood MSCs, which comprise cell populations that share many characteristics with MSCs obtained from other tissues. Robert et al. review the transcriptomic changes that take place during adipogenic, osteogenic, and chondrogenic differentiation of MSCs from various body sites. Kamdje et al. review the ability of the tumor microenvironment to reprogram MSCs toward a phenotype that favors tumoral maintenance. Forsberg et al. addresses the development of MSC-based

Edited and reviewed by:
Valerie Kouskoff,
The University of Manchester, United Kingdom

***Correspondence:**
Lindolfo da Silva Meirelles
lindolfomeirelles@gmail.com

Specialty section:
This article was submitted to Stem Cell Research, a section of the journal Frontiers in Cell and Developmental Biology

Received: *26 January 2021*
Accepted: *01 February 2021*
Published: *18 February 2021*

Citation:
da Silva Meirelles L, Bieback K and Bolontrade MF (2021) Editorial: Current Progress in Mesenchymal Stem/Stromal Cell Research. Front. Cell Dev. Biol. 9:658903. doi: 10.3389/fcell.2021.658903

treatments for human diseases, particularly treatments using MSC-derived exosomes, in contexts like acute radiation syndrome, graft vs. host disease, cardiovascular conditions, and COVID-19. Daltro et al. introduce and review the concept of using MSCs for the treatment of inflammatory/allergic skin disorders such as atopic dermatitis, and suggest that the broad immunomodulatory potential of MSCs on T cells, B cells, and mast cells may prove beneficial in these cases. Damasceno et al. review whether and how genetic engineering can be applied to improve the therapeutic efficacy of MSCs. They summarize the current knowledge on using viral vectors and non-viral methods to express bioactive molecules in the context of cancer treatment and various diseases. Kamal and Kassem review achievements, as well as challenges/hurdles in establishing Wharton's jelly-derived MSCs as therapeutic agents for the treatment of diabetic complications while focusing on the potential of these cells to home and differentiate/replace diseased cells, and to secrete bioactive factors that can modulate immune responses; additionally, these authors stress existing challenges to translate this knowledge from the bench to the bedside. Lavrentieva et al. review possible pitfalls in the production of human MSCs for cell therapies, focusing on the heterogeneity of current strategies used to obtain MSCs for clinical applications. Finally, Ramezankhani et al. summarize authorized advanced therapy medicinal products (ATMPs) currently available and review accomplishments, clinical trial safety, and efficacy data available for various ATMPs during the last two decades. They introduce a classification of the approved ATMPs, providing descriptions together with manufacturer, indication, approval date, regulatory agency, dosage, description, and price data.

Among the original research articles in this Research Topic, two provide aspects of the production of MSCs or extracellular vesicles secreted by them. Stroncek et al. report the variability MSC features when these cells are manufactured using different methods and source materials. Thus, they assess the impact on MSC characteristics when different laboratories propagated MSCs from cultures initiated with bone marrow aliquots derived from the same donor source material. Fuzeta et al. describes a xeno-free microcarrier-based culture system using a vertical-wheel bioreactor and a human platelet lysate culture supplement to achieve scalable production of extracellular vesicles by MSCs obtained from human bone marrow, adipose tissue, and umbilical cord matrix.

The promotion of angiogenesis by MSCs is the focus of two of the original research articles accepted. Kremer et al. compares the angiogenic potential of retinal pericytes and adipose tissue MSCs (ASCs) using angiogenesis assays in addition to transcriptomic and multiplex cytokine analyses; they found that ASCs were able to promote angiogenesis mainly through secretion of vascular-endothelial growth factor, while retinal pericytes did not exhibit pro-angiogenic properties. Whereas, Santos et al. describes the augmentation of the angiogenic potential of bone marrow MSCs by genetically modifying these cells to overexpress leukemia inhibitory factor prior to angiogenesis assays *in vitro* and *in vivo*.

Finally, four original research articles describe findings related to MSC differentiation. Díaz-Flores et al. provide an account of immunohistochemical analyses on archived samples from cases of acute cholecystitis, malignant colonic polyps, and colon adenocarcinomas; their results suggest that the development of myofibroblasts in these samples is linked to the presence of CD34-positive stromal cells. Driesen et al. identify the expression of fibroblast activation protein-α (FAPα) in human dental tissue stem cells, which are an MSC-related cell type. The findings by these authors indicate a relationship of the expression of FAPα with extracellular matrix remodeling and osteoblast function. Dilger et al. describe gap junction-dependent cell-cell communication and the expression pattern of gap junction-building connexins in MSCs during a neuronal differentiation protocol using small molecules, thus providing an account of the generation of immature neuron-like cells that may be of potential interest to explore mechanisms of MSC differentiation. Ji et al. address the mechanism of action of hsa_circ_0026827, demonstrating that it promotes osteoblast differentiation of human dental pulp stem cells via Beclin1 and the RUNX1 signaling pathways, by sponging miR-188-3p.

The fact that so many questions remain open in the MSC research field after decades of development is impressive. The ultimate goal—the widespread therapeutic use of these cells or their acellular products in the clinic—seems to be closer every day, as new clinical trials involving MSCs keep emerging. To achieve this ultimate goal, furthering the knowledge on the mechanisms underlying their potential therapeutic actions is of paramount importance, along with the clinical translation of such knowledge.

AUTHOR CONTRIBUTIONS

All authors listed have made a substantial, direct and intellectual contribution to the work, and approved it for publication.

FUNDING

LdSM acknowledges partial funding by São Paulo Research Foundation (FAPESP), grant number 2015/20206-8. KB acknowledges support from the International Research Training Group DIAMICOM (SP06-GRK1874) funded by the Deutsche Forschungsgemeinschaft (DFG) and the European Union's Horizon 2020 research and innovation programme under the Marie Sklodowska-Curie grant agreement No. 813839 (RenalToolBox). MFB acknowledges funding from the National Agency for Scientific and Technological Promotion, grant number PICT 1974 and Fundación Florencio Fiorini (FFF) - National Academy of Medicine, Argentina.

Conflict of Interest: The authors declare that the research was conducted in the absence of any commercial or financial relationships that could be construed as a potential conflict of interest.

frontiers in Cell and Developmental Biology

BRIEF RESEARCH REPORT
published: 21 January 2020
doi: 10.3389/fcell.2019.00389

Dental Tissue and Stem Cells Revisited: New Insights From the Expression of Fibroblast Activation Protein-Alpha

Ronald B. Driesen[1,2], Petra Hilkens[1,2], Nick Smisdom[3], Tim Vangansewinkel[1,2], Yörg Dillen[1,2], Jessica Ratajczak[1,2], Esther Wolfs[1,2], Pascal Gervois[1,2], Marcel Ameloot[3], Annelies Bronckaers[1,2] and Ivo Lambrichts[1,2]*

[1] Faculty of Medicine, Hasselt University, Diepenbeek, Belgium, [2] Laboratory of Morphology, Biomedical Research Institute, Hasselt University, Diepenbeek, Belgium, [3] Department of Biophysics, Biomedical Research Institute, Hasselt University, Diepenbeek, Belgium

Fibroblast activation protein-α (FAPα) is a membrane protein with dipeptidyl-peptidase and type I collagenase activity and is expressed during fetal growth. At the age of adolescence, FAPα expression is greatly reduced, only emerging in pathologies associated with extracellular matrix remodeling. We determined whether FAPα is expressed in human dental tissue involved in root maturation i.e., dental follicle and apical papilla and in dental pulp tissue. The dental follicle revealed a high concentration of FAPα and vimentin-positive cells within the stromal tissue. A similar observation was made in cell culture and FACS analysis confirmed these as dental follicle stem cells. Within the remnants of the Hertwigs' epithelial root sheath, we observed FAPα staining in the E-cadherin positive and vimentin-negative epithelial islands. FAPα- and vimentin-positive cells were encountered at the periphery of the islands suggesting an epithelial mesenchymal transition process. Analysis of the apical papilla revealed two novel histological regions; the periphery with dense and parallel aligned collagen type I defined as cortex fibrosa and the inner stromal tissue composed of less compacted collagen defined as medulla. FAPα expression was highly present within the medulla suggesting a role in extracellular matrix remodeling. Dental pulp tissue uncovered a heterogeneous FAPα staining but strong staining was noted within odontoblasts. *In vitro* studies confirmed the presence of FAPα expression in stem cells of the apical papilla and dental pulp. This study identified the expression of FAPα expression in dental stem cells which could open new perspectives in understanding dental root maturation and odontoblast function.

Keywords: stem cell, molar, tooth, apical papilla, collagen, vimentin, odontoblast

OPEN ACCESS

Edited by:
Marcela F. Bolontrade, Italian Hospital of Buenos Aires, Argentina

Reviewed by:
Zhi Chen, Wuhan University, China
Gianpaolo Papaccio, Second University of Naples, Italy

****Correspondence:***
Ronald B. Driesen
ronald.driesen@uhasselt.be

Specialty section:
This article was submitted to Stem Cell Research, a section of the journal Frontiers in Cell and Developmental Biology

Received: *04 September 2019*
Accepted: *23 December 2019*
Published: *21 January 2020*

Citation:
Driesen RB, Hilkens P, Smisdom N, Vangansewinkel T, Dillen Y, Ratajczak J, Wolfs E, Gervois P, Ameloot M, Bronckaers A and Lambrichts I (2020) Dental Tissue and Stem Cells Revisited: New Insights From the Expression of Fibroblast Activation Protein-Alpha. Front. Cell Dev. Biol. 7:389. doi: 10.3389/fcell.2019.00389

INTRODUCTION

Fibroblast activation protein alpha (FAPα), also known as seprase, is a type II membrane serine protease which displays functional similarities with prolyl-cleaving peptidases (Chung et al., 2014). The human FAPα gene is located on 2q24.2 and shares 50% homology in amino acids with the dipeptidyl peptidase IV (DPP-IV) enzyme. FAPα promotes type I collagen degradation

through its collagenase activity (Chung et al., 2014). During embryogenesis, FAPα expression is highly upregulated in mesenchymal tissues where it contributes to extracellular matrix remodeling (Niedermeyer et al., 2001). When reaching adolescence, FAPα expression is almost completely lost but it re-emerges in pathologies associated with active tissue remodeling such as myocardial infarction (Tillmanns et al., 2015), pulmonary fibrosis (Fan et al., 2016), and cancer (Wen et al., 2016). At the cellular level, re-expression is found during fibroblast differentiation (Tillmanns et al., 2015) and is linked to circulating levels of TGF-β1 and IL-1β leading to activation of the SMAD pathway (Tillmanns et al., 2015). Loss of FAPα activity impacts the migratory capacity of myofibroblasts but does not affect their proliferation rate (Teichgräber et al., 2015). Recently it has been shown that FAPα is highly expressed in human bone marrow mesenchymal stem cells (BMSCs) (Chung et al., 2014) where it stimulates cell migration via RhoA GTPase activity, independent of its peptidase function.

The discovery of another source of MSCs in dental pulp tissue of third molars (Gronthos et al., 2000) i.e., dental pulp stem cells (DPSCs), led to the identification of a variety of MSCs defined by specific locations in the developing tooth, and the surrounding dental tissue. These include stem cells from the apical papilla (SCAPs), periodontal ligament stem cells (PDLSCs), and dental follicle stem cells (DFSCs). All are classified as MSCs according to the criteria proposed by the International Society for Cellular Therapy (Dominici et al., 2006; Huang et al., 2009). Whether FAPα is expressed in dental stem cells and if it contributes to dental tooth development is currently not known.

In this study, we investigated FAPα expression in the dental follicle and apical papilla, tissues both involved in root formation, and within the dental pulp of third molars of young adolescents. Visualization of FAPα expressing stem cells provided new evidence for the epithelial mesenchymal transition (EMT) within remnants of the Hertwig's epithelial root sheath (HERS) and shed new light on the histological organization of the apical papilla. In addition, FAPα expression was highly pronounced in odontoblasts of the dental pulp suggesting a role in dentinogenesis.

MATERIALS AND METHODS

Isolation and Cell Culture of Stem Cells From Dental Pulp and Apical Papilla

Dental follicles (n = 4) and healthy normal human third molars were collected from patients (14–21 years old) at the Ziekenhuis Maas and Kempen, Bree and ZOL Genk with written informed consent and approved by the medical ethical committee of Hasselt University (protocol 13/0104U). The apical papillae (n = 5) and dental pulp (n = 6) were separated from the teeth and all tissues were collected in α-Minimal Essential Medium (Sigma-Aldrich, Overijse, Belgium) supplemented with 10% heat inactivated fetal calf serum (FCS) (Biochrom AG, Berlin, Germany), 2 mM L-Glutamine, 100 U/ml Penicillin and 100 μg/ml Streptomycin (Sigma-Aldrich). Stem cells were isolated via the explant method as described previously (Hilkens et al., 2013). Briefly, pieces of 1 mm^3 were placed into a 6-well plate containing culture medium. Explants were cultured for 14 days allowing stem cells to grow out of the tissue at 37°C in a humidified atmosphere containing 5% CO_2. Medium was changed twice a week. After 10 to 14 days, 80% to 90% confluency was reached and cells were sub-cultured. For all experiments, cells of passage one to three were used.

Histological Analysis

Tissue samples were fixed in 4% paraformaldehyde overnight and routinely embedded in paraffin. After deparaffinization and rehydration, 7 μm sections were stained for collagen using either Masson's Trichrome or Sirius Red staining. Toluidine blue staining was performed on semi-thin sections of araldite embedded tissue. Prior to staining, samples were fixed with 2% glutaraldehyde in 0.05 M cacodylate buffer, post-fixed in 2% osmium tetroxide and stained with 2% uranyl acetate in 10% acetone. Samples were dehydrated in series of graded acetone concentrations and embedded in araldite according to the pop-off method.

Immunohistochemistry and Immunocytochemistry

Antigen retrieval was performed in deparaffinized tissue sections using citrate buffer (Dako, Glostrup, Denmark) heated in the microwave oven (3 × 5′ cycli). After cooling down for 20′, sections were washed in phosphate buffered saline (PBS) and used for either diaminobenzidine (DAB) or fluorescent immunostaining. For DAB immunostaining, sections were treated with peroxidase block (Dako) for 20′. Afterward sections were washed with PBS and incubated with protein block (Dako) to limit background staining. Consequently, sections were incubated with a primary antibody against FAPα (1:200, Abcam, Ab2844), vimentin (1:100, Abcam, Ab8069), dsPP (1:200, Abcam, Ab216892) diluted in PBS for 1 h at room temperature followed by 3 washes with PBS. As negative control, the primary antibody was omitted from a section. Peroxidase-conjugated secondary antibodies diluted in PBS were applied for 45′ at room temperature followed by 3 washes in PBS. The chromogenic substrate DAB was used to visualize the protein of interest (DAB kit, Dako). Cells were counterstained with Mayer's hematoxylin and mounted using DPX (Dibutylphthalate Polystyrene Xylene) mounting medium. The immune-reactivity was determined using a photomicroscope equipped with an automated camera (Nikon Eclipse 80i, Nikon Co., Japan).

For immunofluorescent staining, sections were treated with protein block, followed by a wash in PBS and incubation with primary antibodies against FAPα (1:200, Abcam, Ab2844), vimentin (1:100, Abcam, Ab8069), E-cadherin (1:200, Abcam, Ab231303), CXCR4 (1:50, Abcam, Ab124824), α-SMA (1:250, Thermo Fisher Scientific, asm-1), and CD44 (1:100, Abcam, Ab194987) overnight in a humidified atmosphere. As negative control, the primary antibody was omitted from a section. The next day, sections were washed with PBS and incubated with fluorochrome conjugated secondary antibodies for 1 h. After 3 washes in PBS, nuclei were counterstained with DAPI for

30 min and sections were mounted in fluorescent embedding medium (Dako). Fluorescent signal was imaged using a Leica fluorescence microscope (DM 4000 B LED) with the Leica Application Suite X software.

Fluorescent Activated Cell Sorting Analysis

Stem cells were seeded in 25 cm^2 culture flasks and were harvested by trypsinization after 7 days. Cells were incubated for at least 1 h at room temperature in PBS with 2% FCS to allow re-expression of receptor proteins at the cell surface. For intracellular staining of vimentin (1:100, Millipore) and nestin (1:100, Dako), cells were first fixed and then permeabilized with the cytofix/cytoperm kit (Becton–Dickinson, San Jose, CA, United States) according to manufacturer's protocol. 0.5×10^5 cells were washed with PBS containing 2% FCS and were incubated for 30 min at room temperature with primary antibodies against either CD24-PE (1:20, eBioscience, San Diego, CA, United States), CD31-PE (1:100, ImmunoTools), CD34-PE (1:100, ImmunoTools), CD44-PE (1:100, Abcam), CD45-PE (1:100, eBioscience), CD90-PE (1:100, eBioscience), CD105-PE (1:100, Abcam), and p75-PE (1:100, Dako). As a negative control for non-specific background staining, appropriate isotype controls were included. Thereafter, cells were washed three times with PBS and if necessary, incubated with secondary antibodies including FITC-labeled goat anti-rabbit (eBioscience) or PE-labeled anti-mouse IgG (Invitrogen) for 45 min at room temperature. Samples were analyzed on a FACScalibur™ flow cytometer equipped with CellQuest software (BD Biosciences, Erembodegem, Belgium).

Second Harmonic Generation and Confocal Microscopy

Second harmonic generation imaging was performed using a Zeiss LSM 880 (Carl Zeiss, Jena, Germany) mounted on an Axio Observer and equipped with a 20× objective (Plan-Apochromat 20×/0.8, Carl Zeiss) (Sanen et al., 2016). A pixel size of 0.69 μm was used with an image resolution of 1024 by 1024 and a pixel dwell time of 8.19 μs. Full tissue sections were imaged by means of tile scans with 10% overlap to enable the stitching of the recorded tiles. Excitation was provided by a femtosecond pulsed laser (MaiTai DeepSee, Spectra-Physics, CA, United States) tuned to a central wavelength of 810 nm. This laser was directed to the sample using a 760 nm shortpass dichroic mirror. The SHG signal and autofluorescence were collected in backward non-descanned mode using a 760 nm short pass dichroic mirror. A BP 350–690 bandpass filter was used to block any scattering infrared light. Finally, a 425 nm dichroic mirror separated SHG from autofluorescence which were subsequently simultanously recorded via, respectively, a 400–410 nm bandpass filter and a 450–650 nm band pass filter, by means of GaAsP detectors (BIG2, Carl Zeiss).

Confocal microscopy was performed using the same system as used for SHG imaging. Fluorescence was collected using a 63× (Plan-Apochromat 63×/1.4 Oil, Carl Zeiss). The resulting pixel size was 0.09 μm with a pixel dwell time of 2.65 μs. 3 laser lines were used for excitation: 488 nm (Ar-ion), 543 nm (HeNe) and 740 nm (MaiTai DeepSee, Spectra-Physics, CA, United States). A 488/543 nm dichroic and a 690 nm shortpass dichroic were used as main beam splitters. The resulting fluorescence was collected using a spectral GaAsP detector selecting 3 different spectral bands: 472–543 nm, 552–695 nm, and 414–472 nm.

Statistical Analysis

Statistical analysis was performed using a Kruskal Wallis one-way ANOVA (non-parametric) on $n = 4$ independent cell cultures from 4 different donors. $p < 0.05$ is considered as statistically significant.

RESULTS

Identification of Fibroblast Activation Protein-α Expressing Stem Cells in the Dental Follicle

The dental follicle determines the growth of the periodontal ligament and the cementum and contains HERS remnants which promote dental root formation (Itaya et al., 2017). Immunofluorescent staining of the dental follicle revealed a high number of stromal cells (**Figure 1A**) which were positive for FAPα but negative for E-cadherin, an epithelial cell adhesion marker. This was contrary to the epithelial rests originating from HERS showing E-cadherin staining between intercellular connections (**Figures 1B–E**). FAPα staining was markedly present in a fraction of the epithelial cells and often co-localized with the nucleus (**Figures 1C–E**). The majority of epithelial cells stained negative for vimentin as demonstrated by immunohistochemistry (**Figure 1F**) and immunofluorescent (**Figure 1G**) staining. However, FAPα positive and vimentin positive cells were encountered at the periphery of the epithelial islands (**Figures 1F,G**). Next, we investigated FAPα and vimentin expression in cell cultures of DFSCs (**Figures 1H,I**). 84 ± 4% of the cells stained positive for FAPα and vimentin (**Figure 1H**, thick arrow) which was significantly higher than the vimentin positive but FAPα negative cells ($p < 0.05$). A total of 15% of the cells were negative for vimentin from which 10 ± 2% stained positive for FAPα (**Figure 1H**; arrowhead) and 5 ± 3.5% were FAPα negative (**Figure 1H**; thin arrow). The cellular localization of FAPα was determined by 3-D volume rendering of confocal z-stack images (**Figure 1J**) showing a diffuse distribution on the plasma membrane and/or a high concentration above the nucleus (**Figure 1K**). Flow cytometry of DFSCs revealed positive expression of the stem cell markers CD44, CD90, and CD105 in almost all cells (**Supplementary Figure 1**) but a lack of expression of CD31, CD34, and CD45. Based on these criteria, the majority of FAPα positive/vimentin positive cells are considered DFSCs.

Fibroblast Activation Protein-α Expression in the Apical Papilla

Third molars of young adolescents have a well-developed apical papilla at the base of the developing root (Sonoyama et al., 2008). Visualization of collagen type I using SHG microscopy

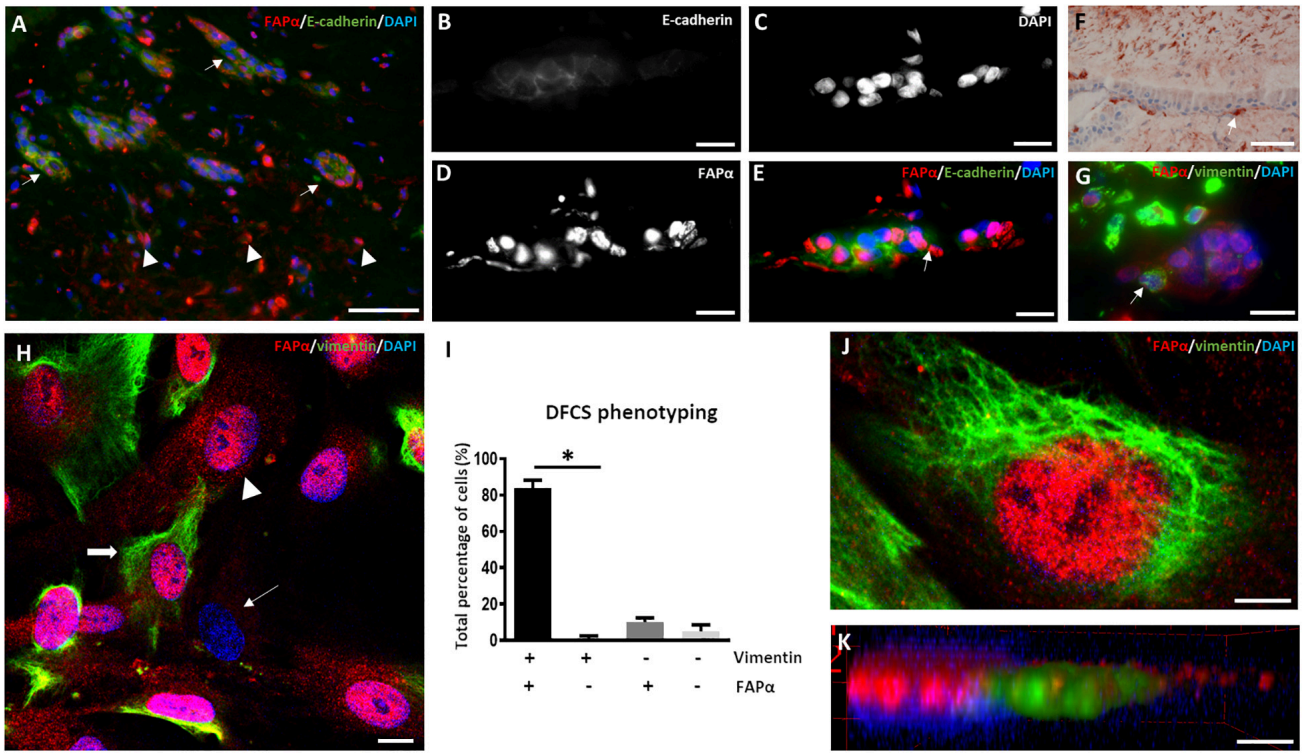

FIGURE 1 | FAPα is expressed in stem cells of the dental follicle. **(A)** Double immunofluorescent staining in dental follicle tissue of FAPα (red), E-cadherin (green), and the nucleus (DAPI, blue). Arrows indicate epithelial rests and arrowheads point to FAPα$^+$/E-cadherin$^-$ cells. **(B–E)** Higher magnification of an epithelial rest displaying E-cadherin **(B)**, nuclei **(C)**, FAPα **(D)**, and the corresponding overlay **(E)**. **(F)** Visualization of mesenchymal cells in the dental follicle using vimentin staining. Note the presence of a vimentin positive cell at the periphery of the epithelial rest (white arrow). **(G)** Double immunofluorescent staining of FAPα and vimentin showing FAPα$^+$/vimentin$^-$ cells in the epithelial rest. A FAPα$^+$/vimentin$^+$ cell is located at the periphery of the epithelial rest. **(H)** Triple immunofluorescent staining of vimentin (green), FAPα (red), and nuclei (blue) in cultured dental follicle stem cells. Indicated cells are FAPα$^+$/vimentin$^+$ (thick arrow), FAPα$^+$/vimentin$^-$ (arrowhead), and FAPα$^-$/vimentin$^-$ (thin arrow). **(I)** Quantification of the different phenotypes based on vimentin and FAPα expression ($n = 4$; $^*p < 0.05$). **(J)** Confocal image of triple immunofluorescent staining of vimentin (green), FAPα (red), and nuclei (DAPI). **(K)** 3-D volume rendering of **(J)** showing localization of FAPα on the plasma membrane. Scale bars represent 4 **(J,K)**, 10 **(B–E,G,H)**, and 50 **(A,F)** μm.

identified two different morphological regions in the apical papilla (**Figure 2A**); the periphery with dense collagen type I and the inner tissue composed of less compacted collagen type I. Semi-thin sections indicated a different cellular orientation within these two regions (**Figure 2B**); (1) the periphery is composed of a single layer of cube-shaped epithelial cells and a sub-epithelial region containing cells with a parallel orientation and (2) the inner region of the apical papilla with randomly oriented cells. Masson's Trichrome staining (**Figure 2C**), Sirius red staining (**Supplementary Figure 2A**) and SHG imaging (**Figure 2D**) confirmed that cells in the periphery are embedded in a tightly organized extracellular matrix displaying a parallel orientation. We defined this region as the cortex fibrosa. Immunohistochemistry showed the presence of FAPα positive cells within the epithelial layer and a lower density of FAPα positive cells in the sub-epithelial region (**Figure 2E**). Double immunofluorescent staining for FAPα and vimentin (**Figure 2F**) confirmed the DAB staining pattern of FAPα and demonstrated absence of vimentin staining in the epithelial layer. The majority of sub-epithelial cells in the cortex fibrosa are vimentin positive with a minority of cells expressing FAPα. The cortex fibrosa encapsulates the inner center which is composed of loose connective tissue with randomly distributed cells as shown by Masson's Trichrome (**Figure 2G**) and Sirius Red (**Supplementary Figure 2B**) staining. SHG imaging confirmed the loose organization of collagen fibers (**Figure 2H**). This inner region which we defined as medulla contained a high concentration of FAPα and vimentin positive cells as shown by immunohistochemistry (**Figure 2I**) and double immunofluorescent staining (**Figure 2J**). Alpha-smooth muscle actin (α-SMA) staining was only restricted to the vasculature (data not shown). Serial sections of the medulla revealed FAPα positive staining in the central peripheral nerve which extends from the dental pulp through the apical papilla (**Figures 2K,L**). Surprisingly, immunofluorescent staining identified round-shaped cells in the inner part of the medulla and in the vicinity of the central nerve which were vimentin negative (**Figures 2M,N**) but still FAPα positive. Additional phenotypical characterization demonstrated that the vimentin expressing cells in the surrounding outer medulla were positive for CD44, a mesenchymal stem cell marker (**Figures 2O–Q**) whereas the vimentin negative fraction inside

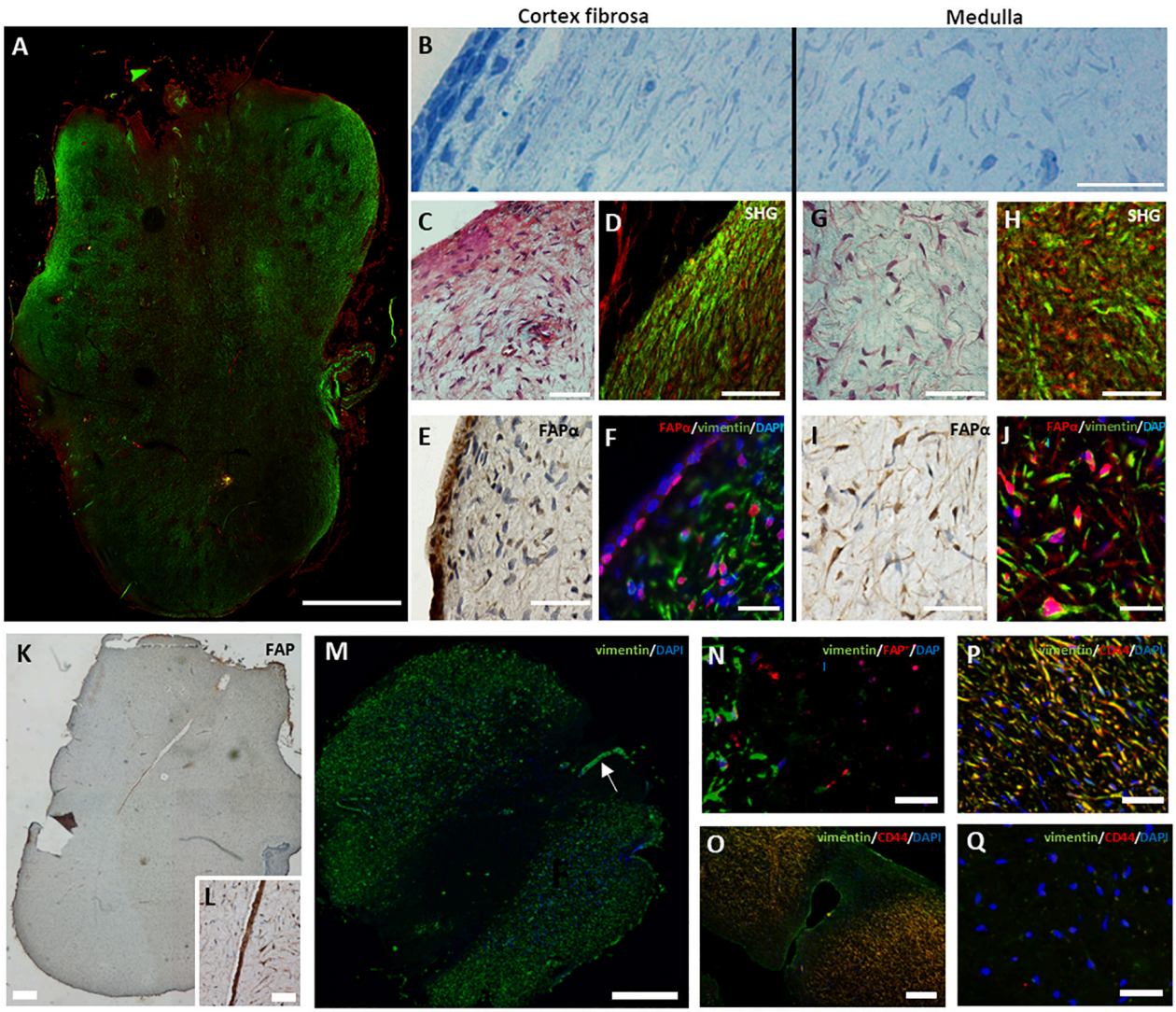

FIGURE 2 | Heterogeneous expression of FAPα in the apical papilla. **(A)** Tile scan of a second harmonic generated overview of a complete apical papilla (green, collagen type I; red, autofluorescence). **(B)** Semi-thin section of an apical papilla stained with toluidine blue showing a parallel orientation of cells at the cortex fibrosa but random orientation inside the medulla. **(C)** Masson's Trichrome staining of the cortex fibrosa showing a high collagen concentration. **(D)** Second harmonic generation imaging of the periphery of the apical papilla (green, collagen type I; red, autofluorescence). **(E)** DAB staining for FAPα reveals a heterogeneous expression pattern at the periphery of the tissue. Note the marked staining of FAPα in the epithelial region. **(F)** Double immunofluorescent staining showing predominantly vimentin positive cells (green) and a small population of $FAP\alpha^+$ (red)/$vimentin^+$ cells. The epithelial region consists of $FAP\alpha^+$ but $vimentin^-$ cells. **(G)** Masson's Trichrome staining of the medulla reveals a loose extracellular matrix with spindle-shaped cells. **(H)** Second harmonic imaging confirms the loose collagen distribution (green). **(I)** DAB staining indicates high expression levels of FAPα in the medulla. **(J)** Immunofluorescent staining reveals a predominant population of $FAP\alpha^+$ (red)/$vimentin^+$ (green) cells. **(K)** FAPα expression in the dental nerve (**K**, magnification in **L**). **(M)** Immunofluorescent staining showing absence of vimentin staining in the inner medulla. Note the presence of the vimentin positive nerve (**M**, arrow). **(N)** Double immunofluorescent staining showing vimentin negative but FAPα positive cells (red) in the inner medulla. **(O–Q)** Double immunofluorescent staining of vimentin (green) and CD44 (red) reveals double positive cells in the outer medulla (yellow) but complete absence of staining in the inner medulla. Scale bars represent 25 **(F,J,O,P,Q,N)**, 50 **(B,C,D,E,G,H,I,L)**, 100 **(J)**, 250 **(K,M)**, and 1000 **(A)** μm.

in the inner medulla stained negative for CD44 (**Figures 2O,Q**). Staining for cytokeratin 19 (data not shown), an epithelial cell marker, revealed no positivity within the vimentin negative cell population. Lastly, we observed FAPα staining within a palisade of columnar shaped cells bordering a small deposit of dentin indicating the presence of odontoblasts (**Supplementary Figures 3A,B**). Within the newly formed dentin, FAPα staining is visualized in small foci suggesting cytoplasmic extensions of odontoblasts in dentinal tubules (**Supplementary Figure 3B**, arrows).

Molecular Characterization of Stem Cells From the Apical Papillas in Culture

After tissue isolation, SCAPs migrated out of tissue explants after 24 to 48 h in culture (**Figure 3A**) and reached confluency

after 10 to 14 days (**Figure 3B**). The majority of SCAPs displayed a spindle-shaped morphology (**Figure 3C**). To evaluate mesenchymal marker expression, immunocytochemistry and FACS analysis were performed. SCAPs stained uniformly for the surface marker CD29 (**Figure 3D**) and a perinuclear expression pattern of CD117 (c-kit) was observed in all SCAPs (**Figure 3E**). A subpopulation of cells showed positive immune-reactivity for CD146 (**Figure 3F**). As shown in the **Supplementary Figure 4**, FACS revealed >95% expression of the mesenchymal stem cell markers CD44, CD90 and CD105, while the expression of hematopoietic stem cell markers CD34 and CD45 were absent (**Supplementary Figure 4**). A SCAPs subpopulation showed immune-positivity for p75 (10.3 ± 3.9%) but no expression of CD24. The majority of cells were positive for vimentin and nestin but SCAPs did not stain for CD31, an endothelial cell marker. Immunocytochemistry showed the presence of FAPα staining mainly on the plasma membrane (**Figure 3G**) but also in the nuclear region and in pseudopodia (**Figure 3H**). Double immunofluorescent staining indicated that the majority (70 ± 3%, n = 5 different donors) of vimentin positive SCAPs were FAPα positive (**Figure 3I**). CXCR4 which is involved in cell migration often co-localized with FAPα in the pseudopodia (**Figure 3J**). The majority of the SCAPs revealed a diffuse α-SMA staining which was absent in tissue sections (**Figure 3K**).

Fibroblast Activation Protein-α Expression in Dental Pulp Tissue and Cultured Stem Cells

Immunohistochemistry of a third molar with intact pulp demonstrated FAPα staining in odontoblasts at the dentin-pulp complex (**Figure 4A**). Higher magnification showed FAPα positive protrusions of odontoblasts extending into dental tubules (**Figure 4B**; white arrows). In extracted dental pulp, odontoblasts were located at the periphery of the tissue and stained positive for FAPα (**Figures 4C,D**) and the specific odontoblast marker dentin sialophosphoprotein (DSPP) (**Figure 4E**). Immunohistochemistry revealed heterogeneous staining of FAPα within the center of the dental pulp (**Figure 4F**). We identified a cell population with FAPα- and vimentin-positive staining (**Figure 4G**, white arrow) pointing to a possible resident stem cell population and a second FAPα negative/vimentin positive cell population (**Figure 4G**, white arrowhead). FAPα staining was not only noted in the nuclei but also in the plasma membrane (**Figure 4H**, white arrow). α-SMA staining (images not shown) was restricted to blood vessels disproving the presence of FAPα and α-SMA positive myofibroblasts within the dental pulp. Immunocytochemistry of cultured DPSCs revealed FAPα staining on the plasma membrane (**Figure 4I**) or in the pseudopodia (**Figure 4J**). FAPα expressing DPSCs had vimentin positive intermediate filaments (**Figure 4K**) but diffuse α-SMA staining (**Figure 4L**). Only few cells displayed α-SMA positive stress fibers (**Figure 4M**) indicating a limited amount of myofibroblasts. The majority of FAPα positive DPSCs showed CXCR4 staining in their cytoplasmic extensions (**Figure 4N**) which frequently co-localized with FAPα (**Figures 4O–Q**).

DISCUSSION

In this study, we investigated the location and role of FAPα expression in dental tissues i.e., dental follicle, apical papilla and dental pulp and in their corresponding stem cells. First, we revealed that the dental follicle contains a rich source of FAPα positive cells which we identified as DFSCs. Within the HERS fragments, epithelial cells were observed showing FAPα expression. HERS cells undergo EMT in the presence of TGF-β1 (Akimoto et al., 2011) which is associated with HERS fragmentation and reduction in E-cadherin expression. Since FAPα expression is regulated by TGF-β1 (Tulley and Chen, 2014), we suggest that FAPα positive epithelial cells in HERS remnants could be part of a TGF-β1 driven EMT process. Collagenase type I activity exerted by FAPα could promote disintegration of the epithelial sheath enabling cell migration. At the periphery of HERS remnants, we observed FAPα and vimentin positive cells which suggests migration of newly differentiated mesenchymal cells into the extracellular matrix. However, we should not exclude the possibility that migration of FAPα positive/vimentin positive DFSCs into the epithelial sheath could cause epithelial degradation (Hirata and Nakamura, 2006).

Numerous studies have focused on the multi-lineage differentiation capacity of SCAPs but detailed knowledge on the histological organization of the apical papilla is lacking. We identified two novel histological regions with different features of FAPα expression. First, the medulla is the largest area of the apical papilla and contains a high concentration of FAPα, vimentin and CD44 positive cells corresponding to SCAPs in culture. Since FAPα exerts a collagenase type I activity, it can be hypothesized that the presence of FAPα in the medulla is associated with a continuous remodeling of the apical papilla during root formation. Secondly, the inner part of the medulla contains a peripheral nerve extending from the dental pulp into the apical papilla which stains positive for FAPα. SCAPs originate from neural crest cells (Chai et al., 2000) and have the capacity for neurogenic differentiation and thus could contribute to peripheral nerve growth (Kim et al., 2017). Interestingly, the region of the peripheral nerve resides a high concentration of round-shaped FAPα$^+$/CD44$^-$/vimentin$^-$ cells. Since vimentin expression is absent in epithelial cells, we hypothesized that these cells could originate from an epithelial source such as HERS. A cytokeratin 19 staining revealed no positivity in this cell population excluding this assumption. Whether these cells belong to an intermediary phenotype of epithelial-mesenchymal cell transition (Klymkowsky and Savagner, 2009) requires further investigation. However, it is tempting to speculate that vimentin$^-$/FAPα$^+$ cells could be involved in maintaining the opening of the root canal during root maturation. The complete medulla is encapsulated by the cortex fibrosa which has a dense extracellular matrix composed of collagen type I. The majority of cells in this region are FAPα negative, vimentin positive and α-SMA negative, typical features of non-differentiated fibroblasts (Tillmanns et al., 2015). This region could provide mechanical support to the apical papilla. Furthermore, we observed FAPα positive

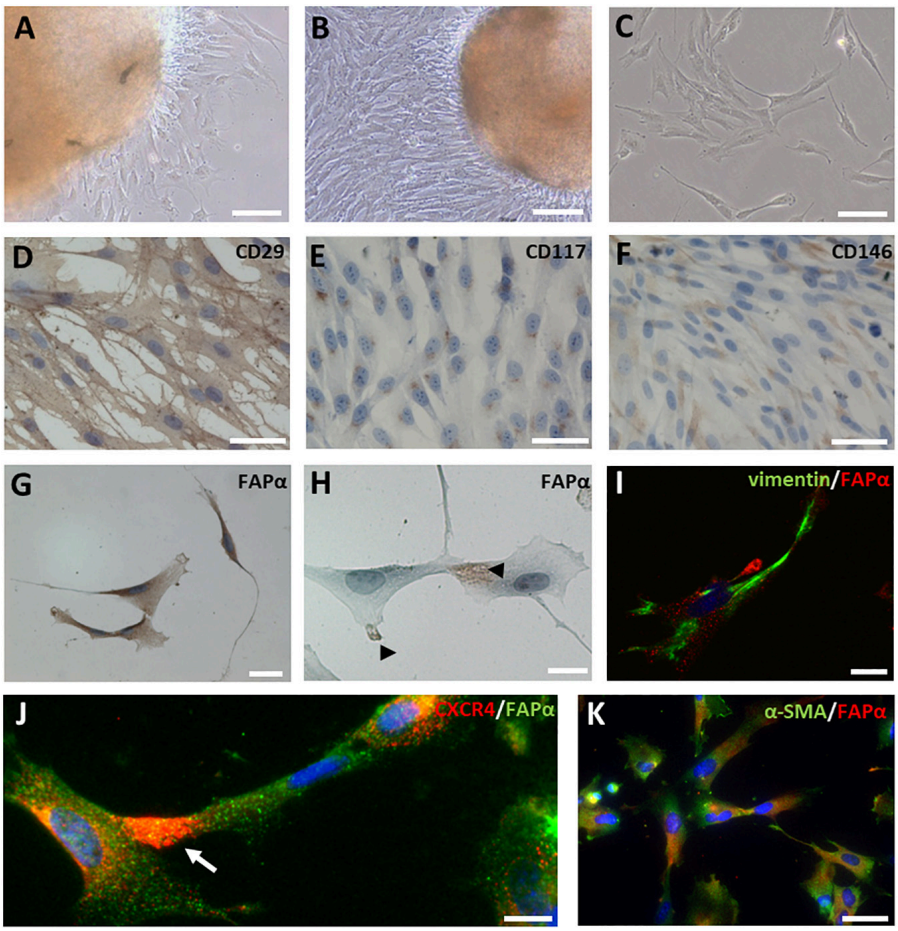

FIGURE 3 | FAPα expression in SCAPs in culture. **(A–C)** SCAPs, isolated via the explant method, migrated out of the tissue explants, and displayed a spindle-shaped morphology. Cells were able to form colonies *in vitro* **(C)**. **(D–H)** Immunocytochemical staining of SCAPs for mesenchymal markers CD29, CD117, CD146, and FAPα. All cells expressed CD29 **(D)** and CD117 **(E)**. A subpopulation of the cells stained positive for CD146 **(F)**. FAPα staining was prominent in all cells and was visible on either the plasma membrane **(G)** or on pseudopodia **(H)**. **(I)** Double immunofluorescent staining **(I–K)** shows that FAPα positive SCAPs (red) co-express vimentin (**I**, green). **(J)** CXCR4 staining (red) was observed in pseudopodia (arrow) of FAPα expressing cells (green). **(K)** Diffuse α-SMA was observed in FAPα^{+} SCAPs (green). Nuclei are counterstained with DAPI (blue). Scale bars represent 20 **(H,I,K)**, 40 **(G)**, 50 **(D–F,J)**, 100 **(A–C)** μm.

odontoblasts inside dentin depositions within the medulla suggesting that FAPα positive SCAPs could act as precursors for odontogenic differentiation as shown before (He et al., 2014; Zhang et al., 2015; Wan et al., 2016). FAPα staining of dental pulp demonstrated that odontoblasts are indeed highly positive for FAPα which could be regulated by high expression of TGF-β receptors I and II (Smith et al., 1998). The function of FAPα in odontoblasts is currently not known but indicates a possible role in dentin formation. Within the dental pulp, FAPα positive cells were not that numerous compared to the medulla of the apical papilla. A considerable fraction of FAPα negative cells stained positive for vimentin but were negative for α-SMA matching the staining profile of non-differentiated fibroblasts. Whether FAPα expression discriminates between dental pulp fibroblasts and stem cells requires further investigation. We conclude that FAPα expression in combination with vimentin identifies heterogeneous cell populations in the apical papilla and dental pulp. However, we should note that there is a discrepancy between the heterogeneous FAPα staining in the tissue and the more homogenous staining in cell culture. This could be due to spontaneous differentiation of stem cells *ex vivo*. This assumption was made by the diffuse α-SMA staining in cultured cells which was absent in tissue. α-SMA expression is enhanced in culture due to the serum in the culture medium and the low compliance of the plastic culture substrate. A microarray study emphasized the role of the micro-environment on SCAPs gene expression as demonstrated by the significant number of differentially expressed genes between SCAPs in culture and from tissue (Diao et al., 2017). Finally, co-expression of FAPα and CXCR4 in the cytoplasmic extensions of cultured SCAPs and DPSCs suggests a joint role in cell migration. SDF-1α stimulates SCAPs chemo-attraction via activation of CXCR4 receptors (Liu et al., 2015) whereas FAPα facilitates cell migration via activation of RhoA GTPase activity as observed in BMSCs (Chung et al., 2014). An interplay between CXCR4 and FAPα could therefore enable

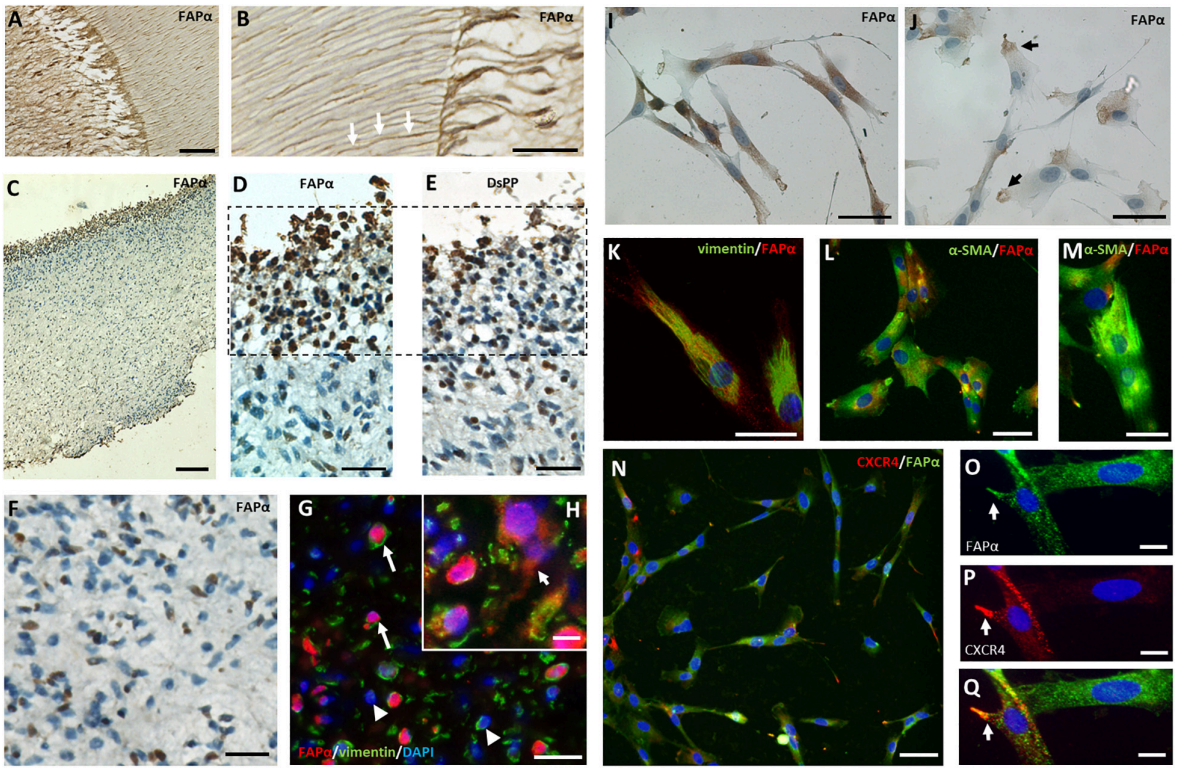

FIGURE 4 | FAPα expression in dental pulp tissue and stem cells. **(A)** Immunohistochemistry staining of FAPα in a decalcified intact molar showing the dentin-pulp region. **(B)** Higher magnification displays FAPα$^+$ odontoblasts with their corresponding protrusions entering the dental tubules. **(C)** FAPα staining of extracted pulp tissue. **(D)** Serial sections demarking the presence of FAPα **(D)** and DSPP **(E)** positive odontoblasts at the periphery of the extracted pulp tissue. **(F)** Immunohistochemistry staining of FAPα in the coronal center of extracted pulp tissue. A heterogeneous population of FAPα expressing cells is visible. **(G,H)** Double immunofluorescent staining of FAPα (red) and vimentin (green) with nuclear counterstaining (DAPI, blue) in matched dental pulp tissue. Indicated cells are FAPα$^+$/vimentin$^+$ (arrow) and FAPα$^-$/vimentin$^+$ (arrowhead). Insert **(H)** showing FAPα + staining in the plasma membrane (arrow). **(I)** Immunocytochemistry staining of FAPα in cultured DPSC's showing localization in the plasma membrane (I) or limited to the pseudopodia **(J)**. Double immunofluorescent staining of cultured DPSCs indicates co-expression of FAPα with either vimentin (**K**, green) or diffuse α-SMA (**L**, green). Only a limited number of cells have organized α-SMA stress fibers **(M)**. **(N–Q)** Double immunofluorescent staining of FAPα (green) and CXCR4 (red) with nuclear counterstaining (DAPI, blue). Co-localization of FAPα **(O)** and CXCR4 **(P)** with the matching overlay image **(Q)**. Scale bars represent 25 **(B,D,E,F,H,K,M,O–Q)**, 50 **(A,I,J,L,N,G)**, and 100 **(C)** μm.

chemo-attraction of SCAPs toward the region of root formation or DPSCs to the dentin border for odontoblast renewal. In addition, FAPα is not only localized on the plasma membrane but also at the nuclear region of dental stem cells. The role of nuclear FAPα is unknown but could share similarities with MMP-7 which after nuclear translocation enhances cell migration (Yingqiu et al., 2016). A further unknown factor is the molecular regulation of FAPα in mesenchymal stem cells and more specifically in dental stem cells. TGF-β1 could act as a possible regulator of FAPα expression since it is present as a latent form within the dentin matrix and it is a potent factor in stimulating odontoblast differentiation (Li et al., 2011). Moreover, it has been shown that the core promotor of FAPα mRNA transcription in humans contains TGF-β-responsive cis-regulatory elements (Zhang et al., 2010). However, other candidates which are reported to induce FAPα expression should not be ruled out including the transcription factors EGR1, TWIST1, and PARAXIS and a plethora of growth factors and cytokines regulating these downstream pathways (Busek et al., 2018).

CONCLUSION

In conclusion, FAPα is considered a novel dental mesenchymal stem cell marker which could offer new future insights in dental root development and odontoblast function.

DATA AVAILABILITY STATEMENT

All datasets generated for this study are included in the article/**Supplementary Material**.

ETHICS STATEMENT

This study protocol was approved by the Medical Ethical Committee of Hasselt University (protocol 13/0104U). All participants gave written informed consent in accordance with the Declaration of Helsinki except for cases where the participant was under the age of 16, where written informed consent was obtained from their legal guardians.

AUTHOR CONTRIBUTIONS

RD and IL designed the research. RD, PH, NS, and AB performed and analyzed the experiments. TV, YD, JR, EW, PG, MA, and IL contributed to the data interpretation and revised the manuscript. RD wrote the manuscript.

FUNDING

TV (GOC1916N), PH (12D8516N), PG (12U7718N), and JR (G089213N) were supported by the Research Foundation-Flanders (FWO-Vlaanderen).

ACKNOWLEDGMENTS

The authors thank Marc Jans for processing and sectioning of araldite embedded samples, Jeanine Santermans for embedding and sectioning of paraffin sections, and Ana Amaya Garrido for her valuable contribution to the experiments.

SUPPLEMENTARY MATERIAL

The Supplementary Material for this article can be found online at: https://www.frontiersin.org/articles/10.3389/fcell.2019.00389/full#supplementary-material

REFERENCES

Akimoto, T., Fujiwara, N., Kagiya, T., Otsu, K., Ishizeki, K., and Harada, H. (2011). Establishment of Hertwig's epithelial root sheath cell line from cells involved in epithelial-mesenchymal transition. *Biochem. Biophys. Res. Commun.* 404, 308–312. doi: 10.1016/j.bbrc.2010.11.112

Busek, P., Mateu, R., Zubal, M., Kotackova, L., and Sedo, A. (2018). Targeting fibroblast activation protein in cancer – Prospects and caveats. *Front. Biosc.* 23:1933–1968. doi: 10.2741/4682

Chai, Y., Jiang, X., Ito, Y., Bringas, P. Jr., Han, J., Rowitch, D. H., et al. (2000). Fate of the mammalian cranial neural crest during tooth and mandibular morphogenesis. *Development* 127, 1671–1679.

Chung, K. M., Hsu, S. C., Chu, Y. R., Lin, M. Y., Jiaang, W. T., et al. (2014). Fibroblast activation protein (FAP) is essential for the migration of bone marrow mesenchymal stem cells through RhoA activation. *PLoS One* 9:e88772. doi: 10.1371/journal.pone.0088772

Diao, S., Lin, X., Wang, L., Dong, R., Du, J., Yang, D., et al. (2017). Analysis of gene expression profiles between apical papilla tissues, stem cells from apical papilla and cell sheet to identify the key modulators in MSCs niche. *Cell Prolif.* 50, 12337. doi: 10.1111/cpr.12337

Dominici, M., Le Blanc, K., Mueller, I., Slaper-Cortenbach, I., Marini, F., Krause, D., et al. (2006). Minimal criteria for defining multipotent mesenchymal stromal cells. The international society for cellular therapy position statement. *Cytotherapy* 8, 315–317. doi: 10.1080/14653240600855905

Fan, M. H., Zhu, Q., Li, H. H., Ra, H. J., Majumdar, S., Gulick, D. L., et al. (2016). Fibroblast activation protein (FAP) accelerates collagen degradation and clearance from lungs in mice. *J. Biol. Chem.* 291, 8070–8089. doi: 10.1074/jbc.M115.701433

Gronthos, S., Mankani, M., Brahim, J., Robey, P. G., and Shi, S. (2000). Postnatal human dental pulp stem cells (DPSCs) in vitro and in vivo. *PNAS* 97, 13625–13630. doi: 10.1073/pnas.240309797

He, W., Zhang, J., Niu, Z., Yu, Q., Wang, Z., Zhang, R., et al. (2014). Regulatory interplay between NFIC and TGF-β1 in apical papilla-derived stem cells. *J. Dent. Res.* 93, 496–501. doi: 10.1177/0022034514525200

Hilkens, P., Gervois, P., Fanton, Y., Vanormelingen, J., Martens, W., Struys, T., et al. (2013). Effect of isolation methodology on stem cell properties and multilineage differentiation potential of human dental pulp stem cells. *Cell Tissue Res.* 353, 65–78. doi: 10.1007/s00441-013-1630-x

Hirata, A., and Nakamura, H. (2006). Localization of perlecan and heparanase in Hertwig's epithelial root sheath during root formation in mouse molars. *J. Histochem. Cytochem.* 54, 1105–1113. doi: 10.1369/jhc.5a6883.2006

Huang, G. T., Gronthos, S., and Shi, S. (2009). Mesenchymal stem cells derived from dental tissues vs. those from other sources: their biology and role in regenerative medicine. *J. Dent Res.* 88, 792–806. doi: 10.1177/0022034509340867

Itaya, S., Oka, K., Ogata, K., Tamura, S., Kira-Tatsuoka, M., Fujiwara, N., et al. (2017). Hertwig's epithelial rooth sheath cells contribute to formation of periodontal ligament through epithelial-mesenchymal transition by TGF-β. *Biomed. Res.* 38, 61–69. doi: 10.2220/biomedres.38.61

Kim, B. C., Jun, S. M., Kim, S. Y., Kwon, Y. D., Choe, S. C., Kim, E. C., et al. (2017). Engineering three dimensional micro nerve tissue using postnatal stem cells from human dental apical papilla. *Biotechnol. Bioeng.* 114, 903–914. doi: 10.1002/bit.26205

Klymkowsky, M. W., and Savagner, P. (2009). Epithelial-mesenchymal transition: a cancer researcher's conceptual friend and foe. *Am. J. Pathol.* 174, 1588–1593. doi: 10.2353/ajpath.2009.080545

Li, Y., Lü, X., Sun, X., Bai, S., Li, S., and Shi, J. (2011). Odontoblast-like cell differentiation and dentin formation induced with TGF-β1. *Arch. Oral Biol.* 56, 1221–1229. doi: 10.1016/j.archoralbio.2011.05.002

Liu, J. Y., Chen, X., Yue, L., Huang, G. T., and Zou, X. Y. (2015). CXC Chemokine receptor 4 is expressed paravascularly in apical papilla and coordinates with stromal cell-derived factor-1α during transmigration of stem cells from apical papilla. *J. Endod.* 41, 1430–1436. doi: 10.1016/j.joen.2015.04.006

Niedermeyer, J., Garin-Chesa, P., Kriz, M., Hilberg, F., Mueller, E., Bamberger, U., et al. (2001). Expression of the fibroblast activation protein during mouse embryo development. *Int. J. Dev. Biol.* 45, 445–447.

Sanen, K., Paesen, R., Lucyk, S., Philips, J., Lambrichts, I., Martens, W., et al. (2016). Label-free mapping of microstructural organization in self-aligning cellular collagen hydrogels using image correlation spectroscopy. *Acta Biomater.* 30, 258–264. doi: 10.1016/j.actbio.2015.10.047

Smith, A. J., Matthews, J. B., and Hall, R. C. (1998). Transforming growth factor-beta 1 (TGF-beta1) in dentine matrix. *Ligand activation and receptor expression. Eur. J. Oral Sci.* 106, 179–184.

Sonoyama, W., Liu, Y., Yamaza, T., Tuan, R. S., Wang, S., Shi, S., et al. (2008). Characterization of the apical papilla and its residing stem cells from human immature permanent teeth: a pilot study. *J. Endod.* 34, 166–171. doi: 10.1016/j.joen.2007.11.021

Teichgräber, V., Monasterio, C., Chaitanya, K., Boger, R., Gordon, K., Dieterle, T., et al. (2015). Specific inhibition of fibroblast activation protein prevents tumor progression in vitro. *Adv. Med. Sci.* 60, 264–272. doi: 10.1016/j.advms.2015.04.006

Tillmanns, J., Hoffmann, D., Habbaba, Y., Schmitto, J. D., Sedding, D., Fraccarollo, D., et al. (2015). Fibroblast activation protein alpha expression identifies activated fibroblasts after myocardial infarction. *J. Mol. Cell. Cardiol.* 87, 194–203. doi: 10.1016/j.yjmcc.2015.08.016

Tulley, S., and Chen, W. T. (2014). Transcriptional regulation of seprase in invasive melanoma cells by transforming growth factor-β signaling. *J. Biol. Chem.* 289, 15280–15296. doi: 10.1074/jbc.M114.568501

Wan, F., Gao, L., Lu, Y., Ma, H., Wang, H., Liang, X., et al. (2016). Proliferation and osteo/odontogenic differentiation of stem cells from apical papilla regulated by Zinc fingers and homeoboxes 2: An in vitro study. *Biochem. Biophys. Res. Commun.* 469, 599–605. doi: 10.1016/j.bbrc.2015.11.135

Wen, X., He, X., Jiao, F., Wang, C., Sun, Y., Ren, X., et al. (2016). Fibroblast activation protein-α-positive fibroblasts promote gastric cancer progression and resistance to immune checkpoint blockade. *Oncol. Res.* 25, 629–640. doi: 10.3727/096504016X14768383625385

Yingqiu, X., Wenfu, L., Shenji, L., Qing, Y., Shawn, G. J., Sandeep, A. S., et al. (2016). MMP-7 interacts with ARF in nucleus to potentiate tumor microenvironments for prostate cancer progression *in vivo*. *Oncotarget* 7, 47609–47619. doi: 10.18632/oncotarget.10251

Zhang, J., Valianou, M., and Cheng, J. D. (2010). Identification and characterization of the promotor of fibroblast activation protein. *Front. Biosci.* 2:1154–1163. doi: 10.2741/e175

Zhang, J., Wang, Z., Jiang, Y., Niu, Z., Fu, L., Luo, Z., et al. (2015). Nuclear factor I-C promotes proliferation and differentiation of apical papilla-derived human stem cells in vitro. *Exp. Cell Res.* 332, 259–266. doi: 10.1016/j.yexcr.2015.01.020

Conflict of Interest: The authors declare that the research was conducted in the absence of any commercial or financial relationships that could be construed as a potential conflict of interest.

frontiers in Cell and Developmental Biology

REVIEW
published: 29 January 2020
doi: 10.3389/fcell.2020.00016

Therapeutic Potential of Wharton's Jelly Mesenchymal Stem Cells for Diabetes: Achievements and Challenges

Mohamed M. Kamal[1,2,3*†‡] *and Dina H. Kassem*[3*†‡]

[1] Pharmacology and Biochemistry Department, Faculty of Pharmacy, The British University in Egypt, Cairo, Egypt, [2] The Center for Drug Research and Development, Faculty of Pharmacy, The British University in Egypt, Cairo, Egypt, [3] Biochemistry Department, Faculty of Pharmacy, Ain Shams University, Cairo, Egypt

OPEN ACCESS

Edited by:
Karen Bieback,
Universität Heidelberg, Germany

Reviewed by:
Philippe Bourin,
Independent Researcher, Toulouse, France
Antonina Lavrentieva,
Leibniz University Hannover, Germany

***Correspondence:**
Mohamed M. Kamal
Mohamed.kamal@bue.edu.eg
Dina H. Kassem
dina_kassem@pharma.asu.edu.eg

†ORCID:
Mohamed M. Kamal
orcid.org/0000-0002-6004-2590
Dina H. Kassem
orcid.org/0000-0001-5102-3235

‡These authors have contributed equally to this work and share first authorship

Specialty section:
This article was submitted to Stem Cell Research, a section of the journal Frontiers in Cell and Developmental Biology

Received: 21 September 2019
Accepted: 10 January 2020
Published: 29 January 2020

Citation:
Kamal MM and Kassem DH (2020) Therapeutic Potential of Wharton's Jelly Mesenchymal Stem Cells for Diabetes: Achievements and Challenges. Front. Cell Dev. Biol. 8:16. doi: 10.3389/fcell.2020.00016

Diabetes mellitus (DM) is an alarming metabolic disease in which insulin secreting β-cells are damaged to various extent. Unfortunately, although currently available treatments help to manage the disease, however, patients usually develop complications, as well as decreased life quality and increased mortality. Thus, efficient therapeutic interventions to treat diabetes are urgently warranted. During the past years, mesenchymal stem cells (MSCs) have made their mark as a potential weapon in various regenerative medicine applications. The main fascination about MSCs lies in their potential to exert reparative effects on an amazingly wide spectrum of tissue injury. This is further reinforced by their ease of isolation and large *ex vivo* expansion capacity, as well as demonstrated multipotency and immunomodulatory activities. Among all the sources of MSCs, those isolated from umbilical cord-Wharton's jelly (WJ-MSCs), have been proved to provide a great source of MSCs. WJ-MSCs do not impose any ethical concerns as those which exist regarding ESCs, and represent a readily available non-invasive source, and hence suggested to become the new gold standard for MSC-based therapies. In the current review, we shall overview achievements, as well as challenges/hurdles which are standing in the way to utilize WJ-MSCs as a novel efficient therapeutic modality for DM.

Keywords: mesenchymal stem cells, diabetes mellitus, umbilical cord, Wharton's jelly, insulin producing cells, pancreatic β-cells, regenerative medicine

INTRODUCTION

Diabetes mellitus (DM) is a devastating metabolic disease in which insulin secreting β-cells in the islets of Langerhans are damaged to different extent. DM occurs when the pancreas fails to produce and secrete sufficient insulin for the maintenance of glucose homeostasis. Unfortunately, the number of patients suffering from DM is rapidly growing which makes it the most prevalent metabolic disease. Nowadays, about 463 million people worldwide are suffering DM with expected increase to about 700 million by the year 2045 (IDF, 2019).

In fact, cell therapy treatment options for diabetic patients are under extensive study. However, limitations of islet transplantation as a cell replacement approach include the unavailability of the donors, the immune rejections and use of immunosuppressive drugs which have several adverse effects and some of them could damage β-cells (Bhonde et al., 2014). Therefore, these

factors strongly encourage the consideration of novel therapeutic interventions such as stem cells' therapies.

Actually, the field of regenerative medicine is rapidly evolving, paving the way for novel therapeutic interventions through cellular therapies which are indeed reshaping the biomedical field (Pileggi, 2012). During the past years, mesenchymal stem cells (MSCs) specifically have made their mark as a potential weapon in various regenerative medicine applications. In fact, during the past decade, there has been a major leap in understanding MSCs due to unraveling many of their exceptional characteristics, as well as the encouraging data from preclinical and clinical studies (Han et al., 2019). Among the various sources of MSCs, umbilical cord (UC) has proved to be a unique source of MSCs, providing several advantages over other sources (El Omar et al., 2014). It is noteworthy that MSCs have been reported to be present in both UC blood (UCB), and UC tissue/matrix – Wharton's jelly (WJ). Nevertheless, they are much more abundant in Wharton's Jelly tissue (Shetty et al., 2010; Arutyunyan et al., 2016). When comparing the success rate for harvesting MSCs, it has been reported to be about 6% from UCB compared to almost 100% from WJ tissue (Shetty et al., 2010). The current review will highlight the achievements, as well as the challenges facing the application of WJ-MSCs as a novel therapeutic modality for DM. Such deep understanding is indeed essential to help the scientific community to overcome those challenges and maximize the therapeutic benefit of WJ-MSCs not only for DM, but also for other disorders.

UMBILICAL CORD WHARTON'S JELLY AS A POTENTIAL SOURCE FOR STEM CELLS

During pregnancy, the placenta and growing fetus are connected by UC. This cord prevents umbilical vessels from kinking, compression, or torsion during movement of the fetus, thus ensuring proper blood supply to the fetus (Kim et al., 2013). Anatomically, the human UC comprises an outer layer of amniotic epithelium enclosing a vein and two arteries embedded within a mucoid connective tissue. The mucoid connective tissue enclosing the three umbilical vessels or the UC matrix is known as "Wharton's jelly." It was first described by Wharton (1656), and is primarily made of collagen and proteoglycans. The discovery that WJ provides a source of MSCs was first highlighted in McElreavey et al. (1991). Not until 2004 when the first report providing robust evidence that WJ-stromal cells can be classified as MSCs was published (Wang et al., 2004).

First discovered in the early seventies, MSCs, a population of plastic-adherent, non-hematopoietic, fibroblast-like cells, were first isolated from bone marrow (BM) (Friedenstein et al., 1970, 1974). Afterward, in 1991, the term "mesenchymal stem cell" also known as *"multipotent mesenchymal stromal cells,"* was proposed based on their properties (Caplan, 1991; Horwitz et al., 2005). In 2006, the International Society for Cellular Therapy (ISCT) defined plastic adherence, expression of mesenchymal markers while lacking hematopoietic markers and ability to differentiate into osteogenic, adipogenic, and chondrogenic lineages as minimal criteria for definition of MSCs (Dominici et al., 2006). So far, MSCs have been isolated from various tissues including adult tissues such as BM, adipose tissue, liver, as well as fetal/perinatal sources like UCB, placenta, and UC matrix (Da Silva Meirelles et al., 2006; Ma et al., 2014). MSCs were proved to have a broad differentiation potential and several lines of evidence support the notion that these cells may cross germinative layers' borders being able to differentiate toward ectoderm-, mesoderm-, and endoderm- derived cell types (Nagai et al., 2007; Anzalone et al., 2011).

Interestingly, WJ-MSCs have exceptional properties in that although they are bona fide MSCs (Troyer and Weiss, 2008), possessing similar properties like their adult BM counterparts, yet, they also retain characteristics of primitive stem cells, like the expression of ESC markers (Fong et al., 2011). They may be representing some intermediate state between adult and embryonic stem cells.

In fact, WJ-MSCs have several advantages over adult MSCs in general. They are easily isolated from UC which is readily available; the UC is considered a medical waste discarded at birth. Thus, unlike BM-MSCs which require painful BM-aspiration, the isolation of WJ-MSCs is non-invasive. Moreover, several reports showed a relatively high expression of pluripotency markers in WJ-MSCs compared to MSCs from other sources, implying a more primitive status (Fong et al., 2011; El Omar et al., 2014). Actually, the transcriptomic profile of WJ-MSCs in comparison to other MSCs is reviewed in detail in a comprehensive review article by El Omar et al. (2014). Most recently, an interesting report showed that WJ-MSCs exhibit a unique gene expression profile compared to BM-MSCs using the high throughput single-cell RNA-sequencing technique. In that report, 436 genes were found to be significantly differentially expressed when comparing the two cell types. Those genes are related to several processes such as chemotaxis, apoptosis, anti-tumor activity, and immuno-modulation. The authors reported that those differences might at least in part explain many of the advantages which WJ-MSCs have over BM-MSCs (Barrett et al., 2018).

Furthermore, WJ-MSCs being isolated from neonatal tissue, they may have retained some primitive characteristics similar to ESC. However, unlike ESCs, WJ-MSCs have no ethical concerns (Hass et al., 2011). Moreover, luckily they do not form teratomas upon transplantation (Rachakatla et al., 2007; Troyer and Weiss, 2008; Gauthaman et al., 2012). This can be explained by their unique transcriptomic profile compared to ESCs. WJ-MSCs have been reported to express low levels of pluripotency markers like POU5F-1, SOX-2 and NANOG as compared to ESCs which explains why they do not develop teratomas (Fong et al., 2011).

Moreover, WJ-MSCs have been particularly found to be immune-privileged after reporting their expression of human leukocyte antigen-G (HLA-G) besides their lack of expression of human leukocyte – antigen D-related (HLA-DR) like other types of MSCs (La Rocca et al., 2009). This suggests an immunosuppressive role for these cells mimicking the process occurring *in vivo* at the fetus-maternal interface (Moffett and Loke, 2003). Additionally, WJ-MSCs have a great potential for banking like their counterparts isolated from UCB whose banking nowadays is a very common practice

(Chatzistamatiou et al., 2014). Taking in consideration all the interesting findings concerned with WJ-MSCs, it has become indeed tempting to nominate them to become the new gold standard for MSCs-based therapies (El Omar et al., 2014).

THERAPEUTIC PROPERTIES AND MECHANISMS OF WJ-MSCs IN DIABETES

Over the past couple of decades, MSCs have indeed made their mark as promising candidates for a wide array of regenerative medicine applications. Originally, MSCs were thought to mediate tissue and organ repair by the virtue of a multilineage differentiation potential that enabled them to replace damaged cells (Mahmood et al., 2003; Murphy et al., 2003). Subsequent findings suggest that in response to tissue injury, MSCs home to the site of damage and encourage repair through the production of trophic factors, including growth factors, cytokines, and antioxidants (Chen et al., 2008; Karp and Leng Teo, 2009), some of which provide the basis for their capacity to modulate immune responses (English et al., 2010). In fact, before carrying out tissue repair functions, MSCs are believed to first prepare the microenvironment by modulating inflammatory processes and releasing various growth factors in response to the inflammation status (Ma et al., 2014).

Generally, clinical applications of MSCs can be attributed to five important biological properties: (a) homing to sites of inflammation following tissue injury when injected intravenously; (b) the secretion of multiple bioactive molecules capable of stimulating recovery of injured cells and inhibiting inflammation; (c) modulating the immune functions (Anzalone et al., 2018), (d) differentiation into various cell types (Wang et al., 2012), and finally (e) as a tool for gene therapy. WJ-MSCs almost use all these properties as a therapeutic potential against DM. We tried to highlight these prominent therapeutic properties and mechanisms of WJ-MSCs related to DM in **Figure 1**.

Homing of WJ-MSCs

One of the major characteristics of MSCs is that they have migratory abilities (Nagyova et al., 2014) that is, after administration, they specifically migrate to the sites of inflammation and tissue damage which is typically associated with cytokine out-burst (Sohni and Verfaillie, 2013; Zachar et al., 2016). This can be referred to as "homing". Actually, the definition of MSCs "homing" is still vague and non-mechanistic. According to a review by Nitzsche and colleagues, they would recommend the definition of homing as the active or passive arrest of a MSC within the vasculature followed by transmigration across the endothelium (Karp and Leng Teo, 2009; Nitzsche et al., 2017).

Stem cells' homing turned out to be more complicated than once expected and the exact mechanism is far from complete elucidation. It is generally assumed to follow the same pattern as leukocyte homing which includes cell contact with the endothelium by tethering and rolling. Usually the adhesion molecules and selectins are involved in this step (Sackstein, 2004). Thorough understanding of homing mechanisms and factors affecting this homing either intrinsic inside the cells or extrinsic inside the host is crucial for the efficacy and safety of the MSCs administration. Homing is involved in either the systemic administration of the MSCs through intravenous

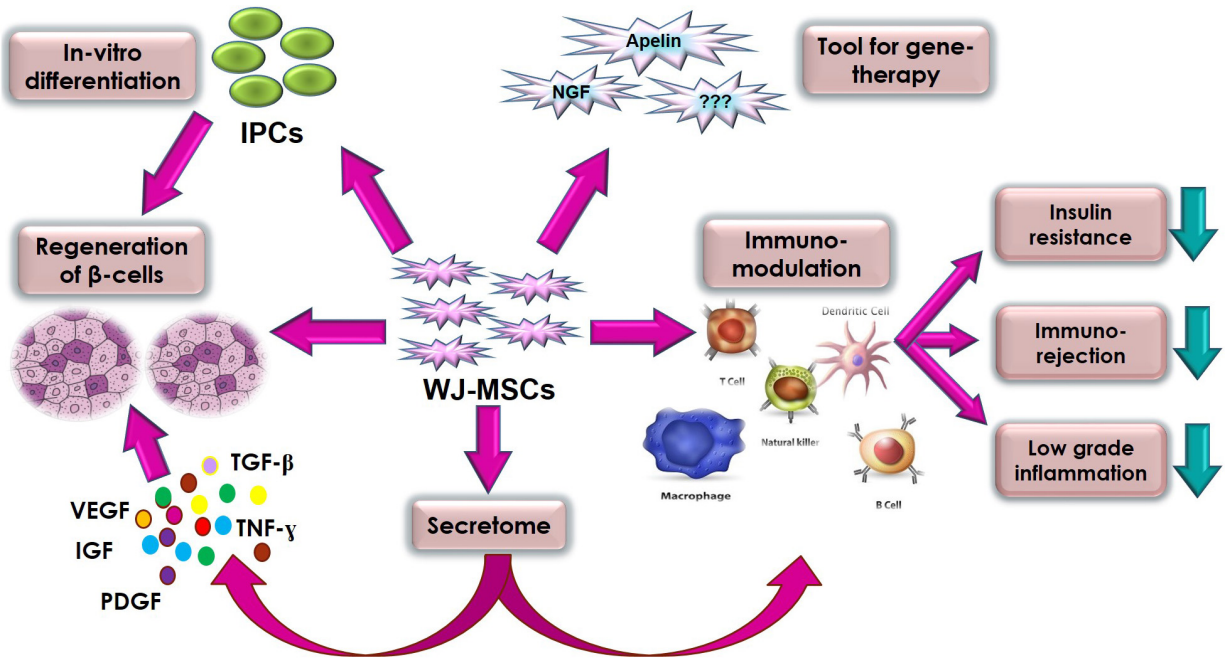

FIGURE 1 | Summary of the various therapeutic properties and mechanisms of action of WJ-MSC in diabetes mellitus.

injection, known as systemic homing. This is a multistep process composed of three distinctive phases: (a) direct administration into the circulation, (b) extravasation at the lesioned tissue vicinity, and (c) interstitial migration toward the target site (Deak et al., 2010). Also, local administration of MSCs involves non-systemic homing which requires either recruitment of local MSC or transplantation of exogenous cells close to the target area within the tissue (Nitzsche et al., 2017). This is especially important as it is now established that factors such as age or passage of the cells (Rombouts and Ploemacher, 2003), source and culturing conditions of MSCs (Wynn et al., 2004; De Becker et al., 2007) and even the host pathological conditions and inflammatory milieu (Schenk et al., 2007), affect the homing capacity and therapeutic efficiency of transplanted cells.

Many studies showed that systemic administration of MSCs from different sources showed an initial entrapment of these cells in different organs such as lungs, spleen, liver and even long bones with subsequent distributions from these organs to different tissues (Gao et al., 2001; Bentzon et al., 2005). Gao et al. showed that following either intra-arterial or intra-venous radioactive labeled MSCs infusion, MSCs were detected primarily in the lungs and then secondarily in the liver and other organs, an effect that was enhanced with vasodilators Gao et al. (2001). This can be associated with huge reduction in the number of cells reaching the target site of injury. Also, this might be associated with unknown effects of these cells on such organs. Actually, it was shown that entrapment of MSCs in liver and spleen may be associated with suppression of T-cell activation (Jellema et al., 2013). Usually the cells could be injected either intravenously (IV) or intra-arterially (IA) for systemic infusion. Usually the IV is the safest, least invasive and easiest to perform, however, it is associated with cells entrapment in the lungs (De Becker and Riet, 2016). On the other hand, the IA injection is more invasive and may be associated with risk of development of microvascular occlusions which is known as passive entrapment (Karp and Leng Teo, 2009). Several excellent reviews have been discussing these MSCs dynamics issues (De Becker and Riet, 2016; Zachar et al., 2016; Nitzsche et al., 2017).

Unfortunately, the study of the homing mechanisms of the WJ-MSCs in general and in diabetes particularly, represents a clear gap of knowledge. One recent study showed that like other MSCs, homing abilities have been reported for injected exogenous WJ-MSCs. An interesting study injected labeled WJ-MSCs into type 2 DM animal model as well as control non-diabetic animals, through the tail vein. In that study, transplanted WJ-MSCs were detected in lung, liver, and spleen in both normal and diabetic mice. However, unlike normal mice, a certain number of WJ-MSCs also homed to the pancreatic islets of diabetic mice, suggesting that homing of WJ-MSCs is closely related to tissue damage (Yin et al., 2018). However, still further studies involving homing of WJ-MSCs are warranted.

Secretome and Paracrine Actions of WJ-MSCs

Interestingly, a growing body of research has revealed that the therapeutic effects of stem cells occur largely via paracrine signaling, and secreted extracellular vesicles/exosomes (Nooshabadi et al., 2018). In agreement with that belief, several studies reported beneficial therapeutic effects of WJ-MSCs-conditioned media (Arno et al., 2014; Fong et al., 2014). Most recently, WJ-MSCs have been reported to mediate their pro-angiogenic activities via secretion of angiogenin, interleukin-8, monocyte chemoattractant protein-1, and vascular endothelial growth factor. The association between their therapeutic pro-angiogenic potential and the secreted levels of those factors was observed in *in vitro* angiogenesis assays, as well as *in vivo* in a rodent model of hind limb ischemia. Moreover, knocking down the expression of those factors by siRNA significantly inhibited the pro-angiogenic activities of WJ-MSCs. Additionally, they found that donor-to-donor variation was commonly observed in WJ-MSCs regarding their secretome profiles, even when using identical culture conditions and passage number (Kim et al., 2019).

Furthermore, paracrine effects of WJ-MSCs have been reported for neuronal regeneration. WJ-MSC-conditioned medium has been reported to enhance Schwann cell viability and proliferation (Guo et al., 2015). Also, BDNF and hepatocyte growth factor (HGF) secreted by WJ-MSCs have been reported to exert neuroprotective effect on damaged neurons (Mukai et al., 2018). In addition, WJ-MSCs conditioned medium has been reported to contain several secreted factors mediating their immune modulatory effects such as IL-2, IL-6, IL-8, IL-12, IL-15, MCP-1, MIP-1, RANTES as well as prostaglandin E2 (PGE2) (Yoo et al., 2009).

Interestingly, WJ-MSCs were also suggested to change their secretome profile based on the context of a lesion or generally the conditions to which they are exposed (Carvalho et al., 2011). In accordance with that, its noteworthy here that most recently, gestational DM has been reported to significantly affect the stemness properties, differentiation potential, oxidative stress, senescence and mitochondrial function of WJ-MSCs of UCs of mothers with gestational DM (Kong et al., 2019).

In addition, WJ-MSCs may mediate their paracrine actions through their extracellular vesicles among which are exosomes. Exosomes are defined as nano-sized bioactive vesicles derived from the cell's endosomal membrane system. They act as shuttles transferring specific cargos of proteins, mRNA, as well as non-coding RNAs like microRNA; as a message in a bottle. Accordingly, they can reprogram the recipient cells and are regarded as "signalosomes" controlling fundamental cellular functions (Bjorge et al., 2017).

In fact, the utilization of WJ-MSCs secretome as a cell-free potentially effective regenerative medicine tool especially for allogenic therapeutic applications is indeed tempting. However, that secretome should be well-characterized and elucidated in detail in order to be utilized properly. Provided that we are witnessing the "OMICS" era, further large-scale proteomics and metabolomics studies are indeed warranted to unravel the exact components of WJ-MSCs secretome, and the mechanisms regulating the secretion of various trophic and immuno-regulatory factors by WJ-MSCs.

Immunomodulatory Effects of WJ-MSCs

Another important feature of WJ-MSCs that actually augments their clinical utility is their low immunogenicity. This is due to the fact that they express MHC class I (HLA-ABC) at low levels but neither class II (HLA-DR) nor co-stimulatory antigens such as CD80, CD86 implicated in activation of both T and B cell responses (Pappa and Anagnou, 2009; Prasanna et al., 2010). In comparison to BM-MSCs, WJ-MSCs does not express HLA-DR upon IFN-γ stimulation. Besides, WJ-MSCs produce huge amounts of immunosuppressant cytokines such as IL-10, TGF-β, IL-6 and VEGF, which have recently been shown to be pivotal in the immunosuppressive capability of MSCs (Weiss et al., 2008). These properties make WJ-MSCs less immunogenic than BM-MSCs making them more amenable for allogeneic transplantation.

Moreover, WJ-MSCs were found to affect almost all cells of the immune system. MSCs, including WJ-MSCs, can suppress the CD3, CD4, and CD8 T-cells (Aggarwal and Pittenger, 2005). Interestingly, WJ-MSCs can suppress allogenic-stimulated immune cells to a greater extent than either BM-MSCs or adipose-derived MSCs (Kim et al., 2013). In addition, WJ-MSCs inhibits the maturation and activation of dendritic cell (DC) precursors by locking the monocytes in an immature DC phenotype (Tipnis et al., 2010). Besides, WJ-MSCs can affect the functions of NK cells (Casado et al., 2013), monocyte/macrophages (Cutler et al., 2010) and even neutrophils and mast cells (Brown et al., 2011). Although many details of these interactions remain to be elucidated, yet, both cell-to-cell contact and soluble factors are thought to be key aspects of WJ-MSCs-mediated immunosuppression (Shi et al., 2010; Ma et al., 2014). These immuno-modulatory effects are the basis of their utility in several diseases such as graft versus host disease (GvHD) (Newell et al., 2014), and DM (Katuchova et al., 2015).

It is noteworthy here to highlight that WJ-MSCs have been reported to exert systemic effects in type 2 DM animal models by modulating macrophages in immune organs, and adipose tissue via increasing M2 (anti-inflammatory) macrophages, causing profound anti-diabetic effects and enhanced insulin sensitivity (Xie et al., 2016; Yin et al., 2018).

Differentiation and Cell Replacement Potential of WJ-MSCs

In addition to immunomodulatory functions and paracrine signaling, the differentiation potential of WJ-MSCs down several lineages adds a lot to their therapeutic potential, not only for DM, but also for a wide array of other diseases (Can et al., 2017). In fact, several pre-clinical studies reported the differentiation potential of WJ-MSCs into insulin producing cells (IPCs) using various induction protocols, and inducing extrinsic factors (Kassem et al., 2016; Pavathuparambil Abdul Manaph et al., 2019).

Additionally, many studies proved the capacity of both differentiated and undifferentiated WJ-MSCs to regulate hyperglycemia in several DM animal models. Interestingly, in order to find out whether undifferentiated WJ-MSCs can differentiate into pancreatic IPCs or not when injected into animal model of DM. Tsai and coworkers, labeled WJ-MSCs using GFP-lentiviral transduction, then injected those cells intravenously into NOD mice. Afterward, co-localization of human C-peptide and GFP was detected in the pancreas; proving that transplanted WJ-MSCs indeed differentiated into IPCs *in vivo* (Tsai et al., 2015). Furthermore, another report highlighted the effect of intravenous infusion of human WJ-MSCs as a therapy by administering them in a type 2 DM rat model. The rats treated with WJ-MSCs exhibited increased numbers of β-cells; suggesting the therapeutic potential of WJ-MSCs in β-cell regeneration (Hu et al., 2014). Moreover, a recent study compared the anti-diabetic regenerative potential of WJ-MSCs compared to BM-MSCs in diabetic rats. WJ-MSCs showed better anti-diabetic effects and potential for pancreatic regeneration (Som and Venkataramana, 2018). WJ-MSCs were also proved better than UCB-MSCs in the same aspect (El-Demerdash et al., 2015).

However, it's important to highlight here that growing body of evidence support the notion that MSCs mostly mediate their therapeutic effects via their secretory/paracrine and immunomodulatory functions rather than their *trans*-differentiation potential *in vivo* (Päth et al., 2019).

WJ-MSCs as a Tool for Gene Therapy

Most recently, an interesting study transduced WJ-MSCs with apelin-expressing lentiviral particles, and those genetically-modified cells were injected into type 2 diabetes rodent model. Infusion of these WJ-MSCs-apelin significantly improved insulin sensitivity, and increased the levels of plasma C-peptide. Moreover, the serum levels of inflammatory cytokines TNF-α and IL-6 decreased, and anti-inflammatory adiponectin levels increased. Also, endogenous pancreatic β-cell proliferation profoundly increased more than 9 folds in the treated group compared to the control group (Gao et al., 2018). Furthermore, WJ-MSCs overexpressing nerve growth factor (NGF) were reported to induce neural regeneration, and to ameliorate symptoms of diabetic cysto-pathy in diabetic rats (WenBo et al., 2017). These reports imply the strong potential of WJ-MSCs to be used as a tool for various gene-therapy applications.

All these therapeutic properties of WJ-MSCs set the stage for these cells to find their ways to clinical trials. In the next section of this review, we will discuss how far these clinical trials went down the way of DM therapy.

CLINICAL APPLICATION OF WJ-MSCs IN DIABETES

Over the last years, various clinical trials have been conducted during the past decade to test the feasibility and efficacy of WJ-MSCs therapy for various disease conditions such as: neurological disorders, cancer, cardiac disease, liver disease, bone/cartilage disease, immunological diseases as well as DM and its complications. Many of these clinical trials have been completed and indeed demonstrated the safety and efficacy of WJ-MSCs (Can et al., 2017). Actually, the public clinical trials database is currently showing about 980 trial investigating MSCs

from various sources for a wide array of therapeutic applications; 64 of these trials are related to DM and its complications *(Accessed on August, 2019)* (ClinicalTrials.gov, 2019).

Regarding the 64 studies currently registered on the public clinical trials database *(Accessed on August, 2019)* investigating MSCs (from various sources) for treating DM and/or its complications, only about 16 of these studies clearly state applying WJ-MSCs as an intervention (ClinicalTrials.gov, 2019). However, unfortunately, many of them are having "unknown-status" labeling, or no reported results. Thus, we tried to summarize the most prominent published completed clinical studies investigating the therapeutic potential of WJ-MSCs for DM together with their reported outcome in **Table 1**. It is noteworthy here, that these are different from other clinical studies utilizing MSCs or even hematopoietic stem cells (HSCs) derived from UCB, which is out of the scope of the current review.

In a clinical study by Hu and coworkers, Out of the 15 treated patients, 3 became insulin independent, and in 8 out of the remaining 12 patients, the daily insulin requirements were reduced by more than 50% compared to their starting baseline (Hu et al., 2013). On the other hand, Liu and coworkers applied WJ-MSCs transplantation in type 2 DM patients with disease duration of about 8.7 ± 4.3 years, and they demonstrated that treatment with WJ-MSCs can indeed improve metabolic control and β-cell function. They also suggested that their mechanism of action may have involved improvements in systemic inflammation as well (Liu et al., 2014). Thus, WJ-MSCs proved to be safe and relatively effective in both type 1 and 2 DM, as well as recently diagnosed or relatively long-standing diabetic patients.

Most recently, an interesting double-blinded randomized placebo-controlled trial has been inaugurated in Sweden and started recruiting patients since January 2018 with estimated measurement of primary outcome in 2020. That study aims to investigate the safety and efficacy of allogenic WJ-MSCs as an investigational medicinal product produced under GMP conditions with minimal batch-to-batch variation (Carlsson and Svahn, 2018). Actually, well-designed large scale randomized clinical trials are indeed warranted to consider not only the safety, but also the optimum dosage regimen and treatment protocol to be followed.

In fact, several meta-analysis studies have been carried out over the past few years attempting to figure out the efficacy of stem cell therapy in DM, and where we are standing exactly. Among these, an interesting comprehensive meta-analysis by El-Badawy and El-Badri included 22 studies investigating stem cell therapy for DM, among which six studies used MSCs. Interestingly, they reported that infusion of WJ-MSCs provided significantly better therapeutic outcome in type-1 DM when compared to BM-MSCs. While BM-mononuclear cells (MNCs) infusion provided better outcome compared to WJ-MSCs in type-2 DM patients. Additionally, they also found that administration of stem cell therapy for recently diagnosed DM was more effective than intervening at later stages. Yet, it's important to keep in mind that those findings are not conclusive and were based on relatively small number of trials and requires confirmation via larger trials (El-Badawy and El-Badri, 2016).

It is important to highlight here that actually most if not all of the clinical studies employing WJ-MSCs are still in early phase I or II. Thus, despite the young age of WJ-MSCs and their ever-growing list of advantages over those isolated from older adult tissue sources like BM or adipose tissue (Kim et al., 2013; El Omar et al., 2014), yet, looks like there is still a long way to go for those cells to reach actual clinical application, and to cut the way from bench to bed-side!

In addition, it is noteworthy here that given the immune-privilege of the WJ-MSCs, their good culture conditions and supported by the above-mentioned studies, WJ-MSCs can be considered as a potential candidate for allogenic transplantation. This may be considered a step forward in development of what is called "off-shelf stem cells drugs." A very recent review addressed this issue and the authors declared that MSCs can effectively be used as an allogenic off-shelf drug despite special concerns of their HLA make up (Kot et al., 2019). This notion requires further investigations and considerations of the challenges that will be further discussed in this review.

CHALLENGES FOR WJ-MSCs TRANSLATION FROM BENCH TO BED-SIDE

Safety Issues

When considering WJ-MSCs as a novel therapeutic intervention not only for DM, but also for other disease conditions, the majority of clinical trials reported the safety and absence of serious acute or chronic adverse effects. Occasionally, transient fever, headache or local pain were reported, yet those adverse events were also reported to resolve spontaneously within few days after transplantation (Can et al., 2017). However, when thinking of WJ-MSCs, being after all a type of stem cells expressing pluripotency factors, and also being applied for allogenic transplantations; in other words, foreign cells supposed to reside and live in the hosting patient/human body for a long term. At that moment, several safety concerns pop up. Such as the possibility of immuno-rejection by the recipient host, the genetic stability, as well as the possible tumorigenicity of those cells.

Actually, what makes MSCs, and especially WJ-MSCs an ideal candidate for regenerative medicine, with potential capabilities not only to regenerate damaged tissues but also to reduce rejection possibilities are their unique immunomodulatory properties (English et al., 2010; Can et al., 2017). These properties provide some sort of relief regarding the concern of possible immuno-rejection.

Nevertheless, WJ-MSCs have been reported to exhibit changes in their gene expression and transcriptomic profile, promoted by prolonged *in vitro* culture till the 12^{th} passage compared to the early 4^{th} passage. Those genes with altered expression have been reported to be related to several processes like: proliferation, differentiation, apoptosis, and inflammation. Briefly, WJ-MSCs according to these findings, showed a progressive decline in their physiological properties with prolonged *in vitro* culture; a phenomenon known as *"Cellular aging"* (Gatta et al., 2013).

TABLE 1 | Clinical studies applying WJ-MSCs for diabetes mellitus.

Patient criteria	Number of cells	Route of delivery	Therapeutic outcome	Adverse effects	References
Type 1 DM – newly onset 29 patients divided into 2 groups: 15 patients received WJ-MSCs and 14 patients received normal saline (control group); randomized double blind placebo-controlled study	1.5–3.2 × 10^7	IV – Parenteral solution Twice, 4 weeks interval	Patients were followed up for 24 months HbA1c and C-peptide values significantly improved	–	Hu et al., 2013
Type 2 DM 22 patients received WJ-MSCs transplantation Non-placebo controlled phase I/II study	1 × 10^6/kg	1 IV and 1 Intra-pancreatic endovascular injection, 5 days interval	Patients were followed up for 12 months HbA1c and glucose levels significantly decreased. Improved C-peptide levels and β-cell function. In addition to reduced systemic inflammation and T lymphocyte counts	Mild fever in 3 of 22 patients on the first operative day Nausea, vomiting and headache in 1 patient, spontaneously recovered within 1 week.	Liu et al., 2014
Type 2 DM 18 patients received WJ-MSCs transplantation	Not specified	3 IV doses	Patients were followed up for 6 months Significant decrease in fasting and post-prandial blood glucose levels, and increase of C-peptide levels and Tregs	4 out of 18 patients had transient slight fever	Kong et al., 2014
Type 1 DM – long standing (2–16 years duration) 21 patients received stem cell therapy (and additional 21 patients acting as control group who did not receive neither stem cell intervention nor placebo).	1.1 × 10^6/kg WJ-MSC –allogenic plus 106.8 × 10^6/kg BM-MNC – autologous	Intra-pancreatic	Patients were followed up for 12 months Significant decrease in FBG and HbA1c levels, increased C-peptide and insulin levels. Significant reduction in insulin dose requirement	Transient abdominal pain observed in 1 patient and spontaneously resolved, and 1 patient with puncture site bleeding resolved with pressure	Cai et al., 2016
Type 2 DM 31 patients received WJ-MSCs and 30 patients received normal saline (control group); randomized double blind placebo-controlled study	1 × 10^6/kg	IV – Parenteral solution Twice, 4 weeks interval	Patients were followed up for 36 months Blood glucose and HbA1c levels significantly decreased. C-peptide levels and pancreatic β-cell function significantly improved. In addition to reduction of insulin and oral hypoglycemic agents dose requirement Reduced incidence of diabetic complications	No serious adverse events reported.	Hu et al., 2016
Diabetic foot 28 patients received WJ-MSCs and 25 patients acting as control group (did not receive WJ-MSCs intervention); randomized study	4.8–8.6 × 10^7 cells	Endovascular infusion and injection around the foot ulcer – Local transplantation	Patients were followed for 3 months Improvements in skin temperature, ankle-brachial pressure index, transcutaneous oxygen tension, and claudication distance. Significant increase in neo-vessels, accompanied by complete or gradual ulcer healing.	–	Qin et al., 2016
Type 2 DM – more than 10 years duration 12 patients were enrolled and randomly divided into two groups: - 6 patients receiving Liraglutide plus WJ-MSCs intervention - 6 patients receiving Liraglutide only (control group) (Article in Chinese)	1 × 10^6 cells/kg	Intra-pancreatic artery infusion on the first day followed by IV infusion on the 8^{th}, 15^{th}, and 22^{nd} day sequentially	Patients were followed for 6 months Significant decrease in FBG, post-prandial glucose and HbA1c levels Significant improvements in C-peptide and HOMA-IR levels	–	Chen et al., 2016

These observations shed light on the crucial importance to keep such possible changes in mind and emphasize the need to carry out essential testing and investigations on the cells to ensure that they are functioning properly and not tumorigenic before their transplantation to the patient.

As for tumorigenicity concern, it is indeed a key hazard which may arise due to transformed cells present in the final administered product, or even possibly developed as a long-term adverse effect of those transplanted cells. Several studies have observed that tumorigenicity may represent a potential adverse effect of MSCs therapy through different mechanisms. First, several studies showed that MSCs may represent the direct cellular origin of cancer, like one study showed that MSCs are source of gastric sarcoma (Kauer et al., 2009; Barkholt et al., 2013; Neri, 2019). Second, MSCs may secrete or produce several inflammatory mediators and chemokines as paracrine factors such as CXCLs or interleukins which were found to support several cancers such as breast or colon cancers (Liu et al., 2011; Tsai et al., 2011). The third mechanism by which MSCs can support tumor formation is the immune suppressive actions of these cells in both innate and adaptive immunity in a way that can promote tumor growth and progression (Lee and Hong, 2017). In fact, several contradictory results have been reported regarding pro- or anti-tumorigenic effects of MSCs. However, as far as our knowledge, so far no cancer was detected in clinical trials using MSCs, a notion supported by relatively recent reviews (Lee and Hong, 2017).

Interestingly, the application of exogenous engineered MSCs has been investigated as a novel anti-cancer strategy (Nowakowski et al., 2016). As for WJ-MSCs specifically, they have been reported to secrete factors causing suppression of cancer growth and inducing apoptosis (Wu et al., 2013; Lin et al., 2014). Generally, WJ-MSCs are reported to be non-tumorigenic, or even anti-tumorigenic and suggested to be a safe promising tool for cancer therapy. But the exact mechanisms of such anti-tumorigenic effect are still far from complete elucidation (El Omar et al., 2014).

Good Manufacturing Practice (GMP) – Compliance

It is important to remember that WJ-MSCs, like all other cell-based therapies are living products constantly interacting with their surrounding environment. This poses new challenges when looking from a pharmaceutical industrial point of view. For example, they cannot be sterilized prior to use to provide strict protection from any contamination transmission to patients. Besides, in order to maintain a consistent product efficacy, with minimal batch-to-batch variation, this requires precise process control and avoidance of adverse changes in heterogeneous populations or the cell environments. Consistent GMP-compliant manufacturing requires high reproducibility with a focus on safety, efficacy, and quality (Stacey et al., 2018).

Basically, WJ-MSCs are considered an advanced therapy medicinal product (ATMP), and should be produced in compliance with GMP (EMA, 2007). These requirements include the following: (a) Tests for virology (HIV-1/2, HBV, HCV, HTLV-1/2, HPV, B-19, CMV, and EBV), syphilis, mycoplasma, and sterility being negative. (b) Phenotype: the percentages of CD73+, CD90+, and CD105+ cells $\geq$ 98% and the percentages of CD34−, CD45−, HLA-DR−, CD14− or CD11b−, CD79a−, or CD19− $\leq$2%. (c) Viability $\geq$ 80% after thawing. (d) The endotoxin content $<$ 2 EU/mL. (e) No significant upregulation of telomerase reverse transcriptase (hTERT) gene and oncogenes during large-scale expansion. (f) No significant downregulation of tumor suppressor genes during large-scale expansion. (g) Confirmed potency (Sensebé et al., 2013; Arutyunyan et al., 2016).

Actually, one of the main concerns regarding using WJ-MSCs for clinical applications is the requirement of *in vitro* expansion which is affected greatly by culture medium. In the same time, production of clinical grade WJ-MSCs requires sterility controls, analysis for viral markers, and genetic testing such as karyotyping. It is important to point here that serum is a very important component of the culture as well as cryopreservation media of WJ-MSCs. It provides nutrients required for the cells' expansion and survival. However, residual proteins from animal serum might cause serious immunological reactions, which could adversely affect the therapeutic potential of the injected cells (Li et al., 2015).

Several studies have suggested alternatives to medium containing FBS or xenogenic serum (Bieback et al., 2009). Some investigators suggested using human serum or platelet-rich plasma (PRP) as an alternative for FBS (Jonsdottir-Buch et al., 2013). Furthermore, an interesting report suggested using PRP isolated from the same UC source, and indeed reported impressive results. Briefly, they collected UCB and UC-tissues from the same donors. The UC tissue was processed to obtain WJ-MSCs, and UCB was used as a source of activated PRP for WJ-MSCs expansion; as a GMP-compliant protocol for clinical applications (Van Pham et al., 2016).

Also, the cryopreservation method, and the optimum agents that should be used are still under debate (Balci and Can, 2013). Dimethyl sulfoxide (DMSO) has always been used as the common-practice cryo-protective agent; protecting the cells from freezing-induced damage. However, DMSO is potentially toxic especially at temperatures greater than 4°C, which complicates direct use of thawed MSCs for clinical applications. Moreover, the use of frozen-thawed MSCs treated with DMSO has been reported to adversely affect patients and cause possible nausea, vomiting, or even death (Thirumala et al., 2013). Importantly, the composition of the cryo-protectant media and the freezing protocol have been found to greatly affect the efficacy of obtaining living healthy cells from thawed UC-tissues (Arutyunyan et al., 2018).

Finally, maintaining cost effectiveness is indeed a very important crucial aspect to consider for manufacturing companies. And when considering scaling-up for generation of efficient cellular therapies from WJ-MSCs, GMP-compliance together with efficient cost-effectiveness is absolutely one of the major challenges facing the translation of WJ-MSCs from bench to bed-side.

Dosage Regimen

Effectiveness of stem cell therapy in DM is multifactorial. Efficiency and therapeutic outcome of injected cells are greatly

affected by the initial source of those cells, the number of injected cells and the route of administration (El-Badawy and El-Badri, 2016). Accordingly, it is indeed essential to optimize the cell dose and frequency, as well as the best route of delivery for every condition. MSCs over the past 2 decades have been mostly administered intravenously (IV). However, in case of local pathological conditions such as spinal cord injuries, *in situ* administration of cells is generally preferable (Can et al., 2017).

For the 7 clinical studies reviewed in **Table 1** which reported beneficial therapeutic effects for WJ-MSCs in DM or DM-related complications, 3 of those studies administered WJ-MSCs solely via IV injection, 1 study transplanted the cells via intra-pancreatic artery (IPA), 2 studies applied both IV and IPA administrations, and the last study injected the cells around the foot ulcer – local transplantation. Interestingly, apart from the route of administration, when considering the dosage regimen, or the frequency of administration, several regimens are also found in literature. Some studies used single dose injection, especially for intra-pancreatic route (Cai et al., 2016). While others used multiple injections ranging from two or more times, separated by varying periods of time (Kong et al., 2014; Chen et al., 2016; Hu et al., 2016). As for the dose/count of the cells to be transplanted, it varied from 0.2×10^6/kg and 8.7×10^6/kg in various disease conditions. Mostly the cell count to be administered is calculated relative to body weight, however, some clinical studies also applied some sort of arbitrary count (not calculated relative to body weight) (Can et al., 2017). Regarding WJ-MSCs transplantation for DM, a dose of 1×10^6/kg was reported several times in the studies reviewed in **Table 1**.

Actually, it is important to highlight here that the number/count of cells, the best route of delivery, the number/frequency of doses, as well as the time intervals between multiple deliveries are indeed very important controversial issues. Further, large scale well-designed randomized placebo-controlled studies are undoubtedly required to resolve these controversies and reach the optimum dosage regimen that should be followed for different types of DM, and DM-related complications.

In conclusion, several issues concerned with obtaining clinical grade WJ-MSCs, and the transition of WJ-MSCs therapy from bench-side to bed-side are still unresolved. Several challenges need to be well-addressed in order to maximize the benefit of WJ-MSCs for various regenerative medicine applications. **Figure 2** provides a summary for the most prominent challenges and hurdles facing WJ-MSCs in order to be translated from bench to bed-side.

WJ-MSCs BANKING AND CLINICALLY RELATED PRODUCTS

WJ-MSCs Banks

The estimation of more than 130 million global annual births worldwide indeed provide a unique opportunity as well as a readily available endless supply of life-saving stem cells, which could be recovered from WJ and UCB, then banked for future autologous or allogenic therapeutic application. It has been more than 20 years since the first human UCB transplant was performed (Munoz et al., 2014). Nowadays, UCB-banks worldwide hold 100s of 1000s of stored cryopreserved UCB units. The methods of collection, cryopreservation and banking of UCB are currently well-established, and thus clinical outcomes continue to improve worldwide for various conditions (Shearer et al., 2017).

However, regarding WJ-MSCs, the best practices for their cryopreservation/thawing and banking processes are still not clear, and not well-standardized. On one hand, the Hellenic UCB-bank reported that viable MSCs can only be isolated from freshly isolated UC-WJ-tissue, and that isolation of WJ-MSCs from frozen tissue fragments was impossible and completely unsuccessful (Chatzistamatiou et al., 2014). On the other hand, another research group from Singapore compared the post-thaw behavior of isolated WJ-MSCs, WJ-tissue, and whole/entire UC segments. Interestingly, they found that viability, proliferation rates, and even apoptotic signals of post-thawed cells which were originally cryopreserved as WJ-MSCs, or isolated from freezed-thawed WJ-tissue were significantly better than those cells derived from freezed-thawed whole UC segments. In conclusion, they reported that freezing WJ-tissue is a simple and reliable method for obtaining large numbers of MSCs to be utilized for cell-based therapies (Fong et al., 2016). Its noteworthy that storage of unprocessed WJ-tissues compared to storing isolated WJ-MSCs could have several advantages; such as minimization of labor and time expenses, as well as better chances for cell isolation and expansion in the future with yet unknown future standards or guidelines (Arutyunyan et al., 2018).

Nowadays, several UCB banks worldwide offer the service of UC-tissue cryo-preservation such as *Cryo-Cell, ViaCord, Cells4Life, CellCare, Cryo-Save*, and others (Arutyunyan et al., 2018). In fact, they encourage storing both UC-tissue and UCB, as the most efficient way to store the child's stem cells. We totally agree with this, taking in consideration the growing body of evidence supporting the regenerative potential of those WJ-MSCs for various disease conditions. However, still the currently used protocols for processing and cryo-preservation of the UC-tissue require careful revision. Standardization of such protocols is indeed warranted to ensure maximum future benefit of these cryopreserved UC-tissues, and to ensure getting clinical grade potentially effective WJ-MSCs for therapeutic applications in the future.

WJ-MSCs and Other UC-Related Products/Trademarks on the Market

In fact according to the European Medicines Agency (EMA), MSCs are considered as ATMP when these cells undergo substantial manipulation or are used for a different essential function. Actually, due to the diversity and complexity of cell-based biopharmaceuticals, the concept behind ATMP development in the EU – the regulation (EC) No. 1394/2007 lays down specific guidelines concerning centralized authorization, supervision and pharmacovigilance, always keeping in mind a strict focus on risk-assessment toward safety of the end user (EMA, 2007). Among the first attempts to produce an ATMP from WJ-MSCs has been the development of UCX®

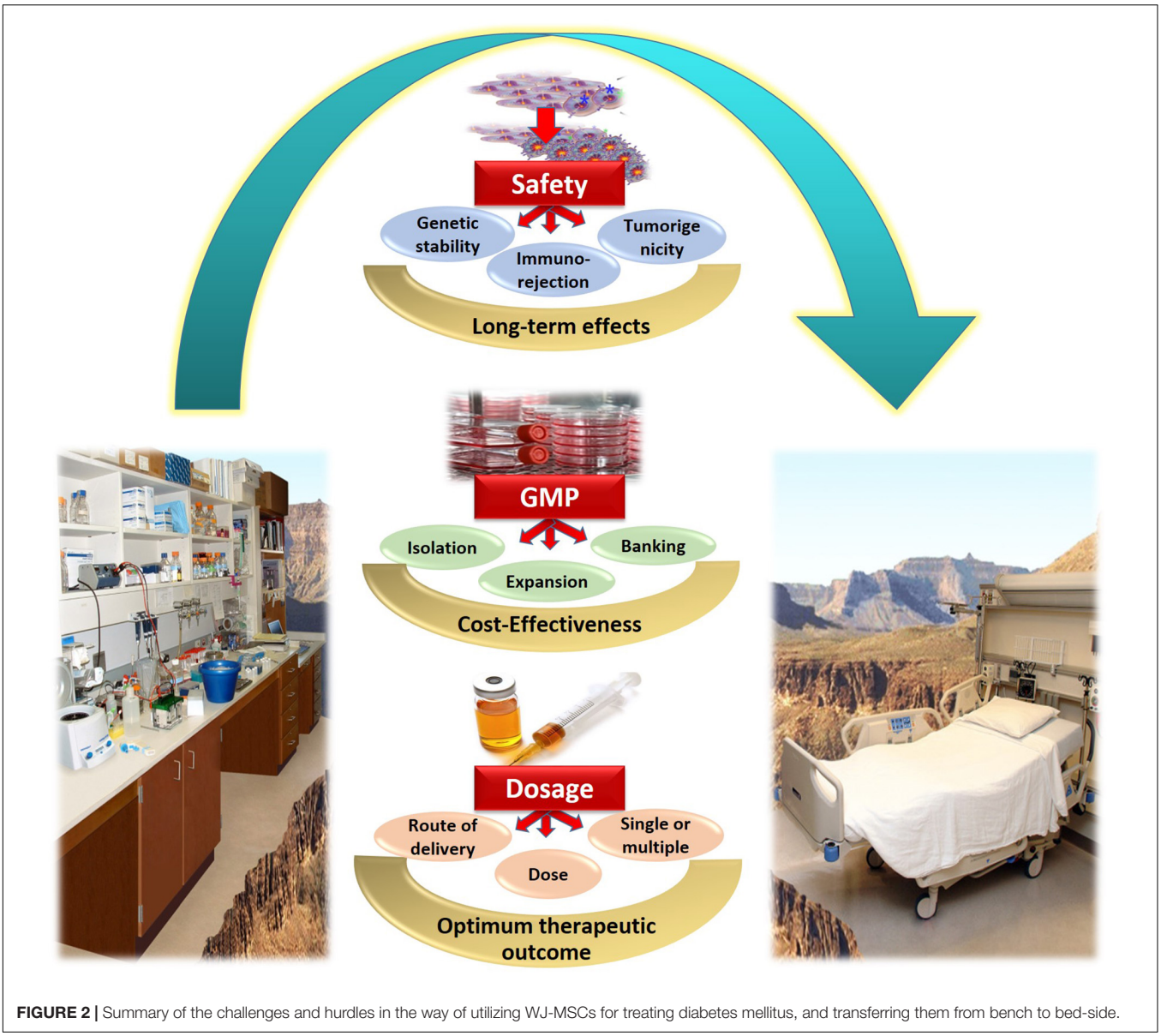

FIGURE 2 | Summary of the challenges and hurdles in the way of utilizing WJ-MSCs for treating diabetes mellitus, and transferring them from bench to bed-side.

manufactured by ECBio (Amadora, Portugal). It has been characterized in terms of cell identity, purity (microbiological, identity, and viability), tumorigenicity and genetic stability (Martins et al., 2014). It is among the first attempts to produce an ATMP from WJ-MSCs in accordance with EMA regulations regarding GMP for producing an ATMP in 2013–2014. However, we believe that its applications are still investigational, like WJ-MSCs in general. This product is an example of a potential product derived from UC tissue – WJ-MSCs, produced on a relatively large scale by ECBio company in accordance with GMP requirement for an ATMP.

Another UC-related trademark in the market is EpiCord®. EpiCord® is a minimally manipulated, dehydrated, devitalized cellular UC allograft commercially available. It is created through a patented PURION Plus process resulting in an allograft material that can be stored in ambient conditions for 5 years. EpiCord® showed indeed very promising results for treating non-healing diabetic foot ulcers (DFU) (Tettelbach et al., 2019). NEOX® Wound Allograft (Amniox Medical, Atlanta, GA, United States) is another UC-related product in the market. NEOX® is cryopreserved human amniotic membrane and UC (AM/UC) tissue dressing indicated for skin ulcers. Efficacy of NEOX® for treating chronic DFUs has been reported, and impressively 87.5% of wounds achieved complete epithelialization within about 14 weeks (Raphael, 2016).

FUTURE PERSPECTIVES

It's noteworthy here, that over the last few years, much attention has been given to decide who would be the winner for diabetes remodeling; ESCs or iPSCs? Additionally, several high

throughput elegant studies have been focusing on generation of IPCs from ESCs (Pagliuca et al., 2014; Vegas et al., 2016; Jacobson and Tzanakakis, 2018; Nair et al., 2019). But still on the other hand, several elegant studies and review articles attempt to investigate the differentiation potential of MSCs into various lineages other than mesoderm (Urrutia et al., 2019). Insulin producing cells is definitely one of these lineages (Enderami et al., 2018; Päth et al., 2019; Pavathuparambil Abdul Manaph et al., 2019). Accordingly, we recommend that interested scientists should also consider developing novel strategies and enhancing induction protocols to generate IPCs from these WJ-MSCs.

Actually, huge line of evidence showed that WJ-MSCs do not impose any ethical concerns or teratoma risk as those which exist regarding ESCs or IPCs and represent a readily available non-invasive source. Besides, several mechanisms have been suggested and discussed in this review for their therapeutic potential in diabetes including differentiation into IPCs, secretion of paracrine and soluble factors and modulating the immune response in the patient. Hence, they are potential candidates to become the next frontier for DM cell therapy.

Whether WJ-MSCs remain immuno-privileged and maintain their hypo-immunogenicity and paracrine effects after differentiation remains an open question requiring further investigations to be unraveled. Also, would it be better to transplant undifferentiated WJ-MSCs or differentiated IPCs as a cell therapy for DM is an open question waiting further elegant well-designed studies to be answered. Additionally, the long-term effects resulting in either cases after transplantation also require further investigations to unravel for how long exactly would the transplanted cells remain efficient and therapeutically effective? For how long will the genetic stability, low immunogenicity, and safety of those transplanted cells be maintained?

Another recent intervention for treating DM is "Stem Cell Educator" therapy. It is one of the relatively recent modalities/interventions being investigated in phase I/II clinical trials for its safety and efficacy to treat DM, or at least improve insulin resistance. For such intervention, a patient's blood is circulated through a closed-loop system that separates MNCs from the patient's whole blood. It briefly co-cultures those MNCs with adherent UCB-derived multipotent stem cells (CB-SCs), and then returns those educated autologous cells back to the patient's blood circulation (Zhao et al., 2013). Given all the remarkable properties of WJ-MSCs, it is indeed tempting to wonder whether they should be also considered to be utilized for this "Stem Cell Educator" intervention like their counterparts CB-SCs.

Finally, the field of extracellular vesicles, especially those derived from MSCs is expanding rapidly. It was suggested that transplanted MSCs could mediate their beneficial therapeutic effects at least partially via secreting various extracellular vesicles such as exosomes which carry several components such as soluble factors and miRNAs (Leibacher and Henschler, 2016). Undoubtedly, future studies are required to better characterize these vesicles and to help further elucidate the therapeutic potential of these WJ-MSCs-derived extracellular cargos.

CONCLUSION

Owing to their unique properties, we believe WJ-MSCs will be frontiers in stem cell therapy. However, several challenges are hindering the transfer of these WJ-MSCs from bench to bed-side. Further elegant large scale well-designed pre-clinical and clinical studies are urgently required to overcome those challenges and sharpen this potential weapon for our battle against DM.

Now understanding their great potential for regenerative medicine, we would recommend WJ-MSCs banking like their counterparts isolated from UCB (for both normal and cesarean labor, at least in hospitals). Actually, given the large number of child-births worldwide, UC provide an unlimited/untapped source of MSCs. Taking in consideration the ever-growing list of advantages and therapeutic effects of WJ-MSCs, not only for DM, but also for various disease conditions, banking of WJ-MSCs and/or UC tissues would indeed turn those UCs from just medical wastes into valuable priceless therapeutic tools. Besides, the medical benefit, this will undoubtedly have a huge economic benefit. We believe, the near future will unravel more interesting findings for WJ-MSCs, and strongly recommend their banking especially for those having family history of DM.

AUTHOR CONTRIBUTIONS

The authors declare that they collected the data and wrote the entire article themselves. MK and DK did not receive any form of sponsorship or honorarium for the material, and equally contributed in writing the current review article.

REFERENCES

Aggarwal, S., and Pittenger, M. F. (2005). Human mesenchymal stem cells modulate allogeneic immune cell responses. *Blood* 105, 1815–1822. doi: 10.1182/blood-2004-04-1559

Anzalone, R., Lo Iacono, M., Loria, T., Di Stefano, A., Giannuzzi, P., Farina, F., et al. (2011). Wharton's jelly mesenchymal stem cells as candidates for beta cells regeneration: extending the differentiative and immunomodulatory benefits of adult mesenchymal stem cells for the treatment of type 1 diabetes. *Stem Cell Rev.* 7, 342–363. doi: 10.1007/s12015-010-9196-4

Anzalone, R., Opatrilova, R., Kruzliak, P., Gerbino, A., and La Rocca, G. (2018). "Chapter 20 - mesenchymal stromal cells from Wharton's jelly (WJ-MSCs): coupling their hidden differentiative program to their frank immunomodulatory phenotype," in *Perinatal Stem Cells*, eds A. Atala, K. J. Cetrulo, R. R. Taghizadeh, S. V. Murphy, and C. L. Cetrulo (Boston, MA: Academic Press), 271–279. doi: 10.1016/b978-0-12-812015-6.00020-0

Arno, A. I., Amini-Nik, S., Blit, P. H., Al-Shehab, M., Belo, C., Herer, E., et al. (2014). Human Wharton's jelly mesenchymal stem cells promote skin wound healing through paracrine signaling. *Stem Cell Res. Ther.* 5, 28–28. doi: 10.1186/scrt417

Arutyunyan, I., Elchaninov, A., Makarov, A., and Fatkhudinov, T. (2016). Umbilical cord as prospective source for mesenchymal stem cell-based therapy. *Stem Cells Int.* 2016:6901286. doi: 10.1155/2016/6901286

Arutyunyan, I., Fatkhudinov, T., and Sukhikh, G. (2018). Umbilical cord tissue cryopreservation: a short review. *Stem Cell Res. Ther.* 9, 236–236. doi: 10.1186/s13287-018-0992-0

Balci, D., and Can, A. (2013). The assessment of cryopreservation conditions for human umbilical cord stroma-derived mesenchymal stem cells towards a potential use for stem cell banking. *Curr. Stem Cell Res. Ther.* 8, 60–72. doi: 10.2174/1574888x11308010008

Barkholt, L., Flory, E., Jekerle, V., Lucas-Samuel, S., Ahnert, P., Bisset, L., et al. (2013). Risk of tumorigenicity in mesenchymal stromal cell-based therapies–bridging scientific observations and regulatory viewpoints. *Cytotherapy* 15, 753–759. doi: 10.1016/j.jcyt.2013.03.005

Barrett, A. N., Fong, C.-Y., Subramanian, A., Liu, W., Feng, Y., Choolani, M., et al. (2018). Human Wharton's jelly mesenchymal stem cells show unique gene expression compared with bone marrow mesenchymal stem cells using single-cell RNA-sequencing. *Stem Cells Dev.* 28, 196–211. doi: 10.1089/scd.2018.0132

Bentzon, J. F., Stenderup, K., Hansen, F. D., Schroder, H. D., Abdallah, B. M., Jensen, T. G., et al. (2005). Tissue distribution and engraftment of human mesenchymal stem cells immortalized by human telomerase reverse transcriptase gene. *Biochem. Biophys. Res. Commun.* 330, 633–640. doi: 10.1016/j.bbrc.2005.03.072

Bhonde, R., Sheshadri, P., Sharma, S., and Kumar, A. (2014). Making surrogate β-cells from mesenchymal stromal cells: perspectives and future endeavors. *Int. J. Biochem. Cell Biol.* 46, 90–102. doi: 10.1016/j.biocel.2013.11.006

Bieback, K., Hecker, A., Kocaömer, A., Lannert, H., Schallmoser, K., Strunk, D., et al. (2009). Human alternatives to fetal bovine serum for the expansion of mesenchymal stromal cells from bone marrow. *Stem Cells* 27, 2331–2341. doi: 10.1002/stem.139

Bjorge, I. M., Kim, S. Y., Mano, J. F., Kalionis, B., and Chrzanowski, W. (2017). Extracellular vesicles, exosomes and shedding vesicles in regenerative medicine - a new paradigm for tissue repair. *Biomater. Sci.* 6, 60–78. doi: 10.1039/c7bm00479f

Brown, J. M., Nemeth, K., Kushnir-Sukhov, N. M., Metcalfe, D. D., and Mezey, E. (2011). Bone marrow stromal cells inhibit mast cell function via a COX2-dependent mechanism. *Clin. Exp. Allergy* 41, 526–534. doi: 10.1111/j.1365-2222.2010.03685.x

Cai, J., Wu, Z., Xu, X., Liao, L., Chen, J., Huang, L., et al. (2016). Umbilical cord mesenchymal stromal cell with autologous bone marrow cell transplantation in established type 1 diabetes: a pilot randomized controlled open-label clinical study to assess safety and impact on insulin secretion. *Diabetes Care* 39, 149–157. doi: 10.2337/dc15-0171

Can, A., Celikkan, F. T., and Cinar, O. (2017). Umbilical cord mesenchymal stromal cell transplantations: a systemic analysis of clinical trials. *Cytotherapy* 19, 1351–1382. doi: 10.1016/j.jcyt.2017.08.004

Caplan, A. (1991). Mesenchymal stem cells. *J. Orthop. Res.* 9, 641–650.

Carlsson, P.-O., and Svahn, M. (2018). Wharton's jelly derived allogeneic mesenchymal stromal cells for treatment of type 1 diabetes: study protocol for a double-blinded, randomized, parallel, placebo-controlled trial. *Clin. Trials Degener. Dis.* 3, 32–37.

Carvalho, M. M., Teixeira, F. G., Reis, R. L., Sousa, N., and Salgado, A. J. (2011). Mesenchymal stem cells in the umbilical cord: phenotypic characterization, secretome and applications in central nervous system regenerative medicine. *Curr. Stem Cell Res. Ther.* 6, 221–228. doi: 10.2174/157488811796575332

Casado, J. G., Tarazona, R., and Sanchez-Margallo, F. M. (2013). NK and MSCs crosstalk: the sense of immunomodulation and their sensitivity. *Stem Cell Rev.* 9, 184–189. doi: 10.1007/s12015-013-9430-y

Chatzistamatiou, T., Papassavas, A., Michalopoulos, E., Gamaloutsos, C., Mallis, P., Gontika, I., et al. (2014). Optimizing isolation culture and freezing methods to preserve Wharton's jelly's mesenchymal stem cell (MSC) properties: an MSC banking protocol validation for the Hellenic cord blood bank. *Transfusion* 54, 3108–3120. doi: 10.1111/trf.12743

Chen, L., Tredget, E., Wu, P., and Wu, Y. (2008). Paracrine factors of mesenchymal stem cells recruit macrophages and endothelial lineage cells and enhance wound healing. *PLoS One* 3:e1886. doi: 10.1371/journal.pone.0001886

Chen, P., Huang, Q., Xu, X. J., Shao, Z. L., Huang, L. H., Yang, X. Z., et al. (2016). The effect of liraglutide in combination with human umbilical cord mesenchymal stem cells treatment on glucose metabolism and β cell function in type 2 diabetes mellitus. *Zhonghua Nei Ke Za Zhi* 55, 349–354.

ClinicalTrials.gov (2019). Available at: https://clinicaltrials.gov/ (accessed August, 2019).

Cutler, A. J., Limbani, V., Girdlestone, J., and Navarrete, C. V. (2010). Umbilical cord-derived mesenchymal stromal cells modulate monocyte function to suppress T cell proliferation. *J. Immunol.* 185, 6617–6623. doi: 10.4049/jimmunol.1002239

Da Silva, Meirelles, L., Chagastelles, P., and Nardi, N. (2006). Mesenchymal stem cells reside in virtually all post-natal organs and tissues. *J. Cell Sci.* 119, 2204–2213. doi: 10.1242/jcs.02932

De Becker, A., and Riet, I. V. (2016). Homing and migration of mesenchymal stromal cells: how to improve the efficacy of cell therapy? *World J. Stem Cells* 8, 73–87. doi: 10.4252/wjsc.v8.i3.73

De Becker, A., Van Hummelen, P., Bakkus, M., Vande Broek, I., De Wever, J., De Waele, M., et al. (2007). Migration of culture-expanded human mesenchymal stem cells through bone marrow endothelium is regulated by matrix metalloproteinase-2 and tissue inhibitor of metalloproteinase-3. *Haematologica* 92, 440–449. doi: 10.3324/haematol.10475

Deak, E., Seifried, E., and Henschler, R. (2010). Homing pathways of mesenchymal stromal cells (MSCs) and their role in clinical applications. *Int. Rev. Immunol.* 29, 514–529. doi: 10.3109/08830185.2010.498931

Dominici, M., Le Blanc, K., Mueller, I., Slaper-Cortenbach, I., Marini, F., Krause, D., et al. (2006). Minimal criteria for defining multipotent mesenchymal stromal cells. The international society for cellular therapy position statement. *Cytotherapy* 8, 315–317. doi: 10.1080/14653240600855905

El Omar, R., Beroud, J., Stoltz, J., Menu, P., Velot, E., and Decot, V. (2014). Umbilical cord mesenchymal stem cells: the new gold standard for mesenchymal stem cell based therapies? *Tissue Eng. Part B Rev.* 20, 523–544. doi: 10.1089/ten.TEB.2013.0664

El-Badawy, A., and El-Badri, N. (2016). Clinical efficacy of stem cell therapy for diabetes mellitus: a meta-analysis. *PLoS One* 11:e0151938. doi: 10.1371/journal.pone.0151938

El-Demerdash, R. F., Hammad, L. N., Kamal, M. M., and El Mesallamy, H. O. (2015). A comparison of Wharton's jelly and cord blood as a source of mesenchymal stem cells for diabetes cell therapy. *Regen. Med.* 10, 841–855. doi: 10.2217/rme.15.49

EMA, (2007). *European Medicines Agency (EMA)*. Available at: https://www.ema.europa.eu/en/human-regulatory/marketing-authorisation/advanced-therapies/advanced-therapy-classification (accessed August, 2019).

Enderami, S. E., Soleimani, M., Mortazavi, Y., Nadri, S., and Salimi, A. (2018). Generation of insulin-producing cells from human adipose-derived mesenchymal stem cells on PVA scaffold by optimized differentiation protocol. *J. Cell. Physiol.* 233, 4327–4337. doi: 10.1002/jcp.26266

English, K., French, A., and Wood, K. (2010). Mesenchymal stromal cells: facilitators of successful transplantation? *Cell Stem Cell* 7, 431–442. doi: 10.1016/j.stem.2010.09.009

Fong, C., Chak, L., Biswas, A., Tan, J., Gauthaman, K., Chan, W., et al. (2011). Human Wharton's jelly stem cells have unique transcriptome profiles compared to human embryonic stem cells and other mesenchymal stem cells. *Stem Cell Rev. Rep.* 7, 1–16. doi: 10.1007/s12015-010-9166-x

Fong, C.-Y., Subramanian, A., Biswas, A., and Bongso, A. (2016). Freezing of fresh Wharton's jelly from human umbilical cords yields high post-thaw mesenchymal stem cell numbers for cell-based therapies. *J. Cell. Biochem.* 117, 815–827. doi: 10.1002/jcb.25375

Fong, C.-Y., Tam, K., Cheyyatraivendran, S., Gan, S.-U., Gauthaman, K., Armugam, A., et al. (2014). Human Wharton's jelly stem cells and its conditioned medium enhance healing of excisional and diabetic wounds. *J. Cell. Biochem.* 115, 290–302. doi: 10.1002/jcb.24661

Friedenstein, A., Chailakhyan, R., Latsinik, N., Panasyuk, A., and Keiliss-Borok, I. (1974). Stromal cells responsible for transferring the microenvironment of the hemopoietic tissues: cloning in-vitro and retransplantation in-vivo. *Transplantation* 17, 331–340. doi: 10.1097/00007890-197404000-00001

Friedenstein, A. J., Chailakhjan, R. K., and Lalykina, K. S. (1970). The development of fibroblast colonies in monolayer cultures of guinea-pig bone marrow and spleen cells. *Cell Prolif.* 3, 393–403. doi: 10.1111/j.1365-2184.1970.tb00347.x

Gao, J., Dennis, J. E., Muzic, R. F., Lundberg, M., and Caplan, A. I. (2001). The dynamic in vivo distribution of bone marrow-derived mesenchymal stem cells after infusion. *Cells Tissues Organs* 169, 12–20. doi: 10.1159/000047856

Gao, L. R., Zhang, N. K., Zhang, Y., Chen, Y., Wang, L., Zhu, Y., et al. (2018). Overexpression of apelin in Wharton' jelly mesenchymal stem cell reverses

insulin resistance and promotes pancreatic β cell proliferation in type 2 diabetic rats. *Stem Cell Res. Ther.* 9:339.

Gatta, V., D'Aurora, M., Lanuti, P., Pierdomenico, L., Sperduti, S., Palka, G., et al. (2013). Gene expression modifications in Wharton's jelly mesenchymal stem cells promoted by prolonged in vitro culturing. *BMC Genomics* 14:635. doi: 10.1186/1471-2164-14-635

Gauthaman, K., Fong, C.-Y., Suganya, C.-A., Subramanian, A., Biswas, A., Choolani, M., et al. (2012). Extra-embryonic human Wharton 's jelly stem cells do not induce tumorigenesis, unlike human embryonic stem cells. *Reprod. Biomed. Online* 24, 235–246.

Guo, Z.-Y., Sun, X., Xu, X.-L., Peng, J., and Wang, Y. (2015). Human umbilical cord mesenchymal stem cells promote peripheral nerve repair via paracrine mechanisms. *Neural Regen. Res.* 10, 651–658.

Han, Y., Li, X., Zhang, Y., Han, Y., Chang, F., and Ding, J. (2019). Mesenchymal stem cells for regenerative medicine. *Cells* 8:886.

Hass, R., Kasper, C., Böhm, S., and Jacobs, R. (2011). Different populations and sources of human mesenchymal stem cells (MSC): a comparison of adult and neonatal tissue-derived MSC. *Cell Commun. Signal.* 9:12. doi: 10.1186/1478-811X-9-12

Horwitz, E., Le Blanc, K., Dominici, M., Mueller, I., Slaper-Cortenbach, I., Marini, F., et al. (2005). Clarification of the nomenclature for MSC: the international society for cellular therapy position statement. *Cytotherapy* 7, 393–395. doi: 10.1080/14653240500319234

Hu, J., Wang, F., Sun, R., Wang, Z., Yu, X., Wang, L., et al. (2014). Effect of combined therapy of human Wharton's jelly-derived mesenchymal stem cells from umbilical cord with sitagliptin in type 2 diabetic rats. *Endocrine* 45, 279–287. doi: 10.1007/s12020-013-9984-0

Hu, J., Wang, Y., Gong, H., Yu, C., Guo, C., Wang, F., et al. (2016). Long term effect and safety of Wharton's jelly-derived mesenchymal stem cells on type 2 diabetes. *Exp. Ther. Med.* 12, 1857–1866. doi: 10.3892/etm.2016.3544

Hu, J., Yu, X., Wang, Z., Wang, F., Wang, L., Gao, H., et al. (2013). Long term effects of the implantation of Wharton's jelly-derived mesenchymal stem cells from the umbilical cord for newly-onset type 1 diabetes mellitus. *Endocr. J.* 60, 347–357. doi: 10.1507/endocrj.ej12-0343

IDF, (2019). *International Diabetes Federation. IDF Diabetes Atlas*, 9th Edn. Available at: http://www.idf.org/diabetesatlas (accessed December, 2019).

Jacobson, E. F., and Tzanakakis, E. S. (2018). Who will win: induced pluripotent stem cells versus embryonic stem cells for β cell replacement and diabetes disease modeling? *Curr. Diab. Rep.* 18:133.

Jellema, R. K., Wolfs, T. G., Lima Passos, V., Zwanenburg, A., Ophelders, D. R., Kuypers, E., et al. (2013). Mesenchymal stem cells induce T-cell tolerance and protect the preterm brain after global hypoxia-ischemia. *PLoS One* 8:e73031. doi: 10.1371/journal.pone.0073031

Jonsdottir-Buch, S. M., Lieder, R., and Sigurjonsson, O. E. (2013). Platelet lysates produced from expired platelet concentrates support growth and osteogenic differentiation of mesenchymal stem cells. *PLoS One* 8:e68984. doi: 10.1371/journal.pone.0068984

Karp, J., and Leng Teo, G. (2009). Mesenchymal stem cell homing: the devil is in the details. *Cell Stem Cell* 4, 206–216. doi: 10.1016/j.stem.2009.02.001

Kassem, D. H., Kamal, M. M., El-Kholy, A. G., and El-Mesallamy, H. O. (2016). Association of expression levels of pluripotency/stem cell markers with the differentiation outcome of Wharton's jelly mesenchymal stem cells into insulin producing cells. *Biochimie* 127, 187–195. doi: 10.1016/j.biochi.2016.05.019

Katuchova, J., Harvanova, D., Spakova, T., Kalanin, R., Farkas, D., Durny, P., et al. (2015). Mesenchymal stem cells in the treatment of type 1 diabetes mellitus. *Endocr. Pathol.* 26, 95–103. doi: 10.1007/s12022-015-9362-y

Kauer, M., Ban, J., Kofler, R., Walker, B., Davis, S., Meltzer, P., et al. (2009). A molecular function map of Ewing's sarcoma. *PLoS One* 4:e5415. doi: 10.1371/journal.pone.0005415

Kim, D., Staples, M., Shinozuka, K., Pantcheva, P., Kang, S., and Borlongan, C. (2013). Wharton's jelly-derived mesenchymal stem cells: phenotypic characterization and optimizing their therapeutic potential for clinical applications. *Int. J. Mol. Sci.* 14, 11692–11712. doi: 10.3390/ijms140611692

Kim, H.-K., Lee, S.-G., Lee, S.-W., Oh, B. J., Kim, J. H., Kim, J. A., et al. (2019). A subset of paracrine factors as efficient biomarkers for predicting vascular regenerative efficacy of mesenchymal stromal/stem cells. *Stem Cells* 37, 77–88. doi: 10.1002/stem.2920

Kong, C.-M., Subramanian, A., Biswas, A., Stunkel, W., Chong, Y.-S., Bongso, A., et al. (2019). Changes in stemness properties, differentiation potential, oxidative stress, senescence and mitochondrial function in Wharton's jelly stem cells of umbilical cords of mothers with gestational diabetes mellitus. *Stem Cell Rev. Rep.* 15, 415–426. doi: 10.1007/s12015-019-9872-y

Kong, D., Zhuang, X., Wang, D., Qu, H., Jiang, Y., Li, X., et al. (2014). Umbilical cord mesenchymal stem cell transfusion ameliorated hyperglycemia in patients with type 2 diabetes mellitus. *Clin. Lab.* 60, 1969–1976.

Kot, M., Baj-Krzyworzeka, M., Szatanek, R., Musial-Wysocka, A., Suda-Szczurek, M., and Majka, M. (2019). The importance of HLA assessment in "off-the-shelf" allogeneic mesenchymal stem cells based-therapies. *Int. J. Mol. Sci.* 20:E5680.

La Rocca, G., Anzalone, R., Corrao, S., Magno, F., Loria, T., Lo Iacono, M., et al. (2009). Isolation and characterization of Oct-4+/HLA-G+ mesenchymal stem cells from human umbilical cord matrix: differentiation potential and detection of new markers. *Histochem. Cell Biol.* 131, 267–282. doi: 10.1007/s00418-008-0519-3

Lee, H. Y., and Hong, I. S. (2017). Double-edged sword of mesenchymal stem cells: cancer-promoting versus therapeutic potential. *Cancer Sci.* 108, 1939–1946. doi: 10.1111/cas.13334

Leibacher, J., and Henschler, R. (2016). Biodistribution, migration and homing of systemically applied mesenchymal stem/stromal cells. *Stem Cell Res. Ther.* 7:7. doi: 10.1186/s13287-015-0271-2

Li, T., Xia, M., Gao, Y., Chen, Y., and Xu, Y. (2015). Human umbilical cord mesenchymal stem cells: an overview of their potential in cell-based therapy. *Expert Opin. Biol. Ther.* 15, 1293–1306. doi: 10.1517/14712598.2015.1051528

Lin, H. D., Fong, C. Y., Biswas, A., Choolani, M., and Bongso, A. (2014). Human Wharton's jelly stem cells, its conditioned medium and cell-free lysate inhibit the growth of human lymphoma cells. *Stem Cell Rev. Rep.* 10, 573–586. doi: 10.1007/s12015-014-9514-3

Liu, S., Ginestier, C., Ou, S. J., Clouthier, S. G., Patel, S. H., Monville, F., et al. (2011). Breast cancer stem cells are regulated by mesenchymal stem cells through cytokine networks. *Cancer Res.* 71, 614–624. doi: 10.1158/0008-5472.CAN-10-0538

Liu, X., Zheng, P., Wang, X., Dai, G., Cheng, H., Zhang, Z., et al. (2014). A preliminary evaluation of efficacy and safety of Wharton's jelly mesenchymal stem cell transplantation in patients with type 2 diabetes mellitus. *Stem Cell Res. Ther.* 5:57. doi: 10.1186/scrt446

Ma, S., Xie, N., Li, W., Yuan, B., Shi, Y., and Wang, Y. (2014). Immunobiology of mesenchymal stem cells. *Cell Death Differ.* 21, 216–225. doi: 10.1038/cdd.2013.158

Mahmood, A., Lu, D., Lu, M., and Chopp, M. (2003). Treatment of traumatic brain injury in adult rats with intravenous administration of human bone marrow stromal cells. *Neurosurgery* 53, 697–703. doi: 10.1227/01.neu.0000079333.61863.aa

Martins, J. P., Santos, J. M., de Almeida, J. M., Filipe, M. A., de Almeida, M. V. T., Almeida, S. C. P., et al. (2014). Towards an advanced therapy medicinal product based on mesenchymal stromal cells isolated from the umbilical cord tissue: quality and safety data. *Stem Cell Res. Ther.* 5:9. doi: 10.1186/scrt398

McElreavey, K., Irvine, A., Ennis, K., and McLean, W. (1991). Isolation, culture and characterisation of fibroblast-like cells derived from the Wharton's jelly portion of human umbilical cord. *Biochem. Soc. Trans.* 19:29S. doi: 10.1042/bst019029s

Moffett, A., and Loke, Y. (2003). The immunological paradox of pregnancy: a reappraisal. *Placenta* 25, 1–8. doi: 10.1016/s0143-4004(03)00167-x

Mukai, T., Tojo, A., and Nagamura-Inoue, T. (2018). Umbilical cord-derived mesenchymal stromal cells contribute to neuroprotection in neonatal cortical neurons damaged by oxygen-glucose deprivation. *Front. Neurol.* 9:466. doi: 10.3389/fneur.2018.00466

Munoz, J., Shah, N., Rezvani, K., Hosing, C., Bollard, C. M., Oran, B., et al. (2014). Concise review: umbilical cord blood transplantation: past, present, and future. *Stem Cells Transl. Med.* 3, 1435–1443. doi: 10.5966/sctm.2014-0151

Murphy, J., Fink, D., Hunziker, E., and Barry, F. (2003). Stem cell therapy in a caprine model of osteoarthritis. *Arthritis Rheum.* 48, 3464–3474. doi: 10.1002/art.11365

Nagai, A., Kim, W., Lee, H., Jeong, H., Kim, K., Hong, S., et al. (2007). Multilineage potential of stable human mesenchymal stem cell line derived from fetal marrow. *PLoS One* 2:e1272. doi: 10.1371/journal.pone.0001272

Nagyova, M., Slovinska, L., Blasko, J., Grulova, I., Kuricova, M., Cigankova, V., et al. (2014). A comparative study of PKH67, DiI, and BrdU labeling techniques for tracing rat mesenchymal stem cells. *In Vitro Cell. Dev. Biol. Anim.* 50, 656–663. doi: 10.1007/s11626-014-9750-5

Nair, G. G., Liu, J. S., Russ, H. A., Tran, S., Saxton, M. S., Chen, R., et al. (2019). Recapitulating endocrine cell clustering in culture promotes maturation of human stem-cell-derived β cells. *Nat. Cell Biol.* 21, 263–274.

Neri, S. (2019). Genetic stability of mesenchymal stromal cells for regenerative medicine applications: a fundamental biosafety aspect. *Int. J. Mol. Sci.* 20:E2406.

Newell, L. F., Deans, R. J., and Maziarz, R. T. (2014). Adult adherent stromal cells in the management of graft-versus-host disease. *Expert Opin. Biol. Ther.* 14, 231–246. doi: 10.1517/14712598.2014.866648

Nitzsche, F., Muller, C., Lukomska, B., Jolkkonen, J., Deten, A., and Boltze, J. (2017). Concise review: MSC adhesion cascade-insights into homing and transendothelial migration. *Stem Cells* 35, 1446–1460. doi: 10.1002/stem.2614

Nooshabadi, V. T., Mardpour, S., Yousefi-Ahmadipour, A., Allahverdi, A., Izadpanah, M., Daneshimehr, F., et al. (2018). The extracellular vesicles-derived from mesenchymal stromal cells: a new therapeutic option in regenerative medicine. *J. Cell. Biochem.* 119, 8048–8073. doi: 10.1002/jcb.26726

Nowakowski, A., Drela, K., Rozycka, J., Janowski, M., and Lukomska, B. (2016). Engineered mesenchymal stem cells as an anti-cancer Trojan horse. *Stem Cells Dev.* 25, 1513–1531. doi: 10.1089/scd.2016.0120

Pagliuca, F., Millman, J., Gurtler, M., Segel, M., Van Dervort, A., Ryu, J., et al. (2014). Generation of functional human pancreatic β cells in vitro. *Cell* 159, 428–439. doi: 10.1016/j.cell.2014.09.040

Pappa, K. I., and Anagnou, N. P. (2009). Novel sources of fetal stem cells: where do they fit on the developmental continuum? *Regen. Med.* 4, 423–433. doi: 10.2217/rme.09.12

Päth, G., Perakakis, N., Mantzoros, C. S., and Seufert, J. (2019). Stem cells in the treatment of diabetes mellitus — Focus on mesenchymal stem cells. *Metabolism* 90, 1–15. doi: 10.1016/j.metabol.2018.10.005

Pavathuparambil Abdul, Manaph, N., Sivanathan, K. N., Nitschke, J., Zhou, X.-F., Coates, P. T., et al. (2019). An overview on small molecule-induced differentiation of mesenchymal stem cells into beta cells for diabetic therapy. *Stem Cell Res. Ther.* 10:293. doi: 10.1186/s13287-019-1396-5

Pileggi, A. (2012). Mesenchymal stem cells for the treatment of diabetes. *Diabetes Metab. Res. Rev.* 61, 1355–1356. doi: 10.2337/db12-0355

Prasanna, S. J., Gopalakrishnan, D., Shankar, S. R., and Vasandan, A. B. (2010). Pro-inflammatory cytokines, IFNgamma and TNFalpha, influence immune properties of human bone marrow and Wharton jelly mesenchymal stem cells differentially. *PLoS One* 5:e9016. doi: 10.1371/journal.pone.0009016

Qin, H. L., Zhu, X. H., Zhang, B., Zhou, L., and Wang, W. Y. (2016). Clinical evaluation of human umbilical cord mesenchymal stem cell transplantation after angioplasty for diabetic foot. *Exp. Clin. Endocrinol. Diabetes* 124, 497–503. doi: 10.1055/s-0042-103684

Rachakatla, R. S., Marini, F., Weiss, M. L., Tamura, M., and Troyer, D. (2007). Development of human umbilical cord matrix stem cell-based gene therapy for experimental lung tumors. *Cancer Gene Ther.* 14, 828–835. doi: 10.1038/sj.cgt.7701077

Raphael, A. (2016). A single-centre, retrospective study of cryopreserved umbilical cord/amniotic membrane tissue for the treatment of diabetic foot ulcers. *J. Wound Care* 25, S10–S17. doi: 10.12968/jowc.2016.25.Sup7.S10

Rombouts, W. J., and Ploemacher, R. E. (2003). Primary murine MSC show highly efficient homing to the bone marrow but lose homing ability following culture. *Leukemia* 17, 160–170. doi: 10.1038/sj.leu.2402763

Sackstein, R. (2004). The bone marrow is akin to skin: HCELL and the biology of hematopoietic stem cell homing. *J. Investig. Dermatol. Symp. Proc.* 9, 215–223. doi: 10.1016/s0022-202x(15)53011-x

Schenk, S., Mal, N., Finan, A., Zhang, M., Kiedrowski, M., Popovic, Z., et al. (2007). Monocyte chemotactic protein-3 is a myocardial mesenchymal stem cell homing factor. *Stem Cells* 25, 245–251. doi: 10.1634/stemcells.2006-0293

Sensebé, L., Gadelorge, M., and Fleury-Cappellesso, S. (2013). Production of mesenchymal stromal/stem cells according to good manufacturing practices: a review. *Stem Cell Res. Ther.* 4:66. doi: 10.1186/scrt217

Shearer, W. T., Lubin, B. H., Cairo, M. S., and Notarangelo, L. D. (2017). Cord blood banking for potential future transplantation. *Pediatrics* 140:e20172695. doi: 10.1542/peds.2017-2695

Shetty, P., Cooper, K., and Viswanathan, C. (2010). Comparison of proliferative and multilineage differentiation potentials of cord matrix, cord blood, and bone marrow mesenchymal stem cells. *Asian J. Transfus. Sci.* 4, 14–24. doi: 10.4103/0973-6247.59386

Shi, Y., Hu, G., Su, J., Li, W., Chen, Q., Shou, P., et al. (2010). Mesenchymal stem cells: a new strategy for immunosuppression and tissue repair. *Cell Res.* 20, 510–518. doi: 10.1038/cr.2010.44

Sohni, A., and Verfaillie, C. M. (2013). Mesenchymal stem cells migration homing and tracking. *Stem Cells Int.* 2013:130763. doi: 10.1155/2013/130763

Som, C., and Venkataramana, N. K. (2018). Evaluation of efficacy and regenerative potential of Wharton's jelly and bone marrow derived mesenchymal stem cells in diabetic rats. *J. Preclin. Clin. Res.* 12, 30–35. doi: 10.26444/jpccr/85329

Stacey, G., Andrews, P., Asante, C., Barbaric, I., Barry, J., Bisset, L., et al. (2018). Science-based assessment of source materials for cell-based medicines: report of a stakeholders workshop. *Regen. Med.* 13, 935–944. doi: 10.2217/rme-2018-0120

Tettelbach, W., Cazzell, S., Sigal, F., Caporusso, J. M., Agnew, P. S., Hanft, J., et al. (2019). A multicentre prospective randomised controlled comparative parallel study of dehydrated human umbilical cord (EpiCord) allograft for the treatment of diabetic foot ulcers. *Int. Wound J.* 16, 122–130. doi: 10.1111/iwj.13001

Thirumala, S., Goebel, W. S., and Woods, E. J. (2013). Manufacturing and banking of mesenchymal stem cells. *Expert Opin. Biol. Ther.* 13, 673–691. doi: 10.1517/14712598.2013.763925

Tipnis, S., Viswanathan, C., and Majumdar, A. S. (2010). Immunosuppressive properties of human umbilical cord-derived mesenchymal stem cells: role of B7-H1 and IDO. *Immunol. Cell Biol.* 88, 795–806. doi: 10.1038/icb.2010.47

Troyer, D., and Weiss, M. (2008). Concise review: Wharton's jelly-derived cells are a primitive stromal cell population. *Stem Cells* 26, 591–599. doi: 10.1634/stemcells.2007-0439

Tsai, K. S., Yang, S. H., Lei, Y. P., Tsai, C. C., Chen, H. W., Hsu, C. Y., et al. (2011). Mesenchymal stem cells promote formation of colorectal tumors in mice. *Gastroenterology* 141, 1046–1056. doi: 10.1053/j.gastro.2011.05.045

Tsai, P.-J., Wang, H.-S., Lin, G.-J., Chou, S.-C., Chu, T.-H., Chuan, W.-T., et al. (2015). Undifferentiated Wharton's jelly mesenchymal stem cell transplantation induces insulin-producing cell differentiation and suppression of T-cell-mediated autoimmunity in nonobese diabetic mice. *Cell Transplant.* 24, 1555–1570. doi: 10.3727/096368914X683016

Urrutia, D. N., Caviedes, P., Mardones, R., Minguell, J. J., Vega-Letter, A. M., and Jofre, C. M. (2019). Comparative study of the neural differentiation capacity of mesenchymal stromal cells from different tissue sources: an approach for their use in neural regeneration therapies. *PLoS One* 14:e0213032. doi: 10.1371/journal.pone.0213032

Van Pham, P., Truong, N. C., Le, P. T.-B., Tran, T. D.-X., Vu, N. B., Bui, K. H.-T., et al. (2016). Isolation and proliferation of umbilical cord tissue derived mesenchymal stem cells for clinical applications. *Cell Tissue Bank.* 17, 289–302. doi: 10.1007/s10561-015-9541-6

Vegas, A. J., Veiseh, O., Gürtler, M., Millman, J. R., Pagliuca, F. W., Bader, A. R., et al. (2016). Long-term glycemic control using polymer-encapsulated human stem cell–derived beta cells in immune-competent mice. *Nat. Med.* 22, 306–311. doi: 10.1038/nm.4030

Wang, H., Hung, S., Peng, S., Huang, C., Wei, H., Guo, Y., et al. (2004). Mesenchymal stem cells in the Wharton's jelly of the human umbilical cord. *Sem Cells* 22, 1330–1337.

Wang, S., Qu, X., and Zhao, R. (2012). Clinical applications of mesenchymal stem cells. *J. Hematol. Oncol.* 5:19. doi: 10.1186/1756-8722-5-19

Weiss, M. L., Anderson, C., Medicetty, S., Seshareddy, K. B., Weiss, R. J., VanderWerff, I., et al. (2008). Immune properties of human umbilical cord Wharton's jelly-derived cells. *Stem Cells* 26, 2865–2874. doi: 10.1634/stemcells.2007-1028

WenBo, W., Fei, Z., YiHeng, D., Wei, W., TingMang, Y., WenHao, Z., et al. (2017). Human umbilical cord mesenchymal stem cells overexpressing nerve growth factor ameliorate diabetic cystopathy in rats. *Neurochem. Res.* 42, 3537–3547. doi: 10.1007/s11064-017-2401-y

Wharton, T. (1656). *Adenographia*. Oxford: Oxford University Press, 242–248.*

Wu, S., Ju, G.-Q., Du, T., Zhu, Y.-J., and Liu, G.-H. (2013). Microvesicles derived from human umbilical cord Wharton's jelly mesenchymal stem cells attenuate bladder tumor cell growth in vitro and in vivo. *PLoS One* 8:e61366. doi: 10.1371/journal.pone.0061366

Wynn, R. F., Hart, C. A., Corradi-Perini, C., O'Neill, L., Evans, C. A., Wraith, J. E., et al. (2004). A small proportion of mesenchymal stem cells strongly expresses functionally active CXCR4 receptor capable of promoting migration to bone marrow. *Blood* 104, 2643–2645. doi: 10.1182/blood-2004-02-0526

Xie, Z., Hao, H., Tong, C., Cheng, Y., Liu, J., Pang, Y., et al. (2016). Human umbilical cord-derived mesenchymal stem cells elicit macrophages into an anti-inflammatory phenotype to alleviate insulin resistance in type 2 diabetic rats. *Stem Cells* 34, 627–639. doi: 10.1002/stem.2238

Yin, Y., Hao, H., Cheng, Y., Gao, J., Liu, J., Xie, Z., et al. (2018). The homing of human umbilical cord-derived mesenchymal stem cells and the subsequent modulation of macrophage polarization in type 2 diabetic mice. *Int. Immunopharmacol.* 60, 235–245. doi: 10.1016/j.intimp.2018.04.051

Yoo, K. H., Jang, I. K., Lee, M. W., Kim, H. E., Yang, M. S., Eom, Y., et al. (2009). Comparison of immunomodulatory properties of mesenchymal stem cells derived from adult human tissues. *Cell Immunol.* 259, 150–156. doi: 10.1016/j.cellimm.2009.06.010

Zachar, L., Bacenkova, D., and Rosocha, J. (2016). Activation, homing, and role of the mesenchymal stem cells in the inflammatory environment. *J. Inflamm. Res.* 9, 231–240. doi: 10.2147/JIR.S121994

Zhao, Y., Jiang, Z., Zhao, T., Ye, M., Hu, C., Zhou, H., et al. (2013). Targeting insulin resistance in type 2 diabetes via immune modulation of cord blood-derived multipotent stem cells (CB-SCs) in stem cell educator therapy: phase I/II clinical trial. *BMC Med.* 11:160. doi: 10.1186/1741-7015-11-160

Conflict of Interest: The authors declare that the research was conducted in the absence of any commercial or financial relationships that could be construed as a potential conflict of interest.

frontiers in Cell and Developmental Biology

REVIEW
published: 14 May 2020
doi: 10.3389/fcell.2020.00326

Mesenchymal Stem Cells and Atopic Dermatitis: A Review

*Sérgio Ricardo Teixeira Daltro[1†], Cássio Santana Meira[1†], Ivanilson Pimenta Santos[1], Ricardo Ribeiro dos Santos[1,2,3] and Milena Botelho Pereira Soares[1,2,3]**

[1] Gonçalo Moniz Institute, Oswaldo Cruz Foundation (FIOCRUZ), Salvador, Brazil, [2] Health Institute of Technology, National Industrial Learning Service - Integrated Manufacturing and Technology Campus (SENAI-CIMATEC), Salvador, Brazil, [3] National Institute of Science and Technology for Regenerative Medicine (INCT-REGENERA), Rio de Janeiro, Brazil

Mesenchymal stem/stromal cells (MSCs) are stromal-derived non-hematopoietic progenitor cells that reside in and can be expanded from various tissues sources of adult and neonatal origin, such as the bone marrow, umbilical cord, umbilical cord blood, adipose tissue, amniotic fluid, placenta, dental pulp and skin. The discovery of the immunosuppressing action of MSCs on T cells has opened new perspectives for their use as a therapeutic agent for immune-mediated disorders, including allergies. Atopic dermatitis (AD), a chronic and relapsing skin disorder that affects up to 20% of children and up to 3% of adults worldwide, is characterized by pruritic eczematous lesions, impaired cutaneous barrier function, Th2 type immune hyperactivation and, frequently, elevation of serum immunoglobulin E levels. Although, in the dermatology field, the application of MSCs as a therapeutic agent was initiated using the concept of cell replacement for skin defects and wound healing, accumulating evidence have shown that MSC-mediated immunomodulation can be applicable to the treatment of inflammatory/allergic skin disorders. Here we reviewed the pre-clinical and clinical studies and possible biological mechanisms of MSCs as a therapeutic tool for the treatment of atopic dermatitis.

Keywords: mesenchymal stem/stromal cells, atopic dermatitis, atopic eczema, immunomodulation, inflammatory skin diseases

OPEN ACCESS

Edited by:
Karen Bieback, Universität Heidelberg, Germany

Reviewed by:
Javier A. Enciso, Universidad Científica del Sur, Peru
Philippe Bourin, Independent Researcher, Toulouse, France

***Correspondence:**
Milena Botelho Pereira Soares
milena@bahia.fiocruz.br

† These authors have contributed equally to this work and share first authorship

Specialty section:
This article was submitted to Stem Cell Research, a section of the journal Frontiers in Cell and Developmental Biology

Received: *29 February 2020*
Accepted: *16 April 2020*
Published: *14 May 2020*

Citation:
Daltro SRT, Meira CS, Santos IP, Ribeiro dos Santos R and Soares MBP (2020) Mesenchymal Stem Cells and Atopic Dermatitis: A Review. Front. Cell Dev. Biol. 8:326. doi: 10.3389/fcell.2020.00326

INTRODUCTION

Atopic dermatitis (AD), commonly known as atopic eczema, is a typical dermal chronic inflammatory disorder characterized by eczematous cutaneous lesions and severe pruritus, representing a significant burden on health-care resources and patients' quality of life (Hoare et al., 2000; Boothe et al., 2017). The prevalence of AD is higher than 20% in children and 1–10% of adults in some countries and continues to increase, affecting not only low-income, but also developed countries (Nutten, 2015; Reed and Blaiss, 2018; Sacotte and Silverberg, 2018).

AD is considered the most expensive cutaneous disorder in the world, followed by acne and psoriasis (Sacotte and Silverberg, 2018). The treatment of AD is based on pharmacological intervention, through the use of corticosteroids, calcineurin inhibitors, leukotriene receptor antagonists and antihistamines (Nakagawa et al., 1994; Berth-Jones et al., 2003; Ring et al., 2012a,b). The use of these classes of drugs, however, not only provides temporary relief of symptoms, but also causes various adverse effects and drug resistance in long-term treatment (Saeki et al., 2016;

Silverberg and Durán-McKinster, 2017). Therefore, the development of safe and effective therapies is necessary for the proper management of patients with AD.

Mesenchymal stem/stromal cells (MSCs), the most common stem cell used in cell therapy field, are multipotent, undifferentiated and self-renewing cells found in many adult and neonatal tissues (Pittenger et al., 1999; Dominici et al., 2006; Wei et al., 2013). MSCs have tissue repair potential through their self-renewal and differentiation abilities and is considered a strong modulator of the immune system through modulation of proliferation, recruitment and function of immune cells from innate and adaptive immune system (Herrero and Pérez-Simón, 2010; Hypnes et al., 2016; Zheng et al., 2018; Poggi and Zocchi, 2019). These features boosted pre-clinical and clinical investigations with the purpose of evaluate MSCs on autoimmune and immune-related diseases, such as asthma, systemic lupus erythematosus, rheumatoid arthritis, multiple sclerosis and skin diseases, such as AD (Sun et al., 2009; Nemeth et al., 2010; Wang et al., 2013; Na et al., 2014; Shin et al., 2017a; Li et al., 2020). In this review, we provide an overview of current reports regarding the use of MSCs as a therapeutic tool in atopic dermatitis, the challenges of conducting MSC studies in AD, as well as future directions needed to develop this field.

ATOPIC DERMATITIS

AD is characterized by severe itchiness, being one of the most common chronic inflammatory skin diseases, affecting up to one-fifth of the population in developed countries (Weidinger and Novak, 2016). AD can occur in any age group or ethnicity, being the most common skin disease in children, especially infants under two years of age. In some countries, especially in Asia and Latin America, it affects around 20% of children (Nagaraja et al., 1996; Odhiambo et al., 2009; Nutten, 2015; Page et al., 2016). Although most cases of childhood AD spontaneously resolve by adulthood, the disease persists in 10–30% of cases (Ellis et al., 2012). More rarely, the first symptoms develop in adulthood, being the prevalence of AD in adults of ˜1–3% (Eichenfield et al., 2014; Nutten, 2015).

The pathogenesis of AD is multifactorial, including genetic factors, epidermal barrier defects and immunopathogenic factors (Meagher et al., 2002). Regarding the immunopathogenic abnormalities, lymphocytes play a critical role, since T helper 2 (Th2) lymphocyte activation and the cytokines released by them lead to elevated production of immunoglobulin E (IgE) (**Figure 1**), increased inflammation in the skin, and aggravate the skin barrier defect in AD (Meagher et al., 2002; Klonowska et al., 2018). The initial course of AD is characterized by a biphasic inflammation, where a Th2 profile predominates, with increased levels of several cytokines, including interleukin-4 (IL-4), IL-13, IL-17, IL-22, IL-31, and thymic stromal lymphopoietin (TSLP) (Olivry et al., 2016; Chaudhary et al., 2019). This immune signature exists in lesional and non-lesional skin, indicating a systemic switch to a Th2 profile. In chronic AD skin lesions, a Th1/Th0 dominance has been described with increased production of interferon-gamma (IFN-γ), IL-6, IL-12 and granulocyte-macrophage colony-stimulating factor (GM-CSF) (**Figure 2**). In addition to cytokines produced from Th1 and Th2 cells, IL-17, produced from Th17 cells, has been reported to contribute to pathogenesis of AD. Interleukin-17 stimulates the production of IL-6 and IL-8 by human keratinocytes, which lead to increased T cell migration to the skin (Nutten, 2015; Miossec and Kolls, 2012; Sidbury and Khorsand, 2017; Campione et al., 2020). Interestingly, MSCs derived from skin samples from patients with chronic AD contributes to pathogenesis of disease through production of several Th1/Th17 cytokines and chemokines, such as CCL2, CCL20, CXCL2, CXCL5, IL-6, IL-8, IL-12, IL-17A, IL-21, transforming growth factor β (TGF-β) and IFN-γ (Orciani et al., 2017).

The clinical manifestations of AD vary with age. Infants (0–2 years) typically present erythematous papules and vesicles on the cheeks, forehead, neck and scalp, whereas children (2 years of age to puberty) exhibit dry skin and lichenified papules and plaques in flexural areas of the limbs. In adulthood, the predominant areas of eczema are the flexural folds, the face and neck, the upper arms and back, hands, feet, fingers and toes (McKenna and Doward, 2008; Weidinger and Novak, 2016; Kapur et al., 2018). Regardless of age, AD affects the patients' quality of life, once implies in sleep deprivation, financial costs and employment loss (Carroll et al., 2005; Lewis-Jones, 2006; Nutten, 2015).

Currently, there is no cure or prevention technique for AD and, therefore, treatment focuses on disease progression control and alleviation of symptoms (Carr, 2013). Due to the multifactorial pathogenetic mechanisms of AD, a single therapeutic approach is hardly capable of achieving disease control. Topical treatment with moisturizers, emollients or corticosteroids, oral therapy with immunomodulators (corticosteroids, calcineurin inhibitors, leukotriene receptor antagonists and antihistamines) and antibiotics have been the basis for the management of atopic dermatitis (Ring et al., 2012a,b; Aoki et al., 2019). In general, topical treatment is the first option of choice, being effective for the most patients with mild disease. Systemic therapy may be offered to those with severe disease or treatment-resistant eczema, however, invariably, in the long term, comes along with side effects (Apfelbacher et al., 2013; Wong et al., 2017; Aoki et al., 2019). New therapeutic approaches, such as monoclonal antibodies, are passing through the drug discovery pipeline and may reinforce the therapeutic arsenal against AD in a near future (Weidinger and Novak, 2016; Snast et al., 2018; Pistone et al., 2019).

MSCs CHARACTERISTICS AND IMMUNOMODULATORY PROPERTIES

MSCs were first described in the 70's as a cell population with the ability of self-renewing and as precursor cells of osteogenic lineage (Friedenstein et al., 1970). Since then, MSCs have been the target of numerous investigations and, due to their therapeutic potential, it is the most studied stem cell type, with more than 1,000 clinical trials, at various phases, recorded in the clinical

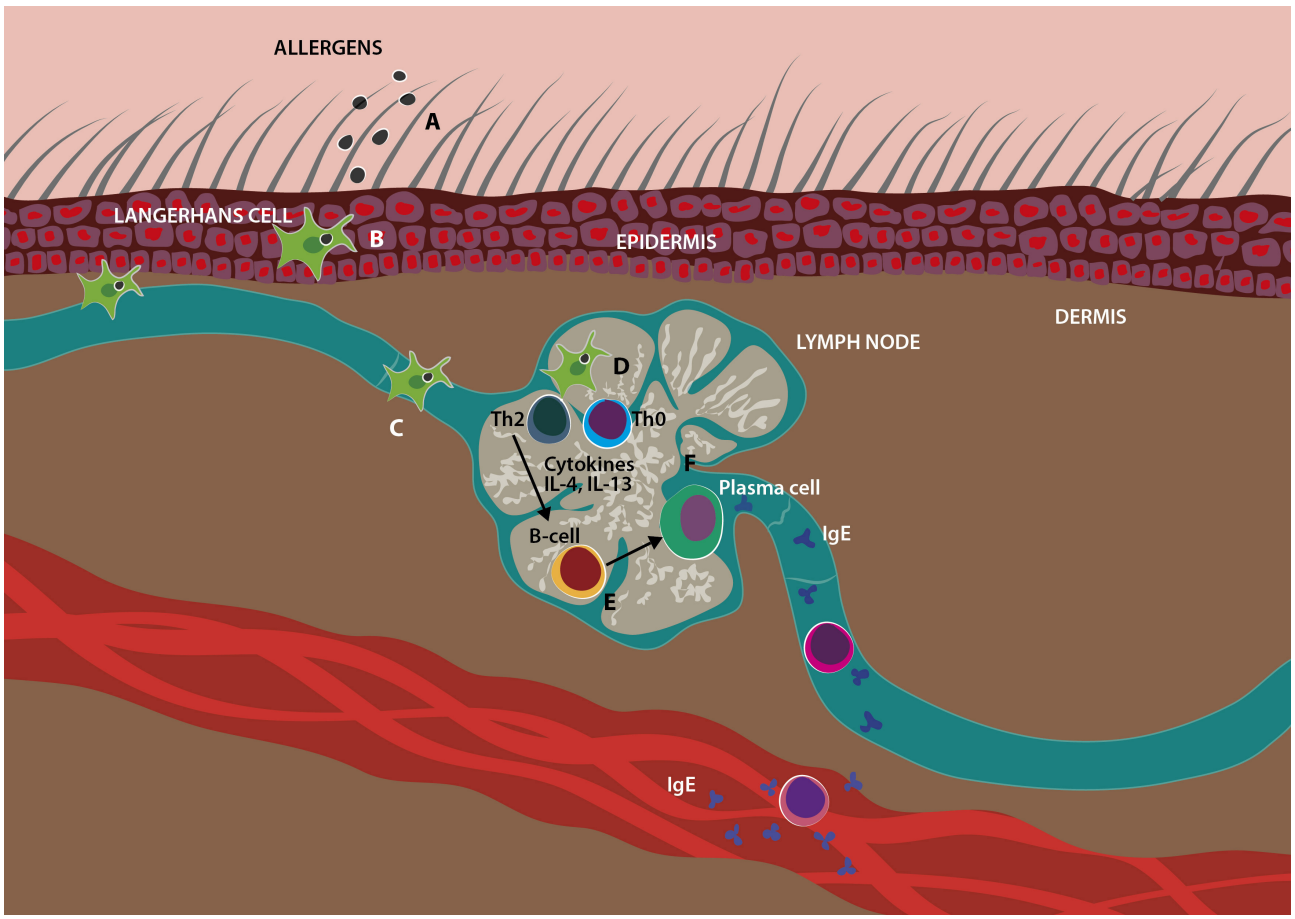

FIGURE 1 | Skin barrier dysfunction undergoing sensitization in AD. Allergens penetrating the skin **(A)** can be captured by Langerhans cells, which migrate to a regional draining lymph nodes **(B,C)**. Langerhans cells present the allergen to a naïve T cells, causing polarization to a Th-2 phenotype which secrete cytokines, such as IL-4 and IL-13 **(D)**, that stimulate B cells to become plasma cells and secrete allergen-specific IgE **(E,F)**.

trials database (clinicaltrials.gov as of January 2020). MSCs have a potential for differentiating into a variety of mesenchymal cell types, including adipocytes, chondrocytes, myoblasts and osteoblasts (Chamberlain et al., 2007; Glenn and Whartenby, 2014). MSCs are a heterogeneous population of cells that can be obtained by different sources, such as adipose tissue, amniotic fluid, bone marrow, dental pulp, skin, placenta, umbilical cord, and umbilical cord blood (Bianco et al., 2001; Lee et al., 2004; Lu et al., 2006; Guimarães et al., 2011; Antoniadou and David, 2016; Loukogeorgakis and De Coppi, 2017). Due to the pleiotropic nature of MSCs, the International Society for Cellular Therapy (ISCT) listed the minimum criteria and markers of MSCs in 2006 (Dominici et al., 2006). Briefly, MSCs should have plastic-adherence when maintained in standard culture conditions, capacity to *in vitro* differentiation into three cells types (adipocytes, chondrocytes and osteoblasts) and positive expression of specific cell surface markers, such as CD73, CD90 and CD105, while being negative to markers such as CD11b, CD14, CD19, CD34, CD45, CD79, and human leukocyte antigen – DR isotype (HLA-DR) (Dominici et al., 2006; Boxall and Jones, 2012).

MSCs emerged as an attractive cell type for the treatment of a variety of diseases, mainly injured tissues and immune-mediated diseases, due to its ability in modulate innate and adaptive immune system (Wei et al., 2013; Glenn and Whartenby, 2014; Golchin et al., 2019). In the innate immune system, MSCs are able to promote macrophage polarization to M2 phenotype (Kim and Hematti, 2009), inhibit the release of antimicrobial products by neutrophils (Raffaghello et al., 2008), suppress degranulation and production of tumor necrosis factor alpha (TNF-α) by mast cells (MC) (Brown et al., 2011), inhibit natural killer cells (NK) activation and production of pro-inflammatory cytokines (Sotiropoulou et al., 2006), and affect dendritic cell (DC) maturation, cytokine secretion and migration to lymph nodes (Chiesa et al., 2011). Regarding the adaptive immune system, MSCs inhibit B cell proliferation and affect antibodies production (Corcione et al., 2005), and, most importantly, affects T cell function, by inhibiting T cell proliferation through arresting at G0/G1 cell cycle phase, suppressing the development of Th1 and Th17 cells and favoring the development of anti-inflammatory Th2 and Treg populations (Di Nicola et al., 2002; Aggarwal and Pittenger, 2005).

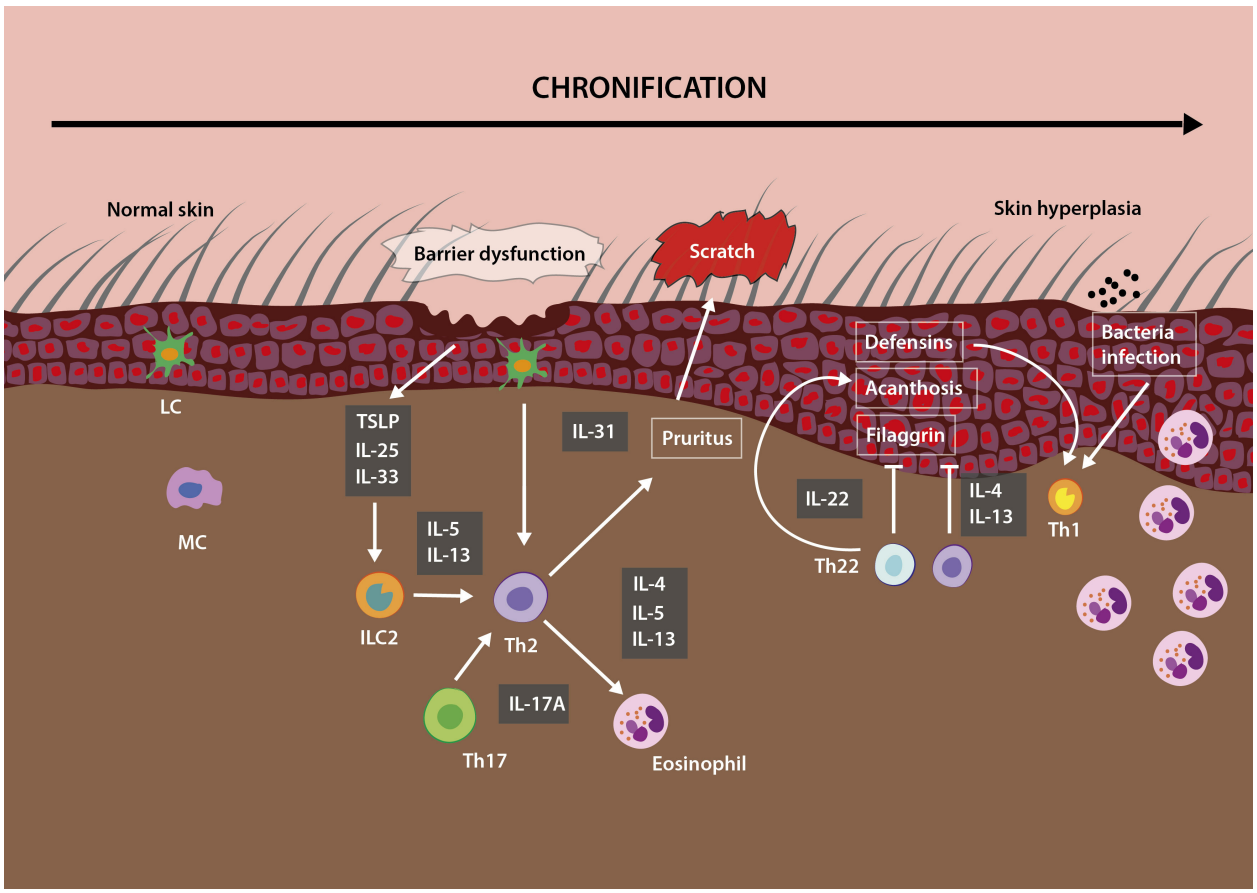

FIGURE 2 | Immune responses involved in chronification of lesions in AD. Scratching resulting from pruritus (the main symptom of AD), makes keratinocytes react by releasing cytokines important for inflammation, including TSLP (thymic stromal lymphopoetin), IL-33, and IL-25. IL-33 activates innate lymphoid cells 2 (ILC2) and Th2 lymphocytes. The release of IL-31 stimulates even more the pruritus. In response to IL-22, keratinocytes proliferate, resulting in diffuse epidermal hyperplasia. Eosinophils accumulate in chronic atopic skin. MC: mast cells; LC: Langerhans cells; ILC2: Innate lymphoid cell 2.

MSCs AND ATOPIC DERMATITIS

Over the last few years, the immunomodulatory effect of MSCs-based therapy has been described in animal models and in human beings, showing a significant improvement in the clinical presentation by inhibiting the activation of T and B cells and, consequently, the release of anti-inflammatory cytokines (IL-10 and TGF-β), by decreasing the proliferation of IL-4 and IFNγ, and by decreasing the production of lgE (Dias et al., 2019).

Although several studies have demonstrated that the allergic progress in AD could be suppressed by MSCs derived from human umbilical cord blood (UCB-MSC), bone marrow (BMMSC) or adipose tissue (AD-MSC) by modulating multiple targets, there are some important issues to be considered in the stem cell-based therapy, such as the stem cell type used, number of cells transplanted, preconditioning of the cell preparation, relevant targets of the therapy, route and frequencyofadministration (Na et al., 2014; Kim et al., 2015; Shin et al., 2017b; Kim D. S. et al., 2018).

Human umbilical cord-derived mesenchymal stem cells (hUCB-MSCs) produced a significant protective and therapeutic effect against *Dermatophagoides farinae* (*Df*)-induced AD in mice by inhibiting MC degranulation. The protective effect was observed more prominently when local subcutaneous (SC) injection of MSCs was performed, when compared with intravenous (IV) administration, showing considerably importance in choosing the route of administration (Shin et al., 2017b). In another study, two different doses (low dose: 2×10^5; high dose: 2×10^6) of human adipose-derived mesenchymal stem cells (hAD-MSCs) were compared in a *Df*-induced mouse AD model (Shin et al., 2017a). The hAD-MSCs were injected intravenously in this study and interestingly, the higher dose of hAD-MSCs significantly reduced the clinical severity of AD in mice compared to the low dose group.

Another example of the complexity of stem cell-based therapy was demonstrated in a study in which hUCB-MSCs were pre-treated with MC granules, enhancing their therapeutic effects, as observed by the attenuation of AD signs in a NC/Nga mouse model. Moreover, it was shown that hUCB-MSCs primed with mast cell granules suppressed the activation of MCs and B lymphocytes more efficiently than naïve MSCs, both *in vitro* and *in vivo* (Lee et al., 2019).

However, the underlying mechanisms by which MSCs attenuate allergic responses is relatively unclear, considering that most studies have not focused on local, lesion specific therapeutic approaches, but rather on the regulation of systemic inflammatory responses (Kim et al., 2017). Accumulating data indicate that MSCs are not spontaneously immunosuppressive, but require stimulation for acquiring their immunomodulatory properties. In particular, the most important priming factors of MSCs are IFN-γ, TNF-α, and IL-1β. The release and binding of IFN-γ on its receptor expressed by MSCs are key steps for the induction of their immunomodulatory properties, not only for various T cell subtypes, but also against B and NK cells (Kim M. et al., 2018; Najar et al., 2018; Wobma et al., 2018). During the synergistic action of IFN-γ and TNF-α, an increased production of IL-6, IL-8, HGF, PGE_2 and cyclooxygenase-2 (COX-2) was observed (Na et al., 2014; Lee and Song, 2018).

EFFECTS OF MSCs ON T CELLS IN THE CONTEXT OF AD

The pathogenesis of AD is mainly associated with T cell abnormalities, especially $CD4^+$ T cells (Leung, 1999; Meagher et al., 2002). Based on the profile of cytokines produced, can be classified in Th1 or Th2 cells, and both cells play a critical role in AD pathogenesis (Hanifin and Chan, 1999; Leung, 1999). In the acute phase, Th2 response predominates with increased levels of several cytokines, including IL-4 and IL-13, which induce the production of IgE by B cells (Chaudhary et al., 2019). During the chronic phase, a predominance of Th1 profile has been described, with increased production of IL-5, IL-12, and IFN-γ, the latter being responsible for inhibiting Th2 lymphocytes (Leung, 1999). Therefore, due to the central role of Th1/Th2 balance in the pathogenesis of AD, any therapy able to modulate these profiles may potentially interfere with the evolution of the disease (Boothe et al., 2017).

Interestingly, MSCs present strong immunomodulatory effects on lymphocyte function (Di Nicola et al., 2002; Aggarwal and Pittenger, 2005; Batorov et al., 2015; Li et al., 2016), including immunomodulatory effects shown in AD models (**Table 1**). In BALB/c mice with AD induced by ovalbumin (OVA), treatment with superoxide dismutase 3-transduced MSCs (SOD3-MSCs) suppressed the recruitment of T cells into the skin and reduced the number of $CD4^+$ and $CD8^+$ T cells in the spleen and lymph node (Sah et al., 2018). A similar inhibitory effect on T cell recruitment to the skin was observed in BALB/c mice with AD induced by *Aspergillus fumigatus* (*Af*) and treated with hUCB-MSCs primed with poly I:C or IFN-γ and in NC/Nga mice with AD induced by *Df* and treated with hUCB-MSCs pretreated with MC granules (Lee et al., 2019; Park et al., 2019).

In vivo findings of T cell inhibition in AD are supported by *in vitro* experiments in which co-cultures of MSCs with T lymphocytes showed suppression of T-cell proliferation and cytokine (IFNγ and IL-4) production (Na et al., 2014). Moreover, inhibition of T-bet and GATA-3 expression, which are transcription factors regulating IFNγ and IL-4 production, respectively, was also observed after treatment with BM-MSCs. Using L-NMMA, a nitric oxide (NO) inhibitor, the suppressive effect of BM-MSCS on T-cell proliferation and IFNγ production, but not IL-4 production, was reversed (Na et al., 2014).

EFFECTS OF MSCs ON B-CELLS AND IgE PRODUCTION IN THE CONTEXT OF AD

B cells play a critical role in the immune system and abnormalities on these cells functions result in a variety of chronic inflammation and autoimmune-mediated disorders, including AD (Simon et al., 2008; Nagel et al., 2009). MSCs are well known as suppressors of B cell function (Corcione et al., 2005; Asari et al., 2009; De Miguel et al., 2012) and, therefore, several studies evaluated their effect on B cells in AD models (**Table 1**).

Initially, Na et al. (2014) evaluated the effects of BM-MSC in BALB/c mice with AD induced by OVA. An intravenous injection of BM-MSCs was shown to suppress AD via inhibition of IgE production by B cells (Na et al., 2014). A reduction in IgE production in sera was also found in NC/Nga mice with AD induced by *Df* and treated with hAD-MSCs or hUCB-MSCs (Shin et al., 2017b; Lee et al., 2019).

In vitro experiments have confirmed the inhibitory effects of different types of MSCs on IgE production by B cells stimulated with lipopolysaccharide (LPS) or anti-CD40, as well as the inhibition of B cell proliferation and maturation (Na et al., 2014; Shin et al., 2017a; Lee et al., 2019). Interestingly, the effects of MSCs on B cell were attenuated with the addition of celecoxib, a selective COX-2 inhibitor (Shin et al., 2017b; Lee et al., 2019). In addition, BM-MSCs-induced IgE suppression is associated downregulation of activation-induced cytidine deaminase (AID) and B lymphocyte-induced maturation protein-1 (BLIMP-1), important regulators for class switch DNA recombination (CSR) and B-cell differentiation (Na et al., 2014). In short, we can see that MSCs modulate the maturation, proliferation and production of IgE, through CSR or COX-2-PGE_2 pathway.

EFFECTS OF MSCs ON MAST CELLS IN THE CONTEXT OF AD

Mast cells regulate trafficking and functions of cells involved in the skin inflammatory response through the release of several soluble mediators, including chemokines, cytokines and growth factors (Liu et al., 2011). In AD, mast cells contribute to the pathogenesis of both acute and chronic lesions, and its presence is supported by higher concentrations of its products such as IL-4, IL-13 and histamine in AD patients (Ring and Thomas, 1989; Hamid et al., 1996; Liu et al., 2011). In addition, mast cell degranulation has been shown to correlate with AD severity (Zhao et al., 2006).

Remarkably, MSCs are able to inhibit mast cell degranulation in AD mouse models (**Table 1**; Kim et al., 2015; Kim M. et al., 2018; Sah et al., 2018; Lee et al., 2019; Park et al., 2019). In NC/Nga mice with AD induced by *Df*, hUCB-MSCs injected

TABLE 1 | Effect of MSCs on experimental animal models of atopic dermatitis.

Model	Animals (strain)	MSCs				
		Source	Route	Effect	Mechanism and note	References
–	Dogs	cAD-MSCs	IV	N	Systemic administration of cADMSCs appears safe but ineffective	Hall et al., 2010
AD (OVA-induced)	Mouse (BALB/c or C3H/HeN)	BM-MSCs	IV	Y	T-cell supression via NO; B cell supression via CSR	Na et al., 2014
AD (*Df*-induced)	Mouse (Nc/Nga)	hUCB-MSCs	SC	Y	Inhibition of MC degranulation throught PG2 and TGFβ1	Kim et al., 2015
AD (*Df*-induced)	Mouse (Nc/Nga)	hAD-MSCs	IV	Y	B cell supresion via (COX)-2	Shin et al., 2017b
AD (DNCB-induced)	Mouse (BALB/c)	hAD-MSCs	IV	Y	Regulating the expression of MIP-2, miR-122a-SOCS1, and Th1/Th2 responses	Kim M. et al., 2018
AD (OVA-induced)	Mouse (BALB/c)	hSOD3-MSCs	SC	Y	Suppression of response elicited by keratinocytes, mast cells, neutrophils, DCs, and T cells through multiple mechanisms	Sah et al., 2018
–	Dogs	cAD-MSCs	IV	Y	Supression of canine PBMC proliferation	Villatoro et al., 2018
AD (*Df*-induced)	Mouse (Nc/Nga)	hUCB-MSCs	SC	Y	Preconditionng of MSC with MC granules optimizes the supression of MC and B cells	Lee et al., 2019
AD (*Af*-induced)	Mouse (BALB/c)	hUCB-MSCs	SC	Y	Control both eosinophil-associated Th2 immunity and neutrophil-related Th17	Park et al., 2019

AD, Atopic dermatitis; OVA, ovalbmin; Df, Dermatophagoides farinae; DNCB, dinitrochlorobenzene; Af, Aspergillus fumigatus; cAD-MSCs, canine adipose-derived mesenchymal stem cells; BM-MSCs, bone marrow-derived mesenchymal stem cells; hUCB-MSCs, human umbilical cord blood mesenchymal stem cells; hAD-MSCs, human adipose-derived mesenchymal stem cells; hSOD3-MSCs, human superoxide dismutase 3- transduced mesenchymal stem cells; IV, intravenous route; SB, subcutaneous route; NO, nitric oxide; CSR, class switch DNA recombination; MC, mast cell; PGE_2, prostaglandin E_2; COX, cyclooxygenase; MIP-2, macrophage inflammatory protein 2; SOCS1, suppressor of cytokine signaling 1; Th1, T helper 1; Th2, T helper 2; DC, dendritic cells; PBMC, peripheral blood mononuclear cell; Th17, T helper 17.

TABLE 2 | Clinical trials of MSCs in AD.

Type	Participants	Stem cells source	Route of administration	Result	References
Phase I; Phase IIa	7 adults; 27 adults	hUCB-MSCs	Subcutaneous	↓ IgE levels ↓ Neutrophil number 6/11 (55%): EASI50 in high dose treated group	Kim et al., 2016
Phase I	13 adults	MSCs	Intravenous	Ongoing	**NCT02888704**
Phase II	118 adults	hAD-MSCs	Intravenous	Recruiting	**NCT04137562**
Phase I; Phase II	20 adults; 72 adults	hBM-MSCs	Intravenous	Not yet recruiting	**NCT04179760**

EASI, Eczema Area and Severity Index; eczema hUCB-MSCs, human umbilical cord blood mesenchymal stem cells; hAD-MSCs, Human adipose tissue mesenchymal stem cells; hBM-MSCs, human bone marrow mesenchymal stem cells. NCT; Identification code given to each clinical study registered on ClinicalTrials.gov.

subcutaneously decreased the number of total degranulated mast cells, as well as the rate of degranulation (Kim et al., 2015; Lee et al., 2019). The inhibitory effect of MSCs on mast cell degranulation was also confirmed in BALB/c mice with AD induced by dinitrochlorobenzene (DNCB) and treated with hAD-MSCs and in BALB/c mice with AD induced by OVA and treated with SOD3-MSCs (Kim D. S. et al., 2018; Sah et al., 2018).

The inhibitory effect of MSC on mast cell degranulation was initially attributed to COX-2-PGE_2 pathway (Kim et al., 2010). Previous reports revealed that human MC express multiple PGE_2 receptors (EP receptors) that activate (EP_3) or inhibit (EP_2) mast cell degranulation (Feng et al., 2006; Kay et al., 2006; Wang and Lau, 2006). The addition of antagonists for the EP_2 and EP_4, but not for the EP_1 and EP_3, reduced the effect of hUCB-MSCs on mast cell degranulation (Kim et al., 2010). In agreement with this finding, MSCs treated with celecoxib, a selective COX-2 inhibitor, have a weak inhibitory effect on mast cell degranulation (Shin et al., 2017a; Lee et al., 2019). Taken together, the data support the involvement of COX-2-PGE_2 pathway on MSC immunosuppression effect of mast cell degranulation.

In addition, Kim et al. (2015), using sirRNA, observed a loss in degranulation-inhibiting effect of MSCs with down-regulation of TGF-β1, which can be explained by the inhibitory effect of TGF-β1 produced on mast cells expression of high-affinity IgE receptor (FcεRI), a critical component for IgE-mediated degranulation (Gomez et al., 2005).

Another mechanism related to MSCs effects on mast cell degranulation is the reduction of reactive oxygen species (ROS) production, since ROS triggers mast cell activation through both FcεRI and histamine H_4 receptor (H4R)-dependent pathways (Son et al., 2006; Swindle et al., 2008; Sah et al., 2018). Moreover, MSCs inhibit nuclear factor-kappa B (NFκB), which has been reported to bind to the H4R promoter region and, thereby, drive H4R upregulation and activation (Cogé et al., 2001).

Due to the promising profile of different types of MSCs to treat AD, several strategies to improve the inhibitory effects of MSCs in

mast cell degranulation and on other immune cells are in process of development. These include the use of MSCs treated with muramyl dipeptide (stimulus for NOD activation) (Kim et al., 2015), MSCs genetically modified to overexpress superoxide dismutase 3 (Sah et al., 2018), hUCB-MSC primed with poly I:C or IFN-γ (Park et al., 2019) and MSCs preconditioning with mast cell granules (Lee et al., 2019). All these strategies were shown to improve the inhibitory effects of MSCs on mast cell degranulation, as well as in other immune cells, such as B and T cells. In addition, extracts from hUCB-MSC and exosomes derived from hAD-MSC also ameliorated AD, reinforcing the importance of the paracrine effects of MSCs in AD context (Cho et al., 2018; Song et al., 2019).

CLINICAL TRIALS OF MSCs THERAPY IN AD

Despite the evidence indicating the benefits of MSCs in the treatment of AD in pre-clinical studies, to the date of this review, only one clinical trial (phase I/IIa) was published with subjects with AD (**Table 2**). A single cell administration hUCB-MSCs subcutaneously was performed in 34 adult participants with moderate-to-severe AD. Using the eczema area and severity index (EASI) score, an improvement in AD symptoms was observed in the groups treated with the two doses (2.5×10^7 cells, low dose; 5×10^7 cells, high dose) tested. In particular, the group treated with the higher dose of hUCB-MSCs showed a 50% reduction in EASI score in 6 of 11 (55%) subjects, without the appearance of side effects. In addition, the serum IgE levels and the number of eosinophils, typical biomarkers of AD, also decreased after treatment (Kim et al., 2017). Despite the encouraging results, this study has limitations, such as the small number of participants, its open label design and the lack of a placebo group. New studies with an experimental design including placebo groups and a larger number of patients, which are ongoing or to be started (**Table 2**), may bring new data to help define the clinical future of MSCs therapy in AD (National Library of Medicine, 2020).

CONCLUSION

Atopic dermatitis has become a significant public health problem due to its increasing prevalence, and there is a need for new therapeutic options for this disease. Evidence of therapeutic efficacy and mechanisms of action produced in pre-clinical studies indicate that MSC-based cell therapy is a promising approach for the treatment of AD. There is a need, however, for the conduction of double-blinded, placebo-controlled studies, to indicate the potential clinical application of MSCs, especially taking into account the complex pathogenesis of AD. Additional studies aiming at uncovering the mechanisms of action of MSC in atopic dermatitis may help define better therapeutic strategies for this disease.

AUTHOR CONTRIBUTIONS

SD and CM designed the study and wrote the manuscript. SD and IS conceived the artwork and performed the bibliographical research. RR and MS supervised the writing. All the authors revised and approved the final version of the manuscript.

FUNDING

The authors of this work acknowledge for the financial support provided by the Brazilian Research Council (CNPq)/MS Grant No. 443909/2018-0.

REFERENCES

Aggarwal, S., and Pittenger, M. E. (2005). Human mesenchymal stem cells modulate allogeneic immune cell responses. *Blood* 105, 1815–1822. doi: 10.1182/blood-2004-04-1559

Antoniadou, E., and David, A. L. (2016). Placental stem cells. *Best Pract. Res. Clin. Obstet. Gynaecol.* 31, 13–29. doi: 10.1016/j.bpobgyn.2015.08.014

Aoki, V., Lorezini, D., Orfali, R. L., Zaniboni, M. C., Oliveira, Z. N. P., Rivitti-Machado, M. C., et al. (2019). Consensus on the therapeutic management of atopic dermatitis- Brazilian Society of Dermatology. *An. Bras. Dermatol.* 94, 67–75. doi: 10.1590/abd1806-4841.2019940210

Apfelbacher, C. J., Van Zuuren, E. J., Fedorowicz, Z., Jupiter, A., Matterne, U., and Weisshaar, E. (2013). Oral H1 antihistamines as monotherapy for eczema. *Cochrane Database Syst. Rev.* 28:CD007770. doi: 10.1002/14651858.CD007770.pub2

Asari, S., Itakura, S., Ferreri, K., Liu, C. P., Kuroda, Y., Kandeel, F., et al. (2009). Mesenchymal stem cells suppress B-cell terminal differentiation. *Exp. Hematol.* 37, 604–615. doi: 10.1016/j.exphem.2009.01.005

Batorov, E. V., Shevela, E. Y., Tikhonova, M. A., Batorova, D. S., Ushakova, G. Y., Sizikova, S. A., et al. (2015). Mesenchymal stromal cells improve early lymphocyte recovery and T cell reconstitution after autologous hematopoietic stem cells transplatation in patients with malignant lymphomas. *Cell. Immunol.* 297, 80–86. doi: 10.1016/j.cellimm.2015.07.001

Berth-Jones, J., Damstra, R. J., Golsch, S., Livden, J. K., Van Hooteghem, O., Allegra, F., et al. (2003). Twice weekly fluticasone propionate added to emolient maintenance treatment to reduce risk of relapse in atopic dermatitis: randomised, double blind, parallel group study. *BMJ* 326:1367. doi: 10.1136/bmj.326.7403.1367

Bianco, P., Rimiucci, M., Gronthos, S., and Robery, P. G. (2001). Bone marrow stromal stem cells: nature, biology, and potential applications. *Stem Cells* 19, 180–192. doi: 10.1634/stemcells.19-3-180

Boothe, D. W., Tarbox, J. A., and Tarbox, M. B. (2017). Atopic dermatitis: pathophysiology. *Adv. Exp. Med. Biol.* 1027, 21–37. doi: 10.1007/978-3-319-64804-0_3

Boxall, S. A., and Jones, E. (2012). Markers for characterization of bone marrow multipotential stromal cells. *Stem Cells Int.* 2012:975871. doi: 10.1155/2012/975871

Brown, J. M., Nemeth, K., Kushnir-Sukhov, N. M., Metcalfe, D. D., and Mezey, E. (2011). Bone marrow stromal cells inhibit mast cell function via a COX2-dependent mechanism. *Clin. Exp. Allergy* 41, 526–534. doi: 10.1111/j.1365-2222.2010.03685.x

Campione, E., Lanna, C., Diluvio, L., Cannizzaro, M. V., Grelli, S., Galluzzo, M., et al. (2020). Skin immunity and its dysregulation in atopic dermatitis, hidradenitis supurativa and vitiligo. *Cell Cycle* 19, 257–267. doi: 10.1080/15384101.2019.1707455

Carr, W. W. (2013). Topical calcineurin inhibitors for atopic dermatitis: review and treatment recomendations. *Paediatr. Drugs* 15, 303–310. doi: 10.1007/s40272-013-0013-9

Carroll, C. L., Balkrishnan, R., Feldman, S. R., Fleischer, A. B., and Manuel, J. C. (2005). The burden of atopic dermatitis: impact on the patient, family, and society. *Pediatr. Dermatol.* 22, 192–199. doi: 10.1111/j.1525-1470.2005.22303.x

Chamberlain, G., Fox, J., Ashton, B., and Middleton, J. (2007). Concise review: mesenchymal stem cells: their phenotype, differentiation capacity, immunological features, and potential for homing. *Stem Cells* 25, 2739–2749. doi: 10.1634/stemcells.2007-0197

Chaudhary, S. K., Singh, S. K., Kumari, P., Kanwal, S., Soman, S. P., Choudhury, S., et al. (2019). Alterations in circulating concentrations of IL-17, IL-31 and total IgE in dogs with atopic dermatitits. *Vet. Dermatol.* 30:383-e114. doi: 10.1111/vde.12762

Chiesa, S., Morbelli, S., Morando, S., Massollo, M., Marini, C., and Bertoni, A. (2011). Mesenchymal stem cells impair *in vivo* T-cell priming by dendritic cells. *Proc. Natl. Acad. Sci. U.S.A.* 108, 17384–17389. doi: 10.1073/pnas.1103650108

Cho, B. S., Kim, J. O., Ha, D. H., and Yi, Y. W. (2018). Exosomes derived from human adipose tissue-derived mesenchymal stem cells alleviate atopic dermatitis. *Stem Cells Res. Ther.* 9:187. doi: 10.1186/s13287-018-0939-5

Cogé, F., Guénin, S. P., Rique, H., Boutin, J. A., and Galizzi, J. P. (2001). Structure and expression of the human histamine H4-receptor gene. *Biochem. Biophys. Res. Commun.* 284, 301–309. doi: 10.1006/bbrc.2001.4976

Corcione, A., Benvenuto, F., Ferretti, E., Giunti, D., Cappiello, V., Cazzanti, F., et al. (2005). Human mesenchymal stem cells modulate B-cell functions. *Blood* 107, 367–372. doi: 10.1182/blood-2005-07-2657

De Miguel, M. P., Fuentes-Julián, S., Blázquez-Martínez, A., Pascual, C. Y., Aller, M. A., Arias, J., et al. (2012). Immunosuppressive properties of mesenchymal stem cells: advances and applications. *Curr. Mol. Med.* 12, 574–591. doi: 10.2174/156652412800619950

Di Nicola, M., Carlo-Stella, C., Magni, M., Milanesi, M., Longoni, P. D., Matteucci, P., et al. (2002). Human bone marrow stromal cells suppress T-lymphocyte proliferation induced by cellular or nonspecific mitogenic stimuli. *Blood* 99, 3838–3843. doi: 10.1182/blood.v99.10.3838

Dias, I. E., Pinto, P. O., Barros, L. C., Viegas, C. A., Dias, I. R., and Carvalho, P. P. (2019). Mesenchymal stem cells therapy in companion animals: useful for immune-mediated diseases? *BMC Vet. Res.* 15:358. doi: 10.1186/s12917-019-2087-2

Dominici, M., Le Blanc, K., Mueller, I., Slaper-Cortenbach, I., Marini, F., and Krause, D. (2006). Minimal criteria for defining multipotent mesenchymal stromal cells. The international society for cellular therapy position statement. *Cytotherapy* 8, 315–317. doi: 10.1080/14653240600855905

Eichenfield, L. F., Tom, W. L., Chamlin, S. L., Feldman, S. R., Hanifin, J. M., Simpson, E. L., et al. (2014). Guidelines of care for the management of atopic dermatitis: section 1. diagnosis and assessment of atopic dermatitis. *J. Am. Acad. Dermatol.* 70, 338–351. doi: 10.1016/j.jaad.2013.10.010

Ellis, C. N., Mancini, A. J., Paller, A. S., Simpson, E. L., and Eichenfield, L. F. (2012). Understanding and managing atopic dermatitis in adult patients. *Semin. Cutan. Med. Surg.* 31(3 Suppl.), S18–S22. doi: 10.1016/j.sder.2012.07.006

Feng, C., Beller, E. M., Bagga, S., and Boyce, J. A. (2006). Human mast cells express multiple EP receptors for prostaglandina E2 that differentially modulate activation responses. *Blood* 107, 3243–3250. doi: 10.1182/blood-2005-07-2772

Friedenstein, A. J., Chailakhjan, R. K., and Lalykina, K. S. (1970). The development of fibroblast colonies in monolayer cultures of guinea-pig bone marrow and spleen cells. *Cell Tissue Kinet.* 3, 393–403. doi: 10.1111/j.1365-2184.1970.tb00347.x

Glenn, J. D., and Whartenby, K. A. (2014). Mesenchymal stem cells: emerging mechanisms of immunomodulation and therapy. *World J. Stem Cells* 26, 526–539. doi: 10.4252/wjsc.v6.i5.526

Golchin, A., Farahany, T. Z., Khojasteh, A., Soleimanifar, F., and Ardeshirylajimi, A. (2019). The clinical trials of mesenchymal stem cell therapy in skin diseases: an update and concise review. *Curr. Stem Cell Res. Ther.* 14, 22–33. doi: 10.2174/1574888X13666180913123424

Gomez, G., Ramirez, C. D., Rivera, J., Patel, M., Norozian, F., Wright, H. V., et al. (2005). TGF-beta 1 inhibits mast cell Fc epsilon RI expression. *J. Immunol.* 174, 5987–5993. doi: 10.4049/jimmunol.174.10.5987

Guimarães, E. T., Cruz, G. S., Jesus, A. A., Lacerda de Carvalho, A. F., Rogatto, S. R., Pereira, L. V., et al. (2011). Mesenchymal and embryonic characteristics of stem cells obtained from mouse dental pulp. *Arch. Oral Biol.* 56, 1247–1255. doi: 10.1016/j.archoralbio.2011.05.008

Hall, M. N., Rosenkrantz, W. S., Hong, J. H., Griffin, C. E., and Mendelsonhn, C. M. (2010). Evaluation of the potential use of adipose-derived mesenchymal stromal cells in the treatment of canine atopic dermatitis: a pilot study. *Vet. Ther.* 11, E1–E14.

Hamid, Q., Naseer, T., Minshall, E. M., Song, Y. L., Boguniewicz, M., and Leung, D. Y. (1996). In vivo expression of IL-12 and IL-13 in atopic dermatitis. *J. Allergy Clin. Immunol.* 98, 225–231. doi: 10.1016/s0091-6749(96)70246-4

Hanifin, J. M., and Chan, S. (1999). Bichemical and imunologic mechanisms in atopic dermatitis: new targets for emerging therapies. *J. Am. Acad. Dermatol.* 41, 72–77. doi: 10.1016/s0190-9622(99)70410-x

Herrero, C., and Pérez-Simón, J. A. (2010). Immunomodulatory effect of mesenchymal stem cells. *Braz. J. Med. Biol. Res.* 43, 425–430. doi: 10.1590/S0100-879X2010007500033

Hoare, C., Li Wan, P. A., and Williams, H. (2000). Systematic review of treatments for atopic eczema. *Health Technol. Assess.* 4, 1–191. doi: 10.1111/bjd.14588

Hypnes, K., Bright, R., Proudman, S., Haynes, D., Gronthos, S., and Bartold, M. (2016). Immunomodulatory properties of mesenchymal stem cell in experimental arthritis in rat and mouse models: a systematic review. *Semin. Arthritis Rheum.* 46, 1–19. doi: 10.1016/j.semarthrit.2016.02.008

Kapur, S., Watson, W., and Carr, S. (2018). Atopic dermatitis. *Allergy Asthma Clin. Immunol.* 14(Suppl. 2):52. doi: 10.1186/s13223-018-0281-6

Kay, L. J., Yeo, W. W., and Peachell, P. T. (2006). Prostaglandin E2 activates EP2 receptors to inhibit human lung mast cell degranulation. *Br. J. Pharmacol.* 147, 707–713. doi: 10.1038/sj.bjp.0706664

Kim, D. S., Jang, I. K., Lee, M. W., Ko, Y. J., Lee, D. H., Lee, J. W., et al. (2018). Enhanced immunosuppressive properties of human mesenchymal stem cells primed by interferon-γ. *EBioMedicine* 28, 261–273. doi: 10.1016/j.ebiom.2018.01.002

Kim, M., Lee, S. H., Kim, Y., Know, Y., Park, Y., Lee, H. K., et al. (2018). Human adipose tissue-derived mesenchymal stem cells attenuate atopic dermatitis by regulating the expression of MIP-2, miR-122a-SOCS1 axis, and Th1/Th2 responses. *Front. Pharmacol.* 9:1175. doi: 10.3389/fphar.2018.01175

Kim, H. S., Lee, J. H., Roh, K. H., Jun, H. J., Kang, K. S., and Kim, T. Y. (2017). Clinical trial of human umbilical cord blood-derived stem cells for the treatment of moderate-to-severe atopic dermatitis: phase I/IIa studies. *Stem Cells* 35, 248–255. doi: 10.1002/stem.2401

Kim, H. S., Yun, J. W., Shin, T. H., Lee, S. H., Lee, B. C., Yu, K. R., et al. (2015). Human umbilical cord blood mesenchymal tem cell-derived PGE2 and TGF-β1 alleviate atopic dermatits by reducing mast cell degranulation. *Stem Cells* 33, 1254–1266. doi: 10.1002/stem.1913

Kim, J., and Hematti, P. (2009). Mesenchymal stem cell-educated macrophages: a novel type of alternatively activated macrophages. *Exp. Hematol.* 37, 1445–1453. doi: 10.1016/j.exphem.2009.09.004

Kim, Y., Eom, S., Kim, K., Lee, Y. S., Choe, J., Hahn, J. H., et al. (2010). Transglutaminase II interacts with rac1, regulates production of reactive oxygen species, expression of snail, secretion of Th2 cytokines and mediates in vitro and in vivo allergic inflammation. *Mol. Immunol.* 47, 1010–1022. doi: 10.1016/j.molimm.2009.11.017

Klonowska, J., Glen, J., Nowicki, R. J., and Trzeciak, M. (2018). New cytokines in the pathogenesis of atopic dermatitis New therapeutic targets. *Int. J. Mol. Sci.* 19:3086. doi: 10.3390/ijms19103086

Lee, B. C., Kim, J. J., Lee, J. Y., Kang, I., Shin, N., Lee, S. E., et al. (2019). Disease-specific primed human adult stem cells effectively ameliorate experimental atopic dermatitis in mice. *Theranostics* 9, 3608–3621. doi: 10.7150/thno.32945

Lee, D. K., and Song, S. U. (2018). Immunomodulatory mechanisms of mesenchymal stem cells and their therapeutical applications. *Cell. Immunol.* 326, 68–78. doi: 10.1016/j.cellimm.2017.08.009

Lee, O. K., Kuo, T. K., Chen, W. M., Lee, K. D., Hsieh, S. L., and Chen, T. H. (2004). Isolation of multipotent mesenchymal stem cells from umbilical cord blood. *Blood* 103, 1669–1675. doi: 10.1182/blood-2003-05-1670

Leung, Y. M. (1999). Pathogenesis of atopic dermatitis. *J. Allergy Clin. Immunol.* 104, S99–S108. doi: 10.1016/s0091-6749(99)70051-5

Lewis-Jones, S. (2006). Quality of life and childhood atopic dermatitis: the misery of living with childhood eczema. *Int. J. Clin. Pract.* 60, 984–992. doi: 10.1111/j.1742-1241.2006.01047.x

Li, H., Tian, Y., Xie, L., Liu, X., Huang, Z., and Su, W. (2020). Mesenchymal stem cells in allergic diseases: current status. *Allergol. Int.* 69, 35–45. doi: 10.1016/j.alit.2019.08.001

Li, X., Xu, Z., Bai, J., Yang, S., Zhao, S., Zhang, Y., et al. (2016). Umbilical cord tissue-derived mesenchymal stem cells induce lymphocyte apoptosis and cell cycle arrest by expression of indoleamine 2,3-dioxygenase. *Stem Cells Int.* 2016:7495135. doi: 10.1155/2016/7495135

Liu, F. T., Goodarzi, H., and Chen, H. Y. (2011). IgE, mast cells, and eosinophils in atopic dermatitis. *Clin. Rev. Allergy. Immunol.* 41, 298–310. doi: 10.1007/s12016-011-8252-4

Loukogeorgakis, S. P., and De Coppi, P. (2017). Concise review: amniotic fluid stem cells: the know, the unknow, and potential regenerative medicine applications. *Stem Cells* 35, 1663–1673. doi: 10.1002/stem.2553

Lu, L. L., Liu, Y. J., Yang, S. G., Zhao, Q. J., Wang, X., Gong, X., et al. (2006). Isolation and characterization of human umbilical cord mesenchymal stem cells with hematopoesis-supportive function and other potentials. *Haematologica* 91, 1017–1026.

McKenna, S. P., and Doward, L. C. (2008). Quality of life of children with atopic dermatitis and their families. *Curr. Opin. Allergy Clin. Immunol.* 8, 228–231. doi: 10.1097/ACI.0b013e3282ffd6cc

Meagher, L. J., Wines, N. Y., and Cooper, A. J. (2002). Atopic dermatitis: review of immunopathogenesis, and advances in immunosuppressive therapy. *Australas. J. Dermatol.* 43, 247–254. doi: 10.1046/j.1440-0960.2002.00610.x

Miossec, P., and Kolls, J. K. (2012). Targeting IL-17 and TH17 cells in chronic Inflammation. *Nat. Rev. Drug Discov.* 11, 763–776. doi: 10.1038/nrd3794

Na, K., Yoo, H. S., Zhang, Y. X., Choi, M. S., Lee, K., Yi, T. G., et al. (2014). Bone marrow-derived clonal mesenchymal stem cells inhibit ovalbumin-induced atopic dermatitis. *Cell Death Dis.* 5:e1345. doi: 10.1038/cddis.2014.299

Nagaraja, R., Kanwar, A. J., Dhar, S., and Singh, S. (1996). Frequency and significance of minor clinical features in various age-related subgroups of atopic dermatits in children. *Pediatr. Dermatol.* 13, 10–13. doi: 10.1111/j.1525-1470.1996.tb01178.x

Nagel, A., Hertl, M., and Eming, R. (2009). B-cell-directed therapy for inflammatory skin diseases. *J. Invest. Dermatol.* 129, 289–301. doi: 10.1038/jid.2008.192

Najar, M., Krayem, M., Merimi, M., Burny, A., Meuleman, N., Bron, D., et al. (2018). Insights into inflammatory priming of mesenchymal stromal cells: functional biological impacts. *Inflamm. Res.* 67, 467–477. doi: 10.1007/s00011-018-1131-1

Nakagawa, H., Etoh, T., Ishibashi, Y., Higaki, Y., Kawashima, M., Torii, H., et al. (1994). Tacrolimus ointment for atopic dermatitis. *Lancet* 344:883.

National Library of Medicine (2020). *ClinicalTrials.gov*. Available online at: https://clinicaltrials.gov/ct2/home (accessed January 20, 2020).

Nemeth, K., Keane-Myers, A., Brown, J. M., Metcalfe, D. D., Gorham, J. D., Bundoc, V. G., et al. (2010). Bone marrow stromal cells use TGF-β to suppress allergic responses in a mouse model of ragweed-induced asthma. *Proc. Natl. Acad. Sci. U.S.A.* 107, 56652–56657. doi: 10.1073/pnas.0910720107

Nutten, S. (2015). Atopic demartitis: global epidemiology and risk factors. *Ann. Nutr. Metab.* 66(Suppl.), 8–18. doi: 10.1159/000370220

Odhiambo, J. A., Williams, H. C., Clayton, T. O., Robertson, C. F., and Asher, M. I. (2009). Global variations in prevalence of eczema symptoms in children from ISAAC phase three. *J. Allergy Clin. Immunol.* 124, 1251–1258. doi: 10.1016/j.jaci.2009.10.009

Olivry, T., Mayhew, D., Paps, J. S., Linder, K. E., Peredo, C., Rajpal, D., et al. (2016). Early activation of Th2/Th22 inflammatory and pruritogenic pathways in acute canine AD skin lesions. *J. Invest. Dermatol.* 136, 1961–1969. doi: 10.1016/j.jid.2016.05.117

Orciani, M., Campanati, A., Caffarini, M., Ganzetti, G., Consales, V., Lucarini, G., et al. (2017). T helper (Th)1, Th17 and Th2 imbalance in mesenchymal stem cells of adult patients with atopic dermatitis: at the origin of the problem. *Br. J. Dermatol.* 176, 1569–1576. doi: 10.1111/bjd.15078

Page, S. S., Weston, S., and Loh, R. (2016). Atopic dermatitis in children. *Aust. Fam. Phys.* 45, 293–296.

Park, A., Park, H., Yoon, J., Kang, D., Kang, M. H., Park, Y. Y., et al. (2019). Priming with toll-like receptor 3 agonist or interferon-gamma enhances the therapeutic effects of human mesenchymal stem cells in a murine model of atopic dermatitis. *Stem Cell Res. Ther.* 10:66. doi: 10.1186/s13287-019-1164-6

Pistone, G., Tilotta, G., Gurreri, R., Castelli, E., Curiale, S., and Bongiorno, M. R. (2019). Real-life practice: rapid improvement in itch symptomatology in patients with atopic dermatitis treated with dupilumab. *J. Dermatolog. Treat.* doi: 10.1080/09546634.2019.1628914 [Epub ahead of print].

Pittenger, M. F., Mackay, A. M., Beck, S. C., Jaiswal, R. K., Douglas, R., Mosca, J. D., et al. (1999). Multilineage potential of adult human mesenchymal stem cells. *Science* 284, 143–147. doi: 10.1126/science.284.5411.143

Poggi, A., and Zocchi, M. R. (2019). Immunomodulatory properties of mesenchymal stromal cells: still unresolved "Yin and Yang". *Curr. Stem. Cell Res. Ther.* 14, 344–350. doi: 10.2174/1574888X14666181205115452

Raffaghello, L., Bianchi, G., Bertolotto, M., Montecucco, F., Busca, A., Dallegri, F., et al. (2008). Human mesenchymal stem cells inhibit neutrophil apoptosis: a model for neutrophil preservation in the bone marrow niche. *Stem Cells* 26, 151–162. doi: 10.1634/stemcells.2007-0416

Reed, B., and Blaiss, M. S. (2018). The burden of atopic dermatitis. *Allergy Asthma Proc.* 39, 406–410. doi: 10.2500/aap.2018.39.4175

Ring, J., Alomar, A., Bieber, T., Deleuran, M., Fink-Wagner, A., Gelmetti, C., et al. (2012a). Guidelines for treatment of atopic eczema (atopic dermatitis) part I. *J. Eur. Acad. Dermatol. Venereol.* 26, 1045–1060. doi: 10.1111/j.1468-3083.2012.04635.x

Ring, J., Alomar, A., Bieber, T., Deleuran, M., Fink-Wagner, A., Gelmetti, C., et al. (2012b). Guidelines for treatment of atopic eczema (atopic dermatitis) part II. *J. Eur. Acad. Dermatol. Venereol.* 26, 1076–1093. doi: 10.1111/j.1468-3083.2012.04636.x

Ring, J., and Thomas, P. (1989). Histamine and atopic eczema. *Acta Derm. Venereol. Suppl.* 144, 70–77.

Sacotte, R., and Silverberg, J. I. (2018). Epidemiology of adult atopic dermatits. *Clin. Dermatol.* 36, 595–605. doi: 10.1016/j.clindermatol.2018.05.007

Saeki, H., Nakahara, T., Tanaka, A., Kabashima, K., Sugaya, M., Murota, H., et al. (2016). Clinical practice guidelines for the management of atopic dermatitis 2016. *J. Dermatol.* 43, 1117–1145. doi: 10.1111/1346-8138.13392

Sah, S. K., Agrahari, G., Nguyen, C. T., Kim, Y. S., Kang, K. S., and Kim, T. Y. (2018). Enhanced therapeutic effects of human mesenchymal stem cells transduced with superoxide dismutase 3 in a murine topic dermatitis-like skin inflammation model allergy. *Allergy* 73, 2364–2376. doi: 10.1111/all.13594

Shin, T. H., Kim, H. S., Choi, S. W., and Kang, K. S. (2017a). Mesenchymal stem cell therapy for inflammatory skin diseases: clinical potential and mode of action. *Int. J. Mol. Sci.* 18, 1–25. doi: 10.3390/ijms18020244

Shin, T. H., Lee, B. C., Choi, S. W., Shin, J. H., Kang, I., Lee, Y. L., et al. (2017b). Human adipose tissue-derived mesenchymal stem cells alleviate atopic dermatits via regulation of B lymphocyte maturation. *Oncotarget* 8, 512–522. doi: 10.18632/oncotarget.13473

Sidburry, R., and Khorsand, K. (2017). Evolving concepts in atopic dermatitis. *Curr. Allergy Asthma Rep.* 17:42. doi: 10.1007/s11882-017-0710-5

Silverberg, N. B., and Durán-McKinster, C. (2017). Special considerations for therapy of pediatric atopic dermatitis. *Dermatol. Clin.* 35, 351–363. doi: 10.1016/j.det.2017.02.008

Simon, D., Hosli, S., Kostylina, G., Yawalkar, N., and Simon, H. U. (2008). Anti-Cd20 (rituximab) treatment improves atopic eczema. *J. Allergy Clin. Immunol.* 121, 122–128. doi: 10.1016/j.jaci.2007.11.016

Snast, I. S., Reiter, O., Hodak, E., Friedland, R., Mimouni, D., and Leshem, Y. A. (2018). Are biological efficacious in atopic dermatits? A systematic review and meta-anaylsis. *Am. J. Clin. Dermatol.* 19, 145–165. doi: 10.1007/s40257-017-0324-7

Son, A., Nakamura, H., Kondo, N., Matsuo, Y., Liu, W., Oka, S., et al. (2006). Redox regulation of mast cell histamine release in thioredoxin-1 (TRX) transgenic mice. *Cell Res.* 16, 230–239. doi: 10.1038/sj.cr.7310031

Song, J. Y., Kang, H. J., Ju, H. M., Park, A., Park, H., Hong, J. S., et al. (2019). Umbilical cord-derived mesenchymal stem cell extracts ameliorate atopic dermatitis in mice by reducing the T cell responses. *Sci. Rep.* 9:6623. doi: 10.1038/s41598-019-42964-7

Sotiropoulou, P. A., Perez, S. A., Gritzapis, A. D., Baxevanis, C. N., and Papamichail, M. (2006). Interactions between human mesenchymal stem cells and natural killer cells. *Stem Cells* 24, 74–85. doi: 10.1634/stemcells.2004-0359

Sun, L., Akiyama, K., Zhang, H., Yamaza, T., Hou, Y., Zhao, S., et al. (2009). Mesenchymal stem cell transplantation reverses multiorgan dysfunction in systemic lupus erythematosus mice and humans. *Stem Cells* 27, 1421–1432. doi: 10.1002/stem.68

Swindle, E. J., DeLeo, F. R., and Metcalfe, D. D. (2008). Intracellular superoxide production by mast cells. *J. Allergy Clin. Immunol.* 121(Suppl. 1):S111. doi: 10.1016/j.jaci.2007.12.441

Villatoro, A. J., Hermida-Prieto, M., Fernández, V., Fariñas, F., Alcoholado, C., and Rodríguez-García, M. I. (2018). Allogeneic adipose-derived mesenchymal stem cell therapy in dogs with refractory atopic dermatitis: clinical efficacy and safety. *Vet. Rec.* 183:654. doi: 10.1136/vr.104867

Wang, L., Wang, L., Cong, X., Liu, G., Zhou, J., Bai, B., et al. (2013). Human umbilical cord mesenchymal stem cell therapy for patients with active rheumatoid arthritis: safety, and efficacy. *Stem Cells Dev.* 22, 3192–3202. doi: 10.1089/scd.2013.0023

Wang, X. L., and Lau, H. Y. A. (2006). Prostaglandin E2 potentiates the immunologically stimulated histamine release from human peripheral blood-derived mast cells through EP1/EP3 receptors. *Allergy* 61, 503–506. doi: 10.1111/j.1398-9995.2006.01043.x

Wei, X., Yang, X., Han, Z. P., Qu, F. F., Shao, L., and Shi, Y. F. (2013). Mesenchymal stem cells: a new trend for cell therapy. *Acta Pharmacol. Sin.* 34, 747–754. doi: 10.1038/aps.2013.50

Weidinger, S., and Novak, N. (2016). Atopic dermatitis. *Lancet* 387, 1109–1122. doi: 10.1016/S0140-6736(15)00149-X

Wobma, H. M., Kanai, M., Ma, S. P., Shih, Y., Li, H. W., Duran-Struuck, R., et al. (2018). Dual IFN-γ/hypoxia priming enhances immunosuppression of mesenchymal stromal cells through regulatory proteins and metabolic mechanisms. *J. Immunol. Regen. Med.* 1, 45–56. doi: 10.1016/j.regen.2018.01.001

Wong, I. T. Y., Tsuyuki, R. T., Cresswell-Melville, A., and Drucker, A. M. (2017). Guidelines for the management of atopic dermatitis (eczema) for pharmacists. *Can. Pharm. J.* 150, 285–297. doi: 10.1177/17151635177 10958

Zhao, L., Jin, H., She, R., Hu, Y., Xiao, C., Yu, Y., et al. (2006). A rodent model for allergic dermatitis induced by flea antigens. *Vet. Immunol. Immunopathol.* 114, 285–296. doi: 10.1016/j.vetimm.2006.08.016

Zheng, G., Huang, R., Qiu, G., Ge, M., Wang, J., Shu, Q., et al. (2018). Mesenchymal stromal cell-derived extracellular vesicles: regenerative and immunomodulatory effects and potential aplicattions in sepsis. *Cell Tissue Res.* 374, 1–15. doi: 10.1007/s00441-018-2871-5 doi: 10.1007/s00441-018-2871-5

Conflict of Interest: The authors declare that the research was conducted in the absence of any commercial or financial relationships that could be construed as a potential conflict of interest.

frontiers in Cell and Developmental Biology

MINI REVIEW
published: 19 May 2020
doi: 10.3389/fcell.2020.00316

Limited Potential or Unfavorable Manipulations? Strategies Toward Efficient Mesenchymal Stem/Stromal Cell Applications

Antonina Lavrentieva[1†], Andrea Hoffmann[2†] and Cornelia Lee-Thedieck[3†]*

[1] Institute of Technical Chemistry, Leibniz University Hannover, Hanover, Germany, [2] Department of Orthopaedic Surgery, Graded Implants and Regenerative Strategies, Hannover Medical School, Hanover, Germany, [3] Institute of Cell Biology and Biophysics, Leibniz University Hannover, Hanover, Germany

OPEN ACCESS

Edited by:
Marcela F. Bolontrade, Consejo Nacional de Investigaciones Científicas y Técnicas (CONICET), Argentina

Reviewed by:
Antonietta Rosa Silini, Fondazione Poliambulanza Istituto Ospedaliero, Italy
Marco Tatullo, University of Bari Medical School, Italy

***Correspondence:**
Cornelia Lee-Thedieck
lee-thedieck@cell.uni-hannover.de

[†] These authors have contributed equally to this work

Specialty section:
This article was submitted to Stem Cell Research, a section of the journal Frontiers in Cell and Developmental Biology

Received: 11 February 2020
Accepted: 09 April 2020
Published: 19 May 2020

Citation:
Lavrentieva A, Hoffmann A and Lee-Thedieck C (2020) Limited Potential or Unfavorable Manipulations? Strategies Toward Efficient Mesenchymal Stem/Stromal Cell Applications. Front. Cell Dev. Biol. 8:316. doi: 10.3389/fcell.2020.00316

Despite almost 50 years of research and over 20 years of preclinical and clinical studies, the question of curative potential of mesenchymal stem/stromal cells (MSCs) is still widely discussed in the scientific community. Non-reproducible treatment outcomes or even absence of treatment effects in comparison to control groups challenges the potential of these cells for routine application both in tissue engineering and in regenerative medicine. One of the reasons of such outcomes is non-standardized and often disadvantageous *ex vivo* manipulation of MSCs prior therapy. In most cases, clinically relevant cell numbers for MSC-based therapies can be only obtained by *in vitro* expansion of isolated cells. In this mini review, we will discuss point by point possible pitfalls in the production of human MSCs for cell therapies, without consideration of material-based applications. Starting with cell source, choice of donor and recipient, as well as isolation methods, we will then discuss existing expansion protocols (two-/three-dimensional cultivation, basal medium, medium supplements, static/dynamic conditions, and hypoxic/normoxic conditions) and influence of these strategies on the cell functionality after implantation. The role of potency assays will also be addressed. The final aim of this mini review is to illustrate the heterogeneity of current strategies for gaining MSCs for clinical applications with their strengths and weaknesses. Only a careful consideration and standardization of all pretreatment processes/methods for the different applications of MSCs will ensure robust and reproducible performance of these cell populations in the different experimental and clinical settings.

Keywords: mesenchymal stem/stromal cell, donor variability, expansion protocols, bioreactor, potency

INTRODUCTION

Mesenchymal stem/stromal cells (MSCs) have the capacity to differentiate into cells and tissues of one germ layer, here the mesodermal lineage, and are consequently multipotent. MSCs also secrete a variety of soluble factors and exosomes and, via contact with host cells, modulate functions of effector cells (Kabat et al., 2020). These features endow them with immunomodulatory, tissue-engrafting, cell-empowering (Najar et al., 2018), migratory, and homing properties. Despite a large history of research and use in clinical trials including some

successful and spectacular examples based on either their differentiating capacities (Horwitz et al., 1999; Horwitz et al., 2002) or their secretory properties (Le Blanc et al., 2004) and nicely summarized in a plethora of reviews (e.g., Ballini et al., 2018 or Kabat et al., 2020), the understanding of MSC biology, their mechanism of action (MoA) in different biological contexts, and their targeted and routine use in the clinics is limited (Hoogduijn and Lombardo, 2019). In this mini review, we propose a hexagon of steps to consider during selection, pretreatment, analysis, and application of MSCs in order to improve the transferability of promising preclinical results into clinical success (**Figure 1**). In the following, the six steps will be discussed in detail.

CELL SOURCE: ADULT TISSUES OR BIRTH-ASSOCIATED TISSUES

Bone marrow (BM) from animals was the protagonist tissue of origin in the 1960s when these cells were first identified (Friedenstein et al., 1968). Meanwhile, MSCs are isolated and expanded from a number of tissues from adult human donors (BM, adipose and dental tissue, muscle, and skin) and from birth-associated human tissues (placenta, amnion, Wharton jelly of the umbilical cord, or umbilical cord blood). Birth-associated tissues offer the advantage of non-invasive acquisition; the cells are in a developmentally early state and have higher immunosuppressive activity (Haase et al., 2009; Deuse et al., 2011; Hass et al., 2011). Despite similarities in morphology, immunophenotype with respect to selected cell surface antigens [while others depend on the tissue source (Lv et al., 2014)] and differentiation *in vitro*, MSCs sourced from distinct tissues may have a different developmental origin (Bosch et al., 2012) and do not necessarily have equivalent biological properties (Reinisch et al., 2015; Sacchetti et al., 2016). This is illustrated by several examples: (i) It was shown that MSC populations from different tissues differed widely in their *in vivo* differentiation potential and transcriptomic signature (Sacchetti et al., 2016). (ii) HLA class I expression was significantly reduced in human amnion MSCs compared to MSCs from BM until passage 6 (Pogozhykh et al., 2015). This indicates that the immunomodulatory and immunoevasive properties of MSCs (Ankrum et al., 2014) from different tissue sources may vary. (iii) Clinical studies using MSCs from BM were considered to be safe even with systemic application by infusion. However, because of the higher expression of tissue factor (also called CD142) on MSCs from adipose or birth-associated tissue compared to MSCs from BM, there is a notably increased risk for incompatibility with blood during intravascular application, caused by the instant blood-mediated inflammatory reaction (IBMIR). This leads to thrombotic complications and reduced engraftment (Moll et al., 2019). In summary, the intended mode of application (systemic or local, cell suspension, or mixed with a carrier system) and MoA of the cells (e. g differentiation into a desired cell type or secretion for immunomodulation) from different sources need to be carefully considered and compared for the choice of tissue source as indicated by forward and backward arrows in **Figure 2A**.

CHOICE OF DONOR AND RECIPIENT

Isolation and expansion of MSCs from human BM were reported in 1992, and in 1999, these cells were administered into human patients (Horwitz et al., 1999). Since that time, as well autologous as allogeneic applications have shown success, with most studies using allogeneic cells (Pittenger et al., 2019). Such allogeneic use is possible because MSCs are considered to be immune evasive (Ankrum et al., 2014). Autologous cells may be an attractive option, available even from perinatal tissue when cryostored—here, however, the system of cryobanks needs to be expanded (Bieback and Brinkmann, 2010; Brown et al., 2019; Kamal and Kassem, 2020). However, the prerequisite for use of autologous cells is that they are not affected by the disease to be treated or by comorbidities. Only an allogeneic setting offers the option to select for cell populations with particular properties (arrows in **Figure 2A**). This choice, however, also depends on the tissue source for cell retrieval. In a proinflammatory environment, the immunosuppressive activity of MSCs is affected with low doses of inflammatory cytokines inducing an immunostimulating phenotype but high doses inducing an immunosuppressive phenotype as demonstrated in a number of studies, e.g., reviewed in Najar et al. (2018). Consequently, the recipients/patients and their disease to be treated may become a decisive factor for success of MSC-based therapies (Martin et al., 2019). **Figure 2A** summarizes some important points.

ISOLATION METHODS

In the case of a fluid tissue such as BM, mononuclear cells are used directly or purified by density gradient centrifugation and plated at defined (clonal or non-clonal) or non-defined cell density. In the case of solid tissues, explant cultures or enzymatic digestion are used (Hoffmann et al., 2017). MSCs are subsequently identified as compact colonies containing spindle-shaped cells. The first passage is usually performed by detaching the cells with a protease once individual clones have reached a certain size as defined by the individual scientist. Although macrophages also grow in a plastic-adherent manner, they do not persist in the cultures as demonstrated by the absence of expression of antigens such as CD11b, CD13, and CD163 (e.g., Schack et al., 2013). Histological investigations with spatial resolution of tissue or single-cell analyses by flow cytometry revealed different subpopulations in different microanatomic sites, even for BM as a single tissue (Rasini et al., 2013) or resulted in isolation of selected subpopulations [CD271: (Kuci et al., 2013), STRO-1: (Shi and Gronthos, 2003)].

Multicolor lentiviral barcode labeling was applied to follow the clonal dynamics of *in vitro* MSC isolation and expansion from pieces of umbilical cord (Selich et al., 2016). MSCs migrating out of the tissue pieces during explant culture initially demonstrated

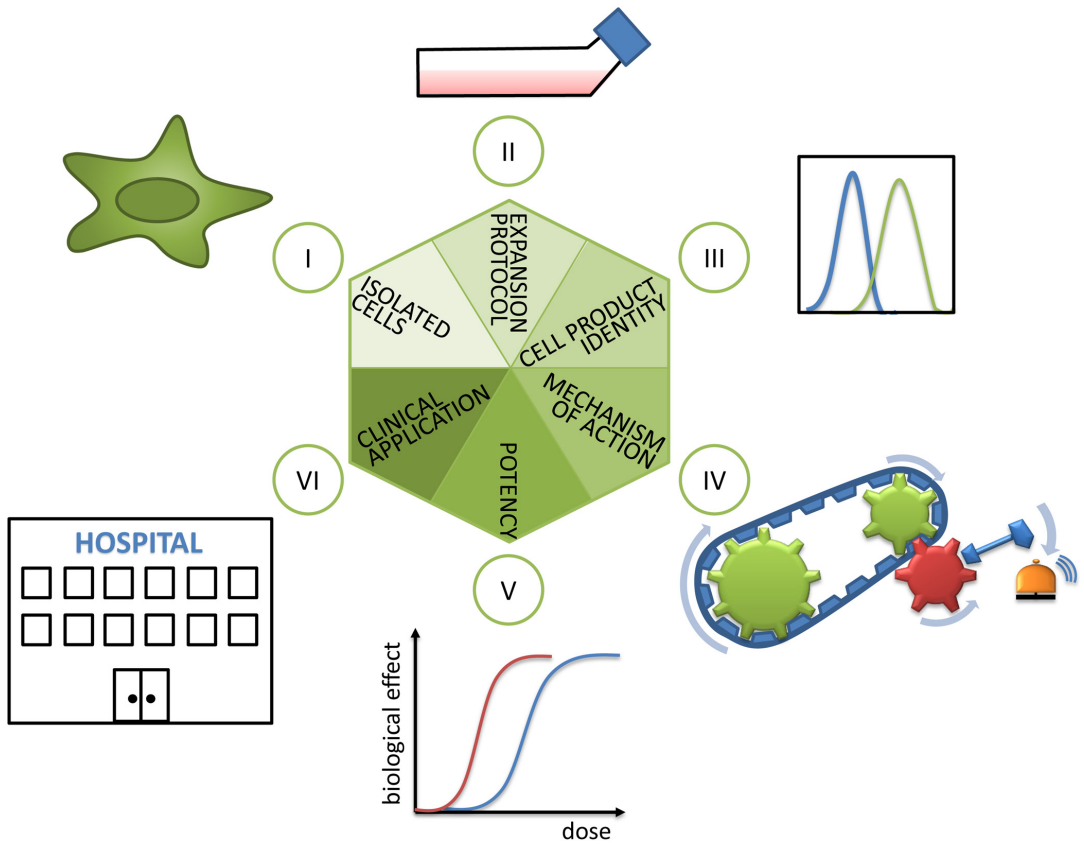

FIGURE 1 | Hexagon toward translating MSCs' promise into clinical reality. (I) As a first step, the isolated cells' identity has to be analyzed. Here, the cell source in terms of donor and tissue of origin, as well as population heterogeneity, plays an important role and is discussed in sections "Cell Source: Adult Tissues or Birth-Associated Tissues", "Choice of Donor and Recipient", "Isolation Methods", and "Biological Properties of MSCs *in vivo*". (II) The decisive role of expansion protocols and (III) cell product identity for preparing MSC products for clinical use are explained in section "Expansion Protocols and Culture Conditions". (IV) The importance of revealing mechanisms of action and (V) choice of valid potency assays or matrix of assays are detailed in section "Potency Assays". (VI) Finally, during clinical application the selection of recipients (reviewed in section "Choice of Donor and Recipient") and measurement of clinical effects have to be considered.

a highly complex mixture of different cell clones. However, with time, a massive reduction in abundance of clones was detected. This led to a preference for only few cell clones within few passages that are necessary to generate clinically relevant cell numbers. Also interesting, initiating novel MSC cultures from the same piece of tissue revealed the existence of more primitive cells as evidenced by a stronger secretion of cytokines after stimulation (Selich et al., 2019). It seems highly likely that similar observations would be found not only for MSCs isolated from solid tissues but also for MSCs from a fluid tissue as BM. Such clonality needs to be considered in the future development of refined cell isolation protocols (**Figure 2A**) as they may result, for example, from more research into the biological properties of these cells *in vivo*.

BIOLOGICAL PROPERTIES OF MSCs *in vivo*

The straightforward preparation of MSCs *in vitro* has enabled an incredible amount of studies. However, the *in vivo* identity and biology are less clear and less well characterized. Researchers identified CD146-positive cells in BM as adventitial reticular cells in the subendothelial layer of sinusoids (Sacchetti et al., 2007) and as the *in vivo* equivalent of *in vitro* MSCs. Self-renewing capacity of CD146-expressing cells as a characteristic of genuine stem cells was demonstrated by secondary passage (Sacchetti et al., 2007) and serial transplantation (Serafini et al., 2014). Independent results demonstrated that MSCs apparently can derive from pericytes ($CD34^{-}CD146^{+}$) and from adventitial cells ($CD34^{+}CD146^{-}$), and they termed them perivascular stromal/stem cells (Corselli et al., 2013). In September 2018, a consortium identified "the human skeletal stem cell" as a self-renewing, multipotent stem cell entity (Chan et al., 2018; Ambrosi et al., 2019). This cell was characterized by surface expression of podoplanin, CD73 (ecto-5'-nucleotidase), and CD164 (Endolyn). It is important to state that most of these studies avoided long-term *in vitro* expansion of their isolated cell populations. From these studies, the possibility emerges that there are several populations of "skeletal stem cells," which await further identification

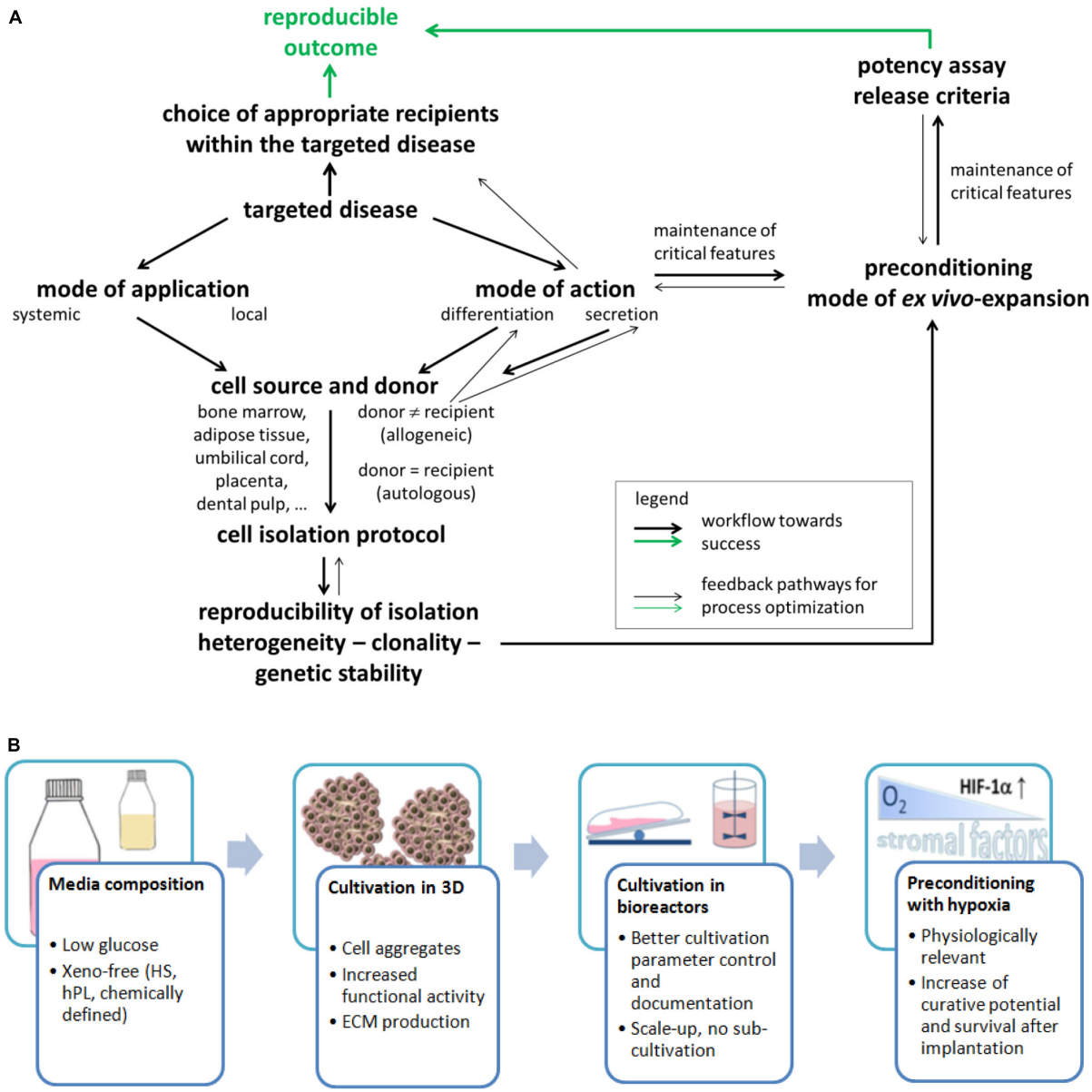

FIGURE 2 | (A) Flowchart of important stages for resolving the challenges on the way toward efficient MSC applications. This will need to consider several important issues that are depicted in the present figure. This will also need a constant reiterative optimization of different aspects compared to the current state of the art. Such a course of action will finally allow enhanced matching of *in vitro* and *in vivo* data and ultimately an enhanced translation of data from laboratory investigations into clinical practice through a reproducible and predictable outcome. **(B)** Important factors and expansion conditions to consider for improving the final MSC product quality.

and characterization, in particular with respect to their MoA and potency.

EXPANSION PROTOCOLS AND CULTURE CONDITIONS

Recent reviews on the clinical development of MSCs highlighted the importance of *ex vivo* MSCs' manipulation (Guadix et al., 2019; Mastrolia et al., 2019; Yuan et al., 2019). *Ex vivo* expansion and preconditioning are considered crucial for cell functionality after implantation. Because the MoA in the treatment of different diseases is not exactly known, it is important to maintain all possible initial MSC functions, including retention of all receptors (to receive external stimuli) and adhesion molecules (for migration, homing, and interaction with other cells), as well as production of cytokines, chemokines, growth factors, and extracellular vesicles (for stromal function). In the following, some factors and conditions that are considered to be important for the final cell product quality are reviewed (**Figure 2B**).

Media Composition: Basal Medium and Supplements

Although long-term (over 40 days) expansion has a negative impact on migration, differentiation, genetic stability, and proliferation of MSCs (Wagner et al., 2009; Hladik et al., 2019), rapid expansion does not guarantee the quality of the cell-based products. Application of high-glucose medium for expansion is considered to enable fast cell growth by the easy availability of glucose (Nuschke et al., 2016); however, glucose concentrations greater than 1 g/L also lead to cellular senescence (Zhang et al., 2017), including telomere shortening and genomic instability (Parsch et al., 2004). It was demonstrated for BM-MSCs that low-glucose Minimum Essential Medium Eagle Alpha Modification (1 g/L glucose) is the better medium choice compared to Dulbecco's Modified Eagle's Medium and Iscove's Modified Dulbecco's Media (Sotiropoulou et al., 2006). In many studies, MSCs were expanded using fetal calf serum (FCS), whereas nowadays the use of FCS for MSC expansion is not favored anymore, because besides the ethical issues of FCS production (collecting the serum from unborn calves), viral, mycoplasm, or prion infections can be transferred to the patient (Bieback, 2013; Jonsdottir-Buch et al., 2013; Hemeda et al., 2014; Mastrolia et al., 2019). Moreover, animal xenogenic compounds (proteins and polysaccharides) from FCS are internalized by the cells and can cause immune response after MSCs implantation, even if autologous cells were used (Spees et al., 2004). As an alternative, human serum or human platelet lysate can be used for MSCs' expansion (Mannello and Tonti, 2007; Bieback, 2013; Hemeda et al., 2014). Chemically defined xeno-free media could provide acceptable cell growth and elimination of the risk of carrying over pathogens (Spees et al., 2004), but the evaluation of functional characteristics of the cells cultivated in such media has to be improved (Lee et al., 2017).

Cultivation in Bioreactors

Traditionally, anchorage-dependent MSCs are expanded in static multiple planar T-flasks or multilayered flasks. Such "open systems" provide only a limited surface area and little control over cultivation parameters, are labor-intensive, and can lead to a high contamination risk and impaired cell function (Bunpetch et al., 2017; Mizukami and Swiech, 2018). In contrast, expansion in bioreactors ("closed systems") provides higher cell yield, full control, and documentation of cultivation parameters, as well as better spatial distribution of nutrients, pH, and oxygen (Bunpetch et al., 2017). Several bioreactor types are used for MSCs' expansion: rotating-bed bioreactors (Neumann et al., 2014), stirred tanks (Sart and Agathos, 2016; Mizukami et al., 2019), bag reactors (Das et al., 2019), hollow fiber (Mennan et al., 2019), and fixed bed reactors (Weber et al., 2010; Osiecki et al., 2015). In the case of stirred tanks or bags, anchorage-dependent MSCs are cultivated as aggregates or on microcarriers (Alimperti et al., 2014; de Soure et al., 2016).

Cultivation in Three-Dimensional Systems and Under Dynamic Conditions

A growing number of publications demonstrate that cultivation/expansion of MSCs in three-dimensional (3D) systems increases their functional activities in terms of angiogenic (Cheng et al., 2013), anti-inflammatory (Bartosh et al., 2010), and immunomodulatory (Noronha et al., 2019) properties. The most common method for 3D MSC cultivation are cell aggregates, generated by hanging drops, ultralow adhesion plates, centrifugation, and structured microwells (Bartosh et al., 2010; de Soure et al., 2016; Egger et al., 2018). To allow better nutrient transport, aggregated cells are then cultivated under dynamic conditions: agitation, stirring, or perfusion. It is important to note that cultivation in 3D aggregates allows MSC expansion in serum-free conditions (Alimperti et al., 2014).

Preconditioning With Hypoxia

Several preconditioning strategies (also called "priming") were developed for MSCs (Hu and Li, 2018; Noronha et al., 2019; Castilla-Casadiego et al., 2020). These strategies include the use of pharmacological or chemical substances, small molecules, cytokines, physical factors, biomaterials, and hypoxia. Here, we focus on priming with hypoxia as it represents a complex, multilevel, and physiologically relevant strategy. Preconditioning of MSCs in hypoxia triggers (via the stabilization of Hypoxia Inducible Factor (HIF)-1α and other adaptation mechanisms) an upregulation of various functions and does not only help MSCs to survive after implantation, but also increases their curative/stromal potential. Exact details of hypoxic treatment protocols are still under discussion: oxygen concentration, duration of preconditioning, MSCs' isolation under hypoxia, and reoxygenation. Oxygen concentration (1–5% O_2) should be low enough to trigger adaptation, but not too low as to cause apoptosis (El-Badawy et al., 2016). Serum deprivation should be avoided during hypoxic conditions, because it also leads to apoptosis (Chen et al., 2018). MSCs isolated from different sources demonstrated higher proliferation and migration rates, metabolic activity, cytokine, and receptor expression, as well as improved immunomodulatory properties and genetic stability under hypoxia (Lavrentieva et al., 2010; Estrada et al., 2012; Haque et al., 2013; Jiang et al., 2015; Choi et al., 2017; Fabian, 2019). Of note, hypoxic conditions should be preferred over using hypoxia-mimicking reagents (e.g., HIF stabilizers), because true hypoxic preconditioning can lead to the involvement of unknown, additional mechanisms beyond the HIF pathways (Pugh and Ratcliffe, 2017; Chakraborty et al., 2019).

POTENCY ASSAYS

While preclinical data on the efficacy of MSCs to treat pathological conditions are promising, translating this into clinical success is not straightforward. The cellular heterogeneity that is, on the one hand, an intrinsic property of cell communities—even in genetically identical cell populations (Wilson et al., 2019)—and on the other hand in case of clinically applied MSCs caused by the factors and parameters discussed above, might be one of the major reasons for the observed discrepancy in MSC efficacy (Galipeau and Sensebe, 2018). Despite these heterogeneities, how can we ensure that preclinical results hold true in clinical studies? The regulatory authorities reply to this question with the demand for potency assays.

The European Medicines Agency EMA defines potency as "the measure of the biological activity using a suitably quantitative biological assay (also called potency assay or bioassay), based on the attribute of the product, which is linked to the relevant biological properties" (European Medicines Agency [EMA], 1999). Furthermore, "A correlation between the expected clinical response and the activity in the biological assay should be established in pharmacodynamic or clinical studies" (European Medicines Agency [EMA], 1999). In other words, potency assays measure the biological activity of a cellular product to ensure its intended function at a specific dose. Thus, the assay is meant to guarantee the comparability of different cellular products and of different lots of one product (Hematti, 2016).

The first prerequisite for defining a valid potency assay is to know the pathophysiology of the disease to be treated with MSCs and to know the MoA by which they exert their effects. The MoA of MSCs is highly dependent on the disease and microenvironmental tissue context in which they are applied. In most cases, the MoA of MSCs is complex involving not only direct but also indirect effects, e.g., via nearby cells. Roughly, the presumed MoA of MSCs can be subdivided into effects related to their following properties: (i) differentiation capacity, (ii) ability to engraft, and (iii) release of paracrine signals (Salvadori et al., 2019). Which capacity contributes to the potency of MSCs in different diseases to which extent is yet to be determined. The situation is further complicated by the phenomena of IBMIR (Moll et al., 2019) and efferocytosis (Galipeau and Sensebe, 2018).

The MoA is the link that is needed for the causal correlation of potency assays that measure a biological activity to the intended clinical response. In some diseases, the MoA might be traced back to one primary activity of MSCs. However, in most cases, MSCs' action is a complex network of direct and indirect effects, and following only one effector pathway might lead to misinterpretable results. Therefore, the International Society for Cellular Therapy recommended developing matrix assay approaches that can cover the multiplicity of pathways involved in the MoA for a certain application (Galipeau et al., 2016). Wide and/or targeted OMICs approaches, particularly transcriptomic and metabolomic analyses, help identifying crucial factors in these networks that can be used as targets in the development of potency assays for MSCs in different diseases (Chinnadurai et al., 2018). Single-cell RNAseq of MSCs (Freeman et al., 2015) even opens the avenue for finding such targets in stemness-related effects that are transmitted by the small fraction of stem cells in the applied MSC populations.

In all cases, where the exact MoA is not fully solved, the dilemma of defining valid potency assays can only be solved by analyzing fundamentally and in detail which cells within the applied MSC population exert which effects in which way.

CONCLUSION

In this mini review, we highlight some important points in the hexagon of steps (**Figure 1**) that are necessary to translate the promising results obtained with MSCs *in vitro* into successful cellular therapies. This includes as a first step ensuring the isolated cells' identity, which is influenced by selection of donors and tissue sources as well as MSC population heterogeneity. In the next steps, optimized and standardized expansion protocols as well as guaranteed quality and identity of the produced cells are essential. At the same time, often unknown MoAs and choosing valid potency assays are currently major challenges in this regard. During the last step—clinical application—the choice of recipients is one decisive parameter. Making informed choices in each of these steps will contribute to improved matching of *in vitro* and *in vivo* data and ultimately an enhanced translation of data from laboratory investigations into clinical practice (**Figure 2A**).

AUTHOR CONTRIBUTIONS

All authors contributed equally to the conception, writing, and editing of the manuscript.

FUNDING

This work has been carried out within the framework of the SMART BIOTECS alliance between the Technische Universität Braunschweig and the Leibniz Universität Hannover. This initiative is supported by the Ministry of Science and Culture (MWK) of Lower Saxony, Germany. CL-T has received funding from the European Research Council (ERC) under the European Union's Horizon 2020 Research and Innovation Programme (Grant Agreement No. 757490). AL research is supported by German Research Foundation (DFG Project 398007461 488 "3D Dual-Gradient Systems for Functional Cell Screening"). AH acknowledges funding by the German Research Foundation with the research unit FOR 2180 "Graded Implants for Tendon-Bone Junctions." The publication of this article was funded by the Open Access Fund of the Leibniz Universität Hannover.

REFERENCES

Alimperti, S., Lei, P., Wen, Y., Tian, J., Campbell, A. M., and Andreadis, S. T. (2014). Serum-free spheroid suspension culture maintains mesenchymal stem cell proliferation and differentiation potential. *Biotechnol. Prog.* 30, 974–983. doi: 10.1002/btpr.1904

Ambrosi, T. H., Longaker, M. T., and Chan, C. K. F. (2019). A revised perspective of skeletal stem cell biology. *Front. Cell Dev. Biol.* 7:189. doi: 10.3389/fcell.2019.00189

Ankrum, J. A., Ong, J. F., and Karp, J. M. (2014). Mesenchymal stem cells: immune evasive, not immune privileged. *Nat. Biotechnol.* 32, 252–260. doi: 10.1038/nbt.2816

Ballini, A., Cantore, S., Scacco, S., Coletti, D., and Tatullo, M. (2018). Mesenchymal stem cells as promoters, enhancers, and playmakers of the translational regenerative medicine 2018. *Stem Cells Int.* 2018, 6927401. doi: 10.1155/2018/6927401

Bartosh, T. J., Ylostalo, J. H., Mohammadipoor, A., Bazhanov, N., Coble, K., Claypool, K., et al. (2010). Aggregation of human mesenchymal stromal cells

(MSCs) into 3D spheroids enhances their antiinflammatory properties. *Proc. Natl. Acad. Sci. U.S.A.* 107, 13724–13729. doi: 10.1073/pnas.1008117107

Bieback, K. (2013). Platelet lysate as replacement for fetal bovine serum in mesenchymal stromal cell cultures. *Transfus Med. Hemother.* 40, 326–335. doi: 10.1159/000354061

Bieback, K., and Brinkmann, I. (2010). Mesenchymal stromal cells from human perinatal tissues: from biology to cell therapy. *World J. Stem Cells* 2, 81–92. doi: 10.4252/wjsc.v2.i4.81

Bosch, J., Houben, A. P., Radke, T. F., Stapelkamp, D., Bunemann, E., Balan, P., et al. (2012). Distinct differentiation potential of "MSC" derived from cord blood and umbilical cord: are cord-derived cells true mesenchymal stromal cells? *Stem Cells Dev.* 21, 1977–1988. doi: 10.1089/scd.2011.0414

Brown, K. S., Rao, M. S., and Brown, H. L. (2019). The future state of newborn stem cell banking. *J. Clin. Med.* 8:117. doi: 10.3390/jcm8010117

Bunpetch, V., Wu, H., Zhang, S., and Ouyang, H. (2017). From "Bench to Bedside": current advancement on large-scale production of mesenchymal stem cells. *Stem Cells Dev.* 26, 1662–1673. doi: 10.1089/scd.2017.0104

Castilla-Casadiego, D. A., Reyes-Ramos, A. M., Domenech, M., and Almodovar, J. (2020). Effects of physical, chemical, and biological stimulus on h-MSC expansion and their functional characteristics. *Ann. Biomed. Eng.* 48, 519–535. doi: 10.1007/s10439-019-02400-3

Chakraborty, A. A., Laukka, T., Myllykoski, M., Ringel, A. E., Booker, M. A., Tolstorukov, M. Y., et al. (2019). Histone demethylase KDM6A directly senses oxygen to control chromatin and cell fate. *Science* 363, 1217–1222. doi: 10.1126/science.aaw1026

Chan, C. K. F., Gulati, G. S., Sinha, R., Tompkins, J. V., Lopez, M., Carter, A. C., et al. (2018*). Identification of the human skeletal stem cell. *Cell* 175, 43.e21–56.e21. doi: 10.1016/j.cell.2018.07.029

Chen, T., Zhu, H., Wang, Y., Zhao, P., Chen, J., Sun, J., et al. (2018). Apoptosis of bone marrow mesenchymal stromal/stem cells via the MAPK and endoplasmic reticulum stress signaling pathways. *Am. J. Transl .Res.* 10, 2555–2566.

Cheng, N. C., Chen, S. Y., Li, J. R., and Young, T. H. (2013). Short-term spheroid formation enhances the regenerative capacity of adipose-derived stem cells by promoting stemness, angiogenesis, and chemotaxis. *Stem. Cells Transl. Med.* 2, 584–594. doi: 10.5966/sctm.2013-0007

Chinnadurai, R., Rajan, D., Qayed, M., Arafat, D., Garcia, M., Liu, Y., et al. (2018). Potency analysis of mesenchymal stromal cells using a combinatorial assay matrix approach. *Cell Rep.* 22, 2504–2517. doi: 10.1016/j.celrep.2018.02.013

Choi, J. R., Yong, K. W., and Wan Safwani, W. K. Z. (2017). Effect of hypoxia on human adipose-derived mesenchymal stem cells and its potential clinical applications. *Cell Mol. Life Sci.* 74, 2587–2600. doi: 10.1007/s00018-017-2484-2

Corselli, M., Crisan, M., Murray, I. R., West, C. C., Scholes, J., Codrea, F., et al. (2013). Identification of perivascular mesenchymal stromal/stem cells by flow cytometry. *Cytometry A* 83, 714–720. doi: 10.1002/cyto.a.22313

Das, R., Roosloot, R., Van Pel, M., Schepers, K., Driessen, M., Fibbe, W. E., et al. (2019). Preparing for cell culture scale-out: establishing parity of bioreactor- and flask-expanded mesenchymal stromal cell cultures. *J. Transl. Med.* 17:241. doi: 10.1186/s12967-019-1989-x

de Soure, A. M., Fernandes-Platzgummer, A., Da Silva, C. L., and Cabral, J. M. (2016). Scalable microcarrier-based manufacturing of mesenchymal stem/stromal cells. *J. Biotechnol.* 236, 88–109. doi: 10.1016/j.jbiotec.2016.08.007

Deuse, T., Stubbendorff, M., Tang-Quan, K., Phillips, N., Kay, M. A., Eiermann, T., et al. (2011). Immunogenicity and immunomodulatory properties of umbilical cord lining mesenchymal stem cells. *Cell Transplant* 20, 655–667. doi: 10.3727/096368910X536473

Egger, D., Tripisciano, C., Weber, V., Dominici, M., and Kasper, C. (2018). Dynamic cultivation of mesenchymal stem cell aggregates. *Bioengineering* 5:48. doi: 10.3390/bioengineering5020048

El-Badawy, A., Amer, M., Abdelbaset, R., Sherif, S. N., Abo-Elela, M., Ghallab, Y. H., et al. (2016). Adipose stem cells display higher regenerative capacities and more adaptable electro-kinetic properties compared to bone marrow-derived mesenchymal stromal cells. *Sci. Rep.* 6:7801. doi: 10.1038/srep37801

Estrada, J. C., Albo, C., Benguria, A., Dopazo, A., Lopez-Romero, P., Carrera-Quintanar, L., et al. (2012). Culture of human mesenchymal stem cells at low oxygen tension improves growth and genetic stability by activating glycolysis. *Cell Death Differ.* 19, 743–755. doi: 10.1038/cdd.2011.172

European Medicines Agency [EMA] (1999). *Biotechnological/Biological Products*. Available: https://www.ema.europa.eu/en/documents/scientific-guideline/ich-q-6-b-test-procedures-acceptance-criteria-biotechnological/biological-products-step-5_en.pdf (accessed 2020/01/15 2020).

Fabian, Z. (2019). The effects of hypoxia on the immune-modulatory properties of bone marrow-derived mesenchymal stromal cells. *Stem Cells Int.* 2019:2509606. doi: 10.1155/2019/2509606

Freeman, B. T., Jung, J. P., and Ogle, B. M. (2015). Single-cell RNA-seq of bone marrow-derived mesenchymal stem cells reveals unique profiles of lineage priming. *PLoS One* 10:e0136199. doi: 10.1371/journal.pone.0136199

Friedenstein, A. J., Petrakova, K. V., Kurolesova, A. I., and Frolova, G. P. (1968). Heterotopic of bone marrow. Analysis of precursor cells for osteogenic and hematopoietic tissues. *Transplantation* 6, 230–247.

Galipeau, J., Krampera, M., Barrett, J., Dazzi, F., Deans, R. J., Debruijn, J., et al. (2016). International society for cellular therapy perspective on immune functional assays for mesenchymal stromal cells as potency release criterion for advanced phase clinical trials. *Cytotherapy* 18, 151–159. doi: 10.1016/j.jcyt.2015.11.008

Galipeau, J., and Sensebe, L. (2018). Mesenchymal stromal cells: clinical challenges and therapeutic opportunities. *Cell Stem Cell* 22, 824–833. doi: 10.1016/j.stem.2018.05.004

Guadix, J. A., Lopez-Beas, J., Clares, B., Soriano-Ruiz, J. L., Zugaza, J. L., and Galvez-Martin, P. (2019). Principal criteria for evaluating the quality, safety and efficacy of hMSC-based products in clinical practice: current approaches and challenges. *Pharmaceutics* 11, 552. doi: 10.3390/pharmaceutics11110552

Haase, A., Olmer, R., Schwanke, K., Wunderlich, S., Merkert, S., Hess, C., et al. (2009). Generation of induced pluripotent stem cells from human cord blood. *Cell Stem Cell* 5, 434–441. doi: 10.1016/j.stem.2009.08.021

Haque, N., Rahman, M. T., Abu Kasim, N. H., and Alabsi, A. M. (2013). Hypoxic culture conditions as a solution for mesenchymal stem cell based regenerative therapy. *Sci. World J.* 2013:632972. doi: 10.1155/2013/632972

Hass, R., Kasper, C., Bohm, S., and Jacobs, R. (2011). Different populations and sources of human mesenchymal stem cells (MSC): a comparison of adult and neonatal tissue-derived MSC. *Cell Commun. Signal.* 9:12. doi: 10.1186/1478-811X-9-12

Hematti, P. (2016). Characterization of mesenchymal stromal cells: potency assay development. *Transfusion* 56, 32S–35S. doi: 10.1111/trf.13569

Hemeda, H., Giebel, B., and Wagner, W. (2014). Evaluation of human platelet lysate versus fetal bovine serum for culture of mesenchymal stromal cells. *Cytotherapy* 16, 170–180. doi: 10.1016/j.jcyt.2013.11.004

Hladik, D., Hofig, I., Oestreicher, U., Beckers, J., Matjanovski, M., Bao, X., et al. (2019). Long-term culture of mesenchymal stem cells impairs ATM-dependent recognition of DNA breaks and increases genetic instability. *Stem Cell Res. Ther.* 10, 218. doi: 10.1186/s13287-019-1334-6

Hoffmann, A., Floerkemeier, T., Melzer, C., and Hass, R. (2017). Comparison of in vitro-cultivation of human mesenchymal stroma/stem cells derived from bone marrow and umbilical cord. *J. Tissue Eng. Regen. Med.* 11, 2565–2581. doi: 10.1002/term.2153

Hoogduijn, M. J., and Lombardo, E. (2019). Mesenchymal stromal cells anno 2019: dawn of the therapeutic era? concise review. *Stem Cells Transl. Med.* 8, 1126–1134. doi: 10.1002/sctm.19-0073

Horwitz, E. M., Gordon, P. L., Koo, W. K., Marx, J. C., Neel, M. D., Mcnall, R. Y., et al. (2002). Isolated allogeneic bone marrow-derived mesenchymal cells engraft and stimulate growth in children with osteogenesis imperfecta: implications for cell therapy of bone. *Proc. Natl. Acad. Sci. U.S.A.* 99, 8932–8937. doi: 10.1073/pnas.132252399

Horwitz, E. M., Prockop, D. J., Fitzpatrick, L. A., Koo, W. W., Gordon, P. L., Neel, M., et al. (1999). Transplantability and therapeutic effects of bone marrow-derived mesenchymal cells in children with osteogenesis imperfecta. *Nat. Med.* 5, 309–313. doi: 10.1038/6529

Hu, C., and Li, L. (2018). Preconditioning influences mesenchymal stem cell properties in vitro and in vivo. *J. Cell Mol. Med.* 22, 1428–1442. doi: 10.1111/jcmm.13492

Jiang, C. M., Liu, J., Zhao, J. Y., Xiao, L., An, S., Gou, Y. C., et al. (2015). Effects of hypoxia on the immunomodulatory properties of human gingiva-derived mesenchymal stem cells. *J. Dent Res.* 94, 69–77. doi: 10.1177/0022034514557671

Jonsdottir-Buch, S. M., Lieder, R., and Sigurjonsson, O. E. (2013). Platelet lysates produced from expired platelet concentrates support growth and osteogenic

differentiation of mesenchymal stem cells. *PLoS One* 8:e68984. doi: 10.1371/journal.pone.0068984

Kabat, M., Bobkov, I., Kumar, S., and Grumet, M. (2020). Trends in mesenchymal stem cell clinical trials 2004-2018: is efficacy optimal in a narrow dose range? *Stem Cells Transl. Med.* 9, 17–27. doi: 10.1002/sctm.19-0202

Kamal, M. M., and Kassem, D. H. (2020). Therapeutic potential of wharton's jelly mesenchymal stem cells for diabetes: achievements and challenges. *Front. Cell Dev. Biol.* 8:16. doi: 10.3389/fcell.2020.00016

Kuci, Z., Seiberth, J., Latifi-Pupovci, H., Wehner, S., Stein, S., Grez, M., et al. (2013). Clonal analysis of multipotent stromal cells derived from CD271+ bone marrow mononuclear cells: functional heterogeneity and different mechanisms of allosuppression. *Haematologica* 98, 1609–1616. doi: 10.3324/haematol.2013.092700

Lavrentieva, A., Majore, I., Kasper, C., and Hass, R. (2010). Effects of hypoxic culture conditions on umbilical cord-derived human mesenchymal stem cells. *Cell Commun. Signal.* 8:8. doi: 10.1186/1478-811X-8-18

Le Blanc, K., Rasmusson, I., Sundberg, B., Gotherstrom, C., Hassan, M., Uzunel, M., et al. (2004). Treatment of severe acute graft-versus-host disease with third party haploidentical mesenchymal stem cells. *Lancet* 363, 1439–1441. doi: 10.1016/S0140-6736(04)16104-7

Lee, M. S., Youn, C., Kim, J. H., Park, B. J., Ahn, J., Hong, S., et al. (2017). Enhanced Cell Growth of adipocyte-derived mesenchymal stem cells using chemically-defined serum-free media. *Int. J. Mol. Sci.* 18:779. doi: 10.3390/ijms18081779

Lv, F. J., Tuan, R. S., Cheung, K. M., and Leung, V. Y. (2014). Concise review: the surface markers and identity of human mesenchymal stem cells. *Stem Cells* 32, 1408–1419. doi: 10.1002/stem.1681

Mannello, F., and Tonti, G. A. (2007). Concise review: no breakthroughs for human mesenchymal and embryonic stem cell culture: conditioned medium, feeder layer, or feeder-free; medium with fetal calf serum, human serum, or enriched plasma; serum-free, serum replacement nonconditioned medium, or ad hoc formula? All that glitters is not gold! *Stem Cells* 25, 1603–1609. doi: 10.1634/stemcells.2007-0127

Martin, I., Galipeau, J., Kessler, C., Le Blanc, K., and Dazzi, F. (2019). Challenges for mesenchymal stromal cell therapies. *Sci. Transl. Med.* 11:eaat2189. doi: 10.1126/scitranslmed.aat2189

Mastrolia, I., Foppiani, E. M., Murgia, A., Candini, O., Samarelli, A. V., Grisendi, G., et al. (2019). Challenges in clinical development of mesenchymal stromal/stem cells: concise review. *Stem Cell Transl. Med.* 8, 1135–1148. doi: 10.1002/sctm.19-0044

Mennan, C., Garcia, J., Roberts, S., Hulme, C., and Wright, K. (2019). A comprehensive characterisation of large-scale expanded human bone marrow and umbilical cord mesenchymal stem cells. *Stem Cell Res. Ther.* 10:99. doi: 10.1186/s13287-019-1202-4

Mizukami, A., and Swiech, K. (2018). Mesenchymal stromal cells: from discovery to manufacturing and commercialization. *Stem Cell Int.* 2018:4083921. doi: 10.1155/2018/4083921

Mizukami, A., Thome, C. H., Ferreira, G. A., Lanfredi, G. P., Covas, D. T., Pitteri, S. J., et al. (2019). Proteomic identification and time-course monitoring of secreted proteins during expansion of human mesenchymal stem/stromal in stirred-tank bioreactor. *Front. Bioeng. Biotechnol.* 7:154. doi: 10.3389/fbioe.2019.00154

Moll, G., Ankrum, J. A., Kamhieh-Milz, J., Bieback, K., Ringden, O., Volk, H. D., et al. (2019). Intravascular mesenchymal stromal/stem cell therapy product diversification: time for new clinical guidelines. *Trends Mol. Med.* 25, 149–163. doi: 10.1016/j.molmed.2018.12.006

Najar, M., Krayem, M., Merimi, M., Burny, A., Meuleman, N., Bron, D., et al. (2018). Insights into inflammatory priming of mesenchymal stromal cells: functional biological impacts. *Inflamm. Res.* 67, 467–477. doi: 10.1007/s00011-018-1131-1

Neumann, A., Lavrentieva, A., Heilkenbrinker, A., Loenne, M., and Kasper, C. (2014). Characterization and application of a disposable rotating bed bioreactor for mesenchymal stem cell expansion. *Bioengineering* 1, 231–245. doi: 10.3390/bioengineering1040231

Noronha, N. C., Mizukami, A., Caliari-Oliveira, C., Cominal, J. G., Rocha, J. L. M., Covas, D. T., et al. (2019). Priming approaches to improve the efficacy of mesenchymal stromal cell-based therapies. *Stem Cell Res. Ther.* 10:131. doi: 10.1186/s13287-019-1224-y

Nuschke, A., Rodrigues, M., Wells, A. W., Sylakowski, K., and Wells, A. (2016). Mesenchymal stem cells/multipotent stromal cells (MSCs) are glycolytic and thus glucose is a limiting factor of in vitro models of MSC starvation. *Stem Cell Res. Ther.* 7:179. doi: 10.1186/s13287-016-0436-7

Osiecki, M. J., Michl, T. D., Kul Babur, B., Kabiri, M., Atkinson, K., Lott, W. B., et al. (2015). Packed bed bioreactor for the isolation and expansion of placental-derived mesenchymal stromal cells. *PLoS One* 10:e0144941. doi: 10.1371/journal.pone.0144941

Parsch, D., Fellenberg, J., Brummendorf, T. H., Eschlbeck, A. M., and Richter, W. (2004). Telomere length and telomerase activity during expansion and differentiation of human mesenchymal stem cells and chondrocytes. *J. Mol. Med.* 82, 49–55. doi: 10.1007/s00109-003-0506-z

Pittenger, M. F., Discher, D. E., Peault, B. M., Phinney, D. G., Hare, J. M., and Caplan, A. I. (2019). Mesenchymal stem cell perspective: cell biology to clinical progress. *NPJ Regen. Med.* 4:22. doi: 10.1038/s41536-019-0083-6

Pogozhykh, O., Pogozhykh, D., Neehus, A. L., Hoffmann, A., Blasczyk, R., and Muller, T. (2015). Molecular and cellular characteristics of human and non-human primate multipotent stromal cells from the amnion and bone marrow during long term culture. *Stem Cell Res. Ther.* 6:150. doi: 10.1186/s13287-015-0146-6

Pugh, C. W., and Ratcliffe, P. J. (2017). New horizons in hypoxia signaling pathways. *Exp. Cell Res.* 356, 116–121. doi: 10.1016/j.yexcr.2017.03.008

Rasini, V., Dominici, M., Kluba, T., Siegel, G., Lusenti, G., Northoff, H., et al. (2013). Mesenchymal stromal/stem cells markers in the human bone marrow. *Cytotherapy* 15, 292–306. doi: 10.1016/j.jcyt.2012.11.009

Reinisch, A., Etchart, N., Thomas, D., Hofmann, N. A., Fruehwirth, M., Sinha, S., et al. (2015). Epigenetic and in vivo comparison of diverse MSC sources reveals an endochondral signature for human hematopoietic niche formation. *Blood* 125, 249–260. doi: 10.1182/blood-2014-04-572255

Sacchetti, B., Funari, A., Michienzi, S., Di Cesare, S., Piersanti, S., Saggio, I., et al. (2007). Self-renewing osteoprogenitors in bone marrow sinusoids can organize a hematopoietic microenvironment. *Cell* 131, 324–336. doi: 10.1016/j.cell.2007.08.025

Sacchetti, B., Funari, A., Remoli, C., Giannicola, G., Kogler, G., Liedtke, S., et al. (2016). No Identical "Mesenchymal Stem Cells" at different times and sites: human committed progenitors of distinct origin and differentiation potential are incorporated as adventitial cells in microvessels. *Stem Cell Rep.* 6, 897–913. doi: 10.1016/j.stemcr.2016.05.011

Salvadori, M., Cesari, N., Murgia, A., Puccini, P., Riccardi, B., and Dominici, M. (2019). Dissecting the pharmacodynamics and pharmacokinetics of MSCs to overcome limitations in their clinical translation. *Mol. Ther. Methods Clin. Dev.* 14, 1–15. doi: 10.1016/j.omtm.2019.05.004

Sart, S., and Agathos, S. N. (2016). Large-scale expansion and differentiation of mesenchymal stem cells in microcarrier-based stirred bioreactors. *Methods Mol. Biol.* 1502, 87–102. doi: 10.1007/7651_2015_314

Schack, L. M., Noack, S., Weist, R., Jagodzinski, M., Krettek, C., Buettner, M., et al. (2013). Analysis of surface protein expression in human bone marrow stromal cells: new aspects of culture-induced changes, inter-donor differences and intracellular expression. *Stem Cell Dev.* 22, 3226–3235. doi: 10.1089/scd.2013.0290

Selich, A., Daudert, J., Hass, R., Philipp, F., Von Kaisenberg, C., Paul, G., et al. (2016). Massive clonal selection and transiently contributing clones during expansion of mesenchymal stem cell cultures revealed by lentiviral RGB-barcode technology. *Stem Cells Transl. Med.* 5, 591–601. doi: 10.5966/sctm.2015-0176

Selich, A., Zimmermann, K., Tenspolde, M., Dittrich-Breiholz, O., Von Kaisenberg, C., Schambach, A., et al. (2019). Umbilical cord as a long-term source of activatable mesenchymal stromal cells for immunomodulation. *Stem Cell Res. Ther.* 10:285. doi: 10.1186/s13287-019-1376-9

Serafini, M., Sacchetti, B., Pievani, A., Redaelli, D., Remoli, C., Biondi, A., et al. (2014). Establishment of bone marrow and hematopoietic niches in vivo by reversion of chondrocyte differentiation of human bone marrow stromal cells. *Stem Cell Res.* 12, 659–672. doi: 10.1016/j.scr.2014.01.006

Shi, S., and Gronthos, S. (2003). Perivascular niche of postnatal mesenchymal stem cells in human bone marrow and dental pulp. *J. Bone Miner Res.* 18, 696–704. doi: 10.1359/jbmr.2003.18.4.696

Sotiropoulou, P. A., Perez, S. A., Salagianni, M., Baxevanis, C. N., and Papamichail, M. (2006). Characterization of the optimal culture conditions for clinical scale

production of human mesenchymal stem cells. *Stem Cells* 24, 462–471. doi: 10.1634/stemcells.2004-0331

Spees, J. L., Gregory, C. A., Singh, H., Tucker, H. A., Peister, A., Lynch, P. J., et al. (2004). Internalized antigens must be removed to prepare hypoimmunogenic mesenchymal stem cells for cell and gene therapy. *Mol. Ther.* 9, 747–756. doi: 10.1016/j.ymthe.2004.02.012

Wagner, W., Bork, S., Horn, P., Krunic, D., Walenda, T., Diehlmann, A., et al. (2009). Aging and replicative senescence have related effects on human stem and progenitor cells. *PLoS One* 4:e5846. doi: 10.1371/journal.pone.0005846

Weber, C., Freimark, D., Portner, R., Pino-Grace, P., Pohl, S., Wallrapp, C., et al. (2010). Expansion of human mesenchymal stem cells in a fixed-bed bioreactor system based on non-porous glass carrier–part A: inoculation, cultivation, and cell harvest procedures. *Int. J. Artif. Organs* 33, 512–525. doi: 10.1177/039139881003300802

Wilson, A., Webster, A., and Genever, P. (2019). Nomenclature and heterogeneity: consequences for the use of mesenchymal stem cells in regenerative medicine. *Regen. Med.* 14, 595–611. doi: 10.2217/rme-2018-0145

Yuan, X., Logan, T. M., and Ma, T. (2019). Metabolism in human mesenchymal stromal cells: a missing link between hmsc biomanufacturing and therapy? *Front. Immunol.* 10:977. doi: 10.3389/fimmu.2019.00977

Zhang, D., Lu, H., Chen, Z., Wang, Y., Lin, J., Xu, S., et al. (2017). High glucose induces the aging of mesenchymal stem cells via Akt/mTOR signaling. *Mol. Med. Rep.* 16, 1685–1690. doi: 10.3892/mmr.2017.6832

Conflict of Interest: The authors declare that the research was conducted in the absence of any commercial or financial relationships that could be construed as a potential conflict of interest.

frontiers in Cell and Developmental Biology

ORIGINAL RESEARCH
published: 09 June 2020
doi: 10.3389/fcell.2020.00387

Pro-angiogenic Activity Discriminates Human Adipose-Derived Stromal Cells From Retinal Pericytes: Considerations for Cell-Based Therapy of Diabetic Retinopathy

Heiner Kremer[1,2†], Julian Gebauer[1,2†], Susanne Elvers-Hornung[1,2], Stefanie Uhlig[1,2,3], Hans-Peter Hammes[4], Elena Beltramo[5], Lothar Steeb[6], Martin C. Harmsen[7], Carsten Sticht[8], Harald Klueter[1,2,9], Karen Bieback[1,2,3,9,10†] and Agnese Fiori[1,2,10†]*

[1] Institute of Transfusion Medicine and Immunology, Medical Faculty Mannheim, Heidelberg University, Mannheim, Germany, [2] German Red Cross Blood Donation Service Baden-Württemberg – Hessen, Mannheim, Germany, [3] FlowCore Mannheim, Medical Faculty Mannheim, Heidelberg University, Mannheim, Germany, [4] 5th Medical Department, Medical Faculty Mannheim, Heidelberg University, Mannheim, Germany, [5] Department of Medical Sciences, University of Turin, Turin, Italy, [6] PeloBiotech GmbH, Martinsried, Germany, [7] Department of Pathology and Medical Biology, University Medical Center Groningen, University of Groningen, Groningen, Netherlands, [8] Center for Medical Research, Medical Faculty Mannheim, Heidelberg University, Mannheim, Germany, [9] Mannheim Institute for Innate Immunoscience, Medical Faculty Mannheim, Heidelberg University, Mannheim, Germany, [10] HEiKA—Heidelberg Karlsruhe Strategic Partnership, Karlsruhe Institute of Technology (KIT), Heidelberg University, Heidelberg, Germany

Diabetic retinopathy (DR) is a frequent diabetes-associated complication. Pericyte dropout can cause increased vascular permeability and contribute to vascular occlusion. Adipose-derived stromal cells (ASC) have been suggested to replace pericytes and restore microvascular support as potential therapy of DR. In models of DR, ASC not only generated a cytoprotective and reparative environment by the secretion of trophic factors but also engrafted and integrated into the retina in a pericyte-like fashion. The aim of this study was to compare the pro-angiogenic features of human ASC and human retinal microvascular pericytes (HRMVPC) *in vitro*. The proliferation and the expression of ASC and HRMVPC markers were compared. Adhesion to high glucose-conditioned endothelial extracellular matrix, mimicking the diabetic microenvironment, was measured. The angiogenesis-promoting features of both cell types and their conditioned media on human retinal endothelial cells (EC) were assessed. To identify a molecular basis for the observed differences, gene expression profiling was performed using whole-genome microarrays, and data were validated using PCR arrays and flow cytometry. Based on multiplex cytokine results, functional studies on selected growth factors were performed to assess their role in angiogenic support. Despite a distinct heterogeneity in ASC and HRMVPC cultures with an overlap of expressed markers, ASC differed functionally from HRMVPC. Most importantly, the pro-angiogenic activity was solely featured by ASC, whereas HRMVPC actively suppressed vascular network formation. HRMVPC, in contrast to ASC, showed impaired adhesion and

OPEN ACCESS

Edited by:
Emmanuel S. Tzanakakis, Tufts University, United States

Reviewed by:
Martina Piccoli, Istituto di Ricerca Pediatrica, Fondazione Città della Speranza, Italy
Giulia Ricci, University of Campania Luigi Vanvitelli, Italy
Cornelis Johannes Forrendinis Van Noorden, VU University Medical Center Amsterdam (VUmc), Netherlands

***Correspondence:**
Karen Bieback
Karen.bieback@medma.uni-heidelberg.de

† These authors have contributed equally to this work

Specialty section:
This article was submitted to Stem Cell Research, a section of the journal Frontiers in Cell and Developmental Biology

Received: *17 February 2020*
Accepted: *29 April 2020*
Published: *09 June 2020*

Citation:
Kremer H, Gebauer J, Elvers-Hornung S, Uhlig S, Hammes H-P, Beltramo E, Steeb L, Harmsen MC, Sticht C, Klueter H, Bieback K and Fiori A (2020) Pro-angiogenic Activity Discriminates Human Adipose-Derived Stromal Cells From Retinal Pericytes: Considerations for Cell-Based Therapy of Diabetic Retinopathy. Front. Cell Dev. Biol. 8:387. doi: 10.3389/fcell.2020.00387

proliferation on the high glucose-conditioned endothelial extracellular matrix. These data were supported by gene expression profiles with differentially expressed genes. The vessel-stabilizing factors were more highly expressed in HRMVPC, and the angiogenesis-promoting factors were more highly expressed in ASC. The vascular endothelial growth factor receptor-2 inhibition efficiently abolished the ASC angiogenic supportive capacities, whereas the addition of angiopoietin-1 and angiopoietin-2 did not alter these effects. Our results clearly show that ASC are pro-angiogenic, whereas HRMVPC are marked by anti-angiogenic/EC-stabilizing features. These data support ASC as pericyte replacement in DR but also suggest a careful risk-to-benefit analysis to take full advantage of the ASC therapeutic features.

Keywords: human adipose-derived stromal cells, human retinal pericytes, diabetic retinopathy, angiogenesis, vascular–endothelial growth factor, angiopoietin

INTRODUCTION

Diabetic retinopathy (DR) is a common microvascular complication of diabetes mellitus with a risk of causing blindness (Stitt et al., 2016; Hammes, 2018). The early stage of the disease, known as non-proliferative DR, is diagnosed by microvascular abnormalities. These are the consequence of a sequela of detrimental events, which involve the whole neurovascular retina and include pericyte dropout, basal lamina thickening, and endothelial, neuronal, and glial dysfunction (Stitt et al., 2016; Fiori et al., 2018; Hammes, 2018). Reactive, uncontrolled mechanisms cause angiogenesis, leading to proliferative DR. To date, treatments of sight-threatening DR include laser photocoagulation, vitreoretinal surgery, corticosteroids, and—more recently—anti-vascular endothelial growth factor (VEGF) drugs to limit and reduce the pathological hyperproliferation of retinal vessels (Stitt et al., 2016; Hammes, 2018). To avoid the associated side effects, cell-based therapies have been suggested (Stitt et al., 2011).

Loss of pericytes appears as the earliest event, causing destabilization of the retinal vessels (Pfister et al., 2013). Destructive signaling pathways involving the angiopoietin–Tie2 axis can lead to pericyte detachment and migration and, sometimes, subsequent apoptosis (Beltramo and Porta, 2013). Therefore, the prevention and/or the containment of DR progression may involve the control of pericyte dropout to promote vascular repair and the reversal of ischemic injury.

Therapy with mesenchymal stromal cells (MSC), especially those sourced from adipose tissue (adipose-derived stromal cells, ASC), emerged as an interesting treatment option for DR due to their pro-regenerative, pro-angiogenic, anti-apoptotic, and anti-inflammatory functions and their close relationship to pericytes (Fiori et al., 2018). Indeed the first hint came from a study where intravenously infused MSC improved the blood–retina barrier integrity (Yang et al., 2010). At this stage, it was not clear whether the observed effect was directly linked to the local action of the infused cells or secondary to lowered hyperglycemia. Subsequent data provided better insight, indicating that ASC not only generate a cytoprotective and regenerative environment by secretion of trophic factors acting on endothelial, neuronal, and glial cells (Ezquer et al., 2016) but also engraft and integrate into the retina in a pericyte-like fashion (Mendel et al., 2013). In different models of DR, ASC wrapped around retinal vessels and expressed α smooth muscle actin (α-SMA) upon intravitreal injection. This went with an improvement of visual function and delay in disease progression (Mendel et al., 2013; Rajashekhar et al., 2014; Hajmousa et al., 2018). *In vitro* tube formation assays complemented these observations, indicating that ASC can support and stabilize capillary structures (Merfeld-Clauss et al., 2010). However, there are discrepant data on whether ASC can effectively migrate, integrate, and differentiate gaining pericyte-like functions or rather exert their function by paracrine effects. Ezquer et al. (2016) observed that the cells remained in the vitreous without signs of differentiation and acted *via* secreted factors. In contrast, (Cronk et al., 2015) observed that only cells, but not the conditioned medium, were vasoprotective. Our previous data indicate that cell–cell interactions *via* NOTCH-2 are required for *in vitro* tube formation, but not for *in vivo* angiogenesis, which appeared to be independent of NOTCH-2, mainly based on paracrine factors (Terlizzi et al., 2018).

Besides the uncertainties in understanding the effective mode of action of MSC/ASC in DR, another concern regarding MSC therapy is that the cells should resist the diabetic microenvironment, which may impair the MSC pro-regenerative function (Cianfarani et al., 2013; Rennert et al., 2014; Cronk et al., 2015). However, others and we have shown that ASC resist hyperglycemic stress and restore the angiogenic properties of endothelial cells (EC) which were suppressed by hyperglycemia (Rajashekhar et al., 2014; Hajmousa et al., 2018; Fiori et al., 2020). Furthermore, the MSC-mediated secretion of pro-angiogenic factors may represent a significant risk as these factors may worsen DR by promoting vessel proliferation (Beltramo et al., 2014). In fact, we observed that the intravitreal injection of MSC into non-diabetic transgenic animals induced cataract, pericyte loss, vascular dysfunction, and inflammatory responses, thus worsening the established retinopathy (Huang et al., 2019).

To clarify whether ASC can take over pericyte functions, we compared the pro-angiogenic and the pericyte-like functions of human ASC and human retinal microvascular pericytes (HRMVPC) *in vitro* to elucidate the differences and the similarities between these two cell types. Intriguingly, the

pro-angiogenic activity was solely featured by ASC, whereas HRMVPC actively suppressed the vascular network formation.

MATERIALS AND METHODS

Cell Culture

All protocols for isolating the primary cells were approved by the Mannheim Ethics Commission II, except for the cells provided by collaboration or commercial sources. All donors gave written informed consent in accordance with the Declaration of Helsinki.

Human umbilical vein endothelial cells (HUVEC), initially used as a model of EC, were isolated as described before (Bieback et al., 2013) and cultivated at 8,000 cells/cm^2 in endothelial cell growth medium-2 (ECGM-2 with 1 g/L glucose; PromoCell, Heidelberg, Germany). HUVEC, derived from different donors, were used from passages 3 to 5. Human retinal microvascular endothelial cells (HRMVEC; two different donor isolates, passage 3; PeloBiotech, Planegg, Germany), used to reflect the microvascular retinal milieu, were cultured similar to HUVEC and used until passage 8. For some experiments, EC were cultured in normal glucose (NG; 1 g/L standard concentration in all culture media used), high glucose (HG; 4.5 g/L), or mannitol as osmotic control, adding additional 3.5 g/L glucose/mannitol to the media. Adipose-derived stromal cells (ASC) were isolated from lipoaspirate as described previously (Bieback et al., 2012). The ASC were cultured at seeding densities of 200 ASC/cm^2 in Dulbecco's modified Eagles medium (DMEM) with 10% human AB serum (1 g/L glucose; PAN Biotech, Aidenbach, Germany and German Red Cross Blood Donor Service, respectively), 1% penicillin/streptomycin (PAN Biotech), and 2% L-glutamine (200 mM; PAN Biotech). Different donor isolates, passages 2 to 4, were used throughout the study to account for donor-specific variances. The immortalized human retinal pericytes (Bmi-HRMVPC; passage 6; kindly provided by Elena Beltramo), initially used for comparison, were cultured by seeding 20,000 cells/cm^2 in DMEM 10% fetal bovine serum (FBS; Sigma-Aldrich Chemie GmbH, Munich, Germany) and used at passages 7 to 8. In addition, three different isolates of primary human retinal microvascular pericytes (HRMVPC, passage 3) were purchased to account for donor-specific differences. The HRMVPC were cultured by seeding 20,000 cells/cm^2 in pericyte growth medium in flasks coated with Speed Coating Solution (all PeloBiotech) and used from passages 4 to 6.

All cells were cultured at 37°C with 5% CO_2 and the medium was changed every 2 to 3 days. All cells were cryopreserved using 90% FBS and 10% dimethyl sulfoxide (Wak-chemie Medical GmbH, Steinbach, Germany).

GFP and dTomato Expressing HUVEC and HRMVEC

To monitor angiogenesis, EC were transduced to express GFP or dTomato. The GFP- or dTomato-expressing plasmids pHR'SIN-cPPT-SEW, together with pCMV-DR8.91 and pMD.G (all kindly provided by Prof. Patrick Maier, Department of Radiation Oncology, University Medical Centre Mannheim, Germany), were used to produce lentiviral vectors through the transient transfection of 293FT cells. The HUVEC and HRMVEC were transduced once in the presence of polybrene (8 μg/ml; Sigma-Aldrich). The transduced GFP- or dTomato-positive EC were sorted using a BD FACSAria IIu (Becton Dickinson, Heidelberg, Germany), collected, and cultured as reported previously. The transduced EC were used from passages 5 to 11.

Comparative Characterization of Human ASC and HRMVPC

The growth curves of ASC, HRMVPC, and Bmi-HRMVPC were assessed by seeding 2,500 cells/cm^2 in 96-well plates in eight technical replicates and recording the increasing confluence every 2 to 4 h using a live imaging device (IncuCyte ZOOM; Essen BioScience, Ann Arbor, MI, United States) (**Supplementary Figure S1**). The percent confluence was determined using an adapted processing definition (IncuCyte® ZOOM software).

Multiparametric flow cytometry was performed on 10,000 trypsinized cells using the titrated antibodies listed in **Supplementary Table S1**, using a BD FACSCanto II (Becton Dickinson) running BD FACSDIVA software. The obtained data were analyzed with FlowJo software (FlowJo, LLC, Ashland, OR, United States). The percentage positivity and the mean fluorescence intensity (MFI) values were calculated against unstained controls. All antibodies were validated using a positive control, except for the regulator of G protein signaling 5 (RGS5), where putative positive controls yielded negative results despite using different antibody clones and direct, indirect, extracellular, and intracellular staining. These data, thus, are not shown.

Interaction of ASC and HRMVPC With High Glucose-Conditioned Endothelial Extracellular Matrix

To compare the interaction between ASC, Bmi-HRMVPC, and HRMVPC on HG-conditioned EC extracellular matrix (ECM), we followed the protocol by Beltramo et al. (2009) with slight modifications. Briefly, the HUVEC (15,000 cells/cm^2) or the HRMVEC (7,500 or 10,000 cells/cm^2) were cultured in 24-well plates. The HUVEC were seeded in 1/4 ECGM-2 (ECGM-2 with 75% reduced growth supplements) at NG or HG conditions. We have previously observed that only upon lowering the growth factor content did the negative HG effects on EC became apparent (Fiori et al., 2020). Mannitol (3.5 g/L) served as osmotic control. The HRMVEC were seeded in standard ECGM-2 at NG or HG conditions. Upon reaching at least 95% confluence, as monitored by kinetic live cell imaging (IncuCyte ZOOM), the EC were washed once with phosphate-buffered saline (PBS) and lysed with 0.25 mM ammonia solution for 3 min. The obtained ECM was washed thrice with PBS and kept wet until use. The intactness of the ECM was verified by brilliant blue stain (**Supplementary Figure S2**). The ASC or HRMVPC were seeded on top of the ECM at a density of 5,000 cells/cm^2. Using kinetic live imaging, adhesion was monitored after 10 and 20 min and proliferation was monitored every 2 h for 2 days. The average single cell area was assessed during adhesion and cell confluence/proliferation using individually adapted segmentation masks/processing definitions

(**Supplementary Figure S2**). Single measurements were excluded when confounded by debris or image analysis errors. The average of the technical replicate values in each individual experiment was normalized to NG control and used to calculate the mean values and the standard deviation for the biological replicates.

Angiogenesis Assays

To assess the vascular network/tube formation of EC and the pro-angiogenic potential of ASC and HRMVPC, two angiogenesis assays were used—one dedicated to assess the supportive action of the ASC/HRMVPC seeded as a monolayer and the other to assess the pro-angiogenic activity of the conditioned medium (CM).

Coculture (CC) Angiogenesis Assay

A total of 30,000 ASC or HRMVPC were seeded per well in a 96-well plate in ¼ ECGM-2 for 1 h, and ¼ ECGM-2 was used to keep the endothelial growth factor concentrations low. Then, 5,000 (in later passages 8,000) GFP or dTomato HUVEC or GFP or dTomato HRMVEC were seeded in ¼ ECGM-2 on top of the monolayer. The cocultures were incubated for 72 h. Visualization of tube formation over time was performed by taking phase-contrast and fluorescent images with the IncuCyte ZOOM imaging device (**Supplementary Figure S3A**). An integrated angiogenesis algorithm measured tube formation by calculating the tube length, area, and number of branch points. After 72 h of coculture, CM was collected and frozen at −80°C. The respective monoculture-derived CM was prepared in parallel; ¼ ECGM-2 served as control.

Basal Lamina Matrix (BM) Angiogenesis Assay

A total of 17,000 GFP or dTomato HRMVEC were seeded per well in a 96-well plate on top of a 50-µl/well layer of a basal lamina matrix (Geltrex^{TM} LDEV-free reduced growth factor matrix; Thermo Fisher Scientific, United States) in ¼ ECGM-2 or CM of the CC angiogenesis assay. Fluorescent images were taken every 30 min with the IncuCyte ZOOM live imaging device (**Supplementary Figure S3A**). Network formation was monitored for up to 6 h and maximum values of branch points ($1/mm^2$) and network length (mm/mm^2) were calculated using either NIH ImageJ with the Angiogenesis Analyzer plugin or the IncuCyte Software. Network branch point metrics were used for statistical analyses. Because ASC showed network formation in the BM angiogenesis assay similar to EC, we did not run direct cocultures in this assay but used it to analyze the CM effects on HRMVEC tube formation.

Conditioned Medium, Inhibitors, and Growth Factor Addition

When specified, CM derived from either CC angiogenesis assays or monocultures, cultured for 72 h in ¼ ECGM-2, was added to both angiogenesis assays instead of the control medium. Furthermore, the following substances were used: recombinant human vascular endothelial growth factor ($rhVEGF_{165}$, 10 ng/ml; PeproTech, London, United Kingdom), angiopoietin-1 and angiopoietin-2 [rhAng-1 and rhAng-2, 400 ng/ml (Teichert et al., 2017); both PeproTech], suramin sodium (anti-angiogenic compound, 100 µM; Santa Cruz Biotechnology, Heidelberg, Germany), and ZM 323881 hydrochloride [selective VEGFR2 antagonist, 1 µM (Busceti et al., 2017); Santa Cruz Biotechnology].

Immunofluorescence Staining

To assess pericyte-like differentiation upon network formation, the expression of pericyte markers α-smooth muscle actin (α-SMA), neural/glial antigen 2 (NG-2), regulator of G protein signaling 5 (RGS5), and platelet-derived growth factor receptor-β (PDGFR-β) (Bergers and Song, 2005) was assessed in CC angiogenesis cocultures. A total of 100,000 ASC/well were seeded in ¼ ECGM-2 medium in eight-well µ-slides (ibidi, Gräfelfing, Germany) and then 20,000 dTomato HRMVEC were seeded on top. Network formation was monitored over 72 h. Then, the wells were washed with PBS and fixed with 2% paraformaldehyde in PBS for 30 min. After washing, the cells were permeabilized with 0.5% Triton X-100. After 15 min of blocking with 2% bovine serum albumin (BSA), 50 µl/well of ready-to-use mouse anti-human α-SMA (Progen, Heidelberg, Germany), mouse anti-human NG-2 (1:100; Santa Cruz Biotechnology), mouse anti-human RGS5 (RGS5 and RGS5-AF647 clone B4, 1:100; Santa Cruz Biotechnology or clone OTI1C1; OriGene Technologies, Rockville, MD, United States), or mouse anti-human PDGFR-β (clone 18A2, 1:100; Santa Cruz Biotechnology) were added and incubated for 1 h in the dark. After washing with 0.1% BSA, secondary antibody anti-mouse-Alexa Fluor 488 F(ab')2 (1:1,000 final dilution, Invitrogen, Thermo Fisher Scientific, Karlsruhe, Germany) was added for 1 h in the dark. The nuclei were counterstained with DAPI (1 µg/ml; Sigma-Aldrich) before embedding the slides in the mounting medium (ibidi). The images were captured using either a Zeiss microscope with AxioVision Rel. 4.7 (Carl Zeiss Microscopy GmbH, Jena, Germany) or an inverse Leica SP5 Mid-multi-photon system (Leica, Wetzlar, Germany) using a × 25 (0.95 NA) water immersion objective or × 40/1.3 NA oil objective (Leica). The negative controls without first antibody showed no staining. RGS5 staining gave negative results and, because antibodies could not be validated using a positive control, the results are not shown.

Microarray and PCR Array Validation

RNA Isolation

The ASC and HRMVPC (three biological replicates each) were cultured for 7 days. Then, the cells were trypsinized, washed, and RNA-isolated using Qiagen RNeasy mini Kit (Qiagen, Hilden, Germany). RNA quality was tested by capillary electrophoresis on an Agilent 2100 bioanalyzer (Agilent, Santa Clara, CA, United States) and high quality (RNA integrity values ≥9) was confirmed.

Microarray

Gene expression profiling was performed using human HTA-2_0-st-type arrays (Affymetrix, Thermo Fisher Scientific). The biotinylated antisense cRNA was prepared, according to the standard labeling protocol, with the GeneChip® WT Plus Reagent Kit and the GeneChip® Hybridization, Wash, and

Stain Kit. The hybridization on the chip was performed on a GeneChip Hybridization oven 640, then dyed in the GeneChip Fluidics Station 450, and thereafter scanned with a GeneChip Scanner 3000.

Bioinformatics

A custom CDF version 22 with ENTREZ-based gene definitions was used to annotate the arrays (Dai et al., 2005). The raw fluorescence intensity values were normalized by applying quantile normalization and RMA background correction. An ANOVA was performed to identify differentially expressed genes using a commercial software package (SAS JMP11 Genomics, version 7; SAS Institute, Cary, NC, United States). A false positive rate of a = 0.05 with FDR correction was taken as the level of significance. Gene Set Enrichment Analysis (GSEA) was used to determine whether the defined sets of genes exhibit a statistically significant bias in their distribution within a ranked gene list using the R software packages EnrichmentBrowser (Geistlinger et al., 2016). KEGG pathway analysis was performed, focusing on apparently relevant pathways[1].

The raw and normalized data are deposited in the Gene Expression Omnibus database (accession no. GSE144605)[2].

PCR Array

The selected genes were validated using RT2 Custom Profiler PCR Arrays (**Supplementary Table S2**; Qiagen, Hilden, Germany), according to the manufacturer's instructions, using a LightCycler® 480 (Roche Life Science, Mannheim, Germany). These PCR arrays were also performed on RNA samples from HUVEC and HRMVEC cultured for 5 days in ¼ ECGM-2 NG/HG (three and one biological replicate, respectively).

Multiplex Cytokine Analysis of Conditioned Media

The angiogenic growth factors in CM derived from either CC angiogenesis assays or monocultures were analyzed with a bead-based immunoassay (LEGENDplex™ Human Angiogenesis Panel 1; BioLegend, San Diego, CA, United States) by following the manufacturer's instructions. Briefly, the samples and the standards were loaded in a 96-well V-bottom plate, followed by incubation with premixed capture beads for 2 h at room temperature (RT) on a plate shaker. After two washing steps with wash buffer, the detection antibodies were added for 1 h at RT to form capture bead/analyte/detection antibody sandwiches. LEGENDplex™ Streptavidin-PE was then added directly after incubation for 30 min at RT. After a final washing step, the samples were transferred to fluorescence-activated cell sorting tubes and analyzed using BD FACS Canto II (Becton Dickinson). The data were analyzed with the LEGENDplex™ data analysis software (BioLegend).

[1]http://www.genome.jp/kegg

[2]http://www.ncbi.nlm.nih.gov/geo/

Statistical Analysis

All results are expressed as mean ± standard deviation; n represents the number of biological replicates or, if not possible to test the different donors, the technical replicates in independent experiments. Statistical analyses were performed using GraphPad Prism 7 (GraphPad Software, San Diego, CA, United States). Differences between experimental groups were analyzed after normality testing by one- or two-way ANOVA (repeated-measures, RM, if applicable) with *post hoc* tests as indicated. $P \leq 0.05$ was considered as statistically significant ($^{*}p \leq 0.05$, $^{**}p \leq 0.01$, $^{***}p \leq 0.001$, and $^{****}p \leq 0.0001$). For comparison and correlation analysis of the microarray, PCR array, and flow cytometry data, the programming language R was used. Volcano plots were generated using the R package ggplot2.

RESULTS

ASC and Retinal Pericyte Morphology and Growth Curves Differ, but the MSC Marker Expression Is Similar

To compare the basic characteristics of ASC and HRMVPC, cell morphology, growth curves, and expression of typical MSC markers were assessed. Both cell types had a typical fibroblastoid morphology, but both immortalized Bmi-HRMVPC, used first for comparison, and HRMVPC, used later to account for potential donor differences, appeared more elongated and slender with an apparently higher light diffraction at the cell borders (**Figure 1A**). Both HRMVPC detached within seconds after adding trypsin, in contrast to ASC that needed approximately 5 min to detach. This suggests that different proteins are involved in cell adhesion, substantiated by the recommended coating for primary HRMVPC. The cell sizes were comparable after trypsinization and ranged between 19 and 21 μm. Both HRMVPC required high seeding densities (split of maximum 1:5), whereas ASC could be seeded at low densities (200 cells/cm^2) to obtain optimal cell proliferation. This also suggests different needs for cell–cell contacts for proliferation. Using live cell imaging, a direct comparison of the growth curves was performed by seeding cells at 2,500 cells/cm^2 and assessing the increase of confluence (**Supplementary Figure S1**). For the first 24 h, the confluence increased indistinguishably, indicating similar kinetics for cell adhesion and spreading (**Figure 1B**). Thereafter, HRMVPC proliferation was very slow in contrast to ASC, which showed a sigmoid curve at reaching 100% confluence after 96 h.

The ASC are characterized by the expression/non-expression of certain surface markers (Dominici et al., 2006; Bourin et al., 2013). Flow cytometry analyses showed that marker expression was largely identical for ASC and HRMVPC (**Figure 1C**). The heterogeneity in endoglin (CD105) expression—two isolates with only 50% of the cells being positive—was surprising for ASC since in previous studies all ASC uniformly expressed CD105 (Kern et al., 2006). The HRMVPC were more heterogeneous than ASC for Thy-1 (CD90, mean 90.7 ± 7.3%, $p \leq 0.01$), CD45 (mean 5.6 ± 3.9%, non-significant), vascular cell adhesion molecule-1

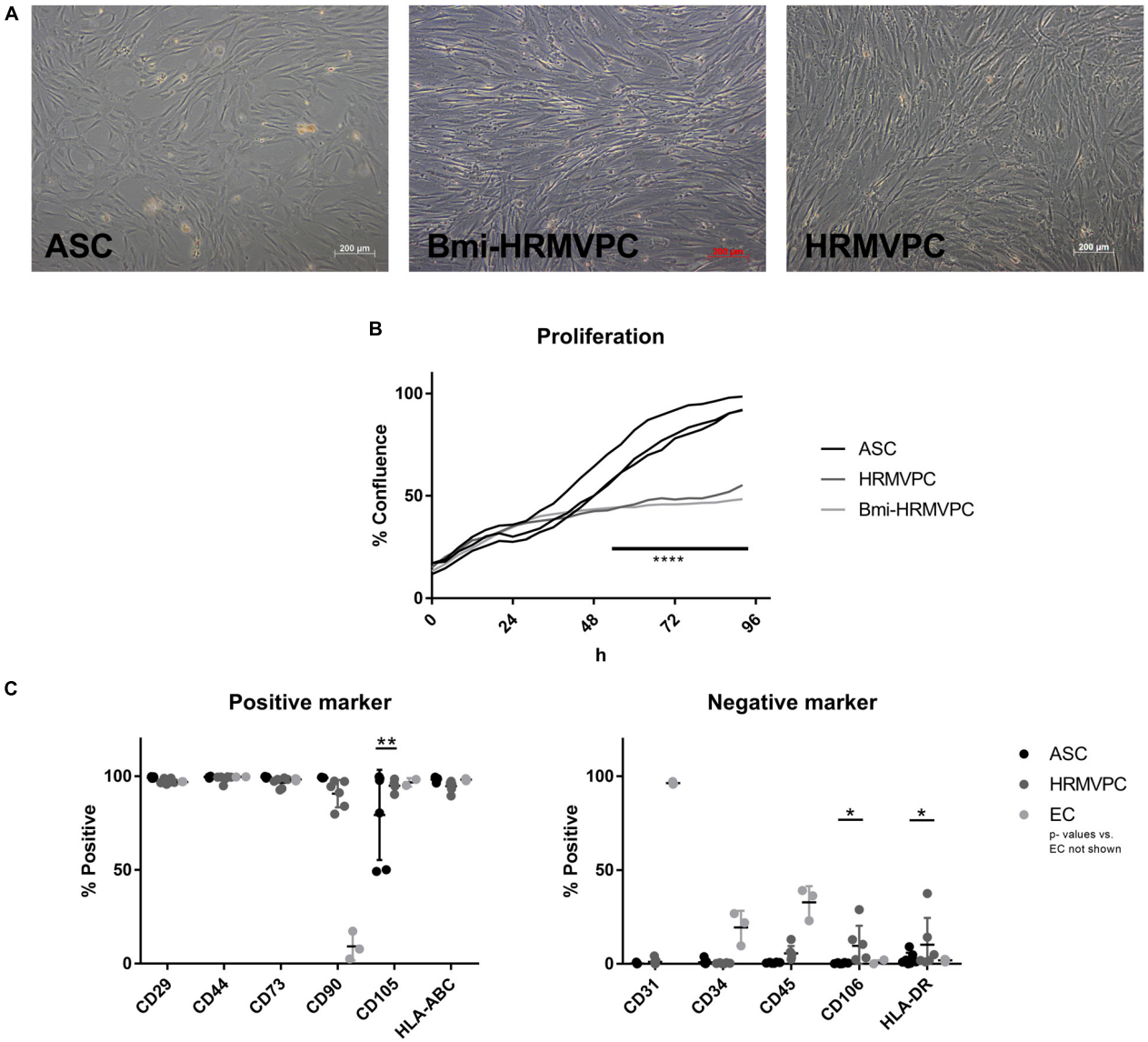

FIGURE 1 | Morphology of adipose-derived stromal cells (ASC) and human retinal microvascular pericytes (HRMVPC) and the growth curves differ, whereas the mesenchymal stromal cells (MSC) marker expression is indistinguishable. **(A)** Representative images of ASC, Bmi-HRMVPC and HRMVPC. **(B)** Growth curves of ASC (three different donors), HRMVPC (one donor), and Bmi-HRMVPC cell line determined by kinetic live imaging (****$p \leq 0.0001$, two-way ANOVA with Sidak's *post hoc* test). **(C)** Surface expression of MSC positive and negative markers for ASC ($n = 7$ different donors), HRMVPC (HRMVPC and Bmi-HRMVPC groups, $n = 6$, biological and technical replicates from three different donors), and endothelial cells (EC; $n = 3$, human umbilical vein endothelial cell and human retinal microvascular endothelial cell groups) (*$p \leq 0.05$ and **$p \leq 0.01$, two-way ANOVA with Tukey's *post hoc* test; significant differences to EC not depicted).

(VCAM-1, CD106, mean: 9.7 ± 10.7%, $p \leq 0.05$), and HLA-DR (mean 10.3 ± 14.3%, $p \leq 0.05$). The EC displayed a significantly differing phenotype as expected (p value not shown).

HRMVPC Show Impaired Interaction With HG-Conditioned EC ECM Compared to ASC

Beltramo et al. (2009) have shown that HG-conditioned EC ECM reduces the adhesion and increases the apoptosis of pericytes, mimicking the pericyte dropout found in DR. Hypothesizing that ASC can resist these changes, adhere, and proliferate, we compared the interaction of ASC and HRMVPC with NG- and HG-conditioned EC ECM. First, we tested HUVEC and then—to better mimic the microvasculature of the retina—HRMVEC. Furthermore, we assessed first immortalized Bmi-HRMVPC and later confirmed these data with primary HRMVPC from different donors. Using live cell imaging, we monitored the kinetics of ASC and HRMVPC interaction with HG-conditioned EC ECM by measuring the percent of cell confluence (**Supplementary Figure S2**). The increase of ASC confluence was higher on EC ECM compared to culture plastic

(**Figure 2A**). The HUVEC ECM, conditioned with NG, HG, or mannitol, did not significantly affect the ASC confluence. HG conditioning rather increased ASC confluence on HUVEC ECM, although non-significant (**Figures 2C,D**). Interestingly, the ASC-improved interaction was not observed when using HRMVEC-derived ECM, reflecting the microvasculature of the retina (**Figure 2E**). As expected, the interaction between HRMVPC and HG-conditioned EC ECM was reduced (**Figures 2B–D**), however, only significant when assessing HRMVEC ECM ($p \leq 0.05$, **Figure 2E**). Nevertheless, compared to ASC, the primary HRMVPC showed reduced confluence levels, which were significant for the first 14 h when assessing the confluence on HUVEC ECM ($p \leq 0.05$, **Figure 2D**) but not when assessing the confluence on HRMVEC ECM (**Figure 2E**).

The differing starting points of the kinetic analysis and the fact that the curves did not separate further over time suggested an early effect of the HG-conditioned ECM, most probably on cell adhesion. Unfortunately, up to now, we were not able to provide conclusive evidence for this. Measuring the cell spreading and counting the adherent cells 10 and 20 min after cell seeding indicated slight but non-significant differences between ASC and HRMVPC, but none when comparing NG- and HG-conditioned EC ECM. The adhesion kinetics, addressing focal adhesion dynamics as previously shown (Dreher et al., 2013), were also inconclusive. We also found no quantifiable measures of HG-induced ECM modifications: staining with an advanced glycation end product-specific antibody (kindly provided by Thomas Fleming, Heidelberg) was only detected in positive controls after methylglyoxal treatment. Quantifying sulfated glycosaminoglycans of NG- and HG-conditioned EC ECM revealed no differences either. Furthermore, no significant changes were found in gene expression upon comparing HRMVEC (not shown as only cells from one donor were tested) and HUVEC cultured for 5 days in NG and HG conditions (**Supplementary Figure S4C**).

Human ASC Are Pro-angiogenic Whereas HRMVPC Do Not Support Angiogenic Network Formation

A key function of pericytes is to control endothelial cell angiogenesis or quiescence (Teichert et al., 2017). To compare how ASC and HRMVPC regulate angiogenesis, we established two kinetic angiogenesis assays *in vitro*—one focusing on cell–cell interactions (direct CC angiogenesis assay) and a second one addressing paracrine factors (BM angiogenesis assay). Both assays evaluate the endothelial cell network formation by live cell imaging (**Supplementary Figure S3A**). The ASC donor-dependently supported endothelial network formation by increasing the network branch points (**Figure 3A**) and the network length (**Supplementary Figure S3B**). This effect was transient, lasting for approximately 48 h, but could be maintained for 3 weeks upon regular medium exchange. In general, the levels of tube formation were stronger in HUVEC compared to HRMVEC (Fiori et al., 2020). In contrast to ASC, HRMVPC did not support network formation, neither of HRMVEC nor of HUVEC (**Figure 3A**). To determine whether this is related to cell–cell or paracrine factor, we compared the CM of ASC and HRMVPC (prepared from CC angiogenesis assays) to $VEGF_{165}$ addition in the BM angiogenesis assay. CM ASC significantly induced network formation similar to $VEGF_{165}$, whereas CM HRMVPC had no effect ($p \leq 0.05$, **Figure 3B**). This indicates that ASC secrete angiogenic factors. Speculating that HRMVPC produce anti-angiogenic/angiostatic factors, we added CM from ASC or HRMVPC cocultures to CC angiogenesis assays, respectively. Indeed CM HRMVPC abolished the supportive function of ASC ($p \leq 0.05$ to $p \leq 0.0001$, **Figure 3C**). CM ASC was not capable of converting HRMVPC to support angiogenesis (non-significant, **Figure 3D**). Interestingly, the ASC from one donor that did not support vascular network formation in the control setting—the same donor as depicted in **Figure 3A** – supported tube formation once CM ASC was added. The ASC, which aligned to and wrapped around the endothelial tube-like structures, showed a strong expression of α-SMA, indicating a pericyte-like differentiation (**Figure 3E**).

These data clearly suggest that ASC exert a pro-angiogenic activity by providing a matrix and by secreting angiogenic factors, whereas HRMVPC do not support and—by secreting anti-angiogenic factors—actively inhibit endothelial tube formation.

Gene and Protein Expression Profiling

Our data suggested that the pro-angiogenic activity discriminates ASC from HRMVPC. To gain further insight into the potential contributing mechanisms, we performed whole-genome microarrays and validated data using PCR arrays, flow cytometry, and immunofluorescence analyses. The microarray gene expression profiling resulted in 2,533 genes more highly expressed in ASC and 2,873 higher in HRMVPC (**Figure 4A**). The KEGG pathway analysis revealed that, in ASC, the more highly expressed genes grouped to genetic information processing, whereas in HRMVPC, the more highly expressed genes grouped to environmental information processing. The selected candidate genes were validated using a PCR array (**Figure 4B**). There was a strong correlation between the microarray and the PCR array data (Spearman $R = 0.95$, $p < 2.2e\text{-}16$).

In order to understand the different adhesion of ASC and HRMVPC to the HG-conditioned EC ECM, we first zoomed into cell adhesion-related genes (based on a NCBI gene query with "cell adhesion AND 'Homo sapiens' [porgn:__txid9606]") and found 434 differentially expressed genes. The integrin subunits alpha 1, 2, 4, and 6 (*ITGA 1*, *2*, *4*, and *6*) appeared to be the most upregulated genes in HRMVPC, whereas ASC expressed integrin subunits alpha 5 and beta 3 (*ITGA5* and *ITGAB3*) to a higher level (**Supplementary Figures S4A,B**). Accordingly, we assessed the surface expression of integrins by flow cytometry. However, only integrin alpha-6 (CD49f) was heterogeneously expressed, higher in HRMVPC (69–95%) than in ASC (13–56%) ($p \leq 0.0001$, **Figure 4C**).

With respect to genes related to ECM, laminin subunit a3 (*LAMA3*), collagen type VIII alpha 1 chain (*COL8A1*), and collagen type XI alpha 1 chain (*COL11A1*) were more highly expressed in HRMVPC, whereas ASC showed a high expression of laminin subunit alpha 1 (*LAMA1*), tenascin C (*TNC*),

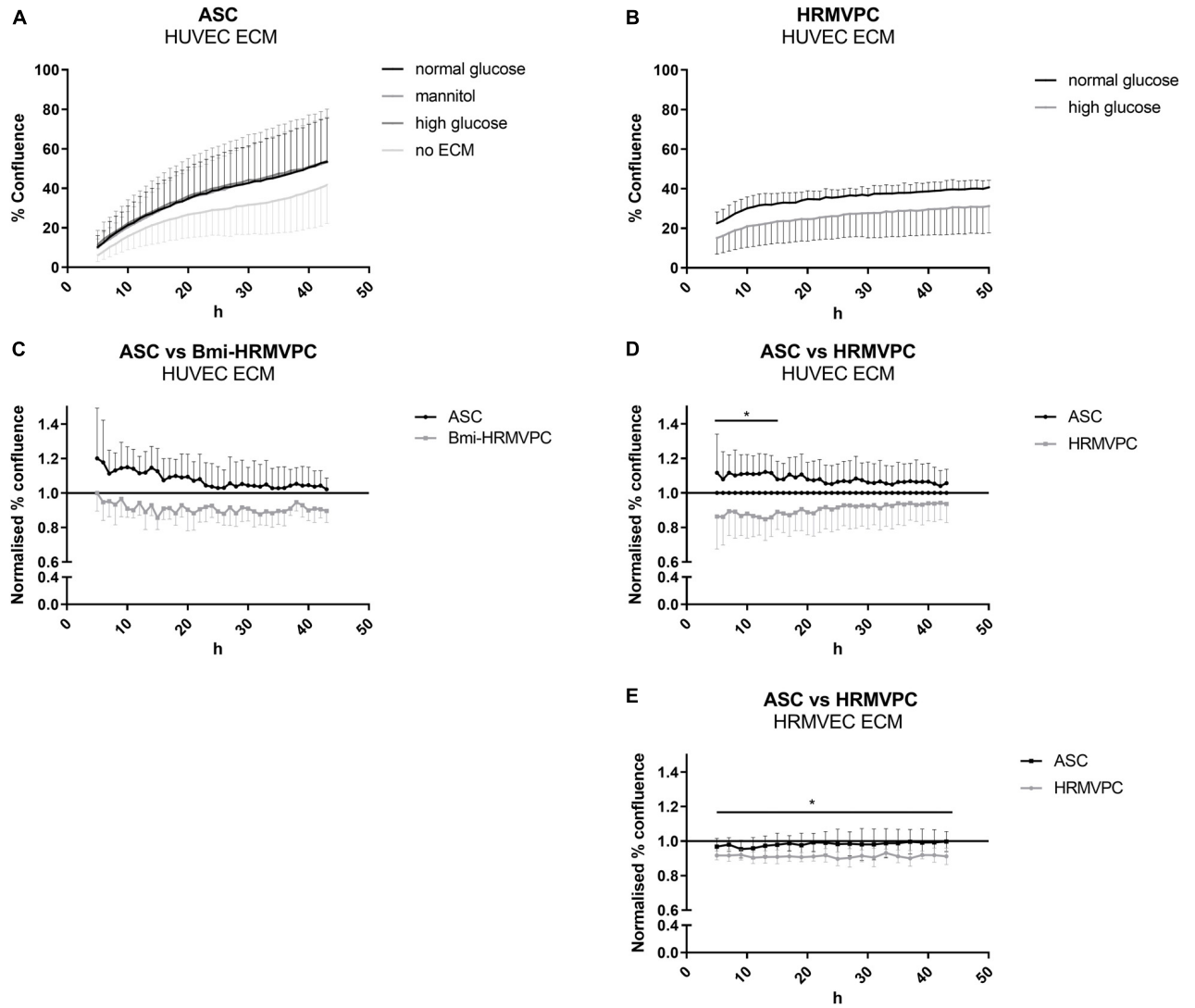

FIGURE 2 | Human retinal microvascular pericytes (HRMVPC) show impaired interaction with high glucose (HG)-conditioned endothelial cells (EC) extracellular matrix (ECM) compared to adipose-derived stromal cells (ASC). The EC, either human umbilical vein endothelial cells (HUVEC) or human retinal microvascular endothelial cells (HRMVEC), were grown until confluence in normal glucose (NG), HG, or mannitol-supplemented medium. Then, the EC ECM was prepared as described in section "Materials and Methods". ASC or HRMVPC were seeded on top, and the increase in confluence was monitored using live cell imaging over 48 h. **(A)** Confluence of ASC seeded on HUVEC ECM conditioned by NG, HG, or mannitol (n = 4 biological replicates; non-significant, two-way RM-ANOVA with Dunnett's *post hoc* test). **(B)** Confluence of HRMVPC seeded on HG-conditioned HRMVEC ECM compared to NG-conditioned ECM (n = 5 independent experiments with HRMVPC from one donor; non-significant, two-way RM-ANOVA with Sidak's *post hoc* test). **(C)** To account for differences in proliferative capacity, confluence data were normalized against the NG-conditioned HUVEC ECM (line at value 1). ASC vs. Bmi-HRMVPC (n = 3 independent experiments with ASC from different donors; non-significant, two-way RM-ANOVA with Sidak's *post hoc* test). **(D)** ASC vs. HRMVPC interaction with NG and HG-conditioned HUVEC ECM (n = 5 independent experiments with ASC from different donors; $^*p \leq 0.05$ for ASC vs. HRMVPC for the first 14 h, two-way RM-ANOVA with Sidak's *post hoc* test). **(E)** ASC vs. HRMPVC interaction with NG and HG-conditioned HRMVEC ECM (n = 3 independent experiments with ASC from different donors; $^*p \leq 0.05$ for HRMVPC interaction with NG and HG-conditioned HRMVEC ECM for all time points, two-way RM-ANOVA with Sidak's *post hoc* test).

and collagen type VI alpha 1 and 2 (*COL6A1* and *COL6A2*) (**Supplementary Figures S4A',B'**). The HRMVPC expressed matrix metalloproteinase-1 (*MMP1*) and metalloproteinase inhibitor 3 (*TIMP3*), which are involved in EC tubular morphogenesis, at significantly higher levels than ASC did.

Finally, we studied the expression of common pericyte markers. Some of the HRMVPC-specific genes appeared with high standardized value scores, indicating relative strength with functional association, within the gene set "pericytes" of the database Harmonizome (Rouillard et al., 2016), such as VEGF receptor 1 (*FLT1*), endothelin (*EDN1*), *RGS5, MMP1*, angiopoietin-1 (*ANGPT1*, Ang-1), and fibulin-1 (*FBLN-1*). None of the ASC-specific genes scored here (**Figure 4A**). Comparing gene expression with protein expression data (flow cytometric MFI values) gave low correlation values (Spearman correlation R = 0.4, p = 0.2) in line with previous

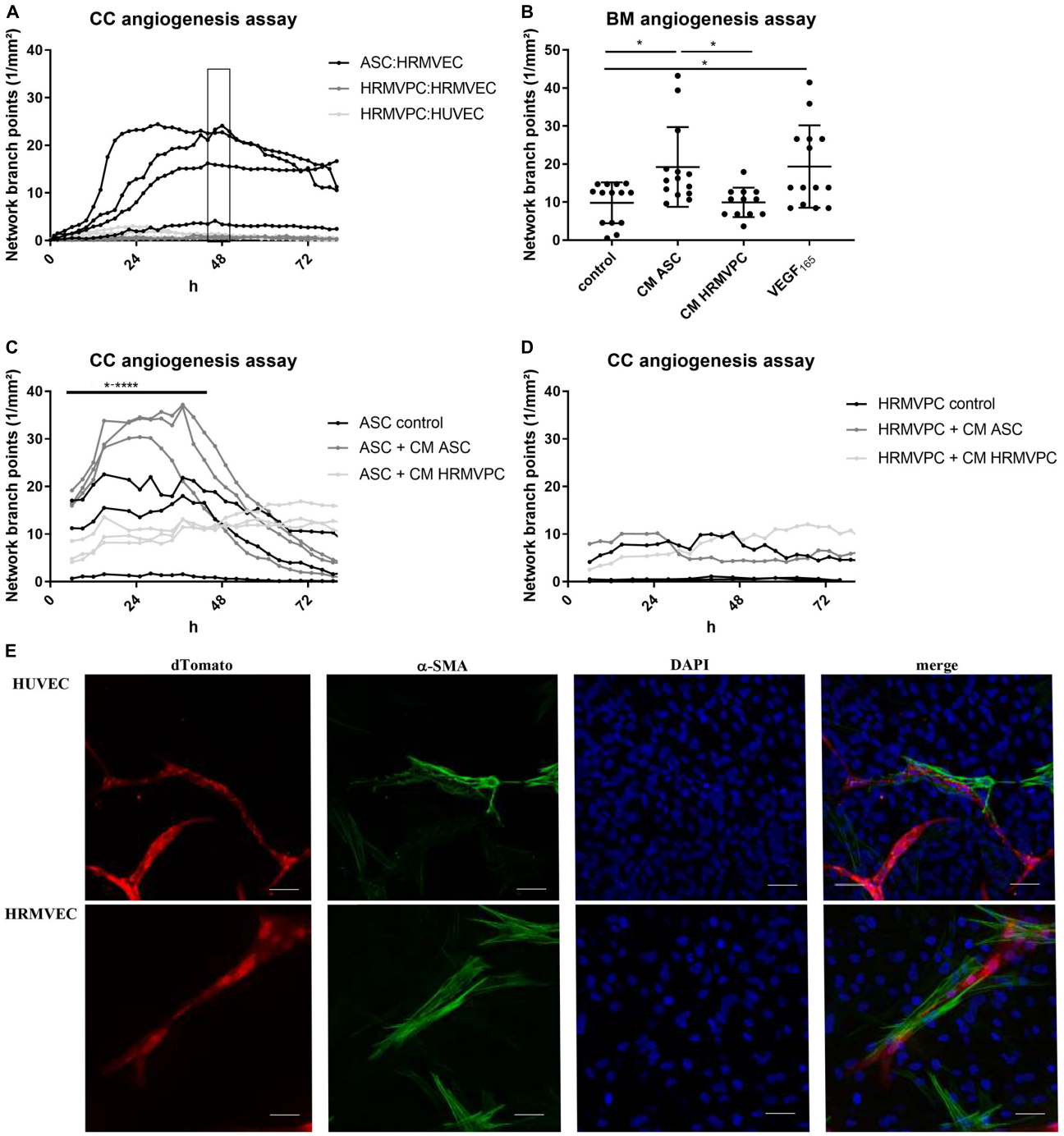

FIGURE 3 | Pro-angiogenic activity discriminates human adipose-derived stromal cells (ASC) and retinal pericytes. **(A)** Vascular network formation in CC angiogenesis assay using network branch point metrics (1/mm^2) of ASC/human retinal microvascular endothelial cells (HRMVEC), human retinal microvascular pericytes (HRMVPC)/HRMVEC, and HRMVPC/human umbilical vein endothelial cells (HUVEC) monitored using live imaging (four different ASC donors, two and three independent experiments with HRMVPC/HRMVEC and HRMVPC/HUVEC, respectively). Medium change is indicated by the box. ASC/HUVEC cocultures are not shown. **(B)** Vascular network formation in a BM angiogenesis assay (n = 11 paired experiments with ASC from 11 different donors and HRMVPC from three different donors in independent experiments; *$p \leq 0.05$, one-way ANOVA with Tukey's *post hoc* test). **(C,D)** Vascular network formation in CC angiogenesis assay, adding ¼ ECGM-2 as control or CC angiogenesis assay-derived CM ASC or CM HRMVPC to ASC/HRMVEC **(C)** or HRMVPC/HRMVEC **(D)** cocultures (n = 3, with three different ASC donors, independent experiments for two HRMVPC donors; *$p \leq 0.05$ to ****$p \leq 0.0001$, two-way RM-ANOVA with Tukey's *post hoc* test). **(E)** Representative images showing the expression of α-smooth muscle actin (α-SMA) in ASC/EC cocultures (dTomato EC, red; α-SMA green; DAPI, blue nuclear counter stain and merge). Scale bar, 50 μm.

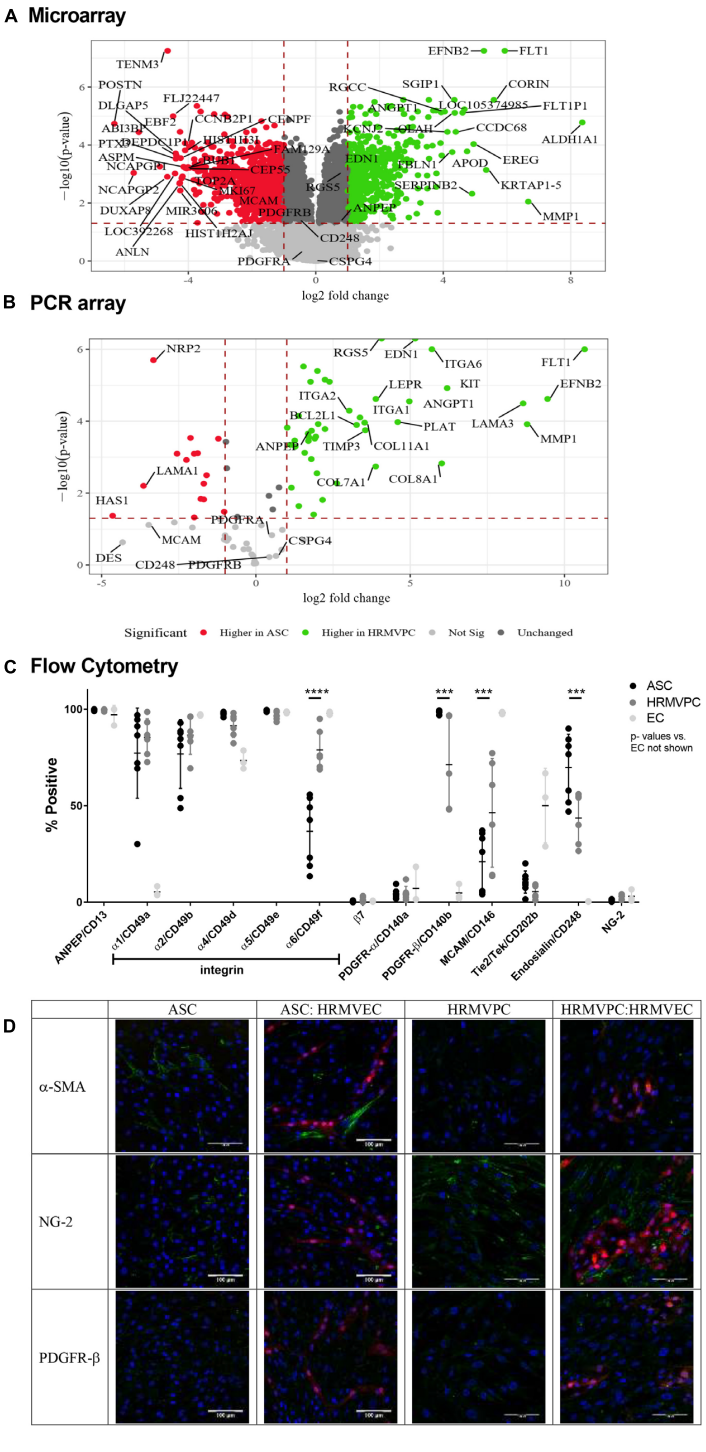

FIGURE 4 | Differential marker expression of adipose-derived stromal cells (ASC) and human retinal microvascular pericytes (HRMVPC) assessed by microarray, PCR array, flow cytometry, and immunofluorescence. **(A)** Volcano plot visualizing the microarray data showing the magnitude of change (log_2-fold change, *x*-axis) vs. statistical significance [$-log_{10}$(*p*-value), *y*-axis] of gene expression of ASC vs. HRMVPC (each $n = 3$ biological replicates). Most differentially expressed genes and putative pericyte markers are labeled. **(B)** Validation of microarray results using PCR array. The correlation is high (Spearman correlation $R = 0.95$, $p < 2.2e\text{-}16$). Most differentially expressed genes and putative pericyte markers are labeled. **(C)** Marker expression in ASC, HRMVPC, and EC measured by flow cytometry. Percent positivity calculated against the unstained control [$n = 7$ different ASC donors, $n = 6$ HRMVPC with three donors in independent experiments, $n = 3$ human umbilical vein endothelial cells and human retinal microvascular endothelial cells (HRMVEC); $^{***}p \leq 0.001$ and $^{****}p \leq 0.0001$, two-way ANOVA with Tukey's *post hoc* test, *p*-values for EC not shown]. Correlation to microarray and PCR array is poor (Spearman correlation $R = 0.4$, $p = 0.2$) using mean fluorescence intensity values. **(D)** Representative pictures of marker expression (green) in ASC, HRMVPC, and the respective cocultures measured by two-photon microscopy. dTomato HRMVEC are shown in red. Scale bar, 100 μm.

reports (Vogel and Marcotte, 2012). The alanyl aminopeptidase (*ANPEP*/CD13) mRNA levels, for instance, appeared to be increased in HRMVPC, whereas the flow cytometry data showed no significant differences in protein expression. In general, flow cytometry revealed a considerable heterogeneity in both ASC and HRMVPC cultures. The percentage of melanoma cell adhesion molecule (CD146)-positive cells was larger within HRMVPC than in ASC (46 ± 28% vs. 21 ± 15%, $p \leq 0.001$, **Figure 4C**), whereas endosialin (CD248) was expressed by a larger fraction of ASC (70 ± 17% vs. 44 ± 13%, $p \leq 0.001$, **Figure 4C**). PDGFR-β (CD140b), generally considered to be a pericyte marker, was expressed by 98 ± 1% of ASC, whereas in HRMVPC cultures the values varied (71 ± 24%, $p \leq 0.001$, **Figure 4C**). PDGFR-β expression was weak in both ASC and HRMVEC after immunofluorescence staining and independent of angiogenic EC coculture (**Figure 4D**). In addition, the common pericyte marker NG-2 was assessed (Bergers and Song, 2005) to validate the array data in which NG-2 did not appear as a differentially expressed gene. NG-2 was positive with immunofluorescence, more in HRMVPC than in ASC, independent of EC coculture (**Figure 4D**), but not detectable by flow cytometry [not detectable by extra- or intracellular staining, most probably related to trypsinization (Schmitt et al., 2018)]. As shown before, those ASC wrapping around the tubular structures in the CC angiogenesis assay were strongly positive for α-SMA (**Figure 4D**). In line with the lack of angiogenenic tube formation, this did not occur in HRMVPC/HRMVEC CC angiogenesis cultures. In monocultures, α-SMA expression was weak and restricted to a fraction of ASC and also of HRMVPC. The gene expression data clearly demonstrated RGS5 as a differentially expressed pericyte marker (**Figure 4A**). However, we were not able to assess RGS5 protein expression by flow cytometry or immunofluorescence since negative results were obtained even in the expected positive controls.

Overall these data demonstrate marked differences in gene expression profiles and document a considerable degree of heterogeneity in ASC and HRMVPC cultures, with an overlap of the expressed markers.

Conditioned Medium Composition Differs Significantly Between ASC and HRMVPC

To explain the different effects of CM ASC and HRMVPC within the angiogenesis assays, we further addressed the differential gene expression of secreted angiogenic and anti-angiogenic/angiostatic factors. Zooming into angiogenesis-related genes (based on a NCBI gene query with "angiogenesis AND 'Homo sapiens' [porgn:__txid9606]"), we found 450 differentially expressed genes within the microarray data sets. *ANGPT1*, *EDN1*, ephrin-B2 (*EFNB2*), Bcl-2-like 1 (*BCL2L1*), and transforming growth factor-beta 2 (*TGFB2*) stood out in HRMVPC, whereas interleukin 6 (*IL-6*) and *VEGF-A* were most upregulated in ASC (**Supplementary Figures S4A",B"**). *TGFB1* and *TGFB3* were also higher in ASC, but at the significant limit.

To validate these results, we quantified the angiogenesis-related growth factors in the CM of ASC and HRMVPC mono- and CC angiogenesis cocultures. We observed some donor-dependent variability, but a paired analysis revealed significant changes that support the gene expression data. In fact, ASC showed a significantly higher production of VEGF in monocultures, which decreased in cocultures, indicating its use ($p \leq 0.0001$, **Figure 5A**). The values exceeded those in HRMVPC cultures ($p \leq 0.05$). The Ang-1 levels, in contrast, were highest in HRMVPC cocultures, which were 2.8-fold higher than in the ASC cocultures ($p \leq 0.05$, **Figure 5B**). The Ang-2 levels increased in both ASC and HRMVPC cocultures compared to those in the monocultures (3.8- and 6.3-fold, respectively, non-significant, **Figure 5C**). Placental growth factor (PlGF), low in all other conditions, was significantly higher in the ASC cocultures ($p \leq 0.001$, **Figure 5D**). The levels of epidermal growth factor (EGF) were high in HRMVEC monocultures but low in all other conditions (non-significant, **Figure 5E**). The PECAM-1 levels were highest in HRMVEC monocultures, significantly reduced in cocultures, and very low in ASC and HRMVPC monocultures ($p \leq 0.01$, **Figure 5F**). The IL-6 levels were significantly increased in ASC cocultures compared to their respective monocultures ($p \leq 0.05$, **Figure 5G**). IL-8 and fibroblast growth factor-beta (FGFb) remained unaffected by the culture condition (**Figures 5H,I**). Importantly, only EGF and FGFb were detectable in ¼ ECGM-2 tested as control. These data suggest that VEGF and PlGF are potential candidates for the observed ASC pro-angiogenic potential, and Ang-1 is a candidate for the HRMVPC anti-angiogenic/angiostatic effects.

VEGFR-2 Inhibition Efficiently Abolishes ASC Angiogenic Supportive Capacities

Especially the high levels of VEGF in ASC/HRMVEC cocultures and Ang-1 in HRMVPC cocultures are in line with their known pro- and anti-angiogenic effects and prompted us to investigate these in more detail. As observed previously (**Figure 3B**), $VEGF_{165}$ had similar effects as CM ASC in promoting tube formation (**Figures 6A,C**). Using suramin as an inhibitor of angiogenesis, the BM matrix dissolved and EC grew to monolayers without forming tube-like structures (not shown). Similar observations were made previously (Prigozhina et al., 2013). Therefore, instead of using suramin, we added the selective VEGFR-2 inhibitor ZM 3238811, which abolished the supportive effect of $VEGF_{165}$ in the ASC coculture angiogenesis assay ($p \leq 0.05$, **Figure 6A**). ZM 3238811 likewise significantly abolished the supportive effect of CM ASC ($p \leq 0.05$, **Figures 6B,C**). As expected, HRMVPC showed no effect on EC tube formation and thus were rather unaffected by the VEGFR-2 inhibitor. Interestingly, in the CC angiogenesis assays on ASC, the inhibitor reduced the network formation affected by CM HRMVPC even further. The inhibitory effect of CM HRMVPC again appeared to be only transient because the branch point values started to increase slightly after 48 h in the ASC cocultures (**Figure 6B**). We verified that the inhibitor did not compromise EC viability. These data suggest that VEGF/VEGFR-2 signaling is required for the pro-angiogenic function of ASC.

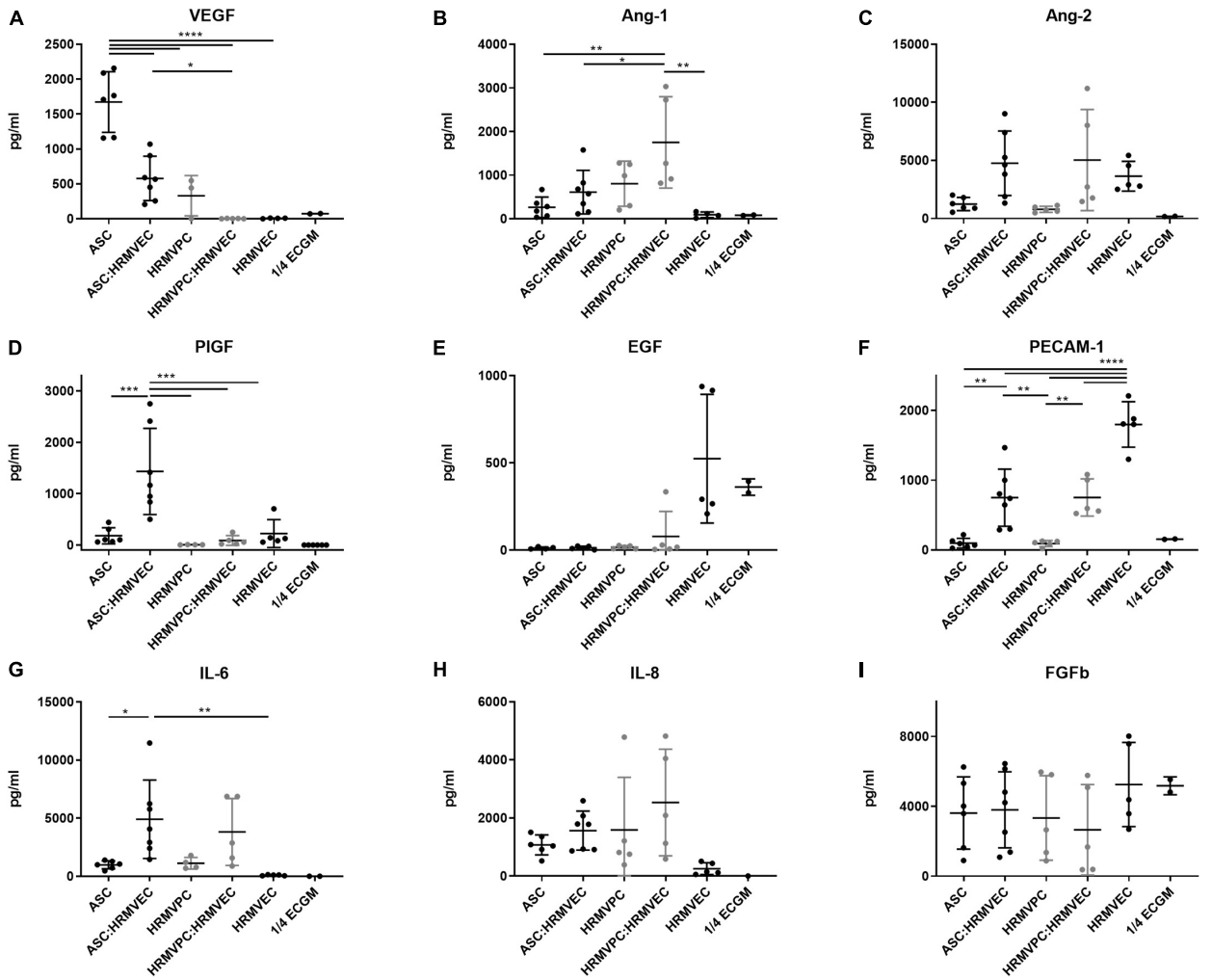

FIGURE 5 | Conditioned medium composition differs significantly between adipose-derived stromal cells (ASC) and human retinal microvascular pericytes (HRMVPC). Angiogenic growth factor levels **(A–I)** of conditioned cell culture supernatants (CM) of mono- or cocultures measured by flow cytometry-based plex assay (*$p \leq 0.05$, **$p \leq 0.01$, ***$p \leq 0.001$, and ****$p \leq 0.0001$, one-way ANOVA with Tukey's *post hoc* test) (ASC from six different donors, HRMVPC from two different donors in independent experiments, 1/4 ECGM-2 $n = 2$ independent experiments).

We considered Ang-1 as an anti-angiogenic effector in CM HRMVPC. However, both Ang-1 and Ang-2—used as control—slightly increased tube formation in the control medium (non-significant, **Figure 6D**). Ang-1 failed to reduce the pro-angiogenic function of CM ASC. In only one culture (Δ), Ang-1 inhibited the pro-angiogenic effect of CM ASC. Other CM ASC showed an even increased angiogenic effect upon adding Ang-1. A similar trend was also found in HRMVPC, where Ang-1 led to a small increase in branching tubular networks. These data suggest that HRMVPC use other/further anti-angiogenic/angiostatic factors than just Ang-1.

DISCUSSION

Diabetic retinopathy is a frequent diabetes-associated complication. Endothelial dysfunction ensues due to pericyte loss. ASC have been suggested as protective and regenerative cellular therapy and functional replacement of pericytes. Indeed the use of ASC in several different animal models of DR brought positive results, preventing retinal degeneration and vessel dysfunction. However, the exact mode of action of MSC in the retinal microenvironment is still unclear. The pericyte-like function and the pro-angiogenic potential are the most likely candidates. To support evidence for this, we compared the pro-angiogenic and the pericyte-like features of ASC and HRMVPC. Our results showed that ASC and HRMVPC: (1) differ in morphology, growth potential, and gene and protein expression (**Figures 1**, **4**), (2) show marked heterogeneity with significantly different percentages of marker-positive cells (**Figure 4**), (3) exhibit different interaction with HG-conditioned EC ECM, mimicking the DR microenvironment (**Figure 2**), and (4) can be clearly discriminated by their angiogenic activity, which involves VEGF, but probably not Ang-1 (**Figures 3–6**).

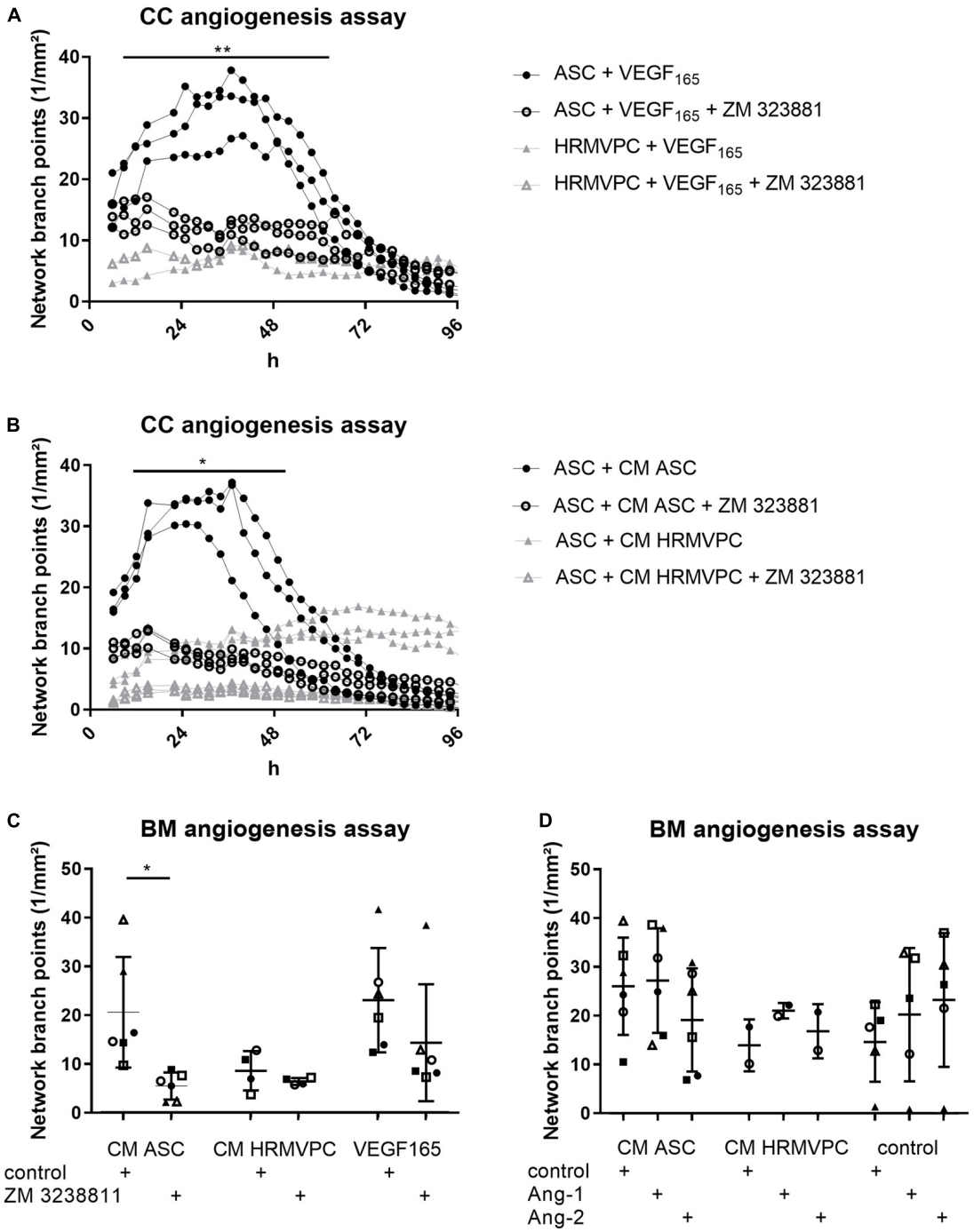

FIGURE 6 | VEGFR-2 inhibition efficiently abolishes adipose-derived stromal cells (ASC) angiogenic supportive capacities, whereas Ang-1 and Ang-2 addition do not alter effects. **(A)** Vascular network formation in CC angiogenesis assay. VEGF and the VEGF inhibitor ZM 3238811 were added to ASC-human retinal microvascular endothelial cell (HRMVEC) or human retinal microvascular pericyte (HRMVPC)/HRMVEC cocultures (three different ASC donors and one HRMVPC donor; $^{**}p \leq 0.01$, two-way RM-ANOVA with Tukey's *post hoc* test). **(B)** Vascular network formation in CC angiogenesis assay. CM ASC or CM HRMVPC are added to ASC/HRMVEC cocultures with the VEGF inhibitor ZM 323881 (three different ASC donors; $^{*}p \leq 0.05$, two-way RM-ANOVA with Tukey's *post hoc* test). **(C)** Vascular network formation in BM angiogenesis assay assessing CM ASC, CM HRMVPC, and $VEGF_{165}$ in the absence and the presence of the VEGF inhibitor ZM 323881 (different ASC donors indicated by different symbols; $^{*}p \leq 0.05$, two-way ANOVA with Sidak's *post hoc* test). **(D)** Vascular network formation in BM angiogenesis assay assessing CM ASC, CM HRMVPC, and control condition in the absence and the presence of recombinant Ang-1 or Ang-2 (different ASC donors or independent HRMVPC experiments indicated by different symbols; non-significant, two-way ANOVA with Tukey's *post hoc* test).

These properties support the use of ASC as cell-based therapy in DR but also raise potential concerns that call for a careful risk-to-benefit analysis.

Distinction Between ASC and HRMVPC

Until now, there is no clear distinction possible between MSC/ASC and pericytes. There is an intense discussion about the *in vivo* identity of MSC that appear to reside in a perivascular location similar to pericytes (Meirelles et al., 2006; Crisan et al., 2008). Perivascular cells express both MSC markers and pericyte markers. Functional tests led to regard MSC as progenitors of pericytes (Crisan et al., 2008; Meirelles et al., 2015; da Silva Meirelles et al., 2016; de Souza et al., 2016; Guimaraes-Camboa et al., 2017; Hardy et al., 2017). Comparing ASC and HRMVPC, we observed differences in morphology and growth potential. In addition, we found a set of differentially expressed genes with a good correlation between microarray and PCR array results. The protein expression analyses, however, resulted in a poor correlation to gene expression, similar to previous reports (Vogel and Marcotte, 2012). Marker expression confirmed a distinct heterogeneity of cell cultures. Many markers were shared, but CD105, CD106, HLA-DR, CD49f, PDGFR-β, CD146, and CD248 revealed a significant variation in the percentage of marker-positive cells, which is in line with previous findings (Blocki et al., 2013; Vezzani et al., 2016).

We now provide evidence that the pro-angiogenic capacity discriminates ASC from HRMVPC. Hypothesizing that ASC may replace pericytes and restore microvascular support in DR, we first compared the interaction between ASC, HRMVPC, and EC ECM by recapitulating the DR-like environment. The significant reduced interaction of HRMVPC with HG-modified EC ECM has been taken as one possible explanation for the pericyte dropout seen in DR (Beltramo et al., 2009). We observed only a slightly impaired adhesion of HRMVPC and no signs of apoptosis. The ASC compared to HRMVPC, however, showed a significantly improved interaction with HG-modified EC ECM. As shown in a previous study (Fiori et al., 2020), the growth factors in the ECGM-2 medium protected EC from HG effects, which is why we reduced their concentration to one quarter. However, despite lowering the concentration, gene expression showed no significant changes between the NG and the HG-cultured EC. Various further analyses did not help to identify the molecular basis for HG-induced ECM changes and the differing interaction of ASC and HRMVPC. Only by using multiple particle tracking microrheology were we able to observe HG-mediated changes in the elasticity of HUVEC ECM, suggesting that the HG effect might relate to the altered mechanical properties of the ECM (Hafner et al, 2020). Whether this is related to physical processes, like osmotic shrinking, or chemical modifications, like glycation, remains to be investigated.

Comparing next the angiogenic properties of ASC and HRMVPC, we showed that the vascular network formation assays can clearly discriminate ASC from HRMVPC. Whereas the ASC induced tube formation, the HRMVPC lacked this support and even actively inhibited network formation, both in a paracrine fashion. The gene expression data supported our observations, indicating a pro-angiogenic profile for ASC and an anti-angiogenic one for HRMVPC.

In CC angiogenesis assays, the ASC underwent a pericyte-like differentiation, characterized by α-SMA-positive cells aligning to the tube-like structures, as shown previously (Merfeld-Clauss et al., 2014). These authors identified that, besides cell–cell contacts, ASC-derived VEGF and HGF and EC-derived PDGF-BB were essential for vascular network formation and linked activin-A to the localized α-SMA expression (Merfeld-Clauss et al., 2010, 2014).

The observed lack of HRMVPC to support tube formation is in line with the vessel-stabilizing function controlling EC sprouting, proliferation, and patterning of remodeling vascular networks (Orlidge and Damore, 1987; Simonavicius et al., 2012). Supporting our findings, Bodnar et al. (2013) described that pericytes, isolated from skeletal muscles, actively prevented basal lamina matrix-induced vessel formation and even induced regression of preformed vascular structures. Contrasting data, however, describe the co-assembly of EC and pericytes in 3D collagen matrices (Stratman et al., 2009). In this serum-free model, hematopoietic growth factors, such as stem cell factor, IL-3, and stromal-derived factor a, were added, which may explain the observed differences. Furthermore, Blocki et al. (2013) reported that placental pericytes were best in supporting and stabilizing the morphologically intact tube structures, comparing pericytes from different tissues, MSC and CD146(+)CD34(-) and CD146(-) BM-MSC. This may suggest that either culture conditions or source and phenotype/marker expressions define function. Interesting candidates for this may be the differentially expressed markers identified in our study. CD248/endosialin, more strongly expressed in HRMVPC than in ASC, has been linked to pericyte-mediated vascular patterning (Simonavicius et al., 2012). The α6β1 integrin/CD49f appears to be required for perivascular localization and α-SMA expression (Carrion et al., 2010, 2013). CD146 expression on MSC seems to be essential for basal lamina matrix-induced tube formation as only CD146(+)CD34(-) MSC stabilized endothelial networks and improved endothelial sprout integrity (Blocki et al., 2013).

Our data hint that soluble factors contribute to the pro- and anti-angiogenic activities of ASC and HRMVPC. We observed that the paracrine anti-angiogenic effect of CM HRMVPC appeared to be transient. The performed growth factor analysis suggested VEGF and PlGF as potential pro-angiogenic factors, significantly enriched in CM from ASC mono- and cocultures, and Ang-1 as potential anti-angiogenic factor in CM from HRMVPC cocultures. Indeed the inhibition of VEGFR-2 abolished the supportive effect of ASC and CM ASC on tube formation, indicating that VEGF/VEGFR-2 signaling is required. Furthermore, in the ASC/HRMVEC coculture, VEGFR-2 inhibition added to the CM HRMVPC effect, confirming the importance of VEGF. In line with this, VEGFR-1 (Flt1) may be involved in mediating the CM HRMVPC anti-angiogenic effect. Flt1, particularly its soluble form, is known to antagonize VEGF–VEGFR2 interaction, and by this, to modulate EC behavior (Eilken et al., 2017),

FLT1 mRNA was significantly more highly expressed by HRMVPC than by ASC.

However, we considered it more likely that Ang-1 is involved because Ang-1–Tie2 signaling is known as an important regulator of the maintenance of a quiescent EC phenotype (Teichert et al., 2017). The significantly higher levels of Ang-1 in HRMVPC cocultures suggested an anti-angiogenic function. However, tube formation was not altered upon adding rhAng-1 or rhAng-2 as control, neither in the control nor in the CM ASC setting. Given the known high complexity and plasticity of pericyte-mediated control of angiogenesis (Teichert et al., 2017), we decided to focus on CM ASC.

We observed a clear ASC donor-dependent level in tube formation, in line with our previous study. In this, we correlated the growth factor concentrations in CM of ASC to the level of vascular network support (Fiori et al., 2020). The levels of all growth factors, except for Ang-1 and VEGF, correlated positively to tube formation. Ang-1 correlated negatively and VEGF showed no correlation, which was surprising given the data shown herein that VEGF appears as the most relevant factor for ASC's pro-angiogenic activity. Unfortunately, in this study, it was not possible to perform similar correlation calculations and especially to analyze the one ASC donor that repeatedly lacked pro-angiogenic activity on its own. Taking both studies together, we propose that ASC secrete VEGF in excess and that the concentration of FGFb, PECAM-1, PlGF, Ang-1, and Ang-2—probably set off against each other—makes up the level of tube formation. In line with this, Lehman et al. (2012) defined the concentrations of 35 pg/ml VEGF, 110 pg/ml IL-8, and 2,050 pg/ml CXCL-5 to be required for angiogenesis induction. In our setting, the levels of both VEGF and IL-8 were higher in ASC mono- and cocultures than these reported minimal concentrations. Although not yet addressed, PlGF appears to be a highly interesting candidate for further investigations. PlGF was found to be increased in ASC derived from patients with coronary artery disease and diabetes mellitus type 2. These, however, exerted significantly reduced angiogenic activity due to increased anti-angiogenic factors (Dzhoyashvili et al., 2014). These data suggest a disturbed homeostasis of pro- and anti-angiogenic factors in these patients.

ASC for Cell-Based Therapy of DR

The underlying question for this study was whether ASC can functionally replace HRMVPC and restore vascular stabilization in DR. As previously introduced, ASC treatment improved visual function and delayed DR progression (Yang et al., 2010; Mendel et al., 2013; Rajashekhar et al., 2014; Ezquer et al., 2016). *In vitro* data from this and our previous studies support this since ASC (1) resist HG-stress (Hajmousa et al., 2016; Fiori et al., 2020), (2) reverse high glucose-induced reduction of angiogenesis in HRMVEC, probably by reducing the oxidative stress levels (Fiori et al., 2020) or the HG-induced proinflammatory activation of EC (Hajmousa et al., 2018), (3) show improved interaction with HG-conditioned HUVEC ECM compared to HRMVPC (shown here), (4) have a pro-angiogenic activity which discriminates them from HRMVPC (shown here), and finally (5) act as functional pericyte-like cells *in vivo* (Hajmousa et al., 2018; Terlizzi et al., 2018).

However, the pro-angiogenic activity of ASC may pose a certain risk for ASC-based therapies. The angiogenic factors are crucial for DR development and progression, with VEGF being the most relevant. That is why ocular anti-VEGF therapy has been introduced (Stitt et al., 2016). In 2017, three patients have been reported to become blind after adipose "stem cell" injection for age-related macular disease treatment (Kuriyan et al., 2017). Ocular hypertension, hemorrhagic retinopathy, vitreous hemorrhage, combined traction, and rhegmatogenous retinal detachment have been reported. Furthermore, in a non-diabetic transgenic model with damage of the neurovascular unit in the retina, intravitreal MSC injection, in fact, worsened the vascular damage by inducing cataract, increasing the loss of pericytes with subsequent retinal vasoregression, and provoking inflammatory responses (Huang et al., 2019). Furthermore, MSC-derived extracellular vesicles have been shown to impair the pericyte-stabilizing function by inducing pericyte detachment, migration, and angiogenesis *in vitro* (Beltramo et al., 2014). Non-clinical data, however, argue in favor of ASC safety and efficacy, showing that MSC readily adapt to the local milieu and orchestrate repair depending on the needs by secreting either pro- or anti-angiogenic factors. Ezquer et al. (2016) at least observed no signs of increased intraocular angiogenic growth factors, rather of the anti-angiogenic factor thrombospondin 1, and no effect on the blood vessels after ASC injection. In a model of corneal wound healing, locally administered MSC likewise efficiently reduced the angiogenic and the inflammatory processes (Oh et al., 2008). Most importantly, Mendel et al. (2013) observed that the ASC therapeutic effects were exactly the needed ones: after vessel destabilization, ASC promoted vessel regrowth, whereas pretreatment with ASC prevented capillary dysfunction. As our observations are based only on *in vitro* experiments, we consider it imperative to investigate the therapeutic mode of action and especially the timing of cell application in suitable non-clinical models in more detail to assure a safe and efficacious therapy. It is also critical to address the question whether to use autologous or allogeneic cells as Cronk et al. (2015) already documented that ASC from diabetic animals have impaired function compared to their healthy counterparts. Furthermore, it would be interesting to understand whether the pro-angiogenic activity is shared by the whole ASC population or belongs to certain subpopulations as already suggested (Blocki et al., 2013; Sherman et al., 2017; Wang et al., 2018). Defining marker combinations that attribute to the observed function may help to fine-tune the therapeutic activity of ASC. The subtypes with increased angiogenic function could be better suited for wound healing approaches, whereas the subtypes with stabilizing features might be advantageous for DR or tumor treatments. Our assay platform, in line with the gene and the protein expression data sets, offers a valuable basis for expansion.

In summary, our data support the use of ASC as candidates for a cell-based therapy in early stages of DR, suggesting that they can replace pericytes and even counteract vasoregression through

the secretion of pro-angiogenic factors, mainly VEGF. However, the ASC-mediated pro-angiogenic activity may pose a risk to disease progression toward proliferative DR. Thus, a deeper study of the pro-angiogenic capacity of ASC may represent the turning point in the development of cell-based approaches in the treatment of DR. We suggest a careful risk-to-benefit analysis, including the characterization of the pro-angiogenic factors and their interaction and the regulation of their secretion, together with the definition of the optimal time point for ASC application, to take full advantage of the ASC therapeutic features.

DATA AVAILABILITY STATEMENT

The datasets generated for this study can be found in the GSE144605.

ETHICS STATEMENT

The studies involving human participants were reviewed and approved by Mannheim Ethics Commission II. The patients/participants provided their written informed consent to participate in this study.

AUTHOR CONTRIBUTIONS

HeK, JG, KB, and AF contributed to the conception, design, acquisition, analysis, interpretation of data, and drafting of the manuscript. SU, EB, LS, MH, and CS contributed to the design and material, performed the analysis, and interpretation of the certain data. H-PH, MH, and HaK contributed to the conception, design, and financial contribution. All authors contributed to the manuscript revision and read and approved the submitted version.

FUNDING

The project was part of the International Research Training Group DIAMICOM (GRK1874-SP06) funded by the Deutsche Forschungsgemeinschaft (AF, H-PH, MH, and KB). In addition, we acknowledged the financial support of the Heidelberg Karlsruhe Strategic Partnership (HEiKA, project 3D-BRB) (KB and AF), of the DDG (JG), and of the DGTI travel fund (JG).

ACKNOWLEDGMENTS

We acknowledged the excellent technical support of the FlowCore facility (Medical Faculty Mannheim). Furthermore, we acknowledged the support of the Core Facility Live Cell Imaging Mannheim at the CBTM (DFG INST 91027/10-1 FUGG).

SUPPLEMENTARY MATERIAL

The Supplementary Material for this article can be found online at: https://www.frontiersin.org/articles/10.3389/fcell.2020.00387/full#supplementary-material

FIGURE S1 | Workflow for kinetic analysis of cell proliferation using IncuCyteZOOM. 1. Using the IncuCyteZOOM live imaging device, phase contrast images of cells are automatically collected at defined time intervals (contrast and brightness of micrographs adapted for better visibility). In general, 4 to 8 replicates are run. 2. With an automated tool, a segmentation mask is assigned that closely resembles the actual cell size, morphology and confluence state. This mask/processing definition can be refined and optimized on different selected micrographs. 3. Using this processing definition, the confluence analysis mask is cross-checked on individual micrographs for each time point and of different experiments and if required further optimized. 4. Kinetic plots of respective analyses metrics are finally generated by the IncuCyte software and results depicted as phase object confluence in percent for each time point. Raw data are exported for further evaluation. Visual confirmation is possible via export of images and movies.

FIGURE S2 | Workflow for analyzing the interaction of ASC and HRMVPC with HG-conditioned EC ECM. 1. Using the IncuCyteZOOM, the proliferation of seeded EC, cultured under NG or HG conditions, is followed (contrast and brightness of micrographs increased). Upon reaching 100% confluence, the ECM is prepared by lysing the EC. 2. Intactness of the ECM is verified by brilliant blue stain. 3. Then ASC or HRMVPC are seeded on the ECM (contrast and brightness of micrograph increased). 8 replicates were run.4. By using an optimized segmentation mask/processing definition, 5. the adhesion and proliferation kinetics are analyzed for each time point using different metrics: number of cells/image, average size of cells and percent confluence, respectively. 6. To allow for quantitative comparison between ASC and HRMVPC, confluence values were normalized against the respective NG-modified EC ECM control, values set as 1.

FIGURE S3 | Kinetic analyses of angiogenesis assays. **(A)** 1. To detect network formation, phase contrast and fluorescence images are automatically recorded at defined time intervals in the IncuCyteZOOM using the tiled field of view (FOV) imaging mode. 3 to 8 replicates were run. 2. Using the integrated Angiogenesis Analysis Module, the fluorescence signal is used to quantify assay metrics: tube length and branch points for each time point. 3. The angiogenesis algorithm assigns a segmentation mask to resemble the vascular network. Exemplary micrographs depict network formation in CC angiogenesis (3A-C) and BM angiogenesis assay (4A, B). 5. Finally, kinetic data of angiogenesis metrics are plotted and exported for further evaluation (5A, B). **(B)** Comparison of network branch points and network length used as metrics to quantify network formation.

FIGURE S4 | Differential gene expression of ASC and HRMVPC, and HUVEC cultured under normal or high glucose conditions. **(A)** Volcano plots visualizing microarray data depicting statistical significance (-log10(p-value), y-axis) versus magnitude of change (log2fold change, x-axis) of gene expression of ASC versus HRMVPC zooming into categories adhesion **(A)**, ECM **(A')** and secreted factors **(A")**, each n = 3 biological replicates. **(B)** Corresponding volcano plots of PCR array data used for validation of microarray data, separating the same categories: adhesion **(B)**, ECM **(B')** and secreted factors **(B")**, each n = 3 biological replicates. There was an overall high correlation between microarray and PCR array data (Spearman correlation $R = 0.95$, $p < 2.2e{-}16$). **(C)** Volcano plot of PCR array data comparing HUVEC cultured for 5d in normal (NG) and high glucose (HG) conditions, n = 3 biological replicates, non-significant. Volcano plots were generated using the R package ggplot2. Similar data were obtained with HRMVECs (not shown, as only n = 1 biological replicate was analyzed in 3 independent experiments).

TABLE S1 | Antibodies used for flow cytometry AF- Alexa Fluor, APC-Allophycocyanin, FITC- Fluorescein isothiocyanate, PE- Phycoerythrin.

TABLE S2 | Gene list, Custom RT2 PCR Array.

REFERENCES

Beltramo, E., Lopatina, T., Berrone, E., Mazzeo, A., Iavello, A., Camussi, G., et al. (2014). Extracellular vesicles derived from mesenchymal stem cells induce features of diabetic retinopathy in vitro. *Acta Diabetol.* 51, 1055–1064. doi: 10.1007/s00592-014-0672-1

Beltramo, E., Nizheradze, K., Berrone, E., Tarallo, S., and Porta, M. (2009). Thiamine and benfotiamine prevent apoptosis induced by high glucose-conditioned extracellular matrix in human retinal pericytes. *Diabetes Metab. Res. Rev.* 25, 647–656. doi: 10.1002/dmrr.1008

Beltramo, E., and Porta, M. (2013). Pericyte loss in diabetic retinopathy: mechanisms and consequences. *Curr. Med. Chem.* 20, 3218–3225. doi: 10.2174/09298673113209990022

Bergers, G., and Song, S. (2005). The role of pericytes in blood-vessel formation and maintenance. *Neuro Oncol.* 7, 452–464. doi: 10.1215/s1152851705000232

Bieback, K., Hecker, A., Schlechter, T., Hofmann, I., Brousos, N., Redmer, T., et al. (2012). Replicative aging and differentiation potential of human adipose tissue-derived mesenchymal stromal cells expanded in pooled human or fetal bovine serum. *Cytotherapy* 14, 570–583. doi: 10.3109/14653249.2011.652809

Bieback, K., Vinci, M., Elvers-Hornung, S., Bartol, A., Gloe, T., Czabanka, M., et al. (2013). Recruitment of human cord blood-derived endothelial colony-forming cells to sites of tumor angiogenesis. *Cytotherapy* 15, 726–739. doi: 10.1016/j.jcyt.2013.01.215

Blocki, A., Wang, Y., Koch, M., Peh, P., Beyer, S., Law, P., et al. (2013). Not all MSCs can act as pericytes: functional in vitro assays to distinguish pericytes from other mesenchymal stem cells in angiogenesis. *Stem Cells Dev.* 22, 2347–2355. doi: 10.1089/scd.2012.0415

Bodnar, R. J., Rodgers, M. E., Chen, W. C., and Wells, A. (2013). Pericyte regulation of vascular remodeling through the CXC receptor 3. *Arteriosc. Thromb. Vasc. Biol.* 33, 2818–2829. doi: 10.1161/ATVBAHA.113.302012

Bourin, P., Bunnell, B. A., Casteilla, L., Dominici, M., Katz, A. J., March, K. L., et al. (2013). Stromal cells from the adipose tissue-derived stromal vascular fraction and culture expanded adipose tissue-derived stromal/stem cells: a joint statement of the International Federation for Adipose Therapeutics and Science (IFATS) and the International Society for Cellular Therapy (ISCT). *Cytotherapy* 15, 641–648. doi: 10.1016/j.jcyt.2013.02.006

Busceti, C. L., Marchitti, S., Bianchi, F., Di Pietro, P., Riozzi, B., Stanzione, R., et al. (2017). Dickkopf-3 upregulates VEGF in cultured human endothelial cells by activating activin receptor-Like Kinase 1 (ALK1) Pathway. *Front. Pharmacol.* 8:111. doi: 10.3389/fphar.2017.00111

Carrion, B., Huang, C. P., Ghajar, C. M., Kachgal, S., Kniazeva, E., Jeon, N. L., et al. (2010). Recreating the perivascular niche ex vivo using a microfluidic approach. *Biotechnol. Bioeng.* 107, 1020–1028. doi: 10.1002/bit.22891

Carrion, B., Kong, Y. P., Kaigler, D., and Putnam, A. J. (2013). Bone marrow-derived mesenchymal stem cells enhance angiogenesis via their alpha6beta1 integrin receptor. *Exp. Cell Res.* 319, 2964–2976. doi: 10.1016/j.yexcr.2013.09.007

Cianfarani, F., Toietta, G., Di Rocco, G., Cesareo, E., Zambruno, G., and Odorisio, T. (2013). Diabetes impairs adipose tissue-derived stem cell function and efficiency in promoting wound healing. *Wound Repair Regen.* 21, 545–553. doi: 10.1111/wrr.12051

Crisan, M., Yap, S., Casteilla, L., Chen, C. W., Corselli, M., Park, T. S., et al. (2008). A perivascular origin for mesenchymal stem cells in multiple human organs. *Cell Stem Cell* 3, 301–313. doi: 10.1016/j.stem.2008.07.003

Cronk, S. M., Kelly-Goss, M. R., Ray, H. C., Mendel, T. A., Hoehn, K. L., Bruce, A. C., et al. (2015). Adipose-derived stem cells from diabetic mice show impaired vascular stabilization in a murine model of diabetic retinopathy. *Stem Cells Transl. Med.* 4, 459–467. doi: 10.5966/sctm.2014-0108

da Silva Meirelles, L., Malta, T. M., Panepucci, R. A., and Da Silva, W. A. Jr. (2016). Transcriptomic comparisons between cultured human adipose tissue-derived pericytes and mesenchymal stromal cells. *Genom. Data* 7, 20–25. doi: 10.1016/j.gdata.2015.11.009

Dai, M. H., Wang, P. L., Boyd, A. D., Kostov, G., Athey, B., Jones, E. G., et al. (2005). Evolving gene/transcript definitions significantly alter the interpretation of GeneChip data. *Nucleic Acids Res.* 33:e17.

de Souza, L. E. B., Malta, T. M., Haddad, S. K., and Covas, D. T. (2016). Mesenchymal Stem cells and pericytes: to what extent are they related? *Stem Cells Dev.* 25, 1843–1852. doi: 10.1089/scd.2016.0109

Dominici, M., Le Blanc, K., Mueller, I., Slaper-Cortenbach, I., Marini, F., Krause, D., et al. (2006). Minimal criteria for defining multipotent mesenchymal stromal cells. The International Society for Cellular Therapy position statement. *Cytotherapy* 8, 315–317. doi: 10.1080/14653240600855905

Dreher, L., Elvers-Hornung, S., Brinkmann, I., Huck, V., Henschler, R., Gloe, T., et al. (2013). Cultivation in human serum reduces adipose tissue-derived mesenchymal stromal cell adhesion to laminin and endothelium and reduces capillary entrapment. *Stem Cells Dev.* 22, 791–803. doi: 10.1089/scd.2012.0051

Dzhoyashvili, N. A., Efimenko, A. Y., Kochegura, T. N., Kalinina, N. I., Koptelova, N. V., Sukhareva, O. Y., et al. (2014). Disturbed angiogenic activity of adipose-derived stromal cells obtained from patients with coronary artery disease and diabetes mellitus type 2. *J. Transl. Med.* 12:337. doi: 10.1186/s12967-014-0337-4

Eilken, H. M., Dieguez-Hurtado, R., Schmidt, I., Nakayama, M., Jeong, H. W., Arf, H., et al. (2017). Pericytes regulate VEGF-induced endothelial sprouting through VEGFR1. *Nat. Commun.* 8:1574. doi: 10.1038/s41467-017-01738-3

Ezquer, M., Urzua, C. A., Montecino, S., Leal, K., Conget, P., and Ezquer, F. (2016). Intravitreal administration of multipotent mesenchymal stromal cells triggers a cytoprotective microenvironment in the retina of diabetic mice. *Stem Cell Res. Ther.* 7:42. doi: 10.1186/s13287-016-0299-y

Fiori, A., Hammes, H. P., and Bieback, K. (2020). Adipose-derived mesenchymal stromal cells reverse high glucose-induced reduction of angiogenesis in human retinal microvascular endothelial cells. *Cytotherapy* 22, 261–275. doi: 10.1016/j.jcyt.2020.02.005

Fiori, A., Terlizzi, V., Kremer, H., Gebauer, J., Hammes, H. P., Harmsen, M. C., et al. (2018). Mesenchymal stromal/stem cells as potential therapy in diabetic retinopathy. *Immunobiology* 223, 729–743. doi: 10.1016/j.imbio.2018.01.001

Geistlinger, L., Csaba, G., and Zimmer, R. (2016). Bioconductor's EnrichmentBrowser: seamless navigation through combined results of set- & network-based enrichment analysis. *BMC Bioinform.* 17:45. doi: 10.1186/s12859-016-0884-1

Guimaraes-Camboa, N., Cattaneo, P., Sun, Y., Moore-Morris, T., Gu, Y., Dalton, N. D., et al. (2017). Pericytes of multiple organs do not behave as mesenchymal stem cells in vivo. *Cell Stem Cell* 20:e345. doi: 10.1016/j.stem.2016.12.006

Hafner, J., Grijalva, D., Ludwig-Husemann, A., Bertels, S., Bensinger, L., Raic, A., et al. (2020). Monitoring matrix remodelling in the cellular microenvironment using microrheology for complex cellular systems. *Acta Biomater.* (in press). doi: 10.1016/j.actbio.2020.04.053

Hajmousa, G., Elorza, A. A., Nies, V. J., Jensen, E. L., Nagy, R. A., and Harmsen, M. C. (2016). Hyperglycemia induces bioenergetic changes in adipose-derived stromal cells while their pericytic function is retained. *Stem Cells Dev.* 25, 1444–1453. doi: 10.1089/scd.2016.0025

Hajmousa, G., Przybyt, E., Pfister, F., Paredes-Juarez, G. A., Moganti, K., Busch, S., et al. (2018). Human adipose tissue-derived stromal cells act as functional pericytes in mice and suppress high-glucose-induced proinflammatory activation of bovine retinal endothelial cells. *Diabetologia* 61, 2371–2385. doi: 10.1007/s00125-018-4713-0

Hammes, H. P. (2018). Diabetic retinopathy: hyperglycaemia, oxidative stress and beyond. *Diabetologia* 61, 29–38. doi: 10.1007/s00125-017-4435-8

Hardy, W. R., Moldovan, N. I., Moldovan, L., Livak, K. J., Datta, K., Goswami, C., et al. (2017). Transcriptional networks in single perivascular cells sorted from human adipose tissue reveal a hierarchy of mesenchymal stem cells. *Stem Cells* 35, 1273–1289. doi: 10.1002/stem.2599

Huang, H., Kolibabka, M., Eshwaran, R., Chatterjee, A., Schlotterer, A., Willer, H., et al. (2019). Intravitreal injection of mesenchymal stem cells evokes retinal vascular damage in rats. *FASEB J.* 33, 14668–14679. doi: 10.1096/fj.201901500R

Kern, S., Eichler, H., Stoeve, J., Kluter, H., and Bieback, K. (2006). Comparative analysis of mesenchymal stem cells from bone marrow, umbilical cord blood, or adipose tissue. *Stem Cells* 24, 1294–1301. doi: 10.1634/stemcells.2005-0342

Kuriyan, A. E., Albini, T. A., Townsend, J. H., Rodriguez, M., Pandya, H. K., Leonard, R. E., et al. (2017). Vision Loss after Intravitreal Injection of Autologous "Stem Cells" for AMD. *N. Engl. J. Med.* 376, 1047–1053. doi: 10.1056/NEJMoa1609583

Lehman, N., Cutrone, R., Raber, A., Perry, R., Van't Hof, W., Deans, R., et al. (2012). Development of a surrogate angiogenic potency assay for clinical-grade stem cell production. *Cytotherapy* 14, 994–1004. doi: 10.3109/14653249.2012.688945

Meirelles, L. D., Malta, T. M., Wagatsuma, V. M. D., Palma, P. V. B., Araujo, A. G., Malmegrim, K. C. R., et al. (2015). Cultured human adipose tissue pericytes and

mesenchymal stromal cells display a very similar gene expression profile. *Stem Cells Dev.* 24, 2822–2840. doi: 10.1089/scd.2015.0153

Meirelles, L. D. S., Chagastelles, P. C., and Nardi, N. B. (2006). Mesenchymal stem cells reside in virtually all post-natal organs and tissues. *J. Cell Sci.* 119, 2204–2213. doi: 10.1242/jcs.02932

Mendel, T. A., Clabough, E. B., Kao, D. S., Demidova-Rice, T. N., Durham, J. T., Zotter, B. C., et al. (2013). Pericytes derived from adipose-derived stem cells protect against retinal vasculopathy. *PLoS One* 8:e65691. doi: 10.1371/journal.pone.0065691

Merfeld-Clauss, S., Gollahalli, N., March, K. L., and Traktuev, D. O. (2010). Adipose tissue progenitor cells directly interact with endothelial cells to induce vascular network formation. *Tissue Eng. Part A* 16, 2953–2966. doi: 10.1089/ten.TEA.2009.0635

Merfeld-Clauss, S., Lupov, I. P., Lu, H., Feng, D., Compton-Craig, P., March, K. L., et al. (2014). Adipose stromal cells differentiate along a smooth muscle lineage pathway upon endothelial cell contact via induction of activin A. *Circ. Res.* 115, 800–809. doi: 10.1161/CIRCRESAHA.115.304026

Oh, J. Y., Kim, M. K., Shin, M. S., Lee, H. J., Ko, J. H., Wee, W. R., et al. (2008). The anti-inflammatory and anti-angiogenic role of mesenchymal stem cells in corneal wound healing following chemical injury. *Stem Cells* 26, 1047–1055. doi: 10.1634/stemcells.2007-0737

Orlidge, A., and Damore, P. A. (1987). Inhibition of capillary endothelial-cell growth by pericytes and smooth-muscle cells. *J. Cell Biol.* 105, 1455–1462. doi: 10.1083/jcb.105.3.1455

Pfister, F., Przybyt, E., Harmsen, M. C., and Hammes, H. P. (2013). Pericytes in the eye. *Pflugers Arch.* 465, 789–796.

Prigozhina, N. L., Heisel, A. J., Seldeen, J. R., Cosford, N. D. P., and Price, J. H. (2013). Amphiphilic suramin dissolves Matrigel, causing an 'inhibition' artefact within in vitro angiogenesis assays. *Int. J. Exp. Pathol.* 94, 412–417. doi: 10.1111/iep.12043

Rajashekhar, G., Ramadan, A., Abburi, C., Callaghan, B., Traktuev, D. O., Evans-Molina, C., et al. (2014). Regenerative therapeutic potential of adipose stromal cells in early stage diabetic retinopathy. *PLoS One* 9:e84671. doi: 10.1371/journal.pone.0084671

Rennert, R. C., Sorkin, M., Januszyk, M., Duscher, D., Kosaraju, R., Chung, M. T., et al. (2014). Diabetes impairs the angiogenic potential of adipose-derived stem cells by selectively depleting cellular subpopulations. *Stem Cell Res. Ther.* 5:79. doi: 10.1186/scrt468

Rouillard, A. D., Gundersen, G. W., Fernandez, N. F., Wang, Z., Monteiro, C. D., Mcdermott, M. G., et al. (2016). The harmonizome: a collection of processed datasets gathered to serve and mine knowledge about genes and proteins. *Database* 2016:baw100. doi: 10.1093/database/baw100

Schmitt, B. M., Laschke, M. W., Rossler, O. G., Huang, W. H., Scheller, A., Menger, M. D., et al. (2018). Nerve/glial antigen (NG) 2 is a crucial regulator of intercellular adhesion molecule (ICAM)-1 expression. *Biochim. Biophys. Acta* 1865, 57–66. doi: 10.1016/j.bbamcr.2017.09.019

Sherman, S. E., Kuljanin, M., Cooper, T. T., Putman, D. M., Lajoie, G. A., and Hess, D. A. (2017). High aldehyde dehydrogenase activity identifies a subset of human mesenchymal stromal cells with vascular regenerative potential. *Stem Cells* 35, 1542–1553. doi: 10.1002/stem.2612

Simonavicius, N., Ashenden, M., Van Weverwijk, A., Lax, S., Huso, D. L., Buckley, C. D., et al. (2012). Pericytes promote selective vessel regression to regulate vascular patterning. *Blood* 120, 1516–1527. doi: 10.1182/blood-2011-01-332338

Stitt, A. W., Curtis, T. M., Chen, M., Medina, R. J., Mckay, G. J., Jenkins, A., et al. (2016). The progress in understanding and treatment of diabetic retinopathy. *Prog. Retin. Eye Res.* 51, 156–186. doi: 10.1016/j.preteyeres.2015.08.001

Stitt, A. W., O'neill, C. L., O'doherty, M. T., Archer, D. B., Gardiner, T. A., and Medina, R. J. (2011). Vascular stem cells and ischaemic retinopathies. *Prog. Retin. Eye Res.* 30, 149–166. doi: 10.1016/j.preteyeres.2011.02.001

Stratman, A. N., Malotte, K. M., Mahan, R. D., Davis, M. J., and Davis, G. E. (2009). Pericyte recruitment during vasculogenic tube assembly stimulates endothelial basement membrane matrix formation. *Blood* 114, 5091–5101. doi: 10.1182/blood-2009-05-222364

Teichert, M., Milde, L., Holm, A., Stanicek, L., Gengenbacher, N., Savant, S., et al. (2017). Pericyte-expressed Tie2 controls angiogenesis and vessel maturation. *Nat. Commun.* 8:16106. doi: 10.1038/ncomms16106

Terlizzi, V., Kolibabka, M., Burgess, J. K., Hammes, H. P., and Harmsen, M. C. (2018). The pericytic phenotype of adipose tissue-derived stromal cells is promoted by NOTCH2. *Stem Cells* 36, 240–251. doi: 10.1002/stem.2726

Vezzani, B., Pierantozzi, E., and Sorrentino, V. (2016). Not all pericytes are born equal: pericytes from human adult tissues present different differentiation properties. *Stem Cells Dev.* 25, 1549–1558. doi: 10.1089/scd.2016.0177

Vogel, C., and Marcotte, E. M. (2012). Insights into the regulation of protein abundance from proteomic and transcriptomic analyses. *Nat. Rev. Genet.* 13, 227–232. doi: 10.1038/nrg3185

Wang, S., Mo, M. H., Wang, J. M., Sadia, S., Shi, B. H., Fu, X. B., et al. (2018). Platelet-derived growth factor receptor beta identifies mesenchymal stem cells with enhanced engraftment to tissue injury and pro-angiogenic property. *Cell. Mol. Life Sci.* 75, 547–561. doi: 10.1007/s00018-017-2641-7

Yang, Z., Li, K., Yan, X., Dong, F., and Zhao, C. (2010). Amelioration of diabetic retinopathy by engrafted human adipose-derived mesenchymal stem cells in streptozotocin diabetic rats. *Graefes Arch. Clin. Exp. Ophthalmol.* 248, 1415–1422. doi: 10.1007/s00417-010-1384-z doi: 10.1007/s00417-010-1384-z

Conflict of Interest: The authors declare that the research was conducted in the absence of any commercial or financial relationships that could be construed as a potential conflict of interest.

frontiers in Cell and Developmental Biology

ORIGINAL RESEARCH
published: 16 June 2020
doi: 10.3389/fcell.2020.00458

Human Mesenchymal Stromal Cell (MSC) Characteristics Vary Among Laboratories When Manufactured From the Same Source Material: A Report by the Cellular Therapy Team of the Biomedical Excellence for Safer Transfusion (BEST) Collaborative

*David F. Stroncek[1,2], Ping Jin[1], David H. McKenna[2,3], Minoko Takanashi[2,4], Magali J. Fontaine[2,5], Shibani Pati[2,6], Richard Schäfer[2,7], Emily Peterson[8], Eric Benedetti[8] and Jo-Anna Reems[2,8]**

[1] Cell Processing Section, Department of Transfusion Medicine, Clinical Center, National Institutes of Health, Bethesda, MD, United States, [2] Biomedical Excellence for Safer Transfusion (BEST), Lebanon, NH, United States, [3] Molecular and Cellular Therapeutics, University of Minnesota, Minneapolis, MN, United States, [4] Center for Stem Cell Biology and Regenerative Medicine, The Institute of Medical Science, The University of Tokyo, Tokyo, Japan, [5] University of Maryland School of Medical Science, Baltimore, MD, United States, [6] University of California, San Francisco, San Francisco, CA, United States, [7] Institute for Transfusion Medicine and Immunohaematology, German Red Cross Blood Donor Service Baden-Württemberg-Hessen gGmbH, Goethe University Hospital, Frankfurt, Germany, [8] Cell Therapy and Regenerative Medicine Facility, University of Utah, Salt Lake City, UT, United States

Background: Culture-derived mesenchymal stromal cells (MSCs) exhibit variable characteristics when manufactured using different methods and different source materials. The purpose of this study was to assess the impact on MSC characteristics when different laboratories propagated MSCs from cultures initiated with BM aliquots derived from the same donor source material.

Methods and Methods: Five aliquots from each of three different BM donors were distributed to five independent laboratories. Three laboratories plated whole BM and two laboratories a mononuclear BM cell fraction. Four laboratories cultured in media supplemented with fetal bovine serum (FBS) and one laboratory used human platelet lysate (hPL). Initial cell seeding densities (i.e., P0) ranged from $19.7 \times 10^3/cm^2$–$282 \times 10^3/cm^2$ and for second seeding (i.e., P1) 0.05×10^3–5.1×10^3 cells/cm^2. Post-thawed MSCs from each laboratory were analyzed for cell viability, immunophenotype, tri-lineage differentiation, fibroblast colony-forming units (CFU-F), gene expression, and immunosuppressive activity.

Results: Transit times from BM collection to receipt by laboratories located in the United States ranged from 16.0–30.0 h and from 41.5–71.5 h for a laboratory in Asia. Post-thaw culture derived MSCs rom BM #1, #2, and #3 exhibited viabilities that ranged from 74–92%, 61–96%, and 23–90%, respectively. CFU activity from BM #1, #2, and

OPEN ACCESS

Edited by:
Marcela F. Bolontrade, Consejo Nacional de Investigaciones Científicas y Técnicas (CONICET), Argentina

Reviewed by:
Antonietta Rosa Silini, Fondazione Poliambulanza Istituto Ospedaliero, Italy
Katharina Schallmoser, Universitätsklinikum Salzburg, Austria

***Correspondence:**
Jo-Anna Reems
joanna.reems@hsc.utah.edu

Specialty section:
This article was submitted to Stem Cell Research, a section of the journal Frontiers in Cell and Developmental Biology

Received: *26 February 2020*
Accepted: *18 May 2020*
Published: *16 June 2020*

Citation:
Stroncek DF, Jin P, McKenna DH, Takanashi M, Fontaine MJ, Pati S, Schäfer R, Peterson E, Benedetti E and Reems J-A (2020) Human Mesenchymal Stromal Cell (MSC) Characteristics Vary Among Laboratories When Manufactured From the Same Source Material: A Report by the Cellular Therapy Team of the Biomedical Excellence for Safer Transfusion (BEST) Collaborative. Front. Cell Dev. Biol. 8:458. doi: 10.3389/fcell.2020.00458

#3 per 200 MSCs plated averaged 45.1 ± 21.4, 49.3 ± 26.8 and 14.9 ± 13.3, respectively. No substantial differences were observed in immunophenotype, and immunosuppressive activities. Global gene expression profiles of MSCs revealed transcriptome differences due to different inter-laboratory methods and to donor source material with the center effects showing greater molecular differences than source material.

Conclusion: Functional and molecular differences exist among MSCs produced by different centers even when the same BM starting material is used to initiate cultures. These results indicated that manufacturing of MSCs by five independent centers contributed more to MSC variability than did the source material of the BM used in this study. Thus, emphasizing the importance of establishing worldwide standards to propagate MSCs for clinical use.

Keywords: mesenchymal stromal cells, bone marrow, variability, quality, transcriptome

INTRODUCTION

MSCs are a diverse population of cells that are under investigation for the treatment of a wide range of diseases and disorders that include graft-versus-host disease (GvHD) (Le Blanc et al., 2008), stroke, (Lalu et al., 2019) Crohn's disease (Forbes, 2017), osteogenesis imperfect (Horwitz et al., 1999), osteoarthritis, (Migliorini et al., 2019) multiple sclerosis (Uccelli et al., 2019), and cardiovascular disease (Yun and Lee, 2019). The possibility of using MSCs to treat such a wide range of conditions is likely attributable to the broad spectrum of biological effects that can be exerted by MSCs via the secretion of paracrine factors such as cytokines, chemokines, and exosomes (Phinney and Pittenger, 2017) or by MSC apoptosis (Galleu et al., 2017). Because MSCs possess these qualities, they are reported to modulate the immune response, reduce inflammation and support tissue repair by promoting cell-to-cell interactions and cellular proliferation (Phinney et al., 2015; Fontaine et al., 2016; Bagno et al., 2018).

Among the first reported successful uses of MSCs was for the treatment of a patient with severe acute GvHD (Le Blanc et al., 2004). Since then, additional reports have surfaced indicating that treatment with allogeneic MSCs can achieve complete responses or show improvement in GvHD (Le Blanc et al., 2008; Prasad et al., 2011; Ball et al., 2013). However, a recent comprehensive review of completed randomized clinical trials (RCTs) that used MSCs for the treatment of GvHD found that MSCs might have little or no effect (Fisher et al., 2019). The RCT results do not support the general conclusion that MSCs are an effective therapy for steroid-refractory acute GvHD despite previously reported positive outcomes (Fisher et al., 2019). The discrepancies found in the effectiveness of using MSCs in clinical studies may be due to the overall quality of the study design (Fisher et al., 2019), the source of MSCs, and/or to differences associated with manufacturing MSCs (Regmi et al., 2019).

At present there is no standardized protocol for culturing MSCs, but more importantly there is no acceptable potency assay for the release of MSCs for clinical therapies that predict their *in vivo* efficacy (Bieback et al., 2019). MSCs are isolated from a number of different tissue source materials (e.g., BM, adipose tissue, placental tissue, etc.) and are manufactured with different culture or preconditioning strategies (Schafer et al., 2016; Bieback et al., 2019). Some of the noted culture variables include the use of different tissue source materials for the same application, different basal medium formulations, medium supplementation, initial seeding densities, the number of passages, and the length of time MSCs are maintained in culture and frozen. Moreover, MSCs from different tissue origin as well as between BM donors may vary in gene expression, phenotype and *in vitro* function (Siegel et al., 2013; Wegmeyer et al., 2013), but the relevance of these heterogeneity generators remains unclear.

The purpose of this study was to focus on determining how much variability was associated with inter-laboratory manufacturing strategies of MSCs when the tissue source material (i.e., BM donations) used to manufacture MSCs was held constant. To address this goal, the study design was to distribute aliquots of the same tissue source material (i.e., BM collections) from three different BM donors, to five independent laboratories. Each laboratory would then use their own MSC isolation and culture strategy to manufacture and cryopreserve the MSCs. The frozen MSCs were sent to a centralized laboratory to assess their characteristics and *in vitro* function.

MATERIALS AND METHODS

Study Design

Single 50–60 mL BM aspirates from the iliac crest were collected from three different volunteer male donors after obtaining informed consent (Lonza Walkersville, Inc., Walkersville, MD,

Abbreviations: 7-AAD, 7-aminoactinomycin D; APC, allophycocyanin; Best, Biomedical Excellence in Safer Transfusion; BM, bone marrow; CFU-F, colony forming unit-fibroblast; FBS, fetal bovine serum; FITC, fluorescein isothiocyanate; GvHD, graft-versus-host disease; hPL, human platelet lysate; LN2, liquid nitrogen; MLR, mixed lymphocyte reaction; MNC, mononuclear cell; MSC, mesenchymal stromal cell; P#, passage number; PCA, principal component analysis; PD, population doubling; PE, phycoerythrin; RCT, randomized control trials.

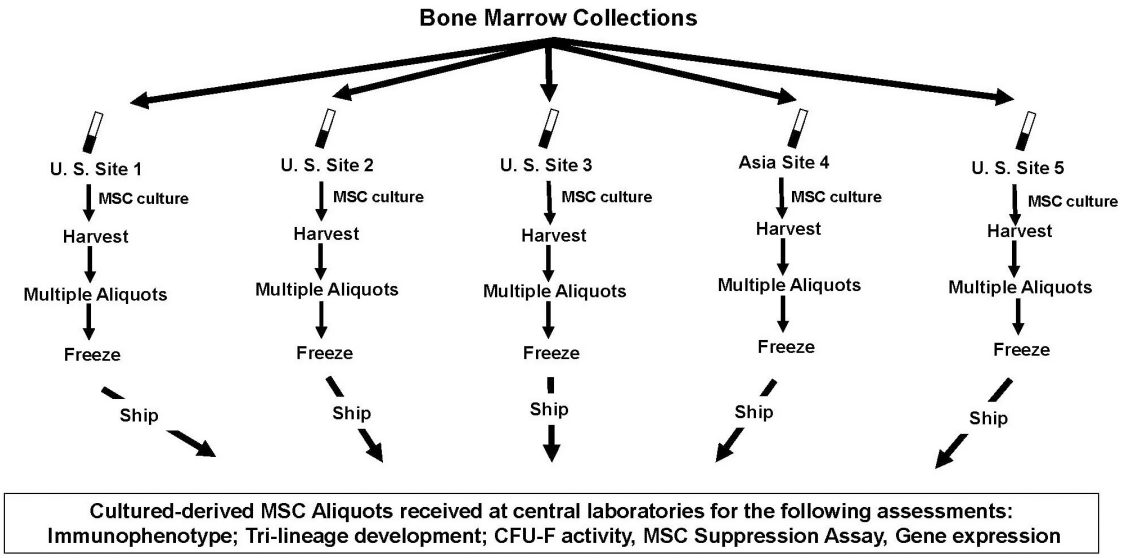

FIGURE 1 | Study design. BM was collected and was divided into 10 mL aliquots (~200 × 10^6 MNC) and from three different donors at three different times by staff at Lonza in Walkersville, MD. Aliquots were shipped overnight to four sites located in the United States to site #4, located in Japan. Upon arrival of the BM aliquots at each site, MSC cultures were initiated according to each site's method for culturing cells. After culturing, the MSCs were harvested, and were then cryopreserved in multiple cryovial aliquots; cryovial aliquots were frozen, and then were sent to centralized labs to perform immunophenoytping, tri-lineage differentiation potential, CFU-F quantification, gene arrays, and MSC immunomodulation.

United States) (**Figure 1**). BM donors #1, #2, and #3 were 21, 24, and 20 years old, respectively. The bone marrow aspirates from each of the first 2 donors, BM #1 and BM #2 were divided into 5 aliquots and BM aspirate from the 3rd donor, BM #3, was divided into six aliquots of approximately 10 mL each. Four sites (#1, #2, #3, and #4) received 1 aliquot of marrow aspirate from all 3 donors; while site #5 received 1 aliquot from BM #1 and BM #2 and 2 aliquots from BM #3. All BM aliquots were shipped to participating facilities, four of which were located within the United States and one site in Japan. FedEx conducted overnight shipments to the United States participating sites using containers with insulated packaging to maintain ambient temperature. Shipment to Japan was facilitated by MNX Global Logistics (Irvine, CA, United States) using the Evo Smart shipper (BioLife Solutions, Bothell, WA, United States) to maintain ambient temperature. Upon arrival of the BM aspirate, each site plated the BM using their own methodology to produce MSC preparations in culture.

MSC Expansion and Cryopreservation

Cell viability and cell count assessments, culture expansions and cryopreservation were performed according to each individual sites preferred method (**Tables 1**–**3**). For all three BM aspirates, two of the sites (site #2 and #3) plated cells from whole BM and two sites (site #1 and #4) plated cells from a mononuclear cell (MNC) fraction (**Table 2**). Site #5 plated whole BM for all three BM aspirates and received an additional BM aliquot from BM donor #3, which they plated cells from a MNC fraction (**Table 2**). Initial and subsequent passage seeding densities are indicated in **Table 3**. The adherent cells were cultured according to each sites' in-house protocol and upon reaching confluence; the cells were harvested and passaged as indicated in **Tables 2**, **3**. Four sites used fetal bovine serum (FBS) as media supplement, and one site used hPL (Cell Xpand^{TM}, University of Utah) (**Table 2**). At the end of each passage, cell counts and viabilities were performed and the number of population doublings (PDs) were calculated according to the following equation: PD(hrs) = t log 2/(log Nf/Ni), where PD = population doubling, t = time in culture, Nf = number of cells harvested, Ni = number of cells seeded. At the end of the culture period, each site prepared multiple aliquots of MSCs and used their own cryopreservation method to freeze the cultured-derived MSCs at a concentration that ranged from 1.0 × 10^6 to 10 × 10^6 cells/mL (**Table 4**). Laboratories routinely tested for bacterial and mycoplasma contamination. Cryopreserved cells were maintained in LN2 storage until they were shipped in LN2 to centralized testing laboratories where they were analyzed for immunophenotype, tri-lineage differentiation potential, CFU-F activity, gene expression, and immunosuppressive activity.

Immunophentyping

Evaluation of post-thaw MSCs generated in culture at each of the 5 sites was conducted by a centralized facility using flow cytometry to determine the expression or lack of expression of surface markers for CD105, CD73, CD90, CD45, CD14, CD34, HLA-DR, and Stro-1. Approximately 250,000 cells were transferred into each of five separate tubes. Cells from one tube were stained with primary antibodies, anti-CD73 conjugated to allophycocyanin (APC) (BD Biosciences), anti-CD90 fluorescein isothiocyanate (FITC) (BD Biosciences) and anti-CD105 phycoerythrin (PE) (Miltenyi Biotec). In a second tube, cells were triple stained with anti-CD45, anti-CD34, and anti-CD14 that were all conjugated with PE-Cy^{TM}5 (BD

TABLE 1 | Cell counting methods used by each site.

	Site #1		Site #2		Site #3		Site #4		Site #5	
	Cell Count	**Viability**	**Cell Count**	**Viability**	**Cell Count**	**Viability**	**Cell Count**	**Viability**	**Cell Count**	**Viability**
Whole BM	Automated (SysmexXS-1000i)	Fluorescent microscope (AO/PI)	Automated (Ad via 1200)	Flow Cytometry (7-AAD)	Manual (hemacytometer)	Light microscope (trypan blue)	Manual (hemacytometer)	Light microscope (trypan blue)	Automated (sysmexXE-5000)	Cellometer (AO/PI)
Passaged Cells	Automated (Sysmex XS-1000i)	Fluorescent microscope (AO/PI)	Cellometer (AO/PI)	Cellometer (AO/PI)	Manual (hemacytometer)	Light microscope (trypan blue)	Manual (hemacytometer)	Light microscope (trypan blue)	Manual (hemacytometer)	Light microscope (trypan blue)

TABLE 2 | Comparison of MSC culture components used by each of the five sites.

Components	Site #1	Site #2	Site #3	Site #4	Site #5
Cells plated	MNC	Whole BM	Whole BM	MNC	Whole BM or MNC
Basal medium	αMEM	αMEM	αMEM	MEM-Eagle	DMEM
Serum supplement	16% FBS	20% FBS	10% FBS	16.5% FBS	10% PL-S
Additional supplements	GlutaMAX	None	L-glutamine	L-glutamine	GlutaMAX
Antibiotics	None	Gentamicin	Pen/Strep	Pen/Strep	Pen/Strep

MNC, ficoll preparation; aMEM, minimum essential medium eagle alpha modification; DMEM, dulbecco's modified eagle medium; FBS, fetal bovine serum; PL-S, serum based platelet lysate; glutaMAX an alternative to L*-glutamine; Pen/Strep, penicillin streptomycin.*

Biosciences). In a third tube cells were stained with anti-Stro1 APC (BioLegend) and anti-HLA-DR FITC (BD Biosciences). Additional tubes were stained with isotype controls and one tube was left unstained as a control. All tubes included the use of 7-aminoactinomycin D (7-AAD) to evaluate cells for viability. Following staining, the cells were washed with PBS-BSA, resuspended in PBS-BSA, and were analyzed on a BD FACSCanto (BD Biosciences) flow cytometer.

Tri-Lineage Differentiation Potential

Adipogenesis, osteogenesis, and chondrogenesis differentiation *in vitro* assays were performed by a centralized laboratory using commercially available StemPro™ kit adipogenesis, StemPro™ kit chondrogenesis and Gibco™ kit osteogenesis as per the manufacturer's differentiation assay protocols. Briefly, cells from each MSC preparation provided by each site were washed and resuspended using Gibco™ MesenPro RS medium (ThermoFisher Scientific). Cells from each MSC preparation were then seeded into four wells (one control well to remain undifferentiated, plus three conditional replicates) of a 12-well tissue-culture plate. Adipogenic (and control) wells were seeded at 1×10^4 cells/cm^2. Osteogenic (and control) wells were seeded at 5×10^3 cells/cm^2. MSC cultures were incubated at 37°C in a humidified atmosphere of 5% CO_2 for 48–50 h, then MesenPro RS medium in the triplicate conditional wells was removed and replaced with either adipogenesis or osteogenesis differentiation medium (StemPro™ kit). The cultures were continued for 12 (adipogenic) or 18–20 (osteogenic) more days. Differentiation medium was exchanged every 2–3 days. Control wells received MesenPro RS media exchanges concurrently as the conditional wells received osteogenesis or adipogenesis media exchanges.

Chondrogenic (and control) wells were each seeded with five "micromass" 5-μL droplets of cells concentrated at 1.6×10^7 cells/mL. Cells were maintained at 37°C in a humidified atmosphere of 5% CO_2 for two hours, after which the StemPro™ Differentiation kit chondrogenesis medium (ThermoFisher Scientific) was added to the triplicate conditional wells and MesenPro RS medium to the controls. Micromass/medium cultures were maintained at 37°C/5% CO_2 for 21 days. Differentiation medium was exchanged every 2–3 days. Control wells received MesenPro RS media exchanges concurrently with

TABLE 3 | Plating densities for each marrow preparation by site and passage.

Culture vessel type and passage number	Number of cells plated/cm^2 (Average ± SD)				
	*Site #1	*Site #2	*Site #3	*Site #4	*Site #5
Culture vessel type	Cell stack	Flasks	Flasks	15 cm dishes	Flasks
Initial seeding to obtain P0 MSCs	136,667 ± 23,094	282,000 ± 5,292	200,407 ± 43,808	19,737 ± 0	240,478 ± 38,708
Second seeding of P0 MSCs to obtain PI MSCs	50 ± 1	3,165 ± 1	2,500 ± 707	2,758 ± 4,425	2,776 ± 1,807
Third seeding of P1 MSCs to obtain P2 MSCs		3,165 ± 1	*4,055		**2,336 ± 232
Fourth seeding of P2 MSCs to obtain P3 MSCs		3,164 ± 1			***2,000

**Average ± Std. Dev. n = 3; **n = 2; ***n = 1.*

TABLE 4 | Cryopreservations methods used by each site.

	Site #1	Site #2	Site #3	Site #4	Site #55
Cell concentration	1–10 × 10^6 Cells/mL	1–10 × 10^6 Cells/mL	1.5–5 × 10^6 Cells/mL	5 × 10^6 Cells/mL	1–5 × 10^6 Cells/mL
Final Freezing Solution	30% Plasmalyte-A, 10% DMSO, 2.5% Human serum albumin	Plasmalyte A, 6% Pentastarch, 5% DMSO, 2%, Human serum albumin	60% D-MEM, 30% Hyclone FBS, 10% DMSO	MEM-Eagle 15% FBS, 10% DMSO	90% FBS, 10% DMSO
Freezing Method	Control Rate Freezer	Mr. Frosty Freezing Container	Mr. Frosty Freezing Container	No Container	Mr. Frosty Freezing Container
	Start Chamber = 0.0°C; Sample = 1.0°C	−80°C O/N; transfer to LN2 freezer	−80°C O/N; transfer to LN2 freezer	−80°C O/N; maintain in −80°C freezer	−80°C O/N; transfer to LN2 freezer
	Ramp 1.0°C/min until Sample = –12.0°C				
	Ramp 20.0°C/min until Chamber = –60.0°C				
	Ramp 15.0°C/min until Chamber = –18.0°C				
	Ramp 1.0°C/min until Sample = –60.0°C				
	Ramp 3.0°C/min until Sample = –100.0°C				
	End and transfer to LN2 Freezer				
Storage freezer	LN2	LN2	LN2	−80°C	LN2

the conditional wells receiving osteogenic or adipogenic media exchange. Control wells received MesenPro RS media exchanges concurrently as the conditional wells received chondrogenesis media exchanges.

Control and differentiated cell cultures were fixed with 10% formalin, and then stained with Oil Red O (adipogenesis), Alizarin Red S (osteogenesis) or Alcian Blue (chondrogenesis) dyes (all from Sigma-Aldrich). Differentiation of cells (or lack thereof) was then scored by three different staff members via visualization under an inverted light microscope from zero to four plus. A score of zero was equal to no differentiation while a score of 4+ was equal to maximum differentiation. A final score was determined as an average of the three scores as assigned by the observers.

Fibroblast Colony-Forming Unit Assay

To determine relative Colony-Forming Unit (CFU-F) activity of for each MSC preparation, a centralized facility received frozen cultured-derived MSCs from each of the five sites derived from BM#1, BM#2, and BM#3. The centralized laboratory thawed and plated the MSCs in triplicate into 6 well plates. Each well was plated with 200 MSCs in a total of 2 mL of MesenCult MSC Basal Medium (StemCell Technologies, Vancouver, Canada). The cells were cultured for 14 days at 37°C with 5% CO_2. After 14 days, the media form each well was aspirated and adherent cells were washed with 2 mL PBS, then 2 mL ice-cold methanol was added to each well for 5 min to fix the cells. The methanol was aspirated and 2 mL Wright-Giemsa Stain (Sigma Aldrich, St. Louis, MO, United States) was added to each well and stained for 10 min. The stain was aspirated and the wells washed twice with 2 mL PBS. The plates were air-dried and colonies were counted using a light microscope.

Mixed Lymphocyte Reaction

The immunosuppressive properties of MSCs were compared using MLR assays (SAIC-Frederic, Frederic, MD, United States). Ficoll-separated peripheral blood mononuclear cells were plated in 96-well plates at 1 × 10^5 responders per well. Responders were co-cultured with 2500 cGy irradiated stimulator peripheral blood mononuclear cells at a concentration of 1 × 10^5 cells per well.

MSCs from different centers were added at concentrations of 1×10^4, 4×10^4, and 10×10^4 cells/well. Culture plates were incubated for 6 days in a humidified 5% CO_2 incubator at 37°C. On the day of harvest, 0.5 μ Ci of ^{3}H-thymidine was added to each well for 4 h with lymphocyte proliferation measured using a liquid scintillation counter. The effect of MSCs on MLR was calculated as the percentage of the suppression compared with the proliferative response of the control without MSCs, where the control was set to 0% suppression. The experiments were performed three times for each variable described.

Global Gene Expression Analysis Using Microarrays

Total RNA extractions were performed on the samples from each of the different centers using RNeasy Mini Kit (Qiagen) according to the manufacturer's protocol. RNA was quantified using Nanodrop 8000 (Thermo Fisher Scientific, Wilmington, DE, United States). Total RNA integrity was evaluated following isolation using a 2100 Bioanalyzer (Agilent Technologies, Santa Clara, CA, United States). Samples with an RNA Integrity Number value ≥8 were used for gene expression analysis.

Microarray gene expression analysis was performed on 4×44 K Whole Human Genome Microarrays (Agilent Technologies, Santa Clara, CA, United States) according to the manufacturer's protocol. In general, 200ng of total RNA from each sample was amplified, labeled, and hybridized on the array chip using a Quick Amp Labeling kit (Agilent). Array images were obtained by Agilent Scanner G2600D. Then images were extracted using Feature Extraction 12.0 software (Agilent). Partek Genomic Suite 6.4 (Partek Inc., St. Louis, MO, United States) was used for data visualization and hierarchical cluster analysis.

Statistical and Microarray Data Analysis

Principal Component Analysis (PCA) was used to visualize the similarities and differences among the samples from different centers. Unsupervised Hierarchical clustering was performed by Partek Genomic Suite using whole gene set to group similar samples into clusters.

The Source of Variation Analysis was performed to present the relative contribution of each factor included in the ANOVA by Partek Genomic Suite and the *F*-value provided by this analysis is the ratio of between group variance/within group variance. A large *F*-value for a factor indicates that between group variation is greater than within group variation.

RESULTS

Bone Marrow Collection and Distribution

BM aspirates (i.e., 50–60 mL each) were collected from three different volunteer donors and the BM from each donor was divided into aliquots of approximately 10 mL each (**Figure 1**). The BM aliquots were shipped to 4 sites located in the United States and to 1 site located in Japan. The average time from the collection to the receipt of the BM at each site is shown in **Table 5**. For those samples transported within the United States the average transit time was approximately 24 h while the average shipment time to the site located in Japan was approximately twice as long. Upon arrival at each site, the initiation of processing was executed within 5 h of receipt of the BM sample (**Table 5**).

TABLE 5 | Average shipping time for marrow collection to manufacturing site and time for receipt of marrow to the initiation of processing.

Site#	Shipping time (hrs)		Receipt to processing processing time (hrs)	
	Average	Range	Average	Range
1	26.8	25.0–27.0	4.3	3.0–6.0
2	28.0	26.5–30.0	3.7	3.0–5.0
3	22.4	16.0–25.8	4.3	2.8–5.0
*4	55.2	41.5–71.5	1.5	0.0–3.5
5	26.2	25.0–27.0	4.3	3.0–6.0

**International.*

Inter-Laboratory Method Comparisons for Producing MSCs in Culture

Each site evaluated the BM aliquots for volume, cell viability, and total number of nucleated cells (**Figure 2**). The requested minimum volume from each of three donors to be supplied by the procurement agency to each site was 10 mL. As shown in **Figure 2A**, all sites received a minimum of 10 mL from each donor with some sites receiving volumes of greater than 10 mL. Cell viabilities as performed by each site (**Table 1**) were typically 98–100%, with one site, site #3, reporting viabilities from 80–90%, and one site, site #5, reporting that one of its aliquots had a viability of approximately 71% (**Figure 2B**). Average viable TNC concentrations for BM aspirates #1, #2, and #3 from the 5 laboratories were $25.5 \pm 6.6 \times 10^6$/mL, $21.8 \pm 4.1 \times 10^6$/mL, and $28.7 \pm 7.1 \times 10^6$/mL with coefficients of variation of 25.7, 21.5, and 24.6%, respectively (**Figure 2C**).

The culture schemes used by each of the five centers are summarized in **Tables 2**, **3**. Two sites used unfractionated whole BM to plate cells, two sites subjected the BM aspirate to a density gradient separation to plate cells from a mononuclear cell fraction (MNC), and one site used either whole marrow or a MNC cell fraction to initiate MSC cultures. Laboratories cultured cells in alpha minimal essential media (MEM), MEM-Eagle or Dulbecco's Modified Eagle Medium (DMEM). Fetal bovine serum (FBS) was used by 4 facilities as a media supplement, and 1 laboratory used a commercially available human platelet lysate-serum (PL-S) (Cell Xpand, University of Utah). The final concentration of FBS ranged from 10% to 20% and the final concentration for PL-S was 10% (**Table 2**). Antibiotics were added to the medium by four of the five centers (**Table 2**). Three sites cultured the cells in T-flasks, one site in a multiple layer flask and one site in dishes of 15 cm diameter (**Table 2**). Primary cultures or the initial seeding cell densities for BM#1, BM#2, and BM#3 ranged from 0.2×10^5 cells/cm^2 to 2.8×10^5 cells/cm^2 (**Table 3**). After the initial seeding, the five sites inoculated MSCs from the primary cultures (i.e., P0) at seeding densities that ranged from 50 cells/cm^2 to 4.0×10^3 cells/cm^2 to obtain P1 MSCs. After harvesting MSCs at P1, sites 1 and 4 cryopreserved their

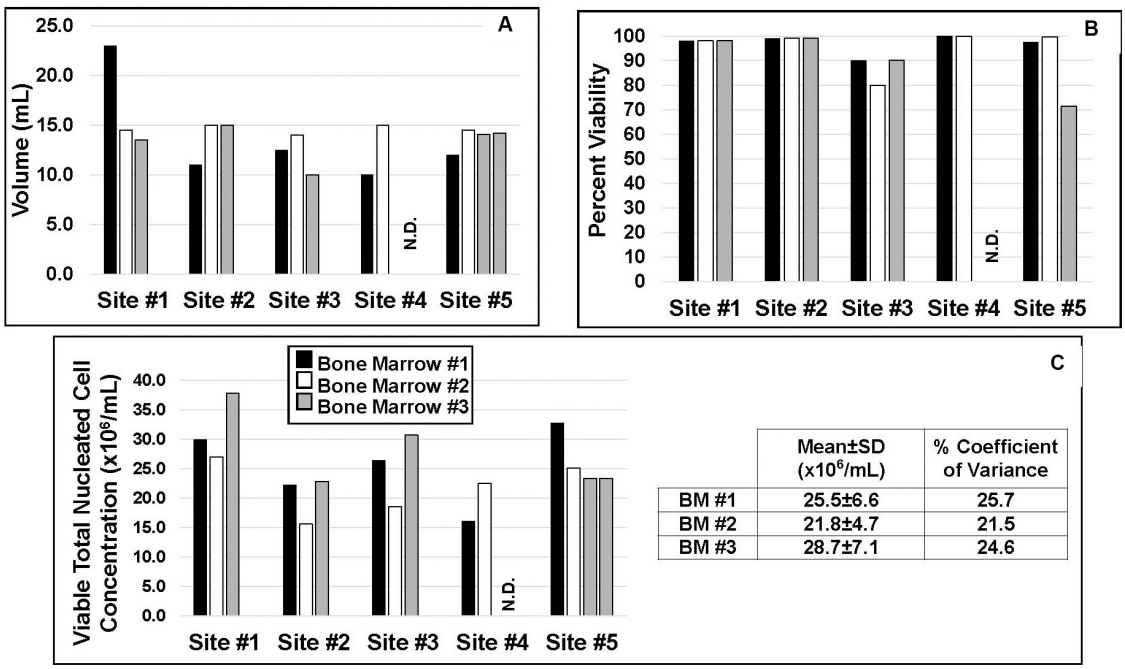

	Mean±SD (x10^6/mL)	% Coefficient of Variance
BM #1	25.5±6.6	25.7
BM #2	21.8±4.7	21.5
BM #3	28.7±7.1	24.6

FIGURE 2 | Characteristics of each of three BM aliquots as evaluated by the respective manufacturing site. **(A)** The volume of BM aspirate received at each site. **(B)** Percent viability of nucleated cells. **(C)** The average concentration of viable total nucleated cells from each of the three donors. The table shows the inter-laboratory Coefficient of Variance for cell concentrations. ND = not done.

cells without any further culturing. Three sites sub-cultured P1 MSCs at seeding densities that ranged from 2.3×10^3 cells/cm^2 to 4.0×10^3 cells/cm^2 to obtain MSCs from a P2 harvest (P2) (**Table 3**). After a P2 harvest, site 3 cryopreserved their cells without any further culturing. Two sites inoculated cultures with P2 MSCs to obtain MSCs that were cryopreserved after passage 3 (P3). No site passaged MSCs beyond P3 (**Table 3**). This translated into overall culture periods that ranged from 21 to 28 days for BM #1, 20 to 34 days for BM #2, and 21 to 35 days for BM #3 (**Figures 3A–C**). We did not only observe inter-laboratory variances for the time cells spent in culture at a particular passage among the five laboratories, but there were also intra-laboratory differences in the amount of time that the MSC cultures from different BM donors spent at a specific passage (**Figures 3A–C**). Each site cryopreserved cells according to their in-house protocol (**Table 4**). Four of the sites used 10% DMSO and one site used 5% DMSO as the final concentration of cryoprotectant. Only one site used a control rate freezer to drop the cyrovial temperature to −100°C, and three sites used a Thermo Scientific Nagene Mr. Frosty Freezing container to drop the temperature to −80°C before transferring to a liquid nitrogen freezer. One site wrapped the cryovials and placed them at −80°C and maintained them at this temperature for shipment to the centralized testing facilities.

In the end, different numbers of passages were executed by the five sites for each of the BM donors. For BM #1, the final harvest of cells for two sites occurred at P1, 1 site at P3 and one site failed to obtain cells. For BM#2, the final harvesting of cells occurred for three of the sites at P1 and for two sites at P3. Finally, for BM#3, three sites harvested at P1, one site at P2 and one site at P3. Overall, this resulted in 14 different final preparations of MSCs that were frozen according to each sites' own specific freezing protocol for maintenance in LN2 prior to their analysis for phenotype and function. In summary, among the five laboratories the variations in methodologies to produce MSCs in culture included: (1) how cells were plated (i.e., cell density, whole BM versus MNC preparations); (2) the culture medium, (3) the time in culture; (8) the number of passages performed before the final cell harvest was cryopreserved and; (9) how each laboratory cryopreserved their cells.

Proliferation Responses

Cellular proliferation responses as measured by theoretical yield and population doubling time from 14 different seeding events from three BM donors from five laboratories are shown in **Figures 3D–F, 4A–C**. Overall, inter-laboratory differences in cell proliferation responses and cell yields were observed from each BM donor. The most notable observations include the following: (1) Cell yields for all three BM donors showed that site #1 consistently produced the most cells and this was accomplished with only a P1 harvest. (2) Site #2 reported cell yields from BM #1 and BM #2 that were comparable to those obtained by site #1, but this was only achieved after site #2 completed a P3 harvest (**Figures 3D,E, 4A,B**). (3) Cell cultures for BM #2 performed by site #5 showed that the cellular proliferation responses lagged relative to the other four sites (**Figures 3E, 4B**). (4) In general proliferation responses from the MSCs isolated from BM #3 were muted relative to the proliferation responses for cells from BM #1

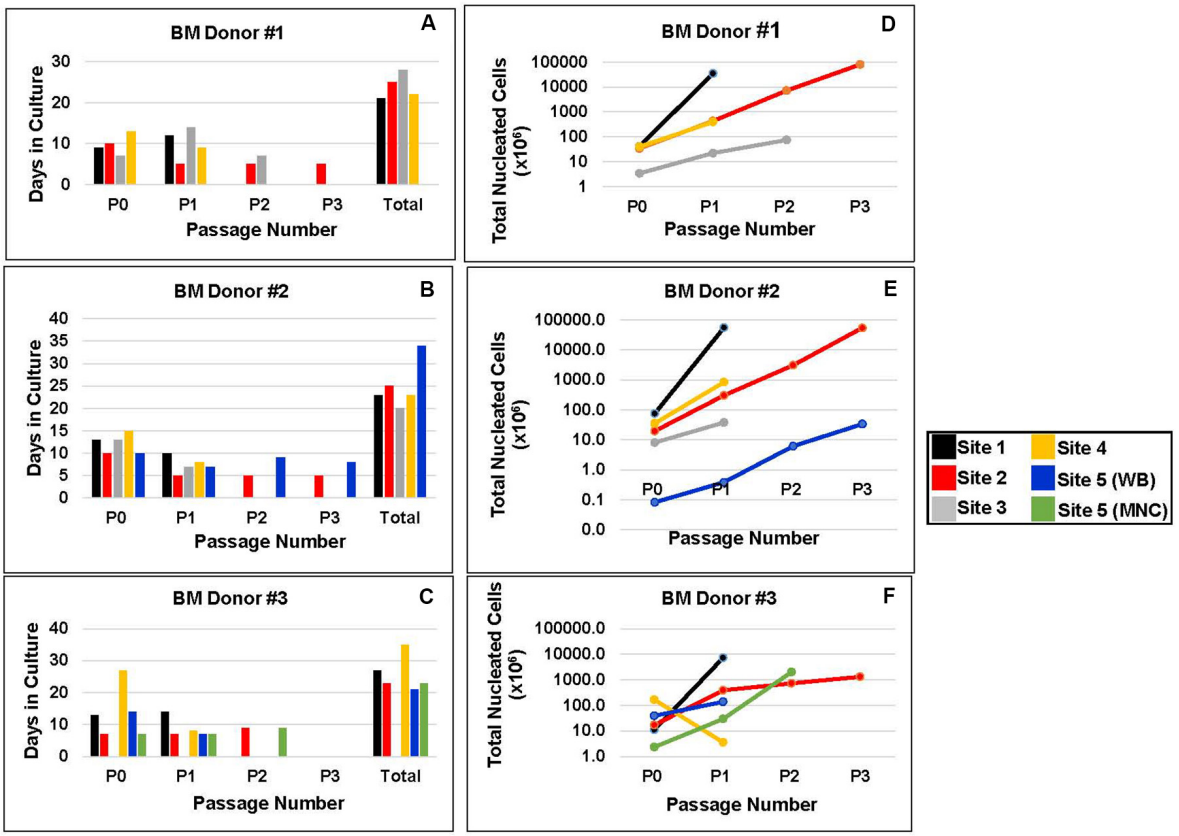

FIGURE 3 | MSC expansion. **(A–C)** The number of passages and the time in culture for each marrow sample as performed by each site. **(D–F)** The theoretical number of adherent cells obtained at the indicated passage by each manufacturing site from each marrow sample. P0 = cell numbers after initial seeding; P1 = cell counts after 2nd seeding; P2 = cell counts after 3rd seeding; and P3 = cell counts after 4th seeding. Since sites did not seed all cells to obtain passages 1, 2, and 3, theoretical cell yields were calculated to predict the number of cells that would have been obtained if all cells had been plated from the previous passage. This was accomplished by first dividing the number of cells harvested by the number of cells seeded for its subsequent passage and then multiplying the actual cell yields obtained for P1, P2, and P3. For example: P1 theoretical cell yields = $(P0_{ay}/P1_{as})xP1_{ay}$. $P0_{ay}$ = actual yield of cells at P0; $P1_{as}$ = actual number of cells seeded to obtain passage 1 cells; $P1_{ay}$ = actual yield of cells at P1.

and BM #2 (compare **Figure 3F** to **Figures 3D,E** and **Figure 4C** to **Figures 4A,B**).

Evaluation of MSCs Post-thaw

To determine whether inter-laboratory manufacturing differences affected the phenotype and function of the cultured MSCs after cryopreservation, the frozen MSCs from 14 final preparations or lots were thawed and examined for cell surface markers, cell viability, CFU-F activity, tri-lineage differentiation potential, immunosuppressive activity, and their gene expression profile. This meant that assays were performed on 14 lots of MSCs that were cryopreserved at different passages during the manufacturing process. Sites #1 and #4 provided 6 lots of P1 MSCs and site #2 provided 3 lots of P3 MSCs from each of the 3 BM donors. Site #3 provided 2 lots of P2 MSCs from BM#1 and BM#2 donors. In addition, site #5 provided 1 lot of P3 MSCs from BM donor #2, and 1 lot of P1 and 1 lot of P2 MSCs from BM donor #3.

To assess whether each of the 14 final preparations of MSCs met the criteria established for a MSC phenotype, each lot of cells was examined by flow cytometry for their expression of cell surface antigens CD105, CD73, CD90 and lack of express for CD45/14/34 and HLA-DR) (Dominici et al., 2006). All final harvests of cells expressed the antigens CD105, CD73, and CD90 and lacked the expression of CD45/14/34 and HLA-DR as well as the Stro-1 antigen without apparent inter-laboratory differences (**Figure 5**).

Next, we examined each of the 14 lots of MSCs to determine whether inter-laboratory differences in culture strategies affected their function. Post-thaw MSC viabilities ranged from 74 to 92% for BM#1, from 61 to 96% for BM#2 and from 23–90% for BM#3 (**Figure 6A**). Site #4 had the lowest viabilities and the poorest CFU-activity for MSCs produced from BM donors #1 and #2. While site #1 had the lowest MSC viabilities and CFU-F activity for BM donor #3. Overall, MSC viabilities and CFU-F activity from BM#3 tended to be lower than for MSCs from BM donors #1 and #2 (**Figures 6B–D**). Inconsistencies in tri-lineage development among the laboratories were also observed and again site#4 showed some of the poorest developmental activity (**Table 6**). Of note is the fact that site#4, which was a

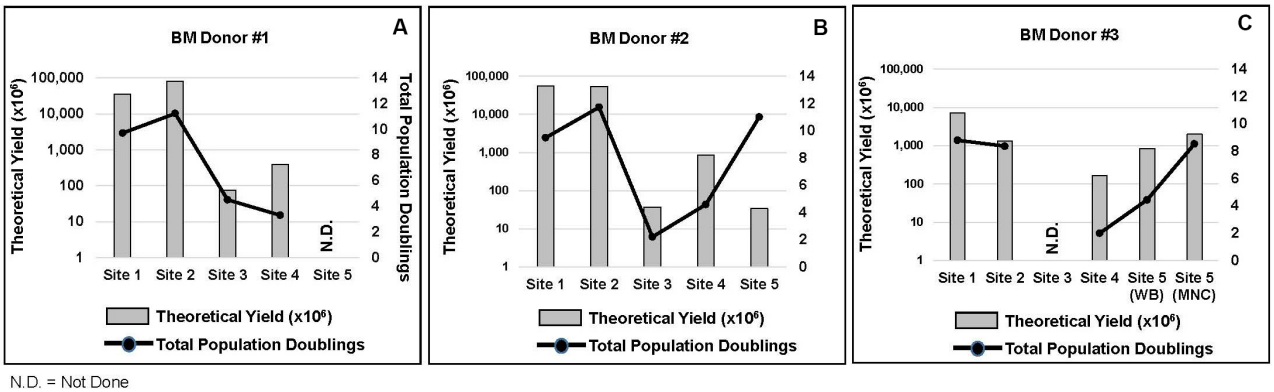

N.D. = Not Done

FIGURE 4 | MSC yields and population doublings. For each BM aspirate and site the theoretical MSC yields and population doubling (PD) are shown. **(A)** Shows the results for BM donor #1, **(B)** the results for BM donor #2 and **(C)** for BM donor #3.

laboratory located in Japan, experienced the longest transport times from BM collection to culture initiation and also shipped their cells at −80°C. Also, greater inconsistencies in tri-lineage development were observed from MSC lots produced from BM#3 than from MSCs isolated from the other two BM donors (**Table 6**). Interestingly, despite poorer viabilities, CFU-F activity and tri-lineage differentiation potential for MSCs from BM#3, the immunosuppressive activity of MSCs from BM#3 were comparable to that of MSCs from BM#1 and BM#2 (**Figure 7**).

Global Gene Expression Analysis

All 14 lots of MSCs were analyzed by global gene expression analysis including PCA and unsupervised hierarchical analysis by using the entire set of expressed genes to identify relationships among the samples. Gene expression of MSC lots clustered by manufacturing site and donors (**Figures 8A,B**). Notably, the MSC lots clustered stronger according to site compared to donors (**Figures 8A,B**). This was confirmed by unsupervised hierarchical clustering analysis showing that the grouping of samples was related to site and donor with sites having a greater effect (**Figure 8C**). To further evaluate the relationship between the effects of manufacturing site and donor variability on MSC characteristics, the entire set of expressed genes from the 14 MSC lots was subjected to source of variation analysis. This analysis confirmed that the variability among MSCs samples was due to both the site and the BM donor, but the manufacturing site had a greater influence on MSC characteristics (**Figure 8C**).

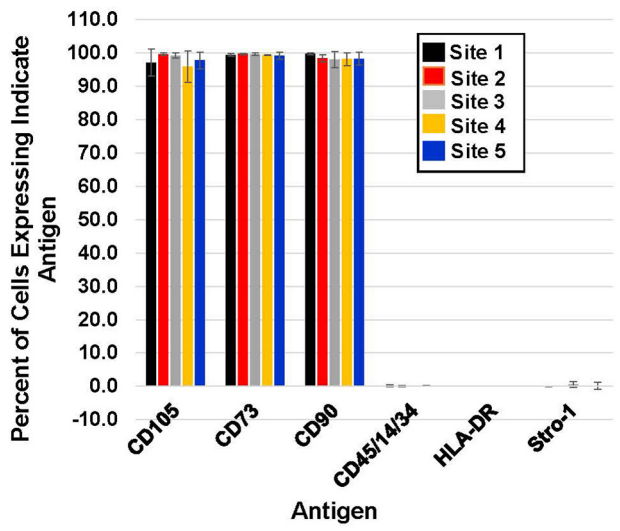

FIGURE 5 | Immunophenotyping of MSCs. 14 lots of cryopreserved MSCs from the five laboratories were analyzed by flow cytometry at a single laboratory. The MSCs were analyzed for the expression of CD105, CD73, CD90, CD45/CD14/CD34, HLA-DR and Stro-1 following thawing.

DISCUSSION

Manufacturing MSCs of consistent quality and potency is important for their utilization as effective clinical therapeutics. For the purpose of this discussion the MSC manufacturing process is divided into the four following steps: (1) Donor selection and BM collection; (2) maintenance and transport of the BM aspirate from the collection site to the processing site; (3) culture strategy (i.e., plating cells, passaging the adherent cells and harvesting the MSCs); and (4) cryopreservation and storage of the manufactured MSCs.

Previously, we reported that MSCs exhibited variable characteristics and functions when multiple participating sites used different tissue sources as well as different manufacturing methods (Liu et al., 2017). Herein, we report that inter-laboratory manufacturing differences make a greater contribution to MSC variability than the differences noted among the BM donors utilized in this study. An observation that suggests that standardizing the manufacturing process of culture-derived MSCs from BM aspirates may lead to reduced variability in MSC characteristics and functions.

Evidence is presented in this study that there are inter-donor differences. Specifically, MSCs from donor #3 were found to

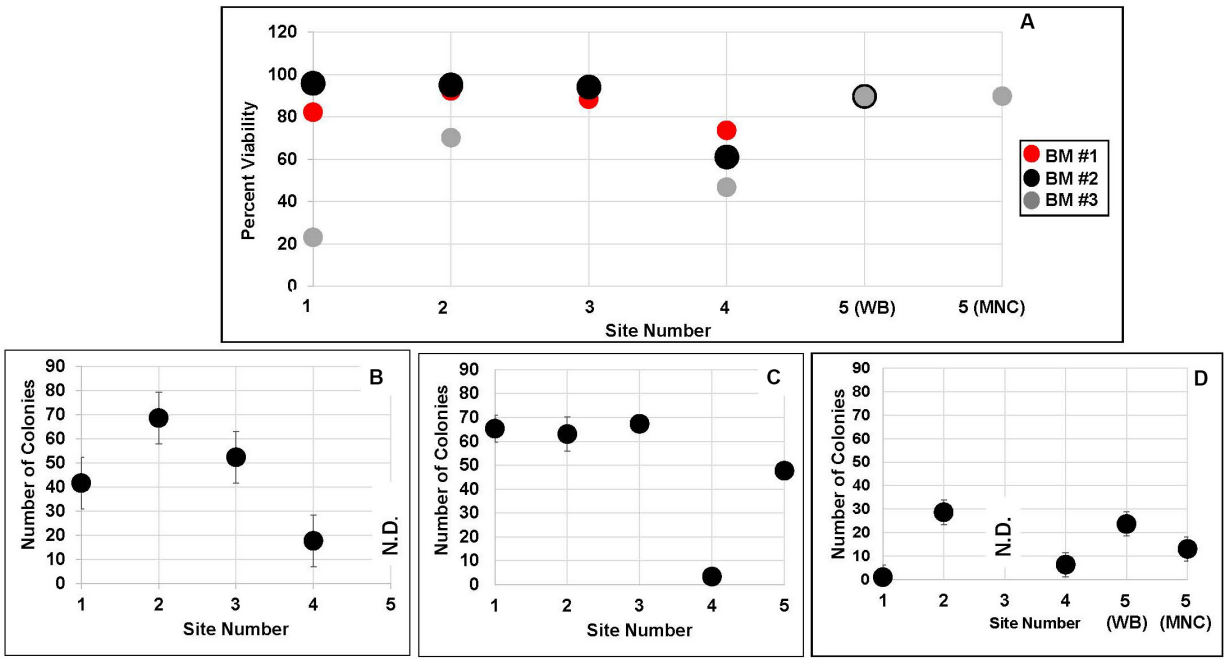

FIGURE 6 | MSC post-thaw viability and CFU activity. **(A)** Percent viabilities for all MSCs produced from the three donors and by the five sites and **(B)** the absolute number of CFU-F colonies produced by MSCs derived at each of five sites from cultures that were initiated with aliquots from **(B)** BM donor #1; **(C)** BM donor #2; and **(D)** BM donor #3. ND = not done.

TABLE 6 | Tri-lineage potential of post-thaw MSCs by manufacturing site.

Adipogenesis				Chrondrogenesis				Osteogenesis			
Site number	**Prep #1**	**Prep #2**	**Prep #3**	**Site number**	**Prep #1**	**Prep #2**	**Prep #3**	**Site number**	**Prep #1**	**Prep #2**	**Prep #3**
	***Average**	***Average**	***Average**		***Average**	***Average**	***Average**				
Site I	2.0	2.3	0.5	Site I	3.0	3.0	0.5	Site I	Pos	Pos	poor diff
Site 2	3.2	4.0	4.0	Site 2	3.0	3.0	3.0	Site 2	Pos	Pos	Pos
Site 3	2.0	4.0	N.D.	Site 3	3.0	3.0	N.D.	Site 3	Pos	Pos	Pos
Site 4	1.0	0.8	0.8	Site 4	3.0	0.0	1.3	Site 4	Pos	Pos	Pos
Site 5 WB	N.D	3.0	3.0	Site 5 WB	N.D.	3.0	3.0	Site 5 WB	N.D.	Pos	Pos
Site 5 MNC	N.D.	N.D.	2.0	Site 5 MNC	N.D.	N.D.	3.0	Site 5 MNC	N.D.	N.D.	Pos
Average	2.0	2.8	2.1	Average	3.0	2.4	2.0				

*Scale 0–4; where 0 = no differentiation and 4 = maximum differentiation. N.D. = Not Done. *n = 3.*

be less proliferative than those from donors #1 and #2 by all sites and formed less CFU-F by four of the five sites. Such variable growth kinetics of MSC preparations have been reported as being attributable to donor-related variables, such as age and sex (Siegel et al., 2013; Detela et al., 2018). This is also highlighted in studies reporting that BM-MSCs from younger donors have distinct molecular signatures and feature superior wound healing efficacy in a mouse model (Siegel et al., 2013; Khong et al., 2019). Although this is a small study, it is unlikely that sex or age is a major contributing factor for the lower proliferative responses from donor #3 as compared to donors #1 and #2 BM aspirates. All of the donors are males and the ages of BM donor #1, #2, and #3 are 21, 24, and 20 years old, respectively.

Manufacturing concepts of MSC therapies vary worldwide with variability in MSC culture strategy and product release specifications (Trento et al., 2018). Consequently, it is not surprising that the inter-laboratory differences of this study, which reflect manufacturing variabilities, resulted in MSCs with variable proliferation rates, total expansion numbers, CFU-F content and MSC tri-lineage differentiation potential. With regard to surface marker expression, we did not find substantial differences among sites. Yet, we tested only for "binaric" (i.e., either high or very low expressed) MSC markers, and not for markers that define MSC subpopulations such as CD271 or CD146 (Tormin et al., 2011; Kuci et al., 2019). Higher resolution analyses quantifying MSC subpopulations might have revealed an impact of the manufacturing strategies

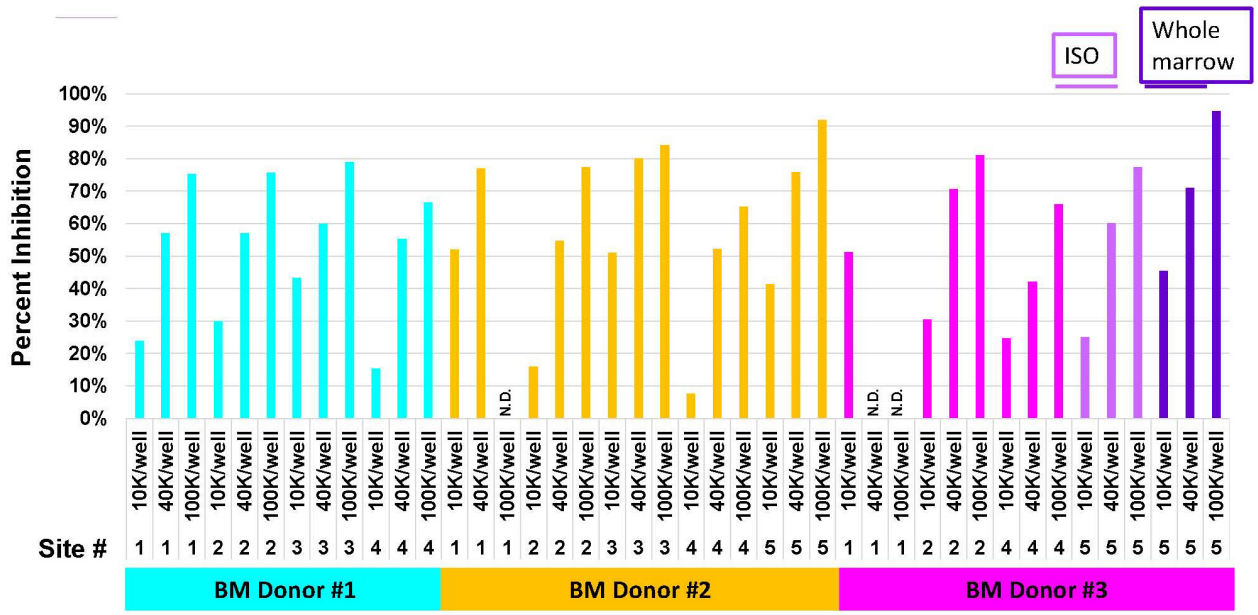

FIGURE 7 | Mixed-Lymphocyte-Reaction of MSCs manufactured from the same three donors at five manufacturing sites. MLR data shows inhibition of lymphocyte proliferation when the BM-derived MSCs were added and the inhibition increased as the ratio of MSCs to lymphocytes increased. Results from three donors and five centers are shown. For some samples no data is shown since not enough MSCs were available to test.

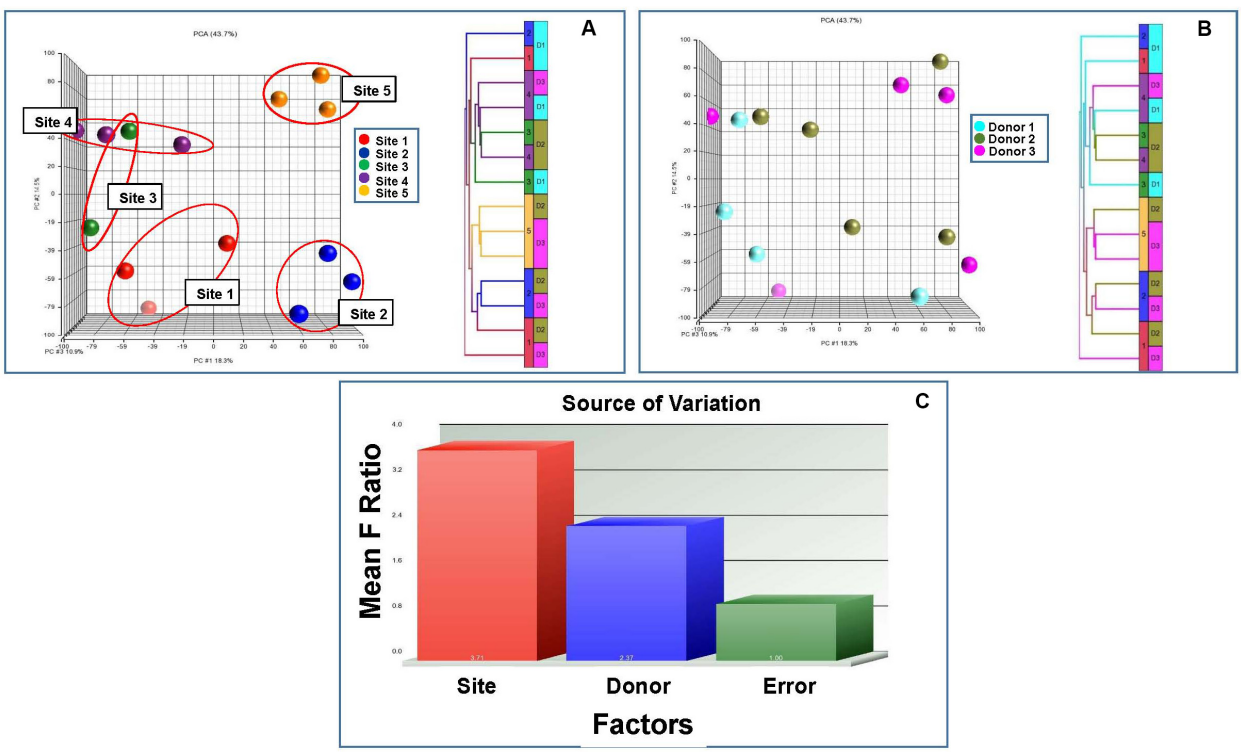

FIGURE 8 | Principle Component Analysis (PCA), unsupervised hierarchical clustering analysis and Source of Variation Analysis of gene expression data from MSCs manufactured from the same three donors by five different manufacturing sites. PCA and unsupervised hierarchical clustering analysis shows that there are differences in MSC transcriptomes due to the manufacturing laboratory and to donor variability. **(A)** The results of PCA analysis for gene expression data of MSC lots are color coded by manufacturing site, **(B)** PCA analysis for gene expression of MSCs are color coded by donor source and **(C)** unsupervised hierarchical clustering analysis. Source of Variation Analysis shows greater transcriptome variation due to laboratory methodology than with donor BM source.

on MSC subpopulation compositions of the products. Another limitation of our study is that not all sites seeded all the available cells from a harvest to produce cells for a subsequent passage. Therefore, theoretical cell yields were calculated to predict the number of cells that would have been obtained if all cells had been plated from the previous passage.

MSCs produced by each site were also evaluated by global gene expression analysis. Differences in gene expression were found that could be attributed to both variability among BM donors and manufacturing site. While the sample size of the study was not large enough to assess the nature of these differences, the analysis showed that the inter-laboratory differences made a greater contribution to MSC variability than did differences among BM donors. This aligns with a recent study reporting that variable *in vitro* expansion strategies (i.e., passaging or "*in vitro* aging") have a stronger impact on MSC molecular phenotype than donor age (Andrzejewska et al., 2019).

There are a number of differences in laboratory practices that likely contributed to the MSC variabilities observed in this study. One such variance in inter-laboratory practices is transport time for the BM harvest to the processing site. Although all BM aliquots were transported at ambient temperatures, transport times at one site varied substantially. Transit times to the four sites located in the United States ranged from 16 to 30 h while for site #4, located in Japan, transit times ranged from 41 to 71 h. Coincidently, the lowest CFU-F content of the manufactured MSCs occurred at site #4. Granting that this is a small data set, if a maintenance temperature of 20–25°C is used, these results indicate that a BM aspirate should probably be processed within 24–36 h of collection. Also, of note is the observation that proliferation capacities and yields of MSCs were greater for sites #1 and #2, which may have been due in part to the use of higher concentrations of FBS as a culture medium supplement by site #1 (16%) and site #2 (20%). Likewise, total population doublings of MSCs cultured using hPL at site #5 were in a higher range as compared to MSC produced by the other sites using FBS. Since hPL is shown to impact MSC biology beyond proliferation, such as in their differentiation potential and immunomodulation capacity (Menard et al., 2013; Bieback et al., 2019). It is likely that the use of hPL is another practice that contributed to MSC variability is the use of hPL by only one site in our study. Other differences in inter-laboratory practices that are associated with culture strategy are likely to have also contributed to MSC variability along with differences in inter-laboratory practices for cryopreservation and storage of MSCs.

These results support the idea that it may be possible to reduce MSC variabilities associated with inconsistencies in inter-laboratory manufacturing practices. Some steps of the manufacturing process may be more amendable to standardization and while others may not be. For instance, since MSCs are used for a number of different clinical applications, a manufacturing process that works the best for one therapy may not produce MSCs with functional qualities that are best for other therapies. Consequently, premature establishment of standards based on a culture strategy for one specific clinical application (i.e., basal medium formulations, medium supplementation, initial seeding densities, the number of passages, and length of time MSCs are maintained in culture) could end up having detrimental consequences for other applications. Conversely, standardizing inter-laboratory practices for manufacturing MSC that are not dependent on intended clinical applications (i.e., donor selection, BM collection, maintenance and transport of the BM aspirate from the collection site to the processing site, cryopreservation and storage) are urgently needed. For example, it would be advantageous for the MSC field to promote the use of superior methods like automated cell counts and the use of fluorescent dyes for viability testing over that of manual cell counts and the use of trypan blue for viability assessments to characterize whole BM aspirates prior to culture initiation (Mascotti et al., 2000).

In the end, the results of this study indicate that even if inter-laboratory manufacturing is standardized, differences among MSC preparations may still exist due to differences in the donor source of cells used for manufacturing MSCs. To build off of this study for the purpose of acquiring more information that may lead to future recommendations about standardizing MSC manufacturing, the BEST collaborative is currently planning a follow-up inter-laboratory study, in which laboratories will use the same source material and the same manufacturing, cryopreservation and storage protocols.

DATA AVAILABILITY STATEMENT

This article contains previously unpublished data. The name of the repository and accession number(s) are not available.

AUTHOR CONTRIBUTIONS

DS and J-AR are responsible for experimental design, lab participation and writing manuscript. DM, MT, MF, and SP labs participated in the study and editing manuscript. PJ, EP, and EB performed the experiments and edited manuscript. RS participated in writing manuscript.

ACKNOWLEDGMENTS

We would like to express our appreciation to MNX Critical Logistics Simplified and Biolife Solutions for supporting the overseas transport of samples for this study. In particular to David Miller and Jim Boss for facilitating the transport. We would also like to express our gratitude to Jiaqiang Ren at the National Institute of Health, Darin Sumstad at the University of Minnesota, and Beate Heissig at the Center for Stem Cell Biology and Regenerative Medicine at the Institute of Medical Science at the University of Tokyo.

REFERENCES

Andrzejewska, A., Catar, R., Schoon, J., Qazi, T. H., Sass, F. A., Jacobi, D., et al. (2019). Multi-parameter analysis of biobanked human bone marrow stromal cells shows little influence for donor age and mild comorbidities on phenotypic and functional properties. *Front. Immunol.* 10: 2474. doi: 10.3389/fimmu.2019.02474

Bagno, L., Hatzistergos, K. E., Balkan, W., and Hare, J. M. (2018). Mesenchymal stem cell-based therapy for cardiovascular disease: progress and challenges. *Mol. Ther.* 26, 1610–1623. doi: 10.1016/j.ymthe.2018.05.009

Ball, L. M., Bernardo, M. E., Roelofs, H., van Tol, M. J., Contoli, B., Zwaginga, J. J., et al. (2013). Multiple infusions of mesenchymal stromal cells induce sustained remission in children with steroid-refractory, grade III-IV acute graft-versus-host disease. *Br. J. Haematol.* 163, 501–509. doi: 10.1111/bjh.12545

Bieback, K., Kuci, S., and Schafer, R. (2019). Production and quality testing of multipotent mesenchymal stromal cell therapeutics for clinical use. *Transfusion* 18, 2164–2173.

Detela, G., Bain, O. W., Kim, H. W., Williams, D. J., Mason, C., Mathur, A., et al. (2018). Donor variability in growth kinetics of healthy hMSCs using manual processing: considerations for manufacture of cell therapies. *Biotechnol. J.* 13:1700085. doi: 10.1002/biot.201700085

Dominici, M., Le Blanc, K., Mueller, I., Slaper-Cortenbach, I., Marini, F., Krause, D., et al. (2006). Minimal criteria for defining multipotent mesenchymal stromal cells. The International Society for Cellular Therapy position statement. *Cytotherapy* 8, 315–317. doi: 10.1080/14653240600855905

Fisher, S. A., Cutler, A., Doree, C., Brunskill, S. J., Stanworth, S. J., Navarrete, C., et al. (2019). Mesenchymal stromal cells as treatment or prophylaxis for acute or chronic graft-versus-host disease in haematopoietic stem cell transplant (HSCT) recipients with a haematological condition. *Cochrane Database Syst. Rev.* 30:CD009768.

Fontaine, M. J., Shih, H., Schafer, R., and Pittenger, M. F. (2016). Unraveling the mesenchymal stromal cells' paracrine immunomodulatory effects. *Transfusion Med. Rev.* 30, 37–43. doi: 10.1016/j.tmrv.2015.11.004

Forbes, G. M. (2017). Mesenchymal stromal cell therapy in crohn's disease. *Dig Dis.* 35, 115–122. doi: 10.1159/000449091

Galleu, A., Riffo-Vasquez, Y., Trento, C., Lomas, C., Dolcetti, L., Cheung, T. S., et al. (2017). Apoptosis in mesenchymal stromal cells induces in vivo recipient-mediated immunomodulation. *Sci. Transl. Med.* 9:eaam7828. doi: 10.1126/scitranslmed.aam7828

Horwitz, E. M., Prockop, D. J., Fitzpatrick, L. A., Koo, W. W., Gordon, P. L., Neel, M., et al. (1999). Transplantability and therapeutic effects of bone marrow-derived mesenchymal cells in children with osteogenesis imperfecta. *Nat. Med.* 5, 309–313. doi: 10.1038/6529

Khong, S. M. L., Lee, M., Kosaric, N., Khong, D. M., Dong, Y., Hopfner, U., et al. (2019). Single-cell transcriptomics of human mesenchymal stem cells reveal age-related cellular subpopulation depletion and impaired regenerative function. *Stem cells.* 37, 240–246. doi: 10.1002/stem.2934

Kuci, S., Kuci, Z., Schafer, R., Spohn, G., Winter, S., Schwab, M., et al. (2019). Molecular signature of human bone marrow-derived mesenchymal stromal cell subsets. *Sci. Rep.* 9:1774.

Lalu, M. M., Montroy, J., Dowlatshahi, D., Hutton, B., Juneau, P., Wesch, N., et al. (2019). From the lab to patients: a systematic review and meta-analysis of mesenchymal stem cell therapy for stroke. *Transl. Stroke Res.* 25, 345–364. doi: 10.1007/s12975-019-00736-5

Le Blanc, K., Frassoni, F., Ball, L., Locatelli, F., Roelofs, H., Lewis, I., et al. (2008). Mesenchymal stem cells for treatment of steroid-resistant, severe, acute graft-versus-host disease: a phase II study. *Lancet* 371, 1579–1586. doi: 10.1016/s0140-6736(08)60690-x

Le Blanc, K., Rasmusson, I., Sundberg, B., Gotherstrom, C., Hassan, M., Uzunel, M., et al. (2004). Treatment of severe acute graft-versus-host disease with third party haploidentical mesenchymal stem cells. *Lancet* 363, 1439–1441. doi: 10.1016/s0140-6736(04)16104-7

Liu, S., de Castro, L. F., Jin, P., Civini, S., Ren, J., Reems, J. A., et al. (2017). Manufacturing differences affect human bone marrow stromal cell characteristics and function: comparison of production methods and products from multiple centers. *Sci. Rep.* 7:46731.

Mascotti, K., McCullough, J., and Burger, S. R. (2000). HPC viability measurement: trypan blue versus acridine orange and propidium iodide. *Transfusion* 40, 693–696. doi: 10.1046/j.1537-2995.2000.40060693.x

Menard, C., Pacelli, L., Bassi, G., Dulong, J., Bifari, F., Bezier, I., et al. (2013). Clinical-grade mesenchymal stromal cells produced under various good manufacturing practice processes differ in their immunomodulatory properties: standardization of immune quality controls. *Stem Cells Dev.* 22, 1789–1801. doi: 10.1089/scd.2012.0594

Migliorini, F., Rath, B., Colarossi, G., Driessen, A., Tingart, M., Niewiera, M., et al. (2019). Improved outcomes after mesenchymal stem cells injections for knee osteoarthritis: results at 12-months follow-up: a systematic review of the literature. *Arch Orthop. Trauma Surg.* 27, 1–6.

Phinney, D. G., Di Giuseppe, M., Njah, J., Sala, E., Shiva, S., St Croix, C. M., et al. (2015). Mesenchymal stem cells use extracellular vesicles to outsource mitophagy and shuttle microRNAs. *Nat. Commun.* 6:8472.

Phinney, D. G., and Pittenger, M. F. (2017). Concise review: MSC-derived exosomes for cell-free therapy. *Stem Cells* 35, 851–858. doi: 10.1002/stem.2575

Prasad, V. K., Lucas, K. G., Kleiner, G. I., Talano, J. A., Jacobsohn, D., Broadwater, G., et al. (2011). Efficacy and safety of ex vivo cultured adult human mesenchymal stem cells (Prochymal) in pediatric patients with severe refractory acute graft-versus-host disease in a compassionate use study. *Biol. Blood Marrow Transpl.* 17, 534–541. doi: 10.1016/j.bbmt.2010.04.014

Regmi, S., Pathak, S., Kim, J. O., Yong, C. S., and Jeong, J. H. (2019). Mesenchymal stem cell therapy for the treatment of inflammatory diseases: challenges, opportunities, and future perspectives. *Eur J Cell Biol.* 14:151041. doi: 10.1016/j.ejcb.2019.04.002

Schafer, R., Spohn, G., and Baer, P. C. (2016). Mesenchymal stem/stromal cells in regenerative medicine: can preconditioning strategies improve therapeutic efficacy? *Transfus. Med. Hemother.* 43, 256–267. doi: 10.1159/000447458

Siegel, G., Kluba, T., Hermanutz-Klein, U., Bieback, K., Northoff, H., and Schafer, R. (2013). Phenotype, donor age and gender affect function of human bone marrow-derived mesenchymal stromal cells. *BMC Med.* 11:146. doi: 10.1186/1741-7015-11-146

Tormin, A., Li, O., Brune, J. C., Walsh, S., Schutz, B., Ehinger, M., et al. (2011). CD146 expression on primary nonhematopoietic bone marrow stem cells is correlated with in situ localization. *Blood* 117, 5067–5077. doi: 10.1182/blood-2010-08-304287

Trento, C., Bernardo, M. E., Nagler, A., Kuci, S., Bornhauser, M., Kohl, U., et al. (2018). Manufacturing mesenchymal stromal cells for the treatment of graft-versus-host disease: a survey among centers affiliated with the european society for blood and marrow transplantation. *Biol. Blood Marrow Transpl.* 24, 2365–2370. doi: 10.1016/j.bbmt.2018.07.015

Uccelli, A., Laroni, A., Brundin, L., Clanet, M., Fernandez, O., Nabavi, S. M., et al. (2019). MEsenchymal StEm cells for Multiple Sclerosis (MESEMS): a randomized, double blind, cross-over phase I/II clinical trial with autologous mesenchymal stem cells for the therapy of multiple sclerosis. *Trials* 20:263.

Wegmeyer, H., Broske, A. M., Leddin, M., Kuentzer, K., Nisslbeck, A. K., Hupfeld, J., et al. (2013). Mesenchymal stromal cell characteristics vary depending on their origin. *Stem Cells Dev.* 22, 2606–2618. doi: 10.1089/scd.2013.0016

Yun, C. W., and Lee, S. H. (2019). Enhancement of functionality and therapeutic efficacy of cell-based therapy using mesenchymal stem cells for cardiovascular disease. *Int. J. Mol. Sci.* 20:982. doi: 10.3390/ijms20040982

Conflict of Interest: The authors declare that the research was conducted in the absence of any commercial or financial relationships that could be construed as a potential conflict of interest.

frontiers in Cell and Developmental Biology

ORIGINAL RESEARCH
published: 26 June 2020
doi: 10.3389/fcell.2020.00470

hsa_circ_0026827 Promotes Osteoblast Differentiation of Human Dental Pulp Stem Cells Through the Beclin1 and RUNX1 Signaling Pathways by Sponging miR-188-3p

Fang Ji[1,2†], Lanying Zhu[3†], Jing Pan[1,2], Zhecheng Shen[1,2], Zhao Yang[1,2], Jian Wang[2,4], Xuebing Bai[2,4], Yueting Lin[2,4] and Jiang Tao[2,4]*

[1] Department of Orthodontics, Ninth People's Hospital, College of Stomatology, Shanghai Jiao Tong University School of Medicine, Shanghai, China, [2] National Clinical Research Center for Oral Diseases, Shanghai Key Laboratory of Stomatology and Shanghai Research Institute of Stomatology, Shanghai, China, [3] Department of Stomatology, Jining Traditional Chinese Medicine Hospital, Shandong, China, [4] Department of General Dentistry, College of Stomatology, Ninth People's Hospital, Shanghai Jiao Tong University School of Medicine, Shanghai, China

OPEN ACCESS

Edited by:
Marcela F. Bolontrade, Consejo Nacional de Investigaciones Científicas y Técnicas (CONICET), Argentina

Reviewed by:
Zhifeng Gu, Affiliated Hospital of Nantong University, China
Andrea Ballini, University of Bari Aldo Moro, Italy

***Correspondence:**
Jiang Tao
doctor_taojiang@126.com

[†]These authors share first authorship

Specialty section:
This article was submitted to Stem Cell Research, a section of the journal Frontiers in Cell and Developmental Biology

Received: 25 March 2020
Accepted: 20 May 2020
Published: 26 June 2020

Citation:
Ji F, Zhu L, Pan J, Shen Z, Yang Z, Wang J, Bai X, Lin Y and Tao J (2020) hsa_circ_0026827 Promotes Osteoblast Differentiation of Human Dental Pulp Stem Cells Through the Beclin1 and RUNX1 Signaling Pathways by Sponging miR-188-3p. Front. Cell Dev. Biol. 8:470. doi: 10.3389/fcell.2020.00470

Previous studies have found that circular RNA (circRNA) hsa_circ_0026827 plays a role during osteoblast differentiation, but the mechanism is unclear. The aim of this study was to illuminate the role of hsa_circ_0026827 in human dental pulp stem cells (DPSCs) during osteoblast differentiation. The results show that hsa_circ_0026827 expression significantly increased during osteoblast differentiation, while knockdown of hsa_circ_0026827 suppressed DPSC-derived osteoblast differentiation. microRNA (miRNA) expression profile analysis showed that downregulation of hsa_circ_0026827 promoted miR-188-3p expression. miR-188-3p downregulation restored osteogenic differentiation of DPSCs after hsa_circ_0026827 was silenced. Luciferase reporter assays verified that miR-188-3p was the target of hsa_circ_0026827 and also demonstrated that Beclin1 and RUNX1 were miR-188-3p downstream targets. miR-188-3p overexpression suppressed DPSC osteogenic differentiation by targeting Beclin-1-mediated autophagy and runt-related transcription factor 1 (RUNX1). *In vivo* studies using a heterotopic bone model also found that hsa_circ_0026827 overexpression plays an important role in promoting heterotopic bone formation. In conclusion, our research indicates that hsa_circ_0026827 promotes osteoblast differentiation of DPSCs via Beclin1 and the RUNX1 signaling pathways by sponging miR-188-3p, which suggests novel therapeutics for osteoporosis treatment.

Keywords: dental pulp stem cells, osteoblast differentiation, hsa_circ_0026827, miR-188-3p, Beclin1, RUNX1

INTRODUCTION

Dental pulp stem cells (DPSCs) belong to a class of multipotent mesenchymal stem cells (MSCs) which can differentiate into distinct specialized cell types such as osteocytes, adipocytes and chondrocytes (Mangano et al., 2010; Spath et al., 2010; Wang et al., 2017). It has been reported that DPSCs are more effective in proliferation and osteogenesis and have lower immunogenicity

than MSCs (Ching et al., 2017). Dental pulp stem cells may thus be useful in oral and maxillofacial reconstruction (Rapino et al., 2019). During osteoblast differentiation, DPSCs express osteoblast differentiation-related biomarkers such as runt-related transcription factor 1 (RUNX1), osteocalcin (OCN), alkaline phosphatase (ALP), and osterix (OSX) (Sharpe, 2016; Victor and Reiter, 2017). Our previous studies have found that downregulation of nuclear factor erythroid 2 related factor promotes autophagy-dependent osteoblastic adipose-derived MSC differentiation (Tao et al., 2016). Although the regulatory role of coding genes in osteoblast differentiation has been broadly studied, the functional contributions of non-coding RNAs, specifically those of circular RNAs (circRNAs), remain unknown.

circRNAs have been shown to be indispensable in post-transcriptional transcriptome regulation (Hansen et al., 2013; Liu et al., 2017). circRNAs are constructed by specific loop splicing and are resistant to RNase R digestion. In contrast to linear RNAs, circRNAs are constructed as a covalently closed continuous loops with their 5′ tails and 3′ heads bound together (Qu et al., 2015). The loop structure is formed via a specific class of alternative splicing event called back-splicing, in which an upstream splice acceptor is joined to a downstream splice donor (Daniel et al., 2015). circRNAs harbor microRNA (miRNA) binding sites, which normally function as miRNA sponges (Hansen et al., 2013). For example, a previous study has validated that circRNA CDR1as acts as an miR-7 inhibitor, which triggers GDF5 upregulation and subsequent p38 and Smad1/5/8 MAPK phosphorylation to enhance osteogenic differentiation of periodontal ligament stem cells (Li et al., 2018). circIGSF11 silencing increases miR-199b-5p expression and enhances osteoblast differentiation (Zhang et al., 2019). circRNA expression profile analysis has demonstrated that hsa_circ_0026827 is abnormally expressed during osteoblast differentiation, but its function is unclear (Zhang et al., 2019).

Thus current investigation aimed to explore the role of hsa_circ_0026827 in DPSC osteoblast differentiation. Our data suggest candidate therapeutic strategies for regeneration of bone and periodontal tissue and also reveal new mechanisms underlying osteogenic differentiation.

MATERIALS AND METHODS

Ethics Statement

All treatments involving animals were approved by the Animal Care Committee of the Ninth People's Hospital, Shanghai Jiao Tong University School of Medicine, Shanghai, China.

DPSC Isolation and Identification

We isolated cells from dental pulp as described in Iezzi et al. (2019). In brief, we gently removed tissue (Gain from Department of Orthodontics, Ninth People's Hospital, Shanghai Jiao Tong University School of Medicine. The Ethics Committee of Ninth People's Hospital, Shanghai Jiao Tong University School of Medicine approval the DPSCs isolation) and immersed it in a digestive solution (4.0 mg/ml dispase and 3.0 mg/ml type I collagenase) for 1 h under at 37°C. We then filtered the digested solution with 70-μm cell strainers to obtain an DPSCs suspension. We plated cells in T25 flasks and cultured them in complete culture medium containing DMEM/F12 with fetal bovine serum (FBS; 10%) and penicillin/streptomycin (1%) at 37°C in 5% CO_2.

We harvested DPSCs in 5 mM ethylene diamine tetraacetic acid (EDTA) in phosphate-buffered saline (PBS) for surface protein flow cytometric analysis. We incubated cells with PE- or FITC-conjugated antibodies against human CD90, CD34, CD29, CD45, CD44, CD73, and CD105 (Becton Dickinson, San Jose, CA, United States). Matched isotype antibodies were employed as controls. We washed cells once with cold PBS containing 2% fetal calf serum. We acquired 1000 labeled cells and analyzed them by a FACScan flow cytometer running CellQuest (Becton Dickinson) (Dominici et al., 2006; Shen et al., 2019).

Plasmid Construction and Transfection

We purchased overexpression plasmids pcDNA3.1-RUNX1 and pcDNA3.1-hsa_circ_0026827 from GeneChem Co., Ltd. (Shanghai, China). We also purchased siRNA against hsa_circ_0026827 (sicircRNA), miR-188-3p inhibitor and mimic from GeneChem. We performed cell transfections using Lipofectamine® 3000 (Invitrogen Life Technologies, United States) following the manufacturer's protocol.

miRNA Microarray Procedures

We used DPSCs for RNA sequencing. We constructed libraries using the Illumina Gene Expression Sample Preparation Kit and sequenced them with the Illumina HiSeqTM 2000 (next generation sequencing) from Beijing Genomics Institute, Beijing, China. In brief, we isolated total RNA from each sample and treated them with DNase I to degrade any potential DNA contamination, then enriched mRNA with oligo (dT) magnetic beads. We mixed enriched mRNA with fragmentation buffer and fragmented it into short fragments (∼200 bp) from which we synthesized the first strand via a random hexamer primer. We synthesized the second strand after adding reaction buffer, RNaseH, dNTPs, and DNA polymerase I to the first strand synthesis mixture. We purified double-stranded cDNA with magnetic beads and added a 3′-terminal single nucleotide adenine. Lastly, we ligated sequencing adaptor to the fragment to amplify it by PCR. We sequenced enriched fragments by the Illumina HiSeq™ 2000 and generated 50-bp raw reads by the Illumina Genome Analyzer II.

Real-Time Quantitative Reverse Transcription PCR Detection

We extracted total RNA using Trizol reagent (Invitrogen, Carlsbad, CA, United States). We utilized RNase-free DNase Set (Qiagen) to erase genomic DNA contamination. We reverse transcribed 1 μg of total RNA using transcriptase (Applied

Abbreviations: 3′UTR, 3′ untranslated region; ALP, alkaline phosphatase; circRNA, circular RNA; DPSCs, dental pulp stem cells; EDTA, ethylene diamine tetraacetic acid; FBS, fetal bovine serum; miRNA, microRNA; MSC, mesenchymal stem cell; OCN, osteocalcin; OSX, osterix; RUNX1, runt-related transcription factor 1.

TABLE 1 | Primers used in this study.

Gene name	Forward (5′-3′)	Reverse (5′-3′)
RUNX1	ACTACCAGCCACCGAGACCA	ACTGCTTGCAGCCTTAAATGACTCT
OCN	AGCCACCGAGACACCATGAGA	GGCTGCACCTTTGCTGGACT
ALP	GAACGTGGTCACCTCCATCCT	TCTCGTGGTCACAATGC
OSX	ACTGCCCCACCCCTTAGACA	GAGGTGCACCCCCAAACCAA
miR-188-3p	ATGTACACAAGCACACCTTCTCATT	TCAGAAAGCTCACCCTCCACCAT
hsa_circ_0026827	GCTGAAGAATTAAATC	CGAAGTTCCGTCTACGGC
U6	CTCGCTTCGGCAGCACA	AACGCTTCACGAATTTGCGT
GAPDH	CGACAGTCAGCCGCATCTT	CCAATACGACCAAATCCGTTG

Biosystems, Foster City, CA, United States) and random primers for cDNA synthesis. Afterward, we performed real-time quantitative reverse transcription PCR (RT-qPCR) utilizing Power SYBR Green PCR Mastermix (Applied Biosystems) on the Applied Biosystems 7500 Real-time Fast PCR System. We carried out PCR in triplicate for every gene. We calculated relative expression by the $2^{-\Delta\Delta Ct}$ method, with glyceraldehyde-3-phosphate dehydrogenase (GAPDH) or U6 for normalization. **Table 1** lists human gene-specific PCR primers.

Dual Luciferase Reporter Assay

We generated reporter plasmids by adding circRNA, Beclin-1 or RUNX1 3′-UTR sequence to the pGL3 vector (Promega, Madison, WI, United States). We co-transfected miR-188-3p mimics and reporter plasmids into 239T cells via Lipofectamine 2000 for the luciferase assay. After culturing for two days, we measured firefly and Renilla luciferase activities through the Dual Luciferase Reporter Assay System (Promega) following standard procedures.

Alkaline Phosphatase Staining

We employed the NBT/BCIP staining kit (CoWin Biotech, Beijing, China) for ALP staining following the manufacturer's protocol. We seeded DPSCs in 24-well plates and cultured them in osteogenic medium (OM) for one or two weeks. We then fixed cells with 4% paraformaldehyde (PFA) for 30 min, followed by incubation in staining reagent in the dark for 20 min.

Mineralization Assay

We seeded DPSCs in 24-well tissue culture plates and cultured them for 1 or 2 weeks in OM so as to measure calcium deposition in the extracellular matrix. We employed a solution of 0.1% Alizarin red S (Sigma-Aldrich, Saint Louis, MO, United States) at pH 4.2 to stain the calcified nodules after fixing DPSCs in 4% PFA.

In vivo Heterotopic Bone Formation Assay

We induced DPSCs under OM for 1 week prior to *in vivo* study. We resuspended cells and incubated them with 7 mm × 5 mm × 2 mm Bio-Oss Collagen scaffolds (Geistlich, GEWO GmbH, Baden-Baden, Germany) for 1 h at 37°C followed by centrifugation at 150 g for 5 min. We then implanted them subcutaneously on the backs of BALB/c homozygous nude (nu/nu) mice (5 mice per group) for 5 weeks old according

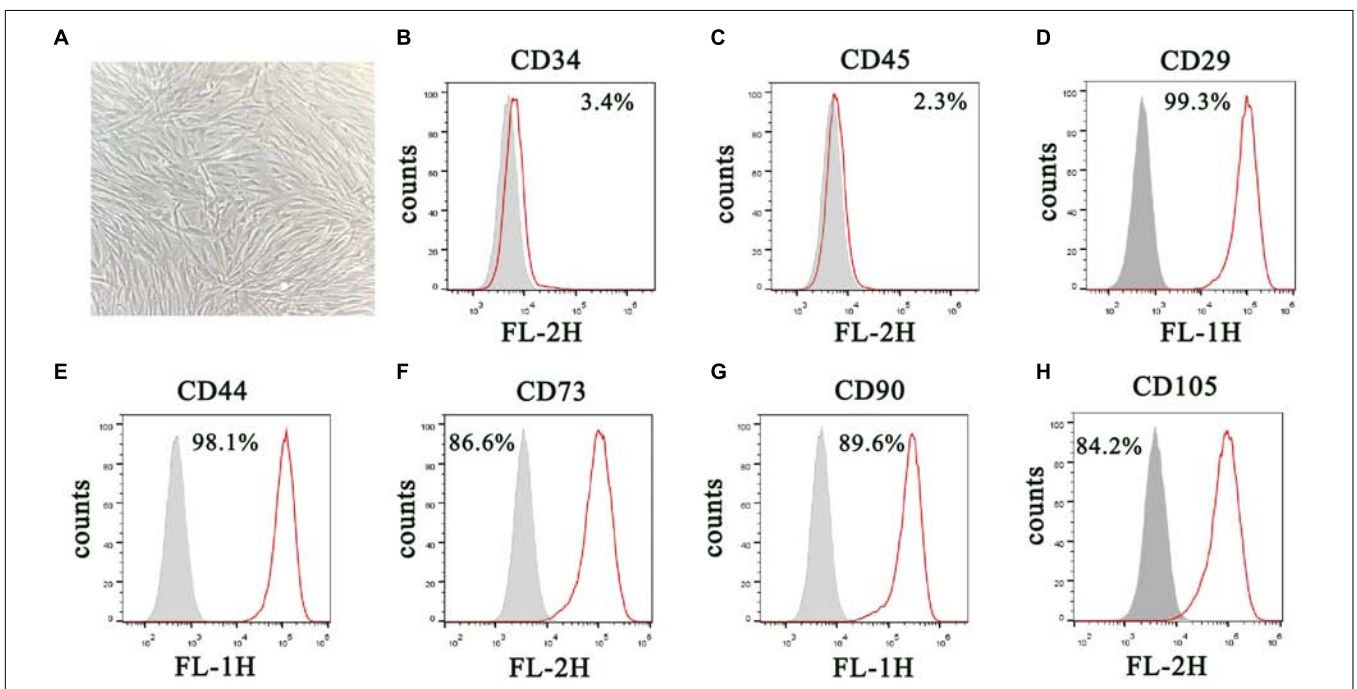

FIGURE 1 | Isolation and characterization of DPSCs. **(A)** Morphology of DPSCs show adoption of fibroblast-like morphology. **(B–H)** Surface protein profiles of DPSCs as analyzed by flow cytometry.

to Jin et al. (2016). We harvested implants after implanted for eight weeks.

Masson's Trichrome, H&E Staining and Immunohistochemical Analysis

We decalcified implanted scaffolds in 10% EDTA, pH 7.4 for 1 month, followed by dehydration and embedding in paraffin. We cut sections of heterotopic bones (5 μm) and stained them with Masson's trichrome and hematoxylin and eosin (H&E). Also, we evaluated sections by immunohistochemical analysis according to Wei et al. (2014). We blocked specimens with 5% normal goat serum for 30 min and then incubated them with primary antibody against OCN (Santa Cruz Biotechnology, Dallas, TX, United States) at 4°C overnight. We then processed sections through an ABC detection kit (Vector Laboratories, Burlingame, CA, United States) and visualized them under an Olympus microscope (Olympus Co., Tokyo, Japan).

Statistical Analysis

Data are displayed as means ± SD (standard deviation). We utilized GraphPad Prism, version 5.0 (GraphPad, La Jolla, CA, United States) to analyze group differences. $P \leq 0.05$ was regarded as statistically significant.

RESULTS

Expression of hsa_circ_0026827 Increased With Osteogenic Differentiation of DPSCs

DPSCs were isolated and displayed a typical cobblestone-like morphology (**Figure 1A**). Immunofluorescence staining showed that isolated DPSCs were negative for CD34 (**Figure 1B**) and CD45 (**Figure 1C**) expression but were positive for mesenchymal cell surface markers CD29 (**Figure 1D**), CD44 (**Figure 1E**), CD73 (**Figure 1F**), CD90 (**Figure 1G**), and CD105 (**Figure 1H**). The osteogenic potential of DPSCs was analyzed with ALP and Alizarin Red S (ARS) staining. Results showed that odontogenic induction promoted osteogenic differentiation of DPSCs in a time-dependent manner (**Figure 2A**). RT-qPCR detection showed that mRNA expression of osteogenic markers *RUNX1*, *ALP*, *OSX* and *OCN* was also consistently and significantly increased during osteogenic differentiation (**Figures 2B–E**).

Previous studies have found that hsa_circ_0026827 expression promotes osteogenic differentiation (Zhang et al., 2019). To determine if hsa_circ_0026827 plays a role in DPSC osteogenic differentiation, we quantified the hsa_circ_0026827 expression level with RT-qPCR and showed that its expression significantly increased during osteogenic differentiation (**Figure 2F**).

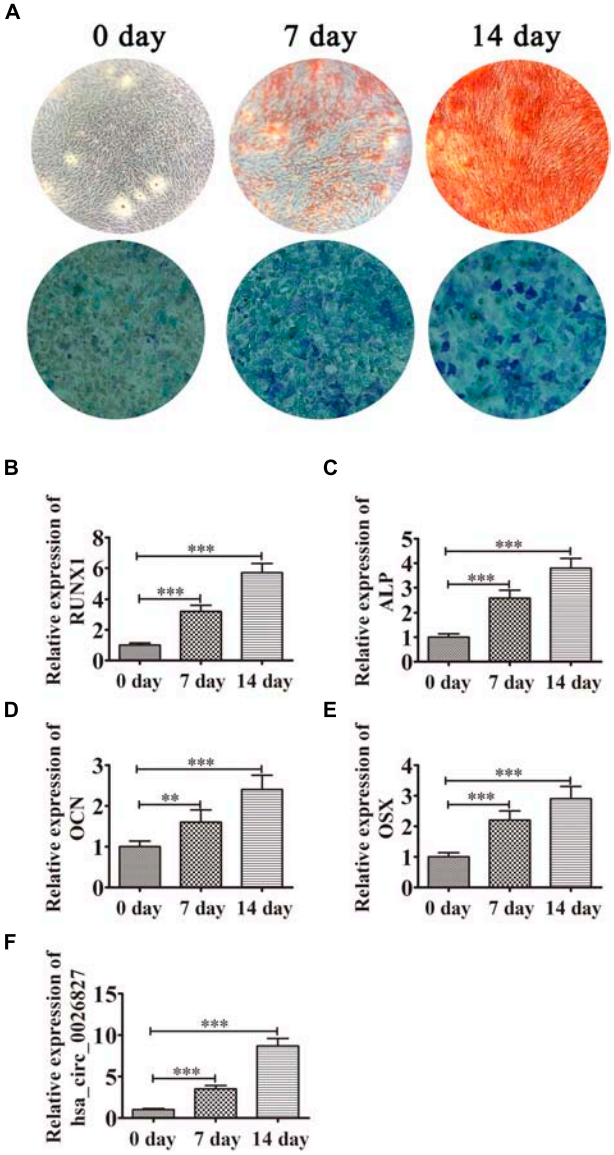

FIGURE 2 | Expression of hsa_circ_0026827 increased with osteogenic differentiation of DPSCs. **(A)** Photographs of ALP (bottom images) and alizarin red staining (top images) show the osteogenic differentiation potential of DPSCs. **(B–E)** RT-qPCR detection shows the expression of RUNX1, OCN, ALP and OSX. Results are presented as means ± SD. $^{**}P < 0.01$, $^{***}P < 0.001$ vs control (0 day). **(F)** RT-qPCR detection shows the expression of hsa_circ_0026827. Results are presented as means ± SD. $^{***}P < 0.001$ vs control (0 day).

hsa_circ_0026827 Knockdown Decreased the Osteogenic Differentiation Potential of DPSCs by Regulating miRNA Expression

To illuminate the function of hsa_circ_0026827, we constructed an siRNA expression vector to silence its expression. The results of ALP and ARS staining demonstrated that DPSC osteogenic differentiation decreased 14 days after osteogenic induction in hsa_circ_0026827-silenced cells (**Figure 3A**). RT-qPCR detection also validated that mRNA expression of osteogenic markers *RUNX1*, *ALP*, *OCN* and *OSX* was significantly decreased during osteogenic differentiation after knockdown of hsa_circ_0026827 (**Figure 3B**). Dental pulp stem cells were then collected for RNA sequencing (RNA-seq) analyses using hierarchical cluster analysis

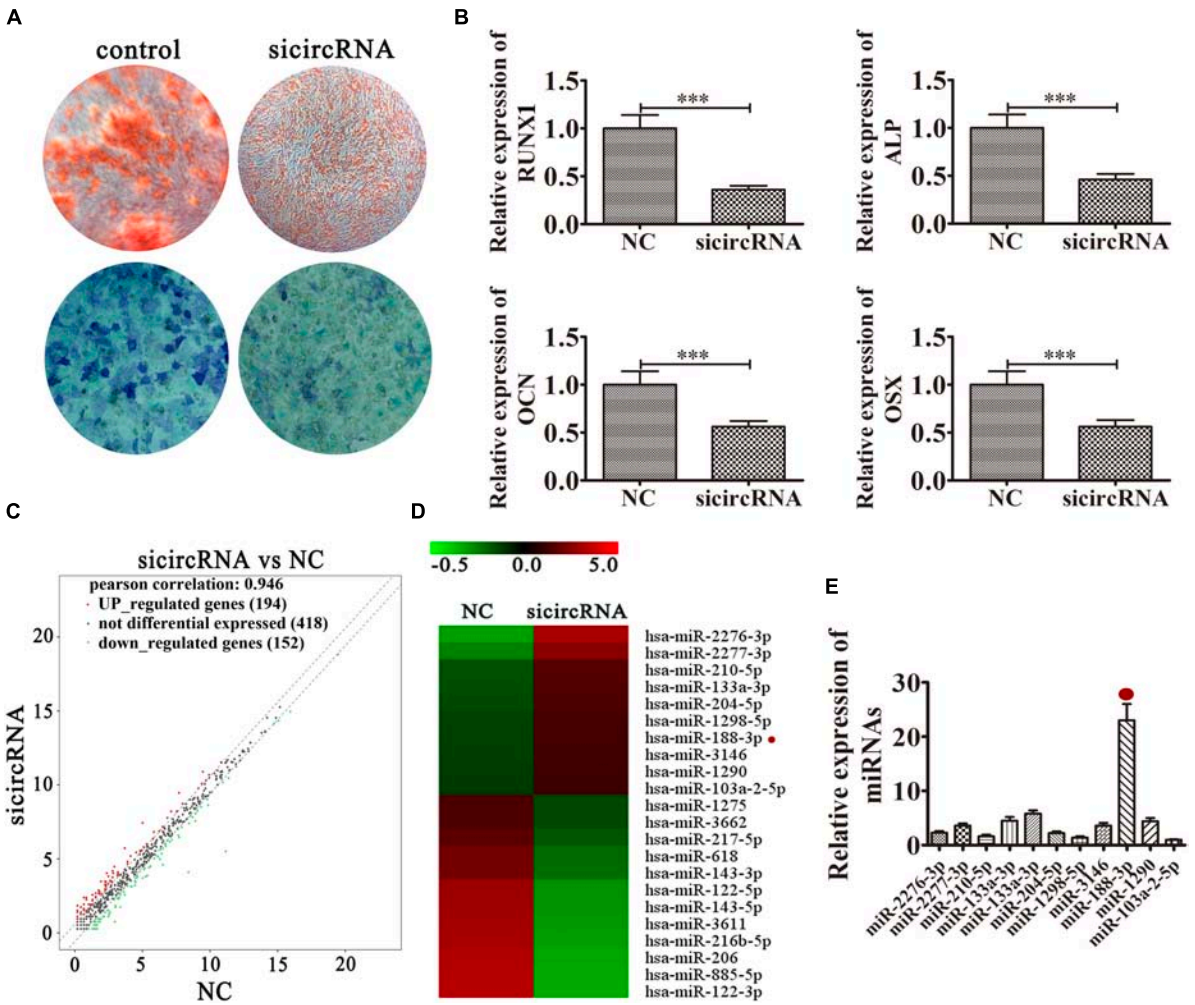

FIGURE 3 | Knockdown of hsa_circ_0026827 decreased the osteogenic differentiation potential of DPSCs by regulating miRNA expression. **(A)** Photographs of ALP (bottom images) and alizarin red staining (top images) show the osteogenic differentiation potential of DPSCs after induction for 14 days. **(B)** RT-qPCR detection shows the expression of RUNX1, OCN, ALP, OSX. Results are presented as means ± SD. ***$P < 0.001$ vs control. **(C)** Hierarchical cluster analysis of the samples found that a total of 194 miRNAs were upregulated and 152 miRNAs were downregulated after hsa_circ_0026827 knockdown in DPSCs. **(D)** Heat map from microarray data showing the differentially expressed miRNAs. **(E)** RT-qPCR analysis shows miRNA relative expression after knockdown of hsa_circ_0026827.

of miRNA expression. The results revealed that 194 miRNAs were upregulated and 152 were downregulated in knockdown cells (**Figure 3C**). Heat maps of microarray data showed differential expression of miRNAs, including upregulation of miR-2276-3p, miR-188-3p, miR-2277-3p, miR-210-5p, miR-133a-3p, miR-204-5p, miR-1298-5p, miR-3146, miR-1290 and miR-103a-2-5p (**Figure 3D**). In particular, RT-qPCR assays indicated that miR-188-3p expression significantly increased after knockdown of hsa_circ_0026827 (**Figure 3E**).

Downregulation of miR-188-3p Restored Osteogenic Differentiation of DPSCs After hsa_circ_0026827 Silencing

To illustrate the interactive relationships between hsa_circ_0026827 and miR-188-3p, binding sites between hsa_circ_0026827 and miR-188-3p were predicted using the Starbase web site.[1] Luciferase vectors containing wild-type or mutated miR-188-3p binding sites were constructed (**Figure 4A**) and co-transfected into DPSCs with miR-188-3p mimic. Luciferase reporter analysis showed that miR-188-3p inhibited luciferase activity in hsa_circ_0026827 wild-type cells without affecting activity in the mutated cells line, suggesting that miR-188-3p was a potential hsa_circ_0026827 target (**Figure 4B**). RT-qPCR detection found that hsa_circ_0026827 expression was significantly reduced after hsa_circ_0026827 downregulation, while transfection with miR-188-3p inhibitor did not affect the recovery of hsa_circ_0026827 expression (**Figure 4C**). RT-qPCR analysis also indicated that silencing hsa_circ_0026827 promoted miR-188-3p expression and treatment with miR-188-3p inhibitor significantly decreased miR-188-3p expression (**Figure 4D**).

[1]http://starbase.sysu.edu.cn/

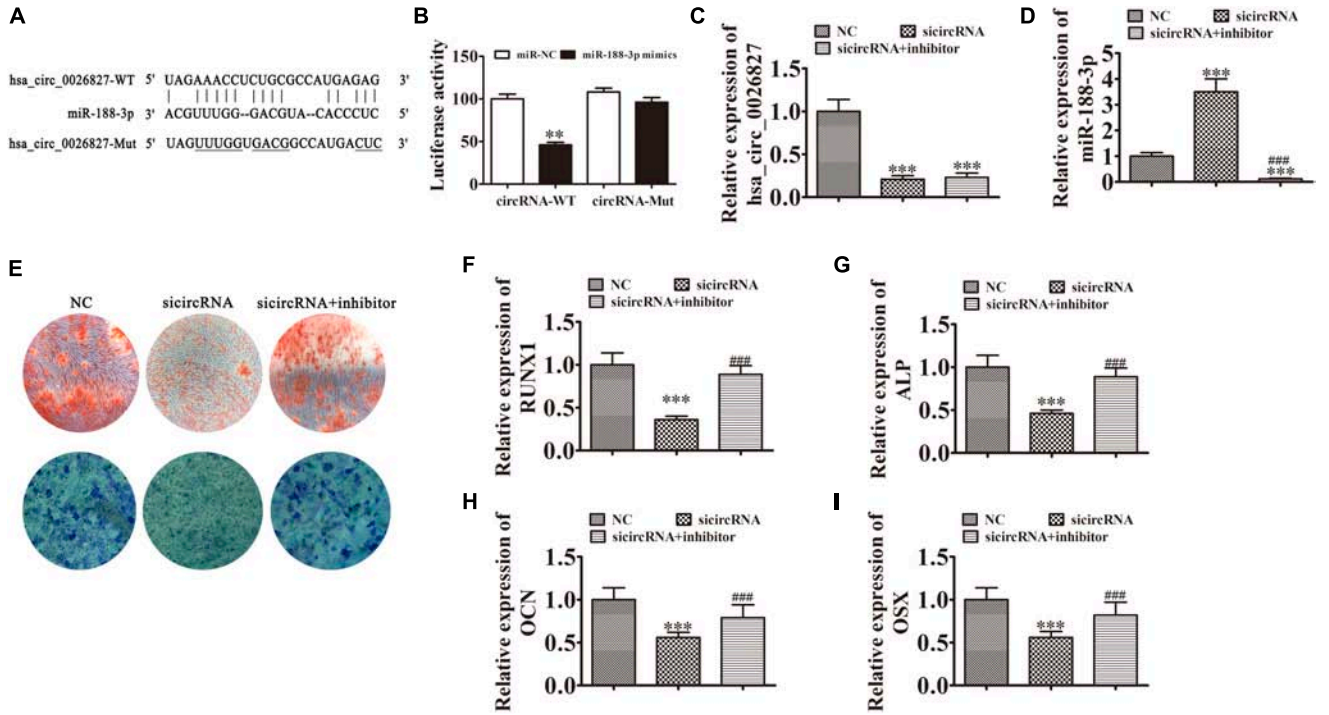

FIGURE 4 | Downregulation of miR-188-3p restored osteogenic differentiation of DPSCs after hsa_circ_0026827 silencing. **(A)** The predicted binding sites of miR-188-3p and hsa_circ_0026827. The mutated (Mut) version of hsa_circ_0026827 is also shown. **(B)** Relative luciferase activity was determined 48 h after transfection with miR-188-3p mimic/normal control (NC) or with wild-type/Mut hsa_circ_0026827 in HEK293T cells. Data are presented as means ± SD. $^{**}P < 0.01$. **(C,D)** RT-qPCR detection shows the expression of hsa_circ_0026827 **(C)** and miR-188-3p **(D)** after transfection with siRNA against hsa_circ_0026827 with and without miR-188-3p inhibitor. Results are presented as means ± SD. $^{***}P < 0.001$ vs NC. $^{\#\#\#}P < 0.001$ vs sicircRNA. **(E)** Photographs of ALP (bottom images) and alizarin red staining (top images) show the osteogenic differentiation potential of DPSCs. **(F–I)** RT-qPCR detection shows the expression of RUNX1, OCN, ALP and OSX. Results are presented as means ± SD. $^{***}P < 0.001$ vs NC. $^{\#\#\#}P < 0.001$ vs sicircRNA.

Results of ALP and ARS staining verified that DPSC osteogenic differentiation 14 days after osteogenic induction was decreased after hsa_circ_0026827 silencing (**Figure 4E**), but downregulation of miR-188-3p restored osteogenic differentiation of DPSCs. RT-qPCR assays also validated that mRNA expression of osteogenic markers *RUNX1*, *ALP*, *OSX*, and *OCN* significantly decreased during osteogenic differentiation after knockdown of hsa_circ_0026827, but miR-188-3p downregulation restored the expression of these markers (**Figures 4F–I**).

miR-188-3p Overexpression Suppressed DPSC Osteogenic Differentiation Through Targeting Beclin-1-Mediated Autophagy

Further experiments found that Beclin-1 was the downstream miR-188-3p target. To examine the relation between Beclin-1 and miR-188-3p, miR-188-3p binding sites in the Beclin-1 3′ untranslated region (3′UTR) were predicted by the Targetscan web site.[2] We then constructed Beclin-1 luciferase vectors containing wild-type or mutated miR-188-3p binding sites and co-transfected them with miR-188-3p mimic into DPSCs (**Figure 5A**). miR-188-3p inhibited luciferase activity in cells containing the wild-type Beclin-1 3′UTR but did not affect mutated cell line activity, indicating that Beclin-1 was a potential miR-188-3p target (**Figure 5B**). RT-qPCR assays found that miR-188-3p expression significantly increased after transfection with miR-188-3p mimic, while transfection with a Beclin-1 overexpression vector did not affect miR-188-3p expression (**Figure 5C**). RT-qPCR detection also found that miR-188-3p overexpression decreased Beclin-1 expression, but transfection with the Beclin-1 overexpression vector significantly enhanced Beclin-1 expression (**Figure 5D**). Immunofluorescence assays showed that miR-188-3p overexpression decreased autophagy plaque formation, but after Beclin-1 overexpression, autophagy of DPSCs recovered under osteogenic differentiation conditions (**Figures 5E,F**).

The results of ALP and ARS staining illustrated that DPSC osteogenic differentiation 14 days after osteogenic induction was decreased by miR-188-3p overexpression (**Figure 5G**), but Beclin-1 overexpression restored the osteogenic differentiation of DPSCs. RT-qPCR detection also verified that mRNA expression of osteogenic markers *RUNX1*, *ALP*, *OSX*, and *OCN* was significantly decreased during osteogenic differentiation after upregulation of miR-188-3p, but

[2]http://www.targetscan.org/vert_71/

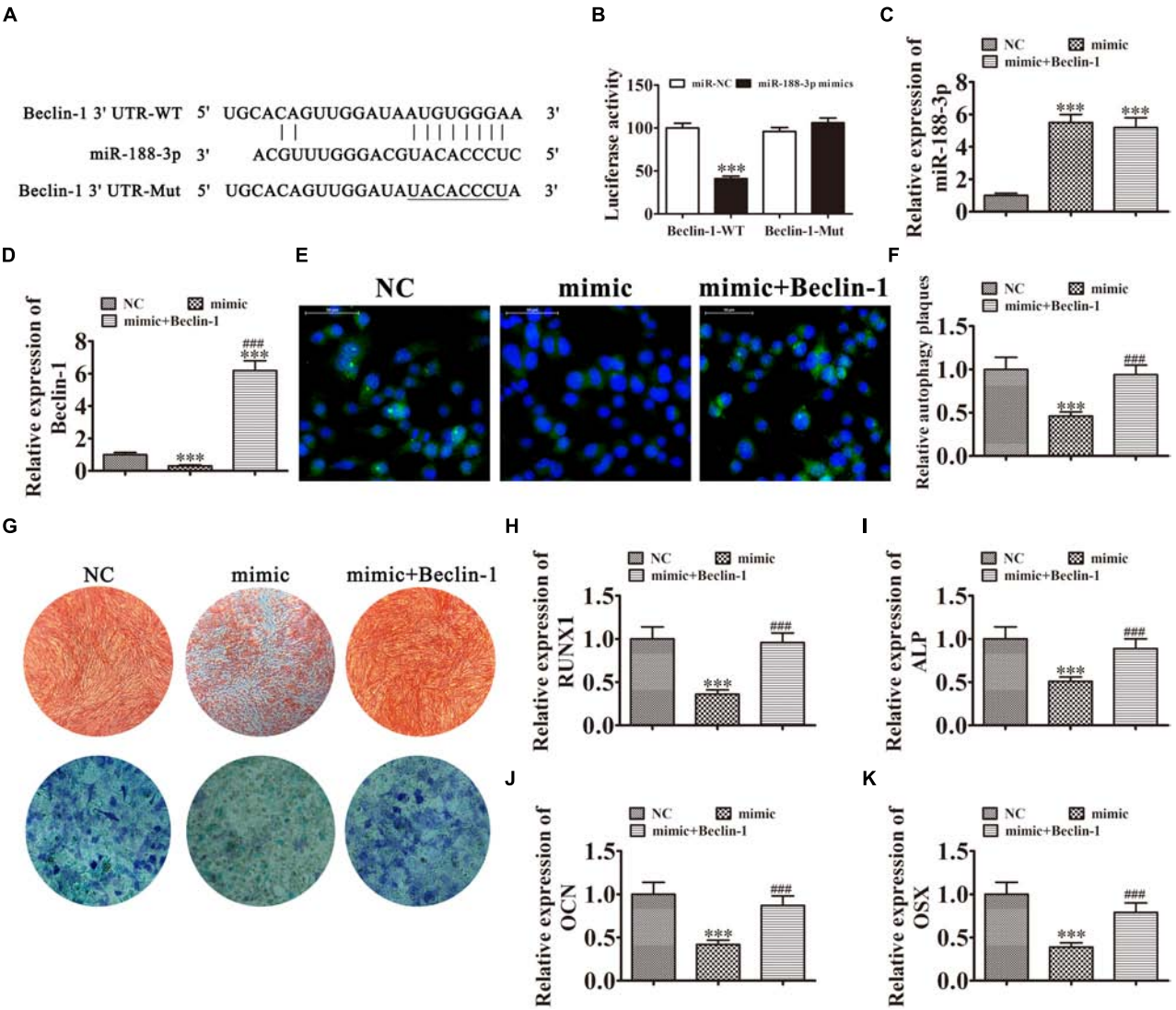

FIGURE 5 | Overexpression of miR-188-3p suppressed osteogenic differentiation of DPSCs by targeting Beclin-1-mediated autophagy. **(A)** The predicted binding sites of miR-188-3p in the 3′UTR of Beclin-1. The mutated (Mut) version of the Beclin-1 3′UTR is also shown. **(B)** Relative luciferase activity was determined 48 h after transfection with miR-188-3p mimic/normal control (NC) or with the wild-type/Mut Beclin-1 3′UTR in HEK293T cells. Data are presented as means ± SD. $^{***}P < 0.001$. **(C,D)** RT-qPCR assays show the expression of miR-188-3p (C) and Beclin-1 **(D)** after transfection with miR-188-3p mimic with and without the Beclin-1 overexpression vector. Results are presented as means ± SD. $^{***}P < 0.001$ vs NC. $^{###}P < 0.001$ vs mimic. **(E,F)** Immunofluorescence detection shows autophagy plaques. Results are presented as means ± SD. $^{***}P < 0.001$ vs NC. $^{###}P < 0.001$ vs mimic. **(G)** Photographs of alizarin red (top images) and ALP staining (bottom images) show the osteogenic differentiation potential of DPSCs. **(H–K)** RT-qPCR analysis shows the expression of RUNX1, OCN, ALP and OSX. Results are presented as means ± SD. $^{***}P < 0.001$ vs NC. $^{###}P < 0.001$ vs mimic.

overexpression of Beclin-1 restored expression of these markers (**Figures 5H–K**).

miR-188-3p Overexpression Suppressed DPSC Osteogenic Differentiation by Targeting RUNX1

In addition to Beclin-1, we determined that RUNX1 was another downstream miR-188-3p target. To examine the interactions between RUNX1 and miR-188-3p, the miR-188-3p binding sites in the RUNX1 3′UTR were predicted through the Targetscan web site tool. We then constructed luciferase vectors containing wild-type or mutated RUNX1 3′UTR sequence (**Figure 6A**) and co-transfected them with miR-188-3p mimic into DPSCs. Luciferase reporter analysis showed that miR-188-3p inhibited luciferase activity in cells containing wild-type RUNX1 3′UTR without affecting mutated cell line activity, suggesting that RUNX1 was a potential miR-188-3p target (**Figure 6B**). RT-qPCR analysis found that miR-188-3p expression significantly increased after transfection with miR-188-3p mimic, while transfection with the RUNX1 overexpression vector did not affect miR-188-3p

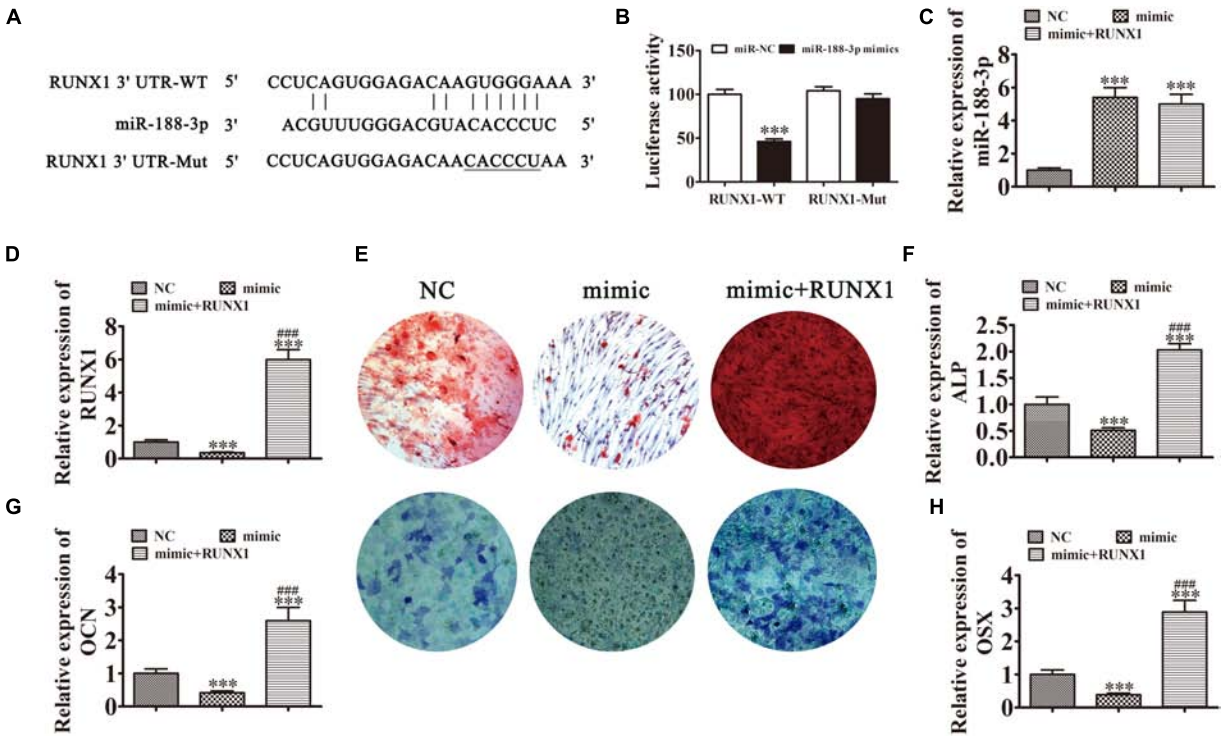

FIGURE 6 | Overexpression of miR-188-3p suppressed osteogenic differentiation of DPSCs by targeting RUNX1. **(A)** The predicted binding sites of miR-188-3p in the 3′UTR of RUNX11. The mutated (Mut) version of the RUNX1 3′UTR is also shown. **(B)** Relative luciferase activity was determined 48 h after transfection with miR-188-3p mimic/normal control (NC) or with the wild-type/Mut RUNX1 3′UTR in HEK293T cells. Data are presented as means ± SD. $^{***}P < 0.001$. **(C,D)** RT-qPCR detection shows the expression of miR-188-3p and RUNX1 after transfection with miR-188-3p mimic with **(C)** and without the RUNX1 overexpression vector **(D)**. Results are presented as means ± SD. $^{***}P < 0.001$ vs NC. $^{###}P < 0.001$ vs mimic. **(E)** Photographs of alizarin red (top images) and ALP staining (bottom images) show the osteogenic differentiation potential of DPSCs. **(F–H)** RT-qPCR detection shows the expression of OCN, ALP and OSX. Results are presented as means ± SD. $^{***}P < 0.001$ vs NC. $^{###}P < 0.001$ vs mimic.

expression (**Figure 6C**). RT-qPCR assays also indicated that miR-188-3p overexpression decreased RUNX1 expression and that transfection with the RUNX1 overexpression vector significantly increased RUNX1 expression (**Figure 6D**).

Detection of ARS and ALP showed that the osteogenic differentiation of DPSCs 14 days after osteogenic induction was decreased after miR-188-3p overexpression (**Figures 6E,F**), but RUNX1 overexpression restored the osteogenic differentiation of DPSCs. RT-qPCR detection also showed that mRNA levels of osteogenic markers *ALP*, *OCN* and *OSX* were significantly decreased during osteogenic differentiation after upregulation of miR-188-3p, but that overexpression of RUNX1 restored the expression of these markers (**Figures 6G,H**).

hsa_circ_0026827 Expression Functions Indispensably in Promoting Heterotopic Bone Formation *in vivo*

To verify whether hsa_circ_0026827 expression can influence bone formation *in vivo*, we loaded DPSCs expressing sh-hsa_circ_0026827, hsa_circ_0026827 or a negative control (NC) onto Bio-Oss Collagen scaffolds and implanted them in nude mouse subcutaneous tissue (five mice per group). A flowchart of the process is shown in **Figure 7A**. We harvested implantation samples and analyzed them after 8 weeks. The bone tissue amount shown in H&E staining and collagen organization displaying a blue color by Masson's trichrome staining was significantly higher in implants containing hsa_circ_0026827 overexpressing cells but were reduced in the sh-hsa_circ_0026827 group. Also, bone trabeculae and osteoblasts were positive for OCN, which can be observed in immunohistochemical staining. The intensity and size of staining increased in the hsa_circ_0026827 overexpression group and decreased in the hsa_circ_0026827 downregulation group (**Figure 7B**).

DISCUSSION

An increasing number of studies have found that MSCs exert different but fundamental roles as promoters, enhancers and playmakers of the translational regenerative medicine (for review see Ballini et al., 2017). Recent reports have demonstrated the therapeutic effects of MSCs in animal models, explained by the ability of MSCs to be activated by signals from injured tissues. In these damaged areas, MSCs showed regenerative behavior (Uccelli and Prockop, 2010; Cantore et al., 2018). Studies have also found that cells from dental tissues have an MSC

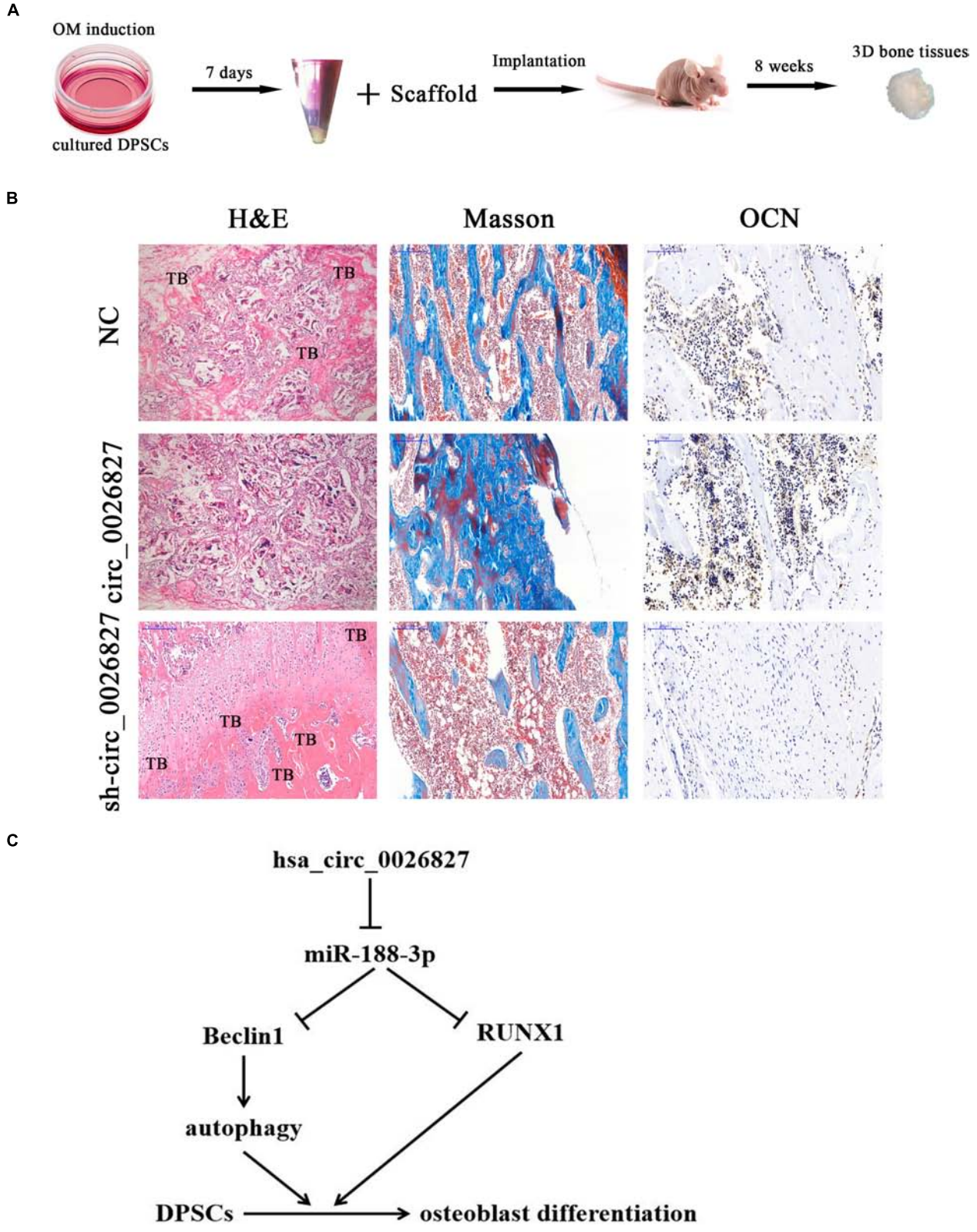

FIGURE 7 | Hsa_circ_0026827 expression plays an important role in promoting heterotopic bone formation *in vivo*. **(A)** Schematic diagram illustrating the experimental setup. **(B)** H&E staining, Masson's trichrome staining, and immunohistochemical staining of OCN in heterotopic bone. **(C)** Proposed mechanism showing how hsa_circ_0026827 may promote bone formation.

phenotype and can differentiate into osteoblastic cells (Brunetti et al., 2018; Ballini et al., 2019a,b), but the regulatory mechanism is unclear. Previous reports indicated that hsa_circ_0026827 was abnormally expressed during osteogenic differentiation. In the current study, found that hsa_circ_0026827 expression in DPSCs significantly increased during osteogenic differentiation. Downregulation of hsa_circ_0026827 suppressed osteogenic differentiation. In order to clarify the regulatory mechanisms, miRNA expression profiles were analyzed and a number of differentially expressed miRNAs were found, including miR-188-3p. The expression of this miRNA significantly increased after downregulation of hsa_circ_0026827. Luciferase reporter assays validated that miR-188-3p was the target of hsa_circ_0026827. Previous studies have found that miR-188 decreased in osteogenic mouse bone marrow stromal stem cells (Wang et al., 2018). BMSC-specific miR-188 inhibition by intra-bone marrow aptamer-antagomiR-188 injection increased bone formation (Li et al., 2015). This study also verified that evoked miR-188-3p expression impaired cell proliferation, especially tumor cells (Pei et al., 2019; Shi et al., 2019).

To further reveal the regulatory mechanisms, the miR-188-3p target was predicted using a bioinformatics website and luciferase reporter assays. The results verified that miR-188-3p could interact with both the RUNX1 and Beclin1 3′UTRs. Overexpressing miR-188-3p suppressed osteogenic differentiation of DPSCs by targeting RUNX1. The RUNX transcription factor family binds DNA as heterodimers with CBFβ, which function critically in embryonic development. Currently, RUNX3, and RUNX1 have been characterized in the RUNX family (Choi et al., 2001). RUNX1 is a crucial transcription factor that regulates hematopoiesis and hematopoietic stem cells. Increasing evidence has shown that RUNX1 takes part in a variety of maturational processes required for skeletal developmental events (Wang et al., 2005; Qin et al., 2015; Lv et al., 2017). Previous studies found that RUNX1 acts as regulator in BMP9-induced MSCs and that MMC osteogenic differentiation occurs primarily through effects on Smad1/5/8 and MAPK signaling (Rahman et al., 2015).

Our study also found that overexpression miR-188-3p suppressed osteogenic differentiation of DPSCs by targeting Beclin-1-mediated autophagy. Autophagy is a natural self-cannibalization procedure that provides orderly degradation and recycling of dysfunctional cellular organelles or macromolecules to guarantee cellular homeostasis (Sbrana et al., 2016). Studies have illustrated that autophagy functions importantly in stemness and self-renewal of MSC regulation (Rodolfo et al., 2016). Autophagy activation can also stimulate osteogenic differentiation, prevent bone loss and improve the cellular oxidative stress environment at the same time (Gomez-Puerto et al., 2016; Wan et al., 2017; Liang et al., 2019). Our study suggests that hsa_circ_0026827 promotes osteogenic differentiation by upregulating Beclin-1-mediated autophagy through sponging of miR-188-3p.

CONCLUSION

This study verified that abnormal hsa_circ_0026827 expression was associated with osteogenic differentiation in DPSCs, which demonstrated that hsa_circ_0026827 promotes osteoblast differentiation of DPSCs via the Beclin1 and RUNX1 signaling pathways by sponging miR-188-3p (**Figure 7C**). The present study not only furthers our understanding of the role of hsa_circ_0026827 in osteogenic differentiation, but also suggests novel therapeutic possibilities for bone regeneration.

DATA AVAILABILITY STATEMENT

The raw data supporting the conclusions of this article will be made available by the authors, without undue reservation, to any qualified researcher.

AUTHOR CONTRIBUTIONS

FJ, LZ, and JT conceived the research and drafted the manuscript with comments from all authors. JP, ZS, ZY, and JW conducted the experiments and analyses. XB and YL participated in experiments and revised the manuscript. All authors approved the final version.

FUNDING

This research was aided by grants from STCSM (18ZR1422700), Interdisciplinary Program of SJTU (YG2019ZDA07), and Innovative Research Team of high-level local universities in Shanghai.

REFERENCES

Ballini, A., Cantore, S., Scacco, S., Perillo, L., Scarano, A., Aityan, S. K., et al. (2019b). A comparative study on different stemness gene expression between dental pulp stem cells vs. dental bud stem cells. *Eur. Rev. Med. Pharmacol. Sci.* 23, 1626–1633.

Ballini, A., Di Benedetto, A., De Vito, D., Scarano, A., Scacco, S., Perillo, L., et al. (2019a). Stemness genes expression in naive vs. osteodifferentiated human dental-derived stem cells. *Eur. Rev. Med. Pharmacol. Sci.* 23, 2916–2923.

Ballini, A., Scacco, S., Coletti, D., Pluchino, S., and Tatullo, M. (2017). Mesenchymal stem cells as promoters, enhancers, and playmakers of the translational regenerative medicine. *Stem. Cells Int.* 2017:3292810. doi: 10.1155/2017/3292810

Brunetti, G., Di Benedetto, A., Posa, F., Colaianni, G., Faienza, M. F., Ballini, A., et al. (2018). High expression of TRAIL by osteoblastic differentiated dental pulp stem cells affects myeloma cell viability. *Oncol. Rep.* 39, 2031–2039.

Cantore, S., Crincoli, V., Boccaccio, A., Uva, A. E., Fiorentino, M., Monno, G., et al. (2018). Recent advances in endocrine, metabolic and immune disorders: mesenchymal stem cells (MSCs) and engineered scaffolds. *Endocr. Metab. Immune Disord. Drug Targets* 18, 466–469. doi: 10.2174/1871530318666180423102905

Ching, H. S., Luddin, N., Rahman, I. A., and Ponnuraj, K. T. (2017). Expression of odontogenic and osteogenic markers in DPSCs and SHED: a review. *Curr. Stem. Cell Res. Ther.* 12, 71–79. doi: 10.2174/1574888x11666160815095733

Choi, J. Y., Pratap, J., Javed, A., Zaidi, S. K., Xing, L., Balint, E., et al. (2001). Subnuclear targeting of Runx/Cbfa/AML factors is essential for tissue-specific differentiation during embryonic development. *Proc. Natl. Acad. Sci. U.S.A.* 98, 8650–8655. doi: 10.1073/pnas.151236498

Daniel, C., Behm, M., and Ohman, M. (2015). The role of Alu elements in the cis-regulation of RNA processing. *Cell Mol. Life Sci.* 72, 4063–4076. doi: 10.1007/s00018-015-1990-3

Dominici, M., Le Blanc, K., Mueller, I., Slaper-Cortenbach, I., Marini, F., Krause, D., et al. (2006). Minimal criteria for defining multipotent mesenchymal stromal cells. International society for cellular therapy position statement. *Cytotherapy* 8, 315–317. doi: 10.1080/14653240600855905

Gomez-Puerto, M. C., Verhagen, L. P., Braat, A. K., Lam, E. W., Coffer, P. J., and Lorenowicz, M. J. (2016). Activation of autophagy by FOXO3 regulates redox homeostasis during osteogenic differentiation. *Autophagy* 12, 1804–1816. doi: 10.1080/15548627.2016.1203484

Hansen, T. B., Jensen, T. I., Clausen, B. H., Bramsen, J. B., Finsen, B., Damgaard, C. K., et al. (2013). Natural RNA circles function as efficient microRNA sponges. *Nature* 495, 384–388. doi: 10.1038/nature11993

Iezzi, I., Cerqueni, G., Licini, C., Lucarini, G., and Mattioli Belmonte, M. (2019). Dental pulp stem cells senescence and regenerative potential relationship. *J. Cell Physiol.* 234, 7186–7197. doi: 10.1002/jcp.27472

Jin, C., Jia, L., Huang, Y., Zheng, Y., Du, N., Liu, Y., et al. (2016). Inhibition of lncRNA MIR31HG promotes osteogenic differentiation of human adipose-derived stem cells. *Stem. Cells* 34, 2707–2720. doi: 10.1002/stem.2439

Li, C. J., Cheng, P., Liang, M. K., Chen, Y. S., Lu, Q., Wang, J. Y., et al. (2015). MicroRNA-188 regulates age-related switch between osteoblast and adipocyte differentiation. *J. Clin. Invest.* 125, 1509–1522. doi: 10.1172/jci77716

Li, X., Zheng, Y., Huang, Y., Zhang, Y., Jia, L., and Li, W. (2018). Circular RNA CDR1as regulates osteoblastic differentiation of periodontal ligament stem cells via the miR-7/GDF5/SMAD and p38 MAPK signaling pathway. *Stem. Cell Res. Ther.* 9:232.

Liang, X., Hou, Z., Xie, Y., Yan, F., Li, S., Zhu, X., et al. (2019). Icariin promotes osteogenic differentiation of bone marrow stromal cells and prevents bone loss in OVX mice via activating autophagy. *J. Cell Biochem.* 120, 13121–13132. doi: 10.1002/jcb.28585

Liu, J., Liu, T., Wang, X., and He, A. (2017). Circles reshaping the RNA world: from waste to treasure. *Mol. Cancer* 16:58. doi: 10.1186/s12943-017-0630-y

Lv, X., Yan, J., Jiang, J., Zhou, X., Lu, Y., and Jiang, H. (2017). MicroRNA-27a-3p suppression of peroxisome proliferator-activated receptor-gamma contributes to cognitive impairments resulting from sevoflurane treatment. *J. Neurochem.* 143, 306–319. doi: 10.1111/jnc.14208

Mangano, C., De Rosa, A., Desiderio, V., d'Aquino, R., Piattelli, A., De Francesco, F., et al. (2010). The osteoblastic differentiation of dental pulp stem cells and bone formation on different titanium surface textures. *Biomaterials* 31, 3543–3551. doi: 10.1016/j.biomaterials.2010.01.056

Pei, J., Zhang, J., Yang, X., Wu, Z., Sun, C., Wang, Z., et al. (2019). TMED3 promotes cell proliferation and motility in breast cancer and is negatively modulated by miR-188-3p. *Cancer Cell Int.* 19:75.

Qin, X., Jiang, Q., Matsuo, Y., Kawane, T., Komori, H., Moriishi, T., et al. (2015). Cbfb regulates bone development by stabilizing Runx family proteins. *J. Bone Miner. Res.* 30, 706–714. doi: 10.1002/jbmr.2379

Qu, S., Yang, X., Li, X., Wang, J., Gao, Y., Shang, R., et al. (2015). Circular RNA: A new star of noncoding RNAs. *Cancer Lett.* 365, 141–148. doi: 10.1016/j.canlet.2015.06.003

Rahman, M. S., Akhtar, N., Jamil, H. M., Banik, R. S., and Asaduzzaman, S. M. T. G. F. - (2015). beta/BMP signaling and other molecular events: regulation of osteoblastogenesis and bone formation. *Bone Res.* 3:15005.

Rapino, M., Di Valerio, V., Zara, S., Gallorini, M., Marconi, G. D., Sancilio, S., et al. (2019). Chitlac-coated thermosets enhance osteogenesis and angiogenesis in a co-culture of dental pulp stem cells and endothelial cells. *Nanomaterials (Basel)* 9:928. doi: 10.3390/nano9070928

Rodolfo, C., Di Bartolomeo, S., and Cecconi, F. (2016). Autophagy in stem and progenitor cells. *Cell Mol. Life Sci.* 73, 475–496.

Sbrana, F. V., Cortini, M., Avnet, S., Perut, F., Columbaro, M., De Milito, A., et al. (2016). The role of autophagy in the maintenance of stemness and differentiation of mesenchymal stem cells. *Stem Cell Rev. Rep.* 12, 621–633. doi: 10.1007/s12015-016-9690-4

Sharpe, P. T. (2016). Dental mesenchymal stem cells. *Development* 143, 2273–2280. doi: 10.1242/dev.134189

Shen, W. C., Lai, Y. C., Li, L. H., Liao, K., Lai, H. C., Kao, S. Y., et al. (2019). Methylation and PTEN activation in dental pulp mesenchymal stem cells promotes osteogenesis and reduces oncogenesis. *Nat. Commun.* 10: 2226.

Shi, W., Zhang, C., Ning, Z., Hua, Y., Li, Y., Chen, L., et al. (2019). Long non-coding RNA LINC00346 promotes pancreatic cancer growth and gemcitabine resistance by sponging miR-188-3p to derepress BRD4 expression. *J. Exp. Clin. Cancer Res.* 38:60.

Spath, L., Rotilio, V., Alessandrini, M., Gambara, G., De Angelis, L., Mancini, M., et al. (2010). Explant-derived human dental pulp stem cells enhance differentiation and proliferation potentials. *J. Cell Mol. Med.* 14, 1635–1644. doi: 10.1111/j.1582-4934.2009.00848.x

Tao, J., Wang, H., Zhai, Y., Park, H., Wang, J., Ji, F., et al. (2016). Downregulation of Nrf2 promotes autophagy-dependent osteoblastic differentiation of adipose-derived mesenchymal stem cells. *Exp. Cell Res.* 349, 221–229. doi: 10.1016/j.yexcr.2016.09.013

Uccelli, A., and Prockop, D. J. (2010). Why should mesenchymal stem cells (MSCs) cure autoimmune diseases? *Curr. Opin. Immunol.* 22, 768–774. doi: 10.1016/j.coi.2010.10.012

Victor, A. K., and Reiter, L. T. (2017). Dental pulp stem cells for the study of neurogenetic disorders. *Hum. Mol. Genet.* 26, R166–R171.

Wan, Y., Zhuo, N., Li, Y., Zhao, W., and Jiang, D. (2017). Autophagy promotes osteogenic differentiation of human bone marrow mesenchymal stem cell derived from osteoporotic vertebrae. *Biochem. Biophys. Res. Commun.* 488, 46–52. doi: 10.1016/j.bbrc.2017.05.004

Wang, L., Chen, K., Wan, X., Wang, F., Guo, Z., and Mo, Z. (2017). NLRP3 inflammasome activation in mesenchymal stem cells inhibits osteogenic differentiation and enhances adipogenic differentiation. *Biochem. Biophys. Res. Commun.* 484, 871–877. doi: 10.1016/j.bbrc.2017.02.007

Wang, Y., Belflower, R. M., Dong, Y. F., Schwarz, E. M., O'Keefe, R. J., and Drissi, H. (2005). Runx1/AML1/Cbfa2 mediates onset of mesenchymal cell differentiation toward chondrogenesis. *J. Bone Miner. Res.* 20, 1624–1636. doi: 10.1359/jbmr.050516

Wang, Y., Liu, W., Liu, Y., Cui, J., Zhao, Z., Cao, H., et al. (2018). Long noncoding RNA H19 mediates LCoR to impact the osteogenic and adipogenic differentiation of mBMSCs in mice through sponging miR-188. *J. Cell Physiol.* 233, 7435–7446. doi: 10.1002/jcp.26589

Wei, J., Li, H., Wang, S., Li, T., Fan, J., Liang, X., et al. (2014). let-7 enhances osteogenesis and bone formation while repressing adipogenesis of human stromal/mesenchymal stem cells by regulating HMGA2. *Stem. Cells Dev.* 23, 1452–1463. doi: 10.1089/scd.2013.0600

Zhang, M., Jia, L., and Zheng, Y. (2019). circRNA expression profiles in human bone marrow stem cells undergoing osteoblast differentiation. *Stem. Cell Rev.* 15, 126–138. doi: 10.1007/s12015-018-9841-x

Conflict of Interest: The authors declare that the research was conducted in the absence of any commercial or financial relationships that could be construed as a potential conflict of interest.

frontiers in Cell and Developmental Biology

REVIEW
published: 08 July 2020
doi: 10.3389/fcell.2020.00561

Adipogenesis, Osteogenesis, and Chondrogenesis of Human Mesenchymal Stem/Stromal Cells: A Comparative Transcriptome Approach

Anny W. Robert, Bruna H. Marcon, Bruno Dallagiovanna and Patrícia Shigunov**

Instituto Carlos Chagas – Fiocruz Paraná, Curitiba, Brazil

OPEN ACCESS

Edited by:
Lindolfo da Silva Meirelles, Universidade Luterana do Brazil, Brazil

Reviewed by:
Maria Fernanda Forni, Yale University, United States
Akiyoshi Uezumi, Tokyo Metropolitan Institute of Gerontology, Japan

***Correspondence:**
Bruno Dallagiovanna
bruno.dallagiovanna@fiocruz.br
Patrícia Shigunov
patricia.shigunov@fiocruz.br; shigu9@yahoo.com.br

Specialty section:
This article was submitted to Stem Cell Research, a section of the journal Frontiers in Cell and Developmental Biology

Received: *31 March 2020*
Accepted: *12 June 2020*
Published: *08 July 2020*

Citation:
Robert AW, Marcon BH, Dallagiovanna B and Shigunov P (2020) Adipogenesis, Osteogenesis, and Chondrogenesis of Human Mesenchymal Stem/Stromal Cells: A Comparative Transcriptome Approach. Front. Cell Dev. Biol. 8:561. doi: 10.3389/fcell.2020.00561

Adipogenesis, osteogenesis and chondrogenesis of human mesenchymal stem/stromal cells (MSC) are complex and highly regulated processes. Over the years, several studies have focused on understanding the mechanisms involved in the MSC commitment to the osteogenic, adipogenic and/or chondrogenic phenotypes. High-throughput methodologies have been used to investigate the gene expression profile during differentiation. Association of data analysis of mRNAs, microRNAs, circular RNAs and long non-coding RNAs, obtained at different time points over these processes, are important to depict the complexity of differentiation. This review will discuss the results that were highlighted in transcriptome analyses of MSC undergoing adipogenic, osteogenic and chondrogenic differentiation. The focus is to shed light on key molecules, main signaling pathways and biological processes related to different time points of adipogenesis, osteogenesis and chondrogenesis.

Keywords: transcriptome, adipogenesis, osteogenesis, chondrogenesis, mesenchymal stem/stromal cell, gene expression profile, cell differentiation

INTRODUCTION

Stem cells are undifferentiated cells that are capable of self-renew and, under appropriate stimuli, differentiate into specific cell lineages (Weissman, 2015). Adult stem cells can be found in all tissues from an adult organism. Because they don't show the biological adverse effects of embryonic stem cells, can be used in autologous transplants and has fewer ethical issues, they have been the focus of basic and clinical research aiming their use in cell-based therapies (Dulak et al., 2015; Visvader and Clevers, 2016).

Mesenchymal stem/stromal cells (MSC) define a specific population of adult stem cells with specific characteristics that make them of high interest for clinical applications. MSC have been used in more than a thousand clinical trials for a wide range of diseases and clinical conditions (ClinicalTrials.gov). MSC have been described as fibroblastic precursors that can be isolated from bone marrow and that were able to differentiate into mesodermal-derived cells (Friedenstein et al., 1966). MSC are mesoderm-derived undifferentiated cells which also show the ability to self-renew and differentiate into a defined set of cell types. When stimulated both *in vivo* or *in vitro* they can differentiate into several mesodermal-derived lineages, in particular chondrogenic, osteogenic and

adipogenic cells. Several reports indicate that these cells can also differentiate into non-mesodermal lineages like hepatocytes, neurons and pancreatic cells (Aurich et al., 2009; Marappagounder et al., 2013; Ghorbani et al., 2018).

Besides its fibroblast-like morphology and the capacity to differentiate in adipocytes, osteocytes and chondrocytes, MSC are defined based on a set of specific surface markers. In 2006, the International Society for Cellular Therapy (ISCT), propose the following phenotypic characteristics for defining MSC: more than 95% of the cells should express the surface proteins CD105, CD73 and CD90, and less than 2% of cells should be positive for the surface markers CD45, CD34, CD14 or CD11b, CD19 or CD79α, and HLA-DR. The set of negative markers avoid contamination with cells from hematopoietic lineage (Dominici et al., 2006). Considering the different sources of MSC, in 2013, the ISCT stated that to characterize mesenchymal/stromal cells isolated from adipose tissue (Bourin et al., 2013). In addition to the positive markers already described (Dominici et al., 2006), others such as CD13, CD29, CD44 (>80% positive cells) can also be included; in relation to the negative ones, CD31 and CD235a could be used. Other markers were also described, but with higher variation in its expression depending on culture conditions and passages (Bourin et al., 2013).

Furthermore, research groups had studied other markers, as STRO-1, CD146, CD271, SSEA-4, CD49f among others, which can be used, e.g., to differentiate populations of stem cells with different potentials (reviewed by Lv et al., 2014; Samsonraj et al., 2017). Despite the advances, controversies still remain regarding the ideal marker or set of markers, since many of them are expressed by other cell types and there may be changes in expression depending on the source or culture method of the MSC. Concerning these differences, the characterization of 246 surface markers in bone marrow and umbilical cord blood-derived MSC showed that both of them highly expressed 18 markers, including the classical ones (CD90, CD105, and CD73) as well as alpha-smooth muscle antigen (SMA), CD13, CD140b, CD276, CD29, CD44, CD59, CD81, CD98, HLA-ABC, and others (Amati et al., 2018). On the other hand, looking for markers that were differentially expressed, it was found that CD143 (an angiotensin-converting enzyme) was highly expressed in bone marrow and adipose tissue-derived MSC in comparison with umbilical cord blood and umbilical cord-derived MSC, suggesting that this marker could differentiate MSC from adult tissues and those derived from perinatal tissues (Amati et al., 2018). In relation to the influence of passage number, analysis of adipose tissue-derived MSC at passages #1 to #8 showed that they changed its immunophenotypic profile based on passage number, although some of the markers presented a variable expression independently from time (Peng et al., 2020).

Mesenchymal stem/stromal cells exist in various tissues being the bone marrow, adipose tissue and umbilical cord blood the preferred source of cells in both basic and clinical research. Their multilineage differentiation potential and their capacity to proliferate *in vitro*, make these cells of great value for tissue engineering (Pittenger et al., 1999; Rebelatto et al., 2008). Though increasing evidence points to a paracrine and an immunomodulatory effect as also responsible for the positive results observed in cell therapies (Gallina et al., 2015; Kuo et al., 2016; Caplan, 2017), their potential to proliferate, differentiate and repopulate the target organ is still a first choice to reconstruct the damaged tissue (Shao et al., 2015; Bacakova et al., 2018; Mazini et al., 2019; Gomez-Salazar et al., 2020).

Cell therapies using adult MSC are slowly being approved for a wide range of diseases, involving different protocols for isolation and commitment to differentiation in specific cell types. Understanding the regulatory pathways and factors involved in the commitment to a specific cell type and understanding the mechanisms that regulate proliferation and differentiation is essential for improvement and successful therapies (Gomez-Salazar et al., 2020).

A cascade of events occurs in the MSC during the differentiation process, generating phenotypic and metabolic transformations. The reduction of the expression of stemness genes and the activation of genes related to the function of a mature phenotype are the first steps of a cascade that will lead to a morphological alteration of the cell. Different studies demonstrated that factors and pathways that stimulate adipogenesis inhibit osteogenesis. Conversely, adipogenic induction inhibits osteogenesis (Beresford et al., 1992; James et al., 2010). The balance between adipogenesis and osteogenesis is important to keep homeostasis in the organism.

In healthy bones, there is a constant process of bone resorption mainly promoted by osteoclasts and the generation of new tissue by osteoblasts. While osteoclasts are derived from the hematopoietic lineage, being formed by the fusion of progenitors from the monocyte/macrophage family (Teitelbaum, 2000), osteoblasts are derived from bone marrow- derived MSC, which may also differentiate into adipogenic lineage (Owen, 1988; Caplan, 1991; Kokabu et al., 2016). An imbalance leading the bone marrow MSC toward a higher rate of adipogenic differentiation to the detriment of osteogenesis is associated with loss of bone mass and diseases, as osteoporosis (Chen et al., 2016; Kokabu et al., 2016).

Moreover, the multilineage potential and the ability to secrete immunomodulatory factors and other signaling molecules made MSC an important source for use in regenerative medicine. Innumerous approaches used MSC as a therapeutic alternative for diverse health problems, which includes, e.g., treatment of obesity (reviewed by Matsushita and Dzau, 2017; Saleh et al., 2018) and for bone repair (reviewed by Shao et al., 2015; Jin and Lee, 2018; Iaquinta et al., 2019), but the mechanism of action of MSC in the body has not yet been fully elucidated, just as many challenges remain in an attempt to improve the proposed therapeutic strategies.

In an attempt to improve our understanding of MSC and its differentiation processes, which could contribute to the development of new therapeutic approaches, several studies have focused on understanding the mechanisms involved in the fate decision of MSC toward adipogenic, osteogenic or chondrogenic differentiation. But despite the advances, these differentiation processes are not completely understood.

The cellular transcriptome can be defined as the total population of RNA molecules in the cell at a particular moment. Measuring the abundance of these transcripts allows us to define

which genes are being expressed, and at what level, under a defined condition. The fate of a stem cell is directed by the gene expression profile at a particular moment and by the interactions among these transcripts and/or transcripts' products (Billing et al., 2016; Hasin et al., 2017; Melamed, 2020). Our understanding of the dynamics of the cell transcriptome was only possible with the emergence of high throughput techniques to characterize the gene expression profile of a cell. At the onset of the century, transcriptomic studies used hybridization-based techniques, such as gene microarrays that allowed the expression of thousands of genes at a time (Clark, 2002; Bertone et al., 2004). However, gene microarrays had technical limitations as they only could analyze known genes, have limited detection of expression signals, false positives because of cross-hybridization between probes and reproducibility issues (Okoniewski and Miller, 2006; Royce et al., 2007).

Since 2008, high-throughput next generation sequencing (NGS) has been used to study the transcriptome. Sequencing the RNA molecules in a cell (RNA-seq) showed to be a powerful tool as it is high-throughput, shows single-base resolution, and doesn't need the previous knowledge of the genes present in the analyzed genome (Mortazavi et al., 2008; Wang et al., 2009). RNA-seq provides precise measurements for messenger abundance and can distinguish new splicing isoforms and allelic expression. Moreover, new species of non-coding RNAs have been identified by RNA-seq analysis which includes small and long regulatory non-coding RNAs (Reuter et al., 2015; Sahraeian et al., 2017). Among these short RNAs are microRNAs (miRNAs), small interfering RNAs (siRNA), and Piwi−interacting RNAs (piRNAs).

miRNAs are small non-coding RNAs that have emerged as crucial post-transcriptional regulators of gene expression. They are single-stranded non-protein coding RNAs of 20–23 nucleotides that regulate both mRNA stability and translation through direct interaction with the transcripts (Bartel, 2009). miRNA have been shown to be important new players in regulation of stem cell development by playing a critical role in differentiation and maintenance of stem cells (Mathieu and Ruohola-Baker, 2013). Long non-coding RNAs (lncRNAs) have arisen as transcriptional and post-transcriptional regulators, acting at various levels of gene expression. They are defined as non-coding RNAs longer than 200 nucleotides and are present both in the nucleus and cytoplasm of the cell. LncRNAs are involved in proliferation and development through controlling the fate of stem cells, generating a complex network of interactions with regulatory proteins and other RNAs (Ulitsky, 2018; Fico et al., 2019; Xie et al., 2019). Finally, circular RNAs (circRNAs) are a different type of non-coding RNA that can form a covalently closed loop structure and are widely distributed in human tissues and organs. circRNA have also been described as regulators of stem cell fate (Wang et al., 2020).

Here we discuss high-throughput studies, using microarray or RNA-seq results, of MSC induced to adipogenesis, osteogenesis and chondrogenesis. As differentiation processes are highly regulated, initially we will present the variables that may influence the results. Then, we will focus the review in exploring the transcriptome or translatome data indicating key molecules, biological processes, signaling pathways and interaction networks that are essential to induce MSC to an adipogenic, osteogenic or chondrogenic phenotype.

MSC Differentiation: Important Features to Take Into Account

The analysis of gene expression during differentiation of MSC involves several variables, as stem/stromal source, protocol for stem/stromal cell isolation and for differentiation induction, time point of analysis during the differentiation process and strategy of analysis.

Regarding MSC source, Rebelatto and collaborators have previously described an efficiency of 100% in isolation of bone marrow and adipose tissue-derived MSC. Interestingly, while both had a similar capacity for chondrogenic and osteogenic differentiation, bone marrow-derived MSC produced more mature adipocytes than adipose tissue-derived MSC (Rebelatto et al., 2008). Nevertheless, using donor-matched samples, Mohamed-Ahmed et al. (2018) showed that adipose tissue-derived MSC had a greater adipogenic and delayed osteogenic capacity when compared to bone marrow MSC. Notably, Mohamed-Ahmed et al. (2018) used MSC isolated from young donors (8–14 years) submitted to iliac crest surgery for treatment of cleft lip and palate, while Rebelatto et al. (2008) used bone marrow from the iliac crest from donors with dilated cardiomyopathy (50–70 years) and adipose tissue from donors undergoing elective bariatric surgery and dermolipectomy procedures (26–50 years).

The same kind of tissue could be isolated from different body sites, by different methodologies and from donors with different features. Adipose tissue, for example, may be obtained as residue from several surgery procedures, as liposuction, eyelid plasty treatment, dermolipectomy among others (**Table 1**). Also, bone marrow may be isolated from iliac crest or metaphysis or proximal diaphysis of the femur (**Table 1**). Donor's age may also influence the features of isolated MSC, but, notably, conflicting results have been found regarding the effects of aging. The yield of MSC per volume of tissue was found to be (Ganguly et al., 2019) or not (Ye et al., 2016; Herrmann et al., 2019) affected by aging. Many studies also reported a decrease in the proliferation rate of MSC isolated from older donors (Marêdziak et al., 2016; Ye et al., 2016; Ganguly et al., 2019), while others did not observe age-related differences in the population doubling time (Herrmann et al., 2019). Similarly, aging was also found to decrease (Ye et al., 2016), increase (Marêdziak et al., 2016), or not affect (Zhu et al., 2009) the adipogenic potential of MSC. However, different studies described a reduced osteogenic and chondrogenic potential in MSC from older donors (Zhu et al., 2009; Choudhery et al., 2014; Marêdziak et al., 2016; Ye et al., 2016).

Interestingly, several studies using donors from the same group (young or aged, for example) obtained variable results (Zhu et al., 2009; Ganguly et al., 2019; Herrmann et al., 2019) and, stromal cells from different sources were found to be similar upon differentiation (Jääger et al., 2012). The conflicting results and the variability reported suggested that

TABLE 1 | Summary of transcriptome studies that analyzed adipogenic and/or osteogenic differentiation of MSC.

MSC tissue source (surgical procedure, donor age)	Immuno-phenotype (% of positive cells)	Time points	Induction media	RNA type isolated for analysis	Method (platform)	References
Adipogenesis						
Adipose tissue (liposuction procedure from abdominal subcutaneous adipose tissue; Ages: 19 to 32 years)	CD73+ CD90+ CD105+ CD34- CD45-	1, 7, 14, 21	DMEM; FBS (10%); PEN [10,000 U/mL]/ STR [10,000 μg/mL] (2%); DEX (1 μM); IBMX (0.5 M); IND (200 μM); INS (10 μg/mL)	Total RNA	Microarray	Ambele et al., 2016
Bone marrow (Ages: NA)	NA	7, 14	MEM-α; FBS (10%); AMPI (100 U/mL); STR (0.1 mg/ml); DEX (1×10^{-7} M); IBMX (0.5 mM); IND (50 mM); bFGF (1ng/mL); UltraGlutamine (2 mM)	Total RNA (ST-DGE) and miRNA (RNA-Seq)	ST-DGE and RNA-Seq (Illumina HiSeq 2000)	Casado-Díaz et al., 2017
Adipose tissue (bariatric surgery; Ages: 23 to 52 years)	NA	3	hMSC Adipogenic Differentiation Bullet Kit (Lonza)	Total and polysome-associated RNA	RNA-Seq (SOLiD4 System)	Spangenberg et al., 2013; Dallagiovanna et al., 2017
Adipose tissue (eyelidplasty treatment; Ages: 20 to 30 years)	NA	1, 7, 14, 21	H-DMEM; FBS (10%); ascorbic acid (5 μg/mL); DEX (1×10^{-7} mol/L); IBMX (0.5 mmol/L)	mRNA and miRNA	Microarray	Hu et al., 2018
Bone marrow (aspiration from iliac crest; Ages: NA)	CD29+ CD44+ CD105+	3	L-DMEM; FBS (10%); DEX (10^{-7} M); IND (50 ug/ml); IBMX (0.45 mM); ascorbate-2 phosphate (50 μg/ml); INS (0.01 mg/ml)	Total RNA	Microarray	Hung et al., 2004
Adipose tissue (liposuction procedure; Ages: 36 to 47 years)	NA	0, 1, 3, 5, 7	Medium 199; FBS (10%); PEN/STR (1%); DEX (1 μM); IND (200 μM); INS (10 μg/mL); methylxanthine (0.5 mM)	Total RNA	RNA-Seq (Illumina HiSeq 2500)	Luan et al., 2015
Adipose tissue (bariatric surgery and dermolipectomy procedures; Ages: 33 to 41 years)	NA	3	DMEM-F12; FBS (15%); PEN (100 U/mL); STR (100 μg/mL); DEX (1 μM); IBMX (500 μM); IND (200 μM); INS (1 μg/mL)	Total and polysome-associated RNA (Ribosome Profiling)	RNA-Seq (SOLiD4 System)	Marcon et al., 2017
Bone marrow (aspiration from iliac crest; Ages: NA)	CD44+ CD73+ CD90+ CD105+ CD166+ CD14- CD34- CD45-	0, 1, 3, 7, 17	DMEM; glucose (4.5 g/L); FBS (10%); DEX (1μM); IND (0.2 mM); IBMX (0.5 mM); INS (10 μg/ml)	Total RNA	Microarray	Menssen et al., 2011

(Continued)

TABLE 1 | Continued

MSC tissue source (surgical procedure, donor age)	Immuno-phenotype (% of positive cells)	Time points	Induction media	RNA type isolated for analysis	Method (platform)	References
Adipose tissue (subcutaneous adipose tissue from panniculectomy and carotid endarterectomies; Ages: NA)	NA	15	DMEM; FBS (10%); DX (1 μM); IBMX (0.5 mM); INS (1 μg/ml)	Total RNA	RNA-Seq single cell	Min et al., 2019
Bone marrow (purchased from BioWhittaker; Ages: NA)	NA	1, 3, 5, 7, 9, 14	H-DMEM; FBS (10%); DEX (1 μM); IND (0.2 mM); IBMX (0.5 mM); INS (0.01 mg/ml)	Total RNA	Microarray	Nakamura et al., 2003
Bone marrow (aspiration from iliac crest; Ages: adult donors)	NA	0, 1, 7, 14, 21	MEM-α; FBS (20%); PEN (100 U/ml); STR (100 μg/ml); L-glutamine (2 mM); DEX (0.5 μM); IBMX (0.5 mM); IND (50 μM)	Total RNA	Microarray	Sekiya et al., 2004
Bone marrow (aspiration from iliac crest; Ages: NA)	CD44+ CD90+ CD105+ CD19- CD34- CD45-	0, 14	MEM-α; FBS (10%); DEX (1 μM); IBMX (0.5 mM); IND (100 μg/mL); INS (0.01 mg/ml)	Total RNA	Microarray	Xu et al., 2016
Bone marrow (Ages: NA)	NA	7, 14, 21, 28	MEM-α; FBS (10%); DEX (1 μM); IBMX (0.5 mM); INS (0.01 mg/ml)	Total RNA	RNA-Seq (Ion)	Yi et al., 2019
Bone marrow (Ages: NA)	NA	0, 7, 14, 21, 28	hMSC Basal Medium (Cyagen); DEX (1.0 μM); IBMX (0.5 mM); INS (0.01 mg/ml)	Total RNA	RNA-Seq (Ion)	Yi et al., 2020a
Bone marrow (Age: 21 years)	NA	0, 7, 14, 21, 28	hMSC basal medium (Cyagen); DEX (1.0 μM); IBMX (0.5 mM); INS (0.01 mg/ml)	miRNA	RNA-Seq (Ion)	Yi et al., 2020b
Bone marrow (Age: 21 years)	NA	0, 7, 14, 21, 28	MEM-α; FBS (10%); DEX (1 μM); IBMX (0.5 mM); INS (0.01 mg/ml)	Total RNA	RNA-Seq (Ion)	Yi et al., 2020c
Adipose tissue (stroma-vascular fraction of white adipose tissue from surgical specimens; Age: 4 months).	NA	0, 3, 8	DMEM/Ham's F12; DEX (1 μM); IBMX (100 μM); INS (0.86 μM); rosiglitazone (1 μM); transferrin (10 μg/ml); triiodothyronine (0.2 nM)	small RNAs	RNA-Seq (SOLiD)	Zaragosi et al., 2011

(Continued)

TABLE 1 | Continued

MSC tissue source (surgical procedure, donor age)	Immuno-phenotype (% of positive cells)	Time points	Induction media	RNA type isolated for analysis	Method (platform)	References
Osteogenesis						
Bone marrow (Ages: 34 to 39 years)	NA	Differentiation: 0, ∼10; Mineralization: ∼24	Differentiation: MEM-α; FBS (10%); PEN (100 U/mL); STR (0.1 mg/mL); ascorbic acid-2 phosphate (0.1 M); DEX (10^{-8} M) Mineralization: + BGP (10 mM)	Total RNA (miRNA)	Microarray	Baglìo et al., 2013
Adipose tissue (liposuction procedure; Ages: 30 to 55 years)	CD73+ CD90+ CD105+ CD34- CD45- CD133-	0, 28	DMEM; FBS (10%); DEX (0.1 mol/L); BGP (10 mmol/L); ascorbic acid-2-phosphate (50 g/mL)	Total RNA	Microarray	Berdasco et al., 2012; Quan et al., 2016; Zhao et al., 2018
hBMSC-telomerase reverse transcriptase (TERT) cells	NA	0, 0.25, 0.5, 1, 3, 7, 10, 13	MEM; FBS (10%); PEN/STR (1%); DEX (10 nM); l-ascorbic acid (0.2 mM); BGP (10mM); 1,25-dihydroxyvitamin D3 (10 mM)	miRNA	RNA-Seq (Illumina HiSeq 2000)	Chang et al., 2018
Adipose tissue (plastic surgery; Ages: middle-aged)	CD73+ CD90+ CD105+ CD14- CD45- CD34 (low)	0, 21	DMEM; glucose (4.5 g/L); FCS (10%); antibiotics (1 %); DEX (1 x 10^{-7} M); ascorbic acid (50 μg/mL)	Total RNA	Microarray	Daniunaite et al., 2015; Zhao et al., 2018
Adipose tissue (liposuction procedure from sub-abdominal region; Ages: 24 to 68 years) and dental pulp (from deciduous teeth; Ages: 6 to 10 years)	CD29+ (>95%) CD73+ (>95%) CD90+ (>95%) CD105+ (>95%) CD31- (<2%), CD34- (<2%) CD45- (<2%)	0, 4, 6	L-DMEM; FBS (10%); ascorbate-2-phosphate (50 μM); BGP (10 mM); DEX (0.1 μM); PEN (100 U/ml); STR (100 g/ml)	Total RNA	Microarray	Fanganiello et al., 2015
Bone marrow (from iliac crest isolated from bone graft surgery; Ages: 19 to 28 years)	CD29+ (>70%) CD44+ (>92%) CD34- (<6%) CD45- (<7%)	14	BGP (10 mM); L-ascorbic acid (50 mM); DEX (100 nM)	Total RNA (miRNA)	Microarray	Gao et al., 2011

(Continued)

TABLE 1 | Continued

MSC tissue source (surgical procedure, donor age)	Immuno-phenotype (% of positive cells)	Time points	Induction media	RNA type isolated for analysis	Method (platform)	References
Bone marrow (from metaphysis and proximal diaphysis of the femur obtained from reconstructive joint surgery; Ages: 46 to 61 years)	Four days after seeding: CD44+ (26%) CD90- CD105- CD166- After confluency and treatment with differentiation medium: CD44+ (>90%)* CD90+ (>90%)* CD105+ (>90%)* CD166+ (>90%)* CD45- (<5%)* CD117- (<5%)*	Differentiation: 0, ∼5.5, ∼10.5, ∼24.2; Mineralization: ∼17.5, ∼23.6, ∼30.7	Differentiation: MEM-α; FBS (10%); PEN (100 U/mL); STR (0.1 mg/mL); ascorbic acid-2 phosphate (100 μM); DEX (10^{-8} M) Mineralization: BGP (10 mM)	Total RNA	Microarray	Granchi et al., 2010
Periodontal ligament (from third molars; Ages: 18 to 20 year)	STRO-1+ CD146+ CD31- CD45-	7	DEX (10 nM), BGP (10 mM) and vitamin C (50 μg/ml).	Total RNA (lncRNA, circRNA, mRNA)	RNA-Seq (Illumina HiSeq2000)	Gu et al., 2017
Bone marrow (Ages: 67 to 74 years)	NA	1, 3, 7	with or without 10^{-7}M DEX	Total RNA	Microarray	Hamidouche et al., 2009; Kang et al., 2019; Yang et al., 2019
Adipose tissue (purchased from Cyagen; Ages: 18 to 45 years)	NA	0, 14	OriCell human ASC Osteogenic Differentiation Medium (Cyagen)	Total RNA (lncRNA, mRNA)	Microarray	Huang et al., 2017; Yu et al., 2018; Wu et al., 2018
Bone marrow (aspiration from iliac crest; Ages: NA)	CD44+ CD73+ CD105+ CD14- CD19- HLA-DR-	0,14	BGP (10 mM); ascorbic acid (50 mM); DEX (100 nM)	Total RNA	Microarray	Jiang et al., 2019
Bone marrow (aspiration from iliac crest; Ages: NA)	CD44+ CD73+ CD90+ CD105+ CD166+ CD11b- CD34- C45- CD117- HLA-DR-	4, 7, 14, 21	DMEM; FBS (10%); PEN (100 U/ml); STR (100 μg/ml); L-glutamine (2 mM); DEX (10 nM); ascorbic-acid-2-phosphate (0.1 mM); BGP (10 mM)	Total RNA	Microarray	Kulterer et al., 2007

(Continued)

TABLE 1 | Continued

MSC tissue source (surgical procedure, donor age)	Immuno-phenotype (% of positive cells)	Time points	Induction media	RNA type isolated for analysis	Method (platform)	References
Dental follicle cells (from third molars; Age: 20 years)	NA	28	MEM-α; FBS (10%); ascorbic acid 2-phosphate (100 μmol/L); KH2PO4 (2.8 mmol/L); DEX sodium phosphate (1×10^{-7} mol/l); HEPES (20 mmol/L)	Total RNA	Microarray	Morsczeck et al., 2009
Periodontal ligament (Ages: NA)	CD29+ CD44+ CD73+ CD90+ CD105+ CD11b- CD14- CD34- CD45-	4,14	MEM-α; FBS (10%); PEN (100 U/mL); STR (100 mg/mL); L-ascorbic acid phosphate magnesium salt (82 μg/mL); BGP (10 mmol/L); DEX (10 nmol/L)	Total RNA	RNA-Seq (SOLiD System)	Onizuka et al., 2016
Adipose tissue (procured from LaCell LLC; Ages: NA)	NA	21	StromaQual; FBS (10%); BGP (10 mM); L-Ascorbic acid 2-phosphate sesquimagnesium salt hydrate (50 μg/ml); DEX (10 nM); 1% antibiotic	Total RNA	RNA-Seq (Ion Proton)	Shaik et al., 2019
hBMSC-telomerase reverse transcriptase (TERT) cells	NA	0, 0.25, 0.5, 1, 3, 6, 9,12	MEM; FCS (10%); PEN/STR (1%); BGP (10 mM); L-ascorbic acid (50 μg/mL); DEX (10 nM); calcitriol (1,25-dihydroxyvitamin D3) (10 nM)	Total RNA	RNA-Seq (Illumina HiSeq 2000)	Twine et al., 2014
Bone marrow (purchased from Cyagen; Ages: 18 to 20 years)	NA	7	STEMPRO osteogenesis differentiation Kit (Invitrogen)	Total RNA (lncRNA, mRNA)	Microarray	Zhang et al., 2017
Bone marrow (purchased from the Shangai Institutes; Ages: NA)	NA	0, 7	MEM-α; FBS (10%); antibiotics (1%); DEX (100 nM); ascorbic acid (0.2 mM); BGP (10 mM)	Total RNA (circRNA, mRNA, miRNA)	Microarray	Zhang M. et al., 2019
Periodontal ligament (from premolars; Ages: 12 to 18 years)	CD73+ CD90+ CD105+	0, 3, 7, 14	MEM-α; FBS (10%); PEN/STR (1%); DEX (100 nM); L-ascorbic acid (200 μM); BGP (10 mM)	Total RNA (circRNA, mRNA) and miRNA	RNA-Seq (HiSeq 2000, Illumina)	Zheng et al., 2017

(Continued)

TABLE 1 | Continued

MSC tissue source (surgical procedure, donor age)	Immuno-phenotype (% of positive cells)	Time points	Induction media	RNA type isolated for analysis	Method (platform)	References
Chondrogenesis						
Bone marrow (Ages: 38 to 58 years)	NA	21	BMP-2-conditioned medium obtained after incubation of chondrogenic medium [DMEM; DEX (0.1 μM); ascorbic acid (0.17 mM); ITS supplement (1%) (Sigma)] on confluent C9 cells for 48 hours	Total RNA	Microarray	Djouad et al., 2009
Bone marrow (from the drill hole of the pedicle during the internal spine fixation; Ages: mean age of 44 years; SD age of 10 years)	NA	3	H-DMEM; FBS (2%); DEX (100 nM); L-ascorbic acid-2 phosphate (50 mM); BD ITS+ Premix (1:100); TGF beta-3 (10 ng/mL)	Total RNA	Microarray	Gong et al., 2018
Bone marrow (from iliac crest; Ages: NA)	CD44+ (>97%) CD73+ (>97%) CD90+ (>75%) CD105+ (>93%) CD45- (<1%)	0, 1, 3, 7, 14, 21	H-DMEM; PEN/STR (1%); ITS+ Premix (Corning) (1%); DEX (100 nM); ascorbic acid (50 μg/mL); L-proline (40 μg/ml); recombinant human TGF beta 3 (rhTGF-b3) (10 ng/ml)	Total RNA	RNA-Seq (HiSeq 2500, Illumina)	Huynh et al., 2019
hMSC (purchased from Cambrex; Ages: NA)	NA	14	Chondrocyte Differentiation Medium Single Quotes Kit CC-4408 (Cambrex)	Total RNA	Microarray	Ikeda et al., 2007
Bone marrow (Ages: NA)	NA	0, 3, 7, 10, 14, 21, 28	H-DMEM; ITS+ (1%); DEX (10^{-7} M); sodium pyruvate (1 mM); ascorbic acid-2 phosphate (120 mM); non-essential amino acids (100 mM); TGF beta-1 (10 ng/mL)	Total RNA	Microarray	Somoza et al., 2018
Adipogenesis and osteogenesis						
Adipose tissue (liposuction procedure; Ages: 27 to 44 years)	CD73+ CD90+ CD105+ CD11b- CD19- CD31- CD34- CD45- CD117- HLA-DR-	1	(Adi) hMSC Adipogenic Differentiation Medium (hMSC Adipogenic Bullet kit, Lonza) (Ost) hMSC Osteogenic Differentiation Medium (hMSC Osteogenic Bullet kit, Lonza)	Total and polysome-associated RNA	RNA-Seq (Illumina HiSeq 2500)	Marcon et al., 2019, 2020; Robert et al., 2018

(Continued)

TABLE 1 | Continued

MSC tissue source (surgical procedure, donor age)	Immuno-phenotype (% of positive cells)	Time points	Induction media	RNA type isolated for analysis	Method (platform)	References
Adipose-derived stem cell-derived cell line	NA	-2, 0, 0.33, 2, 5, 10, 15	(Adi) DMEM/Ham's F12; transferrin (10 μg/ml); INS (0.86 μM); triiodothyronine (0.2 nM); DEX (1 μM); IBMX (100 μM); rosiglitazone (100 nM) (Ost) MEM-α; FCS (10%); L-ascorbic acid phosphate (50 μg/ml); BGP (10 mM); DEX (100 nM)	Total RNA	Microarray	Scheideler et al., 2008
Osteogenesis and chondrogenesis						
Bone marrow (Ages: 33 to 80 years)	CD44+ (100%) CD73+ (100%) CD90+ (>91%) CD105+ (>99%) CD11b- (<1%) CD19- (<1%) CD34- (<1%) CD45- (<1%)	7	(Cho) DMEM; glucose (4.5 g/L); PEN (100 U/mL); STR (100 μg/mL); ITS+ Premix (Corning) (1%); non-essential amino acids (1%); ascorbic acid 2-phosphate (50 μg/mL); DEX (100 nM); TGF beta-1 (10 ng/mL) (Ost) DMEM; glucose (1 g/L); FBS (10%); PEN (100 U/mL); STR (100 μg/mL); ascorbic acid 2-phosphate (50 μg/mL); BGP (5 mM); DEX (10 nM)	Total RNA (RNA-Seq, miRNA and piRNA) and circRNA (Microarray)	RNA-Seq (Illumina NextSeq500) and microarray	Della Bella et al., 2020

(Continued)

TABLE 1 | Continued

MSC tissue source (surgical procedure, donor age)	Immuno-phenotype (% of positive cells)	Time points	Induction media	RNA type isolated for analysis	Method (platform)	References
Adipogenesis, osteogenesis and chondrogenesis						
Adipose tissue (from subcutaneous adipose tissue; Ages: NA) and **fibroblasts** (from dermal skin; Ages: NA)	CD73+ CD105+	0, 1, 2, 3, 4, 5, 6, 7	(Adi) DEX (1 μM); IBMX (500 μM); IND (100 μM); INS (10 μg/ml) (Cho) INS (6.25 μg/ml); L-ascorbic acid 2-phosphate (50 μM); TGF beta-1 (10 ng/mL) (Ost) DEX (100 nM); L-ascorbic acid 2-phosphate (50 μM); BGP (10 mM)	Total RNA	RNA-Seq	Jääger et al., 2012
Bone marrow (Ages: NA)	NA	0, 1, 3, 7 and 21	(Adi) DMEM-F12; newborn calf serum (5%); DEX (1 μM); IBMX (50 μM); IND (60 μM) (Cho) DMEM; DEX (0.1 μM); ascorbate-2 phosphate (0.17 mM); insulin-transferrin-sodium selenite supplement (1%); TGF beta-3 (10 ng/mL) or BMP-2 (100 ng/mL) (Ost) H-DMEM; FCS (10%); BGP (10 mM); DEX (0.1 μM); ascorbic acid (0.05 mM)	Total RNA	Microarray	Mrugala et al., 2009

Adi: adipogenesis; AMPI: ampicillin; bFGF: basic fibroblast-growth factor; BGP: β-glycerophosphate; glycerol 2-phosphate; Cho: chondrogenesis; DEX: dexamethasone; DMEM: Dulbecco's modified Eagles's medium; FBS: fetal bovine serum; FCS: fetal calf serum; H-DMEM: high glucose – Dulbecco's modified Eagles's medium; IBMX: 3—isobutyl—1—methylxanthine; IND: indomethacin; INS: insulin; ITS: Insulin-Transferrin-Selenium; L-DMEM: low glucose – Dulbecco's modified Eagles's medium; MEM-α: minimum Eagles's medium-alpha modification; NA: not available; Ost: osteogenesis; PEN: penicillin; STR: streptomycin; TGF: transforming growth factor.

donors characteristics may not be predictive of the specific MSC phenotype (Ganguly et al., 2019; Herrmann et al., 2019). However, these features are certainly important for the analysis and interpretation of the data obtained from different studies; thus, it must always be clearly described in detail in the methodology section. Another difference that may interfere with the results of MSC studies is related to the cell surface markers expressed by the cells. It is recommended to use at least two positive and two negative markers for immunophenotypic characterization of MSC, commonly based on ISCT statements (Bourin et al., 2013). Surprisingly, not all studies shown a complete phenotypic characterization (**Table 1**). It is important to point out that isolated MSC may have differences in the expression of some markers, which can result in divergences in their proliferation or differentiation potential (Battula et al., 2009; Russell et al., 2010).

For differentiation induction, several protocols have been established to promote adipogenesis, chondrogenesis and osteogenesis which includes the usage of different culture media (**Table 1**), passage number and confluency. In the manuscripts analyzed in this review, the passage at which differentiation was induced ranged from 2-3 (Kulterer et al., 2007; Gu et al., 2017; Huang et al., 2017; Hu et al., 2018; Shaik et al., 2019) to 15 (Ambele et al., 2016). Regarding confluency, some groups reported that the differentiation was induced with subconfluent cells (up to 90% confluence) (Hu et al., 2018; Yi et al., 2019), others used confluent cultures (Zaragosi et al., 2011; Luan et al., 2015; Xu et al., 2016; Min et al., 2019), or even a few days after the cells reached confluence (Scheideler et al., 2008). Confluency and passaging may affect the differentiation potential of MSC (Wall et al., 2007; Safwani et al., 2014; Abo-Aziza and Zaki, 2017; Noda et al., 2019), although some groups did not find this correlation (Kulterer et al., 2007).

Gene expression may be controlled at different levels by epigenetic, transcriptional, post-transcriptional, translational and post-translational mechanisms. The development of different methodologies allowed the analysis of different aspects of gene regulation during the differentiation process of MSC. One of the most common strategies used is the analysis of total mRNA (**Table 1**), which yields information about the identity and abundance of mRNA found in different cell types and populations. Then, differences found at the total mRNA level provide information related to the regulation at the transcriptional level and in mRNA stability, though is not always directly equivalent to their translational rate (Tian et al., 2004; Schwanhäusser et al., 2011), and this kind of approach does not contemplate others important aspects of gene expression regulation (Ingolia, 2016).

The mRNAs associated with polysomes and the rate of translation of the transcripts may also be regulated, modulating protein synthesis. The use of methodologies as the polysome profiling (Spangenberg et al., 2013; Marcon et al., 2020) and the ribosome profiling (Ingolia et al., 2009, 2012; Ingolia, 2016; Marcon et al., 2017) are interesting to investigate these aspects of gene expression. The analysis and comparison of total or ribosome free mRNA fraction with the one associated to polysomes or ribosomes may provide important information about the level at which genes are being regulated, identifying mechanisms of translational efficiency (Marcon et al., 2017) and of coordinated/opposite actions of the transcriptional and the post-transcriptional mechanisms (Marcon et al., 2017; Pereira et al., 2019).

Other approaches focused on the analysis of non-coding RNAs, which have an important role in gene expression regulation. These analyses allow the identification of which micro, long non-coding, circular or other non-coding types of RNAs are specifically found in each phase of the differentiation process.

Following, we will present the findings from studies that used transcriptome analysis to understand the adipogenic, chondrogenic and the osteogenic differentiation process of MSC. Our search was focused in literature that contained results of transcriptomic or gene expression profile studies obtained using high-throughput technologies (microarray, RNAseq) during adipogenesis, osteogenesis or chondrogenesis of human MSC independently from its source. Only studies using *in vitro* differentiation (inductive media) of 2D cultures were considered in this review. Analyzes of various types of RNA, such as mRNAs, miRNAs, lncRNAs and circRNA were contemplated. These studies were summarized in **Table 1**. By compiling and analyzing these manuscripts, we present some of the main processes, pathways and key factors regulated during the differentiation time course that could improve our knowledge regarding osteogenesis, chondrogenesis and adipogenesis (**Figure 1**), highlighting the common and the discrepant findings of each group.

ADIPOGENESIS VS. OSTEOGENESIS: GENERAL ASPECTS

The differentiation process of MSC both into adipocytes and osteocytes *in vitro* takes about 20 days to be accomplished, and can be divided in two main steps: lineage commitment – from MSC to a committed progenitor – and maturation – from progenitors to mature phenotypes (Chen et al., 2016). After the beginning of adipogenic induction, AMP cyclic production is augmented, leading to the phosphorylation of CREB. Transcriptional factors CEBPB and D are also upregulated in the 1st hours of adipogenic treatment. Once activated by phosphorylation, CEBPB binds to regulatory elements and stimulates CEBPA and PPARG transcription. While CEBPB synthesis decays, CEBPA and PPARG transcription is continuously stimulated by CEBPA binding to CEBPs regulatory elements. PPARG transcription is also controlled by transcription factors SREBP1 and KLF family (reviewed by Rosen and MacDougald, 2006; Chen et al., 2016). The later stages of adipogenic differentiation are marked by the expression of fatty acid synthase (FAS), glycerophosphate dehydrogenase, acetyl CoA carboxylase, malic enzyme, glucose transporter type 4 (Glu4), insulin receptor and adipocyte-selective fatty acid binding protein (aP2), and by the formation of lipid, which are characteristic of adipocytes (reviewed by Rosen and Spiegelman, 2000).

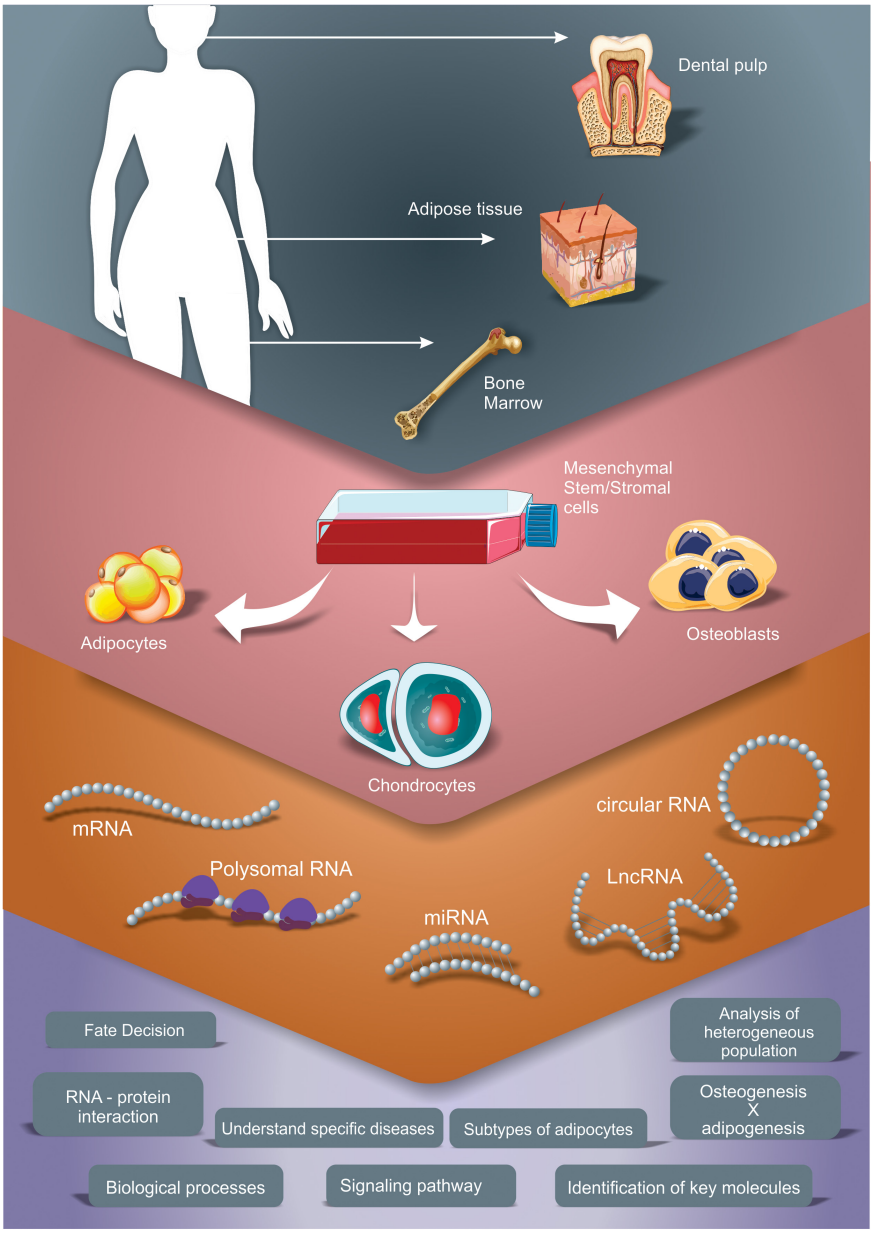

FIGURE 1 | Different transcriptomic approaches to study gene expression profile during adipogenic, chondrogenic and osteogenic differentiation of MSC. The scheme summarizes the studies explored in this review, which used adipose tissue, bone marrow and dental pulp as sources for MSC isolation and performed different induction protocols. Different RNA types were analyzed, as mRNA (by total mRNA, polysome profiling and/or ribosome footprint profiling analysis), microRNA (miRNA), long non-coding RNA (lncRNA) and circular RNA (circRNA). These strategies allow the characterization of main processes, pathways and key factors regulated during the differentiation time course that improve our knowledge regarding osteogenesis, chondrogenesis and adipogenesis.

During early osteogenesis, there is an upregulation of hedgehog proteins, Wnt/β-catenin signaling, BMPs and endocrine hormones, besides epigenetic regulators and growth factors. Then, one of the key factors involved in the osteogenic differentiation, RUNX2, is upregulated. Besides stimulating osteogenesis, RUNX2 also inhibits adipogenesis. But while RUNX2 expression decays along the differentiation process, Osterix and β-catenin upregulation is kept and is important to the maturation of osteoblasts (reviewed by Chen et al., 2016; Pierce et al., 2019). Alkaline phosphatase, osteoprotegerin and type I collagen are also expressed in more advanced stages of osteogenesis, while osteocalcin is related to the terminal differentiation phase (reviewed by Pierce et al., 2019).

One of the main questions about the differentiation process is at what moment during the differentiation time course MSC become committed to a specific phenotype. In our previous works, we observed that, in the first 24 h of osteogenesis of MSC, key genes related to the osteogenic differentiation were not

differentially expressed, notwithstanding we found another set of differentially expressed genes related to ossification and bone mineralization (Robert et al., 2018). Conversely, in MSC treated with adipogenic medium for 24 h, adipogenesis related genes were already differentially expressed, including transcription factors and genes related to lipid metabolism (Marcon et al., 2019), which will be discussed later in this work. Although differentiation genes were already regulated in the first 24 h of induction, the MSC were still not committed with a specific lineage (Spangenberg et al., 2013).

Jääger et al. (2012) compared the gene expression profile of MSC and dermal fibroblasts during adipogenic, osteogenic and chondrogenic differentiation processes over 7 days of differentiation. PCA analysis of the differentially expressed genes suggested that the switch of stromal cell regulatory mechanisms into phenotype-specific regulation happens earlier in adipogenesis than in osteo and chondrogenesis (Jääger et al., 2012). Ambele et al. (2016) suggested that the commitment with the adipogenic lineage only happens after day 7 of induction. On the other hand, Scheideler et al. (2008) analyzed gene expression in adipogenic and osteogenic-induced MSC in different timepoints (8 h, 2, 5, 10 and 15 days of induction), and suggested that lineage commitment to adipogenic or to osteogenic phenotype happens between 2 and 5 days of induction. During this period, they identified 39 genes that were upregulated in MSC induced to osteogenesis and downregulated in adipogenesis induced MSC. Interestingly, 5 of these genes contained binding sites to SREBP. On the other hand, 26 genes were specifically upregulated in adipogenesis and downregulated in osteogenesis, including transcripts containing PPARGDR1 and LXR response elements (Scheideler et al., 2008). These different studies suggest that during early adipogenesis (up to 48 h), MSC already triggered physiological changes that led to changes in gene expression but are still not committed with a lineage specific phenotype. This commitment happens around 2 to 7 days of differentiation, and the variability found may be related to different methodologies used for MSC isolation and induction media/protocol (**Table 1**).

Beside the regulation at the total mRNA level, gene expression during early adipogenesis and osteogenesis is also regulated by controlling the association of transcripts with the translational machinery. This observation has been consistent in studies using different induction times and methodologies for analysis. The comparison of the total and the polysome associated mRNA analysis demonstrated that more genes were identified as differentially expressed in the polysomal fraction during early osteogenesis (Robert et al., 2018). A similar pattern was observed in the first 24 h of adipogenesis (Marcon et al., 2019). On the other hand, after 72 h of adipogenic induction different results were obtained. More genes were identified as differentially expressed in the total fraction than in the polysomal using polysome profiling (Spangenberg et al., 2013). Conversely, using the ribosome profiling methodology more DEG were found in the fraction associated with ribosomes (Marcon et al., 2017). The differences observed in these two studies may be related to differences in the source of MSC (adipose tissue from obese donors underwent to bariatric surgery vs. healthy donors submitted to liposuction surgery) or in the experimental methodology (polysome vs. ribosome profiling) (**Table 1**). Nevertheless, in all the analysis performed, it was demonstrated that the association of mRNAs with the translational machinery is an important step for the regulation of gene expression during the adipogenic and osteogenic differentiation process of MSC.

GENE EXPRESSION PROFILE IN ADIPOGENESIS OF MSC

Initially, the study of the adipogenesis process focused on murine models, such as 3T3-L1 cells (reviewed by Basu et al., 2013; Ruiz-Ojeda et al., 2016). Nakamura et al. (2003) analyzed human MSC induced to adipogenesis for 0, 1, 3, 5, 7, 9 and 14 days. It was found 197 genes modulated over differentiation, with the higher number of upregulated genes on days 3, 7 and 9. Cluster analysis showed that the downregulated genes included markers from other lineages, cytoskeleton and extracellular matrix (ECM). On the other hand, other clusters could be divided into 2 groups: one with genes that were involved in the early stage (days 0–6) and another with genes related to a later stage (days 7–14) of adipogenesis (Nakamura et al., 2003). Among the upregulated genes at early stages were identified CEBPB and D, SWI/ SNF complex (BAF60b) and transcription factors as SLUG, FKHR; at late stage they found CEBPB and D, mitogen-activated protein kinases, CDC2-associated protein, cycline G1, PPARG, CEBPA, FABP-a, LPL and others related to lipid metabolism and adipocyte differentiation (Nakamura et al., 2003). That study, according to the authors, was the first that identified genes related to early stages of adipogenesis, using MSC.

Other gene expression profile analyses during adipogenesis identified several upregulated genes related to metabolism (as gluconeogenesis, fatty acid synthesis), secreted proteins, as apolipoprotein E, TGFb, IGF1 and 2 and seven transcription factors with marker time-dependent increase: ZEB (day 1), ZNF145 (day 7) PPARG (day 14), c-fos (day 14), SOX4 (day 21), CEBPA (day 21), and Forkhead (day 21) (Sekiya et al., 2004). The identification of DEG at 3-day adipogenic induced MSC showed 82 and 31 up and downregulated genes, respectively, many of which had not yet been described as related to the adipogenesis process. Genes related to growth arrest and lipid metabolism (as APOD, PPAP2B, CES2) were among the upregulated ones, while those related to other differentiation lineages, as neural, epithelial or osteogenic, had reduced expression at this time point (Hung et al., 2004). These results indicated an early change in gene expression profile of MSC that were induced to an adipocyte phenotype.

In fact, different groups have demonstrated that in the 1st days of adipogenic induction, the MSC are still not committed with the adipogenic phenotype (Scheideler et al., 2008; Spangenberg et al., 2013), but already have a significant change in the gene expression profile (Scheideler et al., 2008; Spangenberg et al., 2013; Ambele et al., 2016; Marcon et al., 2019). Transcriptomic analysis confirmed the upregulation of key transcriptional factors during early adipogenesis. Different analysis demonstrated that

KLF15 expression was detected in the first 24 h of induction (Ambele et al., 2016; Marcon et al., 2019, 2020), and remained upregulated after 3 (Spangenberg et al., 2013), 7, 14 and 21 (Ambele et al., 2016) days of adipogenic treatment. An augmentation of LMO3, FOXO1, ZBTB16 (Ambele et al., 2016; Marcon et al., 2019) CEBPB and CEBPD (Marcon et al., 2019) mRNA was also detected in the total and in the polysome-associated mRNA fraction (Marcon et al., 2019), suggesting not only an upregulation in terms of mRNA abundance but also in protein synthesis rate.

In the first 24 h of adipogenic differentiation of MSC, it was also demonstrated that the genes related to cell cycle and proliferation were mostly downregulated, and this scenario was accompanied by a decrease in cell proliferation and G1-cell cycle arrest. Interestingly, the downregulation of these transcripts was observed both in the total and in the polysome associated fractions, suggesting that the expression control is mainly promoted by the control of mRNA abundance (Marcon et al., 2019).

After 3 days of adipogenic treatment, genes related to lipid metabolism and adipogenesis are upregulated (Spangenberg et al., 2013; Luan et al., 2015; Marcon et al., 2017). Different studies reported the upregulation of the key transcription factors involved in adipogenesis, PPARG and CEBPA, at this time point (Spangenberg et al., 2013; Luan et al., 2015), but others have reported that those genes were only upregulated after 14 days of adipogenic treatment (Ambele et al., 2016).

In 14 days of adipogenesis, the primary most significant GO categories for upregulated genes were collagen fibril organization, brown fat cell differentiation, and positive regulation of fat cell differentiation (Xu et al., 2016). The main GO categories for downregulated genes were cell cycle, S phase of mitotic cell cycle, and G1/S transition of mitotic cell cycle (Xu et al., 2016), also observed in 24 h by previous studies (Marcon et al., 2019). Notably, it is possible to observe that the inhibition of genes related to cell proliferation or cell cycle were observed at several differentiation time points, indicating a stop of proliferation throughout the commitment to adipocytes.

Investigating the expression profile of mRNA and miRNA, after 7 and 14 days of adipogenesis, Casado-Díaz et al. (2017) identified more than 2000 and 100 regulated mRNAs and miRNAs, respectively. These genes were related to different pathways, including PPARG, lipid, carbohydrate and energy metabolism, redox, membrane-organelle biosynthesis, and endocrine system. The adipogenesis upregulated-genes were clustered into five groups: metabolism, response to stimulus, cell differentiation, biological regulation, and lipid storage. This indicated a relevant activation of cellular metabolism during adipogenesis. On the other hand, the downregulated genes were clustered into seven groups: developmental process, movement and transport, regulation of cellular process, apoptotic process, response to stimulus, cell adhesion and organization of cellular components (Casado-Díaz et al., 2017). Probably cytoskeleton reorganization during adipogenesis might affect survival, adhesion capacity and cell shape. Complementary analysis of mRNA-miRNA interaction showed that repressed miRNA-encoding genes can act downregulating PPARG-related genes, mostly the PPARG activator (PPARGC1A) (Casado-Díaz et al., 2017).

Characterization of early and late stages of adipogenesis showed 85 upregulated genes which were involved in PPARG signaling pathway (RXRA, CEBPA, CES1, PPARG, GPD1), "adipocytokine signaling pathway" (LPL, ADIPOQ, APOE, LGALS3, COL5A3, APOL6, CLEC1A, FLRT3), "adipocyte differentiation pathway" (FABP4, PLIN) and others. Also, they highlighted some other genes that could regulate adipogenesis, as SCARA5 and MRAP (Menssen et al., 2011).

Looking for key genes that could regulate adipogenesis, a temporal gene expression analysis was performed evaluating MSC induced for 7, 14, 21 and 28 days with adipogenic medium (Yi et al., 2019). Among the DEGs, 20 were identified with potential key genes responsible for adipogenesis: the upregulated PPARGC1A, ACACB, ACSL1, FABP4, FASN, IGF1, IRS2, LEP, LEPR, LIPE, PCK1, PDE3B, PLIN1, SCD, SOCS3, STAT3; and the downregulated BDNF, F2R, RAC2, RAPGEF3 (Yi et al., 2019). Previous study, from Casado-Díaz et al. (2017) found the following top upregulated genes during adipogenesis (7 and 14 days): LPL, FABP4, TIMP4, ADIPOQ, PLIN1, AOC3, PPP1R1A and ADH1B. The downregulated genes included some associated to MSC differentiation into osteoblasts as chitinase-3-like (CHI3L1), biglycan (BGN) and "four and a half LIM domains 2" (FHL2) (Casado-Díaz et al., 2017). Interestingly, only PLIN1 and FABP4 were common between both studies. Although both studies used bone marrow MSC and the differentiation medium were very similar, the differences may be due to the presentation of the data: while one indicated the top genes more or less expressed in 7–14 days (Casado-Díaz et al., 2017), the other identified those common in a period of 7-14-21-28 days of differentiation and still appeared in GOs related to adipogenesis (Yi et al., 2019).

GO terms related to metabolism were represented in many analyses of adipogenesis data. Whole transcriptional profiling of cellular metabolism during adipogenesis from MSC explored signaling pathways and metabolism of glucose, amino acid and fatty acid. It was shown that metabolism related pathways and the PI3K−Akt signaling pathway were the most enriched pathways using GO analysis (Yi et al., 2020b). The PI3K−Akt signaling pathway stimulated and directly regulated cellular metabolism by targeting the potential key genes, such as FASN, PCK1, SCD, and SLC2A1 and priming glucose aerobic glycolysis, arginine and proline metabolism, glutathione metabolism, and arachidonic acid metabolism during adipogenesis (Yi et al., 2020b). Also, analyzing polysomal RNA obtained after 3 days of adipogenic induction, it was indicated a change in the energetic profile in induced compared to non-induced cells (Drehmer et al., 2016). The reactive oxygen species (ROS) production, for example, was increased after 3 days of adipogenesis and could be involved in the differentiation process (Drehmer et al., 2016).

Considering the complexity of the gene expression regulation in diverse biological processes, including differentiation, the identification of small and non-coding RNAs that are differentially expressed during adipogenesis of MSC were also performed. Zaragosi et al. (2011) identified twenty-one miRNAs that were upregulated during differentiation, while

five miRNAs were downregulated using deep sequencing. This approach revealed the un-annotated miR-642a-3p as a highly adipocyte-specific miRNA. Inhibition of the miR-30 family blocked adipogenesis, whilst over-expression of miR-30a and miR-30d stimulated this process. One of the miR-30 target is the RUNX2 (osteogenesis transcription factor) which could be, at least in part, responsible for miR-30 positive effects on adipocyte differentiation (Zaragosi et al., 2011). Another study using microarray analysis found 32 miRNAs differentially expressed during adipogenesis, among them is miR27b which was downregulated, while lipoprotein lipase (LPL) mRNA was up-regulated (Hu et al., 2018). miR-27b targeted LPL and inhibits adipogenic differentiation (Hu et al., 2018).

A miRNA expression profile performed by Yi et al. (2020a) found a total of 39, 105, 194, and 112 differentially expressed miRNA at 7, 14, 21, and 28 days of adipogenesis, respectively (Yi et al., 2020a). Among the 25 most significant miRNAs, the majority (14) were upregulated. Of these, nineteen miRNAs potentially targeted for 35 mRNA that were associated, e.g., with lipid droplets formation. Among the identified miRNAs, five were highlighted, including hsa−miR−146a−3p, hsa−miR−4495, hsa−miR−4663, hsa−miR−6069, and hsa−miR−675−3p that could be regulating adipogenesis, once its targets were ACSL1, APOB, METTL7A, PLIN1, and PLIN4, and were potentially involved in lipid droplets formation (Yi et al., 2020a).

Luan et al. (2015) identified 2868 transcripts differentially expressed over days 0, 1, 3, 5, and 7 of adipogenic differentiation of MSC. As expected, the upregulated ones had relation with adipocyte differentiation and function, while de genes downregulated were more related to regulation of cell cycle. Moreover, they found 207 lncRNAs differentially expressed (109 up and 98 downregulated). A "guilt-by-association" analysis pointed out that 26 lncRNAs, all upregulated, assigned for fat-related GO terms, including HSD17B7P2, AQP7P1 and AQP7P3 (Luan et al., 2015).

It was previously demonstrated that a high percentage of lncRNAs are actively mobilized to or from polysomes during early stages of adipogenesis (Dallagiovanna et al., 2017). Non-coding RNAs can also be regulators of gene expression by forming complexes with proteins and other types of RNAs, including mRNAs and miRNAs (Guttman and Rinn, 2012). Dallagiovanna et al. (2017) analyzed the lncRNAs associated with polysomes and identified a great number of lncRNAs regulated in this RNA fraction. Among the differentially expressed lncRNAs, there are pathways related to cell growth and proliferation and a network formed by H19 (*gene* for a long non-coding RNA) interaction partner. Besides that, 43 lncRNAs targeted miRNAs, of which 16 were previously described as having a relevant role in adipogenesis. Between them is lncRNAmir22HG with several binding sites to the miR-30 family and which was more abundant in the control compared to induction (Dallagiovanna et al., 2017). Once that during adipogenesis, lncRNAmir22HG is less abundant, the concentration of those miRNAs might be higher and stimulate the differentiation. Interestingly, previous work had shown that the reduction of mir-30 reduced adipogenesis (Zaragosi et al., 2011). Differences in the analyzed time points and RNAs can generate results that seem conflicting, otherwise indicating the complexity of gene networks that could govern the commitment to the adipogenic lineage.

Yi et al. (2020c) reports global transcriptional profiling of alternative splicing events during adipogenesis from MSC by transcriptome technique. Among the identified 122 alternative splicing events, the three genes including actinin alpha 1 (ACTN1), LDL receptor−related protein 1 (LRP1), and latent transforming growth factor beta binding protein 4 (LTBP4), appeared in multiple alternative splicing types at 7, 14, 21, and 28 days (Yi et al., 2020c). Moreover, the differentially expressed genes displayed changes in the length of their 3′untranslated regions (3′UTR) during the adipogenesis (Spangenberg et al., 2013). The splicing events and changes in UTR regions may be associated with the ability to associate with ribosome or in mRNA half-life.

Mesenchymal stem/stromal cells are heterogeneous with respect to phenotype and function in current isolation and cultivation regimes, which often lead to incomparable experimental results (Mo et al., 2016). The study of transcriptomes of cell populations derived from single MSC before and after adipogenic differentiation and before and after thermogenic activation allowed the identification of a minimum of 4 distinct human adipocyte subtypes that can differentiate from mesenchymal progenitor cells (Min et al., 2019). The new technologies and studies of single cells will be able to expand our knowledge about the different subpopulations of MSC.

GENE EXPRESSION PROFILE IN OSTEOGENESIS OF MSC

The potential of MSC as a therapeutic alternative for bone regeneration led to an attempt to understand the process of osteogenesis *in vitro*. Many of the pathways and molecules involved - and used as differentiation markers - are known (reviewed by James, 2013; Rutkovskiy et al., 2016; Wu et al., 2016), but the complete process of osteogenic commitment is not yet fully understood. Thus, many studies focused on using transcriptome analysis to understand the molecular events, gene expression profiles and post-transcriptional regulation, that are essential for each stage of the MSC osteogenic differentiation process.

The presence of previously known factors related to osteogenesis, such as RUNX2, OCN, ALPL, was confirmed in several studies using transcriptomic analysis (Twine et al., 2014; Shaik et al., 2019). However, depending on the time point analyzed, the classical markers did not appear. For example, the study that evaluated the modulation of gene expression using polysomal mRNA analysis during the first 24 h of osteogenic induction did not find markers of osteoblast commitment, such as RUNX2 and BMP4. On the other hand, it presented other factors related to the ossification process such as BMP6, Forkhead box O1 (FOXO1), osteomodulin (OMD) among others that could have important functions at initial stages of osteogenesis (Robert et al., 2018). Other studies have shown that the expression of RUNX2 and ALPL, for example, appears at later moments of osteogenic differentiation (Twine et al., 2014), but

no regulation was observed after 28 differentiation induction days (Morsczeck et al., 2009).

Granchi et al. (2010) characterized early, intermediate and late stages of osteogenic differentiation in an osteogenic differentiation protocol with two main stages: MSC differentiation (days 5, 10, 24) and MSC mineralization (days 18, 24, 30) (**Table 1**). The main differences were verified at final stages of MSC differentiation and mineralization. Considering the genes upregulated throughout the process, most of them belonged to pathways and GOs related to bone cell biology. Specifically, the upregulated genes at final MSC differentiation were more related to cell communication which involved growth factors and adhesion genes. Genes related to angiogenesis appear in all analyzed time points, but its proportion is higher at initial mineralization process (Granchi et al., 2010). The group also indicated some genes to use as osteogenic markers as ANKH, COMP, DKK1, DKK3, FGF2, ICAM1, SOX9, SPOCK1, and TIMP3 (Granchi et al., 2010).

Another temporal expression profile of mRNAs and miRNAs differentially expressed during osteogenesis were performed comparing eight time points: 0, 6, 12, and 24 h, and 3, 6/7, 9/10, and 12/13 days post-osteogenic differentiation induction (**Table 1**; Twine et al., 2014; Chang et al., 2018). In general, the process was divided into stages including: an early stage, regulating the cell proliferation, an intermediate stage related to the commitment of cell to osteoblasts and matrix maturation, and finally reaching the late stage of matrix mineralization (Chang et al., 2018). These osteogenic stages were also characterized in previous studies, as one that evaluated the regulated mRNAs during 4 time points of the differentiation process, indicating 3 genes, ID4, CRYAB, and SORT1, with potential influence on osteogenesis, and describing the activation of Smad pathways induced by BMPs, TGFb and inhibin in the process (Kulterer et al., 2007).

Looking for genes associated with osteoblast phenotype, Twine et al. (2014) found 332 skeletal related genes in its mRNA dataset. Of these, it was selected 123 genes that could be recognized as markers of osteogenic differentiation. Most of the selected markers were related to secreted proteins and extracellular matrix (more than 50%). In addition, genes with peak expression at the beginning of differentiation (0–24 h) and in the intermediate stage (3–6 days) are related to ECM organization, skeletal system development and processes involved in cellular adhesion. On the other hand, late stages of osteogenesis (9–12 days) were enriched in genes related to osteoblast differentiation, cell migration and others (Twine et al., 2014). Interestingly among the genes with higher counts per million (cpm) values it was found fibronectin (FN1), COL1A1, COL1A2, COL6A3, THBS1 and SPARC, all related to extracellular space or secreted proteins (Twine et al., 2014).

Another possibility for analysis using transcriptome data is the development of interaction networks, not only between genes, but also between GOs and pathway analysis. Recent work has shown more downregulated than upregulated genes after 14 days of osteogenic induction of bone marrow derived-MSC (Jiang et al., 2019). The biological processes and pathways that have been highlighted among downregulated genes were mainly involved in cell proliferation and cell cycle, while extracellular matrix organization and interaction, cell adhesion, complement and coagulation cascades and ossification are highlights among upregulated ones. The pathway network demonstrated that during differentiation there was, for example, interaction between "Focal adhesion" with "ECM-receptor interaction," "Regulation of actin cytoskeleton," and "Cell cycle" pathways (Jiang et al., 2019). Interestingly, biological processes related to cell adhesion, proliferation and communication have also been identified after only 24 h of differentiation (Robert et al., 2018). This shows, along with other studies, the complexity of signaling necessary for an efficient osteogenic differentiation process.

One of the GOs that is common in many of transcriptome analysis during MSC osteogenesis were related to extracellular organization, cell communication and adhesion, both in early and late stages. Recently Shaik et al. (2019) focused on exploring the data related to ECM differentially expressed genes identified after 21 days of osteogenesis. In order to investigate the possible role of ECM and secreted proteins during bone formation and angiogenesis, the group compared their results with matrisome data (Hynes and Naba, 2012; Hynes, 2014) and observed that a great number of glycoproteins, secreted factors, ECM-affiliate genes were upregulated at late stage of osteogenesis. On the other hand, ECM remodeling enzymes, as MMPs and ADAMTS were more downregulated, while many subunits of integrins (ITGA10, 4) showed increased expression compared to undifferentiated MSC (Shaik et al., 2019). Regarding integrin expression and osteogenesis, Hamidouche et al. (2009), showed that the integrin α5 subunit (ITGA5), different from that observed by others (Shaik et al., 2019), is upregulated during osteogenesis and its expression was sufficient to promote osteogenic differentiation (Hamidouche et al., 2009).

The increased presence of secreted pro angiogenic factors, including CXC cytokines, after osteogenesis was another interesting finding (Shaik et al., 2019), indicating the possible regulation of bone development together with the development of new vessels. DEG during only 24 h of osteogenic induction already indicated a process related to vasculature development, GO also found in genes that have high expression after 24 h and 12 days, where VEGF was an example (Twine et al., 2014). The proliferation-related GO is also very common to appear among osteogenesis regulated genes, but while some studies indicate a stop in the cell cycle (Chang et al., 2018; Jiang et al., 2019), others report an increase in proliferation (Robert et al., 2018).

In addition to the possibility of identifying GOs and pathways, there are also studies that focus on identifying transcription factors and/or verifying interaction between genes or proteins, looking for those who have a central role in networks. Analysis of DEG identified over 1, 3 and 7 days of osteogenic differentiation identified some transcription factors as central nodes in interaction networks such as FOS, SOX9, EP300, CREBBP, ESR1 and EGR1 (Kang et al., 2019). Others, based on data from MSC differentiation to osteoblasts during 28 days (Berdasco et al., 2012) showed interesting protein-protein interaction with nodes as VEGFA, IL1B, EDN1, FG2 and others, some of them shared with myogenic induced MSC (Quan et al., 2016).

The osteogenic differentiation potential varies depending on the MSC source. Fanganiello et al. (2015) compared the efficiency of dental pulp (deciduous teeth) derived- MSC (hDPMSC) with adipose tissue derived-MSC (hASC) in promote osteogenic differentiation, using bone marrow MSC (hBMMSC) as control (Fanganiello et al., 2015). Transcriptomic analysis was performed after 4 and 6 days of osteogenesis induction and it was shown that the largest number of regulated genes was found in differentiated cells derived from bone marrow, while the smallest was in hDPMSC. Comparing the data, 11 DEGs were common between hDPMSC and hBMMSC, which were related to osteogenic pathways, but do not appear in hASC. On the other hand, 47 DEG were shared between hBMMSC and hASC, generating pathways such as serine biosynthesis (Fanganiello et al., 2015). Additionally, despite hASC and hDPMSC express osteogenic markers the gene expression was higher in dental derived cells, which showed greater potential for osteogenesis. Looking for markers that could indicate cells with best osteogenic potential, IGF2 and ITGA8 were highlighted considering that both had higher expression over osteogenesis in hDPMSC compared to hASC. Specifically, cells showed more ALP activity and matrix mineralization when IGF2 level was higher. This could indicate that cells with higher levels of IGF2 before the beginning of osteogenic differentiation were more predisposed to the osteogenic phenotype (Fanganiello et al., 2015).

Also, regarding tooth-derived cells, analysis of the transcriptome of dental follicle cells induced to osteogenesis identified that 98 genes were upregulated in the process and were related to extracellular space and immune response (Morsczeck et al., 2009). Interestingly, downregulated genes were also composed of extracellular space proteins, profile also observed in other studies (Shaik et al., 2019). IGF-2, CD14 and transcription factors as KLF9, NR4A3, PRDM1, ALF, TSC22D3 and ZBTB16 were some of the identified upregulated genes in cells induced to osteogenesis (Morsczeck et al., 2009). The zinc finger and BTB domain containing 16 (ZBTB16) was also identified in other data from periodontal ligament-derived MSC differentiated to osteoblasts. It was shown that this zinc finger had increased expression during osteogenesis and its silencing decreased the expression of osteogenic markers (OCN and BSP) and ALP activity (Onizuka et al., 2016). Results from Osx knockdown indicated that expression of ZBTN16 depended of Osx; and, chromatin immunoprecipitation assay also indicated that Osx is an upstream regulator of ZBTB16 (Onizuka et al., 2016).

Considering the differences presented between transcriptomic datasets, joint analysis of different data could result in relevant information for the understanding of osteogenesis. Comparison of datasets could allow the identification of key genes presented in different osteogenic differentiation protocols (Yang et al., 2019) which may indicate an essential role in the differentiation process. Beside that, re-analysis of microarray data from osteogenic differentiated adipose derived-MSC (Berdasco et al., 2012; Daniunaite et al., 2015) showed that 142 and 69 genes were up and downregulated, respectively, in both datasets (Zhao et al., 2018). GO and pathway analysis of DEG indicated that they were enriched in terms associated with "ECM organization," "angiogenesis," "Wnt protein binding," "FXR/RXR activation," and "adipogenesis pathway," among others. Protein-protein interaction network highlighted central nodes composed of, e.g., FOXO1, ID2, IL1B, NID1, PER1, LGR4, STK32B. The reduction of FOXO1, in fact, was shown to be able to reduce expression levels of osteogenic markers and the amount of calcium nodules (Zhao et al., 2018). Thus, FOXO1, identified after 24 h (Robert et al., 2018) and at later stages of osteogenesis (Zhao et al., 2018) could be an important regulator of osteogenesis.

In addition to the mRNA analysis, great interest has arisen trying to understand how the transcribed RNAs could be regulated. Thus, identification of miRNAs, lncRNAs and also circRNAs that are essential to the process allow advances in the understanding of post-transcriptional regulation occurring in the differentiation process.

There are several reports that point out the influence of different miRNAs in regulating pathways related to osteogenesis (reviewed by Martin et al., 2016; Li, 2018). Using 3 MSC donors, a study showed that there is a difference in the differential expression of miRNAs during osteogenesis among the donors: while one of them had more than 50 differentially expressed miRNAs, the other one showed less than 30 (Gao et al., 2011). Considering those that appeared in at least two donors, it was found 8 downregulated (hsa-miR-31a, hsa-miR-106a, hsa-miR-148a, hsa-miR-424, hsa-miR-210, hsa-let-7i, PREDICTED_MIR191, hsa-miR-99a) and 5 upregulated (hsa-miR-30a-5p, hsa-miR-30c, hsa-miR-130a, hsa-miR-15b, hsa-miR-130b) miRNAs (Gao et al., 2011). Some of these miRNAs, e.g., members of the let-7 family and miR-31, have also been reported in other studies, although not always with the same expression profile (Baglìo et al., 2013; Chang et al., 2018).

A miRNA expression profiling analysis during osteogenesis found 29 and 5 miRNAs modulated during differentiation and mineralization stages, respectively (Baglìo et al., 2013). Among the upregulated miRNA, miR-31, miR-145, and miR-504 appear to have potential to regulate Osterix (by binding to the 3'UTR), a known transcriptional factor involved in osteogenesis (Sinha and Zhou, 2013). Indeed, it was demonstrated that the reduction of miR-31 increased Osterix expression, indicating that miR-31 is a regulator of Osterix (Baglìo et al., 2013). Besides that, reduction in miR-31 expression also positively affects expression of RUNX2 and BMPR2 (Gao et al., 2011), indicating that miR-31 could be an important regulator of osteogenesis.

The expression profile analysis of miRNAs during 8 time-points of osteogenic differentiation showed that of the 204 miRNAs filtered, 31 were selected to verify its influence in osteogenesis (Chang et al., 2018). Nineteen showed a decrease in ALPL activity when overexpressed, highlighting the negative effect in osteogenesis of, e.g., miR-512, miR-146a and miR-146b, miR-320a, miR-210, miR-222, miR-423, and miR-138 (Chang et al., 2018).

An interesting approach is to evaluate the potential targets of these miRNAs. miR-30, for example, which is upregulated in differentiation (Gao et al., 2011), has among its targets the CXCL12 (or SDF1), gene that has already been described as having decreased expression in the osteogenesis process (Morsczeck et al., 2009). Another example was the miR-15b, identified as overexpressed by Gao et al. (2011), and with

decreased expression during osteogenesis by Chang et al. (2018). Among the targets of miR-15b is the FGF2 (Gao et al., 2011). The expression levels of this gene showed different profiles in different studies: while some showed a decrease in its expression (Morsczeck et al., 2009; Shaik et al., 2019), other indicated that FGF2 increase over osteogenesis (Granchi et al., 2010) or had a bimodal expression, being overexpressed at the beginning and at the end of differentiation process (Twine et al., 2014). These studies, additionally to the variation in the analyzed time points, presented differences in the methodology for RNAs identification and in the differentiation protocols (**Table 1**). However, all these generated data can be analyzed together, enabling the formation of a complete network.

The important role of lncRNAs in regulating osteogenesis, or even in bone-related diseases, has been explored over the years (reviewed by Silva et al., 2019; Zhang J. et al., 2019). When evaluating gene expression profile of MSC after 7 days of osteogenic induction more than 1200 mRNAs and lncRNAs were differentially expressed in relation to undifferentiated cells, with the majority being upregulated (Zhang et al., 2017). Among the processes and pathways highlighted using mRNA analysis it was shown: response to stimulus, DNA-dependent transcription, cell adhesion, skeletal system development, cytokine-cytokine receptor interaction, ECM-receptor interaction and others. In addition, interaction analysis of mRNAs and lncRNAs identified seven mRNAs (GPX3, TLR2, BDKRB1, FBXO5, BRCA1, MAP3K8, and SCARB1) and six lncRNAs (XR_111050, NR_024031, FR374455, FR401275, FR406817, and FR148647) that could be regulatory genes. XR_111050 when overexpressed enhanced osteogenesis of bone marrow MSC (Zhang et al., 2017).

Another report also demonstrated, after 14 induction days, a great number of regulated lncRNAs of which 88 showed an altered expression of more than 10-fold (55 up and 33 downregulated) (Huang et al., 2017). The most modulated lncRNAs were *uc002lbc.1* and *uc.247+*, up and downregulated, respectively. The same study also analyzed the mRNA profile, finding a great number of downregulated genes (**Table 1**). Despite that, GO analysis of upregulated genes was in agreement with other studies presenting, e.g., ECM organization as one of the main biological processes (Huang et al., 2017). The network of mRNA-lncRNAs highlighted 12 lncRNA interacting with more than 150 mRNAs, as FOXO1, GPM6B, FGF6, OMD, WNT5B. Specific study of lncRNA H19 showed that its expression was reduced during osteogenesis and that its knockdown resulted in the increased expression of osteogenic markers (Huang et al., 2017).

This dataset, generated by Huang et al. (2017), was reanalyzed and new observations regarding the lncRNA-mRNA-miRNA interaction were made. Many genes modulated during osteogenesis were related to the PI3K/Akt signaling pathway, among which IL6 was one of the overrepresented. Co-expression analysis showed a possible interaction with the lncRNA HIF1A-AS2, which in turn could be interacting with miRNAs, including miR-665 (Wu et al., 2018). Silencing and overexpression experiments of these molecules indicated a relationship between HIF1A-AS2 - miR-665 - IL6 and that this core regulates the PI3K/Akt signaling pathway (Wu et al., 2018). In addition, another pathway explored was the toll-like receptor (TLR) signaling pathway. Using similar strategies to previous study (Wu et al., 2018), Yu et al. (2018) observed an interaction between TLR4 (upregulated in osteogenesis) with lncRNA-PCAT1 and miR-145-5p, which were able to regulate the TLR pathway.

Although the function of circRNAs is not completely understood, it is known that they could act in the regulation of gene expression – including pathways related to osteogenesis (reviewed by Huang X. et al., 2019) -, regulating, for example, the expression of its host gene or even function as a miRNA sponge (reviewed by Santer et al., 2019; Yu and Kuo, 2019). Thus, combined analysis of mRNA, miRNA and circRNA have been carried out in an attempt to set up interaction networks and understand how they can contribute to the regulation of osteogenic differentiation.

The number of differentially expressed circRNAs was variable between studies: while one identified over 2000 differentially regulated circRNAs after 7 days (Zhang M. et al., 2019), 2019), other found ∼100–150 circRNAs modulated at different time points of osteogenic differentiation (3, 7 and 14 days) (Zheng et al., 2017). Despite this, the GO analysis both of the mRNAs and of the parental genes of differentially expressed circRNAs highlighted terms related to osteogenesis such as ECM, cell differentiation, plasma membrane, cytoplasmic or membrane bound vesicles and others (Zheng et al., 2017; Zhang M. et al., 2019). Through the construction of a miRNA-circRNA interaction network, the possible relationship between circIGFS11 and miR-199B-5p was indicated: while one has a reduction after 7 days of differentiation, the other increases its expression. Functional tests confirmed that silencing circIGSF11 increased the expression of miR-199b-5p and was able to induce osteoblast differentiation (Zhang M. et al., 2019). The construction of interaction networks also made it possible to identify circRNAs that interacted with miRNAs previously described as having a role in osteogenesis (Zheng et al., 2017). The description of these circRNAs already indicates that they are modulated throughout differentiation, potentially involved in the regulation of their host genes and miRNAs that have positive effects in processes related to osteogenic differentiation.

Thus, it is possible to note the complexity of the osteogenesis process and how the use of transcriptome studies helps to understand it. The identification of biological process or signaling pathways regulated over the differentiation process indicated those that are critical to the osteogenic process, such as those related to the ECM-organization, MAPK and PI3K/Akt pathways. In addition, miRNAs, lncRNAs and circRNAs are an emerging source for the comprehension of regulatory mechanisms of osteogenesis. All these works contribute to the development of the field, as well as helping to understand diseases related to, for example, bone development.

GENE EXPRESSION PROFILE IN CHONDROGENESIS OF MSC

The hyaline cartilage is responsible for the bone formation in the embryo (thought endochondral ossification), and in

adults can be found in costal cartilages, respiratory system, and covering the bone articular surface (reviewed by Carballo et al., 2017). The treatment for cartilage defects, e.g., articular hyaline cartilage defects, is a challenge and the MSC appeared as an alternative for cartilage engineering, since it has the ability to differentiate into chondrocytes *in vitro*. The process of chondrogenic differentiation of MSC is commonly performed with pellet or aggregate culture system, with addition of factors as TGFβ, BMP and/or IGF (reviewed by Boeuf and Richter, 2010; Somoza et al., 2014; **Table 1**). Chondrocytes generated from MSC expressed classical genes/proteins as native chondrocytes, e.g., type II collagen and aggrecan. However, it is also possible to identify hypertrophy-associated genes, as type X collagen, ALP and MMPs (reviewed by Hellingman et al., 2012; Somoza et al., 2014). Thus, differently from normal hyaline cartilage, the *in vitro* differentiation process seems to arrest in early phases of endochondral ossification (Pelttari et al., 2006; Steck et al., 2009; Somoza et al., 2014). Although differentiation protocols are still unable to generate a type of cartilage that resembles articular cartilage in normal physiological conditions of an adult organism, understanding the stages of chondrocyte commitment and comparing it with fetal or adult cells can be of great help in improving the *in vitro* chondrogenesis of MSC.

Since the ECM elements are essential components of cartilage tissue, high expression of ECM related genes, mainly collagens types, was detected in many studies (Ikeda et al., 2007; Djouad et al., 2009; Mrugala et al., 2009; Somoza et al., 2018; Huynh et al., 2019). For example, Ikeda et al. (2007) used the microarray technology to determine the gene expression profiles of MSC following monolayer chondrogenesis after 14 days of induction. The authors identified 23 upregulated and 35 downregulated transcripts, of which 44 and 40%, respectively, were associated to ECM and metabolic pathways. Many collagen types were identified as up (COL10A1, COL11A1) or downregulated (COL6A3), as well as other components uprelated to ECM suchas CLU, SAA1, PTX3, MGP (Ikeda et al., 2007). Interestingly, pathway related to cell growth presented more downregulated genes, e.g., IGFBP2, PDGFB, EMP1, PDGFRA (Ikeda et al., 2007). The last one downregulated only after 3 days of chondrogenesis (Somoza et al., 2018).

In an attempt to identify new factors responsible for chondrogenic differentiation, a gene expression profile of MSC following BMP2-induced chondrogenesis (micropellet) over a 21-day period were performed (Djouad et al., 2009). As expected, the mRNA expression levels of many collagens types characteristics of cartilage tissue (as COL2A1, COL9A2, COL9A3, and COL11A1) were increased in late stage chondrogenesis. Also, aggrecan and cartilage oligomeric protein were upregulated, which are highly and specifically expressed in cartilage, validating the differentiation process. Furthermore, despite the identification of previously known transcription factors associated with chondrogenesis, as SOX9, Twist1 and TCF1, five novel transcription factors were upregulated in differentiation process: FOXO3A, Dlx4, Nessy, Sox13, and Tbox6. Among them, FOXOA3 was shown indeed to be involved to differentiation and apoptosis during chondrogenic differentiation of MSC (Djouad et al., 2009).

Considering the importance of initial signaling in differentiation processes, Gong et al. (2018) performed an analysis of MSC after only 3 days in chondrogenic induction media. Among the genes with a markedly increased expression were DYNC1I1, BNC2, ENPP1, FBXO42, JMYN, FATC1, and PLCE1, while the expression of DNMT3A, PLCG2, ANXA11, GRK6, HSP90B1, KEAP1, and NDST2 were downregulated (Gong et al., 2018). In the GO and pathway analysis, T cell receptor signaling and antigen receptor-mediated signaling were overrepresented while the underrepresented processes included skeletal system, osteoclast differentiation and acute inflammatory response (Gong et al., 2018).

As an effort to investigate the specific molecular signature during chondrogenesis of MSC and elucidate the dynamic of differentiation process, Mrugala et al. (2009) performed a microarray analysis after 1, 3, 7 and 21 days of chondrogenic differentiation, using TGF-β3 or BMP2 induction medium. In addition, adipogenesis and osteogenesis of MSC were also performed and analyzed at the same time points (Mrugala et al., 2009). Comparing the data and selecting the genes that appear only in cells with chondrogenic induction, 318 genes were found as differentially expressed, of which 177 were known sequences. Based on gene expression profile, it was characterized the phases of chondral differentiation: 1) cell attachment and apoptosis, represented by genes as BCL6, ITGA5, NFIL3, CTGF; 2) differentiation induction, including genes such as Wnt5a, Notch3, FOXO1A, FOXO3A, IGFBP1; and 3) Wnt signaling inhibition and hypertrophy with upregulated genes like FKBP5, SLUG, TIMP4, DKK1, APOE/D (Mrugala et al., 2009). Another analysis demonstrated that angiopoietin-like 4 (ANGPTL4) is upregulated during chondrogenesis, mainly at days 1 and 3. Addition of exogenous ANGPTL4 in TGF-β3-induced MSC decrease the expression of classical chondrogenic markers, as aggrecan, COL2A1, COL10A1, and increased the presence of MMPs. On the other hand, knockdown of this gene improved the micromass size and the expression of chondrogenic markers. These results indicated that ANGPTL4 regulates ECM components in chondrogenic differentiation (Mathieu et al., 2014).

Comparison of transcriptome data from *in vitro* MSC chondrogenesis and the normal articular cartilage could allow the identification of common or different signals and regulatory elements, indicating novel strategies that could improve *in vitro* chondrogenic differentiation. A high-throughput analysis of differentially expressed genes of MSC after 3, 7, 10, 14, 21 and 28 days of chondrogenic induction and the characterization of transcriptional regulatory elements from human neonatal articular cartilage showed that more than 500 genes that were highly expressed in neonatal cartilage were not expressed at any time point during *in vitro* chondrogenesis (Somoza et al., 2018). But, interestingly, it was observed that cells at early stages of differentiation (days 3 and 7) were more similar to neonatal cartilage than those from later days, suggesting that, at this time points, it is still possible to interfere and redirect the cells to a specific cartilage phenotype. The data analysis also demonstrated that MSC during chondrogenesis expresses classical markers of hyaline cartilage as aggrecan, SOX9,

COL2 and others, but also expressed COL10, Runx2, ALPL, and MMP13 which are presented in hypertrophic cartilage. This indicates that the markers actually used could not be able to really distinguish an articular cartilage from those generated by MSC differentiation process (Somoza et al., 2018). Comparative analysis demonstrated that among the control elements identified as upregulated in neonate cartilage were the UCMA (Unique Cartilage Matrix-Associated Protein), MSMP (Microseminoprotein, prostate associated), MATN1 (matrilin 1) among others. Furthermore, pathways analysis of the differentially expressed genes in neonatal cartilage (182 up and 191 downregulated) indicated an enrichment in integrin related pathways, as well as those related to VEGFR, ErbB1, IGF1 and others (Somoza et al., 2018). Then these results confirmed the differences between a human cartilage and the *in vitro* chondrogenic differentiation of MSC, but highlight possibilities to improve the protocol.

Similarly, a temporal analysis of MSC after 1, 3, 7, 14, and 21 of chondrogenesis induction confirmed that the *in vitro* derived cartilage, at least in transcriptional level, was different from human articular cartilage from embryonic, adolescent or adult origin (Huynh et al., 2019). Besides, the greatest change in gene expression was observed between day 0 and day 1, with more than 2000 upregulated and 1860 downregulated genes. As expected, during differentiation induction, chondrogenic markers were upregulated as well as naïve MSC markers decrease its expression (Huynh et al., 2019). Gene co-expression network analysis identified a functional module composed of 1172 genes upregulated during differentiation. Analysis of this module indicated that the most enriched pathway was skeletal system development, nevertheless other pathways were also present as ECM and collagen fibril organization, demonstrating the chondrogenic profile. In addition, it was identified a set of transcription factors, including members of SOX family, retinoic acid receptor, FOS/JUN complex and FOXA2, and 230 lncRNAs (Huynh et al., 2019). As previously related (Ikeda et al., 2007), cell proliferation was upregulated at initial time points and downregulated at late stages, while pathways related to chondrogenesis, especially those related to ECM, were upregulated during the entire process at all time points analyzed (Huynh et al., 2019).

Recently several circRNAs, miRNAs and piRNA were differentially expressed after 7 days of chondrogenic and osteogenic induction (Della Bella et al., 2020). This analysis identified 130 up and 97 downregulated circRNAs in chondrogenesis, of which 15 were also identified in osteogenesis. Notably, many of the circRNAs identified share the same precursor gene, as FKBP5, FADS2, ZEB1, and SMYD3, which were also found in osteogenic induced cells. Investigating if the expression of these genes were influenced by dexamethasone, a component of both induction media (**Table 1**), the cells were exposed only to the compound in monolayer or pellet culture. The results indicated that while the expression of FKBP5 was affected by the presence of dexamethasone, FASD2 gene showed no alteration in its levels (Della Bella et al., 2020). FASD2 and FKBP5 were previously identified in chondrogenic induction. The first showed increased expression after 14 days of induction (Ikeda et al., 2007), while FKBP5 was upregulated during chondrogenesis process (Ikeda et al., 2007; Mrugala et al., 2009). Interestingly, the composition of induction medium is different between these studies, not all containing dexamethasone (**Table 1**).

Regarding miRNAs, more than 200 were identified as differentially expressed (102 up and 108 downregulated) in chondrogenic differentiation (Della Bella et al., 2020). Its mRNA targets had relation to PI3K-AKT signaling pathway, NK-kappa B signaling pathway and others. Furthermore, the identification of miRNAs allowed to relate them with the circRNA expressed in chondrogenesis, once they can act as miRNAs sponges. For example, some of circRNAs with binding sites for hsa-miR-665 were upregulated (hsa_circRNA_081069, hsa_circRNA_100833, hsa_circRNA_002161), while the miRNA was downregulated (Della Bella et al., 2020). An interesting observation is that while in osteogenesis only 54 piRNAs were differentially expressed, in chondrogenesis it was identified 131 piRNAs, the most part upregulated (73). But future studies need to be performed to understand the role of this class of RNA in differentiation process (Della Bella et al., 2020).

The data discussed here indicated that, despite the advances, the protocols developed markedly generated chondrocytes with hypertrophic phenotype, generating a cartilage-like tissue different from normal articular cartilage. However, using this information could help to identified the key points that needed to be improved and also new markers that characterize the chondrocytes generated *in vitro* from MSC.

ONE BY ONE: SINGLE CELL TRANSCRIPTOMICS OF HUMAN MSC

Transcriptomic analysis is usually performed in tissue samples, populations of isolated cells or in cells in culture. In every case, there is the assumption that the samples are homogeneous and each cell responds in a similar way to a given stimulus. However, we now know that every cell in a population has a particular response depending on their cell cycle, metabolic state and environmental or positional information. This is of particular concern when studying MSC gene expression profiles. Human MSC have been defined as a heterogeneous population with subpopulations differing in their multipotency and, hence, being a challenge for transcriptome characterization (Wagner et al., 2006; Russell et al., 2010). In this context, single-cell analysis could be a way to bypass the worries of studying heterogenous cell populations.

The combination of FACS or microfluidic cell isolation and high-throughput sequencing, allows the identification of gene expression profiles of isolated cells from a target population (Li et al., 2013; Hedlund and Deng, 2018). First approaches combined single cell isolation and RNA extraction, with expression analysis of a defined set of genes by qPCR or by interrogating microarray devices (e.g., Acosta et al., 2017; Hardy et al., 2017; Khong et al., 2019; in MSC). However, the emergence of next generation sequencing methods enabled transcriptomic studies of single cells to reach higher levels of coverage.

Tang et al. (2009) reported the first single cell transcriptome assay describing the gene expression patterns of cells from murine oocytes and blastomere (Tang et al., 2009). Since then, single cell RNA-seq (scRNAseq) has been applied to analyze a wide range of cell populations under different biological conditions (Hedlund and Deng, 2018; Hwang et al., 2018).

scRNAseq assays in MSC focused mainly on the characterization of the heterogeneity of the isolated populations and in defining the gene expression patterns of cells from different sources. Liu et al. (2019) performed a large scale RNAseq of 24,370 adipose tissue-derived MSC from three different donors. Interestingly, they observed that most of the heterogeneity observed was due to batch effect and cell cycle phase of the cells. After removing the batch and cell cycle effect they obtained a clean gene-expression matrix that is available for further characterization (Liu et al., 2019). In another work, adipose tissue-derived MSC were compared to bone marrow-derived MSC from the same donor. Adipose tissue-derived MSC showed lower transcriptomic heterogeneity, though different subpopulations were observed. Moreover, adipose tissue-derived MSC were less immunogenic with higher immunosuppression capacity (Zhou et al., 2019). Also, in adipose tissue-derived MSC isolated from perivascular adipose tissue two defined subpopulations could be identified after scRNAseq one of them with higher potential to differentiate into smooth muscle lineages (Gu et al., 2019). On the other hand, umbilical blood MSC (hUC-MSC) showed limited heterogeneity even after stimulation with different cytokines. As mentioned before, most of the heterogeneity observed was related to the cell cycle stage of the cells (Huang Y. et al., 2019). Jia et al. (2020) reported opposite results, identifying several clusters in hUC-MSC (Jia et al., 2020). These discrepancy in the results could be due to differences in cell isolation methods or bioinformatic analysis.

Two reports studied gene expression in human primary Wharton's jelly-derived MSC (hWJMSC) by scRNAseq revealed the existence of several distinct subpopulations of MSC. These subpopulations exhibited diverse functional features related to proliferation, development, and inflammation response (Barrett et al., 2019; Sun et al., 2020). Batch effects and cell cycle stage of the cells must be considered, as they can result in major changes in the gene expression patterns observed (Liu et al., 2019; Sun et al., 2020). Even though, scRNAseq emerge as a powerful tool to address the differentiation potential of the subpopulations found among MSC and could also be used to investigate different cell differentiation stages in the differentiation processes.

PERSPECTIVES

The use of stem cells in therapies has gained interest over the past few years. One of its characteristics is the potential for differentiation into mesodermal lineages that include adipocytes, chondrocytes and osteoblasts. The mechanisms of cell differentiation are complex and, despite the advances in the knowledge of the processes, the mechanisms regulating them are not yet fully understood. High-throughput analysis, e.g., transcriptome and translatome, are strategies helping to shed light on the molecular events driving osteogenesis, chondrogenesis and adipogenesis.

Although the advances shown in this review, challenges remain. The variety of differentiation protocols, cell origin, the investigated time points, RNA type used for analysis and sequencing methodology generates a large amount of data that exhibit significant variations in results. On the other hand, these differences can be important to determine which are the determining factors, regardless of the condition, that could stimulate cell differentiation. The studies covered in this review, and still others that have not been cited, contribute to the understanding of the key events, molecules and pathways that lead to adipogenesis, chondrogenesis and/or osteogenesis, as well as in the comprehension of related diseases and the indication of possible therapeutic strategies.

AUTHOR CONTRIBUTIONS

All authors listed have made a substantial, direct and intellectual contribution to the work, and approved it for publication.

FUNDING

This work was supported by FIOCRUZ and CNPq (442324/2019-7).

ACKNOWLEDGMENTS

We thank Dr. Alejandro Correa for help in article selection and revision of the manuscript and Dr. Marco Stimamiglio for help in article selection. We also thank MSc. Wagner Nagib de Souza Birbeire for image design.

REFERENCES

Abo-Aziza, F. A. M., and Zaki, A. A. (2017). The impact of confluence on bone marrow mesenchymal stem (BMMSC) proliferation and osteogenic differentiation. *Int. J. Hematol. Stem Cell Res.* 11, 121–132.

Acosta, J. R., Joost, S., Karlsson, K., Ehrlund, A., Li, X., Aouadi, M., et al. (2017). Single cell transcriptomics suggest that human adipocyte progenitor cells constitute a homogeneous cell population. *Stem Cell Res. Ther.* 8, 4–9. doi: 10.1186/s13287-017-0701-4

Amati, E., Perbellini, O., Rotta, G., Bernardi, M., Chieregato, K., Sella, S., et al. (2018). High-throughput immunophenotypic characterization of bone marrow- and cord blood-derived mesenchymal stromal cells reveals common and differentially expressed markers: identification of angiotensin-converting enzyme (CD143) as a marker differentially expr. *Stem Cell Res. Ther.* 9, 1–11. doi: 10.1186/s13287-017-0755-3

Ambele, M. A., Dessels, C., Durandt, C., and Pepper, M. S. (2016). Genome-wide analysis of gene expression during adipogenesis in human adipose-derived stromal cells reveals novel patterns of gene expression during adipocyte differentiation. *Stem Cell Res.* 16, 725–734. doi: 10.1016/j.scr.2016.04.011

Aurich, H., Sgodda, M., Kaltwasser, P., Vetter, M., Weise, A., Liehr, T., et al. (2009). Hepatocyte differentiation of mesenchymal stem cells from human adipose tissue in vitro promotes hepatic integration *in vivo*. *Gut* 58, 570–581. doi: 10.1136/gut.2008.154880

Bacakova, L., Zarubova, J., Travnickova, M., Musilkova, J., Pajorova, J., Slepicka, P., et al. (2018). Stem cells: their source, potency and use in regenerative therapies with focus on adipose-derived stem cells – a review. *Biotechnol. Adv.* 36, 1111–1126. doi: 10.1016/j.biotechadv.2018.03.011

Baglìo, S. R., Devescovi, V., Granchi, D., and Baldini, N. (2013). MicroRNA expression profiling of human bone marrow mesenchymal stem cells during osteogenic differentiation reveals Osterix regulation by miR-31. *Gene* 527, 321–331. doi: 10.1016/j.gene.2013.06.021

Barrett, A. N., Fong, C. Y., Subramanian, A., Liu, W., Feng, Y., Choolani, M., et al. (2019). Human Wharton's Jelly Mesenchymal Stem Cells Show Unique Gene Expression Compared with Bone Marrow Mesenchymal Stem Cells Using Single-Cell RNA-Sequencing. *Stem Cells Dev.* 28, 196–211. doi: 10.1089/scd.2018.0132

Bartel, D. P. (2009). MicroRNAs: target recognition and regulatory functions. *Cell* 136, 215–233. doi: 10.1016/j.cell.2009.01.002

Basu, U., Romao, J. M., and Guan, L. L. (2013). Adipogenic transcriptome profiling using high throughput technologies. *J. Genomics* 1, 22–28. doi: 10.7150/jgen.3781

Battula, V. L., Treml, S., Bareiss, P. M., Gieseke, F., Roelofs, H., De Zwart, P., et al. (2009). Isolation of functionally distinct mesenchymal stem cell subsets using antibodies against CD56, CD271, and mesenchymal stem cell antigen-1. *Haematologica* 94, 173–184. doi: 10.3324/haematol.13740

Berdasco, M., Melguizo, C., Prados, J., Gómez, A., Alaminos, M., Pujana, M. A., et al. (2012). DNA methylation plasticity of human adipose-derived stem cells in lineage commitment. *Am. J. Pathol.* 181, 2079–2093. doi: 10.1016/j.ajpath.2012.08.016

Beresford, J. N., Bennett, J. H., Devlin, C., Leboy, P. S., and Owen, M. E. (1992). Evidence for an inverse relationship between the differentiation of adipocytic and osteogenic cells in rat marrow stromal cell cultures. *J. Cell Sci.* 102, 341–351.

Bertone, P., Stolc, V., Royce, T. E., Rozowsky, J. S., Urban, A. E., Zhu, X., et al. (2004). Global identification of human transcribed sequences with genome tiling arrays. *Science* 306, 2242–2246. doi: 10.1126/science.1103388

Billing, A. M., Ben Hamidane, H., Dib, S. S., Cotton, R. J., Bhagwat, A. M., Kumar, P., et al. (2016). Comprehensive transcriptomic and proteomic characterization of human mesenchymal stem cells reveals source specific cellular markers. *Sci. Rep.* 6, 1–15. doi: 10.1038/srep21507

Boeuf, S., and Richter, W. (2010). Chondrogenesis of mesenchymal stem cells: role of tissue source and inducing factors. *Stem Cell Res. Ther.* 1, 1–9. doi: 10.1186/scrt31

Bourin, P., Bunnell, B. A., Casteilla, L., Dominici, M., Katz, A. J., March, K. L., et al. (2013). Stromal cells from the adipose tissue-derived stromal vascular fraction and culture expanded adipose tissue-derived stromal/stem cells: a joint statement of the International Federation for Adipose Therapeutics and Science (IFATS) and the international So. *Cytotherapy* 15, 641–648. doi: 10.1016/j.jcyt.2013.02.006

Caplan, A. I. (1991). Mesenchymal stem cells. *J. Orthop. Res.* 9, 641–650. doi: 10.1002/jor.1100090504

Caplan, A. I. (2017). Mesenchymal stem cells: time to change the name! *Stem Cells Transl. Med.* 6, 1445–1451. doi: 10.1002/sctm.17-0051

Carballo, C. B., Nakagawa, Y., Sekiya, I., and Rodeo, S. A. (2017). Basic science of articular cartilage. *Clin. Sports Med.* 36, 413–425. doi: 10.1016/j.csm.2017.02.001

Casado-Díaz, A., Anter, J., Müller, S., Winter, P., Quesada-Gómez, J. M., and Dorado, G. (2017). Transcriptomic analyses of adipocyte differentiation from human mesenchymal stromal-cells (MSC). *J. Cell. Physiol.* 232, 771–784. doi: 10.1002/jcp.25472

Chang, C. C., Venø, M. T., Chen, L., Ditzel, N., Le, D. Q. S., Dillschneider, P., et al. (2018). Global MicroRNA profiling in human bone marrow skeletal—stromal or mesenchymal–stem cells identified candidates for bone regeneration. *Mol. Ther.* 26, 593–605. doi: 10.1016/j.ymthe.2017.11.018

Chen, Q., Shou, P., Zheng, C., Jiang, M., Cao, G., Yang, Q., et al. (2016). Fate decision of mesenchymal stem cells: adipocytes or osteoblasts? *Cell Death Differ.* 23, 1128–1139. doi: 10.1038/cdd.2015.168

Choudhery, M. S., Badowski, M., Muise, A., Pierce, J., and Harris, D. T. (2014). Donor age negatively impacts adipose tissue-derived mesenchymal stem cell expansion and differentiation. *J. Transl. Med.* 12, 1–14. doi: 10.1186/1479-5876-12-8

Clark, T. A. (2002). Genomewide analysis of mRNA processing in yeast using splicing-specific microarrays. *Science* 296, 907–910. doi: 10.1126/science.1069415

Dallagiovanna, B., Pereira, I. T., Origa-Alves, A. C., Shigunov, P., Naya, H., and Spangenberg, L. (2017). lncRNAs are associated with polysomes during adipose-derived stem cell differentiation. *Gene* 610, 103–111. doi: 10.1016/j.gene.2017.02.004

Daniunaite, K., Serenaite, I., Misgirdaite, R., Gordevicius, J., Unguryte, A., Fleury-Cappellesso, S., et al. (2015). Epigenetic regulation of human adipose-derived stem cells differentiation. *Mol. Cell. Biochem.* 410, 111–120. doi: 10.1007/s11010-015-2543-7

Della Bella, E., Menzel, U., Basoli, V., Tourbier, C., Alini, M., and Stoddart, M. J. (2020). Differential regulation of circRNA, miRNA, and piRNA during early osteogenic and chondrogenic differentiation of human mesenchymal stromal cells. *Cells* 9:398. doi: 10.3390/cells9020398

Djouad, F., Bony, C., Canovas, F., Fromigué, O., Rème, T., Jorgensen, C., et al. (2009). Transcriptomic analysis identifies foxo3a as a novel transcription factor regulating mesenchymal stem cell chrondrogenic differentiation. *Cloning Stem Cells* 11, 407–416. doi: 10.1089/clo.2009.0013

Dominici, M., Le Blanc, K., Mueller, I., Slaper-Cortenbach, I., Marini, F., Krause, D., et al. (2006). Minimal criteria for defining multipotent mesenchymal stromal cells. The International Society for Cellular Therapy position statement. *Cytotherapy* 8, 315–317. doi: 10.1080/14653240600855905

Drehmer, D. L., de Aguiar, A. M., Brandt, A. P., Petiz, L., Cadena, S. M. S. C., Rebelatto, C. K., et al. (2016). Metabolic switches during the first steps of adipogenic stem cells differentiation. *Stem Cell Res.* 17, 413–421. doi: 10.1016/j.scr.2016.09.001

Dulak, J., Szade, K., Szade, A., Nowak, W., and Józkowicz, A. (2015). Adult stem cells: hopes and hypes of regenerative medicine. *Acta Biochim. Pol.* 62, 329–337. doi: 10.18388/abp.2015_1023

Fanganiello, R. D., Ishiy, F. A. A., Kobayashi, G. S., Alvizi, L., Sunaga, D. Y., and Passos-Bueno, M. R. (2015). Increased in vitro osteopotential in SHED associated with higher IGF2 expression when compared with hASCs. *Stem Cell Rev. Rep.* 11, 635–644. doi: 10.1007/s12015-015-9592-x

Fico, A., Fiorenzano, A., Pascale, E., Patriarca, E. J., and Minchiotti, G. (2019). Long non-coding RNA in stem cell pluripotency and lineage commitment: functions and evolutionary conservation. *Cell. Mol. Life Sci.* 76, 1459–1471. doi: 10.1007/s00018-018-3000-z

Friedenstein, A. J., Piatetzky-Shapiro, I. I., and Petrakova, K. V. (1966). Osteogenesis in transplants of bone marrow cells. *J. Embryol. Exp. Morphol.* 16, 381–390.

Gallina, C., Turinetto, V., and Giachino, C. (2015). A new paradigm in cardiac regeneration: the mesenchymal stem cell secretome. *Stem Cells Int.* 2015, 765846. doi: 10.1155/2015/765846

Ganguly, P., El-Jawhari, J. J., Burska, A. N., Ponchel, F., Giannoudis, P. V., and Jones, E. A. (2019). The analysis of *in vivo* aging in human bone marrow mesenchymal stromal cells using colony-forming unit-fibroblast assay and the CD45lowCD271+ phenotype. *Stem Cells Int.* 2019:5197983. doi: 10.1155/2019/5197983

Gao, J., Yang, T., Han, J., Yan, K., Qiu, X., Zhou, Y., et al. (2011). MicroRNA expression during osteogenic differentiation of human multipotent mesenchymal stromal cells from Bone Marrow. *J. Cell. Biochem.* 112, 1844–1856. doi: 10.1002/jcb.23106

Ghorbani, S., Tiraihi, T., and Soleimani, M. (2018). Differentiation of mesenchymal stem cells into neuron-like cells using composite 3D scaffold combined with valproic acid induction. *J. Biomater. Appl.* 32, 702–715. doi: 10.1177/0885328217741903

Gomez-Salazar, M., Gonzalez-Galofre, Z. N., Casamitjana, J., Crisan, M., James, A. W., and Péault, B. (2020). Five decades later, are mesenchymal stem cells still relevant? *Front. Bioeng. Biotechnol.* 8:148. doi: 10.3389/fbioe.2020.00148

Gong, M., Liang, T., Zhang, H., Chen, S., Hu, Y., Zhou, J., et al. (2018). Gene expression profiling: identification of gene expression in human MSC chondrogenic differentiation. *Am. J. Transl. Res.* 10, 3555–3566.

Granchi, D., Ochoa, G., Leonardi, E., Devescovi, V., Baglìo, S. R., Osaba, L., et al. (2010). Gene expression patterns related to osteogenic differentiation of bone marrow–derived mesenchymal stem cells during ex vivo expansion. *Tissue Eng. Part C Methods* 16, 511–524. doi: 10.1089/ten.tec.2009.0405

Gu, W., Nowak, W. N., Xie, Y., Le Bras, A., Hu, Y., Deng, J., et al. (2019). Single-cell RNA-Sequencing and metabolomics analyses reveal the contribution of perivascular adipose tissue stem cells to vascular remodeling. *Arterioscler. Thromb. Vasc. Biol.* 39, 2049–2066. doi: 10.1161/ATVBAHA.119.312732

Gu, X., Li, M., Jin, Y., Liu, D., and Wei, F. (2017). Identification and integrated analysis of differentially expressed lncRNAs and circRNAs reveal the potential ceRNA networks during PDLSC osteogenic differentiation. *BMC Genet.* 18:100. doi: 10.1186/s12863-017-0569-4

Guttman, M., and Rinn, J. L. (2012). Modular regulatory principles of large non-coding RNAs. *Nature* 482, 339–346. doi: 10.1038/nature10887

Hamidouche, Z., Fromigué, O., Ringe, J., Häupl, T., Vaudin, P., Pagès, J. C., et al. (2009). Priming integrin α5 promotes human mesenchymal stromal cell osteoblast differentiation and osteogenesis. *Proc. Natl. Acad. Sci. U.S.A.* 106, 18587–18591. doi: 10.1073/pnas.0812334106

Hardy, W. R., Moldovan, N. I., Moldovan, L., Livak, K. J., Datta, K., Goswami, C., et al. (2017). Transcriptional networks in single perivascular cells sorted from human adipose tissue reveal a hierarchy of mesenchymal stem cells. *Stem Cells* 35, 1273–1289. doi: 10.1002/stem.2599

Hasin, Y., Seldin, M., and Lusis, A. (2017). Multi-omics approaches to disease. *Genome Biol.* 18:83. doi: 10.1186/s13059-017-1215-1

Hedlund, E., and Deng, Q. (2018). Single-cell RNA sequencing: technical advancements and biological applications. *Mol. Aspects Med.* 59, 36–46. doi: 10.1016/j.mam.2017.07.003

Hellingman, C. A., Koevoet, W., and van Osch, G. J. V. M. (2012). Can one generate stable hyaline cartilage from adult mesenchymal stem cells? A developmental approach. *J. Tissue Eng. Regen. Med.* 6, e1–e11. doi: 10.1002/term.502

Herrmann, M., Hildebrand, M., Menzel, U., Fahy, N., Alini, M., Lang, S., et al. (2019). Phenotypic characterization of bone marrow mononuclear cells and derived stromal cell populations from human iliac crest, vertebral body and femoral head. *Int. J. Mol. Sci.* 20:3454. doi: 10.3390/ijms20143454

Hu, X., Tang, J., Hu, X., Bao, P., Pan, J., Chen, Z., et al. (2018). MiR-27b impairs adipocyte differentiation of human adipose tissue-derived mesenchymal stem cells by targeting LPL. *Cell. Physiol. Biochem.* 47, 545–555. doi: 10.1159/000489988

Huang, G., Kang, Y., Huang, Z., Zhang, Z., Meng, F., Chen, W., et al. (2017). Identification and characterization of long non-coding RNAs in osteogenic differentiation of human adipose-derived stem cells. *Cell. Physiol. Biochem.* 42, 1037–1050. doi: 10.1159/000478751

Huang, X., Cen, X., Zhang, B., Liao, Y., Zhu, G., Liu, J., et al. (2019). Prospect of circular RNA in osteogenesis: a novel orchestrator of signaling pathways. *J. Cell. Physiol.* 234, 21450–21459. doi: 10.1002/jcp.28866

Huang, Y., Li, Q., Zhang, K., Hu, M., Wang, Y., Du, L., et al. (2019). Single cell transcriptomic analysis of human mesenchymal stem cells reveals limited heterogeneity. *Cell Death Dis.* 10:368. doi: 10.1038/s41419-019-1583-4

Hung, S. C., Chang, C. F., Ma, H. L., Chen, T. H., and Low-Tone Ho, L. (2004). Gene expression profiles of early adipogenesis in human mesenchymal stem cells. *Gene* 340, 141–150. doi: 10.1016/j.gene.2004.06.028

Huynh, N. P. T., Zhang, B., and Guilak, F. (2019). High-depth transcriptomic profiling reveals the temporal gene signature of human mesenchymal stem cells during chondrogenesis. *FASEB J.* 33, 358–372. doi: 10.1096/fj.201800534R

Hwang, B., Lee, J. H., and Bang, D. (2018). Single-cell RNA sequencing technologies and bioinformatics pipelines. *Exp. Mol. Med.* 50:96. doi: 10.1038/s12276-018-0071-8

Hynes, R. O. (2014). Stretching the boundaries of extracellular matrix research. *Nat. Rev. Mol. Cell Biol.* 15, 761–763. doi: 10.1038/nrm3908

Hynes, R. O., and Naba, A. (2012). Overview of the matrisome–an inventory of extracellular matrix constituents and functions. *Cold Spring Harb. Perspect. Biol.* 4:a004903. doi: 10.1101/cshperspect.a004903

Iaquinta, M. R., Mazzoni, E., Bononi, I., Rotondo, J. C., Mazziotta, C., Montesi, M., et al. (2019). Adult stem cells for bone regeneration and repair. *Front. Cell Dev. Biol.* 7:268. doi: 10.3389/fcell.2019.00268

Ikeda, R., Tsukahara, S., Yoshida, K., and Inoue, I. (2007). Gene expression changes during the chondrogenic differentiation of human mesenchymal stem cells. *J. Biol. Sci.* 7, 729–736. doi: 10.3923/jbs.2007.729.736

Ingolia, N. T. (2016). Ribosome footprint profiling of translation throughout the genome. *Cell* 165, 22–33. doi: 10.1016/j.cell.2016.02.066

Ingolia, N. T., Brar, G. A., Rouskin, S., McGeachy, A. M., and Weissman, J. S. (2012). The ribosome profiling strategy for monitoring translation in vivo by deep sequencing of ribosome-protected mRNA fragments. *Nat. Protoc.* 7, 1534–1550. doi: 10.1038/nprot.2012.086

Ingolia, N. T., Ghaemmaghami, S., Newman, J. R. S., and Weissman, J. S. (2009). Genome-wide analysis in vivo of translation with nucleotide resolution using ribosome profiling. *Science* 324, 218–223. doi: 10.1126/science.1168978

Jääger, K., Islam, S., Zajac, P., Linnarsson, S., and Neuman, T. (2012). RNA-seq analysis reveals different dynamics of differentiation of human dermis- and adipose-derived stromal stem cells. *PLoS One* 7:e0038833. doi: 10.1371/journal.pone.0038833

James, A. W. (2013). Review of signaling pathways governing MSC osteogenic and adipogenic differentiation. *Scientifica* 2013, 1–17. doi: 10.1155/2013/684736

James, A. W., Leucht, P., Levi, B., Carre, A. L., Xu, Y., Helms, J. A., et al. (2010). Sonic hedgehog influences the balance of osteogenesis and adipogenesis in mouse adipose-derived stromal cells. *Tissue Eng. Part A* 16, 2605–2616. doi: 10.1089/ten.tea.2010.0048

Jia, Z., Wang, S., and Liu, Q. (2020). Identification of differentially expressed genes by single-cell transcriptional profiling of umbilical cord and synovial fluid mesenchymal stem cells. *J. Cell. Mol. Med.* 24, 1945–1957. doi: 10.1111/jcmm.14891

Jiang, H., Hong, T., Wang, T., Wang, X., Cao, L., Xu, X., et al. (2019). Gene expression profiling of human bone marrow mesenchymal stem cells during osteogenic differentiation. *J. Cell. Physiol.* 234, 7070–7077. doi: 10.1002/jcp.27461

Jin, Y.-Z., and Lee, J. H. (2018). Mesenchymal stem cell therapy for bone regeneration. *Clin. Orthop. Surg.* 10:271. doi: 10.4055/cios.2018.10.3.271

Kang, X., Sun, Y., and Zhang, Z. (2019). Identification of key transcription factors - gene regulatory network related with osteogenic differentiation of human mesenchymal stem cells based on transcription factor prognosis system. *Exp. Ther. Med.* 17, 2113–2122. doi: 10.3892/etm.2019.7170

Khong, S. M. L., Lee, M., Kosaric, N., Khong, D. M., Dong, Y., Hopfner, U., et al. (2019). Single-cell transcriptomics of human mesenchymal stem cells reveal age-related cellular subpopulation depletion and impaired regenerative function. *Stem Cells* 37, 240–246. doi: 10.1002/stem.2934

Kokabu, S., Lowery, J. W., and Jimi, E. (2016). Cell fate and differentiation of bone marrow mesenchymal stem cells. *Stem Cells Int.* 2016, 1–7. doi: 10.1155/2016/3753581

Kulterer, B., Friedl, G., Jandrositz, A., Sanchez-Cabo, F., Prokesch, A., Paar, C., et al. (2007). Gene expression profiling of human mesenchymal stem cells derived from bone marrow during expansion and osteoblast differentiation. *BMC Genomics* 8:70. doi: 10.1186/1471-2164-8-70

Kuo, Y. R., Wang, C. T., Cheng, J. T., Kao, G. S., Chiang, Y. C., and Wang, C. J. (2016). Adipose-derived stem cells accelerate diabetic wound healing through the induction of autocrine and paracrine effects. *Cell Transplant.* 25, 71–81. doi: 10.3727/096368915X687921

Li, B. (2018). MicroRNA regulation in osteogenic and adipogenic differentiation of bone mesenchymal stem cells and its application in bone regeneration. *Curr. Stem Cell Res. Ther.* 13, 26–30. doi: 10.2174/1574888X12666170605112727

Li, Z., Zhang, C., Weiner, L. P., Zhang, Y., and Zhong, J. F. (2013). Molecular characterization of heterogeneous mesenchymal stem cells with single-cell transcriptomes. *Biotechnol. Adv.* 31, 312–317. doi: 10.1016/j.biotechadv.2012.12.003

Liu, X., Xiang, Q., Xu, F., Huang, J., Yu, N., Zhang, Q., et al. (2019). Data descriptor: single-cell RNA-seq of cultured human adipose-derived mesenchymal stem cells. *Sci. Data* 6, 1–8. doi: 10.1038/sdata.2019.31

Luan, A., Paik, K. J., Li, J., Zielins, E. R., Atashroo, D. A., Spencley, A., et al. (2015). RNA sequencing for identification of differentially expressed noncoding transcripts during adipogenic differentiation of adipose-derived stromal cells. *Plast. Reconstr. Surg.* 136, 752–763. doi: 10.1097/PRS.0000000000001582

Lv, F. J., Tuan, R. S., Cheung, K. M. C., and Leung, V. Y. L. (2014). Concise review: the surface markers and identity of human mesenchymal stem cells. *Stem Cells* 32, 1408–1419. doi: 10.1002/stem.1681

Marappagounder, D., Somasundaram, I., Dorairaj, S., and Sankaran, R. (2013). Differentiation of mesenchymal stem cells derived from human bone marrow and subcutaneous adipose tissue into pancreatic islet-like clusters in vitro. *Cell. Mol. Biol. Lett.* 18:75. doi: 10.2478/s11658-012-0040-5

Marcon, B. H., Holetz, F. B., Eastman, G., Origa-Alves, A. C., Amorós, M. A., de Aguiar, A. M., et al. (2017). Downregulation of the protein synthesis machinery is a major regulatory event during early adipogenic differentiation of human

adipose-derived stromal cells. *Stem Cell Res.* 25, 191–201. doi: 10.1016/j.scr.2017.10.027

Marcon, B. H., Shigunov, P., Spangenberg, L., Pereira, I. T., de Aguiar, A. M., Amorín, R., et al. (2019). Cell cycle genes are downregulated after adipogenic triggering in human adipose tissue-derived stem cells by regulation of mRNA abundance. *Sci. Rep.* 9, 1–10. doi: 10.1038/s41598-019-42005-3

Marcon, B. H., Spangenberg, L., Bonilauri, B., Robert, A. W., Angulski, A. B. B., Cabo, G. C., et al. (2020). Data describing the experimental design and quality control of RNA-Seq of human adipose-derived stem cells undergoing early adipogenesis and osteogenesis. *Data Br.* 28:105053. doi: 10.1016/j.dib.2019.105053

Marêdziak, M., Marycz, K., Tomaszewski, K. A., Kornicka, K., and Henry, B. M. (2016). The influence of aging on the regenerative potential of human adipose derived mesenchymal stem cells. *Stem Cells Int.* 2016, 1–15. doi: 10.1155/2016/2152435

Martin, E. C., Qureshi, A. T., Dasa, V., Freitas, M. A., Gimble, J. M., and Davis, T. A. (2016). MicroRNA regulation of stem cell differentiation and diseases of the bone and adipose tissue: perspectives on miRNA biogenesis and cellular transcriptome. *Biochimie* 124, 98–111. doi: 10.1016/j.biochi.2015.02.012

Mathieu, J., and Ruohola-Baker, H. (2013). "Regulation of stem cell populations by microRNAs," in *Advances in Experimental Medicine and Biology*, eds G. Hime and H. Abud (Dordrecht: Springer), 329–351.

Mathieu, M., Iampietro, M., Chuchana, P., Guérit, D., Djouad, F., Noël, D., et al. (2014). Involvement of angiopoietin-like 4 in matrix remodeling during chondrogenic differentiation of mesenchymal stem cells. *J. Biol. Chem.* 289, 8402–8412. doi: 10.1074/jbc.M113.539825

Matsushita, K., and Dzau, V. J. (2017). Mesenchymal stem cells in obesity: insights for translational applications. *Lab. Investig.* 97, 1158–1166. doi: 10.1038/labinvest.2017.42

Mazini, L., Rochette, L., Amine, M., and Malka, G. (2019). Regenerative capacity of adipose derived stem cells (ADSCs), comparison with mesenchymal stem cells (MSC). *Int. J. Mol. Sci.* 20, 1–30. doi: 10.3390/ijms20102523

Melamed, S. (2020). New sequencing methodologies reveal interplay between multiple RNA-binding proteins and their RNAs. *Curr. Genet.* [Epub ahead of print]. doi: 10.1007/s00294-020-01066-y

Menssen, A., Häupl, T., Sittinger, M., Delorme, B., Charbord, P., and Ringe, J. (2011). Differential gene expression profiling of human bone marrow-derived mesenchymal stem cells during adipogenic development. *BMC Genomics* 12:461. doi: 10.1186/1471-2164-12-461

Min, S. Y., Desai, A., Yang, Z., Sharma, A., DeSouza, T., Genga, R. M. J., et al. (2019). Diverse repertoire of human adipocyte subtypes develops from transcriptionally distinct mesenchymal progenitor cells. *Proc. Natl. Acad. Sci. U.S.A.* 116, 17970–17979. doi: 10.1073/pnas.1906512116

Mo, M., Wang, S., Zhou, Y., Li, H., and Wu, Y. (2016). Mesenchymal stem cell subpopulations: phenotype, property and therapeutic potential. *Cell. Mol. Life Sci.* 73, 3311–3321. doi: 10.1007/s00018-016-2229-7

Mohamed-Ahmed, S., Fristad, I., Lie, S. A., Suliman, S., Mustafa, K., Vindenes, H., et al. (2018). Adipose-derived and bone marrow mesenchymal stem cells: a donor-matched comparison. *Stem Cell Res. Ther.* 9, 1–15. doi: 10.1186/s13287-018-0914-1

Morsczeck, C., Schmalz, G., Reichert, T. E., Völlner, F., Saugspier, M., Viale-Bouroncle, S., et al. (2009). Gene expression profiles of dental follicle cells before and after osteogenic differentiation in vitro. *Clin. Oral Investig.* 13, 383–391. doi: 10.1007/s00784-009-0260-x

Mortazavi, A., Williams, B. A., McCue, K., Schaeffer, L., and Wold, B. (2008). Mapping and quantifying mammalian transcriptomes by RNA-Seq. *Nat. Methods* 5, 621–628. doi: 10.1038/nmeth.1226

Mrugala, D., Dossat, N., Ringe, J., Delorme, B., Coffy, A., Bony, C., et al. (2009). Gene expression profile of multipotent mesenchymal stromal cells: identification of pathways common to TGFβ3/BMP2-induced chondrogenesis. *Cloning Stem Cells* 11, 61–75. doi: 10.1089/clo.2008.0070

Nakamura, T., Shiojima, S., Hirai, Y., Iwama, T., Tsuruzoe, N., Hirasawa, A., et al. (2003). Temporal gene expression changes during adipogenesis in human mesenchymal stem cells. *Biochem. Biophys. Res. Commun.* 303, 306–312. doi: 10.1016/S0006-291X(03)00325-5

Noda, S., Kawashima, N., Yamamoto, M., Hashimoto, K., Nara, K., Sekiya, I., et al. (2019). Effect of cell culture density on dental pulp-derived mesenchymal stem cells with reference to osteogenic differentiation. *Sci. Rep.* 9, 1–5. doi: 10.1038/s41598-019-41741-w

Okoniewski, M. J., and Miller, C. J. (2006). Hybridization interactions between probesets in short oligo microarrays lead to spurious correlations. *BMC Bioinformatics* 7:276. doi: 10.1186/1471-2105-7-276

Onizuka, S., Iwata, T., Park, S. J., Nakai, K., Yamato, M., Okano, T., et al. (2016). ZBTB16 as a downstream target gene of osterix regulates osteoblastogenesis of human multipotent mesenchymal stromal cells. *J. Cell. Biochem.* 2434, 2423–2434. doi: 10.1002/jcb.25634

Owen, M. (1988). Marrow stromal stem cells. *J. Cell Sci.* 1988, 63–76. doi: 10.1242/jcs.1988.Supplement_10.5

Pelttari, K., Winter, A., Steck, E., Goetzke, K., Hennig, T., Ochs, B. G., et al. (2006). Premature induction of hypertrophy during in vitro chondrogenesis of human mesenchymal stem cells correlates with calcification and vascular invasion after ectopic transplantation in SCID mice. *Arthritis Rheum.* 54, 3254–3266. doi: 10.1002/art.22136

Peng, Q., Alipour, H., Porsborg, S., Fink, T., and Zachar, V. (2020). Evolution of ASC immunophenotypical subsets during expansion in vitro. *Int. J. Mol. Sci.* 21:1408. doi: 10.3390/ijms21041408

Pereira, I. T., Spangenberg, L., Robert, A. W., Amorín, R., Stimamiglio, M. A., Naya, H., et al. (2019). Cardiomyogenic differentiation is fine-tuned by differential mRNA association with polysomes. *BMC Genomics* 20:219. doi: 10.1186/s12864-019-5550-3

Pierce, J. L., Begun, D. L., Westendorf, J. J., and McGee-Lawrence, M. E. (2019). Defining osteoblast and adipocyte lineages in the bone marrow. *Bone* 118, 2–7. doi: 10.1016/j.bone.2018.05.019

Pittenger, M. F., Mackay, A. M., Beck, S. C., Jaiswal, R. K., Douglas, R., Mosca, J. D., et al. (1999). Multilineage potential of adult human mesenchymal stem cells. *Science* 284, 143–147. doi: 10.1126/science.284.5411.143

Quan, L., Wang, Y., Liang, J., Qiu, T., Wang, H., Zhang, Y., et al. (2016). Screening for genes, transcription factors and miRNAs associated with the myogenic and osteogenic differentiation of human adipose tissue-derived stem cells. *Int. J. Mol. Med.* 38, 1839–1849. doi: 10.3892/ijmm.2016.2788

Rebelatto, C. K., Aguiar, A. M., Moretao, M. P., Senegaglia, A. C., Hansen, P., Barchiki, F., et al. (2008). Dissimilar differentiation of mesenchymal stem cells from bone marrow, umbilical cord blood, and adipose tissue. *Exp. Biol. Med.* 233, 901–913. doi: 10.3181/0712-RM-356

Reuter, J. A., Spacek, D. V., and Snyder, M. P. (2015). High-throughput sequencing technologies. *Mol. Cell* 58, 586–597. doi: 10.1016/j.molcel.2015.05.004

Robert, A. W., Angulski, A. B. B., Spangenberg, L., Shigunov, P., Pereira, I. T., Bettes, P. S. L., et al. (2018). Gene expression analysis of human adipose tissue-derived stem cells during the initial steps of in vitro osteogenesis. *Sci. Rep.* 8, 1–11. doi: 10.1038/s41598-018-22991-6

Rosen, E. D., and MacDougald, O. A. (2006). Adipocyte differentiation from the inside out. *Nat. Rev. Mol. Cell Biol.* 7, 885–896. doi: 10.1038/nrm2066

Rosen, E. D., and Spiegelman, B. M. (2000). Molecular regulation of adipogenesis. *Annu. Rev. Cell Dev. Biol.* 16, 145–171. doi: 10.1146/annurev.cellbio.16.1.145

Royce, T. E., Rozowsky, J. S., and Gerstein, M. B. (2007). Toward a universal microarray: prediction of gene expression through nearest-neighbor probe sequence identification. *Nucleic Acids Res.* 35:e99. doi: 10.1093/nar/gkm549

Ruiz-Ojeda, F. J., Rupérez, A. I., Gomez-Llorente, C., Gil, A., and Aguilera, C. M. (2016). Cell models and their application for studying adipogenic differentiation in relation to obesity: a review. *Int. J. Mol. Sci.* 17, 1–26. doi: 10.3390/ijms17071040

Russell, K. C., Phinney, D. G., Lacey, M. R., Barrilleaux, B. L., Meyertholen, K. E., and O'Connor, K. C. (2010). In vitro high-capacity assay to quantify the clonal heterogeneity in trilineage potential of mesenchymal stem cells reveals a complex hierarchy of lineage commitment. *Stem Cells* 28, 788–798. doi: 10.1002/stem.312

Rutkovskiy, A., Stensløkken, K.-O., and Vaage, I. J. (2016). Osteoblast differentiation at a glance. *Med. Sci. Monit. Basic Res.* 22, 95–106. doi: 10.12659/MSMBR.901142

Safwani, W. K. Z. W., Makpol, S., Sathapan, S., and Chua, K. (2014). Impact of adipogenic differentiation on stemness and osteogenic gene expression in extensive culture of human adipose-derived stem cells. *Arch. Med. Sci.* 3, 597–606. doi: 10.5114/aoms.2014.43753

Sahraeian, S. M. E., Mohiyuddin, M., Sebra, R., Tilgner, H., Afshar, P. T., Au, K. F., et al. (2017). Gaining comprehensive biological insight into the transcriptome

by performing a broad-spectrum RNA-seq analysis. *Nat. Commun.* 8, 1–14. doi: 10.1038/s41467-017-00050-4

Saleh, F., Itani, L., Calugi, S., Grave, R. D., and El Ghoch, M. (2018). Adipose-derived mesenchymal stem cells in the treatment of obesity: a systematic review of longitudinal studies on preclinical evidence. *Curr. Stem Cell Res. Ther.* 13, 466–475. doi: 10.2174/1574888x13666180515160008

Samsonraj, R. M., Raghunath, M., Nurcombe, V., Hui, J. H., van Wijnen, A. J., and Cool, S. M. (2017). Concise review: multifaceted characterization of human mesenchymal stem cells for use in regenerative medicine. *Stem Cells Transl. Med.* 6, 2173–2185. doi: 10.1002/sctm.17-0129

Santer, L., Bär, C., and Thum, T. (2019). Circular RNAs: a novel class of functional RNA molecules with a therapeutic perspective. *Mol. Ther.* 27, 1350–1363. doi: 10.1016/j.ymthe.2019.07.001

Scheideler, M., Elabd, C., Zaragosi, L. E., Chiellini, C., Hackl, H., Sanchez-Cabo, F., et al. (2008). Comparative transcriptomics of human multipotent stem cells during adipogenesis and osteoblastogenesis. *BMC Genomics* 9:340. doi: 10.1186/1471-2164-9-340

Schwanhäusser, B., Busse, D., Li, N., Dittmar, G., Schuchhardt, J., Wolf, J., et al. (2011). Global quantification of mammalian gene expression control. *Nature* 473, 337–342. doi: 10.1038/nature10098

Sekiya, I., Larson, B. L., Vuoristo, J. T., Cui, J. G., and Prockop, D. J. (2004). Adipogenic differentiation of human adult stem cells from bone marrow stroma (MSC). *J. Bone Miner. Res.* 19, 256–264. doi: 10.1359/JBMR.0301220

Shaik, S., Martin, E. C., Hayes, D. J., Gimble, J. M., and Devireddy, R. V. (2019). Transcriptomic profiling of adipose derived stem cells undergoing osteogenesis by RNA-Seq. *Sci. Rep.* 9, 1–17. doi: 10.1038/s41598-019-48089-1

Shao, J., Zhang, W., and Yang, T. (2015). Using mesenchymal stem cells as a therapy for bone regeneration and repairing. *Biol. Res.* 48, 1–7. doi: 10.1186/s40659-015-0053-4

Silva, A. M., Moura, S. R., Teixeira, J. H., Barbosa, M. A., Santos, S. G., and Almeida, M. I. (2019). Long noncoding RNAs: a missing link in osteoporosis. *Bone Res.* 7:10. doi: 10.1038/s41413-019-0048-9

Sinha, K. M., and Zhou, X. (2013). Genetic and molecular control of osterix in skeletal formation. *J. Cell. Biochem.* 114, 975–984. doi: 10.1002/jcb.24439

Somoza, R. A., Correa, D., Labat, I., Sternberg, H., Forrest, M. E., Khalil, A. M., et al. (2018). Transcriptome-wide analyses of human neonatal articular cartilage and human mesenchymal stem cell-derived cartilage provide a new molecular target for evaluating engineered cartilage. *Tissue Eng. Part A* 24, 335–350. doi: 10.1089/ten.tea.2016.0559

Somoza, R. A., Welter, J. F., Correa, D., and Caplan, A. I. (2014). Chondrogenic differentiation of mesenchymal stem cells: challenges and unfulfilled expectations. *Tissue Eng. Part B Rev.* 20, 596–608. doi: 10.1089/ten.teb.2013.0771

Spangenberg, L., Shigunov, P., Abud, A. P. R., Cofré, A. R., Stimamiglio, M. A., Kuligovski, C., et al. (2013). Polysome profiling shows extensive posttranscriptional regulation during human adipocyte stem cell differentiation into adipocytes. *Stem Cell Res.* 11, 902–912. doi: 10.1016/j.scr.2013.06.002

Steck, E., Fischer, J., Lorenz, H., Gotterbarm, T., Jung, M., and Richter, W. (2009). Mesenchymal stem cell differentiation in an experimental cartilage defect: restriction of hypertrophy to bone-close neocartilage. *Stem Cells Dev.* 18, 969–978. doi: 10.1089/scd.2008.0213

Sun, C., Wang, L., Wang, H., Huang, T., Yao, W., Li, J., et al. (2020). Single-cell RNA-seq highlights heterogeneity in human primary Wharton's jelly mesenchymal stem/stromal cells cultured in vitro. *Stem Cell Res. Ther.* 11, 1–16. doi: 10.1186/s13287-020-01660-4

Tang, F., Barbacioru, C., Wang, Y., Nordman, E., Lee, C., Xu, N., et al. (2009). mRNA-Seq whole-transcriptome analysis of a single cell. *Nat. Methods* 6, 377–382. doi: 10.1038/nmeth.1315

Teitelbaum, S. L. (2000). Bone resorption by osteoclasts. *Science* 289, 1504–1508. doi: 10.1126/science.289.5484.1504

Tian, Q., Stepaniants, S. B., Mao, M., Weng, L., Feetham, M. C., Doyle, M. J., et al. (2004). Integrated genomic and proteomic analyses of gene expression in mammalian cells. *Mol. Cell. Proteomics* 3, 960–969. doi: 10.1074/mcp.M400055-MCP200

Twine, N. A., Chen, L., Pang, C. N., Wilkins, M. R., and Kassem, M. (2014). Identification of differentiation-stage specific markers that define the ex vivo osteoblastic phenotype. *Bone* 67, 23–32. doi: 10.1016/j.bone.2014.06.027

Ulitsky, I. (2018). Interactions between short and long noncoding RNAs. *FEBS Lett.* 592, 2874–2883. doi: 10.1002/1873-3468.13085

Visvader, J. E., and Clevers, H. (2016). Tissue-specific designs of stem cell hierarchies. *Nat. Cell Biol.* 18, 349–355. doi: 10.1038/ncb3332

Wagner, W., Feldmann, R. E., Seckinger, A., Maurer, M. H., Wein, F., Blake, J., et al. (2006). The heterogeneity of human mesenchymal stem cell preparations - Evidence from simultaneous analysis of proteomes and transcriptomes. *Exp. Hematol.* 34, 536–548. doi: 10.1016/j.exphem.2006.01.002

Wall, M. E., Bernacki, S. H., and Loboa, E. G. (2007). Effects of serial passaging on the adipogenic and osteogenic differentiation potential of adipose-derived human mesenchymal stem cells. *Tissue Eng.* 13, 1291–1298. doi: 10.1089/ten.2006.0275

Wang, Y., Jiang, Z., Yu, M., and Yang, G. (2020). Roles of circular RNAs in regulating the self-renewal and differentiation of adult stem cells. *Differentiation* 113, 10–18. doi: 10.1016/j.diff.2020.03.001

Wang, Z., Gerstein, M., and Snyder, M. (2009). RNA-Seq: a revolutionary tool for transcriptomics. *Nat. Rev. Genet.* 10, 57–63. doi: 10.1038/nrg2484

Weissman, I. L. (2015). Stem cells are units of natural selection for tissue formation, for germline development, and in cancer development. *Proc. Natl. Acad. Sci. U.S.A.* 112, 8922–8928. doi: 10.1073/pnas.1505464112

Wu, M., Chen, G., and Li, Y. P. (2016). TGF-β and BMP signaling in osteoblast, skeletal development, and bone formation, homeostasis and disease. *Bone Res.* 4:16009. doi: 10.1038/boneres.2016.9

Wu, R., Ruan, J., Sun, Y., Liu, M., Sha, Z., Fan, C., et al. (2018). Long non-coding RNA HIF1A-AS2 facilitates adipose-derived stem cells (ASCs) osteogenic differentiation through miR-665/IL6 axis via PI3K/Akt signaling pathway. *Stem Cell Res. Ther.* 9, 1–13. doi: 10.1186/s13287-018-1082-z

Xie, Z. Y., Wang, P., Wu, Y. F., and Shen, H. Y. (2019). Long non-coding RNA: the functional regulator of mesenchymal stem cells. *World J. Stem Cells* 11, 167–179. doi: 10.4252/WJSC.V11.I3.167

Xu, X., Li, X., Yan, R., Jiang, H., Wang, T., Fan, L., et al. (2016). Gene expression profiling of human bone marrow-derived mesenchymal stem cells during adipogenesis. *Folia Histochem. Cytobiol.* 54, 14–24. doi: 10.5603/FHC.a2016.0003

Yang, W., Xia, Y., Qian, X., Wang, M., Zhang, X., Li, Y., et al. (2019). Correction to: co-expression network analysis identified key genes in association with mesenchymal stem cell osteogenic differentiation (Cell and Tissue Research, (2019), 378, 3, (513-529), 10.1007/s00441-019-03071-1). *Cell Tissue Res.* 378, 561–562. doi: 10.1007/s00441-019-03103-w

Ye, X., Liao, C., Liu, G., Xu, Y., Tan, J., and Song, Z. (2016). Age-related changes in the regenerative potential of adipose-derived stem cells isolated from the prominent fat pads in human lower eyelids. *PLoS One* 11:e0166590. doi: 10.1371/journal.pone.0166590

Yi, X., Liu, J., Wu, P., Gong, Y., Xu, X., and Li, W. (2020a). The key microRNA on lipid droplet formation during adipogenesis from human mesenchymal stem cells. *J. Cell. Physiol.* 235, 328–338. doi: 10.1002/jcp.28972

Yi, X., Liu, J., Wu, P., Gong, Y., Xu, X., and Li, W. (2020b). The whole transcriptional profiling of cellular metabolism during adipogenesis from hMSC. *J. Cell. Physiol.* 235, 349–363. doi: 10.1002/jcp.28974

Yi, X., Wu, P., Liu, J., Gong, Y., Xu, X., and Li, W. (2019). Identification of the potential key genes for adipogenesis from human mesenchymal stem cells by RNA-Seq. *J. Cell. Physiol.* 234, 20217–20227. doi: 10.1002/jcp.28621

Yi, X., Yang, Y., Wu, P., Xu, X., and Li, W. (2020c). Alternative splicing events during adipogenesis from hMSC. *J. Cell. Physiol.* 235, 304–316. doi: 10.1002/jcp.28970

Yu, C. Y., and Kuo, H. C. (2019). The emerging roles and functions of circular RNAs and their generation. *J. Biomed. Sci.* 26, 1–12. doi: 10.1186/s12929-019-0523-z

Yu, L., Qu, H., Yu, Y., Li, W., Zhao, Y., and Qiu, G. (2018). LncRNA-PCAT1 targeting miR-145-5p promotes TLR4-associated osteogenic differentiation of adipose-derived stem cells. *J. Cell. Mol. Med.* 22, 6134–6147. doi: 10.1111/jcmm.13892

Zaragosi, L. E., Wdziekonski, B., Brigand, K. L., Villageois, P., Mari, B., Waldmann, R., et al. (2011). Small RNA sequencing reveals miR-642a-3p as a novel adipocyte-specific microRNA and miR-30 as a key regulator of human adipogenesis. *Genome Biol.* 12:R64. doi: 10.1186/gb-2011-12-7-r64

Zhang, J., Hao, X., Yin, M., Xu, T., and Guo, F. (2019). Long non-coding RNA in osteogenesis. *Bone Jt. Res.* 8, 73–80. doi: 10.1302/2046-3758.82.BJR-2018-0074.R1

Zhang, M., Jia, L., and Zheng, Y. (2019). circRNA expression profiles in human bone marrow stem cells undergoing osteoblast differentiation. *Stem Cell Rev. Rep.* 15, 126–138. doi: 10.1007/s12015-018-9841-x

Zhang, W., Dong, R., Diao, S., Du, J., Fan, Z., and Wang, F. (2017). Differential long noncoding RNA/mRNA expression profiling and functional network analysis during osteogenic differentiation of human bone marrow mesenchymal stem cells. *Stem Cell Res. Ther.* 8, 1–13. doi: 10.1186/s13287-017-0485-6

Zhao, X., Liang, M., Li, X., Qiu, X., and Cui, L. (2018). Identification of key genes and pathways associated with osteogenic differentiation of adipose stem cells. *J. Cell. Physiol.* 233, 9777–9785. doi: 10.1002/jcp.26943

Zheng, Y., Li, X., Huang, Y., Jia, L., and Li, W. (2017). The circular RNA landscape of periodontal ligament stem cells during osteogenesis. *J. Periodontol.* 88, 906–914. doi: 10.1902/jop.2017.170078

Zhou, W., Lin, J., Zhao, K., Jin, K., He, Q., Hu, Y., et al. (2019). Single-cell profiles and clinically useful properties of human mesenchymal stem cells of adipose and bone marrow origin. *Am. J. Sports Med.* 47, 1722–1733. doi: 10.1177/0363546519848678

Zhu, M., Kohan, E., Bradley, J., Hedrick, M., Benhaim, P., and Zuk, P. (2009). The effect of age on osteogenic, adipogenic and proliferative potential of female adipose-derived stem cells. *J. Tissue Eng. Regen. Med.* 3, 290–301. doi: 10.1002/term.165

Conflict of Interest: The authors declare that the research was conducted in the absence of any commercial or financial relationships that could be construed as a potential conflict of interest.

The handling editor declared a past collaboration with one of the authors BD.

frontiers in Cell and Developmental Biology

REVIEW
published: 09 July 2020
doi: 10.3389/fcell.2020.00497

Endometrial and Menstrual Blood Mesenchymal Stem/Stromal Cells: Biological Properties and Clinical Application

Mahmood Bozorgmehr[1,2†], Shanti Gurung[3†], Saeedeh Darzi[4,5†], Shohreh Nikoo[6†], Somaieh Kazemnejad[7†], Amir-Hassan Zarnani[1,8†] and Caroline E. Gargett[4,5*†]*

[1] Reproductive Immunology Research Center, Avicenna Research Institute, Academic Center for Education, Culture and Research (ACECR), Tehran, Iran, [2] Oncopathology Research Center, Iran University of Medical Sciences, Tehran, Iran, [3] Centre for Reproductive Health, Hudson Institute of Medical Research, Melbourne, VIC, Australia, [4] The Ritchie Centre, Hudson Institute of Medical Research, Melbourne, VIC, Australia, [5] Department of Obstetrics and Gynaecology, Monash University, Melbourne, VIC, Australia, [6] Immunology Research Center, Iran University of Medical Sciences, Tehran, Iran, [7] Nanobitechnology Research Center, Avicenna Research Institute, Academic Center for Education, Culture and Research (ACECR), Tehran, Iran, [8] Department of Immunology, School of Public Health, Tehran University of Medical Sciences, Tehran, Iran

OPEN ACCESS

Edited by:
Lindolfo da Silva Meirelles, Universidade Luterana do Brazil, Brazil

Reviewed by:
Francesco De Francesco, Azienda Ospedaliero Universitaria Ospedali Riuniti, Italy
Rachel Chan, The University of Hong Kong, Hong Kong

***Correspondence:**
Amir-Hassan Zarnani
zarnania@tums.ac.ir
Caroline E. Gargett
caroline.gargett@hudson.org.au

† These authors have contributed equally to this work

Specialty section:
This article was submitted to Stem Cell Research, a section of the journal Frontiers in Cell and Developmental Biology

Received: *31 March 2020*
Accepted: *25 May 2020*
Published: *09 July 2020*

Citation:
Bozorgmehr M, Gurung S, Darzi S, Nikoo S, Kazemnejad S, Zarnani A-H and Gargett CE (2020) Endometrial and Menstrual Blood Mesenchymal Stem/Stromal Cells: Biological Properties and Clinical Application. Front. Cell Dev. Biol. 8:497. doi: 10.3389/fcell.2020.00497

A highly proliferative mesenchymal stem/stromal cell (MSC) population was recently discovered in the dynamic, cyclically regenerating human endometrium as clonogenic stromal cells that fulfilled the International Society for Cellular Therapy (ISCT) criteria. Specific surface markers enriching for clonogenic endometrial MSC (eMSC), CD140b and CD146 co-expression, and the single marker SUSD2, showed their perivascular identity in the endometrium, including the layer which sheds during menstruation. Indeed, cells with MSC properties have been identified in menstrual fluid and commonly termed menstrual blood stem/stromal cells (MenSC). MenSC are generally retrieved from menstrual fluid as plastic adherent cells, similar to bone marrow MSC (bmMSC). While eMSC and MenSC share several biological features with bmMSC, they also show some differences in immunophenotype, proliferation and differentiation capacities. Here we review the phenotype and functions of eMSC and MenSC, with a focus on recent studies. Similar to other MSC, eMSC and MenSC exert immunomodulatory and anti-inflammatory impacts on key cells of the innate and adaptive immune system. These include macrophages, T cells and NK cells, both *in vitro* and in small and large animal models. These properties suggest eMSC and MenSC as additional sources of MSC for cell therapies in regenerative medicine as well as immune-mediated disorders and inflammatory diseases. Their easy acquisition via an office-based biopsy or collected from menstrual effluent makes eMSC and MenSC attractive sources of MSC for clinical applications. In preparation for clinical translation, a serum-free culture protocol was established for eMSC which includes a small molecule TGFβ receptor inhibitor that prevents spontaneous differentiation, apoptosis, senescence, maintains the clonogenic $SUSD2^{+}$ population and enhances their potency, suggesting potential for cell-therapies and regenerative medicine. However, standardization of MenSC isolation protocols and culture conditions are major issues requiring further research to maximize their potential for clinical application. Future research will also address crucial safety aspects of eMSC

and MenSC to ensure these protocols produce cell products free from tumorigenicity and toxicity. Although a wealth of data on the biological properties of eMSC and MenSC has recently been published, it will be important to address their mechanism of action in preclinical models of human disease.

Keywords: endometrium, menstrual blood, culture expansion, perivascular MSC, eMSC, MenSC, cell therapy, immunomodulation

INTRODUCTION

Almost all human tissues contain a small resident population of perivascular mesenchymal stem/stromal cells (MSC) (Crisan et al., 2008). MSC have also been identified in a wide variety of small and large mammalian species (Rozemuller et al., 2010), although these have been studied to a lesser degree. Here we discuss a novel source of MSC from the highly regenerative endometrial lining of the uterus (**Figure 1A**), accessible by biopsy in an office-based procedure without an anesthetic, or non-invasively from menstrual blood (**Figure 1B**) (Ulrich et al., 2013). This review will focus on the biological properties and recent functional characterization of endometrial MSC (eMSC) and menstrual blood MSC (MenSC). The reader is referred to a recent comprehensive review providing greater details on earlier studies describing the identification and early characterization of endometrial MSC, MenSC and endometrial stromal fibroblasts (Gargett et al., 2016). Both epithelial progenitors and MSC have been identified in human and mouse endometrium, however, it is the endometrial and menstrual blood MSC that comprise the topic of this review.

Recently the MSC field has been criticized, due to the poor characterization of MSC from various sources, which has resulted in underwhelming outcomes of many clinical trials using MSC (Sipp et al., 2018). Counter arguments reiterate the importance of using the appropriate definition of the cells under study (i.e., perivascular MSC versus fibroblasts) (Galipeau et al., 2019). Integrated transcriptomic profiling of human MSC from different tissues show their segregation by tissue of origin (Roson-Burgo et al., 2016; Menard et al., 2020) and distinct tissue-specific MSC immune signatures that are similar between fresh and cultured MSC from the same tissue source (Menard et al., 2020). Herein we will distinguish between perivascular eMSC and endometrial stromal fibroblasts. We will also differentiate between potential regenerative "stem cell" properties and immunomodulatory function of both eMSC and MenSC. It has become clear that the regenerative properties of MSC are mainly due to the trophic factors they secrete. These stimulate endogenous cells to repair damaged tissues, rather than MSC functioning as true stem cells (Bianco et al., 2013). MSC are reparative rather than regenerative. It is also recognized that MSC have profound immunomodulatory effects on innate and adaptive immune cells that promote healing by reducing inflammation and immune responses (Galipeau and Sensebe, 2018). In this review, we recognize these important developments in the MSC field and our review on endometrial and menstrual blood MSC and fibroblasts has been structured around these themes.

Human endometrium is a dynamic remodeling tissue, undergoing cycles of growth, differentiation and shedding on a monthly basis as part of the menstrual cycle (Gargett et al., 2012). These dynamic processes occur about 400 times in women until menopause (Jabbour et al., 2006). During menstruation, the upper functional layer of endometrial tissue sloughs off and the tissue fragments exit the body in menstrual blood, leaving a residual 1–2 mm of endometrial tissue (basalis) overlying the myometrium (uterine muscle) (**Figures 1A–C**). The raw surface rapidly reepithelializes and the new functional layer (functionalis), comprising epithelial-lined glands and an extensive vascularized stroma regenerates under the influence of rising, circulating estrogen levels (Gargett et al., 2008) in the next cycle. Atrophic postmenopausal endometrium, which transcriptionally resembles cycling basalis endometrium (Nguyen et al., 2012), also regenerates a functionalis-like layer when women take estrogen-only hormone replacement therapy. MSC can be harvested from this regenerated tissue (Ulrich et al., 2014b).

HUMAN ENDOMETRIAL MSC

Endometrial MSC were first identified as clonogenic stromal cells, comprising 1.3% of stromal fibroblasts harvested from hysterectomy tissue, which contains both functionalis and basalis endometrium (Chan et al., 2004). The large stromal colonies, comprised densely packed small cells with a fibroblast-like morphology and distinguishable from self-limiting small, sparsely packed colonies, likely originated from colony forming units-fibroblast (CFU-F) and do not vary in frequency during the menstrual cycle. This and their presence in postmenopausal endometrium indicate hormone independence of endometrial CFU-F (Schwab et al., 2005; Ulrich et al., 2014b). In comparison to single small colonies, individual large CFU-F showed high proliferative capacity, undergoing 30 population doublings (PD) and producing > 600 billion cells (Gargett et al., 2009). Single large endometrial CFU-F underwent self-renewal *in vitro* by serial cloning at very low seeding densities (5–10 cells/cm^2) and differentiated into adipocytes, chondrocytes, myocytes and osteocytes (Gargett et al., 2009). They also expressed the classic pattern of International Society for Cellular Therapies (ISCT) markers (**Table 1**). These properties indicate that human endometrium contains a small population of MSC.

Markers of eMSC

eMSC were identified as perivascular cells by comparing cloning efficiencies of endometrial stromal cells purified using flow

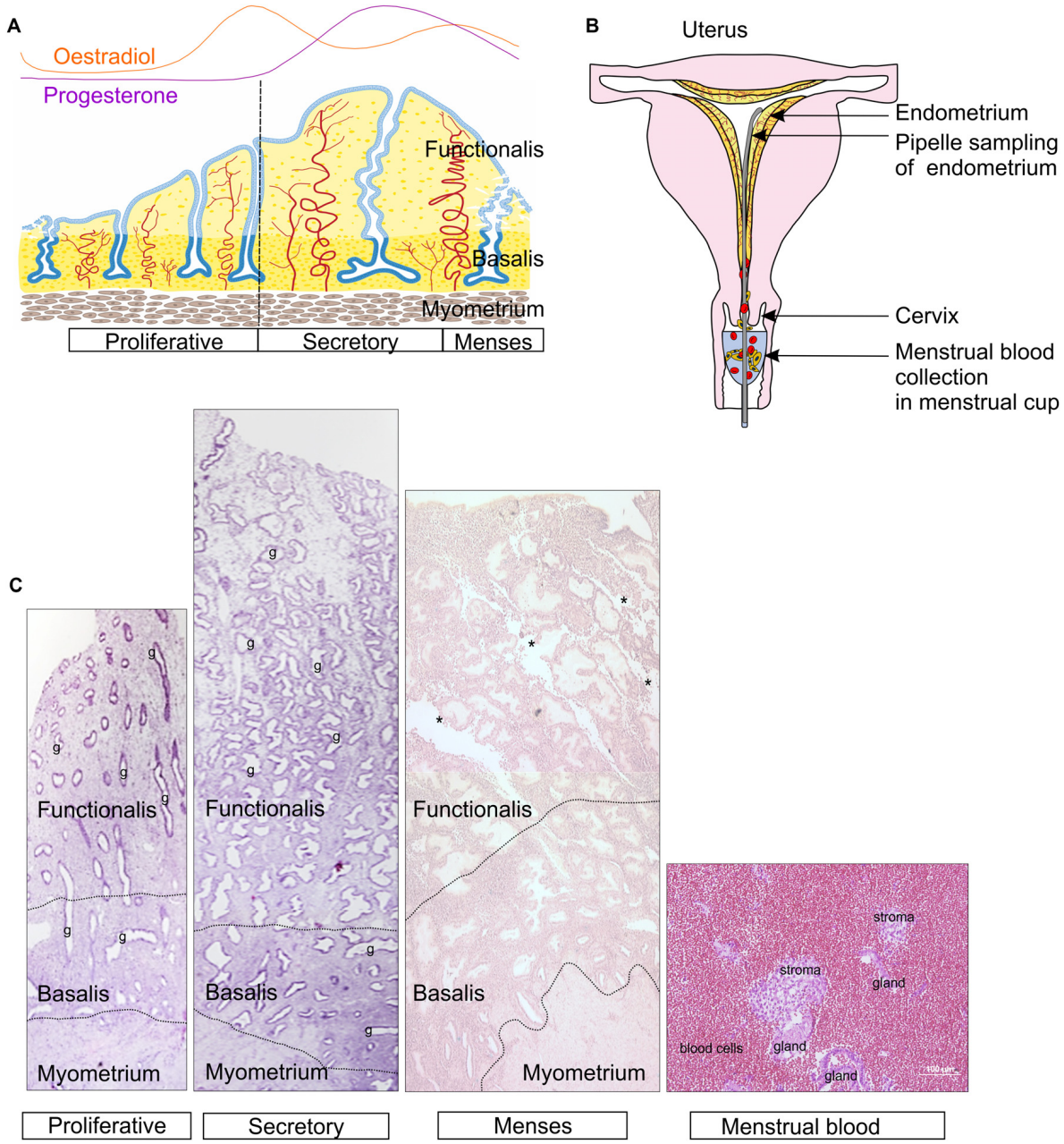

FIGURE 1 | Ovarian and Menstrual cycle, structure of human endometrium and its shedding during menstruation. **(A)** Schematic showing human ovarian hormonal changes corresponding with endometrial growth, differentiation and shedding, during the menstruation, proliferative and secretory phases, respectively, of a menstrual cycle. **(B)** Schematic showing endometrial tissue collection from human endometrium as an office-based procedure using a Pipelle endometrial suction catheter and menstrual fluid using a menstrual cup. **(C)** Histological sections stained with H&E of pre-menopausal human endometrium during the growth (proliferative), differentiation (secretory) and menses stages of the menstrual cycle showing the functionalis, basalis and myometrial layers of the endometrium. *Endometrial tissue breakdown early in the menstrual stage, leaving behind an intact basalis layer. Menstrual blood showing endometrial tissue fragments comprising endometrial stroma, glands and blood cells. Dotted lines define the layers of the endometrium. g, glands. Reproduced with permission from **Figure 1A** from Elsevier (Gargett et al., 2008) and **Figure 1C** from Oxford University Press (Nguyen et al., 2012).

cytometry for several surface markers used for bone marrow MSC (**Figure 2A**) (Schwab et al., 2008). Most CFU-F were from cells co-expressing CD140b and CD146 (Schwab and Gargett, 2007). $CD140b^{+}CD146^{+}$ cells, comprising 1.5% of endometrial stromal cells, were enriched eightfold for CFU-F over unsorted stromal cells and fulfilled the ISCT MSC criteria (Dominici et al., 2006). Their perivascular identity was revealed in both the basalis and functionalis (**Figures 2B,J**), indicating that $CD140b^{+}CD146^{+}$ eMSC could be isolated from endometrial biopsies and would be shed in menstrual blood

(Darzi et al., 2016). Gene profiling CD14b$^+$CD146$^+$ eMSC versus CD140b$^+$CD146$^-$ endometrial fibroblasts showed 762 differentially expressed genes (Spitzer et al., 2012), indicating that perivascular eMSC are distinct from endometrial fibroblasts as for other MSC types (Menard et al., 2020).

Similar to bone marrow MSC, perivascular eMSC are also MSCA-1$^+$ (Sobiesiak et al., 2010), a marker antibody that identifies tissue non-specific aminopeptidase (TNAP), however, this marker is not useful for sorting eMSC as it also marks glandular epithelial cells (**Figures 2G,H**).

To identify a single marker of perivascular eMSC, endometrial stromal cell suspensions were screened with a panel of perivascular and other novel antibodies by flow cytometry and immunohistochemistry of human endometrium (Masuda et al., 2012). Using this strategy, the W5C5 antibody identified a robust marker of stromal cells from pre- and postmenopausal endometrium with MSC properties, enriching clonogenic cells 18-fold over W5C5$^-$ fibroblasts (Masuda et al., 2012; Ulrich et al., 2014b). Sushi Domain-containing 2 (SUSD2) was the antigen identified by the W5C5 antibody (Sivasubramaniyan et al., 2013). SUSD2$^+$ cells comprise 4.1% of endometrial stromal cells and in addition to satisfying the ISCT criteria, they reconstituted stromal tissue *in vivo* under the kidney capsule of NOD-Scid γ (NSG) mice. Non-ISCT markers also expressed by freshly isolated SUSD2$^+$ eMSC include CD117, CD140b, CD146, and STRO-1 (**Figure 2E**). More clonogenic cells were present in the SUSD2$^+$CD146$^+$ and SUSD2^{hi} subpopulations than in the CD140b$^+$CD146$^+$ co-expressing population (Masuda et al., 2012). SUSD2 enables prospective isolation of eMSC from freshly isolated cell suspensions using magnetic bead sorting, providing a more clonogenic population than obtained by flow cytometry sorting, which adversely affects cell viability (Masuda et al., 2012). This is an important consideration for clinical translation.

The specific markers of eMSC show that these cells are located around blood vessels in both the functionalis (**Figures 1**, **2**) indicating they are shed into menstrual fluid as the functionalis breaks down during menstruation (**Figure 1B**). Similarly, stromal fibroblasts are shed into menstrual fluid. Both eMSC and stromal fibroblasts (MenSC) are shed in numbers proportionate to their composition in endometrial functionalis tissue, with eMSC comprising a minority subpopulation. The adult stem cell properties of human eMSC suggest that stromal fibroblasts are their progeny, and to date the only evidence comes from xenografting SUSD2$^+$ eMSC into immunocompromised mice where stromal tissue was generated (Masuda et al., 2012).

Differentiation of eMSC

Physiologically, eMSC around spiral arterioles differentiate into decidual cells under influence of the pregnancy hormone, progesterone, during the secretory stage of the menstrual cycle (Gellersen and Brosens, 2014). This decidual differentiation spreads to the stromal fibroblasts beneath the luminal epithelium. Decidual cells are specialized secretory cells that provide an immunoprivileged environment for an implanting embryo to establish the materno-fetal interface. Subpopulations of eMSC and stromal fibroblasts undergo senescence during the differentiation process (Lucas et al., 2016) and when no embryo implants, progesterone levels fall and menstruation ensues (**Figure 1**).

Transcriptional profiling of endometrial SUSD2$^+$ eMSC and SUSD2$^-$ stromal fibroblasts revealed a distinct gene signature for both cell types following decidual differentiation *in vitro* (Murakami et al., 2014). Known and novel perivascular genes were upregulated in SUSD2$^+$ eMSC, which produced lower levels of inflammatory mediators and chemokines *in vitro* compared to SUSD2$^-$ stromal fibroblasts. Similarly, the inflammatory gene signature of freshly isolated and cultured CD140b$^+$CD146$^+$ eMSC had fewer transcripts than CD140b$^+$CD146$^-$ endometrial stromal fibroblasts (Barragan et al., 2016). Upon decidualization (differentiation) induction SUSD2$^+$ eMSC and SUSD2$^-$ stromal fibroblasts showed greater divergence of their respective secretomes, with the eMSC producing much higher levels of leukemia inhibitory factor and the chemokine CCL7 than stromal fibroblasts. These varying features highlight differences between perivascular eMSC and stromal fibroblasts.

Embryologically, endometrium derives from the mesoderm. Thus, it is not unexpected that endometrial MSC and stromal fibroblasts can be induced to differentiate into mesodermal lineages. Differentiation of eMSC into classic mesodermal lineages *in vitro* as recommended by the ISCT has been shown for clonogenic endometrial stromal cells, SUSD2$^+$ and CD140b$^+$CD146$^+$ cells (Schwab and Gargett, 2007; Gargett et al., 2009; Masuda et al., 2012; Su et al., 2014). Endometrial stromal fibroblasts also show similar mesodermal lineage differentiation, as do bone marrow-derived stromal cells (Haniffa et al., 2009). The reader is referred to table III in Gargett et al. (2016) for a comprehensive list of studies describing mesodermal lineage differentiation of eMSC and endometrial stromal fibroblasts. Differentiation into endodermal lineages include hepatocytes from clonogenic eMSC *in vitro* (Yang et al., 2014) and insulin-and glucagon-secreting pancreatic lineages both *in vitro* and *in vivo* from endometrial stromal fibroblasts (Li et al., 2010; Santamaria et al., 2011). Similarly, cultured endometrial fibroblasts have been differentiated into ectodermal lineages such as dopamine-secreting neurons *in vitro* and *in vivo*, where they may have also induced endogenous neural cell secretion (Wolff et al., 2011). Oligodendrocyte progenitor cells have been differentiated from endometrial stromal fibroblasts (Ebrahimi-Barough et al., 2013). It is not known if eMSC differentiate into ectodermal lineages.

Endometrial MSC in Other Species

The dynamic nature of the endometrium is not limited to humans. Endometrium of other species also undergo proliferation and differentiation, and endure high levels of regeneration during their reproductive life (Rozemuller et al., 2010; Lara et al., 2018). No animal models can replace humans, however, they provide preclinical models bridging the gap between the *in vitro* potential of MSC and future clinical use in humans. The identification of endometrial stromal/stem cells in non-human species has made this possible. Mammalian MSC have been identified in the endometrium (Lara et al., 2018) of mice (Chan and Gargett, 2006; Cervello et al., 2007), guinea pig (Ordener et al., 1993), pig (Miernik and Karasinski, 2012;

TABLE 1 | Comparison of phenotypic markers of endometrial, menstrual, bone marrow, and adipose tissue MSC isolated by plastic adherence or by SUSD2 or CD34 cell sorting.

	Markers (% positive cells)															
MSC type	**CD29**	**CD31**	**CD34**	**CD44**	**CD45**	**CD73**	**CD90**	**CD105**	**CD140b**	**CD146**	**SUSD2**	**STRO1**	**SSEA4**	**OCT4**	**HLA-DR**	**References**
Pericyte $CD146^+CD140b^+$ eMSC in SFM	95.1	–	0	86	0.8	79	–	92	69	37	42.9	–	–	–	–	Rajaraman et al., 2013
Perivascular $SUSD2^+$ eMSC, freshly isolated	11.6	5.3	–	77	4.7	99	71	99	85	28	95	60	–	–	–	Masuda et al., 2012
Perivascular $SUSD2^+$ eMSC in SM	93	2.3	0.5	93	–	99.9	98	99.5	50	1–2	–	0.9	–	–	0	Darzi et al., 2016
Perivascular $SUSD2^+$ eMSC in SFM	–	–	–	-	–	–	–	–	53	1	69	–	–	–	–	Gurung et al., 2015
Perivascular $SUSD2^+$ bmMSC in SM	100	< 1	0	–	0	100	98	100	100	–	–	–	–	–	–	Sivasubramaniyan et al., 2013
Perivascular $SUSD2^+$ bmMSC, freshly isolated	–	26	5	70	90	–	0	20	–	4	–	–	–	–	22	Busser et al., 2015
Perivascular $SUSD2^+$ bmMSC in SM	–	5.3	1.4	83	1.6	–	81	64	–	95	–	–	–	–	1.7	Busser et al., 2015
$CD34^+$ adMSC, freshly isolated	–	38	78	81	57	–	39	28	–	41	–	–	–	–	10	Busser et al., 2015
$CD34^+$ adMSC in SM	–	6.7	17	98	5.8	–	56	79	–	13	–	–	–	–	4.9	Busser et al., 2015
Plastic adherent, passaged, $CD117^+$ MenSC in SM	65	–	5.7	99.8	2.1	–	99.8	99.8	–	–	–	–	90	–	1.6	Patel et al., 2008
Plastic adherent MenSC	99.6	–	0.7	99.4	0.8	99.2	93.1	99.6	–	74.9	–	5.6	–	97.5	0	Musina et al., 2008
Plastic adherent bmMSC	>95	–	0	97.8	0	≥ 90	≥90	≥ 90	≥95	15–20	–	3.8	–	0	0	Vogel et al., 2003; Musina et al., 2008; Bourin et al., 2013
Plastic adherent adMSC	>95	–	0	64	0	25	55	5	–	21	–	0	–	–	1	Gronthos et al., 2001; Mitchell et al., 2006

Adapted from Darzi et al. Stem Cells Translational Medicine 2016 (Darzi et al., 2016) with permission from John Wiley and Sons Publishers. adMSC, Adipose derived MSC; bmMSC, Bone marrow MSC; HLA-DR, Human Leukocyte Antigen DR; MenSC, Menstrual blood MSC; MSC, Mesenchymal Stem/Stromal cell; SFM, DMEM/F12 Serum Free Medium supplemented with EGF and FGF2; SM, DMEM/F12 serum medium contains 10% FBS; –, no data.

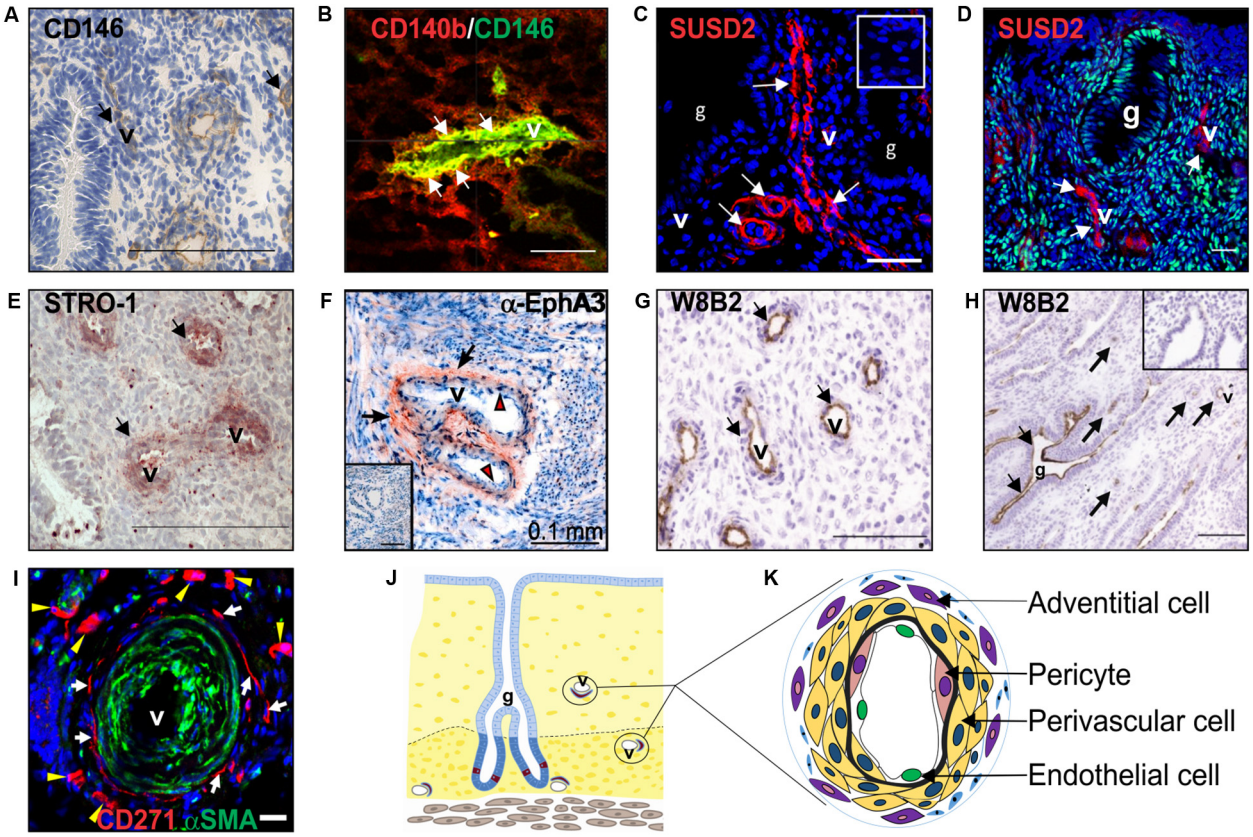

FIGURE 2 | Clonogenic endometrial MSC identified using various surface markers. Surface markers **(A)** CD146, **(B)** co-expression of CD140b/CD146, SUSD2 (red) in **(C)** pre-menopausal and **(D)** postmenopausal endometrium, showing no colocalization with ERα (green), **(E)** STRO-1 and **(F)** EphA3 (red, black arrows), mark clonogenic perivascular eMSC. **(G)** MSCA-1 (TNAP) detected by the W8B2 antibody is expressed by both perivascular and **(H)** epithelial cells in the human endometrium**. (I)** CD271 (red) adventitial perivascular cells mark clonogenic cells in ovine endometrium. **(J)** Schematic of endometrium showing location of endometrial MSC around the vessels. **(K)** Schematic enlargement of blood vessels from **(J)** showing different vascular cell types in the endometrium. Human $CD140b^{+}CD146^{+}$ cells are pericytes (pink cytoplasm), and SUSD2, STRO-1, and EphA3 cells are perivascular cells (yellow cytoplasm). Ovine $CD27^{+}$ cells are adventitial cells (violet cytoplasm). Mouse $CD34^{+}KLF4^{+}$ and LRC cells are also represented by perivascular cells (yellow cytoplasm). Images reprinted with permission from: **(A,E) Figures 1E**, **4C** from Oxford University Press (Schwab et al., 2008), **(B) Figure 4I** from Oxford University Press (Schwab and Gargett, 2007), **(C) Figure 1A** from Bioscientifica (Yang et al., 2019), **(D) Figure 4A** from Oxford University Press (Ulrich et al., 2014b), **(F) Figure 1A** from Public Library of Science (To et al., 2014), **(G,H) Figures 5C,D** from Mary Ann Liebert (Sobiesiak et al., 2010), **(I) Figure 5D** from Public Library of Science (Letouzey et al., 2015) and **(K) Figure 2** from Wiley Online Library (Darzi et al., 2016).

Bodek et al., 2015), sheep (Letouzey et al., 2015; Emmerson et al., 2019), cow (Cabezas et al., 2014), goat (Tamadon et al., 2017), horse (Cabezas et al., 2018) and non-human primates (Padykula et al., 1989; Wolff et al., 2015) (**Table 1**). Label-retention, plastic adherence or specific surface markers have been used to isolate endometrial MSC and demonstrate properties similar to human eMSC and bmMSC.

Murine Label-Retaining Stromal Fibroblasts

Quiescent stem-like endometrial stromal cells were first identified in mice as bromodeoxyuridine label-retaining cells (LRC), which accounted for 6% of the population after 12 weeks of chase in normal cycling mice (Chan and Gargett, 2006). They were localized adjacent to luminal epithelium, near blood vessels and at the endometrial-myometrial junction, similar to their basalis location in human endometrium (Schwab and Gargett, 2007). Stromal LRCs were both $CD31^{-}$ and $CD45^{-}$, indicating they were neither endothelial cells or leukocytes, and perivascular LRCs were αSMA^{+} (Chan and Gargett, 2006). Approximately 16% expressed estrogen receptor-α (ER-α) and were recruited into cell-cycle following estrogen stimulation indicating their involvement in cyclical endometrial regeneration (Chan and Gargett, 2006; Chan et al., 2012). LRCs were also positive for stem cell markers c-Kit and Oct4 (Cervello et al., 2007). However, stem-cell antigen-1 (Sca-1) was not expressed in stromal LRCs (Chan and Gargett, 2006).

Recently, $CD34^{+}KLF^{+}$ endometrial stromal stem/progenitor cells were identified in the perivascular region in the endometrium of a menstruating mouse model (Yin et al., 2019). They expressed the smooth muscle marker, SM22α, and vimentin and upon estrogen stimulation trans-differentiated into gland-like structures lined with E-cadherin-expressing epithelial cells. SUMO-endopeptidase-1 (SENP1)-deletion in $SM22\alpha^{+}$cells induced SUMOylation and activation of ERα

which promoted SM22α$^+$CD34$^+$KLF4$^+$ cell proliferation and transdifferentiation into endometrial epithelium via cyclin D1. Mice share ∼85% of protein-coding regions with humans and have 99% genetic similarity (NIH, 2010), their small size and the development of transgenic humanized mice allow their utility as cost-effective models. More research on mouse eMSC isolation and characterizationis warranted.

Ovine eMSC

Endometrial stromal fibroblasts have been isolated from Fars native sheep uteri as plastic adherent cells (Ghobadi et al., 2018) or clonogenic cells from Border-Leicester-Marino ewes (Letouzey et al., 2015). Plastic adherent cells expressed *CD73* but not *CD34*, with osteogenic and adipogenic differentiation potential and karyotype stability over four passages. Population doubling times were directly related to the cell seeding density and inversely to age of the ewe (**Table 2**). Clonogenic stromal cells were enriched using CD271$^+$CD49f$^-$ surface markers, showing properties similar to bmMSC and human eMSC, with greater clonogenicity, self-renewal by serial cloning compared to CD271$^-$CD49f$^-$ fibroblasts, and differentiated into adipogenic, myogenic, osteogenic and chondrogenic lineages. Apart from CD271, human MSC markers CD44, CD90, CD140b, and CD146 did not cross react with ovine eMSC. The lack of specific ovine marker antibodies has hampered further surface phenotype characterization. Although in a perivascular location, ovine eMSC unlike their human counterpart, were not located in close apposition to vWF$^+$ endothelial cells. Neither did they co-localize with αSMA suggesting they were not pericytes, but rather perivascular adventitial cells, a cell population with similar properties to MSC (Corselli et al., 2012; Crisan et al., 2012). The ability to purify characterized ovine eMSC has enabled the investigation of their use in uro-gynecological disorders such as pelvic organ prolapse (POP) (Letouzey et al., 2015; Emmerson et al., 2019). The domestic ewe has proven a good large animal model because they develop spontaneous POP after vaginal delivery with incidence increasing with parity, similar to women (Couri et al., 2012; Young et al., 2017). Autologous ovine eMSC in a gelatin hydrogel applied onto a polyamide scaffold and implanted into the vagina of the ovine POP model survived for at least 30 days, modulated the inflammatory response, promoting good tissue integration with no postoperative mesh-exposure (Emmerson et al., 2019), one of the main complications associated with human transvaginal mesh (Frankman et al., 2013).

Non-human Primate Endometrial Stromal Cells

Endometrial-derived stromal cells from the non-human primate, green monkey engrafted and differentiated into neuron-like cells when injected into the striatum of males with 1-methyl-4-phenyl-1,2,3,6-tetrahydropyridine (MPTP) induced Parkinson's disease (Wolff et al., 2015). The expanded cells used expressed CD140b, CD146, and CD90, but were otherwise not characterized (Wolff et al., 2015), possibly due to lack of suitable antibodies. The differentiated cells expressed tyrosine hydrolase, a rate limiting enzyme for L-DOPA synthesis, proliferated and produced dopamine metabolites indicating their potential use in cell-based therapies (Wolff et al., 2015). Although non-human primates are ideal for simulating human diseases due to their phylogenetic similarity, their utility in research raises ethical, practical and financial issues.

MENSTRUAL BLOOD MSC (MenSC)

Menstrual blood is a readily accessible, non-invasive source of large numbers of endometrial stem/stromal cells (MenSC) (Ulrich et al., 2013; Darzi et al., 2016), easily collected using a menstrual cup (**Figure 1B**) (Musina et al., 2008; Patel et al., 2008; de Carvalho Rodrigues et al., 2012). Menstrual blood contains fragments of shedding endometrial tissue (**Figure 1C**) which is cultured directly onto plastic similar to bmMSC. Adherent MenSC have typical stromal fibroblast morphology and rapidly propagate with a doubling time of 18–36 h (Meng et al., 2007; Patel et al., 2008). MenSC have higher proliferative capacity, 30–47 PD before senescence, compared to bmMSC, which are generally limited to ∼20 PD (Cui et al., 2007; Allickson et al., 2011). MenSC yield is 2–4-fold higher compared to bmMSC (Alcayaga-Miranda et al., 2015a). As for other adult stem cells, the lifespan of MenSC is relatively short in comparison with human embryonic stem cells (hESC). MenSC only maintain 50% of their telomerase activity at passage 12 compared to hESCs. However, MenSC have more telomerase activity than bmMSC (Patel et al., 2008), perhaps due to the regenerative capacity of the endometrial stroma.

Besides shed endometrial tissue fragments, menstrual fluid also contains peripheral blood. The source of MSC in menstrual fluid could be from bone marrow as well as endometrium. However, peripheral blood contains exceedingly rare bmMSC, as demonstrated by CFU-F analysis. Just 2 CFU-F were found in peripheral blood from 10 patient samples at a frequency of 0–1 CFU-F per 4×10^7 nucleated cells (Kuznetsov et al., 2001). In contrast, menstrual fluid from 18 healthy women contains 600 CFU-F per ml (Alcayaga-Miranda et al., 2015a), suggesting that these CFU-F are derived from the endometrial fragments rather than circulating bone-marrow-derived MSC. Rigorous lineage tracing in chimeric mouse models has also shown that bone marrow stem cells do not contribute to endometrial stromal lineages (Ong et al., 2018). Thus MenSC, comprising mainly endometrial stromal fibroblasts and a small proportion of eMSC found in menstrual fluid are derived from sloughing endometrial tissue rather than non-shedding bone marrow stroma.

Markers of MenSC

MenSC possess the classic ISCT bmMSC markers and are positive for HLA-ABC, negative for HLA-DR and do not express hematopoietic lineage markers (Cui et al., 2007; Meng et al., 2007; Darzi et al., 2012; Kazemnejad et al., 2012; Khanjani et al., 2014; Khanmohammadi et al., 2014). MenSCs, similar to clonogenic eMSC, differ from bmMSC as they do not express STRO-1 (Cui et al., 2007; Meng et al., 2007; Patel et al., 2008; Schwab et al., 2008; Khanmohammadi et al., 2014). Another

TABLE 2 | Endometrial MSC and stromal fibroblasts with MSC properties in mammalian species.

Animal	Cell type	Properties	References
Cow	Plastic adherent stromal cells from early and late luteal phase[a]	• Clonogenic, 0.5–1% cloning efficiency, some alkaline phosphatase positive • Fibroblastic morphology. PDT 20–24 h • Uterine tissue: Express *Stat3*, *Cd44, Cd117*, *Oct4,* and *Sox2* but not *Nanog.* Nuclear Oct4 and Sox2. • Primary culture: Express *Oct4* mRNA, and *Sox2* mRNA and protein but not *Nanog.* • Differentiation: Osteocytes and Chondrocytes (late luteal phase).	Cabezas et al., 2014
Goat	Plastic adherent stromal cells	• Fibroblastic morphology. Clonogenic, PDT ∼ 50–53 h in anestrus stage. • Differentiation: Adipocytes, Osteocytes and Chondrocytes • Stable karyotype during culture expansion	Tamadon et al., 2017
Guinea pig	Plastic adherent stromal cells	• Primary culture: Positive for vimentin, ER and PR; negative for cytokeratin. • Proliferation ↑by EGF and insulin in serum free media. • No effect of ovarian hormones in cell growth despite expression of hormone receptors. • Cultured cells secreted ∼30 different proteins.	Chaminadas et al., 1986; Mahfoudi et al., 1992; Ordener et al., 1993
Horse	Plastic adherent stromal cells	• Clonogenic, highly proliferative cells, PDT 46.4 ± 3.4 h. • Differentiation: Osteocytes and Chondrocytes • Express CD29, CD44, CD90, CD105, MHC class-I but not MHC-II and CD45 • Migrate to chemo-stimulant. • Intrauterine infusion of autologous mucin — stromal cells: survived up to 24 h.	Cabezas et al., 2018 Rink et al., 2018
Mouse	Label-retaining cells (LRC) $CD34^+KLF4^+$ stem progenitor cells	• D3 postnatal BrdU labeling, 12 week-chase; 6% $BrdU^+$ stromal cells. • Location: Perivascular, endometrial-myometrial junction, beneath luminal epithelium • $BrdU^+$ LRC: Some are α-SMA^+, $ER\alpha^+$ (16%) and Ki-67^+ (12%) in response to exogeneous estrogen. • Some co-express c-Kit and OCT4. Do not express C31, Sca-1 and CD45 • Express SM22α and vimentin. • Proliferate ↑, migrate to injured epithelium and undergo MET upon 17-β estradiol stimulation. • SUMOylation augments ERα transcriptional activity with ↑ proliferation and ↓ apoptosis.	Chan and Gargett, 2006; Chan et al., 2012 Cervello et al., 2007 Yin et al., 2019
Monkey	Plastic adherent stromal cells	• Expanded cells are uncharacterised. • Differentiation: Tyrosine hydrolase-expressing neural-like cells *in vivo* • *In vivo*: ↑ level of dopamine metabolite HVA in PD model.	Wolff et al., 2015
Pig	Plastic adherent stromal cells	• Clonogenic, 0.035% clonal efficiency. • Express *CD29*, *CD44*, *CD144*, *CD105*, *CD140b* and *CD31* and pluripotency genes *NANOG* and *OCT4*. • Differentiation: Osteocytes, Adipocytes and Chondrocytes. • Highly proliferative compared to adipose-derive MSC. • Express CD29, CD73, CD90, and CD105 but not CD34 and CD45. • Wnt pathway activation: ↓large colonies and ↑ small colonies. ↓ MSC surface markers. Osteogenic but not adipogenic differentiation. • Wnt pathway inhibition: Clonal efficiency unchanged, MSC markers ↑. • Higher growth rate than AD-MSC. • Express CD73, CD90, and CD105 but not CD34 and CD45. • $CD105^+$ cultured cells differentiation: cardiomyocyte- and insulin-producing β cell-like cells.	Miernik and Karasinski, 2012 Bukowska et al., 2015 Subbarao et al., 2019
Sheep	Plastic adherent stromal cells $CD49f^-CD271^+$ eMSC	• Express *CD73* but not *CD34* and stable karyotype over four passages. • PDT ∼21 h immature and ∼45 h mature ewes. PDT α cell density • Differentiation: Osteocytes, Adipocytes, and Chondrocytes. • Location: adventitia of arterioles and venules. $CD271^+$ αSMA^- cells (**Figure 2I**). • Self-renewal by serial cloning *in vitro*, 5.5% cloning efficiency. • High proliferative, PD time 18.7 h. • Differentiation: Osteocytes, Adipocytes, Chondrocytes and Myocytes. • Express human surface markers CD271 but not CD140b, CD44, CD90, and CD146. • Autologous eMSC on gelatin/polyamide mesh survived 30 d in a sheep model of vaginal prolapse. • ↑*COL1A1*, *COL3A1*, *FBN5*, *ELN,* and elastin. • ↓myofibroblasts and inflammatory response to mesh. • ↓ disrupted muscularis and ↑ elastin fibers • ↑mesh stiffness, compressive extensions, breaking load and no exposure.	Ghobadi et al., 2018; Letouzey et al., 2015; Emmerson et al., 2019

[a]*Luteal phase is the progesterone dominant phase of the estrus cycle; AD-MSC, adipose MSC; ER, estrogen receptor; MET, mesenchymal epithelial transition; PD, Parkinson disease; PDT, population doubling time; PR, progesterone receptor.*

difference is that MenSCs highly express cytoplasmic OCT-4 (Borlongan et al., 2010) which is not expressed by eMSC (Gurung et al., 2015; Gurung et al., 2018b) or conventional bmMSC. Several inconsistencies in MenSC phenotype have been observed for pluripotency markers c-KIT and SSEA-4. Some have reported these markers in isolated MenSCs

(Patel et al., 2008; Borlongan et al., 2010), while others were negative (Cui et al., 2007; Hida et al., 2008; Musina et al., 2008; Khanjani et al., 2015). Others observed a different pattern of these markers in isolated MenSC (Meng et al., 2007; Musina et al., 2008; Darzi et al., 2012; Kazemnejad et al., 2012) including expression of SSEA-4 and/or NANOG in some c-KIT$^+$ cells from cultured menstrual blood (Meng et al., 2007; Patel et al., 2008; Borlongan et al., 2010). Heterogeneity of MenSs cultures may explain these disparities, resulting from differences in menstrual blood sampling day, collection technique and enrichment protocol.

Mesodermal Lineage Differentiation

MenSC have been induced to differentiate into mesodermal lineages characteristic of bmMSC (**Table 3**) to satisfy the minimal criteria for MSC. Similar to marker expression, the degree of MenSC differentiation into mesodermal lineages varies and is dependent on the isolation method (Meng et al., 2007; Darzi et al., 2012; Kazemnejad et al., 2012; Khanjani et al., 2014; Khanjani et al., 2015). MenSCs isolated by density gradient centrifugation and plastic adherence have lower capacity to differentiate toward osteoblasts compared to bmMSC using both cytochemical and molecular analyses (Darzi et al., 2012). In contrast, c-KIT$^+$ MenSC possessed similar differentiation capacity to bmMSC (Patel et al., 2008), although, Alizarin red alone without quantification was used. It is unknown whether c-KIT-sorted MenSC have osteogenic differentiation ability.

Adipogenic differentiation of MenSC isolated by density gradient centrifugation and plastic adherence is limited when assessed by Oil-red O staining (Musina et al., 2008) and significantly lower than umbilical cord MSC (Jin et al., 2013) and bmMSC (Khanmohammadi et al., 2014). Fortification of adipogenic induction medium with rosiglitazone promoted MenSC differentiation into adipocytes as analyzed by molecular and cytochemical techniques (Khanmohammadi et al., 2014). Purifying cultured MenSC using the c-KIT

TABLE 3 | Comparison of *in vitro* differentiation capability of menstrual blood- versus bone marrow-derived mesenchymal stem/stromal cells.

Target lineage	Differentiation medium	Evaluation	Results	References
Chondrocyte	FCS, FGF2, sodium pyruvate, TGFβ3, BMP6, Dex, ITS+1, and ascorbic acid	sGAG Assay, IF, RT-PCR	• High COL2, proteoglycans expression similar to bmMSC • different *COL9A1* and *SOX92A1* to bmMSC	Khanmohammadi et al., 2012
Osteoblast	FCS or HPR, Dex, ascorbic acid, and β-glycerophosphate	Alizarin red, RT-PCR	• ↓ mineralization than bmMSC • Comparable *PTHR, OCN* but lower *ALP* in HPR medium compared to bmMSC.	Darzi et al., 2012
Adipocyte	FBS, Dex, rh-Insulin, IBMX, Indomethacin and ATRA (3 sequential protocols)	Oil red staining, RT- PCR	• Lower differentiation capability compared to bmMSC for all protocols	Khanmohammadi et al., 2014
Decidua-like cells	E_2 and 8-Br-cAMP	FC, IF, RT-PCR	• Markedly higher decidual differentiation than bmMSC	Sugawara et al., 2014
Cardiomyocyte	FBS or serum free medium ± 5-aza, ± FGF2 (2 protocols)	IF, RT-PCR	• Similar ↑ late-stage cardiac markers under 5-aza and FGF2 versus 5-aza alone • ↑ *GJA1* and *TNNT2* in MenSCs while ↑ *GJA1* in bmMSC at the same condition	Rahimi et al., 2014, 2018
Hepatocyte	Three-step protocol – Serum free or FBS medium with EGF, FGF2, DEX, ITS+1, NTA, HGF, and OSM	ICC, RT- PCR, functional assays	• Higher *ALB*, *CYP7A1*compared to bmMSC • Express *ALB* and *CK*-18, secrete albumin and produce glycogen similar to bmMSC	Khanjani et al., 2014
Neural	P4-8F with EGF and FGF2 then BDNF, FBS, horse serum, N2 and all-trans- RA	IF, RT-PCR, EP	• Similar ↑ NES, GFAP, but ↑ *GFAP* in bmMSC • Similar ↑ MAP2, GABABR1/2 and TUBB3 • ↑ K^+, Ca^{2+}, Na^+ channel genes with EP recording	Azedi et al., 2017
	Serum-free N2, B27, FGF2, EGF, IBMX, dbcAMP	ICC, BDNF secretion	• Similar ↑ TUBB3, NEUN, and GFAP to bmMSC • Secretion of BDNF in both MenSCs and bmMSC	Kozhukharova et al., 2018
Glial lineage	Two-step protocol via NSC: P4- 8F medium with EGF and FGF-2 ATRA, FBS, horse serum, N2 and rh-PDGF for glial cells	IF RT-PCR	• Similar ↑ *OLIG2* and NES in NSCs • ↑ GFAP, *OLIG2*, MBP in glial-like cells derived from both MenSCs and bmMSC	Azedi et al., 2014

5-aza, 5-Azacytidine; 8-Br-cAMP, 8-Bromoadenosine 3′,5′-cyclic adenosine monophosphate; ALB, Albumin; ALP, Alkaline phosphatase; ATRA, all-trans retinoic acid; BDNF, brain-derived neurotrophic factor; FGF2, Basic Fibroblast Growth Factor; BGP, β-glycerophosphate; BMP6, Bone morphogenetic protein 6; bmMSC, Bone Marrow derived mesenchymal stem cells; cAMP, Cyclic adenosine monophosphate; CK-18, cytokeratin 18; CYP7A1, cytochrome P450 7A1; dbcAMP, Dibutyryl Cyclic Adenosine Monophosphate; Dex, Dexamethasone; E2, estrogen; EGF, Epidermal growth factor; EP, Electrophysiology; FCS, Fetal calf serum; FC, Flow cytometry; GABABR, gamma aminobutyric acid type b receptor; GFAP, Glial Fibrillary Acidic Protein; GJA1, Gap junction alpha-1 protein; HGF, Hepatocyte growth factor; HPR, human platelet releasate; IBMX, M3-isobutyl-1-methyl-xanthine; ICC, immunocytochemistry; IF, immunofluorescence; ITS+1, insulin–transferrin–selenium, linoleic-BSA; MAP2, Micro-tubule-associated protein; MBP, Myelin basic protein; MenSCs, Menstrual blood-derived mesenchymal stromal cells; NES, Nestin; NEUN, Neuronal Nuclear Protein; NSC, neurosphere-like cells; NTA, Nitrilotriacetic Acid; OCN, Osteocalcin; OSM, Oncostatin M; RA, Retinoic Acid; rh-PDGF, recombinant human platelet-derived growth factor; RT-PCR, Reverse transcription polymerase chain reaction; sGAG, sulfated Glycosaminoglycan; TGFb3, Transforming growth factor b3; TNNT2, Cardiac muscle troponin T.

(CD117) marker resulted in high adipogenic differentiation capacity (60–70%) (Patel et al., 2008), likely due to a more homogeneous MSC population, although it is unknown if CFU-F are also purified in the c-KIT$^+$ subpopulation of cultured MenSC.

Differentiation of MenSC into the chondrocytic lineage has been demonstrated for CD117 purified cells in 2D cultures yielding 45% positive cells, similar to bmMSC (Patel et al., 2008). Unfractionated MenSCs cultured in a 3D nanofibrous scaffold enhanced chondrogenic commitment compared to a 2D culture system (Kazemnejad et al., 2012), with extensive cartilage-like extracellular matrix containing ∼50% more glycosaminoglycan than control MenSCs differentiated in 2D. Chondrogenic differentiation requires very low O_2 tension, which is better established in 3D compared to 2D cultures. MenSCs produce high levels of Activin A, IGF-1, and FGF2, key growth factors involved in chondrogenesis (Ren et al., 2016; Uzieliene et al., 2018).

Co-culture of MenSC with murine cardiomyocytes generated spontaneously beating human cells expressing cardiac specific markers, indicating their differentiation into troponin T-expressing cardiomyocytes (Hida et al., 2008). *In vitro* cardiac differentiation of MenSC was compared with bmMSC using two differentiation protocols and showed that continuous FGF2 was superior to 5-aza-2′-deoxycytidine alone, as shown by increased levels of late-stage cardiac markers (connexin 43 and Troponin T) (**Table 3**). This suggests that FGF2 has a key role in differentiating cardiac cells from MSC sources. MenSC had greater capacity than bmMSC to differentiate toward cardiomyocytes regardless of the differentiation protocol (Rahimi et al., 2014).

Collectively, the differentiation capability of unfractionated MenSC isolated using conventional methods into two mesodermal lineages (osteoblasts and adipocytes) is lower than bmMSC isolated in a similar manner. This suggests differences in tissue specific MSC properties likely reflecting their tissue of origin. Purification of the rarer perivascular MSC with specific markers appears to improve MenSC differentiation, although c-KIT is not expressed on perivascular cells of human endometrium *in vivo* (**Figure 2**), but whether induced in cultured perivascular eMSC is unknown.

Endometrial stromal fibroblasts naturally differentiate into decidualized stromal cells *in vivo*. Decidualization is mediated by estrogen and progesterone, and supports the establishment and continuation of pregnancy. MenSC have been differentiated into decidual-like cells with 8-Br-cAMP and progesterone, showing morphological changes and increased expression of the decidualization markers prolactin and insulin-like growth factor binding protein-1 (IGFBP-1), and attenuated expression of MSC surface markers (Sugawara et al., 2014). Greater secretion of these decidual proteins was observed for MenSC compared to bmMSC and amnion MSC (Domnina et al., 2016). It is possible that easily obtained MenSC could be differentiated into decidual-like cells as a potential strategy to mitigate infertility associated with insufficient endometrial decidualization.

MenSC Differentiation Into Ectodermal and Endodermal Lineages

Cultured MenSC transdifferentiate across lineage boundaries into ectodermal (neurons and glia), and endodermal (hepatocyte) lineages (**Table 3**). c-KIT sorted MenSCs express neuronal phenotypic markers when grown in appropriately conditioned medium (Borlongan et al., 2010). MenSC formed neurosphere-like cells and then differentiated into neural and glial-like cells comparable to bmMSC, and shown by increased expression of classic neural markers (nestin, microtubule-associated protein 2, gamma-aminobutyric acid type B receptor subunit 1 and 2, and tubulin β3 class III) (**Table 3**) (Azedi et al., 2014, 2017).

Differentiation of MenSC into hepatocytes is dependent on the concentrations of hepatocyte growth factor (HGF), oncostatin M (OSM) and removal of serum from the induction medium (Khanjani et al., 2015). Up-regulation of albumin and *CYP7A1* expression was higher in MenSC- compared to bmMSC-derived hepatocyte-like cells, although cytokeratin-18 expression, albumin production and glycogen accumulation were either lower or not different (Khanjani et al., 2014), indicating similarity between MenSCs and bmMSC hepatocyte-like cell differentiation potential.

Unfractionated MenSC have potential to differentiate into keratinocyte-like cells, generating epidermal lineage markers via co-culturing with keratinocytes derived from the foreskin of healthy newborns (Faramarzi et al., 2016; Akhavan-Tavakoli et al., 2017). MenSC were also induced to differentiate into keratinocyte-like cells in 3D culture with human foreskin-derived keratinocytes on a bilayer scaffold composed of amniotic membrane and silk fibroin (Arasteh et al., 2018; Fard et al., 2018). The MenSC-derived keratinocytes expressed keratinocyte-specific markers *K14*, p63 and IVL (involucrin). Generating keratinocytes from MenSC on an efficient natural construct has potential applicability for MSC-based skin wound healing and regeneration (Arasteh et al., 2018; Fard et al., 2018), although these tissue engineering constructs have yet to be evaluated in an animal skin wound repair model.

MenSC show considerable capacity to differentiate into numerous lineages *in vitro*, although have lesser ability for several bmMSC lineages. It would now be important to demonstrate the potential of MenSC to undergo differentiation into these lineages *in vivo* in animal models. Genomic sequencing (e.g., RNAseq) would also shed light on how far down the various lineages MenSC differentiate.

IMMUNOMODULATORY PROPERTIES OF eMSC AND MenSC

Since the first report on the immunomodulatory properties of MSC in 2002 (Bartholomew et al., 2002), numerous studies have shown significant impact of MSC on key cells of the innate and adaptive immune systems (Le Blanc and Mougiakakos, 2012; Wang et al., 2014). These non-stem cell properties have been exemplified in bmMSC (da Silva Meirelles et al., 2006). MSC regulate monocyte infiltration to the site of injury, macrophage

polarization and dendritic cell maturation (Jiang et al., 2005; Kim and Hematti, 2009). MSC also inhibit NK cell proliferation and target cell killing, and secrete IFN-γ (Sotiropoulou et al., 2006). In the adaptive immune system, MSC suppress T cell proliferation, shifting Th17 cells toward T regulatory cells (Tregs) (Di Nicola et al., 2002; Sato et al., 2007). MSC also impede B cell proliferation (Augello et al., 2005; Corcione et al., 2006). Mechanism of interaction relies on direct cell-cell contact and/or MSC secretion of immunosuppressive factors including Indoleamine 2,3 deoxygenase (IDO), prostaglandin E2 (PGE2), nitric oxide (NO), human leukocyte antigen G5 (HLA-G5), IL-10, IL-6 and TGF-β (Di Nicola et al., 2002; Ren et al., 2010). MSC have also been used to successfully treat patients with severe immune disorders, including Graft-Versus-Host Disease (GVHD) and Crohn's disease (Dalal et al., 2012). This extensive literature indicates that MSC have immunosuppressive rather than immunostimulatory functions. Here we review the literature on the immunomodulatory properties of eMSC and MenSCs.

In vitro Immunomodulatory Properties of eMSC

The immunomodulatory properties of perivascular eMSC have only recently been investigated. A transcriptional study on $CD140b^+CD146^+$ eMSC revealed that perivascular eMSC differentially expressed several immunomodulatory genes compared to endometrial stromal fibroblasts (Spitzer et al., 2012) (**Table 4**). A similar gene profile of differentially expressed genes was observed between $SUSD2^+$ perivascular eMSC and $SUSD2^-$ stromal fibroblasts (Murakami et al., 2014) (**Table 4**), including anti-inflammatory *IL10*. The gene profile of perivascular eMSC treated and non-treated with the TGFβ receptor (TGFβR) inhibitor, A83-01 to prevent apoptosis and senescence during culture expansion, revealed upregulation of many immune response genes in treated cells, including interleukins (*IL15, IL33, IL6ST*), TNF and IFNγ related genes, PGE2 synthesis genes (*PLA2G4A, PTGS2/COX-2, PTGES)*, and Toll-like receptors, *TLR2* and *TLR3* (Gurung et al., 2018b). Together, these finding suggest that eMSC have the ability to interact with the immune system in a similar manner to bmMSC, exerting immunosuppressive functions through paracrine mechanisms and by direct contact with the target cell.

eMSC also influence T cell function by suppressing ConA-stimulated murine T lymphocyte proliferation in a dose-dependent manner (Yang et al., 2019). Blocking the TGFβR in eMSC reversed the immunosuppressive effects of eMSC on T cell proliferation, indicating a role for the TGFβ signaling pathway. Of the various mechanisms assessed, neither IL-10, PGE2, TGFβ or Tregs mediated the eMSC anti-proliferative effects on T cells, however, IL-17A and Dickkopf-1 (DKK-1) were secreted and may be candidates involved. Systemic eMSC failed to inhibit swelling in a T cell-mediated mouse model of skin inflammation, suggesting that eMSC have distinct immunomodulatory properties that may not be sufficient to restrain some T cell-mediated events (Yang et al., 2019).

eMSC Effects on Foreign Body Response to Implanted Scaffolds *in vivo*

The immunomodulatory role of perivascular eMSC has been explored in animal models of foreign body response to the implanted biomaterials (**Table 4**). In a nude rat wound healing model, human eMSC seeded on a gelatin-coated polyamide mesh initially increased inflammatory M1 macrophages at the mesh-tissue interface, followed by reduced inflammation around the mesh filaments by switching macrophages from an M1 to a wound healing M2 phenotype. Long term, there were reduced $CD68^+$macrophages at the mesh tissue interface (Ulrich et al., 2014a). Human eMSC seeded on the same polyamide/gelatin mesh inhibited secretion of the inflammatory cytokines IL1β and TNF in early stages of the host response, whereas induced gene expression of anti-inflammatory M2 markers was observed later (Darzi et al., 2018). These responses occurred earlier and were more marked in the immunocompetent than immunocompromised mice. This favorable immunosuppression by eMSC was confirmed subsequently by eMSC-seeded degradable poly(L-lactic acid)-co-poly(ε-caprolactone) (PLACL) nanofibers and 3D bio-printed tissue engineering constructs in the same wound healing immunocompetent mouse models (Mukherjee et al., 2019b; Paul et al., 2019).

In vitro Immunomodulatory Properties of MenSC

The immunomodulatory properties of MenSC have been also been investigated, often in comparison with bmMSC. MenSC effects have been mainly studied on T cell responses. In mixed lymphocyte reactions (MLR), comprising MenSCs mixed with allogenic human peripheral blood mononuclear cells (PBMCs), cellular proliferation, IFN-γ and TNF levels were suppressed, while IL-4 production increased (Murphy et al., 2008). The MenSC suppressive effect on the allogenic MLR was dose-dependent and biphasic, with a high MenSC:PBMC ratio (1/2) suppressing PBMC proliferation and a low ratio (1/32) supporting proliferation (Nikoo et al., 2012). MenSC effects on cytokine levels were similarly concentration dependent with reduced anti-inflammatory $IL4^+IL10^+CD4^+$ T cells at low MenSC:PBMC ratio compared to bmMSC (Luz-Crawford et al., 2016). These effects suggest distinct immunosuppressive activity of MenSC, similar to eMSC and appear less than bmMSC. This may be due to more HLA-DR molecules on the MenSC surface and fewer IFN-γ receptors, and that MenSC produce less IDO, COX2, and Activin A (Luz-Crawford et al., 2016) compared with bmMSC.

Pretreatment (licensing) of bmMSC with an inflammatory stimulus enhances their immunosuppressive properties. In contrast to the anti-proliferative effect of IFN-γ-pre-treated bmMSC on $CD4^+$ T cells, IFN-γ-IFN-g-pre-treated MenSC show a milder response (Aleahmad et al., 2018). Untreated MenSC cocultured with $CD4^+$ T cells at ratios of 1:2–1:8 had a pro-inflammatory effect, increasing the proliferation of anti-CD3/CD28-acitivated T cells, and IFN-γ pretreatment only partially reduced this effect, suggesting that IFN-γ responsiveness

TABLE 4 | Immunomodulatory properties of endometria MSC, stromal fibroblasts, and MenSC.

Cell type	*In vitro* studies	References	Cell type	*In vivo* studies	References
Perivascular endometrial mesenchymal stem cells					
Fresh $CD140b^+CD146^+$ eMSC	• ↑ *JAG1*, *TGFβ1*, *CXCR4*, *IL1RAP*, *IL1RL1* • ↔ *IDO and PGE2*	Spitzer et al., 2012	$SUSD2^+$ eMSC in SM	Skin wound repair rodent models implanted with eMSC seeded scaffolds ➢ **Non-Degradable mesh- Rat** • M1 to M2 switch at 30 days	Ulrich et al., 2014a
$SUSD2^+$ eMSC, Dec-$SUSD2^+$ eMSC	• ↑ *CXCL1*, *CXCL10*, *CCL5*, *IL6*, *IL8* • ↓ *IL33*, *AOC3*, *CCL7*	Murakami et al., 2014		• ↓$CD68^+$ MQ (90 days) ➢ **Non-degradable – NSG and BL6 mice** • C57BL6: ↓ IL1β and TNFα secretion (3d). ↑*Arg, MRC* and *IL10* (3 and 7d).	Darzi et al., 2018
$SUSD2^+$ eMSC cultured in SM	eMSC and mouse splenocytes cocultured • Dose dependently ↓ lymphocyte proliferation • ↑ FOXP3 Treg in co-culture blocked by TGFβ inhibitor • eMSC produced IL17 and DKK-1	Yang et al., 2019		• NSG: ↓ *Arg* (30d), *MRC* (14d). ↓*TNF*α (7 and 30d). ➢ **Degradable Nanofiber – NSG mice** • ↑ Cellular infiltration around scaffold • ↑M2 MQ and few M1 MQ (qualitatively)	Mukherjee et al., 2019b
$SUSD2^+$ eMSC cultured in A83-01/SFM	• ↑ *SOD3*, *SOD2*, *SOCS3*, *CXCL12*, *CXCL16*, *CCL8*, *IL-15*, *IL33*, *IL6, TLR2/3*, *IL1R1*, *IL6R*, *TLR2*, *TLR3, PLA2G4A*, *COX2*, *PTGES, C3, C2*, *CFB*, *CFD* and *CFI* • ↑ CCL2, GM-CSF, IGFBP-2, DKK-1 and EGF. • Secrete IL6, IL8, MCP-1, MIF, MCP-3 and CXCL1.	Gurung et al., 2018b		• *IL1β, TNFα, CCL2, CCL3,4,5,7,12,19 CXCL1,2,10 –CCR1, CCR7* (1w), ↑ *Arg1, Mrc1*, *IL6* and *Il4ra* (6w). ➢ **3D printed mesh – NSG mice** • ↑ M2 MQ and ↓ M1 MQ within implanted biomaterial (1w).	Mukherjee et al., 2020 Paul et al., 2019
Endometrial stromal cells					
Plastic adherent ESC	IFN and TNF stimulated ESC for 3 and 7 days • Express IFN-γ1 and TNF I/II receptors • ↑ expression: HLA-I but not HLA-II • IDO, IL6 and PGE2 production • ↓ contact-induced $CD4^+$ T cell proliferation.	Queckborner et al., 2020	Plastic adherent stromal cells	➢ **EAE in BL6 mouse** • ↓ EAE score • ↓ MN, TH1 and TH17 in CNS • ↑ IL10, IL27 and IDO in mouse splenocytes	Peron et al., 2012
Menstrual blood stem cells					
Plastic adherent MenSC	Proliferation of allogenic PBMCs in MLR • ↓ proliferation at 1:1 and 1:10 (MenSC: PBMC), with higher inhibition at 1:1.	Wang et al., 2012	Plastic adherent MenSC	➢ **DSS induced colitis in BL6 mouse** • ↓ intra-colon IL-2 and TNF-α, ↑ IL-4, IL-10. • ↓ MHC-II expression in splenic DCs.	Cabezas et al., 2014
	Proliferation of allogenic PBMCs in MLR • ↓ proliferation at high MenSC concentrations (1:1 or 1:2; MenSC:PBMC ratios) • ↑ proliferation at low MenSC concentrations (1:32 or 1:64; MenSC:PBMC ratios)	Nikoo et al., 2012		• ↓$CD3^+CD25^+$ and $CD3^+CD8^+$T cells, and ↑ $CD4^+CD25^+Foxp3^+$ Tregs. ➢ **Anti- PD-L1 ± pre-treated MenSCs in DSS induced colitis in mouse.** • ↓ infiltration of immune cells.	Shi et al., 2019
	Mo differentiation and maturation • Interfere with Mo ↑ immature DC: ↓CD80, 86, HLA-DR on DCs. • Interfere early stages DC maturation: ↓ CD14, CD1a on DCs. • ↑IL6 and IL10 in co-culture with Mo.	Bozorgmehr et al., 2014		• ↓ TNFα and IFNγ in serum and colon. • ↓ CD4 and CD8 T cells in colon. • ↓$CD11c^+$MHC-II^+ DC in spleen, total MQ but ↑ M2 MQ. • ↑CD206 cells and $CD4^+CD25^+$ FOXP3 Treg.	
	IL2 supplemented NK cells co-culture with IL1β, IFN ± pre-treated MenSCs • Untreated MenSCs dose dependently ↑ NK cell proliferation • Treated MenSCs ↓ NK cells proliferation. • ↓ NK cell cytotoxicity, GzmA, GzmB and perforin.	Shokri et al., 2019		➢ **DSS induced colitis in mouse.** • ↓ immature splenic plasma cells and deposition of IgG in the colon. • ↑regulatory B cells and IL10. ➢ **CIA and GVHD in mice**	Xu et al., 2018 Luz-Crawford et al., 2016
	PHA-activated PBMC ± IFNγ and IL1β pre-treated MenSCs. • ↓ proliferation at both 1:10 and 1:100 MenSC:PBMC ratios • ↓ %CD4/CD8+ IFNγ+ cells • ↓ %Th17 cells at 1:10 but not in 1:100 MenSC:PBMC ratio	Luz-Crawford et al., 2016		• CIA model: ↑ TNF and IL6 • GVHD: ↑ CD45 cells in the spleen ➢ **Allograft heart transplantation in mouse** • ↓ IgG and IgM production, and B cells activation.	Xu et al., 2017

CIA, collagen-induced arthritis; Dec, decidualised; DSS, dextran sodium sulfate; EAE, Experimental Autoimmune Encephalomyelitis; FOXP3, Forkhead box 3; Gzm, Granzyme; GVHD, Graft versus host disease; HLA, Human leukocyte antigen; IDO, indole-amin-2, 3 dioxygenase; IFN-γ, Interferone-γ; Ig, Immunoglobulin; IL, Interleukine; MES, Melt electrospinning; MHC-II, Major histocompability antigen class-II; MLR, Mixed leukocyte reaction; Mo, Monocyte; MQ, Macrophage; NK, Natura killer; PBMC, Peripheral blood mononuclear cell; PD-L1, Programmed death-ligand 1; PGE 2, Prostaglandin E2; PHA, Phytohemaglutinin; Th, T helper; TNF-α, Tumor necrosis factor-α; Treg, Regulatory T cells.

of MenSC is comparatively lower than bmMSC (**Figure 3**) (Aleahmad et al., 2018). The impact of MenSC on human T cell proliferation *in vitro* is complex and depends on the cytokine milieu, T cell stimulating factors, MenSC/T cell ratio and the co-culture system. MenSC have a weaker and distinct *in vitro* effect on T cell proliferation compared to bmMSC (Aleahmad et al., 2018), possibly similar to the lesser characterized eMSC responses.

As expected, MenSC also have an impact on the innate immune system, including human blood monocyte-derived dendritic cells (MoDCs) (**Table 4**) (Bozorgmehr et al., 2014), NK cells and tissue macrophages. MenSC co-cultured with human monocytes interfered with MoDC differentiation at the phenotypic level. The immature DCs expressed suboptimal co-stimulatory molecules and had low levels of CD40, CD80, CD83 and CD86. MenSC secreted IL-6 and IL-10 (Bozorgmehr et al., 2014), which typically inhibit monocyte to DC differentiation (Allavena et al., 1998; Chomarat et al., 2000). Uterine NK (uNK) cells constitute the main component of the endometrial innate immune system, comprising 50–70% of lymphoid cells in early pregnant endometrium (Moffett-King, 2002). uNK cells function in maintaining a successful pregnancy by preventing allorejection of the embryo and regulating vascular remodeling (Hanna et al., 2006; Kalkunte et al., 2009). Dysregulation of uNK cell function may be involved in the pathogenesis of recurrent pregnancy loss (Dosiou and Giudice, 2005) indicating the importance of tightly regulating uNK cell cytotoxic function. Unstimulated MenSCs induced NK cell proliferation partly due to lower production of IGFBPs 1-4 compared to bmMSC. However, in a pro-inflammatory milieu involving IFN-γ/IL-1β, MenSCs substantially inhibited NK cell proliferation through production of IL-6 and TGF-β (Shokri et al., 2019). IFN-γ/IL-1β-stimulated MenSC also curbed NK cell cytotoxicity by decreasing granzyme A, granzyme B, and perforin expression.

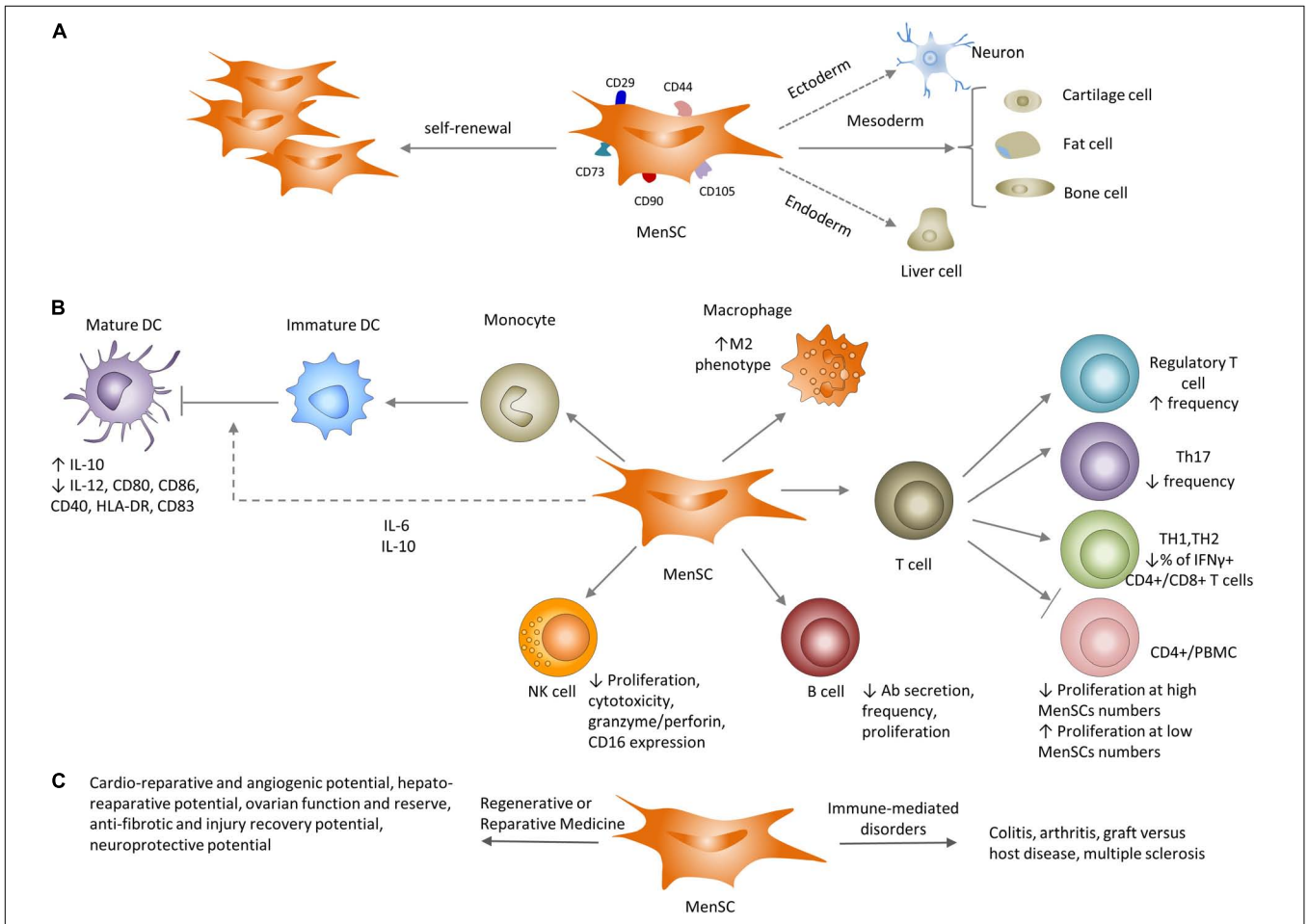

FIGURE 3 | Properties of MenSCs *in vitro* and *in vivo*. **(A)** Similar to their well-known counterparts (bmMSC), MenSCs have the ability to differentiate to cells of different lineages and express typical MSC-associated markers. **(B)** Impact of MenSCs on the adaptive and innate immune systems. MenSCs secrete IL-6 and IL-10 that inhibit optimal maturation of human monocyte-derived dendritic cells (DC). MenSCs shift macrophages toward the M2 (anti-inflammatory) profile. MenSCs either inhibit or support T cell proliferation depending on MenSC/T cell (PBMC) ratio. MenSCs increase Treg frequency, decrease the number of TH17 and IFNγ^{+} CD4^{+}/CD8^{+} T cells and cytotoxic capacity of NK cells. MenSCs decrease antigen-specific antibody secretion and proliferation of B cells. **(C)** Utilization of MenSCs in preclinical settings ranges from immune-mediate disorders: arthritis and GVHD to regenerative and reparative applications: cardio protection, liver and lung fibrosis and neuroprotection.

NK cells also killed MenSC in a MHC- and time-dependent manner. These results suggest a critical role for MenSC in endometrial tissue homeostasis and induction of a pregnancy-friendly phenotype in decidual NK cells.

MenSC Immunomodulatory Effects *in vivo*

Recently it was shown that MenSC influence the humoral immune responses in a mouse model of heart transplantation by attenuating antibody responses (Xu et al., 2017). MenSC injection 24 h following allograft heart transplantation prolonged graft survival in recipient mice by rapidly reducing intragraft deposition of donor-specific IgG and IgM antibodies and reducing donor-specific antibody secreting B cells. It remains to be investigated whether MenSC ameliorate autoantibody production in patients with antibody-mediated autoimmune diseases.

In a murine model of colitis, intravenous MenSC injected 2–8 days after disease induction (Cabezas et al., 2014) increased intra-colon IL-4 and IL-10 and decreased IL-2 and TNF, and splenic dendritic cells expressed lower levels of MHC-II compared to untreated controls (Cabezas et al., 2014). The percentage of $CD3^+CD25^+$ and $CD3^+CD8^+$ T cells was reduced and Tregs increased. MenSC also promoted $F4/80^+CD206^+$ M2 macrophage migration and reduced IgG deposition in the injured colon, decreased splenic plasma cells, increased regulatory B cells (Xu et al., 2018), and appeared to mediate these immunomodulatory effects via PD-L1 (Shi et al., 2019).

Not all studies have corroborated the immunomodulatory effects of MenSC in disease models. MenSC failed to switch T cell-related immune responses toward an anti-inflammatory direction in a murine model of arthritis (Luz-Crawford et al., 2016) (**Table 5**). MenSC injection increased splenic TNF levels and did not reduce lymph node pro-inflammatory Th17 cells and in contrast, bmMSC did not exert any beneficial impacts on disease progression. MenSC injection into a humanized GVHD mouse model, where irradiated NOD-SCID mice received human PBMC, has been efficacious in reducing disease severity (Luz-Crawford et al., 2016). In this acute inflammatory model, intraperitoneal MenSC were superior to bmMSC, in contrast to the arthritis model. MenSC improved intestine structure and survival rate. However, immunosuppressive functions were not observed for MenSC, but rather their effect was attributed to their regenerative capacity. MenSCs expressed high levels of VEGF and FGF2, and induced greater vascularization compared with bmMSC. MenSC also had a greater migratory capacity to target organs due to their higher expression of surface CXCR4.

MenSC also have anti-microbial activity. In a cecal ligation and puncture mouse model of sepsis, the combination of MenSC and antibiotic improved the survival rate of affected animals (up to 95%) compared with control animals receiving either treatment alone. The MenSC/antibiotic combination increased bacterial clearance from blood, and reduced the inflammatory cytokines IL-8, TNF, and MCP in peritoneal fluid, without loss of T and B lymphocytes (Alcayaga-Miranda et al., 2015b).

Taken together, eMSC and MenSC have a range of effects on both arms of the innate and specific immune responses (**Figure 3**), however, the discrepancies between *in vitro* and *in vivo* findings and considerable variation between experimental models necessitate further investigation to identify the underlying mechanisms that orchestrate the cross-talk that MenSC and eMSC utilize to modulate the immune system. Standardization of key variables of human disease and disease models including immune versus non-immune nature of the disease, local versus systemic administration of cells, chronic versus acute disease, and the dose and timing of injected MenSC as well as MSC cell type (perivascular versus unfractionated stromal fibroblast populations) and experimental models as has been promulgated for bmMSC will further increase understanding of the distinct properties of eMSC and MenSC.

THERAPEUTIC POTENTIAL OF eMSC AND MenSC

Challenges for MSC-Based Therapies in Regenerative Medicine

Hundreds of clinical trials of various MSC have overall shown underwhelming results in regenerative medicine applications (Prockop et al., 2014). This is due in part to the use of preclinical mouse studies using syngeneic mice, MHC-matched cells and achievable dosing (Galipeau and Sensebe, 2018). Large animal preclinical models are particularly important to trial MSC before going to the clinic to resolve these issues. To date long term engraftment of substantial numbers of infused MSC has not been demonstrated, rather only a small population (2–10%) remain in the days following administration (Dimmeler et al., 2014). Allogeneic MSC will be rapidly removed by the innate immune system, and while autologous cells may prevail, few appear to integrate into tissues. This lack of MSC integration is due to the ischemic or inflammatory environment of the diseased tissue/organ and loss of vascular niches which may be replaced with fibrosis. Aged tissues and chronic disease can also hinder MSC integration (Dimmeler et al., 2014). Despite these challenges, MSC can have dramatic effects through their paracrine actions, appearing to reset the innate immune system and promoting endogenous cellular repair without substantial integration (Caplan, 2016).

eMSC in Regenerative or Reparative Medicine

Since perivascular eMSC originate from a cyclically regenerating tissue with accompanying angiogenesis (Gargett and Rogers, 2001) they are excellent candidates with therapeutic potential for tissue repair and possibly tissue regeneration. Their pericyte and perivascular identity indicate their specific roles in regulating angiogenesis, inflammation and fibrosis (Thomas et al., 2017), suggesting eMSC are a good candidate for regenerative or reparative medicine.

Endometrium and Decidua Regeneration

As mentioned above, human eMSC differentiate into decidual cells. This property has been harnessed for generating a tissue engineered uterus through repopulating decellularized

extracellular matrix (ECM) constructs with cells, including endometrial stromal fibroblasts (Fu et al., 2014; Hellstrom et al., 2017; Tiemann et al., 2020). This bioengineering approach has been conducted in decellularized uterus from rat (Miyazaki and Maruyama, 2014; Hellstrom et al., 2016; Kuramoto et al., 2018), pig (Campo et al., 2017) and human (Olalekan et al., 2017). Allogeneic endometrial stromal cells and bmMSC seeded into decellularized rat uteri diffused

TABLE 5 | Preclinical and clinical applications of endometrial MSC and Menstrual blood stromal cells.

Disease	Animal model	Findings	References
Perivascular endometrial mesenchymal stem/stromal cells			
Pelvic organ prolapse	• Multiparous sheep, vaginally implanted autologous ovine eMSC seeded PA/G and PA mesh	• 30 days eMSC survival, ↓ myofibroblast, ↑ elastin, ↓ $CD45^+$ leukocytes	Emmerson et al., 2019
	• Rat, SC implantation of DiO-eMSC seeded on PA/G	• ↑ neovascularization (7d), ↓ mesh/tissue stiffness, crimped collagen deposition	Ulrich et al., 2014a
	• Mouse, SC implantation of bio-printed eMSC on 3D printed scaffold	• Better tissue integration, collagen deposition	Paul et al., 2019
	• NSG mouse, implantation of eMSC seeded degradable electrospun nanofiber.	• Better tissue integration, ↑Cellular infiltration into mesh	Mukherjee et al., 2019b
Parkinson disease	• Mouse, immunodeficient and immunocompetent MPTP lesions	• Migrated and differentiated to lesion, ↑ striatal dopamine and its metabolites	Wolff et al., 2011
Endometrial stromal/stem cells (ESC)			
Diabetes mellitus	• Immunocompromised mouse Type I diabetes.	• Insulin production in single cells from kidney capsule	Santamaria et al., 2011
	• ESC differentiated to pancreatic β-like cells were injected into kidney capsule	• minimized diabetes-associated complications • reduced blood glucose • prolonged survival of mice	Li et al., 2010
Menstrual blood stromal/stem cells (MenSCs)			
Myocardial infarction	• Nude rat, GFP labeled MenSCs injected into the center and margin of infarcted area	• Ameliorated left ventricular systolic function • Trans-differentiation to cardiomyocytes • ↓ fibrotic areas	Hida et al., 2008
	• Rat, intracardial injection	• Improved cardiac function • trans-differentiation to cardiomyocytes • ↑ Akt, Erk1/2, Stat3, proliferation and c-kit^+ • ↓ apoptosis and p38 signaling	Jiang et al., 2013
Critical limb ischemia	• BALB/c mice, MenSCs injected into hind-limb of CLI mice	• no muscle necrosis in damaged area	Murphy et al., 2008
Acute liver failure (AFL)	• BALB/c mouse, IV injection of GFP labeled MenSCs	• ↑ Liver regeneration, donor cells homed to injured area, ↓ Ast, Alt, urea and total bilirubin • ↑ hepatic markers Alb, Ck18 and Tat	Fathi-Kazerooni et al., 2017
Liver fibrosis	• ICR mouse, IV injection of GFP labeled MenSCs	• donor cells migrated to injury • ↑ liver function, ↓collagen deposition and activated hepatic satellite cells	Chen et al., 2017b
Premature ovarian failure	• C57BL6 Mouse, tail-vein injection of DiO labeled MenSCs Premature ovarian failure models	• ↑ Amh, Fshr, Ki67, ovarian weight, Plasma E2 levels and normal follicles	Liu et al., 2014; Manshadi et al., 2019
	• C57BL6 Mouse, IV injection of MenSCs	• ↓ apoptosis, restored ovarian function and normalized serum ovarian hormones.	Feng et al., 2019
Poor ovarian response	• POR women, IO injection of MenSCs	• ↑ fertilization rate • ↑ pregnancy rate	Zafardoust et al., 2020
Acute lung injury	• C57BL6 mouse, IV injection of MenSCs	• ↑ pulmonary microvascular permeability, expression of *Pcna*, *Kgf* and *Il-10*	Xiang et al., 2017
	• LPS-induced injury • ICR mouse, IV injection of MenSCs	• ↓ histopathological damage, *Il-1b* expression and Caspase-3 protein expression • ↓ inflammatory response and ↑lung tissue repair	Ren et al., 2018
Pulmonary fibrosis	• C57BL6 mouse, tail-vein injection of MenSCs bleomycin model	• ↓ collagen production, deposition, and wet/dry lung weight	Zhao et al., 2018b
Excisional wound defect	• C57BL6 mouse, intradermal injection of PKH2- labeled MenSCs	• ↑ wound closure, Neovascularization and mature vasculature, collagen content and VEGF	Cuenca et al., 2018
	• Rat, Implantation of amnion seeded with MenSCs	• improved wound closure	Farzamfar et al., 2018
Intrauterine adhesion	• ICR mouse, IV injection of DIL labeled MenSCs	• ↑ endometrial thickness and microvessel density • ↑ conception rate and embryo number	Zhang et al., 2016
Asherman's syndrome	• Infertile women with severe AS, transvaginal delivery of autologous MenSCS	• ↑ endometrial thickness • 2/5 conceived and 1/5 spontaneous pregnancy	Tan et al., 2016
OGD stroke	• Rat, IC and IV injection of MenSCs Neuroprotection model	• ↓ behavioral and histological impairments	Borlongan et al., 2010

(Continued)

TABLE 5 | Continued

Disease	Animal model	Findings	References
Sciatic nerve defect	• Rat, MenSCs seeded neural guidance conduit implanted into nerve defect area	• Improved sciatic functional index • Prevented muscle weight- loss • ↓ HPLT in MenSCs-seeded conduit group	Farzamfar et al., 2017
Alzheimer's disease	• Appswe/PSEN1-overexpressed dE9 mouse • IT injection of MenSCs into hippocampus	• Improved spatial learning and memory • ↓ plaques and hyperphosphorylation • ↑ several Aβ degrading enzymes	Zhao et al., 2018a
Diabetes mellitus	• Mouse type I diabetes, IV injection of MenSCs model of how mice was made diabetic	• ↑ insulin production, normalized glucose level • ↓Weight loss, prolonged life-span • Recovered islet structure	Wu et al., 2014

Aβ, Amyloid beta; Alb, Albumin; Alt, Alanine aminotransferase; Amh, Anti-Müllerian hormone; AS, Asherman's syndrome; Ast, Aspartate transaminase; CD, Cluster of differentiation; CK, Cytokeratin; CLI, Critical limb ischemia; DiO, 3,3′-dioctadecyloxacarbocyanine perchlorate; E2, Estradiol; Fshr, Follicle stimulating hormone receptor; GFP, Green fluorescent protein; HPL, Hot plate latency; IC, Intracerebral; ICR, Imprinting control region; Il, Interleukin; IO, Intraovarian; IT, intrathecal; IV, Intravenous; KGF, Keratinocyte growth factor;, LPS, Lipopolysaccharide; MPTP, 1-methyl-4-phenyl-1,2,3,6-tetrahydropyridine; NSG, NOD scid gamma mouse; OGD, Oxygen glucose deprivation; PA/G, Gelatin coated polyamide; Pcna, Proliferating cell nuclear antigen; POR, Poor ovarian responder; SC, Subcutaneous; TAT, Tyrosine aminotransferase, VEGF, Vascular endothelial growth factor.

into the matrix and expressed the stromal marker vimentin and endothelial marker CD31, demarcated by cytokeratin expressing epithelial cells (Miyazaki and Maruyama, 2014). Transplantation of these uterine constructs into partially excised uteri, regenerated endometrial tissue which differentiated into desmin-expressing decidual-cells and achieved pregnancies (Miyazaki and Maruyama, 2014). There was evidence of fetal development, however, no evidence of placentation at the graft site. In another approach to reconstitute native, functional endometrium, a rat GFP^+ endometrial epithelial cell-sheet was layered on two layers of adherent GFP^+ endometrial stroma cell-sheets and transplanted into a full thickness endometrial defect in a rat model (Kuramoto et al., 2018). Full thickness endometrium with luminal and glandular epithelium and stromal compartments was generated and pregnancy established on the regenerated endometrium with placentation and fetal heart movements detected. Preliminary results using similar approaches in a larger pig model have commenced (Campo et al., 2017). Using human endometrial Side Population cells including stromal cells demonstrated integration of $vimentin^+$ and $cytokeratin^+$ cells in the decellularized pig uterus. In an *in vitro* model, endometrial stromal cells, which likely contained a small population of eMSC, repopulated decellularized human endometrial substrates and proliferated in the scaffold (Olalekan et al., 2017). Most importantly, the cells underwent decidual changes upon stimulation with an estrogen and progesterone treatment protocol mimicking the human 28-day menstrual cycle. The infiltrated cells expressed estrogen and progesterone receptors, and secreted prolactin and IGFBP-1, markers of decidualization. These recent approaches indicate the feasibility of using eMSC and endometrial stromal fibroblasts as cell sources for regenerative medicine in uterine biology.

Pelvic Organ Prolapse

The potential of eMSC in regenerative or reparative medicine has been explored for a common women's gynecological disorder, pelvic organ prolapse (Ulrich et al., 2013; Emmerson and Gargett, 2016; Gargett et al., 2019; Mukherjee et al., 2019a). An autologous approach has been investigated and tissue engineering constructs comprising eMSC and novel non-degradable mesh (Ulrich et al., 2012), degradable nanofiber mesh (Mukherjee et al., 2019b), and 3D bioprinted mesh/eMSC (Paul et al., 2019) have been explored in both rodent and large animal ovine models (Emmerson et al., 2019). In these studies, xenogeneic human eMSC delivered on a mesh in a model of subcutaneous wound repair, exerted a paracrine effect. DiO- or mCherry lentiviral-labeled eMSC implanted on a non-degradable polyamide/gelatin composite mesh, were detectable for 1–2 weeks in immunocompromised rats and mice (Ulrich et al., 2014a; Darzi et al., 2018) and up to 3 days in immune intact mice (Darzi et al., 2018). Despite this, the eMSC exerted marked paracrine effects, promoting early neovascularization, an anti-inflammatory response and supporting the deposition of physiological, crimped collagen rather than scar (Edwards et al., 2015). These changes induced by eMSC resulted in a clinically relevant outcome, a reduction in the stiffness of the mesh/tissue complex in the long term (90 days) (Ulrich et al., 2014a). In studies using degradable PLACL nanofiber/gelatin (Mukherjee et al., 2019b) or 3D printed PCL scaffolds (Paul et al., 2019), m-Cherry-labeled eMSC again reduced the foreign body response, slowed mesh degradation and induced endogenous cell influx into the scaffold *in vivo*, thereby promoting tissue repair. These are outcomes of clinically desired responses, particularly for application in pelvic organ prolapse repair surgery.

To more accurately model the translational approach to be used clinically, autologous, adventitial perivascular ovine eMSC (**Table 2**), labeled with paramagnetic nanoparticles conjugated to FITC were surgically delivered with non-degradable polyamide mesh in an ovine model of vaginal repair (Emmerson et al., 2019). A two-step procedure was required, firstly implanting the mesh followed by separate delivery of the eMSC in a collagen gel onto the mesh and crosslinking with blue light *in situ*, followed by suturing. Approximately 10–20% of the autologous eMSC survived 30 days following implantation. As observed in the rodent models, the eMSC modulated the inflammatory response and reduced myofibroblast accumulation around mesh filaments. Important lessons were learnt using this large animal model, particularly related to the separate delivery of eMSC and

mesh. This modification to our protocol prevented one of the major adverse events associated with transvaginal mesh use, mesh exposure, that had resulted in the banning of polypropylene vaginal mesh by the FDA. This could not have been predicted from using mouse models of skin wound repair and shows the importance of closely recapitulating the clinical condition in large animal models before clinical translation of an MSC-based therapy.

Other Reparative Applications of eMSC

Human and monkey endometrial stromal fibroblasts transdifferentiated into cells with morphological, chemical and electrical activity of dopaminergic neurons have been investigated in several animal models. They engrafted and migrated to site of lesion in chemically induced mouse and green monkey (**Table 2**) models of Parkinson disease, differentiated to neuronal-like cells resulting in increased striatal dopamine and dopamine metabolite concentrations (Wolff et al., 2011, 2015). However, further studies on clinical outcomes such as the behavioral studies are warranted. Type 1 diabetes mellitus is a clinical condition which can benefit from islet-based cell transplantation. The plasticity of human endometrial stromal fibroblasts has been utilized to generate insulin secreting cells. These differentiated cells produced human insulin, decreased blood glucose levels and minimized diabetes-associated complications such as weight loss, dehydration, cataracts, delayed wound healing and sedative behavior in a mouse model of diabetes mellitus (Li et al., 2010; Santamaria et al., 2011). These differentiated cells were more efficient in a 3D construct, and were resistant to oxidative stress, normalized glucose levels and prolonged survival of the recipient mice (Li et al., 2010).

Both eMSC and endometrial fibroblasts show potential in regenerative and reparative medicine, with early studies suggesting capability in tissue engineering approaches using decellularized tissues or biomaterial scaffolds to deliver the cells to tissues requiring regeneration. Mode of action may be both cellular integration and paracrine.

MenSC in Regenerative or Reparative Medicine

MenSC are also an attractive cell source with potential for clinical application. MenSC have been assessed in various preclinical animal models of disease and in regenerative and reparative medicine (**Table 5**). Here, we will briefly review these studies.

Cardio-Reparative Potential

One of the first studies proposing the prospective use of MenSC differentiation in the clinical setting assessed the ability of MenSC to improve cardiac function after myocardial infarction. MenSC transplanted into a rat model ameliorated left ventricular systolic function and diminished fibrotic areas (Hida et al., 2008). *In vivo* differentiation of MenSC to cardiomyocytes in infarcted areas was demonstrated in the absence of recipient and donor cell fusion. Similar outcomes were obtained following MenSC injection into the ischemic zones of an immunocompetent rat model of myocardial infarction (Jiang et al., 2013). The therapy resulted in significant preservation of myocardial viability in the infarct zone and improvement in cardiac function, effects mostly attributed to the paracrine activity of MenSCs rather than transdifferentiation to myocardial cells.

Hepato-Reparative Potential

MenSC's ability to differentiate toward hepatic cells *in vitro* (Khanjani et al., 2015) raised the possibility of MenSC application for treating liver disorders. Both MenSC and bmMSC, with the capacity to differentiate toward hepatocytes, prolonged the survival of mice with acute liver failure. MenSC localized in the damaged liver within 2 h following transplantation. This treatment also improved liver histology and architecture within weeks after MenSC injection. The MenSC therapy reduced serum levels of liver enzymes and metabolites (AST, ALT, urea, and total bilirubin) in the mice. Reduced hepatic degeneration, inflammatory cell infiltrate and collagen fiber deposition and improved glycogen storage were observed following MenSC administration (Fathi-Kazerooni et al., 2017), indicating the protective and reparative role of MenSC in acute liver damage.

It is likely that MenSC improvement of liver function is due to paracrine activity rather than differentiating into hepatocyte-like cells in improving liver fibrosis. In a murine model (Chen et al., 2017b), few MenSC differentiated into hepatocyte-like cells, suggesting the complexity of the *in vivo* milieu influencing MenSC differentiation. MenSC migrated to the fibrotic area, reduced already deposited collagen and significantly improved liver function. Nevertheless, end-stage liver fibrosis with few healthy hepatocytes may be a poor environment for survival of MenSC that also diminishes their ability to potentially differentiate into hepatocyte-like cells. This questions the utility of MenSC as a therapeutic modality to patients with cirrhosis. Further investigation in first reducing fibrosis in cirrhosis using MenSCs before attempting to regenerate hepatic tissue is warranted.

Ovarian Function and Reserve

The reparative capacities of MenSCs was exploited to treat premature ovarian failure (POF) in mouse/rat models (Liu et al., 2014; Feng et al., 2019; Manshadi et al., 2019; Yan et al., 2019). Intra-ovarian or intravenous injection of MenSCs reduced apoptosis and restored ovarian function, shown by expression of the ovarian markers, follicle-stimulating hormone receptor (Fshr), inhibin α/β, anti-Müllerian hormone (Amh), Ddx4 and Vegfa, and rising plasma levels of the ovarian hormones, estrogen and progesterone. Increased numbers of primary, mature and total ovarian follicle numbers were observed. DiI-labeled MenSC localized to GCs of immature ovarian follicles (Manshadi et al., 2019). Microarray analysis revealed greater similarity between mRNA expression patterns in the ovarian cells posttransplantation and human ovarian tissue than the pre-transplantation pattern in MenSCs, suggesting transdifferentiation into ovarian cells or fusion of MenSCs with murine cells (Liu et al., 2014). More importantly, mated mice grafted with MenSCs had more live births indicating the potential of MenSC to repair ovarian function (Feng et al., 2019). Mechanistic analyses revealed that mice treated with MenSCs improved ovarian microenvironment homeostasis through

regulation of the ECM-dependent FAK/AKT signaling pathway (Feng et al., 2019). Similarly, *in vitro*, MenSC increased indices of mouse follicular growth, including survival rate, diameter and antrum formation, *Bmp15* and *Gdf9* expression and maturation rate in a 3D culture system. Secreted progesterone and estradiol increased in co-cultured murine preantral follicles and human MenSC implying a supportive role of MenSCs in follicle development, growth and maturation (Rajabi et al., 2018). In a recent clinical trial in 15 women, intraovarian injection of autologous MenSC in poor ovarian responders increased clinical pregnancy and live births (Zafardoust et al., 2020).

Collectively, MenSC impact on ovarian follicle development through paracrine signaling and potentially transdifferentiation highlights the possible utility of MenSC for ovarian function restoration in patients with POI and also fertility preservation approaches using *in vitro* follicle maturation. These pre-clinical findings and an early phase clinical trial warrant further investigation of the efficacy of MenSC for treatment of POI.

Lung Injury

MenSCs have been used to treat LPS-induced acute lung injury in a murine model (Xiang et al., 2017). Intravenously administered MenSC localized to the injured area and demonstrated repair of lung tissue morphology, improved lung microvascular permeability, and reduced clinical symptoms. MenSC exerted an anti-inflammatory effect, reducing lung inflammatory cells and IL-1β, whereas IL-10 was increased in both lung tissue and broncho-alveolar lavage fluid. Keratinocyte growth factor, which plays a major part in repair of damaged lung was increased, and together with decreased caspase-3 expression further supported the protective impact of the infused MenSC. It is likely that the reparative effect of MenSC can be ascribed to cell-cell contact and/or their paracrine function. Similarly, MenSC injection improved acute lung injury scores through normalization of lung O_2 pressure. MenSC reduced neutrophil frequency, myeloperoxidase activity, and pro-inflammatory cytokines levels in bronchoalveolar fluid (Ren et al., 2018). MenSC injection also reduced inflammation and collagen deposition in a mouse model of bleomycin-induced pulmonary fibrosis (Zhao et al., 2018b). In summary, in acute lung injury and pulmonary fibrosis models, MenSC suppressed innate immune cells, lowered pro-inflammatory cytokines and increased IL-10 in lung, and lung function and morphology were restored, effects likely mediated by paracrine mechanisms.

Skin Wound Repair

The reparative potential of MenSCs in a murine excisional wound splinting model (Cuenca et al., 2018) showed that intradermal injection of MenSCs into a persistent wound improved healing and increased angiogenesis. Two pro-angiogenic genes, *Il-8* and *Vegf* were upregulated in the wounds and there was maturation of wound vasculature. The MenSC-injected group also showed high density, and well-organized collagen fibers, suggesting MenSC have potential application for wound healing and cutaneous regeneration. MenSC seeded on an amniotic membrane improved wound closure in a rat excisional wound defect model (Farzamfar et al., 2018). *In vitro*, MenSCs differentiated into keratinocyte-like cells (Akhavan-Tavakoli et al., 2017), an effect potentiated in 3D culture (Fard et al., 2018) or in a biomimetic nanofibrous scaffold, two approaches that increased the wound healing capacity of MenSC (Arasteh et al., 2018). Such data imply the importance of ECM in the differentiation of MenSC into keratinocyte-like cells and further highlight the value of MenSCs as a potential therapeutic in clinical settings.

Intrauterine Adhesions and Endometrial Decidualization

The reparative potential of MenSC has been explored in a mouse model of endometrial injury and intrauterine adhesion (Zhang et al., 2016), where the endometrium is partially replaced by fibrotic scar tissue (Gargett and Ye, 2012). Intravascular injection of MenSCs rapidly repaired the injury by increasing microvessel density, resulting in increased endometrial thickness. Fertility was restored with a higher conception rate and larger numbers of implanted embryos compared to untreated controls. MenSC-conditioned medium promoted angiogenesis *in vitro* by activating Akt and Erk pathways and overexpression of genes involved in angiogenesis. Autologous cultured MenSCs administered to 7 women with severe Asherman's syndrome, where intrauterine adhesions have replaced the endometrium, increased endometrial thickness to 7 mm in five of seven patients (Tan et al., 2016). Of the four patients who had undergone embryo transfer, two conceived and one had a spontaneous pregnancy, suggesting that MenSC reduced fibrosis and promoted functional endometrial repair of the injured endometrium.

Neuroprotective Potential

The application of MenSC, which can differentiate toward glia and neural cells *in vitro* (**Table 3**), for neuroprotection is an emerging research area. In an adult rat stroke model, intracerebral or intravenous MenSC transplantation ameliorated motor and behavioral symptoms and diminished neuronal cell death (Borlongan et al., 2010). Implantation of MenSC-seeded gelatin-based scaffolds in rats with sciatic nerve defect improved sciatic nerve function and reduced and gastrocnemius muscle loss to a similar level as bridging the nerve defect with autologous resected nerve segment (Farzamfar et al., 2017). MenSC also improved cognition function and memory defects in a mouse APP/PS1 model of Alzheimer's disease (Zhao et al., 2018a). In the hippocampus, more activated microglia were observed which had altered function as less TNF and IL-1β were produced. These activated microglia had higher expression of insulin degrading enzyme and neprilysin, proteases responsible for Aβ plaque degradation. These results highlight the potential of MenSC in improvement of the pathological and cognitive defects in pre-clinical models of Alzheimer disease.

Other Potential Reparative Applications of MenSC

The regenerative ability of MenSC to promote muscle regeneration was demonstrated in a murine Mdx model of Duchenne muscular dystrophy, where skeletal muscles

degenerate from lack of dystrophin. GFP-labeled MenSC were injected intramuscularly, where they fused with murine myoctes and restored dystrophin in the sarcolemma of muscle fibers (Cui et al., 2007). Similarly, MenSC fuse with myocytes in co-culture and subsequently express dystrophin.

MenSC can stimulate the regeneration of pancreatic islet β cells in a murine model (Wu et al., 2014). MenSC transplantation enhanced differentiation of endogenous endocrine progenitor cells into β-cells resulting in more normal islet morphology and structure, with improved hyperglycemia, glucose tolerance, insulin levels, body weight and survival rate. Although not investigated inflammation reduced by MenSC may have also contributed to the observed results.

In summary, MenSC show potential in regenerative medicine, with early studies suggesting capacity to influence tissue regeneration by paracrine mechanism, fusion and enhancement of endogenous tissue stem cell function.

Extracellular Vesicles as a Key Player of MenSC Reparative Function

Increasingly, the effects of MSC are attributed to their ability to secret extracellular vesicles (EVs), including exosomes (Murray and Krasnodembskaya, 2019). MenSCs also produce functionally active EVs that are homogeneous in size (30–170 nM) and express CD81, CD63, and TSG101 (Dalirfardouei et al., 2018). MenSC-EVs contain 895 proteins involved in complement activation, antigen processing and presentation, regulation of adaptive and innate immune responses, apoptosis control and signaling pathways (Marinaro et al., 2019). Licensing MenSCs with pro-inflammatory cytokines such as IFN-γ modulates EV protein cargo, increasing proteins involved in antigen processing and presentation, and miRNA content. MenSC-derived EVs also express high levels of ICAM-1, angiopoetin-2, angiogenin, osteoprotegerin, IL-6, and IL-8. In a mouse model of fulminant hepatic failure, pre-treatment with MenSC-exosomes showed higher survival rates, with reduced serum liver enzymes and pro-inflammatory cytokines, and well-organized hepatic structure (Chen et al., 2017a). Hepatocyte apoptosis and proliferation of liver macrophages were reduced. In a rat model of diabetes, MenSC-derived EVs were tracked in, and enhanced the number of pancreatic β cell islets and raised serum insulin, without impact on non-fasting blood glucose (Mahdipour et al., 2019). MenSC-derived exosomes impacted wound healing in a mouse model of diabetes through M2 macrophage polarization, induction of neoangiogenesis and re-epithelialization (Dalirfardouei et al., 2019).

In summary, the beneficial impacts of MenSC treatment are mostly attributed to the anti-inflammatory properties of MenSC-derived EVs. In some settings the modulatory effects of EVs were superior to the use of intact MenSC. Therapeutic utilization of MenSC-EVs might be advantageous over whole cells by improving the therapeutic index, by introduction of less protein, avoidance of allo- and xenogeneic reactions and their off-the-shelf potential. Nonetheless, their nano-scale size results in rapid clearance from the body necessitating repeated administration in large quantities, although therapy targeted to damaged tissue may overcome this potential challenge. Taken together, MenSC may qualify as a promising therapeutic cell type for future clinical applications. Nevertheless, as with any other treatment modality, the safety of MenSC in the clinical settings needs addressing.

CLINICAL TRANSLATION OF eMSC AND MenSC

There are hundreds of clinical trials using MSC either in progress or completed and thousands of patients have been treated. Apart from several spectacular successes the overall results of these clinical trials have been underwhelming (Prockop et al., 2014). MSC were rushed to the clinic before many issues were resolved, including their mechanism of action and the heterogeneity of MSC products. Heterogeneity arises from variability in isolation methods and during culture expansion (Prockop et al., 2014). Thawing cryostored MSC induces cell injury lasting up to 24 h (Moll et al., 2016), suggesting a lack of fitness for purpose of culture-expanded, thawed MSC (Galipeau and Sensebe, 2018). There is also a need for potency assays based on MSC mechanism of action *in vivo* (Prockop et al., 2014; Galipeau and Sensebe, 2018). These are important considerations for investigators seeking to translate eMSC and MenSC as cell-based therapies.

Serum Free Culture Protocols

The clinical translation of human MSC depends upon largescale production of a homogeneous cell population that is safe and reproducible. Factors contributing to a heterogeneous population are isolation protocol, culture medium and culture environment. The discovery of a single surface marker for human eMSC, SUSD2, has enabled relatively easy purification of a homogeneous starting population. Choice of culture medium and environment majorly influence the generation of large scale homogeneous eMSC and MSC from other sources utilized for clinical use. Until recently, MSC including eMSC have been cultured in fetal calf serum (FCS) containing medium in 20% O_2 environment (Schwab and Gargett, 2007). FCS provides extracellular matrix, growth factors, hormones and many other nutrients promoting cell grow and proliferation (Cantor, 2019). However, FCS is not a defined source of nutrients with batch to batch variation and presence of unknown components that contribute to heterogeneity (Shahdadfar et al., 2005). Some FCS components induce differentiation, reducing the population of potent MSC (Shahdadfar et al., 2005; Labome, 2012). The use of FCS for *in vitro* MSC expansion also carries a rare risk of xeno-immunization and zoonotic transmission (Hawkes, 2015). Defined medium devoid of FCS is required to produce homogeneous, undifferentiated potent MSC using good manufacturing practices (GMP) for safe use in humans. Replacing FCS with human products including human serum, platelet-poor or -rich plasma and platelet lysate have been used (Dessels et al., 2016). Although more physiological, these alternatives have similar composition variability as FCS and may also induce differentiation, resulting in inconsistent, non-reproducible cell products. Gene profiling of primary $CD140b^{+}CD146^{+}$ eMSC showed distinct differences

to endometrial stromal fibroblasts ($CD140b^+CD146^-$) (Spitzer et al., 2012) and extensive eMSC cultivation in FCS medium in 20% O_2 led down-regulation of 81% of eMSC-related genes and up-regulation of 55% of fibroblast-associated genes, verifying culture-induced spontaneous differentiation and reduced functionality (Barragan et al., 2016; Gargett and Gurung, 2016). A defined medium and physiological O_2 environment that generates homogeneous undifferentiated eMSC which are efficacious, safe and reproducible under cGMP guidelines would be appropriate for clinical applications such as pelvic organ prolapse and Asherman's syndrome.

While various serum-free media are available for culturing human MSC, vast research shows that "one size does not fit all," indicting the need to identify the specific niche environment for eMSC. Indeed, eMSC attachment and growth were best supported by a fibronectin matrix in xeno-free DMEM supplemented with FGF2 and EGF (SFM) in 5% O_2, compared to other serum-free commercial media, Lonza-TP-SF and Stem Pro-XF giving similar growth rates to serum-containing medium (Rajaraman et al., 2013). Despite this, like all MSC, the expanded $SUSD2^+$ eMSC spontaneously differentiated to non-clonogenic stromal fibroblasts with loss of the eMSC surface markers SUSD2, CD140b, and CD146 indicating cellular heterogeneity and decreased potency (Gurung et al., 2018b).

Small Molecules to Maintain Undifferentiated eMSC State

Understanding the intrinsic signaling pathways involved in stem-cell fate, self-renewal, proliferation and differentiation, and manipulating them using chemical approaches enables generation of homogeneous potent cells for cell-based therapies (Xu et al., 2008; Li and Ding, 2010). Chemically defined media needs optimization for each cell type using relative cell-growth as a guide. Augmenting SFM with a small molecule (A83-01) targeting the transforming growth factor-β1 receptor (TGFβR) signaling pathway involved in cellular differentiation and enhanced cell growth, mitigated loss of undifferentiated, clonogenic eMSC, overcoming this major bottleneck for clinical translation of eMSC (Gurung et al., 2015, 2018b). A83-01 maintained ISCT properties of eMSC, promoted proliferation of homogeneous $SUSD2^+$ eMSC and prevented apoptosis and senescence. Correlation between SUSD2 expression and TGFβ-induced senescence and cell death was also demonstrated in cancer cells using small interfering RNA and TGFβ (Zhang et al., 2017). The potency of A83-01-treated eMSC was further validated by transcriptome profiling, providing insight into the biological nature of eMSC and the probable therapeutic mode of action (Gurung et al., 2015, 2018b). The complexity of TGFβR signaling in eMSC was defined through identification of ∼1200 differentially regulated genes by A83-01 involved in anti-inflammatory responses, angiogenesis, cell migration and proliferation, collagen fibril and extracellular matrix organization, anti-fibrosis and anti-apoptosis (Gurung et al., 2018b). The potency of A83-01-treated eMSC was established by demonstrating increased expression of recently described bmMSC potency genes; *TWIST1, TWIST2, JAG1, LIFR,* and *SLIT2* (Samsonraj et al., 2015; Gurung et al., 2018b). These and our previous findings also highlighted the need for additional surface markers to identify potent MSC and for specific tissues (Rajaraman et al., 2013; Gurung et al., 2015, 2018b; Samsonraj et al., 2015).

The reparative and regenerative capacity of MSC is mainly driven by the secretome or EVs that promote angiogenesis, ECM regulation, immunoregulation and antimicrobial activity. Transcriptional profiling of A83-01-treated eMSC revealed important cellular secretome-regulating genes involved in angiogenesis, anti-fibrosis and immunomodulation; *HGF, VCAM1, PGF, HPSE, SOD3, SOD2,* and *SOD1*. Secretome analysis of the conditioned medium supported transcriptional findings with increased HGF, PTX3, CCL2, IGFBP-2, CCL2, GM-CSF, IGFBP-2, DKK-1, and EGF and decreased THBS1, EMMPRIN, and OPN. HLA-G, a nonclassical MHC-I molecule, and immunomodulatory cytokine functioning at the maternal-fetal interface and some immune privileged adult tissues, was ubiquitously expressed in A83-01-treated eMSC, together with *HLA-A-C* and *HLA-E* and *F,* but not *HLA-II,* an indicator of good tolerance for allogeneic transplantation. HLA-G has been identified in several MSC types (Selmani et al., 2008; Yang et al., 2012; Naji et al., 2013; Ding et al., 2016), and together with other MHC-I molecules correlates directly to their immunosuppressive effect (Yang et al., 2012). These molecules are surrogate prognostic factors used to monitor disease progression or efficacy of transplantation (Nasef et al., 2007). Likewise, RNA-sequencing revealed the first evidence of the ability of A83-01-treated eMSC to secrete exosomes (Gurung et al., 2018b), that may function in their paracrine action. Further transcriptome analysis showed evidence of the antimicrobial potential of A83-01-treated eMSC partially through the secretion of antimicrobial peptides (AMPs), chromogranin B, liver enriched AMP-2 and secretogranin II (Gurung et al., 2018b). Taken together, these findings signify the clinical potential of eMSC and open avenues to examine their use in regenerative medicine as an "off the shelf" as well as cell-derived therapy.

Safety of eMSC

Spontaneous transformation of MSC is a potential concern for therapeutics, although thorough investigations of earlier studies showed cellular-cross contamination. To date, no cancer due to primary-culture expanded MSC, has been diagnosed in human clinical trials. Nonetheless, the risk of such potential events should be investigated by utilizing surrogate assays, such as telomere length, pluripotency genes, tumor formation, genomic instability, karyotyping and DNA damage response through transcriptomics and *in vitro* and *in vivo* assays. A83-01-expanded eMSC promote telomere stability through *TERC* (Telomerase RNA Component), *TERF1* and *2* (Telomeric Repeat Binding Factors 1 and 2), *TINF2* (TERF1 Interacting Nuclear Factor 2), *TERF2IP* (TERF2 Interacting Protein), *TNKS* (Tankyrase) and *POT1* (Protection of Telomere 1) which collaborate to regulate telomere length and protect cells from chromosomal damage (Gurung et al., 2018b). Using our isolation and expansion protocol, $SUSD2^+$ eMSC do not express pluripotency-associated genes, unlike hESC and iPSCs with unlimited growth and

tumorigenic potential (Gurung et al., 2015; Gurung et al., 2018b). Although SFM/5%O_2/A83-01 culture-expanded eMSC survived longer *in vivo* than culture in FCS/20%O_2 medium, their lifespan was limited and tumors were not detected (Gurung et al., 2018a). Considerable progress has been made in developing expansion protocols for perivascular eMSC showing promise in their safety profile.

Safety of MenSC

Donor Age

Age of donor affects many of MSC functions; cytokine secretion, paracrine activity, anti-apoptotic mechanisms, hematopoietic stem cell supporting capacity and proliferation rate, all of which reduce with aging (Alt et al., 2012). However, the proliferative capacity of MenSC does not appear donor-dependent in individuals aged up to 40 years, but MenSC from older donors had a weaker potential for long-term passaging (Chen et al., 2015).

Passage Number

Menstrual blood can be processed up to 72 h after collection without significant change in properties of the plastic adherent MenSC (Liu et al., 2018). As mentioned, culture expansion of MSC is required to obtain enough cells for preclinical or clinical applications. The proliferation rate of MenSC gradually decreased with increasing passage number (Chen et al., 2015), with highly passaged cells increasing in size, losing fibroblastic morphology and appearing senescent. Important signaling molecules, including MAPK, molecules involved in carcinogenesis (PPAR and P53) and immune responses changed with MenSC passage number. Passaging induces aging of MenSC and alters genes involved in transcriptional regulation, stress response, cell proliferation, development and apoptosis, and karyotype at high passages (P20). MenSC underwent aging after 45 PD (Zemel'ko et al., 2011), but even after 68 PDs of a single MenSC sample, maintained a normal karyotype and did not develop tumors (Meng et al., 2007). Multiplex ligation-dependent probe amplification of MenSC genomic DNA at passages two and twelve showed that MenSC maintained a diploid phenotype without chromosomal aberrations (Khanmohammadi et al., 2014), consistent with other reports of a normal female karyotype without chromosomal aberrations using standard cytogenetics at passage 12 (Cui et al., 2007; Patel et al., 2008). Pluripotency protein expression reduced during passaging of MenSCs, from 97.5% OCT-4^+ cells at the first passage to 19.4% at passage twelve (Khanmohammadi et al., 2014), important for clinical translation. These observations warrant standardization of MenSC isolation and culture protocols for clinical applications.

Safety of MenSC

The risk of tumorigenicity, toxicity, autoimmunity, and/or endometriosis following MenSCs injection are crucial safety issues to be established before using MenSC in the clinic. Angiogenic activity of MenSC, raises concern of promoting tumor progression. In a C6 model of rat glioma MenSCs not only failed to stimulate, but also inhibited tumor growth (Han et al., 2009). MenSCs showed no tumor formation in a xenograft rat model of brain stroke with no concurrent immunosuppression (Borlongan et al., 2010). Several acute and chronic tumorigenicity/toxicity experiments in immunocompromised mice using MenSC in clinically relevant doses showed no toxic effects on body and organ weight, biochemistry following necropsy or histopathological changes at injection sites (Bockeria et al., 2013). Concerns of ectopic bone formation on clinical application of bmMSC, are mitigated by the weak osteogenic differentiation capacity of MenSC and could be advantageous for clinical translation.

The next step prior to clinical development of MenSC is to undertake cell tracking of reliably labeled MenSC *in vivo* and determining their mechanism of action. Also important is the development of relevant large animal pre-clinical models of the targeted disease for evaluating MenSC, to improve the likelihood of translating rodent studies into clinical practice. In 2008, four multiple sclerosis patients were injected both intrathecally and intravenously with *in vitro* expanded allogeneic MenSC. Functional and radiological evaluations demonstrated no disease status progression and none of the treated patients showed allergic reactions or ectopic tissue formation (Zhong et al., 2009). No adverse effects were observed in the patients 4 years later in the last reported follow up (Bockeria et al., 2013). Clearly more investigation is required to determine the safety of MenSC for clinical translation.

Identification of eMSC potency makers and serum-free expansion media have enabled gene sequencing of the primary cells and their expanded progeny (Spitzer et al., 2012; Barragan et al., 2016; Gurung et al., 2018b). Comprehensive RNA-seq analysis of SFM/5%O2/A83-01-treated eMSC described the gene expression profiles and uncovered vast range of regulatory pathways which not only aided in understating their mechanism of action but also suggested their potential for broader applications. Much progress are made in understanding the *in vitro* and *in vivo* roles of eMSC, setting a strong foundation for clinical application. Further research to understand and validate eMSC's potential through careful titration of assays and selection of animal models relative to their potential use is vital.

SUMMARY

eMSC and MenSC have fulfilled the ISCT criteria for MSC, but thus far, no comparative study has been performed to delineate the potential link between these two MSC types. Nonetheless, considering that eMSC comprise a small cell population residing around endometrial blood vessels while MenSC represent majority of endometrial stromal cells, it seems that the latter is more heterogeneous. Although multi-differentiation capacity of eMSC and MenSC has been documented *in vitro*, the reparative properties of these cells *in vivo* seem to stem from their paracrine rather than differentiation capacity and integration into tissue. Akin to MSC from other sources, MenSC and eMSC have profound immunomodulatory effects and attenuate inflammation, although there are distinct differences highlighting their unique tissue of origin. eMSC and MenSC have been evaluated in numerous preclinical animal models of disease showing substantial angiogenic, anti-fibrotic and anti-inflammatory effects although it is too early to draw a firm

conclusion on the same impacts in clinical settings. Culture protocols have been developed that maintain perivascular eMSC in the undifferentiated state during culture expansion, which now need testing in animal models to determine if this more homogeneous MSC product further improves *in vivo* angiogenesis, antifibrosis, anti-inflammatory and prohealing effects. Both eMSC, easily procured without anesthetic, and non-invasively obtained MenSC, imbued with both reparative and immunomodulatory properties are likely promising therapeutic cell types for future clinical applications. Nevertheless, multiple variables need to be standardized particularly heterogeneity of MenSC and the safety and therapeutic potency of eMSC and MenSC in clinical settings needs to be extensively addressed.

AUTHOR CONTRIBUTIONS

CG and A-HZ contributed to the conception and review design and revised the manuscript. MB, SG, SD, SN, SK, A-HZ, and CG wrote sections of the manuscript. All authors contributed to the article and approved the submitted version.

FUNDING

This work was supported by the National Health and Medical Research Council (NHMRC) of Australia Project Grants (ID 1159677 to CG) and Investigator Grant (ID 1173882 to CG) and the Victorian Government's Operational Infrastructure Support Program, and Avicenna Research Institute (ARI) Project Grants (ID 960110-029 to SK).

ACKNOWLEDGMENTS

We are sincerely thankful to Dr. Maryam Tavakoli and Samira Hosseini for their assistance in providing related manuscripts and to Zahra Saffarian for office work.

REFERENCES

Akhavan-Tavakoli, M., Fard, M., Khanjani, S., Zare, S., Edalatkhah, H., Mehrabani, D., et al. (2017). In vitro differentiation of menstrual blood stem cells into keratinocytes: a potential approach for management of wound healing. *Biologicals* 48, 66–73. doi: 10.1016/j.biologicals.2017.05.005

Alcayaga-Miranda, F., Cuenca, J., Luz-Crawford, P., Aguila-Diaz, C., Fernandez, A., Figueroa, F. E., et al. (2015a). Characterization of menstrual stem cells: angiogenic effect, migration and hematopoietic stem cell support in comparison with bone marrow mesenchymal stem cells. *Stem Cell Res. Ther.* 6, 32.

Alcayaga-Miranda, F., Cuenca, J., Martin, A., Contreras, L., Figueroa, F. E., and Khoury, M. (2015b). Combination therapy of menstrual derived mesenchymal stem cells and antibiotics ameliorates survival in sepsis. *Stem Cell Res. Ther.* 6:199.

Aleahmad, M., Ghanavatinejad, A., Bozorgmehr, M., Shokri, M. R., Nikoo, S., Tavakoli, M., et al. (2018). Menstrual Blood-Derived Stromal Stem Cells Augment CD4+ T Cells Proliferation. *Avicenna J. Med. Biotechnol.* 10, 183–191.

Allavena, P., Piemonti, L., Longoni, D., Bernasconi, S., Stoppacciaro, A., Ruco, L., et al. (1998). IL-10 prevents the differentiation of monocytes to dendritic cells but promotes their maturation to macrophages. *Eur. J. Immunol.* 28, 359–369. doi: 10.1002/(sici)1521-4141(199801)28:01<359::aid-immu359>3.0.co;2-4

Allickson, J. G., Sanchez, A. M., Yefimenko, N., Borlongan, C. V., and Sanberg, P. R. (2011). Recent studies assessing the proliferative capability of a novel adult stem cell identified in menstrual blood. *Open Stem Cell J.* 3:4. doi: 10.2174/1876893801103010004

Alt, E. U., Senst, C., Murthy, S. N., Slakey, D. P., Dupin, C. L., Chaffin, A. E., et al. (2012). Aging alters tissue resident mesenchymal stem cell properties. *Stem Cell Res.* 8, 215–225. doi: 10.1016/j.scr.2011.11.002

Arasteh, S., Katebifar, S., Shirazi, R., and Kazemnejad, S. (2018). Differentiation of Menstrual Blood Stem Cells into Keratinocyte-Like Cells on Bilayer Nanofibrous Scaffold. *Methods Mol. Biol.* 2125, 129–156. doi: 10.1007/7651_2018_193

Augello, A., Tasso, R., Negrini, S. M., Amateis, A., Indiveri, F., Cancedda, R., et al. (2005). Bone marrow mesenchymal progenitor cells inhibit lymphocyte proliferation by activation of the programmed death 1 pathway. *Eur. J. Immunol.* 35, 1482–1490. doi: 10.1002/eji.200425405

Azedi, F., Kazemnejad, S., Zarnani, A. H., Behzadi, G., Vasei, M., Khanmohammadi, M., et al. (2014). Differentiation potential of menstrual blood- versus bone marrow-stem cells into glial-like cells. *Cell Biol. Int.* 38, 615–624. doi: 10.1002/cbin.10245

Azedi, F., Kazemnejad, S., Zarnani, A. H., Soleimani, M., Shojaei, A., and Arasteh, S. (2017). Comparative capability of menstrual blood versus bone marrow derived stem cells in neural differentiation. *Mol. Biol. Rep.* 44, 169–182. doi: 10.1007/s11033-016-4095-7

Barragan, F., Irwin, J. C., Balayan, S., Erikson, D. W., Chen, J. C., Houshdaran, S., et al. (2016). Human Endometrial Fibroblasts Derived from Mesenchymal Progenitors Inherit Progesterone Resistance and Acquire an Inflammatory Phenotype in the Endometrial Niche in Endometriosis. *Biol. Reprod.* 94:118.

Bartholomew, A., Sturgeon, C., Siatskas, M., Ferrer, K., McIntosh, K., Patil, S., et al. (2002). Mesenchymal stem cells suppress lymphocyte proliferation in vitro and prolong skin graft survival in vivo. *Exp. Hematol.* 30, 42–48. doi: 10.1016/s0301-472x(01)00769-x

Bianco, P., Cao, X., Frenette, P. S., Mao, J. J., Robey, P. G., Simmons, P. J., et al. (2013). The meaning, the sense and the significance: translating the science of mesenchymal stem cells into medicine. *Nat. Med.* 19, 35–42. doi: 10.1038/nm.3028

Bockeria, L., Bogin, V., Bockeria, O., Le, T., Alekyan, B., Woods, E. J., et al. (2013). Endometrial regenerative cells for treatment of heart failure: a new stem cell enters the clinic. *J. Transl. Med.* 11, 56. doi: 10.1186/1479-5876-11-56

Bodek, G., Bukowska, J., Wisniewska, J., and Ziecik, A. J. (2015). Evidence for the presence of stem/progenitor cells in porcine endometrium. *Mol. Reprod. Dev.* 82, 182–190. doi: 10.1002/mrd.22459

Borlongan, C. V., Kaneko, Y., Maki, M., Yu, S. J., Ali, M., Allickson, J. G., et al. (2010). Menstrual blood cells display stem cell-like phenotypic markers and exert neuroprotection following transplantation in experimental stroke. *Stem Cells Dev.* 19, 439–452. doi: 10.1089/scd.2009.0340

Bourin, P., Bunnell, B. A., Casteilla, L., Dominici, M., Katz, A. J., March, K. L., et al. (2013). Stromal cells from the adipose tissue-derived stromal vascular fraction and culture expanded adipose tissue-derived stromal/stem cells: a joint statement of the International Federation for Adipose Therapeutics and Science (IFATS) and the International Society for Cellular Therapy (ISCT). *Cytotherapy* 15, 641–648. doi: 10.1016/j.jcyt.2013.02.006

Bozorgmehr, M., Moazzeni, S. M., Salehnia, M., Sheikhian, A., Nikoo, S., and Zarnani, A. H. (2014). Menstrual blood-derived stromal stem cells inhibit optimal generation and maturation of human monocyte-derived dendritic cells. *Immunol. Lett.* 162, 239–246. doi: 10.1016/j.imlet.2014.10.005

Bukowska, J., Ziecik, A. J., Laguna, J., Gawronska-Kozak, B., and Bodek, G. (2015). The Importance of the Canonical Wnt signaling pathway in the porcine endometrial stromal stem/progenitor cells: implications for regeneration. *Stem Cells Dev.* 24, 2873–2885. doi: 10.1089/scd.2015.0078

Busser, H., Najar, M., Raicevic, G., Pieters, K., Velez Pombo, R., Philippart, P., et al. (2015). Isolation and Characterization of Human Mesenchymal stromal cell subpopulations: comparison of bone marrow and adipose tissue. *Stem Cells Dev.* 24, 2142–2157. doi: 10.1089/scd.2015.0172

Cabezas, J., Lara, E., Pacha, P., Rojas, D., Veraguas, D., Saravia, F., et al. (2014). The endometrium of cycling cows contains populations of putative mesenchymal progenitor cells. *Reprod. Domest. Anim.* 49, 550–559. doi: 10.1111/rda.12309

Cabezas, J., Rojas, D., Navarrete, F., Ortiz, R., Rivera, G., Saravia, F., et al. (2018). Equine mesenchymal stem cells derived from endometrial or adipose tissue share significant biological properties, but have distinctive pattern of surface markers and migration. *Theriogenology* 106, 93–102. doi: 10.1016/j.theriogenology.2017.09.035

Campo, H., Baptista, P. M., Lopez-Perez, N., Faus, A., Cervello, I., and Simon, C. (2017). De- and recellularization of the pig uterus: a bioengineering pilot study. *Biol. Reprod.* 96, 34–45. doi: 10.1095/biolre/bio143396

Cantor, J. R. (2019). The rise of physiologic media. *Trends Cell Biol.* 29, 854–861. doi: 10.1016/j.tcb.2019.08.009

Caplan, A. I. (2016). MSCs: the sentinel and safe-guards of injury. *J. Cell. Physiol.* 231, 1413–1416. doi: 10.1002/jcp.25255

Cervello, I., Martinez-Conejero, J. A., Horcajadas, J. A., Pellicer, A., and Simon, C. (2007). Identification, characterization and co-localization of label-retaining cell population in mouse endometrium with typical undifferentiated markers. *Hum. Reprod.* 22, 45–51. doi: 10.1093/humrep/del332

Chaminadas, G., Propper, A. Y., Royez, M., Prost, O., Remy-Martin, J. P., and Adessi, G. L. (1986). Culture of epithelial and stromal cells of guinea-pig endometrium and the effect of oestradiol-17 beta on the epithelial cells. *J. Reprod. Fertil.* 77, 547–558. doi: 10.1530/jrf.0.0770547

Chan, R. W., and Gargett, C. E. (2006). Identification of label-retaining cells in mouse endometrium. *Stem Cells* 24, 1529–1538. doi: 10.1634/stemcells.2005-0411

Chan, R. W., Kaitu'u-Lino, T., and Gargett, C. E. (2012). Role of label-retaining cells in estrogen-induced endometrial regeneration. *Reprod. Sci.* 19, 102–114. doi: 10.1177/1933719111414207

Chan, R. W., Schwab, K. E., and Gargett, C. E. (2004). Clonogenicity of human endometrial epithelial and stromal cells. *Biol. Reprod.* 70, 1738–1750. doi: 10.1095/biolreprod.103.024109

Chen, J., Du, X., Chen, Q., and Xiang, C. (2015). Effects of donors' age and passage number on the biological characteristics of menstrual blood-derived stem cells. *Int. J. Clin. Exp. Pathol.* 8:14584.

Chen, L., Xiang, B., Wang, X., and Xiang, C. (2017a). Exosomes derived from human menstrual blood-derived stem cells alleviate fulminant hepatic failure. *Stem Cell Res. Ther.* 8:9.

Chen, L., Zhang, C., Chen, L., Wang, X., Xiang, B., Wu, X., et al. (2017b). Human Menstrual Blood-Derived Stem Cells Ameliorate liver fibrosis in mice by targeting hepatic stellate cells via paracrine mediators. *Stem Cells Transl. Med.* 6, 272–284. doi: 10.5966/sctm.2015-0265

Chomarat, P., Banchereau, J., Davoust, J., and Palucka, A. K. (2000). IL-6 switches the differentiation of monocytes from dendritic cells to macrophages. *Nat. Immunol.* 1, 510–514. doi: 10.1038/82763

Corcione, A., Benvenuto, F., Ferretti, E., Giunti, D., Cappiello, V., Cazzanti, F., et al. (2006). Human mesenchymal stem cells modulate B-cell functions. *Blood* 107, 367–372.

Corselli, M., Chen, C. W., Sun, B., Yap, S., Rubin, J. P., and Peault, B. (2012). The tunica adventitia of human arteries and veins as a source of mesenchymal stem cells. *Stem Cells Dev.* 21, 1299–1308. doi: 10.1089/scd.2011.0200

Couri, B. M., Lenis, A. T., Borazjani, A., Paraiso, M. F., and Damaser, M. S. (2012). Animal models of female pelvic organ prolapse: lessons learned. *Expert Rev. Obstet. Gynecol.* 7, 249–260. doi: 10.1586/eog.12.24

Crisan, M., Corselli, M., Chen, W. C., and Peault, B. (2012). Perivascular cells for regenerative medicine. *J. Cell Mol. Med.* 16, 2851–2860. doi: 10.1111/j.1582-4934.2012.01617.x

Crisan, M., Yap, S., Casteilla, L., Chen, C. W., Corselli, M., Park, T. S., et al. (2008). A perivascular origin for mesenchymal stem cells in multiple human organs. *Cell Stem Cell* 3, 301–313. doi: 10.1016/j.stem.2008.07.003

Cuenca, J., Le-Gatt, A., Castillo, V., Belletti, J., Diaz, M., Kurte, M., et al. (2018). The reparative abilities of menstrual stem cells modulate the wound matrix signals and improve cutaneous regeneration. *Front. Physiol.* 9:464. doi: 10.3389/fphys.2018.00464

Cui, C. H., Uyama, T., Miyado, K., Terai, M., Kyo, S., Kiyono, T., et al. (2007). Menstrual blood-derived cells confer human dystrophin expression in the murine model of Duchenne muscular dystrophy via cell fusion and myogenic transdifferentiation. *Mol. Biol. Cell* 18, 1586–1594. doi: 10.1091/mbc.e06-09-0872

da Silva Meirelles, L., Chagastelles, P. C., and Nardi, N. B. (2006). Mesenchymal stem cells reside in virtually all post-natal organs and tissues. *J. Cell Sci.* 119, 2204–2213. doi: 10.1242/jcs.02932

Dalal, J., Gandy, K., and Domen, J. (2012). Role of mesenchymal stem cell therapy in Crohn's disease. *Pediatr. Res.* 71, 445–451.

Dalirfardouei, R., Jamialahmadi, K., Jafarian, A. H., and Mahdipour, E. (2019). Promising effects of exosomes isolated from menstrual blood-derived mesenchymal stem cell on wound-healing process in diabetic mouse model. *J. Tissue Eng. Regen. Med.* 13, 555–568. doi: 10.1002/term.2799

Dalirfardouei, R., Jamialahmadi, K., and Mahdipour, E. (2018). A feasible method for the isolation of mesenchymal stem cells from menstrual blood and their exosomes. *Tissue Cell* 55, 53–62. doi: 10.1016/j.tice.2018.09.010

Darzi, S., Deane, J. A., Nold, C. A., Edwards, S. E., Gough, D. J., Mukherjee, S., et al. (2018). Endometrial Mesenchymal Stem/Stromal Cells Modulate the Macrophage Response to Implanted Polyamide/Gelatin Composite Mesh in Immunocompromised and Immunocompetent Mice. *Sci. Rep.* 8:6554.

Darzi, S., Werkmeister, J. A., Deane, J. A., and Gargett, C. E. (2016). Identification and characterization of human endometrial mesenchymal stem/stromal cells and their potential for cellular therapy. *Stem Cells Transl. Med.* 5, 1127–1132. doi: 10.5966/sctm.2015-0190

Darzi, S., Zarnani, A. H., Jeddi-Tehrani, M., Entezami, K., Mirzadegan, E., Akhondi, M. M., et al. (2012). Osteogenic differentiation of stem cells derived from menstrual blood versus bone marrow in the presence of human platelet releasate. *Tissue Eng. Part A* 18, 1720–1728. doi: 10.1089/ten.tea.2011.0386

de Carvalho Rodrigues, D., Asensi, K. D., Vairo, L., Azevedo-Pereira, R. L., Silva, R., Rondinelli, E., et al. (2012). Human menstrual blood-derived mesenchymal cells as a cell source of rapid and efficient nuclear reprogramming. *Cell Transplant.* 21, 2215–2224. doi: 10.3727/096368912x653048

Dessels, C., Potgieter, M., and Pepper, M. S. (2016). Making the switch: alternatives to fetal bovine serum for adipose-derived stromal cell expansion. *Front. Cell Dev. Biol.* 4:115. doi: 10.3389/fcell.2016.00115

Di Nicola, M., Carlo-Stella, C., Magni, M., Milanesi, M., Longoni, P. D., Matteucci, P., et al. (2002). Human bone marrow stromal cells suppress T-lymphocyte proliferation induced by cellular or nonspecific mitogenic stimuli. *Blood* 99, 3838–3843. doi: 10.1182/blood.v99.10.3838

Dimmeler, S., Ding, S., Rando, T. A., and Trounson, A. (2014). Translational strategies and challenges in regenerative medicine. *Nat. Med.* 20, 814–821. doi: 10.1038/nm.3627

Ding, D. C., Chou, H. L., Chang, Y. H., Hung, W. T., Liu, H. W., and Chu, T. Y. (2016). Characterization of HLA-G and related immunosuppressive effects in human umbilical cord stroma-derived stem cells. *Cell Transplant.* 25, 217–228. doi: 10.3727/096368915x688182

Dominici, M., Le Blanc, K., Mueller, I., Slaper-Cortenbach, I., Marini, F., Krause, D., et al. (2006). Minimal criteria for defining multipotent mesenchymal stromal cells. the international society for cellular therapy position statement. *Cytotherapy* 8, 315–317. doi: 10.1080/14653240600855905

Domnina, A. P., Novikova, P. V., Fridlyanskaya, I. I., Shilina, M. A., Zenin, V. V., and Nikolsky, N. N. (2016). Induction of decidual differentiation in endometrial mesenchymal stem cells. *Cell Tissue Biol.* 10, 95–99. doi: 10.1134/s1990519x16020048

Dosiou, C., and Giudice, L. C. (2005). Natural killer cells in pregnancy and recurrent pregnancy loss: endocrine and immunologic perspectives. *Endocr. Rev.* 26, 44–62. doi: 10.1210/er.2003-0021

Ebrahimi-Barough, S., Kouchesfahani, H. M., Ai, J., and Massumi, M. (2013). Differentiation of human endometrial stromal cells into oligodendrocyte progenitor cells (OPCs). *J. Mol. Neurosci.* 51, 265–273. doi: 10.1007/s12031-013-9957-z

Edwards, S. L., Ulrich, D., White, J. F., Su, K., Rosamilia, A., Ramshaw, J. A., et al. (2015). Temporal changes in the biomechanical properties of endometrial mesenchymal stem cell seeded scaffolds in a rat model. *Acta Biomater.* 13, 286–294. doi: 10.1016/j.actbio.2014.10.043

Emmerson, S., Mukherjee, S., Melendez-Munoz, J., Cousins, F., Edwards, S. L., Karjalainen, P., et al. (2019). Composite mesh design for delivery of autologous mesenchymal stem cells influences mesh integration, exposure and biocompatibility in an ovine model of pelvic organ prolapse. *Biomaterials* 225:119495. doi: 10.1016/j.biomaterials.2019.119495

Emmerson, S. J., and Gargett, C. E. (2016). Endometrial mesenchymal stem cells as a cell based therapy for pelvic organ prolapse. *World J. Stem Cells* 8, 202–215.

Faramarzi, H., Mehrabani, D., Fard, M., Akhavan, M., Zare, S., Bakhshalizadeh, S., et al. (2016). The potential of menstrual blood-derived stem cells in differentiation to epidermal lineage: A preliminary report. *World J. Plastic Surg.* 5:26.

Fard, M., Akhavan-Tavakoli, M., Khanjani, S., Zare, S., Edalatkhah, H., Arasteh, S., et al. (2018). Bilayer amniotic membrane/nano-fibrous fibroin scaffold promotes differentiation capability of menstrual blood stem cells into keratinocyte-like cells. *Mol. Biotechnol.* 60, 100–110. doi: 10.1007/s12033-017-0049-0

Farzamfar, S., Naseri-Nosar, M., Ghanavatinejad, A., Vaez, A., Zarnani, A. H., and Salehi, M. (2017). Sciatic nerve regeneration by transplantation of menstrual blood-derived stem cells. *Mol. Biol. Rep.* 44, 407–412. doi: 10.1007/s11033-017-4124-1

Farzamfar, S., Salehi, M., Ehterami, A., Naseri-Nosar, M., Vaez, A., Zarnani, A. H., et al. (2018). Promotion of excisional wound repair by a menstrual blood-derived stem cell-seeded decellularized human amniotic membrane. *Biomed. Eng. Lett.* 8, 393–398. doi: 10.1007/s13534-018-0084-1

Fathi-Kazerooni, M., Tavoosidana, G., Taghizadeh-Jahed, M., Khanjani, S., Golshahi, H., Gargett, C. E., et al. (2017). Comparative restoration of acute liver failure by menstrual blood stem cells compared with bone marrow stem cells in mice model. *Cytotherapy* 19, 1474–1490. doi: 10.1016/j.jcyt.2017.08.022

Feng, P., Li, P., and Tan, J. (2019). Human menstrual blood-derived stromal cells promote recovery of premature ovarian insufficiency via regulating the ECM-dependent FAK/AKT signaling. *Stem Cell Rev. Rep.* 15, 241–255. doi: 10.1007/s12015-018-9867-0

Frankman, E. A., Alperin, M., Sutkin, G., Meyn, L., and Zyczynski, H. M. (2013). Mesh exposure and associated risk factors in women undergoing transvaginal prolapse repair with mesh. *Obstet. Gynecol. Int.* 2013:926313.

Fu, R. H., Wang, Y. C., Liu, S. P., Shih, T. R., Lin, H. L., Chen, Y. M., et al. (2014). Decellularization and recellularization technologies in tissue engineering. *Cell Transplant.* 23, 621–630. doi: 10.3727/096368914x678382

Galipeau, J., and Sensebe, L. (2018). Mesenchymal stromal cells: clinical challenges and therapeutic opportunities. *Cell Stem Cell* 22, 824–833. doi: 10.1016/j.stem.2018.05.004

Galipeau, J., Weiss, D. J., and Dominici, M. (2019). Response to Nature commentary "Clear up this stem-cell mess". *Cytotherapy* 21, 1–2. doi: 10.1016/j.jcyt.2018.11.007

Gargett, C. E., Chan, R. W., and Schwab, K. E. (2008). Hormone and growth factor signaling in endometrial renewal: role of stem/progenitor cells. *Mol. Cell. Endocrinol.* 288, 22–29. doi: 10.1016/j.mce.2008.02.026

Gargett, C. E., and Gurung, S. (2016). Endometrial Mesenchymal stem/stromal cells, their fibroblast progeny in endometriosis, and more. *Biol. Reprod.* 94:129.

Gargett, C. E., Gurung, S., Darzi, S., Werkmeister, J. A., and Mukherjee, S. (2019). Tissue engineering approaches for treating pelvic organ prolapse using a novel source of stem/stromal cells and new materials. *Curr. Opin. Urol* 29, 450–457. doi: 10.1097/mou.0000000000000634

Gargett, C. E., Nguyen, H. P., and Ye, L. (2012). Endometrial regeneration and endometrial stem/progenitor cells. *Rev. Endocr. Metab. Disord.* 13, 235–251. doi: 10.1007/s11154-012-9221-9

Gargett, C. E., and Rogers, P. A. (2001). Human endometrial angiogenesis. *Reproduction* 121, 181–186. doi: 10.1530/rep.0.1210181

Gargett, C. E., Schwab, K. E., and Deane, J. A. (2016). Endometrial stem/progenitor cells: the first 10 years. *Hum. Reprod. Update* 22, 137–163.

Gargett, C. E., Schwab, K. E., Zillwood, R. M., Nguyen, H. P., and Wu, D. (2009). Isolation and culture of epithelial progenitors and mesenchymal stem cells from human endometrium. *Biol. Reprod.* 80, 1136–1145. doi: 10.1095/biolreprod.108.075226

Gargett, C. E., and Ye, L. (2012). Endometrial reconstruction from stem cells. *Fertil. Steril.* 98, 11–20. doi: 10.1016/j.fertnstert.2012.05.004

Gellersen, B., and Brosens, J. J. (2014). Cyclic decidualization of the human endometrium in reproductive health and failure. *Endocr. Rev.* 35, 851–905. doi: 10.1210/er.2014-1045

Ghobadi, F., Rahmanifar, F., Mehrabani, D., Tamadon, A., Dianatpour, M., Zare, S., et al. (2018). Endometrial mesenchymal stem stromal cells in mature and immature sheep: An in vitro study. *Int. J. Reprod. Biomed.* 16, 83–92.

Gronthos, S., Franklin, D. M., Leddy, H. A., Robey, P. G., Storms, R. W., and Gimble, J. M. (2001). Surface protein characterization of human adipose tissue-derived stromal cells. *J. Cell. Physiol.* 189, 54–63.

Gurung, S., Deane, J. A., Darzi, S., Werkmeister, J. A., and Gargett, C. E. (2018a). In vivo survival of human endometrial mesenchymal stem cells transplanted under the kidney capsule of immunocompromised mice. *Stem Cells Dev.* 27, 35–43. doi: 10.1089/scd.2017.0177

Gurung, S., Williams, S., Deane, J. A., Werkmeister, J. A., and Gargett, C. E. (2018b). The transcriptome of human endometrial Mesenchymal stem cells under TGFβR inhibition reveals improved potential for cell-based therapies. *Front. Cell Dev. Biol.* 6:164. doi: 10.3389/fcell.2018.00164

Gurung, S., Werkmeister, J. A., and Gargett, C. E. (2015). Inhibition of Transforming Growth Factor-beta Receptor signaling promotes culture expansion of undifferentiated human Endometrial Mesenchymal Stem/stromal Cells. *Sci. Rep.* 5:15042.

Han, X., Meng, X., Yin, Z., Rogers, A., Zhong, J., Rillema, P., et al. (2009). Inhibition of intracranial glioma growth by endometrial regenerative cells. *Cell Cycle* 8, 606–610. doi: 10.4161/cc.8.4.7731

Haniffa, M. A., Collin, M. P., Buckley, C. D., and Dazzi, F. (2009). Mesenchymal stem cells: the fibroblasts' new clothes? *Haematologica* 94, 258–263. doi: 10.3324/haematol.13699

Hanna, J., Goldman-Wohl, D., Hamani, Y., Avraham, I., Greenfield, C., Natanson-Yaron, S., et al. (2006). Decidual NK cells regulate key developmental processes at the human fetal-maternal interface. *Nat. Med.* 12, 1065–1074. doi: 10.1038/nm1452

Hawkes, P. W. (2015). Fetal bovine serum: geographic origin and regulatory relevance of viral contamination. *Bioresour. Bioprocess* 2:34.

Hellstrom, M., Bandstein, S., and Brannstrom, M. (2017). Uterine tissue engineering and the future of uterus transplantation. *Ann. Biomed. Eng.* 45, 1718–1730. doi: 10.1007/s10439-016-1776-2

Hellstrom, M., Moreno-Moya, J. M., Bandstein, S., Bom, E., Akouri, R. R., Miyazaki, K., et al. (2016). Bioengineered uterine tissue supports pregnancy in a rat model. *Fertil. Steril.* 106:487-496.e481.

Hida, N., Nishiyama, N., Miyoshi, S., Kira, S., Segawa, K., Uyama, T., et al. (2008). Novel cardiac precursor-like cells from human menstrual blood-derived mesenchymal cells. *Stem cells* 26, 1695–1704. doi: 10.1634/stemcells.2007-0826

Jabbour, H. N., Kelly, R. W., Fraser, H. M., and Critchley, H. O. (2006). Endocrine regulation of menstruation. *Endocr. Rev.* 27, 17–46. doi: 10.1210/er.2004-0021

Jiang, X. X., Zhang, Y., Liu, B., Zhang, S. X., Wu, Y., Yu, X. D., et al. (2005). Human mesenchymal stem cells inhibit differentiation and function of monocyte-derived dendritic cells. *Blood* 105, 4120–4126. doi: 10.1182/blood-2004-02-0586

Jiang, Z., Hu, X., Yu, H., Xu, Y., Wang, L., Chen, H., et al. (2013). Human endometrial stem cells confer enhanced myocardial salvage and regeneration by paracrine mechanisms. *J. Cell Mol. Med.* 17, 1247–1260. doi: 10.1111/jcmm.12100

Jin, H. J., Bae, Y. K., Kim, M., Kwon, S.-J., Jeon, H. B., Choi, S. J., et al. (2013). Comparative analysis of human mesenchymal stem cells from bone marrow, adipose tissue, and umbilical cord blood as sources of cell therapy. *Int. J. Mol. Sci.* 14, 17986–18001. doi: 10.3390/ijms140917986

Kalkunte, S. S., Mselle, T. F., Norris, W. E., Wira, C. R., Sentman, C. L., and Sharma, S. (2009). Vascular endothelial growth factor C facilitates immune tolerance and endovascular activity of human uterine NK cells at the maternal-fetal interface. *J. Immunol.* 182, 4085–4092. doi: 10.4049/jimmunol.0803769

Kazemnejad, S., Akhondi, M.-M., Soleimani, M., Zarnani, A. H., Khanmohammadi, M., Darzi, S., et al. (2012). Characterization and chondrogenic differentiation of menstrual blood-derived stem cells on a nanofibrous scaffold. *Int. J. Artif. Organs* 35, 55–66. doi: 10.5301/ijao.5000019

Khanjani, S., Khanmohammadi, M., Zarnani, A.-H., Akhondi, M.-M., Ahani, A., Ghaempanah, Z., et al. (2014). Comparative evaluation of differentiation potential of menstrual blood-versus bone marrow-derived stem cells into hepatocyte-like cells. *PLoS One* 9:e86075. doi: 10.1371/journal.pone.0086075

Khanjani, S., Khanmohammadi, M., Zarnani, A.-H., Talebi, S., Edalatkhah, H., Eghtesad, S., et al. (2015). Efficient generation of functional hepatocyte-like cells from menstrual blood-derived stem cells. *J. Tissue Eng. Regen. Med.* 9, E124–E134.

Khanmohammadi, M., Khanjani, S., Bakhtyari, M. S., Zarnani, A. H., Edalatkhah, H., Akhondi, M. M., et al. (2012). Proliferation and chondrogenic differentiation potential of menstrual blood-and bone marrow-derived stem cells in two-dimensional culture. *Int. J. Hematol.* 95, 484–493. doi: 10.1007/s12185-012-1067-0

Khanmohammadi, M., Khanjani, S., Edalatkhah, H., Zarnani, A. H., Heidari-Vala, H., Soleimani, M., et al. (2014). Modified protocol for improvement of differentiation potential of menstrual blood-derived stem cells into adipogenic lineage. *Cell Prolif.* 47, 615–623. doi: 10.1111/cpr.12133

Kim, J., and Hematti, P. (2009). Mesenchymal stem cell-educated macrophages: a novel type of alternatively activated macrophages. *Exp. Hematol.* 37, 1445–1453. doi: 10.1016/j.exphem.2009.09.004

Kozhukharova, I., Zemelko, V., Kovaleva, Z., Alekseenko, L., Lyublinskaya, O., and Nikolsky, N. (2018). Therapeutic doses of doxorubicin induce premature senescence of human mesenchymal stem cells derived from menstrual blood, bone marrow and adipose tissue. *Int. J. Hematol.* 107, 286–296. doi: 10.1007/s12185-017-2346-6

Kuramoto, G., Shimizu, T., Takagi, S., Ishitani, K., Matsui, H., and Okano, T. (2018). Endometrial regeneration using cell sheet transplantation techniques in rats facilitates successful fertilization and pregnancy. *Fertil. Steril.* 110:172-181.e174.

Kuznetsov, S. A., Mankani, M. H., Gronthos, S., Satomura, K., Bianco, P., and Robey, P. G. (2001). Circulating skeletal stem cells. *J. Cell Biol.* 153, 1133–1140.

Labome (2012). Fetal bovine serum. *Material Methods* 2:117.

Lara, E., Rivera, N., Cabezas, J., Navarrete, F., Saravia, F., Rodriguez-Alvarez, L., et al. (2018). Endometrial stem cells in farm animals: potential role in uterine physiology and pathology. *Bioengineering* 5:75. doi: 10.3390/bioengineering5030075

Le Blanc, K., and Mougiakakos, D. (2012). Multipotent mesenchymal stromal cells and the innate immune system. *Nat. Rev. Immunol.* 12, 383–396. doi: 10.1038/nri3209

Letouzey, V., Tan, K. S., Deane, J. A., Ulrich, D., Gurung, S., Ong, Y. R., et al. (2015). Isolation and characterisation of mesenchymal stem/stromal cells in the ovine endometrium. *PLoS One* 10:e0127531. doi: 10.1371/journal.pone.0127531

Li, H. Y., Chen, Y. J., Chen, S. J., Kao, C. L., Tseng, L. M., Lo, W. L., et al. (2010). Induction of insulin-producing cells derived from endometrial mesenchymal stem-like cells. *J. Pharmacol. Exp. Ther.* 335, 817–829.

Li, W., and Ding, S. (2010). Generation of novel rat and human pluripotent stem cells by reprogramming and chemical approaches. *Methods Mol. Biol.* 636, 293–300. doi: 10.1007/978-1-60761-691-7_18

Liu, T., Huang, Y., Zhang, J., Qin, W., Chi, H., Chen, J., et al. (2014). Transplantation of human menstrual blood stem cells to treat premature ovarian failure in mouse model. *Stem Cells Dev.* 23, 1548–1557. doi: 10.1089/scd.2013.0371

Liu, Y., Niu, R., Yang, F., Yan, Y., Liang, S., Sun, Y., et al. (2018). Biological characteristics of human menstrual blood-derived endometrial stem cells. *J. Cell Mol. Med.* 22, 1627–1639. doi: 10.1111/jcmm.13437

Lucas, E. S., Dyer, N. P., Fishwick, K., Ott, S., and Brosens, J. J. (2016). Success after failure: the role of endometrial stem cells in recurrent miscarriage. *Reproduction* 152, R159–R166.

Luz-Crawford, P., Torres, M. J., Noel, D., Fernandez, A., Toupet, K., Alcayaga-Miranda, F., et al. (2016). The immunosuppressive signature of menstrual blood mesenchymal stem cells entails opposite effects on experimental arthritis and graft versus host diseases. *Stem Cells* 34, 456–469. doi: 10.1002/stem.2244

Mahdipour, E., Salmasi, Z., and Sabeti, N. (2019). Potential of stem cell-derived exosomes to regenerate β islets through Pdx-1 dependent mechanism in a rat model of type 1 diabetes. *J. Cell. Physiol.* 234, 20310–20321. doi: 10.1002/jcp.28631

Mahfoudi, A., Fauconnet, S., Bride, J., Beck, L., Remy-Martin, J. P., Nicollier, M., et al. (1992). Serum-free culture of stromal and functionally polarized epithelial cells of guinea-pig endometrium: a potential model for the study of epithelial-stromal paracrine interactions. *Biol. Cell* 74, 255–265. doi: 10.1016/0248-4900(92)90036-z

Manshadi, M. D., Navid, S., Hoshino, Y., Daneshi, E., Noory, P., and Abbasi, M. (2019). The effects of human menstrual blood stem cells-derived granulosa cells on ovarian follicle formation in a rat model of premature ovarian failure. *Microsc. Res. Tech.* 82, 635–642. doi: 10.1002/jemt.23120

Marinaro, F., Gómez-Serrano, M., Jorge, I., Silla-Castro, J. C., Vázquez, J., Sánchez-Margallo, F. M., et al. (2019). Unraveling the molecular signature of extracellular vesicles from endometrial-derived mesenchymal stem cells: potential modulatory effects and therapeutic applications. *Front. Bioeng. Biotechnol.* 7:431. doi: 10.3389/fbioe.2019.00431

Masuda, H., Anwar, S. S., Buhring, H. J., Rao, J. R., and Gargett, C. E. (2012). A novel marker of human endometrial mesenchymal stem-like cells. *Cell Transplant.* 21, 2201–2214. doi: 10.3727/096368911x637362

Menard, C., Dulong, J., Roulois, D., Hebraud, B., Verdiere, L., Pangault, C., et al. (2020). Integrated transcriptomic, phenotypic, and functional study reveals tissue-specific immune properties of mesenchymal stromal cells. *Stem Cells* 38, 146–159. doi: 10.1002/stem.3077

Meng, X., Ichim, T. E., Zhong, J., Rogers, A., Yin, Z., Jackson, J., et al. (2007). Endometrial regenerative cells: a novel stem cell population. *J. Transl. Med.* 5:57.

Miernik, K., and Karasinski, J. (2012). Porcine uterus contains a population of mesenchymal stem cells. *Reproduction* 143, 203–209. doi: 10.1530/rep-11-0202

Mitchell, J. B., McIntosh, K., Zvonic, S., Garrett, S., Floyd, Z. E., Kloster, A., et al. (2006). Immunophenotype of human adipose-derived cells: temporal changes in stromal-associated and stem cell-associated markers. *Stem Cells* 24, 376–385. doi: 10.1634/stemcells.2005-0234

Miyazaki, K., and Maruyama, T. (2014). Partial regeneration and reconstruction of the rat uterus through recellularization of a decellularized uterine matrix. *Biomaterials* 35, 8791–8800. doi: 10.1016/j.biomaterials.2014.06.052

Moffett-King, A. (2002). Natural killer cells and pregnancy. *Nat. Rev. Immunol.* 2, 656–663.

Moll, G., Geissler, S., Catar, R., Ignatowicz, L., Hoogduijn, M. J., Strunk, D., et al. (2016). Cryopreserved or fresh mesenchymal stromal cells: only a matter of taste or key to unleash the full clinical potential of MSC Therapy? *Adv. Exp. Med. Biol.* 951, 77–98. doi: 10.1007/978-3-319-45457-3_7

Mukherjee, S., Darzi, S., Paul, K., Cousins, F. L., Werkmeister, J. A., and Gargett C. E. (2020). Electrospun nanofiber meshes with endometrial MSCs modulate foreign body response by increased angiogenesis, matrix synthesis, and anti-Inflammatory gene expression in mice: Implication in pelvic floor. *Front. Paharmacol.* 11:353. doi: 10.3389/fphar.2020.00353

Mukherjee, S., Darzi, S., Paul, K., Werkmeister, J. A., and Gargett, C. E. (2019a). Mesenchymal stem cell-based bioengineered constructs: foreign body response, cross-talk with macrophages and impact of biomaterial design strategies for pelvic floor disorders. *Interface Focus* 9:20180089. doi: 10.1098/rsfs.2018.0089

Mukherjee, S., Darzi, S., Rosamilia, A., Kadam, V., Truong, Y., Werkmeister, J. A., et al. (2019b). Blended Nanostructured Degradable Mesh with Endometrial Mesenchymal stem cells promotes tissue integration and anti-inflammatory response in vivo for pelvic floor application. *Biomacromolecules* 20, 454–468. doi: 10.1021/acs.biomac.8b01661

Murakami, K., Lee, Y. H., Lucas, E. S., Chan, Y. W., Durairaj, R. P., Takeda, S., et al. (2014). Decidualization induces a secretome switch in perivascular niche cells of the human endometrium. *Endocrinology* 155, 4542–4553. doi: 10.1210/en.2014-1370

Murphy, M. P., Wang, H., Patel, A. N., Kambhampati, S., Angle, N., Chan, K., et al. (2008). Allogeneic endometrial regenerative cells: an "Off the shelf solution" for critical limb ischemia? *J. Transl. Med.* 6:45. doi: 10.1186/1479-5876-6-45

Murray, L. M. A., and Krasnodembskaya, A. D. (2019). Concise review: intercellular communication via organelle transfer in the biology and therapeutic applications of stem cells. *Stem Cells* 37, 14–25. doi: 10.1002/stem.2922

Musina, R. A., Belyavski, A. V., Tarusova, O. V., Solovyova, E. V., and Sukhikh, G. T. (2008). Endometrial mesenchymal stem cells isolated from the menstrual blood. *Bull. Exp. Biol. Med.* 145, 539–543. doi: 10.1007/s10517-008-0136-0

Naji, A., Rouas-Freiss, N., Durrbach, A., Carosella, E. D., Sensebe, L., and Deschaseaux, F. (2013). Concise review: combining human leukocyte antigen G and mesenchymal stem cells for immunosuppressant biotherapy. *Stem Cells* 31, 2296–2303. doi: 10.1002/stem.1494

Nasef, A., Mathieu, N., Chapel, A., Frick, J., Francois, S., Mazurier, C., et al. (2007). Immunosuppressive effects of mesenchymal stem cells: involvement of HLA-G. *Transplantation* 84, 231–237. doi: 10.1097/01.tp.0000267918.07906.08

Nguyen, H. P. T., Sprung, C. N., and Gargett, C. E. (2012). Differential expression of Wnt signaling molecules between pre-and postmenopausal endometrial epithelial cells suggests a population of putative epithelial stem/progenitor cells reside in the basalis layer. *Endocrinology* 153, 2870–2883. doi: 10.1210/en.2011-1839

NIH (2010). *Why Mouse Matters*. Bethesda, MD: National Human Genome Research Institute.

Nikoo, S., Ebtekar, M., Jeddi-Tehrani, M., Shervin, A., Bozorgmehr, M., Kazemnejad, S., et al. (2012). Effect of menstrual blood-derived stromal stem cells on proliferative capacity of peripheral blood mononuclear cells in allogeneic mixed lymphocyte reaction. *J. Obstet. Gynaecol. Res.* 38, 804–809. doi: 10.1111/j.1447-0756.2011.01800.x

Olalekan, S. A., Burdette, J. E., Getsios, S., Woodruff, T. K., and Kim, J. J. (2017). Development of a novel human recellularized endometrium that responds to a 28-day hormone treatment. *Biol. Reprod.* 96, 971–981. doi: 10.1093/biolre/iox039

Ong, Y. R., Cousins, F. L., Yang, X., Mushafi, A. A. A. A., Breault, D. T., Gargett, C. E., et al. (2018). Bone marrow stem cells do not contribute to endometrial cell lineages in chimeric mouse models. *Stem Cells* 36, 91–102. doi: 10.1002/stem.2706

Ordener, C., Cypriani, B., Vuillermoz, C., and Adessi, G. L. (1993). Epidermal growth factor and insulin induce the proliferation of guinea pig endometrial stromal cells in serum-free culture, whereas estradiol and progesterone do not. *Biol. Reprod.* 49, 1032–1044. doi: 10.1095/biolreprod49.5.1032

Padykula, H. A., Coles, L. G., Okulicz, W. C., Rapaport, S. I., McCracken, J. A., King, N. W., et al. (1989). The basalis of the primate endometrium: a bifunctional germinal compartment. *Biol. Reprod.* 40, 681–690. doi: 10.1095/biolreprod40.3.681

Patel, A. N., Park, E., Kuzman, M., Benetti, F., Silva, F. J., and Allickson, J. G. (2008). Multipotent menstrual blood stromal stem cells: isolation, characterization, and differentiation. *Cell Transplant.* 17, 303–311. doi: 10.3727/096368908784153922

Paul, K., Darzi, S., McPhee, G., Del Borgo, M. P., Werkmeister, J. A., Gargett, C. E., et al. (2019). 3D bioprinted endometrial stem cells on melt electrospun poly epsilon-caprolactone mesh for pelvic floor application promote anti-inflammatory responses in mice. *Acta Biomater.* 97, 162–176. doi: 10.1016/j.actbio.2019.08.003

Peron, J. P., Jazedje, T., Brandao, W. N., Perin, P. M., Maluf, M., Evangelista, L. P., et al. (2012). Human endometrial-derived mesenchymal stem cells suppress inflammation in the central nervous system of EAE mice. *Stem Cell Rev. Rep.* 8, 940–952. doi: 10.1007/s12015-011-9338-3

Prockop, D. J., Prockop, S. E., and Bertoncello, I. (2014). Are clinical trials with mesenchymal stem/progenitor cells too far ahead of the science? Lessons from experimental hematology. *Stem Cells* 32, 3055–3061. doi: 10.1002/stem.1806

Queckborner, S., Syk Lundberg, E., Gemzell-Danielsson, K., and Davies, L. C. (2020). Endometrial stromal cells exhibit a distinct phenotypic and immunomodulatory profile. *Stem Cell Res. Ther.* 11:15.

Rahimi, M., Zarnani, A. H., Mobini, S., Khorasani, S., Darzi, M., and Kazemnejad, S. (2018). Comparative effectiveness of three-dimensional scaffold, differentiation media and co-culture with native cardiomyocytes to trigger in vitro cardiogenic differentiation of menstrual blood and bone marrow stem cells. *Biologicals* 54, 13–21. doi: 10.1016/j.biologicals.2018.05.003

Rahimi, M., Zarnani, A.-H., Mohseni-Kouchesfehani, H., Soltanghoraei, H., Akhondi, M.-M., and Kazemnejad, S. (2014). Comparative evaluation of cardiac markers in differentiated cells from menstrual blood and bone marrow-derived stem cells in vitro. *Mol. Biotechnol.* 56, 1151–1162. doi: 10.1007/s12033-014-9795-4

Rajabi, Z., Yazdekhasti, H., Mugahi, S. M. H. N., Abbasi, M., Kazemnejad, S., Shirazi, A., et al. (2018). Mouse preantral follicle growth in 3D co-culture system using human menstrual blood mesenchymal stem cell. *Reprod. Biol.* 18, 122–131. doi: 10.1016/j.repbio.2018.02.001

Rajaraman, G., White, J., Tan, K. S., Ulrich, D., Rosamilia, A., Werkmeister, J., et al. (2013). Optimization and scale-up culture of human endometrial multipotent mesenchymal stromal cells: potential for clinical application. *Tissue Eng. Part C Methods* 19, 80–92. doi: 10.1089/ten.tec.2011.0718

Ren, G., Zhao, X., Zhang, L., Zhang, J., L'Huillier, A., Ling, W., et al. (2010). Inflammatory cytokine-induced intercellular adhesion molecule-1 and vascular cell adhesion molecule-1 in mesenchymal stem cells are critical for immunosuppression. *J. Immunol.* 184, 2321–2328. doi: 10.4049/jimmunol.0902023

Ren, H., Sang, Y., Zhang, F., Liu, Z., Qi, N., and Chen, Y. (2016). Comparative analysis of human Mesenchymal Stem Cells from Umbilical Cord, Dental Pulp, and Menstrual blood as sources for cell therapy. *Stem Cells Int.* 2016, 3516574.

Ren, H., Zhang, Q., Wang, J., and Pan, R. (2018). Comparative effects of umbilical cord-and menstrual blood-derived MSCs in repairing acute lung injury. *Stem Cells Int.* 2018:787362.

Rink, B. E., Beyer, T., French, H. M., Watson, E., Aurich, C., and Donadeu, F. X. (2018). The Fate of Autologous Endometrial Mesenchymal Stromal Cells After Application in the Healthy Equine Uterus. *Stem Cells Dev.* 27, 1046–1052. doi: 10.1089/scd.2018.0056

Roson-Burgo, B., Sanchez-Guijo, F., Del Canizo, C., and De Las Rivas, J. (2016). Insights into the human mesenchymal stromal/stem cell identity through integrative transcriptomic profiling. *BMC Genomics* 17:944. doi: 10.1186/s12864-016-3230-0

Rozemuller, H., Prins, H. J., Naaijkens, B., Staal, J., Buhring, H. J., and Martens, A. C. (2010). Prospective isolation of mesenchymal stem cells from multiple mammalian species using cross-reacting anti-human monoclonal antibodies. *Stem Cells Dev.* 19, 1911–1921. doi: 10.1089/scd.2009.0510

Samsonraj, R. M., Rai, B., Sathiyanathan, P., Puan, K. J., Rotzschke, O., Hui, J. H., et al. (2015). Establishing criteria for human mesenchymal stem cell potency. *Stem Cells* 33, 1878–1891. doi: 10.1002/stem.1982

Santamaria, X., Massasa, E. E., Feng, Y., Wolff, E., and Taylor, H. S. (2011). Derivation of insulin producing cells from human endometrial stromal stem cells and use in the treatment of murine diabetes. *Mol. Ther.* 19, 2065–2071. doi: 10.1038/mt.2011.173

Sato, K., Ozaki, K., Oh, I., Meguro, A., Hatanaka, K., Nagai, T., et al. (2007). Nitric oxide plays a critical role in suppression of T-cell proliferation by mesenchymal stem cells. *Blood* 109, 228–234. doi: 10.1182/blood-2006-02-002246

Schwab, K. E., Chan, R. W., and Gargett, C. E. (2005). Putative stem cell activity of human endometrial epithelial and stromal cells during the menstrual cycle. *Fertil. Steril.* 84(Suppl. 2), 1124–1130. doi: 10.1016/j.fertnstert.2005.02.056

Schwab, K. E., and Gargett, C. E. (2007). Co-expression of two perivascular cell markers isolates mesenchymal stem-like cells from human endometrium. *Hum. Reprod.* 22, 2903–2911. doi: 10.1093/humrep/dem265

Schwab, K. E., Hutchinson, P., and Gargett, C. E. (2008). Identification of surface markers for prospective isolation of human endometrial stromal colony-forming cells. *Hum. Reprod.* 23, 934–943. doi: 10.1093/humrep/den051

Selmani, Z., Naji, A., Zidi, I., Favier, B., Gaiffe, E., Obert, L., et al. (2008). Human leukocyte antigen-G5 secretion by human mesenchymal stem cells is required to suppress T lymphocyte and natural killer function and to induce CD4+CD25highFOXP3+ regulatory T cells. *Stem Cells* 26, 212–222. doi: 10.1634/stemcells.2007-0554

Shahdadfar, A., Fronsdal, K., Haug, T., Reinholt, F. P., and Brinchmann, J. E. (2005). In vitro expansion of human mesenchymal stem cells: choice of serum is a determinant of cell proliferation, differentiation, gene expression, and transcriptome stability. *Stem Cells* 23, 1357–1366. doi: 10.1634/stemcells.2005-0094

Shi, G., Wang, G., Lu, S., Li, X., Zhang, B., Xu, X., et al. (2019). PD-L1 is required for human endometrial regenerative cells-associated attenuation of experimental colitis in mice. *Am. J. Transl. Res.* 11:4696.

Shokri, M. R., Bozorgmehr, M., Ghanavatinejad, A., Falak, R., Aleahmad, M., Kazemnejad, S., et al. (2019). Human menstrual blood-derived stromal/stem cells modulate functional features of natural killer cells. *Sci. Rep.* 9:10007.

Sipp, D., Robey, P. G., and Turner, L. (2018). Clear up this stem-cell mess. *Nature* 561, 455–457. doi: 10.1038/d41586-018-06756-9

Sivasubramaniyan, K., Harichandan, A., Schumann, S., Sobiesiak, M., Lengerke, C., Maurer, A., et al. (2013). Prospective Isolation of Mesenchymal Stem cells from human bone marrow using novel antibodies directed against sushi domain containing 2. *Stem Cells Dev.* 22, 1944–1954. doi: 10.1089/scd.2012.0584

Sobiesiak, M., Sivasubramaniyan, K., Hermann, C., Tan, C., Orgel, M., Treml, S., et al. (2010). The mesenchymal stem cell antigen MSCA-1 is identical to tissue non-specific alkaline phosphatase. *Stem Cells Dev.* 19, 669–677. doi: 10.1089/scd.2009.0290

Sotiropoulou, P. A., Perez, S. A., Gritzapis, A. D., Baxevanis, C. N., and Papamichail, M. (2006). Interactions between human mesenchymal stem cells and natural killer cells. *Stem Cells* 24, 74–85. doi: 10.1634/stemcells.2004-0359

Spitzer, T. L., Rojas, A., Zelenko, Z., Aghajanova, L., Erikson, D. W., Barragan, F., et al. (2012). Perivascular human endometrial mesenchymal stem cells express pathways relevant to self-renewal, lineage specification, and functional phenotype. *Biol. Reprod.* 86:58.

Su, K., Edwards, S. L., Tan, K. S., White, J. F., Kandel, S., Ramshaw, J. A. M., et al. (2014). Induction of endometrial mesenchymal stem cells into tissue-forming cells suitable for fascial repair. *Acta Biomater.* 10, 5012–5020. doi: 10.1016/j.actbio.2014.08.031

Subbarao, R. B., Shivakumar, S. B., Choe, Y. H., Son, Y. B., Lee, H. J., Ullah, I., et al. (2019). CD105(+) Porcine Endometrial Stromal Mesenchymal stem cells

possess differentiation potential toward Cardiomyocyte-like cells and insulin-producing beta cell-like cells in vitro. *Reprod. Sci.* 26, 669–682. doi: 10.1177/1933719118786461

Sugawara, K., Hamatani, T., Yamada, M., Ogawa, S., Kamijo, S., Kuji, N., et al. (2014). Derivation of human decidua-like cells from amnion and menstrual blood. *Sci. Rep.* 4, 1–9.

Tamadon, A., Mehrabani, D., Zarezadeh, Y., Rahmanifar, F., Dianatpour, M., and Zare, S. (2017). Caprine Endometrial Mesenchymal Stromal Stem Cell: Multilineage Potential, Characterization, and Growth Kinetics in Breeding and Anestrous Stages. *Vet. Med. Int.* 2017:5052801.

Tan, J., Li, P., Wang, Q., Li, Y., Li, X., Zhao, D., et al. (2016). Autologous menstrual blood-derived stromal cells transplantation for severe Asherman's syndrome. *Hum. Reprod.* 31, 2723–2729. doi: 10.1093/humrep/dew235

Thomas, H., Cowin, A. J., and Mills, S. J. (2017). The importance of Pericytes in healing: wounds and other pathologies. *Int. J. Mol. Sci.* 18:1129. doi: 10.3390/ijms18061129

Tiemann, T. T., Padma, A. M., Sehic, E., Backdahl, H., Oltean, M., Song, M. J., et al. (2020). Towards uterus tissue engineering: a comparative study of sheep uterus decellularisation. *Mol. Hum. Reprod.* 26, 167–178. doi: 10.1093/molehr/gaaa009

To, C., Farnsworth, R. H., Vail, M. E., Chheang, C., Gargett, C. E., Murone, C., et al. (2014). Hypoxia-controlled EphA3 marks a human endometrium-derived multipotent mesenchymal stromal cell that supports vascular growth. *PLoS One* 9:e112106. doi: 10.1371/journal.pone.0112106

Ulrich, D., Edwards, S. L., Su, K., Tan, K. S., White, J. F., Ramshaw, J. A., et al. (2014a). Human endometrial mesenchymal stem cells modulate the tissue response and mechanical behavior of polyamide mesh implants for pelvic organ prolapse repair. *Tissue Eng. Part A* 20, 785–798.

Ulrich, D., Tan, K. S., Schwab, K., Cheong, A., Deane, J. A., Rosamilia, A., et al. (2014b). Mesenchymal stem/stromal cells in postmenopausal endometrium. *Hum. Reprod.* 29, 1895–1905.

Ulrich, D., Gargett, C. E., Edwards, S., White, J., Rajaraman, G., Tan, K. S., et al. (2012). Human endometrial mesenchymal stem cells and novel meshes as an autologous cell-based therapy for pelvic organ prolapse (POP). *Tissue Eng. Part A* 6:125.

Ulrich, D., Muralitharan, R., and Gargett, C. E. (2013). Toward the use of endometrial and menstrual blood mesenchymal stem cells for cell-based therapies. *Expert Opin. Biol. Ther.* 13, 1387–1400. doi: 10.1517/14712598.2013.826187

Uzieliene, I., Urbonaite, G., Tachtamisevaite, Z., Mobasheri, A., and Bernotiene, E. (2018). The Potential of Menstrual Blood-Derived Mesenchymal stem cells for cartilage repair and regeneration: novel aspects. *Stem Cells Int.* 2018:5748126.

Vogel, W., Grunebach, F., Messam, C. A., Kanz, L., Brugger, W., and Buhring, H. J. (2003). Heterogeneity among human bone marrow-derived mesenchymal stem cells and neural progenitor cells. *Haematologica* 88, 126–133.

Wang, H., Jin, P., Sabatino, M., Ren, J., Civini, S., Bogin, V., et al. (2012). Comparison of endometrial regenerative cells and bone marrow stromal cells. *J. Transl. Med.* 10:207. doi: 10.1186/1479-5876-10-207

Wang, Y., Chen, X., Cao, W., and Shi, Y. (2014). Plasticity of mesenchymal stem cells in immunomodulation: pathological and therapeutic implications. *Nat. Immunol.* 15, 1009–1016. doi: 10.1038/ni.3002

Wolff, E. F., Gao, X. B., Yao, K. V., Andrews, Z. B., Du, H., Elsworth, J. D., et al. (2011). Endometrial stem cell transplantation restores dopamine production in a Parkinson's disease model. *J. Cell Mol. Med.* 15, 747–755. doi: 10.1111/j.1582-4934.2010.01068.x

Wolff, E. F., Mutlu, L., Massasa, E. E., Elsworth, J. D., Eugene Redmond, D. Jr., and Taylor, H. S. (2015). Endometrial stem cell transplantation in MPTP- exposed primates: an alternative cell source for treatment of Parkinson's disease. *J. Cell Mol. Med.* 19, 249–256. doi: 10.1111/jcmm.12433

Wu, X., Luo, Y., Chen, J., Pan, R., Xiang, B., Du, X., et al. (2014). Transplantation of human menstrual blood progenitor cells improves hyperglycemia by promoting endogenous progenitor differentiation in type 1 diabetic mice. *Stem Cells Dev.* 23, 1245–1257. doi: 10.1089/scd.2013.0390

Xiang, B., Chen, L., Wang, X., Zhao, Y., Wang, Y., and Xiang, C. (2017). Transplantation of menstrual blood-derived mesenchymal stem cells promotes the repair of LPS-induced acute lung injury. *Int. J. Mol. Sci.* 18:689. doi: 10.3390/ijms18040689

Xu, X., Li, X., Gu, X., Zhang, B., Tian, W., Han, H., et al. (2017). Prolongation of Cardiac allograft survival by endometrial regenerative cells: focusing on B-cell responses. *Stem Cells Transl. Med.* 6, 778–787. doi: 10.5966/sctm.2016-0206

Xu, X., Wang, Y., Zhang, B., Lan, X., Lu, S., Sun, P., et al. (2018). Treatment of experimental colitis by endometrial regenerative cells through regulation of B lymphocytes in mice. *Stem Cell Res. Ther.* 9:146.

Xu, Y., Shi, Y., and Ding, S. (2008). A chemical approach to stem-cell biology and regenerative medicine. *Nature* 453, 338–344. doi: 10.1038/nature07042

Yan, Z., Guo, F., Yuan, Q., Shao, Y., Zhang, Y., Wang, H., et al. (2019). Endometrial mesenchymal stem cells isolated from menstrual blood repaired epirubicin-induced damage to human ovarian granulosa cells by inhibiting the expression of Gadd45b in cell cycle pathway. *Stem Cell Res. Ther.* 10:4.

Yang, H. M., Sung, J. H., Choi, Y. S., Lee, H. J., Roh, C. R., Kim, J., et al. (2012). Enhancement of the immunosuppressive effect of human adipose tissue-derived mesenchymal stromal cells through HLA-G1 expression. *Cytotherapy* 14, 70–79. doi: 10.3109/14653249.2011.613926

Yang, X., Devianti, M., Yang, Y. H., Ong, Y. R., Tan, K. S., Gurung, S., et al. (2019). Endometrial mesenchymal stem/stromal cell modulation of T cell proliferation. *Reproduction* 157, 43–52. doi: 10.1530/rep-18-0266

Yang, X. Y., Wang, W., and Li, X. (2014). In vitro hepatic differentiation of human endometrial stromal stem cells. In Vitro. *Cell Dev. Biol. Anim.* 50, 162–170. doi: 10.1007/s11626-013-9688-z

Yin, M., Zhou, H. J., Lin, C., Long, L., Yang, X., Zhang, H., et al. (2019). CD34+KLF4+ Stromal Stem Cells Contribute to Endometrial Regeneration and Repair. *Cell Rep* 27:2709-2724.e2703.

Young, N., Rosamilia, A., Arkwright, J., Lee, J., Davies-Tuck, M., Melendez, J., et al. (2017). Vaginal wall weakness in parous ewes: a potential preclinical model of pelvic organ prolapse. *Int. Urogynecol. J.* 28, 999–1004. doi: 10.1007/s00192-016-3206-2

Zafardoust, S., Kazemnejad, S., Darzi, M., Fathi-Kazerooni, M., Rastegari, H., and Mohammadzadeh, A. (2020). Improvement of pregnancy rate and live birth rate in poor ovarian responders by Intraovarian Administration of autologous menstrual blood derived- Mesenchymal Stromal Cells: Phase I/II Clinical Trial. *Stem Cell Rev. Rep.* doi: 10.1007/s12015-020-09969-6 [Epub ahead of print].

Zemel'ko, V. I., Grinchuk, T. M., Domnina, A. P., Artsybasheva, I. V., Zenin, V. V., Kirsanov, A. A., et al. (2011). Multipotent mesenchymal stem cells of desquamated endometrium: isolation, characterization and use as feeder layer for maintenance of human embryonic stem cell lines. *Tsitologiia* 53, 919–929.

Zhang, S., Zeng, N., Alowayed, N., Singh, Y., Cheng, A., Lang, F., et al. (2017). Downregulation of endometrial mesenchymal marker SUSD2 causes cell senescence and cell death in endometrial carcinoma cells. *PLoS One* 12:e0183681. doi: 10.1371/journal.pone.0183681

Zhang, Y., Lin, X., Dai, Y., Hu, X., Zhu, H., Jiang, Y., et al. (2016). Endometrial stem cells repair injured endometrium and induce angiogenesis via AKT and ERK pathways. *Reproduction* 152, 389–402. doi: 10.1530/rep-16-0286

Zhao, Y., Chen, X., Wu, Y., Wang, Y., Li, Y., and Xiang, C. (2018a). Transplantation of human menstrual blood-derived mesenchymal stem cells alleviates Alzheimer's disease-like pathology in APP/PS1 transgenic mice. *Front. Mol. Neurosci.* 11:140. doi: 10.3389/fnmol.2018.00140

Zhao, Y., Lan, X., Wang, Y., Xu, X., Lu, S., Li, X., et al. (2018b). Human endometrial regenerative cells attenuate bleomycin-induced pulmonary fibrosis in mice. *Stem Cells Int.* 2018, 3475137.

Zhong, Z., Patel, A. N., Ichim, T. E., Riordan, N. H., Wang, H., Min, W.-P., et al. (2009). Feasibility investigation of allogeneic endometrial regenerative cells. *J. Transl. Med.* 7:15. doi: 10.1186/1479-5876-7-15

Conflict of Interest: The authors declare that the research was conducted in the absence of any commercial or financial relationships that could be construed as a potential conflict of interest.

frontiers in Cell and Developmental Biology

MINI REVIEW
published: 17 July 2020
doi: 10.3389/fcell.2020.00665

Mesenchymal Stromal Cells and Exosomes: Progress and Challenges

*Matthew H. Forsberg[1], John A. Kink[2,3], Peiman Hematti[2,3] and Christian M. Capitini[1,3]**

[1] Department of Pediatrics, School of Medicine and Public Health, University of Wisconsin-Madison, Madison, WI, United States, [2] Department of Medicine, School of Medicine and Public Health, University of Wisconsin-Madison, Madison, WI, United States, [3] Carbone Cancer Center, University of Wisconsin-Madison, Madison, WI, United States

Due to their robust immunomodulatory capabilities, mesenchymal stem/stromal cells (MSCs) have been used as a cellular therapy for a number of human diseases. Part of the mechanism of action of MSCs is the production of extracellular vesicles (EVs) that contain proteins, nucleic acids, and lipids that transmit signals to recipient cells that change their biologic behavior. This review briefly summarizes the development of MSCs as a treatment for human diseases as well as describes our present understanding of exosomes; how they exert their effects on target cells, and how they are differentiated from other EVs. The current treatment paradigm for acute radiation syndrome (ARS) is discussed, and how MSCs and MSC derived exosomes are emerging as treatment options for treating patients after radiation exposure. Other conditions such as graft-versus-host disease and cardiovascular disease/stroke are discussed as examples to highlight the immunomodulatory and regenerative capacity of MSC-exosomes. Finally, a consideration is given to how these cell-based therapies could possibly be deployed in the event of a catastrophic radiation exposure event.

Keywords: MSCs, extracellular vesicles, exosomes, acute radiation syndrome, macrophages

OPEN ACCESS

Edited by:
Lindolfo da Silva Meirelles, Universidade Luterana do Brazil, Brazil

Reviewed by:
Jeroen J. J. P. van den Beucken, Radboud University Nijmegen Medical Centre, Netherlands
Nicola Baldini, University of Bologna, Italy

****Correspondence:***
Christian M. Capitini
ccapitini@pediatrics.wisc.edu

Specialty section:
This article was submitted to Stem Cell Research, a section of the journal Frontiers in Cell and Developmental Biology

Received: *14 April 2020*
Accepted: *01 July 2020*
Published: *17 July 2020*

Citation:
Forsberg MH, Kink JA, Hematti P and Capitini CM (2020) Mesenchymal Stromal Cells and Exosomes: Progress and Challenges. Front. Cell Dev. Biol. 8:665. doi: 10.3389/fcell.2020.00665

INFUSION OF MSCS FOR TREATING INFLAMMATORY DISEASES

Mesenchymal stem/stromal cells (MSCs) are a potent immunomodulatory cell subset that are readily obtainable and easily expandable *in vitro*. MSCs can be obtained from many different tissues (bone marrow, adipose tissue, peripheral blood, umbilical cord blood), and are being studied for a number of conditions due to their ability to differentiate into various cell types, to migrate to various tissues, and to function as potent immunomodulators (Hass et al., 2011; Musiał-Wysocka et al., 2019). These cells are already approved in Europe for the treatment of complex perianal fistulas in adults with non-active/mildly active luminal Crohn's disease (daradstrocel, Alofisel) and in Japan for steroid-refractory acute graft-versus-host-disease (GVHD) (TEMCELL). A Biologics License Application (BLA) has been submitted to the Food and Drug Administration (FDA) in the United States for steroid refractory acute GVHD in children (remestemcel-L, Ryoncil), with approval expected late 2020. Future BLAs may soon follow since MSCs have shown to be safe or exhibit clinical efficacy for the treatment of other highly inflammatory conditions such as chronic GVHD (Gao et al., 2016; Chen et al., 2019), ankylosing spondylitis (Wang P. et al., 2014), atopic dermatitis (Kim et al., 2017), bronchopulmonary dysplasia (Chang et al., 2014; Ahn et al., 2017), pulmonary emphysema (de Oliveira et al., 2017), non-ischemic cardiomyopathy (Chin et al., 2011; Butler et al., 2017), liver allograft rejection (Shi et al., 2017) and cirrhosis (Zhang et al., 2012;

Suk et al., 2016; Liang et al., 2017), juvenile idiopathic arthritis (Swart et al., 2019), type 1 and type 2 diabetes (Jiang et al., 2011; Cai et al., 2016; Bhansali et al., 2017), rheumatoid arthritis (Park et al., 2018; Shadmanfar et al., 2018; Ghoryani et al., 2019), multiple sclerosis (Mohyeddin Bonab et al., 2007; Karussis et al., 2010; Bonab et al., 2012; Li J.F. et al., 2014; Harris et al., 2018; Riordan et al., 2018), systemic lupus erythematous (Wang D. et al., 2013, 2014), and osteoarthritis (Davatchi et al., 2011, 2016; Koh and Choi, 2012; Orozco et al., 2013; Wong et al., 2013; Vega et al., 2015; Lamo-Espinosa et al., 2016, 2018; Soler et al., 2016; Emadedin et al., 2018; Khalifeh Soltani et al., 2019; Matas et al., 2019).

INFUSION OF MSCS FOR TISSUE REPAIR AND REGENERATION

In part due to their immunomodulatory properties, MSCs have been observed to promote a regenerative environment that aids in the functional recovery of various damaged tissues (Bernardo et al., 2012). MSCs have proven to be safe or exhibited clinical efficacy in the field of regenerative medicine. Examples include improving neurologic function in amyotrophic lateral sclerosis (Petrou et al., 2016; Sykova et al., 2017; Berry et al., 2019), cerebral palsy (Wang X. et al., 2013; Huang et al., 2018), delayed encephalopathy after carbon monoxide poisoning (Wang H. et al., 2016), epilepsy (Hlebokazov et al., 2017), stroke (Bang et al., 2005; Lee et al., 2010), metachromatic leukodystrophy (Koc et al., 2002), and spinal cord injury (Vaquero et al., 2018); improved sexual function in erectile dysfunction (Al Demour et al., 2018); improved motor activity with frailty disorder (Tompkins et al., 2017), and multiple system atrophy (Lee et al., 2008, 2012; Singer et al., 2019); improved cardiovascular function in heart failure (Hare et al., 2012; Golpanian et al., 2015; Mathiasen et al., 2015; Bartolucci et al., 2017), and myocardial ischemia/angina (Hare et al., 2009; Friis et al., 2011; Haack-Sorensen et al., 2013; Karantalis et al., 2014; Kim et al., 2018), improved bone repair in hypophosphatasia (Taketani et al., 2015), lumbar disc degeneration (Orozco et al., 2011; Noriega et al., 2017), osteogenesis imperfecta (Gotherstrom et al., 2014), and osteonecrosis (Hernigou et al., 2018); improved healing from kidney injury (Tan et al., 2012; Saad et al., 2017); improved healing from liver injury related to acute on chronic hepatitis (Shi et al., 2012; Lin et al., 2017) and ischemic biliary lesions following liver transplantation (Zhang et al., 2017); improved hematopoietic recovery (Xiao et al., 2013; Zhang et al., 2013; Xiong et al., 2014); and accelerated wound healing (Falanga et al., 2007). From these indications, remestemcel-L is already in phase III trials for advanced heart failure and chronic low back pain.

POTENTIAL MECHANISMS OF ACTION

Mesenchymal stem/stromal cells have been shown to suppress inflammation through direct cell-to-cell contact in inflamed tissues and through production of numerous anti-inflammatory molecules such as indoleamine 2,3 dioxygenase (IDO) (Su et al., 2014), nitric oxide (NO) (Su et al., 2014), prostaglandin E2 (PGE2) (Hsu et al., 2013), transforming growth factor (TGF)-β (de Araujo Farias et al., 2018), heme oxygenase 1 (HO1) (Chabannes et al., 2007), and hepatocyte growth factor (HGF) (Lee et al., 2018), among others. These molecules suppress the effect of immune cells such as macrophages (Nemeth et al., 2009; Eslani et al., 2018), monocytes (Cutler et al., 2010), dendritic cells (Jiang et al., 2005), B-cells (Corcione et al., 2006), NK cells (Sotiropoulou et al., 2006), and T-cells (Engela et al., 2013; Li M. et al., 2014). In addition to immuno-suppressive molecules, MSCs can influence target cell function through the secretion of large amounts of exosomes. MSC-derived exosomes have been investigated in preclinical models as a potential therapeutic for many of the same conditions that MSCs have shown efficacy in treating, such as wound healing (Fang et al., 2016; Samaeekia et al., 2018), angiogenesis (Teng et al., 2015; Huang et al., 2017), bronchopulmonary dysplasia (Braun et al., 2018), and various autoimmune disorders (Riazifar et al., 2019), but have also shown efficacy in facilitating skeletal muscle regeneration (Nakamura et al., 2015), neurogenesis (Reza-Zaldivar et al., 2019), recovery from stroke (Zhang and Chopp, 2016), and tendon repair (Chamberlain et al., 2019).

To date, no clinical trials infusing MSC-exosomes have been published although some studies have been completed (NCT03384433, NCT02138331) or are recruiting/about to open to accrual (**Table 1**).

This review focuses on recent pre-clinical work on the potential therapeutic uses of MSCs and MSC-exosomes to polarize or "educate" immune cells into anti-inflammatory cells, with treatment of acute radiation syndrome (ARS) and GVHD as models for the systemic effects of the anti-inflammatory properties of MSC-exosomes. The organ-specific regenerative effects of MSC-exosomes are also explored, using cardiovascular disease and stroke as examples. ARS is also used as an example of how MSC derived exosomes could be developed as a cell-based therapeutic, with consideration given to the potential challenges and drawbacks of such an approach. For a thorough review on how MSC exosomes are being used for the treatment of other conditions, a recently published review is highly recommended (Joo et al., 2020).

EXOSOMES: FORMATION, CHARACTERISTICS, AND CARGO

Extracellular vesicles (EVs) are lipid bilayer particles that are released from cells. This diverse family of particles includes microvesicles (MVs), apoptotic bodies, and exosomes. EVs are composed of membrane-bound particles that are classified according to size with exosomes generally defined as 30–150 nm in diameter (Helwa et al., 2017; Bebelman et al., 2018). Exosomes are generally considered to be produced through the inward budding of late stage endosomes, forming multi-vesicular bodies (MVBs) which then release these "buds" (exosomes) upon fusion with the plasma membrane (Hessvik and Llorente, 2018). Due to the fact that exosomes are differentiated from EVs based on their relative size, it can be difficult to separate exosomes from

TABLE 1 | Clinical trials infusing MSC-derived exosomes.

Clinical trial number	Title	Sponsor
NCT03857841	A Safety Study of Intravenous Infusion of Bone Marrow Mesenchymal Stem Cell-derived Extracellular Vesicles (UNEX-42) in Preterm Neonates at High Risk for Bronchopulmonary Dysplasia	United Therapeutics
NCT04173650	A Safety Study of the Administration of MSC Extracellular Vesicles in the Treatment of Dystrophic Epidermolysis Bullosa Wounds	Aegle Therapeutics
NCT04276987	A Pilot Clinical Study on Aerosol Inhalation of the Exosomes Derived From Allogenic Adipose Mesenchymal Stem Cells in the Treatment of Severe Patients With Novel Coronavirus Pneumonia	Jiao Tong University School of Medicine Shanghai, China
NCT04213248	Effect of Umbilical Mesenchymal Stem Cells Derived Exosomes on Dry Eye in Patients With Chronic Graft Versus Host Diseases	Sun Yat-sen University Guangdong, China
NCT04313647	A Tolerance Clinical Study On Aerosol Inhalation of Mesenchymal Stem Cells Exosomes In Healthy Volunteers	Jiao Tong University School of Medicine Shanghai, China
NCT03437759	Mesenchymal Stem Cells Derived Exosomes Promote Healing of Large and Refractory Macular Holes	Tianjin Medical University Hospital Tianjin, China
NCT04270006	Effect of Adipose Derived Stem Cells Exosomes as an Adjunctive Therapy to Scaling and Root Planning in the Treatment of Periodontitis: A Human Clinical Trial	Beni-Suef University Beni-Suef, Egypt

According to clinicaltrials.gov as of 14 April 2020.

smaller EVs. In fact, the formation of a smaller subset of EVs in the size range of what is considered to be exosomes has been observed through the direct budding of the plasma membrane (Casado et al., 2017). Cholesterol, sphingomyelin, ceramide, and various lipid molecules are found in large quantities on the exosomal membrane (Mashouri et al., 2019). Once the exosomes are released into the intercellular space, they can be taken up by recipient cells by endocytosis, receptor–ligand binding, or through direct binding (Kahroba et al., 2019).

Exosomes exert their effects by releasing their contents into the cytosol of recipient cells. Exosome cargo can consist of a number of different molecules such as nucleic acids (DNA, RNA, mRNA miRNA), pro-inflammatory and anti-inflammatory cytokines, enzymes, and various other proteins (Mathivanan et al., 2010; D'Asti et al., 2012). Cytokines can be found not only encapsulated in the exosome, but also imbedded in the exosomal membrane itself (Fitzgerald et al., 2018). The authors of this study hypothesized that exosomes can deliver smaller amounts of cytokines directly to the intended target cell, a more efficient delivery mechanism compared to the traditional cytokine "dump" into the intercellular space (which could be taken up by any cell with a corresponding receptor). Other proteins found in the exosomal membrane such as various heat-shock and signaling proteins have shown to perform immunomodulatory functions as well (Urbanelli et al., 2013; Reddy et al., 2018). A visual representation of exosomes, their formation, and their cargo can be seen in **Figure 1**.

POTENTIAL BENEFITS AND CHALLENGES OF USING MSC-EXOSOMES

Utilizing MSC-exosomes as a therapy has a number of advantages compared to using MSCs themselves. One advantage is that viability is not a concern with exosomes, as they are not cells. This makes exosomes potentially much easier to use post thaw. Indeed, there is preliminary evidence that the thawing process may alter exosomal membranes so that they are absorbed more easily by target cells, although more research is needed to confirm this finding (Cheng et al., 2019). In one report, familial patients who received autologous adipose tissue-derived MSCs all had incidences of pulmonary embolisms related to the infusion (Jung et al., 2013). As MSC-exosomes are not a cellular product, there should be no risk to potential patients of developing pulmonary embolisms. Exosomes can also cross the blood–brain barrier, while MSCs cannot, making MSC-exosomes an

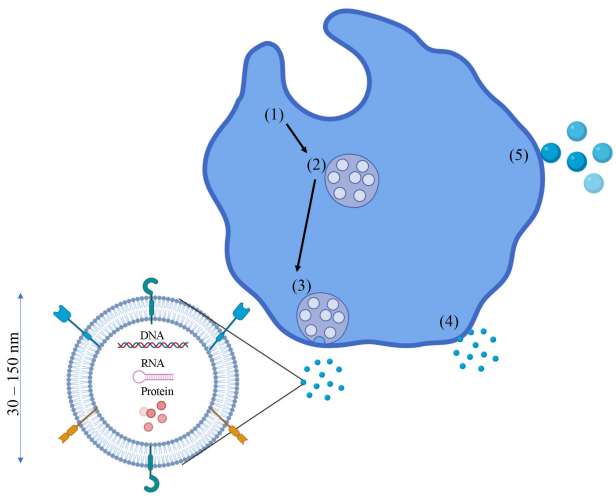

FIGURE 1 | Exosomes: Formation, cargo, and characteristics. Exosome formation typically begins as endosomes (1) begin to bud inward and form multi-vesicular bodies (MVBs) (2). These MVBs then fuse with the plasma membrane (3) and release the exosomes into the intracellular space. However, the plasma membrane can also bleb off small EVs 30–150 nm in diameter which also fall in the same size classification as exosomes, so differentiating the two can be difficult (4). If these plasma membrane blebs are > 150 nm in diameter, they are classified as microvesicles or microparticles (5). Exosomes can contain a number of different molecules as cargo such as proteins/cytokines (free floating and membrane bound), DNA, RNA, and other nucleic acids.

attractive potential therapy option for various degenerative brain disorders (Chen et al., 2016). Just as with any novel therapy, there are challenges that need to be addressed before MSC-exosomes can be used in the clinic. First and foremost there needs to be a method of selecting suitable donors for the production of the MSCs that are used to produce exosomes, as well as the development of an exosome isolation protocol that meets good manufacturing practice (GMP) standards. Additionally, a consistent release criterion (size, surface marker expression, cargo, etc.) needs to be established for the exosomes themselves before they can be infused into potential patients. Depending on the condition being treated, markers need to be identified that distinguish functional from non-functional exosomes. Also, the optimal dose of MSC-exosomes for humans is unknown, which would need to be determined for each condition being treated. Furthermore, the best route of administration (local versus systemic) is unclear, as is the length of time MSC-exosomes remain in the patient before they are cleared by phagocytic cells. These challenges must be overcome and standards must be defined before patients can be tested for the immunomodulatory and regenerative capabilities of MSC-exosomes.

MSC DERIVED EXOSOMES FOR THE TREATMENT OF ARS

Acute radiation syndrome is caused by a high dose of ionizing radiation (>1 GY) over a short period of time (Lopez and Martin, 2011). The most severe side effects of ARS occur due to damage in highly proliferative cells found in the skin, the gastrointestinal tract, and the bone marrow (Heslet et al., 2012). Loss of bone marrow progenitor cells places patients at high risk for infections, as they can no longer produce leukocytes (Dainiak, 2018). The current standard of care for ARS involves the use of supportive care measures such as prophylactic antibiotics, blood and platelet transfusions, and the growth factors granulocyte colony-stimulating factor (G-CSF) and granulocyte-macrophage colony-stimulating factor (GM-CSF) (Waselenko et al., 2004; Gourmelon et al., 2010) which are FDA-approved to treat ARS. These interventions can keep patients alive and provide valuable time to patients who are waiting for an allogeneic hematopoietic stem cell transplant (HSCT) (Weisdorf et al., 2006). However, this process can take several weeks, during which time the patient may die from the initial exposure event. Even if the patient successfully receives a HSCT, this procedure comes with its own set of risks such as engraftment failure and GVHD (Ghimire et al., 2017; Ozdemir and Civriz Bozdag, 2018).

Most cases of ARS are seen in nuclear power plant employees upon accidental exposure resulting from incidents occurring at the plants such as those seen at Chernobyl and Fukushima (Mettler et al., 2007; Cerezo and Macia, 2012). Increasing usage of medical isotopes like iodine-131 to treat cancer has resulted in patients needing to cryopreserve their own (autologous) hematopoietic stem cells prior to treatment so that the bone marrow can be rescued from the cancer treatment. However, due to the current proliferation of nuclear technology worldwide, a mass exposure event from a terrorist attack using an improvised nuclear device or from a nuclear warhead deployed as an act-of-war is also a possibility. ARS could also impact future astronauts as both government agencies like the National Aeronautics and Space Administration (NASA) and private companies push for human voyages back to the moon as well as to Mars. An event such as a solar flare could expose astronauts to a high dose of cosmic radiation (Chancellor et al., 2014). Possible sources of radiation exposure, as well as current treatment options are summarized in **Figure 2**. Due to the current standard of care for ARS as well as the increased risk of exposure events due to accidents at power plants, cancer treatments, political instability, or through the colonization of the inner solar system; a priority has been placed on the development of "off-the-shelf" cell-based therapies that seek to mitigate or even reverse the deleterious effects of ARS.

A number of preclinical studies have shown that MSCs can be used to reverse radiation damage seen in a variety of tissues, including the bone marrow (Fukumoto, 2016). The majority of preclinical work has been done utilizing bone marrow-derived MSCs for treatment of ARS (Lange et al., 2011; Yang et al., 2012). However, adipose tissue derived MSCs have also shown to prolong survival in irradiated mice, as well as enhance the reconstitution of hematopoietic cells (Cousin et al., 2003). Intramuscularly injected human placenta-derived MSCs have also shown the ability to enhance hematopoietic regeneration, reverse severe weight loss, and increase survival in lethally irradiated mice (Gaberman et al., 2013; Pinzur et al., 2018). Interestingly, in a study that exposed C57/BL6 mice to lethal irradiation followed by subsequent treatment with bone marrow-derived syngeneic MSCs within 24 h after exposure, the infused MSCs were cleared from the recipient mice within 3 days (Yang et al., 2012). This finding suggests that the protective effect seen

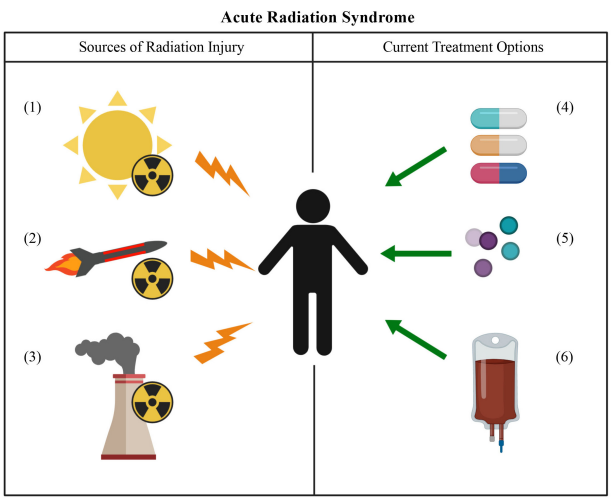

FIGURE 2 | Acute radiation syndrome: sources of injury and current treatment options. Sources of radiation injury can include solar flares (1), nuclear weapons (2), or an accident at a nuclear power plant (3). The current treatment options for ARS involve the use of antibiotics (4) and the growth factors G-CSF and GM-CSF (5). In the more severe cases of ARS, an HSCT may need to be performed (6).

in these mice was not due to the infused MSCs themselves, but rather through endogenous cells that were "educated" by the MSCs. One way in which these target cells could have been educated was by paracrine factors such as EVs produced from MSCs. Indeed, sublethally irradiated C57/BL6 lineage negative bone marrow cells (isolated 7 days after irradiation) showed an increased capacity to engraft in syngeneic recipient mice after being cultured with murine or human MSC-EVs (Wen et al., 2016).

Presently, only one clinical trial using allogeneic ex vivo expanded placental MSCs (PLX-R18, Pluristem Ltd.) is available for ARS, but is not yet recruiting (NCT03797040). However as stated above, it is possible that the benefits of MSCs in ARS may not be from MSCs themselves. Rather, the MSCs may be educating other immune cell subsets such as macrophages to mediate their radioprotective effects (Davies et al., 2017). Human MSC-educated macrophages, or "MEMs," are a high interleukin (IL)-6 and IL-10 producing macrophage subset (Kim and Hematti, 2009) that are more effective than human MSCs alone in treating ARS in an immunocompromised xenogeneic model (Bouchlaka et al., 2017). In this study, MEMs expressed higher levels of inhibitory molecules such as PD-L1 and PD-L2, as well as molecules CD73 and arginase-1, when compared to untreated macrophages. Furthermore, MEMs were found to secrete higher levels of IL-6, while exhibiting a greater capacity to inhibit the proliferation of T-cells while promoting fibroblast proliferation as compared to untreated macrophages. IL-6 is typically considered to be a pro-inflammatory cytokine (Tanaka et al., 2014), although it has also been found in some instances to have anti-inflammatory effects as well as playing a role in tissue regeneration (Scheller et al., 2011; Galun and Rose-John, 2013). In fact, the presence of IL-6 has been associated with reduced inflammation caused by radiation induced injury (Bell et al., 2019). This increased secretion of IL-6 was enhanced when MEMs were "primed" with the TLR-4 ligand lipopolysaccharide (LPS) (Bouchlaka et al., 2017). The role of LPS in promoting the radio-protective effect of MEMs was investigated in a recent study, where LPS induced generation of MSC derived exosomes in a dose-dependent manner (Kink et al., 2019). In this study, human bone marrow-derived MSCs were primed with LPS for 24 h, after which time exosomes were harvested (Kink et al., 2019). The LPS-MSC exosomes (and unprimed MSC exosomes) were then cultured with human macrophages for 3 days, followed by infusion into immunocompromised mice with ARS. Results from this study show that the LPS-primed MSC exosome educated macrophages (LPS EEMs) significantly prolonged survival from ARS, enhanced hematopoietic recovery (by complete blood count and histologic analysis of bone marrow and spleen), and increased phagocytic capacity compared to unprimed MSC exosome educated macrophages (EEMs). The mechanism behind this protective effect is currently unknown, although there are a few intriguing avenues to investigate. The protection may be due to the effects of the increased levels of IL-6 or enhanced expression of PD-L1 found on the surface of the LPS EEMs. This immunomodulatory environment could possibly facilitate the reconstitution of the host mouse bone marrow. In order to investigate these possibilities, researchers could perform a similar study to those mentioned above, except for the inclusion of the administration of IL-6 and/or PD-L1 blocking monoclonal antibodies and observe how the radio-protective effect of the LPS-EEMs is altered. Furthermore, the use of LPS causes some concerns in a clinical setting, as LPS is toxic to humans (Stewart et al., 2006). Therefore, it would be prudent to perform similar experiments using synthetic LPS analogs in place of LPS.

MSC DERIVED EXOSOMES FOR THE TREATMENT OF GVHD AND COVID-19

Due to their immunomodulatory capabilities, MSC-exosomes are an intriguing potential therapy for GVHD. Similar to ARS, GVHD is characterized by damaging proinflammatory responses that affect multiple organs. Immunosuppression with corticosteroids remains the most common treatment for both acute and chronic GVHD, but with sustained response rates around 40–50%, more effective approaches are needed (Garnett et al., 2013). Recent preclinical studies have investigated the use of human MSC-exosomes in mice with acute GVHD. Both umbilical cord derived MSC-exosomes and BM derived MSC exosomes prolonged survival of mice with GVHD compared to controls (Wang L. et al., 2016; Fujii et al., 2018). Furthermore, these studies showed a lower number of T cells, impaired T cell proliferation, and lower levels of proinflammatory cytokines IL-2, TNF-α, and IFN-γ in MSC-exosome treated mice (Wang L. et al., 2016; Fujii et al., 2018). Human BM derived MSC-exosomes have also shown efficacy in mouse models of chronic GVHD. In this study, treated mice showed improved survival, diminished clinical scores, reduced fibrosis in the skin, lung and liver, inhibition of Th17 cells, and induction of IL-10 expressing regulatory cells (Lai et al., 2018). Interestingly, BM derived MSC-exosomes have been given to a human patient with severe therapy-resistant GVHD as an individualized compassionate use treatment (Kordelas et al., 2014). The patient responded well to the therapy, as patient PBMCs showed decreased production of IL-1β, TNF-α, and IFN-γ after the third infusion (Kordelas et al., 2014). Additionally, clinical GVHD symptoms improved significantly, which allowed for a reduced dosage of steroids (Kordelas et al., 2014). The patient remained stable for months before eventually dying 7 months later due to pneumonia (Kordelas et al., 2014). A more recent finding, although not GVHD related, also shows the impact that MSC-exosomes have on reducing inflammatory responses; 24 severe COVID-19 patients were given a dose of ExoFlo^{TM} (a BM derived MSC-exosome product) at a single hospital center (Sengupta et al., 2020). Of these 24 patients, 17 fully recovered, three died, and three remain in intensive care at the time of publication (Sengupta et al., 2020). There were no adverse reactions to ExoFlow^{TM} seen in any of the patients (Sengupta et al., 2020). Patients showed a significant decrease in neutrophil count, an increase in T lymphocyte count, reversal of hypoxia, and downregulation of cytokine storm (Sengupta et al., 2020). More clinical work is needed to determine if MSC-exosomes constitute an effective therapy for inflammatory diseases, but initial results are promising.

MSC DERIVED EXOSOMES FOR THE TREATMENT OF CARDIOVASCULAR DISEASE AND STROKE

Cardiovascular diseases are the leading cause of morbidity and mortality worldwide. One major cause/result of these conditions is the death of cardiomyocytes and the subsequent loss of tissue remodeling capabilities (Olivetti et al., 1996). Cell-based therapies, including MSCs, have been investigated as a potential therapeutic option to help replace the lost cardiomyocytes, and improve heart function (Golpanian et al., 2016; Majka et al., 2017). MSC-exosomes have also shown promise in promoting cardioprotection in a mouse model of myocardial ischemia/reperfusion (I/R) injury, evidenced by reduced infarct size in mice treated with purified MSC-exosomes (Lai et al., 2010). Similarly, in a rat model of myocardial ischemic injury, human umbilical cord MSC-exosomes were found to reduce cardiac cell fibrosis, suppress apoptosis, and promote proliferation (Zhao et al., 2015). In a different study, researchers found that this protective effect of MSC-exosomes was in part due to their ability to deliver miRNAs, specifically miR-19a (Yu et al., 2015). Enhanced myocardial viability has also been observed in an I/R injury mouse model, resulting from increased ATP levels and decreased oxidative stress seen in the heart tissue of mice treated with MSC-exosomes (Arslan et al., 2013). Like cardiovascular disease, stroke is one of the leading causes of death and disability. MSC therapy has shown preclinical and clinical success in promoting recovery from stroke (Zhang and Chopp, 2016), and MSC-exosomes have shown promise in various preclinical models of stroke recovery. In rat models of traumatic brain injury (TBI), administration of MSC-exosomes has been shown to enhance neurogenesis and angiogenesis, and improve spatial learning and sensorimotor functional recovery (Xin et al., 2013a; Zhang et al., 2015). One potential mechanism of the enhanced recovery from TBI is the delivery of the miRNA miR-133b, as MSC-exosomes with elevated miR-133b led to improved axonal remodeling and neurological function when compared to standard MSC-exosomes (Xin et al., 2013b). MSC-exosomes promote tissue repair/remodeling in a number of preclinical disease models in addition to cardiovascular disease/stroke, and provide an exciting potential therapy for patients who suffer from these debilitating conditions.

IMPLEMENTATION OF CELL-BASED THERAPIES FOR ARS

Considerations on how MSCs/MSC-exosomes can be best utilized need to be taken into account on a condition by condition basis. Here, ARS is used as an example to explore what hurdles need to be cleared before MSCs/MSC-exosomes can be used as a treatment for this condition. Cell-based treatment strategies for ARS need to be safe and efficacious in the event of a potentially lethal radiation exposure. To achieve this goal, a number of logistical challenges need to be taken into account. In order to outline the nature of these challenges, and develop strategies to overcome them, the National Institute of Allergy and Infectious Diseases (NIAID) co-sponsored an international workshop in July 2015 in Paris, France, with the Institut de Radioprotection et de Sûreté Nucléaire. A report on this workshop was published in Radiation Research (DiCarlo et al., 2017). In this report, the authors summarize the numerous regulatory hurdles that need to be cleared in order for these cell-based therapies to be approved for human use. Of particular interest was the potential of MSC produced paracrine factors, particularly exosomes, to treat the effects of radiation exposure (Tran et al., 2013). However, the report stated that both cell-based therapies as well as exosomes alone could be used in a mass exposure event (DiCarlo et al., 2017). Patients who were exposed to higher levels of radiation could receive MSCs or MSC exosome educated cells, while the larger number of patients exposed to lower radiation levels (who still have surviving hematopoietic stem cells) could receive MSC exosomes alone to help boost the capacity of their own bone marrow to replenish itself. Importantly, in both of these scenarios, the patient would be receiving an "off-the-shelf" thawed product, so the development of a consistent and effective post-thaw procedure prior to infusion is of upmost importance. Cell-based therapies would likely be stored in a cryopreserved state at a few centralized locations. Therefore, therapeutic cells would need to show efficacy up to 24 or 48 h after the initial radiation exposure in order to account for the time it would take for the product to reach the patient.

CONCLUSION

Mesenchymal stem/stromal cell-exosomes are an emerging treatment for a variety of inflammatory and degenerative conditions, and are beginning to be translated from preclinical models into early phase clinical trials. For ARS, not only will therapies like MSCs, MSC-exosomes, and MSC-educated/MSC exosome-educated macrophages need to be tested for safety and efficacy, but they will also need to retain their function after cryopreservation/thawing so that supplies could be added to a National Stockpile or be transported on a space shuttle. Testing these cell-based options will either require clinical trials in patients with cancer receiving molecularly targeted radioactive therapies that show hematopoietic toxicity requiring growth factors, transfusions or HSCT, or become approved through mechanisms that bypass testing in patients like the FDA two-animal rule (Singh and Olabisi, 2017). Likewise, biomanufacturing standards need to be defined and standardized release criteria need to be developed for MSC-exosomes as they are used to treat other inflammatory conditions such as GVHD or COVID-19, as well as degenerative conditions such as cardiovascular disease and stroke. Depending on the indication, different potency assays may need to be used to verify anti-inflammatory versus tissue regenerative properties of MSC-exosomes. For these milestones to be met, increasing support from government agencies like NIAID, Department of Defense, NASA, and FDA will be needed to insure successful biomanufacturing of MSC-exosomes.

AUTHOR CONTRIBUTIONS

MF drafted the manuscript. JK, PH, and CC revised the manuscript. All authors approved the final version of the manuscript.

FUNDING

This work was supported in part by the Don Anderson GVHD fund and Crystal Carney Fund for Leukemia Research (PH), St. Baldrick's-Stand Up To Cancer Pediatric Dream Team Translational Research Grant SU2C-AACR-DT-27-17, NIH/NCATS UL1TR000427 to the UW ICTR and NIH/NCI P30 CA014520 to the UWCCC (PH and CC), and NIH/NCI R01 CA215461 (CC). Stand Up To Cancer is a division of the Entertainment Industry Foundation. Research grants are administered by the American Association for Cancer Research, the scientific partner of SU2C. The contents of this article do not necessarily reflect the views or policies of the Department of Health and Human Services, nor does mention of trade names, commercial products, or organizations imply endorsement by the US Government. None of these funding sources had any input in the study design, analysis, manuscript preparation, or decision to submit for publication.

REFERENCES

Ahn, S. Y., Chang, Y. S., Kim, J. H., Sung, S. I., and Park, W. S. (2017). Two-year follow-up outcomes of premature infants enrolled in the phase I trial of mesenchymal stem cells transplantation for bronchopulmonary dysplasia. *J. Pediatr.* 185, 49–54.e2. doi: 10.1016/j.jpeds.2017.02.061

Al Demour, S., Jafar, H., Adwan, S., Alsharif, A., Alhawari, H., Alrabadi, A., et al. (2018). Safety and potential therapeutic effect of two intracavernous autologous bone marrow derived mesenchymal stem cells injections in diabetic patients with erectile dysfunction: an open label phase I clinical trial. *Urol. Int.* 101, 358–365. doi: 10.1159/000492120

Arslan, F., Lai, R. C., Smeets, M. B., Akeroyd, L., Choo, A., Aguor, E. N., et al. (2013). Mesenchymal stem cell-derived exosomes increase ATP levels, decrease oxidative stress and activate PI3K/Akt pathway to enhance myocardial viability and prevent adverse remodeling after myocardial ischemia/reperfusion injury. *Stem Cell Res.* 10, 301–312. doi: 10.1016/j.scr.2013.01.002

Bang, O. Y., Lee, J. S., Lee, P. H., and Lee, G. (2005). Autologous mesenchymal stem cell transplantation in stroke patients. *Ann. Neurol.* 57, 874–882. doi: 10.1002/ana.20501

Bartolucci, J., Verdugo, F. J., Gonzalez, P. L., Larrea, R. E., Abarzua, E., Goset, C., et al. (2017). Safety and efficacy of the intravenous infusion of umbilical cord mesenchymal stem cells in patients with heart failure: a phase 1/2 randomized controlled trial (RIMECARD trial [Randomized Clinical Trial of Intravenous Infusion Umbilical Cord Mesenchymal Stem Cells on Cardiopathy]). *Circ. Res.* 121, 1192–1204. doi: 10.1161/circresaha.117.310712

Bebelman, M. P., Smit, M. J., Pegtel, D. M., and Baglio, S. R. (2018). Biogenesis and function of extracellular vesicles in cancer. *Pharmacol. Ther.* 188, 1–11. doi: 10.1016/j.pharmthera.2018.02.013

Bell, B. I., Koduri, S., Salas Salinas, C., Monslow, J., Puré, E., Ben-Josef, E., et al. (2019). Interleukin 6 signaling blockade exacerbates acute and late injury from focal intestinal irradiation. *Int J. Radiat. Oncol. Biol. Phys.* 103, 719–727. doi: 10.1016/j.ijrobp.2018.10.007

Bernardo, M. E., Pagliara, D., and Locatelli, F. (2012). Mesenchymal stromal cell therapy: a revolution in Regenerative Medicine? *Bone Marrow Transplant.* 47, 164–171. doi: 10.1038/bmt.2011.81

Berry, J. D., Cudkowicz, M. E., Windebank, A. J., Staff, N. P., Owegi, M., Nicholson, K., et al. (2019). NurOwn, phase 2, randomized, clinical trial in patients with ALS: safety, clinical, and biomarker results. *Neurology* 93, e2294–e2305. doi: 10.1212/wnl.0000000000008620

Bhansali, S., Dutta, P., Kumar, V., Yadav, M. K., Jain, A., Mudaliar, S., et al. (2017). Efficacy of autologous bone marrow-derived mesenchymal stem cell and mononuclear cell transplantation in type 2 diabetes mellitus: a randomized. Placebo-Controlled Comparative Study. *Stem Cells Dev.* 26, 471–481. doi: 10.1089/scd.2016.0275

Bonab, M. M., Sahraian, M. A., Aghsaie, A., Karvigh, S. A., Hosseinian, S. M., Nikbin, B., et al. (2012). Autologous mesenchymal stem cell therapy in progressive multiple sclerosis: an open label study. *Curr. Stem Cell Res. Ther.* 7, 407–414. doi: 10.2174/157488812804484648

Bouchlaka, M. N., Moffitt, A. B., Kim, J., Kink, J. A., Bloom, D. D., Love, C., et al. (2017). Human mesenchymal stem cell-educated macrophages are a distinct high IL-6-producing subset that confer protection in graft-versus-host-disease and radiation injury models. *Biol. Blood Marrow Transplant.* 23, 897–905. doi: 10.1016/j.bbmt.2017.02.018

Braun, R. K., Chetty, C., Balasubramaniam, V., Centanni, R., Haraldsdottir, K., Hematti, P., et al. (2018). Intraperitoneal injection of MSC-derived exosomes prevent experimental bronchopulmonary dysplasia. *Biochem. Biophys. Res. Commun.* 503, 2653–2658. doi: 10.1016/j.bbrc.2018.08.019

Butler, J., Epstein, S. E., Greene, S. J., Quyyumi, A. A., Sikora, S., Kim, R. J., et al. (2017). Intravenous allogeneic mesenchymal stem cells for nonischemic cardiomyopathy: safety and efficacy results of a phase II-A randomized trial. *Circ. Res.* 120, 332–340. doi: 10.1161/circresaha.116.309717

Cai, J., Wu, Z., Xu, X., Liao, L., Chen, J., Huang, L., et al. (2016). Umbilical cord mesenchymal stromal cell with autologous bone marrow cell transplantation in established type 1 diabetes: a pilot randomized controlled open-label clinical study to assess safety and impact on insulin secretion. *Diabetes Care* 39, 149–157. doi: 10.2337/dc15-0171

Casado, S., Lobo, M. D. V. T., and Paíno, C. L. (2017). Dynamics of plasma membrane surface related to the release of extracellular vesicles by mesenchymal stem cells in culture. *Sci. Rep.* 7:6767.

Cerezo, L., and Macia, I. G. M. (2012). Acute radiation syndrome and Fukushima: A watershed moment? *Rep. Pract. Oncol. Radiother.* 17, 1–3. doi: 10.1016/j.rpor.2012.01.001

Chabannes, D., Hill, M., Merieau, E., Rossignol, J., Brion, R., Soulillou, J. P., et al. (2007). A role for heme oxygenase-1 in the immunosuppressive effect of adult rat and human mesenchymal stem cells. *Blood* 110, 3691–3694. doi: 10.1182/blood-2007-02-075481

Chamberlain, C. S., Clements, A. E. B., Kink, J. A., Choi, U., Baer, G. S., Halanski, M. A., et al. (2019). Extracellular vesicle-educated macrophages promote early Achilles tendon healing. *Stem Cells* 37, 652–662. doi: 10.1002/stem.2988

Chancellor, J. C., Scott, G. B., and Sutton, J. P. (2014). Space radiation: the number one risk to astronaut health beyond low earth orbit. *Life* 4, 491–510. doi: 10.3390/life4030491

Chang, Y. S., Ahn, S. Y., Yoo, H. S., Sung, S. I., Choi, S. J., Oh, W. I., et al. (2014). Mesenchymal stem cells for bronchopulmonary dysplasia: phase 1 dose-escalation clinical trial. *J. Pediatr.* 164, 966–972.e6. doi: 10.1016/j.jpeds.2013.12.011

Chen, C. C., Liu, L., Ma, F., Wong, C. W., Guo, X. E., Chacko, J. V., et al. (2016). Elucidation of exosome migration across the blood-brain barrier model *in vitro*. *Cell. Mol. Bioeng.* 9, 509–529. doi: 10.1007/s12195-016-0458-3

Chen, S., Zhao, K., Lin, R., Wang, S., Fan, Z., Huang, F., et al. (2019). The efficacy of mesenchymal stem cells in bronchiolitis obliterans syndrome after allogeneic HSCT: a multicenter prospective cohort study. *EBioMedicine* 49, 213–222. doi: 10.1016/j.ebiom.2019.09.039

Cheng, Y., Zeng, Q., Han, Q., and Xia, W. (2019). Effect of pH, temperature and freezing-thawing on quantity changes and cellular uptake of exosomes. *Protein Cell* 10, 295–299. doi: 10.1007/s13238-018-0529-4

Chin, S. P., Poey, A. C., Wong, C. Y., Chang, S. K., Tan, C. S., Ng, M. T., et al. (2011). Intramyocardial and intracoronary autologous bone marrow-derived mesenchymal stromal cell treatment in chronic severe dilated cardiomyopathy. *Cytotherapy* 13, 814–821. doi: 10.3109/14653249.2011.574118

Corcione, A., Benvenuto, F., Ferretti, E., Giunti, D., Cappiello, V., Cazzanti, F., et al. (2006). Human mesenchymal stem cells modulate B-cell functions. *Blood* 107, 367–372.

Cousin, B., Andre, M., Arnaud, E., Penicaud, L., and Casteilla, L. (2003). Reconstitution of lethally irradiated mice by cells isolated from adipose tissue. *Biochem. Biophys. Res. Commun.* 301, 1016–1022. doi: 10.1016/s0006-291x(03)00061-5

Cutler, A. J., Limbani, V., Girdlestone, J., and Navarrete, C. V. (2010). Umbilical cord-derived mesenchymal stromal cells modulate monocyte function to suppress T cell proliferation. *J. Immunol.* 185, 6617–6623. doi: 10.4049/jimmunol.1002239

Dainiak, N. (2018). Medical management of acute radiation syndrome and associated infections in a high-casualty incident. *J. Radiat. Res.* 59, ii54–ii64. doi: 10.1093/jrr/rry004

D'Asti, E., Garnier, D., Lee, T. H., Montermini, L., Meehan, B., and Rak, J. (2012). Oncogenic extracellular vesicles in brain tumor progression. *Front. Physiol.* 3:294. doi: 10.3389/fphys.2012.00294

Davatchi, F., Abdollahi, B. S., Mohyeddin, M., Shahram, F., and Nikbin, B. (2011). Mesenchymal stem cell therapy for knee osteoarthritis. Preliminary report of four patients. *Int. J. Rheum. Dis.* 14, 211–215. doi: 10.1111/j.1756-185x.2011.01599.x

Davatchi, F., Sadeghi Abdollahi, B., Mohyeddin, M., and Nikbin, B. (2016). Mesenchymal stem cell therapy for knee osteoarthritis: 5 years follow-up of three patients. *Int. J. Rheum. Dis.* 19, 219–225. doi: 10.1111/1756-185x.12670

Davies, L. C., Boberg, E., and Le Blanc, K. (2017). Commentary: role of mesenchymal stromal cell-mediated crosstalk with macrophages in graft-versus-host disease and tissue repair. *Biol. Blood Marrow Transplant.* 23, 861–862. doi: 10.1016/j.bbmt.2017.04.006

de Araujo Farias, V., Carrillo-Galvez, A. B., Martin, F., and Anderson, P. (2018). TGF-beta and mesenchymal stromal cells in regenerative medicine, autoimmunity and cancer. *Cytokine Growth Factor Rev.* 43, 25–37. doi: 10.1016/j.cytogfr.2018.06.002

de Oliveira, H. G., Cruz, F. F., Antunes, M. A., De Macedo Neto, A. V., Oliveira, G. A., Svartman, F. M., et al. (2017). Combined bone marrow-derived mesenchymal stromal cell therapy and one-way endobronchial valve placement in patients with pulmonary emphysema: a phase i clinical trial. *Stem Cells Transl. Med.* 6, 962–969. doi: 10.1002/sctm.16-0315

DiCarlo, A. L., Tamarat, R., Rios, C. I., Benderitter, M., Czarniecki, C. W., Allio, T. C., et al. (2017). Cellular therapies for treatment of radiation injury: report from a NIH/NIAID and IRSN workshop. *Radiat. Res.* 188, e54–e75. doi: 10.1667/rr14810.1

Emadedin, M., Labibzadeh, N., Liastani, M. G., Karimi, A., Jaroughi, N., Bolurieh, T., et al. (2018). Intra-articular implantation of autologous bone marrow-derived mesenchymal stromal cells to treat knee osteoarthritis: a randomized, triple-blind, placebo-controlled phase 1/2 clinical trial. *Cytotherapy* 20, 1238–1246. doi: 10.1016/j.jcyt.2018.08.005

Engela, A. U., Baan, C. C., Litjens, N. H., Franquesa, M., Betjes, M. G., Weimar, W., et al. (2013). Mesenchymal stem cells control alloreactive CD8(+) CD28(-) T cells. *Clin. Exp. Immunol.* 174, 449–458. doi: 10.1111/cei.12199

Eslani, M., Putra, I., Shen, X., Hamouie, J., Tadepalli, A., Anwar, K. N., et al. (2018). Cornea-derived mesenchymal stromal cells therapeutically modulate macrophage immunophenotype and angiogenic function. *Stem Cells* 36, 775–784. doi: 10.1002/stem.2781

Falanga, V., Iwamoto, S., Chartier, M., Yufit, T., Butmarc, J., Kouttab, N., et al. (2007). Autologous bone marrow-derived cultured mesenchymal stem cells delivered in a fibrin spray accelerate healing in murine and human cutaneous wounds. *Tissue Eng.* 13, 1299–1312. doi: 10.1089/ten.2006.0278

Fang, S., Xu, C., Zhang, Y., Xue, C., Yang, C., Bi, H., et al. (2016). Umbilical cord-derived mesenchymal stem cell-derived exosomal microRNAs suppress myofibroblast differentiation by inhibiting the transforming growth factor-beta/SMAD2 pathway during wound healing. *Stem Cells Transl. Med.* 5, 1425–1439. doi: 10.5966/sctm.2015-0367

Fitzgerald, W., Freeman, M. L., Lederman, M. M., Vasilieva, E., Romero, R., and Margolis, L. (2018). A system of cytokines encapsulated in ExtraCellular vesicles. *Sci. Rep.* 8:8973.

Friis, T., Haack-Sorensen, M., Mathiasen, A. B., Ripa, R. S., Kristoffersen, U. S., Jorgensen, E., et al. (2011). Mesenchymal stromal cell derived endothelial progenitor treatment in patients with refractory angina. *Scand. Cardiovasc. J.* 45, 161–168. doi: 10.3109/14017431.2011.569571

Fujii, S., Miura, Y., Fujishiro, A., Shindo, T., Shimazu, Y., Hirai, H., et al. (2018). Graft-versus-host disease amelioration by human bone marrow mesenchymal stromal/stem cell-derived extracellular vesicles is associated with peripheral preservation of naive T cell populations. *Stem Cells* 36, 434–445. doi: 10.1002/stem.2759

Fukumoto, R. (2016). Mesenchymal stem cell therapy for acute radiation syndrome. *Mil. Med. Res.* 3:17.

Gaberman, E., Pinzur, L., Levdansky, L., Tsirlin, M., Netzer, N., Aberman, Z., et al. (2013). Mitigation of lethal radiation syndrome in mice by intramuscular injection of 3D cultured adherent human placental stromal cells. *PLoS One* 8:e66549. doi: 10.1371/journal.pone.0066549

Galun, E., and Rose-John, S. (2013). The regenerative activity of interleukin-6. *Methods Mol. Biol.* 982, 59–77. doi: 10.1007/978-1-62703-308-4_4

Gao, L., Zhang, Y., Hu, B., Liu, J., Kong, P., Lou, S., et al. (2016). Phase II multicenter, randomized, double-blind controlled study of efficacy and safety of umbilical cord-derived mesenchymal stromal cells in the prophylaxis of chronic graft-versus-host disease after HLA-Haploidentical stem-cell transplantation. *J. Clin. Oncol.* 34, 2843–2850. doi: 10.1200/jco.2015.65.3642

Garnett, C., Apperley, J. F., and Pavlù, J. (2013). Treatment and management of graft-versus-host disease: improving response and survival. *Ther. Adv. Hematol.* 4, 366–378. doi: 10.1177/2040620713489842

Ghimire, S., Weber, D., Mavin, E., Wang, X. N., Dickinson, A. M., and Holler, E. (2017). Pathophysiology of GvHD and other HSCT-related major complications. *Front. Immunol.* 8:79. doi: 10.3389/fimmu.2017.00079

Ghoryani, M., Shariati-Sarabi, Z., Tavakkol-Afshari, J., Ghasemi, A., Poursamimi, J., and Mohammadi, M. (2019). Amelioration of clinical symptoms of patients with refractory rheumatoid arthritis following treatment with autologous bone marrow-derived mesenchymal stem cells: a successful clinical trial in Iran. *Biomed. Pharmacother.* 109, 1834–1840. doi: 10.1016/j.biopha.2018.11.056

Golpanian, S., El-Khorazaty, J., Mendizabal, A., Difede, D. L., Suncion, V. Y., Karantalis, V., et al. (2015). Effect of aging on human mesenchymal stem cell therapy in ischemic cardiomyopathy patients. *J. Am. Coll. Cardiol.* 65, 125–132. doi: 10.1016/j.jacc.2014.10.040

Golpanian, S., Wolf, A., Hatzistergos, K. E., and Hare, J. M. (2016). Rebuilding the damaged heart: mesenchymal stem cells, cell-based therapy, and engineered heart tissue. *Physiol. Rev.* 96, 1127–1168. doi: 10.1152/physrev.00019.2015

Gotherstrom, C., Westgren, M., Shaw, S. W., Astrom, E., Biswas, A., Byers, P. H., et al. (2014). Pre- and postnatal transplantation of fetal mesenchymal stem cells in osteogenesis imperfecta: a two-center experience. *Stem Cells Transl. Med.* 3, 255–264. doi: 10.5966/sctm.2013-0090

Gourmelon, P., Benderitter, M., Bertho, J. M., Huet, C., Gorin, N. C., and De Revel, P. (2010). European consensus on the medical management of acute radiation syndrome and analysis of the radiation accidents in Belgium and Senegal. *Health Phys.* 98, 825–832. doi: 10.1097/hp.0b013e3181ce64d4

Haack-Sorensen, M., Friis, T., Mathiasen, A. B., Jorgensen, E., Hansen, L., Dickmeiss, E., et al. (2013). Direct intramyocardial mesenchymal stromal cell injections in patients with severe refractory angina: one-year follow-up. *Cell Transplant.* 22, 521–528. doi: 10.3727/096368912x636830

Hare, J. M., Fishman, J. E., Gerstenblith, G., Difede Velazquez, D. L., Zambrano, J. P., Suncion, V. Y., et al. (2012). Comparison of allogeneic vs autologous bone marrow-derived mesenchymal stem cells delivered by transendocardial injection in patients with ischemic cardiomyopathy: the POSEIDON randomized trial. *JAMA* 308, 2369–2379.

Hare, J. M., Traverse, J. H., Henry, T. D., Dib, N., Strumpf, R. K., Schulman, S. P., et al. (2009). A randomized, double-blind, placebo-controlled, dose-escalation study of intravenous adult human mesenchymal stem cells (prochymal) after acute myocardial infarction. *J. Am. Coll. Cardiol.* 54, 2277–2286. doi: 10.1016/j.jacc.2009.06.055

Harris, V. K., Stark, J., Vyshkina, T., Blackshear, L., Joo, G., Stefanova, V., et al. (2018). Phase I trial of intrathecal mesenchymal stem cell-derived neural progenitors in progressive multiple sclerosis. *EBioMedicine* 29, 23–30. doi: 10.1016/j.ebiom.2018.02.002

Hass, R., Kasper, C., Böhm, S., and Jacobs, R. (2011). Different populations and sources of human mesenchymal stem cells (MSC): a comparison of adult and neonatal tissue-derived MSC. *Cell Commun. Signal.* 9:12.

Helwa, I., Cai, J., Drewry, M. D., Zimmerman, A., Dinkins, M. B., Khaled, M. L., et al. (2017). A comparative study of serum exosome isolation using differential ultracentrifugation and three commercial reagents. *PLoS One* 12:e0170628. doi: 10.1371/journal.pone.0170628

Hernigou, P., Dubory, A., Homma, Y., Guissou, I., Flouzat Lachaniette, C. H., Chevallier, N., et al. (2018). Cell therapy versus simultaneous contralateral decompression in symptomatic corticosteroid osteonecrosis: a thirty year follow-up prospective randomized study of one hundred and twenty five adult patients. *Int. Orthop.* 42, 1639–1649. doi: 10.1007/s00264-018-3941-8

Heslet, L., Bay, C., and Nepper-Christensen, S. (2012). Acute radiation syndrome (ARS) - treatment of the reduced host defense. *Int. J. Gen. Med.* 5, 105–115.

Hessvik, N. P., and Llorente, A. (2018). Current knowledge on exosome biogenesis and release. *Cell. Mol. Life Sci.* 75, 193–208. doi: 10.1007/s00018-017-2595-9

Hlebokazov, F., Dakukina, T., Ihnatsenko, S., Kosmacheva, S., Potapnev, M., Shakhbazau, A., et al. (2017). Treatment of refractory epilepsy patients with autologous mesenchymal stem cells reduces seizure frequency: an open label study. *Adv. Med. Sci.* 62, 273–279. doi: 10.1016/j.advms.2016.12.004

Hsu, W. T., Lin, C. H., Chiang, B. L., Jui, H. Y., Wu, K. K., and Lee, C. M. (2013). Prostaglandin E2 potentiates mesenchymal stem cell-induced IL-10+IFN-gamma+CD4+ regulatory T cells to control transplant arteriosclerosis. *J. Immunol.* 190, 2372–2380. doi: 10.4049/jimmunol.1202996

Huang, J. H., Yin, X. M., Xu, Y., Xu, C. C., Lin, X., Ye, F. B., et al. (2017). Systemic administration of exosomes released from mesenchymal stromal cells attenuates apoptosis, inflammation, and promotes angiogenesis after spinal cord injury in rats. *J. Neurotrauma* 34, 3388–3396. doi: 10.1089/neu.2017.5063

Huang, L., Zhang, C., Gu, J., Wu, W., Shen, Z., Zhou, X., et al. (2018). A randomized, placebo-controlled trial of human umbilical cord blood mesenchymal stem cell infusion for children with cerebral palsy. *Cell Transplant.* 27, 325–334. doi: 10.1177/0963689717729379

Jiang, R., Han, Z., Zhuo, G., Qu, X., Li, X., Wang, X., et al. (2011). Transplantation of placenta-derived mesenchymal stem cells in type 2 diabetes: a pilot study. *Front. Med.* 5, 94–100. doi: 10.1007/s11684-011-0116-z

Jiang, X. X., Zhang, Y., Liu, B., Zhang, S. X., Wu, Y., Yu, X. D., et al. (2005). Human mesenchymal stem cells inhibit differentiation and function of monocyte-derived dendritic cells. *Blood* 105, 4120–4126. doi: 10.1182/blood-2004-02-0586

Joo, H. S., Suh, J. H., Lee, H. J., Bang, E. S., and Lee, J. M. (2020). Current knowledge and future perspectives on mesenchymal stem cell-derived exosomes as a new therapeutic agent. *Int. J. Mol. Sci.* 21:727. doi: 10.3390/ijms21030727

Jung, J. W., Kwon, M., Choi, J. C., Shin, J. W., Park, I. W., Choi, B. W., et al. (2013). Familial occurrence of pulmonary embolism after intravenous, adipose tissue-derived stem cell therapy. *Yonsei Med. J.* 54, 1293–1296.

Kahroba, H., Hejazi, M. S., and Samadi, N. (2019). Exosomes: from carcinogenesis and metastasis to diagnosis and treatment of gastric cancer. *Cell. Mol. Life Sci.* 76, 1747–1758. doi: 10.1007/s00018-019-03035-2

Karantalis, V., Difede, D. L., Gerstenblith, G., Pham, S., Symes, J., Zambrano, J. P., et al. (2014). Autologous mesenchymal stem cells produce concordant improvements in regional function, tissue perfusion, and fibrotic burden when administered to patients undergoing coronary artery bypass grafting: the Prospective Randomized Study of Mesenchymal Stem Cell Therapy in Patients Undergoing Cardiac Surgery (PROMETHEUS) trial. *Circ. Res.* 114, 1302–1310. doi: 10.1161/circresaha.114.303180

Karussis, D., Karageorgiou, C., Vaknin-Dembinsky, A., Gowda-Kurkalli, B., Gomori, J. M., Kassis, I., et al. (2010). Safety and immunological effects of mesenchymal stem cell transplantation in patients with multiple sclerosis and amyotrophic lateral sclerosis. *Arch. Neurol.* 67, 1187–1194.

Khalifeh Soltani, S., Forogh, B., Ahmadbeigi, N., Hadizadeh Kharazi, H., Fallahzadeh, K., Kashani, L., et al. (2019). Safety and efficacy of allogenic placental mesenchymal stem cells for treating knee osteoarthritis: a pilot study. *Cytotherapy* 21, 54–63. doi: 10.1016/j.jcyt.2018.11.003

Kim, H. S., Lee, J. H., Roh, K. H., Jun, H. J., Kang, K. S., and Kim, T. Y. (2017). Clinical trial of human umbilical cord blood-derived stem cells for the treatment of moderate-to-severe Atopic dermatitis: phase I/IIa studies. *Stem Cells* 35, 248–255. doi: 10.1002/stem.2401

Kim, J., and Hematti, P. (2009). Mesenchymal stem cell-educated macrophages: a novel type of alternatively activated macrophages. *Exp. Hematol.* 37, 1445–1453. doi: 10.1016/j.exphem.2009.09.004

Kim, S. H., Cho, J. H., Lee, Y. H., Lee, J. H., Kim, S. S., Kim, M. Y., et al. (2018). Improvement in left ventricular function with intracoronary mesenchymal stem cell therapy in a patient with anterior wall ST-segment elevation myocardial infarction. *Cardiovasc. Drugs Ther.* 32, 329–338. doi: 10.1007/s10557-018-6804-z

Kink, J. A., Forsberg, M. H., Reshetylo, S., Besharat, S., Childs, C. J., Pederson, J. D., et al. (2019). Macrophages educated with exosomes from primed mesenchymal stem cells treat acute radiation syndrome by promoting hematopoietic recovery. *Biol. Blood Marrow Transplant.* 25, 2124–2133. doi: 10.1016/j.bbmt.2019.07.026

Koc, O. N., Day, J., Nieder, M., Gerson, S. L., Lazarus, H. M., and Krivit, W. (2002). Allogeneic mesenchymal stem cell infusion for treatment of metachromatic leukodystrophy (MLD) and Hurler syndrome (MPS-IH). *Bone Marrow Transplant.* 30, 215–222. doi: 10.1038/sj.bmt.1703650

Koh, Y. G., and Choi, Y. J. (2012). Infrapatellar fat pad-derived mesenchymal stem cell therapy for knee osteoarthritis. *Knee* 19, 902–907. doi: 10.1016/j.knee.2012.04.001

Kordelas, L., Rebmann, V., Ludwig, A. K., Radtke, S., Ruesing, J., Doeppner, T. R., et al. (2014). MSC-derived exosomes: a novel tool to treat therapy-refractory graft-versus-host disease. *Leukemia* 28, 970–973. doi: 10.1038/leu.2014.41

Lai, P., Chen, X., Guo, L., Wang, Y., Liu, X., Liu, Y., et al. (2018). A potent immunomodulatory role of exosomes derived from mesenchymal stromal cells in preventing cGVHD. *J. Hematol. Oncol.* 11, 135–135.

Lai, R. C., Arslan, F., Lee, M. M., Sze, N. S., Choo, A., Chen, T. S., et al. (2010). Exosome secreted by MSC reduces myocardial ischemia/reperfusion injury. *Stem Cell Res.* 4, 214–222. doi: 10.1016/j.scr.2009.12.003

Lamo-Espinosa, J. M., Mora, G., Blanco, J. F., Granero-Molto, F., Nunez-Cordoba, J. M., Lopez-Elio, S., et al. (2018). Intra-articular injection of two different doses of autologous bone marrow mesenchymal stem cells versus hyaluronic acid in the treatment of knee osteoarthritis: long-term follow up of a multicenter randomized controlled clinical trial (phase I/II). *J. Transl. Med.* 16:213.

Lamo-Espinosa, J. M., Mora, G., Blanco, J. F., Granero-Molto, F., Nunez-Cordoba, J. M., Sanchez-Echenique, C., et al. (2016). Intra-articular injection of two different doses of autologous bone marrow mesenchymal stem cells versus hyaluronic acid in the treatment of knee osteoarthritis: multicenter randomized controlled clinical trial (phase I/II). *J. Transl. Med.* 14:246.

Lange, C., Brunswig-Spickenheier, B., Cappallo-Obermann, H., Eggert, K., Gehling, U. M., Rudolph, C., et al. (2011). Radiation rescue: mesenchymal stromal cells protect from lethal irradiation. *PLoS One* 6:e14486. doi: 10.1371/journal.pone.0014486

Lee, E. J., Hwang, I., Lee, J. Y., Park, J. N., Kim, K. C., Kim, G. H., et al. (2018). Hepatocyte growth factor improves the therapeutic efficacy of human bone marrow mesenchymal stem cells via RAD51. *Mol. Ther.* 26, 845–859. doi: 10.1016/j.ymthe.2017.12.015

Lee, J. S., Hong, J. M., Moon, G. J., Lee, P. H., Ahn, Y. H., Bang, O. Y., et al. (2010). A long-term follow-up study of intravenous autologous mesenchymal stem cell transplantation in patients with ischemic stroke. *Stem Cells* 28, 1099–1106. doi: 10.1002/stem.430

Lee, P. H., Kim, J. W., Bang, O. Y., Ahn, Y. H., Joo, I. S., and Huh, K. (2008). Autologous mesenchymal stem cell therapy delays the progression of neurological deficits in patients with multiple system atrophy. *Clin. Pharmacol. Ther.* 83, 723–730. doi: 10.1038/sj.clpt.6100386

Lee, P. H., Lee, J. E., Kim, H. S., Song, S. K., Lee, H. S., Nam, H. S., et al. (2012). A randomized trial of mesenchymal stem cells in multiple system atrophy. *Ann. Neurol.* 72, 32–40.

Li, J. F., Zhang, D. J., Geng, T., Chen, L., Huang, H., Yin, H. L., et al. (2014). The potential of human umbilical cord-derived mesenchymal stem cells as a novel cellular therapy for multiple sclerosis. *Cell Transplant.* 23(Suppl. 1), S113–S122.

Li, M., Sun, X., Kuang, X., Liao, Y., Li, H., and Luo, D. (2014). Mesenchymal stem cells suppress CD8+ T cell-mediated activation by suppressing natural killer group 2, member D protein receptor expression and secretion of prostaglandin E2, indoleamine 2, 3-dioxygenase and transforming growth factor-beta. *Clin. Exp. Immunol.* 178, 516–524. doi: 10.1111/cei.12423

Liang, J., Zhang, H., Zhao, C., Wang, D., Ma, X., Zhao, S., et al. (2017). Effects of allogeneic mesenchymal stem cell transplantation in the treatment of liver cirrhosis caused by autoimmune diseases. *Int. J. Rheum. Dis.* 20, 1219–1226. doi: 10.1111/1756-185x.13015

Lin, B. L., Chen, J. F., Qiu, W. H., Wang, K. W., Xie, D. Y., Chen, X. Y., et al. (2017). Allogeneic bone marrow-derived mesenchymal stromal cells for hepatitis B virus-related acute-on-chronic liver failure: a randomized controlled trial. *Hepatology* 66, 209–219. doi: 10.1002/hep.29189

Lopez, M., and Martin, M. (2011). Medical management of the acute radiation syndrome. *Rep. Pract. Oncol. Radiother.* 16, 138–146.

Majka, M., Sułkowski, M., Badyra, B., and Musiałek, P. (2017). Concise review: mesenchymal stem cells in cardiovascular regeneration: emerging research directions and clinical applications. *Stem Cells Transl. Med.* 6, 1859–1867. doi: 10.1002/sctm.16-0484

Mashouri, L., Yousefi, H., Aref, A. R., Ahadi, A. M., Molaei, F., and Alahari, S. K. (2019). Exosomes: composition, biogenesis, and mechanisms in cancer metastasis and drug resistance. *Mol. Cancer* 18:75.

Matas, J., Orrego, M., Amenabar, D., Infante, C., Tapia-Limonchi, R., Cadiz, M. I., et al. (2019). Umbilical cord-derived mesenchymal stromal cells (MSCs) for knee osteoarthritis: repeated MSC dosing is superior to a single MSC dose and to Hyaluronic acid in a controlled randomized phase I/II trial. *Stem Cells Transl. Med.* 8, 215–224. doi: 10.1002/sctm.18-0053

Mathiasen, A. B., Qayyum, A. A., Jorgensen, E., Helqvist, S., Fischer-Nielsen, A., Kofoed, K. F., et al. (2015). Bone marrow-derived mesenchymal stromal cell treatment in patients with severe ischaemic heart failure: a randomized placebo-controlled trial (MSC-HF trial). *Eur. Heart J.* 36, 1744–1753. doi: 10.1093/eurheartj/ehv136

Mathivanan, S., Ji, H., and Simpson, R. J. (2010). Exosomes: extracellular organelles important in intercellular communication. *J. Proteomics* 73, 1907–1920. doi: 10.1016/j.jprot.2010.06.006

Mettler, F. A. Jr., Gus'kova, A. K., and Gusev, I. (2007). Health effects in those with acute radiation sickness from the Chernobyl accident. *Health Phys.* 93, 462–469. doi: 10.1097/01.hp.0000278843.27969.74

Mohyeddin Bonab, M., Yazdanbakhsh, S., Lotfi, J., Alimoghaddom, K., Talebian, F., Hooshmand, F., et al. (2007). Does mesenchymal stem cell therapy help multiple sclerosis patients? Report of a pilot study. *Iran. J. Immunol.* 4, 50–57.

Musiał-Wysocka, A., Kot, M., and Majka, M. (2019). The pros and cons of mesenchymal stem cell-based therapies. *Cell Transplant.* 28, 801–812. doi: 10.1177/0963689719837897

Nakamura, Y., Miyaki, S., Ishitobi, H., Matsuyama, S., Nakasa, T., Kamei, N., et al. (2015). Mesenchymal-stem-cell-derived exosomes accelerate skeletal muscle regeneration. *FEBS Lett.* 589, 1257–1265. doi: 10.1016/j.febslet.2015.03.031

Nemeth, K., Leelahavanichkul, A., Yuen, P. S., Mayer, B., Parmelee, A., Doi, K., et al. (2009). Bone marrow stromal cells attenuate sepsis via prostaglandin E(2)-dependent reprogramming of host macrophages to increase their interleukin-10 production. *Nat. Med.* 15, 42–49. doi: 10.1038/nm.1905

Noriega, D. C., Ardura, F., Hernandez-Ramajo, R., Martin-Ferrero, M. A., Sanchez-Lite, I., Toribio, B., et al. (2017). Intervertebral disc repair by allogeneic mesenchymal bone marrow cells: a randomized controlled trial. *Transplantation* 101, 1945–1951. doi: 10.1097/tp.0000000000001484

Olivetti, G., Quaini, F., Sala, R., Lagrasta, C., Corradi, D., Bonacina, E., et al. (1996). Acute myocardial infarction in humans is associated with activation of programmed myocyte cell death in the surviving portion of the heart. *J. Mol. Cell Cardiol.* 28, 2005–2016. doi: 10.1006/jmcc.1996.0193

Orozco, L., Munar, A., Soler, R., Alberca, M., Soler, F., Huguet, M., et al. (2013). Treatment of knee osteoarthritis with autologous mesenchymal stem cells: a pilot study. *Transplantation* 95, 1535–1541. doi: 10.1097/tp.0b013e318291a2da

Orozco, L., Soler, R., Morera, C., Alberca, M., Sanchez, A., and Garcia-Sancho, J. (2011). Intervertebral disc repair by autologous mesenchymal bone marrow cells: a pilot study. *Transplantation* 92, 822–828. doi: 10.1097/tp.0b013e3182298a15

Ozdemir, Z. N., and Civriz Bozdag, S. (2018). Graft failure after allogeneic hematopoietic stem cell transplantation. *Transfus. Apher. Sci.* 57, 163–167.

Park, E. H., Lim, H. S., Lee, S., Roh, K., Seo, K. W., Kang, K. S., et al. (2018). intravenous infusion of umbilical cord blood-derived mesenchymal stem cells in rheumatoid arthritis: a phase Ia clinical trial. *Stem Cells Transl. Med.* 7, 636–642. doi: 10.1002/sctm.18-0031

Petrou, P., Gothelf, Y., Argov, Z., Gotkine, M., Levy, Y. S., Kassis, I., et al. (2016). Safety and clinical effects of mesenchymal stem cells secreting neurotrophic factor transplantation in patients with amyotrophic lateral sclerosis: results of phase 1/2 and 2a clinical trials. *JAMA Neurol.* 73, 337–344.

Pinzur, L., Akyuez, L., Levdansky, L., Blumenfeld, M., Volinsky, E., Aberman, Z., et al. (2018). Rescue from lethal acute radiation syndrome (ARS) with severe weight loss by secretome of intramuscularly injected human placental stromal cells. *J. Cachexia Sarcopenia Muscle* 9, 1079–1092. doi: 10.1002/jcsm.12342

Reddy, V. S., Madala, S. K., Trinath, J., and Reddy, G. B. (2018). Extracellular small heat shock proteins: exosomal biogenesis and function. *Cell Stress Chaperones* 23, 441–454. doi: 10.1007/s12192-017-0856-z

Reza-Zaldivar, E. E., Hernandez-Sapiens, M. A., Gutierrez-Mercado, Y. K., Sandoval-Avila, S., Gomez-Pinedo, U., Marquez-Aguirre, A. L., et al. (2019). Mesenchymal stem cell-derived exosomes promote neurogenesis and cognitive function recovery in a mouse model of Alzheimer's disease. *Neural Regen. Res.* 14, 1626–1634.

Riazifar, M., Mohammadi, M. R., Pone, E. J., Yeri, A., Lasser, C., Segaliny, A. I., et al. (2019). Stem cell-derived exosomes as nanotherapeutics for autoimmune and neurodegenerative disorders. *ACS Nano* 13, 6670–6688. doi: 10.1021/acsnano.9b01004

Riordan, N. H., Morales, I., Fernandez, G., Allen, N., Fearnot, N. E., Leckrone, M. E., et al. (2018). Clinical feasibility of umbilical cord tissue-derived mesenchymal stem cells in the treatment of multiple sclerosis. *J. Transl. Med.* 16:57.

Saad, A., Dietz, A. B., Herrmann, S. M. S., Hickson, L. J., Glockner, J. F., Mckusick, M. A., et al. (2017). Autologous mesenchymal stem cells increase cortical perfusion in Renovascular disease. *J. Am. Soc. Nephrol.* 28, 2777–2785. doi: 10.1681/asn.2017020151

Samaeekia, R., Rabiee, B., Putra, I., Shen, X., Park, Y. J., Hematti, P., et al. (2018). Effect of human corneal mesenchymal stromal cell-derived exosomes on corneal epithelial wound healing. *Invest. Ophthalmol. Vis. Sci.* 59, 5194–5200.

Scheller, J., Chalaris, A., Schmidt-Arras, D., and Rose-John, S. (2011). The pro- and anti-inflammatory properties of the cytokine interleukin-6. *Biochim. Biophys. Acta* 1813, 878–888.

Sengupta, V., Sengupta, S., Lazo, A., Woods, P., Nolan, A., and Bremer, N. (2020). Exosomes derived from bone marrow mesenchymal stem cells as treatment for severe COVID-19. *Stem Cells Dev.* 29, 747–754. doi: 10.1089/scd.2020.0080

Shadmanfar, S., Labibzadeh, N., Emadedin, M., Jaroughi, N., Azimian, V., Mardpour, S., et al. (2018). Intra-articular knee implantation of autologous bone marrow-derived mesenchymal stromal cells in rheumatoid arthritis patients with knee involvement: results of a randomized, triple-blind, placebo-controlled phase 1/2 clinical trial. *Cytotherapy* 20, 499–506. doi: 10.1016/j.jcyt.2017.12.009

Shi, M., Liu, Z., Wang, Y., Xu, R., Sun, Y., Zhang, M., et al. (2017). A pilot study of mesenchymal stem cell therapy for acute liver allograft rejection. *Stem Cells Transl. Med.* 6, 2053–2061. doi: 10.1002/sctm.17-0134

Shi, M., Zhang, Z., Xu, R., Lin, H., Fu, J., Zou, Z., et al. (2012). Human mesenchymal stem cell transfusion is safe and improves liver function in acute-on-chronic liver failure patients. *Stem Cells Transl. Med.* 1, 725–731. doi: 10.5966/sctm.2012-0034

Singer, W., Dietz, A. B., Zeller, A. D., Gehrking, T. L., Schmelzer, J. D., Schmeichel, A. M., et al. (2019). Intrathecal administration of autologous mesenchymal stem cells in multiple system atrophy. *Neurology* 93, e77–e87. doi: 10.1212/wnl.0000000000007720

Singh, V. K., and Olabisi, A. O. (2017). Nonhuman primates as models for the discovery and development of radiation countermeasures. *Expert Opin. Drug Discov.* 12, 695–709. doi: 10.1080/17460441.2017.1323863

Soler, R., Orozco, L., Munar, A., Huguet, M., Lopez, R., Vives, J., et al. (2016). Final results of a phase I-II trial using ex vivo expanded autologous Mesenchymal Stromal Cells for the treatment of osteoarthritis of the knee confirming safety and suggesting cartilage regeneration. *Knee* 23, 647–654. doi: 10.1016/j.knee.2015.08.013

Sotiropoulou, P. A., Perez, S. A., Gritzapis, A. D., Baxevanis, C. N., and Papamichail, M. (2006). Interactions between human mesenchymal stem cells and natural killer cells. *Stem Cells* 24, 74–85. doi: 10.1634/stemcells.2004-0359

Stewart, I., Schluter, P. J., and Shaw, G. R. (2006). Cyanobacterial lipopolysaccharides and human health - a review. *Environ. Health* 5:7.

Su, J., Chen, X., Huang, Y., Li, W., Li, J., Cao, K., et al. (2014). Phylogenetic distinction of iNOS and IDO function in mesenchymal stem cell-mediated immunosuppression in mammalian species. *Cell Death Differ.* 21, 388–396. doi: 10.1038/cdd.2013.149

Suk, K. T., Yoon, J. H., Kim, M. Y., Kim, C. W., Kim, J. K., Park, H., et al. (2016). Transplantation with autologous bone marrow-derived mesenchymal stem cells for alcoholic cirrhosis: phase 2 trial. *Hepatology* 64, 2185–2197.

Swart, J. F., De Roock, S., Nievelstein, R. A. J., Slaper-Cortenbach, I. C. M., Boelens, J. J., and Wulffraat, N. M. (2019). Bone-marrow derived mesenchymal stromal cells infusion in therapy refractory juvenile idiopathic arthritis patients. *Rheumatology* 58, 1812–1817. doi: 10.1093/rheumatology/kez157

Sykova, E., Rychmach, P., Drahoradova, I., Konradova, S., Ruzickova, K., Vorisek, I., et al. (2017). Transplantation of mesenchymal stromal cells in patients with

amyotrophic lateral sclerosis: results of phase I/IIa clinical trial. *Cell Transplant.* 26, 647–658. doi: 10.3727/096368916x693716

Taketani, T., Oyama, C., Mihara, A., Tanabe, Y., Abe, M., Hirade, T., et al. (2015). *Ex vivo* expanded allogeneic mesenchymal stem cells with bone marrow transplantation improved osteogenesis in infants with severe hypophosphatasia. *Cell Transplant.* 24, 1931–1943. doi: 10.3727/096368914x685410

Tan, J., Wu, W., Xu, X., Liao, L., Zheng, F., Messinger, S., et al. (2012). Induction therapy with autologous mesenchymal stem cells in living-related kidney transplants: a randomized controlled trial. *JAMA* 307, 1169–1177.

Tanaka, T., Narazaki, M., and Kishimoto, T. (2014). IL-6 in inflammation, immunity, and disease. *Cold Spring Harb. Perspect. Biol.* 6:a016295.

Teng, X., Chen, L., Chen, W., Yang, J., Yang, Z., and Shen, Z. (2015). Mesenchymal stem cell-derived exosomes improve the microenvironment of infarcted myocardium contributing to angiogenesis and anti-inflammation. *Cell. Physiol. Biochem.* 37, 2415–2424. doi: 10.1159/000438594

Tompkins, B. A., Difede, D. L., Khan, A., Landin, A. M., Schulman, I. H., Pujol, M. V., et al. (2017). Allogeneic mesenchymal stem cells ameliorate aging frailty: a phase II randomized, double-blind, placebo-controlled clinical trial. *J. Gerontol. A Biol. Sci. Med. Sci.* 72, 1513–1522. doi: 10.1093/gerona/glx137

Tran, S. D., Liu, Y., Xia, D., Maria, O. M., Khalili, S., Wang, R. W., et al. (2013). Paracrine effects of bone marrow soup restore organ function, regeneration, and repair in salivary glands damaged by irradiation. *PLoS One* 8:e61632. doi: 10.1371/journal.pone.0061632

Urbanelli, L., Magini, A., Buratta, S., Brozzi, A., Sagini, K., Polchi, A., et al. (2013). Signaling pathways in exosomes biogenesis, secretion and fate. *Genes* 4, 152–170. doi: 10.3390/genes4020152

Vaquero, J., Zurita, M., Rico, M. A., Aguayo, C., Bonilla, C., Marin, E., et al. (2018). Intrathecal administration of autologous mesenchymal stromal cells for spinal cord injury: safety and efficacy of the 100/3 guideline. *Cytotherapy* 20, 806–819.

Vega, A., Martin-Ferrero, M. A., Del Canto, F., Alberca, M., Garcia, V., Munar, A., et al. (2015). Treatment of knee osteoarthritis with allogeneic bone marrow mesenchymal stem cells: a randomized controlled trial. *Transplantation* 99, 1681–1690. doi: 10.1097/tp.0000000000000678

Wang, D., Li, J., Zhang, Y., Zhang, M., Chen, J., Li, X., et al. (2014). Umbilical cord mesenchymal stem cell transplantation in active and refractory systemic lupus erythematosus: a multicenter clinical study. *Arthritis Res. Ther.* 16:R79.

Wang, D., Zhang, H., Liang, J., Li, X., Feng, X., Wang, H., et al. (2013). Allogeneic mesenchymal stem cell transplantation in severe and refractory systemic lupus erythematosus: 4 years of experience. *Cell Transplant.* 22, 2267–2277. doi: 10.3727/096368911x582769c

Wang, P., Li, Y., Huang, L., Yang, J., Yang, R., Deng, W., et al. (2014). Effects and safety of allogenic mesenchymal stem cell intravenous infusion in active ankylosing spondylitis patients who failed NSAIDs: a 20-week clinical trial. *Cell Transplant.* 23, 1293–1303. doi: 10.3727/096368913x667727

Wang, X., Cheng, H., Hua, R., Yang, J., Dai, G., Zhang, Z., et al. (2013). Effects of bone marrow mesenchymal stromal cells on gross motor function measure scores of children with cerebral palsy: a preliminary clinical study. *Cytotherapy* 15, 1549–1562. doi: 10.1016/j.jcyt.2013.06.001

Wang, H., Li, Y., Wu, Q., Xu, C., and Liu, Q. (2016). Combination of butylphthalide with umbilical mesenchymal stem cells for the treatment of delayed encephalopathy after carbon monoxide poisoning. *Medicine* 95:e5412. doi: 10.1097/md.0000000000005412

Wang, L., Gu, Z., Zhao, X., Yang, N., Wang, F., Deng, A., et al. (2016). Extracellular vesicles released from human umbilical cord-derived mesenchymal stromal cells prevent life-threatening acute graft-versus-host disease in a mouse model of allogeneic hematopoietic stem cell transplantation. *Stem Cells Dev.* 25, 1874–1883. doi: 10.1089/scd.2016.0107

Waselenko, J. K., Macvittie, T. J., Blakely, W. F., Pesik, N., Wiley, A. L., Dickerson, W. E., et al. (2004). Medical management of the acute radiation syndrome: recommendations of the Strategic National Stockpile Radiation Working Group. *Ann. Intern. Med.* 140, 1037–1051.

Weisdorf, D., Chao, N., Waselenko, J. K., Dainiak, N., Armitage, J. O., Mcniece, I., et al. (2006). Acute radiation injury: contingency planning for triage, supportive care, and transplantation. *Biol. Blood Marrow Transplant.* 12, 672–682. doi: 10.1016/j.bbmt.2006.02.006

Wen, S., Dooner, M., Cheng, Y., Papa, E., Del Tatto, M., Pereira, M., et al. (2016). Mesenchymal stromal cell-derived extracellular vesicles rescue radiation damage to murine marrow hematopoietic cells. *Leukemia* 30, 2221–2231. doi: 10.1038/leu.2016.107

Wong, K. L., Lee, K. B., Tai, B. C., Law, P., Lee, E. H., and Hui, J. H. (2013). Injectable cultured bone marrow-derived mesenchymal stem cells in varus knees with cartilage defects undergoing high tibial osteotomy: a prospective, randomized controlled clinical trial with 2 years' follow-up. *Arthroscopy* 29, 2020–2028. doi: 10.1016/j.arthro.2013.09.074

Xiao, Y., Jiang, Z. J., Pang, Y., Li, L., Gao, Y., Xiao, H. W., et al. (2013). Efficacy and safety of mesenchymal stromal cell treatment from related donors for patients with refractory aplastic anemia. *Cytotherapy* 15, 760–766. doi: 10.1016/j.jcyt.2013.03.007

Xin, H., Li, Y., Cui, Y., Yang, J. J., Zhang, Z. G., and Chopp, M. (2013a). Systemic administration of exosomes released from mesenchymal stromal cells promote functional recovery and neurovascular plasticity after stroke in rats. *J. Cereb. Blood Flow Metab.* 33, 1711–1715. doi: 10.1038/jcbfm.2013.152

Xin, H., Li, Y., Liu, Z., Wang, X., Shang, X., Cui, Y., et al. (2013b). MiR-133b promotes neural plasticity and functional recovery after treatment of stroke with multipotent mesenchymal stromal cells in rats via transfer of exosome-enriched extracellular particles. *Stem Cells* 31, 2737–2746. doi: 10.1002/stem.1409

Xiong, Y. Y., Fan, Q., Huang, F., Zhang, Y., Wang, Y., Chen, X. Y., et al. (2014). Mesenchymal stem cells versus mesenchymal stem cells combined with cord blood for engraftment failure after autologous hematopoietic stem cell transplantation: a pilot prospective, open-label, randomized trial. *Biol. Blood Marrow Transplant.* 20, 236–242. doi: 10.1016/j.bbmt.2013.11.002

Yang, X., Balakrishnan, I., Torok-Storb, B., and Pillai, M. M. (2012). Marrow stromal cell infusion rescues hematopoiesis in lethally irradiated mice despite rapid clearance after infusion. *Adv. Hematol.* 2012:142530.

Yu, B., Kim, H. W., Gong, M., Wang, J., Millard, R. W., Wang, Y., et al. (2015). Exosomes secreted from GATA-4 overexpressing mesenchymal stem cells serve as a reservoir of anti-apoptotic microRNAs for cardioprotection. *Int. J. Cardiol.* 182, 349–360. doi: 10.1016/j.ijcard.2014.12.043

Zhang, Y., Chopp, M., Meng, Y., Katakowski, M., Xin, H., Mahmood, A., et al. (2015). Effect of exosomes derived from multipluripotent mesenchymal stromal cells on functional recovery and neurovascular plasticity in rats after traumatic brain injury. *J. Neurosurg.* 122, 856–867. doi: 10.3171/2014.11.jns14770

Zhang, Y. C., Liu, W., Fu, B. S., Wang, G. Y., Li, H. B., Yi, H. M., et al. (2017). Therapeutic potentials of umbilical cord-derived mesenchymal stromal cells for ischemic-type biliary lesions following liver transplantation. *Cytotherapy* 19, 194–199. doi: 10.1016/j.jcyt.2016.11.005

Zhang, Z., Fu, J., Xu, X., Wang, S., Xu, R., Zhao, M., et al. (2013). Safety and immunological responses to human mesenchymal stem cell therapy in difficult-to-treat HIV-1-infected patients. *AIDS* 27, 1283–1293. doi: 10.1097/qad.0b013e32835fab77

Zhang, Z., Lin, H., Shi, M., Xu, R., Fu, J., Lv, J., et al. (2012). Human umbilical cord mesenchymal stem cells improve liver function and ascites in decompensated liver cirrhosis patients. *J. Gastroenterol. Hepatol.* 27(Suppl. 2), 112–120. doi: 10.1111/j.1440-1746.2011.07024.x

Zhang, Z. G., and Chopp, M. (2016). Exosomes in stroke pathogenesis and therapy. *J. Clin. Invest.* 126, 1190–1197. doi: 10.1172/jci81133

Zhao, Y., Sun, X., Cao, W., Ma, J., Sun, L., Qian, H., et al. (2015). Exosomes derived from human umbilical cord mesenchymal stem cells relieve acute myocardial ischemic injury. *Stem Cells Int.* 2015:761643.

Conflict of Interest: PH and CC are inventors on patents related to this publication. CC reports honorarium from Nektar Therapeutics, who had no input in the study design, analysis, manuscript preparation, or decision to submit for publication.

The remaining authors declare that the research was conducted in the absence of any commercial or financial relationships that could be construed as a potential conflict of interest.

frontiers in Cell and Developmental Biology

ORIGINAL RESEARCH
published: 14 August 2020
doi: 10.3389/fcell.2020.00778

Leukemia Inhibitory Factor (LIF) Overexpression Increases the Angiogenic Potential of Bone Marrow Mesenchymal Stem/Stromal Cells

*Girlaine Café Santos[1,2†], Daniela Nascimento Silva[1,2†], Vitor Fortuna[3], Brysa Mariana Silveira[3], Iasmim Diniz Orge[1,2], Thaís Alves de Santana[1,2], Gabriela Louise Sampaio[1], Bruno Diaz Paredes[4], Ricardo Ribeiro-dos-Santos[1,2,5] and Milena Botelho Pereira Soares[1,2,5]**

[1] Gonçalo Moniz Institute, Oswaldo Cruz Foundation, Salvador, Brazil, [2] Health Institute of Technology, SENAI-CIMATEC, Salvador, Brazil, [3] Health Sciences Institute, Federal University of Bahia, Salvador, Brazil, [4] Research D'Or Institute, Rio de Janeiro, Brazil, [5] National Institute of Science and Technology for Regenerative Medicine, Rio de Janeiro, Brazil

OPEN ACCESS

Edited by:
Lindolfo da Silva Meirelles, Universidade Luterana do Brazil, Brazil

Reviewed by:
Massimo Dominici, University Hospital of Modena, Italy
Melissa Medeiros Markoski, Federal University of Health Sciences of Porto Alegre, Brazil

***Correspondence:**
Milena Botelho Pereira Soares
milena@bahia.fiocruz.br

† These authors have contributed equally to this work

Specialty section:
This article was submitted to Stem Cell Research, a section of the journal Frontiers in Cell and Developmental Biology

Received: *28 February 2020*
Accepted: *24 July 2020*
Published: *14 August 2020*

Citation:
Santos GC, Silva DN, Fortuna V, Silveira BM, Orge ID, de Santana TA, Sampaio GL, Paredes BD, Ribeiro-dos-Santos R and Soares MBP (2020) Leukemia Inhibitory Factor (LIF) Overexpression Increases the Angiogenic Potential of Bone Marrow Mesenchymal Stem/Stromal Cells. Front. Cell Dev. Biol. 8:778. doi: 10.3389/fcell.2020.00778

Mesenchymal stem/stromal cells (MSCs) have the ability to secrete bioactive molecules, exerting multiple biological effects, such as tissue regeneration, reduction of inflammation, and neovascularization. The therapeutic potential of MSCs can be increased by genetic modification to overexpress cytokines and growth factors. Here we produced mouse MSCs overexpressing human leukemia inhibitory factor (LIF) to assess their proangiogenic potential *in vitro* and *in vivo*. Mouse bone marrow-derived MSCs were transduced by using a second-generation lentiviral system to express human LIF. Leukemia inhibitory factor expression was confirmed by RT-qPCR and by ELISA, allowing the quantification of the transcript and secreted protein, respectively. Flow cytometry analysis and trilineage differentiation assay showed that the MSC_LIF cell line maintained the immunophenotype and a multipotency characteristic of MSCs. The immunosuppressive activity of MSC_LIF was confirmed using a lymphoproliferation assay. Moreover, gene expression analysis demonstrated upregulation of genes coding for strategic factors in the neovascularization process, such as angiogenin, IL-8, MCP-1, and VEGF, and for the perivascular cell markers αSMA, Col4a1, SM22, and NG2. To evaluate the pro-angiogenic potential of MSC_LIF, we first tested its effects on endothelial cells obtained from umbilical vein in a scratch wound healing assay. Conditioned medium (CM) from MSC_LIF promoted a significant increase in cell migration compared to CM from control MSC. Additionally, *in vitro* tube formation of endothelial cells was increased by the presence of MSC_LIF, as shown in microvessel sprouting in aortic ring cultures. Finally, an *in vivo* Matrigel plug assay was performed, showing that MSC_LIF were more potent in promoting *in vivo* angiogenesis and tissue vascularization than control MSCs. In conclusion, LIF overexpression is a promising strategy to increase the proangiogenic potential of MSCs and sets precedents for future investigations of their potential applications for the treatment of ischemic diseases and tissue repair.

Keywords: mesenchymal stem/stromal cells, genetic modification, LIF, proangiogenico factors, angiogenesis

INTRODUCTION

The potential of mesenchymal stem/stromal cells (MSCs), a cell population easily obtainable from different sources in the adult organism, has been intensely explored in the past decades for the development of cell and gene therapies. The main therapeutic properties of MSCs are attributed to their ability to secrete an array of soluble bioactive molecules, such as cytokines and growth factors, important in the regulation of several biological processes, including inflammation and fibrosis, cell growth, tissue repair and angiogenesis (Caplan and Dennis, 2006; Parekkadan et al., 2007; Kim et al., 2019). Several studies have investigated the therapeutic potential of MSCs for ischemic diseases, stimulating not only the development of MSCs-based therapies but also the identification of factors and molecules responsible for their pro-angiogenic potential (Gearing et al., 1987). However, differences in potency among cell populations and heterogeneity in the MSC expression profile represent a limitation of their therapeutic use (Murphy et al., 2013).

Leukemia inhibitory factor (LIF), a highly pleiotropic cytokine belonging to the interleukin-6 superfamily, was initially described as an inhibitory factor for myeloid leukemic cells proliferation (Auernhammer and Melmed, 2000). Currently, it is known that LIF acts regulating cell proliferation, differentiation and survival, as well as maintaining the state of pluripotency and self-renewal of stem cell populations, including embryonic stem cells and MSCs (Williams et al., 1988; Jiang et al., 2002; Metcalf, 2003). Other biological properties of LIF include induction of bone remodeling, neuroprotection, cardiac regeneration and regulation of hematopoiesis (Pepper et al., 1995). The role of LIF in angiogenesis has not been completely elucidated, and different studies have shown contradictory responses. The direct effect of LIF on endothelial cells appears to inhibit their angiogenic capacity, while populations of stem cells are stimulated to secrete important proangiogenic growth factors in the presence of LIF, contributing to neovascularization. Thus, the levels of LIF secretion by MSCs may be relevant for the therapeutic effects of these cells (Chen et al., 2014; Nicola and Babon, 2015).

Genetic manipulation of MSCs has been tested as a strategy to generate cells expressing factors capable of increasing or potentiating the biological activities of MSCs, such as migration, survival after transplantation, and secretion of molecules of interest for the treatment of different disease settings (D'souza et al., 2015). This can be achieved by genetic engineering using different viral vectors for transduction or by plasmid transfection. Here we used a second-generation lentiviral system to produce mouse bone marrow-derived MSCs overexpressing LIF (MSC_LIF) to assess their potential on angiogenesis.

MATERIALS AND METHODS

Isolation and Culture of Mouse Bone Marrow MSC

Bone marrow-derived MSCs were obtained from GFP transgenic C57Bl/6 male mice aged 4-8 weeks. The animals were kept in the animal facility of the Center for Biotechnology and Cell Therapy of Hospital São Rafael (Salvador, Brazil), with access to food and water *ad libitum*. The procedures for obtaining the cells were approved by the ethics committee for animal use of Hospital São Rafael (CEUA-HSR 007/18). Bone marrow cells obtained from the tibiae and femurs by flushing were centrifuged at 300 × *g* for 10 min. The pellet was resuspended in 10 ml of Dulbecco's Modified Eagle's Medium (DMEM), supplemented with 10% fetal bovine serum (FBS) and 1% penicillin/streptomycin (all Thermo Fisher Scientific, Waltham, MA, United States) and cultured in plastic flasks in incubator at 37°C with 5% atmospheric CO_2. After two days, the culture medium was completely changed and the non-adherent cells were removed. The adhered cells were cultured at 37°C with 5% atmospheric CO_2 and the medium was changed every 3 days until the monolayer reached 90% confluence. The MSCs were detached using a trypsin-EDTA 0.25% solution (Thermo Fisher Scientific) for expansion and use for transduction.

Lentiviral Production and Transduction of MSCs

MSCs were transduced using non-replicative lentiviral particles carrying the gene of interest (hLIF). The second generation lentiviral system was composed of three vectors: (1) psPAX2, a plasmid packaging (Addgene, Watertown, MA, United States; plasmid # 12260); (2) pMD2.G, envelope protein expressing plasmid (Addgene, plasmid # 12259); and (3) pEGIP, expression vector for stable integration of GFP expression cassette with puromycin selection (Addgene, plasmid # 26777), according to the protocol previously described (Zou et al., 2009). For the generation of the lentiviral *LIF* expressing vector, the coding sequence for the gene was amplified by PCR using pUNO1-hLIFa (Invivogen, San Diego, CA, United States) as template with the primer sequences: hLIF_*Bam*HI_F-CCAACGTGACGGACTTCCC and hLIF_*Bsr*GI_R-TACACGACTATGCGGTACAGC; After cloning, the coding sequence of interest, together with the pEGIP expression vector, were submitted to confirmatory digestion with restriction endonucleases *Bam*HI and *Bsr*GI. After that, the reaction products were subjected to an electrophoretic run in 1% agarose gel in TAE 1X buffer, and the bands with the highest molecular weight, cut and purified. The amplicon was subcloned into the pEGIP vector in the *Bam*HI/*Bsr*GI GFP flanked region (**Figures 1A,B**). The construct was sequenced using the primer F: GGCCAGCTTGGCACTTGATGTA and R: CTAGGAATGCTCGTCAAG. The lentivirus carrying *LIF* was produced in Human embryonic kidney 293Ft (HEK 293FT) cells by transient co-transfection with PSPAX2, PMD2.G and transfer vector pEGIP containing *gfp* or *LIF* as gene inserts, in a proportion of 2:1:3, respectively, using the calcium phosphate method (**Figure 1C**) (Tiscornia et al., 2006). Supernatants from HEK 293FT cells were collected 48 h after transfection and centrifuged at 300 × *g* for 10 min to remove cell debris and filtered through a 0.45 μm pore-size filter. The lentiviral particles were concentrated by ultracentrifugation for 90 min at 50,000 × *g* and 4°C (**Figures 1D,E**). Viral titers were estimated by comparing HEK cells infection with a GFP^+ control lentivirus,

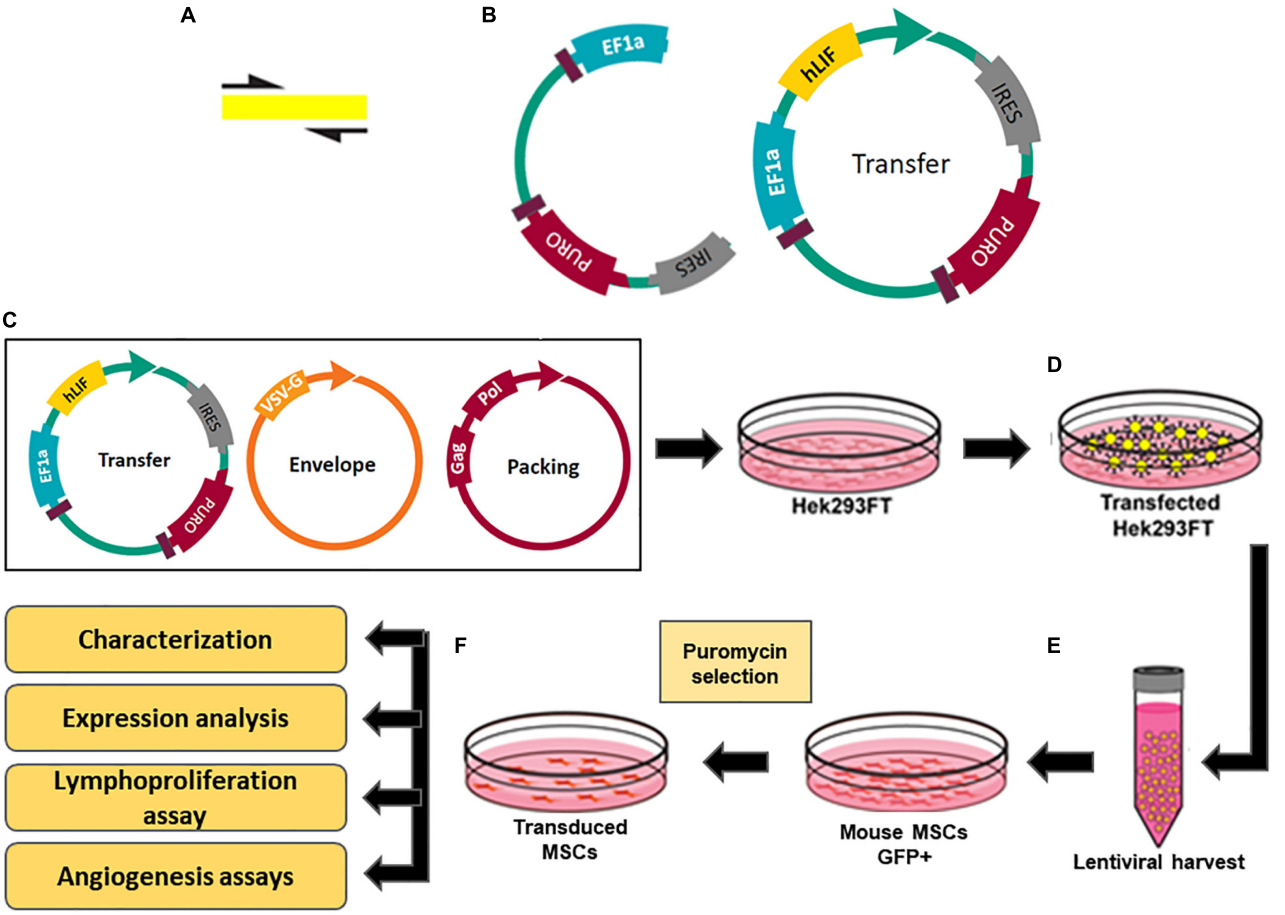

FIGURE 1 | Constructs and experimental design for production of transgenic MSC overexpressing hLIF. **(A)** Amplification of coding region of hLIF; **(B)** Design of pEGIP vector and hLIF lentiviral transfer vector containing EEF1α constitutive promoter and puromycin selection gene. Schematic representation of transgenic MSC lines generation showing **(C)** transfection of Hek293FT cells with the lentiviral system vectors; **(D)** Production of lentiviral particles by the Hek293FT cells; **(E)** Harvest and concentration of lentiviral particles; **(F)** Transduction of MSC with lentivirus and selection of the clones overexpressing human LIF.

generated by the same method, in the dilutions (0, 10^{-1}, 10^{-2}, and 10^{-3}) followed by the evaluation of the percentage of GFP fluorescent HEK cells by flow cytometry after 72 h. To estimate the titers of lentiviral stocks carrying the hLIF gene and empty pEGIP (control), we applied to the formula:

$$title = \left(\frac{F \times C^{o}}{V}\right) \times DF$$

where F is the frequency of positive GFP cells after transduction; C^{o} is the number of cells at the time of infection; V is the volume of the lentiviral solution used for transduction; and DF is the dilution factor (White et al., 1999). The estimated titer for lentivirus stocks carrying the hLIF gene and pEGIP control was 10^{7} TU/mL. The MSCs at passage 5 were seeded in a 6-well plate and maintained in incubator until they reached 80% confluency. The transduction of MSCs was performed by incubating the cells with the lentiviral stocks at 1 MOI of pEGIP LIF or control and 6 μg/ml of polybrene for 24 h. The culture medium was changed and the cells were cultured for 48 h before adding 2 μg/ml of puromycin (Thermo Fisher Scientific) for selection (**Figure 1F**). The cell lines obtained, MCS_LIF (MSC transduced with LIF vector) and MSC_pEGIP (MSC transduced with control vector), as well as the wilt-type MSC, were then expanded for characterization and further experiments.

Quantitative Real-Time PCR

Total RNA was extracted from the MSC and MSC_LIF cell lines using the TRIZOL® extraction reagent (Thermo Fisher Scientific). The quantification of RNA was performed on a NanoDrop™ 1000 spectrophotometer (Thermo Fisher Scientific). The purity of the samples obtained by the ratio A260 nm: A280 nm demonstrated a proportion between 1.8 and 2.0. Aliquots of 1 μg of high quality RNA were used for cDNA synthesis using SuperScript III reverse transcriptase (Invitrogen Waltham, MA, United States) after treatment with DNAse I. To analyze the expression of proangiogenic factors in MSC and MSC_LIF cells, we used the following primer sets purchased from Integrated DNA Technologies™ (Coralville, IA, United States): ACTA2, TAGLN, COL4A1, CCL2, CXCL2, ANG, VEGF, and NG2 (**Table 1**), and Sybr Green (Thermo

TABLE 1 | Oligonucleotide primer sequences.

Primers	Sequences 5′–3′	Amplicon (bp)
LIF_Hs_qPCR_F	CCAACGTGACGGACTTCCC	
LIF_Hs_qPCR_R	TACACGACTATGCGGTACAGC	82
ACTA2_Mm_qPCR_F	GTCCCAGACATCAGGGAGTAA	
ACTA2_Mm_qPCR_R	TCGGATACTTCAGCGTCAGGA	102
TAGLN_Mm_qPCR_F	CCTGGCCGTGAGAACTTCC	
TAGLN_Mm_qPCR_R	CCCAGGTTCATTAGTGTCCGC	189
COL4A1_Mm_qPCR_F	CTGGCACAAAAGGGACGAG	
COL4A1_Mm_qPCR_R	ACGTGGCCGAGAATTTCACC	238
CCL2_Mm_qPCR_F	CACAGATGGCCTTGATGTTG	
CCL2_Mm_qPCR_R	CTCTGGCTCAGCATGACTCC	179
ANG_Mm_qPCR_F	CCAGGCCCGTTGTTCTTGAT	
ANG_Mm_qPCR_R	GGAAGGGAGACTTGCTCATTC	109
VEGF_Mm_qPCR_F	GAGGTCAAGGCTTTTGAAGGC	
VEGF_Mm_qPCR_R	CTGTCCTGGTATTGAGGGTGG	160
NG2_Mm_qPCR_F	GGGCTGTGCTGTCTGTTGA	
NG2_Mm_qPCR_R	TGATTCCCTTCAGGTAAGGCA	132
CXCL2_Mm_qPCR_F	CCAACCACCAGGCTACAGG	
CXCL2_Mm_qPCR_R	GCGTCACACTCAAGCTCTG	108
B2M_Mm_qPCR_F	TTCTGGTGCTTGTCTCACTGA	
B2M_Mm_qPCR_R	CAGTATGTTCGGCTTCCCATTC	104

Fisher Scientific). The reactions were done in triplicate, and the average cycle thresholds (Ct) values were used to calculate the expression of each gene using the B2M gene as a normalizer. The PCR amplification was performed on an ABI7500 real-time PCR system (Thermo Fisher Scientific), under standard thermal cycle conditions.

Enzyme-Linked Immunosorbent Assay

Cell culture supernatants from MSC_LIF were collected after 24, 48, and 72 h of culture and stored at −20°C until use. hLIF concentrations were quantified by enzyme-linked immunosorbent assay (ELISA), using the DuoSet kit (R&D Systems, Minneapolis, MN, United States), according to the manufacturer's instructions. After incubation with a streptoavidin-peroxidase conjugate (Sigma-Aldrich, St. Louis, MO, United States), the reaction was developed using H2O2 and 3,3,5,5-tetramethylbenzidine (Sigma-Aldrich) and the 450 nm wavelength light absorbance read in spectrophotometer (BioTek Instruments, Winooski, VT, United States). Six samples were analyzed per group.

Flow Cytometry Analysis

Mesenchymal stem/stromal cell and MSC_LIF (1×10^5 cells) were resuspended in 0.9% saline solution and incubated for 30 min in flow cytometry tubes with the antibodies Sca1-PE-Cy5.5 (Thermo Fisher Scientific), CD45-APC, CD44-PE (BD Biosciences, Franklin Lakes, NJ, United States), CD29-APC and CD11b-PE (Biolegend, San Diego, CA, United States), or isotype control antibodies (Thermo Fisher Scientific), diluted at 1:100 ratio. After the incubation period, the tubes were centrifuged at $300 \times g$ for 5 min and cells were washed twice with PBS solution. Immunophenotyping analyzes were performed using an LSRFortessa flow cytometer (BD Biosciences). At least 50,000 events were collected and analyzed.

Adipogenic, Osteogenic and Chondrogenic Differentiation

To evaluate the multipotency of the cell lines, the trilineage differentiation assay was performed. In brief, 1×10^4 MSC and MSC_LIF cells were cultured in 24-well plates with complete DMEM (Thermo Fisher Scientific) medium. After reaching 50–60% confluence, the medium was replaced for the specific differentiation media (all from Thermo Fisher Scientific). For adipogenic induction, the cells were cultured in StemPro Adipogenesis Differentiation Kit (Thermo Fisher Scientific) during 14 days, followed by fixation in 4% paraformaldehyde and staining with Oil red solution to observe fat-filled vacuoles. For osteogenic differentiation, the cells were cultured in the StemPro Osteogenesis Differentiation kit (Thermo Fisher Scientific), with changes of half of the differentiation medium every two days. To observe the deposition of a calcium-rich matrix after differentiation, cultures were fixated in 4% paraformaldehyde and stained the cultures with Alizarin red 2%. For chondrogenic differentiation, cells were cultured for 21 days in standard chondrogenic differentiation medium StemPro Chondrogenesis Differentiation kit (Thermo Fisher Scientific). Proteoglycan synthesis was observed by staining with Alcian Blue solution after fixation with 4% paraformaldehyde. The assay was performed in triplicate, and the experiment repeated three times. The images were captured using an AX70 microscope with a digital camera (Olympus, Shinjuku, Tokyo, Japan).

Proliferation Assay

Mesenchymal stem/stromal cell or MSC_LIF cells (5×10^4/well) were cultured in 96-well plates with complete DMEM (Thermo Fisher Scientific) medium. After 72 h, 1 μCi of methyl-^{3}H-thymidine (PerkinElmer, Waltham, MA, United States) was added per well and incubated for 18 h. Cell proliferation was measured as the percent of ^{3}H-thymidine incorporation for MSC or MSC_LIF using a β-plate counter (PerkinElmer). The assay was carried out with six replicates and three independent experiments were performed.

Lymphocyte Proliferation Assay

Splenocytes obtained from C57Bl/6 mice were plated in 96-well plates (8×10^5 cells/well), in a final volume of 200 μL and stimulated with Dynabeads® mouse T-activator CD3/CD28 (bead to cell ratio = 1:1; Themo Fisher Scientific), and co-cultivated in the presence of wild-type or transduced mitomycin-treated MSCs (1:1, 1:10, 1:100, 1:1000 MSCs:Splenocytes ratio) or with supernatant from MSC or MSC_LIF. After 48 h of incubation, plates were pulsed with 1 μCi of methyl-^{3}H-thymidine (PerkinElmer) for 18 h. The cell proliferation was determined by evaluating the ^{3}H-thymidine uptake using a β-plate counter (PerkinElmer). The inhibition of splenocytes proliferation was determined in relation to controls stimulated by anti CD3/CD28 in the absence of MSCs (0:1). The assay

was carried out with six replicate and three independent experiments were performed.

Preparation of Conditioned Medium

Mesenchymal stem/stromal cell and MSC_LIF were seeded in 6-well plates (1×10^6 per well) and incubated in DMEM medium (Thermo Fisher Scientific) supplemented with 10% FBS and 1% penicillin/streptomycin (Thermo Fisher Scientific) until reaching 80% confluence. The culture medium was then removed and the cells were washed with PBS. The conditioned medium was obtained by incubating these cells with 1.5 mL per well of basal EBM-2 medium (Lonza Group, Basel, Switzerland) with 0.3% albumin (Sigma-Aldrich) for 72 h. The cell-free supernatants were obtained by centrifugation at $640 \times g$ for 15 min at 4°C, aliquoted and stored at −80°C until use.

HUVEC Isolation and Culturing

Primary culture and maintenance of human umbilical vein endothelial cells (HUVEC) were performed as described previously (Jaffe et al., 1973). The institutional review board of the Climério de Oliveira Maternity Hospital (CEP – Federal University of Bahia) approved the procedures (approval number 625.059). The HUVECs were cultured in EGM-2/BulletKit medium (Lonza Group) supplemented with 100 U/mL penicillin/streptomycin (Thermo Fisher Scientific) at 37°C in 5% CO_2 and 95% air. Human umbilical vein endothelial cells were seeded on 0.1% gelatin (Sigma-Aldrich) in EGM-2/BulletKit and replaced every 2–3 days. Passages four to six of the HUVECs were used for experiments in this study.

Scratch Wound Healing Assay

Human umbilical vein endothelial cells (2×10^5 per well) were plated in 24-well plates and cultured in EGM2/BulletKit medium (Lonza Group) until they formed a confluent monolayer (about 24 h after incubation). Then, the scratch was performed by scraping the cell monolayer in a straight line, using a p200 pipette tip. Reference points were marked close to the scratches to evaluate the same field during image acquisition. Medium was exchanged to conditioned medium from MSC and MSC-LIF and the plates were incubated at 37°C for 9 or 18 h. EBM-2 medium without supplementation was used as control. Distance between the edges captured using an inverted phase contrast microscope (Leica DMi1) at three points for each well in three timepoints: after performing the scratch (time-point 0), after 9 h in incubation and after 18 h in incubation. The assay was performed in triplicates, and the experiment repeated three times. The open wound area was quantitatively measured using ImagePro Plus 7.0 software (Media Cybernetics, Rockville, MD, United States). Results are represented as a percentage of the migration area, established by subtracting the average distance values obtained at time-point 0 by the values obtained after incubation, according to the formula:

$$\%\ migration\ area = \frac{(Ai - Af)}{Ai}$$

Where, *Ai* represents the initial area of the wound and *Af* represents the final area of the wound after cell migration.

Sprouting Aortic Ring Assay

All procedures were approved by the institutional review board for animal experimentation (CEUA, UFBA-2018-131). The mouse aortic ring assay was performed as described previously (Baker et al., 2012). Thoracic aortas were dissected from male 4–8 weeks-old C57Bl/6 mice. The animals were anesthetized with ketamine and xylazine solution and euthanized by cervical dislocation. The thoracic cavities were opened and the organs carefully separated to expose aortas. Each artery was cut between the anterior end, before the heart and lung insertion, and at the posterior end before branching into the iliac arteries. After removing blood and fat-cover from vessels, the dissected aortas were cut into ∼1.0 mm rings and transferred to Petri dishes with 5 mL serum-starved in DMEM overnight. Next, the aortic rings were randomly placed onto individual wells of a 48-well plate, embedded in 250 μL of fibrin gel and, after polymerization, 1×10^5 MSC or MSC_LIF cells were seeded on top of the gel. Another group was performed by incubating the aortic rings with conditioned medium from MSC or MSC_LIF every 2-3 days. EGM-2/BulletKit medium was used as a positive control (PTV_CTL) and basal EBM-2 media was used as a negative control (NGV_CTL). For 7 days, daily, microvessel sprouting was observed and imaged using an inverted phase-contrast microscope (Leica DMi1). The assay was performed with five replicates per group, and the experiment repeated three times. Quantification of microvessel sprouts number was analyzed using ImagePro Plus 7.0 software (Media Cybernetics).

In vivo Matrigel Plug Assay

In vivo angiogenesis experiments were performed as previously described by Malinda (2009). A mixture of basement membrane matrix (ice-cold phenol red-free, reduced growth factor, Thermo Fisher Scientific) and conditioned medium (0.5 mL, 9:1 proportion) was injected subcutaneously into two-months-old C57Bl/6 wild-type mice ($n = 4$). Each mouse received two implants, totaling eight plugs per group. A buffered saline was included as a negative control during the assay. After 7 days, the mice were euthanized and the plugs were excised, photographed, and processed. Quantification of blood vessels was achieved using immunofluorescent visualization of blood vessels on frozen Matrigel sections and by measuring the amount of hemoglobin (Hb) contained in the plugs. Frozen Matrigel sections were stained with rat anti-mouse CD31 antibody (R&D system, 0.125 μg/mL in BSA/normal serum solution) followed by incubation with Alexa 488-conjugated anti-rat antibody (Molecular Probes, 10 μg/mL in PBS) as described previously by Ribeiro et al. (2019). For quantitation of functional vessels formed, the plugs were homogenized in distilled water and centrifuged at $2{,}400 \times g$ for 5 min. The supernatant was mixed with Drabkin's reagent (Sigma-Aldrich) for measurement of Hb. After 15 min at room temperature, the absorbance of the mixture was measured at 540 nm.

Statistical Analyses

The results of the experiments were analyzed and continuous variables are presented as mean ± SEM. The data were analyzed using Student's *t*-test for comparisons between two groups and 2-way ANOVA, followed by Bonferroni test or ANOVA followed by Newman–Keuls test for multiple-comparison tests, using the software GraphPad Prism version 5.0 (Software Inc., San Diego, CA, United States). *p*-Values < 0.05 were considered statistically significant.

RESULTS

Generation of Transgenic MSC Lines Overexpressing hLIF

Mouse bone marrow-derived MSC were transduced with vectors carrying *LIF* or *gfp* control vector (pEGIP). Digestion with restriction endonucleases confirmed that amplicon was properly subcloned into the pEGIP vector (**Figure 2A**). Transduction was well tolerated by cells, which survived and proliferated during the puromycin selection step (**Figure 2B**), while in non-transduced wells exposure to the antibiotic led to complete cell culture death (**Figure 2C**). Despite maintaining a fibroblast-like morphology, MSC_LIF cells displayed a change in their distribution in culture, showing a tendency to spontaneously organize in circular structures (**Figure 2D**), compared to non-transduced control cultures (**Figure 2E**). The analysis of human LIF expression demonstrated a high expression of the transgene in MSC_LIF cells, while the control MSC (pEGIP) and wild-type cells did not express the human LIF gene ($p < 0.001$) (**Figure 2F**). Furthermore, the production of the protein was confirmed by ELISA, in the supernatants of MSC_LIF cells collected after 24 h ($p < 0.001$), 48 h ($p < 0.001$), and 72 h of culture ($p < 0.001$) (**Figure 2G**).

Characterization of MSC_LIF Cells

The immunophenotyping of the MSC and MSC_LIF cell lines allowed to compare the expression levels of cell markers for mesenchymal cells. Similar to wild-type MSCs, transgenic MSCs showed high expression of the mesenchymal stem cell markers Sca-1, CD29 and CD44, while exhibiting low expression of hematopoietic cell markers CD45 and CD11b (**Table 2**). Moreover, the trilineage assay showed the maintenance of the multipotency of transduced cells, since MSC_LIF differentiated in all three lines (adipogenic, osteogenic and chondrogenic) in a similar fashion compared to the wild-type MSCs (**Figure 3A**). When the proliferative rat was evaluated, we found that the MSC_LIF line had an increased proliferation, when compared to the parental MSC line ($p = 0.0029$) (**Figure 3B**). The immunosuppressive potential of the transduced cells was also investigated by culturing splenocytes stimulated by mitogen (αCD3/αCD28), with MSC (**Figure 4A**) or MSC_LIF (**Figure 4B**) mitomycin-treated cells. The transduced MSC_LIF line, however, showed a similar immunosuppressive capacity than wild-type MSC.

Overexpression of LIF Promotes Upregulation of Pro-angiogenic Factors

Immunostaining and RT-qPCR array were performed to assess whether the overexpression of LIF in MSCs caused changes in the transcription of genes related to angiogenesis. Most of the proangiogenic factors and perivascular cell markers were positively regulated when compared to wild-type MSC cells. Immunofluorescence staining of MSC and MSC_LIF cells with antibodies against the perivascular cell markers showed an increased expression in MSC_LIF, when compared with MSC, for Ng2 ($p = 0.0017$), αSMA ($p = 0.0001$), Sm22 ($p = 0.0375$), and Col4a1 ($p = 0.0032$) (**Figure 5A**). The RT-qPCR analysis confirmed levels significantly higher in the transcripts for these markers in MSC_LIF than in control MSC (**Figure 5B**). In addition, MSC_LIF also showed upregulated gene expression of proangiogenic factors *Vegf* (P = 0.0001), *Cxcl2* (the functional homolog of IL-8 in mice) ($p = 0.0114$), angioginine (*Ang*) ($p = 0.0063$) and *Ccl2*, or MCP-1 ($p = 0.0125$) (**Figure 5C**).

Conditioned Medium From MSC-LIF Promotes *in vitro* Endothelial Cell Migration

Next we assessed the proangiogenic activity of MSC_LIF. As a first step toward investigating whether MSC_LIF produces paracrine factors that promote angiogenesis, conditioned medium (CM) was obtained from MSC and MSC_LIF and tested in an endothelial cell migration assay using HUVEC cells. Conditioned medium-MSC and CM-MSC_LIF conditions significantly facilitated monolayer wound closure in comparison to the vehicle control medium ($p < 0.01$). The migration of HUVECs, however, was significantly greater in the presence of CM-MSC_LIF compared to CM from control cells (**Figure 6**). To investigate the angiogenic effects of MSC_LIF on vascular networks, a mouse aortic ring assay was performed. **Figure 7A** shows the microvessels outgrowth from mouse aortic rings after 5 days of incubation. Mouse aortic explants incubated with PBS alone for 5 days, which showed no microvessel outgrowth, while the aortic rings treated with both CM-MSC and CM-MSC_LIF exhibited an increased outgrowth (**Figure 7A**). The total number and length of the outgrowths, however, were significantly higher in rings incubated in the presence of MSC_LIF cells compared with MSC ($p < 0.001$, at 5 days of incubation), and CM-MSC_LIF also demonstrated better performance when compared with CM-MSC ($p < 0.0001$, at 5 days of incubation) (**Figure 7B**). The CM-MSC_LIF stimulated the formation of tubular networks as early as 4 days following seeding onto the matrix, and the structures were maintained for a minimum of 8 days.

MSC_LIF Promotes *in vivo* Angiogenesis

The effects of CM-MSC and CM-MSC_LIF on *in vivo* angiogenesis were also examined with a Matrigel plug assay. The induction of new blood vessel formation was not evident in the Matrigel plug containing PBS alone. By contrast, the inclusion of either CM significantly induced the development of new blood vessels. The Hb content normalized to the weight of the analyzed Matrigel plug was significantly higher in CM-MSC_LIF plugs in

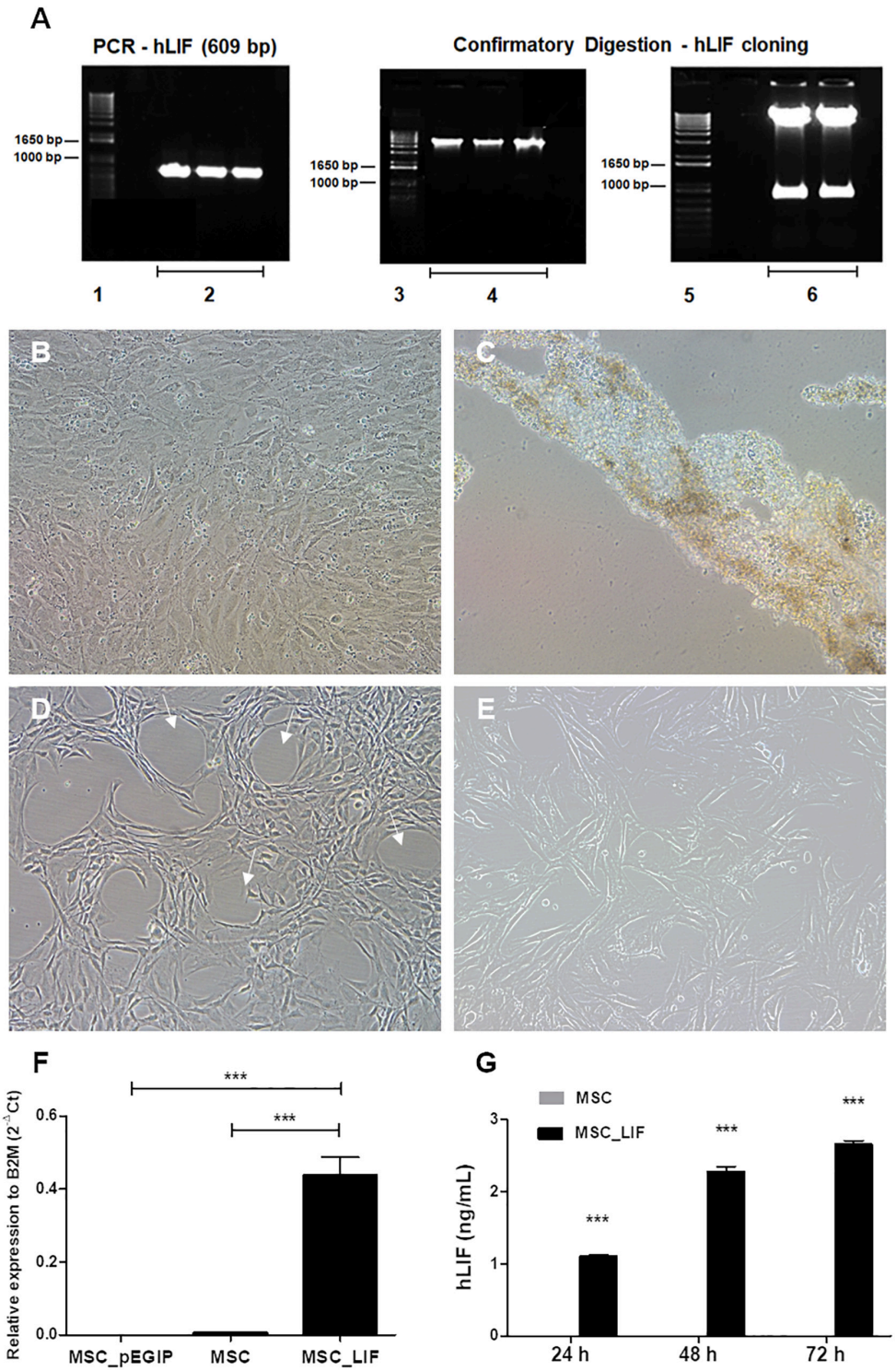

FIGURE 2 | Amplification of the hLIF transgene and confirmatory digestion, antibiotic selection and establishment of stable cell cultures. **(A)** Amplification of the hLIF gene (609 bp) and confirmatory digestion of pEGIP vector after cloning (Caplan and Dennis, 2006; Murphy et al., 2013; Kim et al., 2019), molecular weight marker (Parekkadan et al., 2007), PCR reaction triplicate (Gearing et al., 1987), undigested clones (Auernhammer and Melmed, 2000), and digested clones. **(B,C)** Phase contrast images of the cell culture, showing morphology of MSC_LIF transduced culture and MSC control culture after selection with 2.0 μg/ml of puromycin, respectively. Morphology of expanded cell lines of MSC_LIF **(D)** and MSC wild-type **(E)**. The arrows highlight the halos formed in the MSC_LIF culture after transduction. 100× magnification. mRNA expression analysis of hLIF in MSC_LIF, MSC and MSC_pEGIP **(F)** and detection of the protein in the supernatant after 72 h of culture, by ELISA **(G)**. The two-way ANOVA test and the Bonferroni post-test were used to analyze the differences among the groups. Values are expressed as mean ± SEM of at least three independent experiments. $^{***}p < 0.001$.

comparison to CM-MSC or PBS plugs (0.5 and 3.0 fold higher, respectively) (**Figures 8A,B**). The immunofluorescence staining of Matrigel sections with antibody against endothelial marker showed CD31-positive vascular structures, as well as clusters of individual endothelial cells (**Figure 8C**). A higher density of blood vessels was visualized on CM-MSC_LIF plugs in relation to CM-MSC plugs. Thus, CM-MSC_LIF was more potent than CM-MSC to induce ingrowth of new blood vessels into the Matrigel implant.

TABLE 2 | Flow cytometry analysis of cell surface markers in MSC lines.

Cell marker	MSC_wild-type	MSC_LIF
CD29	98.2% ± 1.52	99.9% ± 0.01
CD44	97.3% ± 2.37	96.3% ± 3.39
CD73	98.5% ± 1.40	99.7% ± 0.05
Sca-1	95.0% ± 5.98	99.0% ± 0.07
CD11b	0.82% ± 0.89	0.90% ± 0.31
CD45	0.35% ± 0.062	0.52% ± 2.04
CD34	0.1% ± 0.99	0.85% ± 0.30

The values represent the mean percentage ± standard deviation of two experiments.

DISCUSSION

The main therapeutic properties of MSCs are attributed to their ability to secrete a series of soluble bioactive molecules, such as cytokines and growth factors, important in the regulation of various biological processes, including angiogenesis (Zhang et al., 2014). With several techniques now available that allow MSCs to be easily manipulated genetically, these cells became excellent vehicles for gene therapy (Porada et al., 2013). In the present

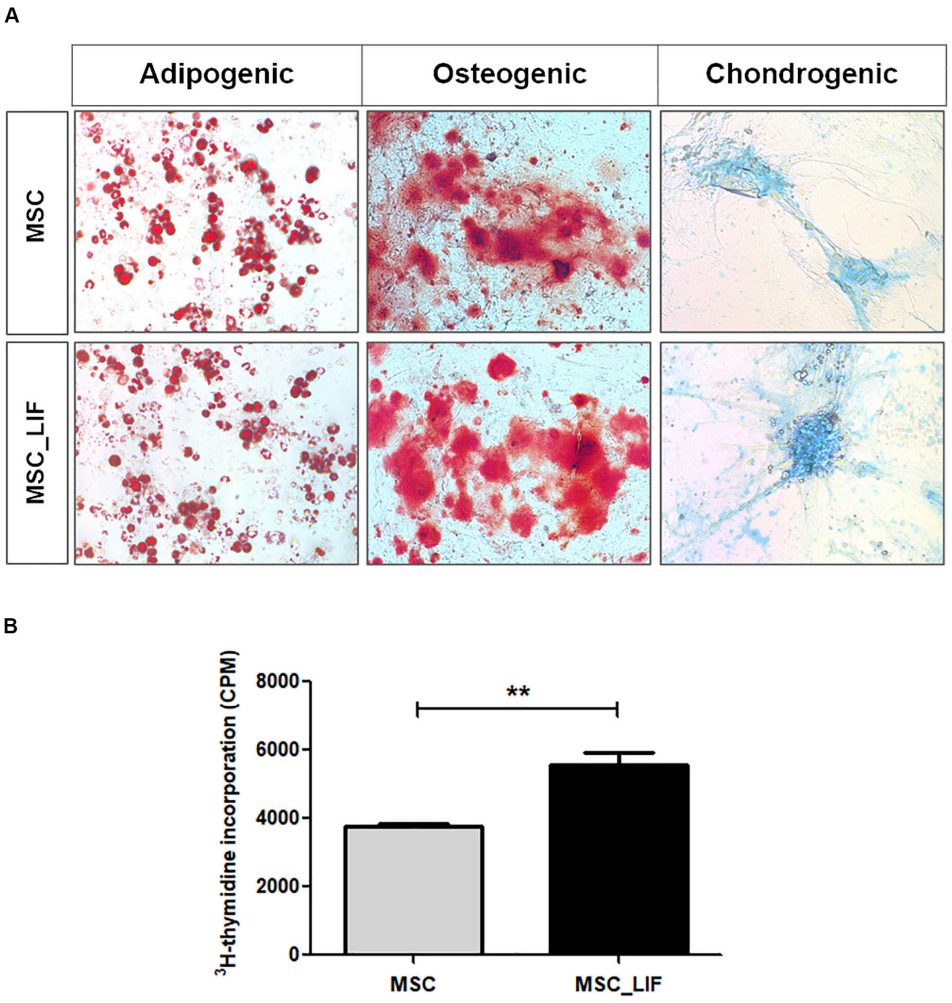

FIGURE 3 | Trilineage differentiation and proliferation assays. **(A)** Cell differentiation of MSC_LIF and MSC was confirmed by staining for adipocytes (Oil red), osteocytes (Alizarin red), and chondrocytes (Alcian blue). Adipogenic and osteogenic differentiation: 200× magnification. Chondrogenic differentiation: 100× magnification. **(B)** The proliferative rate of MSC and MSC_LIF was determined by quantifying the uptake of ^{3}H-thymidine after 18 h of incubation. The Student's *t* test was used to analyze the differences between groups. Values are expressed as mean ± SEM of at least three independent experiments. $^{**}p < 0.01$.

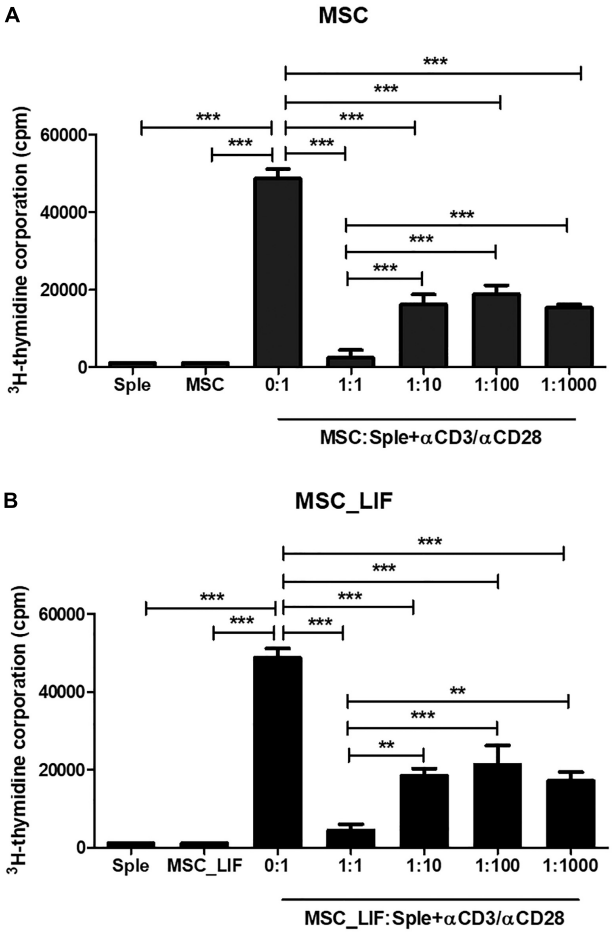

FIGURE 4 | *In vitro* immunomodulatory activity of MSC_LIF. The immunomodulatory potential of MSC **(A)** and MSC_LIF **(B)** cells was determined by quantifying the uptake of ^{3}H-thymidine after co-culturing these cells with splenocytes (Sple) activated with αCD3/αCD28 for 3 days. ANOVA followed by Newman–Keuls post-test were used to analyze the differences among the groups. Values represent means ± SEM of three determinations. $^{**}p < 0.01$; $^{***}p < 0.001$.

study we described the generation of a MSC cell line genetically modified with a lentiviral vector to overexpress LIF.

Several methods have been employed to induce genetic modifications in MSCs, including those using viral vectors or non-viral vectors. Gonçalves et al. (2018) showed that the lentivirus-based transduction method used here is highly efficient and allowed to achieve high levels of expression of the interest transgene without harming the intrinsic properties of the mesenchymal cells (Gonçalves et al., 2018). In our study, the cells obtained were able to produce and secrete hLIF, in addition to maintaining the main characteristics of MSCs, such as the specific immunophenotype, differentiation potential, and immunosuppressive activity. In addition, an increase in the proliferative capacity of MSC_LIF was observed, indicating that the proliferative stimulus of LIF in some cell types can also be seen in MSC (Nicola and Babon, 2015).

Interestingly, the MSC_LIF transcriptomic analysis revealed the positive regulation of four main factors (VEGF, IL-8, MCP1, and Ang) related to vascular regeneration and increased pro-angiogenic potential. The role of LIF in the angiogenic process remains poorly understood. Studies focusing on the influence of LIF on the vascular development have demonstrated that its effects are highly pleiotropic, concentration-dependent and cell-specific for successful angiogenesis. Recently, Mohri et al. (2006) demonstrated that LIF acts at different stages of the mesoderm development process, including the speciation of hematopoietic and endothelial cells and the development of the cardiovascular system. Furthermore, stimulation of Sca-1^+ cardiac stem cells with recombinant LIF resulted in their endothelial differentiation. Parallel to this, Paradis and Gendron (2000) showed that the combined effect of LIF and basic fibroblast growth factor (bFGF) can promote the formation of capillary structures in the EMI embryonic endothelial cell line. In both studies, activation of the STAT3 pathway by LIF was closely related to endothelial differentiation (Paradis and Gendron, 2000; Mohri et al., 2006). Altogether, these studies reinforce the pro-angiogenic potential of LIF.

Previously, Do Rhee et al. (2004) showed that signaling components JAK2, Tyk2, Erk1/2, STAT1, and STAT3 were co-expressed with LIF receptor in perivascular and stromal cells, suggesting that LIF have an effect on other cells, rather than endothelial cells, during vascular development. In our study, LIF transgenic expression did not induce endothelial cell phenotype or expression of endothelial-cell markers (CD31) on MSC, but rather induced the expression of perivascular characteristic markers (Ng2, Acta2, Col4, Tagln). This pattern of transcript expression was confirmed by immunofluorescence staining. In agreement, MSCs derived from human limbal stroma demonstrated increased expression of Pdgfr-b and Acta2, suggestive perivascular markers, and downregulation of endothelial markers (CD31, CD34) when cultivated and expanded in the presence of LIF and b-FGF (Li et al., 2012). In addition, pericyctic populations show high expression of cytokines and immunoregulatory chemokines, including LIF (Gaceb et al., 2018). In muscle pericytes, LIF is related to cardioprotective effects. The transplantation of skeletal muscle pericytes in a model of acute myocardial infarction improved cardiac function by reducing hypoxia and increasing angiogenesis due to increased expression of molecules such as IL-6 and LIF (Chen et al., 2013). Future studies are needed to investigate how LIF transgenic expression might promote perivascular characteristic markers without changing their mesenchymal identity and phenotype.

Recent studies have investigated the applicability of mesenchymal stem cells to ischemic diseases, such as peripheral arterial disease, myocardial infarction and stroke (cerebral ischemia) (Bronckaers et al., 2014). However, many studies have reported on heterogeneous proangiogenic properties of MSC as a bottleneck to improve MSC-based therapies and clinical utility (Du et al., 2016; Pinto et al., 2020). Recently, Kim et al. (2019) have identified the key factors secreted by MSC that correlate to vascular regenerative efficacy in the treatment of ischemic diseases. These trophic factors are considered efficient

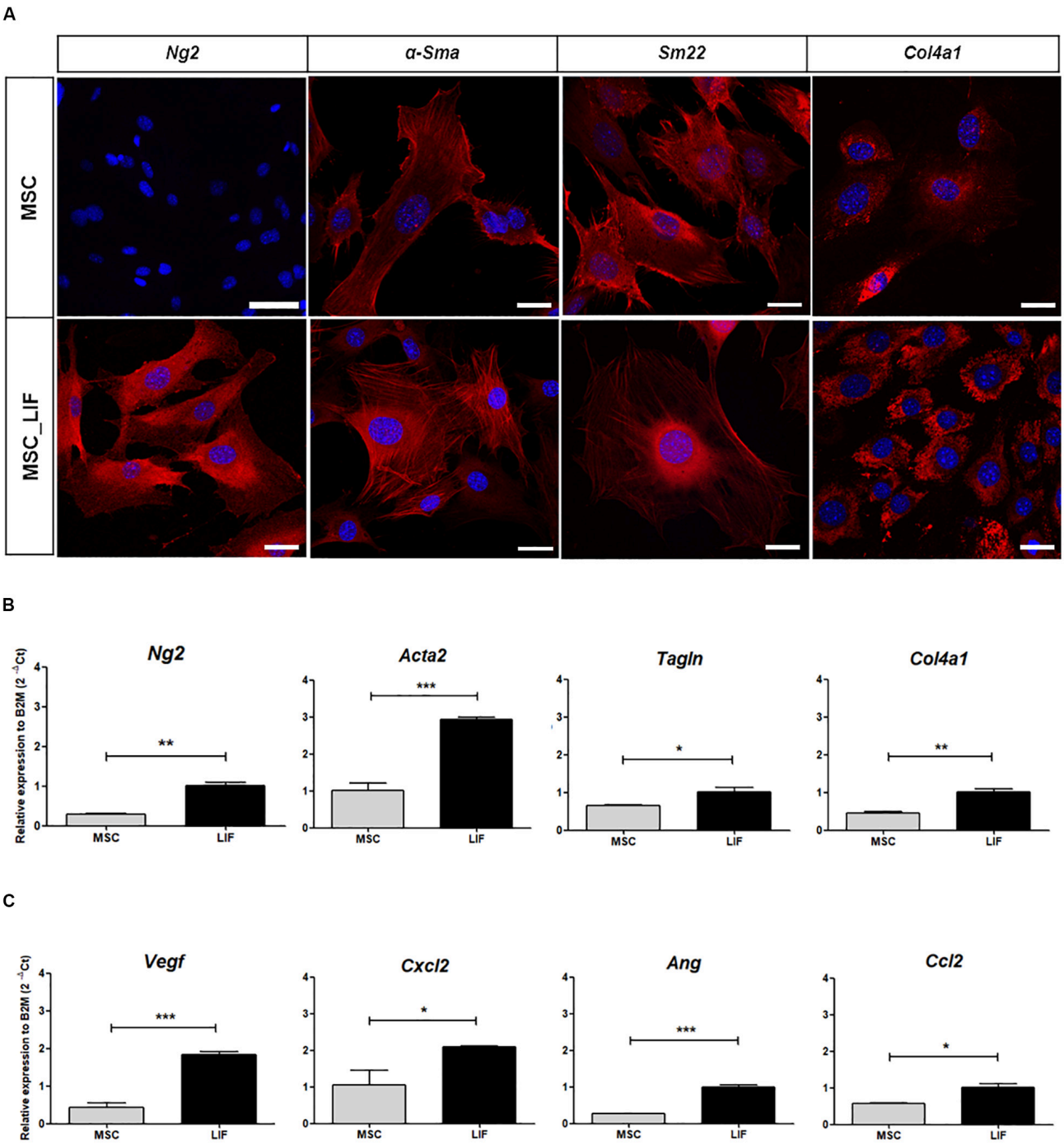

FIGURE 5 | Pro-angiogenic factors expression analysis. **(A)** Immunofluorescence analysis of MSC and MSC_LIF cells with antibodies against Ng2, α-Sma, Sm22 and Col4a1, markers related to perivascular cells (all marked in red). Nuclei are contrasted with DAPI (blue). **(B)** Gene expression analysis of MSC and MSC_LIF to *Ng2*, *Acta2* (α-Sma gene), *Tagln* (Sm22 gene) and *Col4a1*. **(C)** mRNA expression analysis of the pro-angiogenic factors *Vegf*, *Cxcl2*, *Ang* and *Ccl2* (MCP-1 gene) in MSC and MSC_LIF cells. The Student's *t* test was used to analyze the differences between groups. Values are expressed as mean ± SEM of at least three independent experiments. $^{*}p < 0.05$; $^{**}p < 0.01$; $^{***}p < 0.001$. Scale bars of MSC-Ng2 = 75 μm. Scale bar of other images = 25 μm.

biomarkers for predicting the proangiogenic effects of MSCs. In our study, we demonstrated that LIF overexpression was correlated with statistically significant upregulation of four genes *Vegf*, *Ccl2* (functional IL8 homolog in mice), *Cxcl2* (Mcp1 gene) and *Ang*, indicating the proangiogenic potency of LIF_MSCs. Several studies have reported LIF signaling on gene expression during differentiation of MSCs, but the role of LIF on expression of proangiogenic growth factors and cytokines has not been

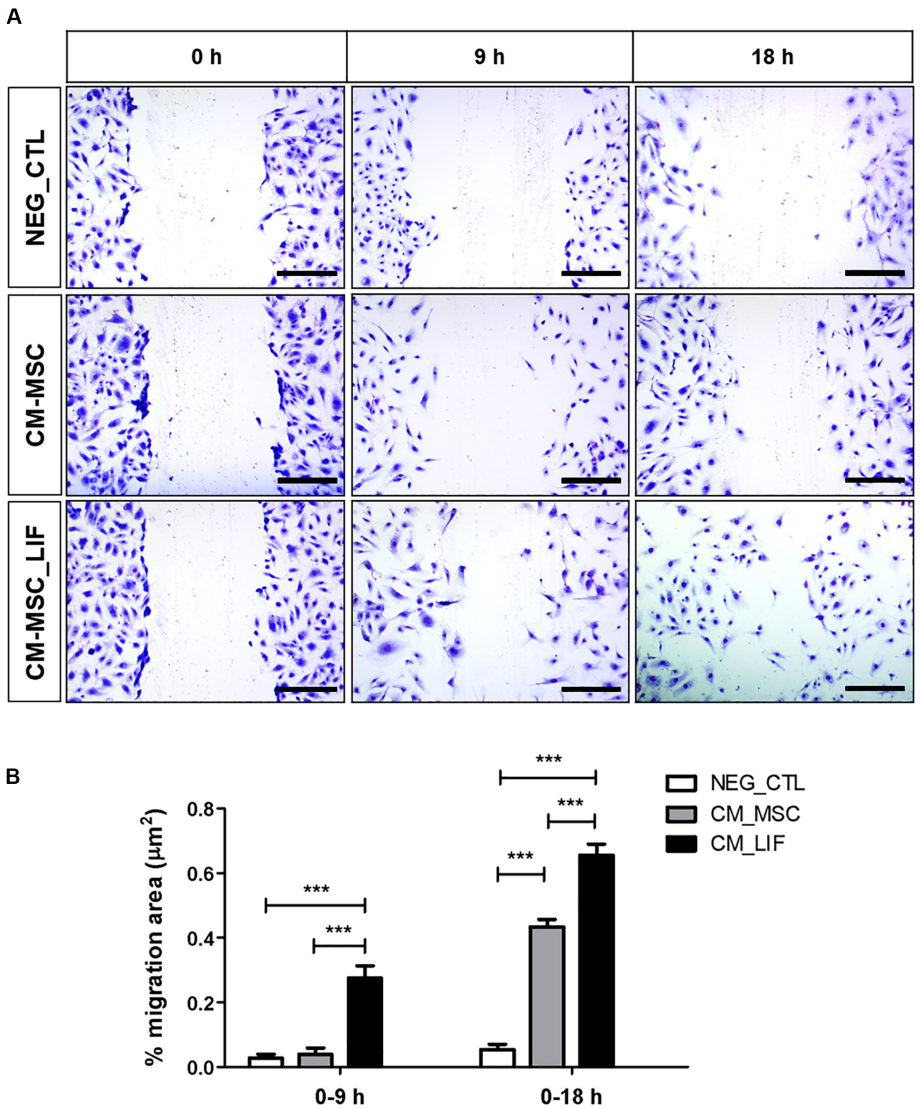

FIGURE 6 | *In vitro* endothelial cell migration. **(A)** Representative image of the migration of HUVEC cells, stained with violet crystal, after 9 or 18 h of incubation in conditioned medium of MSC (CM-MSC) or MSC_LIF (CM-MSC_LIF). **(B)** Quantification of the percentage of variation in the wound area (% migration area). The two-way ANOVA test and the Bonferroni post-test were used to analyze the differences among the groups. Values are expressed as mean ± SEM of at least three independent experiments. ***$p < 0.001$. Scale bars = 250 μm.

demonstrated and deserves attention in future investigations (Oskowitz et al., 2008; Wang et al., 2018, 2019).

In our study, we showed that increased expression of LIF appears to have enriched the secretome of MSC with angiogenic growth factors. Thus, the conditioned medium derived from MSC_LIF (CM-MSC_LIF) stimulated *in vitro* migration of endothelial cells in a conventional two-dimensional assay and enhanced angiogenic sprouting in a three-dimensional model using large vessel (aortic) explants. A similar effect was also observed during co-culture of CTM_LIF with aortic tissue. Finally, in *in vivo* Matrigel assays, the plugs with CM-MSC_LIF displayed significantly higher level of Hb content and were positive stained for CD31-vessels in contrast to control Matrigel plugs. Altogether, these data showed that conditioned medium derived from LIF_MSCs displayed higher proangiogenic activities in comparison to conditioned medium derived from control MSCs.

There is conflicting data on the role of LIF in angiogenesis in the literature, both *in vitro* and *in vivo*. The protective effect of LIF on vasculature by regulating normal vessel density and thickness have been documented in the retina (Yang et al., 2018) while several investigators have reported contradictory effects of LIF on normal and pathological vascular development (Ash et al., 2005; Liu et al., 2019). Liu et al. (2015) reported that LIF stimulates the *in vitro* growth and expansion of Human corneal endothelial cells (HCECs) by blocking contact inhibition via activation of the LIF-Janus kinase 1 signal transducer (JAK1) and transcription signaling activator 3 (STAT3) (Liu et al., 2015).

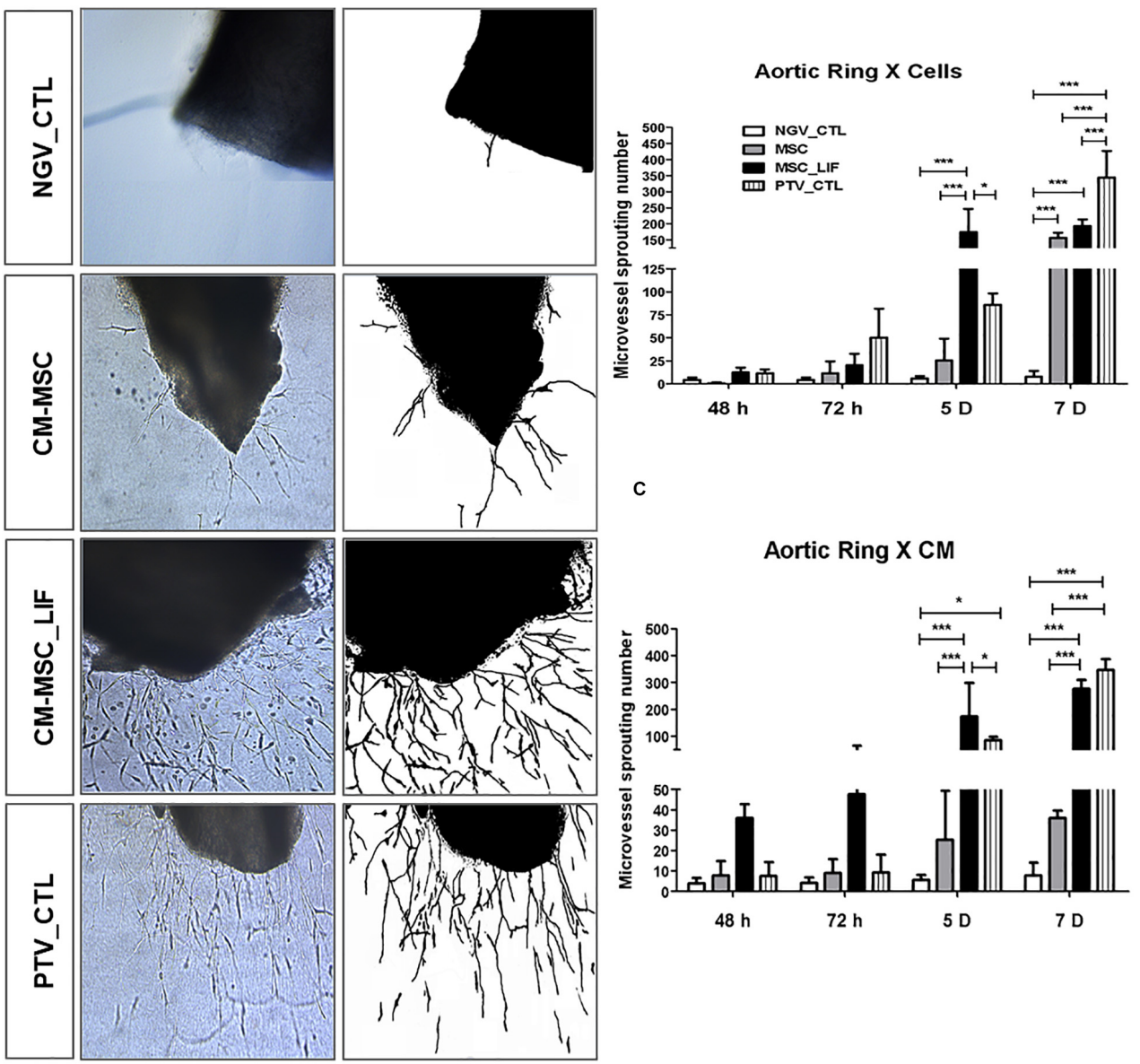

FIGURE 7 | Sprouting of microvessels *in vitro*. **(A)** Representative image of microvessel growth from aortic rings after 5 days of incubation in conditioned medium of MSC (CM-MSC) or MSC_LIF (CM-MSC_LIF). The EBM-2 medium supplemented with recombinant angiogenic factors was used as a positive control (PTV_CTL), and baseline EBM-2 was the negative control (NGV_CTL). Quantification of the number of aortic ring sprouts incubated with **(B)** MSC or MSC_LIF cells or **(C)** conditioned medium from MSC or MSC_LIF on top of the fibrin gel. The two-way ANOVA test and the Bonferroni post-test were used to analyze the differences among the groups. Values are expressed as mean ± SEM of at least three independent experiments. $^{*}p < 0.05$; $^{**}p < 0.01$; $^{***}p < 0.001$.

The retinas of LIF-deficient mice display increased microvessel density due to increased VEGF expression in the vascularized area (Kubota et al., 2008). However, exogenous LIF inhibits VEGF-mediated angiogenesis *in vitro* in bovine aortic endothelial and bovine microvascular endothelial cells (Pepper et al., 1995). Together, these studies have shown that LIF modulates VEGF expression through different mechanisms to ensure adequate capillary density.

In the present study, VEGF and other driving angiogenic factors showed increased transcript expression levels in LIF-overexpressing MSCs, while its conditioned medium showed enhanced proangiogenic potential. These data suggest that the secretory signatures of MSC_LIF and consequently, the therapeutic efficacy of conditioned medium from MSC_LIF can be modulated by LIF overexpression. We propose that the secretion of LIF by LIF-expressing MSCs could enhance its

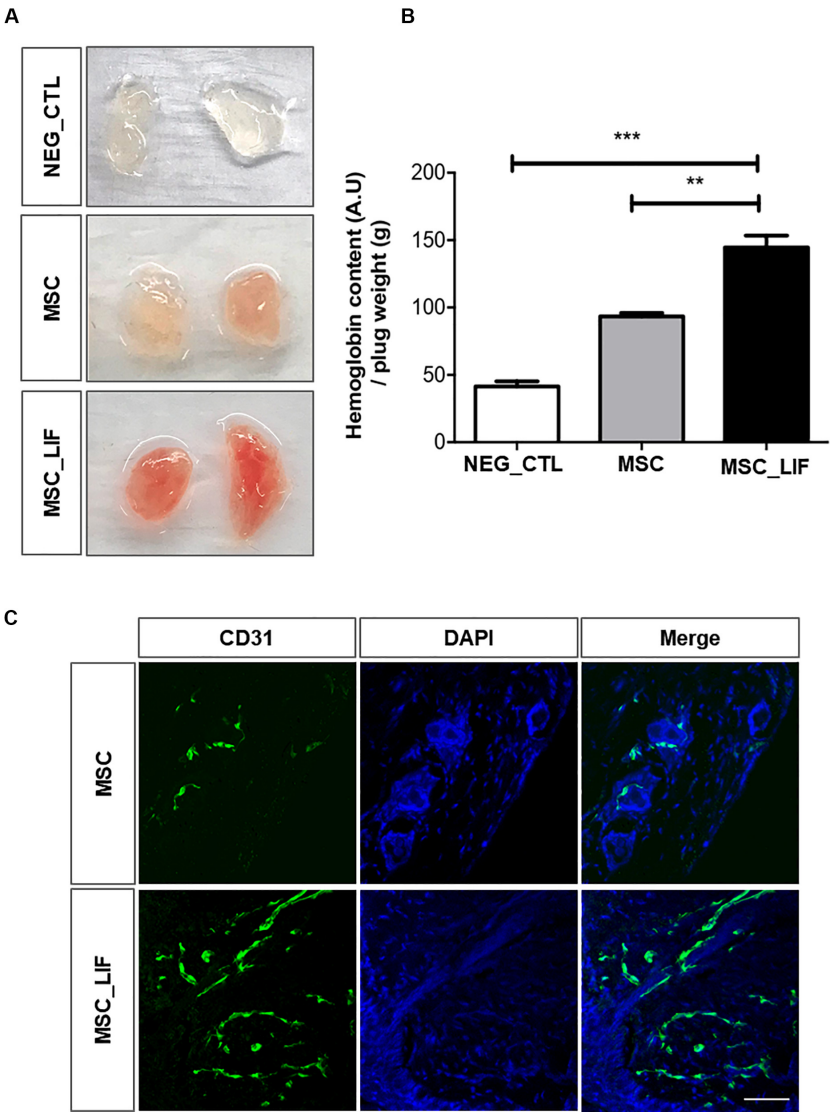

FIGURE 8 | Pro-angiogenic potential of MSC_LIF conditioned medium *in vivo*. Mixture of Matrigel with indicated conditioned medium (MSC or MSC_LIF) or phosphate buffered solution (NEG_CTL) was injected into a mouse ventral area ($n = 3$). After 7 days, Matrigel plugs were measured for hemoglobin (Hb) using Drabkin's solution. **(A)** Representative images and **(B)** quantification of Hb. **(C)** Immunofluorescent staining of frozen Matrigel section with antibodies against endothelial marker CD31 (green). Nuclei are counterstained with DAPI (blue). The two-way ANOVA test and the Bonferroni post-test were used to analyze the differences among the groups. Values are expressed as mean ± SD of at least three independent experiments. $^{**}p < 0.01$; $^{***}p < 0.001$. Scale bars = 50 μm.

proangiogenic effect. Here we found that transcript levels of proangiogenic biomarkers that promote vascular regeneration were increased in response to LIF overexpression, although the molecular mechanisms involved in this process and the secreted factors were not investigated here.

Finally, our study demonstrated that the transgenic expression of LIF in mouse bone marrow-derived mesenchymal stem cells determined a higher proangiogenic activity, via positive regulation of biomarkers related to angiogenic growth. However, the mechanisms of LIF signaling capable of modifying the secretome of MSCs and inducing angiogenesis in ECs remain poorly understood, requiring further investigation. In addition, the therapeutic potential of MSC_LIF in a model that includes all the pathophysiological aspects of ischemic diseases still needs to be investigated.

DATA AVAILABILITY STATEMENT

All datasets generated for this study are included in the article.

ETHICS STATEMENT

The studies involving human participants were reviewed and approved by CEP-Federal University of Bahia. The

patients/participants provided their written informed consent to participate in this study. The animal study was reviewed and approved by CEUA-Hospital São Rafael.

AUTHOR CONTRIBUTIONS

GCS, DS, VF, BS, IO, TS, BP, and GLS contributed to the conception and design, collection and/or assembly of data, data analysis and interpretation, and manuscript writing. RR contributed to the conception and design and financial support. MS contributed to the conception and design, data analysis and interpretation, and manuscript writing. All authors read and approved the final version of the manuscript.

FUNDING

The authors of this work acknowledge for the financial support provided by the Brazilian Research Council (CNPq)/MS grant number 443909/2018-0.

REFERENCES

Ash, J., McLeod, D. S., and Lutty, G. A. (2005). Transgenic expression of leukemia inhibitory factor (LIF) blocks normal vascular development but not pathological neovascularization in the eye. *Mol. Vis.* 11, 298–308.

Auernhammer, C. J., and Melmed, S. (2000). Leukemia-inhibitory factor—neuroimmune modulator of endocrine function. *Endocrine Rev.* 21, 313–345. doi: 10.1210/edrv.21.3.0400

Baker, M., Robinson, S. D., Lechertier, T., Barber, P. R., Tavora, B., D'amico, G., et al. (2012). Use of the mouse aortic ring assay to study angiogenesis. *Nat. Protoc.* 7:89. doi: 10.1038/nprot.2011.435

Bronckaers, A., Hilkens, P., Martens, W., Gervois, P., Ratajczak, J., Struys, T., et al. (2014). Mesenchymal stem/stromal cells as a pharmacological and therapeutic approach to accelerate angiogenesis. *Pharmacol. Ther.* 143, 181–196. doi: 10.1016/j.pharmthera.2014.02.013

Caplan, A. I., and Dennis, J. E. (2006). Mesenchymal stem cells as trophic mediators. *J. Cell. Biochem.* 98, 1076–1084. doi: 10.1002/jcb.20886

Chen, C. W., Okada, M., Proto, J. D., Gao, X., Sekiya, N., Beckman, S. A., et al. (2013). Human pericytes for ischemic heart repair. *Stem cells* 31, 305–316. doi: 10.1002/stem.1285

Chen, G., Xu, X., Zhang, L., Fu, Y., Wang, M., Gu, H., et al. (2014). Blocking autocrine VEGF signaling by sunitinib, an anti-cancer drug, promotes embryonic stem cell self-renewal and somatic cell reprogramming. *Cell Res.* 24, 1121–1136. doi: 10.1038/cr.2014.112

Do Rhee, K., Goureau, O., Chen, S., and Yang, X. J. (2004). Cytokine-induced activation of signal transducer and activator of transcription in photoreceptor precursors regulates rod differentiation in the developing mouse retina. *J. Neurosci.* 24, 9779–9788. doi: 10.1523/jneurosci.1785-04.2004

D'souza, N., Rossignoli, F., Golinelli, G., Grisendi, G., Spano, C., Candini, O., et al. (2015). Mesenchymal stem/stromal cells as a delivery platform in cell and gene therapies. *BMC Med.* 13:186. doi: 10.1186/s12916-015-0426-0

Du, W. J., Chi, Y., Yang, Z. X., Li, Z. J., Cui, J. J., Song, B. Q., et al. (2016). Heterogeneity of proangiogenic features in mesenchymal stem cells derived from bone marrow, adipose tissue, umbilical cord, and placenta. *Stem Cell Res. Therapy* 7:163. doi: 10.1186/s13287-016-0418-9

Gaceb, A., Barbariga, M., Özen, I., and Paul, G. (2018). The pericyte secretome: potential impact on regeneration. *Biochimie* 155, 16–25. doi: 10.1016/j.biochi.2018.04.015

Gearing, D. P., Gough, N. M., King, J. A., Hilton, D. J., Nicola, N. A., Simpson, R. J., et al. (1987). Molecular cloning and expression of cDNA encoding a murine myeloid leukaemia inhibitory factor (LIF). *EMBO J.* 6, 3995–4002. doi: 10.1002/j.1460-2075.1987.tb02742.x

Gonçalves, G. V., Silva, D. N., Carvalho, R. H., Souza, B. S., da Silva, K. N., Vasconcelos, J. F., et al. (2018). Generation and characterization of transgenic mouse mesenchymal stem cell lines expressing hIGF-1 or hG-CSF. *Cytotechnology* 70, 577–591. doi: 10.1007/s10616-017-0131-2

Jaffe, E. A., Nachman, R. L., Becker, C. G., and Minick, C. R. (1973). Culture of human endothelial cells derived from umbilical veins. Identification by morphologic and immunologic criteria. *J. Clin. Investig.* 52, 2745–2756. doi: 10.1172/JCI107470

Jiang, Y., Vaessen, B., Lenvik, T., Blackstad, M., Reyes, M., and Verfaillie, C. M. (2002). Multipotent progenitor cells can be isolated from postnatal murine bone marrow, muscle, and brain. *Exp. Hematol.* 30, 896–904. doi: 10.1016/S0301-472X(02)00869-X

Kim, H. K., Lee, S. G., Lee, S. W., Oh, B. J., Kim, J. H., Kim, J. A., et al. (2019). A subset of paracrine factors as efficient biomarkers for predicting vascular regenerative efficacy of mesenchymal stromal/stem cells. *Stem Cells* 37, 77–88. doi: 10.1002/stem.2920

Kubota, Y., Hirashima, M., Kishi, K., Stewart, C. L., and Suda, T. (2008). Leukemia inhibitory factor regulates microvessel density by modulating oxygen-dependent VEGF expression in mice. *J. Clin. Investig.* 118, 2393–2403. doi: 10.1172/JCI34882

Li, G. G., Chen, S. Y., Xie, H. T., Zhu, Y. T., and Tseng, S. C. (2012). Angiogenesis potential of human limbal stromal niche cells. *Investig. Ophthalmol. Vis. Sci.* 53, 3357–3367. doi: 10.1167/iovs.11-9414

Liu, C. Z., Zhou, H. J., Zhong, J. H., Tang, T., Cui, H. J., Zhou, J. H., et al. (2019). Leukemia inhibitory factor decreases neurogenesis and angiogenesis in a rat model of intracerebral hemorrhage. *Curr. Med. Sci.* 39, 298–304. doi: 10.1007/s11596-019-2034-2

Liu, X., Tseng, S. C., Zhang, M. C., Chen, S. Y., Tighe, S., Lu, W. J., et al. (2015). LIF-JAK1-STAT3 signaling delays contact inhibition of human corneal endothelial cells. *Cell Cycle* 14, 1197–1206. doi: 10.1080/15384101.2015.1013667

Malinda, K. M. (2009). In vivo matrigel migration and angiogenesis assay. *Methods Mol. Biol.* 467, 287–294. doi: 10.1007/978-1-59745-241-0_17

Metcalf, D. (2003). The unsolved enigmas of leukemia inhibitory factor. *Stem Cells* 21, 5–14. doi: 10.1634/stemcells.21-1-5

Mohri, T., Fujio, Y., Maeda, M., Ito, T., Iwakura, T., Oshima, Y., et al. (2006). Leukemia inhibitory factor induces endothelial differentiation in cardiac stem cells. *J. Biol. Chem.* 281, 6442–6447. doi: 10.1074/jbc.M508969200

Murphy, M. B., Moncivais, K., and Caplan, A. I. (2013). Mesenchymal stem cells: environmentally responsive therapeutics for regenerative medicine. *Exp. Mol. Med.* 45:54. doi: 10.1038/emm.2013.94

Nicola, N. A., and Babon, J. J. (2015). Leukemia inhibitory factor (LIF). *Cytokine Growth Fact. Rev.* 26, 533–544. doi: 10.1016/j.cytogfr.2015.07.001

Oskowitz, A. Z., Lu, J., Penfornis, P., Ylostalo, J., McBride, J., Flemington, E. K., et al. (2008). Human multipotent stromal cells from bone marrow and microRNA: regulation of differentiation and leukemia inhibitory factor expression. *Proc. Natl. Acad. Sci. U.S.A.* 105, 18372–18377. doi: 10.1073/pnas.0809807105

Paradis, H., and Gendron, R. L. (2000). LIF transduces contradictory signals on capillary outgrowth through induction of stat3 and (P41/43) MAP kinase. *J. Cell Sci.* 113, 4331–4339.

Parekkadan, B., Van Poll, D., Suganuma, K., Carter, E. A., Berthiaume, F., Tilles, A. W., et al. (2007). Mesenchymal stem cell-derived molecules reverse fulminant hepatic failure. *PLoS One* 2:e000941. doi: 10.1371/journal.pone.0000941

Pepper, M. S., Ferrara, N., Orci, L., and Montesano, R. (1995). Leukemia inhibitory factor (LIF) inhibits angiogenesis in vitro. *J. Cell Sci.* 108, 73–83.

Pinto, D. S., Ahsan, T., Serra, J., Fernandes-Platzgummer, A., Cabral, J. M., and da Silva, C. L. (2020). Modulation of the in vitro angiogenic potential of human mesenchymal stromal cells from different tissue sources. *J. Cell. Physiol.* doi: 10.1002/jcp.29622

Porada, C. D., Stem, C., and Almeida-Porada, G. (2013). The promise of a permanent cure. *NC Med. J.* 74, 526–529.

Ribeiro, T. O., Silveira, B. M., Meira, M. C., Carreira, A. C. O., Sogayar, M. C., Meyer, R., et al. (2019). Investigating the potential of the secretome of mesenchymal stem cells derived from sickle cell disease patients. *PLoS One* 14:e0222093. doi: 10.1371/journal.pone.0222093

Tiscornia, G., Singer, O., and Verma, I. M. (2006). Production and purification of lentiviral vectors. *Nat. Protoc.* 1:241. doi: 10.1038/nprot.2006.37

Wang, T., Yan, R., Xu, X., Yu, H., Wu, J., Yang, Y., et al. (2019). Effects of leukemia inhibitory factor receptor on the adipogenic differentiation of human bone marrow mesenchymal stem cells. *Mol. Med. Rep.* 19, 4719–4726. doi: 10.3892/mmr.2019.10140

Wang, T., Yan, R. Q., Xu, X. Y., Cao, L. L., Liu, J. Y., Zheng, M. R., et al. (2018). Effects of leukaemia inhibitory factor receptor on the early stage of osteogenic differentiation of human bone marrow mesenchymal cells. *Folia Biol.* 64, 186–194.

White, S. M., Renda, M., Nam, N. Y., Klimatcheva, E., Zhu, Y., Fisk, J., et al. (1999). Lentivirus vectors using human and simian immunodeficiency virus elements. *J. Virol.* 73, 2832–2840. doi: 10.1128/jvi.73.4.2832-2840.1999

Williams, R. L., Hilton, D. J., Pease, S., Willson, T. A., Stewart, C. L., Gearing, D. P., et al. (1988). Myeloid leukaemia inhibitory factor maintains the developmental potential of embryonic stem cells. *Nature* 336, 684–687. doi: 10.1038/336684a0

Yang, X. F., Huang, Y. X., Lan, M., Zhang, T. R., and Zhou, J. (2018). Protective effects of leukemia inhibitory factor on retinal vasculature and cells in streptozotocin-induced diabetic mice. *Chin. Med. J.* 131, 75–81. doi: 10.4103/0366-6999.221263

Zhang, B., Yin, Y., Lai, R. C., Tan, S. S., Choo, A. B. H., and Lim, S. K. (2014). Mesenchymal stem cells secrete immunologically active exosomes. *Stem Cells Dev.* 23, 1233–1244. doi: 10.1089/scd.2013.0479

Zou, J., Maeder, M. L., Mali, P., Pruett-Miller, S. M., Thibodeau-Beganny, S., Chou, B. K., et al. (2009). Gene targeting of a disease-related gene in human induced pluripotent stem and embryonic stem cells. *Cell Stem Cell* 5, 97–110. doi: 10.1016/j.stem.2009.05.023

Conflict of Interest: The authors declare that the research was conducted in the absence of any commercial or financial relationships that could be construed as a potential conflict of interest.

frontiers in Cell and Developmental Biology

REVIEW
published: 21 August 2020
doi: 10.3389/fcell.2020.00737

Genetic Engineering as a Strategy to Improve the Therapeutic Efficacy of Mesenchymal Stem/Stromal Cells in Regenerative Medicine

Patricia Kauanna Fonseca Damasceno[1,2], Thaís Alves de Santana[1], Girlaine Café Santos[1], Iasmim Diniz Orge[1,2], Daniela Nascimento Silva[1,2], Juliana Fonseca Albuquerque[1], Giulia Golinelli[3], Giulia Grisendi[3]*, Massimo Pinelli[4], Ricardo Ribeiro dos Santos[1,2,5], Massimo Dominici[3]* and Milena Botelho Pereira Soares[1,2,5]**

[1] Gonçalo Moniz Institute, Oswaldo Cruz Foundation (FIOCRUZ), Salvador, Brazil, [2] Health Institute of Technology, SENAI CIMATEC, Salvador, Brazil, [3] Division of Oncology, Laboratory of Cellular Therapy, University of Modena and Reggio Emilia, Modena, Italy, [4] Division of Plastic Surgery, Department of Medical and Surgical Sciences for Children & Adults, University of Modena and Reggio Emilia, Modena, Italy, [5] National Institute of Science and Technology for Regenerative Medicine (INCT-REGENERA), Rio de Janeiro, Brazil

Mesenchymal stem/stromal cells (MSCs) have been widely studied in the field of regenerative medicine for applications in the treatment of several disease settings. The therapeutic potential of MSCs has been evaluated in studies *in vitro* and *in vivo*, especially based on their anti-inflammatory and pro-regenerative action, through the secretion of soluble mediators. In many cases, however, insufficient engraftment and limited beneficial effects of MSCs indicate the need of approaches to enhance their survival, migration and therapeutic potential. Genetic engineering emerges as a means to induce the expression of different proteins and soluble factors with a wide range of applications, such as growth factors, cytokines, chemokines, transcription factors, enzymes and microRNAs. Distinct strategies have been applied to induce genetic modifications with the goal to enhance the potential of MCSs. This review aims to contribute to the update of the different genetically engineered tools employed for MSCs modification, as well as the factors investigated in different fields in which genetically engineered MSCs have been tested.

Keywords: mesenchymal stem/stromal cells, genetic engineering, regenerative medicine, cell therapy, gene therapy

OPEN ACCESS

Edited by:
Karen Bieback, Heidelberg University, Germany

Reviewed by:
Julie Fradette, Laval University, Canada
Michael Rothe, Hannover Medical School, Germany

****Correspondence:***
Patricia Kauanna Fonseca Damasceno
patriciakauanna@hotmail.com
Giulia Grisendi
giulia.grisendi@unimore.it
Massimo Dominici
massimopinelli1@yahoo.it
Milena Botelho Pereira Soares
milena@bahia.fiocruz.br

Specialty section:
This article was submitted to Stem Cell Research, a section of the journal Frontiers in Cell and Developmental Biology

Received: *28 February 2020*
Accepted: *16 July 2020*
Published: *21 August 2020*

Citation:
Damasceno PKF, de Santana TA, Santos GC, Orge ID, Silva DN, Albuquerque JF, Golinelli G, Grisendi G, Pinelli M, Ribeiro dos Santos R, Dominici M and Soares MBP (2020) Genetic Engineering as a Strategy to Improve the Therapeutic Efficacy of Mesenchymal Stem/Stromal Cells in Regenerative Medicine. Front. Cell Dev. Biol. 8:737. doi: 10.3389/fcell.2020.00737

INTRODUCTION

In the field of stem cell therapy, mesenchymal stem/stromal cells (MSCs) have been widely used in a large number of *in vitro* and *in vivo* studies, as well as in approximately 1000 clinical trials. These are multipotent stem cells that must meet minimum criteria, such as plastic adherence, expression of specific surface markers and the ability to differentiate in adipocytes, chondrocytes and osteocytes (Dominici et al., 2006). Compared to other stem cells, such as embryonic and induced pluripotent stem cells, the use of MSCs has the advantage of being considered safer, regarding the possibility of tumor formation. Additionally, these cells are easier to obtain from different autologous or

allogeneic sources (Kim and Park, 2017). Moreover, MSCs have the capacity to secrete a repertoire of factors with immunomodulatory and anti-apoptotic potential, as well as factors associated to angiogenesis and tissue regeneration (Murphy et al., 2013).

While in numerous studies the therapeutic effects of MSCs have been shown, in others the transplantation of MSCs did not lead to the desired effect, as evaluated in different disease models (Meyer et al., 2006; Huang B. et al., 2012; Sajic et al., 2012). Some studies have shown that transplanted MSCs presented a poor survival rate and proliferation (Shi and Li, 2008; Park J.S. et al., 2015; Li et al., 2016; Silva et al., 2018c; Zhao et al., 2019), possibly due to the hostile microenvironment of lesioned tissues, which could lead to nutrient deprivation and cell death (Moya et al., 2018). Moreover, partial beneficial effects may be enhanced by expression of specific factors capable of promoting desired effects in the target disease setting. Therefore, approaches aiming to enhance the efficacy of MSC transplantation are needed in order to achieve the suitable results.

Genetic engineering of MSCs has been studied in the past years with the purpose of enhancing the therapeutic potential of these cells and improving the outcomes after transplantation. This has been achieved using non-viral or viral vectors to induce the expression of different factors, depending on the desired results, such as increasing their survival and proliferation rate and improving their pro-regenerative capacity (Sage et al., 2016; Foppiani et al., 2019). In this review, we discuss the current methods employed in the generation of genetically modified MSCs and the results obtained with the expression of different factors and the main disease settings in which this modality of cell and gene therapy has been investigated. **Table 1** summarizes the modification agents, cell source, genetic engineering method and applications of diverse studies described in this review.

MSC AS A CELL TARGET FOR GENETIC MODIFICATION AND GENE THERAPY

Several genetic engineering methods to modify the MSCs gene expression profile have been described, as seen in **Table 2**. These techniques can be classified as those using viral vectors or non-viral methods. Replication-deficient viruses are the most used gene transfer tools, mainly due to their high efficiency in DNA transfer when compared to non-viral methods. However, the use of viral vectors in the clinical practice has been limited by the high cost of cell line production and the possibility of adverse immunological reactions, or even the occurrence of insertional mutagenesis, which may lead to the activation of oncogenes (Park J.S. et al., 2015).

Non-viral methods, on the other hand, can be manufactured on a large scale and have low immunogenicity. Currently, the genetic modification of MSCs using non-viral vectors can be performed by physical or chemical methods. The physical methods used in MSCs include electroporation, nucleofection and sonoporation (Otani et al., 2009; Baraniak and Mcdevitt, 2010; Cantinieaux et al., 2013). Chemical methods use lipidic agents, polymers and inorganic nanoparticles (Uchimura et al., 2007; Park et al., 2010). Although the use of non-viral vectors has some advantages for the process of genetic modification of MSCs compared to viral vectors, the impairment of cell viability, low efficiency and transient expression of transgenes make these methods less used in the clinical practice (Marofi et al., 2017).

Viral vectors are the most used tool in the MSC genetic modification protocols, and it has been demonstrated that the high efficiency of viral transduction in these cells (approximately 90%) does not affect their immunophenotypic characteristics, as well as their potential for cell differentiation and secretion of bioactive molecules, which are preserved after genetic modification (Delcayre et al., 2005; Biancone et al., 2012). In addition, viral transduction ensures stable and long-term transcription of the gene of interest and, consequently, a greater efficiency compared to other methods that do not use viral vectors for genetic modification of MSCs (Sage et al., 2016). Currently, there is extensive clinical experience with several types of vectors that include mainly vaccinia, measles, vesicular stomatitis virus (VSV), polio, reovirus, adenovirus, lentivirus, retrovirus, adeno-associated virus (AAV), and herpes virus simplex (HSV). Among those, the most predominant vectors used for cell transduction and transplantation are the lenti- and retroviral vectors. Beyond those applications, AAV vectors have been used as favored vehicle for direct gene delivery to specific tissues (Finer and Glorioso, 2017).

Adenoviral vectors do not integrate into the host genome and can transduce both dividing and quiescent cells with high efficiency. Obtaining high titers of the recombinant vectors is relatively easy with little cytotoxic effect on the packaging cells (Vemula and Mittal, 2010). However, the high immunogenicity and transient expression of the transgene limits its application in clinical practice (Somia and Verma, 2000). Adeno-associated viruses, on the other hand, have no viral gene in its recombinant form used for gene therapy, a characteristic that contributes to a low immunogenicity and pathogenicity. Also, they are dependent on co-infection with other viruses, mainly adenoviruses, in order to replicate. Recombinant adeno-associated viruses episomal DNA is unable to integrate in the host genome, therefore reducing the consistency of transgene expression along the time in proliferating cells (Sage et al., 2016; Naso et al., 2017). However, a limiting factor for the use of AAVs is the action of neutralizing antibodies present in a large part of the population, which drastically reduces their effectiveness *in vivo* (Nayak and Herzog, 2010).

Retroviruses are RNA viruses made up of three essential *genes*: gag, pol and env, which encode the structural protein, reverse transcriptase / integrase and glycoprotein of the viral envelope, respectively. These genes are arranged in separate plasmids and separately for the packaging cells in order to avoid recombination or generation of retroviruses competent for viral replication. Obtaining high viral titers is relatively easy using these vectors; however, the biggest limitation of retroviral vectors is their inability to transduce quiescent cells. Lentiviruses, however, have the property of transducing dividing and quiescent cells (Lewis et al., 1992; Vargas et al., 2016). Currently, lentiviral vectors are

TABLE 1 | Genetic modifications in MSCs and disease models tested.

Factor overexpressed	MSC source	Method	Disease	References
Akt	Mouse bone marrow	Retrovirus	Myocardial infarction	Noiseux et al., 2006
	Rabbit amniotic fluid	Lentivirus	Heart ischemia-reperfusion injury	Wang et al., 2016
	Human umbilical cord	Adenovirus	Acute myocardial infarction	Ma et al., 2017
	Rat bone marrow	Retrovirus	Myocardial infarction	Gnecchi et al., 2006, 2009
Akt and angiopoietin-1 (Ang-1)	Rat bone marrow	Adenovirus	Infarcted heart	Jiang et al., 2006
Akt and Wnt11	Rat bone marrow	AAV	Hypoxia/reoxygenation-induced cardiomyocyte apoptosis	Chen B. et al., 2018
Angiogenin	Yorkshire pig bone marrow	Adenovirus	Myocardial chronic ischemic	Huang et al., 2006
Angiopoietin-1 (Ang1)	Mouse bone marrow	Plasmid transfection	Acute respiratory distress syndrome	Mei et al., 2007
	Rat bone marrow	Lentivirus	Phosgene-induced acute lung injury	Shao et al., 2018
Angiotensin II type 2 receptor	Human bone marrow	Lentivirus	LPS-induced acute lung injury	Xu et al., 2018
Angiotensin-converting enzyme 2 (ACE2)	Mouse bone marrow	Lentivirus	Acute lung injury	He et al., 2015
Arginine decarboxylase	Human adipose tissue	Retrovirus	Spinal cord injury	Park Y.M. et al., 2015
ATP7B	Human bone marrow	Retrovirus	Wilson's disease	Sauer et al., 2010
Basic fibroblast growth factor (bFGF)	Human bone marrow	Lentivirus	Angiogenesis	Fierro et al., 2011
	Rat bone marrow	Lentivirus	Ischemic disease	Zhang J.C. et al., 2014
B-cell lymphoma protein 2 (BCL-2)	Rat bone marrow	AAV	Liver cirrhosis	Jin et al., 2016
Brain-derived neurotrophic factor (BDNF)	Human umbilical cord blood	Plasmid transfection	Neurological injury and disease	Lim et al., 2011
	Human bone marrow	Lentivirus	Neuronal degeneration	Scheper et al., 2019
	Rat bone marrow	Adenovirus	Spinal cord injury	Zhao et al., 2013
	Rat bone marrow	Adenovirus	Neonatal stroke	Van Velthoven et al., 2013
	Rat bone marrow	Lentivirus	Ischemia	Zhou et al., 2017
C1q/tumor necrosis factor-related protein-3 (CTRP3)	Mouse bone marrow	Lentivirus	Myocardial infarction	Zhang Z. et al., 2019
C-C chemokine receptor type 2 (CCR2)	Human bone marrow	Lentivirus	Ischemic stroke	Zhang Y. et al., 2018
C-C chemokine receptor type 1 CCR1	Mouse bone marrow	Retrovirus	Injured myocardium	Huang et al., 2010
Cellular repressor of E1A-stimulated genes (CREG)	Rat bone marrow	Adenovirus	Myocardial infarction	Deng et al., 2010
Cerebral dopamine neurotrophic factor (CDNF)	Rat bone marrow	Lentivirus	Spinal cord injury	Zhao et al., 2014
Ciliary neurotrophic factor (CNTF)	Rat bone marrow	Plasmid transfection	Traumatic injury to the central nervous system	Abbaszadeh et al., 2015
c-MYC	Mouse bone marrow	Retrovirus	Osteosarcoma	Shimizu et al., 2010
Csx/Nkx2.5 and GATA4	Mouse bone marrow	Retrovirus	Stochastic cardiomyogenic fate	Yamada et al., 2007
	Mouse bone marrow	Retrovirus	Myocardial infarction	Gao et al., 2011
CXC chemokine receptor 4 (CXCR4)	Human umbilical cord	Lentivirus	Radiation- induced lung injury	Zhang C. et al., 2019
	Mouse bone marrow	Retrovirus	Breast cancer	Kalimuthu et al., 2017
	Mouse bone marrow	Lentivirus	Inflammatory bowel and cancer	Zheng et al., 2019
	Rat bone marrow	Retrovirus	Myocardial infarction	Cheng et al., 2008
	Rat bone marrow	Adenovirus	Ischemic heart injury	Wu S. Z. et al., 2017
	Rat bone marrow	Lentivirus	Myocardial infarction	Kang et al., 2015
	Mouse bone marrow	Lentivirus	Acute kidney injury	Liu et al., 2013
	Rat bone marrow	Adenovirus	Liver regeneration	Du et al., 2013
	Rat bone marrow	Lentivirus	Myocardial neovascularization	Liang et al., 2012
	Mouse bone marrow	Adenovirus	Myocardial infarction	Huang Z. Y. et al., 2012
	Rat bone marrow	Adenovirus	Myocardial infarction	Zhang et al., 2008
CXC chemokine receptor 7 (CXCR7)	Rat bone marrow	Lentivirus	Acute lung injury	Shao et al., 2019
Cytosine deaminase (CD) and Herpes simplex virus thymidine kinase (HSV-tk)	Human umbilical cord blood	Lentivirus	Ovarian cancer	Jiang et al., 2014

(Continued)

TABLE 1 | Continued

Factor overexpressed	MSC source	Method	Disease	References
Drosophila mothers against decapentaplegic 7 (Smad7)	Rat bone marrow	Lentivirus	Hepatic fibrosis	Wu S. P. et al., 2017
Endothelial nitric oxide synthase (eNOS)	Rat bone marrow	Adenovirus	Endothelial dysfunction	Kanki-Horimoto et al., 2006
	Mouse bone marrow	Adenovirus	Myocardial Infarction	Chen L. et al., 2017
Ephrin-B2	Human bone marrow	Plasmid transfection	Ischemic tissues	Duffy et al., 2010
Erythropoietin (EPO)	Mouse bone marrow	Retrovirus	Myocardial infarction	Copland et al., 2008
	Mouse bone marrow	Retrovirus	Cancer immunotherapy	Campeau et al., 2009
Extracellular regulating kinase 1/2 (ERK1/2)	Rat bone marrow	Lentivirus	Ischemic stroke	Gao et al., 2019
Fibroblast growth factor 21 (FGF21)	Mouse bone marrow	Lentivirus	Traumatic brain injury	Shahror et al., 2019
Fibroblast growth factor 4 (FGF4)	Rat bone marrow	Lentivirus	Liver cirrhosis	Wang et al., 2015
Follistatin-like 1 (Fstl1)	Mouse bone marrow	Lentivirus	Myocardial infarction	Shen et al., 2019
Forkhead box protein (Foxa2)	Human adipose tissue	Plasmid transfection	Acute liver injury	Chae et al., 2019
	Rat bone marrow	Plasmid transfection	Hepatic diseases	Cho J.W. et al., 2012
GATA-4	Mouse bone marrow	Lentivirus	Myocardial infarction	He et al., 2019
	Rat bone marrow	Retrovirus	Myocardial ischemia	Yu B. et al., 2016
	Rat bone marrow	Retrovirus	Heart ischemic injury	Li et al., 2014
Glial-derived neurotrophic factor (GDNF)	Human adipose	Lentivirus	Renal interstitial fibrosis	Wang Z. et al., 2019
	Rat bone marrow	Plasmid transfection	Neurodegenerative diseases	Noori-Zadeh et al., 2014
	Human bone marrow	Adenovirus	Nephrotoxic serum nephritis (NSN)	Huang Z. Y. et al., 2012
	Rat bone marrow	Adenovirus	Intracerebral hemorrhage (ICH)	Yang et al., 2011
Glucocorticoid-induced tumor necrosis factor–related receptor (GITR)	Human bone marrow	Plasmid transfection	Small cell lung cancer	Kopru et al., 2018
Glycogen synthase kinase-3β (GSK-3β)	Mouse bone marrow	Adenovirus	Myocardial infarction	Cho et al., 2011
Granulocyte chemotactic protein (GCP)-2	Human adipose tissue	Lentivirus	Myocardial infarction	Kim et al., 2012
Granulocyte-colony stimulating factor (G-CSF)	Mouse bone marrow	Lentivirus	Chagas disease cardiomyopathy	Silva et al., 2018b
Heme oxygenase-1 (HO-1)	Mouse adipose tissue	Plasmid transfection	Heart ischemic injury	Preda et al., 2014
	Rat bone marrow	Lentivirus	Acute lung injury	Chen X. et al., 2018
	Dog adipose tissue	Lentivirus	Spinal cord injury	Lee et al., 2017
	Human embryonic stem cell	Lentivirus	Myocardial infarction	Kearns-Jonker et al., 2012
	Rabbit adipose tissue	Adenovirus	Myocardial infarction	Yang et al., 2012
Hepatocyte growth factor (HGF)	Human bone marrow	Retrovirus	Bladder outlet obstruction	Song et al., 2012
	Rat bone marrow	Adenovirus	Hepatocirrhosis	Zhang Y. et al., 2018
	Human umbilical cord	Lentivirus	Myocardial infarction	Zhao et al., 2016
	Human bone marrow	Adenovirus	Liver fibrosis	Lai et al., 2015
	Human umbilical cord	Adenovirus	Injured sinonasal mucosa	Li et al., 2015
	Rat bone marrow	Lentivirus	Liver damage caused by radiotherapy	Zhang J. et al., 2014
	Human umbilical cord	Adenovirus	Parkinson's disease	Liu et al., 2014
	Human umbilical cord blood	Plasmid transfection	Liver fibrosis	Seo et al., 2014
	Rat bone marrow	Adenovirus	Pulmonary arterial hypertension	Guo et al., 2013
	Human bone marrow	Lentivirus	Spinal cord injury	Jeong et al., 2012
	Rat bone marrow	Adenovirus	Post-ischemic heart failure	Guo et al., 2008
	Pig adipose tissue	Lentivirus	Intramyocardial transplant	Gómez-Mauricio et al., 2016
Hepatocyte nuclear factor 4α (HNF4α)	Human umbilical cord	Lentivirus	Hepatocellular carcinogenesis (HCC)	Wu et al., 2016
	Mouse bone marrow	Adenovirus	Liver cirrhosis	Ye et al., 2019
Human a1-antitrypsin (hAAT)	Mouse adipose tissue	Lentivirus	Disorders of liver metabolism	Di Rocco et al., 2012

(Continued)

TABLE 1 | Continued

Factor overexpressed	MSC source	Method	Disease	References
Human elastin	Rat bone marrow	Adenovirus	Myocardial infarction	Li et al., 2012
Human N-cadherin	Human umbilical cord blood	Lentivirus	Myocardial infarction	Lee et al., 2012
Hypoxia inducible factor (HIF)-1α.	Human bone marrow	Lentivirus	Angiogenesis	Razban et al., 2012
	Rat bone marrow	Adenovirus	Ischemic cerebrovascular disease	Yang et al., 2014
	Sheep bone marrow	Plasmid transfection	Acute myocardial infarction	Hnatiuk et al., 2016
IL-1Ra	Rats amniotic fluid	Lentivirus	Fulminant hepatic failure	Zheng et al., 2012
IL-33	Rat bone marrow	Lentivirus	Myocardial infarction	Chen Y. et al., 2017
IL-4	Human adipose tissue	Lentivirus	Multiple sclerosis	Payne et al., 2012
Insulin growth factor like-I (IGF-I)	Rat bone marrow	Adenovirus	Myocardial infarction	Haider et al., 2008
	Mouse bone marrow	Retrovirus	Renal failure-induced anemia	Kucic et al., 2008
	Pig adipose tissue	Lentivirus	Intramyocardial transplant	Gómez-Mauricio et al., 2016
	Mouse bone marrow	Retrovirus	Spinal cord injury	Allahdadi et al., 2019
	Mouse bone marrow	Lentivirus Adenovirus	Chagas disease cardiomyopathy	Silva et al., 2018a
	Mouse bone marrow	Adenovirus	Cirrhosis	Fiore et al., 2015
Integrin linked kinase (ILK)	Mini-pig bone marrow	Adenovirus	Myocardial infarction	Mao Q. et al., 2014
	Rats bone marrow	Adenovirus	Myocardial infarction	Mao et al., 2013
Integrin α4	Rat bone marrow	Lentivirus	Cerebral Embolism	Cui et al., 2017
Intercellular Adhesion Molecule 1 (ICAM-1)	Mouse compact bone	Plasmid transfection	Inflammatory bowel disease	Li et al., 2019
Interferon-beta (IFN-β)	Dog adipose tissue	Lentivirus	Melanoma	Han et al., 2015
	Mouse bone marrow	Lentivirus	Breast cancer	Ling et al., 2010
Interleukin-10	Mouse bone marrow	CRISPRa system	Myocardial infarction	Meng et al., 2019
	Rat bone marrow	Lentivirus	Traumatic brain injury	Maiti et al., 2019
	Human amniotic fluid	Adenovirus	Liver fibrosis	Choi et al., 2019
	Mouse bone marrow	Retrovirus	Acute lung injury	Wang et al., 2018
	Human bone marrow	AAV	Acute Ischemic Stroke	Nakajima et al., 2017
	Rat bone marrow	Adenovirus	Myocardial infarction	Meng et al., 2017
Klotho	Mouse bone marrow	Adenovirus	Acute kidney injury	Zhang F. et al., 2018
Large Tumor Suppressor gene 2 (LATS2)	Mouse bone marrow	Lentivirus	Acute respiratory distress syndrome	Dong and Li, 2019
Leptin	Human bone marrow	Lentivirus	Myocardial infarction	Yang et al., 2018
LIM-homeobox transcription factor islet-1 (ISL1)	Human bone marrow	Lentivirus	Myocardial infarction	Xiang et al., 2018
Lipocalin2 (Lcn2)	Rats bone marrow	Plasmid transfection	Kidney injury	Halabian et al., 2014
Liver X receptor-α (LXRα)	Mouse bone marrow	Retrovirus	Pathophysiology of the renin-angiotensin system	Matsushita et al., 2010
Mammalian achaete-scute homologue-1 (Mash1)	Rat bone marrow	Lentivirus	Neurodegenerative disorders	Wang K. et al., 2013
MCT4	Mouse bone marrow	Retrovirus	Myocardial ischemia	Saraswati et al., 2015
miR-1	Mouse bone marrow	Lentivirus	Myocardial infarction	Huang et al., 2013b
miR-101-3p	Human bone marrow	Lentivirus	Oral cancer	Xie et al., 2019
miR-124	Rat bone marrow	Lentivirus	Spinal cord injury	Zou et al., 2014
miR-126	Mouse bone marrow	Lentivirus	Ischemic angiogenesis	Huang et al., 2013a
miR-133	Rat bone marrow	Lentivirus	Acute myocardial infarction	Chen L. et al., 2017
miR-133b	Rat bone marrow	Lentivirus	Stroke	Xin et al., 2017
miR-16−5p	Human bone marrow	Plasmid transfection	Colorectal cancer	Xu et al., 2019
miR-199a	Human bone marrow	Plasmid transfection	Glioma	Yu et al., 2019
miR-199a-3p	Human bone marrow	miRNA transfection	Renal ischemia/reperfusion injury	Zhu et al., 2019

(Continued)

TABLE 1 | Continued

Factor overexpressed	MSC source	Method	Disease	References
miR-211	Rat and human bone marrows	Lentivirus	Adverse post-MI remodeling	Hu et al., 2016
miR-23a	Rat bone marrow	Lentivirus	Myocardial infarction	Mao J. et al., 2014
miR-30b-3p	Mouse bone marrow	Lentivirus	Acute lung injury	Yi et al., 2019
miR-34a	Human bone marrow	Lentivirus	Glioblastoma	Wang B. et al., 2019
miR-705	Mouse bone marrow	Lentivirus	Ischemic brain injury	Ji et al., 2017
miR-let-7d or miR-154	Human bone marrow	Lentivirus	Lung injury	Huleihel et al., 2017
miRNA-181	Human umbilical cord blood	Lentivirus	Myocardial ischemia-reperfusion injury	Wei et al., 2019
miRNA-21	Rat bone marrow	Lentivirus	Intracerebral hemorrhage	Zhang H. et al., 2018
miRNA-21	Rat bone marrow	Lentivirus	Myocardial damage	Zeng et al., 2017
miRNA-25	Rat bone marrow	Lentivirus	Transient spinal cord ischemia	Zhao et al., 2018
as-miR-937	Mouse bone marrow		Alzheimer's Disease	Liu et al., 2015
Monocyte chemoattractant protein-induced protein 1 (MCPIP1)	Mouse bone marrow	Retrovirus	Myocardial repair	Labedz-Maslowska et al., 2015
Neuregulin 1 (NRG1)	Human adipose tissue	Adenovirus	Cerebral ischemia	Ryu et al., 2019
Neuregulin 4 (Nrg4)	Mouse adipose tissue	Lentivirus	Insulin resistance and hepatic steatosis	Wang W. et al., 2019
Neurotrophin-3 (NT-3)	Rat bone marrow	Plasmid transfection	Parkinson disease	Moradian et al., 2017
Nuclear factor (erythroid-derived 2)-like 2 (Nrf2)	Human amniotic fluid	Lentivirus	Acute lung injury	Zhang et al., 2017
Oct4 and *Sox2*	Human adipose tissue	Plasmid transfection	Liver injury	Han et al., 2014
p130 and E2F4	Mouse bone marrow	Lentivirus	Acute respiratory distress syndrome	Zhang X. et al., 2019
PARKIN	Human Wharton's jelly	Plasmid transfection	Parkinson's disease	Bonilla-Porras et al., 2018
Periostin	Rat bone marrow	Lentivirus	Myocardial infarction	Cho Y.H. et al., 2012
Pigment epithelial-derived factor (PEDF)	Human bone marrow	Lentivirus	Hepatocellular carcinoma	Gao et al., 2010
	Human or rat bone marrow	Plasmid transfection	Cerebral ischemia-reperfusion injury	Huang Y. et al., 2018
	Mouse bone marrow	AAV	Glioma	Wang Q. et al., 2013
Receptor activity-modifying protein 1 (RAMP1)	Rabbit bone marrow	Adenovirus	Carotid angioplasty and myocardial infarction	Shi et al., 2014
Receptor tyrosine kinase-like orphan receptor 2 (ROR2)	Mouse bone marrow	Lentivirus	Acute respiratory distress syndrome (ARDS)	Cai et al., 2016
Sirtuin 1 (Sirt 1)	Mouse bone marrow	Adenovirus	Prostate cancer	Yu Y. et al., 2016
Sonic Hedgehog (Shh)	Mouse bone marrow	Lentivirus	Inflamed stomach	Donnelly et al., 2014
	Rat bone marrow	Lentivirus	Spinal cord injury	Jia et al., 2014
SRC3-specific short hairpin RNA (sh-SRC3)	Human bone marrow	Lentivirus	Multiple myeloma	Ji et al., 2017
sST2	Human adipose tissue	Lentivirus	Occupational asthma	Martínez-González et al., 2014
	Human adipose tissue	Lentivirus	Endotoxin-induced acute lung injury	Martínez-González et al., 2013
Stromal cell derived factor-1 (SDF-1)	Rat bone marrow	Lentivirus	Acute myocardial infarction	Unzek et al., 2007
	Mouse bone marrow	Lentivirus	Post-acute myocardial infarction	Mayorga et al., 2017
	Human umbilical cord blood	Plasmid transfection	Myocardial infarction	Gong et al., 2019
	Rat and human bone marrows	Retrovirus	Spinal cord injuries	Stewart et al., 2017
Telomerase (TERT) and myocardin (MYOCD)	Mouse adipose tissue	Lentivirus	Ischemic cardiovascular diseases	Madonna et al., 2019
Thioredoxin-1 (Trx-1)	Human umbilical cord	Adenovirus	Acute radiation injury (ARI)	Hu et al., 2013

(Continued)

TABLE 1 | Continued

Factor overexpressed	MSC source	Method	Disease	References
Tissue matrix metalloproteinase inhibitor 2 (TIMP2)	Human umbilical cord	Lentivirus	Myocardial infarction	Ni et al., 2019
TNF-related apoptosis-inducing ligand (TRAIL)	Human bone marrow	Lentivirus	Non-small cell lung cancer	Xia et al., 2013
	Human adipose tissue	Plasmid transfection	Glioblastoma multiforme	Jiang et al., 2016
	Human adipose tissue	Lentivirus	Pancreatic ductal adenocarcinoma	Spano et al., 2019
	Human bone marrow	Lentivirus	Colorectal carcinoma	Mueller et al., 2011
	Human bone marrow	Lentivirus	Metastatic lung tumors	Loebinger et al., 2009
	Human bone marrow	Lentivirus	Cancer cell lines	Yuan et al., 2017
Transforming growth factor (TGF)β1	Human bone marrow	Lentivirus	Angiogenesis	Fierro et al., 2011
	Rat bone marrow	Lentivirus	Renal ischemia/reperfusion injury	Cai et al., 2019
Tropomyosin receptor kinase A (TrkA)	Rat bone marrow	Lentivirus	Peripheral nerve injury	Zheng et al., 2017
Tumor necrosis factor α (TNF α)	Human adipose tissue	Retrovirus	Lung metastases	Tyciakova et al., 2017
Tyrosine kinase C (TrkC)	Rat bone marrow	Adenovirus	Spinal cord injury	Ding et al., 2013
	Rat bone marrow	Adenovirus	Demyelinated spinal cord	Ding et al., 2015
Urokinase plasminogen activator	Human umbilical cord blood	Adenovirus	Tumor tropism	Pulukuri et al., 2010
Vascular endothelial growth factor (VEGF)	Human bone marrow	Lentivirus	Peripheral nerve injury	Man et al., 2016
	Sheep bone marrow	Plasmid transfection	Myocardial infarction	Locatelli et al., 2015
	Mouse bone marrow	Plasmid transfection	Alzheimer's disease	Garcia et al., 2014
	Rat bone marrow	Lentivirus	Cardiac arrest	Zhou et al., 2017
	Mouse bone marrow	Adenovirus	Heart infarction	Wang et al., 2006
Wnt11	Rat bone marrow	Retrovirus	Cardiac ischemic Injury	Zuo et al., 2012
β-catenin	Mouse bone marrow	Lentivirus	Acute respiratory distress syndrome (ARDS)	Cai et al., 2015

the most used in gene therapy, whether in preclinical or clinical studies, as they guarantee high process efficiency, as shown by the increased number of phase I clinical studies evaluating the safety of gene therapies using lentiviruses conducted in recent years (Milone and O'Doherty, 2018).

Recently, new genetic modification tools arose in order to promote insertion, deletion or correction of genes at specific sites in the genome, and MSCs have been used as a target for these new modifying tools for applications in different diseases (Torres et al., 2014; van den Akker et al., 2016; Gerace et al., 2017; Li et al., 2018; Meng et al., 2019). The site-specific integration of genes can be achieved using tools such as Zinc Finger Nuclease (ZFN), Transcription Activator-Like Effector Nuclease (TALENS) or Clustered Regularly Interspaced Short Palindromic Repeats (CRISPR/Cas9), which are nucleases capable of recognizing and direct the integration of genes in a site-specific manner. These molecular-editing tools can be further explored to improve safety and efficiency of gene insertion/expression (Park J.S. et al., 2015).

APPLICATIONS IN CANCER TREATMENT

Cancer is the second leading cause of global death (WHO, 2020), and conventional chemotherapies have shown poor efficacy for the treatment of cancer in advanced stages. Cell therapy emerged in the last years as a promising tool for cancer treatment. Furthermore, a growing number of cell therapies are being tested in combination with other therapeutic agents, such as checkpoint inhibitors (Li et al., 2017; Hu et al., 2018; Cao et al., 2019).

Along the past years, many studies have been focused on MSCs potential to act as "Trojan horses," promoting the delivery of anticancer immunostimulatory agents, such as chemokines and cytokines, to cancer site due to their tumoral tropism (Hmadcha et al., 2020). The chemokine receptor 4 (CXCR4) plays a critical role in MSCs homing and survival to tumor sites. Overexpression of CXCR4 in adipose tissue (Ad-MSCs) and bone marrow (BMSCs) MSCs promoted anti-tumor activity in different studies (Bobis-Wozowicz et al., 2011). In a mouse model of colitis-associated tumorigenesis, BMSCs transduced with lentiviral vector carrying either CXCR4 had an enhanced homing (2-fold) to inflamed intestinal tissues when compared to control MSCs (Zheng et al., 2019). This higher migratory and engraftment capacity was also observed in an *in vivo* breast cancer mouse model, in which MSCs administered systemically via the tail vein reached the tumors, even though part of the cells remained in the lungs. Moreover, the overexpression of CXCR4 in MSCs increased the accumulation in the tumor compared to non-CXCR4-overexpressing MSCs (Kalimuthu et al., 2017). A study using BMSCs genetically modified to express

TABLE 2 | Genetic engineering methods for MSCs modification.

Genetic engineering methods	Advantages	Limitations
Retrovirus	- Easy manipulation and vector design	- Only transduce dividing cells
	- Stable and efficient gene transfer	- Risk of insertional mutagenesis
	- Extensive cell transduction tropism	
Lentivirus	- Transduce dividing and non-dividing cells	- Risk of insertional mutagenesis
	- Stable and efficient gene transfer	- Size of the therapeutic gene (<10 kb) insert
	- High levels of transgene expression	
	- High titers	
Adenovirus	- Efficient gene transfer	- Transient gene expression
	- Large insert capacity	- High immunogenicity
Adeno-associated virus	- Efficient gene transfer	- Small size of the therapeutic gene insert (<5 kb)
	- Extensive cell transduction tropism	- Low yield (hard to produce)
	- Low immunogenicity	- Transient gene expression in dividing cells
Non-viral (Liposomes and plasmids)	- Low immunogenicity	- Low transfection efficiency
	- Safe manipulation	- Transient gene expression
CRISPR/Cas9, ZFN and TALEN	- Precise gene edition (mutation, insertion, replacement, or deletion)	-Off-target effects risk
	- Relative high efficiency	- Target sequencing must precede a protospacer adjacent motif (PAM) (CRISPR/Cas9) -Not easy to design (ZNF and TALEN)

the CXC receptor 7 (CXCR7), a newly discovered chemokine ligand 12 (CXCL12) receptor that promotes migration to tumor, showed an increase in cell migration and proliferation, which may be attributed to the CXCL12 secreted by MSCs, thus promoting a positive feedback for CXCL12/CXCR7 axis (Liu et al., 2018).

Another explored cancer therapy strategy was the genetic modification of Ad-MSCs to overexpress the cytokine interferon-beta (IFN-β) in an *in vitro* model of canine melanoma. The cytokine family in which IFN-β belongs is known for their antiviral, immunomodulatory and antiproliferative effects. This approach was tested as an adjunctive therapy in order to begin and maintain skin lesion remission caused by pemphigus foliaceus. Ad-MSCs overexpressing IFN-β was associated with pro-apoptotic and growth-inhibitory effects on canine melanoma cells when compared with non-modified MSCs (Han et al., 2015).

The tumor homing of MSCs has been used to deliver TNF-related apoptosis-inducing ligand (TRAIL), known by its anticancer properties. MSCs overexpressing TRAIL (MSC-TRAIL), when co-cultured with tumor cells, induced a 6-fold increase in apoptotic cell death when compared to non-modified MSCs. In addition, these cells were tested in a metastatic lung mouse model, promoting a tumor free rate of 37.5%, whereas no animals were tumor-free in the control MSCs group (Loebinger et al., 2009). Confirmation of the efficacy of MSC-TRAIL *in vivo* were shown by Spano et al. (2019), which tested Ad-MSC-TRAIL in pancreatic cancer, finding a 37% reduction in tumor size in Ad-MSC-TRAIL group compared to non-modified Ad-MSCs, a result which was similar to the that found in the group treated with recombinant TRAIL. Moreover, an increased cytotoxicity of TRAIL-expressing MSCs compared to control MSCs was also seen in a lung cancer *in vivo* model, possibly by enhancing the apoptosis of CLDN7-negative non-small cell lung cancer cells (Xia et al., 2013).

The effects of MSCs-derived exosomes, which are secreted vesicles with an average size of 100 nm originated from the endosomal compartment (Kalluri and LeBleu, 2020), have also been explored in the context of cancer therapy (Gao and Jiang, 2018). Exosomes isolated from MSCs overexpressing microRNAs (MIRs) were also evaluated in different cancer models (Wang B. et al., 2019; Xu et al., 2019; Chen et al., 2020). Treatment with BMSCs-derived exosomes overexpressing miR-16-5p in a mouse model of colorectal cancer (CRC) inhibited invasion, migration and proliferation of malignant cells, and induced a 4-fold higher apoptosis rate *in vitro* compared to control cells (Xu et al., 2019). Exosomes from BMSCs overexpressing miR-34 were 2-fold more potent than control MSCs in inducing the inhibition of invasion, migration, proliferation and tumorigenesis of glioblastoma cells, *in vitro* and *in vivo* (Wang B. et al., 2019). Exosomes from miR-101-3p and miR-199a-overexpressing BMSCs also inhibited invasion, migration and proliferation of oral cancer cells (Xie et al., 2019) and glioma cells (Yu et al., 2019). Furthermore, inhibition of the tumor progression was also observed *in vivo* in a glioma model (Yu et al., 2019).

In a prostate cancer model, administration of BMSCs overexpressing sirtuin 1 led to a decrease in tumor growth and an increase in immune inflammatory response associated with the IFN-γ-induced recruitment and activation of tumoricidal macrophages when compared to non-modified MSCs (Yu Y. et al., 2016). The effects of conditioned medium of umbilical cord-derived MSCs (UC-MSCs) overexpressing hepatocyte nuclear factor 4α (HNF4α), a transcription factor which acts as a master regulator of hepatic differentiation and liver metabolism, has also been evaluated in a mouse model of hepatocellular carcinogenesis (HCC). UC-MSC-HNF4α suppressed metastasis

and proliferation of cancer cells when compared to untreated and control MSCs-treated groups. Furthermore, in an *in vitro* assay, MSC-HNF4α reduced approximately 5-fold the migration and invasion potential of cancer cells compared to controls (Wu et al., 2016).

APPLICATIONS IN CARDIOVASCULAR DISEASES

Novel treatments for improving the heart function are of immense clinical importance, and cell-based therapies show a great promise (Jadczyk et al., 2017). A variety of cell types, including MSCs, have been used in strategies for inducing cardiac regeneration (Madonna et al., 2010). Initially, it was proposed the differentiation of transplanted MSC into cardiomyocytes and vessels as the main mechanism underlying their therapeutic action in cardiovascular diseases (Tomita et al., 1999; Pittenger and Martin, 2004). However, the number of MSCs-derived cells has been shown to be too low to contribute to the functional improvements, and evidence supports the hypothesis that MSC-mediated paracrine mechanisms play an essential role in tissue repair (Luo et al., 2019). Among the mechanisms promoted by MSCs are neovascularization, cytoprotection, endogenous cardiac regeneration, modulation of inflammatory and fibrogenic processes, cardiac contractility and cardiac metabolism (Gnecchi and Cervio, 2013).

Mesenchymal stem/stromal cells have been genetically modified to express factors that resulted in significant improvements in cardiac recovery. Several authors selected factors to be introduced in a gene therapy approach, based on the putative beneficial effects of MSCs described in infarct myocardial models, such as growth factors. MSCs overexpressing vascular endothelial growth factor (VEGF), when delivered by intramyocardial injection, reduced the infarcted area in 31% and improved left ventricular function to almost its baseline when compared with non-transfected MSCs (Locatelli et al., 2015). In a mouse model of myocardial infarction, transplantation of umbilical cord-MSCs overexpressing hepatocyte growth factor (HGF), a pro-regenerative factor, reduced by approximately half the infarcted area when compared with non-transduced cells, in addition to significantly increase the survival rate post-transplant (Zhao et al., 2016). In addition, the pro-survival cytokine insulin-like growth factor (IGF)-1, when overexpressed by BMSCs, reduced by approximately 50% the number of apoptotic myocardial cells post-transplant compared to animals treated with control MSCs, and increased MSC retention in the tissue in an experimental model of myocardial infarction (Haider et al., 2008). Similar results were observed after C1q/tumor necrosis factor-related protein-3 (CTRP3) and CCR1-modified MSCs transplant. MSCs overexpressing CTRP3, which is associated with protective effects after myocardial infarct, had an enhanced survival and retention 7 days post-transplant, approximately three times higher when compared to unmodified control cells (Zhang Z. et al., 2019). Additionally, overexpression of CCR1 increased by ∼90% the chemokinesis of MSC *in vitro* and *in vivo*, also increasing by more than 50% the amount of viable MSCs in the infarcted myocardium area (Huang et al., 2010).

The therapeutic effects of MSCs overexpression growth factors were also studied in a mouse model of cardiomyopathy induced by chronic infection with *Trypanosoma cruzi*, the causative agent of Chagas disease. Administration of genetically modified mesenchymal cells overexpressing granulocyte colony-stimulating factor (G-CSF) were about 2-fold more potent in reducing the number of inflammatory cells and the percentage of fibrosis than control MSCs, acting by increasing the number of myeloid-derived suppressor cells and T regulatory cells (Silva et al., 2018b). In contrast, no increase in anti-inflammatory or antifibrotic activity was seen after transplantation of IGF-overexpressing MSCs in *T. cruzi*-infected animals. However, an increased pro-regenerative activity in skeletal muscle was observed after MSCs-IGF-1 transplantation, compared to control MSCs, increasing the number of myofibers similar to that of uninfected mice (Silva et al., 2018a).

The overexpression of the regulators of cardiogenesis Csx/Nkx 2.5 and GATA-4 was also investigated in a myocardial infarct model. Genetically modified MSCs overexpressing these factors increased the cardiac function by inducing pro-angiogenic effects, significantly increasing microvessel density in the peri-infarct regions and reducing cell loss by apoptosis by approximately 10% compared to animals treated with control MSCs (Gao et al., 2011; He et al., 2019).

In addition to their pro-angiogenic effects, the cellular benefits of MSCs may also be mediated by activating the survival kinase pathways, including Akt activation, in cardiomyocytes in response to MSC-secreted cytokines, promoting a reduction programmed cell death (Jiang et al., 2013). Interestingly, MSCs overexpressing Akt promoted the maintenance of metabolism, glucose uptake and cytosolic pH and prevention of cardiac metabolism remodeling in a myocardial infarct model. Remarkably, for Akt-MSC hearts, systolic performance was only 12% (72 h) to 17% (2 week) lower compared with sham-operated hearts while diastolic performance remained normal. In contrast, for unmodified MSC-treated and untreated infarcted hearts, markers of both systolic and diastolic performance were significantly lower than for sham-operated hearts (Gnecchi et al., 2009). Akt-modified amniotic fluid derived MSCs were also capable of alleviating myocardial injury and contribute to cardiac regeneration in an ischemia-reperfusion injury in a rabbit model, promoting angiogenesis by capillary density enhancement and VEGF expression 2-fold more than control MSCs. Moreover, Akt-expressing MSCs promoted a significant increase in cTNT, GATA-4 and connexin 43 compared to controls (Wang et al., 2016). In addition, purified exosomes from TIMP2- and Akt-modified umbilical cord MSCs promoted improvements in cardiac function, by activating TIMP/Akt pathway (Ni et al., 2019) and increasing platelet-derived growth factor D expression (Ma et al., 2017), in rats submitted to myocardial infarction.

The expression of CXCR4, the stromal cell-derived factor (SDF)-1 receptor, which is largely involved in progenitor homing and survival, has been tested to improve the insufficient cell homing and tissue persistence observed in several preclinical studies. CXCR4-MSCs had a 3-fold increase in cell migration

capacity *in vitro* and *in vivo* in a myocardial infarct model when compared to control MSCs, correlating with an increased expression of metalloproteinases. Additionally, a 4-fold increase in capillary density was found in the hearts of animals treated with CXCR4-MSCs when compared to control MSCs groups (Huang Z. Y. et al., 2012). A significant improvement in cardiac function in CXCR4-MSCs treated animals compared to those treated with control MSCs, which may be explained by the reduction of heart fibrosis and increased angiogenesis post-injury (Huang W. et al., 2012; Mayorga et al., 2017; Wu S. Z. et al., 2017).

Furthermore, anti-inflammatory interleukins and regulators of oxidative factors were explored in the production of genetically engineered MSCs. IL-10 overexpression improved the therapeutic effects of MSCs by reducing by 2.5-fold the production of proinflammatory cytokines (TNF and IL-1β) and promoting a 3-fold reduction of the heart infarct size when compared to control MSCs (Meng et al., 2017, 2019). In addition, injection of MSCs modified to overexpress IL-33, a cytokine known to induce Th2 and Treg responses (Schmitz et al., 2005) resulted in a significant improvement of heart function and reduced inflammation compared to vector control MSCs in rats with myocardial infarction (Chen et al., 2019). MSCs modified to overexpress endothelial nitric oxide synthase (eNOS) were more potent than control MSCs and eNOS adenoviral vector in reducing the myocardial infarct size (4 and 2-fold increase, respectively), corrected hemodynamic parameters and increased the capillary density by increasing nitric oxide production (Chen L. et al., 2017). Moreover, heme oxygenase-1 (HO-1), an enzyme acting on heme degradation, as well as in the generation of cytoprotective agents (Liu and Qian, 2015). Transplantation of HO-1-overexpressing MSCs promoted not only an improvement in angiogenesis in scar areas, but also an increase in connexin 43-positive gap junctions and a higher tyrosine hydroxylase-positive cardiac sympathetic nerves sprouting in a myocardial infarction model (Zeng et al., 2008, 2010; Yang et al., 2012).

Other molecules with diverse mechanisms of action were also explored as modification targets were Follistatin-like 1 and Islet-1. MSCs overexpressing Follistatin-like 1, a pro-survival cardiokine for cardiomyocytes, had increased survival, proliferation and engraftment, thereby improving in about 2-fold their therapeutic efficacy when compared to mcherry transgenic control MSCs in a myocardial infarction model (Shen et al., 2019). Similarly, overexpression of Islet-1, a transcription factor involved in cardiogenesis regulation and a marker of cardiovascular progenitor cells, promoted MSCs survival post-transplant and enhanced their paracrine function (Xiang et al., 2018).

Another strategy studied to improve cell therapies for cardiac diseases is the overexpression of microRNAs in MSCs. Overexpression of mIR-126 in MSCs induced the production of Notch ligand Delta-like-4, which activates the Notch pathway and promotes the production of pro-angiogenic factors, ameliorating the cell therapy efficacy in infarcted hearts by 2-fold compared to control MSCs (Huang et al., 2013b). In a similar way, intramyocardial transplantation of microRNA-1-transfected MSCs was more effective to promote repair of the infarct injury and improvement in heart function by enhancing transplanted cells survival and cardiomyogenic differentiation when compared to mock-transfected MSCs (Huang et al., 2013a). Furthermore, in a model of myocardial ischemic-reperfusion injury, mIR-181a overexpression enhanced the immunosuppressive capacity of MSCs-derived exosomes, improving their therapeutic effect by 2 to 3-fold in reducing the infarct area and increasing the ejection fraction when compared to exosomes produced by control MSCs (Wei et al., 2019). Genetic modification of MSCs to overexpress miR-21 not only promoted an enhanced migration and proliferation rates, but also in angiogenesis and cardiac function. This may be explained by an increase in Bcl-2, Cx43 and VEGF levels and a decrease in Bax, BNP and troponin T, seen in a model of adriamycin-induced myocardial damage (Zeng et al., 2017). Transplantation of MSCs overexpressing miR-133 in a rat model of myocardial infarction reduced fibrosis and promoted an improvement in cardiac function more potently than control vector-MSCs, possibly by reducing *Snail 1* expression (Chen Y. et al., 2017). Finally, in a model of myocardial infarction, intravenous injection of MSCs genetically engineered to overexpress miR-211, known to influence cell migration, promoted a significant increase in migration of MSCs to the injured area and reduction of the infarct size, while PBS or control MSCs did not reduce the infarct size nor promoted functional recovery (Hu et al., 2016).

APPLICATIONS IN LUNG DISEASES

Pulmonary tract pathologies are commonly due to the frequent exposure of the respiratory system to different factors, such as tobacco, toxic smoke or polluted air, which may contribute to the development of acute and chronic disorders, such as infections or autoimmune and inflammatory diseases. Thus, MSCs have been used and genetically modified to express different factors aiming to promote the patients' recovery, since many diseases still do not have an efficient treatment.

Pulmonary arterial hypertension (PAH) has been a target of therapies with modified mesenchymal cells. Guo and collaborators generated rat bone marrow derived MSCs expressing human HGF (MSC-HGF) by transduction with recombinant adenoviral vector (ad-HGF). The treatment with MSC-HGF or MSC-HGF+ recombinant G-CSF promoted a significant reduction in mean pulmonary arterial pressure and hypertrophy in the right ventricle when compared with the control MSCs and untreated groups. In addition, pulmonary perfusion in the MSC-HGF+G-CSF group was improved by increasing the number of blood vessels (∼2-fold more vessels compared with the MSC and untreated group) (Guo et al., 2013). Treatment with MSCs overexpressing the secreted Klotho protein (SKL), a β-glucuronidase that regulates oxidative stress and inflammation, restored pulmonary endothelial dysfunction in a model of monocrotaline-induced PAH, acting by reducing 25% blood vessel thickness and doubling the lumen when compared to the MSCs, MSCs-GFP and untreated groups. MSCs-SKL also slightly attenuated systolic pressure and right

ventricular hypertrophy and had anti-inflammatory effect, reducing by 50% the macrophage infiltration in the lung tissue (Varshney et al., 2016).

In a severe acute lung injury (ALI) mouse model, treatment with bone marrow-derived MSCs modified to express human angiopoietin 1 (Ang1) promoted a significant reduction in airspace inflammation, with 96 % less neutrophils than groups treated with control MSCs or saline. Moreover, Ang 1-MSCs reduced the production of pro-inflammatory cytokines IFN-γ, TNF-α, IL-6 and IL-1β, equal to baseline values observed in naive mice (Mei et al., 2007). In a similar study, MSCs transduced by lentiviral vector to overexpress angiopoietin 1 (MSC-Ang1) also promoted benefits for ALI, reducing the levels of the pro-inflammatory cytokines TGF-β1 and IL-1β and increasing the expression of the anti-inflammatory cytokine IL-10 in the serum and bronchoalveolar lavage fluid, in addition to improving the lung function by increasing the expression of surfactant protein C (Shao et al., 2018).

In vitro studies with alveolar epithelial cells subjected to cigarette smoke extract (CSE) revealed that BMSCs overexpressing Notch1 receptor (MSC-N1ICD) maintained alveolar cells proliferation levels close to those observed in the control not exposed to CSE by activation of PI3K/Akt pathway. Additionally, MSC-N1ICD doubled the expression of CXCR4, promoted a 2-fold greater cell migration when compared to the control MSC groups and prevented apoptosis, as shown by the 50% reduction in caspase-3 expression in alveolar cells when compared to MSC control cells (Cheng et al., 2017). In another study, Cai et al. (2015) reported that MSCs genetically modified to express Wnt/β-catenin contributed *in vivo* with the alveolar epithelium protection, promoting the retention of a greater number of MSCs in the lungs for up to 14 days when compared to the control cell line, as well as an increase (approximately 3-fold) of differentiation of MSCs in type II alveolar epithelial cells and improvements in alveolar epithelial permeability, resulting in a reduction in lung damage.

Mesenchymal stem/stromal cells from different sources have been genetically modified to express different cytokines and chemokines in order to explore the immunomodulatory potential of these cells in lung injury models. The studies demonstrated that MSCs overexpressing IL-10, CXCR4 or CXCR7 caused a decrease in the number of alveolar neutrophils and levels pro-inflammatory cytokines, such as tumor necrosis factor α (TNFα), transforming growth factor (TGF-β1) and IL-6. Moreover, an increase in the survival rate of the animals treated with these genetically modified cells was observed, likely due to the reduction of inflammatory severity and damage to the lungs (Wang et al., 2018; Jerkic et al., 2019; Shao et al., 2019; Zhang C. X. et al., 2019). Differentiation of MSCs into type II alveolar epithelial cells and an increase of alveolar macrophages were also observed (Jerkic et al., 2019; Shao et al., 2019).

Overexpression of enzymes and receptors by MSCs was another approach used in the management of ALI. In a model of LPS-induced lung injury, mouse BMSCs modified by a lentiviral vector to express the angiotensin-converting enzyme 2 (ACE2) induced an improvement in the lung tissue, with decreased inflammatory infiltrate, edema and interstitial hemorrhage and reduction of lung injury score from 13 to 5.7 in WT mice, and to 8.6 in ACE-knockout mice when compared to the MSC and untreated groups. In addition, a decrease in IL-6 and IL-1β levels, as well as an increase in IL-10 levels, was observed in the MSC-ACE2 group compared to the control MSCs (He et al., 2015). Similarly, Martínez-González et al. (2013, 2014) observed that human MSCs derived from adipose tissue overexpressing the soluble IL-1 receptor type 1 (sST2) caused a decrease in histopathological changes associated with lower levels of pro-inflammatory cytokines TNF-α, IL-6, and MIP-2 (1.5 to 3-fold reduction), and 6-fold higher levels of IL-10 in models of ALI and asthma. In a model of ALI in rats, BMSCs overexpressing the enzyme heme-oxygenase-1 (HO-1) promoted the survival and anti-apoptotic activity greater than wild-type BMSCs (Chen X. et al., 2018). The transplantation of MSCs overexpressing the type 2 angiotensin II receptor (AT2R) increased cell migration *in vitro* by 3-fold, inhibited inflammation by decreasing pro-inflammatory cytokines (IL-1β and IL-6) and recovered the injured lung in a model of ALI in mice (Xu et al., 2018), while overexpression of the orphan receptor tyrosine kinase 2 (ROR2) by MSCs not only improved their ability to relieve inflammation and histopathological changes, but also increased their retention in lungs (Cai et al., 2016).

Exosomes derived from MSCs are important sources of microRNAs that provide protection against various diseases. Therefore, increasing the expression of microRNAs in MSC is an interesting alternative for some pulmonary pathologies. In a study that used exosomes derived from MSCs with overexpression of miR-30b-3p in co-culture with alveolar epithelial cells (AECs) challenged with type II LPS, high endocytosis of exosomes rich in miR-30b-3p was found, and this phenomenon was accompanied by reduced expression of SAA3 (protein highly expressed in ALI), increased cell proliferation and inhibition of apoptosis (Yi et al., 2019). BMSCs overexpressing let-7d, an antifibrotic microRNA, were tested in an ALI model in mice, promoting an increase in the production of the anti-inflammatory cytokine IL-1RN (when compared to wild type MSC), a reduction in the number of $CD45^+$ cells (when compared to the untreated group) and decreased collagen transcription levels, even though no significant differences were observed in the Ashcroft score and OH-proline (Huleihel et al., 2017). UC-MSCs overexpressing p130 or E2F4 also proved to be more potent in decreasing tissue damage in the lungs, promoting retention of MSC-p130 and MSC-E2F4 7 days after intratracheal transplantation (50% more retained cells than control groups) and inhibiting fibrosis in a model of severe acute respiratory distress (Zhang X. et al., 2019).

Transcription factors are important regulators of gene expression. The effects of human amniotic MSCs (hAMSCs) modified to express the nuclear factor erythroid-derived 2-like 2 (Nrf2), a transcription factor that regulates the expression of genes related to antioxidant activity, was evaluated in a mouse model of lung injury induced by intratracheal LPS instillation. Nrf2-overexpressing cells were about 2-fold more potent than

control MSCs in reducing apoptosis, fibrosis, edema and pro-inflammatory cytokine levels when injected intravenously (Zhang et al., 2017).

APPLICATIONS IN GASTROINTESTINAL AND LIVER DISEASES

Genetic modification of MSCs is a promising approach widely explored in diverse models of gastrointestinal and liver diseases. The improvement in cell homing and target ability to inflammatory sites, together with the increase in immunosuppression and tissue repair capacity after transplant, are some of the improvements seen in gastrointestinal experimental models of oral mucositis and inflammatory intestinal diseases.

Growth factors have been used as targets for gene therapy in the field of liver disease, as shown in a study in which HGF-overexpressing BMSCs (BMSC-HGF) promoted an improved recovery from liver damage in a model of CCl_4-induced cirrhosis in rats, increasing the expression of hepatic proteins HNF-4α, CK18 and ALB (2 to 3.5-fold greater than untreated control) and reducing the presence of liver injury markers, aspartate aminotransferase (AST), alanine aminotransferase (ALT), and total bilirubin, compared to the other groups tested (Zhang Y. et al., 2018). The therapeutic effects of HGF overexpressing MSCs were also studied in an acute model of radiation-induced liver injury. MSC-HGF showed greater migration and permanence in the injured tissue, increased the proliferation of hepatocytes (about 4-fold greater than untreated control), completely blocked the increase in ALT and AST and prevented apoptosis and liver fibrosis when compared with the other treatments (Zhang J. et al., 2014). In a similar model of chronic injury, MSCs overexpressing fibroblast growth factor 4 (FGF4) also contributed with liver regeneration, promoting greater migration of MSC-FGF4 to cirrhotic livers and increasing the expression of the liver progenitor marker EpCAM by about 4-fold when compared to control groups (Wang et al., 2015).

Hepatic macrophages (Kupffer cells) play a central role in liver fibrosis, being critical in both its promotion and resolution. In a model of chronic thioacetamide poisoning (TAA), MSCs transduced with a lentiviral vector for overexpression of IGF-1 (Ad-MSC-IGF-I) were able to reverse a pro-fibrotic phenotype in Kupffer cells, reducing by half the levels of collagen deposition in the area of the lesion when compared to the vehicle-treated group and downregulating the expression of the pro-fibrogenic genes TGF-β1, α-SMA and collagen 1A2 (COL1A2) (Fiore et al., 2015). Neuregulin 4 (Nrg4) acts in the liver, where it modulates the lipogenesis in hepatocytes by activating the ErbB3/ErbB4 signaling. Thus, the therapeutic potential of Nrg4-overexpressing Ad-MSCs was tested in a model of hepatic steatosis induced by a high-fat diet. Transplantation of MSC-Nrg4 reduced weight gain, decreased serum glucose and insulin levels, in addition to improving glucose intolerance more significantly than treatment with control MSC (Wang W. et al., 2019).

Cytokines and chemokines have also been evaluated in liver and gastrointestinal diseases. Uncontrolled hepatic immune activation is the primary pathological mechanism of fulminant hepatic failure (FHF). The interleukin-1 receptor antagonist (IL-1Ra) plays an anti-inflammatory and anti-apoptotic role in acute and chronic inflammation. The transplantation of MSCs that overexpress this molecule increased survival (63.6% survival in the MSC-IL-1Ra group versus 30.0% and 22.2% in the MSC and vehicle groups). MSC-IL-1Ra increased the fraction of proliferating hepatocytes (23.5%) compared to MSC and control (19.9% and 18.32%, respectively), and improved liver function by negatively regulating inflammatory responses activated by IL-1 *in vivo* (Zheng et al., 2012). In a TAA-induced model of chronic liver fibrosis in mice, engineered MSCs that secrete high levels of IL-10 had a more potent antifibrotic activity and caused the improvement in liver function than control MSCs, which were also able to significantly promote histopathological and functional improvements (Choi et al., 2019).

The role of CXCL2 in oral mucositis was investigated from transplantation of human BMSCs with increased expression of CXCR2 by lentiviral transduction. MSC-CXCR2 exhibited improved ability to migrate in response to CXCL2 *in vitro* (almost 2 times greater than MSC control), indicating greater targeting of these cells to the inflamed mucosa in animal models. MSC-CXCR2 also had a longer residence time in the oral cavity than control MSC and promoted accelerated ulcer healing by reducing pro-inflammatory cytokines, such as TNF-α, IL-1β, and IL-6 and levels of reactive oxygen species (ROS) in epithelial cells were 2-fold lower, while ROS levels were 4-fold lower in tongue fibroblasts (Shen et al., 2018). In a mouse model of inflammatory bowel disease (IBD) induced by sodium dextran sulfate, increased expression of the Intercellular Adhesion Molecule (ICAM)-1 by MSCs have been shown to alleviate inflammatory damage in IBD mice, reducing colon shortening to levels closer to the control without IBD, in addition to halving the number of inflammatory cells when compared to the untreated IBD group. Moreover, ICAM-1 also stimulated the migration of modified MSC to the affected colon (Li et al., 2019).

In addition, the transfer of genes coding for important transcription factors regulating hepatogenesis, such as HNF4α and forkhead box protein (Foxa2), was investigated in the context of liver diseases in association with stem cell therapy. MSCs overexpressing Foxa2, cultured in a 3D system of poly-lactic-co-glycolic acid (PLGA) scaffold, promoted hepatic differentiation, *in vitro* and *in vivo* when implanted into nude mice. Importantly, when implanted into dorsal subcutaneous tissues, Foxa2-overexpressing Ad-MSCs/scaffolds reduced the alterations in liver function markers in the blood and in liver tissue, in an acute liver injury model induced by TAA (Chae et al., 2019). Moreover, Foxa2-MSCs promoted the recovery expressions of liver enzymes close to normal levels, and reduced the fibrotic areas more potently when compared to MSC alone or MSC/vector groups (Cho J.W. et al., 2012). Similarly, HNF-4α-modified MSCs showed increased therapeutic effects in a liver cirrhosis mouse model, where MSC-HNF-4α positively regulated iNOS expression by activating the NF-κB signaling pathway (Ye et al., 2019).

APPLICATIONS IN KIDNEY DISEASES

Nephrological disorders can lead to an increase in mortality and morbidity, especially in cases of acute kidney injury, and may affect the functionality of the organs. The use of genetically modified MSCs has also been investigated in the context of kidney diseases.

Ad-MSCs and BMSCs genetically engineered to overexpress glial cell line-derived neurotrophic factor (GDNF) promoted the switching of macrophages to a reparative phenotype, reduced renal fibrosis and contributed to a recovery in renal function in models of nephrotoxic serum nephritis and unilateral ureteral obstruction (Huang Z. Y. et al., 2012; Wang Z. et al., 2019). In another study, injection of MSC-HGF, in a model of bladder outlet obstruction, not only prevented collagen deposition, with a reduction in collagen area of almost half when compared to the untreated animals, as well as increased cystometric parameters in transplanted animals (Song et al., 2012). In a model of renal failure-induced anemia, MSC-IGF-1 co-implanted with MSCs genetically engineered to secrete erythropoietin (MSC-EPO) promoted a significant hematocrit elevation when compared to the group which received the MSC-EPO + MSC-null, with a difference of approximately 20% after 98 days. Additionally, an improvement in heart function was observed in the animals treated with MSC-EPO + MSC-IGF-1 (Kucic et al., 2008).

Overexpression of cytokines and chemokines in MSCs have also been evaluated in models of kidney diseases. In a model of renal ischemia/reperfusion injury, MSCs genetically modified to overexpress TGF-β1 increased renal function and reduced inflammation by a significant decrease in the pro-inflammatory cytokine expression, such as IL-2, IL-6, and TNF-α, in comparison to the PBS and MSC groups, and an enhancement in IL-10 expression of about 2.5-fold when compared to the sham group (Cai et al., 2019). Lipocalin 2 (Len2), secreted in high levels into the blood and urine after kidney injury may be an important cytoprotective agent against injuries caused by oxidative stress (Roudkenar et al., 2008, 2011). BMSCs overexpressing Len2 prevented cytotoxicity and apoptosis when co-cultured with HK-2 and HEK293 cells in a model of cisplatin-induced kidney injury *in vitro*, with a cell viability of 60% after 70 days when co-cultured with HK-2 cells and 40% with HEK293 cells, while the control groups with only kidney cells co-cultured with MSCs or Mock-MSCs had 20% and less than 10% viability for kidney cells, respectively. Additionally, the percentage of apoptosis in the groups treated with MSC-Len2 was significantly decreased, while HGF, IGF-1 and FGF-2 concentrations were higher in this group when compared to the other treatments (Halabian et al., 2014). BMSCs-CXCR4, were also able to stimulate HGF production when compared to the MSCs alone, although not in the same intensity as the MSC-Len2. Furthermore, an increase in IL-10 and bone morphogenetic protein 7 (BMP-7) was also observed. Increasing in proliferating cells and a decrease in apoptotic cell markers when co-cultured with hypoxia/reoxygenation-pretreated renal tubular epithelial cells (HR-RTECs), as well as renal functional improvement and a decrease in tubular cell death was seen in animals treated with BMSCs-CXCR4 in a model of acute kidney injury (Liu et al., 2013).

Transplantation of BMSCs modified to express the Klotho gene, which is known to be related with the aging process (Kuro-o et al., 1997), promoted antifibrotic effects and led to an increase in proliferation and immuno-regulatory ability of MSCs in a model of acute kidney injury (Zhang F. et al., 2018). Moreover, in a model of ischemia/reperfusion injury, administration of exosomes derived from BMSCs expressing miR-199a-3p had protective effects and decreased inflammatory mediators, as well as the number of apoptotic cells, although this reduction was similar to the group treated with the MSCs (Zhu et al., 2019).

APPLICATIONS IN NEUROLOGICAL DISORDERS

Due to the complexity of the nervous system, many neurological disorders do not have an effective treatment in order to reduce or prevent the damages caused in the nervous tissue. However, MSC cell therapy has been investigated as an option for the treatment of several neurological disorders, and many articles have studied their effects on the nervous system and possible strategies to enhance their therapeutic actions, including genetic engineering.

Mesenchymal stem/stromal cells secrete diverse growth factors related to neurogenesis and neuroprotection, such as brain derived neurotrophic factor (BDNF), Glial cell-derived neurotrophic factor (GDNF), fibroblast growth factor-2 (FGF-2), HGF, IGF-1, nerve growth factor (NGF) and platelet-derived growth factor (PDGF) (Joyce et al., 2010) and, therefore, many studies have been evaluating the effects of MSCs overexpressing these factors for the treatment of neurological disorders in different *in vitro* and *in vivo* models. In a model of diabetic cistopathy, rats that received intrathecal injections of human MSCs derived from umbilical cord modified by lentivirus to overexpress NGF (MSCs-NGF), had a significant improvement in voiding dysfunction, with a 12% and 45% voiding interval higher when compared to the MSC control and untreated diabetic groups, respectively. This effect was related to the differentiation of MSCs-NGF in neurons and glial cells, increasing the control of neuronal functions along the urinary pathway (WenBo et al., 2017). In the *in vitro* model of Parkinson's disease, the conditioned medium MSCs overexpressing HGF showed an increase in the viability of neuron culture 48 h after treatment (about 14% greater than control MSC and 42% greater than untreated cells). In addition, the presence of intracellular free calcium was 2.4-fold lower in the MSC-HGF group and about 2-fold lower in the MSC group when compared to the untreated control, indicating a greater ability of MSC-HGF to maintain the cellular homeostasis (Liu et al., 2014). Supernatant of MSCs overexpressing BDNF from three different donors showed a higher neuroprotective effect *in vitro*, with a neuronal survival rate around 40% when compared to the control-vector infection group (Scheper et al., 2019), while in another study, MSCs also overexpressing BDNF started to express neuronal phenotype markers 1 day after transfection and in the following days, presented a neuron-like morphology when compared to the MSC control, which maintained their fibroblast-like morphology (Lim et al., 2011).

Interestingly, these findings demonstrate that the overexpression of BDNF by MSCs seems to be able to either increase their neuroprotective effects or induce changes in their phenotype to one closer to a neuronal one, suggesting more than one possible effect in the cells.

In another study, MSCs with GDNF overexpression increased the differentiation of neural stem cells (NSCs) when these cells were co-cultured with a 3D microfluidic system. After 5 days in culture, a significant increase in the expression of neuronal markers, such as Tuj1 and MAP2, and in the formation of neurites in NSCs co-cultured with MSC-GDNF when compared to MSC control group was observed. In addition, the authors performed an animal model of hypoxic-ischemic stroke to assess neurobehavioral function. However, even demonstrating promising effects *in vitro*, transplantation of MSC-GDNF did not demonstrate a significant functional increase when compared to control MSC, being superior only to the untreated group (Yang et al., 2015). On the other hand, transplantation of MSCs with increased expression of FGF21 (an important regulator of metabolic pathways) in the brain of mice after traumatic brain injury (TBI) led to a decrease in memory deficits and increased the level of FGF21 in the ipsilateral hippocampus, naturally decreased after TBI. In addition, the MSC-FGF21 group had enhanced neurogenesis and restored the morphology of immature newborn neurons in the hippocampus when compared to the MSC and vehicle groups, which exhibited impaired maturation and deficiency in the neurogenesis process (Shahror et al., 2019).

In a model of spinal cord injury (SCI), bone marrow-derived MSCs overexpressing or not ciliary neurotrophic factor (CNTF) promoted functional recovery, as shown by an improvement in the Basso, Beattie, and Bresnahan (BBB) motor score during the weeks following transplantation, and the H&E staining of the injury site demonstrated that both groups showed a greater cell density in the cavity when compared to untreated group. Nevertheless, even with both cell groups seeming to be able to preserve the nervous tissue, the BMSC-CNTF group displayed a profile more similar to the sham group in comparison to the others (Abbaszadeh et al., 2015). Another study evaluating the effects of MSCs on SCI showed that transplantation of MSCs overexpressing HGF reduced the activation of astrocytes by inhibiting the expression of TGFβ1 and β2, promoting an almost 3-fold decrease in GFAP+ cells in the lesion area, when compared to the control or wild type MSCs, in addition to inducing the reduction of the glial scar, one of the main factors that hinder the functional recovery after SCI (Jeong et al., 2012). BMSCs genetically modified to overexpress the growth factor IGF-1 showed promising effects on neuroprotective and anti-oxidant activity in mice after SCI. When compared to control groups, IGF-1 secretion promoted a 3-fold increase in graft survival in the lesion area, which facilitated the recruitment of endogenous neural progenitor cells, as well as the positive regulation of antioxidant genes, resulting better preservation of neural tissue (myelinated area about 50% greater than that observed in control groups) and significant motor improvement using Basso Mouse Scale (BMS; 6 at the end of the experiment for IGF-1 group vs 4 in control groups) (Allahdadi et al., 2019). In another SCI model, BMSCs overexpressing sonic hedgehog (Shh), a growth factor with multiple functions in the nervous system, were able to reduce tissue damage, with 2 times greater expression of neurofilament 200 (NF200), in addition to promoting functional recovery significant in animals when compared to BMSCs or vehicle groups (Jia et al., 2014). Finally, mice treated with BMSCs genetically modified with brain dopamine factor (CDNF) showed significant functional gains in the BBB score, from week 3 to week 6, when compared to control groups, which did not show significant differences between themselves. In addition, histopathological analyzes indicated greater tissue preservation, with a 6 to 7-fold reduction in the area of cavitary lesions in the MSC-CDNF group when compared to MSC control and untreated groups. Neural fiber recovery was also observed, with improvements in remyelination levels and reduction of neuroinflammation after SCI (Zhao et al., 2014).

A study evaluating the effects of neurotrophin-3 (NT3) overexpression by BMSCs in a model of Parkinson's disease revealed that genetically modified cells protected neuronal tissue and induced differentiation of BMSCs into cells similar to dopaminergic neurons (neuron type affected by Parkinson's disease), as seen by a 5-fold increase in the levels of nurr-1 and wnt-1 in transfected cells, when compared to treatment with wild-type MSCs (Moradian et al., 2017).

VEGF-overexpressing MSCs have been used in different disease models, including neurological diseases. In the treatment of peripheral nerve damage, MSC-VEGF has shown promising results both *in vitro* and *in vivo*, promoting the extension of neurites and maintaining high expression of VEGF in the nerves 2 weeks after grafting (Man et al., 2016). In a model of Alzheimer's disease, also evaluating the effects of MSC-VEGF, genetically modified cells promoted neovascularization in the hippocampus and reduced the presence of beta-amyloid plaques in the dentate gyrus when compared to the vehicle-treated group, although no significant differences were found compared to the MSC group, which also appeared to induce neovascularization (Garcia et al., 2014).

The immunomodulatory effects of genetically modified MSCs to express interleukins have been studied to treat autoimmune diseases, such as multiple sclerosis, or to reduce the damage caused by trauma to the brain or spinal cord in cases of TBI, SCI or stroke. Genetically modified MSCs to express IL-4 (responsible for modulating the autoimmune inflammatory response), for example, exhibited protective effects in a model of multiple sclerosis when transplanted in the early stage of the disease. MSC-IL-4 reduced the expression of pro-inflammatory cytokines such as IFNγ and IL-6, leading to a reduction in disease severity when compared to control groups (Payne et al., 2012). In an acute ischemic stroke model, BMSCs overexpressing IL-10 ameliorate the motor function, posture score and forelimb grip strength. In addition, 72 h after treatment, a decrease in the number of Iba-1 and TNF-α positive cells, of approximately 2-fold more, was seen in BMSC-IL-10 group when compared to the vehicle, while this reduction was of almost half in comparison to the MSC, which also presented a significant difference in relation to the vehicle group

(Nakajima et al., 2017). The effects of BMSC-IL-10 were also evaluated in a TBI model, in which these cells and MSCs alone decreased significantly the expression of cell death markers, such as Bax, cytochrome-C, caspase-3 and p53 when compared to the vehicle group and increase in those related to cell survival (Bcl2) and synaptic transmission (PSD95 and synaptophysin) was seen in BMSC-IL-10, but not in MSCs alone and vehicle groups, which presented differences only in synaptophysin levels. Thus, these results showed the promising effects of BMSC-IL-10 in promoting the protection of neuronal cells following TBI (Maiti et al., 2019). C-C Motif Chemokine Receptor 2 (CCR2) is positively regulated in the first 24 h after ischemic stroke. Therefore, the effects of MSCs genetically modified to express CCR2 were evaluated in a stroke model. In this study, overexpression of CCR2 increased 5-fold approximately the migration of MSCs modified to ischemic region, and it was able to not only decrease ischemic injuries and promote neurological recovery *in vivo*, but demonstrated an important role in protecting the blood-brain barrier and in promoting endothelial regeneration, when compared to the control groups of MSC (Huang Y. et al., 2018).

Overexpression of enzymes and receptors by MSCs, in order to improve the protective effects in tissue regeneration or increase cell survival, has also been studied for the treatment of different neurological disorders. MSCs derived from different sources have been genetically modified to express important enzymes for the CNS. MSCs overexpressing arginine decarboxylase (an enzyme that regulates the synthesis of agmatine, known to confer neuroprotection after brain damage) were tested in an SCI model in rats. Tissue analyzes showed an increase in BDNF expression at the lesion site, and this effect was accompanied by a reduction in the area of fibrotic scar and functional improvement in the group treated with the modified cells. MSCs overexpressing heme oxygenase-1 (an enzyme that modulates the response to oxidative stress after spinal cord trauma) were tested in canine SCI. Overexpression of this molecule led to a functional recovery after transplantation, related to the anti-oxidative effect and to a decrease in the presence of infiltrated cells, fibroblast-like cells and apoptotic cells in the area of the lesion, as well as an increase in the expression of NeuN and β3-tubulin markers when compared with the control groups. In addition, MSCs with increased tropomyosin kinase A (TrkA) receptor, a receptor highly expressed in sensory fibers, were used to repair peripheral nerves in rats. 8 weeks after transplantation, the MSC-TrkA-treated group showed greater axonal growth, with significantly higher expression of the basic myelin protein and superior results of the density of myelinated fibers, in addition to superior functional performance than observed in the control groups (Park Y.M. et al., 2015; Lee et al., 2017; Zheng et al., 2017).

In another study, MSCs derived from Wharton's jelly genetically modified to express PARKIN (an ubiquitin ligase capable of protecting dopaminergic neurons against stress) were tested in the Parkinson's disease model produced by 6-hydroxydopamine-induced toxicity. The overexpression of PARKIN in MSCs was able to significantly reduce the expression of markers of cell death and oxidative stress, in addition to significantly reducing the production of reactive oxygen species (∼ 50% reduction) when compared to wild type and control groups (Bonilla-Porras et al., 2018). Studies in stroke models showed that MSCs overexpressing extracellular regulating kinase 1/2 or integrin α4 not only were able to show induction of neuronal differentiation, proliferation of neural stem cells and a significant functional recovery in mice after the treatment (Gao et al., 2019), but also demonstrated a significant decrease in cell aggregation and improvement of cerebral embolism in rats (Cui et al., 2017).

MicroRNAs have been receiving attention during the past years due to their involvement in the regulation of different and important cellular processes (Clark et al., 2014), as shown in a mouse model of ischemic brain injury, where BMSCs overexpressing miR-705 contributed to ameliorate neurological deficits and to suppress neuronal death, associated with a 2-fold increase in BDNF and VEGF expression when compared to sham and vehicle groups (Ji et al., 2017). Several studies evaluated the effects of exosomes derived from genetically modified MSCs for the treatment of neurological diseases. Exosomes derived from MSCs overexpressing pigment epithelium-derived factor (PEDF) or miR-25 showed neuroprotective effects in models of cerebral ischemia reperfusion and ischemic spinal cord by mechanisms involved in axonal preservation, such as regulation of autophagy and apoptosis or reduction of inflammation and oxidative stress (Huang X. et al., 2018; Zhao et al., 2018). MSCs overexpressing miR-21, miR-124, or miR-133b in models of intracerebral hemorrhage, SCI and stroke, respectively, increased the expression of neuronal markers, such as β-III tubulin and NF200, induced neurite remodeling and outgrowth, reduced neurological damages and promoted functional recovery after treatment (Zou et al., 2014; Xin et al., 2017; Zhang H. et al., 2018).

Transcription factors have also been expressed by MSCs for the treatment of neurological diseases. BMSCs genetically engineered to express hypoxia-inducible factor 1α (HIF-1α) led to motor functional improvement, decreased cerebral infarction and increased by 4-fold the VEGF expression, when compared to the control groups in a model of cerebral artery occlusion (Yang et al., 2014). In another study, Mash1 overexpressing-MSCs enhanced neuronal markers expression, such as NeuN and GAD67, when compared to groups treated with MSCs control cells. In addition, these cells differentiated into cells similar to neurons that showed action potential, as seen by electrophysiological characterization, demonstrating that they were functional *in vitro* (Wang K. et al., 2013).

Genetically modified MSCs have also been combined with other methodologies in order to enhance their effects, as observed in a SCI model, in which the transplantation of BMSCs overexpressing BDNF combined with platelet-rich plasma (PRP) scaffolding promoted an increase in the expression of axonal markers such as NF200, 4 and 8 weeks after transplantation, when compared to groups that received control BMSC cells. Regarding GFAP levels, the BMSC groups, when combined with PRP, showed an increase in the expression of this molecule compared to groups without PRP. In addition, a better functional recovery was observed in the BMSC-BDNF group combined with

PRP, with a significant gain in the BBB index, when compared to the control groups (Zhao et al., 2013). Two studies evaluated the effects of transplanted MSCs genetically engineered to express tyrosine kinase receptor type 3 (TrkC) in combination with electroacupuncture (EA) for the treatment of SCI. An increase in the expression of NT3, an important neurotrophic factor, was seen in the spinal cord, as well as an improvement in the functional recovery in the animals which received this combined therapy. Differentiation of the MSC-TrkC into neuron-like and oligodendrocyte-like cells was also seen, with an expression of NF150 and MOSP almost twice as higher when compared to the control groups. Additionally, a reduction of degenerated myelin and an increase in the number of remyelinating and normal myelinated axons either in MSC combined with EA was observed (Ding et al., 2013, 2015).

CLINICAL TRIALS USING GENETICALLY MODIFIED MSCS

To date, genetically engineered MSCs are being tested only in few clinical studies for the treatment of different diseases. Either by viral or non-viral modification, the clinical use of genetically modified MSCs raises flags about the safety of cell products and quality control that should be carefully executed to guarantee the development of safe and effective alternative treatments.

Application of modified MSCs for genetic diseases treatments is being explored in the clinical research field in cases of severe combined immunodeficiency (SCID). The standard therapy for defective adenosine deaminase (ADA) derived SCID is bone marrow transplant. However, this procedure involves high risks and compatible donors are scarce. To overcome these problems, the collection of hematopoietic stem cells and/or MSCs, derived from the patient's bone marrow, followed by lentiviral transduction to induce correct defective ADA expression and re-implantation into the patient can be considered as a promising strategy for SCID treatment. Therefore, safety and efficiency of an improved self-inactivating lentiviral vector system for therapeutic gene delivery to patients with SCID, due to a defective ADA gene, is being studied in an interventional clinical trial (NCT03645460 ClinicalTrials.gov).

Another ongoing example of safety and efficacy evaluation of a gene transfer phase I/II clinical trial is for treating Fanconi anemia, a rare, inherited disease that is caused by a gene defect that primarily affects an individual's bone marrow, resulting in decreased production of blood cells. In this trial, autologous bone marrow derived MSCs and hematopoietic stem cells are being transduced with a self-inactivating lentiviral vector to functionally correct the defective gene FANCA. Furthermore, the effects of an infusion of these modified cells in order to promote immune reconstitution and long-term correction of Fanconi anemia associated disease symptoms is being evaluated (NCT03351868 ClinicalTrials.gov).

In the oncology field, a first clinical trial in solid tumors was conducted for treatment of advanced gastrointestinal cancer. Subjects were treated with a combination of genetically modified autologous bone marrow derived MSCs expressing the herpes simplex virus thymidine kinase (HSV-TK) (MSC_apceth_101) and ganciclovir, in order to generate a toxic metabolite for the tumor cells. In this study, from the 10 patients treated with this genetically modified MSC, five of them reached a stable disease and a post-study observation demonstrated a median overall survival of 15.6 months. In relation to the immunological markers, a slight increase in baseline levels of IL-6 was seen in 4 of the patients, while 3 demonstrated a slight enhancement in the levels of this cytokine at the end of the study, when compared to the baseline. Additionally, a moderate improvement in baseline levels of IL-8 was seen in 5 patients and 3 of them presented an increase during the time.

Also an enhancement in TNFα/IL-10 ratio, which suggests a higher inflammatory effectiveness and an anti-tumor capacity, was observed in 5 patients as well (von Einem et al., 2019).

In addition, new anticancer immunotherapies are being developed based on the use of recombinant type I IFNs, type I IFN-encoding vectors and type I IFN-expressing cells (Zitvogel et al., 2015). Based on that, a phase I study evaluating the effects of MSCs secreting IFN-β for ovarian cancer therapy is ongoing. The study aims to determine the highest tolerable dose of human MSCs-IFN-β that can be given to patients with ovarian cancer therapy (NCT02530047 ClinicalTrials.gov). The safety and antitumor activity of a modified human MSCs are also being studied in a phase I/II study investigating the outcomes of TRAIL-overexpressing MSCs in addition to chemotherapy, in metastatic non-small cell lung cancer (NCT03298763 ClinicalTrials.gov). In another study, the maximum tolerable dose, safety and efficacy of an intratumoral injection of the IL-12-expressing Human Mesenchymal Stem Cell Vaccine GX-051 are being investigated in subjects with advanced head and neck cancer. IL-12 is a cytokine that induces the production of IFN-γ, an important anti-tumoral factor. This study will evaluate the anti-tumor response, as well as possible changes of IFN-γ and IL-12 levels in blood comparing to the baseline and changes of immune cell distribution in tumor tissue after GX-051 intratumoral injection (NCT02079324 ClinicalTrials.gov).

CONCLUSION

The development of genetic engineering technologies and the continuous improvement in the knowledge of MSCs gene expression enabled the use of genetically modified MSCs with enhanced therapeutic properties compared to wild-type MSCs in a variety of disease models, as discussed in this review. Moreover, many studies described here showed that genetic modification of MSCs improved their paracrine effects, protecting viable cells in a lesion area from further damage and promoting tissue regeneration and significant functional and behavioral recovery in many animal models. However, due to issues concerning the safety and efficacy regarding the use of genetically modified MSCs for treatments, there is a gap between the experimental models and clinical trials, and the few clinical studies were conducted or are being initiated, mainly in the hematology and oncology fields. Additional preclinical studies are needed to ensure the safety

and demonstrate the therapeutic potential of engineered MSCs in more relevant animal models, especially those using medium or large animal models, giving support to the translation of this therapeutic modality into a broad variety of clinical settings.

AUTHOR CONTRIBUTIONS

PD, TS, GS, IO, DS, JA, GGo, GGr, and MP participated in the literature search, wrote the manuscript parts, and prepared the figures and tables. RS, MD, and MS conceived the manuscript concept, wrote, and final edited the manuscript. All authors read and approved the final manuscript.

FUNDING

The authors of this work acknowledge for the financial support provided by the Brazilian National Research Council (CNPq)/MS grant number 443909/2018-0 and INOVA/FIOCRUZ grant number VPPIS-001-FIO-18-70.

ACKNOWLEDGMENTS

The authors wish to thank the support of the Coordenação de Aperfeiçoamento de Pessoal de Nível Superior (CAPES) and Fundação de Amparo à Pesquisa do Estado da Bahia (FAPESB).

REFERENCES

Abbaszadeh, H. A., Tiraihi, T., Noori-Zadeh, A., Delshad, A. R., Sadeghizade, M., and Taheri, T. (2015). Human ciliary neurotrophic factor–overexpressing stable bone marrow stromal cells in the treatment of a rat model of traumatic spinal cord injury. *Cytotherapy* 17, 912–921. doi: 10.1016/j.jcyt.2015.03.689

Allahdadi, K. J., de Santana, T. A., Santos, G. C., Azevedo, C. M., Mota, R. A., Nonaka, C. K., et al. (2019). IGF-1 overexpression improves mesenchymal stem cell survival and promotes neurological recovery after spinal cord injury. *Stem Cell Res. Ther.* 10:146. doi: 10.1186/s13287-019-1223-z

Baraniak, P., and Mcdevitt, T. (2010). Stem cell paracrine actions and tissue regeneration. *Regen. Med.* 5, 121–143. doi: 10.2217/rme.09.74

Biancone, L., Bruno, S., Deregibus, M., Tetta, C., and Camussi, G. (2012). Therapeutic potential of mesenchymal stem cell-derived microvesicles. *Nephrol. Dial. Transpl.* 27, 3037–3042. doi: 10.1093/ndt/gfs168

Bobis-Wozowicz, S., Miekus, K., Wybieralska, E., Jarocha, D., Zawisz, A., Madeja, Z., et al. (2011). Genetically modified adipose tissue-derived mesenchymal stem cells overexpressing CXCR4 display increased motility, invasiveness, and homing to bone marrow of NOD/SCID mice. *Exp. Hematol.* 39, 686–696. doi: 10.1016/j.exphem.2011.03.004

Bonilla-Porras, A. R., Arevalo-Arbelaez, A., Alzate-Restrepo, J. F., Velez-Pardo, C., and Jimenez-Del-Rio, M. (2018). PARKIN overexpression in human mesenchymal stromal cells from Wharton's jelly suppresses 6-hydroxydopamine–induced apoptosis: Potential therapeutic strategy in Parkinson's disease. *Cytotherapy* 20, 45–61. doi: 10.1016/j.jcyt.2017.09.011

Cai, J., Jiao, X., Zhao, S., Liang, Y., Ning, Y., Shi, Y., et al. (2019). Transforming growth factor-β1-overexpressing mesenchymal stromal cells induced local tolerance in rat renal ischemia/reperfusion injury. *Cytotherapy* 21, 535–545. doi: 10.1016/j.jcyt.2018.12.003

Cai, S. X., Liu, A. R., Chen, S., He, H. L., Chen, Q. H., Xu, J. Y., et al. (2015). Activation of Wnt/β-catenin signalling promotes mesenchymal stem cells to repair injured alveolar epithelium induced by lipopolysaccharide in mice. *Stem Cell Res. Ther.* 6:65. doi: 10.1186/s13287-015-0060-y

Cai, S. X., Liu, A. R., Chen, S., He, H. L., Chen, Q. H., Xu, J. Y., et al. (2016). The orphan receptor tyrosine kinase ROR2 facilitates MSCs to repair lung injury in ARDS animal model. *Cell Transplant.* 25, 1561–1574. doi: 10.3727/096368915X689776

Campeau, P. M., Rafei, M., François, M., Birman, E., Forner, K. A., and Galipeau, J. (2009). Mesenchymal stromal cells engineered to express erythropoietin induce anti-erythropoietin antibodies and anemia in allorecipients. *Mol. Ther.* 17, 369–372. doi: 10.1038/mt.2008.270

Cantinieaux, D., Quertainmont, R., Blacher, S., Rossi, L., Wanet, T., Noël, A., et al. (2013). Conditioned medium from bone marrow-derived mesenchymal stem cells improves recovery after spinal cord injury in rats: an original strategy to avoid Cell Transplantation. *PLoS One* 8:e69515. doi: 10.1371/journal.pone.0069515

Cao, Y., Lu, W., Sun, R., Jin, X., Chen, L., He, X., et al. (2019). Anti-CD19 chimeric antigen receptor T cells in combination with nivolumab are safe and effective against relapsed/refractory B-cell non-hodgkin lymphoma. *Front. Oncol.* 9:767. doi: 10.3389/fonc.2019.00767

Chae, Y. J., Jun, D. W., Lee, J. S., Saeed, W. K., Kang, H. T., Jang, K., et al. (2019). The use of Foxa2-overexpressing adipose tissue-derived stem cells in a scaffold system attenuates acute liver injury. *Gut Liver* 13, 450–460. doi: 10.5009/gnl18235

Chen, B., Chen, X., Liu, C., Li, J., Liu, F., and Huang, Y. (2018). Co-expression of Akt1 and Wnt11 promotes the proliferation and cardiac differentiation of mesenchymal stem cells and attenuates hypoxia/reoxygenation-induced cardiomyocyte apoptosis. *Biomed. Pharmacother.* 108, 508–514.

Chen, H.-L., Li, J.-J., Jiang, F., Shi, W.-J., and Chang, G.-Y. (2020). MicroRNA-4461 derived from bone marrow mesenchymal stem cell exosomes inhibits tumorigenesis by downregulating COPB2 expression in colorectal cancer. *Biosci. Biotechnol. Biochem.* 84, 338–346. doi: 10.1080/09168451.2019.1677452

Chen, L., Zhang, Y., Tao, L., Yang, Z., and Wang, L. (2017). Mesenchymal stem cells with eNOS over-expression enhance cardiac repair in rats with myocardial infarction. *Cardiovasc. Drugs. Ther.* 31, 9–18. doi: 10.1007/s10557-016-6704-z

Chen, X., Wu, S., Tang, L., Ma, L., Wang, F., Feng, H., et al. (2018). Mesenchymal stem cells overexpressing heme oxygenase-1 ameliorate lipopolysaccharide-induced acute lung injury in rats. *J. Cell. Physiol.* 234, 7301–7319.

Chen, Y., Zhao, Y., Chen, W., Xie, L., Zhao, Z. A., Yang, J., et al. (2017). MicroRNA-133 overexpression promotes the therapeutic efficacy of mesenchymal stem cells on acute myocardial infarction. *Stem Cell Res. Ther.* 8:268. doi: 10.1186/s13287-017-0722-z

Chen, Y., Zuo, J., Chen, W., Yang, Z., Zhang, Y., Hua, F., et al. (2019). The enhanced effect and underlying mechanisms of mesenchymal stem cells with IL-33 overexpression on myocardial infarction. *Stem Cell Res. Ther.* 10, 1–14. doi: 10.1186/s13287-019-1392-1399

Cheng, Y., Gu, W., Zhang, G., Li, X., and Guo, X. (2017). Activation of Notch1 signaling alleviates dysfunction of bone marrow-derived mesenchymal stem cells induced by cigarette smoke extract. *Int. J. Chron. Obstruct. Pulmon. Dis.* 12, 3133–3147. doi: 10.2147/COPD.S146201

Cheng, Z., Ou, L., Zhou, X., Li, F., Jia, X., Zhang, Y., et al. (2008). Targeted migration of mesenchymal stem cells modified with CXCR4 gene to infarcted myocardium improves cardiac performance. *Mol. Ther.* 16, 571–579. doi: 10.1038/sj.mt.6300374

Cho, J., Zhai, P., Maejima, Y., and Sadoshima, J. (2011). Myocardial injection with GSK-3β–overexpressing bone marrow–derived mesenchymal stem cells attenuates cardiac dysfunction after myocardial infarction. *Circ. Res.* 108, 478–489. doi: 10.1161/CIRCRESAHA.110.229658

Cho, J. W., Lee, C. Y., and Ko, Y. (2012). Therapeutic potential of mesenchymal stem cells overexpressing human forkhead box A2 gene in the regeneration of damaged liver tissues. *J. Gastroenterol. Hepatol.* 27, 1362–1370. doi: 10.1111/j.1440-1746.2012.07137.x

Cho, Y. H., Cha, M. J., Song, B. W., Kim, I. K., Song, H., Chang, W., et al. (2012). Enhancement of MSC adhesion and therapeutic efficiency in ischemic heart using lentivirus delivery with periostin. *Biomaterials* 33, 1376–1385. doi: 10.1016/j.biomaterials.2011.10.078

Choi, J. S., Jeong, I. S., Han, J. H., Cheon, S. H., and Kim, S. W. (2019). IL-10-secreting human MSCs generated by TALEN gene editing ameliorate liver fibrosis through enhanced anti-fibrotic activity. *Biomater. Sci.* 7, 1078–1087. doi: 10.1039/C8BM01347K

Clark, E. A., Kalomoiris, S., Nolta, J. A., and Fierro, F. A. (2014). Concise review: MicroRNA function in multipotent mesenchymal stromal cells. *Stem Cells* 32, 1074–1082. doi: 10.1002/stem.1623

Copland, I. B., Jolicoeur, E. M., Gillis, M. A., Cuerquis, J., Eliopoulos, N., Annabi, B., et al. (2008). Coupling erythropoietin secretion to mesenchymal stromal cells enhances their regenerative properties. *Cardiovasc. Res.* 79, 405–415. doi: 10.1093/cvr/cvn090

Cui, L. L., Nitzsche, F., Pryazhnikov, E., Tibeykina, M., Tolppanen, L., Rytkönen, J., et al. (2017). Integrin α4 overexpression on rat mesenchymal stem cells enhances transmigration and reduces cerebral embolism after intracarotid injection. *Stroke* 48, 2895–2900. doi: 10.1161/STROKEAHA.117.017809.)

Delcayre, A., Estelles, A., Sperinde, J., Roulon, T., Paz, P., Aguilar, B., et al. (2005). Exosome display technology: applications to the development of new diagnostics and therapeutics. *Blood Cell. Mol. Dis.* 35, 158–168. doi: 10.1016/j.bcmd.2005.07.003

Deng, J., Han, Y., Yan, C., Tian, X., Tao, J., Kang, J., et al. (2010). Overexpressing cellular repressor of E1A-stimulated genes protects mesenchymal stem cells against hypoxia-and serum deprivation-induced apoptosis by activation of PI3K/Akt. *Apoptosis* 15, 463–473. doi: 10.1007/s10495-009-0434-437

Ding, Y., Yan, Q., Ruan, J. W., Zhang, Y. Q., Li, W. J., Zeng, Z., et al. (2013). Electroacupuncture promotes the differentiation of transplanted bone marrow mesenchymal stem cells overexpressing TrkC into neuron-like cells in transected spinal cord of rats. *Cell Transplant.* 22, 65–86. doi: 10.3727/096368912X655037

Ding, Y., Zhang, R. Y., He, B., Liu, Z., Zhang, K., Ruan, J. W., et al. (2015). Combination of electroacupuncture and grafted mesenchymal stem cells overexpressing TrkC improves remyelination and function in demyelinated spinal cord of rats. *Sci. Rep.* 5, 1–14. doi: 10.1038/srep09133

Di Rocco, G., Gentile, A., Antonini, A., Truffa, S., Piaggio, G., Capogrossi, M. C., et al. (2012). Analysis of biodistribution and engraftment into the liver of genetically modified mesenchymal stromal cells derived from adipose tissue. *Cell Transplant.* 21, 1997–2008. doi: 10.3727/096368911X637452

Dominici, M., Le Blanc, K., Mueller, I., Slaper-Cortenbach, I., Marini, F. C., Krause, D. S., et al. (2006). Minimal criteria for defining multipotent mesenchymal stromal cells. International Society for Cellular Therapy position statement. *Cytotherapy* 8,315–317. doi: 10.1080/14653240600855905

Dong, L., and Li, L. (2019). Large tumor suppressor gene 2-mediated Hippo signaling pathway regulates the biological behavior of mesenchymal stem cells in vitro. *Zhonghua wei zhong bing ji jiu yi xue* 31, 1143–1148. doi: 10.3760/cma.j.issn.2095-4352.2019.09.017

Donnelly, J. M., Engevik, A., Feng, R., Xiao, C., Boivin, G. P., Li, J., et al. (2014). Mesenchymal stem cells induce epithelial proliferation within the inflamed stomach. *Am. J. Physiol.Gastrointest. Liver Physiol.* 306, G1075-G1088. doi: 10.1152/ajpgi.00489.2012

Du, Z., Wei, C., Yan, J., Han, B., Zhang, M., Peng, C., et al. (2013). Mesenchymal stem cells overexpressing C-X-C chemokine receptor type 4 improve early liver regeneration of small-for-size liver grafts. *Liver Transpl.* 19, 215–225. doi: 10.1002/lt.23577

Duffy, G. P., D'Arcy, S., Ahsan, T., Nerem, R. M., O'Brien, T., and Barry, F. (2010). Mesenchymal stem cells overexpressing Ephrin-B2 rapidly adopt an early endothelial phenotype with simultaneous reduction of osteogenic potential. *Tissue Eng. Part A* 16, 2755–2768. doi: 10.1089/ten.tea.2009.0623

Fierro, F. A., Kalomoiris, S., Sondergaard, C. S., and Nolta, J. A. (2011). Effects on proliferation and differentiation of multipotent bone marrow stromal cells engineered to express growth factors for combined cell and gene therapy. *Stem Cells* 29, 1727–1737. doi: 10.1002/stem.720

Finer, M., and Glorioso, J. (2017). A brief account of viral vectors and their promise for gene therapy. *Gene Ther.* 24, 1–2. doi: 10.1038/gt.2016.71

Fiore, E. J., Bayo, J. M., Garcia, M. G., Malvicini, M., Lloyd, R., Piccioni, F., et al. (2015). Mesenchymal stromal cells engineered to produce IGF-I by recombinant adenovirus ameliorate liver fibrosis in mice. *Stem Cell. Dev.* 24, 791–801. doi: 10.1089/scd.2014.0174

Foppiani, E. M., Candini, O., Mastrolia, I., Murgia, A., Grisendi, G., Samarelli, A. V., et al. (2019). Impact of HOXB7 overexpression on human adipose-derived mesenchymal progenitors. *Stem Cell Res. Ther.* 10, 1–12. doi: 10.1186/s13287-019-1200-1206

Gao, D., and Jiang, L. (2018). Exosomes in cancer therapy: a novel experimental strategy. *Am. J. Cancer Res.* 8, 2165–2175.

Gao, X., Wu, D., Dou, L., Zhang, H., Huang, L., Zeng, J., et al. (2019). Protective effects of mesenchymal stem cells overexpressing extracellular regulating kinase 1/2 against stroke in rats. *Brain Res. Bull.* 149, 42–52. doi: 10.1016/j.brainresbull.2019.04.006

Gao, X. R., Tan, Y. Z., and Wang, H. J. (2011). Overexpression of Csx/Nkx2. 5 and GATA-4 enhances the efficacy of mesenchymal stem Cell Transplantation after myocardial infarction. *Circ. J.* 75, 11,2683–2691. doi: 10.1253/circj.CJ-11-0238

Gao, Y., Yao, A., Zhang, W., Lu, S., Yu, Y., Deng, L., et al. (2010). Human mesenchymal stem cells overexpressing pigment epithelium-derived factor inhibit hepatocellular carcinoma in nude mice. *Oncogene* 29, 2784–2794. doi: 10.1038/onc.2010.38

Garcia, K. D. O., Ornellas, F. L., Matsumoto, P., Patti, C. D. L., Mello, L. E., Frussa-Filho, R., et al. (2014). Therapeutic effects of the transplantation of VEGF overexpressing bone marrow mesenchymal stem cells in the hippocampus of murine model of Alzheimer's disease. *Front Aging Neurosci.* 6:30. doi: 10.3389/fnagi.2014.00030

Gerace, D., Martiniello-Wilks, R., Nassif, N. T., Lal, S., Steptoe, R., and Simpson, A. M. (2017). CRISPR-targeted genome editing of mesenchymal stem cell-derived therapies for type 1 diabetes: a path to clinical success? *Stem Cell Res. Ther.* 8:62. doi: 10.1186/s13287-017-0511-518

Gnecchi, M., and Cervio, E. (2013). "Mesenchymal stem cell therapy for heart disease," in *Mesenchymal Stem Cell Therapy*, eds L. G. Chase and M. C. Vemuri (Totowa, NJ: Humana Press), 241–270. doi: 10.1007/978-1-62703-200-1_13

Gnecchi, M., He, H., Melo, L. G., Noiseaux, N., Morello, F., De Boer, R. A., et al. (2009). Early beneficial effects of bone marrow-derived mesenchymal stem cells overexpressing Akt on cardiac metabolism after myocardial infarction. *Stem Cells* 27, 971–979. doi: 10.1002/stem.12

Gnecchi, M., He, H., Noiseux, N., Liang, O. D., Zhang, L., Morello, F., et al. (2006). Evidence supporting paracrine hypothesis for Akt-modified mesenchymal stem cell-mediated cardiac protection and functional improvement. *FASEB J.* 20, 661–669. doi: 10.1096/fj.05-5211com

Gómez-Mauricio, G., Moscoso, I., Martín-Cancho, M. F., Crisóstomo, V., Prat-Vidal, C., Báez-Díaz, C., et al. (2016). Combined administration of mesenchymal stem cells overexpressing IGF-1 and HGF enhances neovascularization but moderately improves cardiac regeneration in a porcine model. *Stem Cell Res. Ther.* 7:94. doi: 10.1186/s13287-016-0350-z

Gong, X. H., Liu, H., Wang, S. J., Liang, S. W., and Wang, G. G. (2019). Exosomes derived from SDF1-overexpressing mesenchymal stem cells inhibit ischemic myocardial cell apoptosis and promote cardiac endothelial microvascular regeneration in mice with myocardial infarction. *J. Cell. Physiol.* 234, 13878–13893. doi: 10.1002/jcp.28070

Guo, Y., He, J., Wu, J., Yang, L., Dai, S., Tan, X., et al. (2008). Locally overexpressing hepatocyte growth factor prevents post-ischemic heart failure by inhibition of apoptosis via calcineurin-mediated pathway and angiogenesis. *Arch. Med. Res.* 39, 179–188. doi: 10.1016/j.arcmed.2007.11.001

Guo, Y., Su, L., Li, Y., Guo, N., Xie, L., Zhang, D., et al. (2013). The synergistic therapeutic effect of hepatocyte growth factor and granulocyte colony-stimulating factor on pulmonary hypertension in rats. *Heart Vessels* 29, 520–531. doi: 10.1007/s00380-013-0395-391

Haider, H. K., Jiang, S., Idris, N. M., and Ashraf, M. (2008). IGF-1–overexpressing mesenchymal stem cells accelerate bone marrow stem cell mobilization via paracrine activation of SDF-1α/CXCR4 signaling to promote myocardial repair. *Circ. Res.* 103, 11,1300–1308. doi: 10.1161/CIRCRESAHA.108.186742

Halabian, R., Roudkenar, M. H., Jahanian-Najafabadi, A., Hosseini, K. M., and Tehrani, H. A. (2014). Co-culture of bone marrow-derived mesenchymal stem cells overexpressing lipocalin 2 with HK-2 and HEK293 cells protects the kidney cells against cisplatin-induced injury. *Cell Biol. Int.* 39, 152–163. doi: 10.1002/cbin.10344

Han, S. M., Han, S. H., Coh, Y. R., Jang, G., Ra, J. C., Kang, S. K., et al. (2014). Enhanced proliferation and differentiation of Oct4-and Sox2-overexpressing human adipose tissue mesenchymal stem cells. *Exp. Mol. Med.* 46:e101. doi: 10.1038/emm.2014.28

Han, S. M., Park, C. W., Ahn, J. O., Park, S. C., Jung, W. S., Seo, K. W., et al. (2015). Pro-apoptotic and growth-inhibitory effect of IFN-β-overexpressing canine adipose tissue-derived mesenchymal stem cells against melanoma cells. *Anticancer. Res.* 35, 4749–4756.

He, H., Liu, L., Chen, Q., Liu, A., Cai, S., Yang, Y., et al. (2015). Mesenchymal stem cells overexpressing angiotensin-converting enzyme 2 rescue lipopolysaccharide-induced lung injury. *Cell Transplant.* 24, 1699–1715.

He, J. G., Li, H. R., Li, B. B., Xie, Q. L., Yan, D., and Wang, X. J. (2019). Bone marrow mesenchymal stem cells overexpressing GATA-4 improve cardiac function following myocardial infarction. *Perfusion* 34, 696–704. doi: 10.1177/0267659119847442

Hmadcha, A., Martin-Montalvo, A., Gauthier, B. R., Soria, B., and Capilla-Gonzalez, V. (2020). Therapeutic potential of mesenchymal stem cells for cancer therapy. *Front. Bioeng. Biotechnol.* 8:43. doi: 10.3389/fbioe.2020.00043

Hnatiuk, A. P., Ong, S. G., Olea, F. D., Locatelli, P., Riegler, J., Lee, W. H., et al. (2016). allogeneic mesenchymal stromal cells overexpressing mutant human hypoxia-inducible factor 1-α (HIF 1-α) in an ovine model of acute myocardial infarction. *J. Am. Heart Assoc.* 5:e003714. doi: 10.1161/JAHA.116.003714

Hu, J., Yang, Z., Wang, J., Tang, Y., Liu, H., Zhang, B., et al. (2013). Infusion of Trx-1-overexpressing hucMSC prolongs the survival of acutely irradiated NOD/SCID mice by decreasing excessive inflammatory injury. *PLoS One* 8:e78227. doi: 10.1371/journal.pone.0078227

Hu, Q., Sun, W., Wang, J., Ruan, H., Zhang, X., Ye, Y., et al. (2018). Conjugation of haematopoietic stem cells and platelets decorated with anti-PD-1 antibodies augments anti-leukaemia efficacy. *Nat. Biomed. Eng.* 2, 831–840. doi: 10.1038/s41551-018-0310-312

Hu, X., Chen, P., Wu, Y., Wang, K., Xu, Y., Chen, H., et al. (2016). MiR-211/STAT5A signaling modulates migration of mesenchymal stem cells to improve its therapeutic efficacy. *Stem Cells* 34, 1846–1858. doi: 10.1002/stem.2391

Huang, B., Tabata, Y., and Gao, J. Q. (2012). Mesenchymal stem cells as therapeutic agents and potential targeted gene delivery vehicle for brain diseases. *J. Control. Release* 162, 464–473. doi: 10.1016/j.jconrel.2012.07.034

Huang, F., Li, M. L., Fang, Z. F., Hu, X. Q., Liu, Q. M., Liu, Z. J., et al. (2013a). Overexpression of MicroRNA-1 improves the efficacy of mesenchymal stem Cell Transplantation after myocardial infarction. *Cardiology* 125, 18–30. doi: 10.1159/000347081

Huang, F., Zhu, X., Hu, X. Q., Fang, Z. F., Tang, L., Lu, X. L., et al. (2013b). Mesenchymal stem cells modified with miR-126 release angiogenic factors and activate Notch ligand Delta-like-4, enhancing ischemic angiogenesis and cell survival. *Int. J. Mol. Med.* 31, 484–492. doi: 10.3892/ijmm.2012.1200

Huang, J., Zhang, Z., Guo, J., Ni, A., Deb, A., Zhang, L., et al. (2010). Genetic modification of mesenchymal stem cells overexpressing CCR1 increases cell viability, migration, engraftment, and capillary density in the injured myocardium. *Circ. Res.* 106, 1753–1762. doi: 10.1161/CIRCRESAHA.109.196030

Huang, S. D., Lu, F. L., Xu, X. Y., Liu, X. H., Zhao, X. X., Zhao, B. Z., et al. (2006). Transplantation of angiogenin-overexpressing mesenchymal stem cells synergistically augments cardiac function in a porcine model of chronic ischemia. *J. Thorac. Cardiovasc. Surg.* 132, 1329–1338. doi: 10.1016/j.jtcvs.2006.08.021

Huang, W., Wang, T., Zhang, D., Zhao, T., Dai, B., Ashraf, A., et al. (2012). Mesenchymal stem cells overexpressing CXCR4 attenuate remodeling of postmyocardial infarction by releasing matrix metalloproteinase-9. *Stem Cell. Dev.* 21, 778–789. doi: 10.1089/scd.2011.0126

Huang, X., Ding, J., Li, Y., Liu, W., Ji, J., Wang, H., et al. (2018). Exosomes derived from PEDF modified adipose-derived mesenchymal stem cells ameliorate cerebral ischemia-reperfusion injury by regulation of autophagy and apoptosis. *Exp. Cell Res.* 371, 269–277. doi: 10.1016/j.yexcr.2018.08.021

Huang, Y., Wang, J., Cai, J., Qiu, Y., Zheng, H., Lai, X., et al. (2018). Targeted homing of CCR2-overexpressing mesenchymal stromal cells to ischemic brain enhances post-stroke recovery partially through PRDX4-mediated blood-brain barrier preservation. *Theranostics* 8, 5929–5944. doi: 10.7150/thno.28029

Huang, Z. Y., Hong, L. Q., Na, N., Luo, Y., Miao, B., and Chen, J. (2012). Infusion of mesenchymal stem cells overexpressing GDNF ameliorates renal function in nephrotoxic serum nephritis. *Cell Biochem. and Funct.* 30, 139–144. doi: 10.1002/cbf.1827

Huleihel, L., Sellares, J., Cardenes, N., Álvarez, D., Faner, R., Sakamoto, K., et al. (2017). Modified mesenchymal stem cells using miRNA transduction alter lung injury in a bleomycin model. *Am. J. Physiol. Lung Cell. Mol. Physiol.* 313, L92–L103. doi: 10.1152/ajplung.00323.2016

Jadczyk, T., Tfaily, E. B., Mishra, S., Jêdrzejek, M., Bołoz, M., Padmanabhan, P., et al. (2017). *Innovative Diagnostics and Treatment: Nanorobotics and Stem Cells*. Singapore: Springer.

Jeong, S. R., Kwon, M. J., Lee, H. G., Joe, E. H., Lee, J. H., Kim, S. S., et al. (2012). Hepatocyte growth factor reduces astrocytic scar formation and promotes axonal growth beyond glial scars after spinal cord injury. *Exp. Neurol.* 233, 312–322. doi: 10.1016/j.expneurol.2011.10.021

Jerkic, M., Masterson, C., Ormesher, L., Gagnon, S., Goyal, S., Rabani, R., et al. (2019). Overexpression of IL-10 enhances the efficacy of human umbilical-cord-derived mesenchymal stromal cells in *E. coli Pneumosepsis*. *J. Clin. Med.* 8:847. doi: 10.3390/jcm8060847

Ji, M., Wang, W., Li, S., and Hu, W. (2017). Implantation of bone mesenchymal stem cells overexpressing miRNA 705 mitigated ischemic brain injury. *Mol. Med. Rep.* 16, 8323–8328. doi: 10.3892/mmr.2017.7626

Jia, Y., Wu, D., Zhang, R., Shuang, W., Sun, J., Hao, H., et al. (2014). Bone marrow-derived mesenchymal stem cells expressing the Shh transgene promotes functional recovery after spinal cord injury in rats. *Neurosci. Lett.* 573, 46–51. doi: 10.1016/j.neulet.2014.05.010

Jiang, J., Wei, D., Sun, L., Wang, Y., Wu, X., Li, Y., et al. (2014). A preliminary study on the construction of double suicide gene delivery vectors by mesenchymal stem cells and the in vitro inhibitory effects on SKOV3 cells. *Oncol. Rep.* 31, 781–787. doi: 10.3892/or.2013.2898

Jiang, S., Haider, H. K., Idris, N. M., Salim, A., and Ashraf, M. (2006). Supportive interaction between cell survival signaling and angiocompetent factors enhances donor cell survival and promotes angiomyogenesis for cardiac repair. *Circ. Res.* 99, 776–784. doi: 10.1161/01.RES.0000244687.97719.4f

Jiang, X., Fitch, S., Wang, C., Wilson, C., Li, J., Grant, G. A., et al. (2016). Nanoparticle engineered TRAIL-overexpressing adipose-derived stem cells target and eradicate glioblastoma via intracranial delivery. *Proc. Natl. Acad. Sci. U.S.A.* 113, 13857–13862. doi: 10.1073/pnas.1615396113

Jiang, Z., Hu, X., Yu, H., Xu, Y., Wang, L., Chen, H., et al. (2013). Human endometrial stem cells confer enhanced myocardial salvage and regeneration by paracrine mechanisms. *J. Cell Mol. Med.* 17, 1247–1260. doi: 10.1111/jcmm.12100

Jin, S., Li, H., Han, M., Ruan, M., Liu, Z., Zhang, F., et al. (2016). Mesenchymal stem cells with enhanced Bcl-2 expression promote liver recovery in a rat model of hepatic cirrhosis. *Cell Physiol. Biochem.* 40, 1117–1128. doi: 10.1159/000453166

Joyce, N., Annett, G., Wirthlin, L., Olson, S., Bauer, G., and Nolta, J. A. (2010). Mesenchymal stem cells for the treatment of neurodegenerative disease. *Regen. Med.* 5, 933–946. doi: 10.2217/rme.10.72

Kalimuthu, S., Oh, J. M., Gangadaran, P., Zhu, L., Lee, H. W., Rajendran, R. L., et al. (2017). In vivo tracking of chemokine receptor CXCR4-engineered mesenchymal stem cell migration by optical molecular imaging. *Stem Cell. Int.* 2017:8085637. doi: 10.1155/2017/8085637

Kalluri, R., and LeBleu, V. S. (2020). The biology, function, and biomedical applications of exosomes. *Science* 367:6478. doi: 10.1126/science.aau6977

Kang, K., Ma, R., Cai, W., Huang, W., Paul, C., Liang, J., et al. (2015). Exosomes secreted from CXCR4 overexpressing mesenchymal stem cells promote cardioprotection via Akt signaling pathway following myocardial infarction. *Stem Cells Int.* 2015:659890. doi: 10.1155/2015/659890

Kanki-Horimoto, S., Horimoto, H., Mieno, S., Kishida, K., Watanabe, F., Furuya, E., et al. (2006). Synthetic vascular prosthesis impregnated with mesenchymal stem cells overexpressing endothelial nitric oxide synthase. *Circulation* 114, I–327–I–330. doi: 10.1161/CIRCULATIONAHA.105.001586

Kearns-Jonker, M., Dai, W., Gunthart, M., Fuentes, T., Yeh, H. Y., Gerczuk, P., et al. (2012). Genetically engineered mesenchymal stem cells influence gene expression in donor cardiomyocytes and the recipient heart. *J. of Stem Cell Res. Ther.* 2012:005.

Kim, H., and Park, J. (2017). Usage of human mesenchymal stem cells in cell-based therapy: advantages and disadvantages. *Dev. Reprod.* 21, 1–10. doi: 10.12717/DR.2017.21.1.00

Kim, S. W., Lee, D. W., Yu, L. H., Zhang, H. Z., Kim, C. E., Kim, J. M., et al. (2012). Mesenchymal stem cells overexpressing GCP-2 improve heart function through enhanced angiogenic properties in a myocardial infarction model. *Cardiovasc. Res.* 95, 495–506. doi: 10.1093/cvr/cvs224

Kopru, C. Z., Cagnan, I., Akar, I., Esendagli, G., Korkusuz, P., and Gunel-Ozcan, A. (2018). Dual effect of glucocorticoid-induced tumor necrosis factor–related

receptor ligand carrying mesenchymal stromal cells on small cell lung cancer: a preliminary in vitro study. *Cytotherapy* 20, 930–940. doi: 10.1016/j.jcyt.2018.05.002

Kucic, T., Copland, I. B., Cuerquis, J., Coutu, D. L., Chalifour, L. E., Gagnon, R. F., et al. (2008). Mesenchymal stromal cells genetically engineered to overexpress IGF-I enhance cell-based gene therapy of renal failure-induced anemia. *Am. J. Physiol. Renal Physiol.* 295, F488–F496. doi: 10.1152/ajprenal.00044.2008

Kuro-o, M., Matsumura, Y., Aizawa, H., Kawaguchi, H., Suga, T., Utsugi, T., et al. (1997). Mutation of the mouse klotho gene leads to a syndrome resembling ageing. *Nature* 390, 45–51.

Labedz-Maslowska, A., Lipert, B., Berdecka, D., Kedracka-Krok, S., Jankowska, U., Kamycka, E., et al. (2015). Monocyte chemoattractant protein-induced protein 1 (MCPIP1) enhances angiogenic and cardiomyogenic potential of murine bone marrow-derived mesenchymal stem cells. *PLoS One* 10:e0133746. doi: 10.1371/journal.pone.0133746

Lai, L., Chen, J., Wei, X., Huang, M., Hu, X., Yang, R., et al. (2015). Transplantation of MSCs overexpressing HGF into a rat model of liver fibrosis. *Mol. Imaging Biol.* 18, 43–51. doi: 10.1007/s11307-015-0869-x

Lee, E. J., Choi, E. K., Kang, S. K., Kim, G. H., Park, J. Y., Kang, H. J., et al. (2012). N-cadherin determines individual variations in the therapeutic efficacy of human umbilical cord blood-derived mesenchymal stem cells in a rat model of myocardial infarction. *Mol. Ther.* 20, 155–167. doi: 10.1038/mt.2011.202

Lee, S. H., Kim, Y., Rhew, D., Kim, A., Jo, K. R., Yoon, Y., et al. (2017). Effect of canine mesenchymal stromal cells overexpressing heme oxygenase-1 in spinal cord injury. *J. Vet. Sci.* 18, 377–386. doi: 10.4142/jvs.2017.18.3.377

Lewis, P., Hensel, M., and Emerman, M. (1992). Human immunodeficiency virus infection of cells arrested in the cell cycle. *EMBO J.* 11, 3053–3058.

Li, B., Zhang, Y., Li, M., Zhao, X., Xie, H., Guo, X., et al. (2018). Genetic correction of adipose tissue-derived mesenchymal stem cells mediated by TALEN targeting the GDF5 gene. *Int. J. Mol. Med.* 41, 2397–2405. doi: 10.3892/ijmm.2018.3442

Li, H. X., Zhou, Y. F., Jiang, B., Zhao, X., Jiang, T. B., Li, X., et al. (2014). GATA-4 induces changes in electrophysiological properties of rat mesenchymal stem cells. *Biochim. Biophys. Acta* 1840, 2060–2069. doi: 10.1016/j.bbagen.2014.02.020

Li, J., Zheng, C. Q., Li, Y., Yang, C., Lin, H., and Duan, H. G. (2015). Hepatocyte growth factor gene-modified mesenchymal stem cells augment sinonasal wound healing. *Stem Cells Dev.* 24, 1817–1830. doi: 10.1089/scd.2014.0521

Li, L., Chen, X., Wang, W. E., and Zeng, C. (2016). How to improve the survival of transplanted mesenchymal stem cell in ischemic heart? *Stem Cells Int.* 2016:9682757. doi: 10.1155/2016/9682757

Li, S., Siriwon, N., Zhang, X., Yang, S., Jin, T., He, F., et al. (2017). Enhanced cancer immunotherapy by chimeric antigen receptor–modified T cells engineered to secrete checkpoint inhibitors. *Clin. Cancer Res* 23, 6982–6992. doi: 10.1158/1078-0432.CCR-17-0867

Li, S. H., Sun, Z., Guo, L., Han, M., Wood, M. F., Ghosh, N., et al. (2012). Elastin overexpression by cell-based gene therapy preserves matrix and prevents cardiac dilation. *J. Cell Mol. Med.* 16, 2429–2439. doi: 10.1111/j.1582-4934.2012.01560.x

Li, X., Wang, Q., Ding, L., Wang, Y. X., Zhao, Z. D., Mao, N., et al. (2019). Intercellular adhesion molecule-1 enhances the therapeutic effects of MSCs in a dextran sulfate sodium-induced colitis models by promoting MSCs homing to murine colons and spleens. *Stem Cell Res. Ther.* 10, 1–11. doi: 10.1186/s13287-019-1384-1389

Liang, J., Huang, W., Yu, X., Ashraf, A., Wary, K. K., Xu, M., et al. (2012). Suicide gene reveals the myocardial neovascularization role of mesenchymal stem cells overexpressing CXCR4 (MSCCXCR4). *PLoS One* 7:e46158. doi: 10.1371/journal.pone.0046158

Lim, J. Y., Park, S. I., Kim, S. M., Jun, J. A., Oh, J. H., Ryu, C. H., et al. (2011). Neural differentiation of brain-derived neurotrophic factor-expressing human umbilical cord blood-derived mesenchymal stem cells in culture via TrkB-mediated ERK and β-catenin phosphorylation and following transplantation into the developing brain. *Cell Transplant.* 20, 1855–1866. doi: 10.3727/096368910X557236

Ling, X., Marini, F., Konopleva, M., Schober, W., Shi, Y., Burks, J., et al. (2010). Mesenchymal stem cells overexpressing IFN-β inhibit breast cancer growth and metastases through Stat3 signaling in a syngeneic tumor model. *Cancer Microenviron.* 3, 83–95. doi: 10.1007/s12307-010-0041-48

Liu, B., and Qian, J. M. (2015). Cytoprotective role of heme oxygenase-1 in liver ischemia reperfusion injury. *Int. J. Clin. Exp. Med.* 8, 19867–19873.

Liu, L., Chen, J. X., Zhang, X. W., Sun, Q., Yang, L., Liu, A., et al. (2018). Chemokine receptor 7 overexpression promotes mesenchymal stem cell migration and proliferation via secreting Chemokine ligand 12. *Sci. Rep.* 8, 1–10. doi: 10.1038/s41598-017-18509-18501

Liu, N., Patzak, A., and Zhang, J. (2013). CXCR4-overexpressing bone marrow-derived mesenchymal stem cells improve repair of acute kidney injury. *Am. J. Physiol. Renal Physiol.* 305, F1064–F1073. doi: 10.1152/ajprenal.00178.2013

Liu, X. S., Li, J. F., Wang, S. S., Wang, Y. T., Zhang, Y. Z., Yin, H. L., et al. (2014). Human umbilical cord mesenchymal stem cells infected with adenovirus expressing HGF promote regeneration of damaged neuron cells in a Parkinson's disease model. *Biomed. Res. Int.* 2014:909657. doi: 10.1155/2014/909657

Liu, Z., Wang, C., Wang, X., and Xu, S. (2015). Therapeutic effects of transplantation of as-mir-937-expressing mesenchymal stem cells in murine model of alzheimer's disease. *Cell Physiol. Biochem.* 37, 321–330. doi: 10.1159/000430356

Locatelli, P., Olea, F. D., Hnatiuk, A., De Lorenzi, A., Cerdá, M., Giménez, C. S., et al. (2015). Mesenchymal stromal cells overexpressing vascular endothelial growth factor in ovine myocardial infarction. *Gene Ther.* 22, 449–457. doi: 10.1038/gt.2015.28

Loebinger, M. R., Eddaoudi, A., Davies, D., and Janes, S. M. (2009). Mesenchymal stem cell delivery of TRAIL can eliminate metastatic cancer. *Cancer Res.* 69, 4134–4142. doi: 10.1158/0008-5472.CAN-08-4698

Luo, R., Lu, Y., Liu, J., Cheng, J., and Chen, Y. (2019). Enhancement of the efficacy of mesenchymal stem cells in the treatment of ischemic diseases. *Biomed. Pharmacother.* 109, 2022–2034. doi: 10.1016/j.biopha.2018.11.068

Ma, J., Zhao, Y., Sun, L., Sun, X., Zhao, X., Sun, X., et al. (2017). Exosomes derived from AKt-modified human umbilical cord mesenchymal stem cells improve cardiac regeneration and promote angiogenesis via activating platelet-derived growth factor D. *Stem Cells Transl. Med.* 6, 51–59. doi: 10.5966/sctm.2016-2038

Madonna, R., Angelucci, S., Di Giuseppe, F., Doria, V., Giricz, Z., Görbe, A., et al. (2019). Proteomic analysis of the secretome of adipose tissue-derived murine mesenchymal cells overexpressing telomerase and myocardin. *J. Mol. Cell Cardiol.* 131, 171–186. doi: 10.1016/j.yjmcc.2019.04.019

Madonna, R., Rokosh, G., De Caterina, R., and Bolli, R. (2010). Hepatocyte growth factor/Met gene transfer in cardiac stem cells—potential for cardiac repair. *Basic Res. Cardiol.* 105, 443–452. doi: 10.1007/s00395-010-0102-107

Maiti, P., Peruzzaro, S., Kolli, N., Andrews, M., Al-Gharaibeh, A., Rossignol, J., et al. (2019). Transplantation of mesenchymal stem cells overexpressing interleukin-10 induces autophagy response and promotes neuroprotection in a rat model of TBI. *J Cell Mol Med.* 23, 5211–5224. doi: 10.1111/jcmm.14396

Man, A. J., Kujawski, G., Burns, T. S., Miller, E. N., Fierro, F. A., Leach, J. K., et al. (2016). Neurogenic potential of engineered mesenchymal stem cells overexpressing VEGF. *Cell. Mol. Bioeng.* 9, 96–106.

Mao, J., Lv, Z., and Zhuang, Y. (2014). MicroRNA-23a is involved in tumor necrosis factor-α induced apoptosis in mesenchymal stem cells and myocardial infarction. *Exp. Mol. Pathol.* 97, 23–30. doi: 10.1016/j.yexmp.2013.11.005

Mao, Q., Lin, C., Gao, J., Liang, X., Gao, W., Shen, L., et al. (2014). Mesenchymal stem cells overexpressing integrin-linked kinase attenuate left ventricular remodeling and improve cardiac function after myocardial infarction. *Mol. Cell. Biochem.* 397, 203–214. doi: 10.1007/s11010-014-2188-y

Mao, Q., Lin, C. X., Liang, X. L., Gao, J. S., and Xu, B. (2013). Mesenchymal stem cells overexpressing integrin-linked kinase attenuate cardiac fibroblast proliferation and collagen synthesis through paracrine actions. *Mol. Med. Rep.* 7, 1617–1623. doi: 10.3892/mmr.2013.1348

Marofi, F., Vahedi, G., Biglari, A., Esmaeilzadeh, A., and Athari, S. S. (2017). Mesenchymal stromal/stem cells: a new era in the cell-based targeted gene therapy of cancer. *Front. Immunol.* 8:1770. doi: 10.3389/fimmu.2017.01770

Martínez-González, I., Cruz, M. J., Moreno, R., Morell, F., Munoz, X., and Aran, J. M. (2014). Human mesenchymal stem cells resolve airway inflammation, hyperreactivity, and histopathology in a mouse model of occupational asthma. *Stem Cells Dev.* 23, 2352–2363. doi: 10.1089/scd.2013.0616

Martínez-González, I., Roca, O., Masclans, J. R., Moreno, R., Salcedo, M. T., Baekelandt, V., et al. (2013). Human mesenchymal stem cells overexpressing the IL-33 antagonist soluble IL-1 receptor–like–1 attenuate endotoxin-induced

acute lung injury. *Am. J. Respir. Cell Mol. Biol.* 49, 552–562. doi: 10.1165/rcmb.2012-0406OC

Matsushita, K., Morello, F., Wu, Y., Zhang, L., Iwanaga, S., Pratt, R. E., et al. (2010). Mesenchymal stem cells differentiate into renin-producing juxtaglomerular (JG)-like cells under the control of liver X receptor-α. *J. Biol. Chem.* 285, 11974–11982. doi: 10.1074/jbc.M109.099671

Mayorga, M. E., Kiedrowski, M., McCallinhart, P., Forudi, F., Ockunzzi, J., Weber, K., et al. (2017). Role of SDF-1: CXCR4 in impaired post-myocardial infarction cardiac repair in diabetes. *Stem Cells Transl. Med.* 7, 115–124. doi: 10.1002/sctm.17-0172

Mei, S. H., McCarter, S. D., Deng, Y., Parker, C. H., Liles, W. C., and Stewart, D. J. (2007). Prevention of LPS-induced acute lung injury in mice by mesenchymal stem cells overexpressing angiopoietin 1. *PLoS Med.* 4:e269. doi: 10.1371/journal.pmed.0040269

Meng, X., Li, J., Yu, M., Yang, J., Zheng, M., Zhang, J., et al. (2017). Transplantation of mesenchymal stem cells overexpressing IL10 attenuates cardiac impairments in rats with myocardial infarction. *J. Cell. Physiol.* 233, 587–595. doi: 10.1002/jcp.25919

Meng, X., Zheng, M., Yu, M., Bai, W., Zuo, L., Bu, X., et al. (2019). Transplantation of CRISPRa system engineered IL10-overexpressing bone marrow-derived mesenchymal stem cells for the treatment of myocardial infarction in diabetic mice. *J. Biol. Eng.* 13:49. doi: 10.1186/s13036-019-0163-166

Meyer, G. P., Wollert, K. C., Lotz, J., Steffens, J., Lippolt, P., Fichtner, S., et al. (2006). Intracoronary bone marrow cell transfer after myocardial infarction. *Circulation* 113, 1287–1294. doi: 10.1161/CIRCULATIONAHA.105.575118

Milone, M. C., and O'Doherty, U. (2018). Clinical use of lentiviral vectors. *Leukemia* 32, 1529–1541. doi: 10.1038/s41375-018-0106-100

Moradian, H., Keshvari, H., Fasehee, H., Dinarvand, R., and Faghihi, S. (2017). Combining NT3-overexpressing MSCs and PLGA microcarriers for brain tissue engineering: a potential tool for treatment of Parkinson's disease. *Mater. Sci. Eng. C Mater. Biol. Appl.* 76, 934–943. doi: 10.1016/j.msec.2017.02.178

Moya, A., Paquet, J., Deschepper, M., Larochette, N., Oudina, K., Denoeud, C., et al. (2018). Human mesenchymal stem cell failure to adapt to glucose shortage and rapidly use intracellular energy reserves through glycolysis explains poor cell survival after implantation. *Stem Cells* 36, 363–376. doi: 10.1002/stem.2763

Mueller, L. P., Luetzkendorf, J., Widder, M., Nerger, K., Caysa, H., and Mueller, T. (2011). TRAIL-transduced multipotent mesenchymal stromal cells (TRAIL-MSC) overcome TRAIL resistance in selected CRC cell lines in vitro and in vivo. *Cancer Gene Ther.* 18, 229–239. doi: 10.1038/cgt.2010.68

Murphy, M., Moncivais, K., and Caplan, A. (2013). Mesenchymal stem cells: environmentally responsive therapeutics for regenerative medicine. *Exp. Mol. Med.* 45:e54. doi: 10.1038/emm.2013.94

Nakajima, M., Nito, C., Sowa, K., Suda, S., Nishiyama, Y., Nakamura-Takahashi, A., et al. (2017). Mesenchymal stem cells overexpressing interleukin-10 promote neuroprotection in experimental acute ischemic stroke. *Mol. Ther. Methods Clin. Dev.* 6, 102–111. doi: 10.1016/j.omtm.2017.06.005

Naso, M. F., Tomkowicz, B., Perry, W. L., and Strohl, W. R. (2017). Adeno-associated virus (AAV) as a vector for gene therapy. *BioDrugs* 31, 317–334. doi: 10.1007/s40259-017-0234-235

Nayak, S., and Herzog, R. W. (2010). Progress and prospects: immune responses to viral vectors. *Gene Ther.* 17, 295–304. doi: 10.1038/gt.2009.148

Ni, J., Liu, X., Yin, Y., Zhang, P., Xu, Y. W., and Liu, Z. (2019). Exosomes derived from TIMP2-modified human umbilical cord mesenchymal stem cells enhance the repair effect in rat model with myocardial infarction Possibly by the Akt/Sfrp2 pathway. *Oxid. Med. Cell. Longev.* 2019;1958941. doi: 10.1155/2019/1958941

Noiseux, N., Gnecchi, M., Lopez-Ilasaca, M., Zhang, L., Solomon, S. D., Deb, A., et al. (2006). Mesenchymal stem cells overexpressing Akt dramatically repair infarcted myocardium and improve cardiac function despite infrequent cellular fusion or differentiation. *Mol. Ther.* 14, 840–850. doi: 10.1016/j.ymthe.2006.05.016

Noori-Zadeh, A., Mesbah-Namin, S. A., Tiraihi, T., Rajabibazl, M., and Taheri, T. (2014). Non-viral human proGDNF gene delivery to rat bone marrow stromal cells under ex vivo conditions. *J. Neurol. Sci.* 339, 81–86. doi: 10.1016/j.jns.2014.01.025

Otani, K., Yamahara, K., Ohnishi, S., Obata, H., Kitamura, S., and Nagaya, N. (2009). Nonviral delivery of siRNA into mesenchymal stem cells by a combination of ultrasound and microbubbles. *J Controll. Release* 133, 146–153. doi: 10.1016/j.jconrel.2008.09.088

Park, J. S., Na, K., Woo, D. G., Yang, H. N., Kim, J. M., Kim, J. H., et al. (2010). Non-viral gene delivery of DNA polyplexed with nanoparticles transfected into human mesenchymal stem cells. *Biomaterials* 31, 124–132. doi: 10.1016/j.biomaterials.2009.09.023

Park, J. S., Suryaprakash, S., Lao, Y. H., and Leong, K. W. (2015). Engineering mesenchymal stem cells for regenerative medicine and drug delivery. *Methods* 84, 3–16. doi: 10.1016/j.ymeth.2015.03.002

Park, Y. M., Han, S. H., Seo, S. K., Park, K. A., Lee, W. T., and Lee, J. E. (2015). Restorative benefits of transplanting human mesenchymal stromal cells overexpressing arginine decarboxylase genes after spinal cord injury. *Cytotherapy* 17, 25–37. doi: 10.1016/j.jcyt.2014.08.006

Payne, N. L., Dantanarayana, A., Sun, G., Moussa, L., Caine, S., McDonald, C., et al. (2012). Early intervention with gene-modified mesenchymal stem cells overexpressing interleukin-4 enhances anti-inflammatory responses and functional recovery in experimental autoimmune demyelination. *Cell Adh. Migr.* 6, 179–189. doi: 10.4161/cam.20341

Pittenger, M. F., and Martin, B. J. (2004). Mesenchymal stem cells and their potential as cardiac therapeutics. *Circ. Res.* 95, 9–20. doi: 10.1161/01.res.0000135902.99383.6f

Preda, M. B., Rønningen, T., Burlacu, A., Simionescu, M., Moskaug, J. O., and Valen, G. (2014). Remote transplantation of mesenchymal stem cells protects the heart against ischemia-reperfusion injury. *Stem Cells* 32, 2123–2134. doi: 10.1002/stem.1687

Pulukuri, S. M. K., Gorantla, B., Dasari, V. R., Gondi, C. S., and Rao, J. S. (2010). Epigenetic upregulation of urokinase plasminogen activator promotes the tropism of mesenchymal stem cells for tumor cells. *Mol. Cancer Res.* 8, 1074–1083. doi: 10.1158/1541-7786.MCR-09-0495

Razban, V., Lotfi, A. S., Soleimani, M., Ahmadi, H., Massumi, M., Khajeh, S., et al. (2012). HIF-1α overexpression induces angiogenesis in mesenchymal stem cells. *BioRes. Open Access* 1, 174–183. doi: 10.1089/biores.2012.9905

Roudkenar, M. H., Halabian, R., Bahmani, P., Roushandeh, A. M., Kuwahara, Y., and Fukumoto, M. (2011). Neutrophil gelatinase-associated lipocalin: a new antioxidant that exerts its cytoprotective effect independent on Heme Oxygenase-1. *Free Radic. Res.* 45, 810–819. doi: 10.3109/10715762.2011.581279

Roudkenar, M. H., Pour, Z. G., Halabian, R., Roushandeh, A. M., Parichehr, Y., and Baghian, A. G. (2008). Lipocalin 2 acts as a cytoprotective factor against cisplatin toxicity, an in vitro study. *Daru J. Pharm. Sci.* 16, 106–111.

Ryu, S., Lee, J. M., Bae, C. A., Moon, C. E., and Cho, K. O. (2019). Therapeutic efficacy of neuregulin 1-expressing human adipose-derived mesenchymal stem cells for ischemic stroke. *PLoS One* 14:e0222587. doi: 10.1371/journal.pone.0222587

Sage, E., Thakrar, R., and Janes, S. (2016). Genetically modified mesenchymal stromal cells in cancer therapy. *Cytotherapy* 18, 1435–1445. doi: 10.1016/j.jcyt.2016.09.003

Sajic, M., Hunt, D. P., Lee, W., Compston, D. A. S., Schweimer, J. V., Gregson, N. A., et al. (2012). Mesenchymal stem cells lack efficacy in the treatment of experimental autoimmune neuritis despite in vitro inhibition of T-cell proliferation. *PLoS One* 7:e30708. doi: 10.1371/journal.pone.0030708

Saraswati, S., Guo, Y., Atkinson, J., and Young, P. P. (2015). Prolonged hypoxia induces MCT4 expression in MSCs resulting in a secretome that is deleterious to cardiovascular repair. *Stem Cells* 33, 1333–1344. doi: 10.1002/stem.1935

Sauer, V., Siaj, R., Todorov, T., Zibert, A., and Schmidt, H. H. J. (2010). Overexpressed ATP7B protects mesenchymal stem cells from toxic copper. *Biochem. Biophys. Res. Commun.* 395, 307–311. doi: 10.1016/j.bbrc.2010.03.158

Scheper, V., Schwieger, J., Hamm, A., Lenarz, T., and Hoffmann, A. (2019). BDNF-overexpressing human mesenchymal stem cells mediate increased neuronal protection in vitro. *J. Neurosci. Res.* 97, 1414–1429. doi: 10.1002/jnr.24488

Schmitz, J., Owyang, A., Oldham, E., Song, Y., Murphy, E., McClanahan, T. K., et al. (2005). IL-33, an interleukin-1-like cytokine that signals via the IL-1 receptor-related protein ST2 and induces T helper type 2-associated cytokines. *Immunity* 23, 479–490. doi: 10.1016/j.immuni.2005.09.015

Seo, K. W., Sohn, S. Y., Bhang, D. H., Nam, M. J., Lee, H. W., and Youn, H. Y. (2014). Therapeutic effects of hepatocyte growth factor-overexpressing human umbilical cord blood-derived mesenchymal stem cells on liver fibrosis in rats. *Cell Biol. Int.* 38, 106–116. doi: 10.1002/cbin.10186

Shahror, R. A., Linares, G. R., Wang, Y., Hsueh, S. C., Wu, C. C., Chuang, D. M., et al. (2019). Transplantation of mesenchymal stem cells overexpressing Fibroblast Growth Factor 21 facilitates cognitive recovery and enhances neurogenesis in a mouse model of traumatic brain injury. *J. Neurotrauma* 37, 14–26. doi: 10.1089/neu.2019.6422

Shao, Y., Shen, J., Zhou, F., and He, D. (2018). Mesenchymal stem cells overexpressing Ang1 attenuates phosgene-induced acute lung injury in rats. *Inhal. Toxicol.* 30, 313–320. doi: 10.1080/08958378.2018.1521483

Shao, Y., Zhou, F., He, D., Zhang, L., and Shen, J. (2019). Overexpression of CXCR7 promotes mesenchymal stem cells to repair phosgene-induced acute lung injury in rats. *Biomed. Pharmacother.* 109, 1233–1239. doi: 10.1016/j.biopha.2018.10.108

Shen, H., Cui, G., Li, Y., Ye, W., Sun, Y., Zhang, Z., et al. (2019). Follistatin-like 1 protects mesenchymal stem cells from hypoxic damage and enhances their therapeutic efficacy in a mouse myocardial infarction model. *Stem Cell Res. Ther.* 10, 1–14. doi: 10.1186/s13287-018-1111-y

Shen, Z., Wang, J., Huang, Q., Shi, Y., Wei, Z., Zhang, X., et al. (2018). Genetic modification to induce CXCR2 overexpression in mesenchymal stem cells enhances treatment benefits in radiation-induced oral mucositis. *Cell Death Dis.* 9, 1–14. doi: 10.1038/s41419-018-0310-x

Shi, B., Long, X., Zhao, R., Liu, Z., Wang, D., and Xu, G. (2014). Transplantation of mesenchymal stem cells carrying the human receptor activity-modifying protein 1 gene improves cardiac function and inhibits neointimal proliferation in the carotid angioplasty and myocardial infarction rabbit model. *Exp. Biol. Med.* 239, 356–365. doi: 10.1177/1535370213517619

Shi, R. Z., and Li, Q. P. (2008). Improving outcome of transplanted mesenchymal stem cells for ischemic heart disease. *Biochem. Biophys. Res. Commun.* 376, 247–250. doi: 10.1016/j.bbrc.2008.09.004

Shimizu, T., Ishikawa, T., Sugihara, E., Kuninaka, S., Miyamoto, T., Mabuchi, Y., et al. (2010). c-MYC overexpression with loss of Ink4a/Arf transforms bone marrow stromal cells into osteosarcoma accompanied by loss of adipogenesis. *Oncogene* 29, 5687–5699. doi: 10.1038/onc.2010.312

Silva, D. N., Souza, B. S., Azevedo, C. M., Vasconcelos, J. F., de Jesus, P. G., Feitoza, M. S., et al. (2018a). IGF-1-Overexpressing mesenchymal stem/stromal cells promote immunomodulatory and proregenerative effects in chronic experimental chagas disease. *Stem Cells Int.* 2018:9108681. doi: 10.1155/2018/9108681

Silva, D. N., Souza, B. S., Vasconcelos, J. F., Azevedo, C. M., Valim, C. X., Paredes, B. D., et al. (2018b). Granulocyte-Colony stimulating factor-overexpressing mesenchymal stem cells exhibit enhanced immunomodulatory actions through the recruitment of suppressor cells in experimental chagas disease cardiomyopathy. *Front. Immunol.* 9:1449. doi: 10.3389/fimmu.2018.01449

Silva, L. H., Antunes, M. A., Dos Santos, C. C., Weiss, D. J., Cruz, F. F., and Rocco, P. R. (2018c). Strategies to improve the therapeutic effects of mesenchymal stromal cells in respiratory diseases. *Stem Cell Res Ther.* 9:45. doi: 10.1186/s13287-018-0802-808

Somia, N., and Verma, I. M. (2000). Gene therapy: trials and tribulations. *Nat. Rev. Genet.* 1, 91–99. doi: 10.1038/35038533

Song, Y. S., Lee, H. J., Doo, S. H., Lee, S. J., Lim, I., Chang, K. T., et al. (2012). Mesenchymal stem cells overexpressing hepatocyte growth factor (HGF) inhibit collagen deposit and improve bladder function in rat model of bladder outlet obstruction. *Cell Transplant.* 21, 1641–1650. doi: 10.3727/096368912X637488

Spano, C., Grisendi, G., Golinelli, G., Rossignoli, F., Prapa, M., Bestagno, M., et al. (2019). Soluble TRAIL armed human MSC as gene therapy for pancreatic cancer. *Sci. Rep.* 9, 1–14. doi: 10.1038/s41598-018-37433-37436

Stewart, A. N., Kendziorski, G., Deak, Z. M., Brown, D. J., Fini, M. N., Copely, K. L., et al. (2017). Co-transplantation of mesenchymal and neural stem cells and overexpressing stromal-derived factor-1 for treating spinal cord injury. *Brain Res.* 1672, 91–105. doi: 10.1016/j.brainres.2017.07.005

Tomita, S., Li, R. K., Weisel, R. D., Mickle, D. A., Kim, E. J., Sakai, T., et al. (1999). Autologous transplantation of bone marrow cells improves damaged heart function. *Circulation* 100(Suppl._2), II247–II256.

Torres, R., Martin, M. C., Garcia, A., Cigudosa, J. C., Ramirez, J. C., and Rodriguez-Perales, S. (2014). Engineering human tumour-associated chromosomal translocations with the RNA-guided CRISPR–Cas9 system. *Nat. Commun.* 5, 1–8. doi: 10.1038/ncomms4964

Tyciakova, S., Matuskova, M., Bohovic, R., and Kucerova, L. (2017). Mesenchymal stromal cells producing TNFα lack inhibitory effect against A375 experimental lung metastases. *Neoplasma* 64, 222–227. doi: 10.4149/neo_2017_208

Uchimura, E., Yamada, S., Uebersax, L., Fujita, S., Miyake, M., and Miyake, J. (2007). Method for reverse transfection using gold colloid as a nano-scaffold. *J. Biosci. Bioeng.* 103, 101–103. doi: 10.1263/jbb.103.101

Unzek, S., Zhang, M., Mal, N., Mills, W. R., Laurita, K. R., and Penn, M. S. (2007). SDF-1 recruits cardiac stem cell-like cells that depolarize in vivo. *Cell Transplant.* 16, 879–886. doi: 10.3727/096368907783338271

van den Akker, G., van Beuningen, H., Davidson, E. B., and van der Kraan, P. (2016). CRISPR/CAS9 mediated genome engineering of human mesenchymal stem cells. *Osteoarthritis Cartilage* 24:S231. doi: 10.1016/j.joca.2016.01.445

Van Velthoven, C. T., Sheldon, R. A., Kavelaars, A., Derugin, N., Vexler, Z. S., Willemen, H. L., et al. (2013). Mesenchymal stem Cell Transplantation attenuates brain injury after neonatal stroke. *Stroke* 44, 1426–1432. doi: 10.1161/STROKEAHA.111.000326

Vargas, J. E., Chicaybam, L., Stein, R. T., Tanuri, A., Delgado-Cañedo, A., and Bonamino, M. H. (2016). Retroviral vectors and transposons for stable gene therapy: advances, current challenges and perspectives. *J. Transl. Med.* 14, 1–15. doi: 10.1186/s12967-016-1047-x

Varshney, R., Ali, Q., Wu, C., and Sun, Z. (2016). Monocrotaline-induced pulmonary hypertension involves downregulation of antiaging protein klotho and eNOS activity. *Hypertension* 68, 1255–1263. doi: 10.1161/HYPERTENSIONAHA.116.08184

Vemula, S. V., and Mittal, S. K. (2010). Production of adenovirus vectors and their use as a delivery system for influenza vaccines. *Expert Opin. Biol. Ther.* 10, 1469–1487. doi: 10.1517/14712598.2010.519332

von Einem, J. C., Guenther, C., Volk, H. D., Grütz, G., Hirsch, D., Salat, C., et al. (2019). Treatment of advanced gastrointestinal cancer with genetically modified autologous mesenchymal stem cells: Results from the phase 1/2 TREAT-ME-1 trial. *Int. J. Cancer* 145, 1538–1546. doi: 10.1002/ijc.32230

Wang, B., Wu, Z. H., Lou, P. Y., Chai, C., Han, S. Y., Ning, J. F., et al. (2019). Human bone marrow-derived mesenchymal stem cell-secreted exosomes overexpressing microRNA-34a ameliorate glioblastoma development via down-regulating MYCN. *Cell. Oncol.* 42, 783–799. doi: 10.1007/s13402-019-00461

Wang, C., Lv, D., Zhang, X., Ni, Z. A., Sun, X., and Zhu, C. (2018). Interleukin-10-overexpressing mesenchymal stromal cells induce a series of regulatory effects in the inflammatory system and promote the survival of endotoxin-induced acute lung injury in mice model. *DNA Cell Biol.* 37, 53–61. doi: 10.1089/dna.2017.3735

Wang, J., Xu, L., Chen, Q., Zhang, Y., Hu, Y., and Yan, L. (2015). Bone mesenchymal stem cells overexpressing FGF4 contribute to liver regeneration in an animal model of liver cirrhosis. *Int. J. Clin. Exp. Med.* 8, 12774–12782.

Wang, K., Long, Q., Jia, C., Liu, Y., Yi, X., Yang, H., et al. (2013). Over-expression of Mash1 improves the GABAergic differentiation of bone marrow mesenchymal stem cells in vitro. *Brain Res. Bull.* 99, 84–94. doi: 10.1016/j.brainresbull.2013.10.005

Wang, Q., Zhang, Z., Ding, T., Chen, Z., and Zhang, T. (2013). Mesenchymal stem cells overexpressing PEDF decrease the angiogenesis of gliomas. *Biosci. Rep.* 33:e00019. doi: 10.1042/BSR20110124

Wang, W., Zhang, Y., Yang, C., Wang, Y., Shen, J., Shi, M., et al. (2019). Transplantation of neuregulin 4-overexpressing adipose-derived mesenchymal stem cells ameliorates insulin resistance by attenuating hepatic steatosis. *Exp. Biol. Med.* 244, 565–578. doi: 10.1177/1535370219839643

Wang, X., Hu, Q., Mansoor, A., Lee, J., Wang, Z., Lee, T., et al. (2006). Bioenergetic and functional consequences of stem cell-based VEGF delivery in pressure-overloaded swine hearts. *Am. J. Physiol. Heart Circ. Physiol.* 290, H1393–H1405. doi: 10.1152/ajpheart.00871.2005

Wang, Y., Li, Y., Song, L., Li, Y., Jiang, S., and Zhang, S. (2016). The transplantation of Akt-overexpressing amniotic fluid-derived mesenchymal stem cells protects the heart against ischemia-reperfusion injury in rabbits. *Mol. Med. Rep.* 14, 234–242. doi: 10.3892/mmr.2016.5212

Wang, Z., Li, S., Wang, Y., Zhang, X., Chen, L., and Sun, D. (2019). GDNF enhances the anti-inflammatory effect of human adipose-derived mesenchymal stem cell-based therapy in renal interstitial fibrosis. *Stem Cell Res.* 41:101605. doi: 10.1016/j.scr.2019.101605

Wei, Z., Qiao, S., Zhao, J., Liu, Y., Li, Q., Wei, Z., et al. (2019). miRNA-181a over-expression in mesenchymal stem cell-derived exosomes influenced

inflammatory response after myocardial ischemia-reperfusion injury. *Life Sci.* 232:116632. doi: 10.1016/j.lfs.2019.116632

WenBo, W., Fei, Z., YiHeng, D., Wei, W., TingMang, Y., WenHao, Z., et al. (2017). Human umbilical cord mesenchymal stem cells overexpressing nerve growth factor ameliorate diabetic cystopathy in rats. *Neurochem. Res.* 42, 3537–3547. doi: 10.1007/s11064-017-2401-y

WHO (2020). *Cancer*. Available online at: https://www.who.int/health-topics/cancer#tab=tab_1 (accessed February 18, 2019).

Wu, N., Zhang, Y. L., Wang, H. T., Li, D. W., Dai, H. J., Zhang, Q. Q., et al. (2016). Overexpression of hepatocyte nuclear factor 4α in human mesenchymal stem cells suppresses hepatocellular carcinoma development through Wnt/β-catenin signaling pathway downregulation. *Cancer Biol. Ther.* 17, 558–565. doi: 10.1080/15384047.2016.1177675

Wu, S. P., Yang, Z., Li, F. R., Liu, X. D., Chen, H. T., and Su, D. N. (2017). Smad7-overexpressing rat BMSCs inhibit the fibrosis of hepatic stellate cells by regulating the TGF-β1/Smad signaling pathway. *Exp. Ther. Med.* 14, 2568–2576. doi: 10.3892/etm.2017.4836

Wu, S. Z., Li, Y. L., Huang, W., Cai, W. F., Liang, J., Paul, C., et al. (2017). Paracrine effect of CXCR4-overexpressing mesenchymal stem cells on ischemic heart injury. *Cell Biochem. Funct.* 35, 113–123. doi: 10.1002/cbf.3254

Xia, P., Wang, W., and Bai, Y. (2013). Claudin-7 suppresses the cytotoxicity of TRAIL-expressing mesenchymal stem cells in H460 human non-small cell lung cancer cells. *Apoptosis* 19, 491–505. doi: 10.1007/s10495-013-0938-z

Xiang, Q., Liao, Y., Chao, H., Huang, W., Liu, J., Chen, H., et al. (2018). ISL1 overexpression enhances the survival of transplanted human mesenchymal stem cells in a murine myocardial infarction model. *Stem Cell Res. Ther.* 9:51. doi: 10.1186/s13287-018-0803-807

Xie, C., Du, L. Y., Guo, F., Li, X., and Cheng, B. (2019). Exosomes derived from microRNA-101-3p-overexpressing human bone marrow mesenchymal stem cells suppress oral cancer cell proliferation, invasion, and migration. *Mol. Cell. Biochem.* 458, 11–26. doi: 10.1007/s11010-019-03526-3527

Xin, H., Wang, F., Li, Y., Lu, Q. E., Cheung, W. L., Zhang, Y., et al. (2017). Secondary release of exosomes from astrocytes contributes to the increase in neural plasticity and improvement of functional recovery after stroke in rats treated with exosomes harvested from microRNA 133b-overexpressing multipotent mesenchymal stromal cells. *Cell Transplant.* 26, 243–257. doi: 10.3727/096368916X693031

Xu, X. P., Huang, L. L., Hu, S. L., Han, J. B., He, H. L., Xu, J. Y., et al. (2018). Genetic modification of mesenchymal stem cells overexpressing angiotensin II Type 2 receptor increases cell migration to injured lung in LPS-induced acute lung injury mice. *Stem Cells Transl. Med.* 7, 721–730. doi: 10.1002/sctm.17-0279

Xu, Y., Shen, L., Li, F., Yang, J., Wan, X., and Ouyang, M. (2019). microRNA-16-5p-containing exosomes derived from bone marrow-derived mesenchymal stem cells inhibit proliferation, migration, and invasion, while promoting apoptosis of colorectal cancer cells by downregulating ITGA2. *J. Cell. Physiol.* 234, 21380–21394. doi: 10.1002/jcp.28747

Yamada, Y., Sakurada, K., Takeda, Y., Gojo, S., and Umezawa, A. (2007). Single-cell-derived mesenchymal stem cells overexpressing Csx/Nkx2. 5 and GATA4 undergo the stochastic cardiomyogenic fate and behave like transient amplifying cells. *Exp. Cell Res.* 313, 698–706. doi: 10.1016/j.yexcr.2006.11.012

Yang, C., Liu, H., and Liu, D. (2014). Mutant hypoxia inducible factor 1α modified bone marrow mesenchymal stem cells ameliorate cerebral ischemia. *Int. J. Mol. Med.* 34, 1622–1628. doi: 10.3892/ijmm.2014.1953

Yang, C., Zhou, L., Gao, X., Chen, B., Tu, J., Sun, H., et al. (2011). Neuroprotective effects of bone marrow stem cells overexpressing glial cell line-derived neurotrophic factor on rats with intracerebral hemorrhage and neurons exposed to hypoxia/reoxygenation. *Neurosurgery* 68, 691–704.

Yang, F., Wu, R., Jiang, Z., Chen, J., Nan, J., Zhang, N., et al. (2018). Leptin increases mitochondrial OPA1 via GSK3-mediated OMA1 ubiquitination to enhance therapeutic effects of mesenchymal stem Cell Transplantation. *Cell Death Dis.* 9, 1–17. doi: 10.1038/s41419-018-0579-579

Yang, J. J., Yang, X., Liu, Z. Q., Hu, S. Y., Du, Z. Y., Feng, L. L., et al. (2012). Transplantation of adipose tissue-derived stem cells overexpressing heme oxygenase-1 improves functions and remodeling of infarcted myocardium in rabbits. *Tohoku J. f Exp. Med.* 226, 231–241. doi: 10.1620/tjem.226.231

Yang, K., Park, H. J., Han, S., Lee, J., Ko, E., Kim, J., et al. (2015). Recapitulation of in vivo-like paracrine signals of human mesenchymal stem cells for functional neuronal differentiation of human neural stem cells in a 3D microfluidic system. *Biomaterials* 63, 177–188. doi: 10.1016/j.biomaterials.2015.06.011

Ye, Z., Lu, W., Liang, L., Tang, M., Wang, Y., Li, Z., et al. (2019). Mesenchymal stem cells overexpressing hepatocyte nuclear factor-4 alpha alleviate liver injury by modulating anti-inflammatory functions in mice. *Stem Cell Res. Ther.* 10:149. doi: 10.1186/s13287-019-1260-1267

Yi, X., Wei, X., Lv, H., An, Y., Li, L., Lu, P., et al. (2019). Exosomes derived from microRNA-30b-3p-overexpressing mesenchymal stem cells protect against lipopolysaccharide-induced acute lung injury by inhibiting SAA3. *Exp. Cell Res.* 383:111454. doi: 10.1016/j.yexcr.2019.05.035

Yu, B., Yang, Y., Liu, H., Gong, M., Millard, R. W., Wang, Y. G., et al. (2016). Clusterin/Akt up-regulation is critical for GATA-4 mediated cytoprotection of mesenchymal stem cells against ischemia injury. *PLoS One* 11:e0151542. doi: 10.1371/journal.pone.0151542

Yu, L., Gui, S., Liu, Y., Qiu, X., Zhang, G., Zhang, X. A., et al. (2019). Exosomes derived from microRNA-199a-overexpressing mesenchymal stem cells inhibit glioma progression by down-regulating AGAP2. *Aging* 11, 5300–5318. doi: 10.18632/aging.102092

Yu, Y., Zhang, Q., Meng, Q., Zong, C., Liang, L., Yang, X., et al. (2016). Mesenchymal stem cells overexpressing Sirt1 inhibit prostate cancer growth by recruiting natural killer cells and macrophages. *Oncotarget* 7, 71112–71122. doi: 10.18632/oncotarget.12737

Yuan, Z., Kolluri, K. K., Gowers, K. H., and Janes, S. M. (2017). TRAIL delivery by MSC-derived extracellular vesicles is an effective anticancer therapy. *J. Extracell. Vesicles* 6:1265291. doi: 10.1080/20013078.2017.1265291

Zeng, B., Lin, G., Ren, X., Zhang, Y., and Chen, H. (2010). Over-expression of HO-1 on mesenchymal stem cells promotes angiogenesis and improves myocardial function in infarcted myocardium. *J. Biomed. Sci.* 17:80. doi: 10.1186/1423-0127-17-80

Zeng, B., Ren, X., Lin, G., Zhu, C., Chen, H., Yin, J., et al. (2008). Paracrine action of HO-1-modified mesenchymal stem cells mediates cardiac protection and functional improvement. *Cell Biol. Int.* 32, 1256–1264. doi: 10.1016/j.cellbi.2008.07.010

Zeng, Y. L., Zheng, H., Chen, Q. R., Yuan, X. H., Ren, J. H., Luo, X. F., et al. (2017). Bone marrow-derived mesenchymal stem cells overexpressing MiR-21 efficiently repair myocardial damage in rats. *Oncotarget.* 8, 29161–29173. doi: 10.18632/oncotarget.16254

Zhang, C., Zhu, Y., Wang, J., Hou, L., Li, W., and An, H. (2019). CXCR4-Overexpressing Umbilical Cord Mesenchymal Stem Cells Enhance Protection against Radiation-Induced Lung Injury. *Stem Cells Int.* 2019:2457082. doi: 10.1155/2019/2457082

Zhang, D., Fan, G. C., Zhou, X., Zhao, T., Pasha, Z., Xu, M., et al. (2008). Over-expression of CXCR4 on mesenchymal stem cells augments myoangiogenesis in the infarcted myocardium. *J. Mol. Cell Cardiol.* 44, 281–292. doi: 10.1016/j.yjmcc.2007.11.010

Zhang, F., Wan, X., Cao, Y. Z., Sun, D., and Cao, C. C. (2018). Klotho gene-modified BMSCs showed elevated antifibrotic effects by inhibiting the Wnt/β-catenin pathway in kidneys after acute injury. *Cell Biol. Int* 42, 1670–1679. doi: 10.1002/cbin.11068

Zhang, H., Wang, Y., Lv, Q., Gao, J., Hu, L., and He, Z. (2018). MicroRNA-21 overexpression promotes the neuroprotective efficacy of mesenchymal stem cells for treatment of intracerebral hemorrhage. *Front. Neurol.* 9:931. doi: 10.3389/fneur.2018.00931

Zhang, J., Zhou, S., Zhou, Y., Feng, F., Wang, Q., Zhu, X., et al. (2014). Hepatocyte growth factor gene-modified adipose-derived mesenchymal stem cells ameliorate radiation induced liver damage in a rat model. *PLoS One* 9:e114670. doi: 10.1371/journal.pone.0114670

Zhang, J. C., Zheng, G. F., Wu, L., Ou Yang, L. Y., and Li, W. X. (2014). Bone marrow mesenchymal stem cells overexpressing human basic fibroblast growth factor increase vasculogenesis in ischemic rats. *Braz. J. Med. Biol. Res.* 47, 886–894. doi: 10.1590/1414-431X20143765

Zhang, S., Jiang, W., Ma, L., Liu, Y., Zhang, X., and Wang, S. (2017). Nrf2 transfection enhances the efficacy of human amniotic mesenchymal stem cells to repair lung injury induced by lipopolysaccharide. *J. Cell. Biochem.* 119, 1627–1636. doi: 10.1002/jcb.26322

Zhang, X., Chen, J., Xue, M., Tang, Y., Xu, J., Liu, L., et al. (2019). Overexpressing p130/E2F4 in mesenchymal stem cells facilitates the repair of injured alveolar

epithelial cells in LPS-induced ARDS mice. *Stem Cell Res. Ther.* 10:74. doi: 10.1186/s13287-019-1169-1161

Zhang, Y., Li, R., Rong, W., Han, M., Cui, C., Feng, Z., et al. (2018). Therapeutic effect of hepatocyte growth factor-overexpressing bone marrow-derived mesenchymal stem cells on CCl4-induced hepatocirrhosis. *Cell Death Dis.* 9, 1–12. doi: 10.1038/s41419-018-1239-1239

Zhang, Z., Zhu, L., Feng, P., Tan, Y., Zhang, B., Gao, E., et al. (2019). C1q/tumor necrosis factor-related protein-3-engineered mesenchymal stromal cells attenuate cardiac impairment in mice with myocardial infarction. *Cell Death Dis.* 10, 1–15. doi: 10.1038/s41419-019-1760-1765

Zhao, H., Cheng, L., Du, X., Hou, Y., Liu, Y., Cui, Z., et al. (2014). Transplantation of cerebral dopamine neurotrophic factor transducted BMSCs in contusion spinal cord injury of rats: promotion of nerve regeneration by alleviating neuroinflammation. *Mol. Neurobiol.* 53, 187–199. doi: 10.1007/s12035-014-9000-9006

Zhao, L., Hu, C., Zhang, P., Jiang, H., and Chen, J. (2019). Preconditioning strategies for improving the survival rate and paracrine ability of mesenchymal stem cells in acute kidney injury. *J Cell Mol Med.* 23, 720–730. doi: 10.1111/jcmm.14035

Zhao, L., Jiang, X., Shi, J., Gao, S., Zhu, Y., Gu, T., et al. (2018). Exosomes derived from bone marrow mesenchymal stem cells overexpressing microRNA-25 protect spinal cords against transient ischemia. *J. Thorac. Cardiovasc. Surg.* 157, 508–517. doi: 10.1016/j.jtcvs.2018.07.095

Zhao, L., Liu, X., Zhang, Y., Liang, X., Ding, Y., Xu, Y., et al. (2016). Enhanced cell survival and paracrine effects of mesenchymal stem cells overexpressing hepatocyte growth factor promote cardioprotection in myocardial infarction. *Exp. Cell Res.* 344, 30–39. doi: 10.1016/j.yexcr.2016.03.024

Zhao, T., Yan, W., Xu, K., Qi, Y., Dai, X., and Shi, Z. (2013). Combined treatment with platelet-rich plasma and brain-derived neurotrophic factor-overexpressing bone marrow stromal cells supports axonal remyelination in a rat spinal cord hemi-section model. *Cytotherapy* 15, 792–804. doi: 10.1016/j.jcyt.2013.04.004

Zheng, M., Duan, J., He, Z., Wang, Z., Mu, S., Zeng, Z., et al. (2017). Transplantation of bone marrow stromal stem cells overexpressing tropomyosin receptor kinase A for peripheral nerve repair. *Cytotherapy* 19, 916–926. doi: 10.1016/j.jcyt.2017.04.007

Zheng, X. B., He, X. W., Zhang, L. J., Qin, H. B., Lin, X. T., Liu, X. H., et al. (2019). Bone marrow-derived CXCR4-overexpressing MSCs display increased homing to intestine and ameliorate colitis-associated tumorigenesis in mice. *Gastroenterol. Rep.* 7, 127–138. doi: 10.1093/gastro/goy017

Zheng, Y. B., Zhang, X. H., Huang, Z. L., Lin, C. S., Lai, J., Gu, Y. R., et al. (2012). Amniotic-fluid–derived mesenchymal stem cells overexpressing interleukin-1 receptor antagonist improve fulminant hepatic failure. *PLoS One* 7:e41392. doi: 10.1371/journal.pone.0041392

Zhou, L., Lin, Q., Wang, P., Yao, L., Leong, K., Tan, Z., et al. (2017). Enhanced neuroprotective efficacy of bone marrow mesenchymal stem cells co-overexpressing BDNF and VEGF in a rat model of cardiac arrest-induced global cerebral ischemia. *Cell Death Dis.* 8:e2774. doi: 10.1038/cddis.2017.184

Zhu, G., Pei, L., Lin, F., Yin, H., Li, X., He, W., et al. (2019). Exosomes from human-bone-marrow-derived mesenchymal stem cells protect against renal ischemia/reperfusion injury via transferring miR-199a-3p. *J. Cell. Physiol.* 234, 23736–23749. doi: 10.1002/jcp.28941

Zitvogel, L., Galluzzi, L., Kepp, O., Smyth, M. J., and Kroemer, G. (2015). Type I interferons in anticancer immunity. *Nat. Rev. Immunol.* 15, 405–414. doi: 10.1038/nri3845

Zou, D., Chen, Y., Han, Y., Lv, C., and Tu, G. (2014). Overexpression of microRNA-124 promotes the neuronal differentiation of bone marrow-derived mesenchymal stem cells. *Neural Regen. Res.* 9, 1241–1248. doi: 10.4103/1673-5374.135333

Zuo, S., Jones, W. K., Li, H., He, Z., Pasha, Z., Yang, Y., et al. (2012). Paracrine effect of Wnt11-overexpressing mesenchymal stem cells on ischemic injury. *Stem Cells Dev.* 21, 598–608. doi: 10.1089/scd

Conflict of Interest: MD and GGr hold patents in the field of cell and gene therapy and declare a consultancy role, research funding, and stock ownership with Rigenerand Srl.

The remaining authors declare that the research was conducted in the absence of any commercial or financial relationships that could be construed as a potential conflict of interest.

frontiers in Cell and Developmental Biology

BRIEF RESEARCH REPORT
published: 31 August 2020
doi: 10.3389/fcell.2020.00869

Gap Junction Dependent Cell Communication Is Modulated During Transdifferentiation of Mesenchymal Stem/Stromal Cells Towards Neuron-Like Cells

*Nadine Dilger[1], Anna-Lena Neehus[1,2], Klaudia Grieger[1], Andrea Hoffmann[3,4], Max Menssen[5] and Anaclet Ngezahayo[1,6]**

[1] Department of Cell Physiology and Biophysics, Institute of Cell Biology and Biophysics, Leibniz University Hannover, Hanover, Germany, [2] Institute of Experimental Hematology, REBIRTH Research Center for Translational and Regenerative Medicine, Hannover Medical School (MHH), Hanover, Germany, [3] Graded Implants and Regenerative Strategies, Department of Orthopedic Surgery, Hannover Medical School, Hanover, Germany, [4] Lower Saxony Centre for Biomedical Engineering, Implant Research and Development (NIFE), Hanover, Germany, [5] Department of Biostatistics, Institute of Cell Biology and Biophysics, Leibniz University Hannover, Hanover, Germany, [6] Center for Systems Neuroscience, University of Veterinary Medicine Hannover, Hanover, Germany

In vitro transdifferentiation of patient-derived mesenchymal stem/stromal cells (MSCs) into neurons is of special interest for treatment of neurodegenerative diseases. Although there are encouraging studies, little is known about physiological modulations during this transdifferentiation process. Here, we focus on the analysis of gap junction dependent cell-cell communication and the expression pattern of gap junction-building connexins during small molecule-induced neuronal transdifferentiation of human bone marrow-derived MSCs. During this process, the MSC markers CD73, CD90, CD105, and CD166 were downregulated while the neuronal marker Tuj1 was upregulated. Moreover, the differentiation protocol used in the present study changed the cellular morphology and physiology. The MSCs evolved from a fibroblastoid morphology towards a neuronal shape with round cell bodies and neurite-like processes. Moreover, depolarization evoked action potentials in the transdifferentiated cells. MSCs expressed mRNAs encoding Cx43 and Cx45 as well as trace levels of Cx26, Cx37- and Cx40 and allowed transfer of microinjected Lucifer yellow. The differentiation protocol increased levels of Cx26 (mRNA and protein) and decreased Cx43 (mRNA and protein) while reducing the dye transfer. Cx36 mRNA was nearly undetectable in all cells regardless of treatment. Treatment of the cells with the gap junction coupling inhibitor carbenoxolone (CBX) only modestly altered connexin mRNA levels and had little effect on neuronal differentiation. Our study indicates that the small molecule-based differentiation protocol generates immature neuron-like cells from MSCs. This might be potentially interesting for elucidating physiological modifications and mechanisms in MSCs during the initial steps of differentiation towards a neuronal lineage.

Keywords: mesenchymal stem/stromal cells, transdifferentiation, neuron, small molecules, gap junctions, connexins, human

OPEN ACCESS

Edited by:
Marcela F. Bolontrade, Consejo Nacional de Investigaciones Científicas y Técnicas (CONICET), Argentina

Reviewed by:
Aida Salameh, Leipzig University, Germany
Eric C. Beyer, The University of Chicago, United States

****Correspondence:***
Anaclet Ngezahayo
ngezahayo@cell.uni-hannover.de

Specialty section:
This article was submitted to Stem Cell Research, a section of the journal Frontiers in Cell and Developmental Biology

Received: *27 February 2020*
Accepted: *11 August 2020*
Published: *31 August 2020*

Citation:
Dilger N, Neehus A-L, Grieger K, Hoffmann A, Menssen M and Ngezahayo A (2020) Gap Junction Dependent Cell Communication Is Modulated During Transdifferentiation of Mesenchymal Stem/Stromal Cells Towards Neuron-Like Cells. Front. Cell Dev. Biol. 8:869. doi: 10.3389/fcell.2020.00869

INTRODUCTION

Mesenchymal stem/stromal cells (MSCs) are multipotent adult stem cells with the ability to self-renew and to differentiate into osteoblasts, chondrocytes and adipocytes *in vivo* (Berry et al., 1992; Herbertson and Aubin, 1997; Kuznetsov et al., 1997). They can be cultivated for multiple passages. Besides their natural differentiation potential, they can artificially be transdifferentiated into cells of other lineages like cardiomyocytes (Kawada et al., 2004; Huang et al., 2015; Shi et al., 2016) or neuronal cells (Ma et al., 2011; Feng et al., 2014; Qin et al., 2015; Hwang et al., 2017). Therefore, MSCs are thought to open new perspectives for regenerative medicine, as it may be possible to regenerate diverse cell types of the human body from patient-derived MSCs (Phinney and Prockop, 2007; Mollinari et al., 2018).

Neurons are post-mitotic cells that cannot be donated by healthy persons. Therefore, transdifferentiation of neurons from patient-derived cells could be an option in treatment of neurodegenerative diseases. Concerning clinical applications, the usage of small molecules offers perspectives of converting without genetically modifying cells and therefore lower the patients' risk (Qin et al., 2017). Regarding basic research, transdifferentiation offers possibilities to gain more insights into physiological modifications during cell differentiation.

Gap junction mediated cell-cell communication is known to be modulated during neuronal differentiation. Gap junctions are intercellular channels which can assemble to gap junction plaques. They directly connect the cytoplasm of adjacent cells, thus permitting a bidirectional exchange of molecules up to 1–2 kDa like ions, metabolites or second messengers (Söhl and Willecke, 2004; Goodenough and Paul, 2009). Gap junction mediated cell-cell communication thereby allows the progression of electrical and chemical signals in a tissue and has an important impact on physiology, growth and differentiation of cells (Söhl et al., 2005). Gap junctions are composed of oligomerized integral membrane proteins called connexins (Cx), of which 21 isoforms have been identified in humans. The connexin expression pattern is tissue specific and is regulated during cell differentiation (Nielsen et al., 2012).

MSCs are extensively gap junction-coupled and mainly express Cx43, as well as Cx40 and Cx45 (Dorshkind et al., 1993; Bodi et al., 2004; Valiunas et al., 2004). Neurons are also coupled by gap junctions (Lo Turco and Kriegstein, 1991; Bittman et al., 1997) which are mainly composed of the connexins Cx26, Cx30.2, Cx45 and particularly Cx36 (Leung et al., 2002; Kreuzberg et al., 2008; Eugenin et al., 2012; Su et al., 2017). Amongst these, Cx36 is the most prominent neuronal connexin in adult electrical synapses and plays important roles in the developing brain (Belluardo et al., 2000; Condorelli et al., 2000). Gap junction mediated cell-cell communication seems to be essential for neurogenesis, during which the expressed connexin isoforms change (Bosone et al., 2016; Swayne and Bennett, 2016). Along their differentiation, neural progenitor cells need to down-regulate multiple connexin isoforms, especially that of Cx43 and become less gap junction-coupled (Rozental et al., 2000; Rinaldi et al., 2014).

In this report we used small molecule-based transdifferentiation protocols defined by Bi et al. (2010) and Aguilera-Castrejon et al. (2017) to induce the conversion of human bone marrow-derived MSCs into neuronal cells. Analyzing the gap junction coupling during the transdifferentiation process validated that the induced cells are suitable to study physiological modulations in MSCs overcoming mesenchymal cell fate.

MATERIALS AND METHODS

Cell Culture

Human bone marrow-derived MSCs from a healthy female donor were isolated and cultured as described by Jungwirth et al. (2018).

Neuronal Induction of MSCs

MSCs were grown in cell culture plates or seeded onto collagen I-coated glass coverslips and cultivated until they reached a confluency of 70%. Differentiation was induced with differentiation media developed by Bi et al. (2010) and Aguilera-Castrejon et al. (2017) (**Supplementary Table 1**).

The protocol of Bi et al. (2010), further referred to as NIM-1 protocol, describes a pre-induction of MSCs in MSC medium with 1 μM retinoic acid (RA) for 24 h after which the neural differentiation was induced with a neural induction medium (NIM-1) for additional 24 h.

Following the protocol of Aguilera-Castrejon et al. (2017), MSCs were cultivated in a neural induction medium (NIM-2) for 7 days (referred to as 7d NIM-2 protocol). Additionally, the incubation time in NIM-2 was prolonged to 30 days (named 30 d NIM-2 protocol). Before further electrophysiological experiments, cells derived from the 30 d NIM-2 protocol were transferred into a maturation medium (MAT; Hu et al., 2015) for 24 h (referred to as 30 d NIM-2 1d protocol).

Protein and RNA isolation, immunocytochemical staining and physiological analysis were performed after each protocol.

Quantitative Real-Time PCR

Quantitative real-time PCR (qRT-PCR) was used to quantify mRNA expression of MSC and neuronal markers as well as different connexin isoforms. Undifferentiated MSCs were used as control. RNA was isolated using the PeqGOLD Total RNA kit (Peqlab). Thereafter, RNA was reverse transcribed into cDNA using the Maxima First Strand cDNA synthesis kit (Thermo Fisher Scientific, Waltham, MA, United States). 12.5 ng of cDNA were used as template for the qRT-PCR which was performed with the KAPA SYBR FAST Universal mastermix (Kapa Biosystems) in a volume of 10 μL. All primer data are given in **Supplementary Table 3**. Correct amplification was confirmed by sequencing. For each sample and primer pair three technical replicates were analyzed. Each qRT-PCR was run at least three times with cDNA of independent differentiations. The mRNA level of the gene of interest relative to the housekeeping gene *RPS29* was calculated by $2^{-\Delta Ct}$ method.

Immunocytochemistry

The cells were washed with PBS, fixed with 4% formaldehyde or ice-cold acetone/methanol (1:1) and permeabilized and blocked simultaneously in 0.1% Triton X-100 and 1% BSA in PBS. The cells were incubated overnight at 4°C in primary antibody solutions of anti-Cx26 (1:1,000, MABT198, Merck Millipore), anti-Cx43 (1:4,000, C6219, Sigma-Aldrich), anti-Cx45 (1:50, 5C7G1, Thermo Fisher Scientific), anti-Tuj1 (1:1000, 2G10, ab78078, Abcam), anti-Nestin (1:200, SP103, ab105389, Abcam), anti-Map2 (1:50, 4542, Cell Signaling Technology) and anti-NeuN (1:100, A60, MAB377, Merck Millipore). The secondary iFluor^{TM}488-conjugated anti-mouse (1:500, 16448, AAT Bioquest) and anti-rabbit antibodies (1:500, 16608, AAT Bioquest) together with 2 μM DAPI (Sigma-Aldrich) were added to the cells for 1 h at 37°C. The cells were imaged with a Nikon Eclipse TE2000-E C1 confocal laser-scanning microscope (Nikon GmbH).

Western Blot

Total protein of the cells was isolated and the protein concentration was estimated using a Bradford assay (Sigma-Aldrich). 20 μg of total protein were separated by SDS-PAGE and transferred onto a nitrocellulose membrane using semi-dry transfer. Therafter, the membrane was blocked in 5% non-fat dry milk powder in PBS containing 0.1% Tween 20 (PBS-T). Primary antibody incubation was performed overnight at 4°C. The primary antibodies anti-β-tubulin (1:2,000, T4026, Sigma-Aldrich), anti-GAPDH (1:100,000, ab181602, Abcam), anti-Cx43 (1:7,500, C6219, Sigma-Aldrich), anti-Cx26 (1:1,000, MABT198, Merck Millipore), anti-Cx45 (1:500, 5C7G1, Thermo Fisher Scientific), anti-Tuj1 (1:2,000, ab78078, Abcam) and anti-NeuN (1:200, MAB377, Merck Millipore) were diluted in PBS-T. Depending on the molecular weight of the target proteins, either GAPDH or β-tubulin was used as internal standard. The following day, the secondary anti-rabbit antibody (A9169, Sigma-Aldrich), diluted in PBS-T (1:40,000), was added to the membrane for 1 h at room temperature, followed by the secondary anti-mouse antibody (A9044, Sigma-Aldrich), diluted 1:40,000 in PBS-T for another 1 h incubation at room temperature. The membrane was imaged with ECL substrate. The western blot experiments were performed four times and analyzed with the gel analyzer tool of Fiji (Schindelin et al., 2012). The measured band intensities were first normalized to the loading control (GAPDH or β-tubulin) and secondly to the undifferentiated MSC samples.

Dye Transfer Experiments

Gap junction coupling was analyzed by dye transfer experiments with Lucifer Yellow (LY) lithium salt (Biotium). Cells grown on coverslips were transferred into a perfusion chamber filled with 500 μL of a bath solution (140 mM NaCl, 5 mM KCl, 10 mM HEPES, 1 mM $MgCl_2$, 10 mM glucose, 2 mM $CaCl_2$ at pH 7.4 and 295 mosmol/L). A whole-cell patch-clamp configuration was established onto the central cell of the observed area using an EPC 10 USB double patch-clamp amplifier (HEKA). The patch pipette was filled with a LY (1 mg/mL)-containing pipette solution (145 mM K-gluconate, 5 mM KCl, 10 mM HEPES, 2.5 mM MgATP, 5 mM glucose, 0.5 mM Na_2ATP, 1 mM EGTA, 0.5 mM $CaCl_2$ at pH 7.4 and 295 mosmol/L). The dye was allowed to diffuse into the patched cell for 10 min before the pipette was removed. LY was excited at 410 nm. For each experiment, fluorescence images were captured before establishing the whole-cell patch-clamp configuration, during the experiment and after removal of the pipette. The micrographs were analyzed using Fiji (Schindelin et al., 2012). Images taken before the experiment were subtracted from images captured after pipette removal. To quantify cell coupling, the integrated density of the fluorescence signal was measured in all cells except for the patched cell and then normalized to the integrated density of the patched cell. This ratio will further be referred to as LY dye coupling rate.

Electrophysiology

The whole-cell configuration was established onto a cell using the same setup and conditions as described above for dye transfer experiments. The bath and pipette solutions were identical except for LY lacking in the pipette solution. Patch pipettes showed electrical resistances of 4–6 MΩ. Cells were clamped to −60 mV and action potentials were induced in current-clamp mode by injecting depolarizing currents.

Statistical Analysis

All statistical analyses were run using R and linear models were fit by the lm() function (R Core Team, 2019). Model based least-square means were compared using the emmeans package version 1.3.4 (Lenth, 2019) with $\alpha = 0.05$. All data sets and corresponding R-code are available under https://github.com/MaxMenssen/Dilger_et_al_2020.

Analyzing the qRT-PCR data, $2^{-\Delta Ct}$ values were ln-transformed and modeled based on runs and treatments separately for each gene of interest. Least-square means were compared between the control group and further treatments.

$2^{-\Delta Ct}$ values for the CBX data were split by genes of interest. For each gene, ln-transformed $2^{-\Delta Ct}$ values were modeled based on run, treatments, CBX concentrations and the interaction between treatments and concentrations. Comparisons of means were run such that means were compared against MSC without CBX and against 7 d NIM-2 without CBX.

Western blot data was split by proteins. Normalized protein expression was ln-transformed and modeled depending on runs and treatments. Since normalization set control values to one, the treatment means were tested to be significantly different from one.

For the dye transfer data, the minimum coupling rate was added to all coupling rates and was ln-transformed and modeled based on different treatments. Subsequently, mean comparisons between control and treatments were run.

RESULTS

The goal of this study was to analyze the connexin expression and gap junction mediated cell-cell communication during

transdifferentiation of MSCs into neuronal cells. MSCs from human bone marrow proliferated and formed an adherent monolayer of cells with fibroblast-like morphology (**Figure 1A**). We used the protocols NIM-1, 7 d NIM-2, 30 d NIM-2 and 30 d NIM-2 1 d MAT, based on the publications of Bi et al. (2010) and Aguilera-Castrejon et al. (2017), to develop MSCs into neuronal cells.

Following the conversion of the MSCs into neuron-like cells, we analyzed changes in cell morphology and expression level of the MSC markers CD73 (*NT5E*), CD90 (*THY1*), CD105 (*ENG*) and CD166 (*ALCAM*), the neuronal stem cell marker Nestin (*NES*), the neuronal markers Tuj1 (*TUBB3*), NeuN (*RBFOX3*) and MAP-2 (*MAP2*) and the transcription factors Brn-2 (*POU3F2*), SOX-2 (*SOX2*) and MyT1-L (*MYT1L*) (**Figure 1**, for gene/protein equivalents also see **Supplementary Table 2**).

The applied transdifferentiation protocols reduced proliferation and induced a morphological development from fibroblast-like cells to cells with round cell bodies and long cell processes (**Figures 1A,D**). At mRNA level, the MSCs expressed *NT5E*, *THY1*, *ENG* and *ALCAM* as well as *NES* and *TUBB3*. The NIM-1 protocol down-regulated *NT5E*, *THY1*, and *ALCAM*, while *MAP2* was upregulated. Differentiating the MSCs with the NIM-2 protocols reduced the mRNA levels of *NT5E*, *THY1*, *ENG*, *ALCAM*, *NES*, *MAP2* and *POU3F2*. The induction with the 30 d NIM-2 and 30 d NIM-2 1 d MAT protocols reinforced the down-regulation of *THY1* and *ALCAM* (**Figure 1B**). The muscle specific markers *ACTA2*, *TAGLN*, *MYL2* and *SMYD1* were not upregulated at mRNA level during differentiation.

At protein level, the expression of Nestin, MAP-2, Tuj1 and NeuN was analyzed by Western blotting and immunocytochemical staining (**Figures 1C,D**). Immunocytochemistry revealed no expression of Nestin, MAP-2 and NeuN in MSCs which was not altered by the NIM-2 differentiation protocols. Only the NIM-1 protocol resulted in slightly increased expression of NeuN, which was mainly located in the nucleus, and of Nestin. Tuj1 was detectable in MSCs, while the differentiation protocols 7 d NIM-2, 30 d NIM-2 as well as 30 d NIM-2 1 d MAT increased the Tuj1 signal after differentiation (**Figure 1D**). To quantify the protein expression, Western blotting experiments were performed of the most unambiguously expressed neuronal marker Tuj1, which is a marker for immature neurons. For comparison, NeuN, a marker for mature neurons, was also analyzed by Western blotting experiments. The expression of Tuj1 in MSCs and its upregulation by the differentiation procedures were confirmed (**Figure 1C**). NeuN was barely detectable in MSCs via Western blot but a basal expression was measurable. This was not the case when the cells were differentiated by NIM-2 which down-regulated NeuN. Only the NIM-1 protocol had an inducing effect on NeuN although the samples were heterogeneous in their expression level (**Figure 1C**).

To further characterize the differentiation of the MSCs into neuron-like cells, electrophysiological measurements were performed. MSCs differentiated by the 30 d NIM-2 1 d MAT protocol showed resting membrane potentials of −60 mV and responded to the injection of depolarizing currents by firing action potentials. The action potentials were scarcely overshooting and the cells did not sufficiently repolarize to allow repetitive action potentials during the depolarization interval (**Figure 2A**).

Gap junctions are known to have an impact on cell differentiation and are essential for electrical synapses in neuronal networks. We therefore analyzed the influence of the gap junction dependent cell-to-cell communication during the neuronal transdifferentiation of MSCs into neuron-like cells.

MSCs were coupled by gap junctions as LY was able to diffuse into numerous neighboring cells during dye transfer experiments. The differentiation protocols 7 d NIM-2, 30 d NIM-2 and 30 d NIM-2 1 d MAT reduced the capability of dye transfer, whereas it was not affected by the NIM-1 protocol (**Figures 2B,C**). Although time-dependent effects cannot be completely excluded, the results suggest an effect on gap junction coupling.

In order to identify the expressed connexins forming the gap junctions, qRT-PCR and Western blotting experiments were performed as well as immunocytochemistry staining of the most prominent connexins (**Figure 3**). In MSCs the qRT-PCR results revealed strong expression of *GJA1* (Cx43), while *GJC1* (Cx45) was less present. Even weaker expressed were *GJA4* (Cx37), *GJA5* (Cx40) and *GJB2* (Cx26). *GJD2* (Cx36) was barely detectable. The NIM-1 protocol down-regulated *GJA1* and *GJC1* but did not affect the other connexin isoforms. The differentiation with the NIM-2 protocols down-regulated *GJA4*, *GJA5*, *GJA1* and *GJC1* whereas the *GJB2* expression was up-regulated. The mRNA level of *GJD2* was not affected by any of the applied protocols (**Figure 3A**).

The results of the qRT-PCR analysis of *GJB2*, *GJA1* and *GJC1* were re-examined at protein level. In contrast to the qRT-PCR results, Cx45 was barely detectable in MSCs by Western blot and its expression did not change after treatment with the NIM-1 or NIM-2 protocols. On the other hand, Cx43 was clearly detectable and appeared to be strongly expressed in MSCs and NIM-1-induced cells. After differentiation with NIM-2 protocols the Cx43 expression was reduced compared to MSCs. Cx26, which was the only up-regulated connexin at mRNA level after differentiation, was barely detectable in MSCs and NIM-1-differentiated cells by Western blot, but upregulated after NIM-2 differentiation (**Figure 3B**). Immunocytochemistry staining of these connexins confirmed the Western blotting results showing cell membrane associated staining and gap junction plaque formation (**Figure 3C**).

Different carbenoxolone (CBX) concentrations were added to NIM-2 during the 7 days differentiation to test whether gap junction blocking has an effect on the differentiation progress. In parallel, we added the identical concentrations of CBX to the MSC growth medium for 7 days as control. The gap junction inhibitor CBX did not influence the morphology of control MSCs nor the morphological changes induced by the 7 d NIM-2 protocol (data not shown). qRT-PCR experiments showed that *THY1*, *ENG*, *TUBB3*, *MAP2* and *POU3F2* were slightly reduced by addition of CBX in MSCs, while *NT5E*, *THY1*, *NES*, *TUBB3*, *MAP2*, *POU3F2* and *MYT1L* were altered in 7 d NIM-2-differentiated cells (**Figure 4A**). Concerning

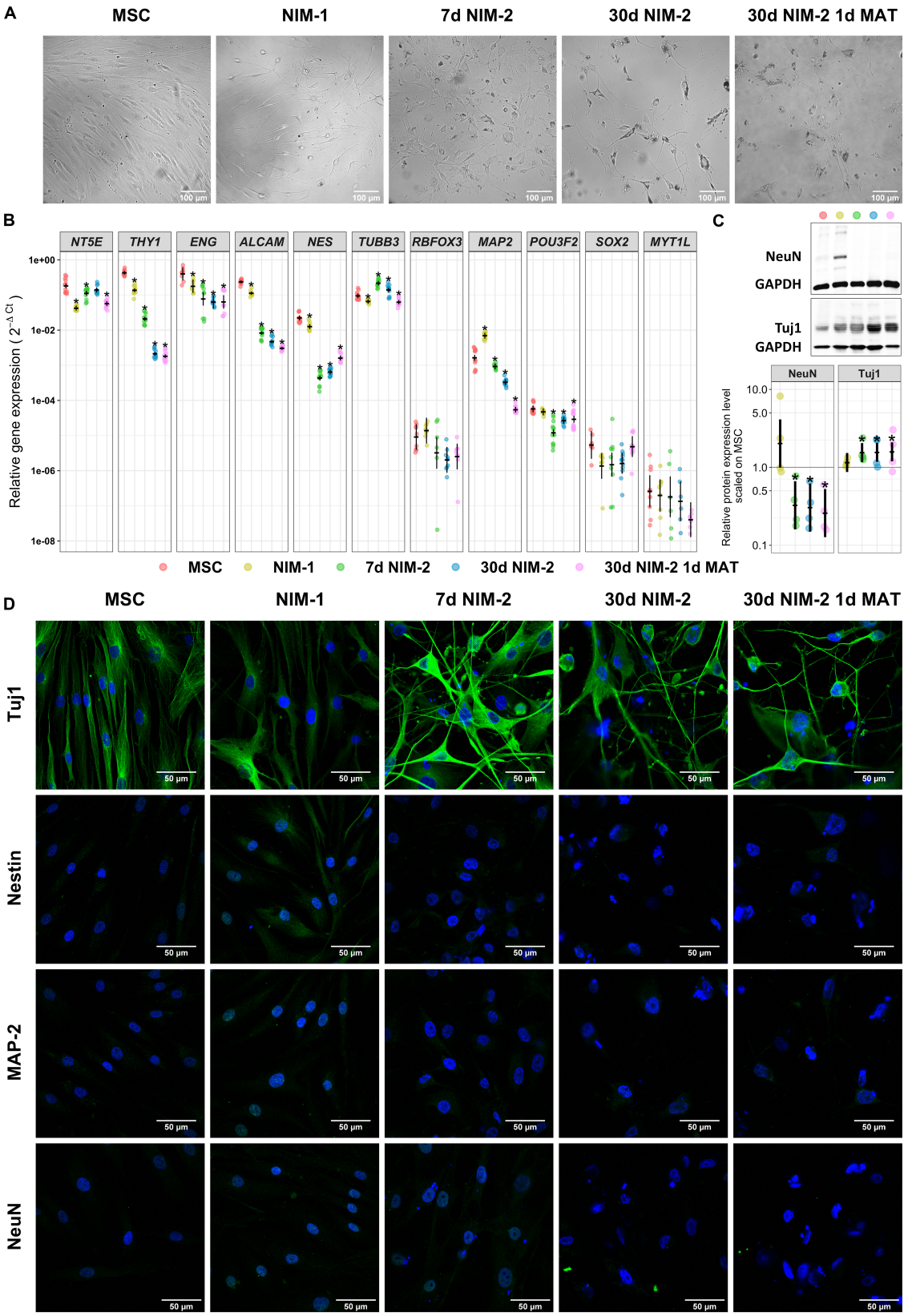

FIGURE 1 | Continued

FIGURE 1 | Transdifferentiation of MSCs into neuron-like cells. **(A)** Bright-field images of MSCs before and after the differentiation procedures. Note the morphology changes of the cells into cells with round cell bodies and long cell processes. The scale bars represent 100 μm. **(B)** Gene expression analysis of MSC markers (*NT5E*, *THY1*, *ENG*, *ALCAM*) and neuronal markers (*NES*, *TUBB3*, *RBFOX3*, *MAP2*, *POU3F2*, *SOX2*, *MYT1L*) by qRT-PCR. **(C)** Western blotting of the neuronal markers Tuj1 and NeuN. Exemplary blots are shown in the upper panel. A quantitative analysis normalized to GAPDH and control MSCs is shown in the lower panel. **(D)** Immunocytochemistry staining of the neuronal markers Tuj1, Nestin, MAP2 and NeuN in MSCs and the differentiated cells. The protein of interest is visualized by secondary antibodies labeled with iFluor^{TM}488 (green) while the nuclei are stained with DAPI (blue). The scale bars represent 50 μm in panels **(B,C)** (lower panel) the original data points are plotted in colorful dots. The horizontal lines indicate model-based least-square means together with their 95%-confidence intervals (vertical lines). The * marks significant mean differences ($\alpha = 0.05$) between MSCs and the differentiated cells.

the connexin expression, *GJB2*, *GJA1* and *GJC1* were the connexins affected by CBX presence during 7 d NIM-2-induced transdifferentiation (**Figure 4B**).

DISCUSSION

In this study, gap junction mediated cell communication was studied during neuronal differentiation by analyzing the expression pattern of connexin isoforms and performing dye transfer experiments to study the functionality of the formed gap junction channels. To induce a neuronal transdifferentiation of human bone marrow-derived MSCs, we used and adjusted the small-molecule based NIM-1 and NIM-2 protocols by Bi et al. (2010) and Aguilera-Castrejon et al. (2017), who discussed the impact of the applied small molecules in detail, whereby the effects of single small molecules vary with concentration and composition (Qin et al., 2017). Analyzing the resulting morphological development, changes in the expression pattern of neuronal markers as well as action potential measurements of the developed cells allowed a characterization of the induced neuron-like cells.

All tested protocols were able to stop cell proliferation and induced a morphological development of MSCs towards neuron-like cell shapes with round cell bodies and long neurite-like processes. Similar morphological changes were observed when neuronal cells were induced either by transfection with neuronal lineage transcription factors (Vierbuchen et al., 2010; Pang et al., 2011) or by small molecules (Bi et al., 2010; Alexanian et al., 2013; Aguilera-Castrejon et al., 2017) and therefore represent a first indication for neuronal differentiation. Moreover, we found that the expression of typical MSC markers was reduced, which suggests a loss of mesenchymal stem cell properties and ongoing differentiation. The multi-lineage progenitor cell marker *NES* was down-regulated in NIM-2-differentiated cells while its level was not altered in NIM-1-differentiated cells. As the Nestin expression is down-regulated when neuronal stem cells stop proliferating and enter the neuronal differentiation (Zhang and Jiao, 2015) it could be possible that NIM-2-induced cells were further developed than the NIM-1-differentiated cells which more resembled neural progenitor cells. Underlining this assumption, the differentiation with the NIM-2 protocols up-regulated the immature neuronal marker Tuj1 at both mRNA (*TUBB3*) and protein level while the NIM-1 protocol did not change its expression. Although *MAP2* was increased at mRNA level after NIM-1 differentiation it could not be detected at protein level. Generally, the effects of the induction with NIM-2 were reinforced when the differentiation time was extended to 30 days. The maturation did not perceivably alter the marker expression pattern of the differentiated cells but stabilized the cells and enabled a stable whole-cell patch-clamp configuration to perform electrophysiological measurements and induce action potentials. These action potentials lasted longer than expected from neurons (Hodgkin and Huxley, 1952; Jiang et al., 2015) and were neither strongly overshooting nor repetitive. They more resembled action potentials measured in immature neurons (Ma et al., 2011; Connor et al., 2018), smooth muscle cells or cardiomyocytes (Voitychuk et al., 2012; Manchanda et al., 2019). However, a myogenic differentiation was considered unlikely as muscle specific markers were not upregulated at mRNA level (**Supplementary Figure 1**). Taken together, our data indicate an appreciable degree of neuronal differentiation as shown before by Bi et al. (2010) and Aguilera-Castrejon et al. (2017). The cells appear further developed than neuronal stem or progenitor cells although they do not show the characteristics of fully mature neurons. These induced cells therefore offered the possibility for further developmental studies of connexin expression and gap junction coupling in MSCs overcoming the mesenchymal cell fate.

Dye transfer experiments revealed that undifferentiated MSCs were well gap junction-coupled, which is consistent with the findings of other authors who showed extensive gap junction coupling in MSCs (Dorshkind et al., 1993; Valiunas et al., 2004). Although neurons are also coupled by gap junctions (Gutnick and Prince, 1981; Noctor et al., 2001) we saw a significant reduction of the LY dye coupling rate in NIM-2-differentiated cells suggesting a reduction in the number of gap junction channels what has already been observed in neurons (Eugenin et al., 2012). The gap junction coupling rate of the NIM-1-induced neural progenitor-like cells was not altered compared to the control MSCs. This finding is consistent with the conception that gap junction coupling is abundant and essential for neuronal stem and progenitor cells (Duval et al., 2002) as gap junction coupling is a crucial element for cell survival and the maintenance of the self-renewal state of stem cells (Cheng et al., 2004; Todorova et al., 2008).

Cx43, Cx40 and Cx45 play the major role in the gap junction coupling capabilities of MSCs (Bodi et al., 2004; Valiunas et al., 2004). We expected that the differentiation of MSCs into neuron-like cells would down-regulate mesenchymal connexins like Cx43, Cx40 and Cx37 while up-regulating neuronal connexins like Cx26, Cx45 and especially Cx36 (Rozental et al., 2000; Söhl et al., 2005; Eugenin et al., 2012; Su et al., 2017). Our analysis of connexin expression in the transdifferentiated neuron-like cells showed a significant

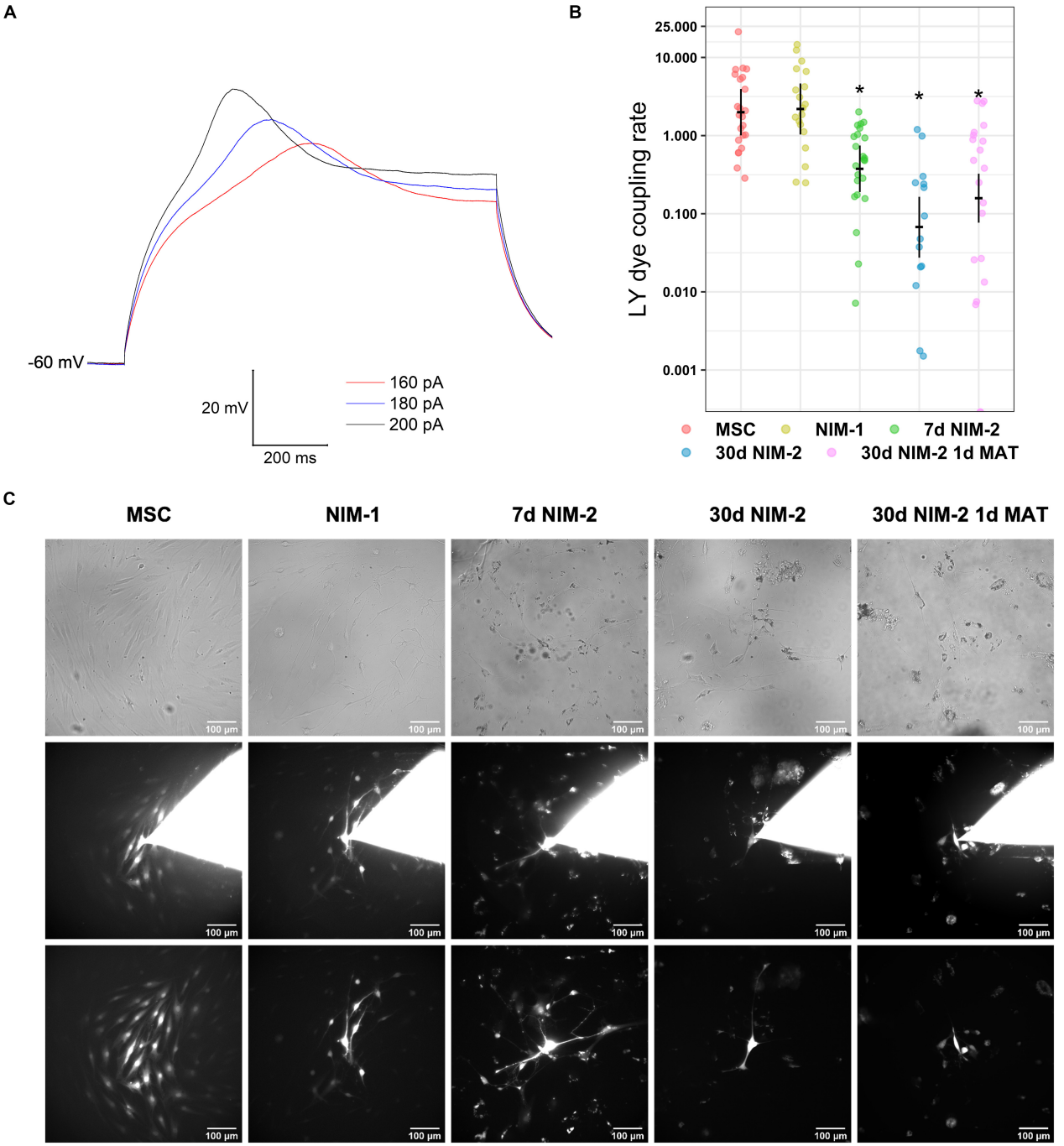

FIGURE 2 | Electrophysiological properties and gap junction coupling in differentiated MSCs. **(A)** Membrane potential recordings in a 30 d NIM-2 1 d MAT-differentiated cell measured in the whole-cell patch-clamp configuration. Action potentials were evoked by the injection of depolarizing currents of 160–200 pA. **(B)** Quantification of the dye transfer experiments. The original data points are plotted in colorful dots. The horizontal lines indicate model-based least-square means together with their 95%-confidence intervals (vertical lines). The * marks significant mean differences ($\alpha = 0.05$) between MSCs and the differentiated cells. **(C)** Exemplary micrographs of LY dye transfer experiments. Phase contrast images captured before the experiment are shown in the first row. The second row shows the cells during the dye transfer experiment with the patch pipette still attached onto the cell. In the third row, micrographs of the dye transfer experiment are displayed, which were captured after removing the patch pipette to evaluate the degree of gap junction coupling. The scale bars indicate 100 µm.

down-regulation of the mesenchymal connexins Cx43, Cx40 and Cx37 and an upregulation of Cx26, th ereby confirming our expectations. These changes in the connexin expression pattern correlated with a reduction of the gap junction coupling rate showing that the upregulation of Cx26 alone was not sufficient to maintain a high gap junction coupling rate. The

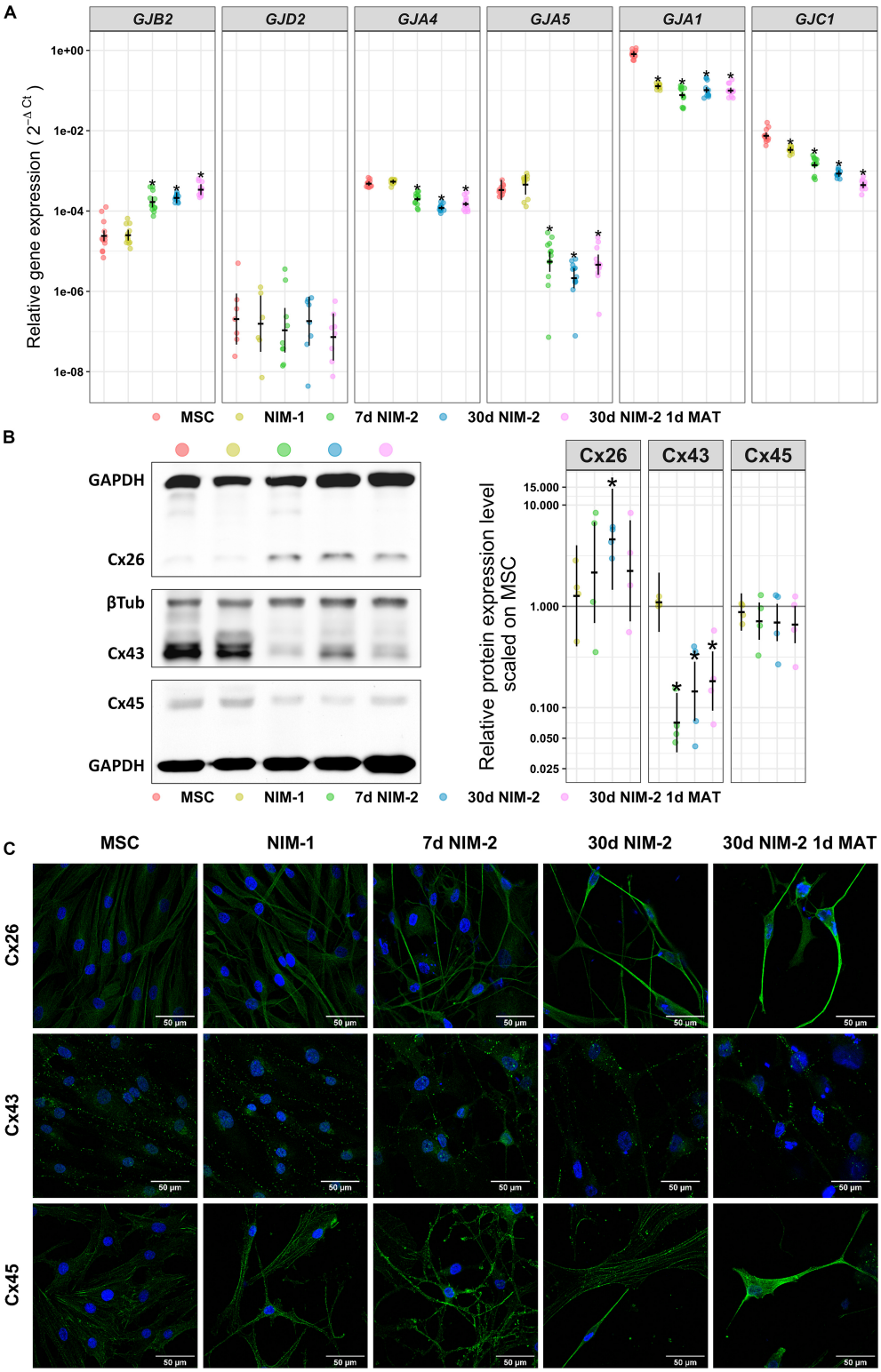

FIGURE 3 | Connexin expression in MSCs and NIM-1- and NIM-2-differentiated cells. **(A)** qRT-PCR analysis of *GJB2, GJA4*, *GJA5*, *GJA1*, and *GJC1* as well as neuronal *GJD2*. **(B)** Western blot analysis of the connexin expression in MSCs and differentiated cells. Exemplary blots are shown on the left and its quantification on the right. **(C)** Immunocytochemistry staining of Cx26, Cx43 and Cx45 (green) and the nuclei (DAPI, blue). The scale bars represent 50 µm. In panels **(A,B)** (right panel) the original data points are plotted in colorful dots. The horizontal lines indicate model-based least-square means together with their 95%-confidence intervals (vertical lines). The * marks significant mean differences ($\alpha = 0.05$) between MSCs and the differentiated cells.

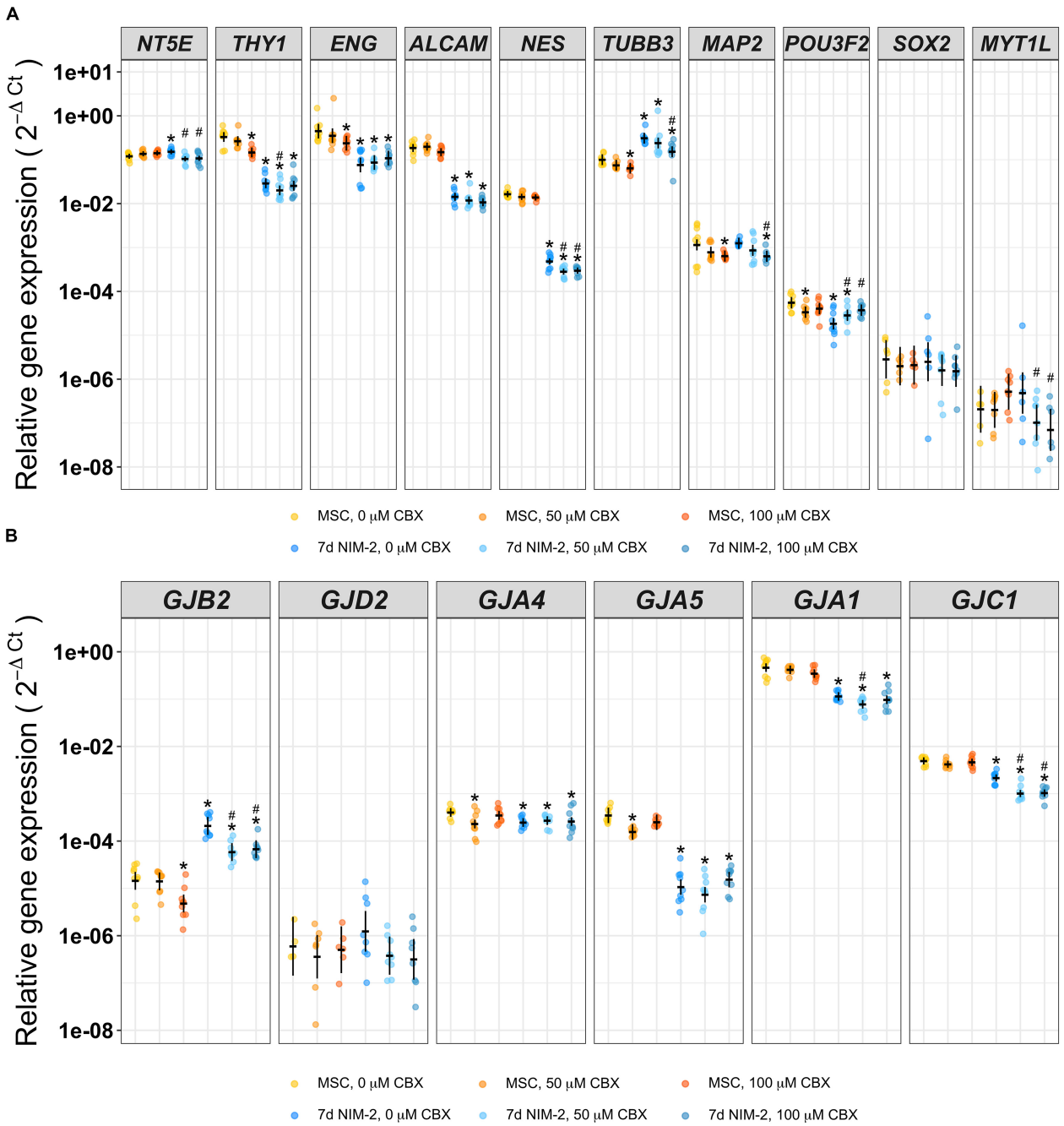

FIGURE 4 | Differentiation of MSCs in presence of the gap junction inhibitor CBX. mRNA of MSCs supplemented with 0 μM, 50 μM or 100 μM CBX for 7 days and of 7 d NIM-2-treated MSCs supplemented with identical concentrations of CBX was analyzed by qRT-PCR. The original data points are plotted in colorful dots. The horizontal lines indicate model-based least-square means together with their 95%-confidence intervals (vertical lines). The * marks significant mean differences ($\alpha = 0.05$) between MSC 0 μM and the other treatments while the # marks significant mean differences ($\alpha = 0.05$) of 7 d NIM-2 in presence of 50 μM CBX and 7 d NIM-2 in presence of 100 μM CBX compared to 7 d NIM-2 in presence of 20 μM CBX. **(A)** qRT-PCR analysis of MSC and neuronal markers. **(B)** qRT-PCR analysis of *GJB2, GJA4*, *GJA5*, *GJA1*, *GJC1* and *GJD2*.

presence of Cx26 *in vivo* is essential for a proper neuronal development, synapse formation in the neocortex and animal behavior (Su et al., 2017) and could be considered as another indicator for neuronal development of the MSCs. Cx36 is predominantly found in neurons. It has important roles in synapse activities and in the developing brain (Condorelli et al., 2000; Gulisano et al., 2000). Its presence would therefore be expected in fully developed neurons but was

not found after transdifferentiation, indicating an incomplete differentiation. For Cx43 it has been shown that its extensive expression in human neural progenitor cells (Rozental et al., 2000) promoted growth factor dependent proliferation and repressed neural differentiation (Lemcke and Kuznetsov, 2013). To promote neuronal differentiation Cx43 has to be down-regulated (Rinaldi et al., 2014) and an uncoupling of the neural progenitor cells has to take place (Rozental et al., 2000). We could measure a significant decrease of Cx43 level although it was still stronger expressed than the other analyzed connexins after differentiation. Despite incomplete down-regulation of mesenchymal connexins, the reduction of gap junction coupling could indicate a differentiation progress towards a neuronal fate, since the suppression of gap junction coupling is described as prerequisite for exiting the cell cycle and inducing differentiation (Rozental et al., 2000; Lemcke and Kuznetsov, 2013; Lemcke et al., 2013; Rinaldi et al., 2014). As the unspecific gap junction inhibitor CBX, which is known to efficiently and rapidly close gap junction channels, did not accelerate the NIM-2-induced differentiation, it seems that the reduction of gap junction coupling might be necessary for complete neuronal development but was no promoting signal for the induction of differentiation.

CONCLUSION

We could show an electrophysiological excitability of neuronal-like cells derived by a small molecule-based conversion of human MSCs into cells of neuronal lineage. MSC markers were down-regulated and the neuronal marker Tuj1 was up-regulated during differentiation while the cells developed a neuron-like morphology and, more importantly, physiological and functional properties of early neuronal cells. The connexin expression was modulated during differentiation while the gap junction coupling of the induced neuronal cells was almost entirely suppressed. This reduction of gap junction coupling is a prerequisite for neuronal differentiation but appears to be no driving mechanism itself. The here presented transdifferentiation approach towards neuron-like cells, however, revealed severe limitations both in phenotypic (gene and protein expressions) and in functional abilities of the cells. In the future, apart from small molecules, transcription factor-based reprogramming might be pursued as a more efficient and stable alternative.

DATA AVAILABILITY STATEMENT

All datasets generated for this study are included in the article/**Supplementary Material**. Additionally, all datasets and corresponding R-code are available under https://github.com/MaxMenssen/Dilger_et_al_2020.

ETHICS STATEMENT

The studies involving MSCs isolated from bone marrow of a human donor were reviewed and approved by the Ethics committee of Hannover Medical School. The donor provided written informed consent to donate tissue.

AUTHOR CONTRIBUTIONS

ND and AN designed the research and wrote the manuscript. ND, A-LN, and KG performed and analyzed the experiments. AH isolated and provided the MSCs. A-LN, KG, AH, and MM contributed to the data interpretation and revised the manuscript. MM was responsible for the data processing, as well as the statistical analysis. The manuscript was proofread by all authors. All authors contributed to the article and approved the submitted version.

FUNDING

This study was supported by the German Research Foundation (HO 2058/10-1 to AH and NG 4/10-1 to AN; AOBJ: 606578).

ACKNOWLEDGMENTS

The publication of this article was funded by the Open Access Fund of Leibniz Universität Hannover. We thank the reviewers for working on the manuscript and their helpful comments.

SUPPLEMENTARY MATERIAL

The Supplementary Material for this article can be found online at: https://www.frontiersin.org/articles/10.3389/fcell.2020.00869/full#supplementary-material

REFERENCES

Aguilera-Castrejon, A., Pasantes-Morales, H., Montesinos, J. J., Cortés-Medina, L. V., Castro-Manrreza, M. E., Mayani, H., et al. (2017). Improved Proliferative Capacity of NP-Like Cells Derived from Human Mesenchymal Stromal Cells and Neuronal Transdifferentiation by Small Molecules. *Neurochem. Res.* 42, 415–427. doi: 10.1007/s11064-016-2086-7

Alexanian, A. R., Liu, Q.-S., and Zhang, Z. (2013). Enhancing the efficiency of direct reprogramming of human mesenchymal stem cells into mature neuronal-like cells with the combination of small molecule modulators of chromatin modifying enzymes, SMAD signaling and cyclic adenosine monophosphate levels. *Int. J. Biochem. Cell Biol.* 45, 1633–1638. doi: 10.1016/j.biocel.2013.04.022

Belluardo, N., Mudò, G., Trovato-Salinaro, A., Le Gurun, S., Charollais, A., Serre-Beinier, V., et al. (2000). Expression of connexin36 in the adult and developing rat brain. *Brain Res.* 865, 121–138. doi: 10.1016/s0006-8993(00)02300-3

Berry, L., Grant, M. E., McClure, J., and Rooney, P. (1992). Bone-marrow-derived chondrogenesis in vitro. *J. Cell Sci.* 101(Pt 2), 333–342.

Bi, Y., Gong, M., Zhang, X., Zhang, X., Jiang, W., Zhang, Y., et al. (2010). Pre-activation of retinoid signaling facilitates neuronal differentiation of

mesenchymal stem cells. *Dev. Growth. Differ.* 52, 419–431. doi: 10.1111/j.1440-169x.2010.01182.x

Bittman, K., Owens, D. F., Kriegstein, A. R., and LoTurco, J. J. (1997). Cell coupling and uncoupling in the ventricular zone of developing neocortex. *J. Neurosci.* 17, 7037–7044. doi: 10.1523/jneurosci.17-18-07037.1997

Bodi, E., Hurtado, S. P., Carvalho, M. A., Borojevic, R., and Campos de Carvalho, A. C. (2004). Gap junctions in hematopoietic stroma control proliferation and differentiation of blood cell precursors. *An. Acad. Bras. Cienc.* 76, 743–756. doi: 10.1590/s0001-37652004000400009

Bosone, C., Andreu, A., and Echevarria, D. (2016). GAP junctional communication in brain secondary organizers. *Dev. Growth Differ.* 58, 446–455. doi: 10.1111/dgd.12297

Cheng, A., Tang, H., Cai, J., Zhu, M., Zhang, X., Rao, M., et al. (2004). Gap junctional communication is required to maintain mouse cortical neural progenitor cells in a proliferative state. *Dev. Biol.* 272, 203–216. doi: 10.1016/j.ydbio.2004.04.031

Condorelli, D. F., Belluardo, N., Trovato-Salinaro, A., and Mudò, G. (2000). Expression of Cx36 in mammalian neurons. *Brain Res. Brain Res. Rev.* 32, 72–85. doi: 10.1016/s0165-0173(99)00068-5

Connor, B., Firmin, E., McCaughey-Chapman, A., Monk, R., Lee, K., Liot, S., et al. (2018). Conversion of adult human fibroblasts into neural precursor cells using chemically modified mRNA. *Heliyon* 4:e00918. doi: 10.1016/j.heliyon.2018.e00918

Dorshkind, K., Green, L., Godwin, A., and Fletcher, W. H. (1993). Connexin-43-type gap junctions mediate communication between bone marrow stromal cells. *Blood* 82, 38–45. doi: 10.1182/blood.v82.1.38.bloodjournal82138

Duval, N., Gomès, D., Calaora, V., Calabrese, A., Meda, P., and Bruzzone, R. (2002). Cell coupling and Cx43 expression in embryonic mouse neural progenitor cells. *J. Cell Sci.* 115, 3241–3251.

Eugenin, E. A., Basilio, D., Saez, J. C., Orellana, J. A., Raine, C. S., Bukauskas, F., et al. (2012). The role of gap junction channels during physiologic and pathologic conditions of the human central nervous system. *J. Neuroimmune Pharmacol.* 7, 499–518. doi: 10.1007/s11481-012-9352-5

Feng, N., Han, Q., Li, J., Wang, S., Li, H., Yao, X., et al. (2014). Generation of highly purified neural stem cells from human adipose-derived mesenchymal stem cells by Sox1 activation. *Stem Cells Dev.* 23, 515–529. doi: 10.1089/scd.2013.0263

Goodenough, D. A., and Paul, D. L. (2009). Gap junctions. *Cold Spring Harb. Perspect. Biol.* 1:a002576. doi: 10.1101/cshperspect.a002576

Gulisano, M., Parenti, R., Spinella, F., and Cicirata, F. (2000). Cx36 is dynamically expressed during early development of mouse brain and nervous system. *Neuroreport* 11, 3823–3828. doi: 10.1097/00001756-200011270-00045

Gutnick, M. J., and Prince, D. A. (1981). Dye coupling and possible electrotonic coupling in the guinea pig neocortical slice. *Science* 211, 67–70. doi: 10.1126/science.7444449

Herbertson, A., and Aubin, J. E. (1997). Cell sorting enriches osteogenic populations in rat bone marrow stromal cell cultures. *Bone* 21, 491–500. doi: 10.1016/s8756-3282(97)00197-x

Hodgkin, A. L., and Huxley, A. F. (1952). A quantitative description of membrane current and its application to conduction and excitation in nerve. *J. Physiol.* 117, 500–544. doi: 10.1113/jphysiol.1952.sp004764

Hu, W., Qiu, B., Guan, W., Wang, Q., Wang, M., Li, W., et al. (2015). Direct conversion of normal and alzheimer's disease human fibroblasts into neuronal cells by small molecules. *Cell Stem Cell* 17, 204–212. doi: 10.1016/j.stem.2015.07.006

Huang, Y.-S., Li, I.-H., Chueh, S.-H., Hueng, D.-Y., Tai, M.-C., Liang, C.-M., et al. (2015). Mesenchymal stem cells from rat olfactory bulbs can differentiate into cells with cardiomyocyte characteristics. *J. Tissue Eng. Regen. Med.* 9, E191-201. doi: 10.1002/term.1684

Hwang, D. W., Kwon, H. W., Jang, J., Jung, H. J., Kim, K. R., and Lee, D.-S. (2017). Neuron-Specific fluorescence reporter-based live cell tracing for transdifferentiation of mesenchymal stem cells into neurons by chemical compound. *Stem Cells Int.* 2017:8452830. doi: 10.1155/2017/8452830

Jiang, X., Shen, S., Cadwell, C. R., Berens, P., Sinz, F., Ecker, A. S., et al. (2015). Principles of connectivity among morphologically defined cell types in adult neocortex. *Science* 350:aac9462. doi: 10.1126/science.aac9462

Jungwirth, N., Salinas Tejedor, L., Jin, W., Gudi, V., Skripuletz, T., Stein, V. M., et al. (2018). Mesenchymal Stem Cells Form 3D Clusters Following Intraventricular Transplantation. *J. Mol. Neurosci.* 65, 60–73. doi: 10.1007/s12031-018-1070-x

Kawada, H., Fujita, J., Kinjo, K., Matsuzaki, Y., Tsuma, M., Miyatake, H., et al. (2004). Nonhematopoietic mesenchymal stem cells can be mobilized and differentiate into cardiomyocytes after myocardial infarction. *Blood* 104, 3581–3587. doi: 10.1182/blood-2004-04-1488

Kreuzberg, M. M., Deuchars, J., Weiss, E., Schober, A., Sonntag, S., Wellershaus, K., et al. (2008). Expression of connexin30.2 in interneurons of the central nervous system in the mouse. *Mol. Cell Neurosci.* 37, 119–134. doi: 10.1016/j.mcn.2007.09.003

Kuznetsov, S. A., Friedenstein, A. J., and Robey, P. G. (1997). Factors required for bone marrow stromal fibroblast colony formation in vitro. *Br. J. Haematol.* 97, 561–570. doi: 10.1046/j.1365-2141.1997.902904.x

Lemcke, H., and Kuznetsov, S. A. (2013). Involvement of connexin43 in the EGF/EGFR signalling during self-renewal and differentiation of neural progenitor cells. *Cell. Signal.* 25, 2676–2684. doi: 10.1016/j.cellsig.2013.08.030

Lemcke, H., Nittel, M.-L., Weiss, D. G., and Kuznetsov, S. A. (2013). Neuronal differentiation requires a biphasic modulation of gap junctional intercellular communication caused by dynamic changes of connexin43 expression. *Eur. J. Neurosci.* 38, 2218–2228. doi: 10.1111/ejn.12219

Lenth, R. (2019). *emmeans: Estimated Marginal Means, aka Least-Squares Means. R package version 1.3.4*. Available online at: https://CRAN.R-project.org/package=emmeans (accessed April 15, 2020).

Leung, D. S. Y., Unsicker, K., and Reuss, B. (2002). Expression and developmental regulation of gap junction connexins cx26, cx32, cx43 and cx45 in the rat midbrain-floor. *Int. J. Dev. Neurosci.* 20, 63–75. doi: 10.1016/s0736-5748(01)00056-9

Lo Turco, J. J., and Kriegstein, A. R. (1991). Clusters of coupled neuroblasts in embryonic neocortex. *Science* 252, 563–566. doi: 10.1126/science.1850552

Ma, K., Fox, L., Shi, G., Shen, J., Liu, Q., Pappas, J. D., et al. (2011). Generation of neural stem cell-like cells from bone marrow-derived human mesenchymal stem cells. *Neurol. Res.* 33, 1083–1093. doi: 10.1179/1743132811Y.0000000053

Manchanda, R., Appukuttan, S., and Padmakumar, M. (2019). Electrophysiology of syncytial smooth muscle. *J. Exp. Neurosci.* 13, 1179069518821917. doi: 10.1177/1179069518821917

Mollinari, C., Zhao, J., Lupacchini, L., Garaci, E., Merlo, D., and Pei, G. (2018). Transdifferentiation: a new promise for neurodegenerative diseases. *Cell Death Dis.* 9:830. doi: 10.1038/s41419-018-0891-4

Nielsen, M. S., Nygaard Axelsen, L., Sorgen, P. L., Verma, V., Delmar, M., and Holstein-Rathlou, N.-H. (2012). Gap junctions. *Compr. Physiol.* 2, 1981–2035. doi: 10.1002/cphy.c110051

Noctor, S. C., Flint, A. C., Weissman, T. A., Dammerman, R. S., and Kriegstein, A. R. (2001). Neurons derived from radial glial cells establish radial units in neocortex. *Nature* 409, 714–720. doi: 10.1038/35055553

Pang, Z. P., Yang, N., Vierbuchen, T., Ostermeier, A., Fuentes, D. R., Yang, T. Q., et al. (2011). Induction of human neuronal cells by defined transcription factors. *Nature* 476, 220–223. doi: 10.1038/nature10202

Phinney, D. G., and Prockop, D. J. (2007). Concise review: mesenchymal stem/multipotent stromal cells: the state of transdifferentiation and modes of tissue repair-current views. *Stem Cells* 25, 2896–2902. doi: 10.1634/stemcells.2007-0637

Qin, H., Zhao, A., and Fu, X. (2017). Small molecules for reprogramming and transdifferentiation. *Cell Mol. Life. Sci.* 74, 3553–3575. doi: 10.1007/s00018-017-2586-x

Qin, Y., Zhou, C., Wang, N., Yang, H., and Gao, W.-Q. (2015). Conversion of Adipose Tissue-Derived Mesenchymal Stem Cells to Neural Stem Cell-Like Cells by a Single Transcription Factor, Sox2. *Cell Reprogram* 17, 221–226. doi: 10.1089/cell.2015.0001

R Core Team (2019). *R: A Language and Environment for Statistical Computing. R version 3.6.1*. Vienna: R Foundation for Statistical Computing.

Rinaldi, F., Hartfield, E. M., Crompton, L. A., Badger, J. L., Glover, C. P., Kelly, C. M., et al. (2014). Cross-regulation of Connexin43 and \beta-catenin influences differentiation of human neural progenitor cells. *Cell Death Dis.* 5:e1017. doi: 10.1038/cddis.2013.546

Rozental, R., Srinivas, M., Gökhan, S., Urban, M., Dermietzel, R., Kessler, J. A., et al. (2000). Temporal expression of neuronal connexins during hippocampal

ontogeny. *Brain Res. Brain Res. Rev.* 32, 57–71. doi: 10.1016/s0165-0173(99)00096-x

Schindelin, J., Arganda-Carreras, I., Frise, E., Kaynig, V., Longair, M., Pietzsch, T., et al. (2012). Fiji: an open-source platform for biological-image analysis. *Nat. Methods* 9, 676–682. doi: 10.1038/nmeth.2019

Shi, S., Wu, X., Wang, X., Hao, W., Miao, H., Zhen, L., et al. (2016). Differentiation of bone marrow mesenchymal stem cells to cardiomyocyte-like cells is regulated by the combined low dose treatment of transforming growth factor-\beta1 and 5-Azacytidine. *Stem Cells Int.* 2016, 3816256. doi: 10.1155/2016/3816256

Söhl, G., Maxeiner, S., and Willecke, K. (2005). Expression and functions of neuronal gap junctions. *Nat. Rev. Neurosci.* 6, 191–200. doi: 10.1038/nrn1627

Söhl, G., and Willecke, K. (2004). Gap junctions and the connexin protein family. *Cardiovasc. Res.* 62, 228–232. doi: 10.1016/j.cardiores.2003.11.013

Su, X., Chen, J.-J., Liu, L.-Y., Huang, Q., Zhang, L.-Z., Li, X.-Y., et al. (2017). Neonatal CX26 removal impairs neocortical development and leads to elevated anxiety. *Proc. Natl. Acad. Sci. U.S.A.* 114, 3228–3233. doi: 10.1073/pnas.1613237114

Swayne, L. A., and Bennett, S. A. L. (2016). Connexins and pannexins in neuronal development and adult neurogenesis. *BMC Cell Biol.* 17(Suppl. 1):10. doi: 10.1186/s12860-016-0089-5

Todorova, M. G., Soria, B., and Quesada, I. (2008). Gap junctional intercellular communication is required to maintain embryonic stem cells in a non-differentiated and proliferative state. *J. Cell. Physiol.* 214, 354–362. doi: 10.1002/jcp.21203

Valiunas, V., Doronin, S., Valiuniene, L., Potapova, I., Zuckerman, J., Walcott, B., et al. (2004). Human mesenchymal stem cells make cardiac connexins and form functional gap junctions. *J. Physiol.* 555, 617–626. doi: 10.1113/jphysiol.2003.058719

Vierbuchen, T., Ostermeier, A., Pang, Z. P., Kokubu, Y., Südhof, T. C., and Wernig, M. (2010). Direct conversion of fibroblasts to functional neurons by defined factors. *Nature* 463, 1035–1041. doi: 10.1038/nature08797

Voitychuk, O. I., Asmolkova, V. S., Gula, N. M., Sotkis, G. V., Galadari, S., Howarth, F. C., et al. (2012). Modulation of excitability, membrane currents and survival of cardiac myocytes by N-acylethanolamines. *Biochim. Biophys. Acta* 1821, 1167–1176. doi: 10.1016/j.bbalip.2012.05.003

Zhang, J., and Jiao, J. (2015). Molecular biomarkers for embryonic and adult neural stem cell and neurogenesis. *Biomed. Res. Int.* 2015:727542. doi: 10.1155/2015/727542

Conflict of Interest: The authors declare that the research was conducted in the absence of any commercial or financial relationships that could be construed as a potential conflict of interest.

frontiers in Cell and Developmental Biology

ORIGINAL RESEARCH
published: 18 September 2020
doi: 10.3389/fcell.2020.544845

Presence/Absence and Specific Location of Resident CD34+ Stromal Cells/Telocytes Condition Stromal Cell Development in Repair and Tumors

Lucio Díaz-Flores[1], Ricardo Gutiérrez[1], Ma Pino García[2], Miriam González-Gómez[1], Lucio Díaz-Flores Jr.[1], Hugo Álvarez-Argüelles[1] and José Luis Carrasco[1]*

[1] Department of Basic Medical Sciences, Faculty of Medicine, University of La Laguna, Tenerife, Spain, [2] Department of Pathology, Eurofins® Megalab–Hospiten Hospitals, Tenerife, Spain

OPEN ACCESS

Edited by:
Lindolfo da Silva Meirelles, Universidade Luterana do Brazil, Brazil

Reviewed by:
Dragos Cretoiu, Carol Davila University of Medicine and Pharmacy, Romania
Helen Cristina Miranda, Case Western Reserve University, United States

***Correspondence:**
Lucio Díaz-Flores
kayto54@gmail.com

Specialty section:
This article was submitted to Stem Cell Research, a section of the journal Frontiers in Cell and Developmental Biology

Received: *22 March 2020*
Accepted: *21 August 2020*
Published: *18 September 2020*

Citation:
Díaz-Flores L, Gutiérrez R, García MP, González-Gómez M, Díaz-Flores L Jr, Álvarez-Argüelles H and Luis Carrasco J (2020) Presence/Absence and Specific Location of Resident CD34+ Stromal Cells/Telocytes Condition Stromal Cell Development in Repair and Tumors. Front. Cell Dev. Biol. 8:544845. doi: 10.3389/fcell.2020.544845

CD34+ stromal cells/telocytes (CD34+SCs/TCs) can have a role as mesenchymal precursor cells. Our objective is to assess whether the myofibroblastic stromal cell response in repair and in desmoplastic reactions in tumors depend on the presence or absence of resident CD34+SCs/TCs in specific regions/layers of an organ and on the location of their possible subpopulations. For this purpose, using conventional and immunohistochemical procedures, we studied specimens of (a) acute cholecystitis, with early repair phenomena (n: 6), (b) surgically resected segments of colon tattooed with India ink during previous endoscopic removal of malignant polyps, with macrophage infiltration and stromal cell reaction (n: 8) and (c) infiltrative adenocarcinomas of colon, with desmoplastic reaction (n: 8). The results demonstrated (a) stromal myofibroblastic reaction during repair and tumor desmoplasia in most regions in which resident CD34+SCs/TCs are present, (b) absence of stromal myofibroblastic reaction during repair in the mucosa of both organs in which resident CD34+SCs/TCs are absent and (c) permanence of CD34+SCs/TCs as such, without myofibroblastic response, in smooth muscle fascicles, nerves, and Meissner and Auerbach plexuses, in which the CD34+SCs/TCs mainly undergo reactive phenomena. Therefore, the development of activated αSMA+ myofibroblasts in these conditions requires the presence of resident CD34+SCs/TCs and depends on their location. In conclusion, the facts support the hypotheses that CD34+SCs/TCs participate in the origin of myofibroblasts during repair and tumor stroma formation, and that there is a heterogeneous population of resident CD34+SCs/TCs with different roles.

Keywords: gallbladder, colon, repair, tumor stroma, CD34+ stromal cells/telocytes

INTRODUCTION

CD34+ stromal cells are present in the connective tissue of multiple anatomical sites. A new cellular type named telocyte was identified by electron microscopy and described in 2010 (Popescu and Faussone-Pellegrini, 2010; Faussone Pellegrini and Popescu, 2011; Popescu, 2011). This cell type largely corresponds to the CD34+ stromal cells observed in light microscopy

(Rusu et al., 2016; Manetti et al., 2019). Several roles have been hypothesized for CD34+ stromal cells/telocytes (CD34+SCs/TCs) in (a) the maintenance and modulation of tissue homeostasis, including organization and control of the extracellular matrix, structural support, creation of microenvironments, integration of tissue components, control and regulation of other cells, and immunomodulation (Faussone Pellegrini and Popescu, 2011; Popescu, 2011; Popescu and Nicolescu, 2013; Díaz-Flores et al., 2014, 2016a; Cretoiu et al., 2016, 2020; Vannucchi et al., 2016) regeneration and repair (Faussone Pellegrini and Popescu, 2011; Popescu, 2011; Popescu et al., 2011; Ceafalan et al., 2012; Bani and Nistri, 2014; Díaz-Flores et al., 2015a,b, 2016b; Vannucchi et al., 2016). In regeneration, CD34+SCs/TCs act on neighboring parenchymal stem cells, regulating their proliferation and maturation (Faussone-Pellegrini and Bani, 2010; Popescu, 2011; Ceafalan et al., 2012; Gherghiceanu and Popescu, 2012; Rusu et al., 2016; Vannucchi and Faussone-Pellegrini, 2016; Cretoiu et al., 2017; Manetti et al., 2019). In repair through granulation tissue, CD34+SCs/TCs play an important role as precursor cells. Thus, they can change their location, relationship, proliferative activity, morphology, and immunohistochemical profile. For example, they can lose CD34 expression and gain alpha-smooth muscle actin (αSMA) expression, acquiring myofibroblastic characteristics (Nakayama et al., 2000, 2001, 2003; Barth et al., 2002a,b, 2004, 2005; Chauhan et al., 2003; Ramaswamy et al., 2003; Kuroda et al., 2005a,c; Ebrahimsade et al., 2007; Nimphius et al., 2007; Wessel et al., 2008; Díaz-Flores et al., 2015a,b, 2016b). The vascular/perivascular niche (da Silva Meirelles et al., 2006, 2015, 2016; Díaz-Flores et al., 2015a,b; Corrêa Bellagamba et al., 2018) is one of the principal sources of mesenchymal precursor cells that participate in tissue repair. Among these precursor cells are CD34+SCs/TCs, which are located around the abluminal surface of the pericytes and of the vascular smooth muscle cells. Thus, the CD34-stained vessels show a double-ring appearance (CD34+ endothelium and CD34+SCs/TCs), owing to two concentric circles "sandwiching" the unstained media layer (smooth muscle or pericytic layer) (Pusztaszeri et al., 2006; Lin et al., 2008, 2010; Díaz-Flores et al., 2015a,b).

Therefore, CD34+SCs/TCs can have multiple functions, which may depend on the location of their subpopulations (region-specific roles) (Pieri et al., 2008; Vannucchi et al., 2013; Díaz-Flores et al., 2016a; Cretoiu et al., 2017). In addition, they can be absent in some vessels and some regions or layers of an organ. Consequently, studying the stromal cell population (CD34+SCs/TCs and myofibroblasts) during repair, including tumor stroma formation as a special type of repair, in different areas of an organ, can reveal whether the response depends on (a) the regional presence or absence of CD34+SCs/TCs (general role of CD34+SCs/TCs in repair) and (b) the area in which these cells are located (different role of CD34+SCs/TCs subpopulations depending on location).

Given the above, the objective of this work is to assess whether the response of the stromal cell population in repair through granulation tissue, including tumor stromal formation, depends on the presence or absence of CD34+SCs/TCs and on their location within the organ. For this purpose, we study (1) the normal distribution of CD34+SCs/TCs in the different layers of the gallbladder and colon, and (2) the stromal cell response during repair in these organs, including the following processes (a) acute cholecystitis with initial and specific repair phenomena, (b) surgically resected segments of the colon after endoscopic resection of malignant polyps and India ink tattoos, leading to macrophage infiltration and stromal cell reaction, and (c) infiltrating colon adenocarcinomas with an important stromal reaction (desmoplastic reaction).

MATERIALS AND METHODS

Human Tissue Samples

The archives of Histology and Anatomical Pathology of the Departments of Basic Medical Sciences of La Laguna University, University Hospital, and Eurofins® Megalab–Hospiten Hospitals of the Canary Islands were searched for cases presenting the process outlined above, of which demonstrative samples were selected, including acute cholecystitis with initial and specific repair phenomena (n: 6), surgically resected segments of colon, following previous resection of malignant polyps (Parra-Blanco et al., 2006), tattooed with India ink (n: 8) and infiltrative adenocarcinomas of colon (n: 8), with later repair phenomena. In addition to confirming the results in different conditions and organs, an important objective is therefore to confirm the facts over time. Non-affected gallbladders and regions of the colon without pathologic findings (colectomies with a margin longer than 10 cm from the lesion) were also selected. Ethical approval for this study was obtained from the Ethics Committee of La Laguna University (Comité de Ética de la Investigación y de Bienestar Animal, CEIBA 2020-0382), including the dissociation of the samples from any information that could identify the patient. The authors therefore had no access to identifiable patient information.

Light Microscopy

Specimens for conventional light microscopy were fixed in a buffered neutral 4% formaldehyde solution, embedded in paraffin and cut into 3 μm-thick sections. Sections were stained with Hematoxylin–Eosin (HE), PAS–Alcian Blue and Masson trichrome.

Immunohistochemistry

Histologic sections, 3 μm-thick, were attached to silanized slides. After pre-treatment for enhancement of labeling, the sections were blocked with 3% hydrogen peroxide and then incubated with primary antibodies (10–40 min). The primary antibodies (Dako, Glostrup, Denmark) used in this study were CD34 monoclonal mouse anti-human, clone QBEnd-10, (dilution 1:50), catalog No. IR632, αSMA monoclonal mouse anti-human, clone 1A4 (dilution 1:50), catalog No. IR611 and podoplanin monoclonal mouse anti-human, clone D2-40 (dilution 1:50), catalog No. M3619. The immunoreaction was developed in a solution of diaminobenzidine and the sections were then briefly counterstained with hematoxylin,

dehydrated in ethanol series, cleared in xylene and mounted in Eukitt®. Positive and negative controls were used. For the double immunostaining, we used anti-CD34 or anti-podoplanin antibodies (diaminobenzidine, DAB, as chromogen) and anti-αSMA (aminoethylcarbazole, AEC, substrate–chromogen).

Immunofluorescence in Confocal Microscopy

For immunofluorescence, tissue sections were obtained as described above. For antigen retrieval, sections were deparaffinized and boiled for 20 min in sodium citrate buffer 10 mM (pH 6), rinsed in *Tris*-buffered saline (TBS, pH 7.6, 0.05 M), and incubated with the following primary antibodies diluted in TBS overnight in a humid chamber at room temperature: mouse monoclonal anti-CD34, code no. IR63261, Dako (ready to use), and goat polyclonal anti-actin (1/50 dilution, C-11, sc-1615, Santa Cruz Biotechnology). For the double immunofluorescence staining, sections were incubated with the mixture of monoclonal and polyclonal primary antibodies (mouse monoclonal anti-CD34 and goat polyclonal anti-actin). The next day, the slides were rinsed in TBS and incubated for 1 h at room temperature in the dark with the secondary biotinylated goat anti-rabbit IgG (H+L) (1:500, Code: 65-6140, Invitrogen, San Diego, CA, United States) and Alexa Fluor 488 goat anti-mouse IgG (H+L) antibody (1:500, Code: A11001, Invitrogen), followed by incubation with Streptavidin Cy3 conjugate (1:500, Code: SA1010, Invitrogen) for 1 h at room temperature in the dark. Nuclei were detected by DAPI staining (Chemicon International, Temecula, CA, United States). After washing in TBS, sections were exposed to a saturated solution of Sudan black B (Merck, Barcelona, Spain) for 20 min to block autofluorescence. They were rinsed in TBS and cover-slipped with DABCO (1%) and glycerol-PBS (1:1). Negative controls were performed in the absence of primary antibodies. Fluorescence immunosignals were obtained using a Fluoview 1000 laser scanning confocal imaging system (Olympus Optical).

RESULTS

CD34+SCs/TCs in the Normal Gallbladder

Depending on the gallbladder layer (**Figure 1A**), the distribution of CD34+SCs/TCs was as follows: (1) absence in the lamina propria of the mucosa (**Figure 1B**) (although some of these cells were observed underlying the glands in the gallbladder neck), (2) presence in variable numbers in the other layers (**Table 1**), including the fibrovascular connective tissue that separates the muscle bundles of the muscularis propria (**Figures 1C,D** and insert), the perimuscular subserosal layer of connective tissue (**Figure 1D** and insert) and the serosa, in which CD34+SCs/TCs are generally arranged in strands parallel to the serosa surface (**Figure 1E**). When present, CD34+SCs/TCs were located in the perivascular niche (around pericytes) (**Figures 1F,G**), in the adventitia of greater vessels (around vascular smooth muscle cells) (**Figure 1H**), in the connective interstitium, and around and within nerves (**Figure 1I**). They were also seen in contact with the endothelium or smooth muscle cells in lymphatic vessels, including capillaries, pre-collectors (**Figure 1J**) and collectors, which were relatively frequent in the gallbladder serosa.

Stromal Cells During Repair in Acute Cholecystitis

In general, the gallbladders with acute cholecystitis showed findings of early repair, including vasodilation, edema, angiogenic phenomena, margination, extravasation and infiltration of the leukocytes, and an increase in the number, size and characteristics of stromal cells (hereinafter activated stromal cells) (**Figure 2A**). These activated stromal cells were either CD34+ (CD34+SCs/TCs) or αSMA+ (myofibroblasts) (**Figure 2A** and insert). However, the mucosa, when conserved, did not show activated stromal cells (**Figure 2B**). An important population of activated αSMA+ CD34- stromal cells was observed in the fibrovascular connective tissue that separates the muscle bundles in the muscularis propria (**Figure 2**) and in the perimuscular subserosal layer of connective tissue (**Figures 2A**, **3A**). Therefore, loss of CD34 expression and gain of αSMA expression (myofibroblastic phenotype) occurred in these areas. In the serosa layer, increased CD34+ stromal cells were observed underlying the perimuscular subserosal layer (**Figure 3A**) and between the strands described in normal conditions. Conversely, the perimuscular subserosal layer (as aforementioned) and the strands presented numerous αSMA+ stromal cells (myofibroblastic phenotype). Thus, bands of cells expressing CD34 or αSMA were seen between the subserosal limit of the muscularis propria and the serosal surface. The weak expression of podoplanin that CD34+SCs/TCs normally present became occasionally intense in stromal cells (**Figure 3B**) which conserved their CD34 positivity. Abundant reactive CD34+SCs/TCs were observed in the nerves. Occasionally, cells expressing both markers were seen (**Figure 3C**).

CD34+SCs/TCs in the Normal Intestinal Wall

Depending on the intestinal layer, the CD34+SCs/TCs showed the following distribution: (1) Absence in the mucosa (**Figure 4A**), except in the areas underlying the tubular glands and the muscularis mucosae, where they were present in variable numbers (**Figures 4B,C**). (2) Presence in variable numbers (**Table 1**) in (a) the submucosa (**Figure 4C**), including perivascular niches (around the pericytes), the adventitia of the largest vessels (around vascular smooth muscle cells), the interstitium, the nerves and the Meissner plexus, (b) the muscularis propria, including the muscle fascicles (within and around them) (**Figures 4D–F**), nerves and the myenteric plexus (**Figure 4G**), close to the c-kit+ interstitial cells of Cajal, and (c) the serosa, including perivascular niches, adventitia of larger vessels, interstitium, nerves and adipose tissue.

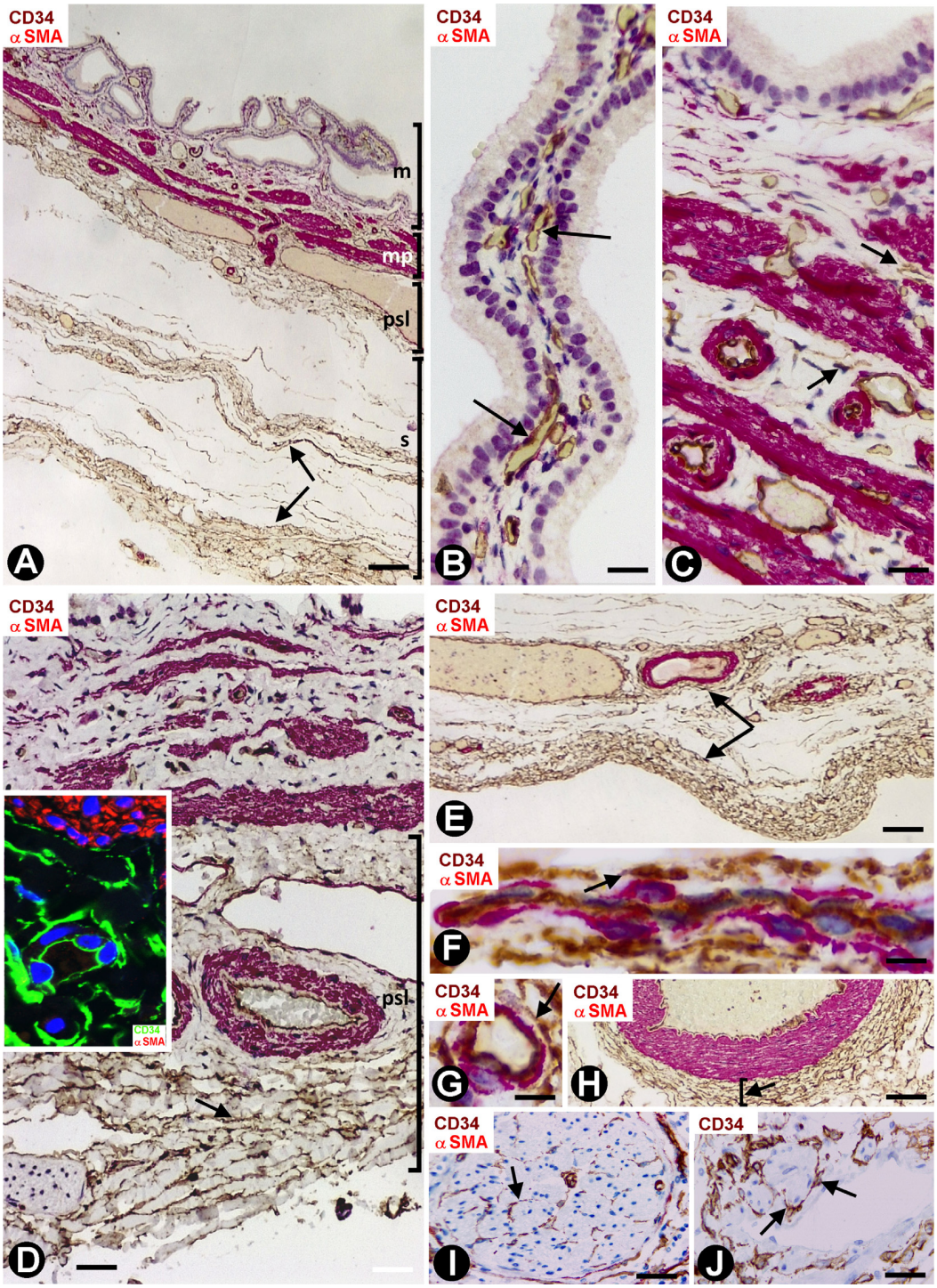

FIGURE 1 | CD34+ SCFTs in the normal gallbladder. **(A–I)** Sections double-stained with anti-CD34 (brown) and anti-αSMA (red). **(J)** Section stained with anti-CD34 (brown). **(A)** Panoramic view of gallbladder wall layers, mucosa (m), muscularis propria (mp) (smooth muscle cells: red), perimuscular subserosal layer (psl) and serosa (s), in which a different distribution of CD34+SCs/TCs (brown) is observed, predominantly in the perimuscular subserosal layer and in strands in the serosa (arrows), parallel to the serosa surface. **(B)** Absence of CD34+SCs/TCs in the corium of the mucosa; the endothelial cells are the only cells stained with anti-CD34 (arrows). Note that CD34+SCs/TCs are also absent in the perivascular spaces, which may or may not contain pericytes. **(C,D)** CD34+SCs/TCs (arrows) in the muscularis propria. In panel **(D)**, observe numerous CD34+SCs/TCs (brown, arrow) in the perimuscular subserosa layer (psl). In the insert, smooth muscle cells (αSMA+, red) and CD34+SCs/TCs (green). **(E)** Abundant CD34+SCs/TCs (brown, arrows) in parallel strands in the serosa. **(F–J)** Details of the location of CD34+SCs/TCs in vessels, nerves, and lymphatics (arrows). Note CD34+SCs/TCs around pericytes in the pericytic microvasculature (**F,G**, arrows), in the adventitia of an artery (**H**, arrow), in a nerve (**I**, arrow) and in a lymphatic pre-collector (**J**, arrow). Bar: **(A)** 160 μm; **(B)** 20 μm; **(C,H–I)** 40 μm; **(D)** 60 μm; **(E)** 80 μm; **(F,G)** 10 μm.

TABLE 1 | Presence/Absence and semiquantification of CD34+SCs/TCs in normal conditions, and CD34+SCs/TCs and αSMA+cells (myofibroblasts) during repair and tumoral stroma formation.

	Gallbladder			Colon				
	Normal conditions	Repair in cholecystitis		Normal conditions	Repair in surgical resected segments after malignant polyps removed and India ink tattoo		Desmoplastic reaction in Invasive adenocarcinomas of colon	
	CD34+SCs/TCs	CD34+SCs/TCs	αSMA+ cells (myofibroblasts)	CD34+SCs/TCs	CD34+SCs/TCs	αSMA+ cells (myofibroblasts)	CD34+SCs/TCs	αSMA+ cells (myofibroblasts)
Mucosa of both organs	−	−	−	−	−	−	−	+/−
Perimuscular subserosal layer of gallbladder Submucosa of colon	++	−	+++	+++	−−	+++	−	+++
Muscularis propria	++/−	++	−	++/−	++	−	++	−−
Adventitia of arteries	++	++	+/−	++	++	+/−	++	+/−
Nerves in bath organs Meissner and myenteric plexuses in colon	++	+++	−	++	+++	−	+++	−
Serosa	+++/−	−	+++	+++/−	−	+++	−	+++

Stromal Cells in Segments of Colon Tattooed With India Ink, Following Previous Resection of Malignant Polyps

We observed an intense infiltrate of macrophages, isolated or forming small groups, and varying numbers (**Table 1**) of activated stromal cells in the segments of colon, following resection of malignant polyps tattooed with India ink. In the mucosa, the stromal cell reaction was not evident (**Figure 5A**). Stromal cells expressing αSMA (myofibroblastic phenotype) were observed between the macrophages in the submucosa (**Figures 5A–C**) and serosa, CD34+SCs/TCs were not observed in these layers. However, activated stromal cells remained positive for anti-CD34 and were negative for anti-αSMA in the adventitia of submucosal and serosal medium sized vessels (**Figures 5B,C**), and between (**Figure 5D**) and within (**Figure 5E**) the muscle fascicles, nerves (**Figure 5F**) and myenteric plexuses (**Figure 5G**) in the muscularis layer.

Stromal Cells in Infiltrative Carcinomas of Colon

Infiltrative adenocarcinomas of the colon showed a desmoplastic reaction in the submucosa (**Figure 6A**) and serosa (**Figure 6B**), in which numerous elongated stromal cells around the neoplastic glands presented αSMA expression (myofibroblastic phenotype) (**Figures 6A,B**) and were negative for anti-CD34 (**Figure 6C**). In the mucosa, the desmoplastic reaction was irregular and scarce (**Figures 6D–G**). Thus, activated αSMA+ stromal cells were absent in some regions of the mucosa (**Figure 6D**), whereas αSMA+ stromal cells were seen around the neoplastic glands in other regions (**Figures 6F,G**). CD34+SCs/TCs were also absent around the neoplastic glands in the mucosa (**Figure 6E**), which generally were in vicinity to fragmented muscularis mucosa. An irregular stromal reaction was also observed in the connective tracts between the muscle fascicles of the muscularis propria, with presence of activated cells showing αSMA (**Figure 7A**) and CD34 (**Figures 7B,C**) expression. Likewise, CD34+SCs/TCs were present in the muscle fascicles (**Figures 7D,E**), nerves (**Figure 7F**) and myenteric plexuses (**Figure 7G**). In the serosa, intimal thickening was also observed in medium-caliber arteries, with presence of αSMA myointimal cells (**Figure 7H**) and adventitial CD34+SCFTs (**Figure 7I**).

Common Findings and Their Variations in the Histological Samples Evaluated

The data described were present in all histological samples in the groups studied except those of the gallbladder serosa with acute cholecystitis and the colon mucosa with invasive carcinoma. In four cases of gallbladder with acute cholecystitis, the response affected the entire serosa, and in the other two cases, it was zonal. In the colon mucosa with invasive adenocarcinoma, the stromal response was absent in four cases and scarce in the other four cases.

DISCUSSION

We report that the repair response in different processes of the gallbladder and colon, including stroma formation in tumors, depends on the regional presence or absence of CD34+SCs/TCs (there is no myofibroblast response

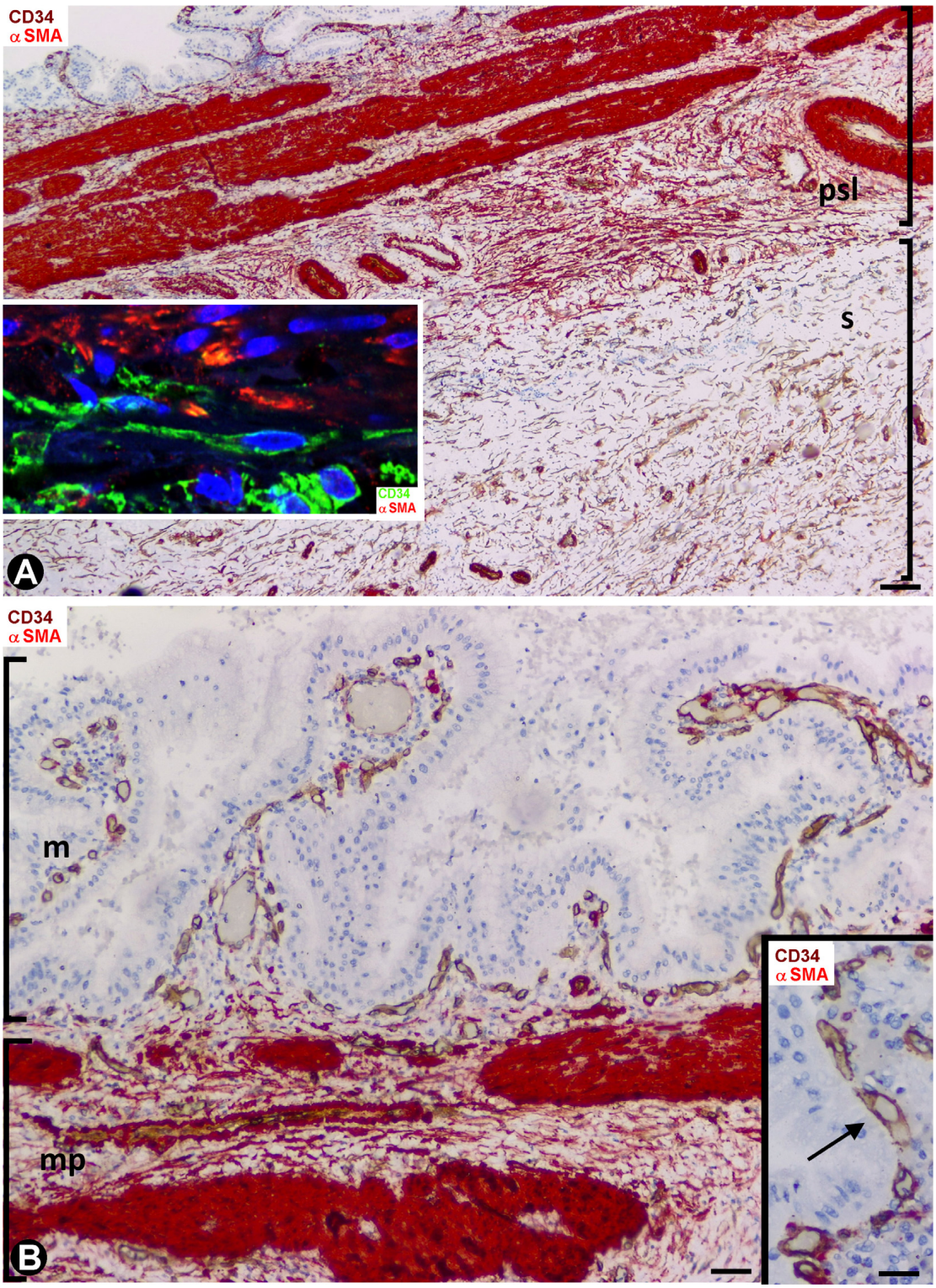

FIGURE 2 | Stromal cells during repair in acute cholecystitis. Double staining with anti-CD34 (brown) and anti-αSMA (red). **(A)** Panoramic view of the gallbladder wall showing a high αSMA expression (deep red) in smooth muscle cells of the lamina propria and of vascular media layer, and moderate expression in myofibroblasts (numerous in the perimuscular serosal layer: psl). Note persistence of CD34+SCs/TCs (brown) in the area of serosa underlying the perimuscular serosa layer. In the insert, a zone of transition between αSMA+ cells (myofibroblasts, red) and CD34+SCs/TCs (green) is shown by fluorescent immunostaining in confocal microscopy. **(B)** Absence of activated stromal cells in the mucosa, whereas αSMA+ activated stromal cells (red) are present between the muscle fascicles (deep red) of the muscularis propria. In the insert, detail of the vessels (arrows) in the mucosa. Bar: **(A)** 60 μm, **(B)** 40 μm; Insert: 20 μm.

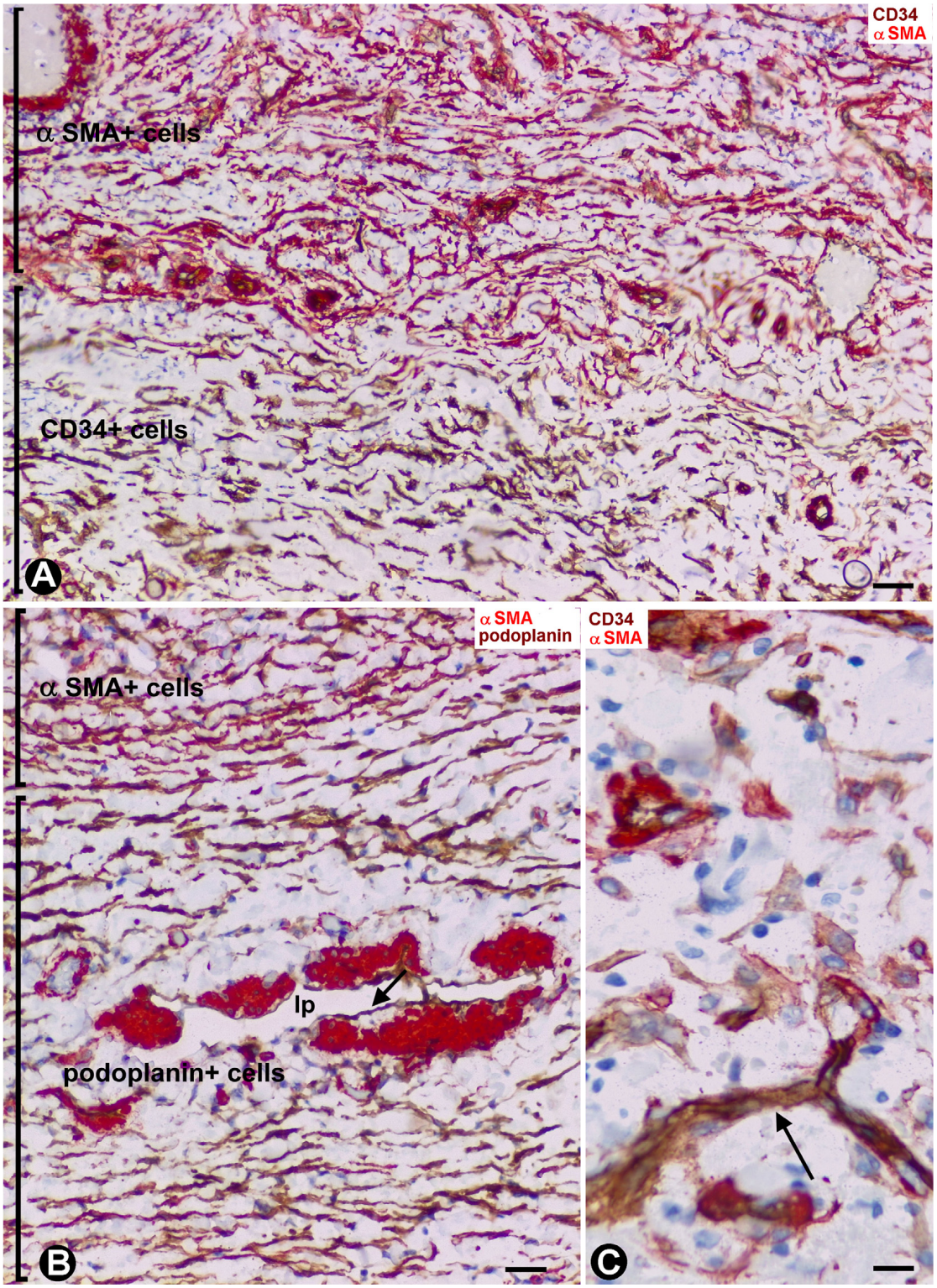

FIGURE 3 | Stromal cells during repair in acute cholecystitis. **(A,C)** Double staining with anti-CD34 (brown) and anti-αSMA (red). **(B)** Double staining with anti-αSMA and anti-podoplanin. **(A)** αSMA+ activated stromal cells (myofibroblastic phenotype, red) observed in the perimuscular subserosal layer, alternating with a subjacent band of CD34+ activated stromal cells (brown). **(B)** αSMA activated stromal cells of a strand of the serosal layer are observed alternating with a band of podoplanin+ cells, which also express CD34 (not shown). Note the presence of a lymphatic pre-collector vessel (LpV) with podoplanin+ endothelial cells (arrow) and groups of SMCs (red) in its wall. **(C)** Cells expressing CD34 (brown) and αSMA (red). A capillary is also observed (arrow) Bar: **(A,B)** 40 μm; **(C)** 10 μm.

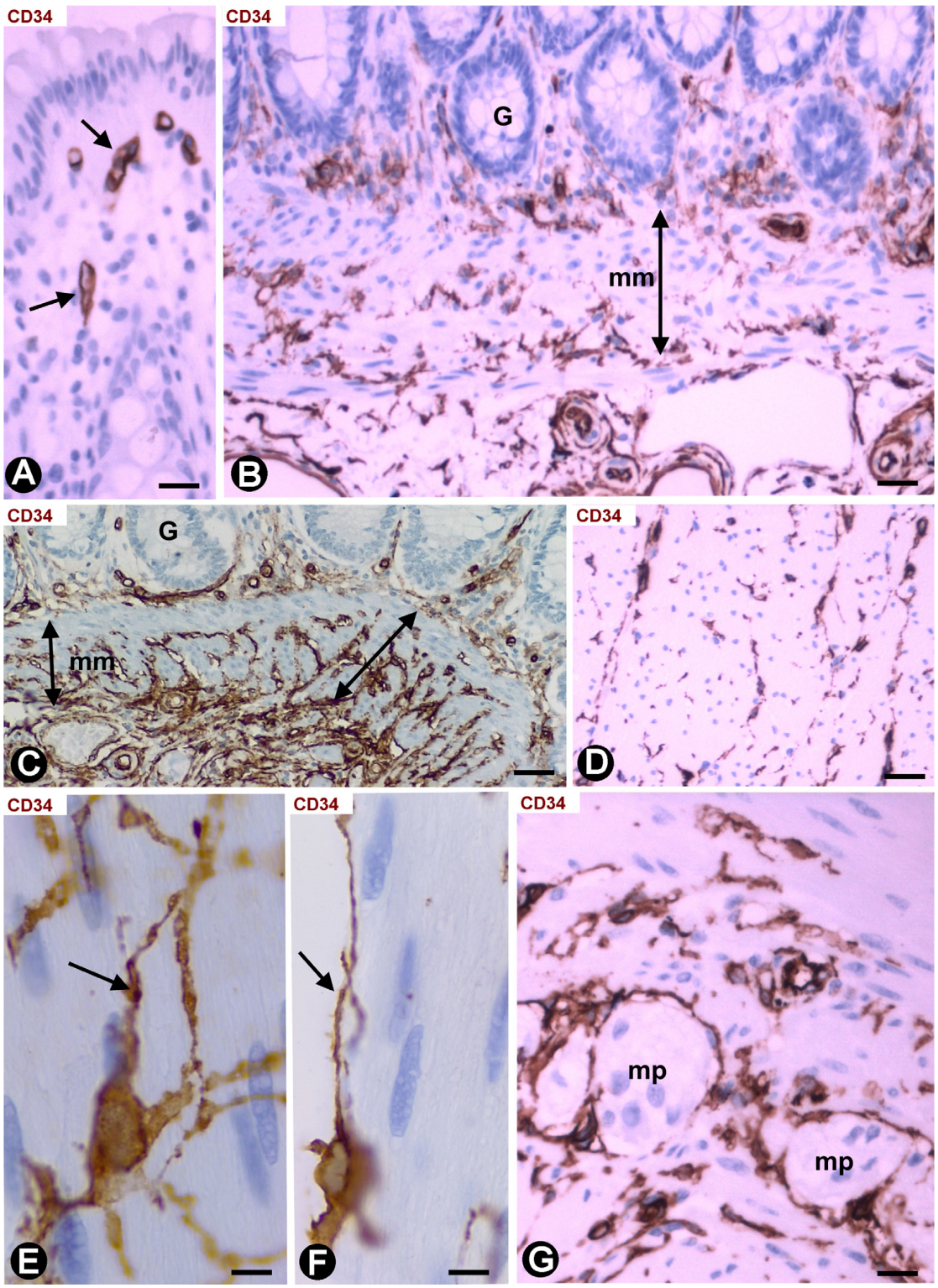

FIGURE 4 | CD34+SCs/TCs in the normal intestinal wall. Sections stained with anti-CD34. **(A)** Absence of CD34+SCs/TCs in the chorion of the mucosa underlying the epithelium (only the endothelial cells express CD34, arrow). **(B,C)** Varying numbers of CD34+SCs/TCs (brown) in the areas between the base of the mucosa tubular glands and the muscularis mucosae (mm). A portion of the submucosa with abundant CD34+SCs/TCs (brown) is also observed in panel **(C)**. **(D)** CD34+SCs/TCs (brown) are seen within and around the muscle fascicles of the muscularis propria. **(E,F)** Details of the CD34+SCs/TCs within (**E**, arrow) and around (**F**, arrow) the muscle fascicles. **(G)** CD34+SCs/TCs in myenteric plexuses (mp). Bar: **(A,G)** 20 μm; **(B–D)** 40 μm; **(E,F)** 10 μm.

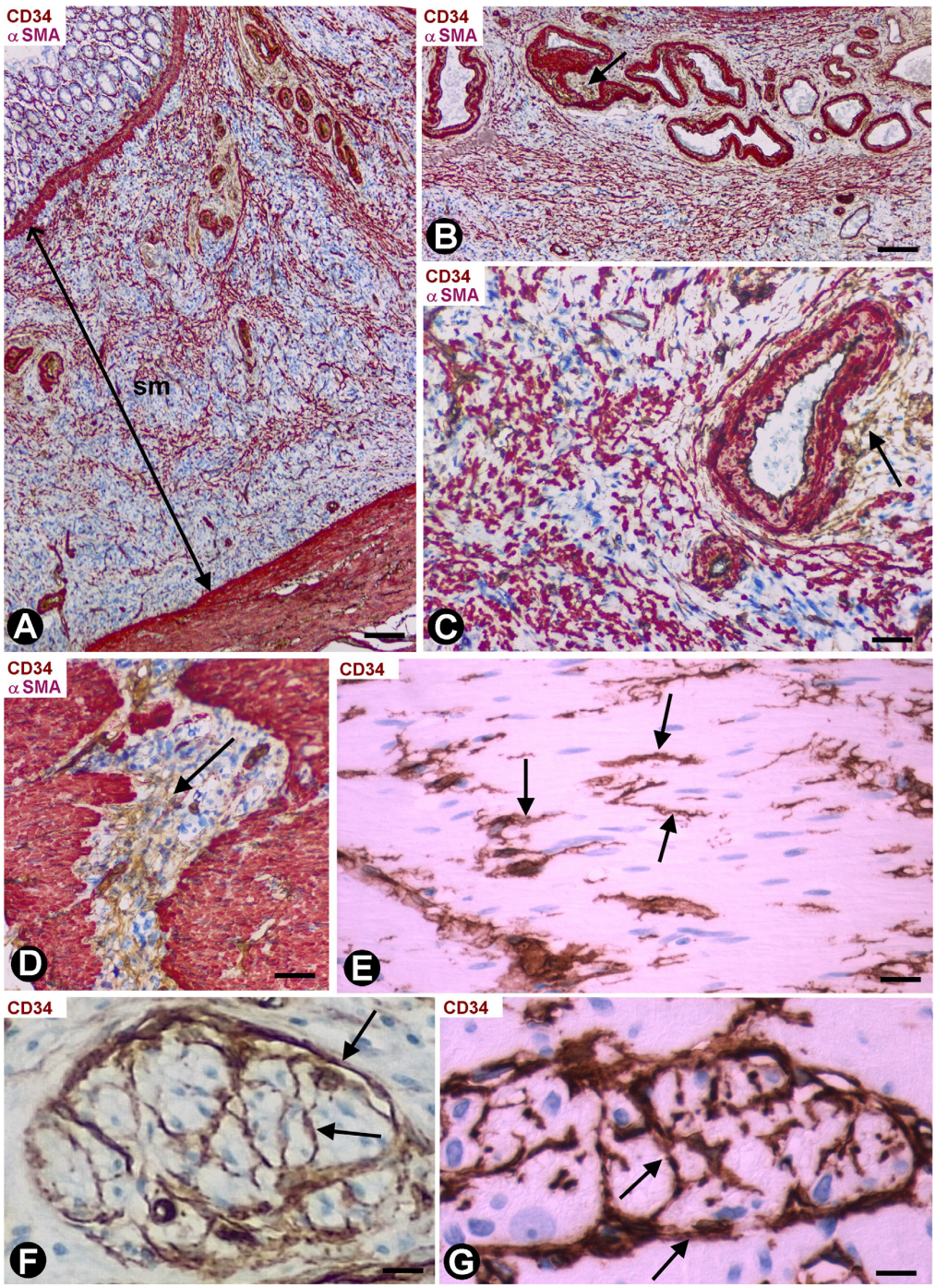

FIGURE 5 | Stromal cells in segments of colon following resection of malignant polyps, tattooed with India ink, and with an intense infiltrate of macrophages. **(A)** Activated stromal cells are present in the submucosa and absent in the mucosa. Note that the activated stromal cells in the submucosa (sm) are αSMA+ (red). Infiltrates of macrophages are also observed in the mucosa and submucosa. **(B,C)** Absence of stromal cell reaction in the adventitia of large submucosal vessels, in which the CD34+SCs/TCs (brown, arrows) are conserved. **(D,E)** Activated CD34+SCs/TCs (brown) in the connective tissue between (**D**, arrow) and within (**E**, arrows) muscle fascicles. **(F,G)** Presence of CD34+SCs/TCs (brown) in a nerve (**F**, arrows) and in a myenteric ganglion (**G**, arrows). **(A–D)** Double staining with anti-CD34 (brown) and anti-SMA (red). **(E–G)** Sections stained with anti-CD34. Bar: **(A)** 60 μm; **(B)** 40 μm; **(C–F)** 20 μm; **(G)** 15 μm.

where resident CD34+SCs/TCs are absent) and on their location within the organ (with or without myofibroblast response). These findings support the hypothesis that resident CD34+SCs/TCs play an important role as stromal precursor cells in tissue repair and tumor stroma formation, and that there is a heterogeneous population of

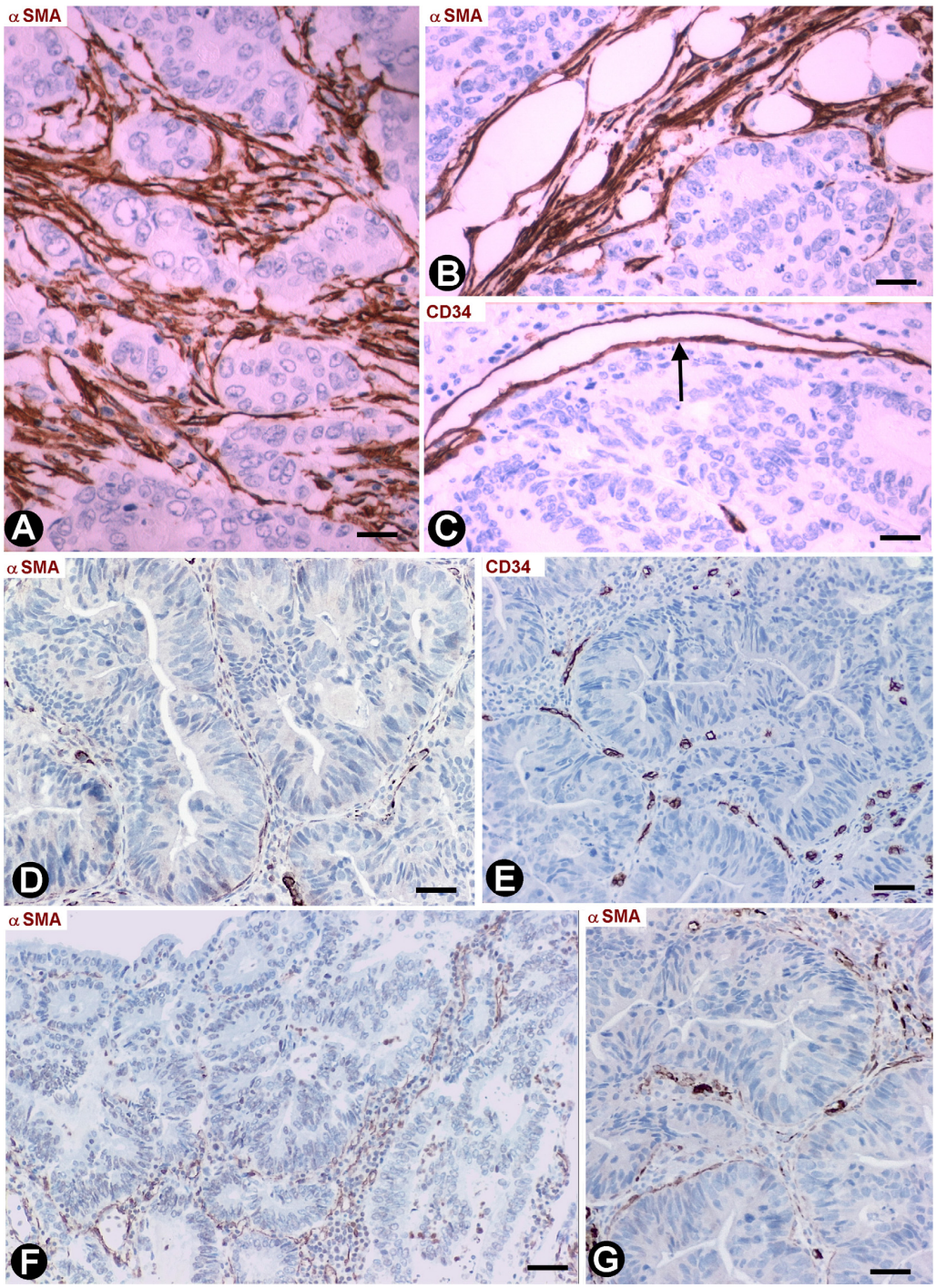

FIGURE 6 | Stromal cells in infiltrative carcinomas of colon. **(A,B,D,F,G)** Sections stained with anti-αSMA. **(C,E)** Sections stained with anti-CD34. **(A,B)** αSMA+ stromal cells (brown) are observed around neoplastic glands in the submucosa **(A)** and serosa **(B)**. **(C)** Absence of CD34+SCs/TCs around neoplastic glands in the submucosa. Note that the endothelial cells are the only cells expressing CD34 (arrow). **(D–G)** Neoplastic glands in the mucosa. The stromal cell reaction is scarce and irregular with few αSMA+ cells (brown) **(D,F,G)**. CD34+SCs/TCs s are absent **(E)**. Bar: **(A)** 20 μm; **(B–G)** 40 μm.

resident CD34+SCs/TCs with different roles. We consider these issues below.

We have used the term CD34+SCs/TCs because telocytes identified in electron microscopy largely correspond to CD34+ stromal cells observed in light microscopy (Rusu et al., 2016; Manetti et al., 2019). However, further studies, including transmission electron microscopy observation, are required. Indeed, the advantage of immunohistochemistry in light

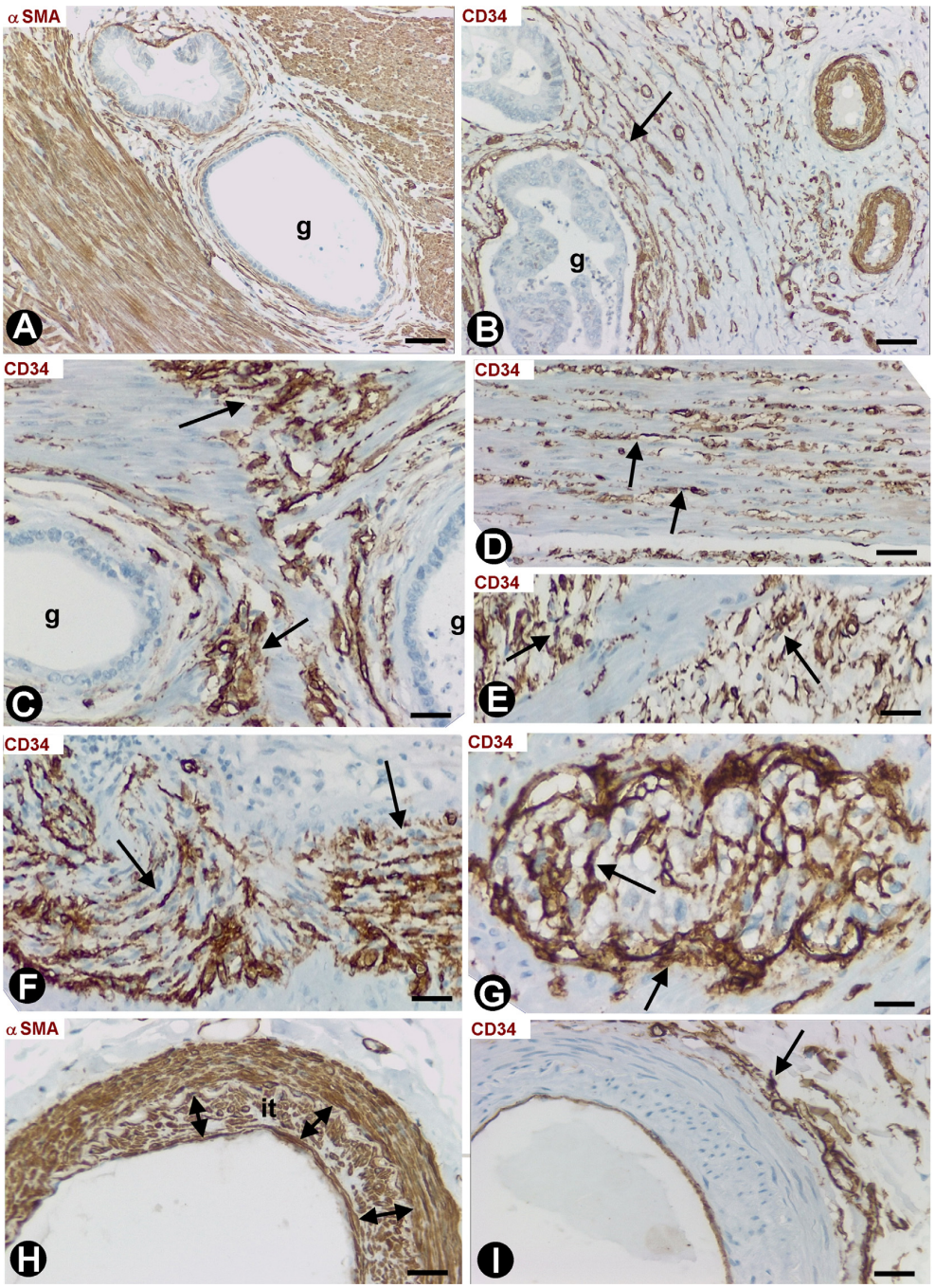

FIGURE 7 | Stromal cells in infiltrative carcinomas of colon. **(A,H)** Sections stained with anti-αSMA. **(B–G,I)** Sections stained with anti-CD34. **(A)** Scarce αSMA+stromal cells (arrow) around neoplastic glands (g) present in the connective tracts between the muscle fascicles of the muscularis propria. **(B,C)** Activated CD34+SCs/TCs (brown, arrow) neighboring neoplastic glands (g) in the muscularis propria. **(D–G)** activated CD34+SCs/TCs within (**D**, arrow) and between (**E**, arrow) muscle fascicles, a nerve (brown, arrow) and a myenteric plexus (brown, arrow). **(H)** Intimal thickening formed by αSMA+ cells is observed in an artery of the serosa. **(I)** Adventitial CD34+SCs/TCs (brown, arrow) are seen in an artery with intimal thickening. Bar: **(A–F,H,I)** 20 μm; **(G)** 10 μm.

microscopy is that it enables the observation of CD34+SC/TCs in extensive areas, while electron microscopy allows a better identification of telocytes.

Resident CD34+SCs/TCs are located in multiple anatomical sites, including vessels (around pericytes in pericytic microvasculature and in the adventitia of larger vessels), loose connective tissue, capsules, fibrous tracts, adipose tissue, cardiac, smooth and skeletal muscle, nerves, and around glands and skin annexes (Pieri et al., 2008; Bani et al., 2010; Popescu and Faussone-Pellegrini, 2010;

Popescu et al., 2011; Nicolescu and Popescu, 2012; Nicolescu et al., 2012; Vannucchi et al., 2014; Díaz-Flores et al., 2016a). Conversely, resident CD34+SCs/TCs are not observed in some organic regions. Examples of organs with or without CD34+SCs/TCs, depending on the layer examined, are the gallbladder and the intestine, whose mucosa is devoid of CD34+SCs/TCs (except occasional presence between the base of glands and the muscularis propria in the gallbladder and the muscularis mucosae in the intestine), whereas CD34+SCs/TCs are present in the other layers. These observations in the intestine coincide with those of other authors (Nakayama et al., 2000: Pieri et al., 2008; Vannucchi et al., 2013). Hinescu et al. (2007) have described interstitial Cajal-like cells expressing CD117 and CD34 in the lamina propria of the gallbladder, which can also coincide with subepithelial cells in the base of the glands near the muscularis propria in the gallbladder neck.

Given the above, we chose the gallbladder and colon to study the CD34+SC/TC and myofibroblast response during repair for the following reasons: these organs contain layers with or without resident CD34+SC/TCs, with a well-known CD34+SC/TC distribution, above all in the intestine; and they present repair phenomena in certain diseases, which require surgical removal. Another advantage is knowing this response *in situ* and in humans. One disadvantage could be that the study is based on snapshot observations. However, the observation of repair phenomena at different stages (initial stage in the gallbladder and more advanced in the colon) has allowed us to confirm the facts over time. Indeed, in acute cholecystitis, whose treatment is usually the urgent laparoscopic removal of the gallbladder, the repair phenomena were at an early phase. Conversely, following resection of malignant polyps and India ink tattoo, repair was more advanced in the colon, in which no urgent secondary surgical intervention after pathological diagnosis is the treatment.

The data described were present in most of the histologic samples with exceptions. The different extension of the lesion in the serosa of the gallbladder may be related to the intensity of the process. The variable response in the intestinal mucosa affected by invasive adenocarcinoma will be discussed below.

That growth and development of activated αSMA+ myofibroblasts were lacking during repair in the mucosa of the gallbladder and colon, in which CD34+SCs/TCs are absent (Nakayama et al., 2000; Pieri et al., 2008; Vannucchi et al., 2013), shows that CD34+SCs/TCs are essential to this process of myofibroblast development, supporting the hypothesis that myofibroblasts in repair can originate from CD34+SCs/TCs (resident CD34+SDs/TCs as precursor cells) (Nakayama et al., 2001, 2002a,b; Barth et al., 2002a, 2005; Ramaswamy et al., 2003; Kuroda et al., 2005b; Ebrahimsade et al., 2007; Nimphius et al., 2007; Wessel et al., 2008; Díaz-Flores et al., 2015a,b, 2016b).

There are numerous studies about cells expressing CD34 with different phenotypes, mainly in bone marrow and blood samples (CD34+ hematopoietic cells). We have circumscribed our observations to resident CD34+SC/TC behavior during repair. The results demonstrate different responses of CD34+SCs/TCs, depending on their location, with myofibroblast growth and development and CD34+SCs/TC disappearance (e.g., submucosa and serosa of colon, and perimuscular serosal layer of gallbladder) or with no myofibroblast development and persistence of reactive CD34+SCs/TCs (e.g., nerves, ganglia and smooth muscle fascicles). This CD34+SC/TC behavior also supports the hypothesis of heterogeneous subpopulations of CD34+SCs/TCs with different roles (Pieri et al., 2008; Vannucchi et al., 2013; Cretoiu et al., 2017). Whether or not these cells with different roles have a different phenotype requires verification.

Interpretation of the stromal cell response in tumors depending on location is more difficult, since tumor type may also influence the response. Thus, although there is a phenotypic shift from CD34+SCs/TCs toward αSMA+ myofibroblasts in numerous malignant invasive epithelial tumors (Nakayama et al., 2000, 2001, 2003; Barth et al., 2002a,b, 2004, 2005; Chauhan et al., 2003; Ramaswamy et al., 2003; Kuroda et al., 2005a,c; Nimphius et al., 2007; Wessel et al., 2008), the reaction is not constant. For example, CD34+SCs/TCs are preserved (reactive stromal cells are CD34+) in most lobular carcinoma of the breast, with no transformation into reactive αSMA+ stromal cells (Ebrahimsade et al., 2007). For this reason, we selected invasive adenocarcinomas of the colon in which reactive αSMA+ stromal cells are always present in the layers beyond the muscularis mucosae (Nakayama et al., 2000).

Our results concur with the study of Nakayama et al. (2000) on the activated stromal cells (growth and development of myofibroblasts and loss of CD34+SCs/TCs) in colonic adenocarcinomas. However, when we considered the stromal response in specific locations in the colon wall, the permanence of CD34+SCs/TCs, without myofibroblastic transformation, is a constant phenomenon in the muscle fascicles, nerves, and Meissner and Auerbach plexuses. Therefore, the response in these specific locations is similar to that observed in the repair processes outlined above, also suggesting the heterogeneity of the CD34+SCs/TCs. Nevertheless, the presence or not of αSMA+ cells around neoplastic glands in the mucosa is more difficult to interpret. It could be due to the persistence of pericryptal cells, normally present in the intestinal mucosa, or to infiltration of neoplastic glands surrounded by αSMA+ cells from the submucosa, a question that requires further study.

An important finding in the colonic infiltrating carcinomas was the frequent intimal thickening in arteries located in the serosa, which were in proximity to but not in contact with neoplastic glands. The adventitia participates in artery remodeling (Shen et al., 2016) and the role of the adventitial CD34+SCs/TCs in the arterial intimal thickening in adenocarcinomas of colon also requires further study.

CONCLUSION

We demonstrate that, during repair in the gallbladder and colon, αSMA+ myofibroblasts develop in areas in which resident CD34+SCs/TCs are present, but not where these cells are absent. Likewise, αSMA+ cells can or cannot develop depending

on the regional-specific location of resident CD34+SCs/TCs. These findings support the hypotheses that myofibroblasts in repair originate from CD34+SCs/TCs and that subpopulations of CD34+SCs/TCs have different roles. Further studies are required in this field, including electron microscopy observation.

DATA AVAILABILITY STATEMENT

The raw data supporting the conclusions of this article will be made available by the authors, without undue reservation.

ETHICS STATEMENT

Ethical approval for this study was obtained from the Ethics Committee of La Laguna University (Comité de Ética de la Investigación y de Bienestar Animal, CEIBA 2020-0382), including the dissociation of the samples from any information that could identify the patient. The authors therefore had no access to identifiable patient information.

AUTHOR CONTRIBUTIONS

LD-F designed the study, acquired, analyzed and interpreted the data, and drafted and revised the manuscript. RG contributed to the study design, analyzed and interpreted the data, and drafted and revised the manuscript. MG analyzed and interpreted the data. MG-G interpreted immunofluorescence in confocal microscopy. LD-F Jr., HA-A, and JC analyzed and interpreted the data and revised the manuscript. All authors listed have reviewed and approved the final version of the manuscript for submission.

ACKNOWLEDGMENTS

The authors would like to thank Kim Eddy for the English revision.

REFERENCES

Bani, D., Formigli, L., Gherghiceanu, M., and Faussone-Pellegrini, M. S. (2010). Telocytes as supporting cells for myocardial tissue organization in developing and adult heart. *J. Cell Mol. Med.* 14, 2531–2538. doi: 10.1111/j.1582-4934.2010.01119.x

Bani, D., and Nistri, S. (2014). New insights into the morphogenic role of stromal cells and their relevance for regenerative medicine. Lessons from the heart. *J. Cell Mol. Med.* 18, 363–370. doi: 10.1111/jcmm.12247

Barth, P. J., Moll, R., and Ramaswamy, A. (2005). Stromal remodeling and SPARC (secreted protein acid rich in cysteine) expression in invasive ductal carcinomas of the breast. *Virch. Arch.* 446, 532–536. doi: 10.1007/s00428-005-1256-9

Barth, P. J., Ebrahimsade, S., Ramaswamy, A., and Moll, R. (2002a). CD34+ fibrocytes in invasive ductal carcinoma, ductal carcinoma in situ, and benign breast lesions. *Virch. Arch.* 440, 298–303. doi: 10.1007/s004280100530

Barth, P. J., Ramaswamy, A., and Moll, R. (2002b). CD34(+) fibrocytes in normal cervical stroma, cervical intraepithelial neoplasia III, and invasive squamous cell carcinoma of the cervix uteri. *Virch. Arch.* 441, 564–568. doi: 10.1007/s00428-002-0713-y

Barth, P. J., Schenck zu Schweinsberg, T., Ramaswamy, A., and Moll, R. (2004). CD34+ fibrocytes, alpha-smooth muscle antigen-positive myofibroblasts, and CD117 expression in the stroma of invasive squamous cell carcinomas of the oral cavity, pharynx, and larynx. *Virch. Arch.* 444, 231–234. doi: 10.1007/s00428-003-0965-1

Ceafalan, L., Gherghiceanu, M., Popescu, L. M., and Simionescu, O. (2012). Telocytes in human skin–are they involved in skin regeneration? *J. Cell Mol. Med.* 16, 1405–1420. doi: 10.1111/j.1582-4934.2012.01580.x

Chauhan, H., Abraham, A., Phillips, J. R., Pringle, J. H., Walker, R. A., and Jones, J. L. (2003). There is more than one kind of myofibroblast: analysis of CD34 expression in benign, in situ, and invasive breast lesions. *J. Clin. Pathol.* 56, 271–276. doi: 10.1136/jcp.56.4.271

Corrêa Bellagamba, B., Grudzinski, P. B., Ely, P. B., Nader, P. J. H., Nardi, N. B., and da Silva Meirelles, L. (2018). Induction of expression of CD271 and CD34 in mesenchymal stromal cells cultured as spheroids. *Stem Cells Int.* 2018:7357213. doi: 10.1155/2018/7357213

Cretoiu, D., Radu, B. M., Banciu, A., Banciu, D. D., and Cretoiu, S. M. (2017). Telocytes heterogeneity: From cellular morphology to functional evidence. *Semin. Cell. Dev. Biol.* 64, 26–39. doi: 10.1016/j.semcdb.2016.08.023

Cretoiu, D., Roatesi, S., Bica, I., Plesca, C., Stefan, A., Bajenaru, O., et al. (2020). Simulation and modeling of telocytes behavior in signaling and intercellular communication processes. *Int. J. Mol. Sci.* 21, 2615. doi: 10.3390/ijms21072615

Cretoiu, D., Xu, J., Xiao, J., and Cretoiu, S. M. (2016). Telocytes and their extracellular vesicles-evidence and hypotheses. *Int. J. Mol. Sci.* 17, 1322. doi: 10.3390/ijms17081322

da Silva Meirelles, L., Bellagamba, B. C., Camassola, M., and Nardi, N. B. (2016). Mesenchymal stem cells and their relationship to pericytes. *Front. Biosci.* 21:130–156. doi: 10.2741/4380

da Silva Meirelles, L., Chagastelles, P. C., and Nardi, N. B. (2006). Mesenchymal stem cells reside in virtually all post-natal organs and tissues. *J. Cell. Sci.* 119, 2204–2213. doi: 10.1242/jcs.02932

da Silva Meirelles, L., Malta, T. M., Panepucci, R. A., and da Silva, W. A. Jr. (2015). Transcriptomic comparisons between cultured human adipose tissue-derived pericytes and mesenchymal stromal cells. *Genom. Data* 7, 20–25. doi: 10.1016/j.gdata.2015.11.009

Díaz-Flores, L., Gutiérrez, R., Díaz-Flores, L. Jr., Goméz, M. G., Sáez, F. J., and Madrid, J. F. (2016a). Behaviour of telocytes during physiopathological activation. *Semin. Cell Dev. Biol.* 55, 50–61. doi: 10.1016/j.semcdb.2016.01.035

Díaz-Flores, L., Gutiérrez, R., García, M. P., González, M., Díaz-Flores, L., and Madrid, J. F. (2016b). Telocytes as a source of progenitor cells in regeneration and repair through granulation tissue. *Curr. Stem Cell Res. Ther.* 11, 395–403. doi: 10.2174/1574888x10666151001115111

Díaz-Flores, L., Gutiérrez, R., García, M. P., Sáez, F. J., Aparicio, F., Díaz-Flores, L., et al. (2014). Uptake and intracytoplasmic storage of pigmented particles by human CD34+ stromal cells/telocytes: endocytic property of telocytes. *J. Cell Mol. Med.* 18, 2478–2487. doi: 10.1111/jcmm.12437

Díaz-Flores, L., Gutiérrez, R., García, M. P., González, M., Sáez, F. J., Aparicio, F., et al. (2015a). Human resident CD34+ stromal cells/telocytes have progenitor capacity and are a source of αSMA+ cells during repair. *Histol. Histopathol.* 30, 615–627. doi: 10.14670/HH-30.615

Díaz-Flores, L., Gutiérrez, R., Lizartza, K., Goméz, M. G., García, M. D. P., Sáez, F. J., et al. (2015b). Behavior of in situ human native adipose tissue CD34+ stromal/progenitor cells during different stages of repair. Tissue-resident CD34+ stromal cells as a source of myofibroblasts. *Anat. Rec.* 298, 917–930. doi: 10.1002/ar.23086

Ebrahimsade, S., Westhoff, C. C., and Barth, P. J. (2007). CD34+ fibrocytes are preserved in most invasive lobular carcinomas of the breast. *Pathol. Res. Prac.* 203, 695–698. doi: 10.1016/j.prp.200

Faussone Pellegrini, M. S., and Popescu, L. M. (2011). Telocytes. *Biomol. Concepts* 2, 481–489. doi: 10.1515/BMC.2011.039

Faussone-Pellegrini, M. S., and Bani, D. (2010). Relationships between telocytes and cardiomyocytes during pre- and post-natal life. *J. Cell Mol. Med.* 14, 1061–1063. doi: 10.1111/j.1582-4934.2010.01074.x

Gherghiceanu, M., and Popescu, L. M. (2012). Cardiac telocytes - their junctions and functional implications. *Cell Tissue Res.* 348, 265–279. doi: 10.1007/s00441-012-1333-8

Hinescu, M. E., Ardeleanu, C., Gherghiceanu, M., and Popescu, L. M. (2007). Interstitial Cajal-like cells in human gallbladder. *J. Mol. Histol.* 38, 275–284. doi: 10.1007/s10735-007-9099-0

Kuroda, N., Guo, L., Miyazaki, E., Hamauzu, T., Toi, M., Hiroi, M., et al. (2005a). The appearance of myofibroblasts and the disappearance of CD34-positive stromal cells in the area adjacent to xanthogranulomatous foci of chronic cholecystitis. *Histol. Histopathol.* 20, 127–133. doi: 10.14670/HH-20.127

Kuroda, N., Jin, Y. L., Hamauzu, T., Toi, M., Miyazaki, E., Hiroi, M., et al. (2005b). Consistent lack of CD34-positive stromal cells in the stroma of malignant breast lesions. *Histol. Histopathol.* 20, 707–712. doi: 10.14670/HH-20.707

Kuroda, N., Nakayama, H., Miyazaki, E., Toi, M., Hiroi, M., and Enzan, H. (2005c). The distribution of CD34-positive stromal cells and myofibroblasts in colorectal carcinoid tumors. *Histol. Histopathol.* 20, 27–33. doi: 10.14670/HH-20.27

Lin, C. S., Xin, Z. C., Deng, C. H., Ning, H., Lin, G., and Lue, T. F. (2010). Defining adipose tissue-derived stem cells in tissue and in culture. *Histol. Histopathol.* 25, 807–815. doi: 10.14670/HH-25.807

Lin, G., Garcia, M., Ning, H., Banie, L., Guo, Y. L., Lue, T. F., et al. (2008). Defining stem and progenitor cells within adipose tissue. *Stem Cells Dev.* 17, 1053–1063. doi: 10.1089/scd.2008.0117

Manetti, M., Tani, A., Rosa, I., Chellini, F., Squecco, R., Idrizaj, E., et al. (2019). Morphological evidence for telocytes as stromal cells supporting satellite cell activation in eccentric contraction-induced skeletal muscle injury. *Sci. Rep.* 9:14515. doi: 10.1038/s41598-019-51078-z

Nakayama, H., Enzan, H., Miyazaki, E., Kuroda, N., Naruse, K., and Hiroi, M. (2000). Differential expression of CD34 in normal colorectal tissue, peritumoral inflammatory tissue, and tumour stroma. *J. Clin. Pathol.* 53, 626–629. doi: 10.1136/jcp.53.8.626

Nakayama, H., Enzan, H., Miyazaki, E., Kuroda, N., Naruse, K., Kiyoku, H., et al. (2001). CD34 positive stromal cells in gastric adenocarcinomas. *J. Clin. Pathol.* 54, 846–848. doi: 10.1136/jcp.54.11.846

Nakayama, H., Enzan, H., Miyazaki, E., Moriki, T., Toi, M., and Zhang, Y. (2002a). CD34-positive stromal cells and alpha-smooth muscle actin-positive stromal cells in the tumor capsule of skin sweat gland neoplasms. *Pathol. Int.* 52, 25–30. doi: 10.1046/j.1440-1827.2002.01317.x

Nakayama, H., Enzan, H., Miyazaki, E., and Toi, M. (2002b). Alpha smooth muscle actin positive stromal cells in gastric carcinoma. *J. Clin. Pathol.* 55, 741–744. doi: 10.1136/jcp.55.10.741

Nakayama, H., Enzan, H., Yamamoto, M., Miyazaki, E., Hidaka, C., Okumichi, T., et al. (2003). CD34-positive stromal cells in primary lung carcinomas. *Oncol. Rep.* 10, 1313–1316.

Nicolescu, M. I., Bucur, A., Dinca, O., Rusu, M. C., and Popescu, L. M. (2012). Telocytes in parotid glands. *Anat. Rec.* 295, 378–385. doi: 10.1002/ar.21540

Nicolescu, M. I., and Popescu, L. M. (2012). Telocytes in the interstitium of human exocrine pancreas: ultrastructural evidence. *Pancreas* 41, 949–956. doi: 10.1097/MPA.0b013e31823fbded

Nimphius, W., Moll, R., Olbert, P., Ramaswamy, A., and Barth, P. J. (2007). CD34+ fibrocytes in chronic cystitis and noninvasive and invasive urothelial carcinomas of the urinary bladder. *Virch. Arch.* 450, 179–185. doi: 10.1007/s00428-006-0347-6

Parra-Blanco, A., Gimeno-García, A. Z., Nicolás-Pérez, D., García, C., Medina, C., Díaz-Flores, L., et al. (2006). Risk for high-grade dysplasia or invasive carcinoma in colorectal flat adenomas in a Spanish population. *Gastroenterol. Hepatol.* 29, 602–609. doi: 10.1016/s0210-5705(06)71700-9

Pieri, L., Vannucchi, M. G., and Faussone-Pellegrini, M. S. (2008). Histochemical and ultrastructural characteristics of an interstitial cell type different from ICC and resident in the muscle coat of human gut. *J. Cell. Mol. Med.* 12, 1944–1955. doi: 10.1111/j.1582-4934.2008.00461.x

Popescu, L. M. (2011). The tandem: telocytes-stem cells. *Int. J. Biol. Biomed. Eng.* 5, 83–92.

Popescu, L. M., and Faussone-Pellegrini, M. S. (2010). Telocytes - a case of serendipity: the winding way from Interstitial Cells of Cajal (ICC), via Interstitial Cajal-Like Cells (ICLC) to telocytes. *J. Cell. Mol. Med.* 14, 729–740. doi: 10.1111/j.1582-4934.2010.01059.x

Popescu, L. M., Manole, E., Serboiu, C. S., Manole, C. G., Suciu, L. C., Gherghiceanu, M., et al. (2011). Identification of telocytes in skeletal muscle interstitium: Implication for muscle regeneration. *J. Cell Mol. Med.* 15, 1379–1392. doi: 10.1111/j.1582-4934.2011.01330.x

Popescu, L. M., and Nicolescu, M. I. (2013). "Telocytes and stem cells," in *Resident Stem Cells and Regenerative Therapy*, eds R. Coeli dos Santos Goldenberg and A. C. Campos de Carvalho (Waltham, MA: Academic Press/Elsevier), 205–231. doi: 10.1016/b978-0-12-416012-5.00011-6

Pusztaszeri, M. P., Seelentag, W., and Bosman, F. T. (2006). Immunohistochemical expression of endothelial markers CD31, CD34, von Willebrand factor, and Fli-1 in normal human tissues. *J. Histochem. Cytochem.* 54, 385–395. doi: 10.1369/jhc.4A6514.2005

Ramaswamy, A., Moll, R., and Barth, P. J. (2003). CD34+ fibrocytes in tubular carcinomas and radial scars of the breast. *Virch. Arch.* 443, 536–540. doi: 10.1007/s00428-003-0855-6

Rusu, M. C., Cretoiu, D., Vrapciu, A. D., Hostiuc, S., Dermengiu, D., Manoiu, V. S., et al. (2016). Telocytes of the human adult trigeminal ganglion. *Cell. Biol. Toxicol.* 32, 199–207. doi: 10.1007/s10565-016-9328-y

Shen, Y., Wu, Y., Zheng, Y., Ao, F., Kang, K., Wan, Y., et al. (2016). Responses of adventitial CD34(+) vascular wall-resident stem/progenitor cells and medial smooth muscle cells to carotid injury in rats. *Exp. Mol. Pathol.* 101, 332–340. doi: 10.1016/j.yexmp.2016.11.004

Vannucchi, M. G., Bani, D., and Faussone-Pellegrini, M. S. (2016). Telocytes contribute as cell progenitors and differentiation inductors in tissue regeneration. *Curr. Stem Cell Res. Ther.* 11, 383–389. doi: 10.2174/1574888x10666150528142741

Vannucchi, M. G., Traini, C., Guasti, D., Del Popolo, G., and Faussone-Pellegrini, M. S. (2014). Telocytes subtypes in human urinary bladder. *J. Cell Mol. Med.* 18, 2000–2008. doi: 10.1111/jcmm.12375

Vannucchi, M. G., Traini, C., Manetti, M., Ibba-Manneschi, L., and Faussone-Pellegrini, M. S. (2013). Telocytes express PDGFRα in the human gastrointestinal tract. *J. Cell. Mol. Med.* 17, 1099–1108. doi: 10.1111/jcmm.12134

Vannucchi, M. G., and Faussone-Pellegrini, M. S. (2016). "The telocyte subtypes," in *Telocytes. Advances in Experimental Medicine and Biology*, Vol. 913, eds X. Wang and D. Cretoiu (Singapore: Springer).

Wessel, C., Westhoff, C. C., Nowak, K., Moll, I., and Barth, P. J. (2008). CD34(+) fibrocytes in melanocytic nevi and malignant melanomas of the skin. *Virch. Arch.* 453, 485–489. doi: 10.1007/s00428-008-0667-9

Conflict of Interest: The authors declare that the research was conducted in the absence of any commercial or financial relationships that could be construed as a potential conflict of interest.

frontiers in Cell and Developmental Biology

ORIGINAL RESEARCH
published: 03 November 2020
doi: 10.3389/fcell.2020.553444

Scalable Production of Human Mesenchymal Stromal Cell-Derived Extracellular Vesicles Under Serum-/Xeno-Free Conditions in a Microcarrier-Based Bioreactor Culture System

Miguel de Almeida Fuzeta[1,2], Nuno Bernardes[1], Filipa D. Oliveira[2], Ana Catarina Costa[1], Ana Fernandes-Platzgummer[1], José Paulo Farinha[3], Carlos A. V. Rodrigues[1], Sunghoon Jung[4], Rong-Jeng Tseng[5], William Milligan[5], Brian Lee[4], Miguel A. R. B. Castanho[2], Diana Gaspar[2], Joaquim M. S. Cabral[1] and Cláudia Lobato da Silva[1]**

[1] iBB-Institute for Bioengineering and Biosciences and Department of Bioengineering, Instituto Superior Técnico, Universidade de Lisboa, Lisbon, Portugal, [2] Instituto de Medicina Molecular, Faculdade de Medicina, Universidade de Lisboa, Lisbon, Portugal, [3] Centro de Química Estrutural and Department of Chemical Engineering, Instituto Superior Técnico, Universidade de Lisboa, Lisbon, Portugal, [4] PBS Biotech Inc., Camarillo, CA, United States, [5] AventaCell Biomedical Corp., Atlanta, GA, United States

Mesenchymal stromal cells (MSC) hold great promise for tissue engineering and cell-based therapies due to their multilineage differentiation potential and intrinsic immunomodulatory and trophic activities. Over the past years, increasing evidence has proposed extracellular vesicles (EVs) as mediators of many of the MSC-associated therapeutic features. EVs have emerged as mediators of intercellular communication, being associated with multiple physiological processes, but also in the pathogenesis of several diseases. EVs are derived from cell membranes, allowing high biocompatibility to target cells, while their small size makes them ideal candidates to cross biological barriers. Despite the promising potential of EVs for therapeutic applications, robust manufacturing processes that would increase the consistency and scalability of EV production are still lacking. In this work, EVs were produced by MSC isolated from different human tissue sources [bone marrow (BM), adipose tissue (AT), and umbilical cord matrix (UCM)]. A serum-/xeno-free microcarrier-based culture system was implemented in a Vertical-Wheel^{TM} bioreactor (VWBR), employing a human platelet lysate culture supplement (UltraGRO^{TM}-PURE), toward the scalable production of MSC-derived EVs (MSC-EVs). The morphology and structure of the manufactured EVs were assessed by atomic force microscopy, while EV protein markers were successfully identified in EVs by Western blot, and EV surface charge was maintained relatively constant (between -15.5 ± 1.6 mV and -19.4 ± 1.4 mV), as determined by zeta potential measurements. When compared to traditional culture systems under static conditions (T-flasks), the VWBR system allowed the production of EVs at higher

OPEN ACCESS

Edited by:
Lindolfo da Silva Meirelles, Universidade Luterana do Brazil, Brazil

Reviewed by:
Laura Iop, University of Padua, Italy
Milena Botelho Pereira Soares, Gonçalo Moniz Institute (IGM), Brazil

***Correspondence:**
Nuno Bernardes
nuno.bernardes@tecnico.ulisboa.pt
Cláudia Lobato da Silva
claudia_lobato@tecnico.ulisboa.pt

Specialty section:
This article was submitted to Stem Cell Research, a section of the journal Frontiers in Cell and Developmental Biology

Received: *18 April 2020*
Accepted: *05 October 2020*
Published: *03 November 2020*

Citation:
de Almeida Fuzeta M, Bernardes N, Oliveira FD, Costa AC, Fernandes-Platzgummer A, Farinha JP, Rodrigues CAV, Jung S, Tseng R-J, Milligan W, Lee B, Castanho MARB, Gaspar D, Cabral JMS and da Silva CL (2020) Scalable Production of Human Mesenchymal Stromal Cell-Derived Extracellular Vesicles Under Serum-/Xeno-Free Conditions in a Microcarrier-Based Bioreactor Culture System. Front. Cell Dev. Biol. 8:553444. doi: 10.3389/fcell.2020.553444

concentration (i.e., EV concentration in the conditioned medium) (5.7-fold increase overall) and productivity (i.e., amount of EVs generated per cell) (3-fold increase overall). BM, AT and UCM MSC cultured in the VWBR system yielded an average of $2.8 \pm 0.1 \times 10^{11}$, $3.1 \pm 1.3 \times 10^{11}$, and $4.1 \pm 1.7 \times 10^{11}$ EV particles ($n = 3$), respectively, in a 60 mL final volume. This bioreactor system also allowed to obtain a more robust MSC-EV production, regarding their purity, compared to static culture. Overall, we demonstrate that this scalable culture system can robustly manufacture EVs from MSC derived from different tissue sources, toward the development of novel therapeutic products.

Keywords: extracellular vesicles, mesenchymal stromal cells (MSC), scalable production, bioreactors, serum-/xenogeneic-free

INTRODUCTION

Mesenchymal stromal cells (MSC) exhibit multilineage differentiation ability, as well as intrinsic immunomodulatory and trophic activities, standing as promising candidates for tissue engineering and cell-based therapies (Caplan and Dennis, 2006; da Silva Meirelles et al., 2009). MSC are able to inhibit apoptosis and scarring (fibrosis), promote angiogenesis and support growth and differentiation of progenitor cells into functional regenerative units (Caplan and Dennis, 2006; da Silva Meirelles et al., 2009). The array of beneficial effects attributed to MSC has made them one of the most studied cells in clinical trials (Heathman et al., 2015). The trophic activity of MSC relies greatly on the secretion of bioactive factors that assist in repair and regeneration processes through paracrine signaling (Caplan and Dennis, 2006; da Silva Meirelles et al., 2009).

Recently, increasing evidence suggests that several MSC-associated paracrine therapeutic features are mediated by extracellular vesicles (EVs) (Bruno et al., 2009; Lai et al., 2010; Lener et al., 2015; Börger et al., 2017). EVs, such as exosomes and microvesicles, are lipid membrane enclosed structures actively secreted by cells. These vesicles have emerged as relevant mediators of intercellular communication, through the transfer of a cargo of proteins and RNA (i.e., microRNA and mRNA), which trigger alterations on host cells (Raposo et al., 1996; Ratajczak et al., 2006; Valadi et al., 2007). Their small size (generally 50 – 1000 nm) and resemblance to the cell membrane makes EVs ideal candidates to cross biological barriers, thus providing high biocompatibility to target cells (Alvarez-Erviti et al., 2011; El Andaloussi et al., 2013; Van Niel et al., 2018).

EV can be used in therapeutic settings through two different approaches. On one hand, EVs are able to mediate some of the therapeutic effects from their cells of origin (Lai et al., 2010; Bruno et al., 2012). Therefore, EVs could be potentially used in substitution of their cell of origin, as a cell-free therapy triggering equivalent therapeutic effect. On the other hand, EVs can be used as drug delivery vehicles, by loading EVs with therapeutic cargo, as an alternative to synthetic drug delivery systems (Batrakova and Kim, 2015).

MSC are particularly interesting for EV production for a number of reasons. MSC are considered immune evasive cells and the safety of their administration has already been confirmed in a number of clinical trials (Lalu et al., 2012). Therefore, it is reasonable to assume that MSC-derived EVs (MSC-EVs) are not prone to immune reaction from the host immune system (Mendt et al., 2018; Elahi et al., 2020), and promising for the development of allogeneic (i.e., off-the-shelf) therapeutic products. MSC are intrinsically therapeutic, with promising applications for multiple diseases and MSC-EVs convey similar benefits as well (Lener et al., 2015; Phinney and Pittenger, 2017). Finally, MSC show great ability for expansion when cultured *ex vivo* and robust expansion platforms have already been established (Rafiq et al., 2013; dos Santos et al., 2014; Schirmaier et al., 2014; Carmelo et al., 2015; Mizukami et al., 2016; Lawson et al., 2017).

Despite the promising potential of EVs for therapeutic applications, robust manufacturing processes that would increase the consistency and scalability of EV production are still lacking. Similarly to the cell therapy context, where large cell numbers per dose are required (Ren et al., 2012; Golpanian et al., 2016; Wysoczynski et al., 2018), very large numbers of EVs are expected to be required for clinical use (e.g., each patient may require 0.5 – 1.4×10^{11} EVs, Kordelas et al., 2014). In order to achieve such large production capacities, robust and scalable manufacturing processes need to be developed.

The development of cell-based therapies faces multiple challenges (recently reviewed de Almeida Fuzeta et al., 2019) and these also apply to manufacturing of EV products. One of these challenges is the use of appropriate cell culture medium. The most commonly used culture medium supplement in *ex vivo* expansion platforms of MSC is fetal bovine serum (FBS), which presents several disadvantages when considering the production of cell-based therapies for human use due to their animal origin. As an alternative to animal derived products, serum-/xenogeneic-free (S/XF) culture supplements have been developed, such as human platelet lysates (hPL).

Another major challenge is determining the appropriate cell culture platform for scalable manufacturing of cell-based therapies (de Almeida Fuzeta et al., 2019). In order to achieve large product batches for clinical use, culture platforms require scalability as well as the ability to monitor and control culture parameters, which cannot be accomplished in traditional static culture systems. Multiple bioreactor configurations operating in dynamic culture conditions have been developed for this

purpose (de Soure et al., 2016; de Almeida Fuzeta et al., 2019). Expansion of MSC immobilized on microcarriers has been explored in stirred-tank bioreactor configurations (de Soure et al., 2016; de Almeida Fuzeta et al., 2019). These bioreactors use an agitation system to maintain microcarriers in suspension and allow medium homogenization. However, agitation impacts cellular physiology due to increased shear stress.

In order to improve agitation patterns in cell culture, PBS Biotech has developed scalable Vertical-Wheel^{TM} bioreactors (VWBR) that can provide gentle and uniform mixing with minimal shear stress. A vertically rotating wheel promotes radial and axial fluid flow and creates a more homogeneous hydrodynamic environment compared with traditional stirred-tank bioreactors. In addition, the Vertical-Wheel^{TM} impeller can fully suspend microcarriers with minimal power input and thus minimize shear stress effects (Croughan et al., 2016). Moreover, this technology is scalable, being available at working volumes that range from 100 mL up to 500 L. Recently, VWBR have been successfully applied in microcarrier-based cell culture processes for the expansion of MSC from multiple sources (Sousa et al., 2015; de Sousa Pinto et al., 2019), as well as for human induced pluripotent stem cells (Rodrigues et al., 2018; Nogueira et al., 2019).

In this work, EVs were produced by MSC isolated from different human tissue sources, namely bone marrow (BM), adipose tissue (AT), and umbilical cord matrix (UCM). A S/XF microcarrier-based culture system was implemented in a single-use VWBR, employing a hPL culture supplement (UltraGRO^{TM}-PURE), toward the production of MSC-EVs.

When compared with traditional static culture systems (i.e., T-flasks), the bioreactor-based culture system allowed a substantial improvement in EV production. This culture system is expected to contribute to robustly manufacture human MSC-EVs in a scalable manner, which can be applied as intrinsic medicines or as delivery vehicles in different therapeutic settings.

MATERIALS AND METHODS

MSC Isolation From Human Samples

Human MSC used in this study are part of the cell bank available at the Stem Cell Engineering Research Group (SCERG), iBB-Institute for Bioengineering and Biosciences at Instituto Superior Técnico (IST). MSC were previously isolated/expanded according to protocols previously established at iBB-IST. UCM MSC were isolated in hPL-supplemented medium according to the protocol described by de Soure et al. (2017). BM MSC were isolated in hPL-supplemented medium by adapting the protocol for cell isolation using FBS-supplemented medium described by dos Santos et al. (2010). AT MSC were originally isolated in FBS-supplemented medium according to Oliveira et al. (2012), cryopreserved and later adapted for 1 or 2 passages to hPL-supplemented medium. Originally, human tissue samples were obtained from local hospitals under collaboration agreements with iBB-IST (bone marrow: Instituto Português de Oncologia Francisco Gentil, Lisboa; adipose tissue: Clínica de Todos-os-Santos, Lisboa; umbilical cord: Hospital São Francisco Xavier, Lisboa, Centro Hospitalar Lisboa Ocidental, Lisboa). All human samples were obtained from healthy donors after written informed consent according to the Directive 2004/23/EC of the European Parliament and of the Council of 31 March 2004 on setting standards of quality and safety for the donation, procurement, testing, processing, preservation, storage and distribution of human tissues and cells (Portuguese Law 22/2007, June 29), with the approval of the Ethics Committee of the respective clinical institution. Human MSC from the different sources (BM, AT, and UCM) were cryopreserved in a liquid/vapor-phase nitrogen container.

MSC Expansion in Static Conditions

In general, MSC expansion in static conditions was performed as previously described (de Sousa Pinto et al., 2019). In summary, previously isolated BM, AT and UCM MSC were thawed and plated on T-flasks (Falcon), at a cell density between 3000–6000 cell/cm^2. MSC were cultured in low glucose (1 g/L) Dulbecco's Modified Eagle's Medium (DMEM) (Gibco, Life Technologies), supplemented with 5% v/v of the human platelet lysate (hPL) UltraGRO^{TM}-PURE (AventaCell Biomedical) and Antibiotic-Antimycotic (1x) (Gibco, Life Technologies).

Cells were maintained at 37°C and 5% CO_2 in a humidified atmosphere and culture medium was changed every 3–4 days. At 70–80% cell confluence, MSC were detached from the flasks using the xeno-free cell detachment solution TrypLE^{TM} Select (1x) (Gibco, Life Technologies) for 7 min at 37°C. Cell number and viability were determined using the Trypan Blue (Gibco, Life Technologies) exclusion method.

After thawing, MSC were passaged at least once before either final inoculation in T-flasks for EV production under static conditions or inoculation in VWBR. MSC were always plated at 3000 cell/cm^2. For each cell source, MSC from three independent donors (n = 3) in passages (P) from P4 to P5 were used to inoculate either the final T-flasks for EV production or the VWBR [specifically, BM1 (P4); BM2 (P5); BM3 (P4); AT1 (P4); AT2 (P4); AT3 (P5); UCM1 (P4); UCM2 (P4); UCM3 (P5)] (**Figure 1**).

MSC-EV Production Under Static Conditions

For the production of MSC-EVs under static conditions, previously cultured MSC were passaged to T-175 flasks, at 3000 cells/cm^2. Cells were cultured in the same conditions described before for MSC expansion under static conditions. When maximum cell confluency in the flasks was achieved (90–100%), cells were washed once with basal DMEM low glucose (i.e., supplemented only with Antibiotic-Antimycotic) and subsequently cultured for 48 h in basal DMEM low glucose (20 mL per T-175), for medium conditioning. At the end of the 48 h period, the conditioned medium was recovered, centrifuged (360 × g, 10 min) to remove cell debris and stored at 4°C for less than 1 week until processing for EV isolation.

After recovery of the conditioned medium, MSC were detached from the flasks and cell number was determined as previously described. Cells were re-suspended in

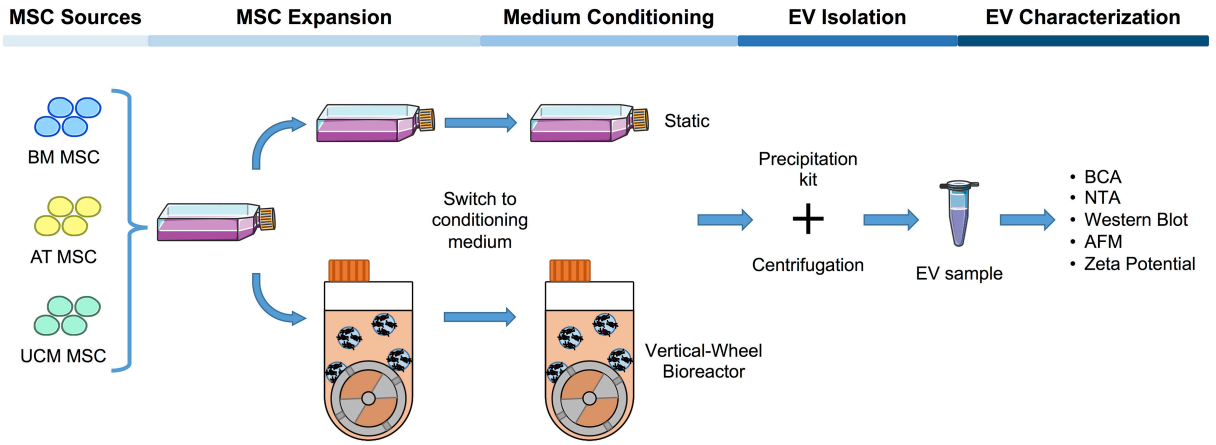

FIGURE 1 | Workflow of the production and characterization of MSC-EVs in bioreactors and static systems. MSC were isolated from three different human tissue sources: BM, AT, and UCM. Firstly, MSC were expanded in static conditions (i.e., T-flasks) in hPL supplemented DMEM. These cells were subsequently used to inoculate a VWBR (5M cells; 100 mL final working volume), as well as to maintain a static culture in T-175 flasks. For each cell source, MSC from three independent donors (n = 3; BM1, 2, 3; AT1, 2, 3; UCM1, 2, 3) were used to inoculate either the final T-flasks for EV production or the VWBR, in passages from P4 to P5 [specifically, BM1 (P4); BM2 (P5); BM3 (P4); AT1 (P4); AT2 (P4); AT3 (P5); UCM1 (P4); UCM2 (P4); UCM3 (P5)]. Upon reaching stationary growth phase in VWBR or maximum confluency in static, the culture medium was changed for supplement-free culture medium and culture was maintained for 48 h. Over this period, culture medium was enriched in EVs secreted by cultured MSC. This conditioned culture medium was recovered and EVs were isolated by precipitation using a commercially available kit. Finally, EV production was quantified in both static and dynamic systems and samples were characterized using multiple techniques. MSC, mesenchymal stromal cells; EV, extracellular vesicles; VWBR, Vertical-Wheel^{TM} bioreactor; hPL, human platelet lysate; BM, bone marrow; AT, adipose tissue; UCM, umbilical cord matrix; NTA, nanoparticle tracking analysis; AFM, atomic force microscopy. The cells, T-flask and Eppendorf cartoons were obtained from Smart Servier Medical Art (https://smart.servier.com).

phosphate-buffered saline (PBS) for pelleting and stored at −80°C until further analysis (i.e., Western blots).

MSC Expansion and MSC-EV Production in the Bioreactor Culture System

Expansion of human MSC in VWBR was generally performed as previously described (de Sousa Pinto et al., 2019). In summary, previously isolated and expanded human MSC were inoculated in a PBS 0.1 MAG bioreactor (PBS Biotech Inc.) with a working volume of 100 mL. Animal product-free SoloHill plastic microcarriers (PALL) were used in order to provide a surface for MSC to adhere and proliferate. Inoculation in the VWBR was performed in 60 mL of the same culture medium used for static conditions (i.e., DMEM low glucose, 5% v/v UltraGRO^{TM}-PURE, Antibiotic-Antimycotic 1x), with an initial MSC number of 5×10^6 and 2 g of microcarriers. The VWBR was placed at 37°C and 5% CO_2 in a humidified atmosphere.

After an initial intermittent agitation regime, a continuous agitation mode was set at 25 rpm, as previously described (de Sousa Pinto et al., 2019). This agitation rate was always maintained, except for AT MSC culture, which required an increment in the agitation rate to 30 rpm at day 2 or 3 of culture and to 35 rpm at day 4 or 5, due to increased medium viscosity and the subsequent formation of cell aggregates.

After 2 days of culture, 40 mL of fresh culture medium with a glucose pulse (3 g/L) was added to the VWBR, achieving a final working volume of 100 mL. From this day onward, 25% v/v of culture medium was exchanged every 24 h, with the addition of fresh culture medium supplemented with a glucose pulse (3 g/L). Cell growth and viability were assessed every day, as previously described (de Soure et al., 2017). Growth rate was determined by performing an exponential fitting to experimental data corresponding to the exponential growth phase. Cell visualization on microcarriers was performed by staining the cells with 4′,6-diamidino-2- phenylindole (DAPI, Sigma, 1.5 μg/mL in PBS), as previously described (de Soure et al., 2017).

When MSC cultures reached stationary growth and the maximum cell concentration was achieved, the MSC expansion stage of the process was concluded and the EV production stage started. The culture medium was removed from the VWBR, after a 10 min sedimentation of cells attached to microcarriers inside the vessel. The VWBR was washed with 60 mL basal DMEM low glucose medium, at 30 rpm agitation, in order to remove hPL components. The cells on microcarriers were sedimented once again for 10 min and the washing medium was removed. MSC were kept in culture in the VWBR for 48 h in 60 mL basal DMEM low glucose medium, in the same conditions (i.e., agitation speed, temperature, O_2 and CO_2 concentrations) used for MSC expansion.

At the end of the 48 h period, the whole culture volume was recovered from the VWBR and transferred to 50 mL tubes (Falcon), where cells on microcarriers were sedimented for 10 min. The MSC conditioned medium was recovered and centrifuged at 360 × g for 10 min, to remove remaining microcarriers, cells and cell debris. Conditioned medium was stored at 4°C for less than 1 week until processing for EV isolation. After recovery of the conditioned medium, cells

attached to microcarriers were re-suspended in PBS and stored at −80°C for further analysis (i.e., Western blots).

Isolation of EVs From MSC Cultures

EV were isolated using the Total Exosome Isolation reagent (Invitrogen, Life Technologies), according to the manufacturer instructions. Briefly, MSC conditioned medium was centrifuged for 30 min at 2000 × *g*, to remove cell debris and incubated overnight at 4°C with the isolation reagent. This mixture was then centrifuged for 1 h at 10000 × *g* and 4°C. The supernatant was discarded and the EV fraction was recovered by thoroughly washing the walls of the centrifuge tube with PBS 1x (Invitrogen, Life Technologies) in UltraPure™ DNase/RNase-Free Distilled Water (Invitrogen, Life Technologies). EV samples were re-suspended in a PBS volume corresponding to a concentration factor of 20x to 70x relatively to the processed conditioned medium volume. EV samples were frozen at −80°C in aliquots (50–100 μL), in order to minimize freeze-thawing cycles.

Comprehensive Characterization of Manufactured EVs

Protein Quantification

Total protein was quantified in EV samples using the Pierce™ BCA Protein Assay Kit (Thermo Scientific), according to manufacturer instructions for the microplate procedure. Samples were quantified either undiluted or after a 2x dilution. Three replicates were quantified for each sample. Sample concentration was determined by applying a linear fit to the bovine serum albumin (BSA) standards and using the resulting equation to determine each sample concentration from its absorbance measurement.

Nanoparticle Tracking Analysis

EV size distribution profiles and concentration measurements were obtained by nanoparticle tracking analysis (NTA), using a NanoSight LM14c instrument equipped with a 405 nm laser (Malvern) and NTA software version 3.1 (Malvern). Silica 100 nm microspheres (Polysciences, Inc.) were routinely analyzed to check instrument performance (Gardiner et al., 2013). NTA acquisition and post-acquisition settings were optimized and kept constant for all samples. These settings were established using silica 100 nm microspheres (Gardiner et al., 2013) and subsequently adjusted for optimal detection of MSC-EVs.

EV samples were diluted in 2 mL of PBS 1x in UltraPure™ DNase/RNase-Free Distilled Water, to obtain a final concentration in the range of 5×10^8 to 3×10^9 particles/mL. Samples were measured using a camera level of 13. Acquisition temperature was controlled and maintained at 20°C. Each sample was recorded 10 times for 30 s, using fresh sample for each acquisition (by pushing the sample syringe). The detection chamber was thoroughly washed with PBS between each sample measurement. A threshold level of 7 was applied for video processing. Each video recording was analyzed to obtain the size and concentration of EVs.

Western Blot

Cells were lysed with Catenin lysis buffer (1% Triton X-100, Sigma, 1% Nonidet P-40, Sigma, in PBS) supplemented with protease inhibitor (Sigma) and phosphatase inhibitor (Sigma) for 10 min on ice and then centrifuged at 14000 × *g* for 10 min at 4°C to remove insoluble material. Supernatants were recovered and used as whole cell lysates (WCL). For CD63 and CD81 detection, cells and EV samples were lysed with RIPA lysis buffer (150 mM NaCl, 25 mM Tris pH 7.4, 1% Nonidet P-40, 0.5% sodium deoxycholate, 0.1% SDS) and sonicated (three rounds of 5 s, at 50% intensity). Total protein content in WCL and EV samples was quantified using the BCA kit as previously described.

Both WCL and EV samples were mixed with sample buffer in reducing conditions and heated to 100°C for 10 min. For CD63 and CD81 detection, urea containing sample buffer was used. All samples were loaded (6–30 μg of total protein) in 4–12% Bis–Tris polyacrylamide gels (Invitrogen, Life Technologies), in equal protein content for each gel, and subjected to electrophoresis.

Proteins were transferred into nitrocellulose membranes using a Power Blotter System (Invitrogen, Life Technologies). Membranes were blocked with 5% w/v non-fat dry milk solution in tris-buffered saline (TBS) Tween 20 buffer 1x (Thermo Fisher Scientific), for 1 h with mild orbital agitation at room temperature and incubated with primary antibodies overnight at 4°C. For CD63 and CD81 detection, membranes were blocked with 5% BSA solution in TBS Tween 20 buffer 1x. Finally, membranes were incubated with HRP conjugated secondary antibodies for 1 h at room temperature and Pierce™ ECL Western Blotting Substrate (Thermo Fisher Scientific) was applied for membrane revelation.

Primary antibodies included anti-Calnexin (1:1000, BD), anti-Synthenin (1:1000, Abcam), anti-CD63 (1:1000, Genetex), anti-CD81 (1:500, Abcam) and anti-GAPDH (1:1000, Santa Cruz). Secondary antibodies included Goat anti-Mouse IgG (H + L) Cross-Adsorbed Secondary Antibody, HRP (1:5000, Invitrogen, Life Technologies) and Goat anti-Rabbit IgG HRP-conjugated (1:1000, R&D Systems). Image acquisition was performed on iBright™ CL1500 Imaging System (Invitrogen, Life Technologies).

Atomic Force Microscopy Imaging

EV samples were prepared for atomic force microscopy (AFM) imaging in freshly cleaved mica without any previous dilution. A volume ranging between 30–70 μL was used and samples were allowed to deposit during 30 min to 2 h. After this period, the samples were washed with filtered MilliQ water and air dried. AFM imaging was performed with a JPK Nano Wizard IV mounted on a Zeiss Axiovert 200 inverted microscope (Carl Zeiss). The AFM head is equipped with a 15 μm z-range linearized piezoelectric scanner and an infrared laser. Uncoated silicon ACL cantilevers from AppNano were used, with resonance frequencies and spring constants ranging between 160–225 kHz and 36–90 N/m, respectively. Scan speeds were between 0.1 and 0.3 Hz. Total areas with 10 × 10 μm were scanned with a 512 × 512 pixel resolution, in AC mode. Height and error images were recorded, and line fitted. Image processing was performed on JPK SPM data processing software version spm-6.0.55.

Zeta Potential

EV samples were diluted to a final protein concentration of 25 μg/mL, in PBS. Samples were loaded into disposable zeta cells with gold electrodes and allowed to equilibrate for 15 min at 37°C. Zeta potential measurements consisted in a set of 15 runs, each one resulting from an automatically defined number of subruns (ranging from 10 to 100) performed on the Zetasizer Nano ZS (Malvern), at a constant voltage of 40 V.

Lactate Dehydrogenase Activity Measurements

Cell culture medium samples from VWBR cultures were recovered daily and centrifuged at 360 × *g* for 10 min, to remove remaining microcarriers, cells and cell debris. Lactate dehydrogenase (LDH) activity was quantified in cell culture supernatants using the Pierce LDH Cytotoxicity Assay Kit (Thermo Scientific) by adapting the manufacturer instructions for the microplate procedure. The same procedure was applied to a positive control (1 μL LDH Positive Control in 10 mL of 10% BSA in PBS). Three replicates were quantified for each sample. The LDH activity was reported as the quotient between the LDH activity of each sample and the LDH activity of the positive control, according with the following equation.

$$LDH\ activity(\%) = \frac{LDH_{sample}}{LDH_{pos.control}} \times 100$$

Statistical Analysis

Statistical analysis was performed using GraphPad Prism 8 Software. Results are presented as mean ± standard error of the mean (SEM) of the values obtained from different MSC donors (i.e., biological replicates) or as mean ± standard deviation (SD) of the values from technical replicates. Paired *t*-test was applied to evaluate the statistical significance of the differences in EV concentration and specific EV concentration in the conditioned medium from MSC cultures in static and VWBR systems. These data sets passed normality tests. *P*-values result from two-tailed tests with a 95% confidence interval. Differences were considered significant at $P < 0.05$ and statistical output was represented as $^{**} < 0.01$.

RESULTS

MSC Expansion and Medium Conditioning for MSC-EV Production From Three Different Human Sources (BM, AT and UCM) Was Achieved in the Bioreactor Culture System

Bioreactors have been implemented as scalable platforms for MSC manufacturing. Building on previous work from our group (de Sousa Pinto et al., 2019), a S/XF microcarrier-based culture system implemented in a VWBR originally targeting MSC expansion was adapted to the production of cell-derived products such as MSC-EVs and compared with traditional static culture systems (i.e., T-flasks) (**Figure 1**).

BM, AT and UCM MSC were successfully expanded in the VWBR system (**Figure 2A**, upper panel). The expansion of BM MSC was the most heterogeneous among donors ($n = 3$), with final post-expansion cell numbers ranging between $12.0 \pm 3.6 \times 10^6$ and $53.4 \pm 5.5 \times 10^6$, depending on BM donor. The expansion culture period also ranged from 7 to 11 days in BM MSC cultures. AT and UCM MSC expansion curves were more homogeneous, reaching an average of $29.2 \pm 1.7 \times 10^6$ and $19.9 \pm 2.4 \times 10^6$ cells, respectively, at the end of the expansion period. This expansion period was 7 days for AT MSC and 9–10 days for UCM MSC.

Estimated adhesion efficiency of MSC to microcarriers after VWBR inoculation was higher for AT MSC (110 ± 12%), followed by BM MSC (68 ± 17%) and UCM MSC (55 ± 4%) (**Table 1**). AT MSC adhered and started proliferating in less than 24 h, which resulted in estimated adhesion efficiencies higher than 100%. BM MSC showed the highest average growth rate ($0.47 \pm 0.05\ day^{-1}$), which was very similar to AT MSC ($0.45 \pm 0.06\ day^{-1}$), while UCM MSC showed the lowest growth rate ($0.35 \pm 0.09\ day^{-1}$), as a consequence of the lower initial adhesion efficiency observed.

In general, BM and AT MSC maintained cell viability close to 100% throughout culture (**Figure 2A**, lower panel). Cell viability suffered more oscillations in UCM MSC cultures, especially in the first days of culture.

Throughout the culture period, microcarrier colonization by cells increased progressively as MSC expanded (**Figure 2B**). The increasing microcarrier occupancy was followed by microcarrier aggregation, as MSC expansion reached higher cell numbers. We observed that cell expansion stopped when large microcarrier aggregates were formed, likely due to lack of surface available to attach and proliferate (**Figures 2A,B**).

In some cultures, a significant decrease in cell number was observed at the start of the medium conditioning stage, immediately after the culture medium was changed from hPL-supplemented medium to supplement-free culture medium. This can be explained, at least partially, by a possible removal of microcarriers during medium change operation, resulting in a loss of cells from the vessel. Additionally, it should be noticed that microcarrier aggregation might affect our estimation of cell numbers at this stage. In the medium conditioning stage, MSC were cultured for 48 h in a supplement-free medium, which could be a stress factor for cell culture. Although a decrease in the cell number was occasionally observed during the 48 h medium conditioning period, this was an exception rather than the rule (**Figure 2A**). High cell viabilities were maintained (**Figure 2A**) and there were no visible differences in microcarrier occupancy during this stage (**Figure 2B**). Still, in order to thoroughly assess if MSC were experiencing induced cell stress, the levels of LDH activity in culture were monitored during the 48 h conditioning period. LDH activity can be used as a readout of cell stress, as this toxic compound is released to cell culture medium upon plasma membrane damage (Racher et al., 1990). LDH activity did not change significantly over this period for any of the MSC sources (**Figure 2C**). Therefore, there were no indications that MSC were experiencing significant stress in stirred culture due to the absence of hPL in the 48 h conditioning period.

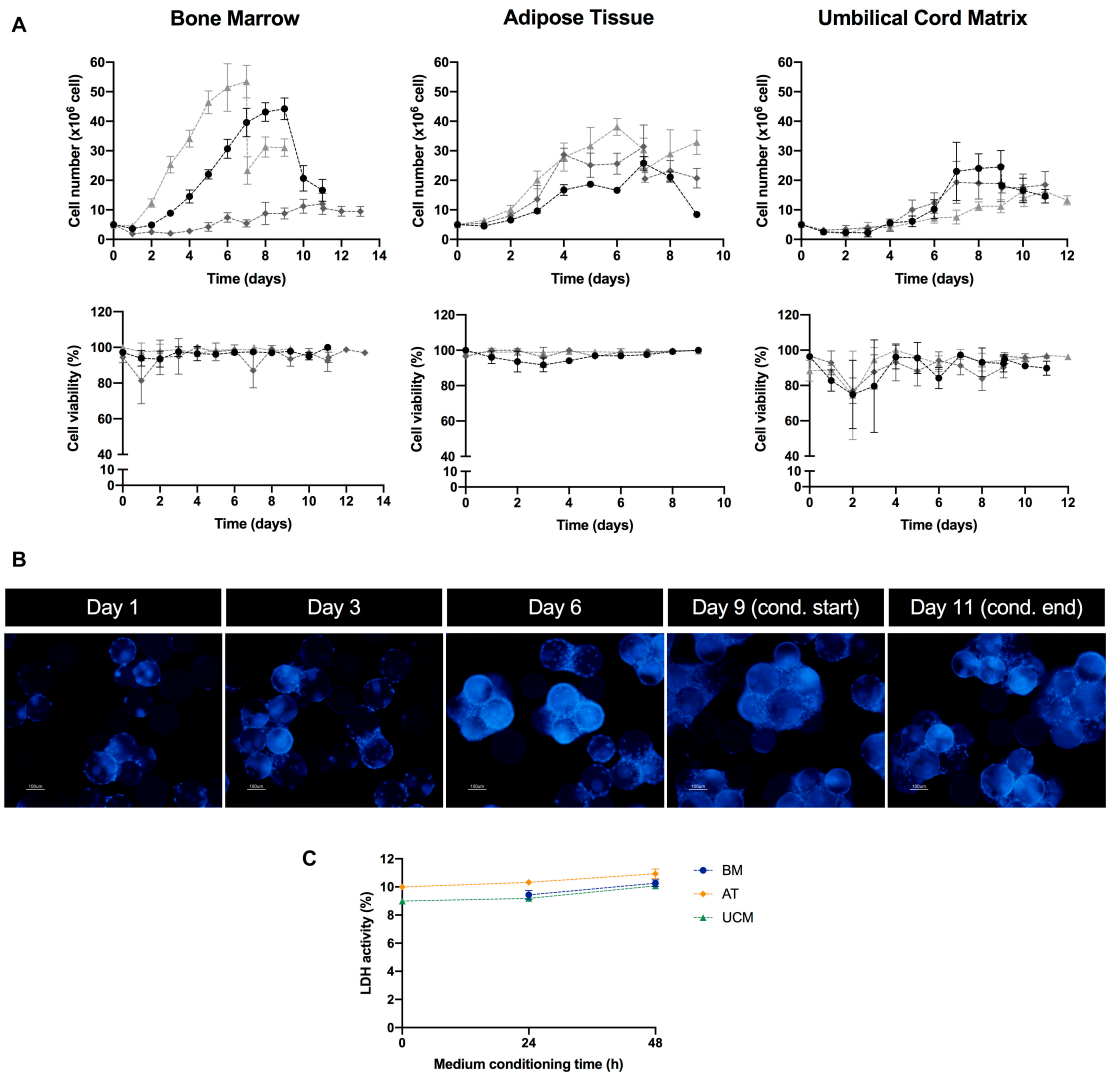

FIGURE 2 | MSC culture in the microcarrier-based bioreactor system. **(A)** Evolution of cell number (upper panel) and cell viability (lower panel) over culture period time, for MSC from three different human tissue sources (bone marrow, adipose tissue, and umbilical cord matrix). MSC from three different donors (i.e., three biological replicates) were used per tissue source, which are represented in three different shades of gray. Two data points are presented for the same day when the medium conditioning stage (i.e., EV production) started. Results are presented as mean ± SD of cell count for each time point. **(B)** Representative images of microcarrier occupation by MSC throughout culture. Cell nuclei were stained with DAPI and images were acquired using a fluorescence microscope. In this case, EV production started on day 9 of culture and finished on day 11. Scale bar = 100 μm. **(C)** LDH activity profile during the medium conditioning (i.e., EV production) stage in the VWBR system. Culture medium samples were taken at 0, 24, and 48 h after medium conditioning started. Results from one experiment for each MSC source (BM, AT, and UCM). Results are presented as mean ± SD (n = 3). LDH, lactate dehydrogenase; VWBR, Vertical-Wheel^{TM} bioreactor; BM, bone marrow; AT, adipose tissue; UCM, umbilical cord matrix.

Characterization of MSC-EVs Reveals Improved Properties Upon Bioreactor Manufacturing

EV were successfully isolated from the conditioned medium of MSC cultures. We were able to identify the presence of EVs from static and bioreactor cultures of MSC, from the 3 different sources (i.e., BM, AT and UCM) through AFM (**Figure 3A** and **Supplementary Figure 1**). Individual vesicles of different sizes were observed, as well as vesicle aggregates. The formation of aggregates and collapsed vesicles may be caused by sample processing techniques, which involve sample dehydration. Larger vesicles were observed for AT MSC (**Figure 3A**). These vesicles may have a higher tendency to aggregate or even fuse together due to the higher medium viscosity observed in AT MSC cultures.

The production of EVs was also confirmed by Western blot analysis (**Figure 3B** and **Supplementary Figure 2**). The EV protein markers synthenin, CD63 and CD81 were successfully detected in EV samples, while the negative EV protein marker calnexin (a protein from the endoplasmic reticulum) was present in cells, but absent in EV samples, as expected (**Figure 3Bi**). In general, synthenin and CD63 presence were verified for

TABLE 1 | Parameters from cultures of MSC from three different human sources (BM, AT, and UCM) in bioreactors.

	Adhesion efficiency	Growth rate (day^{-1})	Duplication time (day)
BM	68 ± 17%	0.47 ± 0.05	1.49 ± 0.13
AT	110 ± 12%	0.45 ± 0.06	1.60 ± 0.19
UCM	55 ± 4%	0.35 ± 0.09	2.30 ± 0.61

Average initial cell adhesion efficiency, growth rate and duplication time for each MSC source. Adhesion efficiency was estimated by dividing the total cell number 24 h after inoculation (day 1) by the cell number used in bioreactor inoculation (day 0). Three biological replicates (i.e., MSC from three different human donors) were used for each MSC source (n = 3). Results are presented as mean ± SEM.

MSC-EVs obtained from both static and bioreactor systems, using MSC from the 3 different tissue sources (**Figure 3Bii**). Interestingly, both synthenin and CD63 presence were increased when EVs were obtained from bioreactors. Contrarily to EVs, cells showed higher synthenin expression under static conditions compared to the bioreactor. CD81 was detected in EVs obtained from BM and AT MSC obtained from both static and bioreactor systems, but not from UCM MSC. CD81 was detected in higher quantity in EVs obtained from AT MSC cultured in bioreactors, compared with static conditions.

The surface charge of MSC-EVs was also quantified. MSC-EVs presented a negative surface charge, as determined through zeta potential measurements (**Figure 3C**). Overall, no significant differences were observed in the zeta potential between samples obtained from static or bioreactor platforms, neither between different MSC tissue sources. The zeta potentials ranged between −15.5 ± 1.6 mV and – 19.4 ± 1.4 mV.

The size distribution of MSC-EVs was determined by NTA. In general, MSC-EV samples showed a size distribution profile mostly enriched in small EVs (<200 nm) (**Figures 4A,B**). Although EVs derived from AT MSC showed a more homogeneous size distribution when obtained from the bioreactor compared to static cultures, no significant difference was observed for other MSC sources. The sizes of EVs produced from AT MSC in the static platform were significantly larger, possibly due to vesicle aggregation or fusion. Therefore, the bioreactor system reveals potential to produce EVs with lower size dispersity, as observed for AT MSC-EVs.

Bioreactor Culture Improves the Production of MSC-EVs

MSC-EVs produced in the bioreactor system were quantified by NTA after EV isolation and compared with MSC-EVs obtained from static cultures. When EVs were produced in the bioreactor system, their concentration was significantly increased (**Figure 5A**), at an overall fold increase of 5.7 ± 0.9 (**Table 2**). When analyzed individually, we observed a fold increase of 4.0 ± 0.6 for BM MSC, 4.4 ± 1.2 for AT MSC and 8.8 ± 3.8 for UCM MSC, when EVs were produced in the bioreactor system (**Table 2**). Bioreactor cultured UCM MSC yielded the highest average EV concentration in the conditioned medium ($6.9 \pm 1.7 \times 10^9$ particles/mL) (**Figure 5A**). The average EV concentration in bioreactor cultures was similar for BM and AT MSC ($4.6 \pm 0.2 \times 10^9$ and $5.1 \pm 2.1 \times 10^9$ particles/mL, respectively), although the latter presented higher heterogeneity between experiments.

In order to evaluate if the conditions in the bioreactor might modulate the intrinsic capacity of cultured MSC for the production of EVs compared to static conditions, we estimated the EV productivity (i.e., specific EV concentration, per cell) by dividing the concentration of EVs (from NTA) by the cell concentration at the beginning of the conditioning period. When EVs were produced in the bioreactor system, EV productivity increased compared with static culture (**Figure 5B**) at an overall fold increase of 3.0 ± 0.5 (**Table 2**). Although this difference was not statistically significant (which is likely due to the heterogeneities between the different tissue sources and donors used), the bioreactor system allowed an improved productivity of MSC-EVs for most of the MSC donors used (i.e., in six out of eight MSC donors).

EV productivity increased in the bioreactor by a fold increase of 1.4 ± 0.3 for BM MSC, 3.7 ± 1.0 for AT MSC and 3.9 ± 1.4 for UCM MSC (**Table 2**), compared with static conditions. Bioreactor cultured UCM MSC yielded the highest average EV productivity ($2.7 \pm 0.6 \times 10^4$ particles/cell) (**Figure 5B**). The average EV productivity in bioreactor cultures was similar for BM and AT MSC ($1.6 \pm 0.5 \times 10^4$ and $1.7 \pm 0.6 \times 10^4$ particles/cell, respectively).

A particle to protein ratio (PPR) was also determined by dividing the EV concentration (determined by NTA) by the total protein concentration in the same sample (determined through BCA protein assay). The PPR can be used to assess the purity of an EV sample, as the higher is this ratio, the lower is the amount of co-isolated protein contaminants, thus the higher is the sample purity (Webber and Clayton, 2013). EV samples from BM and UCM MSC cultures presented a more homogeneous PPR in the bioreactor system than in static conditions (**Figure 5C**). EV samples from AT MSC cultures presented a homogeneous PPR for both culture platforms, but the average PPR was slightly higher in the bioreactor. Overall, the PPR was relatively constant in the bioreactor system, ranging between 1.63×10^8 and 3.40×10^8 particles/μg protein (**Figure 5C**). PPR was much more heterogeneous in static conditions (i.e., T-flasks), ranging between 3.47×10^7 and 9.88×10^8 particles/μg protein. Additionally, the median PPR was higher for the EVs produced in the bioreactor system.

DISCUSSION

MSC hold great promise for the development of cell-based therapies for a variety of disorders. MSC-derived products such as MSC-EVs offer the opportunity to develop new therapeutic products benefiting from MSC regenerative properties in cell-free formulations. These cell-free therapies are expected to present significant advantages, obviating the complexity and safety issues in utilizing cells themselves as therapeutic systems in a clinical context (Batrakova and Kim, 2015; Conlan et al., 2017).

MSC-EVs can be used as intrinsically therapeutic products, by mediating some of the effects conveyed by MSC. MSC-EVs present therapeutic properties for neurological, cardiovascular,

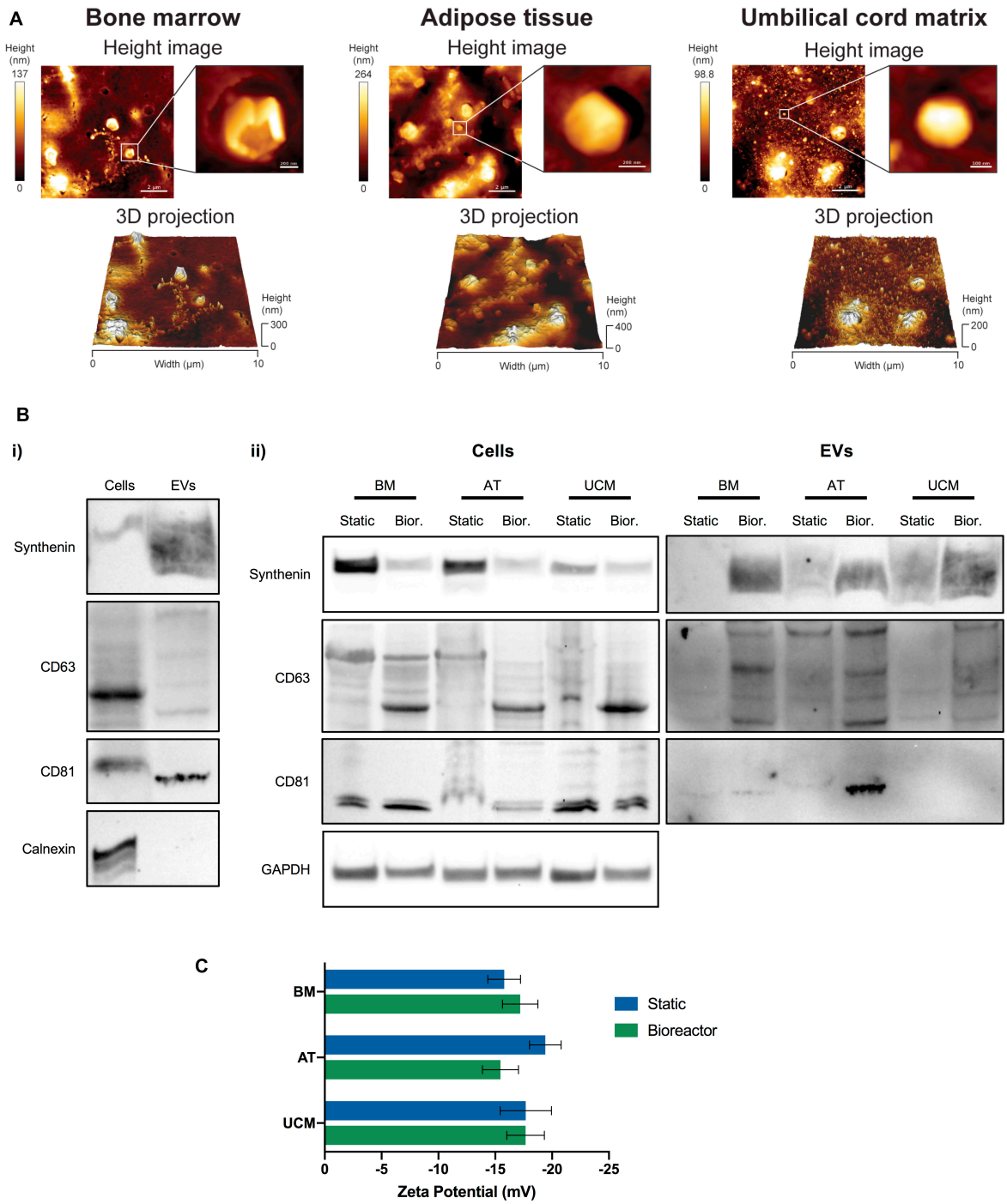

FIGURE 3 | Characterization of MSC-EVs. **(A)** Representative AFM images of MSC-EVs obtained in the VWBR system, using MSC from three different human tissue sources (bone marrow, adipose tissue, and umbilical cord matrix). AFM height images (top) and respective 3D projections (bottom), capturing a total area of 10 × 10 μm. A close-up image focusing on a single EV is presented for each AFM height image. **(B)** Western blots of MSC lysates and MSC-EV samples. **(i)** Representative Western blot images of synthenin, CD63, CD81 and calnexin detection in MSC-EVs and corresponding WCL (i.e., cells) obtained from VWBR cultures. (ii) Western blot detection of synthenin, CD63 and CD81 in MSC-EV samples and corresponding WCL (i.e., cells), obtained from BM, AT and UCM MSC after EV production in static and VWBR systems. Detection of the housekeeping protein GAPDH in the same WCL preparations. **(C)** Zeta potential measurements of the surface charge of MSC-EVs (mV), obtained in either static or VWBR systems, using MSC from three different human sources (BM, AT, and UCM). Results correspond to one representative experiment for each condition. Results are presented as mean ± SD. AFM, atomic force microscopy; WCL, whole cell lysates; BM, bone marrow; AT, adipose tissue; UCM, umbilical cord matrix; VWBR, Vertical-Wheel^{TM} bioreactor.

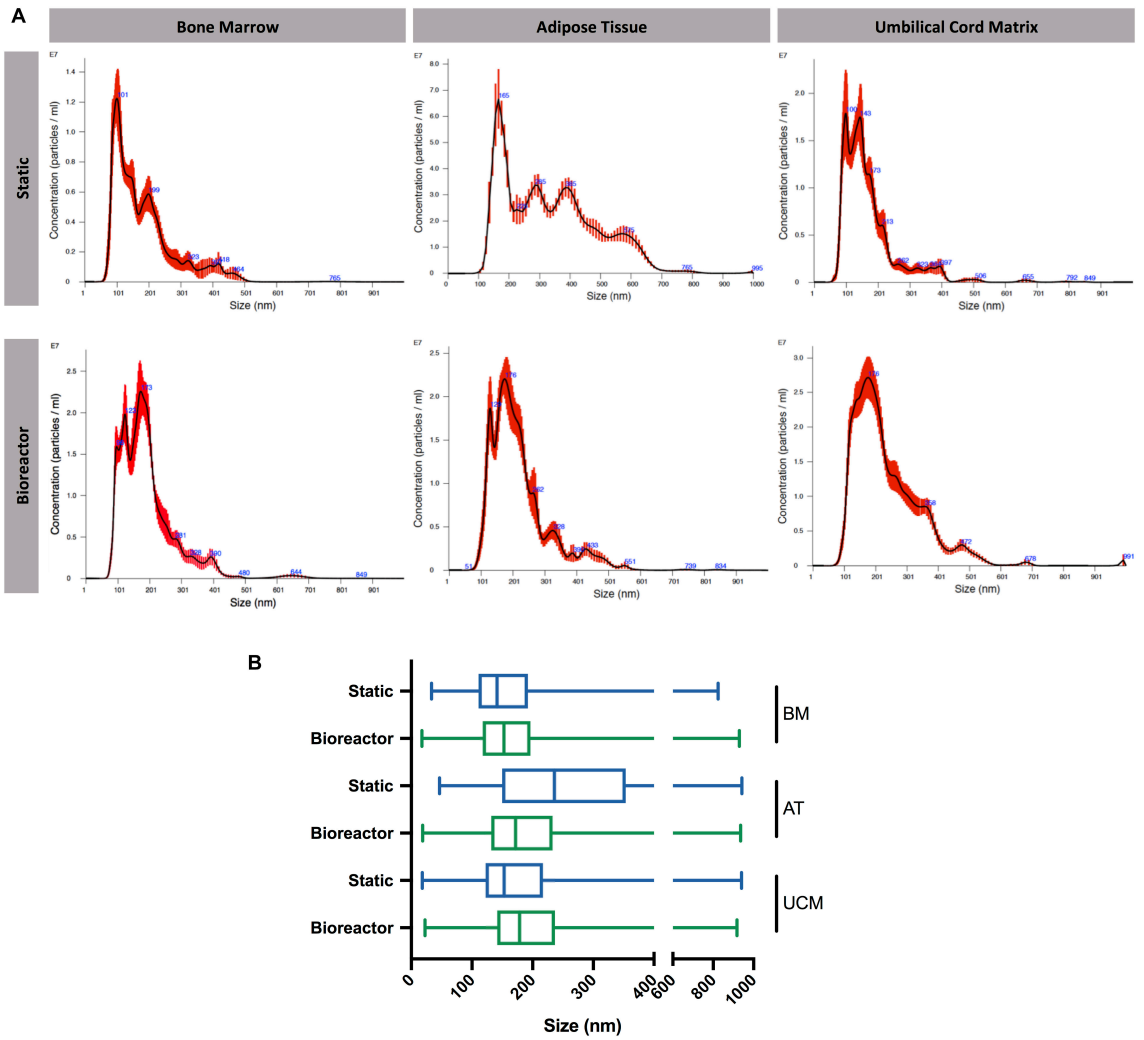

FIGURE 4 | Size distribution of MSC-EVs. **(A)** Representative size distribution curves of EV samples obtained from BM, AT, and UCM MSC, cultured in static or Vertical-Wheel^{TM} bioreactor systems. **(B)** Box plots representing the size distribution profiles of EV samples obtained from BM, AT, and UCM MSC, cultured in static or Vertical-Wheel^{TM} bioreactor systems. The minimum, 1st quartile, median, 3rd quartile and maximum values are represented for each condition. MSC from three different donors were used for each tissue source (i.e., $n = 3$ biological replicates). BM, bone marrow; AT, adipose tissue; UCM, umbilical cord matrix.

immunological, kidney and liver diseases, among others (Phinney and Pittenger, 2017; Keshtkar et al., 2018; Elahi et al., 2020). MSC-EVs have been described to reduce myocardial ischemia/reperfusion injury in mice (Lai et al., 2010) and also allowed improved recovery from acute kidney injury (Bruno et al., 2012) and from stroke (Doeppner et al., 2015). Indeed, there are multiple studies describing their pro-angiogenic (Bian et al., 2014; Vrijsen et al., 2016) and wound healing capacity (Zhang et al., 2015; Fang et al., 2016).

Alternatively, EVs can be engineered toward the development of novel drug delivery systems (DDS). Drug loaded EVs can be used to transport and deliver therapeutic cargo to target diseased cells and tissues (Batrakova and Kim, 2015; Vader et al., 2016). These natural DDS could be an appealing alternative to the more established synthetic DDS, by avoiding toxicity and rapid clearance from the organism, as well as a better membrane matching capacity (Batrakova and Kim, 2015). Dendritic cell-derived EVs were able to deliver siRNA to the brain in mice, demonstrating their potential use as targeted therapy for neurological diseases (Alvarez-Erviti et al., 2011). Macrophage-derived EVs loaded with catalase provided increased neuroprotective effects in *in vitro* and *in vivo* models of Parkinson's disease, compared to free catalase (Haney et al., 2015). Recently, multiple studies have successfully developed EVs as DDS for cancer therapy (Pascucci et al., 2014; Tian et al., 2014; Kim et al., 2016, 2018; Kooijmans et al., 2016, 2018; Jia et al., 2018; Li et al., 2018). Intravenously injected EVs from dendritic cells delivered doxorubicin specifically to tumor tissues in mice, leading to the inhibition of tumor growth with lower toxcicity (Tian et al., 2014). MSC incubated with a high Paclitaxel concentration secreted EVs loaded with this drug, successfully inhibiting tumor growth *in vitro* (Pascucci et al.,

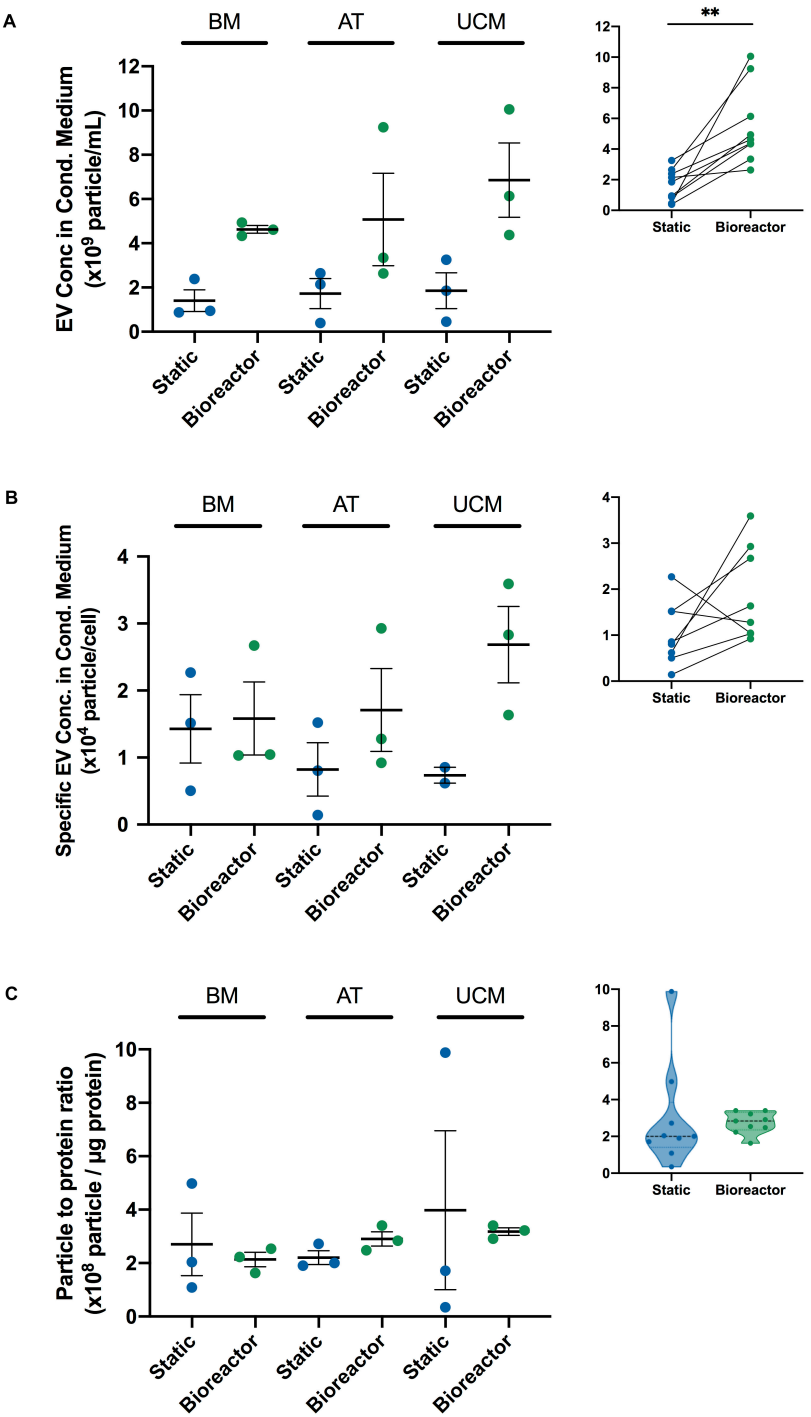

FIGURE 5 | Comparing MSC-EV production in bioreactor and static culture systems, using MSC from different sources. **(A)** EV concentration (particles/mL) in the cell culture conditioned medium from BM, AT, and UCM MSC cultures in static and Vertical-Wheel^{TM} bioreactor systems. MSC from three different donors were used for each tissue source (i.e., $n = 3$ biological replicates). Results are presented as mean ± SEM ($n = 3$). Upper-right panel: Summarized paired analysis comparing EV concentration in static and Vertical-Wheel^{TM} bioreactor systems, for each MSC donor. Paired statistical analysis (paired t-test $^{**}P = 0.0027$) ($n = 9$). **(B)** Specific EV concentration (particles/cell) in the cell culture conditioned medium from BM, AT, and UCM MSC cultures in static and Vertical-Wheel^{TM} bioreactor systems. MSC from three different donors were used for each tissue source. In static cultures, each T-175 yielded 1.2 – 6.6 × 10^6 cells upon 4 – 9 days of expansion, regardless of the cell tissue source. Results are presented as mean ± SEM ($n = 3$; $n = 2$ for UCM-static). Upper-right panel: Summarized paired analysis comparing specific EV concentration in static and Vertical-Wheel^{TM} bioreactor systems, for each MSC donor. **(C)** Particle to protein ratios (PPR) (particle/µg protein) of EV samples obtained from BM, AT and UCM MSC, cultured in static and Vertical-Wheel^{TM} bioreactor systems. MSC from three different donors were used for each tissue source. Results are presented as mean ± SEM ($n = 3$). Upper-right panel: Violin plot of PPR of MSC-EV samples obtained in static and Vertical-Wheel^{TM} bioreactor systems.

TABLE 2 | Fold changes in EV concentration and EV productivity in the cell culture conditioned medium from the bioreactor system compared to static conditions.

	EV concentration fold change (bioreactor/static)	EV productivity fold change (bioreactor/static)
BM	4.0 ± 0.6	1.4 ± 0.3
AT	4.4 ± 1.2	3.7 ± 1.0
UCM	8.8 ± 3.8	3.9 ± 1.4
Global	5.7 ± 0.9	3.0 ± 0.5

Results from each of the 3 MSC sources used (BM, AT, and UCM), as well as global fold change averages from all the sources. Three biological replicates (i.e., MSC from three different human donors) were used for each MSC source (n = 3). For each MSC source, results are presented as the average of fold changes for each donor, in order to account for biological diversity. Global fold changes are presented as the average of fold changes from each MSC source. Results are presented as mean ± SEM.

2014). Additionally, EVs can be further engineered to improve specificity and retention on target cells and tissues (Jia et al., 2018; Kooijmans et al., 2016, 2018).

Despite the promising potential of EVs for therapeutic applications, large EV doses are expected to be required to achieve therapeutic effects in clinical settings. This requires the development of robust manufacturing processes that could increase the consistency and scalability of EV production, which are currently lacking.

The present work aimed to establish a scalable culture platform for the manufacturing of MSC-EVs in S/XF culture conditions. This was achieved by building on previous work from our group where a S/XF microcarrier-based culture system was implemented in single-use bioreactors (VWBR), employing a hPL culture supplement (UltraGRO^{TM}-PURE) for MSC expansion (de Sousa Pinto et al., 2019). In the present study, EVs were produced by MSC isolated from 3 different human tissue sources (BM, AT and UCM) in a process that comprises a cell expansion stage and a culture medium conditioning stage.

S/XF culture conditions were implemented by exclusively applying products without any animal components, namely hPL as a culture supplement used in the cell expansion stage, instead of the more commonly used FBS, as well as animal product-free plastic microcarriers and TrypLE as a cell detaching solution. Multiple studies have revealed hPL-supplemented media to be efficient for the isolation and expansion of MSC from various origins (Doucet et al., 2005; Kinzebach et al., 2013; Reinisch et al., 2015), cultured both in static and dynamic systems (de Soure et al., 2017; de Sousa Pinto et al., 2019), as well as for the expansion of other cell types (Naveau et al., 2010; Mazzocca et al., 2012; Hofbauer et al., 2014; Hildner et al., 2015). However, the fact that hPL products originate from human donors presents some constraints, such as the risk of transmission of human diseases by viruses, ill-definition and the possibility of triggering immune responses (Hemeda et al., 2014). The ideal option for production of clinical-grade cell based therapies would be a chemically defined, animal component-free medium (including human). However, there are very few of these options available, namely for MSC culture. Therefore, presently, hPL seems to be the most promising and cost-effective alternative to FBS supplementation in cell culture medium for now, being more readily translatable to a clinical setting, especially considering that gamma irradiated hPL products allowing significant viral reduction have already been developed (Huang et al., 2019).

Culture medium supplements such as FBS and hPL have a large amount of protein and vesicle contents, presenting an additional challenge for their use in EV manufacturing. These components are prone to be co-isolated with the EV fraction, thus contaminating the end product (Witwer et al., 2019). For this reason, we removed hPL at the end of the MSC expansion period and hPL-free medium was used for the medium conditioning period. MSC were cultured for 48 h in this supplement-free medium, which could be a stress factor for cell culture. However, we did not observe any significant reduction in cell number, cell viability or microcarrier occupancy during this stage. Furthermore, LDH activity did not change significantly over this period for any of the MSC sources. Therefore, there were no indications that MSC were experiencing significant stress in culture, due to the absence of hPL in the 48 h conditioning period. Still, MSC might potentially undergo some alterations over this period. Minimal identity criteria commonly used to define multipotent MSC could suffer modifications, namely their *in vitro* multilineage differentiation capacity or their immunophenotype (i.e., expressing CD73, CD90, and CD105, lacking the expression of hematopoietic and endothelial markers CD11b, CD14, CD19, CD34, CD45, CD79a and HLA-DR) (Viswanathan et al., 2019). Of notice, MSC expanded in the VWBR system maintain the typical MSC immunophenotype, as previously reported by our group (de Sousa Pinto et al., 2019). Further work could be performed by comparing the MSC features before and after the culture medium conditioning period.

Bioreactor systems such as VWBR present several advantages for the manufacturing of cell-based therapies. Cell culture on microcarriers in suspension inside a bioreactor allows an increase of available surface area per volume ratio, enabling higher cell concentrations in culture. Bioreactors also allow the implementation of culture monitoring and control systems, providing an additional advantage to optimize culture conditions, by adjusting feeding regimes and physicochemical parameters (e.g., O_2 concentration and pH) according to real-time culture measurements.

In this work, we established a bioreactor process in 100 mL VWBR vessels. This process can be scaled-up to VWBR with a working volume of 3 L or higher (up to 500 L), which include an integrated control system, allowing for a controlled manufacturing process. To the best of our knowledge, this study is the first to establish a S/XF microcarrier-based culture system in bioreactors for the manufacturing of MSC-EVs, using MSC from 3 different human tissue sources (BM, AT and UCM). It is also the first to implement the VWBR configuration for EV production. Cell expansion in this bioreactor culture system allowed an increase in EV concentration in the conditioned medium when compared to traditional static systems (5.7 ± 0.9 global fold increase), partly due to higher cell concentrations obtained in VWBR. However, in addition to that, the EV productivity (i.e., specific EV concentration) also increased in bioreactors (3.0 ± 0.5 global fold increase), meaning that each cell secreted more EVs when MSC were cultured in the VWBR, compared to

static conditions. Although this difference was not found to be statistically significant, this was likely due to the heterogeneities between different tissue sources and donors. For example, if we had not considered the results from one of the BM MSC donors (for which EV productivity decreased in the bioreactor, contradicting the observed general tendency of our study), this difference would be statistically significant. This reinforces the relevance of testing MSC from multiple tissue donors in order to account for intrinsic biological variability. Of notice, this study was performed using MSC from 3 different donors for each tissue source, comprising a total 9 random human donors. Still, further work may be performed with additional donors in order to more thoroughly account for donor variability and its impact. Altogether, the higher EV concentrations achieved in VWBR were due to higher cell densities, as well as to higher EV productivities by MSC.

Overall, in the conditions of our study, UCM MSC allowed the highest EV concentration and EV productivity in the bioreactor system. They also showed the highest fold increase in both parameters when compared to static systems. Therefore, UCM seems to be the MSC source that benefits the most from cultivation in the VWBR system, being the most promising of the three tissue sources studied for scalable MSC-EV production. This is in line with previous work where UCM MSC have been described to allow higher EV productivity than BM and AT MSC in static culture (Haraszti et al., 2018).

Nonetheless, the real applicability of these MSC-EVs depends on their biological function. Given their different tissue origins, we can expect that EVs obtained from cells derived from each MSC source will have different functional characteristics. Indeed, different intrinsic therapeutic features have been described for MSC derived from different tissues (Ribeiro et al., 2013). In order to develop therapeutic products, based on the MSC-EVs manufactured in this work, additional functional studies will be required. These could include, for example, (i) scratch assays or tube formation assays using endothelial cells to determine the ability of MSC-EVs to promote angiogenesis in the context of vascular repair (Vrijsen et al., 2016) or (ii) cell uptake assays to determine EV uptake by target cancer cells, to assess their potential as drug delivery vehicles for cancer therapy (Kooijmans et al., 2018).

The increase observed in EV productivity in VWBR can be explained by multiple reasons. EV secretion by MSC may have been stimulated by fluid flow, promoted by the VWBR mixing system. Fluid flow has already been described to stimulate EV secretion in osteocytes through a Ca^{2+}-mediated response (Morrell et al., 2018). Additionally, when MSC were cultured in the bioreactor system, cells attached to the surface of plastic microcarriers and proliferated. Later in culture, microcarrier aggregates were formed and, consequently, MSC formed aggregates as well, as previously observed (Frauenschuh et al., 2007; Eibes et al., 2010). MSC culture in spheroids has been described to lead to higher secretion of paracrine factors (Bhang et al., 2011; Costa et al., 2017), as well as to an increased secretion of microvesicles (Cha et al., 2018). Hence, aggregate formation could be leading to an increased EV secretion in the VWBR system. Finally, MSC cultured in the VWBR system are likely to be exposed to lower oxygen concentrations than in static platforms. The VWBR agitation system allows mixing of the cell culture medium, achieving a homogeneous oxygen concentration. However, there is no aeration system in the 100 mL VWBR, so oxygen exchange occurs only at the surface gas-liquid interface. Considering the differences between the geometries of the VWBR vessel and the T-flask, oxygen concentration would be expectedly lower in the VWBR system than in static. This could potentially be a contributing factor for the observed increase in EV secretion when cells were expanded in the bioreactor system. Previous studies have demonstrated an increase in EV secretion when different cell types (including MSC) were cultured under hypoxic conditions (ranging from 0.1 to 3% O_2, compared to controls) (King et al., 2012; Salomon et al., 2013; Panigrahi et al., 2018). Although all of these factors might lead to an increased EV productivity in the VWBR, additional studies would be needed to determine their actual contributions.

Zeta potential measurements revealed that the surface charge of obtained MSC-EVs were generally similar, regardless the production platform and MSC source used, ranging between -15.5 ± 1.6 mV and -19.4 ± 1.4 mV. These surface charges are moderately negative, as it was expected considering that EVs are cell-derived nanoparticles, therefore containing negatively charged phospholipids. The values of zeta potential obtained herein were in line with other studies reporting zeta potential measurements for EVs derived from cell culture (Akagi et al., 2014; Hood et al., 2014; Kesimer and Gupta, 2015; Rupert et al., 2017).

Further EV characterization revealed that bioreactors improved not only EV quantity but also their purity, as assessed by Western blot and PPR. Western blot analysis revealed that synthenin, CD63 and CD81 (key proteins involved in EV biogenesis and commonly used as protein markers) were in general more abundant in EVs obtained from bioreactors than from their static counterparts (**Figure 3Bii**). Therefore, EVs from bioreactors seem to have a higher purity than EVs obtained from static system, since a higher amount of synthenin, CD63 and CD81 were detected for the same amount of total protein. This observation corroborates the increased EV concentration in VWBR identified by NTA. The fact that bioreactor EV samples showed increased levels of EV protein markers validates the hypothesis that the increased concentration of particles detected by NTA corresponds to an increased concentration of EVs and not of protein aggregates.

EV purity was also assessed by estimating the PPR for each EV sample (Webber and Clayton, 2013). PPR was more homogeneous and reproducible in EV samples obtained from bioreactors compared to those produced under static conditions and the median PPR was higher in the bioreactor system (**Figure 5C**). A more homogeneous environment in VWBR offers a more reproducible process for different sources and donors. Constant agitation provides the cells with a more homogeneous access to nutrients, thus allowing a more robust MSC-EV manufacturing process. Therefore, the bioreactor platform established in this work is expected to allow the robust production of MSC-EVs at higher purities, compared to static systems.

In our previous work focused on the establishment of a S/XF microcarrier-based culture system in single-use bioreactors (VWBR) (de Sousa Pinto et al., 2019), an economic evaluation revealed that the application of this culture system allowed a cost reduction for MSC manufacturing when compared to static cell culture using T-flasks. Therefore, it can be expected that the application of this bioreactor system will also allow a cost reduction for the production of MSC-EVs, compared to static platforms.

A few manufacturing processes for the production of EVs have been previously studied. The Integra CELLine culture system is a static platform that has been used to optimize EV production (Mitchell et al., 2008). This is a two-compartment culture flask with a semi-permeable membrane separating a cell-containing compartment from a larger medium compartment. When mesothelioma and NK cells were cultured in this system, a 12-fold and a 8-fold increase in EV (protein) concentration was observed, respectively, compared to traditional T-flasks (Mitchell et al., 2008). This system also allowed a 13- to 16-fold increase in EV (protein) concentration from bladder carcinoma cells (Jeppesen et al., 2014). The CELLine system allows culture medium change while EVs are retained in the cell compartment, enabling higher EV concentrations. However, this static system has limited scalability, thus not being the most suitable option for large-scale EV production.

Watson and colleagues developed a hollow-fiber bioreactor platform for the production of HEK-derived EVs (Watson et al., 2016). The authors reported a 10-fold increase in EV concentration compared with static culture, which was sustained by an increased purity (both increased PPR and protein marker expression). However, EV size distribution profiles were more dispersed in the bioreactors, which is the opposite from what we observed in our study with the VWBR system. Mendt and colleagues manufactured BM MSC-derived EVs in a closed system, hollow-fiber bioreactor, named Quantum (Mendt et al., 2018). They were able to achieve 1.04×10^{10} particles/mL on average, which was higher, but comparable with the EV concentrations we obtained in the VWBR system ($5.5 \pm 0.8 \times 10^{9}$ particles/mL) herein.

Hollow-fiber bioreactors (i.e., without mechanical agitation) provide surface immobilization of cells on the fibrous material and represent a suitable configuration to obtain an increased EV concentration in culture, since culture medium can be recirculated while EVs are retained by the hollow-fiber membranes. However, stirred bioreactors as the VWBR may allow a better fine-tuning of EV production by manipulating process parameters. For example, agitation may play an important role in EV secretion, since fluid flow seems to have impact on this process. Further studies may be developed in the VWBR, testing the impact of agitation on EV production. Other process parameters, such as oxygen concentration, temperature and pH, are also likely to play a role in EV secretion by cultured MSC and are more easily controlled in a VWBR, especially when integrated with a control system. Further studies addressing the impact of these parameters on EV production using the VWBR system would be relevant to fine-tune and optimize MSC-EV production.

CONCLUSION

In this study, we have successfully developed a scalable S/XF microcarrier-based bioreactor culture system for the robust production of MSC-EVs, using MSC from 3 different human tissue sources (BM, AT, and UCM). This system allowed the production of MSC-EVs at higher concentration and productivity when compared to traditional static culture systems. It also allowed to obtain a more robust MSC-EV manufacturing process, regarding their purity. Further developments of this system will need to take into consideration a proper balance between EV production and function. Additional studies will be required to characterize the therapeutic potential of these MSC-EVs. The MSC-EVs obtained through this scalable platform are promising for the development of multiple therapeutic products and DDS, targeting a variety of diseases.

DATA AVAILABILITY STATEMENT

The original contributions presented in the study are included in the article/**Supplementary Material**, further inquiries can be directed to the corresponding authors.

AUTHOR CONTRIBUTIONS

MAF, NB, AF-P, DG, JC, and CS designed the research study. MAF performed the MSC-EV production and isolation. MAF and NB performed the characterization and data analysis. AC assisted on MSC-EV production. AF-P supported the establishment and management of the MSC bank. FO, MC, and DG were responsible for zeta potential and AFM characterization. JF assisted on NTA. CR, SJ, and BL supported the development of the Vertical-Wheel^{TM} bioreactor system. R-JT and WM supported the use of the human platelet lysate culture supplement (UltraGRO^{TM}-PURE) for cell isolation and expansion. MAF, NB, and CS wrote the manuscript. All the authors critically revised and approved the final manuscript.

FUNDING

Funding received by iBB-Institute for Bioengineering and Biosciences from the Portuguese Foundation for Science and Technology (FCT) (UID/BIO/04565/2020) and through the projects PTDC/EQU-EQU/31651/2017, PTDC/BBB-BQB/1693/2014, and PTDC/BTM-SAL/31057/2017 is acknowledged. Funding received from POR de Lisboa 2020 through the project PRECISE – Accelerating progress toward the new era of precision medicine (Project N. 16394) is also acknowledged. MAF (PD/BD/128328/2017)

and FO (PD/BD/135046/2017) acknowledge FCT for the Ph.D. fellowships and DG (SFRH/BPD/109010/2015) for the Post-Doctoral fellowship.

ACKNOWLEDGMENTS

We thank Inês Ferreira and Rita Oliveira (CEDOC - Chronic Diseases Research Center, NOVA Medical School/Faculdade de Ciências Médicas, Universidade NOVA de Lisboa) for their insightful support in Western blot protocols.

SUPPLEMENTARY MATERIAL

The Supplementary Material for this article can be found online at: https://www.frontiersin.org/articles/10.3389/fcell.2020.553444/full#supplementary-material

REFERENCES

Akagi, T., Kato, K., Hanamura, N., Kobayashi, M., and Ichiki, T. (2014). Evaluation of desialylation effect on zeta potential of extracellular vesicles secreted from human prostate cancer cells by on-chip microcapillary electrophoresis. *Jpn. J. Appl. Phys.* 53:06JL01. doi: 10.7567/jjap.53.06jl01

Alvarez-Erviti, L., Seow, Y., Yin, H., Betts, C., Lakhal, S., and Wood, M. J. A. (2011). Delivery of siRNA to the mouse brain by systemic injection of targeted exosomes. *Nat. Biotechnol.* 29, 341–345. doi: 10.1038/nbt.1807

Batrakova, E. V., and Kim, M. S. (2015). Using exosomes, naturally-equipped nanocarriers, for drug delivery. *J. Control. Release* 219, 396–405. doi: 10.1016/j.jconrel.2015.07.030

Bhang, S. H., Cho, S. W., La, W. G., Lee, T. J., Yang, H. S., Sun, A. Y., et al. (2011). Angiogenesis in ischemic tissue produced by spheroid grafting of human adipose-derived stromal cells. *Biomaterials* 32, 2734–2747. doi: 10.1016/j.biomaterials.2010.12.035

Bian, S., Zhang, L., Duan, L., Wang, X., Min, Y., and Yu, H. (2014). Extracellular vesicles derived from human bone marrow mesenchymal stem cells promote angiogenesis in a rat myocardial infarction model. *J. Mol. Med.* 92, 387–397. doi: 10.1007/s00109-013-1110-5

Börger, V., Bremer, M., Ferrer-Tur, R., Gockeln, L., Stambouli, O., Becic, A., et al. (2017). Mesenchymal stem/stromal cell-derived extracellular vesicles and their potential as novel immunomodulatory therapeutic agents. *Int. J. Mol. Sci.* 18:1450. doi: 10.3390/ijms18071450

Bruno, S., Grange, C., Collino, F., Deregibus, M. C., Cantaluppi, V., Biancone, L., et al. (2012). Microvesicles derived from mesenchymal stem cells enhance survival in a lethal model of acute kidney injury. *PLoS One* 7:e33115. doi: 10.1371/journal.pone.0033115

Bruno, S., Grange, C., Deregibus, M. C., Calogero, R. A., Saviozzi, S., Collino, F., et al. (2009). Mesenchymal stem cell-derived microvesicles protect against acute tubular injury. *J. Am. Soc. Nephrol.* 20, 1053–1067. doi: 10.1681/asn.2008070798

Caplan, A. I., and Dennis, J. E. (2006). Mesenchymal stem cells as trophic mediators. *J. Cell. Biochem.* 98, 1076–1084. doi: 10.1002/jcb.20886

Carmelo, J. G., Fernandes-Platzgummer, A., Diogo, M. M., da Silva, C. L., and Cabral, J. M. S. (2015). A xeno-free microcarrier-based stirred culture system for the scalable expansion of human mesenchymal stem/stromal cells isolated from bone marrow and adipose tissue. *Biotechnol. J.* 10, 1235–1247. doi: 10.1002/biot.201400586

Cha, J. M., Shin, E. K., Sung, J. H., Moon, G. J., Kim, E. H., Cho, Y. H., et al. (2018). Efficient scalable production of therapeutic microvesicles derived from human mesenchymal stem cells. *Sci. Rep.* 8:1171.

Conlan, R. S., Pisano, S., Oliveira, M. I., Ferrari, M., and Mendes Pinto, I. (2017). Exosomes as reconfigurable therapeutic systems. *Trends Mol. Med.* 23, 636–650. doi: 10.1016/j.molmed.2017.05.003

Costa, M. H. G., McDevitt, T. C., Cabral, J. M. S., da Silva, C. L., and Ferreira, F. C. (2017). Tridimensional configurations of human mesenchymal stem/stromal cells to enhance cell paracrine potential towards wound healing processes. *J. Biotechnol.* 262, 28–39. doi: 10.1016/j.jbiotec.2017.09.020

Croughan, M. S., Giroux, D., Fang, D., and Lee, B. (2016). "Novel single-use bioreactors for scale-up of anchorage-dependent cell manufacturing for cell therapies," in *Stem Cell Manufacturing*, eds J. M. S. Cabral, C. L. da Silva, L. G. Chase, and M. M. Diogo (Amsterdam: Elsevier), 105–139. doi: 10.1016/B978-0-444-63265-4.00005-4

da Silva Meirelles, L., Fontes, A. M., Covas, D. T., and Caplan, A. I. (2009). Mechanisms involved in the therapeutic properties of mesenchymal stem cells. *Cytokine Growth Factor Rev.* 20, 419–427. doi: 10.1016/j.cytogfr.2009.10.002

de Almeida Fuzeta, M., Branco, A. D. M., Fernandes-Platzgummer, A., Lobato da Silva, C., and Cabral, J. M. S. (2019). "Addressing the manufacturing challenges of cell-based therapies," in *Advances in Biochemical Engineering/Biotechnology*, Vol. 171, eds A. Silva, J. Moreira, J. Lobo, and H. Almeida (Berlin: Springer), 225–278. doi: 10.1007/10_2019_118

de Soure, A. M., Fernandes-Platzgummer, A., da Silva, C. L., and Cabral, J. M. S. (2016). Scalable microcarrier-based manufacturing of mesenchymal stem/stromal cells. *J. Biotechnol.* 236, 88–109. doi: 10.1016/j.jbiotec.2016.08.007

de Soure, A. M., Fernandes-Platzgummer, A., Moreira, F., Lilaia, C., Liu, S.-H., Ku, C.-P., et al. (2017). Integrated culture platform based on a human platelet lysate supplement for the isolation and scalable manufacturing of umbilical cord matrix-derived mesenchymal stem/stromal cells. *J. Tissue Eng. Regen. Med.* 11, 1630–1640. doi: 10.1002/term.2200

de Sousa Pinto, D., Bandeiras, C., de Almeida Fuzeta, M., Rodrigues, C. A. V., Jung, S., Hashimura, Y., et al. (2019). Scalable manufacturing of human mesenchymal stromal cells in the vertical-wheel bioreactor system: an experimental and economic approach. *Biotechnol. J.* 14:1800716. doi: 10.1002/biot.201800716

Doeppner, T. R., Herz, J., Görgens, A., Schlechter, J., Ludwig, A.-K., Radtke, S., et al. (2015). Extracellular vesicles improve post-stroke neuroregeneration and prevent postischemic immunosuppression. *Stem Cells Transl. Med.* 4, 1131–1143. doi: 10.5966/sctm.2015-0078

dos Santos, F., Andrade, P. Z., Boura, J. S., Abecasis, M. M., da Silva, C. L., and Cabral, J. M. S. (2010). Ex vivo expansion of human mesenchymal stem cells: a more effective cell proliferation kinetics and metabolism under hypoxia. *J. Cell. Physiol.* 223, 27–35.

dos Santos, F., Campbell, A., Fernandes-Platzgummer, A., Andrade, P. Z., Gimble, J. M., Wen, Y., et al. (2014). A xenogeneic-free bioreactor system for the clinical-scale expansion of human mesenchymal stem / stromal cells. *Biotechnol. Bioeng.* 116, 1116–1127. doi: 10.1002/bit.25187

Doucet, C., Ernou, I., Zhang, Y., Llense, J. R., Begot, L., Holy, X., et al. (2005). Platelet lysates promote mesenchymal stem cell expansion: a safety substitute for animal serum in cell-based therapy applications. *J. Cell. Physiol.* 205, 228–236. doi: 10.1002/jcp.20391

Eibes, G., dos Santos, F., Andrade, P. Z., Boura, J. S., Abecasis, M. M. A., da Silva, C. L., et al. (2010). Maximizing the ex vivo expansion of human mesenchymal stem cells using a microcarrier-based stirred culture system. *J. Biotechnol.* 146, 194–197. doi: 10.1016/j.jbiotec.2010.02.015

El Andaloussi, S., Lakhal, S., Mäger, I., and Wood, M. J. A. (2013). Exosomes for targeted siRNA delivery across biological barriers. *Adv. Drug Deliv. Rev.* 65, 391–397. doi: 10.1016/j.addr.2012.08.008

Elahi, F. M., Farwell, D. G., Nolta, J. A., and Anderson, J. D. (2020). Preclinical translation of exosomes derived from mesenchymal stem/stromal cells. *Stem Cells* 38, 15–21. doi: 10.1002/stem.3061

Fang, S., Xu, C., Zhang, Y., Xue, C., Yang, C., Bi, H., et al. (2016). Umbilical cord-derived mesenchymal stem cell-derived exosomal MicroRNAs suppress myofibroblast differentiation by inhibiting the transforming growth factor-β/SMAD2 pathway during wound healing. *Stem Cells Transl. Med.* 5, 1425–1439. doi: 10.5966/sctm.2015-0367

Frauenschuh, S., Reichmann, E., Ibold, Y., Goetz, P. M., Sittinger, M., and Ringe, J. (2007). A microcarrier-based cultivation system for expansion of primary mesenchymal stem cells. *Biotechnol. Prog.* 23, 187–193. doi: 10.1021/bp060155w

Gardiner, C., Ferreira, Y. J., Dragovic, R. A., Redman, C. W. G., and Sargent, I. L. (2013). Extracellular vesicle sizing and enumeration by nanoparticle tracking analysis. *J. Extracell. Vesicles* 2:19671. doi: 10.3402/jev.v2i0.19671

Golpanian, S., Schulman, I. H., Ebert, R. F., Heldman, A. W., DiFede, D. L., Yang, P. C., et al. (2016). Concise review: review and perspective of cell dosage and routes of administration from preclinical and clinical studies of stem cell therapy for heart disease. *Stem Cells Transl. Med.* 5, 186–191. doi: 10.5966/sctm.2015-0101

Haney, M. J., Klyachko, N. L., Zhao, Y., Gupta, R., Plotnikova, E. G., He, Z., et al. (2015). Exosomes as drug delivery vehicles for Parkinson's disease therapy. *J. Control. Release* 207, 18–30.

Haraszti, R. A., Miller, R., Stoppato, M., Sere, Y. Y., Coles, A., Didiot, M. C., et al. (2018). Exosomes produced from 3D cultures of MSCs by tangential flow filtration show higher yield and improved activity. *Mol. Ther.* 26, 2838–2847. doi: 10.1016/j.ymthe.2018.09.015

Heathman, T. R., Nienow, A. W., McCall, M. J., Coopman, K., Kara, B., and Hewitt, C. J. (2015). The translation of cell-based therapies: clinical landscape and manufacturing challenges. *Regen. Med.* 10, 49–64. doi: 10.2217/rme.14.73

Hemeda, H., Giebel, B., and Wagner, W. (2014). Evaluation of human platelet lysate versus fetal bovine serum for culture of mesenchymal stromal cells. *Cytotherapy* 16, 170–180. doi: 10.1016/j.jcyt.2013.11.004

Hildner, F., Eder, M. J., Hofer, K., Aberl, J., Redl, H., van Griensven, M., et al. (2015). Human platelet lysate successfully promotes proliferation and subsequent chondrogenic differentiation of adipose-derived stem cells: a comparison with articular chondrocytes. *J. Tissue Eng. Regen. Med.* 9, 808–818. doi: 10.1002/term.1649

Hofbauer, P., Riedl, S., Witzeneder, K., Hildner, F., Wolbank, S., Groeger, M., et al. (2014). Human platelet lysate is a feasible candidate to replace fetal calf serum as medium supplement for blood vascular and lymphatic endothelial cells. *Cytotherapy* 16, 1238–1244. doi: 10.1016/j.jcyt.2014.04.009

Hood, J. L., Scott, M. J., and Wickline, S. A. (2014). Maximizing exosome colloidal stability following electroporation. *Anal. Biochem.* 448, 41–49. doi: 10.1016/j.ab.2013.12.001

Huang, C., Liang, F., Lin, Y., Chen, Y., Tseng, R., and Huang, M. (2019). Gamma irradiation of human platelet lysate: validation of efficacy for pathogen reduction and assessment of impacts on hpl performance. *Cytotherapy* 21, S82–S83.

Jeppesen, D. K., Nawrocki, A., Jensen, S. G., Thorsen, K., Whitehead, B., Howard, K. A., et al. (2014). Quantitative proteomics of fractionated membrane and lumen exosome proteins from isogenic metastatic and nonmetastatic bladder cancer cells reveal differential expression of EMT factors. *Proteomics* 14, 699–712. doi: 10.1002/pmic.201300452

Jia, G., Han, Y., An, Y., Ding, Y., He, C., Wang, X., et al. (2018). Biomaterials NRP-1 targeted and cargo-loaded exosomes facilitate simultaneous imaging and therapy of glioma in vitro and in vivo. *Biomaterials* 178, 302–316. doi: 10.1016/j.biomaterials.2018.06.029

Keshtkar, S., Azarpira, N., and Ghahremani, M. H. (2018). Mesenchymal stem cell-derived extracellular vesicles: novel frontiers in regenerative medicine. *Stem Cell Res. Ther.* 9:63.

Kesimer, M., and Gupta, R. (2015). Physical characterization and profiling of airway epithelial derived exosomes using light scattering. *Methods* 87, 59–63. doi: 10.1016/j.ymeth.2015.03.013

Kim, M. S., Haney, M. J., Zhao, Y., Mahajan, V., Deygen, I., Klyachko, N. L., et al. (2016). Development of exosome-encapsulated paclitaxel to overcome MDR in cancer cells. *Nanomedicine* 12, 655–664. doi: 10.1016/j.nano.2015.10.012

Kim, M. S., Haney, M. J., Zhao, Y., Yuan, D., Deygen, I., Klyachko, N. L., et al. (2018). Engineering macrophage-derived exosomes for targeted paclitaxel delivery to pulmonary metastases: in vitro and in vivo evaluations. *Nanomedicine* 14, 195–204. doi: 10.1016/j.nano.2017.09.011

King, H. W., Michael, M. Z., and Gleadle, J. M. (2012). Hypoxic enhancement of exosome release by breast cancer cells. *BMC Cancer* 12:421. doi: 10.1186/1471-2407-12-421

Kinzebach, S., Dietz, L., Klüter, H., Thierse, H. J., and Bieback, K. (2013). Functional and differential proteomic analyses to identify platelet derived factors affecting ex vivo expansion of mesenchymal stromal cells. *BMC Cell Biol.* 14:48. doi: 10.1186/1471-2121-14-48

Kooijmans, S. A. A., Fliervoet, L. A. L., Van Der Meel, R., Fens, M. H. A. M., Heijnen, H. F. G., Van Bergen En Henegouwen, P. M. P., et al. (2016). PEGylated and targeted extracellular vesicles display enhanced cell specificity and circulation time. *J. Control. Release* 224, 77–85. doi: 10.1016/j.jconrel.2016.01.009

Kooijmans, S. A. A., Gitz-Francois, J. J. J. M., Schiffelers, R. M., and Vader, P. (2018). Recombinant phosphatidylserine-binding nanobodies for targeting of extracellular vesicles to tumor cells: a plug-and-play approach. *Nanoscale* 10, 2413–2426. doi: 10.1039/c7nr06966a

Kordelas, L., Rebmann, V., Ludwig, A. K., Radtke, S., Ruesing, J., Doeppner, T. R., et al. (2014). MSC-derived exosomes: a novel tool to treat therapy-refractory graft-versus-host disease. *Leukemia* 28, 970–973. doi: 10.1038/leu.2014.41

Lai, R. C., Arslan, F., Lee, M. M., Sze, N. S. K., Choo, A., Chen, T. S., et al. (2010). Exosome secreted by MSC reduces myocardial ischemia/reperfusion injury. *Stem Cell Res.* 4, 214–222. doi: 10.1016/j.scr.2009.12.003

Lalu, M. M., McIntyre, L., Pugliese, C., Fergusson, D., Winston, B. W., Marshall, J. C., et al. (2012). Safety of cell therapy with mesenchymal stromal cells (safecell): a systematic review and meta-analysis of clinical trials. *PLoS One* 7:e47559. doi: 10.1371/journal.pone.0047559

Lawson, T., Kehoe, D. E., Schnitzler, A. C., Rapiejko, P. J., Der, K. A., Philbrick, K., et al. (2017). Process development for expansion of human mesenchymal stromal cells in a 50L single-use stirred tank bioreactor. *Biochem. Eng. J.* 120, 49–62. doi: 10.1016/j.bej.2016.11.020

Lener, T., Gimona, M., Aigner, L., Börger, V., Buzas, E., Camussi, G., et al. (2015). Applying extracellular vesicles based therapeutics in clinical trials - an ISEV position paper. *J. Extracell. Vesicles* 4:30087.

Li, Y., Gao, Y., Gong, C., Wang, Z., Xia, Q., Gu, F., et al. (2018). A33 antibody-functionalized exosomes for targeted delivery of doxorubicin against colorectal cancer. *Nanomedicine* 14, 1973–1985. doi: 10.1016/j.nano.2018.05.020

Mazzocca, A. D., McCarthy, M. B. R., Chowaniec, D. M., Dugdale, E. M., Hansen, D., Cote, M. P., et al. (2012). The positive effects of different platelet-rich plasma methods on human muscle, bone, and tendon cells. *Am. J. Sports Med.* 40, 1742–1749. doi: 10.1177/0363546512452713

Mendt, M., Kamerkar, S., Sugimoto, H., McAndrews, K. M., Wu, C. C., Gagea, M., et al. (2018). Generation and testing of clinical-grade exosomes for pancreatic cancer. *JCI Insight* 3:e99263.

Mitchell, J. P., Court, J., Mason, M. D., Tabi, Z., and Clayton, A. (2008). Increased exosome production from tumour cell cultures using the Integra CELLine culture system. *J. Immunol. Methods* 335, 98–105. doi: 10.1016/j.jim.2008.03.001

Mizukami, A., Fernandes-platzgummer, A., Carmelo, J. G., Swiech, K., Covas, D. T., Cabral, J. M. S., et al. (2016). Stirred tank bioreactor culture combined with serum- / xenogeneic-free culture medium enables an efficient expansion of umbilical cord-derived mesenchymal stem / stromal cells. *Biotechnol. J.* 11, 1048–1059. doi: 10.1002/biot.201500532

Morrell, A. E., Brown, G. N., Robinson, S. T., Sattler, R. L., Baik, A. D., Zhen, G., et al. (2018). Mechanically induced Ca2+ oscillations in osteocytes release extracellular vesicles and enhance bone formation. *Bone Res.* 6:6.

Naveau, A., Lataillade, J.-J., Fournier, B. P., Couty, L., Prat, M., Ferre, F. C., et al. (2010). Phenotypic study of human gingival fibroblasts in a medium enriched with platelet lysate. *J. Periodontol.* 82, 632–641. doi: 10.1902/jop.2010.100179

Nogueira, D. E. S., Rodrigues, C. A. V., Carvalho, M. S., Miranda, C. C., Hashimura, Y., Jung, S., et al. (2019). Strategies for the expansion of human induced pluripotent stem cells as aggregates in single-use Vertical-WheelTM bioreactors. *J. Biol. Eng.* 13:74.

Oliveira, P. H., Boura, J. S., Abecasis, M. M., Gimble, J. M., da Silva, C. L., and Cabral, J. M. S. (2012). Impact of hypoxia and long-term cultivation on the genomic stability and mitochondrial performance of ex vivo expanded human stem/stromal cells. *Stem Cell Res.* 9, 225–236. doi: 10.1016/j.scr.2012.07.001

Panigrahi, G. K., Praharaj, P. P., Peak, T. C., Long, J., Singh, R., Rhim, J. S., et al. (2018). Hypoxia-induced exosome secretion promotes survival of African-American and Caucasian prostate cancer cells. *Sci. Rep.* 8:3853.

Pascucci, L., Coccè, V., Bonomi, A., Ami, D., Ceccarelli, P., Ciusani, E., et al. (2014). Paclitaxel is incorporated by mesenchymal stromal cells and released in exosomes that inhibit in vitro tumor growth: a new approach for drug delivery. *J. Control. Release* 192, 262–270. doi: 10.1016/j.jconrel.2014.07.042

Phinney, D. G., and Pittenger, M. F. (2017). Concise review: MSC-derived exosomes for cell-free therapy. *Stem Cells* 35, 851–858. doi: 10.1002/stem.2575

Racher, A. J., Looby, D., and Griffiths, J. B. (1990). Use of lactate dehydrogenase release to assess changes in culture viability. *Cytotechnology* 3, 301–307. doi: 10.1007/bf00365494

Rafiq, Q. A., Brosnan, K. M., Coopman, K., Nienow, A. W., and Hewitt, C. J. (2013). Culture of human mesenchymal stem cells on microcarriers in a 5 l stirred-tank bioreactor. *Biotechnol. Lett.* 35, 1233–1245. doi: 10.1007/s10529-013-1211-9

Raposo, G., Nijman, H. W., Stoorvogel, W., Liejendekker, R., Harding, C. V., Melief, C. J., et al. (1996). B lymphocytes secrete antigen-presenting vesicles. *J. Exp. Med.* 183, 1161–1172. doi: 10.1084/jem.183.3.1161

Ratajczak, J., Miekus, K., Kucia, M., Zhang, J., Reca, R., Dvorak, P., et al. (2006). Embryonic stem cell-derived microvesicles reprogram hematopoietic progenitors: evidence for horizontal transfer of mRNA and protein delivery. *Leukemia* 20, 847–856. doi: 10.1038/sj.leu.2404132

Reinisch, A., Etchart, N., Thomas, D., Hofmann, N. A., Fruehwirth, M., Sinha, S., et al. (2015). Epigenetic and in vivo comparison of diverse MSC sources reveals an endochondral signature for human hematopoietic niche formation. *Blood* 125, 249–260. doi: 10.1182/blood-2014-04-572255

Ren, G., Chen, X., Dong, F., Li, W., Ren, X., Zhang, Y., et al. (2012). Concise review: mesenchymal stem cells and translational medicine: emerging issues. *Stem Cells Transl. Med.* 1, 51–58. doi: 10.5966/sctm.2011-0019

Ribeiro, A., Laranjeira, P., Mendes, S., Velada, I., Leite, C., Andrade, P., et al. (2013). Mesenchymal stem cells from umbilical cord matrix, adipose tissue and bone marrow exhibit different capability to suppress peripheral blood B, natural killer and T cells. *Stem Cell Res. Ther.* 4:125. doi: 10.1186/scrt336

Rodrigues, C. A. V., Silva, T. P., Nogueira, D. E. S., Fernandes, T. G., Hashimura, Y., Wesselschmidt, R., et al. (2018). Scalable culture of human induced pluripotent cells on microcarriers under xeno-free conditions using single-use vertical-WheelTM bioreactors. *J. Chem. Technol. Biotechnol.* 93, 3597–3606. doi: 10.1002/jctb.5738

Rupert, D. L. M., Claudio, V., Lässer, C., and Bally, M. (2017). Methods for the physical characterization and quantification of extracellular vesicles in biological samples. *Biochim. Biophys. Acta* 1861, 3164–3179. doi: 10.1016/j.bbagen.2016.07.028

Salomon, C., Ryan, J., Sobrevia, L., Kobayashi, M., Ashman, K., Mitchell, M., et al. (2013). Exosomal signaling during hypoxia mediates microvascular endothelial cell migration and vasculogenesis. *PLoS One* 8:e68451. doi: 10.1371/journal.pone.0068451

Schirmaier, C., Jossen, V., Kaiser, S. C., Jüngerkes, F., Brill, S., Safavi-Nab, A., et al. (2014). Scale-up of adipose tissue-derived mesenchymal stem cell production in stirred single-use bioreactors under low-serum conditions. *Eng. Life Sci.* 14, 292–303. doi: 10.1002/elsc.201300134

Sousa, M. F. Q., Silva, M. M., Giroux, D., Hashimura, Y., Wesselschmidt, R., Lee, B., et al. (2015). Production of oncolytic adenovirus and human mesenchymal stem cells in a single-use, Vertical-Wheel bioreactor system: impact of bioreactor design on performance of microcarrier-based cell culture processes. *Biotechnol. Prog.* 31, 1600–1612. doi: 10.1002/btpr.2158

Tian, Y., Li, S., Song, J., Ji, T., Zhu, M., Anderson, G. J., et al. (2014). A doxorubicin delivery platform using engineered natural membrane vesicle exosomes for targeted tumor therapy. *Biomaterials* 35, 2383–2390. doi: 10.1016/j.biomaterials.2013.11.083

Vader, P., Mol, E. A., Pasterkamp, G., and Schiffelers, R. M. (2016). Extracellular vesicles for drug delivery. *Adv. Drug Deliv. Rev.* 106, 148–156. doi: 10.1016/j.addr.2016.02.006

Valadi, H., Ekström, K., Bossios, A., Sjöstrand, M., Lee, J. J., and Lötvall, J. O. (2007). Exosome-mediated transfer of mRNAs and microRNAs is a novel mechanism of genetic exchange between cells. *Nat. Cell Biol.* 9, 654–659. doi: 10.1038/ncb1596

Van Niel, G., D'Angelo, G., and Raposo, G. (2018). Shedding light on the cell biology of extracellular vesicles. *Nat. Rev. Mol. Cell Biol.* 19, 213–228. doi: 10.1038/nrm.2017.125

Viswanathan, S., Shi, Y., Galipeau, J., Krampera, M., Leblanc, K., Martin, I., et al. (2019). Mesenchymal stem versus stromal cells: international society for cell & gene therapy (ISCT®) mesenchymal stromal cell committee position statement on nomenclature. *Cytotherapy* 21, 1019–1024. doi: 10.1016/j.jcyt.2019.08.002

Vrijsen, K. R., Maring, J. A., Chamuleau, S. A. J., Verhage, V., Mol, E. A., Deddens, J. C., et al. (2016). Exosomes from cardiomyocyte progenitor cells and mesenchymal stem cells stimulate angiogenesis via EMMPRIN. *Adv. Healthc. Mater.* 5, 2555–2565. doi: 10.1002/adhm.201600308

Watson, D. C., Bayik, D., Srivatsan, A., Bergamaschi, C., Valentin, A., Niu, G., et al. (2016). Efficient production and enhanced tumor delivery of engineered extracellular vesicles. *Biomaterials* 105, 195–205. doi: 10.1016/j.biomaterials.2016.07.003

Webber, J., and Clayton, A. (2013). How pure are your vesicles? *J. Extracell. Vesicles* 2:19861. doi: 10.3402/jev.v2i0.19861

Witwer, K. W., Van Balkom, B. W. M., Bruno, S., Choo, A., Dominici, M., Gimona, M., et al. (2019). Defining mesenchymal stromal cell (MSC)-derived small extracellular vesicles for therapeutic applications. *J. Extracell. Vesicles* 8:1609206. doi: 10.1080/20013078.2019.1609206

Wysoczynski, M., Khan, A., and Bolli, R. (2018). New paradigms in cell therapy: repeated dosing, intravenous delivery, immunomodulatory actions, and new cell types. *Circ. Res.* 123, 138–158. doi: 10.1161/circresaha.118.313251

Zhang, B., Wang, M., Gong, A., Zhang, X., Wu, X., Zhu, Y., et al. (2015). HucMSC-exosome mediated-Wnt4 signaling is required for cutaneous wound healing. *Stem Cells* 33, 2158–2168. doi: 10.1002/stem.1771

Conflict of Interest: SJ is employee of PBS Biotech, Inc. BL is CEO and co-founder of PBS Biotech, Inc. These collaborating authors participated in the development of the bioreactor systems used in the manuscript. R-JT and WM are employees of AventaCell Biomedical Corp. These collaborating authors participated in the development of the culture medium supplement used in the manuscript. This does not alter the authors adherence to all the policies of the journal on sharing data and materials.

The remaining authors declare that the research was conducted in the absence of any commercial or financial relationships that could be construed as a potential conflict of interest.

frontiers in Cell and Developmental Biology

REVIEW
published: 19 November 2020
doi: 10.3389/fcell.2020.545126

Tumor Microenvironment Uses a Reversible Reprogramming of Mesenchymal Stromal Cells to Mediate Pro-tumorigenic Effects

Armel H. Nwabo Kamdje[1], Paul F. Seke Etet[1,2], Richard Simo Tagne[1], Lorella Vecchio[2], Kiven Erique Lukong[3] and Mauro Krampera[4]*

[1] Department of Physiological Sciences and Biochemistry, Faculty of Medicine and Biomedical Sciences (FMBS), University of Ngaoundéré, Ngaoundéré, Cameroon, [2] Center for Sustainable Health and Development, Garoua, Cameroon, [3] Department of Biochemistry, Microbiology and Immunology, College of Medicine, University of Saskatchewan, Saskatoon, SK, Canada, [4] Section of Hematology, Stem Cell Research Laboratory, Department of Medicine, University of Verona, Verona, Italy

OPEN ACCESS

Edited by:
Lindolfo da Silva Meirelles, Universidade Luterana do Brazil, Brazil

Reviewed by:
Gianandrea Pasquinelli, University of Bologna, Italy
Sofia Avnet, Rizzoli Orthopedic Institute (IRCCS), Italy

***Correspondence:**
Armel H. Nwabo Kamdje
armel.nwabo@gmail.com

Specialty section:
This article was submitted to Stem Cell Research, a section of the journal Frontiers in Cell and Developmental Biology

Received: *24 March 2020*
Accepted: *28 October 2020*
Published: *19 November 2020*

Citation:
Nwabo Kamdje AH, Seke Etet PF, Simo Tagne R, Vecchio L, Lukong KE and Krampera M (2020) Tumor Microenvironment Uses a Reversible Reprogramming of Mesenchymal Stromal Cells to Mediate Pro-tumorigenic Effects. Front. Cell Dev. Biol. 8:545126. doi: 10.3389/fcell.2020.545126

The role of mesenchymal stromal cells (MSCs) in the tumor microenvironment is well described. Available data support that MSCs display anticancer activities, and that their reprogramming by cancer cells in the tumor microenvironment induces their switch toward pro-tumorigenic activities. Here we discuss the recent evidence of pro-tumorigenic effects of stromal cells, in particular (i) MSC support to cancer cells through the metabolic reprogramming necessary to maintain their malignant behavior and stemness, and (ii) MSC role in cancer cell immunosenescence and in the establishment and maintenance of immunosuppression in the tumor microenvironment. We also discuss the mechanisms of tumor microenvironment mediated reprogramming of MSCs, including the effects of hypoxia, tumor stiffness, cancer-promoting cells, and tumor extracellular matrix. Finally, we summarize the emerging strategies for reprogramming tumor MSCs to reactivate anticancer functions of these stromal cells.

Keywords: stromal cells, tumorigenic effects, anticancer effects, tumor microenvironment, reprogramming

INTRODUCTION

Mesenchymal stromal cells (MSCs) are multipotent stem cells capable of differentiating into various cell types of the mesodermal lineage, including adipocytes, endothelial cells, fibroblasts, chondrocytes, osteoblasts, and myocytes (Dominici et al., 2006), and possibly into non-mesodermal cell types, such as neural, pancreatic, hepatic, and gastric cells (Oswald et al., 2004; Cislo-Pakuluk and Marycz, 2017; Luo et al., 2020; Xuan et al., 2020). They are a heterogeneous mesenchymal cell population, which resides in the stroma of various tissues and organs and expressing the membrane markers CD105, CD73, and CD90, but not HLA-DR, CD14, CD19, CD31, CD34, and CD45 (Dominici et al., 2006; Nwabo Kamdje et al., 2011). MSCs are a key tool in tissue engineering and regenerative medicine, because they are easily collected and thanks to their ability to migrate and home into damaged tissues where they (i) interact with the microenvironment to drive tissue repair; (ii) transdifferentiate into new cells to restore and/or replace damaged tissues; (iii) rescue organ functions, thanks to their high proliferation, adhesion, migration, differentiation, and immunoregulatory properties (Barberini et al., 2014; Chi et al., 2014; Li et al., 2015). MSC properties

are mainly dependent of components of their secretome including numerous factors favoring tissue repair, such as angiopoietin-1 (Ang1), vascular epidermal growth factor (EGF), endothelial growth factor (VEGF), transforming growth factor-beta (TGF-β), hepatocyte growth factor (HGF), fibroblast growth factor (FGF), granulocyte-colony stimulating factor (G-CSF), platelet-derived growth factor (PDGF), interleukin 6 (IL-6) and IL-12, chemokine (C-C motif) ligand 7 (CCL7) and CCL25, and C-X-C motif chemokine 8 (CXCL8), CXCL9, CXCL16, and CCL20 (Ishiki et al., 1992; Li et al., 2013; Wang et al., 2013; Liu et al., 2014; Windmolders et al., 2014; Sesia et al., 2015; Rolandsson Enes et al., 2016; Tsiklauri et al., 2018; Gyukity-Sebestyen et al., 2019; Ozdemir et al., 2019).

However, MSCs also reside in the tumor microenvironment, where they were reported to promote pivotal tumorigenic processes such as: (i) malignant transformation; (ii) cancer cell maintenance and stemness; (iii) cancer stem cell niche formation, including angiogenesis and neovascularization; (iv) metastasis formation; and (v) resistance to anticancer drugs [for review see Seke Etet et al. (2013), Nwabo Kamdje et al. (2014), Atiya et al. (2020), Osman et al. (2020)]. On the other hand, MSC-derived stromal cells restraining cancer growth have been reported in the tumor microenvironment (Bu et al., 2019; Mizutani et al., 2019; Tew et al., 2019) and growing evidence supports that the pro-tumorigenic effects of MSCs emerge from cell reprogramming by the tumor microenvironment (Coffman et al., 2019; Mandal et al., 2019; Al-Jawadi et al., 2020; Boada et al., 2020). Herein, we provide an overview and discuss emerging data supporting MSC reprogramming by the tumor microenvironment and recent reports supporting the existence of stromal cells restraining cancer growth in the tumor microenvironment.

MSC PRO-TUMORIGENIC EFFECTS: IMMUNOSUPPRESSION AND METABOLIC CHANGES

Some of the most reported pro-tumorigenic effects of MSCs include their roles in the metabolic and cellular senescence-like changes, typically observed in various cancers and in the tumor microenvironment-mediated immunosuppression (**Figure 1**).

Cancer-Associated Metabolic Changes

The Warburg effect, a metabolic hallmark of tumor cells, is the fact that cancer cells produce most of their ATP via glycolysis, even under aerobic conditions, although it is a less efficient pathway compared to oxidative phosphorylation and despite their greater need for energy [for review see Xu et al. (2015), Fu et al. (2017)]. For instance, pancreatic cancer cells can utilize "metabolic reprogramming," through the enhancement of glycolysis with increased lactate production and glycolytic enzyme overexpression, to satisfy their energy demand and support malignant behavior, despite a hypoxic and nutrient-deficient microenvironment (Yang et al., 2020). Growing evidence supports that stromal cells trigger the Warburg effect in cancer cells. For instance, the bone marrow (BM)-derived MSCs co-cultured with leukemia cells under normoxic conditions revealed reduced mitochondrial membrane potential and pyruvate metabolism in the both cell types (Samudio et al., 2008). Interestingly, mitochondrial membrane potential reduction was mediated in leukemia cells by an uncoupling protein 2 (UCP2)-dependent mechanism, suggesting that MSCs facilitated the Warburg effect in cancer cells by activating highly conserved mammalian UCPs. On the same hand, a study carried out on bevacizumab-resistant glioblastoma, suggested that inside the hypoxic microenvironment, chemoresistance in cancer cells occurs through: (i) metabolic reprogramming, characterized with suppressed oxidative phosphorylation and upregulated glycolysis; (ii) perivascular invasiveness along remaining blood vessels in a VEGF- and neo-angiogenesis-independent manner; and (iii) enrichment of tumor-initiating stem cells residing in the perivascular niche close to residual blood vessels (Chandra et al., 2020). Such observations are the basis of studies aiming at targeting signaling molecules pivotal for cancer cell glycolysis [for review see Xu et al. (2015)].

An early study aimed at determining whether the Warburg effect is due mainly to the hypoxic microenvironment, or to inherent metabolic alterations in transformed MSCs, revealed that aerobic glycolysis results from MSC oncogenic adaptation to bioenergetic requirements. Authors observed that in some circumstances, transformed MSCs may also rely on increased in oxidative phosphorylation (Funes et al., 2007). However, the study revealed a reversible increase in the transcription of glycolytic enzymes genes, in tumors generated by transformed MSCs, indicating a metabolic support of MSCs for surrounding cells of the tumor to its microenvironment. Similar observations led to the development of a new hypothesis for stromal cell support to cancer cell metabolism, the reverse Warburg effect [for review see Xu et al. (2015), Fu et al. (2017)]. Basically, cancer cells induce oxidative stress in neighboring stromal cells such as MSC-derived fibroblasts by secreting reactive oxygen species (ROS). In stromal cells, ROS trigger aerobic glycolysis and the production of lactate, pyruvate, and other high energy metabolites. Finally, the latter are transported to adjacent cancer cells where they sustain the energy need and various signaling pathways driving tumor progression, metastasis, and chemoresistance (Fu et al., 2017). This new approach focused on tumor cell metabolism, pointed out many targets in tumor microenvironment and cancer cell machinery for anticancer therapy.

A wealth of other reports also supports the involvement of stromal cells in the metabolic changes supporting tumorigenic processes. For instance, In breast cancer, depending on ROS, hypoxia, and glucose availability in the microenvironment, tumor-initiating cells are capable to switch toward oxidative phosphorylation and glycolysis. This adaptative metabolic switch is controlled at least in part by stromal cells to confer a survival advantage to malignant cells (Walsh et al., 2019). Lung et al. (2019) reported that the expression of estrogen receptor-α (ER), the target of endocrine therapies in breast cancer, is regulated by the BM microenvironment. In this study, the induction of ESR1 mRNA and ER protein downregulation, through a MAPK-independent mechanism, was achieved by the treatment of breast cancer cells with conditioned culture media from either cancer-activated BM stromal cells or HS5 BM stromal cell line

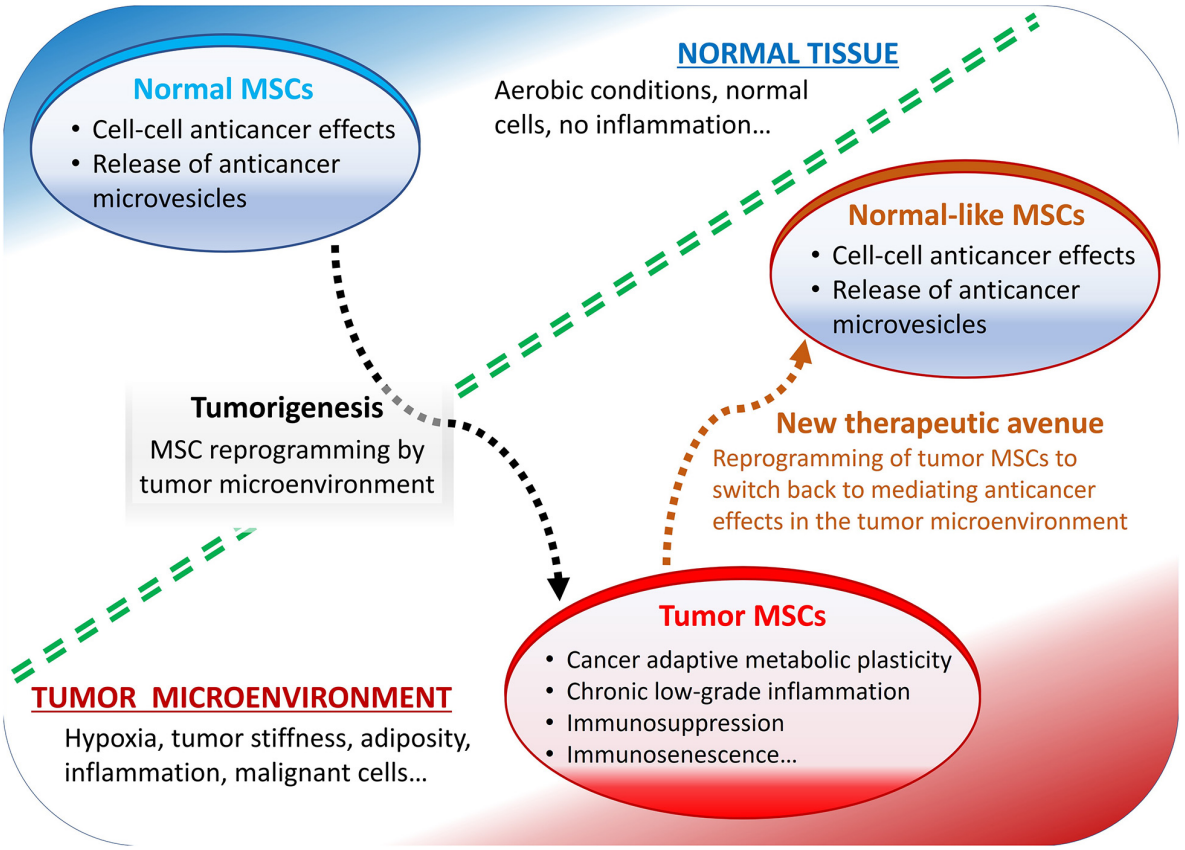

FIGURE 1 | Summary of mesenchymal stromal cells (MSCs) role in the tumor microenvironment. Normally, MSCs mediate anticancer effects but reprogrammed by tumor microenvironment they display pro-tumorigenic effects.

(Lung et al., 2019). In addition, thyroid hormones, which are well-established pro-tumorigenic players, may stimulate tumor growth and neovascularization in various solid cancers by activating MSCs through a non-classical integrin αvβ3 signaling (Schmohl et al., 2019). Moreover, the EGF-like superfamily member EGFL6 would promote tumor growth by mediating a cross-talk between stromal and cancer cells that would contribute to stemness and epithelial-mesenchymal transition (EMT), an important tumorigenic mechanism where epithelial cells become MSCs by losing their cell polarity and adhesion ability, and by gaining migratory and invasive properties (An et al., 2019). Altogether, these observations confirm that targeting cancer cell energy metabolism is still a sound anticancer strategy, and point out stromal cells as major players in cancer cell energy metabolism.

Immunosenescence and Immunosuppression

Immunosuppression and immunosenescence are two major immunological phenomena observed in the tumor microenvironment. Like aging processes, cancers environment is characterized by a chronic inflammation ("inflammaging") and cellular senescence ("immunosenescence"). The role of stromal cells' immunomodulation in shaping a senescent microenvironment in broad spectrum of human malignancies, especially tumorigenesis, has been documented extensively [for review see Salminen et al. (2020), Thomas et al. (2020)]. For instance, BM stromal cells from patients with myelodysplastic syndrome display a senescence phenotype induced by S100A9-induced Toll-like receptor 4 (TLR4), NLRP3 inflammasome activation and IL-1β secretion (Shi et al., 2019). Senescent breast luminal cells promoted carcinogenesis by activating MSC-derived fibroblasts through the inflammatory cytokine IL-8 (Al-Khalaf et al., 2019). Acute myeloid leukemia (AML) blasts induced a senescence-associated secretory phenotype (SASP) in BM stromal cells through a p16INK4a-dependent mechanism, which encompassed the irreversible arrest of cell proliferation and the secretion of a set of chemokines, proinflammatory cytokines, and growth factors (Abdul-Aziz et al., 2019). MSCs promoted the progression of gastric cancer cells through the release of CXCL16, which activates STAT3-mediated expression of Ror1 in the cancer cells (Ikeda et al., 2020). In oral mucosa carcinogenesis, MSCs increased immunosuppressive functions on T cell proliferation and pro-tumorigenic effects of tumor resident MSCs correlated with higher expressions of cellular proliferative status indicator Ki67 (Chen et al., 2019a). STAT4 over-expression in gastric cancer cells made normal fibroblasts

acquire cancer-associated fibroblast (CAF)-like features through wnt/β-catenin-dependent signaling (Zhou et al., 2019a). A recent study using MSCs expanded from BM and prostate cancer tissue from independent donors showed that tumor-infiltrating MSCs are major drivers of the immunosuppressive tumor microenvironment in prostate cancer (Krueger et al., 2019). The authors reported the ability of prostate cancer-infiltrating MSCs to suppress T-cell proliferation through immunosuppressive properties comparable to canonical BM-derived MSCs. The suppression of proliferation mediated by prostate cancer-infiltrating MSCs was dose-dependent, and the expressions of PD-L1 and PD-L2 were upregulated on T-cells in the presence of IFN-γ and TNF-α (Krueger et al., 2019). In another study, the transcriptome analysis of MSCs from multiple myeloma patients revealed constitutive abnormalities in immune system activation, cell cycle progression, and osteoblastogenesis that were maintained even in the absence of tumor cells, thus strongly suggesting that MSCs may contribute to the immune evasion and bone lesions frequently found in multiple myeloma (Fernando et al., 2019). Altogether, these observations also point out stromal cells as major players in tumorigenesis and reveal more targets for pharmacological anticancer therapy.

Although it is well-established that MSCs are major drivers of the immunomodulation observed in solid tumor microenvironment, many others cell components can cooperate with MSCs to modulate immune response. In AML,CXCL8 supports the survival and proliferation of leukemic cells via the PI3K/AKT signaling pathway. In the affected BM microenvironment CXCL8 is mainly secreted by MSCs (Cheng et al., 2019). Study on other bone marrow disorders show that and MSCs to shape the Microenvironment at least partly by inducing suppressive monocytes and dampening NK cell functions (Sarhan et al., 2020).

EVIDENCE OF STROMAL CELL PROGRAMMING BY TUMOR MICROENVIRONMENT

A growing body of evidence supports that stromal cells follow the program dictated by their microenvironment.

Tumor Microenvironment Effects on Stromal Cells

Early studies addressing the composition of the tumor microenvironment, reported an atypical cellular and molecular microenvironment supporting carcinogenesis and chemoresistance (Garcia-Hernandez et al., 2017; Pelizzo et al., 2018). Recently, Coffman et al. (2019) reported that ovarian carcinoma-associated MSCs, which are critical stromal progenitor cells promoting tumor cell growth, cancer stemness and chemoresistance, arose from a process of tumor-mediated reprogramming of local tissue MSCs. This study also provided strong evidence that tumor-mediated MSC conversion is tissue- and cancer-type dependent, requiring tumor-secreted factors and hypoxia (Coffman et al., 2019). In other studies, gene expression signatures and mesenchymal shift in quiescent glioblastoma cells, a source of tumor recurrence in highly malignant glioblastoma, was observed following their interactions with niche microenvironment (Tejero et al., 2019). Breast tumor microenvironment transformed naive MSCs into tumor-forming cells in nude mice. Indeed, MSCs pre-exposed to conditioned medium or purified exosomes derived from breast cancer cells (MDA-MB-231) formed a tumor-like mass rich in stromal tissue by 14 weeks when injected into mammary glands of nude mice (Worner et al., 2019). Similarly, CCL5 secreted by classic Hodgkin lymphoma cells recruited MSCs and monocytes, enhancing MSC proliferation and CCL5 secretion. Conditioned medium from these educated MSCs increased tumor cell growth and monocyte migration (Casagrande et al., 2019). Similarly TLR4 signaling educated MSCs to promote tumor microenvironment transformation in multiple myeloma (Giallongo et al., 2019).

Exosomes including extracellular vesicles (EVs) represent a mean used by tumor cells to educate MSCs in the microenvironment. In chronic myeloid leukemia (CML), leukemia cells altered the cellular and immune-related properties of BM-MSCs and macrophages *in vitro* by the mean of exosomes (Jafarzadeh et al., 2019). Consistently, Zannoni et al. (2019) reported that EVs released by monocytes from chronic myelomonocytic leukemia patients conferred a procoagulant state favorable for cancer progression, through a tissue factor-dependent mechanism mediated by MSCs. In glioma, exosomes from cancer cells induced a tumor-like phenotype in MSCs by activating glycolysis (Ma et al., 2019). In gastric cancer, tumor cell-derived exosomes affected the immunomodulatory functions of MSCs by activating the NF-kB signaling pathway, which in turn mediates support to tumor growth by maintaining the inflammatory environment and enhancing the ability of MSCs to activate immune cells (Shen et al., 2019).

In addition, pre-metastatic niche in distant organs may be created, at least in part, by the transfer of EVs secreted by tumor-associated macrophages (TAMs) to stromal cells, such as fibroblasts, peritoneal mesothelial cells (PMCs), and endothelial cells (Umakoshi et al., 2019). Long-term culture of human MDA-MB-231 breast cancer cells with normal human MSCs was associated with the formation of three-dimensional (3D) tumor spheroids *in vitro*, with a 14-fold enhanced expression of the breast tumor marker urokinase plasminogen activator (uPA; Melzer et al., 2019). Similarly, MSCs cultured with colorectal cancer cells showed increased invasiveness and proliferative abilities due to increased TGF-β1 and decreased p53 levels (Oh et al., 2020). In another study, TGF-β1 promoted the migration and invasion of HCT116 and HT29 colorectal cancer cells, and induced the differentiation of MSCs into CAFs through a JAK/STAT3 signaling-depended mechanism (Tan et al., 2019).

The available data also support detrimental cross-talks between stromal and cancer cells. For instance, reciprocal reprogramming of cancer stem cells (CSCs) and associated MSCs may promote tumor progression in gastric cancer (Shamai et al., 2019). Similarly, asporin, a factor secreted by MSCs following cellular interactions within the tumor microenvironment, altered the tumor microenvironment and inhibited MSC differentiation

to drive metastatic progression through CD49d/CD29 signaling (Hughes et al., 2019). Moreover, Dabbah et al. (2019) reported that microvesicles derived from BM MSCs of multiple myeloma patients increased the tumorigenicity of MM cells (Hughes et al., 2019). In this study, CD49d and CD29 integrin overexpression in MM-MSC microvesicles were associated with patient staging and response to treatment. The concomitant inhibition of these molecules resulted in reduced uptake of EVs by MM-MSC (but not normal donor MSC microvesicles), and downregulation of aggressiveness markers, thus enhancing response to chemotherapy (Dabbah et al., 2019). Interestingly, this study also suggested that the reciprocal interactions of malignant cells and MSCs in breast cancer microenvironment may result in the transformation of naive MSCs into cells capable of forming explants in nude mice (Dabbah et al., 2019).

Overall, together with evidence of MSC role in cancer metabolism discussed in section 1.1, these data suggest that tumorigenesis is triggered and driven by a bidirectional cross-talks between MSCs and tumor environment. Therefore, unraveling the signaling molecules involved in these pro-tumorigenic cross-talks may lead to the identification of novel targets for anti-cancer therapy. Promising reports using this approach include a recent study that addressed the potential roles and mechanisms of long non-coding RNAs in EMT and in the maintenance of CSC-like properties in non-small cell lung cancer (NSCLC). Using A549 and H1299 human NSCLC cell lines, L9981 and 95D highly metastatic NSCLC cell lines, and NL9980 and 95C low-metastatic NSCLC cell lines., the authors observed that knockdown of long non-coding RNA linc-ITGB1 inhibited the expression of various markers of cancer stemness and CSC formation by reducing the expression of the EMT-related transcription factor Snail. Rewardingly, the overexpression of Snail reversed the inhibitory effects of linc-ITGB1 knockdown (Guo et al., 2019). Further studies should characterize and target the signaling pathways supporting the reprogramming of stromal cells by cancer cells, as well as other interactions between these cells that support tumorigenesis.

Hypoxia and Tumor Stiffness

Tumor stiffness and hypoxia are key conditions of the solid tumor microenvironment, known to promote tumor survival, progression and metastasis. Hypoxia-driven phosphorylated glycoprotein such as osteopontin, promoted stem cell-like properties and EMT in pancreatic cancer cells in a paracrine manner, through integrin αvβ3-Akt/Erk- forkhead box protein M1 (FOXM1) signaling (Cao et al., 2019). Hypoxia-induced EMT was observed in non-small-cell lung cancer (Chen et al., 2019b) where hypoxia induced the acquisition of cancer stem cell features through CXCR4 activation (Kang et al., 2019). In fact earlier reports pointed out HIF-1 as a link between hypoxia, inflammation, and cancer [for review see Balamurugan (2016), Shi et al. (2018)]. Growing evidence suggests that stromal cells mediate the pro-tumorigenic effects of hypoxia and tumor stiffness. Notably, MSC-derived CAFs were suggested as the link between biophysical forces and pro-metastatic signaling in colon cancer, as they respond to increased stiffness of the tumor microenvironment by activating TGF-β family members and the signaling of the strong pro-metastatic cytokine activin A (Bauer et al., 2020). On the same hand, microvesicles derived from human BM-MSCs supported human osteosarcoma (U2OS) cell growth under hypoxia conditions both *in vitro* and *in vivo* through PI3K/AKT and HIF-1α-dependent mechanisms (Lin et al., 2019). In addition, interactions of cancer cells and stromal cells in hypoxic microenvironment were found to drive EMT through NOTCH and c-MET signaling, inducing an immunosuppressive response within the microenvironment in pancreatic ductal adenocarcinoma (PDA; Daniel et al., 2019).

In a study addressing the end-stage of myeloma cell mobilization from the BM into peripheral blood (PB), hypoxic BM niches, together with a pro-inflammatory microenvironment resulting from the interactions between tumor cells and BM stromal cells, were able to induce an arrest in proliferation, thus forcing tumor cells to circulate into the peripheral blood to seek other BM niches (Garces et al., 2020). These observations suggest that hypoxic BM niches are key players in metastatic processes. In agreement with this view, it has been observed in an *in vivo* mouse syngeneic tumor model, that hypoxic BM stromal cells-derived exosomal miRNAs promoted metastasis of lung cancer cells via STAT3-induced EMT (Zhang et al., 2019a,b). Consistently, Saforo et al. (2019) described an *in vitro* cell culturing system incorporating elements of the *in vivo* lung environment, including physiological hypoxia (5% O2) and lung fibroblast-derived extracellular matrix. Through this culture system, a rapid expansion of stromal progenitors from patient's lung tumor resections was achieved. These progenitor cells retained the secretion of factors associated with cancer progression, the expression of pluripotency markers, and the ability to enhance tumor cell growth and metastasis (Saforo et al., 2019). The ability of hypoxia-conditioned MSCs to promote cancer progression was also observed in hepatocellular carcinoma but the effect was dependent of yes-associated protein (YAP)-mediated lipogenesis reprogramming (Liu et al., 2019). In Glioblastoma, the glioblastoma stem-like cells (GSCs) phenotype, the worst prognostic marker of Glioblastoma, was reported to persist due to hypoxic microenvironment-dependent release of extracellular adenosine, which in turn, promote cell migration, invasion and tumor recurrence through the activation of the A3 Adenosine Receptor (A3AR; Torres et al., 2019).

Altogether, these data suggest that hypoxia, tumor stiffness, and inflammation are among the major drivers of the pro-tumorigenic reprogramming of stromal cells in the tumor microenvironment.

Extracellular Matrix Involvement

Emerging data strongly suggest that the tumor extracellular matrix (ECM) also contributes to tumor microenvironment effects on stromal cells. For example, after showing that multiple myeloma (MM) cells, cultured with BM-MSCs, co-modulated the phenotype of MM cells in a MAPKs/translation initiation (TI)-dependent manner, Ibraheem et al. (2019) reported that even the decellularized ECM of BM-MSCs from MM patients was able to induce comparable pro-tumorigenic effects (Ref). A number of changes in microRNAs was shown to affect MM phenotype and the activation of MAPK/TI, EMT, proliferation, and CXCR4,

with a role for BM-MSCs secretome and microvesicles. On the other hand, the decellularized ECM of BM-MSCs from normal donors mediated anticancer effects, including a rapid and persistent decrease in MAPK/TI activation, proliferation, cell count, viability, migration, and invasion (Ibraheem et al., 2019). These authors also provided evidence of a synergism between the ECM and microvesicles in the modulation of MM cell response to chemotherapy as well as in the hierarchy and interdependence of MAPKs/TI/autophagy/phenotype cascade. These observations suggested that to reprogram MSCs for pro-tumorigenic effects, the ECM also needs to be reprogrammed by cancer-promoting cells. For example, senescent MSCs actively remodeled the surrounding ECM to drive breast cancer cells to a more-invasive phenotype (Ghosh et al., 2020). Consistently, matrix metalloproteinase-9 (MMP-9) produced by leukemia cells facilitated tumor progression via remodeling of the ECM of the BM microenvironment. This is supported by the fact that MMP-9-deficiency in the BM microenvironment reduced leukemia-initiating cells and prolonged survival of mice with BCR-ABL1-positive B-cell acute lymphoblastic leukemia (B-ALL; Verma et al., 2020).

Three-dimensional culture studies with cancer and stromal cells in ECM and multiplex quantitative analysis method, reprensent majors tool to tacle signaling molecules and mechanisms used by reprogrammed ECM to drive MSC pro-tumorigenic effects, (Hwang et al., 2019; Maliszewska-Olejniczak et al., 2019). Therefore, a recent study using such approach in hepatocellular carcinoma (HCC), showed that cell repopulation of cirrhotic scaffolds displayed a unique up-regulation of genes related to EMT and TGF-β signaling as well as high concentration of endogenous TGF-β1 in comparison to healthy scaffolds and TGF-β1-induced phosphorylation of canonical proteins Smad2/3 (Mazza et al., 2019). This study characterized the inherent features of ECM microenvironment from human cirrhotic liver acting as key pro-tumorigenic components in HCC development.

Impact of Adiposity

It is well-established that fat tissue overgrowth in obesity promotes tumor progression [for reviews of earlier reports see Park et al. (2014), Iyengar et al. (2016), Quail and Dannenberg (2019)]. Using a xenograft model of early multiple myeloma, it has been shown that bone niche switching towards a "fatty" marrow supports the development of malignant cells during carcinogenesis. In this study, MSCs mainly gave rise to adipocytes supporting tumor growth by increasing the survival and chemoresistance of malignant cells (Berlier et al., 2019). Su et al. (2019) compared lean and obese mice grafted with prostate tumors and showed that obesity promotes EMT in cancer cells and tumor invasion into the surrounding fat tissue. In this study, adipose stromal cells induced EMT in prostate cancer cells and rendered them more migratory and chemo-resistant. By contrast, interference of adipose stromal cell capabilities suppressed both EMT and chemoresistance to docetaxel, cabazitaxel, and cisplatin chemotherapy in human prostate cancer cells (Su et al., 2019). It has been suggested that that adipose-derived factors may play a role in MSC-mediated pro-tumorigenic effects. For instance, the adipokine chemerin, a cell differentiation promoter and leukocyte chemoattractant factor established as a major player in obesity-mediated support of cancer progression, was reported to promote the growth, proliferation migration, invasion, and metastasis of cancer cells. The effects of the adipokine chemerin were achieved through the recruitment of tumor-associated MSCs and the stimulation of angiogenesis pathways in endothelial cells through chemerin receptor 1 (CMKLR1), chemerin receptor 2 (GPR1), and CCLR2 signaling (Goralski et al., 2019). Interestingly, in a culture system established to investigate the paracrine effects of MSCs on the migration and invasion potential of this aggressive breast cancer cell line, human adipose-derived MSCs promoted EMT in MCF7 breast cancer cells by cross-interacting with the TGF-β/Smad and PI3K/AKT signaling pathways, suggesting that stromal cells are key players in obesity-mediated tumor progression (Wu et al., 2019). There is probably a pro-tumorigenic cross-talk between adipose tissue and tumor stromal cells, particularly in obesity-like contexts. Adipose-derived signaling molecules might be among the drivers of pro-tumorigenic reprogramming of stromal cells by cancer cells. The evidence of stromal cell programming by tumor microenvironment suggest that non programmed cells could mediate anticancer effects in contrast with their educated counterpart.

EVIDENCE OF STROMAL CELLS MEDIATING ANTICANCER EFFECTS

Emerging data support that non-tumor associated MSCs mediate anticancer effects and suggest the existence of stromal cells mediating anticancer effects in the tumor microenvironment, notably, MSCs slowing tumor progression and cancer-restraining CAFs.

Naïve Stromal Cells Mediate Anticancer Effects

To address the antitumor potential of non-tumor associated-MSCs, Francois et al. (2019), treated immunocompetent rat models of colorectal carcinogenesis with non-tumor BM-derived MSCs, observing inhibition of cancer progression. This effect was partially due to the control of the tumor microenvironmental immunity as shown by (i) the modulation of effector cells, such as regulatory T cells (Tregs), CD8+ cells and NK cells; (ii)macrophage reprogramming into regulatory cells performing phagocytosis with reduced production of proinflammatory cytokines; (iii) the restoration ofTh17 activity and (iv) 50% decrease in the infiltration rate of CD68+ cells, and two-fold increase of CD3+ cells (Francois et al., 2019). In another study, intra-BM but not the systemic administration of BM MSCs from healthy donors reduced tumor burden and prolonged survival of the leukemia-bearing mice (Xia et al., 2020). In this study, the MSC senescence observed during disease progression was stopped and the BM microenvironment was restored, with functional recovery of host myelopoiesis and improvement of thrombopoiesis. Moreover, in a bioluminescence imaging study monitoring the effects of human umbilical cord-derived MSCs in mouse hepatoma tumor models with H7402 cell

line, MSC microenvironment effectively inhibited the growth of cancer cells (Liu et al., 2019). Interestingly, human BM MSC-derived exosomes overexpressing miR-34a inhibited glioblastoma development (Wang et al., 2019). Two other microRNAs, associated with the capacity of MSCs to attenuate cancer growth have also been identified, namely miR-150 and miR-7 (Wang et al., 2019). Mandal et al. (2019) reported that perinatal tissue MSCs encapsulated with the sodium alginate biomaterial for isolation from tumor microenvironment displayed: (i) increased proliferation with enhanced expressions of pluripotency genes, EMT, immune-modulation and angiogenesis; (ii) increased expression of the tumor invasion suppressor protein E-cadherin; (iii) and increased secretions of VEGF, TGF-β, TNF-α, IFN-γ, IL-10 and IL-6, and IL-3β. Furthermore, treatment of CSCs derived from MDA-MB-231 and MCF7 breast cancer cell lines with encapsulated MSCs lowered CSC viability and migration, with downregulation of markers related to angiogenesis, EMT and proliferation, and upregulation of Wnt antagonists sFRP4 and DKK1 (Mandal et al., 2019). Taken together, these data suggest that non-tumor associated MSCs mediate anticancer effects and support that MSC pro-tumorigenic effects result from tumor reprogramming.

Early clinical and experimental studies in mouse models suggested the existence of at least two types of MSC-derived CAFs: they extensively studied cancer-promoting CAFs and the cancer-restraining CAFs, which were poorly investigated due to the lack of markers [for review see Bu et al. (2019)]. In a recent study using stromal cell lines derived from central nervous system (CNS) metastasis of breast and lung cancer patients, a cell population with tumor inhibitory functions, expressing high levels of collagen and displaying gene expression signatures of CAFs, MSCs, and EMT, was isolated and characterized in cancer metastasis microenvironment (Tew et al., 2019). Some very interesting recent reports have proposed markers to identify cancer-restraining CAFs. The study of Mizutani et al. (2019) has reported the glycosylphosphatidylinositol-anchored protein Meflin as a potential marker of cancer-restraining CAFs. These authors observed that the tissue infiltration of Meflin-positive CAFs correlated with favorable patient outcome in pancreatic ductal adenocarcinoma. Meflin deficiency or downregulated resulted in markedly faster tumor progression in a pancreatic ductal adenocarcinoma mouse model. Consistently, the overexpression of Meflin in CAFs or the delivery of a Meflin-expressing lentivirus into the tumor stroma were sufficient to suppress the growth of xenograft tumors (Mizutani et al., 2019). This new marker paves the way to isolation and further characterization of CAFs exerting anti-tumoral effects.

Overall, *in vitro* studies and studies using naïve MSCs, i.e., MSCs that were not in contact with tumor microenvironment, support the anti-tumor effects of MSCs. But these anti-cancer functions can be markedly reduced by the direct crosstalk with tumor bulk or tumor stromal elements. Interestingly, Early studies addressing the immunological hallmarks of MSCs in the tumor microenvironment revealed various molecular mechanisms through which MSCs may modulate the immune response in the cancer microenvironment. This indicated that it may be possible to convert the microenvironment from immunosuppressive to immunostimulant feature [for review see Turley et al. (2015), Poggi et al. (2018)]. These reports paved the way for studies attempting to reprogram tumor stromal cells for anticancer effects.

Attempts to Reprogram Tumor Stromal Cells for Anticancer Effects

A bulk of recent reports propose promising strategies for reprogramming microenvironmental stromal cells to mediate only anticancer effects. For instance, treatments with various flavonoids and non-flavonoid polyphenolic compounds from medicinal plants alleviated multidrug resistance in breast, prostate, lung and colorectal cancer with survival benefits in patients. These effects were achieve through the modulation of inflammatory responses, their antioxidant capacity, and the inactivation of oncogenes, the inhibition of angiogenesis, proliferation, survival, and metastasis [for review see Costea et al. (2020)]. On the same hand, unlike conditioned medium from human adipose MSCs, eicosapentanoic acid-treated adipose MSCs reduced mRNA levels of the tumor-associated genes FASN, STAT3, cIAP-2 in MDA-MB-231 and MCF-7 breast cancer cell lines. Functionaly, cancer cell lines treated in these conditions displayed reduced glycolysis, inflammation and motility *in vivo* (Al-Jawadi et al., 2020). In addition, treatment with 5-Azacytidine restored IL-6-increased production in MSCs collected from myelodysplastic patients (Boada et al., 2020). Engineered human placenta-derived MSCs, armed with a double fusion gene containing the herpes simplex virus truncated thymidine kinase and firefly luciferase, inhibited the tumorigenesis mediated by the HT29 colon cancer cell line in nude mice (Yang et al., 2019). Similarly, as compared to short-culture CAFs, prolonged culture of heterogeneous prostatic CAFs resulted in marked decreases in the expression of proliferative endothelial cell surface marker endoglin (CD105), and loss of their tumor expansion potential in 3D-cultures and patient-derived xenograft tissues (Kato et al., 2019).

Furthermore, irradiated endothelial cells decreased the malignancy of liver cancer cells in a culture system using conditioned medium from endothelial cells, suggesting that irradiated endothelial cells are key players in the therapeutic effects of radiotherapy (Kim et al., 2019). Similarly, a study addressing the response of human MSCs to low-dose photodynamic therapy revealed that this treatment may increase MSC immunogenicity and promote angiogenic potential (Udartseva et al., 2019). In this *in vitro* study, low-dose photodynamic therapy: (i) induced the reorganization of MSC cytoskeleton, with decrease in cell motility; (ii) induced the inhibition of GSK-3 and the activation of Erk1/2 signaling in MSCs; (iii) significantly upregulated the secretion of VEGF-A, IL-8, PAI-1, MMP-9, and other proangiogenic factors by MSCs; (iv) dramatically inhibited the secretion of pro-tumorigenic macrophage infiltration marker CCL2 (MCP-1) by MSCs and decreased MSC viability and immunogenicity when cultured with lymphocytes. In another study, MSCs loaded with photosensitizer MnO2@Ce6 successfully shipped these

nanoparticles into lung cancer tumor sites, enhancing the effects of photodynamic therapy *in vivo* (Cao et al., 2020). In sarcomas, tumor-initiating cells are thought to derive from MSCs, modified MSC were successfully used to deliver TNF-related apoptosis-inducing ligand (TRAIL) to induce tumor apoptosis, open novel therapeutic opportunities (Grisendi et al., 2015). Altogether, these observations confirm that it is possible to reprogram tumor stromal cells to mediate anticancer effects, and warrant further studies aimed at developing therapies using this approach. We propose that reprogrammed tumor MSCs loaded with photosensitizer MnO2@Ce6 or other nanoparticles with anticancer effects could display strong anticancer effects *in vivo*, as this approach will couple the MSC anticancer effects with the anticancer effects of nanoparticles (Ref).

CONTROVERSY SOURCES AND IMPLICATIONS FOR MSC THERAPEUTIC USE

Other Sources of Controversy on the Roles of Stromal Cells in Tumorigenesis

Beyond the fact that MSC effects in the tumor microenvironment depend on the interactions with the adipose tissue and malignant cells (pro-tumorigenic when there are cross-talks and anticancer effects when there are poor interactions) and with the ECM programming (pro- or anticancer) to support differences between *in vitro* and *in vivo* studies, controversies on the roles of stromal cells in the tumor microenvironment may also emerge from MSC origin and the cancer type. This hypothesis is fully supported by a report of Quach et al. (2019) where the inhibition of the glypican-1 (GPC-1) prostate cancer biomarker in the aggressive prostate cancer cell line PC-3 decreased cell growth and migration *in vitro*, but increased PC-3 tumor size in NCr nude mice xenografts. Authors also observed that GPC-1 inhibition in an aggressive prostate cancer cell line, the DU-145 cells, increased cancer cell proliferation and migration, suggesting that GPC-1 accounts among the factors that drive cancer cell line-dependent responses to stromal cells Reduced cell growth observed in GPC-1 knockdown PC-3 cells was rescued by culturing the cells with MSCs and CAFs. Further, the treatment of these stromal cells with tumor-conditioned media from PC-3 cells transfected with GPC-1 shRNA increased the expression of extracellular matrix components, endocrine and paracrine biomolecules, and migration markers (Quach et al., 2019). In another study, despite *in vivo* observations revealing the ability of IGF/IGF-IR signaling to induce drug resistance and influence the ability to form metastasis via the induction of EMT in pancreatic cancer, the activation of this signaling pathway by stromal cells failed to induce EMT in cultures with MiaPaCa-2, AsPC-1, Capan-2, BxPC-3, and Panc1 pancreatic cancer cell lines (Kopantzev et al., 2019), suggesting a key role for tumor microenvironment for the pro-tumorigenic effects of this MSC-activated signaling pathway.

When assessing how breast cancer cells from different stages of the metastatic cascade convert MSCs into tumor-associated MSCs, it was observed that only MDA-MB-231 breast cancer secretomes, but not MCF-7 cells or sublines isolated from bone, lung, and brain metastases, converted MSCs into tumor-associated MSCs in bioengineered 3D microenvironments (Blache et al., 2019). These observations further confirm that MSCs from tumor microenvironment are reprogrammed by cancer-initiating cells and primary tumor ECM to mediate pro-tumorigenic effects, and that without such reprogramming the stromal cells may rather mediate anticancer effects. On the same hand, in co-cultures with stem cell-like (CD133+) cells from urinary bladder cancer cell lines, adipose-derived MSCs produced soluble mediators that: (i) increased the phosphorylation of molecules involved in cancer progression and drug resistance, such as p70 S6K, ERK1/2, and AKT1/2/3 in CD133+ cells (5,637 cell line); but instead, (ii) decreased the phosphorylation of those involved in PI3K/Akt and MAPK signaling molecules in CD133+ cells (HB-CLS-1 cell line; Maj et al., 2019). In this study, there seemed to be a controversy on the effect of MSCs on urinary bladder cancer lines *in vitro*, as MSCs induced pro-tumorigenic effects in culture with 5637 cell line and anticancer effects in culture with HB-CLS-1 cell line. However, this difference may actually suggest that unlike the first, the latter cell line was not able to reprogram MSCs for pro-tumorigenic effects, hence, MSCs mediated anticancer effects.

However, considering that naïve MSCs promoted anticancer effects in most reports, treatment of MDAMB231 and MCF7 human breast cancer cells with medium containing EVs from naïve MSC cultures promoted the *in vitro* proliferation and migration of cancer cells through ERK signaling (Zhou et al., 2019b). We hypothesize that these effects may be due to differences in the origin of MSCs, as unlike in most reports, in this study human umbilical cord MSCs, and not BM or adipose-derived MSCs were used. A comparative study of subcutaneous and visceral adipose-derived MSCs revealed various functional similarities and differences, despite similar surface markers (Ritter et al., 2019). Notably, visceral MSCs secreted higher levels of inflammatory cytokines (IL-6, IL-8, and TNF-α) and had more active sonic hedgehog pathway than subcutaneous MSCs. Moreover, fetal and adult lung MSCs possess lung-specific properties, unlike BM MSC (Rolandsson Enes et al., 2016). A study profiling the transcriptomes of 361 single MSCs derived from two umbilical cords (UC-MSCs), harvested at different passages and stimulated with or without inflammatory cytokines, revealed that UC-MSCs are a well-organized population with limited heterogeneity, as compared to other MSC types (Huang et al., 2019). These data support strong differences between MSC lines based on their origin, and even raise caution for the therapeutic use of some MSC lines in cancer context.

Implications for MSC Use for Tissue Regeneration in Cancer Patients

Because MSCs are able to increase cancer cell malignancy *in vitro,* early studies raised the danger of the application of human MSCs in regenerative medicine for patients with history of

breast cancer, small cell ovarian cancer and other malignancies (Kucerova et al., 2011; Yang et al., 2015). Although subsequent reports from *in vitro* studies provided encouraging results for potential use of MSCs from patients for post-anticancer therapy tissue regeneration, there are still some concerns. For instance, an *in vitro* biosafety profile evaluation of MSCs derived from the BM of sarcoma patients showed that the *in vitro* expansion of MSCs from osteosarcoma (OS) and Ewing sarcoma (EWS) patients does not favor malignant transformation, but instead of that these MSCs displayed comparable morphology, immunophenotype, differentiation potential, proliferation rate, and telomerase activity to MSCs from healthy donors, indicating that OS and EWS patients may benefit from an autologous MSCs-based bone reconstruction after anticancer chemotherapy (Lucarelli et al., 2014). However, these promising findings, which need to be confirmed *in vivo*, were mitigated by the observation of chromosomal aberrations in MSCs after culture, raising caution and confirming the need for rigorous phenotypic, genetic and functional evaluation of the biosafety of MSCs from patients before clinical use. Interestingly, reports from exploratory studies in mice confirmed the therapeutic potential of MSCs for repairing damaged tissues after anticancer chemotherapy *in vivo*, thus after elimination of most of the primary tumor tissue that could have reprogrammed MSCs to mediate pro-tumorigenic effects [for review see Bussard et al. (2016), Baghban et al. (2020)]. Notably, human adipose-derived MSCs displayed repairing properties in damaged thymus following chemotherapy in mouse models of blood cancer, with improvements in the thymic structure and functions, as shown by the proportion of circulating and splenic Treg cells and the recovery of T-cell subpopulations (Zhan et al., 2019). However, the caution remains, not because of the possibility of reprogramming of MSCs for pro-tumorigenic effects, considering that anticancer chemotherapy normally eliminates most of the primary tumor tissue, but because we still need studies proving phenotypic, genetic and functional biosafety of MSCs in cancer context. Autologous MSC use may require a biosafety evaluation for each patient considering the clinical implications of using damaged MSCs.

CONCLUDING REMARKS

The available data support that stromal cells normally have anticancer cancer effects. MSCs reprogrammed by cancer cells in the tumor microenvironment undergo a switch towards pro-tumorigenic activities, including their support to cancer cells in part through the metabolic reprogramming necessary to satisfy the energy demand and malignant behavior of the latter in a hypoxic and nutrient-deficient microenvironment. Tumor microenvironment reprograms MSCs thanks to hypoxia and the extracellular matrix cross-talks with MSCs. Interestingly, promising emerging reports suggest strategies for reprogramming microenvironmental stromal cells, which in turn switch back to naïve MSCs capable to function as anti-cancer agents. These reprogramming treatment include MSCs treatment with polyphenolic compounds from medicinal plants, with eicosapentanoic acid, or with 5-Azacytidine. . .. Taken together, the available data suggests that targeting the tumor microenvironment could be a promising therapeutic strategy in cancer, and that it is possible to reprogram tumor stromal cells to revert back to anticancer effects. These strategies should be further developed in the search for anticancer therapies, in particular for refractory cancers.

AUTHOR CONTRIBUTIONS

All authors listed have made a substantial, direct and intellectual contribution to the work, and approved it for publication.

REFERENCES

Abdul-Aziz, A. M., Sun, Y., Hellmich, C., Marlein, C. R., Mistry, J., Forde, E., et al. (2019). Acute myeloid leukemia induces protumoral p16INK4a-driven senescence in the bone marrow microenvironment. *Blood* 133, 446–456. doi: 10.1182/blood-2018-04-845420

Al-Jawadi, A., Rasha, F., Ramalingam, L., Alhaj, S., Moussa, H., Gollahon, L., et al. (2020). Protective effects of eicosapentaenoic acid in adipocyte-breast cancer cell cross talk. *The Journal of nutritional biochemistry* 75, 108244. doi: 10.1016/j.jnutbio.2019.108244

Al-Khalaf, H. H., Ghebeh, H., Inass, R., and Aboussekhra, A. (2019). Senescent Breast Luminal Cells Promote Carcinogenesis through Interleukin-8-Dependent Activation of Stromal Fibroblasts. *Molecular and cellular biology* 39,

An, J., Du, Y., Fan, X., Wang, Y., Ivan, C., Zhang, X. G., et al. (2019). EGFL6 promotes breast cancer by simultaneously enhancing cancer cell metastasis and stimulating tumor angiogenesis. *Oncogene* 38, 2123–2134. doi: 10.1038/s41388-018-0565-9

Atiya, H., Frisbie, L., Pressimone, C., and Coffman, L. (2020). Mesenchymal Stem Cells in the Tumor Microenvironment. *Advances in experimental medicine and biology* 1234, 31–42. doi: 10.1007/978-3-030-37184-5_3

Baghban, R., Roshangar, L., Jahanban-Esfahlan, R., Seidi, K., Jaymand, M., Kolahian, S., et al. (2020). Tumor microenvironment complexity and therapeutic implications at a glance. *Cell communication and signaling : CCS* 18, 59.

Balamurugan, K. (2016). HIF-1 at the crossroads of hypoxia, inflammation, and cancer. *International journal of cancer* 138, 1058–1066. doi: 10.1002/ijc.29519

Barberini, D. J., Freitas, N. P., Magnoni, M. S., Maia, L., Listoni, A. J., Heckler, M. C., et al. (2014). Equine mesenchymal stem cells from bone marrow, adipose tissue and umbilical cord: immunophenotypic characterization and differentiation potential. *Stem cell research & therapy* 5, 25. doi: 10.1186/scrt414

Bauer, J., Emon, A. B. M., Staudacher, J. J., Thomas, A. L., Mancinelli, G., Krett, N., et al. (2020). Increased stiffness of the tumor microenvironment in colon cancer stimulates cancer associated fibroblast-mediated prometastatic activin A signaling. *Scientific reports* 10, 50.

Berlier, J. L., Rethnam, M., Banu Binte Abdul Majeed, A., and Suda, T. (2019). Modification of the bone marrow MSC population in a xenograft model of early multiple myeloma. *Biochemical and biophysical research communications* 508, 1175–1181. doi: 10.1016/j.bbrc.2018.11.178

Blache, U., Horton, E. R., Xia, T., Schoof, E. M., Blicher, L. H., Schonenberger, A., et al. (2019). Mesenchymal stromal cell activation by breast cancer secretomes in bioengineered 3D microenvironments. *Life science alliance* 2,

Boada, M., Echarte, L., Guillermo, C., Diaz, L., Tourino, C., and Grille, S. (2020). 5-Azacytidine restores interleukin 6-increased production in mesenchymal stromal cells from myelodysplastic patients. *Hematology, transfusion and cell therapy*

Bu, L., Baba, H., Yoshida, N., Miyake, K., Yasuda, T., Uchihara, T., et al. (2019). Biological heterogeneity and versatility of cancer-associated fibroblasts in the tumor microenvironment. *Oncogene* 38, 4887–4901. doi: 10.1038/s41388-019-0765-y

Bussard, K. M., Mutkus, L., Stumpf, K., Gomez-Manzano, C., and Marini, F. C. (2016). Tumor-associated stromal cells as key contributors to the tumor microenvironment. *Breast cancer research : BCR* 18, 84.

Cao, J., Li, J., Sun, L., Qin, T., Xiao, Y., Chen, K., et al. (2019). Hypoxia-driven paracrine osteopontin/integrin alphavbeta3 signaling promotes pancreatic cancer cell epithelial-mesenchymal transition and cancer stem cell-like properties by modulating forkhead box protein M1. *Molecular oncology* 13, 228–245. doi: 10.1002/1878-0261.12399

Cao, W., Liu, B., Xia, F., Duan, M., Hong, Y., Niu, J., et al. (2020). MnO2@Ce6-loaded mesenchymal stem cells as an "oxygen-laden guided-missile" for the enhanced photodynamic therapy on lung cancer. *Nanoscale* 12, 3090–3102. doi: 10.1039/c9nr07947e

Casagrande, N., Borghese, C., Visser, L., Mongiat, M., Colombatti, A., and Aldinucci, D. (2019). CCR5 antagonism by maraviroc inhibits Hodgkin lymphoma microenvironment interactions and xenograft growth. *Haematologica* 104, 564–575. doi: 10.3324/haematol.2018.196725

Chandra, A., Jahangiri, A., Chen, W., Nguyen, A. T., Yagnik, G., Pereira, M. P., et al. (2020). Clonal ZEB1-driven mesenchymal transition promotes targetable oncologic anti-angiogenic therapy resistance. *Cancer research*

Chen, Y., Wang, X., Fang, J., Song, J., Ma, D., Luo, L., et al. (2019a). Mesenchymal stem cells participate in oral mucosa carcinogenesis by regulating T cell proliferation. *Clinical immunology (Orlando, Fla.)* 198, 46–53. doi: 10.1016/j.clim.2018.12.001

Chen, Y. L., Zhang, Y., Wang, J., Chen, N., Fang, W., Zhong, J., et al. (2019b). A 17 gene panel for non-small-cell lung cancer prognosis identified through integrative epigenomic-transcriptomic analyses of hypoxia-induced epithelial-mesenchymal transition. *Molecular oncology* 13, 1490–1502. doi: 10.1002/1878-0261.12491

Cheng, J., Li, Y., Liu, S., Jiang, Y., Ma, J., Wan, L., et al. (2019). CXCL8 derived from mesenchymal stromal cells supports survival and proliferation of acute myeloid leukemia cells through the PI3K/AKT pathway. *FASEB journal : official publication of the Federation of American Societies for Experimental Biology* 33, 4755–4764. doi: 10.1096/fj.201801931r

Chi, Y., Han, Z. B., Xu, F. Y., Wang, Y. W., Feng, X. M., Chen, F., et al. (2014). Adipogenic potentials of mesenchymal stem cells from human bone marrow, umbilical cord and adipose tissue are different. *Zhongguo shi yan xue ye xue za zhi* 22, 588–594.

Cislo-Pakuluk, A., and Marycz, K. (2017). A Promising Tool in Retina Regeneration: Current Perspectives and Challenges When Using Mesenchymal Progenitor Stem Cells in Veterinary and Human Ophthalmological Applications. *Stem cell reviews and reports* 13, 598–602. doi: 10.1007/s12015-017-9750-4

Coffman, L. G., Pearson, A. T., Frisbie, L. G., Freeman, Z., Christie, E., Bowtell, D. D., et al. (2019). Ovarian Carcinoma-Associated Mesenchymal Stem Cells Arise from Tissue-Specific Normal Stroma. *Stem cells (Dayton, Ohio)* 37, 257–269. doi: 10.1002/stem.2932

Costea, T., Vlad, O. C., Miclea, L. C., Ganea, C., Szollosi, J., and Mocanu, M. M. (2020). Alleviation of Multidrug Resistance by Flavonoid and Non-Flavonoid Compounds in Breast, Lung, Colorectal and Prostate Cancer. *International journal of molecular sciences* 21,

Dabbah, M., Jarchowsky-Dolberg, O., Attar-Schneider, O., Tartakover Matalon, S., Pasmanik-Chor, M., and Drucker, L. (2019). Multiple myeloma BM-MSCs increase the tumorigenicity of MM cells via transfer of VLA4 enriched microvesicles. *Carcinogenesis*

Daniel, S. K., Sullivan, K. M., Labadie, K. P., and Pillarisetty, V. G. (2019). Hypoxia as a barrier to immunotherapy in pancreatic adenocarcinoma. *Clinical and translational medicine* 8, 10.

Dominici, M., Le Blanc, K., Mueller, I., Marini, F., Krause, D., and Deans, R. (2006). Minimal criteria for defining multipotent mesenchymal stromal cells. *The International Society for Cellular Therapy position statement, Cytotherapy* 8, 315–317. doi: 10.1080/14653240600855905

Fernando, R. C., Mazzotti, D. R., Azevedo, H., Sandes, A. F., Rizzatti, E. G., and Dalboni, M. A. (2019). Transcriptome Analysis of Mesenchymal Stem Cells from Multiple Myeloma Patients Reveals Downregulation of Genes Involved in Cell Cycle Progression. *Immune Response, and Bone Metabolism, Scientific reports* 9, 1056.

Francois, S., Usunier, B., Benderitter, M., Douay, L., Gorin, N. C., Larsen, A. K., et al. (2019). Mesenchymal Stem Cell Administration Attenuates Colon Cancer Progression by Modulating the Immune Component within the Colorectal Tumor Microenvironment. *Stem cells translational medicine* 8, 285–300. doi: 10.1002/sctm.18-0117

Fu, Y., Liu, S., Yin, S., Niu, W., Xiong, W., Tan, M., et al. (2017). The reverse Warburg effect is likely to be an Achilles' heel of cancer that can be exploited for cancer therapy. *Oncotarget* 8, 57813–57825. doi: 10.18632/oncotarget.18175

Funes, J. M., Quintero, M., Henderson, S., Martinez, D., Qureshi, U., Westwood, C., et al. (2007). Transformation of human mesenchymal stem cells increases their dependency on oxidative phosphorylation for energy production. *Proceedings of the National Academy of Sciences of the United States of America* 104, 6223–6228. doi: 10.1073/pnas.0700690104

Garces, J. J., Simicek, M., Vicari, M., Brozova, L., Burgos, L., Bezdekova, R., et al. (2020). Transcriptional profiling of circulating tumor cells in multiple myeloma: a new model to understand disease dissemination. *Leukemia* 34, 589–603. doi: 10.1038/s41375-019-0588-4

Garcia-Hernandez, M. L., Uribe-Uribe, N. O., Espinosa-Gonzalez, R., Kast, W. M., Khader, S. A., and Rangel-Moreno, J. (2017). A Unique Cellular and Molecular Microenvironment Is Present in Tertiary Lymphoid Organs of Patients with Spontaneous Prostate Cancer Regression. *Frontiers in immunology* 8:563.

Ghosh, D., Mejia Pena, C., Quach, N., Xuan, B., Lee, A. H., and Dawson, M. R. (2020). Senescent mesenchymal stem cells remodel extracellular matrix driving breast cancer cells to a more-invasive phenotype. *Journal of cell science* 133,

Giallongo, C., Tibullo, D., Camiolo, G., Parrinello, N. L., Romano, A., Puglisi, F., et al. (2019). TLR4 signaling drives mesenchymal stromal cells commitment to promote tumor microenvironment transformation in multiple myeloma. *Cell death & disease* 10, 704.

Goralski, K. B., Jackson, A. E., McKeown, B. T., and Sinal, C. J. (2019). More Than an Adipokine: The Complex Roles of Chemerin Signaling in Cancer. *International journal of molecular sciences* 20,

Grisendi, G., Spano, C., Rasini, V., Veronesi, E., Prapa, M., Petrachi, T., et al. (2015). Mesenchymal progenitors expressing TRAIL induce apoptosis in sarcomas. *Stem cells (Dayton, Ohio)* 33, 859–869. doi: 10.1002/stem.1903

Guo, L., Sun, C., Xu, S., Xu, Y., Dong, Q., Zhang, L., et al. (2019). Knockdown of long non-coding RNA linc-ITGB1 inhibits cancer stemness and epithelial-mesenchymal transition by reducing the expression of Snail in non-small cell lung cancer. *Thoracic cancer* 10, 128–136. doi: 10.1111/1759-7714.12911

Gyukity-Sebestyen, E., Harmati, M., Dobra, G., Nemeth, I. B., Mihaly, J., Zvara, A., et al. (2019). Melanoma-Derived Exosomes Induce PD-1 Overexpression and Tumor Progression via Mesenchymal Stem Cell Oncogenic Reprogramming. *Frontiers in immunology* 10:2459.

Huang, Y., Li, Q., Zhang, K., Hu, M., Wang, Y., Du, L., et al. (2019). Single cell transcriptomic analysis of human mesenchymal stem cells reveals limited heterogeneity. *Cell death & disease* 10, 368.

Hughes, R. M., Simons, B. W., Khan, H., Miller, R., Kugler, V., Torquato, S., et al. (2019). Asporin Restricts Mesenchymal Stromal Cell Differentiation, Alters the Tumor Microenvironment, and Drives Metastatic Progression. *Cancer research* 79, 3636–3650. doi: 10.1158/0008-5472.can-18-2931

Hwang, H. J., Oh, M. S., Lee, D. W., and Kuh, H. J. (2019). Multiplex quantitative analysis of stroma-mediated cancer cell invasion, matrix remodeling, and drug response in a 3D co-culture model of pancreatic tumor spheroids and stellate cells. *Journal of experimental & clinical cancer research : CR* 38, 258.

Ibraheem, A., Attar-Schneider, O., Dabbah, M., Dolberg Jarchowsky, O., Tartakover Matalon, S., and Lishner, M. (2019). BM-MSCs-derived ECM modifies multiple myeloma phenotype and drug response in a source-dependent manner. *Translational research : the journal of laboratory and clinical medicine* 207, 83–95. doi: 10.1016/j.trsl.2019.01.003

Ikeda, T., Nishita, M., Hoshi, K., Honda, T., Kakeji, Y., and Minami, Y. (2020). Mesenchymal stem cell-derived CXCL16 promotes progression of gastric cancer cells by STAT3-mediated expression of Ror1. *Cancer science*

Ishiki, Y., Ohnishi, H., Muto, Y., Matsumoto, K., and Nakamura, T. (1992). Direct evidence that hepatocyte growth factor is a hepatotrophic factor for liver regeneration and has a potent antihepatitis effect in vivo. *Hepatology (Baltimore, Md.)* 16, 1227–1235. doi: 10.1016/0270-9139(92)90019-6

Iyengar, N. M., Gucalp, A., Dannenberg, A. J., and Hudis, C. A. (2016). Obesity and Cancer Mechanisms: Tumor Microenvironment and Inflammation. *Journal of clinical oncology : official journal of the American Society of Clinical Oncology* 34, 4270–4276. doi: 10.1200/jco.2016.67.4283

Jafarzadeh, N., Safari, Z., Pornour, M., Amirizadeh, N., Forouzandeh Moghadam, M., and Sadeghizadeh, M. (2019). Alteration of cellular and immune-related properties of bone marrow mesenchymal stem cells and macrophages by K562 chronic myeloid leukemia cell derived exosomes. *Journal of cellular physiology* 234, 3697–3710. doi: 10.1002/jcp.27142

Kang, N., Choi, S. Y., Kim, B. N., Yeo, C. D., Park, C. K., Kim, Y. K., et al. (2019). Hypoxia-induced cancer stemness acquisition is associated with CXCR4 activation by its aberrant promoter demethylation. *BMC cancer* 19:148.

Kato, M., Madhav, A., Haldar, S., Tripathi, M., Billet, S., Mishra, R., et al. (2019). Heterogeneous cancer-associated fibroblast population potentiates neuroendocrine differentiation and castrate resistance in a CD105-dependent manner. *Oncogene* 38, 716–730. doi: 10.1038/s41388-018-0461-3

Kim, S. D., Yi, J. M., and Park, M. T. (2019). Irradiated endothelial cells modulate the malignancy of liver cancer cells. *Oncology letters* 17, 2187–2196.

Kopantzev, E. P., Kopantseva, M. R., Grankina, E. V., Mikaelyan, A., Egorov, V. I., and Sverdlov, E. D. (2019). Activation of IGF/IGF-IR signaling pathway fails to induce epithelial-mesenchymal transition in pancreatic cancer cells. *Pancreatology : official journal of the International Association of Pancreatology (IAP) .. [et al.]* 19, 390–396. doi: 10.1016/j.pan.2019.01.010

Krueger, T. E., Thorek, L. J. D., Meeker, A. K., Isaacs, J. T., and Brennen, W. N. (2019). Tumor-infiltrating mesenchymal stem cells: Drivers of the immunosuppressive tumor microenvironment in prostate cancer? *The Prostate* 79, 320–330. doi: 10.1002/pros.23738

Kucerova, L., Kovacovicova, M., Polak, S., Bohac, M., Fedeles, J., Palencar, D., et al. (2011). Interaction of human adipose tissue-derived mesenchymal stromal cells with breast cancer cells. *Neoplasma* 58, 361–370. doi: 10.4149/neo_2011_05_361

Li, C. Y., Wu, X. Y., Tong, J. B., Yang, X. X., Zhao, J. L., Zheng, Q. F., et al. (2015). Comparative analysis of human mesenchymal stem cells from bone marrow and adipose tissue under xeno-free conditions for cell therapy. *Stem cell research & therapy* 6, 55.

Li, D., Wang, N., Zhang, L., Hanyu, Z., Xueyuan, B., Fu, B., et al. (2013). Mesenchymal stem cells protect podocytes from apoptosis induced by high glucose via secretion of epithelial growth factor. *Stem cell research & therapy* 4, 103. doi: 10.1186/scrt314

Lin, S., Zhu, B., Huang, G., Zeng, Q., and Wang, C. (2019). Microvesicles derived from human bone marrow mesenchymal stem cells promote U2OS cell growth under hypoxia: the role of PI3K/AKT and HIF-1alpha. *Human cell* 32, 64–74. doi: 10.1007/s13577-018-0224-z

Liu, X., Chen, H., Zhu, W., Chen, H., Hu, X., Jiang, Z., et al. (2014). Transplantation of SIRT1-engineered aged mesenchymal stem cells improves cardiac function in a rat myocardial infarction model. *The Journal of heart and lung transplantation : the official publication of the International Society for Heart Transplantation* 33, 1083–1092. doi: 10.1016/j.healun.2014.05.008

Liu, Y., Ren, H., Zhou, Y., Shang, L., Zhang, Y., Yang, F., et al. (2019). The hypoxia conditioned mesenchymal stem cells promote hepatocellular carcinoma progression through YAP mediated lipogenesis reprogramming. *Journal of experimental & clinical cancer research : CR* 38, 228.

Lucarelli, E., Bellotti, C., Mantelli, M., Avanzini, M. A., Maccario, R., Novara, F., et al. (2014). In vitro biosafety profile evaluation of multipotent mesenchymal stem cells derived from the bone marrow of sarcoma patients. *Journal of translational medicine* 12, 95. doi: 10.1186/1479-5876-12-95

Lung, D. K., Warrick, J. W., Hematti, P., Callander, N. S., Mark, C. J., Miyamoto, S., et al. (2019). Bone Marrow Stromal Cells Transcriptionally Repress ESR1 but Cannot Overcome Constitutive ESR1 Mutant Activity. *Endocrinology* 160, 2427–2440. doi: 10.1210/en.2019-00299

Luo, Y., Kishi, S., Sasaki, T., Ohmori, H., Mori, S., Goto, K., et al. (2020). Targeting claudin-4 enhances chemosensitivity in breast cancer. *Cancer science* 1, 1.

Ma, Z., Cui, X., Lu, L., Chen, G., Yang, Y., Hu, Y., et al. (2019). Exosomes from glioma cells induce a tumor-like phenotype in mesenchymal stem cells by activating glycolysis. *Stem cell research & therapy* 10, 60.

Maj, M., Kokocha, A., Bajek, A., and Drewa, T. (2019). The effects of adipose-derived stem cells on CD133-expressing bladder cancer cells. *Journal of cellular biochemistry*

Maliszewska-Olejniczak, K., Brodaczewska, K. K., Bielecka, Z. F., Solarek, W., Kornakiewicz, A., Szczylik, C., et al. (2019). Development of extracellular matrix supported 3D culture of renal cancer cells and renal cancer stem cells. *Cytotechnology* 71, 149–163. doi: 10.1007/s10616-018-0273-x

Mandal, S., Arfuso, F., Sethi, G., Dharmarajan, A., and Warrier, S. (2019). Encapsulated human mesenchymal stem cells (eMSCs) as a novel anti-cancer agent targeting breast cancer stem cells: Development of 3D primed therapeutic MSCs. *The international journal of biochemistry & cell biology* 110, 59–69. doi: 10.1016/j.biocel.2019.02.001

Mazza, G., Telese, A., Frenguelli, L., Levi, A., Marrali, M., Longato, L., et al. (2019). Cirrhotic Human Liver Extracellular Matrix 3D Scaffolds Promote Smad-Dependent TGF-beta1 Epithelial Mesenchymal Transition. *Cells* 9,

Melzer, C., von der Ohe, J., Otterbein, H., Ungefroren, H., and Hass, R. (2019). Changes in uPA, PAI-1, and TGF-beta Production during Breast Cancer Cell Interaction with Human Mesenchymal Stroma/Stem-Like Cells (MSC). *International journal of molecular sciences* 20,

Mizutani, Y., Kobayashi, H., Iida, T., Asai, N., Masamune, A., Hara, A., et al. (2019). Meflin-Positive Cancer-Associated Fibroblasts Inhibit Pancreatic Carcinogenesis. *Cancer research* 79, 5367–5381. doi: 10.1158/0008-5472.can-19-0454

Nwabo Kamdje, A. H., Mosna, F., Bifari, F., Lisi, V., Bassi, G., Malpeli, G., et al. (2011). Notch-3 and Notch-4 signaling rescue from apoptosis human B-ALL cells in contact with human bone marrow-derived mesenchymal stromal cells. *Blood* 118, 380–389. doi: 10.1182/blood-2010-12-326694

Nwabo Kamdje, A. H., Seke Etet, P. F., Vecchio, L., Muller, J. M., Krampera, M., and Lukong, K. E. (2014). Signaling pathways in breast cancer: therapeutic targeting of the microenvironment. *Cellular signalling* 26, 2843–2856. doi: 10.1016/j.cellsig.2014.07.034

Oh, I. R., Raymundo, B., Kim, M., and Kim, C. W. (2020). Mesenchymal stem cells co-cultured with colorectal cancer cells showed increased invasive and proliferative abilities due to its altered p53/TGF-beta1 levels. *Bioscience, biotechnology, and biochemistry* 84, 256–267. doi: 10.1080/09168451.2019.1676692

Osman, A., Afify, S. M., Hassan, G., Fu, X., Seno, A., and Seno, M. (2020). Revisiting Cancer Stem Cells as the Origin of Cancer-Associated Cells in the Tumor Microenvironment: A Hypothetical View from the Potential of iPSCs. *Cancers* 12,

Oswald, J., Boxberger, S., Jorgensen, B., Feldmann, S., Ehninger, G., Bornhauser, M., et al. (2004). Mesenchymal stem cells can be differentiated into endothelial cells in vitro. *Stem cells (Dayton, Ohio)* 22, 377–384. doi: 10.1634/stemcells.22-3-377

Ozdemir, B. O. R., Ozdemir, A. T., Sariboyaci, A. E., Uysal, O., Tuglu, M. I., and Kirmaz, C. (2019). The investigation of immunomodulatory effects of adipose tissue mesenchymal stem cell educated macrophages on the CD4 T cells. *Immunobiology* 224, 585–594. doi: 10.1016/j.imbio.2019.04.002

Park, J., Morley, T. S., Kim, M., Clegg, D. J., and Scherer, P. E. (2014). Obesity and cancer–mechanisms underlying tumour progression and recurrence. *Nature reviews. Endocrinology* 10, 455–465. doi: 10.1038/nrendo.2014.94

Pelizzo, G., Veschi, V., Mantelli, M., Croce, S., Maltese, A., Catenacci, L., et al. (2018). Microenvironment in neuroblastoma: isolation and characterization of tumor-derived mesenchymal stromal cells. *BMC cancer* 18:1176.

Poggi, A., Varesano, S., and Zocchi, M. R. (2018). How to Hit Mesenchymal Stromal Cells and Make the Tumor Microenvironment Immunostimulant Rather Than Immunosuppressive. *Frontiers in immunology* 9:262.

Quach, N. D., Kaur, S. P., Eggert, M. W., Ingram, L., Ghosh, D., Sheth, S., et al. (2019). Paradoxical Role of Glypican-1 in Prostate Cancer Cell and Tumor Growth. *Scientific reports* 9, 11478.

Quail, D. F., and Dannenberg, A. J. (2019). The obese adipose tissue microenvironment in cancer development and progression. *Nature reviews. Endocrinology* 15, 139–154. doi: 10.1038/s41574-018-0126-x

Ritter, A., Friemel, A., Roth, S., Kreis, N. N., Hoock, S. C., Safdar, B. K., et al. (2019). Subcutaneous and Visceral Adipose-Derived Mesenchymal Stem Cells: Commonality and Diversity. *Cells* 8,

Rolandsson Enes, S., Andersson Sjoland, A., Skog, I., Hansson, L., Larsson, H., Eriksson, L., et al. (2016). MSC from fetal and adult lungs possess lung-specific properties compared to bone marrow-derived MSC. *Scientific reports* 6, 29160.

Saforo, D., Omer, L., Smolenkov, A., Barve, A., Casson, L., Boyd, N., et al. (2019). Primary lung cancer samples cultured under microenvironment-mimetic

conditions enrich for mesenchymal stem-like cells that promote metastasis. *Scientific reports* 9, 4177.

Salminen, A., Kaarniranta, K., and Kauppinen, A. (2020). ER stress activates immunosuppressive network: implications for aging and Alzheimer's disease. *Journal of molecular medicine (Berlin, Germany)* 98, 633–650. doi: 10.1007/s00109-020-01904-z

Samudio, I., Fiegl, M., McQueen, T., Clise-Dwyer, K., and Andreeff, M. (2008). The warburg effect in leukemia-stroma cocultures is mediated by mitochondrial uncoupling associated with uncoupling protein 2 activation. *Cancer research* 68, 5198–5205. doi: 10.1158/0008-5472.can-08-0555

Sarhan, D., Wang, J., Hallstrom, C., Verneris, M. R., Grzywacz, B., Warlick, E., et al. (2020). Mesenchymal stromal cells shape the MDS microenvironment by inducing suppressive monocytes that dampen NK cell function. *JCI insight*

Schmohl, K. A., Mueller, A. M., Dohmann, M., Spellerberg, R., Urnauer, S., Schwenk, N., et al. (2019). Integrin alphavbeta3-Mediated Effects of Thyroid Hormones on Mesenchymal Stem Cells in Tumor Angiogenesis. *Thyroid : official journal of the American Thyroid Association* 29, 1843–1857. doi: 10.1089/thy.2019.0413

Seke Etet, P. F., Vecchio, L., Bogne Kamga, P., Nchiwan Nukenine, E., Krampera, M., and Nwabo Kamdje, A. H. (2013). Normal hematopoiesis and hematologic malignancies: role of canonical Wnt signaling pathway and stromal microenvironment. *Biochimica et biophysica acta* 1835, 1–10. doi: 10.1016/j.bbcan.2012.08.002

Sesia, S. B., Duhr, R., Todorov, A., Schaeren, S., Padovan, E., Spagnoli, G., et al. (2015). Anti-inflammatory/tissue repair macrophages enhance the cartilage-forming capacity of human bone marrow-derived mesenchymal stromal cells. *Journal of cellular physiology* 230, 1258–1269. doi: 10.1002/jcp.24861

Shamai, Y., Alperovich, D. C., Yakhini, Z., Skorecki, K., and Tzukerman, M. (2019). Reciprocal Reprogramming of Cancer Cells and Associated Mesenchymal Stem Cells in Gastric Cancer. *Stem cells (Dayton, Ohio)* 37, 176–189. doi: 10.1002/stem.2942

Shen, Y., Xue, C., Li, X., Ba, L., Gu, J., Sun, Z., et al. (2019). Effects of Gastric Cancer Cell-Derived Exosomes on the Immune Regulation of Mesenchymal Stem Cells by the NF-kB Signaling Pathway. *Stem cells and development* 28, 464–476. doi: 10.1089/scd.2018.0125

Shi, L., Zhao, Y., Fei, C., Guo, J., Jia, Y., Wu, D., et al. (2019). Cellular senescence induced by S100A9 in mesenchymal stromal cells through NLRP3 inflammasome activation. *Aging* 11, 9626–9642. doi: 10.18632/aging.102409

Shi, Y., Wang, Y., Li, Q., Liu, K., Hou, J., Shao, C., et al. (2018). Immunoregulatory mechanisms of mesenchymal stem and stromal cells in inflammatory diseases. *Nature reviews. Nephrology* 14, 493–507. doi: 10.1038/s41581-018-0023-5

Su, F., Ahn, S., Saha, A., DiGiovanni, J., and Kolonin, M. G. (2019). Adipose stromal cell targeting suppresses prostate cancer epithelial-mesenchymal transition and chemoresistance. *Oncogene* 38, 1979–1988. doi: 10.1038/s41388-018-0558-8

Tan, H. X., Cao, Z. B., He, T. T., Huang, T., Xiang, C. L., and Liu, Y. (2019). TGFbeta1 is essential for MSCs-CAFs differentiation and promotes HCT116 cells migration and invasion via JAK/STAT3 signaling. *OncoTargets and therapy* 12, 5323–5334. doi: 10.2147/ott.s178618

Tejero, R., Huang, Y., Katsyv, I., Kluge, M., Lin, J. Y., Daviaud, N., et al. (2019). Gene signatures of quiescent glioblastoma cells reveal mesenchymal shift and interactions with niche microenvironment. *EBioMedicine* 42, 252–269. doi: 10.1016/j.ebiom.2019.03.064

Tew, B. Y., Legendre, C., Gooden, G. C., Johnson, K. N., Martinez, R. A., Kiefer, J., et al. (2019). Isolation and characterization of patient-derived CNS metastasis-associated stromal cell lines. *Oncogene* 38, 4002–4014. doi: 10.1038/s41388-019-0680-2

Thomas, R., Wang, W., and Su, D. M. (2020). Contributions of Age-Related Thymic Involution to Immunosenescence and Inflammaging. *Immunity & ageing : I & A* 17, 2.

Torres, A., Erices, J. I., Sanchez, F., Ehrenfeld, P., Turchi, L., Virolle, T., et al. (2019). Extracellular adenosine promotes cell migration/invasion of Glioblastoma Stem-like Cells through A3 Adenosine Receptor activation under hypoxia. *Cancer letters* 446, 112–122. doi: 10.1016/j.canlet.2019.01.004

Tsiklauri, L., Werner, J., Kampschulte, M., Frommer, K. W., Berninger, L., Irrgang, M., et al. (2018). Visfatin alters the cytokine and matrix-degrading enzyme profile during osteogenic and adipogenic MSC differentiation. *Osteoarthritis and cartilage* 26, 1225–1235. doi: 10.1016/j.joca.2018.06.001

Turley, S. J., Cremasco, V., and Astarita, J. L. (2015). Immunological hallmarks of stromal cells in the tumour microenvironment. *Nature reviews. Immunology* 15, 669–682. doi: 10.1038/nri3902

Udartseva, O. O., Zhidkova, O. V., Ezdakova, M. I., Ogneva, I. V., Andreeva, E. R., Buravkova, L. B., et al. (2019). Low-dose photodynamic therapy promotes angiogenic potential and increases immunogenicity of human mesenchymal stromal cells. *Journal of photochemistry and photobiology. B, Biology* 199, 111596. doi: 10.1016/j.jphotobiol.2019.111596

Umakoshi, M., Takahashi, S., Itoh, G., Kuriyama, S., Sasaki, Y., Yanagihara, K., et al. (2019). Macrophage-mediated transfer of cancer-derived components to stromal cells contributes to establishment of a pro-tumor microenvironment. *Oncogene* 38, 2162–2176. doi: 10.1038/s41388-018-0564-x

Verma, D., Zanetti, C., Godavarthy, P. S., Kumar, R., Minciacchi, V. R., Pfeiffer, J., et al. (2020). Bone marrow niche-derived extracellular matrix-degrading enzymes influence the progression of B-cell acute lymphoblastic leukemia. *Leukemia*

Walsh, H. R., Cruickshank, B. M., Brown, J. M., and Marcato, P. (2019). The Flick of a Switch: Conferring Survival Advantage to Breast Cancer Stem Cells Through Metabolic Plasticity. *Frontiers in oncology* 9:753.

Wang, B., Wu, Z. H., Lou, P. Y., Chai, C., Han, S. Y., Ning, J. F., et al. (2019). Human bone marrow-derived mesenchymal stem cell-secreted exosomes overexpressing microRNA-34a ameliorate glioblastoma development via down-regulating MYCN. *Cellular oncology (Dordrecht)* 42, 783–799. doi: 10.1007/s13402-019-00461-z

Wang, N., Zhang, R., Wang, S. J., Zhang, C. L., Mao, L. B., Zhuang, C. Y., et al. (2013). Vascular endothelial growth factor stimulates endothelial differentiation from mesenchymal stem cells via Rho/myocardin-related transcription factor–a signaling pathway. *The international journal of biochemistry & cell biology* 45, 1447–1456. doi: 10.1016/j.biocel.2013.04.021

Windmolders, S., De Boeck, A., Koninckx, R., Daniels, A., Bracke, M., Hendrikx, M., et al. (2014). Mesenchymal stem cell secreted platelet derived growth factor exerts a pro-migratory effect on resident Cardiac Atrial appendage Stem Cells. *Journal of molecular and cellular cardiology* 66, 177–188. doi: 10.1016/j.yjmcc.2013.11.016

Worner, P. M., Schachtele, D. J., Barabadi, Z., Srivastav, S., Chandrasekar, B., Izadpanah, R., et al. (2019). Breast Tumor Microenvironment Can Transform Naive Mesenchymal Stem Cells into Tumor-Forming Cells in Nude Mice. *Stem cells and development* 28, 341–352. doi: 10.1089/scd.2018.0110

Wu, S., Wang, Y., Yuan, Z., Wang, S., Du, H., Liu, X., et al. (2019). Human adiposederived mesenchymal stem cells promote breast cancer MCF7 cell epithelialmesenchymal transition by cross interacting with the TGFbeta/Smad and PI3K/AKT signaling pathways. *Molecular medicine reports* 19, 177–186.

Xia, C., Wang, T., Cheng, H., Dong, Y., Weng, Q., Sun, G., et al. (2020). Mesenchymal stem cells suppress leukemia via macrophage-mediated functional restoration of bone marrow microenvironment. *Leukemia*

Xu, X. D., Shao, S. X., Jiang, H. P., Cao, Y. W., Wang, Y. H., Yang, X. C., et al. (2015). Warburg effect or reverse Warburg effect? A review of cancer metabolism. *Oncology research and treatment* 38, 117–122. doi: 10.1159/000375435

Xuan, W., Khan, M., and Ashraf, M. (2020). Extracellular Vesicles From Notch Activated Cardiac Mesenchymal Stem Cells Promote Myocyte Proliferation and Neovasculogenesis. *Frontiers in cell and developmental biology* 8:11.

Yang, J., Lv, K., Sun, J., and Guan, J. (2019). Anti-tumor effects of engineered mesenchymal stem cells in colon cancer model. *Cancer management and research* 11, 8443–8450. doi: 10.2147/cmar.s209880

Yang, J., Ren, B., Yang, G., Wang, H., Chen, G., You, L., et al. (2020). The enhancement of glycolysis regulates pancreatic cancer metastasis. *Cellular and molecular life sciences : CMLS* 77, 305–321. doi: 10.1007/s00018-019-03278-z

Yang, Y., Bucan, V., Baehre, H., von der Ohe, J., Otte, A., and Hass, R. (2015). Acquisition of new tumor cell properties by MSC-derived exosomes. *International journal of oncology* 47, 244–252. doi: 10.3892/ijo.2015.3001

Zannoni, J., Mauz, N., Seyve, L., Meunier, M., Brault, J., Jouzier, C., et al. (2019). Tumor microenvironment and clonal monocytes from chronic myelomonocytic leukemia induce a procoagulant climate. *Blood advances* 3, 1868–1880. doi: 10.1182/bloodadvances.2018026955

Zhan, Y., Wang, L., Liu, G., Zhang, X., Yang, J., Pan, Y., et al. (2019). The Reparative Effects of Human Adipose-Derived Mesenchymal Stem Cells in the Chemotherapy-Damaged Thymus. *Stem cells and development* 28, 186–195. doi: 10.1089/scd.2018.0142

Zhang, L. N., Huang, Y. H., and Zhao, L. (2019b). Fusion of macrophages promotes breast cancer cell proliferation, migration and invasion through activating epithelial-mesenchymal transition and Wnt/beta-catenin signaling pathway. *Archives of biochemistry and biophysics* 676, 108137. doi: 10.1016/j.abb.2019.108137

Zhang, X., Sai, B., Wang, F., Wang, L., Wang, Y., Zheng, L., et al. (2019a). Hypoxic BMSC-derived exosomal miRNAs promote metastasis of lung cancer cells via STAT3-induced EMT. *Molecular cancer* 18, 40.

Zhou, X., Li, T., Chen, Y., Zhang, N., Wang, P., Liang, Y., et al. (2019b). Mesenchymal stem cellderived extracellular vesicles promote the in vitro proliferation and migration of breast cancer cells through the activation of the ERK pathway. *International journal of oncology* 54, 1843–1852.

Zhou, Y., Zhong, J. H., Gong, F. S., and Xiao, J. (2019a). MiR-141-3p suppresses gastric cancer induced transition of normal fibroblast and BMSC to cancer-associated fibroblasts via targeting STAT4. *Experimental and molecular pathology* 107, 85–94. doi: 10.1016/j.yexmp.2018.11.014

Conflict of Interest: The authors declare that the research was conducted in the absence of any commercial or financial relationships that could be construed as a potential conflict of interest.

frontiers in Cell and Developmental Biology

REVIEW
published: 17 December 2020
doi: 10.3389/fcell.2020.547653

Two Decades of Global Progress in Authorized Advanced Therapy Medicinal Products: An Emerging Revolution in Therapeutic Strategies

Roya Ramezankhani[1,2†], Shukoofeh Torabi[1,2†], Neda Minaei[1,2], Hoda Madani[1,2], Siamak Rezaeiani[1,3], Seyedeh Nafiseh Hassani[3,4], Adrian P. Gee[5], Massimo Dominici[6], Daniela Nascimento Silva[7,8], Hossein Baharvand[3,4,9] and Ensiyeh Hajizadeh-Saffar[1,2,4]*

[1] Department of Regenerative Medicine, Cell Science Research Center, Royan Institute for Stem Cell Biology and Technology, Academic Center for Education, Culture and Research, Tehran, Iran, [2] Department of Applied Cell Sciences, Faculty of Basic Sciences and Advanced Medical Technologies, Royan Institute, Academic Center for Education, Culture and Research, Tehran, Iran, [3] Department of Stem Cells and Developmental Biology, Cell Science Research Center, Royan Institute for Stem Cell Biology and Technology, Academic Center for Education, Culture and Research, Tehran, Iran, [4] Advanced Therapy Medicinal Product Technology Development Center, Royan Institute for Stem Cell Biology and Technology, Academic Center for Education, Culture and Research, Tehran, Iran, [5] Division of Hematology and Oncology, Department of Pediatrics, Baylor College of Medicine, Houston, TX, United States, [6] Division of Oncology, Department of Medical and Surgical Sciences for Children & Adults, University of Modena and Reggio Emilia, Modena, Italy, [7] Karolinska Institutet, Stockholm, Sweden, [8] Health Institute of Technology, SENAI-CIMATEC, Salvador, Brazil, [9] Department of Developmental Biology, University of Science and Culture, Tehran, Iran

The introduction of advanced therapy medicinal products (ATMPs) to the global pharma market has been revolutionizing the pharmaceutical industry and has opened new routes for treating various types of cancers and incurable diseases. In the past two decades, a noticeable part of clinical practices has been devoting progressively to these products. The first step to develop such an ATMP product is to be familiar with other approved products to obtain a general view about this industry trend. The present paper depicts an overall perspective of approved ATMPs in different countries, while reflecting the degree of their success in a clinical point of view and highlighting their main safety issues and also related market size as a whole. In this regard, published articles regarding safety, efficacy, and market size of approved ATMPs were reviewed using the search engines PubMed, Scopus, and Google Scholar. For some products which the related papers were not available, data on the relevant company website were referenced. In this descriptive study, we have introduced and classified approved cell, gene, and tissue engineering-based products by different regulatory agencies, along with their characteristics, manufacturer, indication, approval date, related regulatory agency, dosage, product description, price and published data about their safety and efficacy. In addition, to gain insights about the commercial situation of each product, we have gathered accessible sale reports and market size information that pertain to some of these products.

Keywords: advanced therapy medicinal products, ATMP, safety, efficacy, market size

OPEN ACCESS

Edited by:
Marcela F. Bolontrade, Consejo Nacional de Investigaciones Científicas y Técnicas (CONICET), Argentina

Reviewed by:
Patrick Celis, European Medicines Agency, United Kingdom
Mariana G. Garcia, Austral University, Argentina

****Correspondence:***
Ensiyeh Hajizadeh-Saffar
Hajizadeh.ehs@royaninstitute.org; hajizadeh.ehs@gmail.com

† These authors have contributed equally to this work

Specialty section:
This article was submitted to Stem Cell Research, a section of the journal Frontiers in Cell and Developmental Biology

Received: *31 March 2020*
Accepted: *16 September 2020*
Published: *17 December 2020*

Citation:
Ramezankhani R, Torabi S, Minaei N, Madani H, Rezaeiani S, Hassani SN, Gee AP, Dominici M, Silva DN, Baharvand H and Hajizadeh-Saffar E (2020) Two Decades of Global Progress in Authorized Advanced Therapy Medicinal Products: An Emerging Revolution in Therapeutic Strategies. Front. Cell Dev. Biol. 8:547653. doi: 10.3389/fcell.2020.547653

INTRODUCTION

Based on Directive 2001/83/EC, medicinal products in Europe have been defined as any substance or combination of substances that have the capability to treat or prevent diseases in humans or may be used with the purpose to restore, correct, or modify physiological functions in conjunction with the capability to be used for medical diagnosis in humans. With the advent of new gene and/or cell therapies and in order to assure their appropriate quality, safety, and efficacy, these therapies were introduced into the European medicinal product legislation in June 2003 as a new class of medicinal products, which were later called ATMPs. In 2007, Regulation (EC) No. 1394/2007, a specific regulation for ATMPs, was established by the EU Commission. This regulation divides ATMPs into four distinct types: GTMPs, SCTMPs, TEPs, and the combined ATMPs (cATMPs). GTMPs are products directly related to therapeutic, prophylactic, or diagnostic effects with a recombinant nucleic acid sequence. SCTMPs are products that contain substantially manipulated cells or tissues, or the cells or tissues not intended to be used for the same essential function(s) in the recipient and the donor. TEPs are engineered cells or tissues that have the properties of regenerating, repairing, or replacing human tissue, all in accordance with the medicinal products general definition and finally cATMPs comprise another type of these products and contain one or several medical devices that are an integral part of the GTMPs, SCTMPs, or TEPs (Hanna et al., 2016a; Detela and Lodge, 2019). Also, each regulatory authority may provide a certain type of definition for ATMPs. For example, in US according to FDA, advanced therapies are regulated as biologic products, similar to EU classification. Biological products consist of allergenic products that includes allergen extracts, allergen patch tests, and antigen skin tests, blood and blood products, vaccines, xenotrasplants, and ATMPs which constitutes two subcategories: CGTs (Integra, 2019). "Cellular immunotherapies, cancer vaccines, and other types of both autologous and allogeneic cells for certain therapeutic indications, including hematopoietic stem cells and adult and embryonic stem cells that have been subject to substantial *ex vivo* manipulation constitute cellular therapy based products, while modifying the expression of a gene or changing the biological properties of living cells for therapeutic use compose human gene therapy based products" (Genzyme, 2019). Moreover, "combination products include products that are comprised of two or more regulated components, i.e., drug/device, biologic/device, drug/biologic, or drug/device/biologic." The MFDS in South Korea also define the cell therapy product as "a medicinal product manufactured through physical, chemical, and/or biological manipulation, such as *in vitro* culture of autologous, allogeneic, or xenogeneic cells. However, this definition does not apply to a case where a medical doctor performs minimal manipulation (e.g., simple separation, washing, freezing, thawing, and other manipulations, while maintaining biological properties) that does not cause safety problems of the cells in the course of surgical operation or treatment at a medical center." And a gene therapy product is defined as "a genetic material or a medicinal product containing such genetic material intended to be administered to human beings for treatment of disease (Choi et al., 2015). The regulatory guidelines regarding the (pre)submission, details of approval procedures, marketing authorization etc. have described thoroughly elsewhere (Detela and Lodge, 2019; EU, 2020; Luria et al., 2020). The need to establish effective therapeutic approaches to treat incurable diseases, notably, inherited genetic conditions, blood related disorders, malignancies, neurodegenerative diseases, tissue regeneration, and provide a bridge for patients awaiting organ transplantation has encouraged the increased use of ATMPs in medical

Abbreviations: 6MWT, 6-minute walk test; AALS, Appel ALS; AAV, adeno-associated virus; ABPI, ankle brachial pressure index; ACKFBC, Allogeneic Cultured Keratinocytes and Fibroblasts in Bovine Collagen; ADA-SCID, adenosine deaminase severe combined immunodeficiency; ADC, adipose tissue-derived cell; ADL, activities of daily living; AL, allogeneic; ALS, amyotrophic lateral sclerosis; ALSFRS, Amyotrophic Lateral Sclerosis Functional Rating Scale; AMDDC, autologous monocyte-derived mature dendritic cell; AMI, acute myocardial infarction; ASD, atrial septal defect; AT, autologous; ATMP, advanced therapy medicinal product; AT-MSC, adipose tissue-derived mesenchymal stem cell; AVN, avascular necrosis; AVR, aortic valve reconstruction; B-ALL, B-cell precursor acute lymphoblastic leukemia; BCVA, best-corrected visual acuity; BM-MSC, bone marrow-derived mesenchymal stem cell; CAGR, compound annual growth rate; CAR, chimeric antigen receptor; CD, Crohn's disease; CEA, cultured epidermal autograft; CFDA, China Food and Drug Administration; CLI, critical limb ischemia; COBLT, cord blood transplantation; CR, complete remission; CRT, cardiac resynchronization therapy; *CTLA4Ig*, cytotoxic T-lymphocyte associated protein 4 immunoglobulin; DB, dermal burn; DC, dendritic cell; DCGI, Drug Controller General of India; DDB, deep dermal burn; DFS, disease-free survival; DFU, diabetic foot ulcer; DLBCL, diffuse large B-cell lymphoma; DRR, durable response rate; DTH, delayed type hypersensitivity; EFS, event-free survival; EMA, European Medicines Agency; FDA, Food and Drug Administration; FST, full-field light sensitivity testing; FVC, forced vital capacity; GACI, gel-type autologous chondrocyte implantation; GM-CSF, granulocyte macrophage colony stimulating factor; GTMP, Gene Therapy Medicinal Product; GvHD, graft-versus-host disease; HAS, Heath Administration of Singapore; HCEpC, human corneal epithelial cell; HDFn, human dermal fibroblasts, neonatal; HEKn, human epidermal keratinocytes, neonatal; HPC, hematopoietic progenitor cell; HNSCC, head and neck squamous cell carcinoma; *hRPE65*, human retinal pigment epithelium 65 kDa; HSCT, hematopoietic stem cell transplantation; HSV, herpes simplex virus; ICRS, International Cartilage Repair Society; IFN-γ, interferon gamma; IKDC, International Knee Documentation Committee; irRC, immune-related response criteria; KLH, keyhole limpet hemocyanin; KOOS, knee injury and osteoarthritis outcome score; KSS, Knee Society Scoring system; LCC, living cellular construct; LPLD, lipoprotein lipase deficiency; LVEDV, left ventricular end-diastolic volume; LVEF, left ventricular ejection fraction; LVESV, end-systolic volume; LVRR, left ventricular reverse remodeling; mCRPC, metastatic castration-resistant prostate cancer; MFDS, Ministry of Food and Drug Safety; MLMT, multi-luminance mobility test; MOCART, Magnetic Resonance Observation of Cartilage Repair Tissue; MOH, Ministry of Health; mPP, modified per protocol; MSC, mesenchymal stem cell; MSS, MRI Scoring of Severity; NGFR, nerve growth factor receptor; NLF, nasolabilal fold; NRM, non-relapse mortality; NSCLC, non-small cell lung carcinoma; OA, osteoarthritis; OCD, osteochondritis dissecans; OR, overall response; ORR, objective response rate; ORR, overall response rate; ORR, overall remission rate; OS, overall survival; PAD, peripheral artery disease; PAP, prostatic acid phosphatase; PBMNC, peripheral-blood mononuclear cell; Pca, prostate cancer; PCI, percutaneous coronary intervention; PFU, plaque forming unit; PMBCL, primary mediastinal large B-cell lymphoma; PMDA, Pharmaceuticals and Medical Devices Agency; PR, partial remission; PRP, platelet-rich plasma; PWD, pain-free walking distance; QOL, quality of life; r/r, relapsed or refractory; RECIST, Response Evaluation Criteria in Solid Tumor; RFS, recurrence free survival; RFS, relapse-free survival; SCTMP, somatic cell therapy medicinal product; SDCS, skeletal myoblast-derived cell sheet; SOC, standard of care; SPECT, single-photon emission computed tomography; SRA, sports and recreational activity; TBSA, total body surface area; TEAEs, treatment emergent adverse events; TEP, tissue engineered product; TGA, Therapeutic Goods Administration; TL-pulsed DC, tumor lysate-pulsed dendritic cell; TNC, total nucleated cell; TREC, T-cell receptor excision circle; TTF, time to treatment failure; TTP, time to progression; UCCBB, University of Colorado Cord Blood Bank; SMA, spinal muscular atrophy; SMN, survival motor neuron; VAS, visual analog scale; VEGF, vascular endothelial growth factor; VG, vector genome; VLU, venous leg ulcer; VP, viral particle; VSD, ventricular septal defect; Xn, xenogeneic.

sciences. Interestingly, a significant growth in the research and development phase along with the clinical use of ATMPs has been observed in recent years. In this regard, based on the results of three clinical trials databases: ClinicalTrials.gov, the International Clinical Trials Registry Platform (ICTRP) of the World Health Organization (WHO), and EudraCT, 939 clinical trials of ATMPs conducted between 1999 and June 2015 (Hanna et al., 2016b). This would indicate an increase in investment by big pharma sponsors for ATMPs (Ten Ham et al., 2018). Of note, potential challenges that exist in terms of the development of ATMPs include the specific requirements for high-technology equipment, difficulty with manufacturing processes, complicated trial design, establishment of robust assays for validation of identity and functionality, achieving an expected high efficacy, avoidance of probable long-term adverse events, regulatory considerations in terms of regulatory cost burden and timelines etc., and, in particular, financial issues that provide situations where the product cannot be sold at a sufficiently high price to establish a commercially viable product (Mount et al., 2015; Elsanhoury et al., 2017; Lee, 2018). ATMPs are based on a diverse set of most advanced technologies (Elsanhoury et al., 2017), therefore, there is an increased need for the technical/academic personnel involved directly and professionally in ATMP development (Lee, 2018). Besides, regarding the rare nature of the diseases that ATMPs are mostly developed for, there are concerns in relation with trial design such as the low number of patients, insufficient knowledge respecting the disease pathogenesis and some issues with the interpretation of endpoints for new indications (Lee, 2018). Also, the statistical analysis of safety and efficacy is affected by the limited number of participants (Viganò et al., 2018). On the other hand, validating these products particularly with regard to identity, purity, and potency is of great importance. The restricted accessible appropriate standards and reference material along with an inadequacy in certain guidelines are the other challenges in this regard (McConaghie, 2017).

Financial issues may be one of the main challenges that can negatively influence the company and consumers. A well-known example, Glybera, is a gene therapy based drug for a rare familial LPLD (European Medicines Agency, 2020b). Its marketing authorization expired on October 28, 2017 following a decision by the marketing authorization holder to not apply for a renewal. The drug was proven to be a commercial failure because a single dose treatment cost over one million euro per patient, in addition to the low market size due to the fact that LPLD is a ultra-rare disease (Senior, 2017; Cuende et al., 2018).

Cuende et al. (2018) previously described cell therapy products with market authorization (Food and Drug Administration, 2019a), in this extensive review thanks to available information in the regulatory agencies and related company's web resources, articles, and other data sources, we in-depth dissected and classified cell, gene, and tissue engineering products (**Tables 1–3**). Data are presented in detailed tables that has been categorized in terms of product's definition, manufacturer, indication, approval date and related regulatory agency, product dosage and description, price, and related references. In addition, based on clinical trials data, we have further discussed each ATMP's safety and efficacy points, categorized by the common indication within each group. Also included is a definition of the available market sizes and sale reports for the related products in an attempt to clarify the commercial point of view for each of the GTMPs, SCTMPs, and TEPs fields.

To achieving this end, published articles regarding the characteristics, safety and efficacy, and market size of approved ATMPs were reviewed using the search engines PubMed, Scopus, and Google Scholar. For some products which the related papers were not available, data on the relevant company website was used as reference. The type of documents used to obtain the data were original articles, review articles, HTML documents, and official websites of each product manufacturer. Search terms included MeSH (Medical Subject Headings) terms, "ATMP" "CTMP" "GTMP" "TEP" and also "product name" in addition to each terms of "efficacy" "safety" "adverse events" "price" and "market size." The cut-off date for the data search was May 2020.

Collectively, this paper aims to provide a comprehensive insight for development of other cell therapy products for stakeholders, sponsors, manufacturing companies, regulatory agencies, and researchers interested in entering this research pathway.

CLASSIFICATION OF ADVANCED THERAPY MEDICINAL PRODUCTS

To the best of our knowledge, worldwide, there are 64 approved ATMPs by taking into consideration that Prochymal, a CTMP product, approved by both the FDA and Health Canada, and the GTMP product, Kymriah, is being approved by the FDA, EMA, and Health Canada. In addition, the FDA and EMA both approved another GTMP product, Yescarta. Obviously, the CTMP group, with 34 products, is the largest class. The TEP and GTMP groups, with 20 and 10 products, follow in order. **Figure 1** shows that United States, by authorizing 23 ATMPs (11 CTMPs, 7 TEPs, and 5 GTMPs), is the pioneer country in this field followed by South Korea with 15 ATMPs (13 CTMPs and 2 TEPs). **Figure 2** shows the indications of each of the ATMP categories, which emphasizes the importance of the indications related to hematologic along with skin and soft tissue disorders (**Figure 2A**), skin and soft tissue related disorders (**Figure 2B**), and oncology (**Figure 2C**) in the CTMPs, TEPs, and GTMPs, respectively. It can be concluded that most CTMPs and GTMPs have an autologous source (**Figure 2A,C**), while TEPs involve 45 percent of allogeneic and 40 percent of autologous products (**Figure 2B**).

SAFETY AND EFFICACY OF ADVANCED THERAPY MEDICINAL PRODUCTS (ATMPs)

Cell Therapy Medicinal Products (CTMPs)

CTMPs can be divided into eight distinct groups with respect to the indication for which they have been developed: hematologic

TABLE 1 | List of approved cell therapy medicinal products (CTMPs).

No.	Trade name/proper name	Manufacturer	Indication	Approved by/date	Product dosage	Product form	Product description	AT/AL	Price
1	Hemacord (Food and Drug Administration, 2019g) HPC, cord blood	New York Blood Center, Inc. (United States)	HSCT	US FDA 2011 November	A minimum of 5×10^8 total nucleated cells with at least 1.25×10^6 viable CD34 + cells at the time of cryopreservation	Bag	Human cord blood-derived HPCs	AL	NA/ Generally, an average allogeneic HSCT costs US $200,000
2	HPC, cord blood (Food and Drug Administration, 2019f)	Clinimmune Labs, UCCBB (United States)	HSCT	US FDA 2012 May	A minimum dose of 2.5×10^7 nucleated cells/kg at cryopreservation	Bag	Human cord blood-derived HPCs	AL	
3	Ducord HPC, cord blood (Food and Drug Administration, 2019e)	Duke University School of Medicine (United States)	HSCT	US FDA 2012 October	A minimum dose of 2.5×10^7 nucleated cells/kg at cryopreservation	Bag	Human cord blood-derived HPCs	AL	
4	Allocord HPC, cord blood (Yeh et al., 2018; Food and Drug Administration, 2019h)	SSM Health Cardinal Glennon Children's Hospital (United States)	HSCT	US FDA 2013 May	A minimum of 5×10^8 TNC with at least 1.25×10^6 viable CD34 + cells at cryopreservation	Bag	Human cord blood-derived HPCs	AL	
5	HPC, cord blood (RxList, 2018)	LifeSouth Community Blood Centers, Inc. (United States)	HSCT	US FDA 2013 June	2.5×10^7 nucleated cells/kg	Bag	Human cord blood-derived HPCs	AL	
6	HPC, cord blood (Food and Drug Administration, 2019c)	Bloodworks (United States)	HSCT	US FDA 2016 January	Minimum dose of 2.5×10^7 nucleated cells/kg at cryopreservation Each bag: 5×10^8 TNC with a minimum of 1.25×10^6 CD34 + cells in 25 ml	Bag	Human cord blood-derived HPCs	AL	
7	Celevecord HPC, cord blood (Food and Drug Administration, 2019d)	Cleveland Cord Blood Center (United States)	HSCT	US FDA 2016 September	A minimum dose of 2.5×10^7 nucleated cells/kg at cryopreservation	Bag	Human cord blood-derived HPCs	AL	
8	HPC, cord blood (Food and Drug Administration, 2019b)	MD Anderson Cord Blood Bank (United States)	HSCT	US FDA 2018 June	2.5×10^7 nucleated cells/kg	Bag	Human cord blood-derived HPCs	AL	
9	Azficel-T laViv (Fibrocell Science Inc., 2013; S-Biomedics Ltd., 2019a)	Fibrocell Technologies, Inc. (United States)	Moderate to severe NLF wrinkles	US FDA 2011 June	$\sim 18 \times 10^6$ autologous fibroblasts in 1.2 ml suspension/three treatment sessions spaced at intervals of 3 to 6 weeks	Vial	Human fibroblasts	AT	$19,900 for a patient's full course of treatment

(Continued)

TABLE 1 | Continued

No.	Trade name/proper name	Manufacturer	Indication	Approved by/date	Product dosage	Product form	Product description	AT/AL	Price
10	Provenge Sipuleucel-T (Timmerman, 2010; Food and Drug Administration, 2019j)	Dendreon, Corp. (United States)	Asymptomatic or minimally symptomatic metastatic castrate resistant (hormone refractory) PCA	US FDA 2010 April EMA 2010 September	Minimum of 50 million activated CD54 + cells, suspended in 250 mL of Lactated Ringer's solution	Bag	PBMNCs (primarily DCs) activated with PAP and GM-CSF	AT	$93,000 for 3 infusions
11	Prochymal BM-MSCs (Rattue, 2012; Mills, 2019)	Mesoblast, Ltd., International (Australia)	Acute and refractory GvHD	US FDA 2015 June Health Canada 2012 May	Intravenous administration: Low (2 million cells/kg) High (8 million cells/kg)	Bag	Human BM-MSCs	AL	$200,000 per treatment
12	Alofisell (Cx601) Darvadstrocel (Cho et al., 2015; NICE, 2019; Specialist pharmecy service, 2020)	TiGenix (United States) and Takeda (United Kingdom)	Complex perianal fistulas in CD	EMA 2018 March	5 million MSCs/ml suspension Treatment: 4 vials	Vial	Human adipose tissue- derived MSCs	AL	~ $47,485 per treatment
13	KeraHeal (Biosolution Ltd., 2019a,b; Medical observer, 2019)	Biosolution, Co., Ltd. (South Korea)	Deep 2^{nd} degree burn (> 30% of the TBSA) and 3^{rd} degree burn (>10% of the TBSA)	South Korea MFDS 2006 May	1 ml skin-derived keratinocytes suspension/100–400 cm^2	Vial	Human skin-derived keratinocytes	AT	~ $3,561/100–400 cm^2 per vial
14	Queencell (Anterogen Co., 2020; Ministry of Food and Drug Safety, 2020)	Anterogen (South Korea)	Subcutaneous tissue defects	South Korea MFDS 2010 March	Minimally manipulated ADC $\geq 1.0 \times 10^6$/vial (1 mL). Cell volume: according to size of the subcutaneous fat defect site.	Vial	Human adipose tissue-derived adipose cell	AT	NA
15	CureSkin (Sang-jun, 2010; Biomedic, 2019; S-Biomedics Ltd., 2019b)	S. Biomedics (South Korea)	Depressed acne scars	South Korea MFDS 2010 May	50 to 100 μl (2.0×10^7 cells/ml) of dermal fibroblasts per intradermal injection three times biweekly injection	Vial	Human dermal fibroblasts	AT	A 500-won coin-sized scar: ~ $6,300 and the whole face: $11,700
16	KeraHeal-Allo (Joo-sung, 2016; Biosolution Ltd., 2019c)	Biosolution, Co., Ltd. (South Korea)	Deep 2^{nd} degree burns	South Korea MFDS 2015 October	One syringe (2.0×10^7 skin-derived keratinocytes/1.5 ml) to the image area of 100 cm^2	Pre-filled syringe	Human skin-derived keratinocytes suspended in a thermosensitive hydrogel	AL	~ $628 per 1.5-ml
17	Rosmir (Doo-hyun, 2018; Tego Science, 2020a,b)	Tego Sciences (South Korea)	Nasojugal groove	South Korea MFDS 2017 December	2×10^7 fibroblasts cells per packaging unit; single intradermal administration	Vial	Human fibroblasts	AT	More than ~ $ 81.38 per injection

(Continued)

TABLE 1 | Continued

No.	Trade name/proper name	Manufacturer	Indication	Approved by/date	Product dosage	Product form	Product description	AT/AL	Price
18	Chondron (Naver, 2019; Sewon Cellontech Ltd., 2019a)	Sewon Cellontech, Corp. (South Korea)	Focal knee cartilage defect	South Korea MFDS 2001 January	1 to 6 vials per patient >12 million cultured chondrocytes per vial	Vial	Human chondrocytes	AT	∼$5,890 per treatment
19	RMS- Ossron (Sewon Cellontech Ltd., 2019b)	Sewon Cellontech, Co., Ltd. (South Korea)	Bone defects	South Korea MFDS 2009 August	1 to 6 vials containing > 12 million cultured osteoblasts per vial (0.4 ml)	Vial	Human osteoblasts	AT	NA
20	Cartistem (Cade Hildreth, 2018; Medipost, 2019; SCT, 2019)	Medipost (South Korea)	Knee osteoarthritis (ICRS grade IV)	South Korea MFDS 2012 January	500 $\mu L/cm^2$ depending on the lesion (7.5×10^6 cells in 1.5 ml)	Vial	Human umbilical cord blood-derived MSCs	AL	$19,000–21,000 for the standard treatment and an additional $10,000 for each extra treatment
21	CreaVax-RCC (Woo, 2007; Ministry of Food and Drug Safety, 2019a)	JW CreaGene (South Korea)	Metastatic renal cell carcinoma for which nephrectomy can be performed	South Korea MFDS 2007 May	8 doses (4 times, once every 2 weeks); each vial: 5.0×10^7 dendritic cells in 2 ml	Vial	Human DCs	AT	∼ $27,000 (eight treatments)
22	Immuncell-LC (Sun-kyu, 2016; Ministry of Food and Drug Safety, 2019b)	Green Cross Cell, Corp. (South Korea)	Post-surgical recurrence of hepatocellular carcinoma	South Korea MFDS 2007 August	Each administration: 200 ml over a spot that contains $1.0 \times 10^9 \sim 2.0 \times 10^{10}$ activated T-cells (16 doses)	Bag	Human activated T lymphocytes	AT	>$4,500 per dose
23	Cupistem (Cade Hildreth, 2018; Anterogen Co., 2019; Ministry of Food and Drug Safety, 2019c)	Anterogen (South Korea)	Crohn's fistula	South Korea MFDS 2012 January	Fistula diameter: (a) ≤ 1 cm (3.0×10^7 AT-MSCs in 1 ml) (b) $1 < X < 2$ cm (6.0×10^7 AT-MSCs in 2 ml)	Vial	Human adipose tissue-derived MSCs	AT	$3,000–5,000 per treatment
24	Cellgram-AMI (Doo-hyun, 2019)	FCB Pharmicell (South Korea)	AMI	South Korea MFDS 2011 July	(a) Under 60 kg = 10 mL/5.0×10^7 BM-MSCs (b) 61 ∼ 80 kg = 14 mL/7.0×10^7 BM-MSCs c. Over 81 kg = 18 mL/9×10^7 BM-MSCs	Pre-filled syringe	Human BM- MSCs	AT	$15,000 for one shot
25	Neuronata-R (Han-soo, 2018; Corestem Inc., 2019)	Corestem (South Korea)	ALS (Lou Gehrig's Disease)	South Korea MFDS 2014 July	(0.1 ml/kg) 1.0×10^6 BM-MSCs in 4 ml self-cerebrospinal fluid Twice every 4 weeks	Pre-filled syringe	Human BM-MSCs	AT	∼$55,000 annually (24 treatments)
26	Cartigrow (Das, 2018; FAQ, 2019)	Regrow Biosciences, Pvt. Ltd. (India)	Knee/ankle cartilage loss	India DCGI 2017 April	48 million chondrocytes	Vial	Human chondrocytes	AT	$1,988 per treatment

(Continued)

TABLE 1 | Continued

No.	Trade name/proper name	Manufacturer	Indication	Approved by/date	Product dosage	Product form	Product description	AT/AL	Price
27	Ossgrow (Das, 2018; Regrow Biosciences Pvt. Ltd., 2019)	Regrow Biosciences, Pvt. Ltd. (India)	Early-stage AVN of hip	India DCGI 2017 April	1.2×10^7 autologous bone cells/0.4 ml	Vial	Human osteoblasts	AT	$1,988 per treatment
28	Apceden AMDDC (Apac Biotech, 2019; Safer, 2019)	APAC Biotech (India)	Prostate, ovarian, colorectal and NSCLC	India DCGI 2017 March	6 doses (4–5 million mature DCs per dose) in 14 weeks	Vial	Monocyte-derived mature DCs	AT	$7,100–9,940 per treatment
29	Stempeucel (Jayaraman, 2016; Stempeutics Research Pvt Ltd., 2019)	Stempeutics Research (India)	CLI due to thromboangiitis obliterans (Buerger's disease)	India DCGI 2016 May	Intramuscular injection of 1 or 2 million cells/kg body weight	Vial	Human BM-MSCs	AL	$2200 per treatment
30	Chondrocytes-T-Ortho-ACI Cartogen (Orthocell, 2018, 2019)	Orthocell (Australia)	Cartilage damage (chondromalacia patella or OCD) 18–55 years	Australia TGA 2017 March	2–5 million cells suspended in 1.0 ml of assembly medium	Bag	Human chondrocytes	AT	$4,500 per treatment
31	Temcell HS (StreetInsider, 2015; Jcr Pharmaceuticals Co., 2020)	JCR Pharmaceuticals (Japan)	Acute and refractory GvHD	Japan PMDA 2015 September	Intravenous infusion of 2 million cells/kg (each bag contains 72 million cells in 18 ml of saline) 4 ml per minute twice weekly at an interval of 3 days or more for 4 weeks	Bag	Human BM-MSCs	AL	$7,600 per bag
32	RenuDermcell (CellTech, 2019)	Cell Tech Pharmed (Iran)	Facial wrinkles and acne scars, atrophic skin lesions following skin trauma	Iran FDA 2018 January	Intradermal injection of a minimum of 3.0×10^7 cells. Usually three repeated times	Vial	Human dermal fibroblasts	AT	NA
33	MesestroCell (CellTech, 2019)	Cell Tech Pharmed (Iran)	OA and knee joint arthritis	Iran FDA 2018 January	A minimum intra-articular injection of 2.0×10^7 cells/knee, totally 4.0×10^7 cells for both knees	Vial	BM-MSCs	AT	NA
34	RecolorCell (CellTech, 2019)	Cell Tech Pharmed (Iran)	Different types of vitiligo: focal; segmental generalized	Iran FDA 2019 February	Approximately 70,000 cells/cm^2 area of vitiligo patches; This product is effective for vitiligo patches < 200 cm^2	Vial	Human keratinocytes and melanocytes	AT	NA

ADC, adipose tissue-derived cell; AL, allogeneic; ALS, amyotrophic lateral sclerosis; AMDDC, autologous monocyte-derived mature dendritic cell; AMI, acute myocardial infarction; AT, autologous; AT-MSCs, adipose tissue-derived mesenchymal stem cell; AVN, avascular necrosis; BM-MSC, bone marrow-derived mesenchymal stem cell; CD, Crohn's disease; CLI, critical limb ischemia; DC, dendritic cell; DCGI, Drug Controller General of India; DFU, diabetic foot ulcer; EMA, European Medicines Agency; FDA, Food and Drug Administration; GM-CSF, granulocyte macrophage colony stimulating factor; GvHD, graft-versus-host disease; HCEpC, human corneal epithelial cell; HPC, hematopoietic progenitor cell; HSCT, hematopoietic stem cell transplantation; ICRS, International Cartilage Repair Society; MFDS, Ministry of Food and Drug Safety; MSC, mesenchymal stem cell; NA, not available; NLF, nasolabial fold NSCLC, non-small cell lung carcinoma; OA, osteoarthritis; OCD, osteochondritis dissecans; PAP, prostatic acid phosphatase; Pca, prostate cancer; PBMNC, peripheral-blood mononuclear cell; PMDA, Pharmaceuticals and Medical Devices Agency; TBSA, total body surface area; TGA, Therapeutic Goods Administration; TNC, total nucleated cell; UCCBB, University of Colorado Cord Blood Bank.
All prices are in USD.

TABLE 2 | List of approved gene therapy medicinal products (GTMPs).

No.	Trade name/proper name	Manufacturer	Indications	Approved by/date	Dosage	Product form	Description	AT/ AL	Price
1	Kymriah Tisagenlecleucel (Miller, 2018; Food and Drug Administration, 2019k)	Novartis Pharmaceuticals, Corp. (United States)	Refractory B-ALL or in second or later relapse for patients up to 25 years of age	US FDA 2017 August	Intravenous administration of 0.2–5.0 $\times$ 10^6 cells/kg for $\leq$ 50 kg, and 0.1–2.5 $\times$ 10^8 cells/kg for $>$ 50 kg B-cell ALL patients up to 25 years of age and 0.6–6.0 $\times$ 10^8 cells for adult r/r DLBCL	Bag	CD19-targeted genetically modified T-lymphocytes	AT	$475,000 for ALL and $373,000 for DLBCL
2	Yescarta Axicabtageneciloleucel (Clarke and Berkrot, 2019; Food and Drug Administration, 2019l)	Kite Pharma, Inc. (United States)	Adult patients with r/r large B-cell lymphoma after two or more lines of systemic therapy, including DLBCL not otherwise specified, primary mediastinal large B-cell lymphoma, high grade B-cell lymphoma, and DLBCL arising from follicular lymphoma	US FDA 2017 October	2 $\times$ 10^6 CAR-T cells/kg	Bag	CD19-targeted genetically modified T lymphocytes	AT	$373,000 per treatment
3	Zolgensma Onasemnogene abeparvovec-xioi (Food and Drug Administration, 2019m)	AveXis (United States)	Pediatric patients $<$ 2 years of age with SMA and bi-allelic mutations in the *SMN1* gene	US FDA 2019 May	1.1 $\times$ 10^{14} to 1.4 $\times$ 10^{14} vg/kg	Vial	AAV9 vector containing functional copy of the SMN1 gene	-	$2.1 million per treatment
4	Kymriah Tisagenlecleucel (European Medicines Agency, 2019)	Novartis Pharmaceuticals, Corp. (United States)	Patients up to 25 years of age with refractory B-ALL, who are in relapse post-transplantation or in second or later relapse, and adult patients with r/r DLBCL after two or more lines of systemic therapy	EMA 2018 August	Intravenous administration of 0.2–5.0 $\times$ 10^6 cells/kg for $\leq$ 50 kg, and 0.1–2.5 $\times$ 10^8 cells/kg for $>$ 50 kg B-cell ALL patients up to 25 years of age and 0.6–6.0 $\times$ 10^8 cells for adult r/r DLBCL	Bag	CD19- targeted genetically modified T-lymphocytes	AT	$475,000 for ALL, and $373,000 for DLBCL
5	Yescarta Axicabtagene ciloleucel (Clarke and Berkrot, 2019; Yeskarta)	Kite Pharma, Inc. (United States)	Adult patients with r/r DLBCL and PMBCL after 2 or more lines of systemic therapy	EMA 2018 August	2 $\times$ 10^6 CAR-T cells/kg	Bag	CD19-targeted genetically modified T- lymphocytes	AT	$373,000 per treatment

(Continued)

TABLE 2 | Continued

No.	Trade name/proper name	Manufacturer	Indications	Approved by/date	Dosage	Product form	Description	AT/ AL	Price
6	Imlygic Talimogene laherparepvec [Imlygic, 2017; IMLYGIC (talimogene laherparepvec) | FDA, 2020]	Amgen, Inc. (United States)	Unresectable cutaneous, subcutaneous, and nodal lesions in recurrent melanoma after initial surgery	US FDA 2015 October EMA 2015 December	An initial dose of up to 4×10^6 PFU/ml, followed by subsequent doses of up to 4 ml at a concentration of 10^8 PFU/ml	Vial	Live, attenuated HSV-1 genetically modified to express hGM-CSF	-	$65,000 per treatment
7	Zalmoxis (Zalmoxis, 2016; MolMed, 2019)	Molmed S.p.A. (Italy)	Haploidentical-HSCT adult patients with high-risk hematological malignancies	EMA 2016 August Withdrawn 2019 October	$1 \pm 0.2 \times 10^7$ cells/kg	Bag	Genetically modified T-lymphocyte with a retroviral vector encoding ΔLNGFR and HSV-TK	AL	$170,000 (Italy) $186,000 (Germany)
8	Strimvelis (Mullin, 2019; Stem Cell Research, 2019)	GlaxoSmithKline (GSK, United Kingdom)	ADA-SCID	EMA 2016 May	The recommended dose range is between 2 and 20 million CD34 + cells/kg	Bag	Transduced CD34 + cells with a retroviral vector encoding human ADA	AT	$648,000 per treatment
9	Luxturna Voretigeneparvovec-rzyl (Berkrot, 2018; Food and Drug Administration, 2019n)	Spark Therapeutics, Inc. (United States)	Biallelic RPE65 mutation-associated retinal dystrophy	US FDA 2017 December EMA 2018 September	Sub-retinal injection of 1.5×10^{11} AAV vector genomes in a total volume of 0.3 ml for each eye	Vial	Live, non-replicating AAV2 genetically modified to express hRPE65 gene	-	$425,000 per eye
10	Gendicine (Rosen, 2012; Sibiono, 2019)	Shenzhen SiBiono Gene Tech, Co., Ltd. (China)	Late-stage HNSCC or terminal-stage non-HNSCC tumors	CFDA 2003 October	Administration of $1–4 \times 10^{12}$ VP once every 3–7 days over a course of 3–8 weeks	Vial	Recombinant adenovirus expressing human p53	-	Up to $100,000 per dose
11	Oncorine (SunWay Biotech, 2019)	Shanghai Sunway Biotech (China)	Nasopharyngeal carcinoma	CFDA 2005 November	5×10^{11} VP for 5 consecutive days	Vial	Recombinant human adenovirus type 5 with E1B-55kD and E3 region deletion	-	NA

(Continued)

TABLE 2 | Continued

No.	Trade name/proper name	Manufacturer	Indications	Approved by/date	Dosage	Product form	Description	AT/ AL	Price
12	Kymriah Tisagenlecleucel (Novartis., 2019b)	Novartis Pharmaceuticals Canada, Inc. (Canada)	3–25 year old patients with refractory B-ALL, relapsed after allogeneic SCT or ineligible for SCT, or with second or later relapse, and adult patients with r/r large B-cell lymphoma after two or more lines of systemic therapy including DLBCL not otherwise specified, high grade B-cell lymphoma and DLBCL arising from follicular lymphoma	Health Canada 2018 September	Intravenous administration of 0.2–5.0 $\times$ 10^6 cells/kg for $\leq$50 kg, and 0.1–2.5 $\times$ 10^8 cells/kg for $>$ 50 kg B-cell ALL patients up to 25 years of age and 0.6–6.0 $\times$ 10^8 cells for adult relapsed or refractory diffuse large B-cell lymphoma	Bag	CD19-targeted genetically modified T-lymphocytes	AT	$475,000 per treatment
13	Neovasculgen Cambiogeneplasmid (NOVARTIS, 2019a)	Human Stem Cells Institute (Russia)	PAD, including CLI caused by atherosclerosis	MOH of the Russia Federation 2011 December	2 sequential injections (i.e., 2 vials) of 1.2 mg of pCMV-veg f165 with an interval of 14 days	Vial	Plasmid encoding the CMV-VEGF (165 aa) gene	-	$\sim$ $6600 per treatment
14	Zynteglo (ClinicalTrials, 2020)	bluebird bio (Netherlands) B.V.	Patients up to 12 years old with beta thalassemia who require regular blood transfusions	EMA 2019 May	1.2–20 $\times$ 10^6 cells/mL dispersion for infusion	Bag	CD34 + cells encoding βA-T87Q-globin gene	AT	$1.78 million

AAV, adeno-associated virus; ADA-SCID, adenosine deaminase severe combined immunoeficiency; AL, allogeneic; AT, autologous; B-ALL, B-cell precursor acute lymphoblastic leukemia; CAR, chimeric antigen receptor; CFDA, China Food and Drug Administration; CLI, critical limb ischemia; DLBCL, diffuse large B-cell lymphoma; EMA, European Medicines Agency; FDA, Food and Drug Administration; GM-CSF, granulocyte macrophage colony-stimulating factor; HNSCC, head and neck squamous cell carcinoma; hRPE65, human retinal pigment epithelium 65 kDa; HSCT, hematopoietic stem cell transplantation; HSV, herpes simplex virus; NA, not available; MOH, Ministry of Health; NGFR, nerve growth factor receptor; PAD, peripheral artery disease; PFU, plaque forming unit; PMBCL, primary mediastinal large B-cell lymphoma; r/r, relapsed or refractory; SMA, spinal muscular atrophy; SMN, survival motor neuron; VEGF, vascular endothelial growth factor; VG, vector genome; VP, viral particle.
All prices are in USD.

TABLE 3 | List of approved tissue-engineered products (TEPs).

No.	Trade name/proper name	Manufacturer	Indications	Approvedby/date	Dosage	Product form	Description	AT/ AL	Price
1	Apligraf (Organogenesis Inc., 2019c, 2020)	Organogenesi, Inc. and Novartis AG (United States)	Chronic VLU, DFU	US FDA 2000 June	Circular disk with a diameter and thickness of 75 and 0.75 mm in size	Bag	Bi-layer bioengineered skin with inner layer of HDFn and outer layer of HEKn	AL	$1,500–2500 per treatment
2	Dermagraft (Organogenesis Inc., 2019d)	Organogenesis, Inc. (United States)	Full-thickness DFU > 6 weeks extended through the dermis without tendon, muscle, joint capsule, or bone exposure	US FDA 2001 September	2 × 3-inch sheets	Bag	Fibroblasts on a piece of bio-absorbable scaffold	AL	$1,700 per treatment
3	Aurix (Napodano, 2015; Nuo Therapeutics Inc., 2019)	Nuo Therapeutics, Inc. (United States)	All types of ulcers (DFU, pressure, VLU, etc.)	US FDA 2007 September	Depends on the size and condition of the wound	Gel	PRP hematogel	AL	$430 per treatment
4	Epicel Cultured epidermal autografts (Genzyme, 2019; Schlatter, 2019)	Vericel, Corp. (United States)	Deep dermal or full thickness burns	US FDA 2007 October	50 cm^2 sheets with a thickness of 2–8 cell layers	Sheet	Cultured keratinocytes on murine 3T3 fibroblasts (each graft is attached to petrolatum gauze backing with titanium surgical clips)	AT	$6,000 to $10,000 per 1% TBSA
5	Gintuit ACKFBC (Food and Drug Administration, 2019o)	Organogenesis, Inc. (United States)	Surgically created vascular wound bed in the treatment of mucogingival conditions	US FDA 2012 March	Sheets with a diameter and thickness of 75 and 0.75 mm, respectively, which consist of ∼4 million cells	Sheet	Cultured neonatal keratinocytes and fibroblasts on bovine collagen	AL	NA
6	Omnigraft Dermal Regeneration Matrix (Food and Drug Administration, 2019p; Integra, 2019)	Integra LifeSciences, Corp. (United States)	DFU	US FDA 2016 January	Sheets with two sizes of 4 × 4 and 7 × 7 cm^2	Sheet	Bi-layered bioengineered scaffold, including an inner layer of bovine collagen and chondroitin, and an outer layer consisting of thin silicone	Xn	$499.00 per Kit
7	MACI (Bloomberg Businessweek, 2018; Food and Drug Administration, 2019q)	Vericel, Corp. (United States)	Single or multiple symptomatic full-thickness cartilage defects of the knee with or without bone involvement in adults	US FDA 2016 December EMA 2013 June	3 × 5 cm^2 sheets, consist of 500,000 cells per cm^2	Sheet	Cultured chondrocytes on a porcine type I/III collagen membrane	AT	$40,000 per each scaffold

(Continued)

TABLE 3 | Continued

No.	Trade name/proper name	Manufacturer	Indications	Approvedby/date	Dosage	Product form	Description	AT/ AL	Price
8	Holoclar (EMC Inc., 2020; European Medicines Agency, 2020c)	Chiesi Farmaceutici S.p.A (Italy)	Severe limbal stem cell deficiency	EMA 2015 February	79,000–316,000 cells/cm^2	Sheet	HCEpC containing stem cells	AT	~ $102,977 per treatment per eye
9	Spherox (European Medicines Agency, 2020d; Startseite., 2020)	CO.DON AG (Germany)	Symptomatic articular cartilage defects of the femoral condyle and the patella of the knee with defect sizes up to 10 cm^2 in adults	EMA 2017 July	10–70 spheroids/cm^2	Tube	Tissue spheroids of human matrix-associated chondrocytes	AT	~ $12224 per treatment
10	Holoderm (Kim, 2014; Food and Drug Administration, 2019i; Tego Science, 2019e)	Tego Science (South Korea)	Deep 2^{nd} and 3^{rd} degree burns	South Korea MFDS 2002 December	56 cm^2/piece consisting of 1–4 billion keratinocytes	Sheet	Cultured keratinocyte sheet	AT	$697.76 per each cm^2
11	Kaloderm (Jae-hyeon, 2018; Global Sources, 2019)	Tego Science (South Korea)	Deep 2^{nd} degree burns and DFU	South Korea MFDS 2005 March (for burns) 2010 January (for DFU)	Each sheet contains $> 2 \times 10^7$ cells backed by vaseline gauze. The amount is determined considering the size and condition of the wound.	Sheet	Cultured keratinocytes sheet	AL	$26.5 per 1 cm^2 for products with 56 cm^2 units
12	CardioCel Pure collagen scaffold (Taylor and Francis Group, 2015; Anteris Technologies Limited, 2019)	Admedus (Singapore)	ASD and VSD	Australia HAS 2014 November	Sheets with three sizes of 4×4, 5×8, and 14×7 cm^2	Sheet	Tissue engineered bovine pericardium	Xn	$421.13 per sheet
13	JACE Epidermis-derived cell sheet (Drew, 2015; Pharmaceuticals and Medical Devices Agency, 2019)	J-TEC (Japan)	Scars, vitiligo, nevi (birthmarks), ulcers, skin-graft donor sites, severe burns: DDB + DB $\geq$ 30%	Japan PMDA 2007 October	A sheet consists of 1×10^4 cells/cm^2	Sheet	Keratinocytes sheet cultured on 3T3-J2 cells	AT	S$3,140 per 8×10 inch sheet
14	JACC AT Chondrocyte (Japan Tissue Engineering Co Ltd., 2020)	J-TEC (Japan)	Cartilage defect area >2–4 cm with no alternative therapy	Japan PMDA 2012 July	The quantity of mixture determined by the size of the cartilage defect: defect area x 0.3 ml (final cell density = 2×10^6 cells/mL, 1.33% collagen)	Pre-field syringe	Cultured chondrocytes in atelocollagen gel	AT	$21,300 per knee
15	HeartSheet SDCS (Pharmaceuticals and Medical Devices Agency, 2019; Pricing of Approved Cell Therapy, 2019)	Terumo, Corp. (Japan)	Severe heart failure due to ischemic heart disease	Japan PMDA 2015 September	5 skeletal myoblast-derived cell sheets (containing 3×10^8 cells)	Sheet	Skeletal myoblast sheet	AT	A kit: $56000 B kit: $15000 (Each treatment 1 A kit and 5 B kits)

(Continued)

TABLE 3 | Continued

No.	Trade name/proper name	Manufacturer	Indications	Approvedby/date	Dosage	Product form	Description	AT/ AL	Price
16	Artificial transfected pigskin (Cheng et al., 2016)	Chongqing Zongshen Junhui Biotechnology (China)	Burns and other traumatic wounds	China CFDA 2007	NA	Sheet	Bama miniature pig fresh skin tissue transfected with CTLA4Ig gene	Xn	NA
17	Bilayer artificial skin (Cheng et al., 2016)	Shaanxi Eyre skin Biological Engineering (China)	Deep 2^{nd} degree burn wound, not more than 3^{rd} degree burn wound 20 cm^2 (diameter <5 cm)	China CFDA 2007	NA	Sheet	A bilayer artificial skin with the epidermal layer composed of human epidermal cells and the dermal fibroblasts from human and bovine collagen	AL	NA
18	Amniosin (SinaCell Enterprise Knowledge Management, 2019)	SinaCell (Iran)	Corneal ulcer, full-thickness DFU > 6 weeks extended through the dermis without tendon, muscle, joint capsule, or bone exposure	Iran FDA 2017 March	One piece of 2 × 2 cm^2 implanted	Sheet	Acellular human amniotic membrane-derived dressing	AL	NA
19	Cell-Amniosin (SinaCell Enterprise Knowledge Management, 2019)	SinaCell (Iran)	Full-thickness DFU > 6 weeks extended through the dermis without tendon, muscle, joint capsule, or bone exposure	Iran FDA 2017 March	One piece of 2 × 2, 3 × 3, 5 × 5, 5 × 10, or 10 × 10 cm^2 implanted weekly until the ulcer is healed	Sheet	Cellular human amniotic membrane-derived dressing	AL	NA
20	Amniodisk (SinaCell Enterprise Knowledge Management, 2019)	SinaCell (Iran)	Corneal ulcer, conjunctival and epithelial damage	Iran FDA 2020 September	One piece of 15 mm circular shape sheet	Sheet	Dehydrated human amniotic membrane-derived ocular allograft	AL	NA

ACKFBC, allogeneic cultured keratinocytes and fibroblasts in bovine collagen; AL, allogeneic; ASD, atrial septal defect; AT, autologous; CFDA, China Food and Drug Administration; CTLA4Ig, cytotoxic T-lymphocyte associated protein 4 immunoglobulin; DDB, deep dermal burn; DB, dermal burn; DFU, diabetic foot ulcer; EMA, European Medicines Agency; FDA, Food and Drug Administration; HAS, Heath Administration of Singapore; HDFn, human dermal fibroblasts (neonatal); HEKn, human epidermal keratinocytes (neonatal); MFDS, Ministry of Food and Drug Safety; NA, not available; PMDA, Pharmaceuticals and Medical Devices Agency; PRP, platelet-rich plasma; SDCS, skeletal myoblast-derived cell sheet; TBSA, total body surface area; VLU, venous leg ulcer; VSD, ventricular septal defect; Xn, xenogeneic. All prices are in USD.

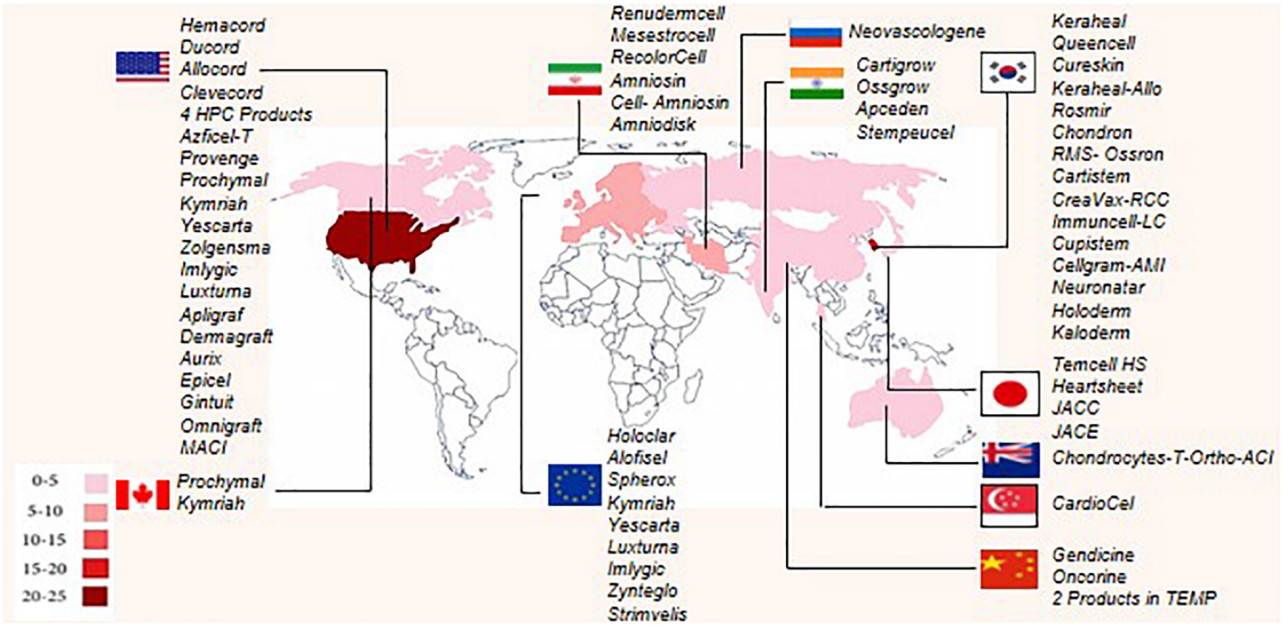

FIGURE 1 | Number of authorized ATMPs worldwide, according to country. Each country has been determined by specific color, and based on the number of authorized ATMPs. United States, South Korea, and the European Union have the highest number of approved ATMPs.

disorders, skin and soft tissue related issues, orthopedic diseases, oncology, and immunological, cardiovascular, neurological, and ocular related disorders.

For hematologic disorders, Hemacord (US FDA.2011), Ducord (US FDA.2012), Allocord (US FDA.2013), Clevecord (US FDA.2016), and four other HPC based products are approved for hematopoietic stem cell transplantations. Each product related efficacy has been compared against two studies: the COBLT study and another study with retrospective information from docket and public data (RxList, 2018; Food and Drug Administration, 2019b,c,d,e,f,g,h) with regards to neutrophil recovery at day 42, platelet recovery at day 100 (20,000/μL and 50,000/μL), and erythrocyte recovery at day 100. After receiving a TNC dose of $\geq 2.5 \times 10^7$/kg HPC, from multiple cord blood banks, the estimated values were as follows: neutrophils (76%), platelets (20,000/μL [57%] and 50,000/μL [46%]), and erythrocyte (65%) recovery in the COBLT study. The docket and public data information show an estimated neutrophil recovery of 77% and platelet recovery (50,000/μL) of 45%. On the other hand, the three parameters for neutrophil recovery and platelet recovery (20,000/μL and 50,000/μL) parameters were 88, 87, and 79% for Allocord; 96, 92, and 83% for Clevecord; 95, 92, and 71% for Ducord; 79, 62, and 55% for HPCs Cord Blood from Clinimmune Labs; 88.2, 73.6, and 43% for HPCs Cord Blood from MD Anderson Cord Blood Bank; 91, 95, and, 95% for HPCs Cord Blood from LifeSouth; and 82, 66, and 50% for HPCs Cord Blood from Bloodworks, respectively. In addition, the reported data related to the Hemacord study were 83% (neutrophil) and 77% platelet (20,000/μL) recovery. The median time for neutrophil recovery, platelet recovery (20,000/μL and 50,000/μL), and erythrocyte recovery were 27, 90, 113, and 64 days in the COBLT study, respectively. The median time for neutrophil recovery and platelet recovery (50,000/μL) were 25 and 122 days according to docket and public data information. The median time of neutrophil recovery and platelet recovery (20,000/μL and 50,000/μL) were 21, 48, and 56 days for Allocord; 18, 41, and 43 days for Clevecord; 21, 46, and 61 days for Ducord; 25, 55, and 49 days for HPCs Cord Blood from Clinimmune labs; 19, 47, and 65 days for HPCs Cord Blood from MD Anderson Cord Blood Bank; 22, 44, and 70 days from HPCs Cord Blood from LifeSouth; and 21.5, 46, and 53 days for HPCs Cord Blood from Bloodworks, respectively. Also, 20 days for neutrophil recovery and 45 days for platelet recovery (20,000/μL) were reported for Hemacord. The most important adverse events related to the safety of these products included hypersensitivity reactions, infusion reactions, graft-versus-host disease, engraftment syndrome and graft failure, malignancies of donor origin, transmission of serious infections, and transmission of rare genetic diseases.

For skin and soft tissue related disorders, CureSkin (South Korea MFDS.2010), Queencell (South Korea MFDS.2010), Azficel-T (US FDA.2011), Rosmir (South Korea MFDS.2017), and RenudermCell (Iran FDA.2018) are approved to treat acne scars and facial wrinkles, KeraHeal (South Korea MFDS.2006) and KeraHeal-allo (South Korea MFDS.2015) are approved for skin burns and finally RecolorCell (Iran FDA.2019) is indicated for different types of Vitiligo. The effectiveness of Azficel-T was demonstrated in two studies consist of 421 total patients at 3 and 6 months follow up. The self- and physician-reported assessments indicated 57 and 33% improvements in the first study, and 45 and 19% in the second study for patients who

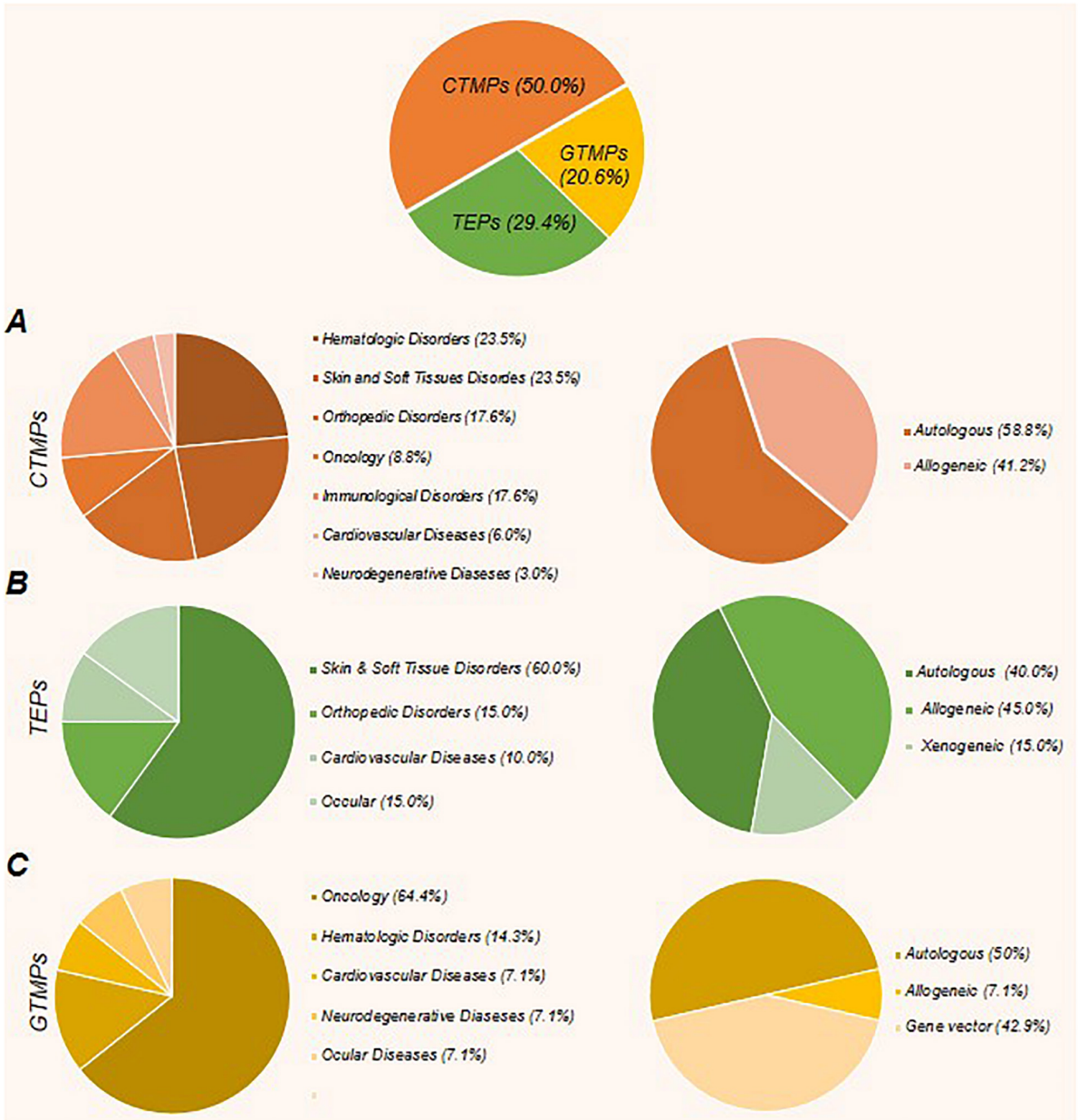

FIGURE 2 | The percent of approved cell, gene, and tissue engineering products, along with their related indications and product type (autologous or allogeneic). **(A)** The CTMPs with 34 members constitute the largest class of ATMPs. Most of these products have an autologous source. Hematologic disorders, along with skin and soft tissue related disorders and orthopedic disorders constitute the main fields. **(B)** The TEPs, with 20 products, represent the next largest class of ATMPs. The most emphasized indications in this class are skin and soft tissue related disorders, orthopedic disorders, and cardiovascular diseases, respectively, and the percentage of allogeneic products are more than autologous products. **(C)** GTMPs with 10 products comprise the last class. The first common indications are oncology, hematologic disorders, and cardiovascular diseases, respectively. Similar to CTMPs, GTMP members mostly have autologous sources.

received Azficel-T. A two-point improvement in NLF wrinkles was reported after 6 months. The most common adverse events were injection-site redness, bruising, swelling, pain, hemorrhage, edema, nodules, papules, irritation, dermatitis, and pruritus (S-Biomedics Ltd., 2019a). Qualitative data regarding the efficacy of CureSkin shows its superior effect in the healing process of depressed acne scars (S-Biomedics Ltd., 2012). Moreover, according to the product's brochure, the most common reported adverse events after repeated administration of CureSkin was erythema at the injection site. Common adverse events for Rosmir included eye irritation and allergic rhinitis (Yim et al., 2011; Tego Science, 2019a). Regarding KeraHeal efficacy, the take rate of 1:4–6 meshed autografts along with KeraHeal in 29 patients with burn injuries was estimated to be 96 and 100%

at 2 and 4 weeks after treatment, respectively. A reduction in Vancouver burn scar scale at 8, 12, and 24 weeks following the treatment was observed (Yoon et al., 2017). The primary outcome used to show the KeraHeal-allo efficacy was the period of re-epithelialization, which occurred 2.5 or 2.8 days faster in the treated sites in comparison with the control. No associated adverse events were reported with these two products (Park et al., 2017).

For orthopedic disorders, Cartistem (South Korea MFDS.2012) and MesestroCell (Iran FDA.2018) are approved for knee osteoarthritis; Chondron (South Korea MFDS.2001), Cartigrow (India DCGI.2017), and Chondrocytes-T-Ortho-ACI (Australia TGA.2017) are approved for defective knee cartilage. Ossron (South Korea MFDS.2009) and Ossgrow (India DCGI.2017) are approved for repair of bone defects. The safety and efficacy of Cartistem was assessed in a phase I/II clinical trial with 7 years long−term follow−up in seven patients with osteoarthritis of the knee joint with Kellgren−Lawrence (K−L) grade 3 and painful full−thickness cartilage defects. Results have shown repaired tissue at 12-weeks post-transplantation, while arthroscopic examination and biopsy at 1 year showed stable regenerated cartilage. Furthermore, the 100-mm VAS score for pain and the IKDC subjective score were improved at 24 weeks post-transplantation and maintained for up to 7 years. A high glycosaminoglycan content in the regenerated cartilage at 3 years was determined through the mean relative change in R1 (ΔR1) index. Mild to moderate adverse events included arthralgia, back pain, and bladder distension. No particular adverse reactions were noted over 7 years of clinical follow-up (Choi et al., 2010). Following the Chondron transplantation in 98 patients with articular cartilage injury of the knee joint and 13∼25-month follow-up, assessments showed a notable improvement in the Knee Society Scoring system (tKSS)-A (pain) and tKSS-B (function) scores. A total of 2.04% of the patients experienced adverse events related to GACI due to 'catching symptom' (Bauer et al., 2012). The safety, tolerability, and efficacy of Chondrocytes-T-Ortho-ACI are reported from clinical trials of 1077 reported cases that showed significant improvements in the KOOS subscales and in the 6MWT during 36 months of post-surgery follow up in comparison with the pre-operative group. MRI analysis also showed significant post-operative progression; however, this observation was not sustained until the study end point. The most common adverse events encountered during these clinical trials included engraft failure, cartilage hypertrophy, incomplete drug effect, and graft delamination (Kim et al., 2009). Safety and efficacy of Ossron and Ossgrow have been assessed in a clinical trial of 64 patients with long-bone shaft fractures during 2 months. The average callus formation score was significantly higher in the experimental group at 1 and 2 months of follow up, while the osteoblast injection response was not statistically different between younger and older patients. No adverse effects were observed in association with the osteoblast injection (Kim et al., 2007).

In oncology, CreaVax-RCC (South Korea MFDS.2007) is approved for metastatic renal cell carcinoma, Immuncell-LC (South Korea MFDS.2007) is approved for post-surgical recurrence of hepatocellular carcinoma, Sipuleucel-T (Provenge) (US FDA.2010/EMA.2010) is approved for mCRPC, and finally, Apceden (India DCGI.2017) is approved for Prostate, ovarian, colorectal, and NSCLC. The safety and efficacy of CreaVax-RCC was assessed in nine patients suffering from metastatic renal cell carcinoma with a median follow-up of 17.5 months. This treatment had the ability to prompt an immune response against the tumor. Out of nine patients, one experienced a PR and a decrease in the size of lung metastases; five had stable disease; and three had evidence of progressive disease after one cycle of immunotherapy. The results of the DTH skin test with KLH or TL-pulsed DCs determined that three patients with no initial DTH reactivity and three patients with a positive initial DTH response to KLH- or TL-pulsed DC had positive reactions to both after immunotherapy and experienced raised skin reactions after the vaccination. In addition, there was an elevation in the number of tumor specific interferon gamma (IFN-γ)-producing cells after one cycle of the vaccination. No severe adverse effects have been reported (Lee et al., 2015). In the Immuncell-LC phase III clinical trial, 230 patients with HCC were assigned randomly to receive immunotherapy 16 times during 60 weeks or no adjuvant therapy (controls). RFS and RFS rates were considered to be the primary outcomes. Overall survival (OS), cancer-specific survival, the OS rate, and cancer-specific survival rate criteria accounted for secondary outcomes. The RFS time for the immunotherapy group was 44 months in comparison with 30 months in the control group. The RFS rate for both groups declined during 12, 24, 36, and 48 months post-treatment; however, the amount of statistically significant rates per month were higher in the immunotherapy group. Both the OS rate and cancer-specific survival rate decreased in the immunotherapy and control groups during 12, 24, 36, and 48 months. Again, the amounts of the statistical rates per month were higher in the treatment group. Serious adverse events were reported in the immunotherapy group and included hemorrhage from esophageal varices, hepatic vein stenosis, herpes zoster, laceration, meniscus lesion, humerus fracture, foot fracture, bladder neoplasm, and high frequency ablation (Kantoff et al., 2010). In a phase III clinical trial, 341 patients with mCRPC received Stempeucel-T (Provenge). There was a relative decline of 22% in the risk of death observed in the sipuleucel-T group compared with the placebo group. This reduction resulted in a 4.1-month improvement in median patient survival. The most common adverse events were chills, fever, and headache. These adverse events were more frequent in the sipuleucel-T group than in the placebo group (Bapsy et al., 2014). Safety and efficacy of Apceden was assessed in a multicenter phase II clinical trial in India that enrolled 51 patients with refractory solid cancers. A significant improvement regarding QOL and overall median survival in patients with objective response was observed. The TTP analysis showed a notable delay in the onset of disease development. There was an increase in the mean CD4:CD8 ratio in the immune response evaluation, along with an ORR of 28.9 and 42.1% by RECIST and irRC, respectively. One adverse event, an episode of rigors together with mild fever during a single infusion was reported (Prasad et al., 2011).

Immunological disorders have four approved products. Prochymal (Health Canada.2012, US FDA.2015) together with

Temcell HS (Japan PMDA.2015) are produced to treat GvHD. Cupistem (South Korea MFDS.2012) and Alofisel (EMA.2018) are two other products in this group. First one is indicated for reducing the inflammation in Crohn's Fistula and the latter is indicated for treatment of complex perianal fistulas in adult patients with non-active/mildly active luminal Crohn's disease. In one trial, Prochymal was used to treat refractory grades III and IV acute GvHD in 12 children. The results indicated that allogeneic HSCT was well-tolerated. The survival rate was 42% after a median follow up of 611 days. The OS for patients who achieved CR was estimated to be 68% at 2 years (Muroi et al., 2016). Temcell HS was evaluated in a phase I/II study of 25 patients with steroid-refractory grade III or IV acute GvHD. A statistically significant consistent CR for grade III or IV steroid-refractory acute GvHD was shown from 4 to 52 weeks of follow up. At 52 weeks, 48% of the patients who achieved CR were still alive. In addition, the survival of patients who had an OR, which is the sum of the CR and PR, was substantially higher than those with no OR. Responses in children were better than adults. The most common adverse events were leukocytopenia, thrombocytopenia, anemia, sepsis, hypertension, microangiopathy, liver dysfunction, and chronic GvHD (European Medicines Agency, 2020a).

The assessment efficacy and safety of Alofisel compared to placebo was considered in a pivotal Phase III clinical trial. In this study 212 perianal fistulising CD patients (107 receiving Alofisel Cx601 and 105 receiving placebo) was screened over 24, 52, and 104 weeks. Full analysis of the efficacy data showed combined remission of perianal fistulising CD and absence of collections $>$ 2 cm of the treated fistula confirmed by MRI images, at week 24. The combined remission in the active group was 49.5% (53/107) and in the placebo group were 34.5% (36/105). Presented data from week 52 showed statistically significant effects in favor of Alofisel treatment, and finally in patients who entered the 104 weeks follow-up (25 Alofisel, 15 placebo), the rate of clinical remission was 56 and 40% in the active and placebo group, respectively (Cho et al., 2015). In a phase II clinical trial fistula healing was evaluated 24 months after the administration of Cupistem in 43 patients. Cupistem seemed to be efficient considering the results of the mPP analysis 24 months after transplantation where 80.8% of the patients showed complete fistula healing. In order to assess the sustainability of the initial response, complete closure in 83.3% of the 24 patients who had evidence of complete closure at the 8^{th} week after the injection still had complete closure at year 2. The most common adverse reactions were abdominal pain, eczema and exacerbation of crohn's disease, anal inflammation, diarrhea, and fever. None of the observed adverse events were considered to be related to the product (Kim et al., 2018).

Cardiovascular diseases are the next category in the field of CTMPs. Cellgram-AMI (South Korea MFDS.2011) for AMI and Stempeucel (India DCGI.2016) for CLI due to thromboangiitis obliterans (Buerger's disease) are in this group. In a clinical study, for evaluating the safety and efficacy of Cellgram-AMI, 26 patients with successful PCI for acute ST-segment elevation anterior wall myocardial infarction were assigned to either a control group (n = 12) or Cellgram group (n = 14) and were follow-up for 4-month. Patients who received Cellgram-AMI had improved Left ventricular function as shown by a substantial progress in overall LVEF, measured by SPECT and echocardiography 3 months after the BM-MSC injection and 4 months after PCI. This improvement continued to the 12^{th} month follow up as assessed by echocardiography. However, the baseline and 4-month LVEDV and LVESV values did not significantly change. No adverse events, in-stent restenosis, or proarrhythmic effects were noted in both groups during the 4 and 12-month follow up periods (Gupta et al., 2017). A phase II study in India assessed the safety and efficacy of Stempeucel. This study placed 90 patients with CLI due to Buerger's disease into two dose groups. The rest pain and ulcer size per month were the primary outcomes. Both decreased in comparison with the SOC group. The secondary outcomes of ABPI, amount of total walking distance, and QOL activity score of units per month increased for both doses. Skin ulcer and gangrene in the 1×10^6 and 2×10^6 cells/kg groups, respectively, were the most frequently reported TEAEs. They were considered either remotely related or unrelated to Stempeucel (Oh et al., 2015).

The only related **neurological disorder** was ALS for which the product Neuronata-R (South Korea MFDS.2014) has been approved. In a phase I clinical trial to evaluate the safety of of Neuronata-R, seven patients with definite or probable ALS received two intrathecal injections of Neuronata-R and were follow-up for 12 months. The ALSFRS score, AALS score, and FVC were used to assess treatment efficacy. It was shown that none of the mentioned parameters declined rapidly and that the decrease in ALSFRS-R score during the 6 months follow up was more gradual than the observed decrease in the lead-in period, while these scores remained persistent for 6 months after the first injection of MSCs. None of the patients experienced serious adverse events during the 12-month follow-up period (Zhang et al., 2018).

Gene Therapy Medicinal Products (GTMPs)

The GTMPs have been developed for oncology, hematologic, cardiovascular, neurodegenerative, and ocular diseases.

In oncology related indications, Gendicine (CFDA.2003) is the first approved gene therapy product to treat head and neck squamous cell carcinoma, Imlygic (US FDA/EMA.2015) is approved for melanoma treatment, and Kymriah (US FDA.2017-EMA/Health Canada.2018) and Yescarta (US FDA.2017-EMA.2018) are two products used for hematologic malignancies. To evaluate the safety and efficacy of Gendicine, there are over 30 clinical study related publications. This product was assessed in a large number of clinical studies that included more than 30,000 patients. The results showed remarkable safety records along with improvements in efficacy, including tumor shrinkage and an enhanced QOL. The average response rate for CR and PR reached 90%. After the 5-year follow up, a large group of patients were still alive. The most common adverse events include fever, arthralgia, and myalgia (Andtbacka et al., 2015). In a phase III clinical trial, an intralesional injection of Imlygic was compared with subcutaneous administration of GM-CSF in

patients with advanced melanoma. The mean treatment duration was 23 in the Imlygic group and 10 weeks in the GM-CSF group. The median OS was determined to be 23.3 in the patients treated with Imlygic compared with 18.9 months in patients who received GM-CSF. The DRR and ORR were considerably higher in the Imlygic arm. Additional efficacy criteria included the median TTF and median time to response which were 8.2 and 4.1 months in Imlygic treated group versus 2.9 and 3.7 months in the GM-CSF arm. The most common reported adverse events were fatigue, chills, and pyrexia (Maude et al., 2018). In a phase II clinical trial, 75 pediatric and young adults with relapsed or refractory B-ALL received Kymriah. The ORR was 81% at 3 months of follow-up. EFS and OS rates were calculated 73 and 90% at 6 months, and 50 and 76% at 12 months, respectively. The median duration of remission and EFS were not reached, while the rate for RFS was 80 and 59% at 6 and 12 months, respectively, among patients who responded to treatment. The most common non-hematological adverse reaction in 77% of patients was cytokine release syndrome. Also, neurologic events occurred in 40% of patients (Schuster et al., 2019). In another phase II clinical trial, to evaluate the efficacy of Kymriah therapy, 93 patients with relapsed or refractory DLBCL were infused with Kymriah and the median follow up time was 14 months. The best OR was 52%, 40% of the patients had complete responses and 12% had partial responses in a median of 2 months. After 12 months of the initial response, the rate of RFS was estimated to be 65% (79% among patients with a complete response). Also, cytokine release syndrome (58%), anemia (48%), and pyrexia (35%) were the most common adverse events of any grade (Neelapu et al., 2017). In a phase II clinical trial, Yescarta was administrated to 101 patients with DLBCL and PMBCL. The ORR and the complete response rate were 82 and 54%, respectively. The OS rates at 6, 12, and 18 months were 78, 59, and 52%. CAR T cell levels in the blood peaked within 14 days and were detectable in most patients at 180 days after the Yescarta infusion. The most serious adverse reactions included cytokine release syndrome and neurologic events (Cicalese et al., 2016).

For hematologic disorders, Strimvelis (EMA.2016) is developed to treat adenosine deaminase deficiency derived severe combined immunodeficiency (ADA-SCID) and Zynteglo (EMA.2019) is approved to treat Patients up to 12 years old with beta thalassemia who require regular blood transfusions.

In a phase II clinical trial, 18 patients with ADA-SCID received Strimvelis. The OS in a median follow-up of 6.9 years was 100% and there were increased numbers of CD3 +, CD4 +, CD8 + T cells, and CD16 + CD56 + NK cells as an outcome of immune reconstitution. A slower increase in CD19 + B-cells was reported. The TREC and lymphocyte ADA enzyme activity both increased in peripheral blood lymphocytes after treatment. Venous red blood cell deoxyadenosine nucleotide levels were <100 nmol/ml. The most frequent adverse events were respiratory and gastrointestinal tract infections (Karponi and Zogas, 2019). Five completed and ongoing clinical trials are existed regarding Zynteglo, HGB-205, HGB-204, HGB-207, HGB-212, and LTF-303. During HGB-204 and HGB-205 clinical trials, it was revealed that 11 of 18 and all of 4 enrolled patients with transfusion-dependent beta (β)-thalassemia (TDT) in each study met the primary endpoint which was the elimination of RBC transfusion requirement, respectively. HGB-207, HGB-212 clinical trials and a long-term follow-up study named LTF-303 constitute the ongoing clinical trials. So far, 17 of 20 and 6 of 11 enrolled patients in HGB-207, HGB-212 clinical trials have shown transfusion independency, respectively (European Medicines Agency, 2020e). Thrombocytopenia constituted the only serious adverse reaction related to Zynteglo. Moreover, there were common adverse reactions attributed to Zynteglo containing leukopenia, neutropenia, hot flush, dyspnea, pain in extremity, non-cardiac chest pain, and one very common adverse reaction as abdominal pain (ClinicalTrials, 2020).

Some of the common side effects reported in patients receiving Zynteglo^{TM} during the clinical trials were a low count of thrombocytes, numbness in hands and feet, pain in the bone, nausea, headache, and low blood calcium levels (Deev et al., 2018).

A phase I/IIa clinical trial for Neovasculgen (Russian MOH.2011), as the single product in the **cardiovascular diseases class**, verified the safety of this product. In phase IIb/III trials that enrolled 100 patients (75 in the treatment and 25 in the control group), PWD was estimated to have increased significantly by 110% at 6 months in the treatment group. Moreover, PWD increased in the Neovasculgen treated group by 167% at 1 year and 191% at 2 years after treatment. There were no reported adverse events (Deev et al., 2015a, 2017; NOVARTIS, 2019a). Finally, the safety and efficacy of Zolgensma (US FDA.2019) one of the recent gene therapy products for **neurodegenerative related diseases** is being evaluated in an ongoing phase III STR1VE trial that enrolled 21 SMA pediatric patients with biallelic mutations in the survival motor neuron (SMN1) gene. As of the March 2019 data cutoff, remarkable survival rates, improved rapid motor function, and the capability to sit without support were among the most momentous results related to the efficacy of this product. The most common adverse events were elevated aminotransferases and vomiting (Russell et al., 2017). Luxturna (US FDA.2017/EMA.2018), the only gene product related to **ocular diseases** was assessed in a phase III clinical trial of 31 patients with RPE65-mediated inherited retinal dystrophy. The mean bilateral MLMT score was 1.8 light levels in the intervention group and 0.2 in the control group. Mean FST improved by more than two log units by day 30 in the intervention group, whereas the control group had no meaningful change. However, BCVA showed a numerical improvement among both groups. The most common adverse events included increased intraocular pressure, cataracts, retinal tears, and eye inflammation (Edmonds, 2009).

Tissue-Engineered Products (TEPs)

Skin and soft tissue related disorders, orthopedic, cardiovascular and ocular disorders are four indications for authorized TEPs.

For skin and soft tissue disorders, Apligraf (US FDA.2000), Dermagraft (US FDA.2001), Aurix (US FDA.2007), Omnigraft (US FDA.2016), Amniocin (Iran FDA.2017), and Cell-Amniosin (Iran FDA.2017) are developed to treat Chronic VLU and/or DFU. Holoderm (South Korea MFDS.2002), Epicel (US FDA.2007), and JACE (Japan PMDA.2007) are approved for

skin burns and finally, Kaloderm (South Korea MFDS.2005, for burns/2010, DFU) is approved for both DFU and deep 2^{nd} degree burns. The safety and efficacy Apligraf compared to standard therapy was assessed in 106 patients with neuropathic DFUs during 12 weeks. Kaplan–Meier curves indicated that the Apligraf treated group had a significantly faster complete wound closure in comparison with the standard treatment; after 12 weeks, 51.5% of patients who received Apligraf had achieved complete wound closure compared with 26.3% in the control group. The reported related adverse events consist of suspected wound local infection, cellulitis, and exudate (Marston et al., 2003). A clinical study of 314 patients with chronic DFUs evaluated the safety and efficacy of Dermagraft. The results showed a trend toward a shorter time for complete wound healing using Dermagraft. In addition, 30.0% of Dermagraft patients achieved complete wound closure compared with 18.3% of control patients after 12 weeks. No specific related adverse events were reported and the incidence of ulcer infection, cellulitis, or osteomyelitis was significantly lower in the Dermagraft treated patients versus the control patients (Driver et al., 2006). A clinical study of Aurix for 72 patients who suffered from non-healing DFU showed that 91% of long-term non-healing wounds responded to treatment with a 64% reduction in volume during 15 days or less. They researchers observed that 81.3% of Aurix treated wounds, which were less than 7 cm^2, healed completely within 6.2 weeks in comparison with saline gel. In addition, the Kaplan–Meier time-to-healing was significantly better in the Aurix group. No product-related serious adverse events were reported (Driver et al., 2015). The results of the study that evaluated the safety and efficacy of Omnigraft in comparison to standard wound care in 307 patients with neuropathic DFU demonstrated improved life quality, approximately 5 weeks faster wound closure, and 19% increased healing rate in patients treated with Omnigraft (Tego Science, 2019b). Allergic reaction was the most concern about the safety of Omnigraft. We were unable to locate any data that pertained to the efficacy of Holoderm; however, according to the product brochure, abnormal cellular responses such as dyskeratosis or parakeratosis may occur following the use of Holoderm-derived epidermis (Food and Drug Administration, 2019i). The survival rate of Epicel was assessed in three studies. In the first study, the OS rate was 86.6% for overall patients and 89.3% for pediatric patients at 3 months after the initial implantation. In the second study, an OS rate of 88.3% in pediatric patients compared with 81.3% in the total population was reported. In the third study, the treatment group had a 90% survival rate compared to 37.5% for the control group. The most common adverse reactions were infections, graft shear, blisters, drainage, sepsis, graft detachment, and renal failure (Matsumura et al., 2016). The CEA JACE safety and efficacy was evaluated through a 6-year multicenter clinical trial for treatment of burns that covered more than 30% of the TBSA. The mean CEA take rate at 4 weeks post-engraftment was 66%, while the use of combined treatments such as artificial dermis or a wide split-thickness auto or a patch graft significantly elevated this rate. The most common adverse events were skin ulcers or auto graft detachment; however, death and sepsis, which were reported as serious adverse events during later periods, did not appear to be related to CEA (Tego Science, 2019c). Treatment of DFU with Kaloderm has shown that 12 weeks after treatment, all patients in the keratinocyte-treated group and 69% of patients in the control group experienced complete wound healing. No adverse events were reported in relation with the wound dressings. In terms of skin burns, the product packaging insert for Kaloderm stated that, no adverse reaction has been reported other than a possible occasional infection at the site, dermatitis, exudate formation, weak edema, hypersensitivity, and pain. In addition, Kaloderm can promote the re-epithelialization of deep abdominal cavity burns (McGuire et al., 2011; You et al., 2012).

Gintuit (US FDA.2012) is approved for surgically created **vascular wound** in the treatment of mucogingival conditions, the results of a clinical trial with 96 patients during 6 months follow up showed that the LCC mediated $\geq$ 2 mm regenerated keratinized gingiva in 81 of 85 patients and $\geq$ 1 mm in all patients, while the color and texture was similar to the adjacent tissue. The most common adverse events included sinusitis, nasopharyngitis, respiratory tract infections, aphthous stomatitis, and the local effects of oral surgery (Tohyama et al., 2009).

In orthopedics disorders, JACC (Japan PMDA.2012), MACI (US FDA.2016/EMA.2013) and Spherox (EMA.2017), are used to treat cartilage defects. JACC was studied through a multi-center clinical trial for transplanting autologous cultured chondrocytes in 27 patients with cartilage lesions who were evaluated at 3, 6, 12, and 24 months after the implantation surgery. Elimination of locked knee together with decreased pain were observed following the transplantation. Also, substantial progression of the original knee-function scale and the clinical scores based on the Lysholm Knee Scoring Scale, and observation of the natural appearance in 92% of patients as indicated by arthroscopic assessment showed restorative promotion of articular cartilage in the knees (Saris et al., 2014). There were few adverse events, except for two cases of graft detachment. The efficiency of a MACI implant has been assessed and its superiority versus microfracture treatment was evaluated in the SUMMIT clinical trial of 144 patients. The results at week 104 revealed significant improvement with MACI in the three KOOS subscales of pain, SRA, and ADL when compared with the microfracture group. Serious adverse reactions reported for MACI were arthralgia, cartilage injury, meniscus injury, treatment failure, and osteoarthritis (Armoiry et al., 2018). In a phase III clinical trial, Spherox was compared with the microfracture treatment in 102 patients. The mean overall KOOS in patients treated with Spherox increased from 56.6 $\pm$ 15.4 at baseline to 78.7 $\pm$ 18.6 after 12 months, with a further increase to 81.5 $\pm$ 17.3 after 24 months. However, the MOCART scores did not change significantly among the two groups (Becher et al., 2017). In a phase II clinical trial, 73 patients with cartilage defects received transplants of three different doses (low, medium, and high) and were subsequently followed until 36 months. Severe adverse events included meniscus lesion with the low dose; syncope and joint effusion with the medium dose; and arthralgia, joint effusion, and chondropathy with the high dose (Nordmeyer et al., 2018).

For cardiovascular diseases, CardioCel (Singapore HAS.2014) is approved to treat ASD and VSD and Heartsheet (Japan PMDA.2015) is developed for severe heart failure

due to ischemic heart disease. In a study, CardioCel patches were applied on 40 patients for 2 years. While the probability of stopping the development of the combined end point that consisted of death, additional surgery, and a moderate degree of aortic valve dysfunction after AVR was 92 ± 5% at 12 months, this probability reduced to 28 ± 9% at 36 months after surgery. In this study, 23% of patients experienced an event during follow up, which included death and additional surgery due to stenosis, aortic valve insufficiency, and aortic valve endocarditis (Imamura et al., 2016). Heartsheet was evaluated in a phase II multi-center clinical trial of autologous skeletal myoblast sheet transplantation in seven patients with advanced heart failure compared with a control group receiving CRT in a 1 year follow upLVRR and heart failure symptoms improved in the treatment group and a lower rate of cardiac death during 800 days of follow up was observed. Common adverse events experienced by all of the patients during the study included arrhythmia, wound complications, hypokalemia, and post-operative fever (Rama et al., 2010). **For ocular disorder**, Amniodisk (Iran FDA.2020) is approved for Corneal ulcer, conjunctival and epithelial damage and Holoclar (EMA.2015) is approved for severe limbal stem cell deficiency. In a retrospective case series study, 106 patients with corneal damage received Holoclar. As the human limbal stem cells are recognized through p63 transcription factor expression, the clinical outcome assessment was conducted according to the percentage of p63-bright holoclone-forming stem cells in culture. If this percentage was greater than 3%, then the transplantation was considered successful. The success, partial success, and failure rates in the transplantation process were 76.6, 13.1, and 10.3% of the treated eyes, respectively (European Medicines Agency, 2015). The most common adverse reactions were blepharitis and corneal epithelium defects (Market Research, 2020).

MARKET SIZE OF ADVANCED THERAPY MEDICINAL PRODUCTS (ATMPs)

Price and market size are two main issues that should be emphasized for guarantee of product survival in the market. We have attempted to provide information of the market size of most products introduced in this paper by preferably accessing the appropriate company's available data on the Internet. All product prices are presented in USD to be comparable. The information regarding the market size of each mentioned product was collected by using company's IR book, website, and market research websites. The disease markets were considered based on the related CAGRs, following with the data respecting each product.

Thus far, the area of diseases that is targeted by ATMPs are divided into hematological disorders, skin and soft tissue disorders, orthopedic disorders, immunological disorders, cardiovascular diseases, neurodegenerative diseases, ocular diseases, and cancers. The market size of each mentioned diseases can be classified based on the industrial analysis and CAGR. According to Mordorintelligence, the largest predicted CAGR from 2020 till 2025 belongs to dermatology (Cancer Therapy Market, 2020) therapeutics market (8.95%) and cancers (Autoimmune Disease Diagnostics Market, 2020), autoimmune disorders (Orthopedic Devices Market, 2020), orthopedic disorders (Cardiovascular Devices Market, 2020), cardiovascular diseases (CellTech, 2019) and the hematology (Hematology Market, 2020) field come in the next places with the CAGRs of 8.37, 8.3, 7.2, 6.2, and 5%, respectively. Also, predicted CAGRs for markets of soft tissue (Soft Tissue Repair Market, 2020) repair, neurodegenerative diseases (Neurodegenerative Disease Market, 2020), and ophthalmic disorders (Ophthalmic Drugs Market, 2020) from 2019 till 2024 are 5.8, 5.5, and 4.6%. Therefore, beginning with dermatology therapeutics, Fibrocell Science has announced that the sale of Azficel-T increased approximately $0.3 million, or 63.4%, for the year ending December 31, 2016 compared to 2015 (Fibrocell Science Inc., 2020) Apligraf and Dermagraft have experienced strong sales growth, with more than one million units of each one, shipped for patient use until April 2016 (Organogenesis Inc., 2019a) along with approximately one million patient units for Apligraf until September 2017 (Organogenesis Inc., 2019b). Nuo Therapeutics estimated a turn in the Aurix sales from $0.495 million in 2014, to peak sales over $50 million (Napodano, 2015). Based on Vericel investor reports, Epicel has been administered to approximately 100 patients in the U.S. annually, and it could achieve $23.1 million net revenue by December 31, 2018 (Vericel Corporation, 2019). According to the company's IR book, the operating margin of Tego Science Company for Kaloderm and Holoderm products was $10.9 million in 2006, which reached $23.4 million in 2013. Sales of Kaloderm were lower in 2006; however, by 2013, sales of Kaloderm were significantly higher than Holoderm (Tego Science, 2019d). As stated by Biosolution Company's IR book, 15% of the market in 2008 in South Korea belonged to KeraHeal in comparison with competitive products. This amount rose to more than 70% in 2012. Regarding the market size, the number of patients in 2017 was approximately 410 with the sales percent of nearly $9.5 million. The number of patients is expected to reach approximately 450 in 2021 with an estimated sales of $42.6 million (Bio Solution Co Ltd., 2019). In 2017, the first year that KeraHeal-Allo was released, it occupied 20% of the market. It was estimated that this product would experience rapid growth in sales during 2019. Regarding market size, in 2017 there were approximately 203,000 persons with a sale of $7.5 million. The numbers of patients are expected to reach 217,000 persons in 2021 with an estimated sales of $56 million (Bio Solution Co Ltd., 2019). The J-TEC company in 2009 has estimated that the market size of JACE would be approximately 100 to 300 million US dollars only in Japan (Joo-sung, 2016). In the cancer area, the Green Cross Cell company IR book estimated that the market potential for Immuncell-LC for only the US will be about $6 billion, with the targeted market consisting of liver cancer, brain tumors, and pancreatic cancer (Green Cross Cell, 2019). Also, several approved GTMP therapeutics, Kymriah, Yescarta, Imlygic, Zalmoxis, Gendicine, and Oncorine are indicated for oncology related diseases. Kymriah grew strongly in Europe and US in the first quarter of 2020, with a

net sale of $93 million (Globenewswire, 2020). Also, Yescarta's sale during the first quarter of 2019 was $96 million compared to $40 million for the same period in 2018 (Business Wire, 2020). Amgen, the manufacturer of Imlygic, has not disclosed Imlygic sales in its quarterly results presentations. However, EvaluatePharma reported consensus analyst forecasts of $45 million and $250 million for worldwide Imlygic sales in 2016 and 2022, respectively (Imlygic, 2017). Financial reports in 2012 revealed that over 6000 patients diagnosed with various types of solid cancers in China received Gendicin, which had a CAGR from 2004 to 2011 of 68.3% (Kudrin, 2018). Sales of Gendicin were $3.6 million in 2007 and $16 million in 2008. However, the sales of Oncorine were unsatisfactory in China (<$1.2) due to its high price in 2009 (Kudrin, 2018). Products indicted for immunological disorders show that Alofisel is forecasted by Evaluate Pharma that the worldwide consensus sales will reach $529 million in 2024 (Mesoblast Limited, 2020). In terms of the Cupistem market in South Korea, the number of CD patients increased from approximately 15,000 in 2010 to almost 20,000 in 2014, while an increased prevalence has also been observed (Green Cross Cell, 2019). Sales of Temcell HS were $14.3 million in FY 2017, which showed a 124.3% increase compared to previous fiscal years (HIYAKU, 2019). For orthopedic disorders, in the beginning of 2019, Cartistem sold $11.1 million and the revenues for its sale accounted for 34.4% of the total sales in the first 6 months of 2019 (Korea Biomedical, 2020). Chondron sales for cartilage cell therapy in 2012 were approximately $13.8 million and increased to approximately $17.8 million in 2014 (Mksvc, 2019). In addition, Cartigrow has been used in 140,000 knee replacement cases annually (Das, 2018). According to Orthocel, Chondrocytes-T-Ortho-ACI is currently marketed in Australia, New Zealand, Hong Kong, Singapore, the United States, Europe, and China. Total revenues for its sale reached $739,100 during the 2018 fiscal year (FY). Moreover, the revenue forecast for Chondrocytes-T-Ortho-ACI until the FY 2028 is an estimated $340,203,044 (Hice, 2018). According to a 2018 report published in the standard business website, Ossgrow is used in 108,000 cases of total hip replacement in India each year (Das, 2018). TMACI, Spherox, and JACC are other approved therapeutics for orthopedic disorders. Vericel Company announced that MACI generated net revenues of approximately $67.7 million in the year ending December 31, 2018 (Vericel Corporation, 2019). CO.DON AG, launched Spherox for distribution in European countries in September 2017, starting from Germany. In Germany, the market volume addressed by CO.DON AG, approximated 20,000 annual treatments. With a population of 82.2 million, this meant that in Germany about 0.025% of the population could receive treatment with Spherox per year. Expressed in a conservative perspective, the potential for more than 115,000 knee-joint treatments per year was calculated in Europe. Marketing approval of Spherox was received in May 2017 from EMA (CODON, 2019). According to the J-TEC company's IR book, the sales of JACC between FY 2011–2012 were reported to be $10.8 million compared to $371280 at its launch in 2003 (PMDA, 2011). In the field of cardiovascular diseases, according to the FCB Pharmicell Company IR book for Cellgram-AMI, in the South Korea the number of patients with AMI in 2015 was 87,984. The total amount of medical care costs for AMI in the same year was $1749 million (Pharmicell Ltd., 2020). Assessment of Neovasculogen, a product for cardiovascular diseases in Russia, indicated that 5 million people have been diagnosed with PAD. Also, the number of patients with CLI annually amounts up to 145,000, of which around 25% die (Deev et al., 2015b; NOVARTIS, 2019a). Also, the market size for Stempeucel is approximately $1.5 billion worldwide (Lane, 2016). Moreover, the annual reports from Admedus indicated that they achieved revenues of $6.9M million by selling their ADAPT®, bio-scaffold tissue technology, realted products (including CardioCel® Neo, VascuCel®) in North America, Europe, the MENA region, Asia, Australia, and New Zealand (Cardiocel, 2017). Products based on human cord blood derived HPCs, cover the market of hematologic disorders. Cord blood, as stem cell sources for patients without a donor, has its own market with more than 2000 cord blood hematopoietic stem cell transplants performed each year (WHO, 2013). The other approved product in this field is Zalmoxis. In 2018, Molmed Company projected peak sales of around 100 $ million to be achieved by 2026 for Zalmoxis (Spark Therapeutics Inc., 2019). However, very recently MolMed decided to the withdraw the drug's conditional marketing authorization (CMA) after Phase III clinical trial results showed that the drug offered no benefit on DFS (Sharma, 2019) and stopped investing in the product. Revenues for Zalmoxis in 2018 is estimated at approximately $4.6 million (MolMed, 2018). In the neurological disorders, by taking into account the production of Nuronata-r in January 2015 and based on sales for June 2015 that were approximately $1.6 million, 2016 sales were estimated to be approximately $4.8 million with a rapid sales growth compared to other stem cell treatments. Also, the domestic patient sales in 2018 were expected to reach near $16.6 million which, together with overseas patients, the final number would be approximately $37.4 million (Commercialized Stem Cell Corestem Inc., 2020). Finally, Spark Therapeutics reported that in the year ended December 31, 2018, they recognized $64.7 million in total revenue, of which $27.0 million was net product sales of LUXTURNA (Spark Therapeutics Inc., 2019).

Overall, also it is worthy to note that according to the Seoane-Vazquez et al. (2019), the treatment cost of Kymriah, sipuleucel-T, Imlygic, and autologous cultured chondrocytes was higher in the United States than in Europe.

CONCLUSION AND FUTURE REMARKS

Cellular therapies have attracted tremendous attention from numerous researchers, clinicians and from industry, specifically for incurable diseases. As it can be concluded from **Tables 1–3**, most of the approved products in the recent years belong to the CTMPs, although a decrease in the total amount of approved products occurred in 2013 and 2014, which may be occurred due to financial and regulatory restriction issues. For the next years, there was an increased trend with five products approved in 2017 (**Figure 3A**). The year 2007 witnessed an increase in the number

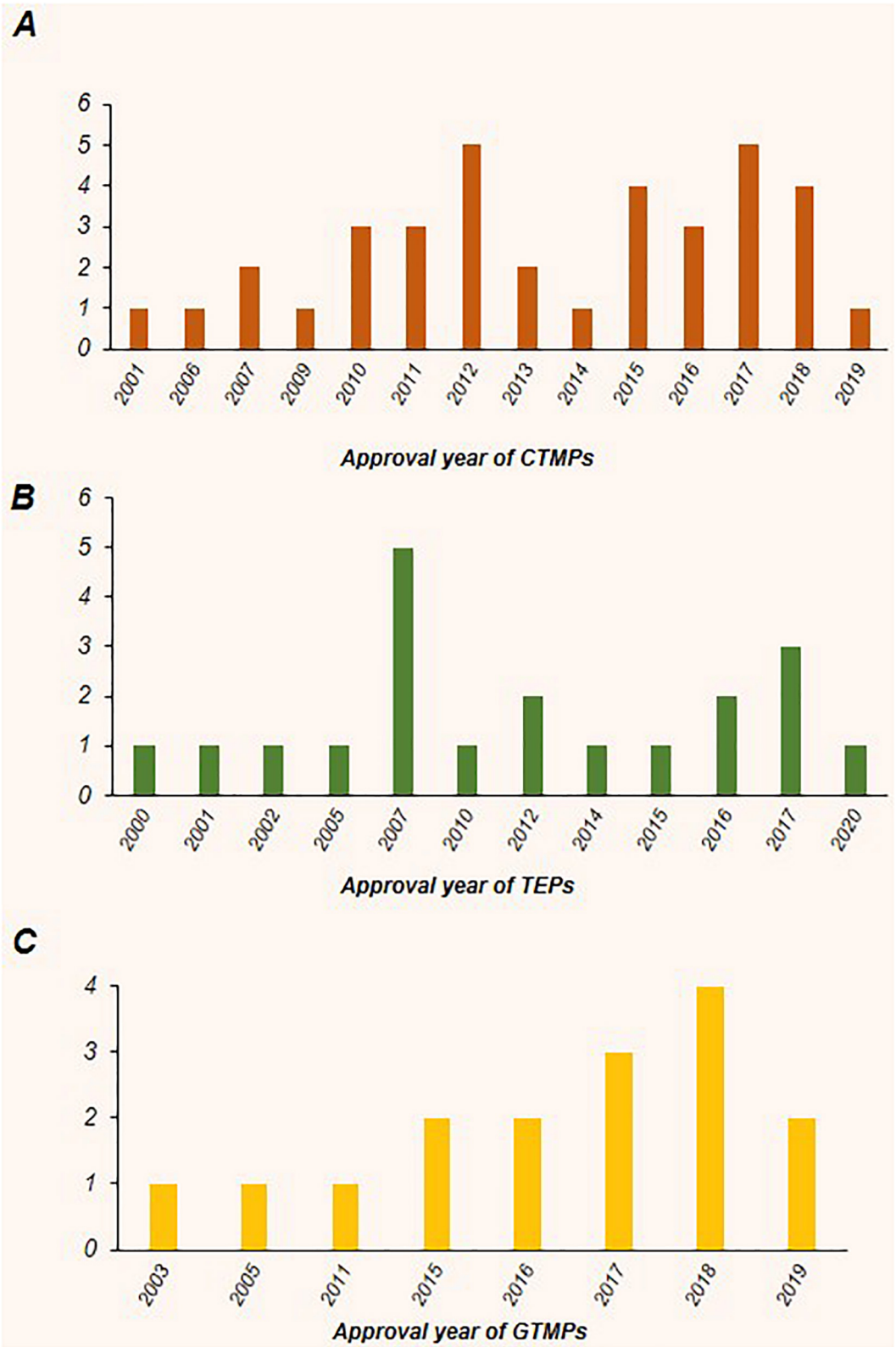

FIGURE 3 | The annual trend of approval for CTMPs, GTMPs, and TEPs worldwide. Most of the products were recently approved. **(A)** In terms of CTMPs, despite a decrease in the number of approved products in 2013 and 2014, a second increased trend can be observed with five products approved in 2017. **(B)** For TEPs, the year 2007 with five approved products showed an increase in the total trend; however, there was a subsequent decrease in the following years. **(C)** There is a noticeable growth trend with respect to gene therapy medicinal products (GTMPs).

of approved TEP products; however, in the next years this amount decreased and this field has not experienced any evident growth trend, which can be seen in two other products (**Figure 3B**). GTMPs have faced an obvious progressive trend regarding the number of approved products and this is clearly apparent from the growth in the trend of these products, which may be due to entrance of big pharma in this field to develop a treatment for refractory conditions or rare diseases which do not have an effective pharmaceutical drug. The latest approved product, Zynteglo, is placed in this class (**Figure 3C**). It is expected that with the current advances in genetic engineering, products in this field would experience significant growth in following years. The origin of these products is an important subject since the use of autologous, allogeneic or xenogeneic cell sources would have a substantial effect on the financial policies of the companies that produce the regenerative medicine product and the related regulatory agencies. The allogeneic based products have a preferred advantage regarding their capability to be adapted for scale up strategies and also catching large market through massive export. However, as mentioned before, most members of CTMPs and GTMPs have an autologous source, due to the medicinal constraints in regards with immune rejection and the extensive required safety tests for allogeneic cells, while the cells used in tissue engineering based products with local indications, have the higher percentage for allogeneic rather than autologous products and have a greater market and higher sales (Kim et al., 2019). Altogether, it seems that with release of guidelines in different regulatory agencies the regulatory problem could be overcome in next years and trend of allogeneic products would raise noticeably. Market size and price are two main determinants of a product success or failure. Glybera with a both low market size and high price is one example of how these two factors can affect the survival of a certain ATMP in the market. Generally, the average prices for GTMPs are higher in comparison to CTMPs and TEPs. ATMPs related treatments despite their great therapeutic potential are very costly and there are challenges regarding their reimbursement issues. The high price of ATMPs is the result of several factors; high manufacturing costs, complex quality control tests, expensive raw materials, requirement of cold chains for transfer, intellectual property rules, small target populations (in some of cases) and strict regulatory inspections are among the most important reasons.

Due to the significant therapeutic potential of ATMPs for serious conditions in comparison with conventional drugs, as one of the major growth drivers for market, their market share is anticipated to be increasing. Respecting to the new slow shift toward personalized medicine while ATMPs are one of the high potential players in this regard, increasing the value of ATMPs global market size is highly expected. This idea is strongly supported by entrance of big pharma to this field in recent years. Moreover, the market interest has largely affected the number of developed products. This can be seen, for instance, in the percent of approved products for skin related application, as they are placed in the first position of TEPs (60%) and also CTMPs (23.5%).

Overall, the criteria regarding the efficacy of each ATMPs, shows optimistic results and the total numbers of adverse events are not dramatic. Cellular therapy is expected to be a promising area used for treatment of a noticeable quantity of incurable disorders. However, limiting factors regarding the development and uses of ATMPs should be still overcome, including the demand for high-technology systems for cell manufacturing and delivery (reducing production times and costs), vectors for gene modification availability and production, establishment of assays to validate products potency to ultimately improve treatment efficacy while avoiding adverse events and, last but not least the costs of these products and their reimbursability. On the other hand, since regenerative medicine strategies might become a solution for treatment of still incurable diseases and due to massive public and private investments, it is rational to claim that this field has the potential to overcome many of the mentioned limitations in a near future to reach a revolutionary phase in both the pharmaceutical industry and in the clinics.

AUTHOR CONTRIBUTIONS

HB, ST, EH-S, and RR conceived the manuscript concept, wrote and final edited the manuscript. All authors participated in the literature search, wrote the manuscript parts, prepared the figures and tables, and read and approved the final manuscript.

FUNDING

We gratefully appreciate supportive colleagues in Royan Advanced Therapy Medicinal Product Technology Development Center (ATMP-TDC) and Dr. Massoud Vosough, who helped us in this project. This study was financially supported by the grant from the "Italian Ministry of Research and University – Dipartimenti Eccellenti 2017 (MD)" and "Royan Institute and Ministry of Health and Medical Education (MoH, no. 700/147)".

REFERENCES

Andtbacka, R. H. I., Kaufman, H. L., Collichio, F., Amatruda, T., Senzer, N., Chesney, J., et al. (2015). Talimogene laherparepvec improves durable response rate in patients with advanced melanoma. *J. Clin. Oncol.* 33, 2780–2788.

Anteris Technologies Limited (2019). *CardioCel Admedus*. Available online at: https://admedus.com/solutions/adapt/cardiocel/ (accessed May 10, 2019).

Anterogen Co. (2019). 안트로젠. Available online at: http://anterogen.com/main/en/sub02_01.html?type= (accessed Jun 23, 2019).

Anterogen Co. (2020). 안트로젠. Available online at: http://anterogen.com/main/en/sub02_01_02.html?type=2 (accessed May 15, 2020).

Apac Biotech (2019). *Approved Immunotherapy Treatment Centre India*. Available online at: http://apacbiotech.com/ (accessed May 9, 2019).

Armoiry, X., Cummins, E., Connock, M., Metcalfe, A., Royle, P., and Johnston, R. (2018). *Autologous Chondrocyte Implantation with Chondrosphere for Treating Articular Cartilage Defects in the Knee: An Evidence Review Group Perspective of a NICE Single Technology Appraisal. Pharmacoeconomics*. Available online at: http://www.ncbi.nlm.nih.gov/pubmed/30426462 (accessed May 10, 2019).

Autoimmune Disease Diagnostics Market (2020). *Growth, Trends, and Forecasts*. Available online at: https://www.mordorintelligence.com/industry-reports/global-autoimmune-disease-diagnostics-market (accessed May 24, 2020).

Bapsy, P. P., Sharan, B., Kumar, C., Das, R. P., Rangarajan, B., Jain, M., et al. (2014). Open-label, multi-center, non-randomized, single-arm study to evaluate the safety and efficacy of dendritic cell immunotherapy in patients with refractory solid malignancies, on supportive care. *Cytotherapy* 16, 234–244. doi: 10.1016/j.jcyt.2013.11.013

Bauer, S., Khan, R. J. K., Ebert, J. R., Robertson, W. B., Breidahl, W., Ackland, T. R., et al. (2012). Knee joint preservation with combined neutralising High tibial osteotomy (HTO) and matrix-induced autologous chondrocyte implantation (MACI) in younger patients with medial knee osteoarthritis: a case series with prospective clinical and MRI follow-up over 5years. *Knee* 19, 431–439. doi: 10.1016/j.knee.2011.06.005

Becher, C., Laute, V., Fickert, S., Zinser, W., Niemeyer, P., John, T., et al. (2017). Safety of three different product doses in autologous chondrocyte implantation: results of a prospective, randomised, controlled trial. *J. Orthop Surg. Res.* 12:71.

Berkrot, B. (2018). *Spark's Price for Luxturna Blindness Gene Therapy Too High: ICER - Reuters. Reuters Helath News*. Available online at: https://www.reuters.com/article/us-spark-icer/sparks-price-for-luxturna-blindness-gene-therapy-too-high-icer-idUSKBN1F1298 (accessed May 10, 2019).

Bio Solution Co Ltd. (2019). *Improve the Quality of Your Life by Cell-Based Biotechnology BIOSOLUTION. Investor Relations 2*. Available online at: https://file.irgo.co.kr/data/BOARD/ATTACH_PDF/5dc0bf4035c46328f53a815b9d3d8bf7.pdf (accessed May 11, 2019).

Biomedic (2019). *S-Biomedic*. Available online at: https://www.sbiomedic.com/ (accessed Jun 23,2019).

S-Biomedics Ltd. (2012). 제정일자. *rosmir*. Available online at: http://sthepharm.com/download/cure_skin_kr.pdf (accessed June 29, 2012).

Biosolution Ltd. (2019a). (*Cell therapy Products*) *Biosolution Co., Ltd. View|Biological Products | Minisry of Food and Drug Safety*. Available online at: https://www.mfds.go.kr/eng/brd/m_30/view.do?seq=71374 (accessed Jun 23, 2019).

Biosolution Ltd. (2019b). 바이오솔루션. Available online at: http://www.biosolutions.co.kr/eng/product/medicine1.asp (accessed Jun 23, 2019).

Biosolution Ltd. (2019c). (*Cell therapy products*) *Biosolution Co., Ltd. View|Biological Products | Minisry of Food and Drug Safety*. Available online at: http://www.mfds.go.kr/eng/brd/m_30/view.do?seq=71374 (accessed May 9, 2019).

Bloomberg Businessweek (2018). *Michelle Fay Cortez. This Implant Helps Heal Knees With a Patient's Own Cartilage - Bloomberg. Bloomberg Businessweek*. Available online at: https://www.bloomberg.com/news/articles/2018-09-22/this-implant-helps-heal-knees-with-a-patient-s-own-cartilage (accessed May 10, 2019).

Business Wire (2020). *Gilead Sciences Announces First Quarter 2019 Financial Results | Business Wire*. Available online at: https://www.businesswire.com/news/home/20190502005790/en/Gilead-Sciences-Announces-Quarter-2019-Financial-Results (accessed May 24, 2020).

Cade Hildreth (2018). *Pricing of Approved Cell Therapy Products. Bioinformant*. Available online at: https://bioinformant.com/price-of-cell-therapy-pro. Available online at: https://bioinformant.com/price-of-cell-therapy-pro (accessed March 22, 2018).

Cancer Therapy Market (2020). *Growth, Trends, and Forecast (2020 - 2025)*. Available online at: https://www.mordorintelligence.com/industry-reports/cancer-therapy-market (accessed May 24, 2020).

Cardiocel (2017). *Admedus Annual Report 2*. Available online at: https://cdn.admedus.com/2018/08/10114914/2016-2017-Annual-Report.pdf (accessed August 8, 2017).

Cardiovascular Devices Market (2020). *Growth, Trends, and Forecasts (2020 - 2025)*. Available online at: https://www.mordorintelligence.com/industry-reports/global-cardiovascular-devices-market-industry (accessed May 24, 2020).

CellTech (2019). *Products - CellTech*. Available online at: http://en.celltech.ir/products/ (accessed May 9, 2019).

Cheng, B., Lu, S., and Fu, X. (2016). Regenerative medicine in China: main progress in different fields. *Mil. Med. Res.* 3:24.

Cho, Y. B., Park, K. J., Yoon, S. N., Song, K. H., Kim, D. S., and Jung, S. H. (2015). Long-term results of adipose-derived stem cell therapy for the treatment of crohn's fistula. *Stem Cells Transl. Med.* 4, 532–537. doi: 10.5966/sctm.2014-0199

Choi, M., Han, E., Lee, S., Kim, T., and Shin, W. (2015). *Regulatory Oversight of Gene Therapy and Cell Therapy Products in Korea. Advances in Experimental Medicine and Biology*. New York, NY: Springer, 163.

Choi, N.-Y., Kim, B.-W., Yeo, W.-J., Kim, H.-B., Suh, D.-S., Kim, J.-S., et al. (2010). Gel-type autologous chondrocyte (ChondronTM) implantation for treatment of articular cartilage defects of the knee. *BMC Musculoskelet Disord* 11:103.

Cicalese, M. P., Ferrua, F., Castagnaro, L., Pajno, R., Barzaghi, F., Giannelli, S., et al. (2016). Update on the safety and efficacy of retroviral gene therapy for immunodeficiency due to adenosine deaminase deficiency. *Blood* 128, 45–54.

Clarke, T., and Berkrot, B. (2019). *FOOD AND DRUG ADMINISTRATION Approves Gilead Cancer Gene therapy; Price set at $373,000 - Reuters. Reuters Helath News*. Available online at: https://www.reuters.com/article/us-gilead-sciences-Food and Drug Administration/Food and Drug Administration-approves-gilead-cancer-gene-therapy-price-set-at-373000-idUSKBN1CN35H/ (accessed May 10, 2019).

ClinicalTrials (2020). *Zynteglo for Transfusion-Dependent Beta-Thalassemia, Europe*. Available online at: https://www.clinicaltrialsarena.com/projects/zynteglo-beta-thalassemia/ (accessed May 27, 2020).

CODON (2019). *Financial Reports. Interim Consolidated Financial Statements 1 January to 30 June 2*. Available online at: https://www.codon.de/en/investoren/financial-reports (accessed May 15, 2020).

Commercialized Stem Cell Corestem Inc. (2020). Available online at: https://dokumen.tips/documents/the-commercialized-stem-cell-corestem-inc-ir-bookpdf-bbc-research.html (accessed May 13, 2020).

Corestem Inc. (2019). (*Cell Therapy Products*) *Corestem, Inc. View|Biological Products | Minisry of Food and Drug Safety*. Available online at: http://www.mfds.go.kr/eng/brd/m_30/view.do?seq=70956 (accessed May 9, 2019).

Cuende, N., Rasko, J. E. J., Koh, M. B. C., Dominici, M., and Ikonomou, L. (2018). Cell, tissue and gene products with marketing authorization in 2018 worldwide. *Cytotherapy* 20, 1401–1401. doi: 10.1016/j.jcyt.2018.09.010

Das, S. (2018). *Mumbai's Regrow Biosciences Develops Cell Therapy for Bone Joint Disorders | Business Standard News*. Available online at: https://www.business-standard.com/article/companies/mumbai-s-regrow-biosciences-develops-cell-therapy-for-bone-joint-disorders-118091000783_1.html (accessed May 11, 2019).

Deev, R. V., Bozo, I. Y., Mzhavanadze, N. D., Voronov, D. A., Gavrilenko, A. V., Chervyakov, Y. V., et al. (2015a). pCMV- vegf165 intramuscular gene transfer is an effective method of treatment for patients with chronic lower limb ischemia. *J. Cardiovasc Pharmacol. Ther.* 20, 473–482. doi: 10.1177/1074248415574336

Deev, R. V., Drobyshev, A. Y., Bozo, I. Y., and Isaev, A. A. (2015b). Ordinary and activated bone grafts: applied classification and the main features. *Biomed. Res. Int.* 2015, 1–19. doi: 10.1155/2015/365050

Deev, R., Plaksa, I., Bozo, I., and Isaev, A. (2017). Results of an international postmarketing surveillance study of pl-VEGF165 safety and efficacy in 210 patients with peripheral arterial disease. *Am. J. Cardiovasc. Drugs* 17, 235–242. doi: 10.1007/s40256-016-0210-3

Deev, R., Plaksa, I., Bozo, I., Mzhavanadze, N., Suchkov, I., Chervyakov, Y., et al. (2018). Results of 5-year follow-up study in patients with peripheral artery disease treated with PL-VEGF165 for intermittent claudication. *Ther. Adv. Cardiovasc. Dis.* 12, 237–246. doi: 10.1177/1753944718786926

Detela, G., and Lodge, A. (2019). EU regulatory pathways for ATMPs: standard, accelerated and adaptive pathways to marketing authorisation. *Mol. Ther. Methods Clin. Dev.* 13, 205–232. doi: 10.1016/j.omtm.2019.01.010

Doo-hyun, A. (2018). *Cell Therapy Rosmir to Target Anti-Wrinkle Market - Korea Biomedical Review. Koreabiomed*. Available online at: http://www.koreabiomed.com/news/articleView.html?idxno=2617 (accessed May 15, 2020).

Doo-hyun, N. (2019). *Will Korea's First Stem Cell Therapy Pass Reexamination? - Korea Biomedical Review. Koreabiomed*. Available online at: http://www.koreabiomed.com/news/articleView.html?idxno=585 (accessed Jun 23, 2019).

Drew, S. W. (2015). *JACE*. Available online at: https://haseloff.plantsci.cam.ac.uk/resources/SynBio_reports/BEM-FinalReport-Web.pdf (accessed March 6, 2015).

Driver, V. R., Hanft, J., Fylling, C. P., and Beriou, J. M. (2006). Autologel diabetic foot ulcer study group. a prospective, randomized, controlled trial of autologous

platelet-rich plasma gel for the treatment of diabetic foot ulcers. *Ostomy Wound Manage* 52, 68–70.

Driver, V. R., Lavery, L. A., Reyzelman, A. M., Dutra, T. G., Dove, C. R., Kotsis, S. V., et al. (2015). A clinical trial of integra template for diabetic foot ulcer treatment. *Wound Repair Regen* 23, 891–900. doi: 10.1111/wrr.12357

Edmonds, M. (2009). European and australian apligraf diabetic foot ulcer study group. apligraf in the treatment of neuropathic diabetic foot ulcers. *Int. J. Low Extrem Wounds* 8, 11–18. doi: 10.1177/1534734609331597

Elsanhoury, A., Sanzenbacher, R., Reinke, P., and Abou-El-Enein, M. (2017). *Accelerating Patients' Access to Advanced Therapies in the EU, Molecular Therapy - Methods and Clinical Development*, Cambridge, MA: Cell Press, 15–19.

EMC Inc. (2020). *Holoclar - Summary of Product Characteristics* (*SmPC*) - (*emc*). Available online at: https://www.medicines.org.uk/emc/product/8033/smpc (accessed May 11, 2020).

EU (2020). *Study on the Regulation of Advanced Therapies in Selected Jurisdictions - Publications Office of the EU*. Available online at: https://op.europa.eu/en/publication-detail/-/publication/78af6082-bc4a-11e6-a237-01aa75ed71a1 (accessed May 24, 2020).

European Medicines Agency (2015). *Holoclar*. Available online at: https://www.ema.europa.eu/en/medicines/human/EPAR/holoclar (accessed March 2, 2015).

European Medicines Agency (2019). *kymriah2*. Available online at: https://www.ema.europa.eu/en/medicines/human/EPAR/kymriah#overview-section (accessed June 15, 2019).

European Medicines Agency (2020a). *Alofisel | European Medicines Agency*. Available online at: https://www.ema.europa.eu/en/medicines/human/EPAR/alofisel (accessed May 11, 2020).

European Medicines Agency (2020b). *Glybera | European Medicines Agency*. Available from: https://www.ema.europa.eu/en/medicines/human/EPAR/glybera. [Accessed on 2020 Nov 19].

European Medicines Agency (2020c). *Holoclar | European Medicines Agency*. Available online at: https://www.ema.europa.eu/en/medicines/human/EPAR/holoclar (accessed May 11, 2020).

European Medicines Agency (2020d). *Spherox*. Available online at: https://www.ema.europa.eu/en/medicines/human/EPAR/spherox 31 (January 6, 2020).

European Medicines Agency. (2020e). *Zynteglo | European Medicines Agency*. Available from: https://www.ema.europa.eu/en/medicines/human/EPAR/zynteglo. [accessed on Nov 19, 2020].

FAQ (2019). *Patient FAQ'S FOR CARTIGROW*. Available online at: https://www.regrow.in/pdf/FAQ-FOR-CARTIGROW.PDF (accessed May 9, 2019).

Fibrocell Science Inc. (2013). *EXTON P. Fibrocell Science Pursues Premium Aesthetic Market Position for LAVIV® | Business Wire. -Fibrocell Science, Inc*. Available online at: https://www.businesswire.com/news/home/20130424006764/en/Fibrocell-Science-Pursues-Premium-Aesthetic-Market-Position (accessed May 9, 2019).

Fibrocell Science Inc. (2020). *Annual Reports*. Available online at: http://www.annualreports.com/HostedData/AnnualReportArchive/f/NASDAQ_FCSC_2013.pdf (accessed May 24, 2020).

Food and Drug Administration (2019a). *Cord Blood - MD Anderson Cord Blood Bank*. Available online at: https://www.FoodandDrugAdministration.gov/vaccines-blood-biologics/cellular-gene-therapy-products/hpc-cord-blood-md-anderson-cord-blood-bank (accessed May 9, 2019).

Food and Drug Administration (2019b). *Cord Blood - Bloodworks | FOOD AND DRUG ADMINISTRATION*. Available online at: https://www.Food and Drug Administration.gov/vaccines-blood-biologics/cellular-gene-therapy-products/hpc-cord-blood-bloodworks (accessed May 9, 2019).

Food and Drug Administration (2019c). *CLEVECORD (HPC Cord Blood)*. Available online at: https://www.Food and Drug Administration.gov/vaccines-blood-biologics/cellular-gene-therapy-products/clevecord-hpc-cord-blood (accessed May 9, 2019).

Food and Drug Administration (2019d). *DUCORD (HPC Cord Blood)*. Available online at: https://www.Food and Drug Administration.gov/vaccines-blood-biologics/cellular-gene-therapy-products/ducord-hpc-cord-blood (accessed May 9, 2019).

Food and Drug Administration (2019e). *HPC, Cord Blood*. Available online at: https://www.Food and Drug Administration.gov/vaccines-blood-biologics/cellular-gene-therapy-products/hpc-cord-blood (accessed May 9, 2019).

Food and Drug Administration (2019f). *HEMACORD (HPC, cord blood)*. Available online at: https://www.Food and Drug Administration.gov/vaccines-blood-biologics/cellular-gene-therapy-products/hemacord-hpc-cord-blood (accessed May 9, 2019).

Food and Drug Administration (2019g). *HPC, Cord Blood - LifeSouth*. Available online at: https://www.Food and Drug Administration.gov/vaccines-blood-biologics/cellular-gene-therapy-products/hpc-cord-blood-lifesouth (accessed May 9, 2019).

Food and Drug Administration (2019h). *Laviv (Azficel-T) | Food And Drug AdministratioN*. Available online at: https://www.Food and Drug Administration.gov/vaccines-blood-biologics/cellular-gene-therapy-products/laviv-azficel-t (accessed May 9, 2019).

Food and Drug Administration (2019i). *Epicel (Cultured Epidermal Autografts) | Food And Drug Administration*. Available online at: https://www.Food and Drug Administration.gov/vaccines-blood-biologics/approved-blood-products/epicel-cultured-epidermal-autografts (accessed May 10, 2019).

Food and Drug Administration (2019j). *PROVENGE* (*sipuleucel-T*) | *FOOD AND DRUG ADMINISTRATION*. Available online at: https://www.Food and Drug Administration.gov/vaccines-blood-biologics/cellular-gene-therapy-products/provenge-sipuleucel-t (accessed May 9, 2019).

Food and Drug Administration (2019k). *KYMRIAH* (*tisagenlecleucel*). Available online at: https://www.Food and Drug Administration.gov/vaccines-blood-biologics/cellular-gene-therapy-products/kymriah-tisagenlecleucel (accessed May 10, 2019).

Food and Drug Administration (2019l). *YESCARTA* (*axicabtagene ciloleucel*). Available online at: https://www.Food and Drug Administration.gov/vaccines-blood-biologics/cellular-gene-therapy-products/yescarta-axicabtagene-ciloleucel (accessed May 10, 2019).

Food and Drug Administration (2019m). *ZOLGENSMA | FOOD AND DRUG ADMINISTRATION*. Available online at: https://www.Food and Drug Administration.gov/vaccines-blood-biologics/zolgensma (accessed June 23, 2019).

Food and Drug Administration (2019n). *Package Insert - LUXTURNA* (*voretigene neparvovec-rzyl*). Available online at: www.Food and Drug Administration.gov/medwatch. (accessed May 10, 2019).

Food and Drug Administration (2019o). *GINTUIT (Allogeneic Cultured Keratinocytes and Fibroblasts in Bovine Collagen)*. Available online at: https://www.Food and Drug Administration.gov/vaccines-blood-biologics/cellular-gene-therapy-products/gintuit-allogeneic-cultured-keratinocytes-and-fibroblasts-bovine-collagen (accessed May 10, 2019).

Food and Drug Administration (2019p). *Integra® Omnigraft™ Dermal Regeneration Matrix-Smart Solutions for Serious Wounds. Patient Guide to Healing Diabetic Foot Ulcers*. Available online at: https://www.accessdata.Food and Drug Administration.gov/cdrh_docs/pdf/P900033S042c.pdf (accessed May 10, 2019).

Food and Drug Administration (2019q). *MACI (Autologous Cultured Chondrocytes on a Porcine Collagen Membrane)*. Available online at: https://www.Food and Drug Administration.gov/vaccines-blood-biologics/cellular-gene-therapy-products/maci-autologous-cultured-chondrocytes-porcine-collagen-membrane (accessed May 10, 2019).

Food and Drug Administration (2020a). *Cellular & Gene Therapy Products | FOOD AND DRUG ADMINISTRATION*. Available online at: https://www.Food and Drug Administration.gov/vaccines-blood-biologics/cellular-gene-therapy-products (accessed May 11, 2020).

Food and Drug Administration (2020b). *yeskarta*. Available online at: https://www.Food and Drug Administration.gov/vaccines-blood-biologics/cellular-gene-therapy-products/yescarta-axicabtagene-ciloleucel (accessed may 28, 2020).

Food and Drug Administration (2020c). *IMLYGIC* (*talimogene Laherparepvec*) | *FOOD AND DRUG ADMINISTRATION*. Available online at: https://www.Food and Drug Administration.gov/vaccines-blood-biologics/cellular-gene-therapy-products/imlygic-talimogene-laherparepvec (accessed May 14, 2020).

Genzyme (2019). *Biosurgery Genzyme. Epicel® (cultured epidermal autografts) HDE# BH990200 Patient Information*. Available online at: https://www.Food and Drug Administration.gov/media/103055/download (accessed May 10, 2019).

Global Sources (2019). *KALODERM | Global Sources*. Available online at: https://www.globalsources.com/si/AS/Tego-Science/6008850646004/pdtl/KALODERM/1131606547.htm (accessed May 10, 2019).

Globenewswire (2020). *Novartis Operational Performance*. Available online at: https://www.globenewswire.com/news-release/2020/04/28/2022974/0/en/Novartis-maintains-strong-operational-performance-in-Q1-confirms-FY-2020-guidance-at-this-time-and-advances-a-broad-range-of-efforts-to-support-the-global-response-to-COVID-19.html (accessed April 28, 2020).

Green Cross Cell (2019). 세포치료 전문기업 *GC* 녹십자셀 *2018*년 *7*월 *24*일 *[Internet]*. Available online at: https://file.irgo.co.kr/data/BOARD/ATTACH_PDF/da48452112f0f845a6b9e1ffd028dab3.pdf (accessed May 11, 2019).

Gupta, P. K., Krishna, M., Chullikana, A., Desai, S., Murugesan, R., Dutta, S., et al. (2017). Administration of adult human bone marrow-derived, cultured, pooled, allogeneic mesenchymal stromal cells in critical limb ischemia due to buerger's disease: phase ii study report suggests clinical efficacy. *Stem Cells Transl. Med.* 6, 689–699. doi: 10.5966/sctm.2016-0237

Hanna, E., Rémuzat, C., Auquier, P., and Toumi, M. (2016a). Advanced therapy medicinal products: current and future perspectives. *J. Mark Access. Heal Policy* 4:31.

Hanna, E., Rémuzat, C., Auquier, P., and Toumi, M. (2016b). Risk of discontinuation of advanced therapy medicinal products clinical trials. *J. Mark Access Heal Policy*. 16:367.

Han-soo, L. (2018). *Corestem's NeuroNata-R Marks Increase in Foreign Patients - Korea Biomedical Review. Koreabiomed*. Available online at: http://www.koreabiomed.com/news/articleView.html?idxno=2138 (accessed May 9, 2019).

Hematology Market (2020). *Growth, Trends, and Forecast (2020-2025)*. Available online at: https://www.mordorintelligence.com/industry-reports/global-hematology-market-industry (accessed May 24, 2020).

Hice, R. (2018). *orthoACI. Global Equity Research led*. Available online at: https://www.orthocell.com.au/s/Orthocell-Limited-Report-April-3-2018-gpnh.pdf (accessed April 3, 2018).

HIYAKU (2019). *quot;HIYAKU"*. Available online at: http://www.jcrpharm.co.jp/wp2/wp-content/uploads/2018/09/ee53eae8e85c0d1d22ce14ee9f0c91a5.pdf (accessed May 11, 2019).

Iglesias-López, C., Agustí, A., Obach, M., and Vallano, A. (2019). Regulatory framework for advanced therapy medicinal products in europe and united states. *Front. Pharmacol.* 10:569.

Imamura, T., Kinugawa, K., Sakata, Y., Miyagawa, S., Sawa, Y., Yamazaki, K., et al. (2016). Improved clinical course of autologous skeletal myoblast sheet (TCD-51073) transplantation when compared to a propensity score-matched cardiac resynchronization therapy population. *J. Artif. Organs* 19, 80–86. doi: 10.1007/s10047-015-0862-9

Imlygic (2017). *Viralytics*. Available online at: https://www.edisoninvestmentresearch.com/?ACT=18&ID=18566&LANG= (accessed April 19, 2017).

Integra (2019). *DFU4041S, Integra OmniGraft Dermal Regeneration Matrix Kit w/Stapler 4cm x 4cm - eSutures*. Available online at: https://www.esutures.com/product/1-expired/105-integra/848-duraplasty/46286263-integra-omnigraft-dermal-regeneration-matrix-kit-wstapler-4cm-x-4cm-DFU4041S/ (accessed May 10, 2019).

Jae-hyeon, S. (2018). *Will Tego Science Win reimbursement for Diabetic foot Ulcer Treatment? - Korea Biomedical Review. Koreabiomed*. Available online at: http://www.koreabiomed.com/news/articleView.html?idxno=3971 (accessed May 10, 2019).

Japan Tissue Engineering Co Ltd. (2020). *Autologous Cultured Cartilage* (*Regenerative Medicine Business*)*?:Japan Tissue Engineering Co., Ltd.* (*J-TEC*). Available from: http://www.jpte.co.jp/english/business/Regenerative/cultured_cartilage.html [accessed on Nov 19, 2020].

Japan Tissue Engineering Ltd. (2009). *Biotech Gate (Company Database)*. Available online at: http://www.jpte.co.jp/english/ir/BIOTECH_report.pdf (acessed May 14, 2020).

Jayaraman, K. S. (2016). *Stempeucel. Natureasia*. Available online at: https://www.natureasia.com/en/nindia/article/10.10 (accessed 15 May 2016).

Jcr Pharmaceuticals Co. (2020). *Products | JCR Pharmaceuticals Co., Ltd.* Available online at: https://www.jcrpharm.co.jp/en/site/en/biopharmaceutical/product_tem.html (accessed May 14, 2020).

Joo-sung, K. (2016). 식약처-심평원은 왜 이 약에 집착할까*? [Internet]*. Available online at: http://www.pressian.com/news/article/?no=140360 (accessed May 9, 2019).

Kantoff, P. W., Higano, C. S., Shore, N. D., Berger, E. R., Small, E. J., Penson, D. F., et al. (2010). Sipuleucel-T immunotherapy for castration-resistant prostate cancer. *N. Engl. J. Med.* 363, 411–422.

Karponi, G., and Zogas, N. (2019). *Gene Therapy for Beta-Thalassemia: Updated Perspectives, Application of Clinical Genetics*, Vol. 12.? Macclesfield: Dove Medical Press Ltd, 167.

Kim, J. H., Lee, Y., Bae, Y.-S., Kim, W. S., Kim, K., and Im, H. Y. (2007). Phase I/II study of immunotherapy using autologous tumor lysate-pulsed dendritic cells in patients with metastatic renal cell carcinoma. *Clin. Immunol.* 125, 257–267. doi: 10.1016/j.clim.2007.07.014

Kim, J.-S. (2014). 화상세포치료제 급여산정 무슨일 있었나? - 메디칼업저버. *Medical Observer*. Available online at: http://www.monews.co.kr/news/articleView.html?idxno=70997 (accessed May 10, 2019).

Kim, S. H., Cho, J. H., Lee, Y. H., Lee, J. H., Kim, S. S., Kim, M. Y., et al. (2018). Improvement in left ventricular function with intracoronary mesenchymal stem cell therapy in a patient with anterior wall st-segment elevation myocardial infarction. *Cardiovasc Drugs Ther.* 32, 329–338. doi: 10.1007/s10557-018-6804-z

Kim, S.-J., Shin, Y.-W., Yang, K.-H., Kim, S.-B., Yoo, M.-J., Han, S.-K., et al. (2009). A multi-center, randomized, clinical study to compare the effect and safety of autologous cultured osteoblast(OssronTM) injection to treat fractures. *BMC Musculoskelet Disord* 10:20.

Kim, Y. S., Smoak, M. M., Melchiorri, A. J., and Mikos, A. G. (2019). An overview of the tissue engineering market in the United States from 2011 to 2. *Tissue Eng. Part A* 25, 1–8. doi: 10.1089/ten.tea.2018.0138

Korea Biomedical (2020). *Sae-im J. Medipost's Stem Cell Therapy, Cord Blood Bank Show Solid Growth - Korea Biomedical Review*. Available online at: http://www.koreabiomed.com/news/articleView.html?idxno=6289 (accessed May 14, 2020).

Kudrin, A. (2018). Business models and opportunities for cancer vaccine developers. *Hum. Vaccin. Immunother.* 8, 1431–1438. doi: 10.4161/hv.20629

Lane, E. (2016). *Stempeutics' Buerger's Disease Cell Therapy Gets Conditional Nod in India | FiercePharma. Pharma Asia*. Available online at: https://www.fiercepharma.com/pharma-asia/stempeutics-buerger-s-disease-cell-therapy-gets-conditional-nod-india (accessed May 14, 2020).

Lee, B. (2018). *9 Challenges Keeping Cell And Gene Therapy Executives Up At Night. RepliCel Life Sciences Inc*. Available online at: https://www.cellandgene.com/doc/challenges-keeping-cell-and-gene-therapy-executives-up-at-night-0001 (accessed May 27, 2020).

Lee, J. H., Lee, J.-H., Lim, Y.-S., Yeon, J. E., Song, T.-J., and Yu, S. J. (2015). Adjuvant immunotherapy with autologous cytokine-induced killer cells for hepatocellular carcinoma. *Gastroenterology* 148, 1383–1391. doi: 10.1053/j.gastro.2015.02.055

Luria, B. S. X. R., Castelo, F. F., Vandromme, M., Monteiro, S., Portuguesa, B. A., Rogelio, P. C. A., et al. (2020). *BIOREG* (SOE3/P1/E750)-Co-financed by the INTERREG IVB SUDOE Program with ERDF funds Handbook about Regulatory Guidelines and Procedures for the Preclinical and Clinical Stages of Advanced Therapy Medicinal Products (ATMPs) Reviewers: Editor. Available online at: www.ddrmedic.com (accessed May 24, 2020).

Market Research (2020). *Consulting, Reports, Advisory, Sizing | Consulting - Client Research, Market Analysis | Competitive Landscape Analysis | Global Strategic Business Reports | Custom Market Research - Mordor Intelligence*. Available online at: https://www.mordorintelligence.com/industry-reports/dermatological-therapeutics-market (accessed May 23, 2020).

Marston, W. A., Hanft, J., Norwood, P., and Pollak, R. (2003). Dermagraft diabetic foot ulcer study group. the efficacy and safety of dermagraft in improving the healing of chronic diabetic foot ulcers: results of a prospective randomized trial. *Diabetes Care* 26, 1701–1705. doi: 10.2337/diacare.26.6.1701

Matsumura, H., Matsushima, A., Ueyama, M., and Kumagai, N. (2016). Application of the cultured epidermal autograft "JACE®" for treatment of severe burns: results of a 6-year multicenter surveillance in Japan. *Burns* 42, 769–776. doi: 10.1016/j.burns.2016.01.019

Maude, S. L., Laetsch, T. W., Buechner, J., Rives, S., Boyer, M., Bittencourt, H., et al. (2018). Tisagenlecleucel in children and young adults with b-cell lymphoblastic leukemia. *N. Engl. J. Med.* 378, 439–448.

McConaghie, A. (2017). *Glybera, The Most Expensive Drug in the World, to be Withdrawn After Commercial Flop -. Pharmaphorum*. Available

online at: https://pharmaphorum.com/news/glybera-expensive-drug-world-withdrawn-commercial-flop/ (accessed May 14, 2020).

McGuire, M. K., Scheyer, E. T., Nevins, M. L., Neiva, R., Cochran, D. L., Mellonig, J. T., et al. (2011). Living Cellular construct for increasing the width of keratinized gingiva: results from a randomized, within-patient, controlled trial. *J. Periodontol.* 82, 1414–1423. doi: 10.1902/jop.2011.100671

Medical observer (2019). 말 많던 화상약제 케라힐, 결국 감사원 감사 결정 - 메디칼업저버. Available online at: http://www.monews.co.kr/news/articleView.html?idxno=75292 (accessed Jun 23, 2019).

Medipost (2019). *The Future of Biotechnology*. Available online at: http://www.medi-post.com/front/eng/stemcell/cartistem.do (accessed Jun 23, 2019).

Mesoblast Limited (2020). *(ASX:MSB) - Msb, Page-2 - HotCopper | ASX Share Prices, Stock Market & Share Trading Forum*. Available online at: https://hotcopper.co.nz/threads/msb.4694211/page-2 (accessed May 17, 2020).

Miller, J. (2018). *Novartis wins EU Approval for Blood Cancer Therapy Kymriah - Reuters. Reuters Helath News*. Available online at: https://www.reuters.com/article/us-novartis-cancer/novartis-wins-eu-approval-for-blood-cancer-therapy-kymriah-idUSKCN1LC0CU/ (accessed May 10, 2019).

Mills, R. (2019). *Counting Coup: Is Osiris Losing Faith in Prochymal? | SCSI Stem Cell Stock Index. Osiris Therapeutics*. Available online at: http://busaconsultingllc.com/scsi/organelles/counting_coup_prochymal.php (accessed May 9, 2019).

Ministry of Food and Drug Safety (2019a). (*Cell therapy products*) *JW CreaGene Corporation View|Biological Products | Minisry of Food and Drug Safety*. Available online at: http://www.mfds.go.kr/eng/brd/m_30/view.do?seq=71375 (accessed May 9, 2019).

Ministry of Food and Drug Safety (2019b). (*Cell Therapy Prodcuts*) *Green Cross Cell Corp. View|Biological Products* |. Available online at: https://www.mfds.go.kr/eng/brd/m_30/view.do?seq=70951 (accessed Jun 23, 2019).

Ministry of Food and Drug Safety (2019c). *Minisry of Food and Drug Safety*. Available online at: https://www.mfds.go.kr/eng/index.do (accessed Jun 23, 2019)

Ministry of Food and Drug Safety (2020). (*Cell Therapy Products*) *ANTEROGEN View|Biological Products | Minisry of Food and Drug Safety*. Available online at: https://www.mfds.go.kr/eng/brd/m_30/view.do?seq=71337&srchFr=&srchTo=&srchWord=&srchTp=&itm_seq_1=0&itm_seq_2=0&multi_itm_seq=0&company_cd=&company_nm=&page=1 (accessed May 15, 2020).

Mksvc (2019). 플랜트사업부 수주 증가로 턴어라운드. Available online at: http://file.mk.co.kr/imss/write/20150724104734_mksvc01_00.pdf (accessed May 11, 2019).

MolMed (2018). *Annual Report as of December 31st, 2018*. Available online at: https://www.molmed.com/sites/default/files/2019-11/EN 31 12 2018_ last.pdf (accessed May 27, 2020).

MolMed (2019). *MolMed S.p.A*. Available online at: https://www.molmed.com/search/node/Zalmoxis?page=2 (accessed May 10, 2019).

Mount, N. M., Ward, S. J., Kefalas, P., and Hyllner, J. (2015). *Cell-Based Therapy Technology Classifications and Translational Challenges, Philosophical Transactions of the Royal Society B: Biological Sciences*, London: Royal Society, 370.

Mullin, E. (2019). *A Year After Approval, Gene-Therapy Cure Gets Its First Customer - MIT Technology Review. MIT thechnology review*. Available online at: https://www.technologyreview.com/s/604295/a-year-after-approval-gene-therapy-cure-gets-its-first-customer/ (accessed May 10, 2019).

Muroi K, Miyamura K, Okada M, Yamashita T, Murata M, Ishikawa T, et al. (2016). Bone marrow-derived mesenchymal stem cells (JR-031) for steroid-refractory grade III or IV acute graft-versus-host disease: a phase II/III study. *Int. J. Hematol.* 103, 243–50.

Napodano, J. (2015). *aurix. Nuo Therapeutics, Inc*. Available online at: http://s1.q4cdn.com/460208960/files/May-15-2015_NUOT_Napodano_v001_v296b7.pdf (accessed May 15, 2015).

Naver (2019). 콘드론 : 네이버 블로그. Available online at: https://m.blog.naver.com/azure0321/150107641730 (accessed Jun 23, 2019).

Neelapu, S. S., Locke, F. L., Bartlett, N. L., Lekakis, L. J., Miklos, D. B., Jacobson, C. A., et al. (2017). Axicabtagene Ciloleucel CAR T-Cell Therapy in Refractory Large B-Cell Lymphoma. *N. Engl. J. Med.* 377, 2531–2544.

Neurodegenerative Disease Market (2020). *Growth, Trends, and Forecast (2019-2024)*. Available online at: https://www.mordorintelligence.com/industry-reports/neurodegenerative-disease-market (accessed May 24, 2020).

NICE (2019). *2 Information About Darvadstrocel | Darvadstrocel for Treating Complex Perianal Fistulas in Crohn's Disease | Guidance | NICE. National Institute for Health and Care Excellence*. Available online at: https://www.nice.org.uk/guidance/ta556/chapter/2-Information-about-darvadstrocel (accessed May 11, 2020).

Nordmeyer, S., Murin, P., Schulz, A., Danne, F., Nordmeyer, J., Kretzschmar, J., et al. (2018). Results of aortic valve repair using decellularized bovine pericardium in congenital surgery. *Eur. J. Cardio. Thoracic Surg.* 54, 986–992. doi: 10.1093/ejcts/ezy181

NOVARTIS (2019a). *MEDIA RELEASE COMMUNIQUE AUX MEDIAS MEDIENMITTEILUNG AveXis receives Food And Drug Administration approval for Zolgensma®, the First and Only Gene Therapy for Pediatric Patients with Spinal Muscular Atrophy (SMA)*. Available online at: http://www.novartis.com (accessed Jun 23, 2019).

Novartis. (2019b). *Novartis Receives Health Canada approval of its CAR-T cell therapy, Kymriah™ (tisagenlecleucel) | Novartis Canada*. Available online at: https://www.novartis.ca/en/news/media-releases/novartis-receives-health-canada-approval-its-car-t-cell-therapy-kymriah (accessed May 10, 2019).

Nuo Therapeutics Inc. (2019). *Treatment For Tunneling, Sinus Tracts & More - Aurix System*. Available online at: http://www.nuot.com/aurix-system/ (accessed May 10, 2019).

Oh, K.-W., Moon, C., Kim, H. Y., Oh, S., Park, J., Lee, J. H., et al. (2015). Phase I trial of repeated intrathecal autologous bone marrow-derived mesenchymal stromal cells in amyotrophic lateral sclerosis. *Stem Cells Transl. Med.* 4, 590–597. doi: 10.5966/sctm.2014-0212

Ophthalmic Drugs Market (2020). *Growth, Trends, and Forecast (2019-2024)*. Available online at: https://www.mordorintelligence.com/industry-reports/global-opthalmic-drugs-market (accessed May 24, 2020).

Organogenesis Inc. (2019a). *Canton, Mass / San Diego C. Organogenesis Secures $30 Million in Financing to Fund Aggressive Expansion of Commercial Operations and Product Portfolio | Organogenesis Holdings Inc*. Available online at: https://investors.organogenesis.com/news-releases/news-release-details/organogenesis-secures-30-million-financing-fund-aggressive (accessed May 11, 2019).

Organogenesis Inc. (2019b). *CANTON M. Organogenesis Names New Chief Commercial Officer and Chief Operating Officer | Organogenesis Holdings Inc.* Available online at: https://investors.organogenesis.com/news-releases/news-release-details/organogenesis-names-new-chief-commercial-officer-and-chief (accessed May 11, 2019).

Organogenesis Inc. (2019c). *Apligraf?: What is Apligraf?* Available online at: http://www.apligraf.com/professional/what_is_apligraf/index.html (accessed May 10, 2019).

Organogenesis Inc. (2019d). *About Dermagraft*. Available online at: http://www.dermagraft.com/patient/about-dermagraft/ (accessed May 10, 2019).

Organogenesis Inc. (2020). *apligraft*. Available online at: http://www.apligraf.com/professional/pdf/PaymentRateSheetHospitalOutpatient.pdf (accessed May 5, 2020).

Orthocell (2018). (*ASX: OCC*) *Growing with CelGro®. NDF research*. Available online at: https://static1.squarespace.com/static/55d2ae4ce4b0e20eb51007ce/t/5aafccb4575d1ff97c019043/1521470660673/2018+03+20+Orthocell+report+from+NDF+Research_Final.pdf (accessed May 9, 2019).

Orthocell (2019). *Cartilage Regeneration — Orthocell*. Available online at: https://www.orthocell.com.au/ortho-aci/ (accessed May 9, 2019).

Orthopedic Devices Market (2020). *Growth, Trends, and Forecasts (2020 - 2025)*. Available online at: https://www.mordorintelligence.com/industry-reports/global-orthopedic-devices-market-industry (accessed May 24, 2020).

Park, Y.-B., Ha, C.-W., Lee, C.-H., Yoon, Y. C., and Park, Y.-G. (2017). Cartilage regeneration in osteoarthritic patients by a composite of allogeneic umbilical cord blood-derived mesenchymal stem cells and hyaluronate hydrogel: results from a clinical trial for safety and proof-of-concept with 7 years of extended follow-Up. *Stem Cells Transl. Med.* 6, 613–621. doi: 10.5966/sctm.2016-0157

Pharmaceuticals and Medical Devices Agency (2019). *List of Approved Products | Pharmaceuticals and Medical Devices Agency*. Available online at: https://www.pmda.go.jp/english/review-services/reviews/approved-information/0002.html (accessed May 10, 2019).

Pharmicell Ltd. (2020). Available online at: http://www.pharmicell.com/ (accessed May 24, 2020).

PMDA (2011). *Hata D S Ph D Ken ichiro Hata DDS KD. PMDA 4th International Symposium on Biologics PMDA 4th International Symposium on Biologics J-TEC's Perspective: The Clinical Development of the Autologous cell/Tissue-Based Medicinal Products cell/Tissue Based Medicinal Products*. Available online at: https://www.pmda.go.jp/files/000152967.pdf (accessed May 14, 2020).

Prasad, V. K., Lucas, K. G., Kleiner, G. I., Talano, J. A. M., Jacobsohn, D., Broadwater, G., et al. (2011). Efficacy and Safety of ex vivo cultured adult human mesenchymal stem cells (prochymaltm) in pediatric patients with severe refractory acute graft-versus-host disease in a compassionate use study. *Biol. Blood Marrow Transplant* 17, 534–541. doi: 10.1016/j.bbmt.2010.04.014

Pricing of Approved Cell Therapy (2019). Available online at: https://bioinformant.com/price-of-cell-therapy-products/ (accessed May 9, 2019).

Rama, P., Matuska, S., Paganoni, G., Spinelli, A., De Luca, M., and Pellegrini, G. (2010). Limbal stem-cell therapy and long-term corneal regeneration. *N. Engl. J. Med.* 363, 147–155. doi: 10.1056/nejmoa0905955

Rattue, P. (2012). *Prochymal–First Stem Cell Drug Approved. Medical News Today*. Available online at: https://www.medicalnewstoday.com/articles/245704.php (accessed May 9, 2019).

Regrow Biosciences Pvt.Ltd. (2019). Available online at: https://www.regrow.in/ (accessed May 9, 2019).

Rosen, L. (2012). *Gene Therapy Product Gets Green Light With More Comng Soon*. Available online at: https://www.21stcentech.com/biomedicine-update-commercial-gene-therapy-treatments-starting-2013/ (accessed May 10, 2019).

Russell, S., Bennett, J., Wellman, J. A., Chung, D. C., Yu, Z.-F., Tillman, A., et al. (2017). Efficacy and safety of voretigene neparvovec (AAV2-hRPE65v2) in patients with RPE65 -mediated inherited retinal dystrophy: a randomised, controlled, open-label, phase 3 trial. *Lancet* 390, 849–860.

RxList (2018). *Allocord (Cord Blood Injectable Suspension for Intravenous Use): Side Effects, Interactions, Warning, Dosage & Uses*. Available online at: https://www.rxlist.com/allocord-drug.html (accessed May 9, 2019).

Safer (2019). *Cancer Therapy Trials in India Show Promise*. Available online at: http://www.delhidailynews.com/news/Safer-cancer-therapy-trials-in-India-show-promise-1400044111/ (accessed May 9, 2019).

Sang-jun, P. (2010). 자가세포 이용 흉터 치료제 '큐어스킨' 출시 - 메디칼업저버. *Medical observer*. Available online at: http://www.monews.co.kr/news/articleView.html?idxno=36759 (accessed Jun 23, 2019).

Saris, D., Price, A., Widuchowski, W., Bertrand-Marchand, M., Caron, J., Drogset, J. O., et al. (2014). Matrix-applied characterized autologous cultured chondrocytes versus microfracture. *Am. J. Sports Med.* 42, 1384–1394. doi: 10.1177/0363546514528093

S-Biomedics Ltd. (2019a). 체세포 치료제 - *S.BIOMEDICS [Internet]*. Available online at: http://http://sbiomedics.com/체세포 치료제 (accessed May 10, 2019).

S-Biomedics Ltd. (2019b). (*Cell therapy products*) *S.Biomedics Co., Ltd. View|Biological Products | Minisry of Food and Drug Safety*. Available online at: https://www.mfds.go.kr/eng/brd/m_30/view.do?seq=71390 (accessed Jun 23, 2019).

Schlatter, S. (2019). *Epicel Skin Grafts*. Available online at: http://www.Food and Drug Administration.gov/cdrh/mda/docs/H990002.html (accessed May 10, 2019).

Schuster, S. J., Bishop, M. R., Tam, C. S., Waller, E. K., Borchmann, P., McGuirk, J. P., et al. (2019). Tisagenlecleucel in adult relapsed or refractory diffuse large B-cell lymphoma. *N. Engl. J. Med.* 380, 45–56.

SCT (2019). *Stem-art*. Available online at: http://www.stem-art.com/Library/Miscellaneous/SCT products Sheet 1.pdf (accessed April 5, 2019).

Senior, M. (2017). After Glybera's withdrawal, what's next for gene therapy? *Nat. Biotechnol.* 35, 491–492. doi: 10.1038/nbt0617-491

Seoane-Vazquez, E., Shukla, V., and Rodriguez-Monguio, R. (2019). Innovation and competition in advanced therapy medicinal products. *EMBO Mol Med.* 11:3.

Sewon Cellontech Ltd. (2019a). (*Cell therapy products*) *Sewon Cellontech Co., LTD. View|Biological Products | Minisry of Food and Drug Safety*. Available online at: https://www.mfds.go.kr/eng/brd/m_30/view.do?seq=70954&srchFr=&srchTo=&srchWord=&srchTp=&itm_seq_1=0&itm_seq_2=0&multi_itm_seq=0&company_cd=&company_nm=&page=1 (accessed Jun 23, 2019).

Sewon Cellontech Ltd. (2019b). (*Cell therapy products*) *Sewon Cellontech Co., LTD. View|Biological Products | Minisry of Food and Drug Safety*. Available online at: http://www.mfds.go.kr/eng/brd/m_30/view.do?seq=70954 (accessed May 9, 2019).

Sharma, V. (2019). *Disappointing End For MolMed's Zalmoxis Cell Therapy In EU?:: Pink Sheet. Pharmaintelligence*. Available online at: https://pink.pharmaintelligence.informa.com/PS140998/Disappointing-End-For-MolMeds-Zalmoxis-Cell-Therapy-In-EU (accessed Jan 13, 2020).

Sibiono (2019). *Weblet Importer*. Available online at: http://www.sibiono.com/en/index.aspx (accessed May 10, 2019).

SinaCell Enterprise Knowledge Management (2019). *Home English - SinaCell Co*. Available online at: http://sinacellco.com/?lang=en (accessed May 10, 2019).

Soft Tissue Repair Market (2020). *Growth, Trends, and Forecast (2019-2024)*. Available online at: https://www.mordorintelligence.com/industry-reports/soft-tissue-repair-market (accesed May 24, 2020).

Spark Therapeutics Inc. (2019). *Spark Therapeutics Reports Second Quarter 2018 Financial Results and Recent Business Progress | Spark Therapeutics Inc. – IR Site*. Available online at: http://ir.sparktx.com/news-releases/news-release-details/spark-therapeutics-reports-second-quarter-2018-financial-results (accessed May 11, 2019).

Specialist pharmecy service (2020). *Darvadstrocel – Medicines – SPS - Specialist Pharmacy Service – The First stop for Professional Medicines Advice. Specialist Pharmecy Service*. Available online at: https://www.sps.nhs.uk/medicines/darvadstrocel/ (accessed May 11, 2020).

Startseite. (2020). *Startseite*. Available from: https://www.codon.de/. (accessed on Nov 19, 2020).

Stem Cell Research (2019). *Stem Cell Blog - Cell Therapy 2016 – Year in Review (part 1) | Cell Trials*. Available online at: http://celltrials.info/2016/12/31/cell-therapy-2016-year-review-1/ (accessed May 10, 2019).

Stempeutics Research Pvt Ltd. (2019). *Stem Cell, stempeucel, stempeutron, stempeucare, USA Patents, Cuticera, Manipal Group, Cipla*. Available online at: http://www.stempeutics.com/ (accessed May 9, 2019).

StreetInsider (2015). *Mesoblast's (MESO) Japan Licensee Receives Pricing for TEMCELL HS Inj. For Treatment of aGVHD. Streetinsider*. Available online at: https://www.streetinsider.com/Corporate+News/Mesoblasts+%28MESO%29+Japan+Licensee+Receives+Pricing+for+TEMCELL+HS+Inj.+For+Treatment+of+aGVHD/11109517.html (accessed May 14, 2020).

Sun-kyu, K. (2016). 더벨 - 국내 최고 자본시장(*Capital Markets*) 미디어. Available online at: http://www.thebell.co.kr/free/content/ArticleView.asp?key=201602030100007350000448&lcode=00 (accessed Jun 23, 2019).

SunWay Biotech (2019). 上海三维生物技术有限公司. Available online at: http://www.sunwaybio.com.cn/en/product.html (accessed May 10, 2019).

Taylor and Francis Group (2015). *cardiocel*. Available online at: https://www.tandfonline.com/doi/full/10.1586/17434440.2015.985651?scroll=top&needAccess=true (accessed April 10, 2015).

Tego Science (2019a). 로스미르® *CELL THERAPY?:: TECO SCIENCE [Internet]*. Available online at: http://www.tegoscience.com/kor/product/view.do?prdSeq=13 (accessed May 10, 2019).

Tego Science (2019b). 홀로덤® *CELL THERAPY?:: TECO SCIENCE [Internet]*. Available online at: http://www.tegoscience.com/kor/product/view.do?prdSeq=7 (accessed May 10, 2019).

Tego Science (2019c). 칼로덤® *CELL THERAPY?:: TECO SCIENCE [Internet]*. Available online at: http://www.tegoscience.com/kor/product/view.do?prdSeq=12 (accessed May 10, 2019).

Tego Science (2019d). 본 자료는 제안된 *IPO* 공모와 관련하여 기관투자가와 일반투자자들을 대상으로 실시되는 *PRESENTATION* 에서의 정보제공을 목적으로 테고사이언스㈜ *[Internet]. INVESTOR RELATIONS 2*. Available online at: http://w3.kirs.or.kr/download/broadcast/테고사이언스_IR Book.pdf (accessed May 11, 2019).

Tego Science (2019e). (*Cell therapy products*) *Tego Science, Inc View|Biological Products | Minisry of Food and Drug Safety*. Available online at: http://www.mfds.go.kr/eng/brd/m_30/view.do?seq=71359 (accessed May 10, 2019).

Tego Science (2020a). 홍보 < *PR/IR?:: TECO SCIENCE*. Available online at: http://www.tegoscience.com/kor/board/view.do?seq=309 (accessed May 15, 2020).

Tego Science (2020b). (*Cell therapy products*) *Tego Science, Inc View|Biological Products | Minisry of Food and Drug Safety*. Available online at: https://www.mfds.go.kr/eng/brd/m_30/view.do?seq=71359 (accessed May 15, 2020).

Ten Ham, R. M. T., Hoekman, J., Hövels, A. M., Broekmans, A. W., Leufkens, H. G. M., and Klungel, O. H. (2018). Challenges in advanced therapy medicinal

product development: a survey among companies in Europe. *Mol. Ther. Methods Clin. Dev.* 11, 121–130. doi: 10.1016/j.omtm.2018.10.003

Timmerman, L. (2010). *Xconomy: Dendreon Sets Provenge Price at $93,000, Says Only 2,000 People Will Get it in First Year*. Available online at: https://xconomy.com/seattle/2010/04/29/dendreon-sets-provenge-price-at-93000-says-only-2000-people-will-get-it-in-first-year/ (accessed May 9, 2019).

Tohyama, H., Yasuda, K., Minami, A., Majima, T., Iwasaki, N., Muneta, T., et al. (2009). Atelocollagen-associated autologous chondrocyte implantation for the repair of chondral defects of the knee: a prospective multicenter clinical trial in Japan. *J. Orthop. Sci.* 14, 579–588. doi: 10.1007/s00776-009-1384-1

Vericel Corporation (2019). *Seeking Alpha*. Available online at: https://seekingalpha.com/filing/4373677 (accessed May 11, 2019).

Viganò, M., Budelli, S., Lavazza, C., Montemurro, T., Montelatici, E., De Cesare, S., et al. (2018). Tips and tricks for validation of quality control analytical methods in good manufacturing practice mesenchymal stromal cell production. *Stem Cells Int.* 2018:3038565.

WHO (2013). *Haematopoietic Stem Cell Transplantation HSCtx*. Geneva: WHO.

Woo, S. J. (2007). 약업닷컴 (약업신문) - 뉴스 :: 민・관 협력 항암제 개발 개가 *[Internet]*. Available online at: http://m.yakup.com/?m=n&mode=view&nid=90918 (accessed May 9, 2019).

Yeh, A. C., Khan, M. A., Harlow, J., Biswas, A. R., Akter, M., Ferdous, J., et al. (2018). Hematopoietic stem-cell transplantation in the resource-limited setting: establishing the first bone marrow transplantation unit in bangladesh. *J. Glob. Oncol.* 4, 1–10. doi: 10.1007/978-3-319-59358-6_1

Yim, H., Yang, H. T., Cho, Y. S., Seo, C. H., Lee, B. C., and Ko, J. H. (2011). Clinical study of cultured epithelial autografts in liquid suspension in severe burn patients. *Burns* 37, 1067–1071. doi: 10.1016/j.burns.2011.03.018

Yoon, J., Yang, H.-T., Yim, H., Cho, Y.-S., Kym, D., and Hur, J. (2017). Effectiveness and safety of a thermosensitive hydrogel cultured epidermal allograft for burns. *Adv Skin Wound Care* 30, 559–564. doi: 10.1097/01.asw.0000526882.14740.01

You, H.-J., Han, S.-K., Lee, J.-W., and Chang, H. (2012). Treatment of diabetic foot ulcers using cultured allogeneic keratinocytes-A pilot study. *Wound Repair Regen* 20:334.

Zalmoxis (2016). Available online at: https://www.ema.europa.eu/en/medicines/human/EPAR/zalmoxis (accessed September 5, 2016).

Zhang, W.-W., Li, L., Li, D., Liu, J., Li, X., Li, W., et al. (2018). The first approved gene therapy product for cancer Ad- p53 (Gendicine): 12 Years in the clinic. *Hum. Gene Ther.* 29, 160–179. doi: 10.1089/hum.2017.218

Conflict of Interest: The authors declare that the research was conducted in the absence of any commercial or financial relationships that could be construed as a potential conflict of interest.

Advantages of publishing in Frontiers

OPEN ACCESS
Articles are free to read for greatest visibility and readership

FAST PUBLICATION
Around 90 days from submission to decision

HIGH QUALITY PEER-REVIEW
Rigorous, collaborative, and constructive peer-review

TRANSPARENT PEER-REVIEW
Editors and reviewers acknowledged by name on published articles

Frontiers
Avenue du Tribunal-Fédéral 34
1005 Lausanne | Switzerland

Visit us: www.frontiersin.org
Contact us: frontiersin.org/about/contact

REPRODUCIBILITY OF RESEARCH
Support open data and methods to enhance research reproducibility

DIGITAL PUBLISHING
Articles designed for optimal readership across devices

FOLLOW US
@frontiersin

IMPACT METRICS
Advanced article metrics track visibility across digital media

EXTENSIVE PROMOTION
Marketing and promotion of impactful research

LOOP RESEARCH NETWORK
Our network increases your article's readership